

THESE TERMS GOVERN YOUR USE OF THIS DOCUMENT

Your use of this Ontario Geological Survey document (the “Content”) is governed by the terms set out on this page (“Terms of Use”). By downloading this Content, you (the “User”) have accepted, and have agreed to be bound by, the Terms of Use.

Content: This Content is offered by the Province of Ontario’s *Ministry of Northern Development and Mines* (MNDM) as a public service, on an “as-is” basis. Recommendations and statements of opinion expressed in the Content are those of the author or authors and are not to be construed as statement of government policy. You are solely responsible for your use of the Content. You should not rely on the Content for legal advice nor as authoritative in your particular circumstances. Users should verify the accuracy and applicability of any Content before acting on it. MNDM does not guarantee, or make any warranty express or implied, that the Content is current, accurate, complete or reliable. MNDM is not responsible for any damage however caused, which results, directly or indirectly, from your use of the Content. MNDM assumes no legal liability or responsibility for the Content whatsoever.

Links to Other Web Sites: This Content may contain links, to Web sites that are not operated by MNDM. Linked Web sites may not be available in French. MNDM neither endorses nor assumes any responsibility for the safety, accuracy or availability of linked Web sites or the information contained on them. The linked Web sites, their operation and content are the responsibility of the person or entity for which they were created or maintained (the “Owner”). Both your use of a linked Web site, and your right to use or reproduce information or materials from a linked Web site, are subject to the terms of use governing that particular Web site. Any comments or inquiries regarding a linked Web site must be directed to its Owner.

Copyright: Canadian and international intellectual property laws protect the Content. Unless otherwise indicated, copyright is held by the Queen’s Printer for Ontario.

It is recommended that reference to the Content be made in the following form:

Ontario Geological Survey 2012. Summary of Field Work and Other Activities 2012; Ontario Geological Survey, Open File Report 6280, 476p.

or, for partial Content

Béland Otis, C. 2012. Preliminary results: potential Ordovician shale gas units in southern Ontario; *in* Summary of Field Work and Other Activities 2012, Ontario Geological Survey, Open File Report 6280, p.29-1 to 29-12.

Use and Reproduction of Content: The Content may be used and reproduced only in accordance with applicable intellectual property laws. *Non-commercial* use of unsubstantial excerpts of the Content is permitted provided that appropriate credit is given and Crown copyright is acknowledged. Any substantial reproduction of the Content or any *commercial* use of all or part of the Content is prohibited without the prior written permission of MNDM. Substantial reproduction includes the reproduction of any illustration or figure, such as, but not limited to graphs, charts and maps. Commercial use includes commercial distribution of the Content, the reproduction of multiple copies of the Content for any purpose whether or not commercial, use of the Content in commercial publications, and the creation of value-added products using the Content.

Contact:

FOR FURTHER INFORMATION ON	PLEASE CONTACT:	BY TELEPHONE:	BY E-MAIL:
The Reproduction of the Content	MNDM Publication Services	Local: (705) 670-5691 Toll-Free: 1-888-415-9845, ext. 5691 (inside Canada, United States)	Pubsales.ndm@ontario.ca
The Purchase of MNDM Publications	MNDM Publication Sales	Local: (705) 670-5691 Toll-Free: 1-888-415-9845, ext. 5691 (inside Canada, United States)	Pubsales.ndm@ontario.ca
Crown Copyright	Queen’s Printer	Local: (416) 326-2678 Toll-Free: 1-800-668-9938 (inside Canada, United States)	Copyright@gov.on.ca



**Ontario Geological Survey
Open File Report 6280**

**Summary of Field Work
and Other Activities
2012**

2012



ONTARIO GEOLOGICAL SURVEY

Open File Report 6280

Summary of Field Work and Other Activities 2012

by

Ontario Geological Survey

Edited by G.P. Beakhouse, R.D. Dyer, R.M. Easton, O.M. Burnham, B.R. Berger, A.F. Bajc, S. Préfontaine, S.M. Hamilton, F.R. Brunton, J.R. Parker and E.J. Debicki

2012

Parts of this publication may be quoted if credit is given. It is recommended that reference to this publication be made in the following form:

Béland Otis, C. 2012. Preliminary results: potential Ordovician shale gas units in southern Ontario; *in* Summary of Field Work and Other Activities 2012, Ontario Geological Survey, Open File Report 6280, p.29-1 to 29-12.

Users of OGS products are encouraged to contact those Aboriginal communities whose traditional territories may be located in the mineral exploration area to discuss their project.

Open File Reports of the Ontario Geological Survey are available for viewing at the John B. Gammon Geoscience Library in Sudbury and at the regional Mines and Minerals office whose district includes the area covered by the report (see below).

Copies can be purchased at Publication Sales and the office whose district includes the area covered by the report. Although a particular report may not be in stock at locations other than the Publication Sales office in Sudbury, they can generally be obtained within 3 working days. All telephone, fax, mail and e-mail orders should be directed to the Publication Sales office in Sudbury. Purchases may be made using cash, debit card, VISA, MasterCard, American Express, cheque or money order. Cheques or money orders should be made payable to the *Minister of Finance*.

John B. Gammon Geoscience Library
933 Ramsey Lake Road, Level A3
Sudbury, Ontario P3E 6B5

Tel: (705) 670-5615

Publication Sales
933 Ramsey Lake Rd., Level A3
Sudbury, Ontario P3E 6B5

Tel: (705) 670-5691 (local)
Toll-free: 1-888-415-9845 ext. 5691
Fax: (705) 670-5770
E-mail: pubsales.ndm@ontario.ca

Regional Mines and Minerals Offices:

Kenora - Suite 104, 810 Robertson St., Kenora P9N 4J2

Kirkland Lake - 10 Government Rd. E., Kirkland Lake P2N 1A8

Red Lake - Box 324, Ontario Government Building, Red Lake P0V 2M0

Sault Ste. Marie - 875 Queen St. E., Suite 6, Sault Ste. Marie P6A 6V8

Southern Ontario - P.O. Bag Service 43, 126 Old Troy Rd., Tweed K0K 3J0

Sudbury - 933 Ramsey Lake Rd., Level A3, Sudbury P3E 6B5

Thunder Bay - Suite B002, 435 James St. S., Thunder Bay P7E 6S7

Timmins - Ontario Government Complex, P.O. Bag 3060, Hwy. 101 East, South Porcupine P0N 1H0

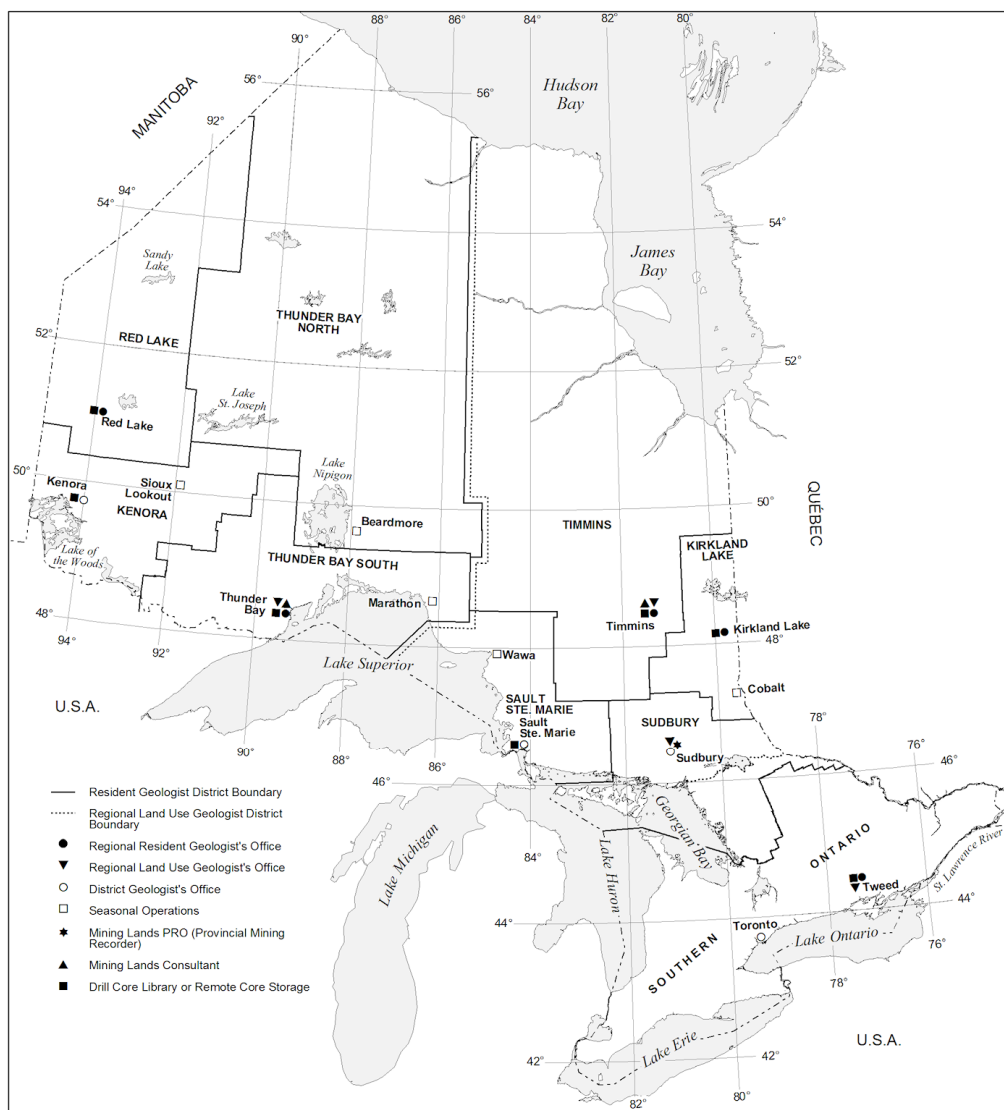
This report has not received a technical edit. Discrepancies may occur for which the Ontario Ministry of Northern Development and Mines does not assume any liability. Source references are included in the report and users are urged to verify critical information. Recommendations and statements of opinions expressed are those of the author or authors and are not to be construed as statements of government policy.

If you wish to reproduce any of the text, tables or illustrations in this report, please write for permission to the Team Leader, Publication Services, Ministry of Northern Development and Mines, 933 Ramsey Lake Road, Level A3, Sudbury, Ontario P3E 6B5.

Cette publication est disponible en anglais seulement.

Parts of this report may be quoted if credit is given. It is recommended that reference be made in the following form:

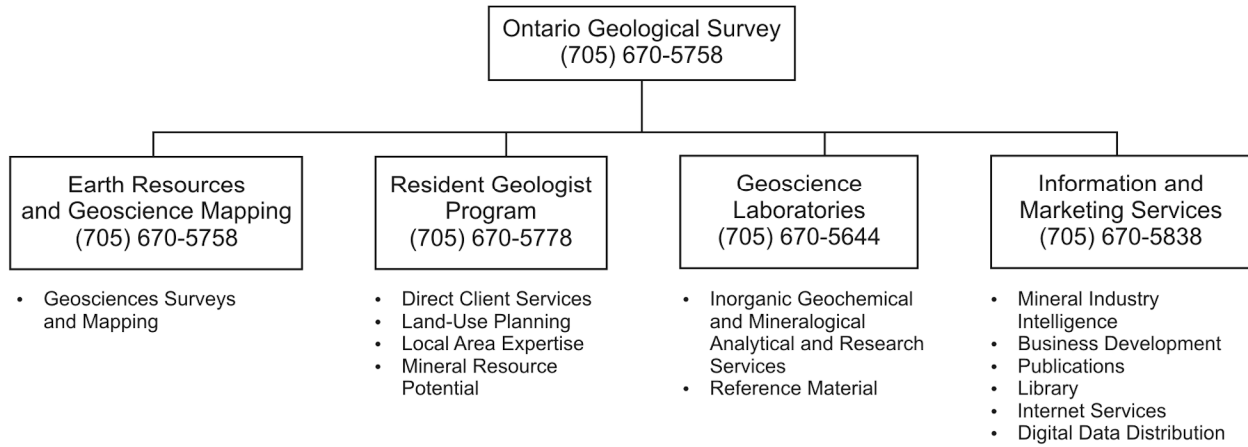
Béland Otis, C. 2012. Preliminary results: potential Ordovician shale gas units in southern Ontario; in Summary of Field Work and Other Activities 2012, Ontario Geological Survey, Open File Report 6280, p.29-1 to 29-12.



Mines and Minerals Division Regional and District Offices

CITY	ADDRESS	OFFICE(S)	TELEPHONE	FAX
Kenora	Suite 104, 810 Robertson St., Kenora P9N 4J2	○ ■	(807) 468-2819	(807) 468-2930
Red Lake	227 Howey Street, P.O. Box 324, Red Lake P0V 2M0	● ■	(807) 727-2464	(807) 727-3553
Thunder Bay – North	Suite B002, 435 James St. S., Thunder Bay P7E 6S7	● ■ ▼ ▲	(807) 475-1331 (807) 475-1311	(807) 475-1112 (807) 475-1112
Thunder Bay – South	Suite B002, 435 James St. S., Thunder Bay P7E 6S7	● ■ ▼ ▲	(807) 475-1331 (807) 475-1311	(807) 475-1112 (807) 475-1112
Sault Ste. Marie	Suite 6, 875 Queen St. E., Sault Ste. Marie P6A 2B3	○ ■	(705) 945-6931	(705) 945-6935
Timmins	Ontario Government Bldg., P.O. Bag 3060, 1270 Hwy 101 East, South Porcupine P0N 1H0	● ■ ▼ ▲	(705) 235-1619 (705) 235-1600	(705) 235-1620 (705) 235-1610
Kirkland Lake	10 Government Rd. E., P.O. Box 100, Kirkland Lake P2N 3M6	● ■	(705) 568-4518	(705) 568-4524
Sudbury	Willet Green Miller Centre, Level A3, 933 Ramsey Lake Rd., Sudbury P3E 6B5	○ ▼ ★	(705) 670-5735 (705) 670-5887 (705) 670-5742	(705) 670-5770 (705) 670-5807 (705) 670-5681
Tweed (Southern Ontario)	P.O. Bag Service 43, 126 Old Troy Rd., Tweed K0K 3J0	● ■ ▼	(613) 478-3161	(613) 478-2873

Ministry of Northern Development and Mines



Contents

Office of the Director, Ontario Geological Survey

1. The Ontario Geological Survey Branch *J.A. Fyon*

Earth Resources and Geoscience Mapping Section

2. Earth Resources and Geoscience Mapping Section: Program and Project Overview *J.R. Parker*

Precambrian Geology – Northeastern Ontario

3. Project Unit 11-001. Interpretation of Geochemistry in the South of Gogama Area *B.R. Berger*
4. Project Unit 11-001. Report on Geochronology for the South of Gogama Area *B.R. Berger and R.W.D. Lodge*
5. Project Unit 11-008. Geology and Mineral Potential of Price and Thorneloe Townships, Abitibi Greenstone Belt *S. Préfontaine*
6. Project Unit 06-002. Geology and Mineral Potential of Nursey Township, Abitibi Greenstone Belt *L. Robichaud*

Precambrian Geology – Northwestern Ontario

7. Project Unit 09-006. Western Wabigoon Subprovince Synthesis Project *G.P. Beakhouse*
8. Project Unit 11-011. Metamorphism in the Western Wabigoon Subprovince: Insights from the Bending Lake Area *M. Duguet and G.P. Beakhouse*
9. Project Unit 11-002. New Geochemical and Geochronological Results from the Rowan Lake Area, Northwestern Ontario *D. Lewis, S.L. Kamo and R.W.D. Lodge*
10. Project Unit 10-010. Preliminary Results of Uranium–Lead Geochronology from the Shebandowan Greenstone Belt, Wawa Subprovince *R.W.D. Lodge*

Precambrian Geology – Far North

11. Project Unit 10-002. Uranium–Lead Geochronological Results from the Keezhik Lake and Miminiska Lake Area, Fort Hope Greenstone Belt, Eastern Uchi Subprovince *S. Buse and M.A. Hamilton*

Precambrian Geology – Proterozoic and Grenville Province

12. Project Unit 11-004. Geology and Mineral Potential of the Brudenell Area, Northeastern Central Metasedimentary Belt, Grenville Province, with an Emphasis on the Syenitic Rocks *R.M. Easton*
13. Project Unit 11-003. Geology and Mineral Potential of the Admaston–Horton Area, Northeastern Central Metasedimentary Belt, Grenville Province *M. Duguet, S.J. Magnus and L. Ratcliffe*
14. Project Unit 11-005. Geology and Mineral Potential of the Raglan Hills Metagabbro, Northeastern Central Metasedimentary Belt, Grenville Province *S.J. Magnus, B. Cousens and R.M. Easton*
15. Project Unit 11-013. Major Element, Trace Element and Isotope Geochemistry of Plutons Intruded Circa 1090 to 1065 Ma in the Southeastern Central Metasedimentary Belt, Grenville Province *J. Cutts, R.M. Easton and S.D. Carr*

16. Project Unit 12-003. Lithological and Structural Mapping of Albanel Township, Southern and Superior Provinces *D. Lewis*
17. Project Unit 12-004. Preliminary Results from the Otter–Morin Townships Bedrock Mapping Project, Southern and Superior Provinces *C.A. Gordon*
18. Project Unit 11-007. Whole Rock and Isotope Data from the Midcontinent Rift: Implications for Crustal Contamination History *R.M. Cundari, P. Hollings, M.C. Smyk, J.F. Scott and D.A. Campbell*

Geophysics

19. Summary of Geophysical Projects and Activities *D.R.B. Rainsford and T.L. Muir*

Aggregate Resources and Industrial Minerals

20. Summary of Aggregate Resource and Industrial Mineral Projects and Activities, Southern Ontario *V.L. Lee and D.J. Rowell*
21. Project Unit 12-008. Aggregate Resources of the County of Perth, Southwestern Ontario *D.J. Rowell*
22. Project Unit 12-012. The St. Edmund Formation—The Next Major Bedrock-Derived Aggregate Source in Ontario? *D.J. Rowell and F.R. Brunton*

Surficial Mapping and Sampling

23. Project Unit 08-005. Surficial Mapping in the Detour Lake–Burntbush Areas: A Progress Report *C. Gao*
24. Project Unit 08-008. Field Investigations for Remote Predictive Terrain Mapping in the Far North of Ontario *P.J. Barnett and K.H. Yeung*
25. Project Unit 08-008. Quaternary Stratigraphy of the Ridge River Area in Support of Far North Terrain Mapping *M.K. Nguyen, S.R. Hicock and P.J. Barnett*

Surficial Geochemistry

26. Project Unit 11-027. Greenstone Area High-Density Lake Sediment and Water Survey, Northwestern Ontario *R.D. Dyer and H.E. Burke*
27. Project Unit 12-013. Current Lake Area High-Density Lake Sediment and Water Survey, Northwestern Ontario *R.D. Dyer*
28. Project Unit 11-024. McFaulds Lake (“Ring of Fire”) Area Lake Sediment and Water Sampling Pilot Study, Far North, Ontario *R.D. Dyer*

Paleozoic Geology and Energy Studies

29. Project Unit 09-024. Preliminary Results: Potential Ordovician Shale Gas Units in Southern Ontario *C. Béland Otis*
30. Project Unit 10-028. Update on the Hudson Platform Paleozoic Mapping Project: Results from the Northwestern Moose River Basin *D.K. Armstrong*

Groundwater Studies

31. Project Unit 10-026. An Update on Three-Dimensional Mapping of Quaternary Deposits in the Southern Part of the County of Simcoe, Southern Ontario *A.F. Bajc, D.R.B. Rainsford and R.P.M. Milligan*
32. Project Unit 08-003. Conceptual Geologic Model for the Orangeville Moraine Three-Dimensional Project *A.K. Burt*
33. Project Unit 12-005. The Mount Forest–Elmira Study: A New Three-Dimensional Quaternary Mapping Project *A.K. Burt*
34. Project Unit 12-006. A Preliminary Assessment of Subsurface Sediments in the Central Norfolk Sand Plain, Norfolk County and the County of Oxford, Southern Ontario *A.S. Marich*
35. Project Unit 11-032. Regional-Scale Groundwater Mapping in Early Silurian Carbonate Rocks of the Niagara Escarpment Cuesta: Multi-Level Monitoring Well Sampling *E.H. Priebe, F.R. Brunton and V.L. Lee*
36. Project Unit 07-025. Description and Mitigation of Domestic Well Sampling Biases *S.M. Hamilton and V.L. Lee*
37. Project Unit 07-025. Ambient Groundwater Geochemistry Project of the Ottawa–St. Lawrence River Area *C.N. Freckelton and S.M. Hamilton*
38. Project Unit 07-025. Assessing Laboratories' Capabilities for Water Analysis: Results of a Round-Robin Study *O.M. Burnham, J. Schroeder and S.M. Hamilton*

Geoscience Laboratories

39. Revision of the Calibration for Major Element Analysis of Geological Samples by Wavelength Dispersive X-Ray Fluorescence at the Geoscience Laboratories *G.L. Keating and O.M. Burnham*
40. QA/QC: Summary of 2010–2012 Quality-Control Data at the Geoscience Laboratories *J. Hargreaves*

Targeted Geoscience Initiative 4 (TGI-4)

41. Update on Research Activities in the Targeted Geoscience Initiative 4 Magmatic-Hydrothermal Nickel-Copper-Platinum Group Elements Ore System Subproject: System Fertility and Ore Vectors *D.E. Ames, S.A.S. Dare, J.J. Hanley, P. Hollings, S.E. Jackson, P.J. Jugo, D.J. Kontak, R.L. Linnen and I.M. Samson*
42. Overview of the High-Magnesium Ultramafic to Mafic Systems Subproject under the Targeted Geoscience Initiative 4: An Ontario Perspective *M.G. Houlé, C.M. Lesher and R.T. Metsaranta*
43. Project Unit 10-004. Progress on the McFaulds Lake (“Ring of Fire”) Region Data Compilation and Bedrock Geology Mapping Project *R.T. Metsaranta and M.G. Houlé*
44. Preliminary Results of Chromite Geochemistry at the Black Label, Black Thor and Big Daddy Chromite Deposits, McFaulds Lake Greenstone Belt, Ontario *J.E. Laarman, R.L. Barnett and N.A. Duke*
45. Multiple Sulphur Isotopes as a Method to Evaluate Sulphur Sources and a Potential Exploration Tool in the Komatiite-Associated Nickel-Copper-(Platinum Group Elements) Hart Deposit, Shaw Dome, Abitibi Greenstone Belt, Ontario *R.S. Hiebert, A. Bekker, M.G. Houlé, C.M. Lesher and B.A. Wing*

46. Geochemistry of Chromite from the Alexo Komatiite, Dundonald Township: Preliminary Results from Electron Microprobe and Laser Ablation Inductively Coupled Plasma Mass Spectrometric Analyses *J. Méric, P. Pagé, S.-J. Barnes and M.G. Houlé*
47. Targeted Geoscience Initiative 4. Lode Gold Deposits in Ancient Deformed and Metamorphosed Terranes: The Role of Extension in the Formation of Timiskaming Basins and Large Gold Deposits, Abitibi Greenstone Belt—A Discussion *W. Bleeker*
48. Targeted Geoscience Initiative 4. Lode Gold Deposits in Ancient Deformed and Metamorphosed Terranes: Geological Setting of Banded Iron Formation–Hosted Gold Mineralization in the Geraldton Area, Northern Ontario *B. Lafrance, Z. Tóth, B. Dubé and P. Mercier-Langevin*

Index of Authors

Metric Conversion Table

**Office of the Director,
Ontario Geological Survey**

1. The Ontario Geological Survey Branch—2012

J.A. Fyon¹

¹Director, Ontario Geological Survey

INTRODUCTION

The vision of the Ontario Geological Survey (OGS) is “a leading provider of reliable, credible, accessible geoscience for the public good”. Our mission is to provide the citizens and institutions of Ontario with earth science data, information, and knowledge to meet Ontario’s economic and quality of life priorities. Our geoscience program is designed around, and to address, the public policy priorities of the Ontario Government:

- job creation / economic development
- quality of life
- education as that relates to Aboriginal relationships

The OGS helps to address these public policy priorities by providing geoscience data, information, and expert knowledge about the rocks; surficial deposits, and the land forms; mineral, energy, and groundwater resources; and the geological history that ties all of these together. This same geological information is available to inform decisions and guide actions related to environmental baseline characterization, public health and safety, and climate change issues affecting rural as well as metropolitan areas across all of Ontario. The OGS works from Pelee Island, in Lake Erie, to the land just south of the Pen Islands in Hudson Bay. To inform the broad range of public policy priorities and, therefore, to achieve our mission, the OGS focusses on ensuring our geoscience data, information, and knowledge are reliable, accurate, independent, and accessible to Ontario and global citizens.

The OGS is committed to

- linking our geoscience activities to key Ontario government public policy and societal issues that will be informed by considering public geoscience knowledge;
- “growing” the breadth and accessibility of geoscience information describing Ontario in order to address increasingly complex and inter-related public policy and societal issues;
- learning from each other including our external Aboriginal and non-Aboriginal collaborators and partners;
- leading the development and application of geoscience methodologies and approaches to help expand and enhance Ontario’s geoscience information base available to address public policy priorities, now, and in the future;
- remaining focussed on our primary geological mapping function.

OGS GEOSCIENCE CONTEXT

In support of Ontario government priorities, the OGS geoscience program provides up-to-date knowledge on Ontario’s rocks, deposits left by the glaciers, and the Earth resources contained within the rocks and glacial deposits. The Earth resources include metallic and non-metallic mineral resources,

*Summary of Field Work and Other Activities 2012,
Ontario Geological Survey, Open File Report 6280, p.1-1 to 1-9.*

groundwater, and renewable (e.g., ground heat) and non-renewable (e.g., hydrocarbon) energy endowment and potential. OGS products include data sets, reports, maps, and knowledge about the two-dimensional (2-D) and three-dimensional (3-D) geology, landscape, and Earth resources inventories and potential.

The OGS carries out field-based investigations to define and understand geological processes and the earth resources to support mineral investment priorities and inferences about the state of the environment, natural hazards, public health and safety, and climate change adaptation. We collaborate with provincial, national, and international geoscience partners to create a more robust provincial geoscientific evidence base to support policy and decisions on sustainable use of land, minerals, energy, and groundwater, and living with environmental change. As the steward of Ontario's public geoscience data and information, the OGS provides public access to these information and knowledge holdings.

OGS FUNCTIONS AND ORGANIZATION

The OGS activities are grouped around 4 core functions (Figure 1.1): a) geological mapping and surveying; b) geoservices based on chemical and physical analyses of inorganic geological materials; cartographic, editorial, and publication services; library services; warehouse services; and mineral sector information gathering and analysis; c) local area mineral investment expertise that includes inventorying and assessing Ontario's Earth resource potential; and d) marketing of the OGS role and Ontario's investment opportunities.

After careful analysis at the Division and OGS Branch level, as part of an OGS strategic analysis and a Divisional organization design analysis, the OGS merged its 2 geological mapping units, the Precambrian Geoscience Section and the Sedimentary Geoscience Section, into a new unit named the *Earth Resources and Geoscience Mapping Section*, led by Jack Parker, Senior Manager. In addition to the new *Earth Resources and Geoscience Mapping Section*, the OGS comprises 4 other administrative units: Director's Office, Geoscience Laboratories, Information and Marketing Services, and the Resident Geologist Program (*see* chart, this volume, page iv).

Ontario Geological Survey - Functional View

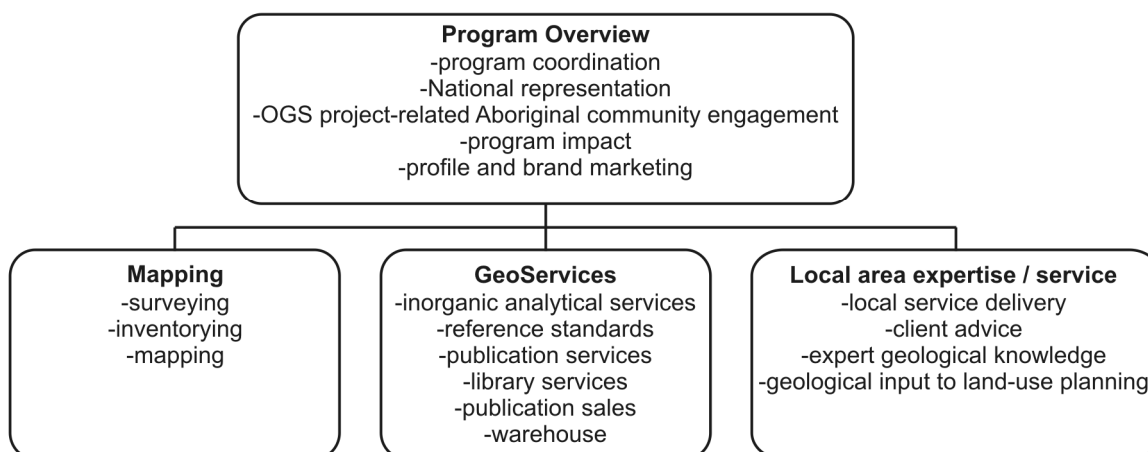


Figure 1.1. Ontario Geological Survey functional organization chart.

OGS STRATEGIC PRIORITIES

To address the Government priorities, the OGS documents Ontario's geology, and the results are communicated to clients in a way that helps to inform policy formulation and decision-making (Table 1.1). The fundamental geological and Earth resources descriptions of Ontario can be re-framed to speak more directly to specific public interests:

- framework bedrock and surficial geoscience, including mineral, energy, and groundwater inventory and potential
- environment-related geoscience
- health- and safety-relevant geoscience
- geoscience to inform land-use planning
- climate change-related geoscience
- recruitment, retention, and retirement management tactics
- marketing to promote value of geoscience (branding and profile)
- design and implementation of a new investment attraction marketing strategy

OGS STRATEGIC OPERATIONAL PRIORITIES

The primary emphasis of the OGS geoscience program during the year remains focussed on

- Geoscience
 - generation 1, 2, and 3 (regional, local, and very detailed) geological mapping across all of Ontario
 - multidisciplinary and collaborative geoscience studies of the McFaulds Lake ("Ring of Fire") region, Far North
 - karst distribution and implications for public safety and groundwater
 - 2-D and 3-D groundwater aquifer mapping
 - energy-related geoscience in the south and Far North
 - geological context for chemical and physical characteristics of groundwater and the environment
 - documentation of Earth resources inventory (mineral, groundwater, energy)
- Investment attraction marketing strategy
- Aboriginal engagement and consultation
 - OGS program-related Aboriginal community engagement, collaboration, and consultation
- Communication
 - communication of OGS goods and services to technical and non-technical audiences in forms relevant to different users and using social media
- Recruitment and retention of professional and technical staff
- Participation in the modernization of Ontario's *Mining Act*

Table 1.1. Linkage between the Ontario Geological Survey geoscience program and key public policy interests.

Public Policy Interest	OGS Geoscience Program Initiative	Application and Results
Investment - economy	Mineral-related geoscience	Mineral resource investment opportunities. Insights gained from the “Ring of Fire” area, which are relevant elsewhere in Ontario. Mineral investment attraction, jobs, sustainable communities.
	Energy-related geoscience	Energy investment opportunity. New green energy resources; new Far North energy options; geothermal energy industry and science, technology, research, and development opportunities.
	Groundwater aquifer geoscience	Groundwater opportunity and opportunity cost. Location, capacity, quality, and opportunities related to bedrock and surficial groundwater aquifers.
Security of energy supply and green, renewable energy	Energy-related geoscience	New green energy resources; new Far North energy options; geothermal energy industry and science, technology, research, and development opportunities.
Groundwater resources (and source water protection)	Groundwater aquifer mapping geoscience	3-D groundwater aquifer models that identify prospective groundwater-bearing units, areas of groundwater recharge and susceptibility to contamination warranting protection
	Bedrock mapping of karst distribution	Areas of potential groundwater recharge and contamination warranting protection
Environment	Stream sediment geochemistry across southern Ontario	Baseline inorganic geochemistry and its geological context for metals and other inorganic geochemical components in the environment to help identify natural and anthropogenic sources and to inform regulatory enforcement and standard setting by Ministry of Environment.
Public health and safety	Bedrock mapping of karst distribution	Identification of hazard lands related to natural geological processes.
	Ambient groundwater geochemical characterization	Baseline inorganic geochemistry and geological context for groundwater to identify natural geological sources and relation to potential public health concerns.
	Bedrock mapping of natural concentrations of metals and other compounds in rocks	Distribution of natural metals and other compounds that occur naturally in the rocks (e.g., uranium, arsenic, methane, fluoride) to inform regulators and health specialists of potential dangers to public health.
	Surficial geology mapping	Distribution of near-surface unconsolidated material, such as sensitive clays, that is subject to landslides to inform regulators and health specialists of potential dangers to public health.
Land-use planning	Regional, local, and detailed geology and Earth resources inventory	Land-use plans informed by an understanding of the economic mineral, energy, and groundwater opportunities, and the health, safety, and environment considerations defined by what lies beneath the surface of the Earth.
Climate change	Regional geological mapping of bedrock and surficial materials	Fundamental geological information describing the composition of geological materials required to inform climate change modelling – for example, questions such as what metals exist in what form in the geological material, and will those materials be released to the environment in response to changes in water table and temperature.

Reaching a secure, clean, and green energy future while reducing carbon dioxide emissions remains an Ontario priority. The OGS energy-related geoscience helps provide information about Ontario's natural and unconventional gas potential of southern Ontario and the Far North, where there is an Aboriginal interest to migrate away from expensive diesel generation of electricity, as a means to bridge between traditional and green renewable energy sources. In addition, the low-temperature geothermal potential of southern Ontario continues to be investigated with interest from major municipalities. The OGS is collaborating with the Geological Survey of Canada on several Near North and Far North geoscience projects under the Targeted Geoscience Initiative and Geo-mapping for Energy and Minerals (GEM) initiative. This collaboration is yielding new insights about the geology and Earth resources potential of Ontario.

While the OGS is not directly involved in modelling climate change, understanding the geological landscape of Ontario is an important aspect of constraining models for climate change impact and adaptation. Because geoscience is a proxy for the Earth, it is important to understand the links between climate change, bedrock and surficial geology, implications for metals within the near-surface geological environment, ground stability, and groundwater sustainability and quality.

OGS Operational Priorities

The 2011–2012 OGS operational priority is focussed on:

- generation and acquisition of generation 1, 2, and 3 geoscience information relevant to economic prosperity (minerals, groundwater, and energy), environment (groundwater, environmental geochemistry, and climate change), and public health and safety (karst, and groundwater geochemistry) across all of Ontario
- strategic investment attraction strategy.

Within this operational priority, the OGS geoscience program is focussed on several technical initiatives, framed in a geographic context:

- Pan-Ontario initiatives
 - provincial-scale metallogenic compilation and inventory studies
 - integration of geophysics and bedrock geology mapping
- Far North geoscience initiative, in support of development in the “Ring of Fire” and the Far North land-use planning initiative
 - regional and local surficial, bedrock, mineral occurrence, energy, geochemical, geophysical surveying, and Earth resources potential estimation
 - development of an approach to estimate metallic mineral potential across the Far North in layered geological settings
 - some projects are collaborations with the Laurentian University Living With Lakes Centre and the Geological Survey of Canada (Targeted Geoscience Initiative and Geo-mapping for Energy and Minerals)
- Near North geological surveying
 - northwest: geology and metallogeny of northwestern Ontario under the bedrock geology and metallogeny of northwest Ontario initiative
 - northeast: bedrock, surficial, and energy geology and metallogeny of northeastern Ontario

- Southern geoscience surveying
 - Proterozoic bedrock geology initiative including bedrock mapping
 - regional and local surficial, bedrock, mineral occurrence, shale gas and geothermal energy, groundwater aquifer, ambient groundwater chemistry, aggregate, industrial mineral, karst type and distribution, geochemical, and Earth resources potential estimation, including 3-D geologic model development relevant to groundwater aquifer distributions
- Business process initiatives
 - documenting OGS success stories
 - strategic hiring and mentoring
 - OGS Branch-wide Aboriginal engagement, relationship building, information sharing, and consultation
- Revamp the investment attraction strategy

STRATEGIC INVESTMENT ATTRACTION

As a result of a competitive review of the Ministry's investment attraction marketing activities, the OGS is developing and implementing a new investment attraction marketing strategy. The key efforts are focussing on

- defining our marketing targets (direct mining investment, "Junior" exploration companies not operating in Ontario, and "Junior" companies operating in Ontario)
- refining existing and developing new marketing vehicles (branding and tag line, direct marketing campaign, collateral marketing materials, Web site revamp, off-the-shelf products, International Business Development Representative's and Senior Economic Development Officer's tool box, targeted events, speaking engagements, strategic selling training, and customer relationship management process)
- tracking and measuring performance

REFORMING AND MODERNIZING ONTARIO'S *MINING ACT*

On October 21, 2009, the Act to amend the *Mining Act* (Bill 173) passed third reading in the legislature. Ontario Geological Survey staff are involved in aspects of external communication and information delivery about the new regulatory changes and the use of geoscience to address public policy priorities. OGS has no regulatory authority so our role is to speak to the value and role of geoscience in the lives of Ontario citizens.

GEOSCIENCE AND OTHER COLLABORATIONS

The OGS collaborates with other jurisdictions and organizations as a delivery model to help "grow" the geoscience knowledge about Ontario and to help achieve other science documentation and communication goals.

The 2 Federal geoscience programs that involve OGS staff are the Targeted Geoscience Initiative 4 (TGI-4) and the Geo-mapping for Energy and Minerals Initiative (GEM) (*see* Parker, this volume, Article 2). The GEM Hudson Platform initiative continued in the Far North with a focus on the surficial geology, the Paleozoic geology, and the implications for Earth resources. A science collaboration with the Laurentian University Living With Lakes Centre and the Climate Change Centre is in place, and a collaboration with MIRARCO on an energy project is evolving—all in collaboration with Aboriginal communities.

The OGS continues its geoscience collaborations with a number of other organizations and Ministries, including Laurentian University, Carleton University, Lakehead University, University of Ottawa, McMaster University, Western University (formerly the University of Western Ontario), Science North, conservation authorities (Grand River Conservation Authority, Lake Simcoe Conservation Authority, Nottawasaga Conservation Authority), the City of Guelph, the Regional Municipality of Waterloo, the Greenstone Economic Development Corporation, the Ontario Ministry of Natural Resources, the Ontario Ministry of Environment, the United States Geological Survey, and the Geological Survey of Canada.

ABORIGINAL ENGAGEMENT AND RELATIONSHIP BUILDING

The OGS engages and collaborates with Aboriginal communities to meet both OGS program and some community-based land-related interests. Subject to a collaboration agreement, the OGS may provide geoscience and mineral sector information to Aboriginal communities in support of community decisions, logistical field support for community-based Traditional Ecological Mapping projects, and bridging between the community and independent experts capable of informing community interests that lie outside the OGS mandate. This engagement and communication is a foundation to our field project implementation and helps inform community and related Government decisions.

Roles and responsibilities related to engagement, relationship building, information exchange, and consultation are divided across the OGS. For field mapping projects in the Far North, the OGS Director and Senior Managers are involved at the outset of engagement with an Aboriginal community to establish a basis for communication and collaboration. Once a basis for mutual benefit and communication is established, and a mutually beneficial collaboration is established, technical managers and staff become directly involved with the community during technical design, implementation, and sharing the results of the geoscience project. The OGS Director and Senior Managers maintain an ongoing relationship with the community following completion of the mapping project. The OGS Resident Geologist Program staff maintain communication with Aboriginal communities in their district to address questions about geoscience, mineral sector activity in the region, and to assist in addressing questions related to the content of material related to the quarterly delivery of mineral sector activity by the Ministry of Northern Development and Mines (MNDM).

INTERJURISDICTIONAL REPRESENTATION

The OGS Director represents Ontario's geoscience interests to several interjurisdictional committees. The intent is to assure the geoscience interests of Ontario are understood and accommodated, to establish synergies between jurisdictions required to address trans-border geological topics (e.g., groundwater), and to learn from these other jurisdictions so that the OGS remains informed of program-related policies, programs, and practices that may be of value to Ontario. Interjurisdictional representation by the OGS Director includes

- Canada's National Geological Surveys Committee
- Canada's Committee of Provincial and Territorial Geologists
- Great Lakes Geological Mapping Coalition (Indiana, Illinois, Michigan, Ohio, Ontario, Pennsylvania, Wisconsin, Minnesota, and New York)

Technical committees support these national and international committees to help ensure appropriate technical and scientific benefits are shared.

ONTARIO GEOLOGICAL SURVEY STAFF CHANGES

Several new staff joined the OGS or successfully competed for new positions within the OGS during the past year:

- Earth Resources and Geoscience Mapping Section
 - Steven Meade, Precambrian Geoscientist, Sudbury
 - Jose Schroeder, Geological Assistant, Sudbury
- Resident Geologist Program
 - Cheryl MacDonald, Administrative Assistant, Thunder Bay
 - Shannon Zurevinski, MDI Geologist, Northwest
 - Lesley-Anne Bardeggia, District Geological Assistant, Sudbury
 - Mark Puumala, Regional Resident Geologist, Thunder Bay South
 - Gerry White, Regional Resident Geologist, Thunder Bay North
 - Mark Smyk, Regional Manager, Northwest
 - Suzanne Halet, First Nation Mineral Information Officer, Northeast
 - Carole Larche, District Geological Assistant, Timmins
 - Catherine Daniels, Regional Land Use Geologist, Northeast
- Information & Marketing Services
 - Paula Takats, Geoscience Editor, Publication Services, Sudbury
- Geoscience Laboratories
 - Jennifer Hargreaves, Quality Assurance Co-ordinator, Sudbury
 - Annette Gladu, Solution Preparation Technologist
 - Keith McCormick, Sample Preparation Technologist

In late 2011 and within the first 9 months of 2012, after many years of service, 4 OGS staff retired: Jim Ireland (Senior Manager, Resident Geologist Program), Hugh Lockwood (Regional Land Use Planner, Northwest), Charles Carter (Operations Manager, Warehouse), and John Scott (Regional Resident Geologist, Thunder Bay).

PROVINCIAL AND TERRITORIAL GEOLOGISTS MEDAL

In September 2012, Dr. Andy Bajc, Earth Resources and Geoscience Mapping Section, was awarded Canada's Provincial and Territorial Geologists Medal—a national recognition for the outstanding work as a Provincial Geologist. Previous OGS recipients of the national gold medal included Dr. Peter Barnett (2003), Dr. Greg Stott (2006), and Dr. Michael Easton (2008).

FUTURE

To date, the OGS information holdings include 9777 maps, 3244 reports, 578 data releases; including the 14 new reports, 147 new maps, and 23 new data releases published since August 31, 2011. Our most popular Web site, OGSEarth, was visited over 20 000 times between August 31, 2011, and September 30, 2012.

The OGS continues to

- implement the enhanced geoscience program applied to economic development, environment, public health and safety, and climate change
- advocate for balanced land-use planning through the provision of modern geoscience data and knowledge
- identify geological characteristics relevant to Ontario's public health and safety
- publish and market information on Ontario's landmass and its mineral, energy, and water resource endowments
- develop new geoscience products that help present our complex geoscience data in a form that is understood by non-geoscience users, including the development of products that use Google Earth™ mapping service ("OGSEarth"), which shows great promise as the medium to broaden the access and awareness of OGS geoscience goods and services to both traditional and non-traditional users

Public geoscience plays an important role in helping support public-policy decision makers, investors, and other users of the near surface of the Earth. Societal needs are increasingly complex and require a sound and objective understanding and application of geoscience to help assess and frame the complex options available. The OGS is working to supply or facilitate access to the geoscience knowledge needed to support the public policy and societal issues.

Earth Resources and Geoscience Mapping Section

2. Earth Resources and Geoscience Mapping Section: Program and Project Overview

J.R. Parker¹

¹Earth Resources and Geoscience Mapping Section, Ontario Geological Survey

GOAL AND RESPONSIBILITY OF THE SECTION

The Sedimentary and Precambrian Geoscience sections of the Ontario Geological Survey (OGS) were merged in 2012 to form the Earth Resources and Geoscience Mapping Section (ERGMS). This new combined section rolls the “mapping function” of the OGS into one business unit resulting in greater consistency of management and improved integration of multidisciplinary geoscience projects.

The goal of the ERGMS is to improve the understanding of geology and Earth resources of Ontario and to convey this knowledge to the public through multiyear, multidisciplinary geoscience projects that address critical geoscience problems in key geographic areas. These studies may be delivered as part of the ERGMS geoscience mapping function or through collaborative geoscience projects or initiatives.

The ERGMS is responsible for

- mapping Ontario’s Precambrian and Phanerozoic bedrock geology and understanding various metal and mineral deposit settings at a regional scale;
- mapping and sampling Ontario’s Quaternary sediments to understand regional distribution, composition and glacial history of the surficial stratigraphy as well as identifying aggregate resources and indicator minerals to evaluate regional mineral potential, in particular, for areas under thick Quaternary deposits;
- mapping Ontario’s overburden and bedrock groundwater resources at a regional scale and understanding the geochemical effects of groundwater interactions with rock and surficial media;
- regional ground and airborne geophysical data and derivative products in support of the bedrock geology and groundwater mapping programs;
- regional surficial geochemistry of water and other surficial media (e.g., lake and stream sediments, peat, etc.) to identify anomalies and better understand geochemical processes in the near-surface environment;
- mapping Ontario’s aggregate and industrial minerals to provide current inventories and quality assessments of aggregate and industrial mineral resource potential;
- mapping Ontario’s traditional and unconventional non-renewable energy resources to identify new energy sources and better understand the effect of hydrocarbon interaction on groundwater resources.

The program direction and strategic thrusts of the ERGMS address the results-based plan and core business of the Ministry of Northern Development and Mines (MNDM). Government priorities (Table 2.1) are achieved through a variety of strategies and initiatives that consist of one or more projects. Therefore, project planning, development, evaluation, selection and implementation are based on strategies and initiatives designed to achieve alignment of individual projects with Ministry and Government priorities.

*Summary of Field Work and Other Activities 2012,
Ontario Geological Survey, Open File Report 6280, p.2-1 to 2-17.*

Table 2.1. Government Priorities as linked to current projects of the Earth Resources and Geoscience Mapping Section: 2012–2013.

Region	Government Priority	Strategy	Objective	Initiative	Activity	Current Projects
Far North	Economy: <ul style="list-style-type: none"> • aggregate material is essential to infrastructure development and growth • understanding the geology and Earth resource potential of Ontario attracts investment dollars, triggers economic development and assists in closing the socio-economic gap between Aboriginal and non-Aboriginal Ontarians; contribute geoscience data to assess non-renewable potential for the Far North as a transition source and to support remote development 	In collaboration, apply geoscience techniques to assess Earth resource potential to meet societal and government priorities	Provide the geologic framework to support earth resource exploration (minerals, metals and energy), land-use planning, economic and infrastructure development and provide a geoscience baseline to help assess cumulative impacts of development by collecting, interpreting, synthesizing and disseminating geoscience information	“Ring of Fire” Initiative; Far North Land Use Planning Initiative; Geo-mapping for Energy and Minerals (GEM) – Federal Program; Targeted Geoscience Initiative 4 (TGI-4) – Federal Program	Precambrian Bedrock Mapping	a) <i>Bedrock geology and compilation of the McFaulds region: multiyear bedrock mapping, core re-logging and compilation in the “Ring of Fire”</i> b) <i>Regional characterization of ultramafic to mafic intrusions in the Oxford–Sull and Uchi domains, Superior Province</i> c) <i>Petrology of iron-vanadium-titanium mafic intrusions in the McFaulds Lake greenstone belt: MSc thesis study</i> d) <i>Study of the ultramafic to mafic Black Label–Black Thor intrusive complex in the McFaulds Lake greenstone belt: PhD thesis study</i> e) <i>Geology of the Fort Hope greenstone belt: multiyear bedrock geology mapping of the entire greenstone belt</i>
	Improving Quality of Life: <ul style="list-style-type: none"> • collection of new, accurate geoscience data informs land-use planning for protection of natural beauty + development of resources and for healthy families + communities; provide a foundation to help assess cumulative impact on the land from development and climate change 				Surficial Mapping and Sampling	f) <i>Far North terrain mapping project: remote sensing and data interpretation; reconnaissance mapping</i> g) <i>Quaternary glaciation and stratigraphy of the Ridge River area in northern Ontario: MSc thesis study</i> h) <i>Surficial deposits sampling in the “Ring of Fire” region: overburden sampling for indicator minerals, i.e., gold, diamonds, platinum group metals, base metals and REE</i> i) <i>Geochemistry of detrital chromite: investigating their use as a vector to nickel-copper-PGE, chromium and iron-titanium-vanadium deposits</i>

Table 2.1, continued.

Region	Government Priority	Strategy	Objective	Initiative	Activity	Current Projects
Far North, continued	continued from p.2-2	continued from p.2-2	continued from p.2-2	“Ring of Fire” Initiative; Far North Land Use Planning Initiative; Geo-mapping for Energy and Minerals (GEM) – Federal Program; Targeted Geoscience Initiative 4 (TGI-4) – Federal Program	Surficial Geochemistry	j) <i>McFaulds Lake area lake sediment and water sampling pilot study: high-density lake sediment and water geochemistry pilot survey – mineral exploration and baseline environmental data</i>
					Geophysical Mapping	k) <i>Regional airborne magnetometer survey: Winisk River Region, Hudson Bay Lowland</i>
						l) <i>Regional airborne magnetometer survey: Fort Severn Region, Hudson Bay Lowland</i>
						m) <i>Airborne gravity gradiometer and magnetic survey, McFaulds Lake greenstone belt</i>
						n) <i>Geophysical modelling of regional airborne gravity survey data</i>
Near North - Northeast	see p.2-2 for details	see p.2-2 for details	see p.2-2 for details	Abitibi Initiative	Paleozoic Bedrock Mapping	o) <i>Paleozoic stratigraphy and hydrocarbon resource potential of the Hudson Platform: bedrock mapping and core logging to upgrade geoscience data for Paleozoic strata in the Hudson Bay Lowland and re-evaluate hydrocarbon resource potential</i>
					Precambrian Bedrock Mapping	a) <i>Barlett and Hallday domes bedrock mapping: 1:20 000 scale bedrock mapping in Midlothian, Nursey and several other townships</i>
						b) <i>Geology of Price and Thorneloe townships: 1:20 000 scale bedrock mapping and diamond-drill core logging with focus on gold potential</i>
						c) <i>Geological mapping and compilation of the Burntish-Normetal volcanic belt – bedrock mapping and compilation with a focus on volcanogenic base metal mineralization</i>
						d) <i>Montclerg gold deposit, Abitibi greenstone belt, east Timmins region, Ontario: stratigraphy, lithogeochemistry, mineralization and nature of vein fluids</i>
						e) <i>Evaluation of gold mineralization in the Matachewan, Shining Tree, Chester Township and Northern Cobalt Embayment</i>

Table 2.1, continued.

Region	Government Priority	Strategy	Objective	Initiative	Activity	Current Projects
Near North - Northeast, continued	continued from p.2-3	continued from p.2-3	continued from p.2-3	Proterozoic Initiative	Precambrian Bedrock Mapping, continued	f) <i>Geology of Varley-Albanel townships: 1:20 000 scale bedrock mapping with focus on mineral potential</i>
						g) <i>Geology of Morin-Otter townships: 1:20 000 scale bedrock mapping with focus on mineral potential</i>
						h) <i>Geology of the Pecors-Whiskey area: 1:20 000 scale bedrock geology mapping, diamond-drill core logging and compilation to better understand the stratigraphy, structure and setting of uranium mineralization</i>
						i) <i>East Bull Lake Intrusion copper-nickel-PGE element dispersion case study</i>
Near North - Northwest	see p.2-2 for details	see p.2-2 for details	see p.2-2 for details	Metallogeny and Geology of Northwest Ontario	Surficial Geochemistry Surficial Mapping and Sampling	j) <i>Surficial mapping and till sampling in the Detour Lake-Burntbrush area</i>
						k) <i>Surficial mapping and till sampling in the Cobalt-New Liskeard-Englehart area</i>
						l) <i>Surficial mapping and till sampling in the Chapleau area</i>
						a) <i>Western Wabigoon Synthesis: multiyear 1:100 000 scale bedrock geology compilation and synthesis of the western Wabigoon Subprovince</i>
						b) <i>Geodynamic setting of volcanogenic massive sulphide mineralization in the Wawa Subprovince: PhD thesis study</i>
				Proterozoic Initiative		c) <i>Geochemistry of granitic rocks in the Quetico Subprovince: BSc thesis study</i>
						d) <i>Geology of the Rowan Lake area: 1:50 000 scale bedrock geology mapping to better understand the geology, structure and setting of gold mineralization</i>
						e) <i>Geoscience studies of Mesoproterozoic Midcontinent Rift-related mafic intrusions: ongoing reconnaissance sampling of intrusions near Thunder Bay to characterize geochemistry and assess mineral potential – MSc thesis study</i>

Table 2.1, *continued*.

Region	Government Priority	Strategy	Objective	Initiative	Activity	Current Projects
Near North - Northwest, <i>continued</i>	<i>continued</i> from p.2-4	<i>continued</i> from p.2-4	<i>continued</i> from p.2-4	Surficial Geochemistry of Northern Ontario Initiative	Surficial Mapping and Sampling	f) <i>Regional till sampling at Mowe Lake: surficial mapping and geochemical sampling (till and stream sampling)</i>
					Geochemical Mapping	g) <i>Greenstone area high-density lake sediment and water geochemistry survey: Municipality of Greenstone</i>
						h) <i>Separation Lake area high-density lake sediment and water geochemistry survey: Rex-Werner-Separation lakes area</i>
						i) <i>Current Lake area high density lake sediment and water survey pilot study: Current Lake Area north of Thunder Bay</i>
						j) <i>Mine Centre high-density lake sediment and water geochemistry survey: Mine Centre</i>
South	<i>see</i> p.2-2 for details	<i>see</i> p.2-2 for details	<i>see</i> p.2-2 for details	Proterozoic Initiative	Precambrian Bedrock Mapping	a) <i>Geology of Admaston area: multiyear 1:20 000 scale bedrock mapping of the Renfrew region to better understand the geology and metallogeny, Grenville Province</i>
						b) <i>Geology of the Brudenell area: multiyear 1:50 000 scale bedrock and compilation mapping project to improve understanding of the geology and mineral deposits of the northwest Central Metasedimentary Belt, Grenville Province</i>
						c) <i>Origin and tectonic history of the circa 1090 to 1070 million-year-old plutons in the southeastern Central Metasedimentary Belt, Grenville Province: MSc thesis study</i>
						d) <i>Nickel-copper mineralization at the Raglan Hills gabbro, Grenville Province: MSc thesis study</i>

Table 2.1, continued.

Region	Government Priority	Strategy	Objective	Initiative	Activity	Current Projects
South, continued	Green Energy Transition: • identification of renewable (ground heat) to non-renewable (natural gas) energy options that occur in the subsurface	Apply and integrate geoscience techniques and data related to groundwater, regional surface and subsurface geology, and natural gas properties to assess energy potential and implications for environment, groundwater quality, and public health	Provide a geoscience framework to assess energy potential in the south and Far North and the relationship between the geology and groundwater quality and public health and safety	Energy Initiative	Gas Assessment of Paleozoic Shales	e) <i>Shale gas assessment of the Devonian Kettle Point Formation and Ordovician shale units: multiyear program to assess shale gas potential of various bedrock shale units in southern Ontario</i> (Note the linkage to the Ambient Groundwater projects in the south and the Far North Geo-mapping for Energy and Minerals (GEM) energy projects)
	Economy: • energy options in the south (and Far North) related to renewable (ground heat) and non-renewable (natural gas) energy options that occur in the subsurface Improving Quality of Life: • impact of natural gas on groundwater quality and implications for health and safety					
	Improving Quality of Life: • identification of natural and anthropogenic metals and organic components in the environment mitigates the impact of geohazards on public health and safety	In collaboration with Ministry of Environment, apply geoscience techniques in areas of environmental priority to identify natural and anthropogenic hazards	Provide the geologic context for identification and interpretation of natural and anthropogenic threats to the environment, water quality issues, and geohazards by collecting, interpreting, synthesizing and disseminating geoscience information	Environmental Initiative	Stream Sediment Sampling and Analysis	f) <i>Southern Ontario stream sediment geochemistry survey: continued analysis of organic and inorganic compounds in collected stream sediment samples, southern Ontario</i>

Table 2.1, continued.

Region	Government Priority	Strategy	Objective	Initiative	Activity	Current Projects
South, continued	Economy: • aggregate material is essential to infrastructure development and growth	Apply geoscience techniques in areas of aggregate resource priority to meet societal and government priorities	Provide the geoscience framework for identification of aggregate and industrial mineral resources for land-use planning and for resource and infrastructure development by collecting, interpreting, synthesizing and disseminating geoscience information.	Aggregate Resources Initiative	Aggregate Resources Mapping and Inventory	g) <i>Renfrew County ARIP</i> : continue aggregate resources inventory h) <i>Lanark County ARIP</i> : complete aggregate resources inventory
	Infrastructure Investments: • aggregate resource supply is essential to infrastructure investments					i) <i>Ottawa ARIP</i> : complete aggregate resources inventory j) <i>Perth County ARIP</i> : complete aggregate resources inventory
	Improving Quality of Life: • collection of new, accurate geoscience data on aggregate resources informs land-use planning for protection of natural beauty + development of resources required to support healthy families + communities					k) <i>Simcoe County ARIP</i> : complete aggregate resources inventory
				Industrial Minerals Inventory Initiative	Industrial Minerals Resource Evaluation	l) <i>Shale resources study</i> : industrial minerals study to update shale geochemistry data
	Economy: • water is essential to growth	Apply geoscience techniques in areas of groundwater priority to meet societal and government priorities	Provide the geoscience framework for groundwater use, protection, and planning by collecting, interpreting, synthesizing and disseminating geoscience information	Three-Dimensional (3-D) Surficial Sediment Mapping Initiative	Surficial Mapping and Sampling	m) <i>Three-dimensional (3-D) mapping of Quaternary deposits in the southern part of Simcoe County</i> : multiyear project to generate 3-D geologic overburden model for groundwater assessment
	Improving Quality of Life: • abundant clean water is a prerequisite for healthy families + communities (Places to Grow; climate change)					n) <i>Sedimentological study of postglacial glaciolacustrine deposits in the Alliston area, southern Ontario</i> : MSc thesis study
	• understanding groundwater systems (<i>Clean Water Act</i> ; Greenbelt) will enable protection of natural beauty + resources					o) <i>Three-dimensional (3-D) mapping of the Orangeville-Fergus area</i> : multiyear project to generate 3-D geologic overburden model for groundwater assessment in the Orangeville-Fergus area
	• identification of groundwater quality issues and geohazards mitigates public health and safety issues					p) <i>Three-dimensional (3-D) mapping of Quaternary deposits in the Mount Forest-Elmira area</i> : multiyear project to generate 3-D geologic overburden model for groundwater assessment. First-year: literature review and ground geophysical gravity survey
						q) <i>Norfolk County – Tier 3 groundwater study</i> : logging overburden cores to generate geologic framework for Norfolk region

Table 2.1, continued.

Region	Government Priority	Strategy	Objective	Initiative	Activity	Current Projects
South, continued	continued from p.2-7	continued from p.2-7	continued from p.2-7	Three-Dimensional (3-D) Bedrock Mapping	Paleozoic Bedrock Mapping	r) <i>Bedrock aquifer, karst and Early Silurian sequence stratigraphy mapping project - Guelph to Owen Sound:</i> groundwater flow characterization, mapping karst distribution, bedrock core logging, water sampling and isotope studies s) <i>Bedrock aquifer mapping of the Niagara Escarpment cuesta:</i> support bedrock aquifer, karst and Silurian sequence stratigraphy project through FLUTE™ water sampling and mapping
				Ambient Groundwater Geochemistry Mapping	Geochemical Mapping	t) <i>Ambient Groundwater and Geochemistry Project:</i> field sampling of overburden and bedrock wells in Ottawa region to assess geochemical and other water parameters
				Geophysical Techniques in Support of Surficial Mapping	Geophysical Mapping	u) <i>South Simcoe airborne time-domain electromagnetic (TDEM) survey:</i> to support 3-D surficial mapping v) <i>Regional ground gravity survey in the Forest Hill-Elmira area:</i> to support 3-D surficial mapping
				Provincial-scale Metallogenic Inventory	Precambrian Bedrock Mapping; Geoscience Data Inventory and Compilation	a) <i>Document the distribution of regional settings and characteristics of mineralized, intermediate to felsic plutonic systems</i> b) <i>Evolved (FL- to FILL-type) felsic metavolcanic rocks (e.g., rhyolite) across the Superior Province to highlight regions with high base-metal potential</i> c) <i>Metamorphic patterns in Archean greenstone belts</i> d) <i>Maintain geochronology database for Ontario</i>
Pan-Provincial	<p>Economy:</p> <ul style="list-style-type: none"> understanding the geology and Earth resource potential of Ontario attracts investment dollars and triggers economic development <p>Improving Quality of Life:</p> <ul style="list-style-type: none"> collection of new, accurate geoscience data informs land-use planning for protection of natural beauty + development of resources and for healthy families + communities 	<p>Apply geoscience techniques to assess Earth resource potential to meet societal and government priorities</p>	<p>Provide the geoscience framework to support earth resource exploration (minerals, metals and energy), land use planning, economic and infrastructure development and provide a geoscience baseline to help assess cumulative impacts of development by collecting, interpreting, synthesizing and disseminating geoscience information</p>			

The ERGMS supported 63 active projects during the 2012–2013 fiscal year, which includes 42 active core projects (*see* Table 2.1) and 21 active collaborative projects, which include 1 project with the Ministry of the Environment; 7 projects with the Geological Survey of Canada (GSC); 3 projects providing “in-kind” support to the Discover Abitibi Initiative (DAI); and 10 projects with universities (Table 2.2). Locations for projects for which there are corresponding articles in this volume are depicted on Figures 2.1 and 2.2.

From November 2011 to November 2012 inclusive, the ERGMS produced 20 Preliminary Maps, 6 Open File Reports (OFR), 16 Miscellaneous Releases—Data (MRD), 2 Aggregate Resource Inventory Papers (ARIP), 2 Groundwater Resource Studies (GRS), 4 Geophysical Data Sets (GDS) and 35 airborne geophysical survey maps. The ERGMS staff presented numerous technical talks and posters at various geoscience forums and meetings throughout the year.

PROGRAM DIRECTION: STRATEGIES

Core Geoscience Program

The ERGMS strategies and objectives (*see* Table 2.1) are derived from MNDM business goals and goals that were established in the OGS Strategic Plan.

The purpose of the ERGMS strategies is to focus staff and resources in key geological areas or geoscience themes, over a period of 3 to 5 years, to contribute to expanding the geoscience database of Ontario; support sustainable development and effective land-use planning; provide the geoscience framework for groundwater use, public health and safety and the public good; support and attract new mineral investment; build new collaborations with Aboriginal communities, private sector, academe and federal government; and collaborate with other ministries on initiatives of mutual interest. These strategies are addressed through a series of initiatives built upon one or more projects (*see* Table 2.1). In addition, ERGMS participates in several collaborative projects (*see* Table 2.2) to complement existing staff skills and capacity and to expand the amount of geoscience data that describe Ontario. Collaborative projects are an important means to extend government resources and to capitalize on resources and expertise available in other government geological surveys, universities or industry.

The ERGMS program is organized into 5 technical strategies or objectives to provide the geoscience framework or context to

1. support earth resource exploration (minerals, metals and energy), land-use planning, economic and infrastructure development and provide a geoscience baseline to help assess cumulative impacts of development by collecting, interpreting, synthesizing and disseminating geoscience information;
2. assess energy potential in the south and Far North and the relationship between the geology and groundwater quality and public health and safety;
3. identify and interpret natural and anthropogenic threats to the environment, water-quality issues and geohazards by collecting, interpreting, synthesizing and disseminating geoscience information;
4. identify and inventory aggregate and industrial mineral resources for land-use planning and resource and infrastructure development by collecting, interpreting, synthesizing and disseminating geoscience information;
5. identify and inventory groundwater resources for use, protection, and planning by collecting, interpreting, synthesizing and disseminating geoscience information.

Table 2.2. Earth Resources and Geoscience Mapping Section collaborative initiatives, 2012–2013.

Initiative	Project	Project Collaborator(s)	Project Progress
Three-Dimensional (3-D) Surficial Sediment Mapping	MSc thesis study of the sedimentology of postglacial glaciolacustrine deposits in the Alliston area	McMaster University	1:50 000 scale Quaternary map to be published in 2013
Far North Land Use Planning Initiative	MSc thesis study of the Quaternary glaciation and stratigraphy of the Ridge River area in northern Ontario	Western University	<i>Summary of Field Work</i> article in 2012
“Ring of Fire” Initiative	McFaulds Lake area lake sediment and water sampling pilot study	Living with Lakes (LWL) Centre, Cooperative Freshwater Ecology Unit, Laurentian University	Ongoing study
Environmental Initiative	Southern Ontario stream-sediment geochemistry survey	Ministry of the Environment	Ongoing; Miscellaneous Release—Data in 2012
Abitibi Initiative	Bedrock geology mapping and compilation in the Burntbrush–Normétal volcanic belt	Discover Abitibi, Ore Systems Consulting	Miscellaneous Release—Data in 2013
	Monticlerg gold deposit, Abitibi greenstone belt, east Timmins region, Ontario: stratigraphy, lithogeochemistry, mineralization and nature of vein fluids	Discover Abitibi, Ore Systems Consulting, Laurentian University	Miscellaneous Release—Data in 2013
	Evaluation of gold mineralization in the Matachewan, Shining Tree, Chester Township and Northern Cobalt Embayment	Discover Abitibi, Laurentian University, Western University, University of Waterloo	Miscellaneous Release—Data in 2013
Proterozoic Initiative	MSc thesis study of nickel-copper mineralization at the Raglan Hills gabbro, Grenville Province	Carleton University, First Nickel Inc.	Second year of multiyear project, contribution to a <i>Summary of Field Work</i> article in 2012
	MSc thesis study on the origin and tectonic history of the <i>circa</i> 1090 to 1070 million-year-old plutons in the southeastern Central Metasedimentary Belt, Grenville Province	Carleton University	Second year of multiyear project, contribution to a <i>Summary of Field Work</i> article in 2012
	Geological, paleomagnetic, geochemical and geochronological studies of Mesoproterozoic Midcontinent Rift–related mafic intrusions near Thunder Bay	Lakehead University	Ongoing; Miscellaneous Release—Data in 2013
Metallogeny and Geology of Northwest Ontario	BSc thesis to study geochemistry and petrography of Quetico Subprovince granitoid rocks, located north of Thunder Bay	Lakehead University	Ongoing; Miscellaneous Release—Data in 2013
	PhD thesis study of the geodynamic setting of volcanogenic massive sulphide mineralization in the Wawa Subprovince	Mineral Exploration Research Centre (MERC)–Laurentian University	OGS–Laurentian University Graduate Mapping School Program; <i>Summary of Field Work</i> article in 2012; Miscellaneous Release—Data in 2013

Table 2.2, continued.

Initiative	Project	Project Collaborator(s)	Project Progress
Collaborative Projects with the GSC:	Paleozoic stratigraphy and hydrocarbon resource potential of the Hudson Platform	Geological Survey of Canada	Ongoing data collection and compilation
	Airborne magnetic geophysical survey of the Fort Severn region in the Hudson Bay Lowland	Geological Survey of Canada	Data to be collected in fall–winter 2012–2013
Geo-mapping for Energy and Minerals (GEM) Initiative			
Collaborative Projects with the GSC:	MSc thesis study of petrology of iron-vanadium-titanium mafic intrusions in the McFaulds Lake greenstone belt	Lakehead University, Geological Survey of Canada, Noront Resources Ltd., MacDonald Mines Exploration Ltd.	Analytical support for MSc thesis study which is in progress
	PhD thesis study of the ultramafic to mafic Black Label–Black Thor intrusive complex in the McFaulds Lake greenstone belt	Laurentian University, Geological Survey of Canada, Cliffs Natural Resources Inc.	Analytical support for PhD thesis study which is in progress
Targeted Geoscience Initiative 4 (TGI-4)	Geochemistry of detrital chromite: investigating their use as a vector to nickel-copper-platinum group elements (PGE), chromium and iron-titanium-vanadium deposits	Geological Survey of Canada	Ongoing
	Airborne gravity gradiometer and magnetic geophysical survey, McFaulds Lake greenstone belt	Geological Survey of Canada	Ongoing
	Geophysical modelling of regional airborne gravity survey data	Geological Survey of Canada	Ongoing
	Regional characterization of ultramafic to mafic intrusions in the Oxford–Stull and Uchi domains, Superior Province	Geological Survey of Canada	Ongoing
	Bedrock geology mapping, diamond-drill core re-logging and compilation of the McFaulds Lake (“Ring of Fire”) region	Geological Survey of Canada	Ongoing project with first maps anticipated in 2013

INITIATIVES

The ERGMS initiatives are based on geographic or functional groupings and are made up of 1) team initiatives (i.e., Abitibi Initiative) consisting of individual projects that are designed to meet an overall goal; 2) interjurisdictional team initiatives, such as the Targeted Geoscience Initiative 4 (TGI-4) and Geo-mapping for Energy and Minerals (“GEM”) initiative, that consist of individual and joint OGS and GSC projects that are also designed to meet an overall goal or objective; and 3) individual, focussed projects. The major initiatives of the ERGMS are subdivided into 8 broad categories outlined below and in Table 2.1.

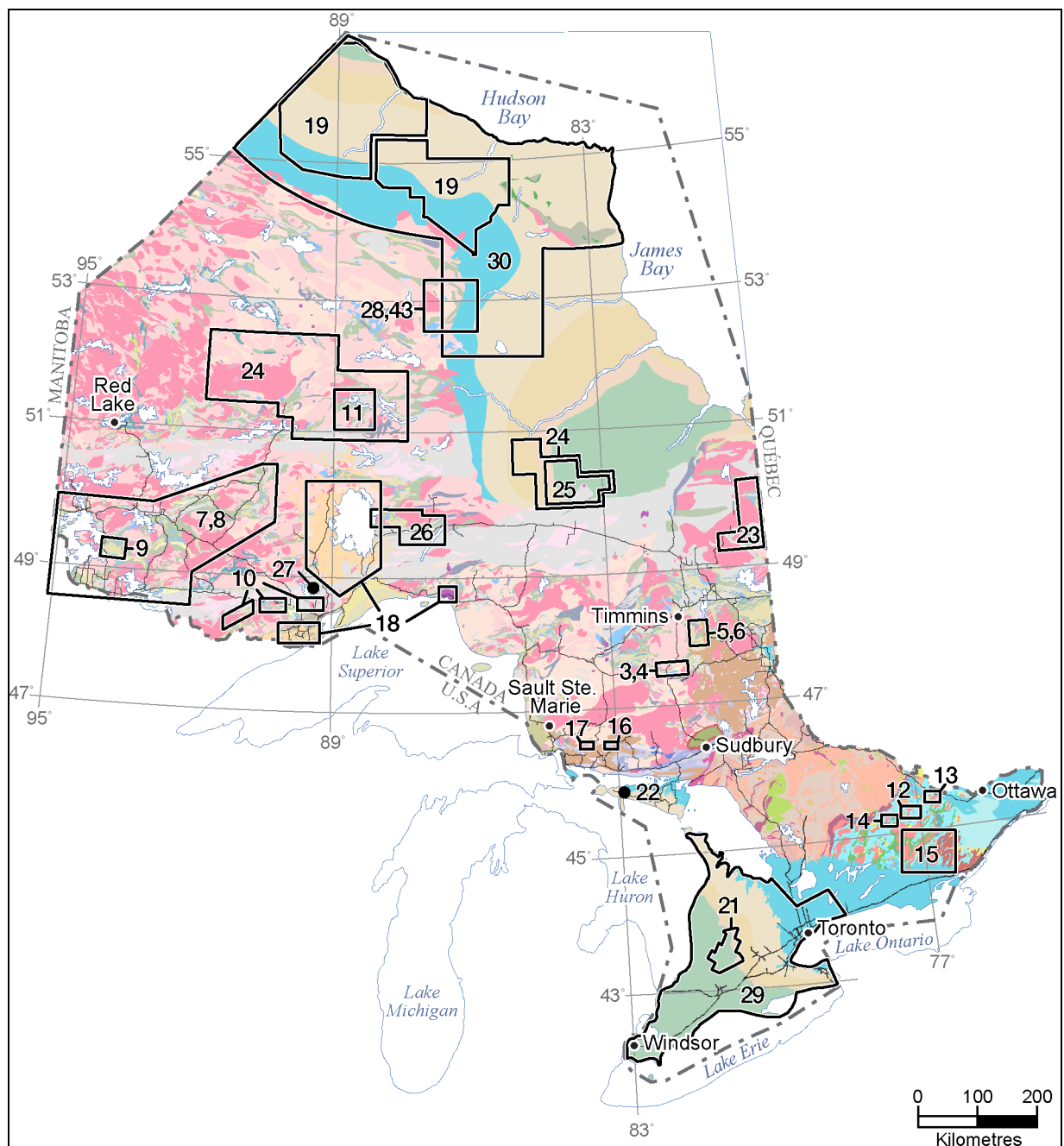


Figure 2.1. Location of Earth Resources and Geoscience Mapping Section projects described in *Summary of Field Work and Other Activities, 2012*. Numbers correspond to article numbers.

Initiatives that involve collaborative project agreements with the GSC:

- Targeted Geoscience Initiative 4 (TGI-4) nickel-copper-PGE-chromium projects and lode gold projects;
- Geo-mapping for Energy and Minerals (GEM) initiative projects.

Initiatives involving provincial-scale metallogenic compilation and inventory studies:

- documentation of specific types of mineralization;
- inventories of various tectonic settings relevant to mineral exploration.

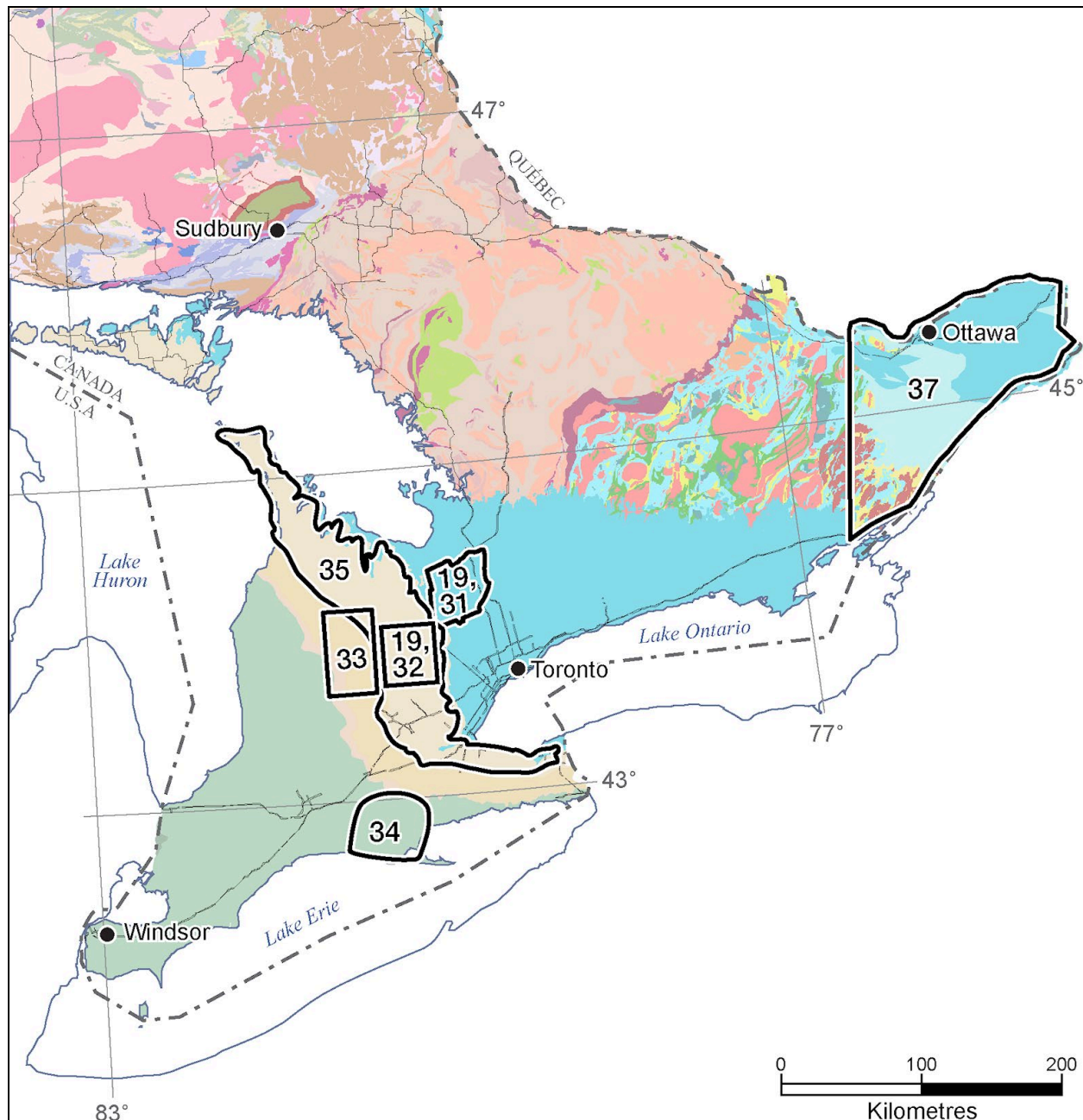


Figure 2.2. Location of Earth Resources and Geoscience Mapping Section groundwater projects described in *Summary of Field Work and Other Activities, 2012*. Numbers correspond to article numbers.

Initiatives based on geographic area:

- Abitibi initiative;
- “Ring of Fire” initiative;
- Far North Land Use Planning initiative;
- metallogeny and geology of northwestern Ontario;
- surficial geochemistry of northern Ontario;
- Proterozoic initiative.

Initiatives involving aggregate and industrial mineral resource compilation and inventory studies:

- documentation and inventory of aggregates resources;
- inventories of industrial mineral resources.

Initiatives involving support of the groundwater program:

- three-dimensional surficial sediment mapping initiative;
- three-dimensional Paleozoic bedrock mapping initiative;
- ambient groundwater geochemistry mapping initiative;
- environmental initiative.

Initiatives involving documentation, compilation and inventory studies of energy resources:

- documentation of hydrocarbons in Paleozoic rocks.

Initiatives involving geophysical projects:

- geophysics and bedrock geology mapping integration initiative;
- geophysics and rock properties data set initiative;
- geophysical techniques in support of surficial sediment mapping.

Initiatives that develop and manage client, stakeholder and First Nation relationships:

- external and internal committees;
- regional associations;
- maintaining relationships and exchanging technical information with First Nation communities.

COMMUNITY-GUIDED GEOSCIENCE

The ERGMS provided “in-kind” support to the final year of the Discover Abitibi Initiative (DAI) by continuing to support 3 geoscience projects: the Burntbrush–Normétal mapping project; a study of the Montclerg gold deposit; and an evaluation of gold mineralization in the Matachewan, Shining Tree, Chester Township and Northern Cobalt Embayment. Results of these projects will be published in 2013.

COLLABORATIVE PROJECTS WITH THE GEOLOGICAL SURVEY OF CANADA

The Targeted Geoscience Initiative 4 (TGI-4) commenced in 2011 and is a five-year, collaborative, federal geoscience program with a mandate to generate new geoscience knowledge in support of deep exploration (this volume, Targeted Geoscience Initiative 4 Section, Articles 41 to 48). To accomplish this objective, the Geological Survey of Canada, as part of the Earth Sciences Sector (ESS) of Natural Resources Canada (NRCan), has implemented an extensive program with activities focussed on regions in and around established and emerging mineral camps. In addition, TGI-4 will lead the development of new geoscience-based techniques to better vector toward buried mineral deposits.

The GSC and OGS, industry and academe are collaborating on geoscience projects located throughout Ontario that are focussed on nickel-copper-PGE-chromium (Ames et al., this volume, Article 41; Houlé, Leshar and Metsaranta, this volume, Article 42; Laarman, Barnett and Duke, this volume, Article 44; Hiebert et al., this volume, Article 45; Méric et al., this volume, Article 46) and lode gold deposits (Bleeker, this volume, Article 47; Lafrance et al., this volume, Article 48).

Collaborative GSC–OGS projects in the McFaulds Lake (“Ring of Fire”) region (Houlé, Leshar and Metsaranta, this volume, Article 42) include

- ongoing bedrock geology mapping, diamond-drill core re-logging and compilation as part of a multiyear ERGMS–GSC collaborative project as OGS “in-kind” support to TGI-4 (Metsaranta and Houlé, this volume, Article 43);
- regional characterization of ultramafic to mafic intrusions in the Oxford–Stull and Uchi domains, which includes participation of ERGMS staff;
- ongoing interpretation of the airborne gravity gradiometer and magnetic geophysical survey conducted in the McFaulds Lake greenstone belt, which includes participation of ERGMS staff;
- ongoing geophysical modelling of regional airborne gravity survey data from the McFaulds Lake greenstone belt, which includes participation of ERGMS staff;
- a study of the geochemistry of detrital chromite and investigating its use as a vector to nickel-copper-PGE, chromium and iron-titanium-vanadium deposits, which includes participation of ERGMS and OGS Geoscience Laboratories staff;
- co-support of a Master of Science (MSc) thesis at Lakehead University to study the petrology and iron-vanadium-titanium mineralization of the Thunderbird and Macdonald mafic to ultramafic intrusions in the McFaulds Lake greenstone belt, which includes participation of ERGMS staff and analytical support from the OGS Geoscience Laboratories;
- co-support of a PhD thesis at Laurentian University to study the ultramafic to mafic Black Label–Black Thor intrusive complex in the McFaulds Lake greenstone belt, which includes analytical support from the OGS Geoscience Laboratories.

The ERGMS is conducting 2 projects that complement targeted geoscience activities by the GSC, as part of their Geo-mapping for Energy and Minerals (GEM) initiative, which, in turn, is focussed on geological mapping for informed resource development in the extreme Far North of Canada (generally north of latitude 60°). The first project is a study of Paleozoic stratigraphy and hydrocarbon resource potential of the Hudson Platform, which involves bedrock mapping, diamond-drill core logging and compilation to upgrade geoscience data for Paleozoic strata in the Hudson Bay Lowland and re-evaluate hydrocarbon resource potential (Armstrong, this volume, Article 30). The second project is an airborne magnetic gradiometer geophysical survey of the Fort Severn region in the Hudson Bay Lowland, which will provide information for mineral exploration, land-use planning and energy development as part of the Ontario government’s Far North Land-Use Planning Initiative (Rainsford and Muir, this volume, Article 19).

OTHER COLLABORATIVE PROJECTS

Other collaborative projects conducted by the ERGMS in 2012 (*see* Table 2.2) are as follows:

- support of a Master of Science (MSc) thesis study of the Quaternary glaciation and stratigraphy of the Ridge River area in northern Ontario (Nguyen, Hicock and Barnett, this volume, Article 25);
- collaboration with Living with Lakes (LWL) Centre, Cooperative Freshwater Ecology Unit, Laurentian University on the McFaulds Lake area lake sediment and water sampling pilot study: by sharing water chemistry data (Dyer, this volume, Article 28);

- support of a PhD thesis study of the geodynamic setting of volcanogenic massive sulphide mineralization in the Wawa Subprovince as part of the OGS Graduate Mapping School Program with Laurentian University (Lodge, this volume, Article 10);
- support of a Bachelor of Science (BSc) thesis to study geochemistry and petrography of Quetico Subprovince granitoid rocks, located north of Thunder Bay;
- ongoing geological, paleomagnetic, geochemical and geochronological thesis studies of Mesoproterozoic Midcontinent Rift-related mafic intrusions near Thunder Bay, which is a collaboration, including thesis support, with Lakehead University (Cundari et al., this volume, Article 18);
- support of a Master of Science (MSc) thesis study on the origin and tectonic history of the *circa* 1090 to 1070 million-year-old plutons in the southeastern Central Metasedimentary Belt, Grenville Province, as part of a collaboration with Carleton University (Cutts, Easton and Carr, this volume, Article 15);
- support of a Master of Science (MSc) thesis study of nickel-copper mineralization in the Raglan Hills gabbro, Grenville Province, as part of a collaboration with Carleton University (Magnus, Cousens and Easton, this volume, Article 14);
- collaborate with Ministry of the Environment on a regional stream water sampling project across southern Ontario (Dyer and Burke 2012);
- support of a Master of Science (MSc) thesis study of the sedimentology and postglacial glaciolacustrine history of the Alliston area, southern Ontario.

PROVINCIAL-SCALE METALLOGENIC COMPILATION AND INVENTORY STUDIES

The ERGMS continued 4 ongoing, multiyear, provincial-scale projects that fall under the initiative to create inventories of various tectonic settings relevant to mineral exploration, as follows:

- ongoing documentation and distribution of FI-, FII- and FIII-type, potentially volcanogenic massive sulphide (VMS) deposit-productive felsic metavolcanic rocks in Ontario. Miscellaneous Release—Data 298 (Berger and Chartrand 2012) represents a compilation and interpretation of rhyolite occurrences in northwestern Ontario and in the Grenville Province. The compilation is intended to provide the user with an approximate location, physical character, age and chemical nature of the various “rhyolite” units in Ontario.
- ongoing documentation of mineralized intermediate to felsic plutonic systems in the Superior Province primarily focussed on documentation of gold mineralization related to felsic to intermediate plutonic rocks in the Wabigoon Subprovince;
- update and maintain the geochronology database for Ontario. The current geochronology database will be updated and converted to a Microsoft® Access® database and geographic information system (GIS) format.
- documentation of metamorphic patterns in Archean greenstone belts with work initially focussing on the Wabigoon Subprovince (Duguet and Beakhouse, this volume, Article 8).

INTERJURISDICTIONAL AND COMMITTEE REPRESENTATION

Staff of the ERGMS represented the Ministry of Northern Development and Mines, the OGS and other geoscience organizations on several interjurisdictional committees, internal committees and associations during the 2012–2013 fiscal year, which are summarized below:

- North American Commission on Stratigraphic Nomenclature (representing the Geological Association of Canada)
- Paleontology Division of the Geological Association of Canada
- Targeted Geoscience Initiative 4 nickel-copper-PGE-chromium and lode gold project teams
- TGI 4–National Geological Surveys Committee (NGSC) Subcommittee
- Great Lakes Geologic Mapping Coalition
- Canadian Mining Industry Research Organization (CAMIRO) Geophysics Expert Committee
- CAMIRO Geochemical Expert Committee
- Conservation Authorities Geosciences Committee
- Canadian Exploration Geophysical Society (KEGS) Scholarship Foundation
- Far North Information and Knowledge Management Working Group
- MNDM Management Health and Safety Committee
- MNDM Green Team
- MNDM Information Technology–Information Management (IT/IM) Strategy Committee
- MNDM Mining 101 Steering Group
- Geoscience Laboratories (Geo Labs)–ERGMS Working Group
- Willet Green Miller Centre (WGMC) Joint Health and Safety Committee
- GIS in the Ontario Public Service (OPS) License Management Task Force
- Ontario Public Service (OPS) GIS Summit/GIS Day Planning Committee
- National Geoscience Information Management Group
- Canadian Working Group on Regional Groundwater Flow Systems of the International Association of Hydrogeologists
- Thesis committees and adjunct professorships at universities (Laurentian University, Carleton University, Ohio State University, Western University, Chinese Academy of Sciences)
- Prospectors and Developers Association of Canada (PDAC) Health and Safety Committee (representing the Committee of Provincial and Territorial Geological Surveys)
- Prospectors and Developers Association of Canada (PDAC) Student–Industry Mineral Exploration Workshop

STAFFING CHANGES IN THE SECTION

S. Meade, J. Schroeder, C.N. Freckelton and H.E. Burke accepted positions with the ERGMS as Precambrian Geoscientist, Geological Assistant and Surficial Geochemists, respectively.

REFERENCES

- Berger, B.R. and Chartrand, J.E. 2012. Ontario rhyolite database—northwestern Ontario and the Grenville Province; Ontario Geological Survey, Miscellaneous Release—Data 298.
- Dyer, R.D. and Burke, H.E. 2012. Preliminary data release, southern Ontario stream sediment geochemistry survey; Ontario Geological Survey, Miscellaneous Release—Data 302.

3. Project Unit 11-001. Interpretation of Geochemistry in the South of Gogama Area

B.R. Berger¹

¹Earth Resources and Geoscience Mapping Section, Ontario Geological Survey

INTRODUCTION

This article reports on the whole-rock and trace-element geochemistry for 92 samples collected to supplement geological mapping in the south of Gogama area (Berger 2011, 2012a). The Ontario Geological Survey (OGS) routinely uses geochemical data to characterize and discriminate among various rock types encountered during field mapping, to aid petrogenetic interpretation and to help recognize areas with potential for economic mineralization. The geochemical data for these analyses are included in Berger (2012b).

The south of Gogama area (Figure 3.1) is underlain by Archean supracrustal rocks composed of mafic, intermediate and felsic metavolcanic rocks and clastic metasedimentary rocks that form a narrow linear belt connecting the Swayze greenstone belt to the west with the Shining Tree greenstone belt to the east. These rocks are intruded by members of 2 granitoid batholiths (Kenogamissi batholith and Ramsey–Algoma granitoid complex) and mafic to felsic members of a synvolcanic intrusive complex (Chester intrusive complex).

SUPRACRUSTAL ROCKS

Mafic Metavolcanic Rocks

Mafic metavolcanic rocks occur along the contact with the Kenogamissi batholith on the north side of the supracrustal rocks and as a 900 m wide unit in the east part of the map area (*see* Figure 3.1). Amphibolite and massive flows are most common, pillowed flows and schistose mafic rocks are less common, tuff breccia and tuff are rare. Ultramafic metavolcanic rocks were not observed and the geochemical data confirm that no rocks with ultramafic chemistry are present in the map area. Extended element plots for the several mafic metavolcanic rocks show that the majority display flat rare earth element (REE) profiles typical of tholeiitic magmas (Figure 3.2) (Henderson 1984). However, tantalum, niobium and titanium are weakly depleted and are commonly observed features of magmas generated in subduction zones associated with arc tholeiites (Wyman, Kerrich and Polat 2002).

Ayer et al. (in press) note similar geochemical features for many of the mafic metavolcanic rocks in the Shining Tree greenstone belt suggesting that there is correlation with the volcanic units immediately east of the map area. However, the geochemistry was not specific to any of the lithotectonic assemblages, so discrimination among assemblages in the map area cannot be based on geochemistry of the mafic metavolcanic rocks.

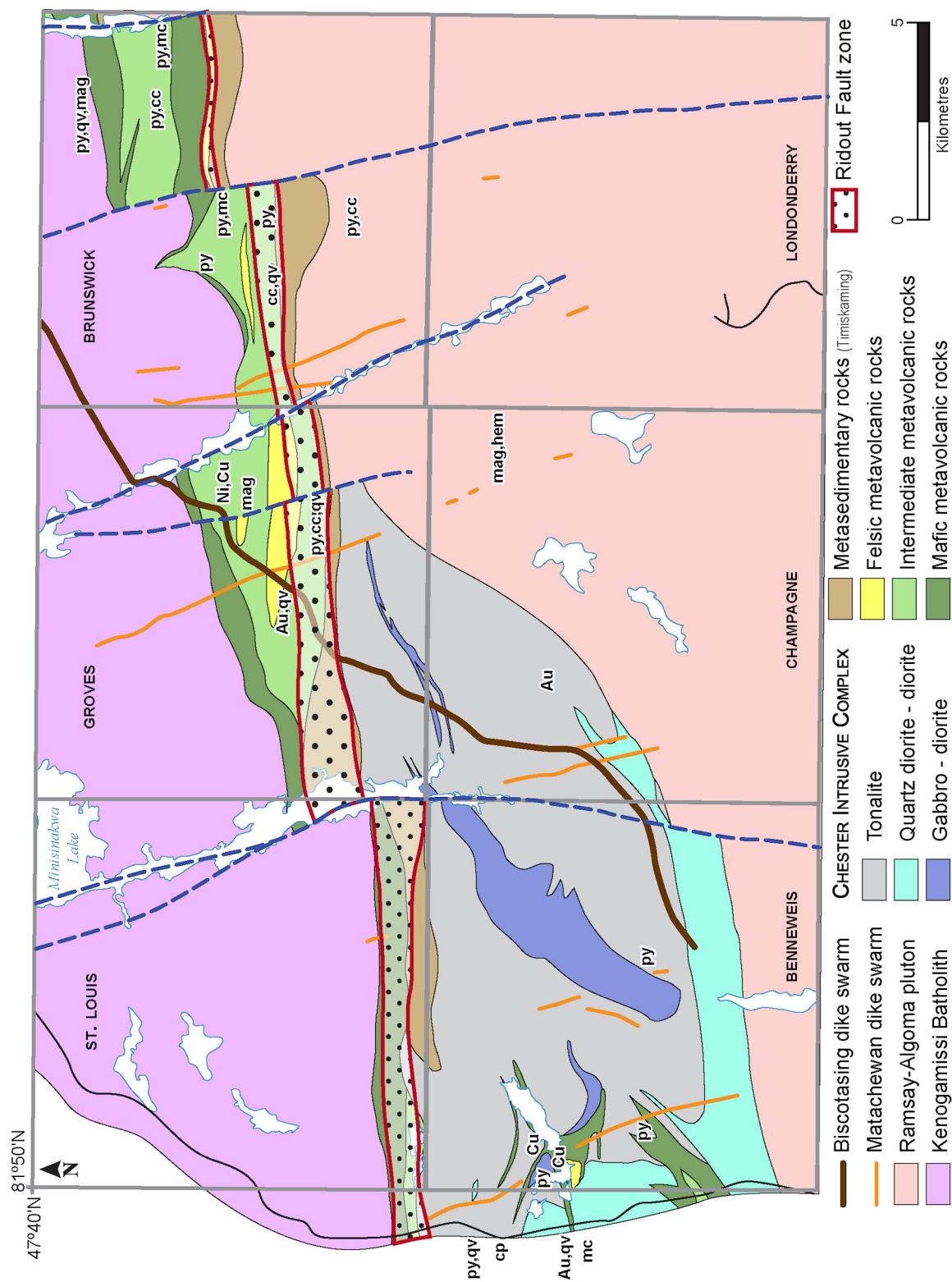


Figure 3.1. General geology of the south of Gogama area (based on Berger 2012b). Abbreviations: Au, gold; cc, carbonate alteration; cp, chalcopyrite; Cu, copper; hem, hematite; mag, magnetite; mc, malachite; Ni, nickel; py, pyrite; qv, quartz vein.

Intermediate and Felsic Metavolcanic Rocks

Intermediate and felsic metavolcanic rocks underlie parts of Brunswick Township and Groves Township (*see* Figure 3.1) where they occur mainly as epiclastic and pyroclastic tuff breccia, lapilli tuff, and tuff units. Massive, autobrecciated and rare magnetite-chlorite matrix breccia felsic flows occur locally in Groves Township. Felsic and intermediate schist is common in the Ridout fault zone. Felsic lapillistone, lapilli tuff and rare spherulitic flows occur as isolated rafts and screens in the Chester tonalite in Benneweis and east Chester townships. Felsic metavolcanic rocks west of the map area have a U/Pb zircon age of 2739 ± 1 Ma correlative with the Pacaud assemblage (van Breemen, Heather and Ayer 2006; Ayer et al. 2002). Previously determined ages for intermediate and felsic metavolcanic rocks east of the map area are 2707 ± 1 Ma (Tisdale assemblage) in Kelvin Township, 2687 ± 1 Ma (Porcupine assemblage) in Natal Township and 2741 ± 9.8 Ma (Pacaud assemblage) in Fawcett Township (Ayer et al. 2003).

Geochemical data indicate that the intermediate and felsic metavolcanic rocks can be subdivided into 2 groups (Figure 3.3). Group 1 rocks are characterized by fractionated light rare earth element (LREE) and flat heavy rare earth element (HREE) patterns on extended element plots (Figure 3.3a). These rocks also have elevated thorium, depleted europium, very strongly depleted titanium and Zr/Y between 3 and 8 or transitional geochemical affinity (Leshner et al. 1986; Ayer et al., in press). These patterns are similar to FII rhyolites that are interpreted to be derived from magmas generated from partial melts of basalts in upper crustal magma chambers (Hart, Gibson and Leshner 2004; Leshner et al. 1986.) The FII rhyolites in other parts of the Abitibi Subprovince are associated with volcanogenic massive sulphide (VMS) deposits (e.g., Selbaie and Normétal in Quebec) and this suggests that there is potential for base metal mineralization in the Gogama area (Leshner et al. 1986; Barrett et al., in press). Group 1 intermediate and felsic rocks occur mostly as large rafts, inclusions and screens in the Chester intrusive complex and are inferred to be the extrusive equivalents of the tonalite phase of the complex (*see* “Chester Intrusive Complex”). The tonalite was determined to be approximately 2740 Ma, which falls within the range of the Pacaud assemblage for the Abitibi greenstone belt (van Breemen, Heather and Ayer 2006; Ayer et al. 2002). Therefore, the Pacaud assemblage in the Swayze and Shining Tree greenstone belts has potential for VMS mineralization.

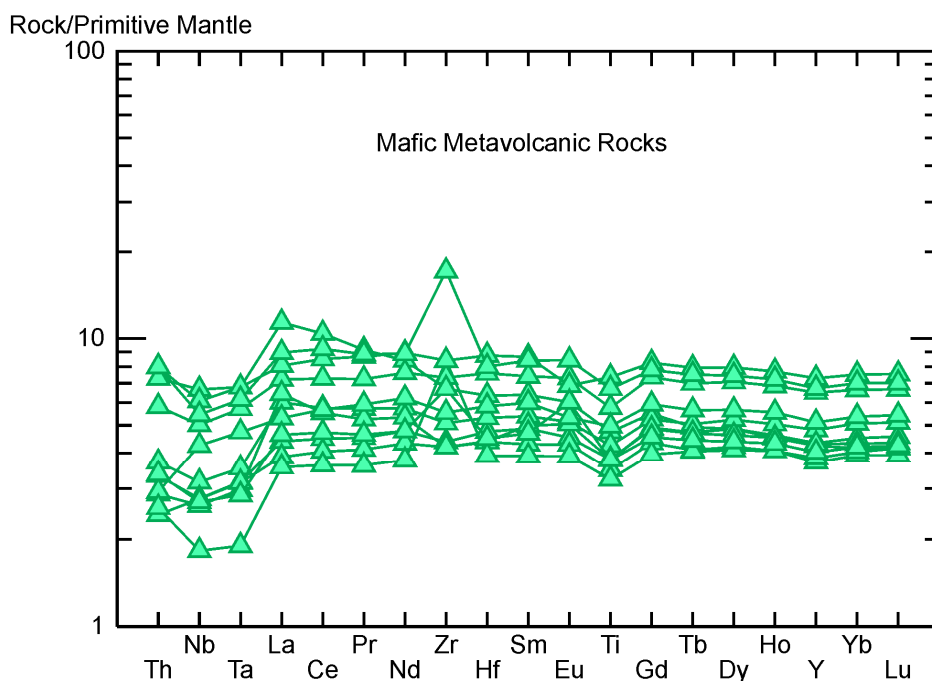


Figure 3.2. Extended element plot for mafic metavolcanic rocks in the south of Gogama area. Note: all geochemical diagrams were generated using Terra Soft Inc. IGPET (version March 8, 2008) software; REE data are normalized *after* Sun and McDonough (1989).

Group 1 felsic metavolcanic rocks are also observed in Groves Township where they occur as hydrothermal breccia and schist in the Ridout fault zone (Photo 3.1). The felsic metavolcanic rocks in this part of Groves Township should be thoroughly explored for their base metal and gold potential.

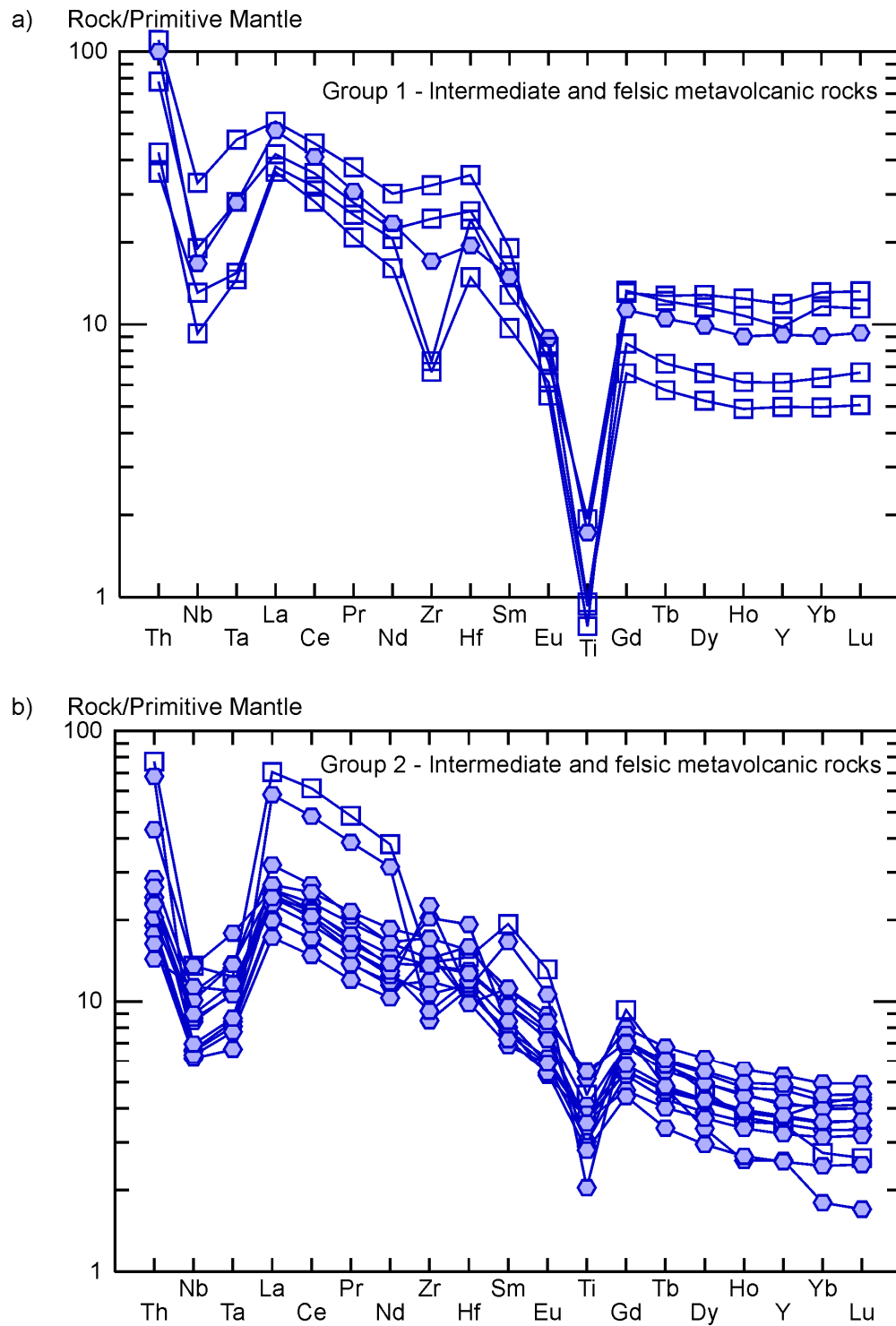


Figure 3.3. Extended element plots for intermediate and felsic metavolcanic rocks in the south of Gogama area. a) Group 1: similar REE patterns to FII rhyolite; and b) Group 2: similar REE patterns to FI rhyolite (cf. Leshner et al. 1986). REE data are normalized *after* Sun and McDonough (1989).

Group 2 intermediate and felsic metavolcanic rocks are characterized by negatively sloped REE patterns with moderately elevated thorium, moderately depleted titanium, no europium anomalies and Zr/Y greater than 6 or calc-alkalic geochemical affinity (Figure 3.3b) (Leshner et al. 1986; Ayer et al., in press). These patterns are similar to FI felsic metavolcanic rocks as described by Leshner et al. (1986). These rocks are interpreted to have been derived from partial melting at lower crustal depths with rapid ascent to the surface. The FI felsic rocks are much less likely to be associated with VMS deposits than FII or FIII rhyolites (Leshner et al. 1986; Hart, Gibson and Leshner 2004). Group 2 rocks occur mostly in the east part of the map area, but are also known as far west as Minisinakwa Lake in St. Louis Township (*see* Figure 3.1).

Ayer et al. (in press) indicate that intermediate and felsic metavolcanic rocks in the Shining Tree greenstone belt are calc-alkalic, transitional or alkalic in geochemical affinity. The alkalic volcanic rocks appear to be restricted to the Porcupine assemblage precluding its presence in the map area. The calc-alkalic and transitional rocks are more widely distributed with no apparent correlation with assemblages in the Shining Tree greenstone belt. Ayer et al. (in press) did not classify the intermediate and felsic metavolcanic rocks as FI or FII type according to Leshner et al. (1986) or Hart, Gibson and Leshner (2004) and this, again, precludes direct comparison to metavolcanic rocks in the map area.

Clastic Metasedimentary Rocks

Clastic metasedimentary rocks, composed mostly of matrix- to clast-supported conglomerate with lesser massive sandstone and derived schist, form a linear unit along the south side of the supracrustal rocks in the map area (*see* Figure 3.1). This unit is correlated with the Timiskaming assemblage based on clast composition (tonalite clasts are a major component; Photo 3.2), quartz-rich sand matrix, the inferred unconformity with the Ramsey–Algoma granitoid complex to the south and inferred deposition in an alluvial–fluvial environment.



Photo 3.1. Example of FII rhyolite breccia in Groves Township interpreted as hydrothermal, possibly related to VMS-style mineralization.

Geochemistry of clastic metasedimentary rocks typically reflects the mixing of the various provenances of the detritus. Figure 3.4 shows a strong similarity in trace-element geochemistry among all metasedimentary rocks with the intermediate to felsic metavolcanic rocks and the nearby felsic intrusions in the map area. There is little similarity with mafic rocks and this suggests that these rock types had only a minor contribution to detritus or that the mafic component was overwhelmed by felsic detritus. The geochemical patterns displayed in Figure 3.4 are similar to Timiskaming assemblage clastic metasedimentary rocks in other parts of the Abitibi greenstone belt (Berger 2002).

PLUTONIC ROCKS

Kenogamissi Batholith

The Kenogamissi batholith is a complex amalgamation of several plutons of various compositions and diverse ages that occurs along the north edge of the map area (*see* Figure 3.1) (Beakhouse 2011; van Breemen, Heather and Ayer 2006; Benn 2004). Tonalite, gneissic tonalite, granodiorite and potassium feldspar megacrystic granite occur in the map area; geochemical data for all rock types display strong niobium and tantalum depletion and negatively sloped REE patterns (Figure 3.5). These patterns are similar to those for the many phases described by Beakhouse (2011).

Beakhouse (2011) indicated that the early high-alumina tonalite–trondhjemite–granodiorite (TTG) plutons of the Kenogamissi batholith were emplaced over a protracted interval (2737 to 2698 Ma) synchronous with the Pacaud, Stoughton–Roquemaure, Kidd–Munro and Blake River volcanic assemblages (cf. Ayer et al. 2002). Younger (2685 to 2680 Ma) diorite-quartz monzodiorite plutons postdate the volcanism and have geochemistry compatible with sanukitoid petrogenesis (Beakhouse 2011). The geochemical data for rocks in the map area support this interpretation.



Photo 3.2. Tonalite clast in sandstone from Brunswick Township; the matrix is typical of conglomerates in the map area interpreted as Timiskaming assemblage.

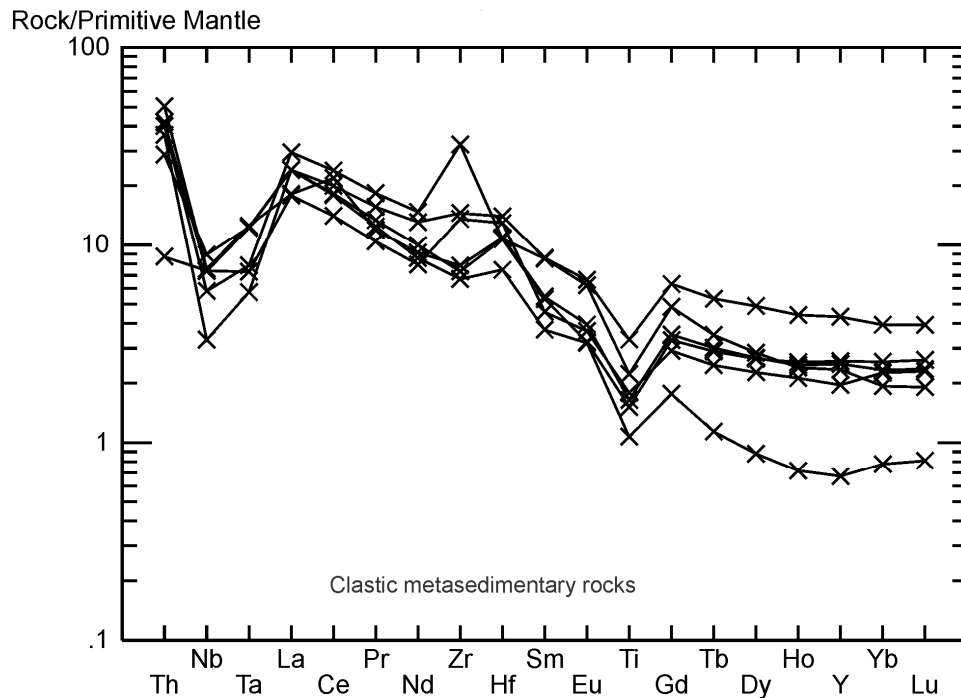


Figure 3.4. Extended element plot for clastic metasedimentary rocks in the south of Gogama area. Patterns are similar to clastic metasedimentary rocks in other parts of the Abitibi greenstone belt correlated with the Timiskaming assemblage. REE data are normalized *after* Sun and McDonough (1989).

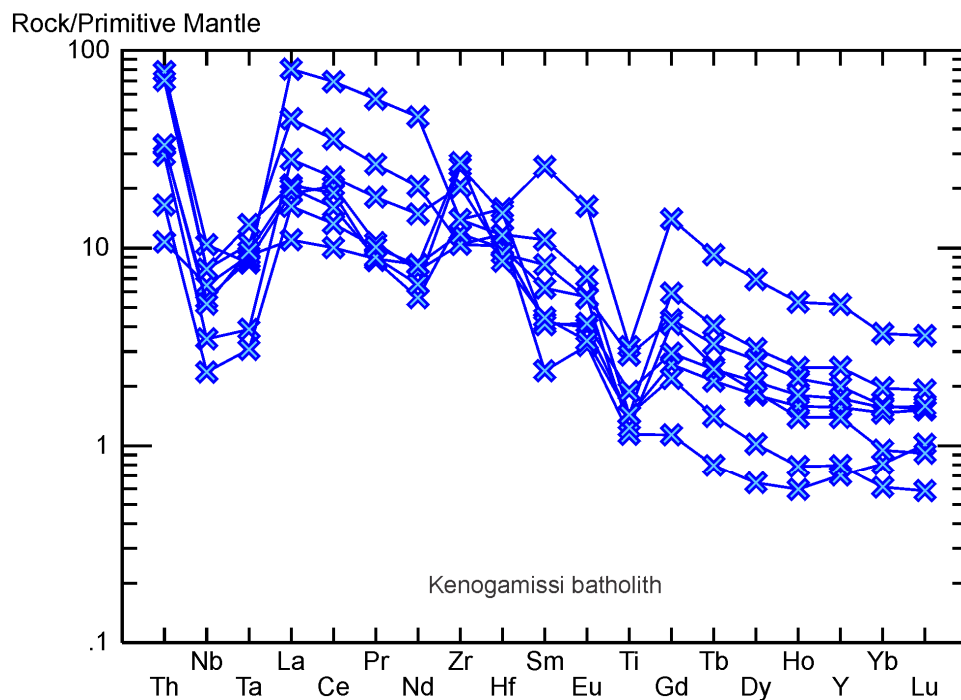


Figure 3.5. Extended element plot for intermediate and felsic intrusive rocks of the Kenogamissi batholith without regard to age. Negative niobium, tantalum and titanium anomalies for all samples suggest derivation of magmas from subduction-related processes. REE data are normalized *after* Sun and McDonough (1989).

Chester Intrusive Complex

The Chester intrusive complex is a multiphase intrusion that underlies the southwestern part of the map area and extends to the west where it is host to the disseminated gold-copper Côté Lake deposit (Trelawney Mining and Exploration Inc., news release, February 24, 2012). Tonalite, diorite, quartz diorite and gabbro are the main phases of the intrusion and field relationships, which, combined with recent U/Pb zircon ages, indicate that these rocks are approximately contemporaneous between 2741 and 2738 Ma (Trelawney Mining and Exploration Inc., news release, February 24, 2011). Pegmatitic and coarse-grained gabbro cut by narrow tonalite dikes comprise a separate phase in the central part of Benneweis Township (*see* Figure 3.1). The gabbro appears to be a cumulate phase of the Chester intrusive complex and is characterized by a diffuse high airborne magnetic response (Ontario Department of Mines–Geological Survey of Canada 1963). This phase of the intrusion is distinctive in the field and geochemically displays flat REE patterns with positive europium and titanium anomalies and with weakly depleted niobium and tantalum (Figure 3.6). These patterns are consistent with the interpretation that the gabbro is a cumulate phase of the intrusive complex.

Medium-grained equigranular gabbro, diorite and quartz diorite are common in the west and southwest portion of the Chester intrusive complex. These rock types are commonly equigranular mesocratic rocks, but also occur as breccias with tonalitic matrix, as xenoliths within the tonalite and as dikes cutting the nearby tonalite. Geochemically, these rocks display fractionated REE patterns, no or weakly depleted europium and titanium anomalies, weakly to moderately depleted niobium and tantalum and elevated thorium (*see* Figure 3.6). These patterns are similar to, and overlap with, geochemical patterns for the Chester tonalite with which the gabbro, diorite and quartz diorite are inferred to be genetically related (*see* text below).

White weathering, medium-grained, equigranular to quartz porphyritic tonalite is the most common phase of the Chester intrusive complex in the map area (*see* Figure 3.1). Tonalite is most commonly massive, but is locally brecciated near the contacts with the diorite-quartz diorite phases of the intrusion and is locally schistose along its northern boundary with the Ridout fault zone. Tonalite dikes cut the gabbro, diorite and quartz diorite phases, but diorite dikes are commonly observed cutting the tonalite especially in eastern Benneweis Township and parts of Champagne Township. The tonalite is geochemically characterized by fractionated LREE, pronounced negative europium anomalies and elevated flat HREE (Figure 3.7), virtually identical to the group 1, FII felsic metavolcanic rocks described above. Further, the Chester tonalite is also characterized by pronounced negative niobium, tantalum and titanium anomalies as is typical of magmas generated by subduction-related processes. The FII geochemical affinity of Chester tonalite strongly suggests that the felsic metavolcanic rocks may be fertile for VMS mineralization as is observed in other parts of the Abitibi greenstone belt (cf. Leshner et al. 1986; Barrett et al., in press). This is further reinforced by the whole-rock geochemistry of the tonalite that locally displays strong sodium depletion (0.78% Na₂O at 76% SiO₂) characteristic of VMS-style hydrothermal alteration (Lydon 1988).

The Chester tonalite is inferred by the author to represent a subvolcanic magma chamber for the Pacaud assemblage felsic metavolcanic rocks in the map area and to the west in the Swayze greenstone belt. The tonalite is inferred to have intruded to a high crustal level based on the number and large size of greenstone rafts and xenoliths in the intrusion and on the presence of miarolitic cavities and graphic-textured minerals (indicative of rapid cooling) (Kontak 2012). The Côté Lake disseminated gold-copper deposit is hosted by the Chester intrusive complex and is interpreted to be hypogene mineralization in a porphyry-style setting (Kontak 2012; Trelawney Mining Inc., news release, February 24, 2012). Porphyry-style mineralization occurs in modern settings at convergent-plate margins in continental crust or volcanic-arc settings over subduction zones (McMillan and Panteleyev 1988; Garwin 2011). If the porphyry model is confirmed, there is a good probability that similar types of subvolcanic intrusions to

the Abitibi greenstone belt lie southwest and west of the Côté Lake deposit. The area immediately south of the Swayze greenstone belt and south to Elizabeth and Margaret townships should be examined for possible mineralized subvolcanic intermediate and felsic plutons.

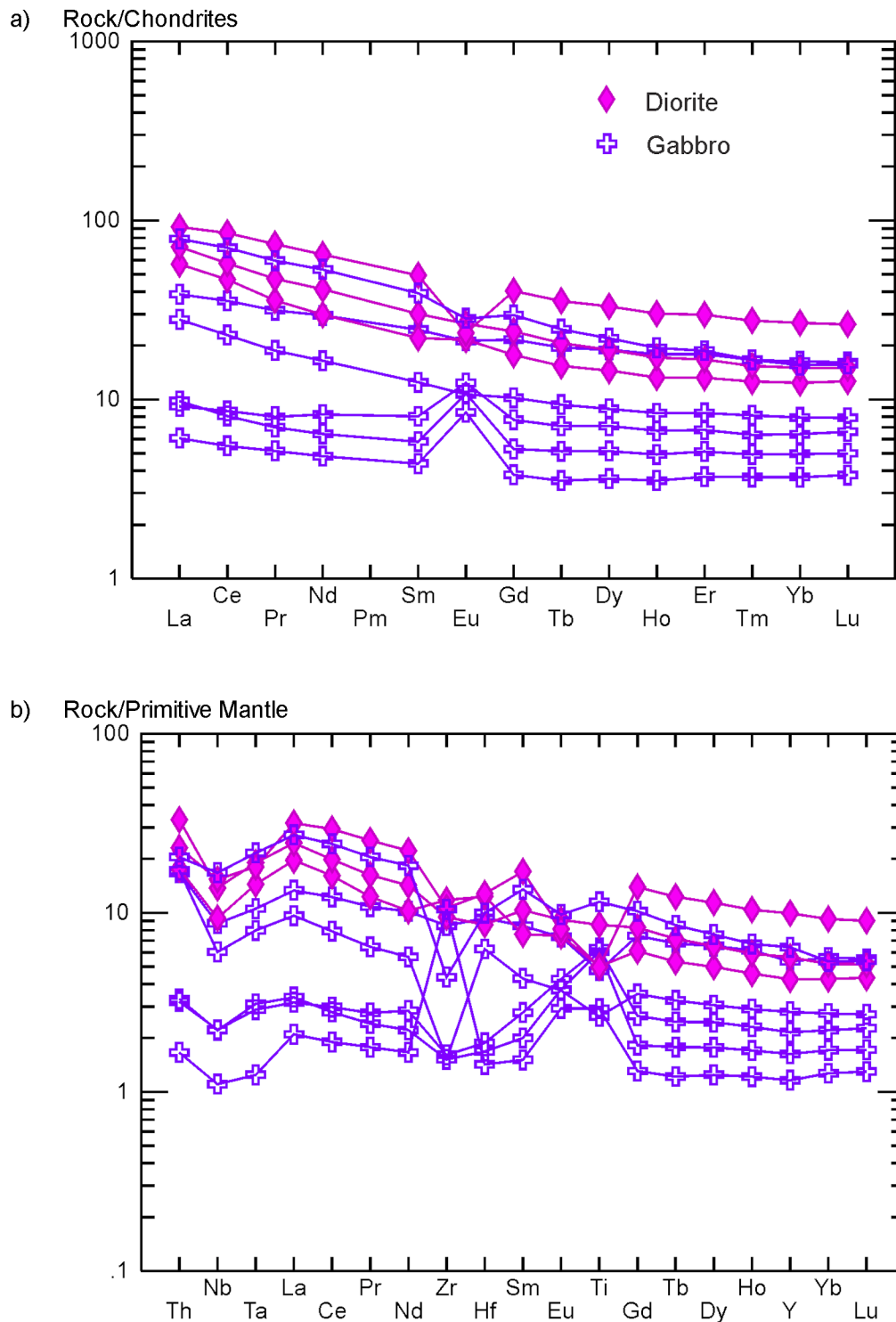


Figure 3.6. Rare earth and extended element plots for mafic and intermediate plutonic phases of the Chester intrusive complex: a) REE plot for gabbro, diorite and quartz diorite phases; and b) extended element plot for gabbro, diorite and quartz diorite phases. REE data are normalized *after* Sun and McDonough (1989).

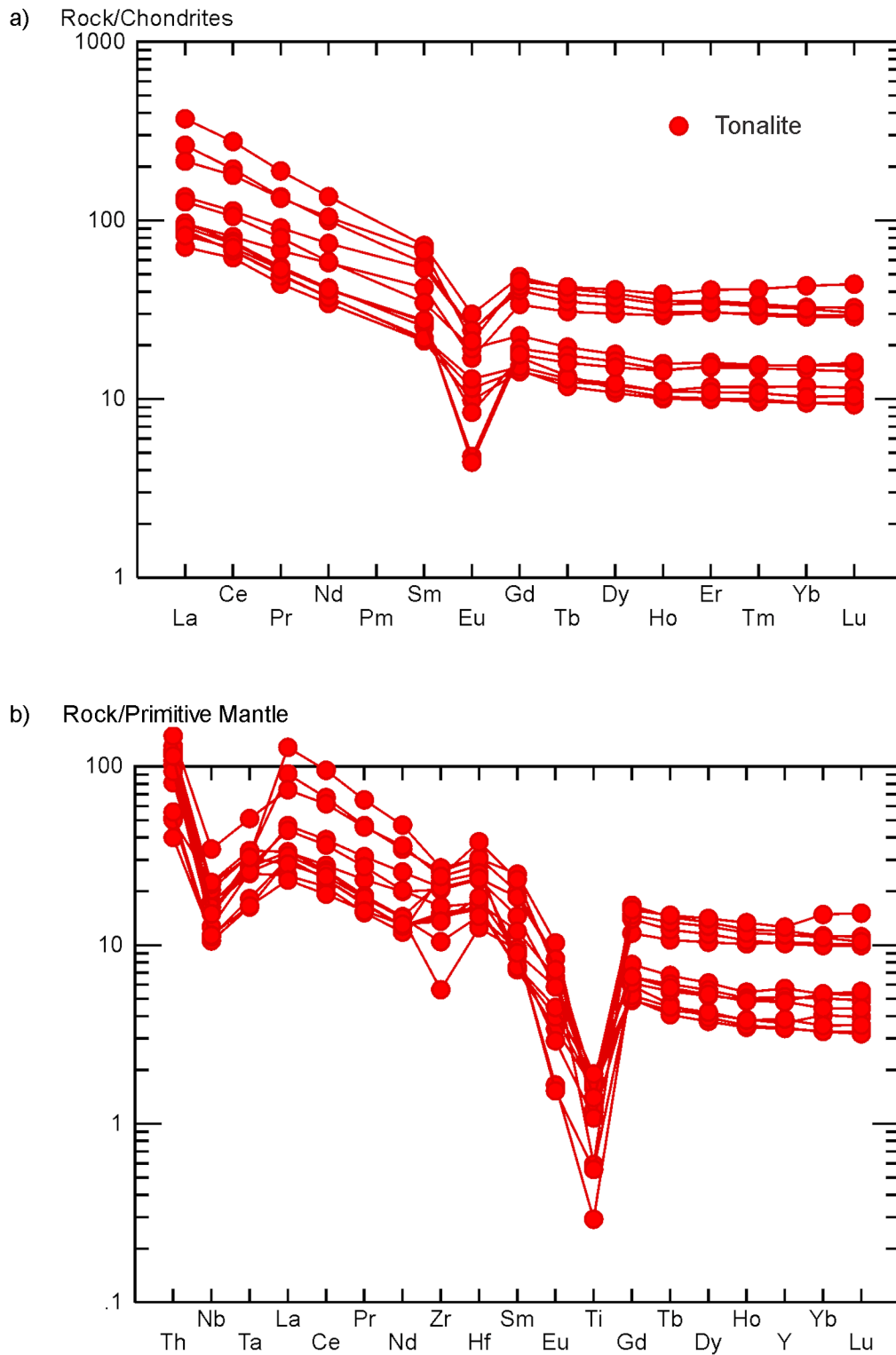


Figure 3.7. Rare earth and extended element plots for felsic plutonic rocks of the Chester intrusive complex: a) REE plot for tonalite; note similarity to FII rhyolite; and b) extended element plot for tonalite. REE data are normalized *after* Sun and McDonough (1989).

Ramsey–Algoma Granitoid Complex

White to pink weathering, medium- to coarse-grained, equigranular tonalite and granodiorite underlie the southeastern part of the map area. These rocks comprise a single weakly deformed pluton that is part of the Ramsey–Algoma granitoid complex, also referred to as the Ramsey–Algoma intrusive complex of the Ramsey–Algoma terrane (Ayer et al. 2010; van Breemen, Heather and Ayer 2006). The tonalite and granodiorite are in apparent unconformable contact with the Timiskaming assemblage clastic metasedimentary rocks. Geochemical analyses of representative samples of this intrusion show tightly clustered fractionated REE patterns with pronounced negative tantalum, niobium and titanium anomalies (Figure 3.8). This intrusion is remarkably homogeneous in texture and geochemistry over a large surface area (~225 km²) unlike the other granitic intrusions in the map area. However, the contact between the Chester intrusive complex and this intrusion is poorly exposed and field relationships are often confused because the tonalite phase of both intrusions is similar in appearance. Distinction between the Chester tonalite and the Ramsey–Algoma tonalite-granodiorite is important as the Chester tonalite is a potential host to gold mineralization wherever it occurs. Fortunately, the 2 tonalites are distinct geochemically. The difference in REE characteristics is illustrated in Figure 3.9a and the 2 tonalites are readily separated on the granite discrimination plot shown in Figure 3.9b. Mineral explorationists may find these types of discrimination plots useful when trying to separate the 2 intrusions in the map area.

CONCLUSIONS

Whole-rock and trace-element geochemistry aids identification and classification of the supracrustal and plutonic rocks in the mapped area south of Gogama. Intermediate and felsic metavolcanic rocks are subdivided into 2 groups based on REE and trace-element geochemistry. Group 1 has geochemical patterns similar to FII rhyolites that are potential hosts to economic volcanogenic massive sulphide (VMS) deposits (cf. Leshner et al. 1986). Group 2 has geochemical patterns similar to FI rhyolites that are less likely to host base metal mineralization. However, further work is required to link the metavolcanic rocks in the map area with those in the Shining Tree greenstone belt based on geochemistry alone.

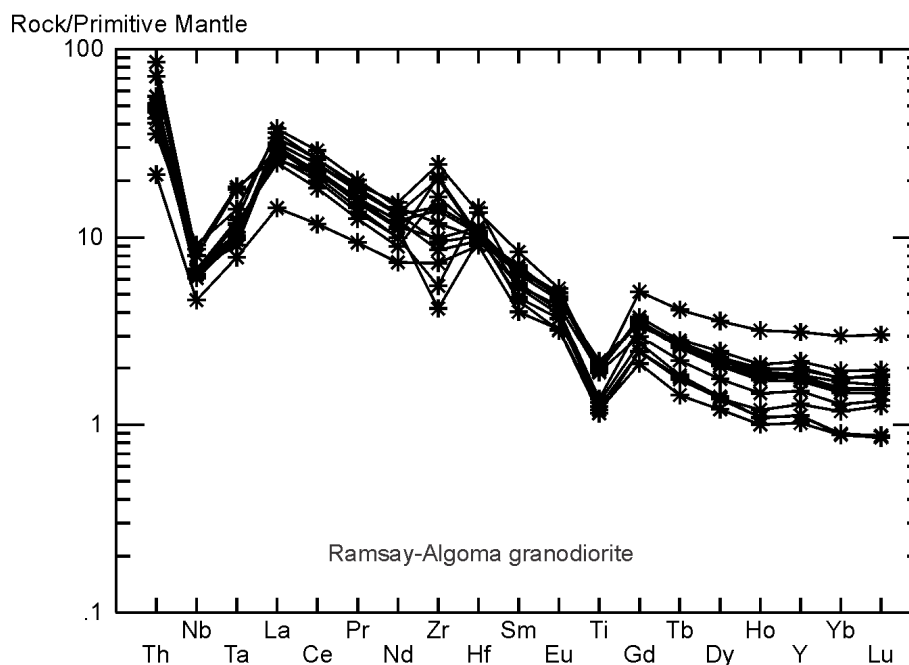


Figure 3.8. Extended element plot for felsic intrusive rocks of the Ramsey–Algoma granitoid complex. REE data are normalized *after* Sun and McDonough (1989).

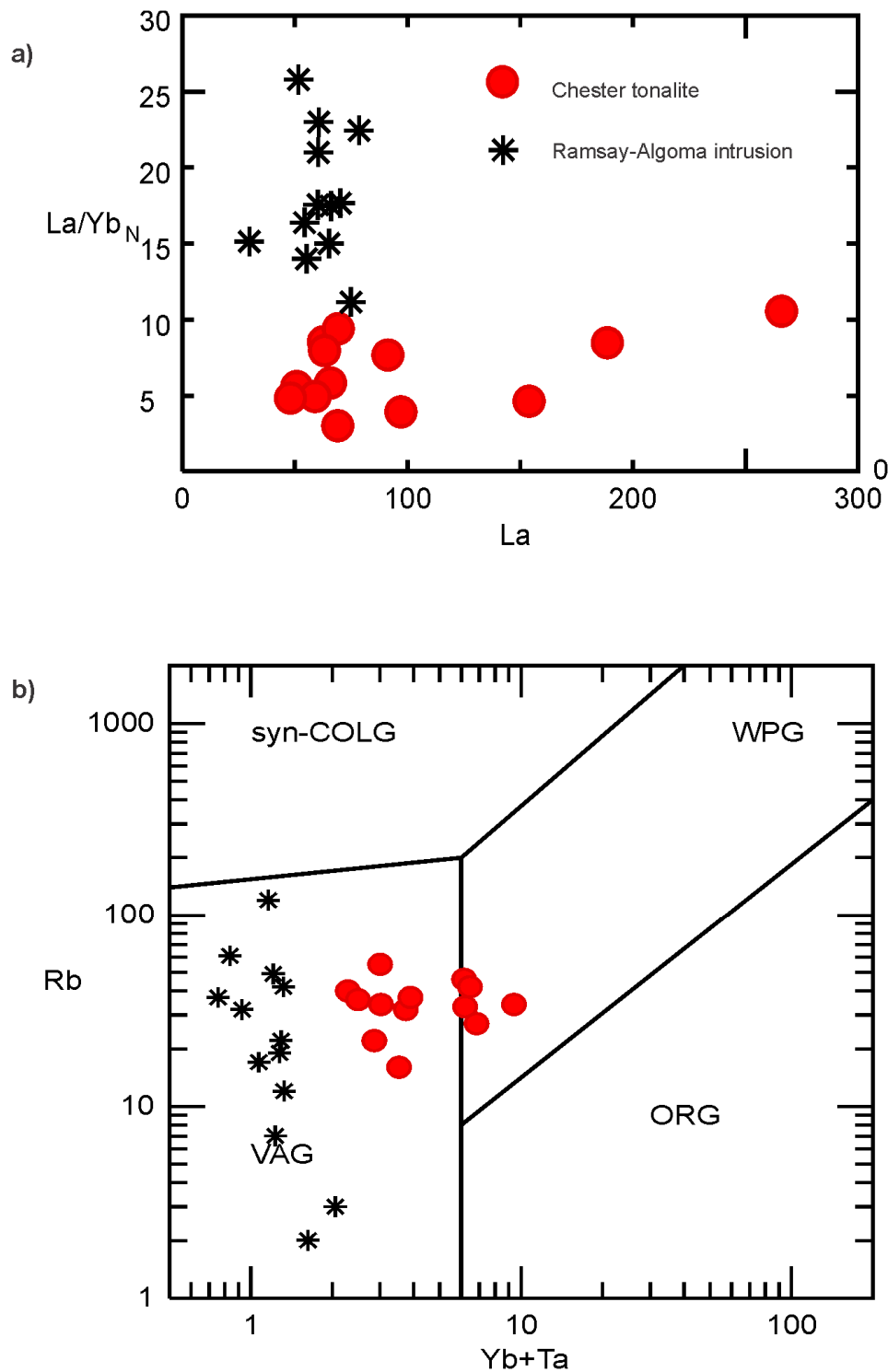


Figure 3.9. Discrimination plots showing the distinction between the felsic plutonic rocks of the Chester intrusive complex and the Ramsey-Algoma granitoid complex. a) La versus $(La/Yb)_N$. b) Yb+Ta versus Rb; fields are syn-COLG, syn-collisional granite; WPG, within-plate granite; ORG, ocean ridge granite; VAG, volcanic arc granite (*after* Pearce, Harris and Tindle 1984). REE data are normalized *after* Sun and McDonough (1989).

The various phases of the Chester intrusive complex display geochemical patterns that are consistent with derivation by fractionation. Coarse-grained gabbro, interpreted as a cumulate, is distinct in the field, but retains weak niobium and tantalum depletions (*see* Figure 3.6b) that genetically link it to the other intrusive phase. Diorite, quartz diorite and medium-grained gabbro display REE and trace-element patterns that overlap those of the more abundant tonalite phase of the intrusion. Geochemical patterns of the tonalite are similar to those for FII rhyolites and the tonalite is interpreted as a subvolcanic magma chamber to the nearby FII intermediate and felsic metavolcanic rocks.

REFERENCES

- Ayer, J., Amelin, Y., Corfu, F., Kamo, S., Ketchum, J., Kwok, K. and Trowell, N. 2002. Evolution of the southern Abitibi greenstone belt based on U-Pb geochronology: autochthonous volcanic construction followed by plutonism, regional deformation and sedimentation; *Precambrian Research*, v.115, p.63-95.
- Ayer, J.A., Chartrand, J.E., Trowell, N.F. and Wilson, A.C. 2010. Geological compilation of the Maple Mountain area, Abitibi greenstone belt; Ontario Geological Survey, Preliminary Map P.3620, scale 1:100 000.
- Ayer, J.A., Kontak, D.J., Linnen, R.L. and Lin, S. eds. in press. Results from the Shining Tree, Chester Township and Matachewan gold projects and the northern Cobalt embayment polymetallic vein project; Ontario Geological Survey, Miscellaneous Release—Data 294.
- Ayer, J.A., Trowell, N.F., Josey, S., Nevills, M. and Valade, L. 2003. Geological compilation of the Matachewan area, Abitibi greenstone belt; Ontario Geological Survey, Preliminary Map P.3527, scale 1:100 000.
- Barrett, T.J., Ayer, J.A., Ordóñez-Calderón, J.C. and Hamilton, M.A. in press. Geological mapping and compilation of the Burntbush–Normétal volcanic belt, Abitibi greenstone belt, Ontario–Quebec; Ontario Geological Survey, Miscellaneous Release—Data 299.
- Beakhouse, G.P. 2011. The Abitibi Subprovince plutonic record: tectonic and metallogenic implications; Ontario Geological Survey, Open File Report 6268, 155p.
- Benn, K. 2004. Late Archean Kenogamissi Complex, Abitibi Subprovince, Ontario: doming, folding and deformation-assisted melt remobilisation during syntectonic batholith emplacement; *in* Fifth Hutton Symposium, The origin of granites and related rocks, Transactions of the Royal Society of Edinburgh (Earth Sciences), v.95, pts.1-2, p.297-307.
- Berger, B.R. 2002. Geological synthesis of the Highway 101 area, east of Matheson, Ontario; Ontario Geological Survey, Open File Report 6091, 124p.
- 2011. Geological investigations south of Gogama; *in* Summary of Field Work and Other Activities, 2011, Ontario Geological Survey, Open File Report 6270, p.3-1 to 3-5.
- 2012a. Precambrian geology, south of Gogama area; Ontario Geological Survey, Preliminary Map P.3762—Revised, scale 1:50 000.
- 2012b. Geology, petrography, geochemistry and photographs of the south of Gogama area; Ontario Geological Survey, Miscellaneous Release—Data 292.
- Garwin, S. 2011. Porphyry-copper-gold deposits: characteristics and economic significance; short course presentation, Prospectors and Developers Association of Canada, Annual Convention, 2011.
- Hart, T.R., Gibson, H.L. and Leshner, C.M. 2004. Trace element geochemistry and petrogenesis of felsic volcanic rocks associated with volcanogenic massive Cu-Zn-Pb sulphide deposits; *Economic Geology*, v.99, p.1003-1013.
- Henderson, P. ed. 1984. Rare earth element geochemistry; Elsevier, Amsterdam, *Developments in Geochemistry* 2, 510p.

- Kontak, D.J. 2012. Is Canada's oldest Au deposit an Archean analogue for a porphyry system? The 2740 Ma Côte Lake Au-(Cu) deposit, northern Ontario; presentation, Laurentian University, Department of Earth Sciences, seminar, March 9, 2012.
- Leshner, C.M., Goodwin, A.M., Campbell, I.H. and Gorton, M.P. 1986. Trace-element geochemistry of ore associated and barren, felsic metavolcanic rocks in the Superior Province, Canada; *Canadian Journal of Earth Sciences*, v.23, p.222-237.
- Lydon, J.W. 1988. Volcanogenic massive sulphide deposits, parts 1 and 2; *in* Ore deposit models, Geological Association of Canada, Geoscience Canada Reprint Series 3, p.145-182.
- McMillan, W.J. and Panteleyev, A. 1988. Porphyry copper deposits; *in* Ore deposit models, Geological Association of Canada, Geoscience Canada Reprint Series 3, p.45-58.
- Ontario Department of Mines–Geological Survey of Canada 1963. Gogama, Ontario; Ontario Department of Mines–Geological Survey of Canada, Aeromagnetic Map 1528G, scale 1:63 360.
- Pearce, J.A., Harris, B.W. and Tindle, A.G. 1984. Trace element discrimination diagrams for the tectonic interpretation of granitic rocks; *Journal of Petrology*, v.25, p.956-983.
- Sun, S.-S. and McDonough, W.F. 1989. Chemical and isotopic systematics of oceanic basalts: implications for mantle composition and processes; *in* Magmatism in the ocean basins, The Geological Society, Special Publication No.42, p.313-345.
- van Breemen, O., Heather, K.B. and Ayer, J.A. 2006. U-Pb geochronology of the Neoarchean Swayze sector of the southern Abitibi greenstone belt; Geological Survey of Canada, Current Research 2006-F1, 32p.
- Wyman, D.A., Kerrich, R. and Polat, A. 2002. Assembly of Archean cratonic mantle lithosphere and crust: plume–arc interaction in the Abitibi–Wawa subduction – accretion complex; *Precambrian Research*, v.115, p.37-62.

4. Project Unit 11-001. Report on Geochronology for the South of Gogama Area

B.R. Berger¹ and R.W.D. Lodge²

¹Earth Resources and Geoscience Mapping Section, Ontario Geological Survey, Sudbury, Ontario P3E 6B5

²Department of Earth Sciences, Laurentian University, Sudbury, Ontario P3E 2C6

INTRODUCTION

Four samples were selected for U/Pb geochronological analysis from the south of Gogama area in 2011 (Figure 4.1). Three samples were submitted to Laurentian University for analysis by laser ablation inductively coupled plasma mass spectrometry (LA-ICP-MS) and 1 sample was submitted to the Jack Satterly Geochronology Laboratory in Toronto for thermal ionization mass spectrometric (TIMS) analysis. This article reports the results for the 3 samples submitted to Laurentian University. The result from the TIMS analysis was pending at time of writing. Geochronology sampling has several purposes, with the main intent designed to provide absolute age constraints on the geology in the area. This knowledge permits correlation of geological units within the map area as well as in other parts of the Abitibi greenstone belt. Geochronology also aids interpretation of timing for sedimentation and deformation and provides constraints on timing of major mineralization.

LASER ABLATION INDUCTIVELY COUPLED PLASMA MASS SPECTROMETRIC ANALYSES AT LAURENTIAN UNIVERSITY

The samples were crushed, milled and passed over a Wilfley[®] table to yield a heavy mineral pre-concentrate. This pre-concentrate was split into a series of magnetic fractions. The least magnetic fraction passed through heavy liquids to separate zircons and other heavy minerals (pyrite, apatite, etc). Zircons were then picked from each sample and mounted in one-inch epoxy pucks that were polished down to a 1 µm paste.

All grains were analyzed at Laurentian University using a 193 nm ArF excimer laser (Resonetics RESolution M-50) to vaporize material from each grain with a spot size of 17 µm. The ablated material was carried via a gaseous stream of helium (600 mL/minute), argon (740 mL/minute), and nitrogen (6 mL/minute) to a Thermo X Series II quadrupole ICP-MS where it was then analyzed for uranium, thorium and lead content. Ablation occurred in ultra-pure helium, with minimal mercury blanks. Additional elements were analyzed to confirm composition (zircon) and to qualitatively assess alteration or lead-contamination (mercury, bismuth, strontium) of each grain, but were not calibrated to determine their absolute concentration.

The uranium, thorium and lead data were calibrated using the 91500 zircon geostandard, which has an accepted age of 1065.3±0.3 Ma (Wiedenbeck et al. 1995). Quality control of the calibration was completed by analyzing other geostandard zircons: Plešovice with an accepted age of 337.13±0.37 Ma (Plešovice quarry zircon, Blanský les granulite body, Bohemian Massif, Czech Republic: Sláma et al. 2008) and Temora-2 with an accepted age of 416.75±0.24 Ma (Temora-2 zircon is from the Middledale gabbroic diorite, Temora, New South Wales, Australia: Black et al. 2003). Concordia diagrams for the standards were obtained and proved to be in agreement with the respective accepted ages (for calculation procedure, see Ludwig 1998) before the sample zircons were analyzed.

*Summary of Field Work and Other Activities 2012,
Ontario Geological Survey, Open File Report 6280, p.4-1 to 4-10.*

© Queen's Printer for Ontario, 2012

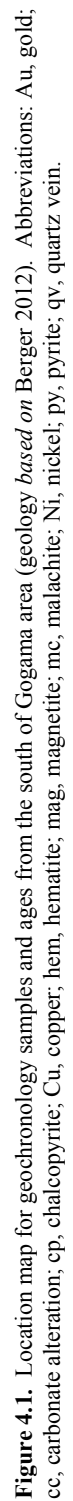


Table 4.1. Number of zircons and useful analyses for all samples in this study.

Sample	Zircons Picked	Useful Analyses
11-BRB-070	50	40
11-BRB-132	143	129
11-BRB-136	49	41

Each individual zircon analysis was inspected in terms of signal intensity as a function of time so as to distinguish distinct zones of different Th/U, $^{207}\text{Pb}/^{206}\text{Pb}$, ^{204}Pb , ^{88}Sr and/or ^{209}Bi . Zones of signal showing evidence for alteration (high ^{88}Sr) or Pb-contamination (high ^{204}Pb , ^{209}Bi , erratic $^{207}\text{Pb}/^{206}\text{Pb}$ ages) were not selected for integrations for final age determination of the zircon.

Uranium–lead concordia diagrams were constructed using Iolite (Paton et al. 2011) and VizualAge (Petrus and Kamber 2012) programs, and are included in the discussions below. Histograms were generated for analysis of detrital zircon populations. After treating the data as discussed above, the number of useful analyses for each sample may be less than the total number of zircons picked. Highly contaminated and altered zircons were excluded from the final concordia diagram and data tables because of unreliable age determinations. Concordia ages and data represent the least-altered and least-contaminated ablated zones of the zircons. The number of grains picked and useful analyses obtained for each sample is summarized in Table 4.1.

RESULTS

Sample 11-BRB-070 Biotite Granodiorite

Londonderry Township, 458216E 5264032N, NAD83, Zone 17

The pink, medium-grained, equigranular biotite granodiorite is the major phase of a felsic pluton that underlies the southeastern part of the map area (*see* Figures 4.1 and 4.2a). The sample was selected for geochronology to determine the age of felsic plutonism in this part of the map area, to test the potential correlation with the Chester intrusive complex, for which an age of 2741 ± 1 Ma was determined previously (Kontak 2012), and to constrain the age of the nearby greenstone belt.

The zircons picked from this sample were largely euhedral with well-formed crystal faces. Grains range from large elongated prisms to small, stubby and equant. Grains are clear to cloudy and are lightly coloured.

All data obtained from this sample produced a tight group of concordant ages with minor lead-loss moving data along a distinct concordia line toward the origin. When best analyses were isolated (concordant, stable signal, etc.), they provided a concordant age of 2695.7 ± 3.0 Ma and this is interpreted to represent the magmatic age of the sample (Figure 4.2b). There are potentially some inherited zircons at approximately 2720 Ma.

Geochemical analyses indicate that the granodiorite intrusion is remarkably homogenous with pronounced negative tantalum and niobium anomalies, elevated light rare earth and depleted heavy rare earth element abundances (Berger, this volume, Article 3). Geological mapping indicates that the granodiorite intruded the Chester intrusive complex (Groves Township portion) and may be part of the Ramsey–Algoma granitoid complex of the Abitibi Subprovince. The age from this sample is in agreement with a sample collected approximately 16 km to the southwest and reported at 2695 ± 12 Ma by Ayer et al. (2010). These ages have no comparable extrusive equivalents in the nearby greenstone belts, further suggesting the granodiorite pluton is part of the Ramsey–Algoma granitoid complex.

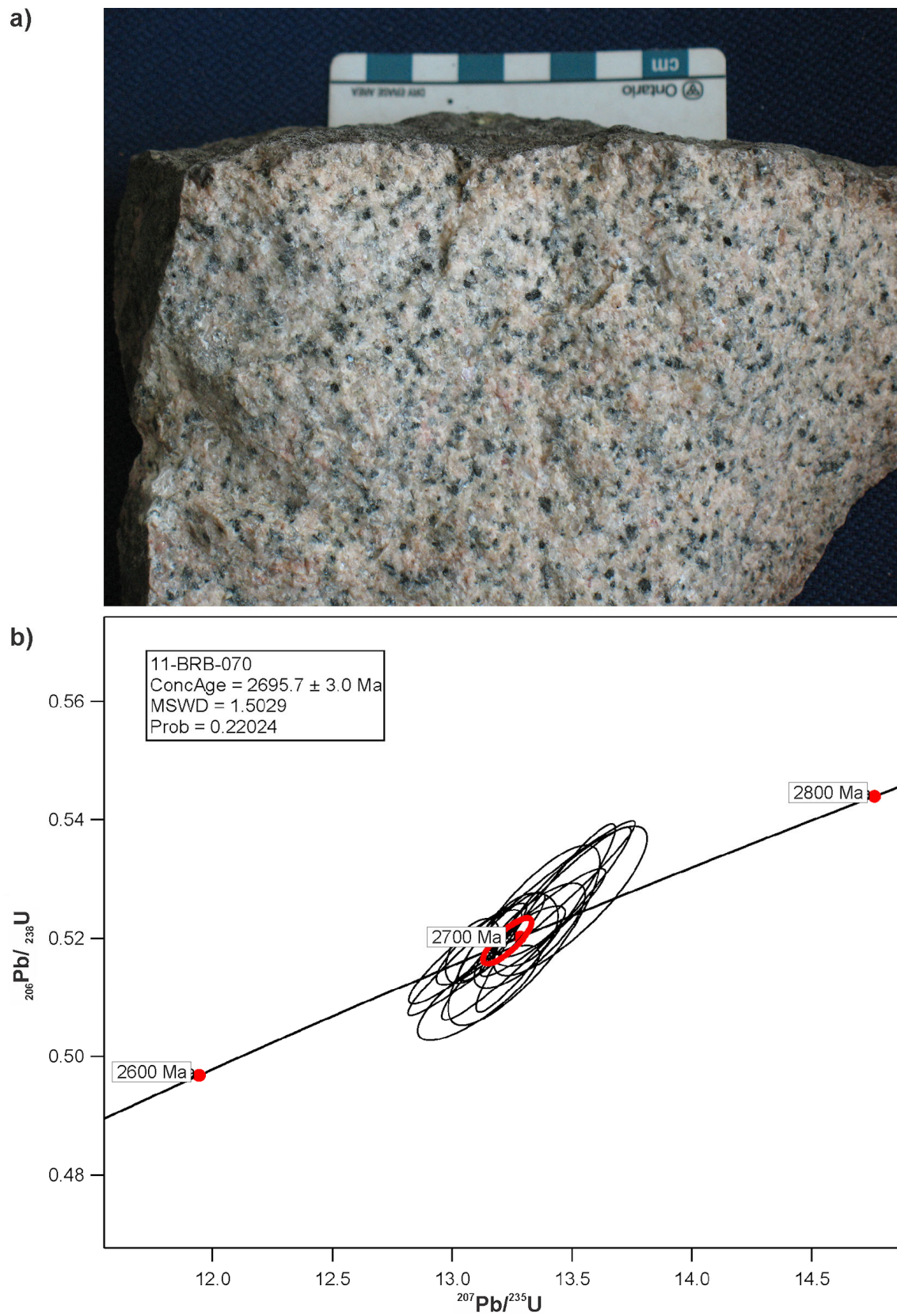


Figure 4.2. a) Photograph of sample 11-BRB-070 granodiorite; and b) concordia plot for concordant zircons.

Sample 11-BRB-136 Biotite Tonalite to Granodiorite

Brunswick Township, 460371E 5272417N, NAD83, Zone 17

The sample is a coarse-grained, equigranular biotite tonalite that appears to be contiguous with the granodiorite phase of the intrusion represented by sample 11-BRB-070 (*see* “Sample 11-BRB-070 Biotite Granodiorite”; *see* Figures 4.1 and 4.3a). The sampled tonalite crops out 100 m south of clastic metasedimentary rocks that have been correlated by the senior author with the Timiskaming assemblage and that physically resemble the cobbles in the nearby conglomerates. The tonalite was sampled to provide an absolute age for the felsic pluton, to provide correlation with other felsic plutons in the map area and to aid determination of the maximum age of sedimentation in the Timiskaming assemblage. Zircons in this sample were found to be largely euhedral with well-formed crystal faces. Most crystals are stubby to moderately prismatic, with a few that are elongated, needle-like crystals. They are typically weakly coloured and have moderate opacity.

Some zircon crystals in this sample had moderate lead-loss and lead-contamination as evidenced by the ages plotting away from concordia and being shifted toward the origin. Despite this, there was a very good grouping of concordant ages that produced an age of 2718.1 ± 3.5 Ma, which is interpreted to be the magmatic age of the sample (Figure 4.3b). There were no obvious inherited zircons.

This tonalite physically resembles the Chester intrusive complex tonalite, but is slightly coarser grained and visual separation of the 2 rock types is very difficult in the field. Geochemically, however, sample 11-BRB-136 is very similar to the granodiorite sampled above, which is very different than the Chester intrusive complex (*see* Berger, this volume, Article 3).

Sample 11-BRB-132 Sandstone Matrix to Conglomerate

Brunswick Township, 460155E 5273493N, NAD83, Zone 17

Clastic metasedimentary rocks correlated with the Timiskaming assemblage are composed mostly of conglomerate with lesser quartz-rich sandstone, arkose and rare mudstone-siltstone. Medium- and coarse-grained granitoid clasts are common and are characteristic of the Timiskaming assemblage throughout the Abitibi Subprovince (Legault and Hattori 1994; Mueller and Corcoran 1998). A sample of coarse sandstone matrix from a conglomerate unit was selected for geochronology to determine ages of detrital zircons in order to provide a maximum age for sedimentation in the Timiskaming assemblage in the south of Gogama area and to determine if nearby felsic plutons may have been potential sources for the numerous granitoid clasts in the conglomerate (Figure 4.4a).

Zircon grains in this sample were found to be largely euhedral with well-formed crystal faces. Despite being a sedimentary rock, the grains show minimal rounding of edges. Most grains are stubby to moderately prismatic with minor elongated needle-like prisms.

The detrital grains of this sample formed a broad range of ages between *circa* 2680 and 2765 Ma with the main peak at *circa* 2730 Ma (Figure 4.4b). There may be a second peak at *circa* 2695 Ma. The maximum age of the basin is interpreted to be 2680 Ma based on the youngest concordant zircons. The youngest single zircon analyzed is 2678 ± 8.7 Ma. It should be noted that the zircons were not thermally annealed or chemically abraded; therefore, the age of the youngest zircon must be interpreted with caution. All grains were polished prior to analysis and generally this material would have been ground away during polishing. However, it is possible that the ablated (analyzed) part of the zircon may be entirely or partially from a metamorphic rim formed after deposition of the conglomerate. This could potentially give an age that is younger than the original source rock of the zircon.

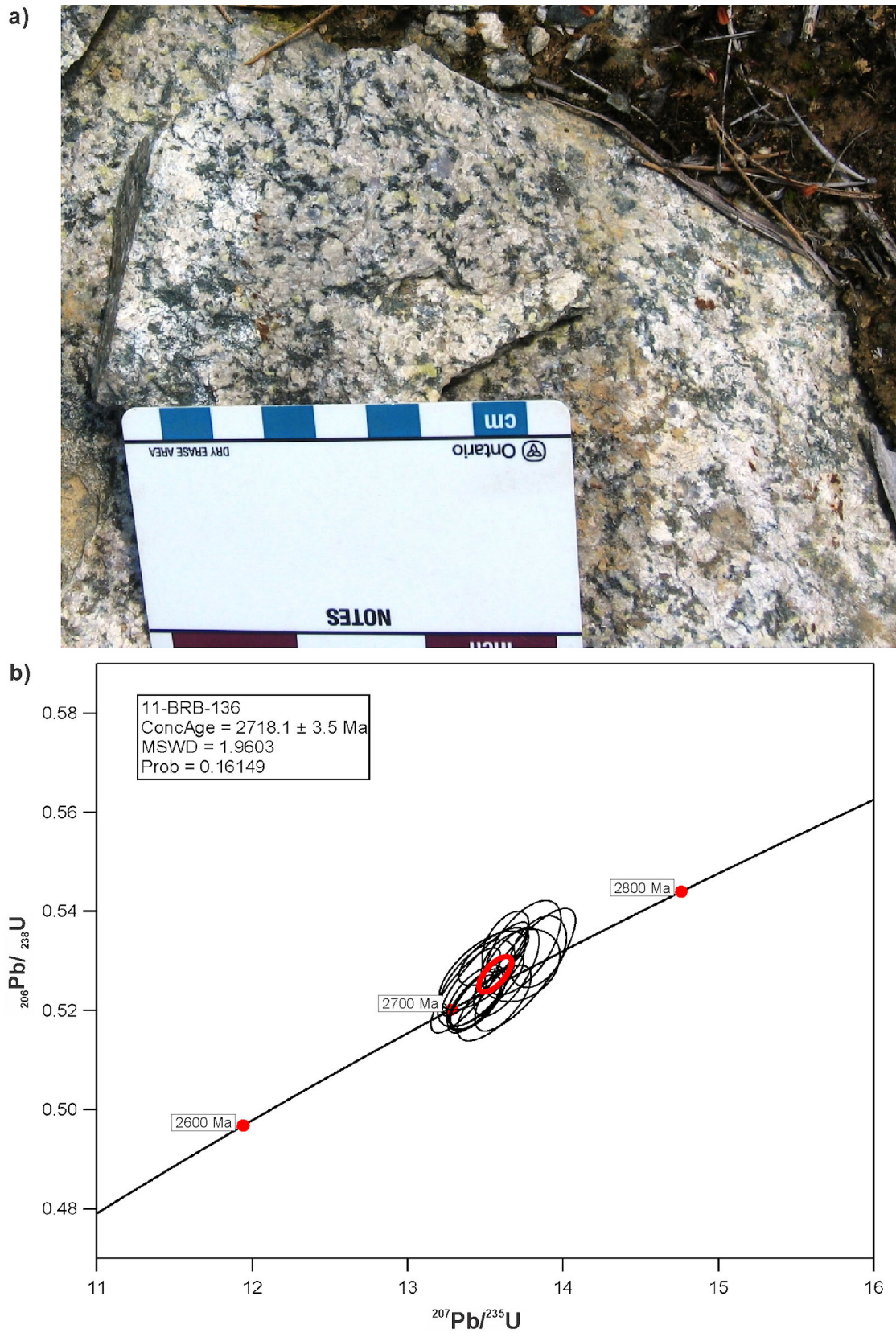


Figure 4.3. a) Photograph of sample 11-BRB-136 tonalite; and b) concordia plot for concordant zircons.

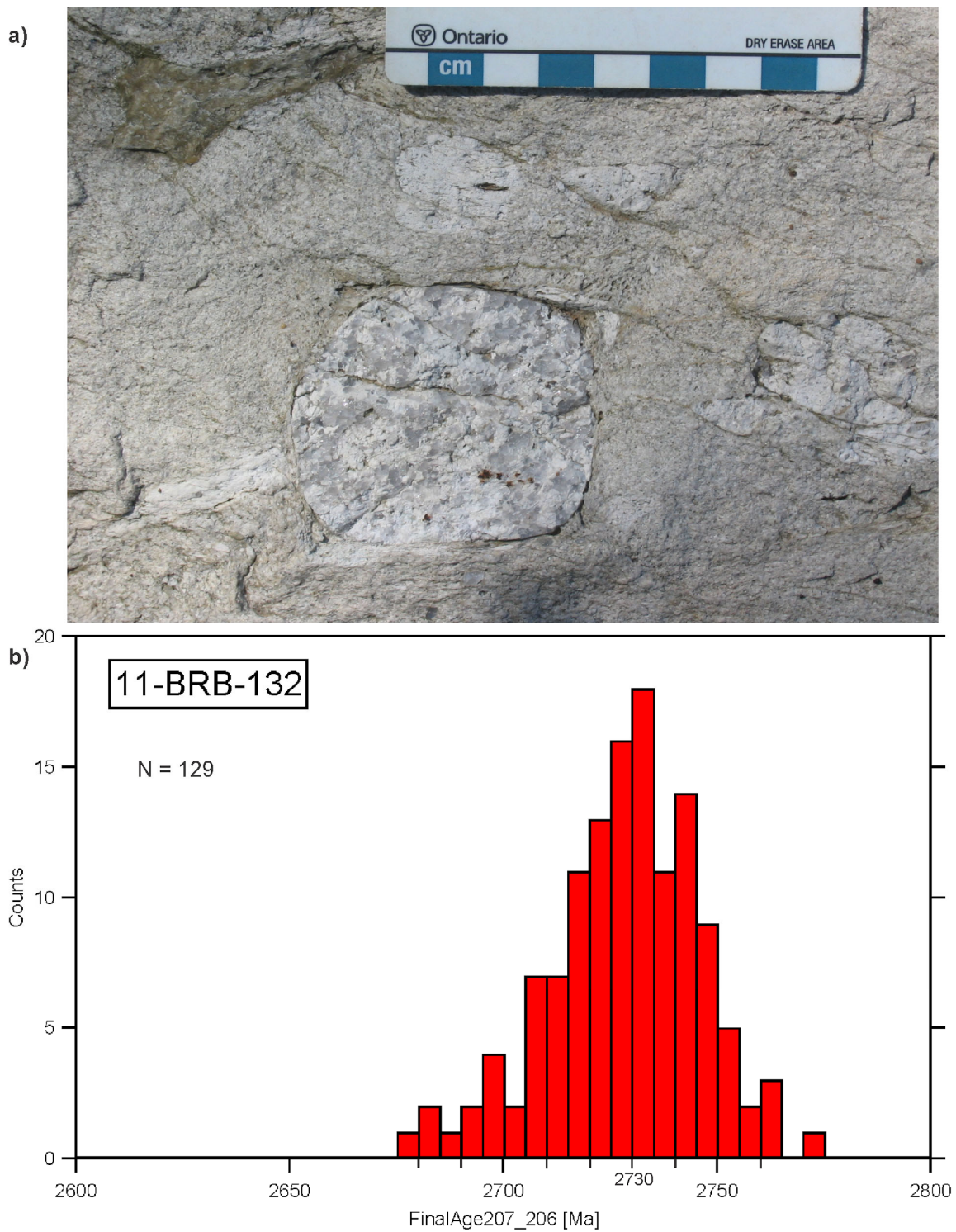


Figure 4.4. a) Photograph of sample 11-BRB-132 conglomerate-sandy matrix (note tonalite clasts) selected for geochronology; and b) histogram of ages for detrital zircons from sandy matrix.

INTERPRETATION

The biotite granodiorite (sample 11-BRB-070) with an age of 2695.7 ± 3 Ma and the coarse-grained tonalite (sample 11-BRB-136) adjacent to the supracrustal rocks in Brunswick Township with an age of 2718.1 ± 3.5 Ma are geochemically similar and appear to be gradational in the field. It is interpreted that the tonalite (sample 11-BRB-136) is an older phase of the same pluton that produced the granodiorite (sample 11-BRB-070) and that the inherited zircons in sample 11-BRB-070 were derived from this tonalite. This assumption further suggests that felsic magmatism in this part of the map area was protracted over approximately 20 million years and became progressively more potassic over this interval (tonalite to granodiorite). The granodiorite is of a similar age to gneissic tonalite south of the map area, which is correlated with the Ramsey–Algoma terrane (Ayer et al. 2010). The Ramsey–Algoma granodiorite intruded the Chester intrusive complex (Groves Township portion), and this field relationship combined with the geochemistry and geochronology serve to clearly define the limits of the 2 major intrusions. This is important for mineral exploration as the Chester intrusive complex is host to the Côté Lake gold deposit and is a prospective target for future gold discoveries wherever it occurs.

Detrital zircons indicate a maximum age for sedimentation of less than 2680 Ma for clastic metasedimentary rocks in the map area (sample 11-BRB-132). The majority of detrital zircons are older than 2730 Ma corresponding with the Pacaud assemblage metavolcanic rocks and the Chester intrusive complex (*see* Figure 4.4b; Kontak 2012; van Breemen, Heather and Ayer 2006). This indicates, as expected, a proximal source for most detritus in the Timiskaming assemblage. However, many detrital zircons are younger than 2730 Ma and their provenance may be volcanic and/or plutonic. The Kenogamissi batholith, located north of the supracrustal rocks, is composed of several plutons of appropriate age that could have provided detritus to the metasedimentary package. Clasts in conglomerate observed on the east shore of Mattagami Lake closely resemble Kenogamissi batholith granodiorite observed approximately 1.5 km to the northwest on the west shore of the lake. Late-stage north-side-up movement is apparent on the Ridout fault zone and it is reasonable to assume that the Kenogamissi batholith is a likely provenance for many of the younger zircons (Berger 2011; Beakhouse 2011). However, tonalite clasts in the metasedimentary rocks resemble the tonalite pluton, with an age of 2718.1 ± 3.5 Ma (sample 11-BRB-136), immediately south of the greenstone belt. Further, there is a small detrital population at 2695 Ma similar in age to the granodiorite in the south part of the map area. Detailed physical and geochemical analysis of the detrital zircons and zircons from the various plutonic phases is required to further constrain provenance.

The clastic metasedimentary rocks in the map area are on strike with similar rocks in the Swayze greenstone belt to the west and are contiguous with clastic metasedimentary rocks in the Shining Tree greenstone belt to the east. Heather (2001) mapped the Ridout Group of coarse clastic metasedimentary rocks intercalated with metavolcanic rocks in the Swayze greenstone belt west of the map area and determined from detrital zircon ages a maximum age of sedimentation at *circa* 2683 Ma. Ayer et al. (in press) determined from detrital and magmatic zircon ages that coarse clastic metasedimentary rocks intercalated with coeval metavolcanic rocks had a maximum age of sedimentation of 2680 Ma in the Shining Tree area immediately east of the map area. It is concluded that all of these metasedimentary rocks are coeval and formed a single more-or-less continuous depositional basin across the south part of the Abitibi Subprovince. The maximum age of sedimentation is similar to metasedimentary rocks in the Matachewan area, Midlothian Township and the main part of the Porcupine assemblage in the Timmins area, but are older than ages for the Timiskaming assemblage metasedimentary rocks at Kirkland Lake and Timmins (van Breemen, Heather and Ayer 2006; Ayer et al. 2010, 2003, 2002; Ayer and Trowell 2000).

Assignment of these metasedimentary rocks of the Ridout Group, Shining Tree greenstone belt and in the map area to a supracrustal assemblage is controversial. Jackson and Fyon (1991), Heather (2001), Ayer et al. (2002) and Berger (2011) correlated these rocks with the Timiskaming assemblage (2676 to

2670 Ma) based on the interpretation that conglomerates and associated sandstone were deposited in an alluvial–fluvial environment that rested unconformably on top of metavolcanic rocks. In parts of the Swayze greenstone belt, similar metasedimentary rocks also appear to have experienced less deformation than underlying metavolcanic rocks (Heather 2001). Ayer et al. (in press) correlated the Shining Tree metasedimentary rocks with the Porcupine assemblage (2690 to 2680 Ma) based mainly on the similarity of ages with intercalated shoshonitic metavolcanic rocks. However, the coarse clastic metasedimentary rocks are composed of conglomerate, commonly with tonalite and iron formation clasts, volcanoclastic sandstone and arenite that is rarely cross-bedded and is similar to conglomerate observed in the map area. An alluvial–fluvial depositional environment is interpreted for these metasedimentary rocks (Ayer et al., in press). Porcupine assemblage metasedimentary rocks are generally inferred to be deep-water turbidite-facies sediments elsewhere in the Abitibi greenstone belt (Ayer et al. 2002). Therefore, recognition of shallow-water facies sediments in the Porcupine assemblage has important implications for stratigraphic correlation, tectonic reconstruction of the Abitibi Subprovince and gold metallogenesis. For example, Porcupine assemblage conglomerates were previously interpreted as either submarine fan–channel fill (Ayer et al. 2002; Berger 1994) or fault-scarp deposits (Berger 1999, 2002) that contained only local provenance clasts. Such deposit types are distinctly different than alluvial–fluvial Timiskaming assemblage conglomerates that contain extra basinal granitoid clasts. If the conglomerates and associated metasedimentary rocks in the Shining Tree area are part of the Porcupine assemblage, then depositional facies and clast populations can no longer be used to distinguish between assemblages. Further, if shallow-water facies with extra basinal clasts (e.g., tonalite) are present in the Porcupine assemblage, then extensive continental hinterland was developed much earlier in the tectonic evolution of the Abitibi Subprovince than previously thought. There is a close spatial and temporal relationship between gold mineralization, Timiskaming sedimentation and alkalic magmatism. If the Porcupine and Timiskaming assemblages represent similar tectonic and depositional environments, then both should be equally prospective targets for gold mineralization. Alternatively, if the major gold mineralizing systems are associated with the younger and more alkaline tectonic environments, then mineral exploration should focus on these criteria rather than the depositional environments of the associated metasedimentary rocks.

REFERENCES

- Ayer, J., Amelin, Y., Corfu, F., Kamo, S., Ketchum, J., Kwok, K. and Trowell, N. 2002. Evolution of the southern Abitibi greenstone belt based on U-Pb geochronology: autochthonous volcanic construction followed by plutonism, regional deformation and sedimentation; *Precambrian Research*, v.115, p.63-95.
- Ayer, J.A., Chartrand, J.E., Trowell, N.F. and Wilson, A.C. 2010. Geological compilation of the Maple Mountain area, Abitibi greenstone belt; Ontario Geological Survey, Preliminary Map P.3620, scale 1:100 000.
- Ayer, J.A., Kontak, D.J., Linnen, R.L. and Lin, S. eds. in press. Results from the Shining Tree, Chester Township and Matachewan gold projects and the northern Cobalt embayment polymetallic vein project; Ontario Geological Survey, Miscellaneous Release—Data 294.
- Ayer, J.A. and Trowell, N.F. 2000. Geological compilation of the Kirkland Lake area, Abitibi greenstone belt; Ontario Geological Survey, Preliminary Map P.3425, scale 1:100 000.
- Ayer, J.A., Trowell, N.F., Josey, S., Nevills, M. and Valade, L. 2003. Geological compilation of the Matachewan area, Abitibi greenstone belt; Ontario Geological Survey, Preliminary Map P.3527, scale 1:100 000.
- Beakhouse, G.P. 2011. The Abitibi Subprovince plutonic record: tectonic and metallogenic implications; Ontario Geological Survey, Open File Report 6268, 155p.
- Berger, B.R. 1994. Geology of Matheson and Evelyn townships, District of Cochrane; Ontario Geological Survey, Open File Report 5900, 109p.

- . 1999. Geology of Murphy and Wark townships, District of Cochrane; Ontario Geological Survey, Open File Report 5994, 64p.
- . 2002. Geological synthesis of the Highway 101 area, east of Matheson, Ontario; Ontario Geological Survey, Open File Report 6091, 124p.
- . 2011. Geological investigations south of Gogama; *in* Summary of Field Work and Other Activities, 2011, Ontario Geological Survey, Open File Report 6270, p.3-1 to 3-5.
- . 2012. Precambrian geology, south of Gogama area; Ontario Geological Survey, Preliminary Map P.3762–Revised, scale 1:50 000.
- Black, L.P., Kamo, S.L., Allen, C.M., Aleinikoff, J.N., Davis, D.W., Korsch, R.J. and Foudoulis, C. 2003. TEMORA 1: a new zircon standard for Phanerozoic U-Pb geochronology; *Chemical Geology*, v.200, p.155-170.
- Heather, K.B. 2001. The geological evolution of the Archean Swayze greenstone belt, Superior Province, Canada; unpublished PhD thesis, Keele University, Keele, England, 370p.
- Jackson, S.L. and Fyon, J.A. 1991. The western Abitibi Subprovince in Ontario; *in* Geology of Ontario, Ontario Geological Survey, Special Volume 4, Part 1, p.405-482.
- Kontak, D.J. 2012. Is Canada's oldest Au deposit an Archean analogue for a porphyry system? The 2740 Ma Côte Lake Au-(Cu) deposit, northern Ontario; presentation, Laurentian University, Department of Earth Sciences, seminar, March 9, 2012.
- Legault, M.I. and Hattori, K. 1994. Provenance of igneous clasts in conglomerate of the Archaean Timiskaming Group, Kirkland Lake area, Abitibi greenstone belt, Canada; *Canadian Journal of Earth Sciences*, v.31, p.1749-1762.
- Ludwig, K.R. 1998. On the treatment of concordant uranium-lead ages; *Geochimica et Cosmochimica Acta*, v.62, p.665-676.
- Mueller, W.U. and Corcoran, P.L. 1998. Late orogenic basins in the Archaean Superior Province, Canada: characteristics and inferences; *Sedimentary Geology*, v.120, p.177-203.
- Paton, C., Hellstrom, J., Paul, B., Woodhead, J. and Hergt, J. 2011. Iolite: freeware for the visualization and processing of mass spectrometer data; *Journal of Analytical Atomic Spectrometry*, v.26, p.2508-2518.
- Petrus, J.A. and Kamber, B.S. 2012. VizualAge: a novel approach to laser ablation ICP-MS U-Pb geochronology data reduction; *Geostandards and Geoanalytical Research*, v.36, p.247-270, DOI: 10.1111/j.1751-1908X.2012.00158.x.
- Sláma, J., Košler, J., Condon, D.J., Crowley, J.L., Gerdes, A., Hanchar, J.M., Horstwood, M.S.A., Morris, G.A., Nasdala, L., Nöberg, N., Schaltegger, U., Schoene, B., Turbrett, M. and Whitehouse, M.J. 2008. Plešovice zircon - a new natural reference material for U-Pb and Hf isotopic microanalysis; *Chemical Geology*, v.249, p.1-35.
- van Breemen, O., Heather, K.B. and Ayer, J.A. 2006. U-Pb geochronology of the Neoarchean Swayze sector of the southern Abitibi greenstone belt; Geological Survey of Canada, Current Research 2006-F1, 32p.
- Wiedenbeck, M., Allé, P., Corfu, F., Griffen, W.L., Meier, M., Oberli, F., Von Quadt, A., Roddick, J.C. and Spiegel, W. 1995. Three natural zircon standards for U-Th-Pb, Lu-Hf, trace element and REE analyses; *Geostandards Newsletter*, v.19, p.1-23.

5. Project Unit 11-008. Geology and Mineral Potential of Price and Thorneloe Townships, Abitibi Greenstone Belt

S. Préfontaine¹

¹Earth Resources and Geoscience Mapping Section, Ontario Geological Survey

INTRODUCTION

In 2006, the Ontario Geological Survey (OGS) started a multiyear geological bedrock mapping project of the Bartlett Dome and Halliday Dome areas (Project Unit 06-002) as part of an ongoing project to update geological mapping in the Abitibi greenstone belt. The project was completed this summer with 1:20 000 scale mapping of the eastern part of Price Township as well as Nursey Township (Robichaud, this volume, Article 6). Reconnaissance in Midlothian, Doon, Beemer and Moher townships was carried out for geological verification purposes. The goals of this multiyear project are to 1) update the geological mapping in the Bartlett Dome and Halliday Dome areas as well as to complete the recent mapping; 2) clarify and characterize the major lithological units; 3) better understand the stratigraphy; and 4) evaluate the mineral potential of the area.

Thorneloe Township and the western part of Price Township were mapped at a scale of 1:20 000 this summer to complete geological mapping west of the Mattagami River fault and to complement mapping by Vaillancourt, Pickett and Dinel (2000) and Hall and Smith (2002).

GENERAL GEOLOGY

The Abitibi greenstone belt consists of a stratigraphically continuous succession of Archean metavolcanic and metasedimentary rocks that developed in an ensimatic tectonic setting (Ayer, Amelin et al. 2002). These rocks have been subdivided into 8 temporally constrained lithotectonic assemblages by Ayer, Amelin et al. (2002), Ayer et al. (1999a, 1999b) and Ayer, Ketchum and Trowell (2002). Six of these assemblages are dominantly volcanic: Pacaud, Deloro, Stoughton–Roquemaure, Kidd–Munro, Tisdale and Blake River; and 2 are dominantly sedimentary: Porcupine and Timiskaming. More recently, Thurston et al. (2008) have proposed some revision to the Abitibi-wide stratigraphy and reaffirmed the autochthonous development of the volcanic stratigraphy. They propose subdividing the Abitibi greenstone belt into 7 discrete volcanic episodes: pre-2750 Ma; 2750–2735 Ma (Pacaud); 2734–2724 Ma (Deloro); 2723–2720 Ma (Stoughton–Roquemaure); 2720–2710 Ma (Kidd–Munro); 2710–2704 Ma (Tisdale); and 2704–2695 Ma (Blake River), followed by 2 successor sedimentary basins, referred to as the Porcupine-type (2690–2682 Ma) and Timiskaming-type (2676–2670 Ma) basins. Significant depositional gaps marked by chemical sediments are found between and within many of the assemblages.

The Bartlett Dome (Figure 5.1) was mapped in previous years (Houlé 2006, 2007; Houlé and Solgadi 2007; Houlé, Baldwin and Thurston 2008; Houlé, Préfontaine and Brown 2008; Houlé, Solgadi and Préfontaine 2009; Préfontaine et al. 2009; Duguet et al. 2010). The Archean supracrustal rocks in the Bartlett Dome area are composed of a lower sequence of mafic and rare ultramafic metavolcanic rocks with rare felsic metavolcanic rocks correlated with the lower 2734–2724 Ma episode (Deloro); a middle sequence of intermediate to felsic metavolcanic rocks with regionally extensive metasedimentary units correlated with the upper 2734–2724 Ma episode (Deloro); and an upper sequence of mafic and ultramafic metavolcanic

*Summary of Field Work and Other Activities 2012,
Ontario Geological Survey, Open File Report 6280, p.5-1 to 5-14.*

rocks with lesser intermediate to felsic metavolcanic rocks and semi-continuous metasedimentary rocks correlated with the 2710–2704 Ma episode (Tisdale) (Houlé 2006, 2007; Houlé and Solgadi 2007; Houlé, Baldwin and Thurston 2008; Houlé, Préfontaine and Brown 2008; Houlé, Solgadi and Préfontaine 2009; Préfontaine et al. 2009; Duguet et al. 2010). The Bartlett Dome is considered to be the continuation of the Shaw Dome, which is a shallow-dipping anticline. The Shaw Dome comprises volcano-sedimentary strata that young outward from the centre of the anticline. The oldest to youngest strata comprise 1) coherent intermediate volcanic flows of the 2734–2724 Ma episode (Deloro) capped by 3 regionally extensive iron formation units; 2) felsic volcanoclastic rocks intercalated with komatiitic dikes, sills, lavas, and less extensive iron formations in the lower part of the 2710–2704 Ma episode (Tisdale); 3) intercalated tholeiitic mafic and komatiitic volcanic rocks in the middle part of the 2710–2704 Ma episode (Tisdale); and 4) calc-alkalic felsic to intermediate volcanic rocks in the upper part of the 2710–2704 Ma episode (Tisdale) (Vaillancourt, Pickett and Diné 2000; Hall, MacDonald and Diné 2003; Houlé, Hall and Tremblay 2004a, 2004b; Houlé and Guilmette 2005; Houlé and Hall 2006, 2007).

The stratigraphy changes west of the Mattagami River fault. The 2734–2724 Ma volcanic episode (Deloro) is represented by dominantly mafic metavolcanic rocks with minor intermediate to felsic metavolcanic rocks and chemical metasedimentary rocks. These are located at the western edge of the Kenogamissi batholith (Hall and Smith 2002). The northern and central rocks are interpreted to be part of the 2720–2710 Ma volcanic episode (Kidd–Munro). The northern section is dominated by a series of intermediate to felsic volcanoclastic rocks with minor coherent flows. The more central portion is dominated by mafic metavolcanic rocks with minor komatiitic rocks and metasedimentary rocks. Overlying the metavolcanic package are turbiditic metasedimentary rocks interpreted to be part of the 2690–2682 Ma Porcupine-type sedimentary basin.

The supracrustal rocks are intruded by large felsic intrusions (e.g., Adams pluton and the Kenogamissi batholith) and other smaller, ultramafic to felsic intrusions. Mafic Proterozoic dikes correlated with the Sudbury, Matachewan and Abitibi swarms intruded the Archean rocks.

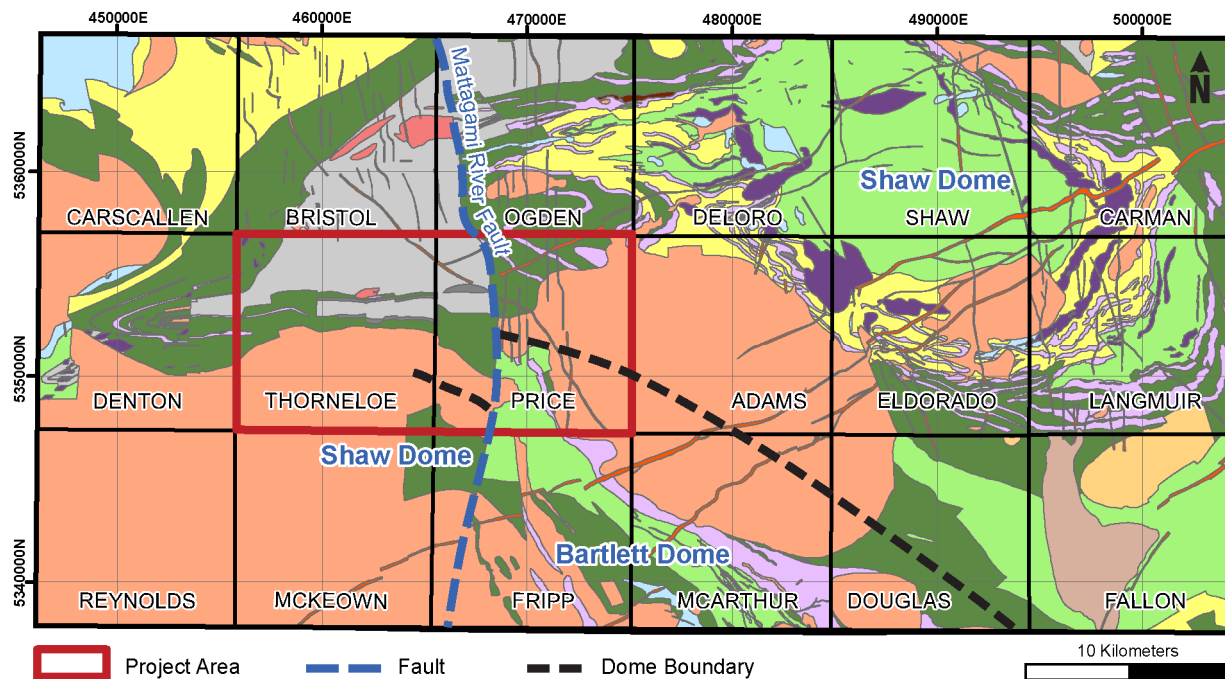


Figure 5.1. General location map of the Shaw and Bartlett domes and the west side of the Mattagami River fault area. The red outline indicates the area of bedrock mapping in 2012 in Price and Thorneloe townships. The black dashed line marks the approximate boundary between the Bartlett Dome and the Shaw Dome. Location information provided as Universal Transverse Mercator (UTM) co-ordinates using North American Datum 1983 (NAD83) in Zone 17 (*modified after Ayer and Chartrand 2011*).

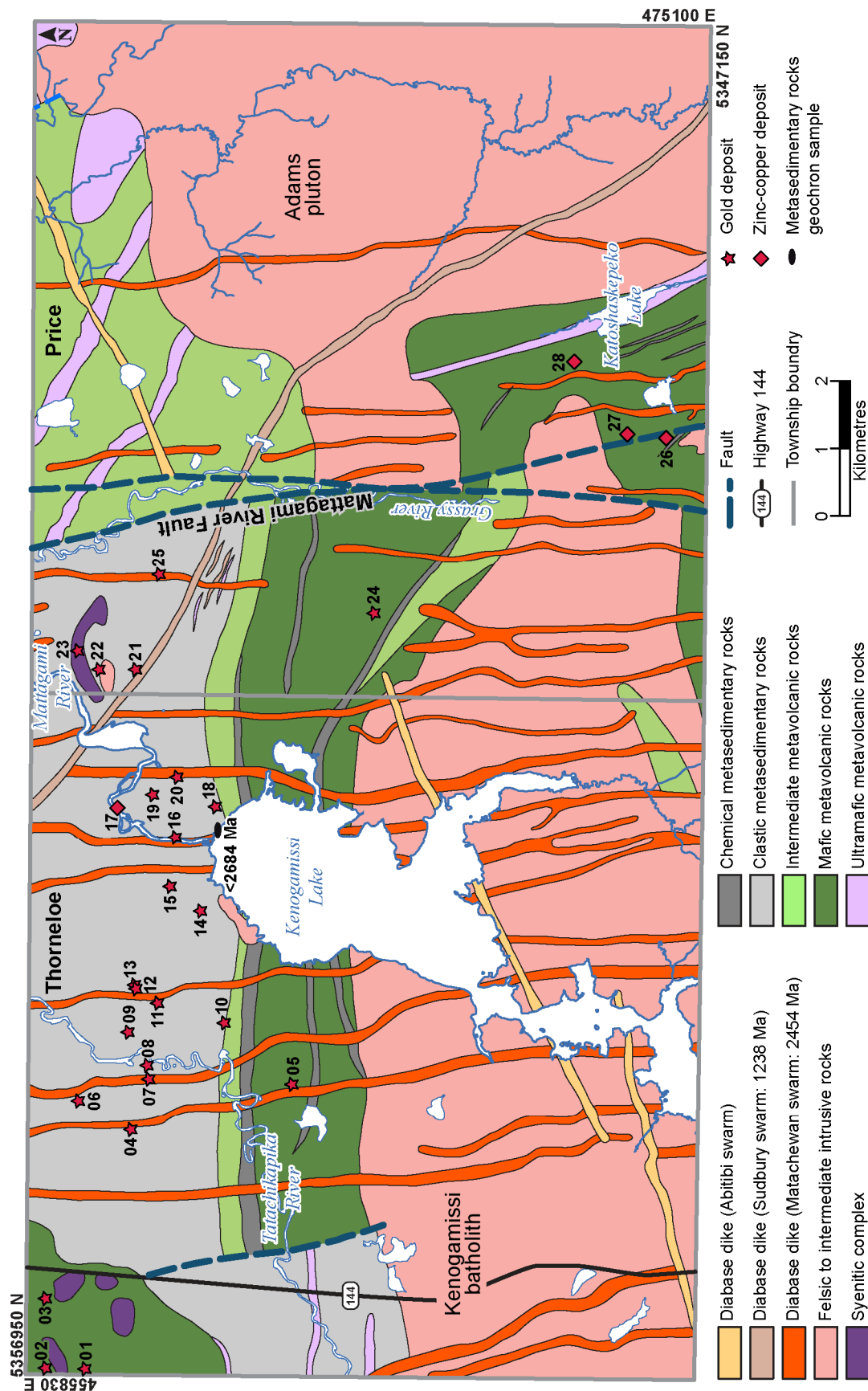


Figure 5.2. Simplified lithostructural map of Price and Thorneioe townships, south of Timmins, Abitibi greenstone belt. Numbers beside deposit symbols are keyed to properties listed in Table 5.1. Location information provided as UTM co-ordinates using NAD83 in Zone 17.

GEOLOGY OF PRICE AND THORNELOE TOWNSHIPS

Price and Thorneloe townships were previously mapped by Ferguson and Harding (1959a, 1959b), Choudhry (1982), and a map was compiled by Pyke (1982). Houlé and Hall (2006) did some reconnaissance mapping in the eastern part of Price Township. The geology in these 2 townships can be correlated with the Shaw Dome, the Bartlett Dome and geology west of the Mattagami River fault (*see* Figure 5.1).

Shaw Dome

The Shaw Dome rocks east of the Mattagami River fault are located in the northern portion of Price Township (*see* Figures 5.1 and 5.2). There are very few (5) outcrops exposed because extensive overburden covers most of this area and no drill holes are known to the author. Reliance on airborne geophysical data was necessary to interpret geology in this area (Ontario Geological Survey 2003a, 2003b, 2004, 2007). Mafic metavolcanic rocks with minor ultramafic rocks correlated with the 2710–2704 Ma volcanic episode (Tisdale) are interpreted to underlie this area (*see* Figure 5.2). West of the Mattagami River fault, the Shaw Dome rocks are located in the southern part of Price Township and extend into Thorneloe Township (*see* Figures 5.1 and 5.2); they are dominantly mafic metavolcanic rocks with one outcrop of intermediate metavolcanic rocks.

GEOLOGY

In the northeastern portion, both outcrops of mafic metavolcanic rocks are massive with some possible pillowed flows locally. Some feldspar-filled amygdules were observed as well as local gabbroic textures. Some ultramafic rocks occur within this dominantly mafic package of rock. The ultramafic rocks are generally massive to spinifex textured, with one area exposing variable size spinifex (Photo 5.1A) with a possible flow-top breccia suggesting that these are metavolcanic rocks. This would be consistent with the geology in Ogden Township interpreted by Houlé and Hall (2006).

In the southern area, the mafic to intermediate metavolcanic rocks are dominantly massive flows that are recrystallized and commonly display gneissic textures. They are generally moderately to locally strongly foliated (Photo 5.1B) and are often crosscut by intermediate to felsic dikes. One outcrop contained possible plagioclase-filled amygdules.

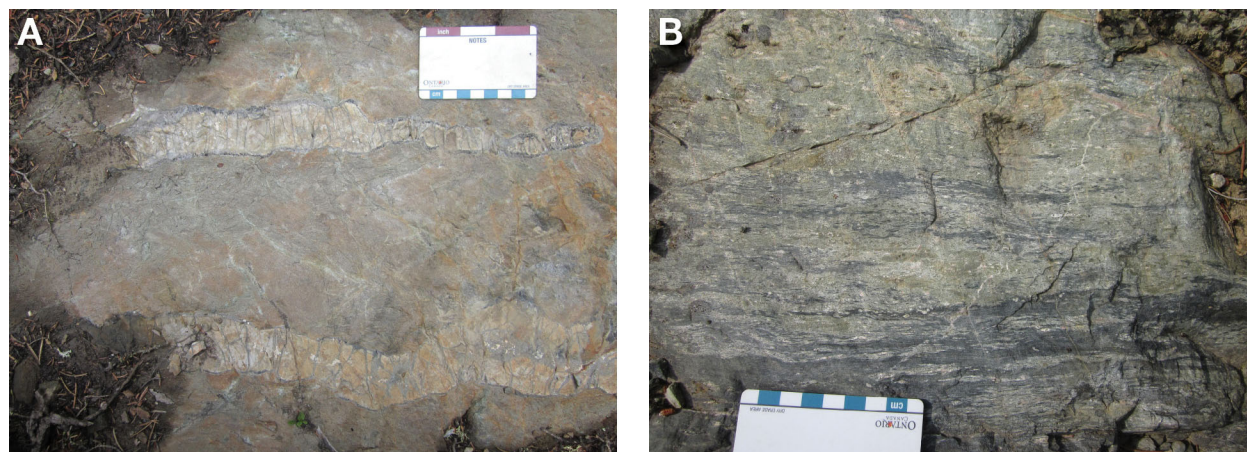


Photo 5.1. Typical lithologies found in the Shaw Dome area. A) Spinifex-textured ultramafic flow crosscut by plagioclase-phyric Matachewan diabase dike, located in the northeastern corner of Price Township (UTM 471510E 5355779N). B) Foliated metavolcanic rocks displaying epidote alteration typical of the alteration in the metavolcanic rocks at the boundary of the Kenogamissi batholith. Located in southern Price Township west of the Mattagami River fault (UTM 467478E 5347348N). UTM co-ordinates provided using NAD83 in Zone 17.

ALTERATION AND VEINING

In general, little alteration was observed in the northern area; however, one mafic metavolcanic outcrop displayed significant silicification exposed over at least 2 m. North of this outcrop (350 m), mafic metavolcanic rocks are crosscut by a 30 cm quartz-feldspar-sulphide vein and minor quartz veinlets along the foliation. In the southern area, epidote alteration occurs in veins and in patches especially near the contact with the Kenogamissi batholith (*see* Photo 5.1B).

STRUCTURE

A consistent northeast-striking foliation is observed within the 5 outcrops located in the northeast of Price Township. This foliation seems to be aligned with the contact between the Adams pluton and the supracrustal rocks. Similarly, there is a moderate to strong foliation that is aligned with the contact between the Kenogamissi batholith and the rocks of the Shaw Dome located in the south-central part of the map area. One outcrop in the southern portion displayed folding with an axial plane striking 287°, which is consistent with the regional folding pattern observed in Bartlett Township (Houlé, Solgadi and Préfontaine 2009).

METAMORPHISM

Observations made during the summer mapping suggest that the rocks located in the northern area are consistent with greenschist-facies metamorphism. Thompson (2005) identified actinolite and hornblende in mafic metavolcanic rocks and clinoamphibole in ultramafic rocks, suggesting that the rocks in this area are in the upper greenschist to transitional (to amphibolite) metamorphic facies. Based on this summer's mapping, the metamorphic grade of the southern portion of the Shaw Dome would be upper greenschist, transitional to amphibolite.

Bartlett Dome

The Bartlett Dome rocks are located southeast of the Mattagami River fault in Price Township (*see* Figure 5.1). In comparison to the northern part of Price Township, the southern part has more outcrops. Nevertheless, the interpretation of the geology of this area was aided by airborne geophysical data (Ontario Geological Survey 2003a, 2003b, 2004, 2007). The geology consists dominantly of mafic metavolcanic rocks with minor volcanoclastic rocks, clastic and chemical metasedimentary rocks as well as ultramafic metavolcanic rocks (*see* Figure 5.2).

GEOLOGY

The base of the stratigraphic succession in this area is composed of mafic metavolcanic rocks. These rocks are massive, recrystallized and locally display gabbroic texture. They are often intruded by intermediate to felsic intrusive rocks that become more prominent toward the Adams pluton and the Kenogamissi batholith and commonly occur in gneissic textured metavolcanic rocks. Intercalated with the mafic volcanic rocks are relatively thin and discontinuous units of intermediate volcanoclastic and clastic rocks with iron formation that vary from tuff, lapilli tuff and tuff breccia to argillite, siltstone and sandstone. These rocks are intercalated with oxide-facies iron formation composed of alternating magnetite-rich layers and chert layers ranging in thickness from 1 to 10 cm (Photo 5.2A). Chert-breccia was observed in one locality and all of the iron formation contains disseminated sulphide minerals commonly resulting in rusty zones. The volcano-sedimentary base of the Bartlett Dome is interpreted to be part of the 2734–2724 Ma volcanic episode (Deloro).

Overlying the 2734–2724 Ma volcanic episode (Deloro) are ultramafic and mafic metavolcanic rocks of the 2710–2704 Ma volcanic episode (Tisdale). Ultramafic rocks are mostly massive with local areas of spinifex (Photo 5.2B) and are interpreted to be the extension of the komatiitic sheet flows mapped in McArthur Township (Houlé 2006, 2007). Massive mafic metavolcanic rocks, observed in only one outcrop, overlie the ultramafic rocks.

ALTERATION AND VEINING

Epidote is the dominant alteration mineral and is found as either patches or veins in the mafic metavolcanic rocks and, locally, in the intermediate volcanoclastic and clastic metasedimentary rocks. The alteration is stronger near the contact between the supracrustal rocks and the Kenogamissi batholith than near the contact of the Adams pluton. Minor quartz and quartz-feldspar veins are observed throughout this section.

STRUCTURE

The stratigraphy of the Bartlett Dome trends north and youngs toward the east. Foliations broadly follow the contacts of the dominant intrusions (i.e., Kenogamissi batholith and Adams pluton) and 2 sets of lineations were observed. Southeast-plunging mineral lineations are dominant in the southern part of Price Township. The second lineation plunging northeast is dominantly found in the northern edge of the Bartlett Dome, although it was locally identified in the south. One outcrop demonstrated folding with an east-trending axial plane consistent with the regional folding pattern found in Bartlett Township (Houlé, Solgadi and Préfontaine 2009).

METAMORPHISM

Most of the rocks in this area are upper greenschist to lower amphibolite metamorphic facies as indicated by the presence of garnet and possibly cordierite in some of the intermediate volcanoclastic and clastic metasedimentary rocks. Thompson (2005) identified biotite and biotite-hornblende mineral assemblages in the meta-quartzofeldspathic rocks and actinolite-hornblende mineral assemblage in mafic metavolcanic rocks. These mineral assemblages are indicative of upper greenschist to transitional (to amphibolite) facies (Thompson 2005).

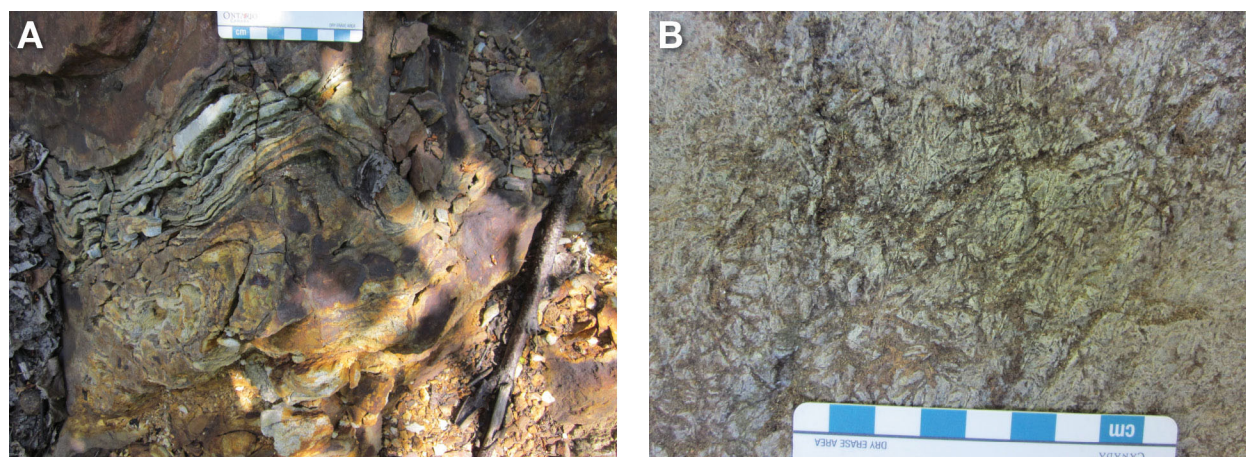


Photo 5.2. Typical lithologies found in the Bartlett Dome area. A) Folded oxide-facies iron formation with chert layers and sulphide mineralization. Located west of Katoshaskepeko Lake (UTM 470656E 5347973N). B) Spinifex-textured ultramafic flow similar to the spinifex-textured flow found in McArthur Township. Located on the shore of Katoshaskepeko Lake (UTM 470847E 5348363N). UTM co-ordinates provided using NAD83 in Zone 17.

West of the Mattagami River Fault

This package of rocks covers all of Thorneloe Township and the western part of Price Township, west of the Mattagami River fault. There is extensive Quaternary cover. Most of the outcrops are located in the southern area and are either diabase dikes or felsic to intermediate intrusive rocks of the Kenogamissi batholith. To aid the mapping of this section, core from 33 diamond-drill holes were re-logged and several drill logs were reinterpreted. Geophysical data are key to the interpretation of the units because of the lack of outcrop (Ontario Geological Survey 2003a, 2003b, 2004, 2007). More work is needed in this area to have a better understanding of the geology; thus, the descriptions and interpretations are preliminary.

The geology of this area is separated into an older volcanic episode and a younger sedimentary episode. Both the metavolcanic and metasedimentary rocks are interpreted to be folded with an east-trending axial plane (*see* Figure 5.1). Based on an age (2717.1 ± 2.6 Ma; Ayer and Chartrand 2011) obtained from a location in Bristol Township, the metavolcanic rocks are interpreted to belong to the 2720–2710 Ma volcanic episode (Kidd–Munro). These rocks are composed of mafic and intermediate metavolcanic rocks with minor chemical metasedimentary rocks and are located near the southern boundary of the Kenogamissi batholith as well as the most northwestern corner of Thorneloe Township (*see* Figure 5.2). Clastic metasedimentary rocks located in the northern part of the map area are correlated with the 2690–2682 Ma sedimentary episode (Porcupine) (*see* Figure 5.2).

GEOLOGY

There is little exposure and few diamond-drill holes located at the contact of the Kenogamissi batholith, where most of the rocks of the 2720–2710 Ma volcanic episode lie. The exposures of mafic metavolcanic rocks are dominantly massive, recrystallized and locally display gneissic textures. The more intermediate metavolcanic rocks have either pyroclastic or volcanoclastic tuff and tuff breccia. The metavolcanic rocks are moderately to locally strongly foliated and are crosscut by intermediate to felsic dikes of the Kenogamissi batholith. Intercalated with the metavolcanic rocks are chemical and clastic metasedimentary rocks. Two outcrops of oxide-facies iron formation were observed, composed of magnetite-rich layers, chert layers and clastic metasedimentary rock layers. The clastic metasedimentary rocks are intermediate to felsic siltstone and sandstone. One outcrop of ultramafic rocks, on either side of Highway 144, is interpreted to be an extension of the ultramafic metavolcanic unit mapped to the west by Hall and Smith (2002); however, no evidence of primary volcanic or intrusive textures was observed on the outcrop. The ultramafic rock is medium-grained, equigranular and crosscut by serpentine veins with generally little deformation, although, locally, small shears were observed. The northwestern part of Thorneloe Township is dominated by mafic metavolcanic rocks that are massive to pillowed displaying local amygdules; possible hyaloclastite was observed in diamond-drill core. These rocks are often crosscut by hematite-altered felsic intrusions.

The north-central part of the map area is interpreted to be underlain by clastic metasedimentary rocks of the 2690–2682 Ma sedimentary episode (Porcupine). Siltstone with lesser amounts of sandstone and mudstone and rare conglomerate were observed and are commonly laminated and interbedded. Beds in the siltstone and sandstone generally range in thickness from a few centimetres to several decimetres (Photo 5.3A). The sandstone varies in grain size from very fine grained to very coarse grained. The sandstone is commonly arenite with lithic clasts of mafic composition, dark mudstone and fuchsite-altered clasts. The mudstone is often graphitic and generally has beds of less than 10 cm in thickness. However, in the northeastern corner of Thorneloe Township, several diamond-drill holes contain hundreds of metres of graphitic mudstone. Very few conglomeratic rocks were observed. One type of conglomerate has a green fine-grained matrix with rounded clasts of much more felsic composition than the matrix (Photo 5.3B). This conglomerate was observed on the northern shore of Kenogamissi Lake and was also observed in 1 diamond-drill hole; an age of less than 2684 Ma was reported for this conglomerate by Ayer et al. (2005). The other

type of conglomerate is more suggestive of a debris flow. The matrix is a graphitic mudstone with clasts that are generally sedimentary in origin; however, exotic clasts such as feldspar porphyry were also observed.

Iron formation, mafic and ultramafic rocks were also observed in the north-central part of the map area. These units may be structurally emplaced in the Porcupine metasedimentary rocks; however, this is not clear in the observed diamond-drill core. The oxide-rich iron formation is generally thin (50 cm) and includes sulphide mineral-rich (pyrite and pyrrhotite) layers. It is intercalated with clastic and volcanoclastic rocks. Minor chert beds were observed. The mafic and ultramafic rocks are generally moderately to strongly deformed and are often banded or patchy with carbonate alteration (calcite and ankerite).

Intermediate to felsic porphyritic dikes intrude the metavolcanic and metasedimentary rocks of this area. The dikes contain quartz phenocrysts, feldspar phenocrysts or phenocrysts of both quartz and feldspar that are a few millimetres in size. These dikes are moderately altered (*see* “Alteration and Veining”). In addition to the porphyritic intrusions, a syenitic complex was also mapped (Photo 5.3C). It was observed in diamond-drill core from the northwestern corner of Thorneloe Township and interpreted from diamond-drill logs in the northwestern corner of Price Township. This unit varies in composition from ultramafic to felsic

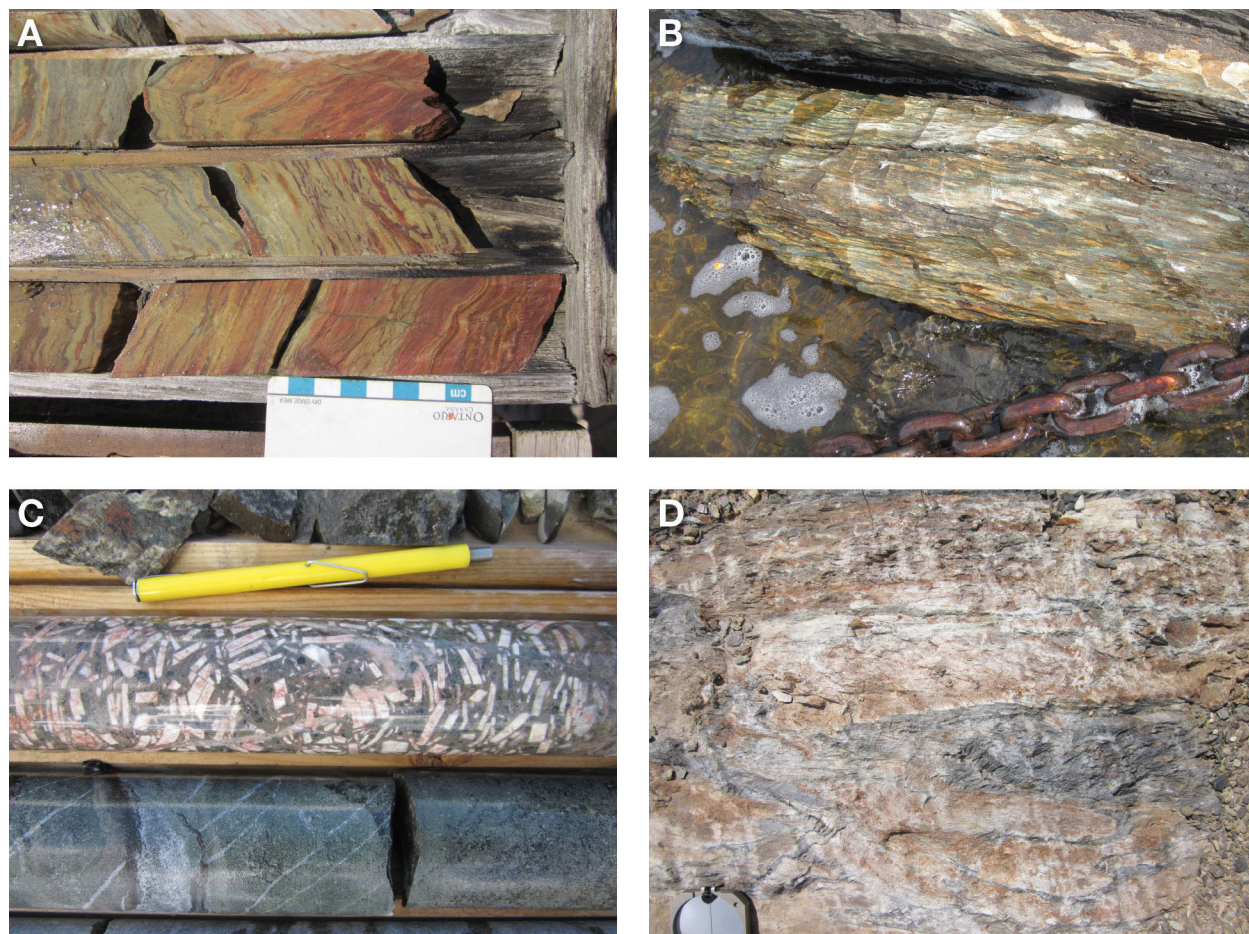


Photo 5.3. Typical lithologies found in the Thorneloe–Denton–Bristol–Carscallen townships area. A) Strongly altered with sericite (yellow) and hematite (red) metasedimentary rocks. Located north-central part of Thorneloe Township (collar UTM 460629E 5355338N). B) Strongly foliated mafic matrix conglomerate located on the north shore of Kenogamissi Lake (UTM 463592E 5354200N). C) Syenite complex displaying more felsic (top) potassium feldspar-rich and mafic (bottom) with dark layers of garnet. Located in the northwestern part of Thorneloe Township (collar UTM 457058E 5356206N). D) Strongly deformed metasedimentary rocks located north of Kenogamissi Lake displaying iron-carbonate alteration (UTM 462407E 5354511N). UTM co-ordinates provided using NAD83 in Zone 17.

with a great variation in potassium feldspar content (0 to 80%). Locally, the potassium feldspar is megacrystic up to 5 cm in length. Gradational contacts from ultramafic to felsic compositions were observed, but there is also a more felsic component crosscutting the more mafic component with sharp contacts observed. Locally, felsic patches are found in a mafic to ultramafic matrix. Biotite, garnet, apatite and titanite were either observed or mentioned in the diamond-drill logs indicating that this syenitic complex has an alkalic affinity. Several syenite to monzonite dikes with thicknesses of less than 1 m were observed crosscutting the metavolcanic and metasedimentary rocks. They are probably related to the syenite complex.

ALTERATION AND VEINING

Virtually every rock is altered west of the Mattagami River fault. Sericite is dominant and is present in all rocks with the possible exception of the graphitic mudstone and in the porphyritic intrusions. Alteration intensity varies greatly from weak to intense where no textures or bedding is preserved (*see* Photo 5.3A). Sericite is usually pervasive although, locally, it occurs in patches and some quartz-feldspar veins have a sericite halos. Chlorite alteration is found both in the metasedimentary and the metavolcanic rocks. The chlorite alteration intensity varies, but it was never observed to totally obliterate textures and bedding; unlike the sericite alteration, the chlorite alteration is generally pervasive but locally patchy. Hematite was observed to be pervasive as well as stratabound and is often associated with the syenite to monzonite dikes and intrusions. The hematite alteration is observed in the metavolcanic rocks, metasedimentary rocks and porphyritic intrusions and varies greatly in intensity (*see* Photo 5.3A). Locally, it can also be associated with sericite and magnetite. Iron carbonate was generally observed in veins, but, locally, the alteration was pervasive and varied in intensity. Epidote alteration is dominantly found in the mafic metavolcanic rocks either as veins or as patches. Silicification of metasedimentary rocks as well as porphyritic intrusions was observed; silicification is generally pervasive, but not very extensive. Wisps of fuchsite were observed in the metasedimentary rocks as well as in the porphyritic intrusions. Fuchsite seems to appear when the sericite alteration is strong to intense. Calcite was observed especially in the metavolcanic rocks located in the northwestern corner of Thornehoe Township; it is weakly pervasive and observed in veins.

Several compositions of veins were observed. The more prolific, but generally not very thick (a few centimetres), were quartz-feldspar veins. They often have a dark matrix where arsenopyrite was observed. Quartz and iron carbonate veins were observed crosscutting the metasedimentary rocks. Minor calcite, hematite, epidote and tourmaline were all identified during the mapping. Locally, white quartz veins, as thick as 1 m, were observed in the diamond-drill core.

STRUCTURE

Most of the rocks west of the Mattagami River fault display at least 2 foliations that are generally perpendicular to each other. The intensity of the foliation varies, locally weak but generally moderate to strong. Several areas were observed to have strong to intense foliation, often occurring when sericite alteration is intense, making the core very fissile. The Porcupine–Destor deformation zone (PDDZ) is interpreted to be located at the boundary of the metavolcanic rocks and the metasedimentary rocks, just north of Kenogamissi Lake. There were several shear zones observed in diamond-drill core located north in the metasedimentary rocks: it is possible that the PDDZ is located further north of Kenogamissi Lake or alternatively these shear zones are splays off of the main PDDZ.

Several S- and Z-symmetry folds and kinks were observed and several top reversals were also noted in diamond-drill core. Where folding was intense, the bedding was very chaotic in the core. In one metasedimentary rock outcrop, 3 foliations and 2 different folding events were measured (Photo 5.3D). It is interpreted that, regionally, the rocks are folded around east- to northeast-striking fold axes.

METAMORPHISM

Most of the area west of the Mattagami River fault is at the lower greenschist metamorphic facies. In the western part of Thorneloe Township, around the northwest-trending fault, were observed an actinolite-chlorite-epidote-albite mineral assemblage indicating either lower or upper greenschist facies, an actinolite-hornblende mineral assemblage indicating a transitional (to amphibole) facies and, finally, a hornblende-calcic plagioclase mineral assemblage indicating an amphibolite-facies metamorphism (Thompson 2005).

Intermediate to Felsic Intrusions

Two main felsic to intermediate intrusions were mapped: the Kenogamissi batholith and the Adams pluton. For a description and the petrogenesis of the Kenogamissi batholith and the Adams pluton, *see* Beakhouse (2011).

Proterozoic Intrusions

Proterozoic quartz gabbro and gabbro intrusions observed in the study area are correlated with the Matachewan, Sudbury and Abitibi dike swarms. The Matachewan dike swarm is the predominant swarm in the area and trends north to northwest. The Sudbury dikes define a northwest trend and are observed crosscutting the northeastern part of Price Township. Finally, the Abitibi dike swarm trends northeast. All of the dike swarms are moderately magnetic and typically show a distinct high aeromagnetic signature on airborne geophysical maps (Ontario Geological Survey 2003a, 2003b, 2004, 2007).

SUMMARY OF MINERAL DEPOSIT INVENTORY (MDI) SITES

Summarized in Table 5.1 are 28 Mineral Deposit Inventory (MDI) sites, 24 of which are related to gold mineralization (*see* Figure 5.2; *see* Table 5.1). In addition, the Timmins West gold mine is located in Bristol Township just north of Thorneloe Township. For more information on the Timmins West Mine, refer to a report by Crick et al. (2012). Similarly, the Lake Shore Gold Corp., Gold River property, which occupies most of the northern half of Thorneloe Township, is well described in a technical report by Samson, Kusins and Powers (2012).

Major gold deposits are believed to occur in fault splays associated with major fault structure or “breaks” such as the PDDZ (Colvine et al. 1988); however, Berger (2003) noted that some major gold deposits, such as the Holloway Mine and the Glimmer Mine, also occur within the main part of the PDDZ east of Timmins. In the map area, the PDDZ is interpreted to extend along the north edge of Kenogamissi Lake. The main type of gold mineralization at the Gold River property is associated with metavolcanic rocks that are interpreted to be structurally emplaced within metasedimentary rocks. The potential structural emplacement of metavolcanic rocks into the metasedimentary rocks and the location of the PDDZ suggest that the central part of Thorneloe Township is a prospective area for gold mineralization. The central part of Thorneloe Township has had little exploration, unlike the area to the north of Thorneloe Township, which has undergone extensive exploration. Even though there is no evidence for a major break or even splays in the northwest part of Thorneloe Township, the contact between the metavolcanic rocks and the metasedimentary rocks is a prospective area because of the possible structural contact between those 2 rock types.

Ultramafic rocks are interpreted to lie in the northeastern portion of Price Township; however, little exploration has been done in the northern part of Price Township. These ultramafic rocks are interpreted to be part of the Shaw Dome, which contains several nickel-copper-platinum group element (PGE) mines and occurrences.

Table 5.1. Main characteristics of the Mineral Deposit Inventory (MDI) sites in Thorne and Price townships.

Occurrence	Map ID*	Commodity	Best Historic Value	Hosted Units
Battle Mountain DDH MC-97-18 MDI42A05SE00054	1	Au	up to 1.70 g/t Au	Mafic metavolcanic rocks and porphyry
Highway 144 option / Syenite discovery / Lake Shore 144 zone / Lake Shore DDH HWY-11-12 MDI000000001321	2	Au	up to 16.75 g/t Au	Porphyritic syenite
Battle Mountain DDH MC97-20 / Mahoney Creek property MDI42A05NE00113	3	Au	up to 5.91 g/t Au	Mafic metavolcanic rocks and quartz veins
Golden River west zone / Thorne property / Thorne west zone / Band-Ore horizon / Gold River trend MDI42A05SE00065	4	Au	Measured resources of 690 000 t at 6.06 g/t Au	Both in quartz veins in metasedimentary rocks and in metasedimentary rocks
Keno zone / Thorne property / Band-Ore DDH GS-03-01 MDI42A05SE00071	5	Au	up to 0.5 g/t Au	Metasedimentary rock and porphyry
Red Porphyry zone / Thorne property / Golden River west zone MDI42A05SE00069	6	Au	Indicated resources of 93 000 t at 4.57 g/t Au	Both in porphyry and metasedimentary rocks
Sand Hill porphyry zone / Band-Ore DDH GW-04-11 / Golden River west zone MDI42A05SE00072	7	Au	Indicated resources of 93 000 t at 4.57 g/t Au	Both in porphyry and metasedimentary rocks
No. 14 zone / Thorne property / Band-Ore DDH GW-03-15 / Golden River west zone MDI42A05SE00068	8	Au	Indicated resources of 93 000 t at 4.57 g/t Au	Both in quartz veins in metasedimentary rocks and in metasedimentary rocks
Esso Kapika zone / Robele Joint Venture / Esso DDH T-36 / Gertie Gold Syndicate DDH7 / Golden River east zone MDI42A05SE00006	9	Au	Indicated resources of 597 000 t at 6.39g/t Au	Both in quartz carbonate vein in metasedimentary rocks and metasedimentary rocks
Thibeault horizon / Band-Ore DDH GS-03-10 MDI42A05SE00070	10	Au	up to 1.7 g/t Au	Metasedimentary rocks
Footwall fault zone / Thorne property / Lower Footwall fault zone / Golden River west MDI42A05SE00067	11	Au	Measured resources of 690 000 t at 6.06 g/t Au	Both in quartz veins in metasedimentary rocks and in metasedimentary rocks
South zone / Thorne property / Band-Ore horizon / South fault zone / Golden River east zone MDI42A05SE00066	12	Au	Indicated resources of 597 000 t at 6.39 g/t Au	Both in quartz carbonate vein in metasedimentary rocks and metasedimentary rocks
Golden River east zones / Thorne east zone / Band-Ore horizon / Band-Ore DDH TH96-12 / Thorne property / Gold River trend MDI42A05NE00121	13	Au	Measured resources of 690 000 t at 6.06 g/t Au	Both in quartz carbonate veins and quartz vein in sheared metasedimentary rocks
Joseph Thibeault property, Thibeault–Derby Group / Maryland Gold Mines property MDI42A05SE00029	14	Au	up to \$14.80 (avg: \$20.67 per troy ounces gold in 1923)	Sheared metasedimentary rocks
Falconbridge 617-3-86 / Constate option PN 617 / Derby claims / Thibeault–Derby Group / Maryland Porcupine property MDI42A05SE00010	15	Au	up to 2470 ppb Au	Quartz veins in intermediate volcaniclastic rocks or metasedimentary rocks
Black Pearl DH BKP-T8 MDI000000000447	16	Au	up to 0.176 oz/t Au	Quartz vein in metasedimentary rocks
Black Pearl DH BKP-T20 MDI000000000446	17	Cu	up to 1.4% Cu	Quartz carbonate hosted in metasedimentary rocks
Swanson occurrence / English–Swanson Group / Constate East Thorne and Price Group, Wawatin Group / Bonhomme sample 58314 MDI42A06SW00004	18	Au	up to 14.13 g/t Au	Both in quartz carbonate vein in sheared metasedimentary rocks and in the sheared metasedimentary rocks
Black Pearl DDH KKP-T6 MDI000000000444	19	Au	up to 0.96 oz/t Au	Metasedimentary rocks
Porcupine Joint Venture / DH CP04-03 MDI000000000442	20	Au	up to 2.92 g/t Au	Quartz vein hosted in metasedimentary rocks

Table 5.1, continued.

Occurrence	Map ID*	Commodity	Best Historic Value	Hosted Units
Kangas DDH MK-938 MDI42A06SW00033	21	Au	up to 2026 ppb Au	Intermediate volcanoclastic rock or metasedimentary rocks host
Lake Shore Gold DDH PR06-04 MDI000000001396	22	Au, As	up to 1.01 g/t Au and up to 1255 ppm As	Quartz vein in mafic metavolcanic rocks
Chevron DDH PO-88-2 / Croxall-Kangas option / Croxall DDH JC-941 / Temex DDH TC09-01 MDI42A06SW00009	23	Au	up to 2.88 g/t Au in the metasedimentary rocks, up to 5.28 g/t Au in the porphyry	Quartz carbonate hosted in both ankeritized and sheared metasedimentary rock and feldspar porphyry
Golddale MDI42A06SW00008	24	Au	up to 0.08 oz/t Au	Iron formation hosted with intermediate metavolcanic hanging wall and footwall
Porcupine JV CK03-02 / Kangas-Croxall property MDI42A06SW00035	25	Au	up to 0.55 g/t Au	Quartz carbonate vein hosted in ultramafic intrusive
Dwyer-Mousseau gold showing MDI42A06SW00034	26	Cu, Pb, Zn, (Au)	up to 3.86% Cu, up to 2.10% Pb, up to 7.84% Zn (up to 20.72 oz/t Au (location uncertain))	Brecciated quartz vein hosted in iron formation
Dwyer-Mousseau Copper / Samin Canada DDH P-83-1 / claim 39859 MDI42A06SW00025	27	Cu, Zn, Pb	up to 6.10% Cu, up to 1.12% Pb, up to 1.98% Zn	Both in mafic metavolcanic rocks and iron formation
F. Latimer property MDI000000001395	28	Zn, (Cu)	up to 1.10% Zn (up to 0.05% Cu)	Mafic to intermediate metavolcanic rocks

* refers to deposit number on Figure 5.2. **Source:** Mineral Deposit Inventory (MDI2) recently updated by A.C. Wilson, Mineral Deposit Compilation Geologist, Timmins, Ontario.

ACKNOWLEDGMENTS

This project has benefited from the assistance of Kyle Whitney and Nicholas Wray. The author is very thankful to Lake Shore Gold Corp. and their staff, in particular Jacques Samson and Keith Green. Without access to the drill core, this project would not have been possible. Patrick Gervais is thanked for drafting and finalizing figures for this report. The authors appreciate all the support from the staff of the Timmins Resident Geologist Office, especially Brian Atkinson and Ann Wilson for their help during the field season. Insightful discussions and comments from colleagues such as Ben Berger, Ontario Geological Survey, and Michel Houllé, Geological Survey of Canada, were greatly appreciated. Thanks are extended to Cindy, Ben and Roy of the Warne Logging and Sawmill; to Bruce and Jennifer from the Golden Eagle Camp; as well as to Russ and Linda from the Green Wilderness Lodge for their assistance during the field season.

REFERENCES

- Ayer, J., Amelin, Y., Corfu, F., Kamo, S., Ketchum, J., Kwok, K. and Trowell, N. 2002. Evolution of the southern Abitibi greenstone belt based on U-Pb geochronology: autochthonous volcanic construction followed by plutonism, regional deformation and sedimentation; *Precambrian Research*, v.115, p.63-95.
- Ayer, J.A. and Chartrand, J.E. 2011. Geological compilation of the Abitibi greenstone belt; Ontario Geological Survey, Miscellaneous Release—Data 282.
- Ayer, J.A., Ketchum, J.W.F. and Trowell, N.F. 2002. New geochronological and neodymium isotopic results from the Abitibi greenstone belt, with emphasis on the timing and the tectonic implications of Neoproterozoic sedimentation and volcanism; *in* Summary of Field Work and Other Activities 2002, Ontario Geological Survey, Open File Report 6100, p.5-1 to 5-16.

- Ayer, J.A., Thurston, P.C., Bateman, R., Dubé, B., Gibson, H.L., Hamilton, M.A., Hathway, B., Hocker, S.M., Houlé, M.G., Hudak, G., Ispolatov, V.O., Lafrance, B., Leshner, C.M., MacDonald, P.J., Péloquin, A.S., Piercey, S.J., Reed, L.E. and Thompson, P.H. 2005. Overview of results from the Greenstone Architecture Project: Discover Abitibi Initiative; Ontario Geological Survey, Open File Report 6154, 146p.
- Ayer, J.A., Trowell, N.F., Amelin, Y. and Corfu, F. 1999a. Geological compilation of the Abitibi greenstone belt in Ontario: toward a revised stratigraphy based on compilation and new geochronology results; *in* Summary of Field Work and Other Activities 1998, Ontario Geological Survey, Miscellaneous Paper 169, p.14-24.
- Ayer, J.A., Trowell, N.F., Madon, Z., Kamo, S., Kwok, Y.Y. and Amelin, Y. 1999b. Compilation of the Abitibi greenstone belt in the Timmins–Kirkland Lake area: revisions to stratigraphy and new geochronological results; *in* Summary of Field Work and Other Activities 1999, Ontario Geological Survey, Open File Report 6000, p.4-1 to 4-14.
- Beakhouse, G.P. 2011. The Abitibi Subprovince plutonic record: tectonic and metallogenic implications; Ontario Geological Survey, Open File Report 6268, 161p.
- Berger, B.R. 2003. Geological synthesis of the Highway 101 area, east of Matheson, Ontario; Ontario Geological Survey, Open File Report 6091, 124p.
- Choudhry, A.G. 1982. Precambrian geology of Thorneloe Township, Cochrane District; Ontario Geological Survey, Preliminary Map P.2502, scale 1:15 840.
- Colvine, A.C., Fyon, J.A., Heather, K.B., Marmont, S., Smith, P.M. and Troop, D.G. 1988. Archean Lode gold deposits in Ontario; Ontario Geological Survey, Miscellaneous Paper 139, 136p.
- Crick, D., Koch, R., Kusins, R., Powers, D. and Buss, B. 2012. 43-101 Technical report, prefeasibility study and mineral reserve estimate for Timmins West Mine, Timmins, Ontario, Canada, for Lake Shore Gold Corp., May 14, 2012; Technical Report under NI 43-101, filed May 18, 2012, with SEDAR[®], see [SEDAR Home Page](#), 613p.
- Duguet, M., Préfontaine, S., Brown, G.H., Houlé, M.G. and Cole, E. 2010. Precambrian geology of Semple Township; Ontario Geological Survey, Preliminary Map P.3618, scale 1:20 000.
- Ferguson, S.A. and Harding, W.D. 1959a. Price Township; Ontario Department of Mines, Preliminary Map P.30, scale 1:15 840.
- 1959b. Thorneloe Township; Ontario Department of Mines, Preliminary Map P.29, scale 1:15 840.
- Hall, L.A.F., MacDonald, C.A. and Dinel, E.R. 2003. Precambrian geology of Deloro Township; Ontario Geological Survey, Preliminary Map P.3528, scale 1: 20 000.
- Hall, L.A.F. and Smith, M.D. 2002. Precambrian geology of Denton and Carscallen townships, Timmins West area; Ontario Geological Survey, Open File Report 6093, 75p.
- Houlé, M.G. 2006. Geological and mineral potential of McArthur Township in the Bartlett Dome, Abitibi greenstone belt; *in* Summary of Field Work and Other Activities 2006, Ontario Geological Survey, Open File Report 6192, p.6-1 to 6-14.
- 2007. Precambrian geology of McArthur Township; Ontario Geological Survey, Preliminary Map P.3583, scale 1:20 000.
- Houlé, M.G., Baldwin, G. and Thurston, P.C. 2008. Day 3: Physical volcanology of the Bartlett dome; *in* Field trip guidebook to the stratigraphy and volcanology of supracrustal assemblages hosting base metal and gold mineralization in the Abitibi greenstone belt, Timmins, Ontario; Ontario Geological Survey, Open File Report 6225, p.59-73.
- Houlé, M.G. and Guilmette, C. 2005. Precambrian geology of Carman and Langmuir townships; Ontario Geological Survey, Preliminary Map P.3268, scale 1:20 000.

- Houlé, M.G. and Hall, L.A.F. 2006. Lithogeochemical data compilation for the Shaw Dome area: Shaw, Adams, Eldorado, Carman, Langmuir, Deloro and Price townships; Ontario Geological Survey, Miscellaneous Release—Data 211.
- 2007. Geological compilation of the Shaw Dome area, northeastern Ontario; Ontario Geological Survey, Preliminary Map P.3595, scale 1:50 000.
- Houlé, M.G., Hall, L.A.F. and Tremblay, E. 2004a. Precambrian geology of Eldorado and Adams townships; Ontario Geological Survey, Preliminary Map P.3542, scale 1:20 000.
- 2004b. Precambrian geology of Shaw Township; Ontario Geological Survey, Preliminary Map P.3541, scale 1:20 000.
- Houlé, M.G., Préfontaine, S. and Brown, G.H. 2008. Geology and mineral potential of English and Zavitz townships in the Bartlett dome, Abitibi greenstone belt; *in* Summary of Field Work and Other Activities 2008, Ontario Geological Survey, Open File Report 6225, p.10-1 to 10-17.
- Houlé, M.G. and Solgadi, F. 2007. Geological and mineral potential of Bartlett and Geikie townships in the Bartlett dome, Abitibi greenstone belt; *in* Summary of Field Work and Other Activities 2007, Ontario Geological Survey, Open File Report 6213, p.7-1 to 7-15.
- Houlé, M.G., Solgadi, F. and Préfontaine, S. 2009. Precambrian geology of Bartlett and Geikie townships; Ontario Geological Survey, Preliminary Map P.3612, scale 1:20 000.
- Ontario Geological Survey 2003a. Ontario airborne geophysical surveys, magnetic and electromagnetic data, grid and profile data, Geosoft® format, Timmins area; Ontario Geological Survey, Geophysical Data Set 1004.
- 2003b. Single master gravity and aeromagnetic data for Ontario, Geosoft® format; Ontario Geological Survey, Geophysical Data Set 1036.
- 2004. Ontario airborne geophysical surveys, magnetic and electromagnetic data, grid and profile data, Geosoft® format and vector data, Shaw Dome area (Discover Abitibi: PU02-047); Ontario Geological Survey, Geophysical Data Set 1046.
- 2007. Ontario airborne geophysical surveys, magnetic and electromagnetic data, grid and profile data, ASCII and Geosoft® formats and vector data, Bartlett Dome area MEGATEM® II; Ontario Geological Survey, Geophysical Data Set 1057.
- Préfontaine, S., Duguet, M., Cole, E.M. and Brown, G.H. 2009. Geology, mineral potential and preliminary geological interpretation of the Bartlett and Halliday domes, Abitibi greenstone belt, *in* Semple and Hutt townships, Ontario; *in* Summary of Field Work and Other Activities 2009, Ontario Geological Survey, Open File Report 6240, p.5-1 to 5-17.
- Pyke, D.R. 1982. Geology of the Timmins area, District of Cochrane; Ontario Geological Survey, Report 219, 141p., accompanied by Map 2455, scale 1:50 000.
- Samson, J., Kusins, R. and Powers, D. 2012. Technical report on the update of mineral resource estimate of the Gold River property, Thorneloe Township, Timmins, Ontario, Canada, for Lake Shore Gold Corp. and West Timmins Mining Inc., April 5, 2012; Technical Report under NI 43-101, filed April 5, 2012, with SEDAR®, see [SEDAR Home Page](#), 289p.
- Thompson, P.H. 2005. A new metamorphic framework for gold exploration in the Timmins–Kirkland Lake area, western Abitibi greenstone belt: Discover Abitibi Initiative; Ontario Geological Survey, Open File Report 6162, 104p.
- Thurston, P.C., Ayer, J.A., Goutier, J. and Hamilton, M.A. 2008. Depositional gaps in Abitibi greenstone belt stratigraphy: a key to exploration for syngenetic mineralization; *Economic Geology*, v.103, p.1097-1134.
- Vaillancourt, C., Pickett, C.L. and Dinel, E. 2000. Precambrian geology, Timmins West – Bristol and Ogden townships; Ontario Geological Survey, Preliminary Map P.3436, scale 1:20 000.

6. Project Unit 06-002. Geology and Mineral Potential of Nursey Township, Abitibi Greenstone Belt

L. Robichaud¹

¹Earth Resources and Geoscience Mapping Section, Ontario Geological Survey

INTRODUCTION

The mapping carried out in Nursey Township is part of a multiyear bedrock mapping project that began in 2006 with the objective of updating the geological knowledge of the Bartlett and Halliday domes in the southern part of the Timmins mining camp. During the summer of 2012, mapping, at a scale of 1:20 000, focussed on Nursey Township (Figure 6.1). The objectives of this project are to 1) perform the geological mapping in Nursey Township, which has not previously been mapped at this scale; 2) characterize the major lithological units and stratigraphy; and 3) evaluate the mineral potential of the area.

GENERAL GEOLOGY

The Abitibi greenstone belt consists of stratigraphically continuous successions of Archean metavolcanic and metasedimentary rocks (Ayer et al. 2002). Thurston et al. (2008) proposed a revised nomenclature of the Abitibi greenstone belt subdividing it into 7 discrete volcanic episodes: pre-2750 Ma, 2750–2735 Ma (Pacaud), 2734–2724 Ma (Deloro), 2723–2720 Ma (Stoughton–Roquemaure), 2720–2710 Ma (Kidd–Munro), 2710–2704 Ma (Tisdale) and 2704–2695 Ma (Blake River). These episodes are followed by the emplacement of 2 sedimentary basins: 2690–2685 Ma (Porcupine-type) and 2676–2670 Ma (Timiskaming-type). Depositional gaps marked by chemical sedimentary rocks break up the succession within many of the assemblages.

The Bartlett Dome (*see* Figure 6.1) was mapped in previous years (Houlé 2006, 2007; Houlé and Solgadi 2007; Houlé, Baldwin and Thurston 2008; Houlé, Préfontaine and Brown 2008; Houlé, Solgadi and Préfontaine 2009; Préfontaine et al. 2009; Duguet et al. 2010). Préfontaine (this volume, Article 5) mapped the eastern half of Price Township in order to complete mapping in the Bartlett Dome. The Bartlett Dome is subdivided into 3 sequences: a lower sequence consisting predominantly of mafic and ultramafic metavolcanic rocks with intermittent felsic metavolcanic rocks (2734–2724 Ma volcanic episode (Deloro)); a middle sequence of intermediate to felsic metavolcanic rocks with widespread metasedimentary units (2734–2724 Ma volcanic episode (Deloro)); and an upper sequence of mafic and ultramafic metavolcanic rocks with minor intermediate to felsic metavolcanic rocks and metasedimentary rocks (2710–2704 volcanic episode (Tisdale)) (Houlé 2006, 2007; Houlé and Solgadi 2007; Houlé, Baldwin and Thurston 2008; Houlé, Préfontaine and Brown 2008; Houlé, Solgadi and Préfontaine 2009; Préfontaine et al. 2009; Duguet et al. 2010).

The Halliday Dome (*see* Figure 6.1) was partially mapped in previous years (Préfontaine et al. 2009; Duguet et al. 2010; Préfontaine and Magnus 2010, 2012; Préfontaine 2011). The westernmost part of the Halliday Dome is interpreted to extend into Nursey Township, and was mapped this year (area outlined in red on Figure 6.1). The Halliday Dome predominantly consists of felsic to intermediate metavolcanic rocks with minor metasedimentary rocks (2710–2704 volcanic episode (Tisdale)). These are overlain by

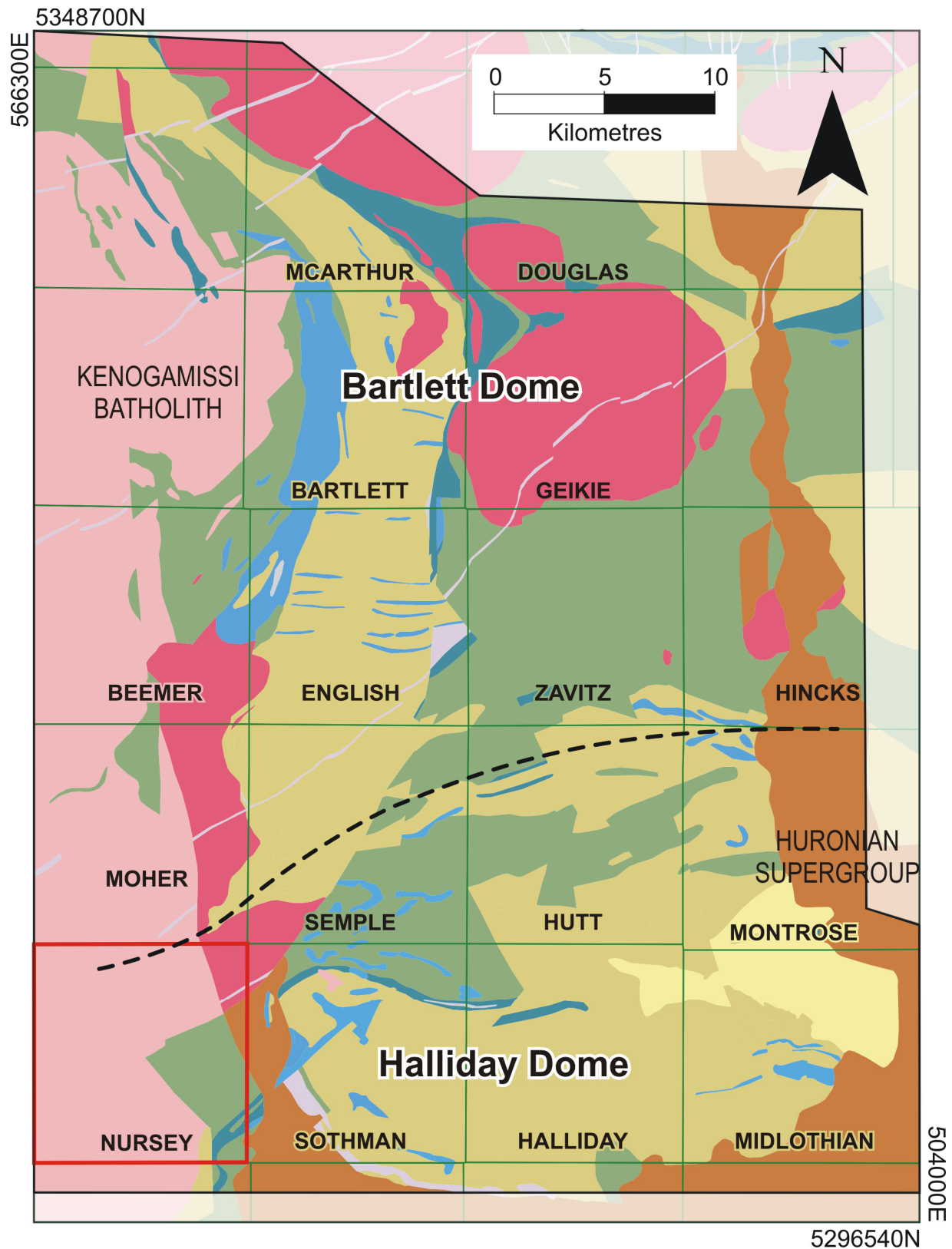


Figure 6.1. General location map of the eastern part of the Kenogamissi batholith. Nursey Township (lower left) is outlined in red. The black dashed line marks the approximate location of the boundary separating the Bartlett and Halliday domes. Universal Transverse Mercator (UTM) co-ordinates are provided in Zone 17 using North American Datum 1983 (NAD83).

metasedimentary and ultramafic rocks (2676–2670 Ma sedimentary basin (Timiskaming) or 2690–2685 Ma sedimentary basin (Porcupine)) (Préfontaine et al. 2009; Duguet et al. 2010; Préfontaine and Magnus 2010, 2012; Préfontaine 2011).

The supracrustal rocks in the Bartlett and Halliday domes are intruded by large felsic to intermediate intrusions (e.g., Adams pluton, Geikie pluton and the Kenogamissi batholith) as well as other smaller, felsic to ultramafic intrusions. Proterozoic dikes of the Sudbury, Biscotasing, Nipissing and Matachewan swarms also intruded the supracrustal rocks. The Bartlett and Halliday domes are delimited by the Kenogamissi batholith to the west and by the Shaw Dome to the north, and are unconformably overlain by Proterozoic Huronian Supergroup metasedimentary rocks to the east and south (Gowganda Formation) (see Figure 6.1). Stratigraphy from the Halliday Dome is deemed to be a continuation of the Bartlett Dome.

GEOLOGY OF NURSEY TOWNSHIP

The geology of Nursey Township (Figure 6.2) has not been mapped previously at the 1:20 000 scale; however, limited work of small-scale mapping and compilation mapping has been performed (Mullen 1983; Hrabi 1993; Rogers 1995). The Kenogamissi batholith underlies the western and northern portions of the map area; mafic and ultramafic metavolcanic flows underlie the southeastern section of the map area. Archean rocks are unconformably overlain by Huronian Supergroup metasedimentary rocks east of Sinclair Lake. Supracrustal rocks are also intruded by Proterozoic gabbroic dikes and intrusions.

Quaternary coverage in Nursey Township is extensive and considerably limits exposure. There is a denser concentration of outcrops in the centre of the field area, and some areas have little to no exposure. A Quaternary map (Alcock and Miller 2001) was used to determine which areas to target for mapping and the interpretation of the map was aided by aeromagnetic geophysical data (Ontario Geological Survey 2003).

Ultramafic Metavolcanic Rocks

The ultramafic metavolcanic rocks located in the southeastern and northeastern part of Nursey Township (see Figure 6.2) are dominated by massive flows that are dark grey to blackish green on the fresh surface and brownish when weathered. Rare spinifex texture can also be observed in the southern ultramafic metavolcanic rocks. The ultramafic metavolcanic rocks are typically altered with calcite and sporadic magnesite and green mica (Photo 6.1A). In the northeastern portion of the map, metasedimentary rocks are exposed within the ultramafic metavolcanic flows. This unit consists of a matrix-supported conglomerate interbedded with argillite layers. Clasts sizes vary from a few centimetres to 20 cm and are subrounded to well rounded.

Brecciated ultramafic flows are common on the shoreline of Sinclair Lake and in the northeastern part of the township. The angular to subrounded fragments in these brecciated flows vary in size from a few centimetres to several decimetres. The matrix is beige to white and consists of calcite. These flows are unreliable in providing stratigraphic facing direction. This stratigraphic unit can be traced in outcrops into Sothman and Halliday townships to the east and reinforces the interpretation that the supracrustal rocks in Nursey Township are part of the Halliday Dome.

Mafic Metavolcanic Rocks

Mafic metavolcanic rocks dominate the central part of Nursey Township, with smaller units occurring in the southeast and northeast of the map area (see Figure 6.2). The mafic metavolcanic flows are mostly massive (Photo 6.1B), with pillowed flows exposed in one outcrop located on the southern boundary of the map area. Pillow tops in this outcrop indicate stratigraphic facing to the west at 285°. The mafic metavolcanic flows are typically well foliated and chloritized with minor hematite or epidote.

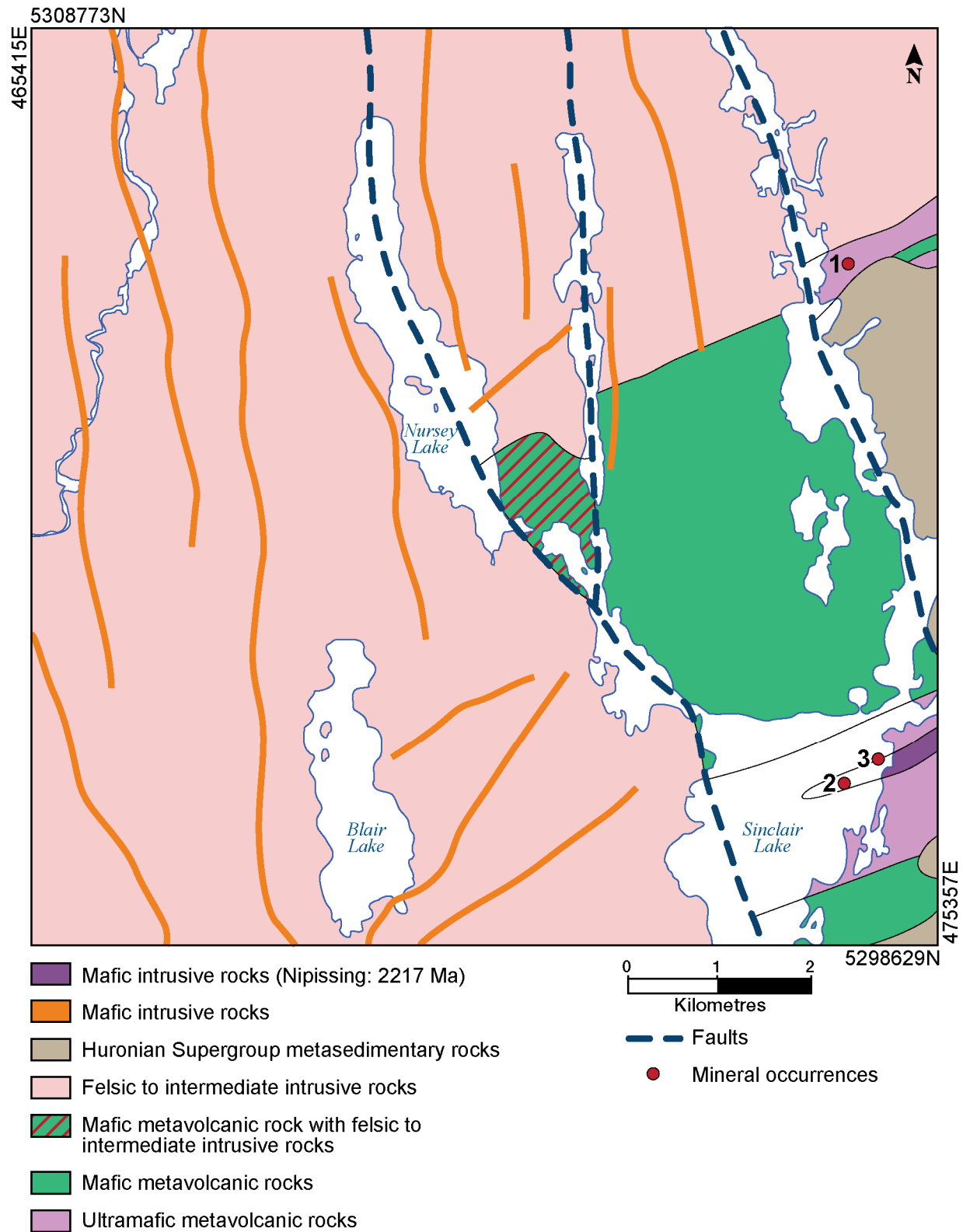


Figure 6.2. Simplified lithological map of Nursey Township. Numbers beside mineral occurrence points are related to properties listed in Table 6.1. UTM co-ordinates are provided in Zone 17 using NAD83.

The mafic metavolcanic rocks interlayered with felsic to intermediate intrusive rocks (*see* hatched area in Figure 6.2) are generally amphibolitized and have a strong foliation, sometimes exhibiting a gneissic texture (Photo 6.1C). Alternating layers of granitic material and mafic metavolcanic rocks form the gneissic texture, varying in proportion and thickness. Increased hematite and epidote alteration as well as foliated quartz veins are often observed proximal to the contact. Felsic to intermediate dikes crosscut this area, becoming more prominent nearer the Kenogamissi batholith.

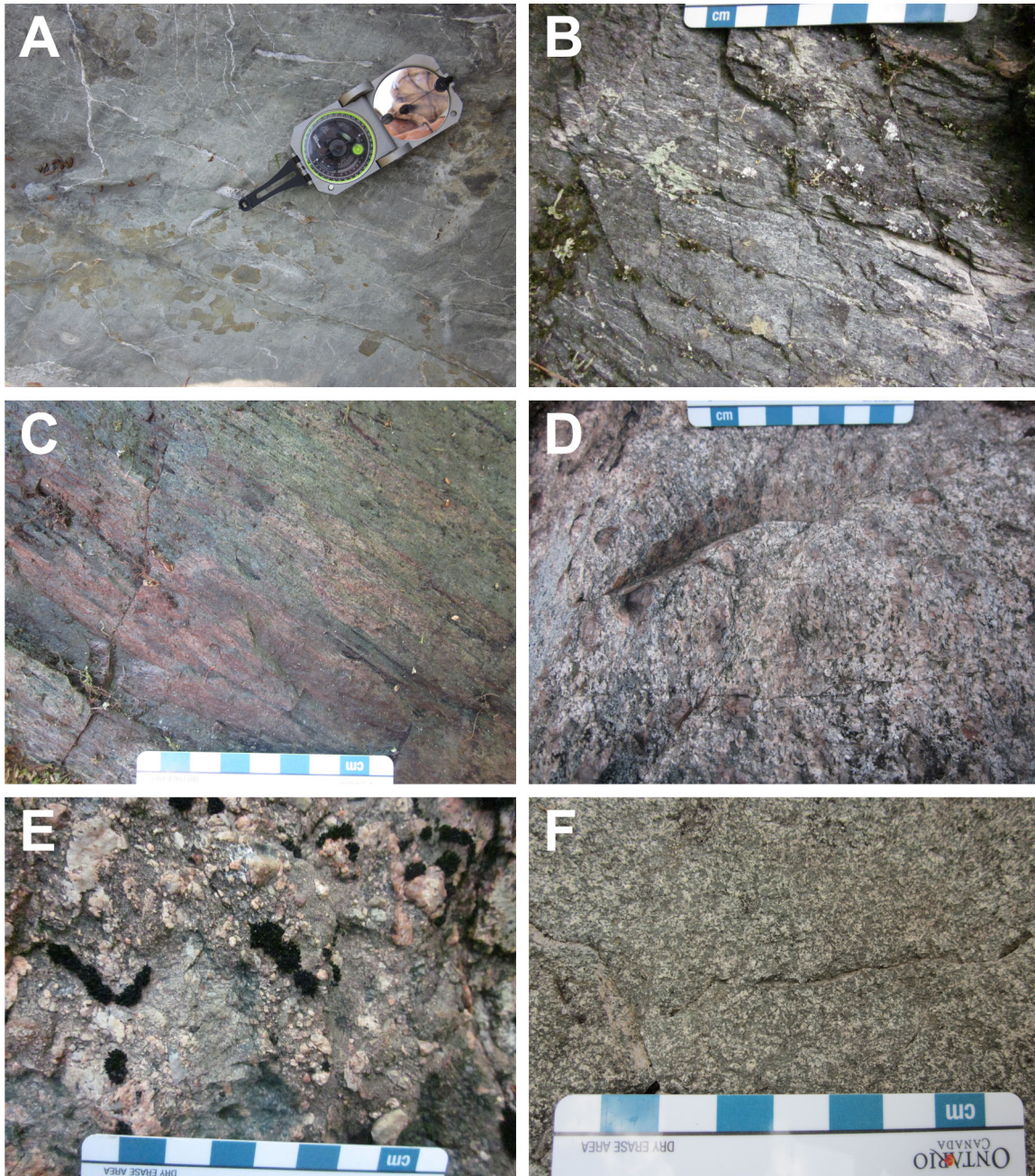


Photo 6.1. A) Altered ultramafic metavolcanic rocks displaying calcite and magnesite alteration (UTM 474553E 5306192N). B) Moderately foliated massive mafic metavolcanic rocks (UTM 471622E 5304650N). C) Gneissic texture showing an even distribution of mafic metavolcanic and granitic material (UTM 472613E 5302698N). D) Potassium feldspar megacrystic granite (UTM 471456E 5304779N). E) Polymictic conglomerate, with subrounded to rounded clasts of the Huronian Supergroup (UTM 474910E 5303722N). F) Diabase texture in Proterozoic Matachewan dike (UTM 474656E 5300519N). UTM coordinates are provided in Zone 17 using NAD83.

Archean Intrusions

Several dikes of varying composition intrude the supracrustal rocks in Nursey Township. Several lamprophyre dikes intrude the ultramafic metavolcanic rocks in the southeastern corner of the study area. In the central portion of the map area, 2 ultramafic dikes and a syenite dike intrude mafic metavolcanic rocks. The lamprophyres are fine to medium grained and are up to 50 cm wide. The ultramafic dikes are foliated, medium- to coarse-grained peridotites with talc alteration noted in one of the exposures. The syenite dike is composed almost entirely of potassium feldspar, with less than 5% quartz and 10% plagioclase, with no mafic minerals present. The syenite is interpreted to postdate the ultramafic intrusion based on intrusive contact relationships.

The Kenogamissi batholith is the latest Archean intrusion in Nursey Township, postdating the lamprophyre, ultramafic and syenite dikes. Beakhouse (2011) describes the Kenogamissi batholith as a foliated composite intrusion of tonalite to granodiorite, cut by later, nonfoliated to weakly foliated plutons (hornblende granodiorite, biotite granodiorite to granite and diorite). Geochronologic data indicate that the Kenogamissi batholith was emplaced over 70 million years, from 2747 to 2698 Ma. The later intrusions range in age from 2684 to 2681 Ma for dioritic units and from 2676 to 2673 Ma for granitic phases.

The Kenogamissi batholith occupies the entire western half of Nursey Township and extends to the northeastern border of the map area (*see* Figure 6.2). It varies in composition from granite to tonalite, containing both biotite and amphibole, with biotite as the dominant mineral. The westernmost part of the batholith is predominantly granodiorite with some tonalite. The eastern part of the intrusion has a more granitic composition, with lesser granodiorite and diorite phases. The more granitic phases are pinkish on fresh and weathered surfaces, whereas the more tonalitic phases are whitish grey on fresh surfaces and weather buff grey. The diorite phase is whitish grey and is devoid of deformation features or alteration. Some of the more granitic phases contain potassium feldspar megacrysts that can be up to 1 cm in size (Photo 6.1D). Pegmatitic and aplitic granitic dikes are also found near the margins of the batholith. Quartz veins as well as hematite and epidote alteration are common within the Kenogamissi batholith.

Huronian Supergroup Metasedimentary Rocks

The Huronian Supergroup metasedimentary rocks (Photo 6.1E) in Nursey Township are interpreted to be part of the Gowganda Formation of the Cobalt Group. The Gowganda Formation unconformably overlies the Archean rocks in the eastern part of Nursey Township (*see* Figure 6.2). Polymictic, poorly sorted, matrix-supported conglomerate is the predominant rock type. The matrix is typically sandy and clasts are subrounded to rounded and range from 1 to 20 cm in size. Clast compositions include granite to tonalite, gabbro, quartzite, sandstone and mudstone clasts. In some areas, the rocks are composed of sandstone consisting of fine to medium sand with rare clasts not exceeding 6 cm. One outcrop of mudstone on the shore of Sinclair Lake consists of grey to green, laminated silty material with a few clasts.

Where bedding is observed in the sandstone and conglomerate, it is typically moderately dipping 35 to 60°, with diverging dip directions. The dip of bedding in these rocks, combined with opposing facing directions, suggests that the Huronian Supergroup metasedimentary rocks are folded and form an anticline.

Proterozoic Intrusions

Proterozoic intrusions are gabbroic in composition (Photo 6.1F). The majority of the dikes trend roughly north, but a few are northeast trending. These dikes generally have strong, linear aeromagnetic signatures and were mostly defined by using aeromagnetic data (Ontario Geological Survey 2003). These are predominantly medium-grained gabbros, frequently having a diabase texture and containing a small

amount of sulphide minerals (typically <1%). Some of the dikes display saussuritized plagioclase. Most of the dikes have been interpreted to be part of the Matachewan dike swarm, because of their orientation and the presence of porphyritic plagioclase. The other northeast-trending dikes are believed to be part of the Biscotasing swarm and are mostly defined by airborne geophysics.

An intrusion of the Nipissing gabbro is also exposed in the southeast corner of the study area, occurring within ultramafic metavolcanic flows. The gabbro extends into Sothman Township, suggesting that the rocks are related to each other. Similarly, there are Nipissing intrusions in Kemp and Mond townships to the southeast of Nursey Township (Machado 2002; Machado and Longu  p  e 2002).

STRUCTURAL GEOLOGY

The foliation in Nursey Township has a relatively consistent orientation throughout the supracrustal rocks, becoming more pronounced closer to the Kenogamissi batholith. The foliation generally trends west-southwest or north-northeast. The dip is highly variable, ranging from 30 to 80  ; the dip direction is north-northwest and east-southeast. The foliation bends along some of the faults that cut through the area. Evidence for regional folding was observed within the ultramafic and mafic metavolcanic rocks in the central and eastern parts of Nursey Township. The fold in the ultramafic metavolcanic rocks is an open M fold, and the fold within the mafic metavolcanic rocks is isoclinal. The axial plane of the folds trends west-northwest and follows the foliation in the central part of the township.

The Kenogamissi batholith is weakly to strongly foliated. The foliation is roughly parallel to that of the supracrustal rocks, generally trending west-southwest or north-northeast. The dip is variable, ranging from 30 to 80  , dipping toward the north-northwest and east-southeast.

Major faults, roughly north-northeast trending, cut across the map area and extend through Sinclair and Nursey lakes (*see* Figure 6.2). Hrab   (1993) suggested multiple reactivations of these faults, and estimated sinistral strike-slip displacement between 3 and 6 km. Opposing bedding in the Huronian Supergroup metasedimentary rocks suggest that these have been folded into an anticline.

PRELIMINARY INTERPRETATIONS

The metavolcanic rocks of Nursey Township are interpreted to be part of the Tisdale assemblage that extends west from Sothman and Halliday townships. Previously, Mullen (1982) and Rogers (1995) suggested that the metavolcanic rocks in Nursey Township could be related to those in the Shining Tree area to the south. The continuation of brecciated ultramafic metavolcanic rocks eastward into Sothman and Halliday townships supports the interpretation that the stratigraphy in Nursey Township is part of the Halliday Dome. However, the lack of adequate material for geochronology and the presence of a major fault between the 2 areas make this a tentative interpretation.

ECONOMIC POTENTIAL

A few commodities have been reported in Nursey Township, based on mineral exploration programs by mining companies and prospectors. A total of 3 Mineral Deposit Inventory (MDI) sites are reported in the study area (*see* Figure 6.2). Table 6.1 summarizes the known mineral occurrences in Nursey Township.

The Mineral Data Inventory (MDI) and the bedrock mapping highlight a few key commodities in the study area such as gold, nickel and zinc. Lesser amounts of nickel, copper and cobalt are documented at the Rawson Island showing, but their values are slightly below the occurrence limits in MDI.

Table 6.1. Main characteristics of the Mineral Deposit Inventory sites in Nursey Township.

Occurrence	Map ID*	Commodities	Best Historic Value	Hosted Units
Sirola Gold Mines property MDI41P14NW00021	1	Au, Ni	up to 0.22 oz/t Au, 0.15% Ni	Mafic intrusive within ultramafic metavolcanic rocks
Rawson Island showing MDI000000001385	2	Zn (Ni, Cu, Co)	up to 10 000 ppm Zn (0.125% Ni, 0.194% Cu, 187 ppm Co)	Ultramafic metavolcanic rocks
First Island Sample 1627	3	Ni	up to 1900 ppm Ni	Ultramafic metavolcanic rocks

*Refers to deposit number on Figure 6.2.

Source: Mineral Deposit Inventory (MDI) updated June 2012 by A.C. Wilson, Resident Geologist Office, Timmins, Ontario.

Little exploration has been done in Nursey Township; however, the presence of sulphide-bearing ultramafic rocks, notably in the southeastern part of the map area, provide new targets for mineral exploration related to nickel-copper-platinum group elements (PGE). In addition, SGX Resources Inc.'s property located northeast and east of the field area in Sothman Township has 2 notable gold mineralized zones, the Edleston zone and the Sirola zone, in ultramafic metavolcanic flows. The Edleston zone has values up to 57.4 g/t Au over 3.3 m, including 0.4 m with 540.3 g/t Au (SGX Resources Inc., Timmins South property, www.sgxresources.com/mndata/sgx/uploaded_files/2012-09-19-Edleston.pdf, [accessed September 19, 2012]). The Sirola zone has values up to 6.1 g/t Au (Ontario Geological Survey 2011). Considering that the geology of Sothman Township is interpreted to extend westward into Nursey Township and gold mineralization has been reported in the northeast part of Nursey Township (MDI site 1, *see* Table 6.1 and Figure 6.2), the northeastern part of Nursey Township, thus, is considered to be a significant exploration target for gold mineralization.

ACKNOWLEDGMENTS

This project has benefited from the assistance of Kyle Whitney and Nicholas Wray. The author appreciates all the support from the staff of the Timmins Resident Geologist Office, in particular Ann Wilson. Sonia Préfontaine and Ben Berger are thanked for their valuable insight, interpretation and discussions. Patrick Gervais is thanked for drafting figures for this report. Thanks are extended to Cindy, Ben and Roy of the Warne Logging and Sawmill tourist camp; and to Russ and Linda from the Green Wilderness Lodge for their assistance during the field season.

REFERENCES

- Alcock, P.W. and Miller, M.J. 2001. Quaternary geology of the Sinclair Lake area; Ontario Geological Survey, Map 2653, scale 1:50 000.
- Ayer, J., Amelin, Y., Corfu, F., Kamo, S., Ketchum, J., Kwok, K. and Trowell, N. 2002. Evolution of the southern Abitibi greenstone belt based on U-Pb geochronology: autochthonous volcanic construction followed by plutonism, regional deformation and sedimentation; *Precambrian Research*, v.115, p.63-95.
- Beakhouse, G.P. 2011. The Abitibi Subprovince plutonic record: tectonic and metallogenic implications; Ontario Geological Survey, Open File Report 6268, 161p.
- Duguet, M., Préfontaine, S., Brown, G.H., Houlé, M.G. and Cole, E. 2010. Precambrian geology of Semple Township; Ontario Geological Survey, Preliminary Map P.3618, scale 1:20 000.
- Houlé, M.G. 2006. Geological and mineral potential of McArthur Township in the Bartlett Dome, Abitibi greenstone belt; *in* Summary of Field Work and Other Activities 2006, Ontario Geological Survey, Open File Report 6192, p.6-1 to 6-14.
- . 2007. Precambrian geology of McArthur Township; Ontario Geological Survey, Preliminary Map P.3583, scale 1:20 000.

- Houlé, M.G., Baldwin, G. and Thurston, P.C. 2008. Day 3: Physical volcanology of the Bartlett Dome; *in* Field trip guidebook to the stratigraphy and volcanology of supracrustal assemblages hosting base metal and gold mineralization in the Abitibi greenstone belt, Timmins, Ontario; Ontario Geological Survey, Open File Report 6225, p.59-73.
- Houlé, M.G., Préfontaine, S. and Brown, G.H. 2008. Geology and mineral potential of English and Zavitz townships in the Bartlett Dome, Abitibi greenstone belt; *in* Summary of Field Work and Other Activities 2008, Ontario Geological Survey, Open File Report 6225, p.10-1 to 10-17.
- Houlé, M.G. and Solgadi, F. 2007. Geological and mineral potential of Bartlett and Geikie townships in the Bartlett Dome, Abitibi greenstone belt; *in* Summary of Field Work and Other Activities 2007, Ontario Geological Survey, Open File Report 6213, p.7-1 to 7-15.
- Houlé, M.G., Solgadi, F. and Préfontaine, S. 2009. Precambrian geology of Bartlett and Geikie townships; Ontario Geological Survey, Preliminary Map P.3612, scale 1:20 000.
- Hrabi, R.B. 1993. Supracrustal assemblages and structural geology in the Midlothian Lake–Peterlong Lake area, Abitibi Subprovince; unpublished MSc thesis, Queen’s University, Kingston, Ontario, 147p.
- Machado, G. 2002. Geology of Burrows, Kemp and Mond townships, Shining Tree area; Ontario Geological Survey, Open File Report 6077, 41p.
- Machado, G. and Longuépée, H. 2002. Precambrian geology of Burrows, Kemp and Mond townships; Ontario Geological Survey, Preliminary Map P.3765, scale 1:20 000.
- Mullen, D.V. 1983. Report on the geology of the Sothman greenstone belt, District of Sudbury and Temiskaming, Ontario; Falconbridge Limited, internal report, 53p.
- Ontario Geological Survey 2003. Ontario airborne geophysical surveys, magnetic and electromagnetic data, grid and vector data, ASCII format, Halliday Dome area, MEGATEM® II survey; Ontario Geological Survey, Geophysical Data Set 1043a.
- 2011. Mineral Deposit Inventory–2011; Ontario Geological Survey, Mineral Deposit Inventory, December 2011 release, Sherwood prospect, MDI41P14NW00003.
- Préfontaine, S. 2011. Geology and mineral potential of Midlothian Township, Halliday Dome, Abitibi greenstone belt; *in* Summary of Field Work and Other Activities 2011, Ontario Geological Survey, Open File Report 6270, p.4-1 to 4-12.
- Préfontaine, S., Duguet, M., Cole, E.M. and Brown, G.H. 2009. Geology, mineral potential and preliminary geological interpretation of the Bartlett and Halliday domes, Abitibi greenstone belt, in Semple and Hutt townships, Ontario; *in* Summary of Field Work and Other Activities 2009, Ontario Geological Survey, Open File Report 6240, p.5-1 to 5-17.
- Préfontaine, S. and Magnus, S.J. 2010. Geology and mineral potential of Sothman and Halliday townships, Halliday Dome, Abitibi greenstone belt; *in* Summary of Field Work and Other Activities 2010, Ontario Geological Survey, Open File Report 6260, p.6-1 to 6-20.
- 2012. Precambrian geology of Sothman and Halliday townships; Ontario Geological Survey, Preliminary Map P.3765, scale 1:20 000.
- Rogers, M.C. 1995. Geological and exploration data compilation map of the Grassy River area; Ontario Geological Survey, Preliminary Map P.3343, scale 1:50 000.
- Thurston, P.C., Ayer, J.A., Goutier, J. and Hamilton, M.A. 2008. Depositional gaps in Abitibi greenstone belt stratigraphy: a key to exploration for syngenetic mineralization; *Economic Geology*, v.103, p.1097-1134.

7. Project Unit 09-006. Western Wabigoon Subprovince Synthesis Project

G.P. Beakhouse¹

¹Earth Resources and Geoscience Mapping Section, Ontario Geological Survey

INTRODUCTION

This contribution summarizes some of the results from field observations carried out during the 2012 field season. Field work was concentrated in the Sioux Lookout area in an area approximately bounded by longitudes 91°45' and 92°30'W and latitudes 49°50' and 50°15'N.

GENERAL GEOLOGICAL SETTING

The Sioux Lookout greenstone belt is bounded to the north by the Winnipeg River Subprovince and to the south by the Basket Lake batholith and consists of a number of east-northeast-trending panels that are alternately dominated by metavolcanic or metasedimentary rocks (Figure 7.1). The proportion of metasedimentary rocks (the prefix “meta” is hereafter omitted) within this belt is unusually high relative to other portions of the western Wabigoon Subprovince and Superior Province greenstone belts in general.

Following some early reconnaissance mapping (summarized in subsequent publications referred to below), the abundance of sedimentary rocks, together with their exceptional preservation and relatively good exposure, attracted the attention of Francis Pettijohn who undertook some of the pioneering investigations attempting to apply classic stratigraphic and sedimentological principles to Archean rocks (Pettijohn 1934, 1935, 1936, 1943). Pettijohn introduced stratigraphic nomenclature that has been adopted, but revised or not consistently applied by subsequent workers (Johnston 1969, 1972; Walker and Pettijohn 1971; Turner and Walker 1973; Page 1984; Devaney 2000); consequently, in the ensuing discussion, this nomenclature will be used to facilitate comparison of different interpretations with the goal of moving toward a less interpretative, more descriptive nomenclature.

FIELD OBSERVATIONS AND INTERPRETATIONS

The following section describes the character of the component panels of the Sioux Lookout greenstone belt and some of the critical observations and/or interpretations derived from field work done in 2012. The locations of the features discussed are indicated in Figure 7.1.

The Botham Bay volcanics unit (“BBV” on Figure 7.1) constitutes part of the northern volcanic belt (Trowell, Blackburn and Edwards 1980). The belt consists almost entirely of basaltic flows (with a high proportion of these being pillowed) with volumetrically minor but widespread interflow sedimentary units. The sedimentary units consist mainly of chert and magnetite ironstone, although a minor detrital or tuffaceous component may be present locally. The BBV is an overturned southward-facing homocline (dips characteristically approximately 65 to 70° to the north). The intensity of strain varies in a fairly systematic way through the unit. The southern half of the unit exhibits exceptionally low strain with even, very delicate volcanic structures (e.g., thin spalled pillow rinds within interpillow carbonate still partially

*Summary of Field Work and Other Activities 2012,
Ontario Geological Survey, Open File Report 6280, p.7-1 to 7-6.*

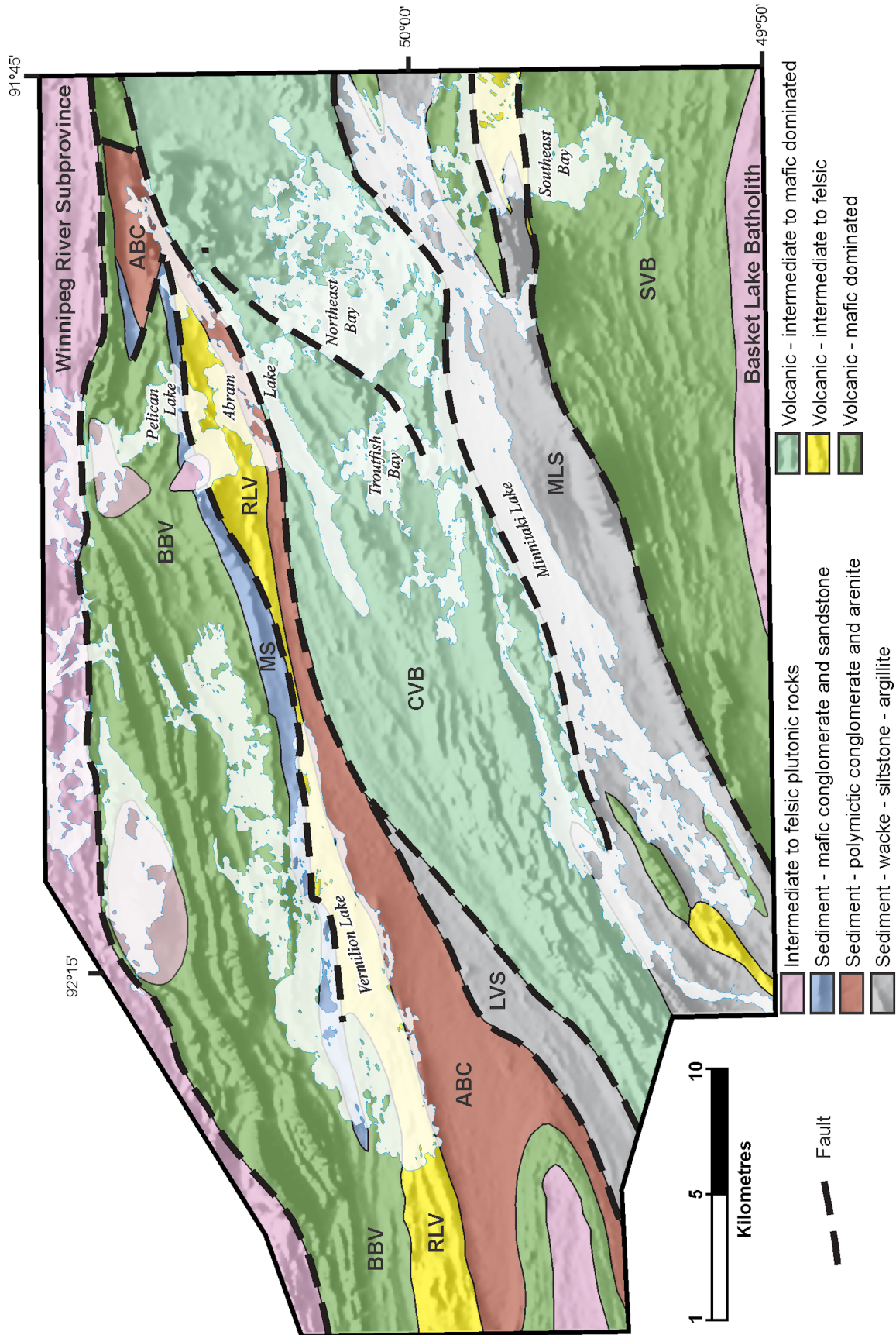


Figure 7.1. General geological map of the Sioux Lookout area draped over a shaded image of the first vertical derivative of the total magnetic field. Abbreviations discussed in text include ABC, Ament Bay conglomerates; BBV, Botham Bay volcanics; CVB, central volcanic belt; LVS, Little Vermilion sediments; MLS, Minnitaki Lake sediments; MS, mafic sediments; RLV, Redhat Lake volcanics; SVB, southern volcanic belt.

attached to selva) being preserved. The northern quarter of the unit is characterized by pervasive intense strain, particularly near the northern contact with the Winnipeg River Subprovince, which is interpreted to be a fault that is extensively modified by the emplacement of abundant younger intrusive phases. That portion of the stratigraphy between these areas of low and high strain is characterized by heterogeneous strain with the most intense strain partitioned into flow contacts.

To the west of Vermilion Lake, the BBV are directly overlain by a sequence of intermediate to felsic volcanic rocks that have been informally referred to as the Redhat Lake volcanics (Page 1984; “RLV” on Figure 7.1). Although facing indicators are not abundant within this unit, it is provisionally interpreted to be a south-facing, overturned homoclinal sequence that is apparently conformably overlying the BBV in the area to the west of Vermilion Lake. Fragmental intermediate volcanic rocks ranging from coarse tuff-breccia to feldspar crystal tuff (feldspar phenocrysts are also commonly present within coarser lithic fragments) greatly predominate within the unit. More massive felsic volcanic rocks, representing a possible flow and/or dome complex (Page 1984), are restricted to the basal portion of the sequence west of Vermilion Lake.

Intermediate fragmental rocks exposed on islands in the southern portion of Vermilion Lake and portions of Pelican Lake and Abram Lake are provisionally interpreted here to be lateral equivalents of the Redhat Lake volcanics. This interpretation differs from some earlier workers (Johnston 1972; Turner and Walker 1973) who variously interpreted these rocks to be correlative with various portions of the Patara and Abram sediments. This interpretation is similar to that advanced by Devaney (2000), although he also proposed a correlation with the Daredevil tuff (discussed below) that is not supported by observations made as part of this investigation. Tuffaceous units greatly predominate over coarser fragmental units in the Abram Lake area in particular suggesting that this portion of the unit may be a distal facies equivalent of the flow and/or dome complex and coarser fragmental deposits in the area west of Vermilion Lake.

Between the west end of Vermilion Lake and Pelican Lake, a unit of mafic sediments (“MS” on Figure 7.1) are in contact with the BBV. These mafic sediments have been placed within the Patara sediments by all previous workers; however, the interpretation of the significance of the unit has varied widely. Most workers have followed Pettijohn (1934) in interpreting these mafic sediments to be a dominantly homoclinal (albeit with local folding), south-facing “slope wash” deposit (sourced from the BBV) postdating BBV volcanism. This interpretation carries the implication that the Botham Bay volcanics–mafic sediments contact is either conformable or represents only a minor unconformity. A sample of mafic conglomerate collected for U/Pb geochronology had very few zircons, but 2 of these zircons suggested an age of approximately 2703 Ma (Fralick and Davis 1999). In part based on this relatively young detrital age, Devaney (2000) proposed that this was one of the youngest units within the Sioux Lookout greenstone belt and further suggested a coarsening-upward sequence (presumably north facing) and the presence of a profound angular unconformity at the Botham Bay volcanics–mafic sediments contact. Observations made as part of this study suggest that the mafic sediments are generally southward younging with a mafic conglomerate base grading upward into finer grained mafic sandstones and siltstones. The northern portion of the unit displays minimal strain and is generally conformable with bedding in the underlying BBV. The mafic clasts that predominate within the conglomerates closely resemble basalts in the underlying BBV; the only other clasts present locally are minor chert and/or ironstone clasts similar to those occurring as a minor component of the BBV and clasts of vein quartz. Minor folding is most prevalent near the south contact of the unit. The south contact of the mafic sediments with the Redhat Lake volcanics is not exposed, but exposures near the south contact are commonly highly strained with intense iron carbonate alteration suggesting that the contact may be a fault. These observations are provisionally interpreted to indicate that the mafic sediments are derived from the BBV and that the north contact is a minor erosional unconformity, whereas the mafic sediments are in fault contact with the Redhat Lake volcanics. The geochronological relationships require further investigation.

Previous workers have proposed formal stratigraphic nomenclature for a belt of sedimentary rocks extending from the Abram Lake area to the Little Vermilion Lake area with the Abram Group comprising the basal Ament Bay Formation, which is overlain successively by the Daredevil Formation and the Little Vermilion Formation (Pettijohn 1934; Turner and Walker 1973). Based on field relationships and absolute age constraints discussed below, this stratigraphic coherence is no longer tenable and the contact between the Ament Bay unit and the Daredevil unit is interpreted here to be a fault (*see also* discussion in Devaney (2000)).

Coarse polymictic conglomerates with generally subordinate sandstones characterize a unit assigned by all previous workers to the Ament Bay Formation that are referred to herein as the Ament Bay conglomerates (“ABC” on Figure 7.1). The conglomerates are massive to thickly bedded and lack grading and the sandstones commonly display large-scale cross-bedding—features that led Turner and Walker (1973) to infer a subaerial alluvial fan depositional environment for the unit. Clasts range up to very large boulders (~1 m diameter) and include both a range of mafic to felsic metavolcanic rocks and massive to well-foliated granitoid rocks as well as subordinate chemical sedimentary rocks and vein quartz. The well-foliated to gneissic character of many of the granitoid boulders is consistent with their derivation from the adjacent Winnipeg River Subprovince—an interpretation supported by the presence of granitoid clasts older than any known western Wabigoon Subprovince granitoid rocks (Davis, Sutcliffe and Trowell 1988). Davis, Sutcliffe and Trowell (1988) also established a young maximum depositional age of 2698 ± 4 Ma.

In the Little Vermilion Lake area, the top of the Ament Bay conglomerates are in contact with a thin, strongly deformed, felsic crystal (feldspar and quartz) tuff (previously assigned to the Daredevil Formation), which is overlain to the south by a sequence of wacke, siltstone and argillite (previously assigned to Little Vermilion Formation). Two zircon fractions from the tuff unit are slightly discordant with $^{207}\text{Pb}/^{206}\text{Pb}$ ages of 2713 and 2719 Ma (Davis, Sutcliffe and Trowell 1988) and either must be inherited zircons or the Daredevil tuff must be older than the apparently underlying Ament Bay conglomerates. Although further geochronological study is planned, the latter interpretation is provisionally interpreted to be the most likely; consequently, the localization of high strain in the tuff is attributed to the presence of a fault at the contact. The Daredevil tuff, together with the overlying wacke–siltstone–argillite sequence may represent a coherent stratigraphic assemblage that is informally referred to here collectively as the Little Vermilion sediments (“LVS” on Figure 7.1).

The central volcanic belt (“CVB” on Figure 7.1), although portrayed simply on published detailed maps (Johnston 1969, 1972), displays remarkable lithological diversity and internal complexity. This diversity and complexity is most striking in the Troutfish Bay and Northeast Bay areas where it has been studied by R.O. Page (Page and Clifford 1977; R.O. Page, unpublished data (*see* “Acknowledgments”)). On a regional scale, massive and pillowed (the latter commonly variolitic) mafic volcanic rocks predominate over subordinate felsic volcanic rocks. In the western portion of Minnitaki Lake, distinctive plagioclase \pm amphibole (after pyroxene?) porphyritic intermediate flows and fragmental rocks are also well represented. Geochemical analyses of these intermediate rocks are pending, but these units are anticipated to have compositions approximating andesite. Somewhat similar units were identified in the central volcanic belt in Laval Township where they were interpreted to be calc-alkalic basalt to andesite distinct from tholeiitic basalt–rhyolite occurring in the same area (Berger 1990).

The central volcanic belt is generally southward facing, although local reversals occur in several areas; consequently, the central volcanic belt structurally overlies the Ament Bay conglomerates and Little Vermilion sediments (*see* Figure 7.1). Geochronological evidence suggests that the central volcanic belt is older than these units occurring to the west; consequently, this constitutes an “old over young” relationship that has been interpreted to indicate that the northern contact of the central volcanic belt is a thrust fault (Davis, Sutcliffe and Trowell 1988; Blackburn et al. 1991). This interpretation is consistent with the presence of a narrow zone of high strain associated with the contact.

The Minnitaki Lake sediments (“MLS” on Figure 7.1) consist of thin to thick bedded wacke–siltstone–argillite with local intercalated conglomerate beds. A major magnetite ironstone unit is interlayered with the sediments near the southern contact of the unit. Bedding is generally relatively even and continuous and graded bedding, scoured bases and small-scale ripple cross-laminations are common; large-scale cross-bedding was not observed. These characteristics suggest deposition from turbidity currents below wave base (Walker and Pettijohn 1971). In the Southeast Bay area, the sediments are interpreted to interfinger with fragmental intermediate to felsic volcanic rocks. The relationship of the sediments to a number of mafic volcanic units illustrated within the area underlain by the Minnitaki Lake sediments (*see* Figure 7.1) are unclear. Portions of the Minnitaki Lake sediments are characterized by abundant, short wavelength, tight to isoclinal folding.

The southern volcanic belt (“SVB” on Figure 7.1) is not well exposed in the area investigated in 2012. The unit is apparently composed mainly of massive to pillowed mafic volcanic rocks, although several thin intermediate to felsic fragmental units were observed in one exposure in the central portion of the unit south of the entrance to Troutfish Bay.

ACKNOWLEDGMENTS

The author was capably assisted in the field by Brian Pisani. Discussions with Teal Riley, especially with regard to some of the volcanoclastic rocks, are greatly appreciated. Richard Page generously provided access to unpublished maps and other information and insight concerning the Sioux Lookout belt in general and the central volcanic belt in particular.

REFERENCES

- Berger, B.R. 1990. Precambrian geology, Laval and Hartman townships; Ontario Geological Survey, Report 272, 74p., accompanied by Map 2534.
- Blackburn, C.E., Johns, G.W., Ayer, J. and Davis, D.W. 1991. Wabigoon Subprovince; *in* Geology of Ontario, Ontario Geological Survey, Special Volume 4, Part 1, p.303-381.
- Davis, D.W., Sutcliffe, R.H. and Trowell, N.F. 1988. Geochronological constraints on the tectonic evolution of a Late Archean greenstone belt, Wabigoon Subprovince, northwest Ontario, Canada; *Precambrian Research*, v.39, p.171-191.
- Devaney, J.R. 2000. Regional geology of the Sioux Lookout orogenic belt, western Wabigoon Subprovince: stages of Archean volcanism, sedimentation, tectonism and mineralization; Ontario Geological Survey, Open File Report 6017, 151p.
- Fralick, P. and Davis, D.W. 1999. The Seine–Coutchiching problem revisited: sedimentology, geochronology and geochemistry of sedimentary units in the Rainy Lake and Sioux Lookout areas; *in* 1999 Western Superior Transect Fifth Annual Workshop, Lithoprobe Secretariat, University of British Columbia, Lithoprobe Report #70, p.66-75.
- Johnston, F.J. 1969. Geology of the western Minnitaki Lake area, District of Kenora; Ontario Department of Mines, Report 75, 28p., accompanied by Map 2155.
- 1972. Geology of the Vermilion–Abram lakes area, District of Kenora.; Ontario Department of Mines, Report 101, 56p., accompanied by Maps 2242 and 2243.
- Page, R.O. 1984. Geology of the Lateral Lake area, District of Kenora; Ontario Geological Survey, Open File Report 5518, 175p., accompanied by Preliminary Maps P.2371 and P.2372.

- Page, R.O. and Clifford, P.M. 1977. Physical volcanology of an Archean vent complex, Minnitaki Lake area, northwestern Ontario; *in* Current Research Part A, Geological Survey of Canada, Paper 77-1A, p.441-443.
- Pettijohn, F.J. 1934. Conglomerate of Abram Lake, and its extensions; Geological Society of America Bulletin, v.45, p.479-505.
- 1935. Stratigraphy and structure of Vermilion Township, District of Kenora, Ontario; Geological Society of America Bulletin, v.46, p.1891-1908.
- 1936. Early Precambrian varved slate in northwestern Ontario; Geological Society of America Bulletin, v.47, p.621-628.
- 1943. Archean sedimentation; Geological Society of America Bulletin, v.54, p.925-972.
- Trowell, N.F., Blackburn, C.E. and Edwards, G.R. 1980. Preliminary synthesis of the Savant Lake–Crow Lake metavolcanic-metasedimentary belt, northwestern Ontario, and its bearing upon mineral exploration; Ontario Geological Survey, Miscellaneous Paper 89, 30p.
- Turner, C.C. and Walker, R.G. 1973. Sedimentology, stratigraphy and crustal evolution of the Archean greenstone belt near Sioux Lookout, Ontario; Canadian Journal of Earth Sciences, v.10, p.817-845.
- Walker, R.G. and Pettijohn, F.J. 1971. Archean sedimentation: analysis of the Minnitaki basin, northwestern Ontario, Canada; Geological Society of America Bulletin, v.82, p.2099-2130.

8. Project Unit 11-011. Metamorphism in the Western Wabigoon Subprovince: Insights from the Bending Lake Area

M. Duguet¹ and G.P. Beakhouse¹

¹Earth Resources and Geoscience Mapping Section, Ontario Geological Survey

INTRODUCTION

The results discussed in this report represent the first phase of a multiyear thematic study addressing metamorphic patterns in Archean greenstone belts. The initial phases of this project are focussed on the western Wabigoon Subprovince and complement ongoing or recently completed detailed mapping and regional synthesis projects. The first phase of the project is designed to fill a knowledge gap regarding the metamorphism of the western Wabigoon Subprovince. The metamorphic study carried out in this project will modernize a component of the geological record that has never been addressed on a regional basis. The addition of these data and their interpretation will enhance the usefulness of both older (much of the area was last mapped in the 1960s and 1970s) and more recent mapping. The main focus of the initial stages of this work is the Bending–Stormy lakes area and builds on the results from recent mapping and other investigations carried out by D. Stone (Stone 2009, 2010; Stone, Paju and Smyk 2011; Stone, Hellebrandt and Lange 2011a, 2011b) (Figure 8.1).

RATIONALE FOR THE STUDY

The importance of characterizing regional metamorphic conditions and patterns in order to understand the geological record and tectonic settings has long been recognized in younger orogenic belts (Miyashiro 1961, 1973; Brown 2009), but is only beginning to be addressed in Archean terranes. One crucial impediment to investigation of Archean terranes has been the lack of appropriate tools to evaluate metamorphic conditions, particularly in greenstone-granite terranes in which high-variance mineral assemblages associated with mafic to felsic igneous rocks predominate and metapelitic rock are erratically distributed. It is only over the 10 last years that the tools to deal with these types of rocks have been developed. We have reached a stage where it is now possible to retrieve, with an acceptable level of precision and accuracy, first-hand thermobarometric data from Archean rocks. The methodology used for this study is described in detail in the next section.

METHODOLOGY

The project is based on a three-stage approach, the design of which draws on some aspects of a comprehensive investigation carried out in the Yilgarn craton (Goscombe et al. 2009).

- The first stage requires a compilation of the existing data, selection of potential targets for data acquisition and the design of a geodatabase. An inventory of specific diagnostic mineral assemblages and textural analysis is a crucial part of this process. Garnet-bearing samples are investigated first since they are the most suited to give acceptable precision in a thermobarometric study. Mineral assemblages within alteration zones are also examined, as the generally lower variance of these assemblages compared to the country rocks makes them more suitable for thermobarometry. They are also especially relevant to exploration for a variety of types of mineralization.

*Summary of Field Work and Other Activities 2012,
Ontario Geological Survey, Open File Report 6280, p.8-1 to 8-12.*

© Queen's Printer for Ontario, 2012

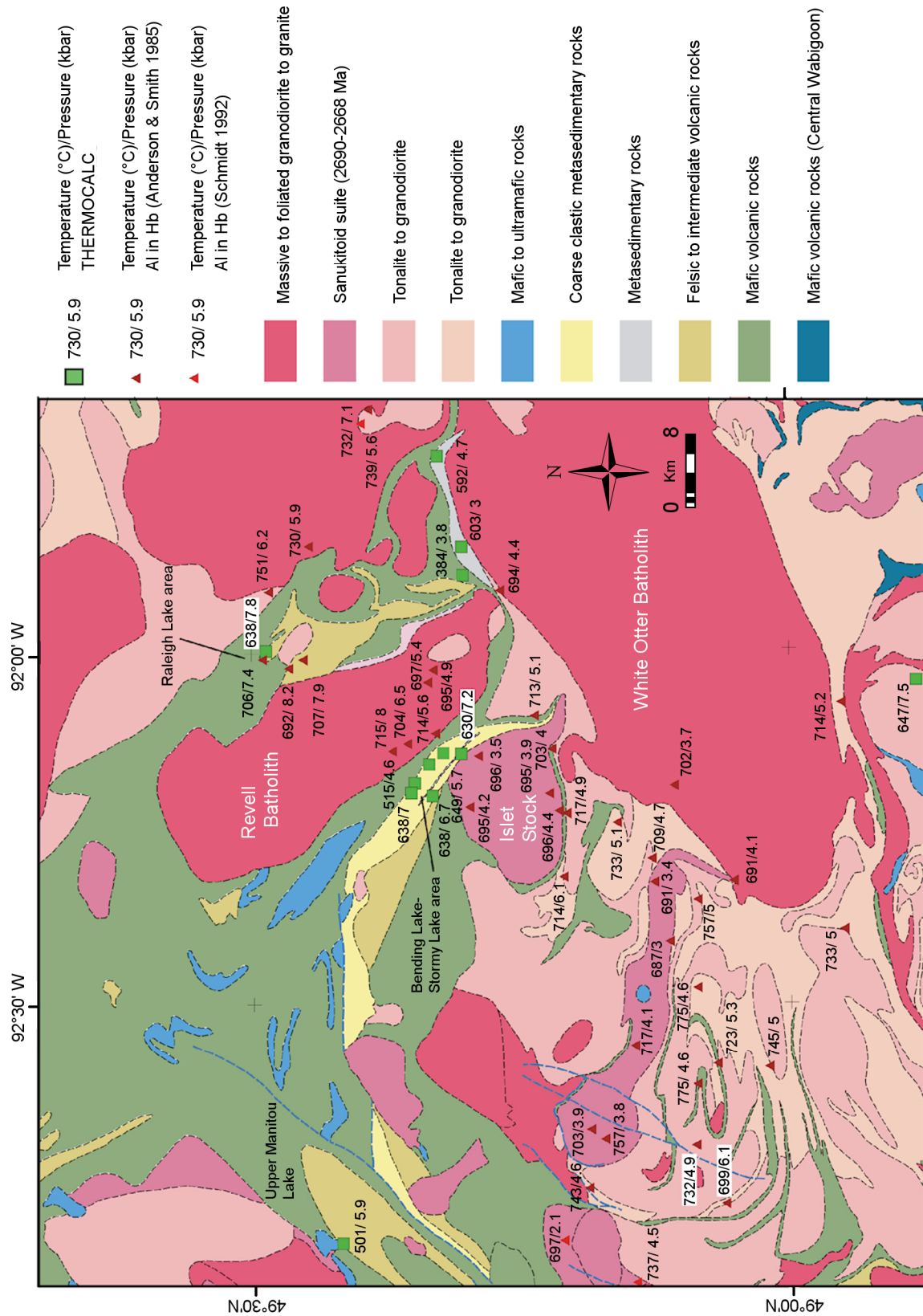


Figure 8.1. Simplified geological map of Bending Lake area and surroundings in the western Wabigoon Subprovince. Locations of samples with calculated $P-T$ conditions shown on the figure. Abbreviations: Al, aluminum; Hb, hornblende.

- The second stage consists of obtaining thermobarometric data from suitable assemblages. The aim is to cover as large an area as possible with reliable thermobarometric data.

Two methodologies have been used so far. The first approach was to use multiequilibria thermobarometry with the Average-PT mode of THERMOCALC v3.33 with the internally consistent thermodynamic database tcds55 (Holland and Powell 1990, 1998, www.metamorph.geo.uni-mainz.de/thermocalc/index.html [accessed October 11, 2012]) mostly on garnet-bearing supracrustal rocks. The activities of the different end-members were calculated with the AX software (Holland 2009). For hornblende-bearing plutonic rocks with appropriate mineral assemblages, a more conventional approach was used; namely, the aluminum-in-hornblende barometer (Anderson and Smith 1995; Schmidt 1992) and the plagioclase-hornblende thermometer (Holland and Blundy 1994). Despite the fact that the aluminum-in-hornblende barometer is calibrated directly from natural assemblages, it is the only known method to calculate pressure from plutonic rocks that are regionally extensive in Archean greenstone terranes. Most of the aluminum-in-hornblende data were compiled from Stone's work done over the last decade. Pressures retrieved from this latter method are crosschecked wherever possible with THERMOCALC results from nearby supracrustal rocks. If inconsistencies are found, then the Average-PT results prevail.

- The third stage is to investigate the pressure–temperature (P – T) path characteristics of regional metamorphism. This is done using isochemical P – T – X diagram (or pseudosection) modelling based on an internally consistent thermodynamic database and updated activity models for mineral phases. This allows us to model, for a given bulk chemical composition and a chosen P – T space, the different predicted mineral assemblages and their compositions for each (P , T) point. The main goal is to visualize, in the P – T space, the sequence of mineral assemblages that a rock may experience given different P – T trajectories. Moreover, chemical zoning of mineral phases may also be modelled in order to extract the P – T conditions at which they began to grow. Several software packages, such as THERMOCALC (Powell and Holland 1988), Perple_X (Connolly 1990, 2009, www.perplex.ethz.ch/ [accessed October 11, 2012]) or THERIAK_DOMINO (de Capitani and Petrakakis 2010), are available for such modeling. Each has their advantages and disadvantages. For this study, Perple_X was chosen because of its highly automated capabilities which allows for rapid output.

RESULTS

Petrography

Garnet-bearing metasedimentary rocks and amphibolites were investigated during this study. The mineral assemblages are presented in Table 8.1 along with the thermobarometric results. Metasedimentary rocks display various peak mineral assemblages such as quartz + muscovite + plagioclase + biotite + staurolite + garnet + ilmenite, plagioclase + quartz + biotite + garnet + staurolite + ilmenite, plagioclase + quartz + biotite + garnet + ilmenite, quartz + plagioclase + biotite + muscovite + garnet + sillimanite. Amphibolites are characterized by assemblages such as hornblende + plagioclase + garnet + quartz, plagioclase + quartz + hornblende + biotite + garnet, plagioclase + quartz + hornblende + biotite + garnet + epidote.

Porphyroblasts of staurolite typically overprint the main foliation and engulfed garnet porphyroblasts (Photos 8.1A and 8.1B). Both staurolite and garnet porphyroblasts are optically zoned with inclusion-rich cores and inclusion-free rims. The textural relationships of staurolite indicate that it formed syn to late in the metamorphic history of the samples. The timing of garnet deformation–recrystallization relationships is inconclusive in the metasedimentary rocks, but it is either syntectonic to posttectonic in the amphibolites. Furthermore, there may be several generations of garnet present (Photo 8.1C). Some samples present evidences of retrogression such as garnet dissolution (Photo 8.1D) or in the case of the amphibolites, well-developed secondary assemblages, composed of chlorite + grünerite + clinozoisite or chlorite + clinozoisite after garnet, are present. The range of textural relationships of the various porphyroblasts with

Table 8.1. THERMOCALC Average pressure-temperature ($P-T$) results for garnet-bearing samples (see Appendix 8.1 for mineral and endmember abbreviations).

Sample	Location	Easting (m) ¹	Northing (m) ¹	Parageneses ²	Endmembers ²	T (°C) ³	T Std.Dev. (°C) ³	P (kilobars) ³	P Std.Dev. (kilobars) ³	Cor ⁴	Sigfit ⁵ (cutoff)	$X_{(H_2O)}$	n^6
09DS164	Bending Lake	562148	5461837	pl+qtz+hbl+bt+grt	phl-ann-east-py-gr-alm- an-ab-tr-fact-ts-gl-q- H ₂ O	630	106	7.20	1.50	0.65	1.36 (1.54)	1.00	6
09DS171	Bending Lake	562200	5463700	hbl+pl+grt+qtz	phl-ann-east-py-gr-alm- an-ab-tr-fact-ts-q-H ₂ O	593	103	5.90	1.80	0.51	1.58 (1.61)	1.00	5
09DS175	Bending Lake	558100	5467000	qtz+mu+pl+bt+st+grt	phl-ann-east-py-gr-alm- an-ab-mst-fst-mu-cel- fccl-pa-q-H ₂ O	638	35	7.0	1.3	0.76	1.37 (1.45)	0.30	8
09DS177	Bending Lake	557800	5464750	qtz+mu+pl+bt+st+grt	phl-ann-east-py-gr-alm- an-ab-mst-fst-mu-cel- fccl-pa-q-H ₂ O	638	33	6.6	1.3	0.79	1.22 (1.54)	0.30	6
09ML15	Bending Lake	561047	5465140	pl+qtz+bt+grt+st	phl-ann-east-py-gr-alm- an-mst-fst-q-H ₂ O	649	122	5.70	2.60	0.85	1.43 (1.73)	1.00	4
11GB425	Upper Manitou Lake	511589	5474018	qtz+bt+pl+mu+chl+zo +grt	phl-ann-east-py-gr-alm- an-cz-clin-daph-ames- mu-cel-fcel-q-H ₂ O	509	11	5.90	0.50	0.56	1.17 (1.42)	1.00	9
96DS01	Raleigh Lake	572689	5482007	qtz+mu+pl+bt+st+grt	phl-ann-east-py-gr-alm- an-ab-mst-fst-mu-q- H ₂ O	638	46	7.80	1.00	0.58	0.92 (1.61)	1.00	6
96DS103	NW of White Otter batholith	592839	5464356	qtz+pl+bt+mu+grt+sill	phl-ann-east-py-gr-alm- an-sill-q-H ₂ O	592	125	4.70	1.80	0.76	0.05 (1.96)	1.00	3
96DS14	NW of White Otter batholith	583489	5461857	qtz+bt+pl+mu+sill+grt	phl-ann-east-py-gr-alm- an-sill-q-H ₂ O	603	120	3.00	1.80	0.72	0.29 (1.96)	1.00	3

Multi-equilibrium calculations were realized with the mode Average-PT of THERMOCALC v3.33 (Powell and Holland 1988, 1994). These results are obtained using the chemical compositions of matrix minerals and garnet rims.

¹UTM co-ordinates are given in NAD83, Zone 15.

²For mineral abbreviations, see Appendix 8.1.

³ T = temperature, P = pressure; the P and T uncertainties ("Std. Dev." in the table) correspond to 1σ .

⁴Cor = the coefficient of correlation.

⁵Diagnostic parameter called "Sigfit" being lower than the "cutoff" value given in parentheses for all samples; it can be considered that the solution found for $P-T$ is consistent with the input data within their uncertainties.

⁶ n = the number of reactions used for calculations.

the main foliation and the conspicuous retrogression in some samples suggest that the metamorphism in this area was either polyphase or was protracted relative to the duration of deformation.

In order to perform thermobarometry, chemical analyses of mineral phases were obtained using the Ontario Geological Survey Geoscience Laboratories (Geo Labs) Cameca SX-100 electron microprobe. Particular attention was paid to internal chemical zoning within garnet porphyroblasts. Both traverse and X-ray mapping were performed. Chemistry from one garnet of the sample 09ML15 is presented on Figure 8.2. Chemical zoning within this garnet is concentric and is characterized by a continuous enrichment in pyrope (magnesium) and almandine (iron) end-members from core to rim coeval with a decrease in spessartine (manganese) and grossular (calcium) contents. This type of zoning has been classically interpreted as resulting from chemical fractionation during garnet growth (Spear et al. 1990).

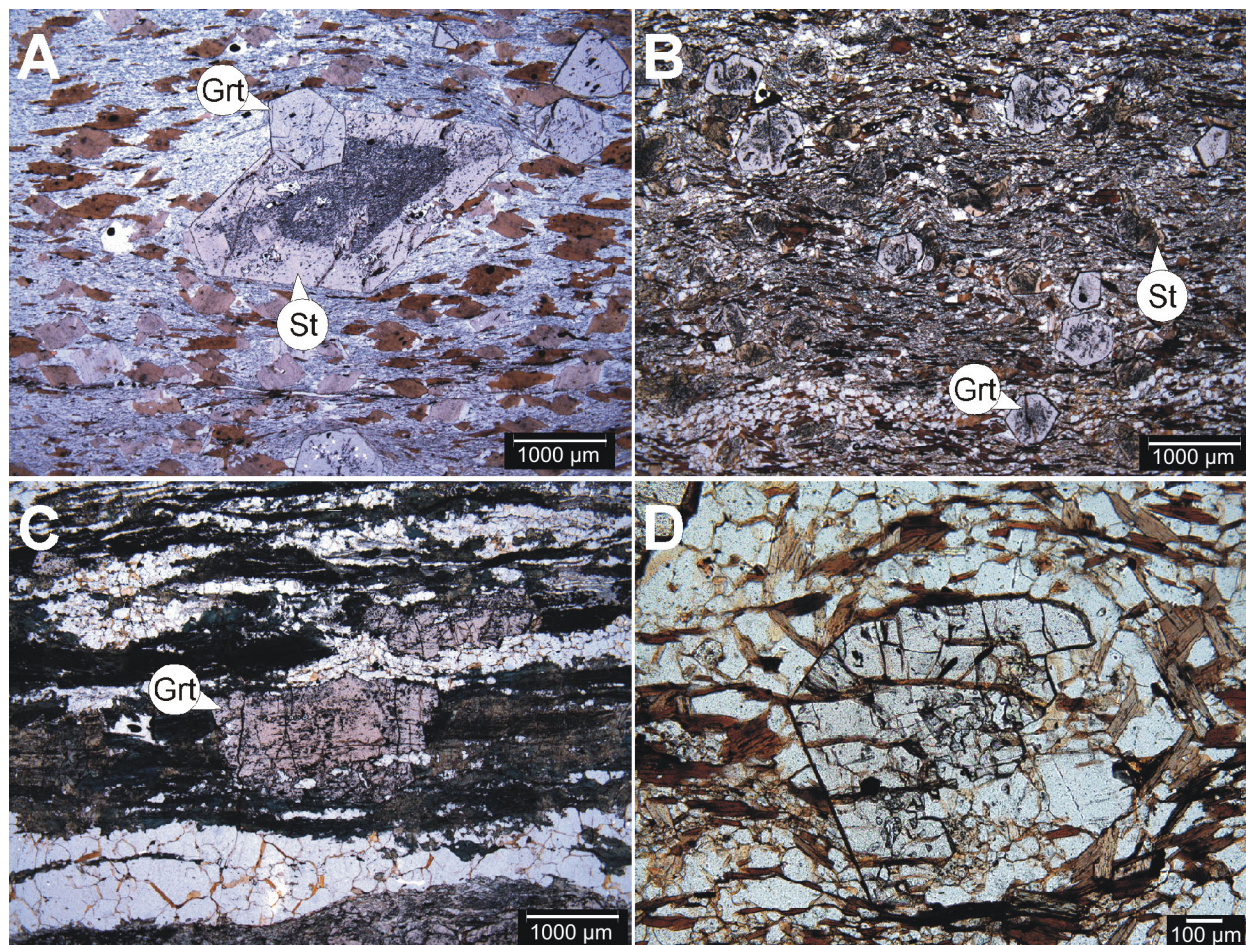


Photo 8.1. **A)** Plane-polarized light photomicrograph of sample 09DS177 showing a euhedral staurolite (St) porphyroblast engulfing a garnet (Grt) porphyroblast. The staurolite is optically zoned with a graphite inclusion-rich core. The scale bar at the bottom right is 1000 µm long. **B)** Plane-polarized light photomicrograph of sample 09ML15 showing a euhedral garnet and staurolite porphyroblasts. Both staurolite and garnet are optically zoned with inclusion-rich cores and inclusion-free rims. The scale bar at the bottom right is 1000 µm long. **C)** Plane-polarized light photomicrograph of sample 09ML17 showing a garnet porphyroblast cross-cutting the main foliation. Its growth is late regarding to the main foliation. The scale bar at the bottom right is 1000 µm long. **D)** Plane-polarized light photomicrograph of sample 09ML16 showing a garnet porphyroblast displaying retrogression feature. The garnet is partly dissolved in its half right side into plagioclase-quartz-biotite aggregate. The scale bar at the bottom right is 100 µm long.

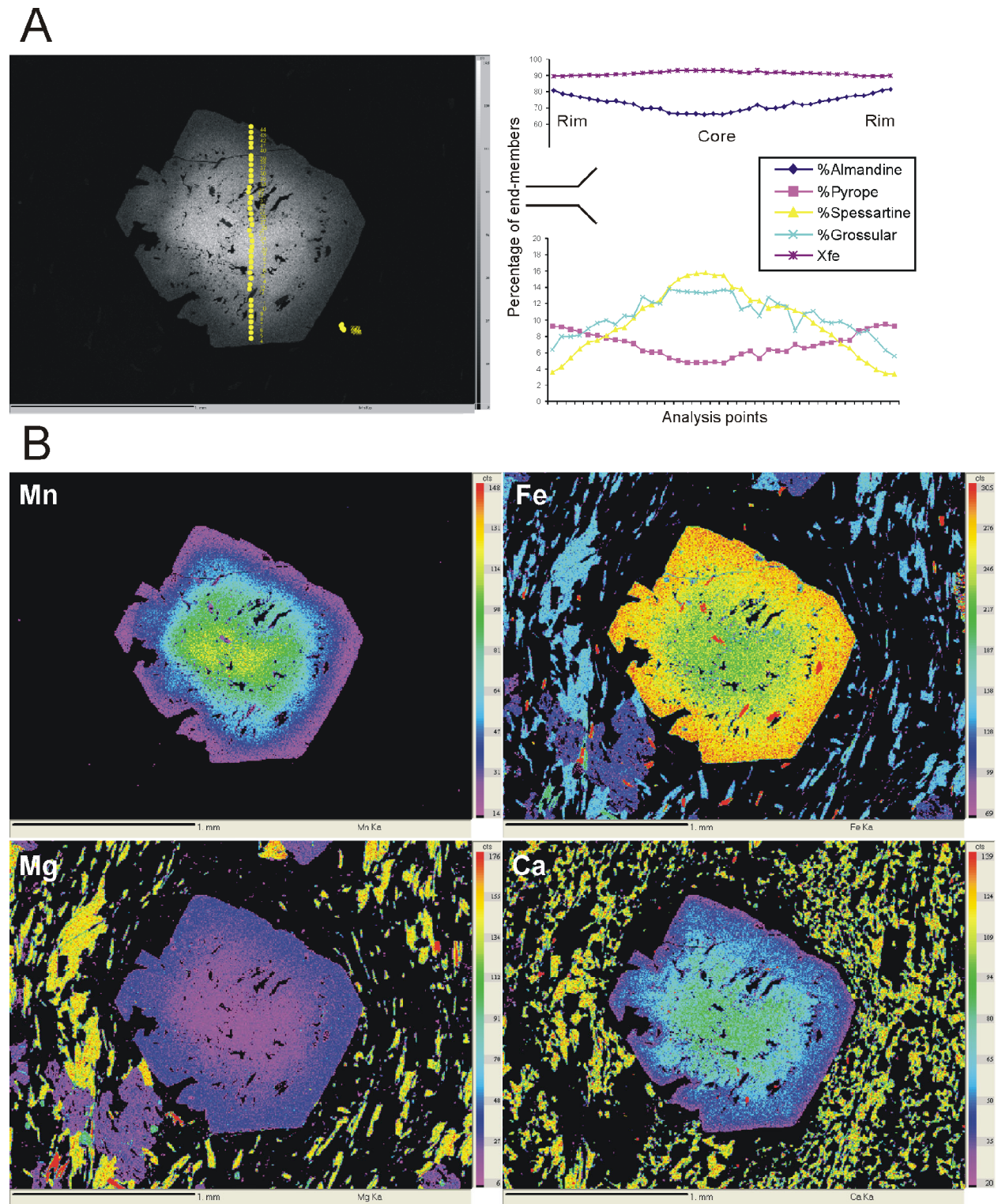


Figure 8.2. A) Sample 09ML15. Scanning electron microscope (SEM) imagery showing the punctual analyse traverse performed on the garnet. The diagram on the right displays the relative proportion of end members (almandine, pyrope, grossular and spessartine) from core to rims.

B) X-ray elements mapping performed on this garnet for manganese (Mn), iron (Fe), magnesium (Mg) and calcium (Ca). Colour scales on the right of each pictures is proportional to the relative concentration of the different elements expressed in counts. High concentrations are pictured by warm colours; lower concentrations are represented by colder colours.

Multiequilibria and Conventional Thermobarometry

Thermobarometric results are presented in Figure 8.1 and Table 8.1. Microprobe results indicate that garnet was the only phase which displayed strong chemical zoning. Thus, garnet-rim analyses along with analyses from matrix phases were chosen for thermobarometric calculations. Calculated metamorphic conditions for the Bending Lake area located on the south flank of the Revell batholith yielded temperatures between 595 and 650°C with pressure ranging from 5.7 to 7 kilobars. Within error, these results are consistent with each other. They are also consistent with the pressures calculated from the oldest facies of the Revell batholith, which has an age of 2732.3 ± 0.8 Ma (Stone et al. 2011a). Generally, the plagioclase-hornblende thermometer (Holland and Blundy 1994) used here to calculate temperature for hornblende-bearing plutons consistently gives higher temperatures than those found in the supracrustal rocks. These higher temperatures are interpreted to be a result of cooling of the plutonic rocks during crystallization.

On the northern margin of the Revell batholith in the Raleigh Lake area, a single garnet-staurolite-bearing metasedimentary sample yielded a temperature of 638°C and a pressure of 7.8 kilobars. This pressure matches those calculated from various nearby tonalitic stocks emplaced into the supracrustal rocks (*see* Figure 8.1).

Much lower pressure, usually around 3 to 4 kilobars, was found within all the late-tectonic to posttectonic plutons indicating they were emplaced at higher crustal levels than the earlier plutons and that the associated uplift followed the onset of regional metamorphism. These types of plutons are emplaced between 2695 and 2700 Ma throughout the western Wabigoon Subprovince (Davis and Edwards 1986; Davis, Blackburn and Krogh 1982) and characteristically have a sanukitoid chemical affinity. Similar timing of sanukitoid plutonism relative to regional metamorphism and uplift has been described from other portions of the Superior Province (Beakhouse 2011; Beakhouse and Davis 2005; Beakhouse, Lin and Kamo 2011).

Some supracrustal rocks seem to have only experienced this low-pressure-high-temperature event since no trace of the earlier medium-pressure event was found in the investigated samples. The garnet-bearing parageneses are characterized by the transition of andalusite to sillimanite, which can only occur at relatively low pressure (3 to 4 kilobars). This supracrustal package, composed of metasedimentary rocks and located on the northwest margin of the White Otter batholith, consistently gave pressure between 3 and 4.7 kilobars for temperature ranging from 400 to 600°C, the with the higher temperatures being found closer to the plutons (*see* Figure 8.1; *see* Table 8.1).

Isochemical Section Modelling

An isochemical section (or pseudosection) was constructed for sample 09ML15 with the software Perple_X v6.6 (Connolly 1990, 2009) using the internally consistent thermodynamic data set hp04ver translation for Perple_X of the database tcd55s (Holland and Powell 1990, 1998: using last update from 2005) (Figure 8.3). Calculations were conducted in the system $\text{MnO}-\text{Na}_2\text{O}-\text{CaO}-\text{K}_2\text{O}-\text{FeO}-\text{MgO}-\text{Al}_2\text{O}_3-\text{SiO}_2-\text{H}_2\text{O}-\text{TiO}_2$ (MnNCKFMASHTi) under conditions of water saturation. Quartz was considered in excess. The chemical composition of the sample, as determined by X-ray fluorescence (XRF) at the Geo Labs is given in Figure 8.3. Solid solution models were used for muscovite (Coggon and Holland 2002), chlorite (extended from Holland, Baker and Powell 1998), biotite (Tajčmanová, Connolly and Cesare 2009), garnet (Holland, Baker and Powell 1998), staurolite (Mahar et al. 1997; Holland and Powell 1998), chloritoid (Mahar et al. 1997; Holland and Powell 1998), cordierite (Mahar et al. 1997; Holland and Powell 1998), ilmenite (model IlGkPy for Perple_X) and feldspar (Fuhrman and Lindsley 1988).

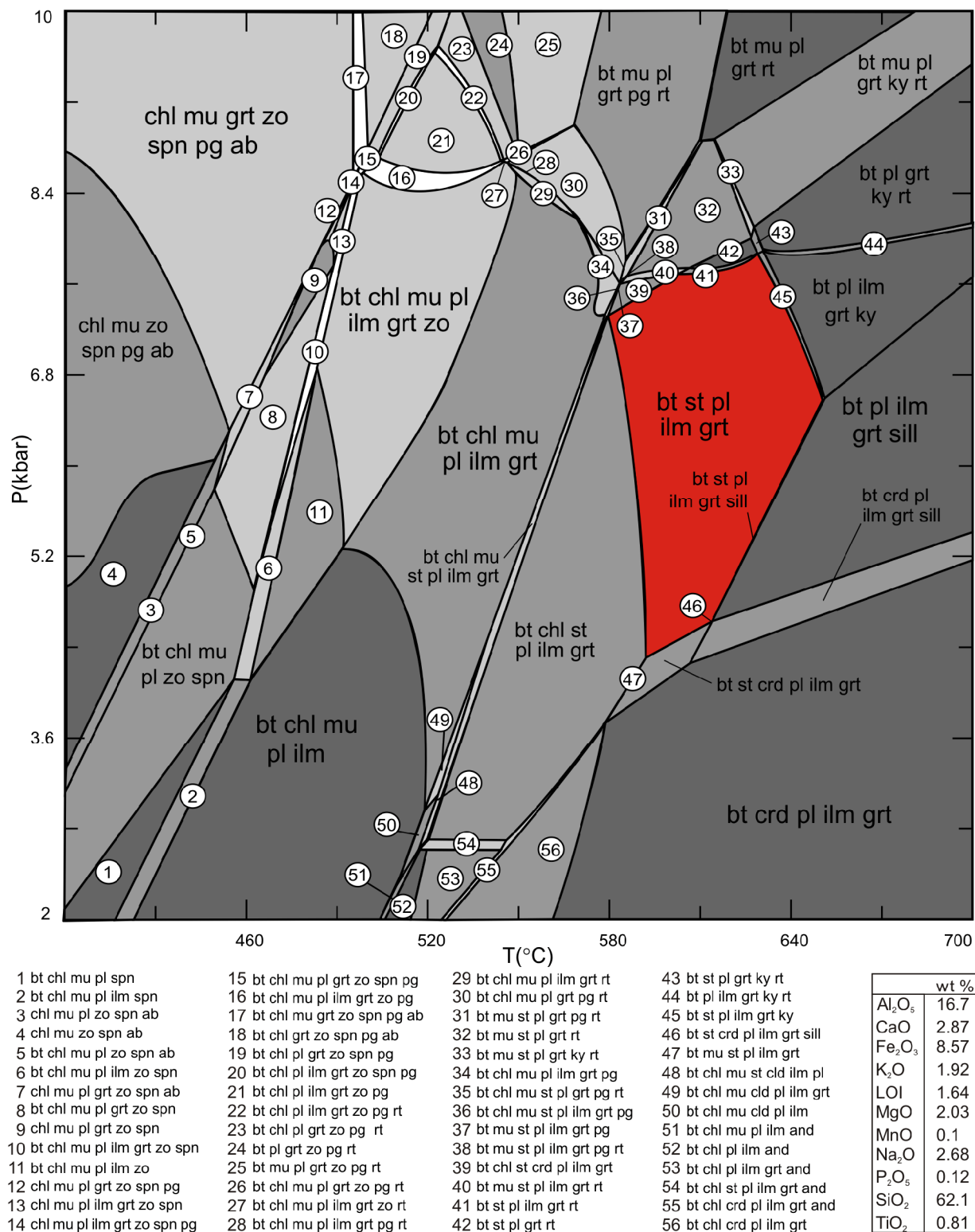


Figure 8.3. Isochemical section (or pseudosection) (P - T diagram) built in the system MnO-Na₂O-CaO-K₂O-FeO-MgO-Al₂O₃-SiO₂-H₂O-TiO₂ (MnNCKFMASHTi) for sample 09ML15. Water (H₂O) and quartz are considered in excess for calculation. The modelled mineralogical assemblage matching the observed one is coloured in red on the figure. See Appendix 8.1 for endmember and mineral abbreviations. The software Perple_x v6.6 (Connolly 1990, 2009) with the internally consistent thermodynamic data set hp04ver translation for Perple_x of the database tcd55s (Holland and Powell 1990, 1998; last update in 2005) was used.

The P – T section was drawn from 400 to 700°C for a pressure range from 2 to 10 kilobars. At low to medium pressure, the garnet-in reaction occurs around 510°C in the biotite + chlorite + muscovite + plagioclase + ilmenite + quartz field. Muscovite reacts out at 520°C very quickly after staurolite appears in the mineralogical assemblage. Chlorite reacts out at 580°C. The observed mineral assemblage plagioclase + quartz + biotite + garnet + staurolite occurs in the P – T space from 580 to 640°C and from 4 to 8.2 kilobars. The P – T range predicted by *Perple_X* for this mineral assemblage matches the result found by the Average-PT mode of THERMOCALC (see Table 8.1).

Isopleth modelling provides the P – T conditions at which the garnet started to grow. Garnet-core isopleths (X_{Mn} , X_{Fe} , X_{Ca}) were plotted in the P – T diagram (Figure 8.4) along with the garnet-in reaction, the stability field of staurolite and the isopleth X_{st} ($\text{Fe}/(\text{Fe}+\text{Mg})$) for staurolite. Garnet-core isopleths crosscut each other at a high angle at 527°C and 5.2 kilobars very close to the garnet-in reaction. Compared with the multiequilibria thermobarometry and considering the garnet zoning pattern, this garnet experienced a temperature increase of 130°C for a moderate pressure increase of 0.5 kilobars. Nonetheless, the climax pressure calculated for sample 09ML15 is lower than nearby samples (sample 09DS175 and 09DS177) that yielded pressure as high as 7.2 kilobars. Sample 09ML15 (as nearby sample 09ML16, see Photo 8.1D) may have been affected by retrogression, which would shift plagioclase

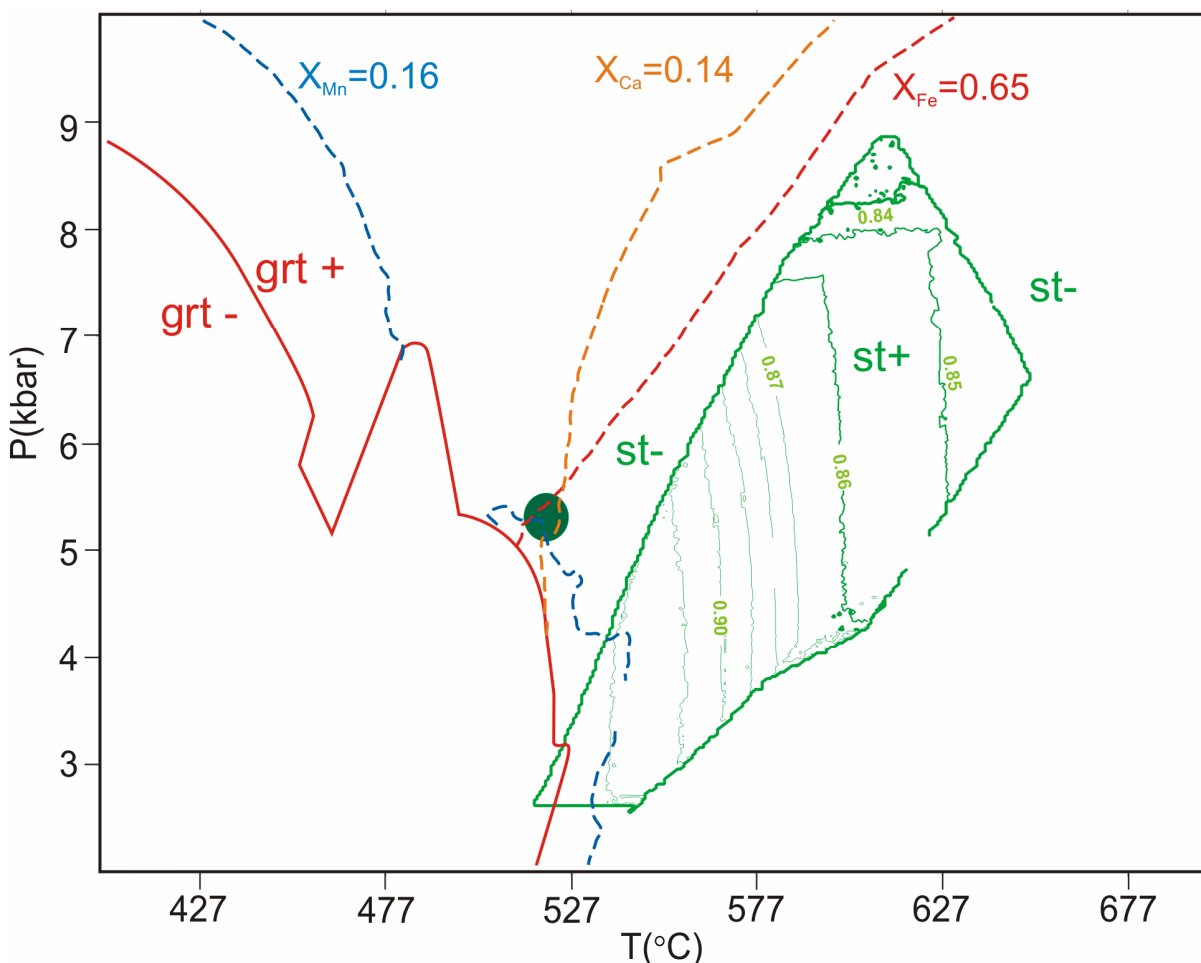


Figure 8.4. Pressure–temperature (P – T) diagram for sample 09ML15 plotting the garnet-core isopleths X_{Mn} ($X_{\text{Mn}} = \text{Mn}/(\text{Mn}+\text{Mg}+\text{Fe}+\text{Ca})$), X_{Ca} ($X_{\text{Ca}} = \text{Ca}/(\text{Mn}+\text{Mg}+\text{Fe}+\text{Ca})$) and X_{Fe} ($X_{\text{Fe}} = \text{Fe}/(\text{Mn}+\text{Mg}+\text{Fe}+\text{Ca})$). Their intersection gives the P – T conditions at which the garnet had started to grow (green circle). The garnet-in (grt+) reaction is displayed by the red line. The stability field of staurolite (st) is displayed by the green curve along with the isopleth X_{st} ($X_{\text{st}} = \text{Fe}/(\text{Fe}+\text{Mg})$).

chemistry toward a more albitic composition, thereby decreasing pressure by as much as 2 kilobars. Moreover, microprobe analysis of X_{st} yielded values close to 0.84, which plot in the isochemical section above 5 kilobars for a temperature of 627°C. Nevertheless, the pressure of 5.7 kilobars calculated for sample 09ML15 is, within error, similar to the pressure calculated for 09DS175 and 09DS177. The P – T path deduced from the isochemical section of the sample 09ML15 is very close to isobaric heating providing that the increase of pressure is real. This last aspect will warrant further studies.

CONCLUSION

This metamorphic and thermobarometric study focussing on garnet-bearing supracrustal rocks obtained surprisingly higher P – T conditions than previously thought for the area. The highest conditions are found on each flank of the Revell batholith and are as high as 7.8 kilobars. The metamorphism of these supracrustal rocks is likely coeval with the emplacement of the oldest tonalitic suite (*circa* 2730 Ma) in the area. This medium-temperature and medium- to high-pressure metamorphism likely occurred early in the history of this portion of the Wabigoon Subprovince. The Wabigoon Subprovince was subsequently affected by a lower pressure metamorphism that retrogressed the previous mineral assemblages and which may have been coeval with the emplacement of the sanukitoid suite between 2695 and 2700 Ma.

Some questions remain concerning the timing of this early event, its relationships with deformation and plutonism, its geodynamical context and its regional extent. In the Upper Manitou Lake area (*see* Figure 8.1), 40 km to the west, a garnet-bearing metasedimentary rock sample yielded a pressure of 5.9 kilobars for a temperature of 509°C (*see* Table 8.1). Between the Bending Lake area to the east and the Upper Manitou Lake area to the west is a 40 km long greenstone belt composed mostly of mafic volcanic and plutonic rocks which was metamorphosed under greenschist-facies conditions. Such greenschist mineral assemblages are commonly thought to have developed under comparatively low-pressure conditions, but the results presented here suggest that this interpretation should be re-evaluated.

ACKNOWLEDGMENTS

Denver Stone (formerly OGS) and David Lewis (OGS) are warmly thanked for their great interest in the project. Their work and sampling are contributing greatly to the extension of the geodatabase. Dave Crabtree (Geoscience Laboratories) performed X-ray mapping on the garnet-bearing samples and provided invaluable expertise with the microprobe work.

REFERENCES

- Anderson, J.L. and Smith, D.R. 1995. The effects of temperature and fO_2 on the Al-in-hornblende barometer; *American Mineralogist*, v.80, p.549-559.
- Beakhouse, G.P. 2011. The Abitibi Subprovince plutonic record: tectonic and metallogenic implications; Ontario Geological Survey, Open File Report 6268, 161p.
- Beakhouse, G.P. and Davis, D.W. 2005. Evolution and tectonic significance of intermediate to felsic plutonism associated with the Hemlo greenstone belt, Superior Province, Canada; *Precambrian Research*, v.137, p.61-92.
- Beakhouse, G.P., Lin, S. and Kamo, S.L. 2011. Magmatic and tectonic emplacement of the Pukaskwa batholith, Superior Province, Ontario, Canada; *Canadian Journal of Earth Sciences*, v.48, p.187-204.
- Brown, M. 2009. Metamorphic patterns in orogenic systems and the geological record; *in* *Accretionary orogens in space and time*, The Geological Society [London], Special Publication No.318, p.37-74.
- Coggon, R. and Holland, T.J.B. 2002. Mixing properties of phengitic micas and revised garnet-phengite thermobarometers; *Journal of Metamorphic Geology*, v.20, p.683-696.

- Connolly, J.A.D. 1990. Multivariable phase diagrams – an algorithm based on generalized thermodynamics; *American Journal of Science*, v.290, p.666-718.
- 2009. The geodynamic equation of state: what and how; *Geochemistry, Geophysics, Geosystems*, v.10, paper Q10014, 19p. DOI:10.1029/2009GC002540.
- Davis, D.W., Blackburn, C.E. and Krogh, T.E. 1982. Zircon U–Pb ages from the Wabigoon–Manitou Lakes region, Wabigoon Subprovince, northwest Ontario; *Canadian Journal of Earth Sciences*, v.19, p.254-266.
- Davis, D.W. and Edwards, G.R. 1986. Crustal evolution of Archean rocks in the Kakagi Lake area, Wabigoon Subprovince, Ontario, as interpreted from high-precision U–Pb geochronology; *Canadian Journal of Earth Sciences*, v.23, p.182-192.
- de Capitani, C. and Petrakakis, K. 2010. The computation of equilibrium assemblage diagrams with THERIAK/DOMINO software; *American Mineralogist*, v.95, p.1006-1016.
- Fuhrman, M. and Lindsley, D. 1988. Ternary-feldspar modeling and thermometry; *American Mineralogist*, v.73, p.201-215.
- Goscombe, B., Blewett, R.S., Czarnota, K., Groenewald, P.B. and Maas, R. 2009. Metamorphic evolution and integrated terrane analysis of the eastern Yilgarn Craton: rationale, methods, outcomes and interpretation; *Geoscience Australia, Record 2009/23*, 270p.
- Holland, T.J.B. 2009. AX: a program to calculate activities of mineral endmembers from chemical analyses (usually determined by electron microprobe); Department of Earth Sciences, University of Cambridge, Cambridge, United Kingdom, www.esc.cam.ac.uk/research/research-groups/holland/ax. [software downloaded February 5, 2009; site accessed October 9, 2012]
- Holland, T. and Blundy, J. 1994. Non-ideal interactions in calcic amphiboles and their bearing amphibole plagioclase thermometry; *Contributions to Mineralogy and Petrology*, v.116, p.433-447.
- Holland, T.J.B. and Powell, R. 1990. An enlarged and updated internally consistent thermodynamic dataset with uncertainties and correlations: the system K_2O - Na_2O - CaO - MgO - MnO - FeO - Fe_2O_3 - Al_2O_3 - TiO_2 - SiO_2 - C - H_2 - O_2 ; *Journal of Metamorphic Geology*, v.8, p.89-124.
- 1998. An internally consistent thermodynamic dataset for phases of petrological interest; *Journal of Metamorphic Geology*, v.16, p.309-343.
- Holland, T., Baker, J. and Powell, R. 1998. Mixing properties and activity-composition relationships of chlorites in the system MgO - FeO - Al_2O_3 - SiO_2 - H_2O ; *European Journal of Mineralogy*, v.10, p.395-406.
- Kretz, R. 1983. Symbols for rock-forming minerals; *American Mineralogist*, v.68, p.277-279.
- Mahar, E.M., Baker, J.M., Powell, R., Holland, T.J.B. and Howell, N. 1997. The effect of Mn on mineral stability in metapelites; *Journal of Metamorphic Geology*, v.15, p.223-238.
- Miyashiro, A. 1961. Evolution of metamorphic belts; *Journal of Petrology*, v.2, p.277-311.
- 1973. *Metamorphism and metamorphic belts*; George Allen and Unwin Ltd., London, 492p.
- Powell, R. and Holland, T.J.B. 1988. An internally consistent thermodynamic dataset with uncertainties and correlations: 3: application, methods, worked examples and a computer program; *Journal of Metamorphic Geology*, v.6, p.173-204.
- 1994. Optimal geothermometry and geobarometry; *American Mineralogist*, v.79, p.120-133.
- Schmidt, M.W. 1992. Amphibole composition in tonalite as a function of pressure: an experimental calibration of the Al-in-hornblende barometer; *Contributions to Mineralogy and Petrology*, v.110, p.304-310.
- Spear, F.S., Kohn, M.J., Florence, F. and Menard, T. 1990. A model for garnet and plagioclase growth in pelitic schists: implications for thermobarometry and *P-T* path determinations; *Journal of Metamorphic Geology*, v.8, p.683-696.

- Stone, D. 2009. Geology of the Bending Lake area, northwestern Ontario; *in* Summary of Field Work and Other Activities 2009, Ontario Geological Survey, Open File Report 6240, p.14-1 to 14-7.
- 2010. Geology of the Stormy Lake area, northwestern Ontario; *in* Summary of Field Work and Other Activities 2010, Ontario Geological Survey, Open File Report 6260, p.13-1 to 13-12.
- Stone, D., Paju, G. and Smyk, E. 2011. Precambrian geology of the Stormy Lake area; Ontario Geological Survey, Preliminary Map P.2515, scale 1:20 000.
- Stone, D., Hellebrandt, B. and Lange, M. 2011a. Precambrian geology of the Bending Lake area (north sheet); Ontario Geological Survey, Preliminary Map P.3623, scale 1:20 000.
- 2011b. Precambrian geology of the Bending Lake area (south sheet); Ontario Geological Survey, Preliminary Map P.3624, scale 1:20 000.
- Tajčmanová, L., Connolly, J.A.D. and Cesare, B. 2009. A thermodynamic model for titanium and ferric iron solution in biotite; *Journal of Metamorphic Geology*, v.27, p.153-165.

Appendix 8.1. Endmember (*from* THERMOCALC v3.33: Holland and Powell 1998) and mineral abbreviations (*from* Kretz 1983) used in this article.

Abbreviation	Endmember	Abbreviation	Mineral
ab	albite	ab	albite
alm	almandine	and	andalusite
ames	amesite	bt	biotite
an	anorthite	chl	chlorite
ann	annite	crd	cordierite
cel	celadonite	cld	chloritoid
clin	clinochlore	cz	clinozoisite
cz	clinozoisite	ep	epidote
daph	daphnite	grt	garnet
east	eastonite	grun	grünerite
fact	ferro-actinolite	hbl	hornblende
fcel	ferroceladonite	ilm	ilmenite
fst	ferrostauroilite	ky	kyanite
gl	glaucophane	mu	muscovite
gr	grossular	pg	paragonite
hbl	hornblende	pl	plagioclase
ilm	ilmenite	qtz	quartz
ky	kyanite	rt	rutile
mst	magnesiostauroilite	sill	sillimanite
mu	muscovite	spn	sphene (titanite)
pa	paragonite	st	staurolite
phl	phlogopite	zo	zoisite
py	pyrope		
q	quartz		
ru	rutile		
sill	sillimanite		
tr	tremolite		
ts	tschermakite		

9. Project Unit 11-002. New Geochemical and Geochronological Results from the Rowan Lake Area, Northwestern Ontario

D. Lewis¹, S.L. Kamo² and R.W.D. Lodge³

¹Earth Resources and Geoscience Mapping Section, Ontario Geological Survey, Sudbury, Ontario P3E 6B5

²Jack Satterly Geochronology Laboratory, University of Toronto, Toronto, Ontario M5S 3B1

³Department of Earth Sciences, Laurentian University, Sudbury, Ontario P3E 2C6

INTRODUCTION

A multi-year 1:20 000 scale mapping project of the bedrock geology of the Rowan–Cedartree–Kakagi lakes area was initiated during the summer field season of 2011, commencing with the Rowan Lake area. The study builds on high-quality lithostratigraphic mapping (Kaye 1973) and was intended to focus on the gold potential of the area. A major part of the study is the investigation of the geochemistry and geochronology of rock units. During the 2011 field season, 109 rock samples were taken for geochemical analyses and 2 samples were taken for geochronological analyses.

REGIONAL GEOLOGY

In the following discussion, since all rocks have undergone metamorphism, the “meta” prefix is omitted for the sake of brevity. The Rowan Lake area is located 30 km east of Sioux Narrows, Ontario, and is underlain by Archean rocks of the western Wabigoon Subprovince (Trowell, Blackburn and Edwards 1980). At Rowan Lake, the rocks consist primarily of mafic, intermediate and felsic metavolcanic rocks with minor metasedimentary rocks, and are intruded by various mafic to felsic plutonic rocks including the Nolan Lake stock (Figure 9.1). The volcanic rocks are divisible into 2 distinct sequences: the Rowan Lake volcanics consisting predominantly of mafic volcanic rocks, and the Cameron Lake volcanics that exhibit greater compositional diversity (*see* Figure 9.1; Blackburn and Hailstone 1984; Melling 1986). All observed facing indicators suggest that the Cameron Lake volcanics are younger than the Rowan Lake volcanics (Kaye 1973; Lewis and Woolgar 2011), although the presence of faults near or along rock contacts may have locally complicated the stratigraphic section (*see* Lewis and Woolgar 2012).

GEOCHEMISTRY

In the Rowan Lake area, 109 bedrock samples were collected (Figure 9.2) and were analyzed for major and trace elements at the OGS Geoscience Laboratories (Geo Labs), Sudbury, Ontario. All samples were crushed using an agate mill (or a high chrome steel mill for mineralized samples or samples of quartz veins) and dissolved using a closed vessel multi-acid digestion. Major elements were analyzed by X-ray fluorescence (XRF) and trace elements were analyzed by inductively coupled plasma mass spectrometry (ICP–MS). For simplicity, the samples have been divided into mafic and felsic subsets and the most highly altered samples have been disregarded for this report.

Mafic to Intermediate Volcanic and Plutonic Rocks

Mafic volcanic rocks (67 samples) are plotted on major and trace element discrimination diagrams (Figure 9.3). On silica (SiO_2) versus total alkali ($\text{Na}_2\text{O} + \text{K}_2\text{O}$) diagrams (LeBas et al. 1986), the samples range in composition from microbasalt to basaltic andesite, although the most common are basalt and basaltic andesite (Figure 9.3A). Immobile lanthanum–yttrium–niobium (La–Y–Nb) discrimination plots for modern-day tectonic settings of Cabanis and Lecolle (1989) divide these basaltic rocks into calc-alkalic and tholeiitic back-arc basin–normal mid-ocean ridge basalt (NMORB) groupings (Figure 9.3B).

The calc-alkalic rocks are characterized by a moderately fractionated rare element profile, with enriched light rare earth elements (LREE) and a more flat heavy REE (HREE) slope with some samples displaying a weak to moderate negative europium anomaly (Figure 9.3C). They are also characterized by strongly negative niobium, tantalum and titanium anomalies when normalized to primitive mantle (Figure 9.3D), which is characteristic of modern-day arc volcanism (Cox, Bell and Pankhurst 1979; Henderson 1984; LeBas et al. 1986).

The tholeiitic rocks are characterized by a flat but enriched profile with weak positive to weak negative europium anomalies (Figure 9.3E). When normalized to primitive mantle, the rocks display a relatively flat profile with depleted thorium and niobium and slightly negative titanium anomalies (Figure 9.3F). These anomalies are consistent with modern-day back-arc basin volcanism (*see* Figure 9.3B).

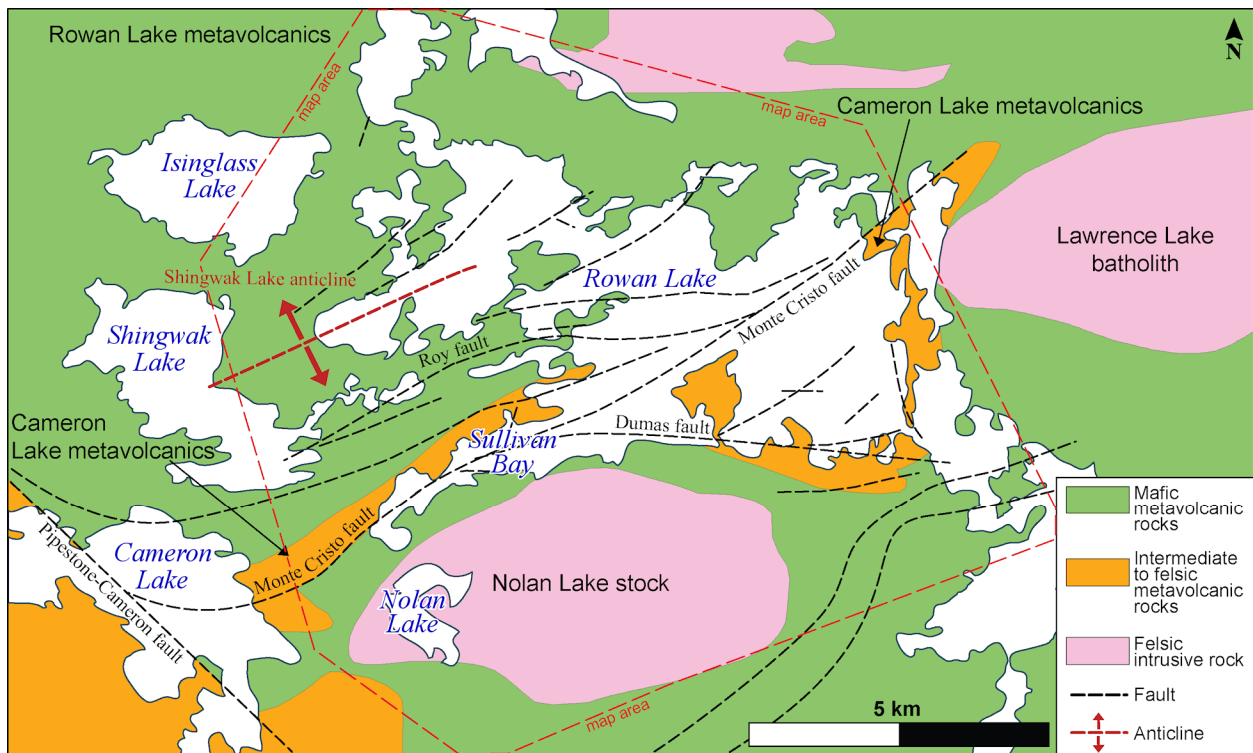


Figure 9.1. Simplified lithologic map of the Rowan Lake area showing the location of the Rowan Lake volcanics, the Cameron Lake volcanics, the Nolan Lake stock, the Lawrence Lake batholith, the Pipestone–Cameron fault, the Monte Cristo fault, the Roy fault and the Shingwak Lake anticline. Mafic rocks south of the Monte Cristo fault have not been studied in detail. Co-ordinates are based on North American Datum 1983 (NAD83), Zone 15.

Intermediate to Felsic Volcanic and Plutonic Rocks

Felsic volcanic and plutonic rocks (14 samples) are plotted on major and trace element discrimination diagrams (Figure 9.4). On silica (SiO_2) versus total alkali ($\text{Na}_2\text{O}+\text{K}_2\text{O}$) diagrams (LeBas et al. 1986), the samples range in composition from trachydacite to dacite to rhyolite (Figure 9.4A). Immobile element ytterbium versus tantalum and yttrium versus niobium plots of Pearce, Harris and Tindle (1984) indicate 2 groupings, with one of these lying entirely within the modern-day volcanic-arc field and the other straddling the modern-day volcanic arc–within-plate field boundary (Figures 9.4B and 9.4C, respectively).

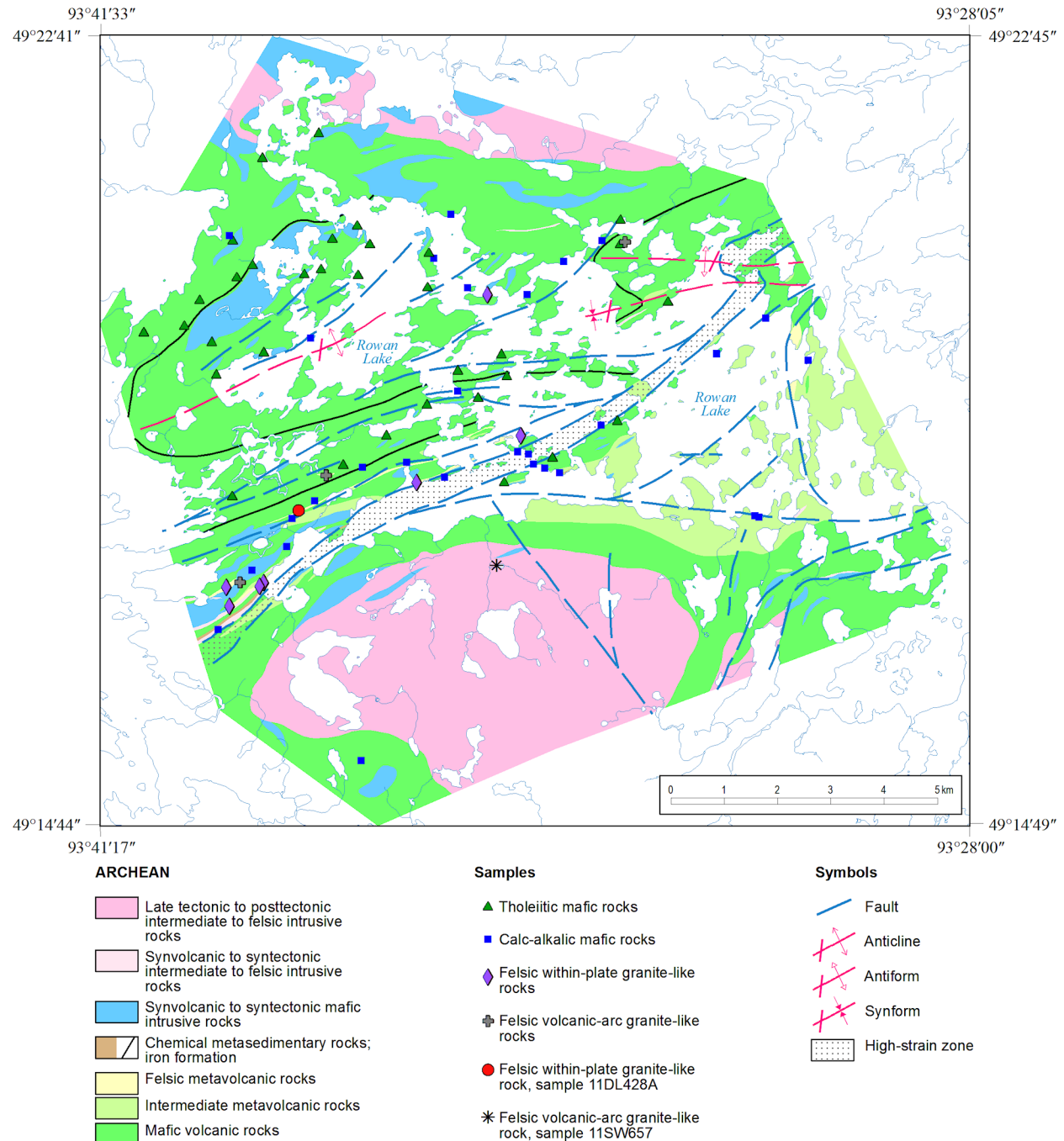


Figure 9.2. Geologic map of the Rowan Lake area showing the distribution of sample locations (*modified from Lewis and Woolgar 2012*). The symbols for rock sample types are also used in Figures 9.3 and 9.4.

The rocks from the group straddling the within-plate field (*see* Figure 9.4B) have elevated REE abundances with moderately fractionated LREE, unfractionated HREE and moderate to very weak negative europium anomalies (Figure 9.4D). On primitive-mantle-normalized REE spider diagrams, these within-plate rocks are characterized by negative niobium, tantalum and titanium anomalies (Figure 9.4E).

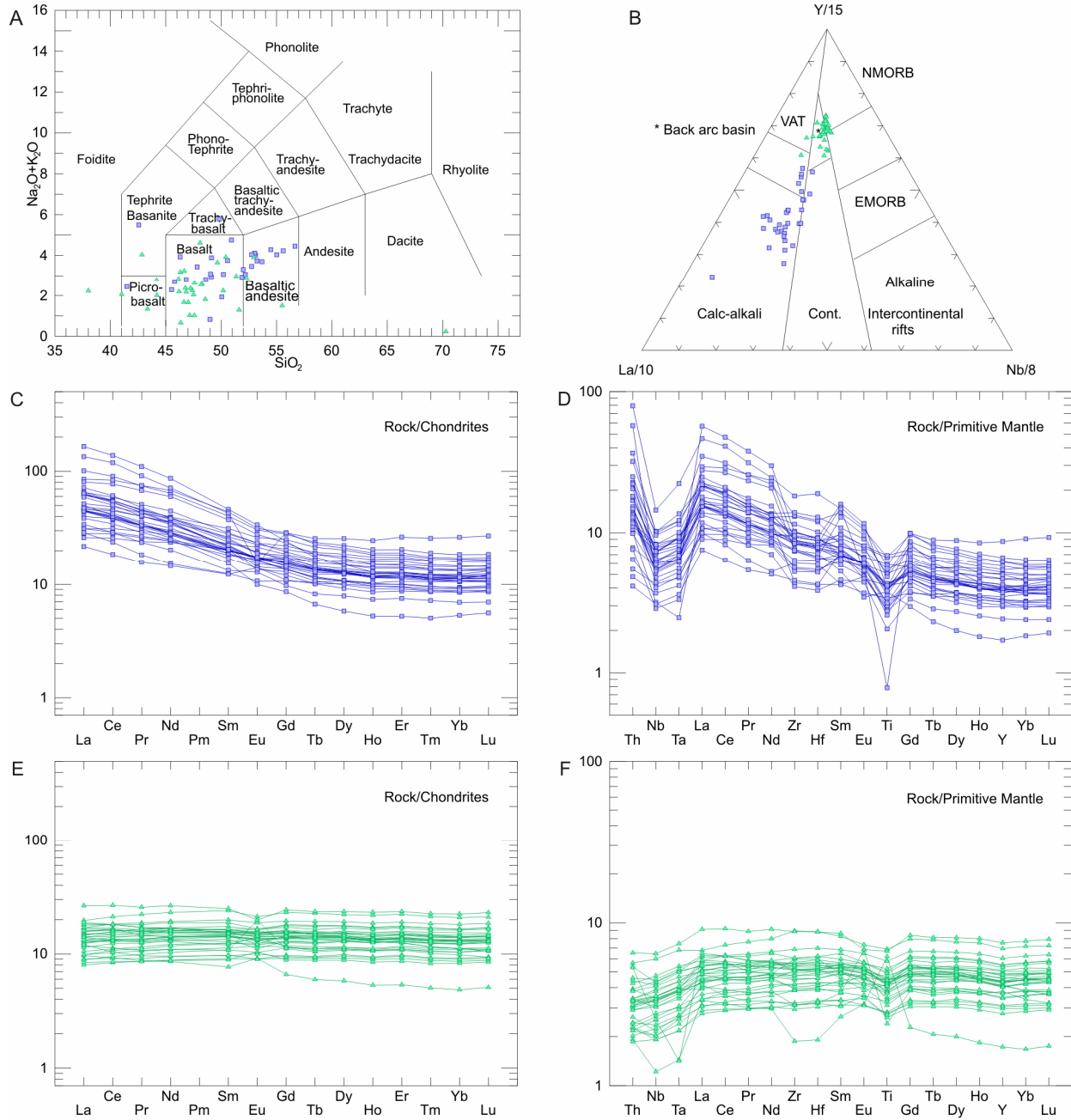


Figure 9.3. Geochemical discrimination diagrams of the mafic volcanic and plutonic rocks from the Rowan Lake area. A) Silica (SiO_2) versus total alkali ($\text{Na}_2\text{O} + \text{K}_2\text{O}$) plot of LeBas et al. (1986). B) Lanthanum–yttrium–niobium (La–Y–Nb) discrimination diagram of Cabanis and Lecolle (1989). Abbreviations: Cont., continental arc; EMORB, enriched mid-ocean ridge basalt; NMORB, normal mid-ocean ridge basalt; VAT, volcanic arc tholeiite. C) Chondrite-normalized rare earth element (REE) plot of the calc-alkalic mafic rocks. D) Primitive mantle-normalized REE plot of the calc-alkalic mafic rocks. E) Chondrite-normalized REE plot of the tholeiitic mafic rocks. F) Primitive mantle-normalized REE plot of the tholeiitic mafic rocks. All normalization values from Sun and McDonough (1989).

Some of these samples are characterized by elevated yttrium (36 to 47 ppm) and zirconium (220 to 274 ppm). These characteristics are similar to those attributed to FII rhyolites (Leshner et al. 1986; Hart, Gibson and Leshner 2004) that may indicate favourable environments for volcanogenic massive sulphide (VMS)-style mineralization.

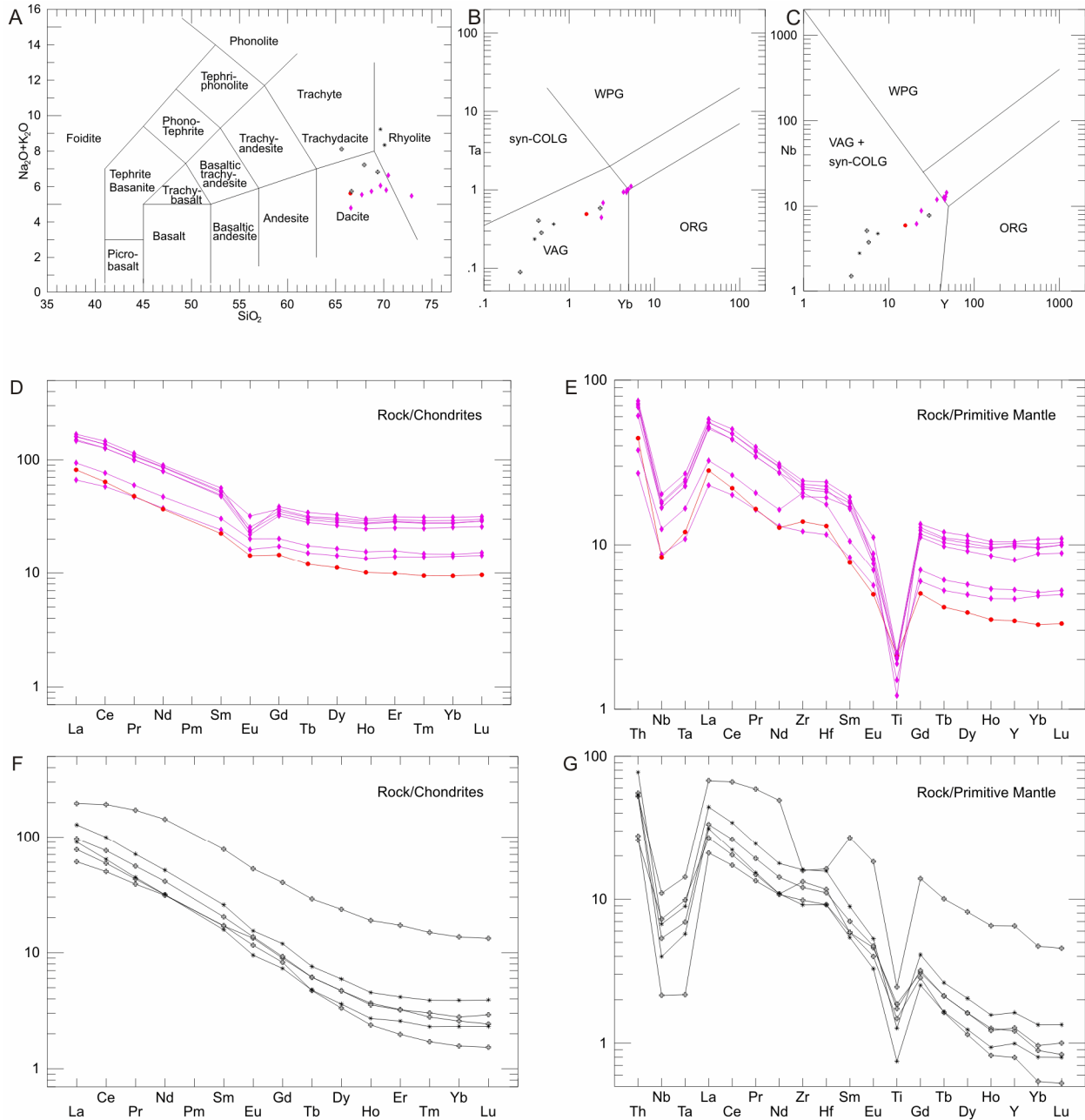


Figure 9.4. Geochemical discrimination diagrams of the felsic volcanic and plutonic rocks from the Rowan Lake area. A) Silica (SiO_2) versus total alkali ($\text{Na}_2\text{O}+\text{K}_2\text{O}$) plot of LeBas et al. (1986). B) Ytterbium (Yb) versus tantalum (Ta) discrimination diagram of Pearce, Harris and Tindle (1984). Abbreviations: COLG, syn-collisional granite; ORG, ocean ridge granite; VAG, volcanic arc granite; WPG, within-plate granite. C) Yttrium (Y) versus niobium (Nb) discrimination diagram of Pearce, Harris and Tindle (1984); abbreviations as for Figure 9.4B. D) Chondrite-normalized REE plot of the within-plate-type felsic rocks. E) Primitive mantle-normalized REE plot of the within-plate-type felsic rocks. F) Chondrite-normalized REE plot of the volcanic-arc boundary-type felsic rocks. G) Primitive mantle-normalized REE plot of the volcanic-arc boundary-type felsic rocks. All normalization values from Sun and McDonough (1989).

In contrast to the within-plate type, the group of samples plotting distinctly within the volcanic-arc field are characterized by strongly fractionated REE with extremely depleted HREE abundances and negligible europium anomalies (Figures 9.4F and 9.4G). These characteristics are more typical of the FI rhyolites (Leshner et al. 1986) that predominate within Archean greenstone belts.

GEOCHRONOLOGY

Two (2) samples were submitted for U/Pb geochronological analysis; the results are presented in this report. Sample 11DL428B, from a felsic volcanic unit, was analyzed at the Jack Satterly Geochronology Laboratory at the University of Toronto; and sample 11SW657, from a felsic intrusive unit, was analyzed at Laurentian University, Sudbury, Ontario.

Analytical Methodology

THERMAL IONIZATION MASS SPECTROMETRIC ANALYSIS AT THE UNIVERSITY OF TORONTO

The sample was crushed, milled, and passed over a Wilfley[®] table to obtain a pre-concentrate of heavy minerals. The pre-concentrate was then split into magnetic fractions before the least magnetic fraction was passed through heavy liquids to separate zircons and other heavy minerals (pyrite, apatite, etc). Zircons were then hand picked from the heavy minerals separates. Zircons were thermally annealed and chemically abraded with hydrofluoric (HF) acid modified from Mattinson (2005) and analyzed using isotope dilution thermal ionization mass spectrometry (ID-TIMS). Uranium and lead were isolated from the zircon solutions and analyzed with a VG354 mass spectrometer using a Daly detector in pulse counting mode. For zircon, all common lead was assigned to a procedural lead blank. Thermal mass discrimination corrections are 0.10% per atomic mass unit. Decay constants are those of Jaffey et al. (1971). All age errors quoted in the text and error ellipses in the concordia diagrams are given at the 95% confidence (2 sigma (2 σ)) interval. Uranium-lead age calculations and plotting were done using Isoplot 3.00 (Ludwig 2003).

LASER ABLATION INDUCTIVELY COUPLED PLASMA MASS SPECTROMETRIC ANALYSIS AT LAURENTIAN UNIVERSITY

The sample was crushed, milled and passed over a Wilfley[®] table to yield a heavy mineral pre-concentrate. This pre-concentrate was split into a series of magnetic fractions. The least magnetic fraction passed through heavy liquids to separate zircons and other heavy minerals (pyrite, apatite, etc). Zircons were then picked from each sample and mounted in one-inch epoxy pucks that were polished down to a 1 μ m paste. All grains were analyzed at Laurentian University using a 193 nm ArF excimer laser (Resonetics RESolution M-50) to vaporize material from each grain with a spot size of 17 μ m. The ablated material was carried via a gaseous stream of helium (600 mL/minute), argon (740 mL/minute), and nitrogen (6 mL/minute) to a Thermo X Series II quadrupole ICP-MS where it was then analyzed for uranium, thorium and lead content. Ablation occurred in ultra-pure helium, with minimal mercury blanks. The U/Pb concordia diagram was constructed using Iolite (Paton et al. 2011) and VizualAge (Petrus and Kamber 2012) programs. The concordia ages and data represent the least-altered and least-contaminated ablated zones of the zircons; highly contaminated and altered zircons were excluded. For information about standards used, *see* Lodge (this volume).

Sample 11DL428B Felsic Volcanic Flow

This fine- to medium-grained felsic volcanic flow is conformable within the volcanic stratigraphy in the Rowan Lake area. Abundant, generally unaltered, euhedral zircon grains were recovered and a selection of these gem-like grains was chemically abraded. Four single zircon grains (Z1-Z4) are concordant and have similar $^{207}\text{Pb}/^{206}\text{Pb}$ ages with a weighted mean of $2732 \pm 2 \text{ Ma}$ (2σ ; MSWD=2.1; Figure 9.5). This is interpreted as the age of the felsic volcanic unit and provides an estimate on the time of volcanism of the Cameron Lake volcanic rocks.

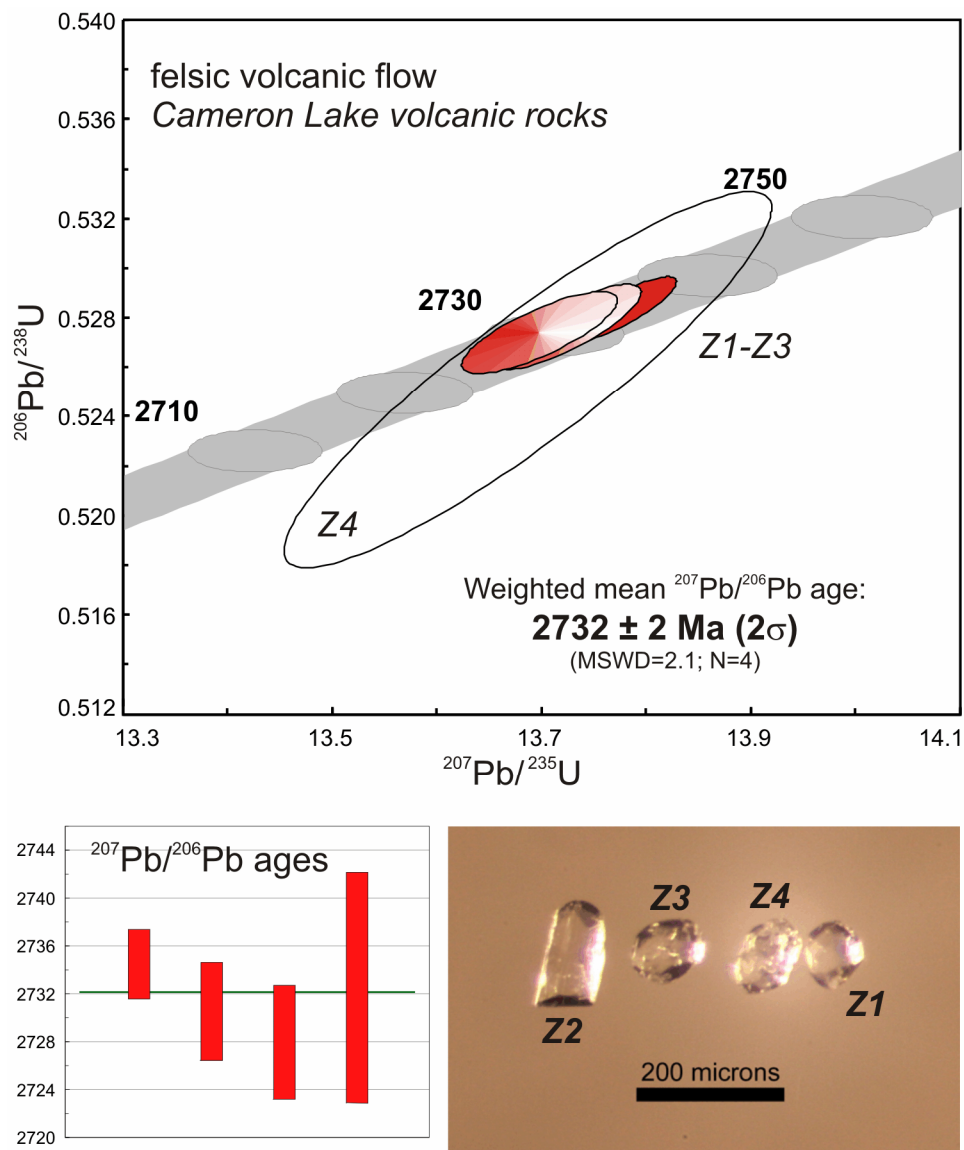


Figure 9.5. Concordia plot and photomicrograph of zircons for sample 11DL428B.

Sample 11SW657 Felsic Intrusive Rock

This medium-grained felsic intrusive rock is from the Nolan Lake stock (*see* Figure 9.1). Zircon grains in this sample were found to be largely euhedral with well-formed crystal faces (Figure 9.6). Most grains were weakly coloured stubby to prismatic crystals with a moderate to high opacity. The majority of the analyses are reversely discordant and the reason for this is unclear. The data are approximately co-linear with a concordia intercept age of 2705 ± 4 Ma (*see* Figure 9.6) that approximates the timing of emplacement of the Nolan Lake stock. There are no obvious older inherited grains.

DISCUSSION

Results from the geochemical investigation of volcanic rocks in the Rowan Lake area reveal a bimodal assemblage consisting of mafic (basalt to basaltic andesite) and more felsic (dacite to rhyolite) components. The mafic component is divisible into tholeiitic and calc-alkalic endmembers. The Rowan Lake volcanics are predominantly tholeiitic in composition, but they also contain interlayered calc-alkalic mafic rocks with the latter being most abundant within the Cameron Lake volcanics. The felsic compositions include components with similarities to both FI and FII rhyolites. The FII rhyolites occur within the Cameron Lake volcanics and may indicate that this assemblage is prospective host for base-metal VMS deposits.

A U/Pb TIMS age for a volcanic unit within the Cameron Lake volcanics is interpreted to indicate a crystallization age of 2732 ± 2 Ma. This age is similar to other ages for volcanic rocks in proximity to the Atikwa batholith (Davis, Blackburn and Krogh 1982). A U/Pb LA-ICP-MS age for the late tectonic Nolan Lake stock is approximately 2705 ± 4 Ma. Evidence presented elsewhere (Lewis and Woolgar 2011) indicates that the contact metamorphic aureole of the Nolan Lake stock predates a late component of dextral displacement on the Monte Cristo shear zone; consequently, the age for the stock also represents a maximum age for this component of deformation.

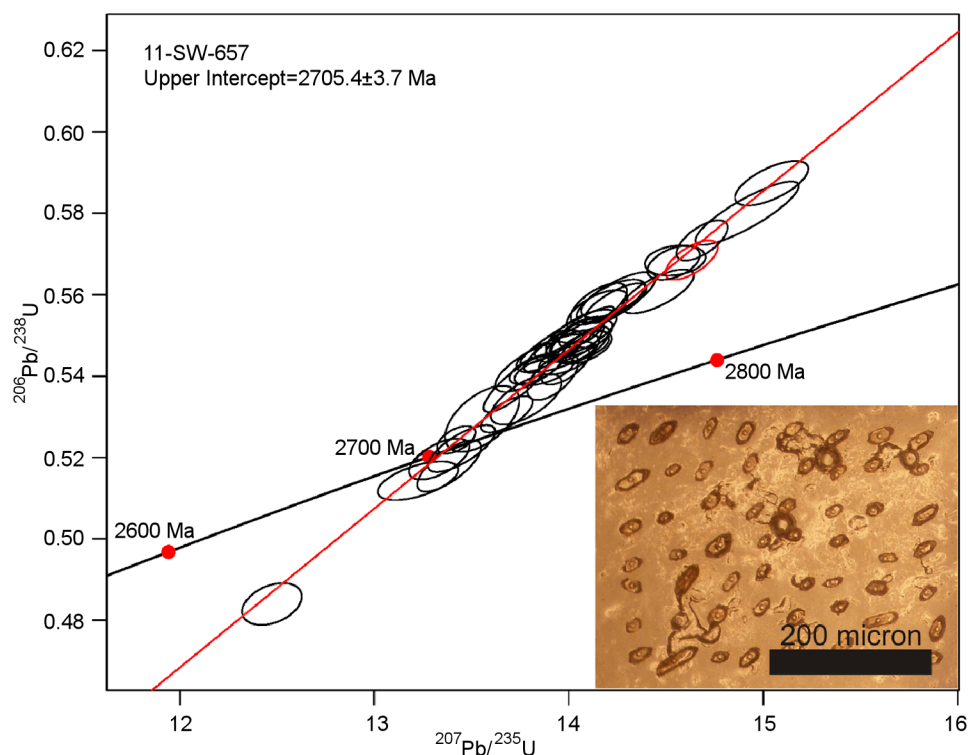


Figure 9.6. Concordia plot and photomicrograph of zircons for sample 11SW657.

REFERENCES

- Blackburn, C.E. and Hailstone, M.R. 1984. The geological environment of gold mineralization, Cameron–Rowan lakes, northwestern Ontario; presentation, Ontario Geological Survey Geoscience Research Seminars, December 6-7, 1983, Toronto, Ontario, 13p.
- Cabanis, B. and Lecolle, M. 1989. Le diagramme La/10-Y/15-Nb/8; un outil pour la discrimination des séries volcaniques et la mise en évidence des processus de mélange et/ou de contamination crustale; *Comptes Rendus de l'Académie des Sciences, Série II, Mécanique, physique, chimie, sciences de l'univers, sciences de la terre*, v.309, p.2023-2029.
- Cox, K.G., Bell, J.D. and Pankhurst, R.J. 1979. The interpretation of igneous rocks; Allen and Unwin, London, 450p.
- Davis, D.W., Blackburn, C.E. and Krogh, T.E. 1982. Zircon U-Pb ages from the Wabigoon–Manitou Lakes region, Wabigoon Subprovince, northwest Ontario; *Canadian Journal of Earth Sciences*, v.19, p.254-266.
- Hart, T.R., Gibson, H.L. and Leshner, C.M. 2004. Trace element geochemistry and petrogenesis of felsic volcanic rocks associated with volcanogenic massive Cu-Zn-Pb sulphide deposits; *Economic Geology*, v.99, p.1003-1013.
- Henderson, P. ed. 1984. Rare earth element geochemistry; Elsevier, Amsterdam, *Developments in Geochemistry* 2, 510p.
- Jaffey, A.H., Flynn, K.F., Glendenin, L.E., Bentley, W.C. and Essling, A.M. 1971. Precision measurement of half-lives and specific activities of ²³⁵U and ²³⁸U; *Physical Reviews*, v.4, p.1889-1906.
- Kaye, L. 1973. Rowan Lake area, District of Kenora; Ontario Geological Survey, Preliminary Map P.831, scale 1:15 840.
- LeBas, M.J., LeMaitre, R.W., Streckeisen, A. and Zanettin, B. 1986. A chemical classification of volcanic rocks based on the total alkali silica diagram; *Journal of Petrology*, v.27, p.745-750.
- Leshner, C.M., Goodwin, A.M., Campbell, I.H. and Gorton, M.P. 1986. Trace-element geochemistry of ore-associated and barren, felsic metavolcanic rocks in the Superior Province, Canada; *Canadian Journal of Earth Sciences*, v.23, p.222-237.
- Lewis, D. and Woolgar, S. 2011. Structural controls and alteration patterns of gold mineralization at Rowan Lake, northwest Ontario; *in* Summary of Field Work and Other Activities 2011, Ontario Geological Survey, Open File Report 6270, p.10-1 to 10-9.
- 2012. Precambrian geology of the Rowan Lake area, northwestern Ontario; Ontario Geological Survey, Preliminary Map P.3766, scale 1:20 000.
- Ludwig, K.R. 2003. User's manual for Isoplot 3.00. A geochronological toolkit for Microsoft® Excel®; Berkley Geochronology Center, Special Publication No. 4, 71p.
- Mattinson, J. 2005. Zircon U-Pb chemical abrasion (CA-TIMS) method: combined annealing and multi-step partial dissolution analysis for improved precision and accuracy of zircon ages; *Chemical Geology*, v.220, p.47-66.
- Melling, D.R. 1986. The occurrence of gold in the Cameron–Rowan Lake area: Preliminary report on the Monte Cristo and Victor Island gold prospects in the Monte Cristo shear zone; *in* Summary of Field Work and Other Activities 1986, Ontario Geological Survey, Miscellaneous Paper 132, p.252-260.
- Paton, C., Hellstrom, J., Paul, B., Woodhead, J. and Hergt, J. 2011. Iolite: freeware for the visualization and processing of mass spectrometer data; *Journal of Analytical Atomic Spectrometry*, v.26, p.2508-2518.
- Pearce, J.A., Harris, B.W. and Tindle, A.G. 1984. Trace element discrimination diagrams for the tectonic interpretation of granitic rocks; *Journal of Petrology*, v.25, p.956-983.

- Petrus, J.A. and Kamber, B.S. 2012. VizualAge: a novel approach to laser ablation ICP-MS U-Pb geochronology data reduction; *Geostandards and Geoanalytical Research*, v.36, p.247-270, DOI: 10.1111/j.1751-1908X.2012.00158.x.
- Sun, S-S. and McDonough, W.F. 1989. Chemical and isotopic systematics of oceanic basalts: implications for mantle compositions and processes; *in* *Magmatism in ocean basins*, The Geological Society, Special Publication No.42, p.313-345.
- Trowell, N.F., Blackburn, C.E and Edwards, G.R. 1980. Preliminary geological synthesis of the Savant Lake–Crow Lake metavolcanic–metasedimentary belt, northwest Ontario and its bearing upon mineral exploration; Ontario Geological Survey, Miscellaneous Paper 89, 30p.

10. Project Unit 10-010. Preliminary Results of Uranium–Lead Geochronology from the Shebandowan Greenstone Belt, Wawa Subprovince

R.W.D. Lodge^{1,2}

¹Mineral Exploration Research Centre, Department of Earth Sciences, Laurentian University, Sudbury, Ontario P3E 2C6

²Earth Resources and Geoscience Mapping Section, Ontario Geological Survey, Sudbury, Ontario P3E 6B5

INTRODUCTION

This article is the third report (*see* previous reports Lodge 2010, 2011) that summarizes some of the results of an ongoing four-year PhD thesis study designed to compare the geodynamic setting of volcanogenic massive sulphide (VMS) mineralization in the Shebandowan, Vermilion, Winston Lake and Manitouwadge greenstone belts along the northern boundary of the Wawa Subprovince adjacent to the Quetico Subprovince (Figure 10.1). This research is supported by the Ontario Geological Survey and the Department of Earth Sciences at Laurentian University through the Ontario Geological Survey–Laurentian University Graduate Mapping School Program.

Mapping during the summers of 2010 and 2011 focussed on investigating the volcanology and geodynamic setting of the Shebandowan, Vermilion, Winston Lake and Manitouwadge greenstone belts. Mapping and sampling were completed along semilinear, regional-scale transects through representative strata within each greenstone belt to determine geodynamic environment and petrogenetic processes of each belt as they relate to VMS-potential. During mapping, more than 800 rock samples were from these belts. Of these samples, 400 were chosen for full geochemical analyses, 70 for neodymium and lead isotopic analyses, 7 for magmatic zircon U/Pb geochronologic analysis, and 7 for detrital zircon U/Pb geochronologic analysis.

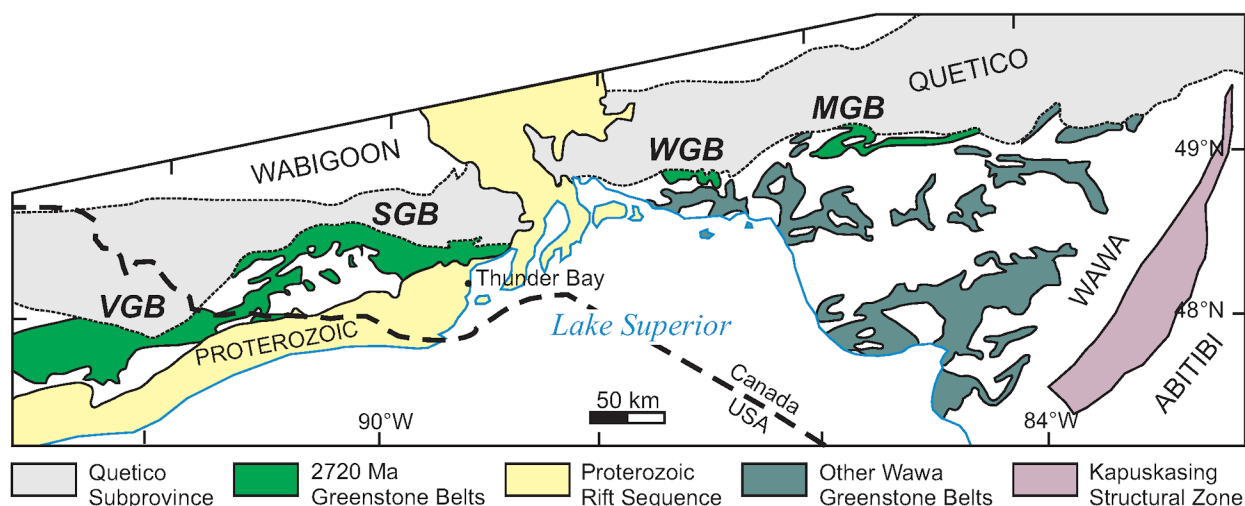


Figure 10.1. General geology of the Wawa Subprovince of the Superior Craton. Abbreviations: MGB, Manitouwadge greenstone belt; SGB, Shebandowan greenstone belt; VGB, Vermilion greenstone belt; WGB, Winston Lake greenstone belt. “Abitibi”, “Quetico”, “Wabigoon” and “Wawa” labels refer to subprovinces of the Archean Superior Province. Figure from Lodge (2011).

Summary of Field Work and Other Activities 2012,
Ontario Geological Survey, Open File Report 6280, p.10-1 to 10-10.

© Queen’s Printer for Ontario, 2012

This report will discuss the preliminary results of the U/Pb geochronology of samples collected from the Shebandowan greenstone belt in 2010 and 2011.

ANALYTICAL METHODS

Three samples were submitted to the Jack Satterly Geochronology Laboratory at the University of Toronto for high-precision U/Pb age determinations by thermal ionization mass spectrometry (TIMS) analysis. One sample for lower-precision U/Pb ages and 5 samples for detrital zircon ages were sent to the laser ablation inductively coupled plasma mass spectrometry (LA-ICP-MS) lab at Laurentian University for analyses. The methodology for zircon separation was the same at both laboratories. Samples were crushed, milled, and passed over a Wilfley[®] table to obtain a pre-concentrate of heavy minerals. The pre-concentrate was then split into magnetic fractions before the least magnetic fraction was passed through heavy liquids to separate zircons and other heavy minerals (pyrite, apatite, etc). Zircons were then hand picked from the heavy minerals separates.

Thermal Ionization Mass Spectrometric Analysis at University of Toronto

The zircons from each sample were thermally annealed and chemically abraded with hydrofluoric (HF) acid using the methodologies outlined by Mattinson (2005) for improved precision of calculated ages for analyzed zircon grains. These processes chemically homogenize the grain and remove the outermost layer of the grains where lead-loss is most likely to occur. Following treatment of the grains, 3 to 5 “ideal” zircons were hand picked on the basis of crystal quality and clarity. These zircons were then dissolved in accordance to the procedures outlined by Krogh (1973). Uranium and lead were separated using anion exchange columns before analysis (Gerstenberger and Haase 1997). Uranium-lead age determinations and plotting of concordia diagrams were completed using Isoplot for Microsoft[®] Excel[®] (Ludwig 2012) and calculated using the U/Pb decay constants from Jaffey et al. (1971).

Laser Ablation Inductively Coupled Plasma Mass Spectrometric Analysis at Laurentian University

Untreated zircons were hand picked and mounted in epoxy for analysis by LA-ICP-MS. All grains were analyzed using a 193 nm ArF excimer laser to vaporize material from each grain with a spot size of 17 μm . The ablated material was carried via a gaseous stream of helium, argon and nitrogen to a Thermo X Series II quadrupole ICP-MS where it was then analyzed for uranium, thorium and lead content. Uranium-thorium-lead data were calibrated using the 91500 zircon geostandard (Wiedenbeck et al. 1995), and quality control was completed with analysis of 2 additional geostandards: the Plešovice (Plešovice quarry zircon, Blanský les granulite body, Bohemian Massif, Czech Republic: Sláma et al. 2008) and Temora-2 (Temora-2 zircon is from the Middledale gabbroic diorite, Temora, New South Wales, Australia: Black et al. 2003). Age determinations of each standard had to be within error from the published accepted age before proceeding with analysis and age determination of sample zircons. Each individual zircon analysis was inspected in terms of signal intensity as a function of time so as to distinguish distinct zones of different Th/U, $^{207}\text{Pb}/^{206}\text{Pb}$, ^{204}Pb , ^{88}Sr and/or ^{209}Bi . Zones of signal showing evidence of alteration (high ^{88}Sr) or common-lead contamination (high ^{204}Pb , ^{209}Bi , erratic $^{207}\text{Pb}/^{206}\text{Pb}$ ages) were not integrated for final age determination of the zircon. Uranium-lead concordia diagrams were constructed using Iolite (Paton et al. 2011) and VizualAge (Petrus and Kamber 2012) programs. Histograms were generated using Isoplot for Microsoft[®] Excel[®] (Ludwig 2012).

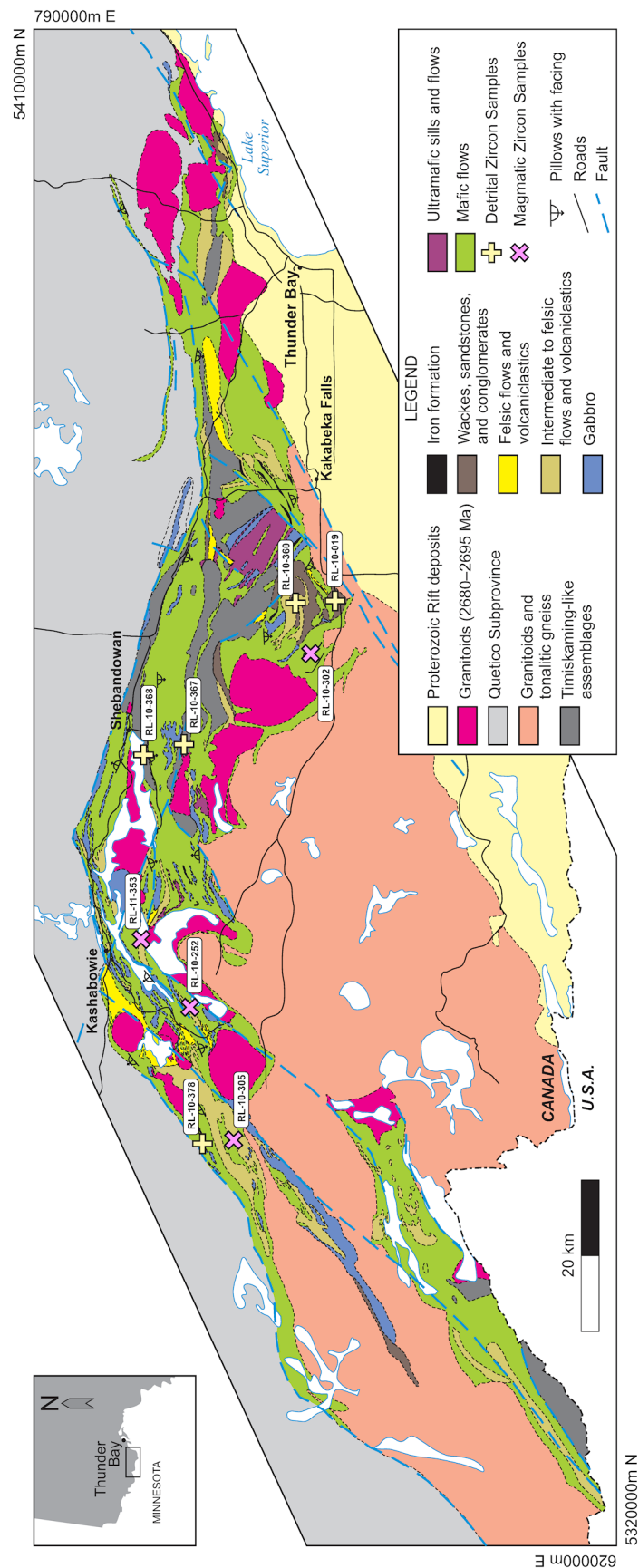


Figure 10.2. Regional geology of the Shebandowan greenstone belt showing locations of samples taken for U/Pb geochronological analysis. Figure *modified from* Lodge (2011) and compiled and *modified from* Santiaguda (2001a, 2001b). Universal Transverse Mercator (UTM) co-ordinates are provided using North American Datum 1983 (NAD83), Zone 15.

Table 10.1. Details of samples collected from the Shebandowan greenstone belt.

Sample	Township or Area	UTM Zone	Easting (m)	Northing (m)	Method	Age Type
RL-10-019	Marks	16	291133	5364950	LA-ICP-MS	Detrital
RL-10-252	Burchell Lake Area	15	680320	5379603	TIMS	Volcanic
RL-10-302	Aldina	16	283069	5365089	TIMS	Volcanic
RL-10-360	Adrian	16	290767	5369539	LA-ICP-MS	Detrital
RL-10-367	Duckworth	15	715382	5387512	LA-ICP-MS	Detrital
RL-10-368	Conacher	15	715817	5383007	LA-ICP-MS	Detrital
RL-10-378	Moss	15	662733	5377895	LA-ICP-MS	Detrital
RL-11-305	Moss	15	664180	5375812	TIMS	Volcanic
RL-11-353	Greenwater Lake Area	15	688477	5387009	LA-ICP-MS	Volcanic

All UTM co-ordinates are reported in NAD83. Abbreviations: LA-ICP-MS, laser ablation inductively coupled plasma mass spectroscopy; TIMS, thermal ionization mass spectroscopy.

By using VizualAge to determine U/Pb ages (Petrus and Kamber 2012), most of the data points were near concordant and only a few samples that were more than 10% discordant were rejected from the final data set. Magmatic ages were determined in VizualAge by statistical analysis of clustered and overlapping data points. The average error for the $^{207}\text{Pb}/^{206}\text{Pb}$ ages for individual grains averaged 20 to 40 m.y., but was often as low as 10 to 15 m.y. Therefore, trends in the age of the population are more relevant for interpreting the data rather than the age of individual grains in detrital zircon analysis.

RESULTS AND DISCUSSION

Geochronologic sampling in the Shebandowan greenstone belt (*see* Figure 10.2 for sample locations) focussed on establishing the age of volcanism in VMS-prospective strata throughout the belt. Detrital zircon analysis was conducted on 5 samples from various metasedimentary basins to better understand the provenance of the detritus, tectonic evolution of the belt and metallogenic significance of the basins. Previous geochronological studies in the Shebandowan greenstone belt (Corfu and Stott 1986, 1998; Hart 2007) established 3 main assemblages: Greenwater (*circa* 2720 Ma), Kashabowie (*circa* 2695 Ma) and Shebandowan (*circa* 2680 to 2690 Ma). The details of each sample analyzed are summarized in Table 10.1.

Detrital zircon analyses for each of the samples produced ages that are significantly younger than 2680 Ma (Figure 10.3), which is the previous youngest age for a unit in the Shebandowan greenstone belt (Corfu and Stott 1998). These younger ages are interpreted to be the result of analyzing a metamorphic rim or overgrowth. Detrital grains were untreated before picking and mounting for analysis and, therefore, these younger zircon growths may have been preserved despite abrasion during polishing. Therefore, the youngest ages (post-2680 Ma) most likely reflect younger regional thermal events and not a younger sedimentary provenance.

Sample RL-10-019 Thinly Bedded Wacke

This sample is a dark, thinly bedded wacke to sandstone taken from a roadside outcrop on Adrian Lake Road in Marks Township. Bedding is planar and ranges in thickness from 1 to 3 cm in the sampled outcrop. Other outcrops in the immediate area are sandstones and heterolithic paraconglomerates that are interpreted to be deposited in a shallow marine to fluvial environment (Rogers and Berger 1995). Erosional features such as channel structures are present in nearby outcrops.

Detrital zircons from this sample ($n = 143$) are generally small, equant to slightly prismatic crystals. They are typically euhedral with slightly rounded crystal facies. Grains have a high to moderate level of

opacity and are colourless to weakly coloured. All analyzed grains fall within 10% discordance. The calculated $^{207}\text{Pb}/^{206}\text{Pb}$ ages for the detrital zircons are graphically summarized as a histogram in Figure 10.3. A preliminary version of this data is presented in Lodge (2010).

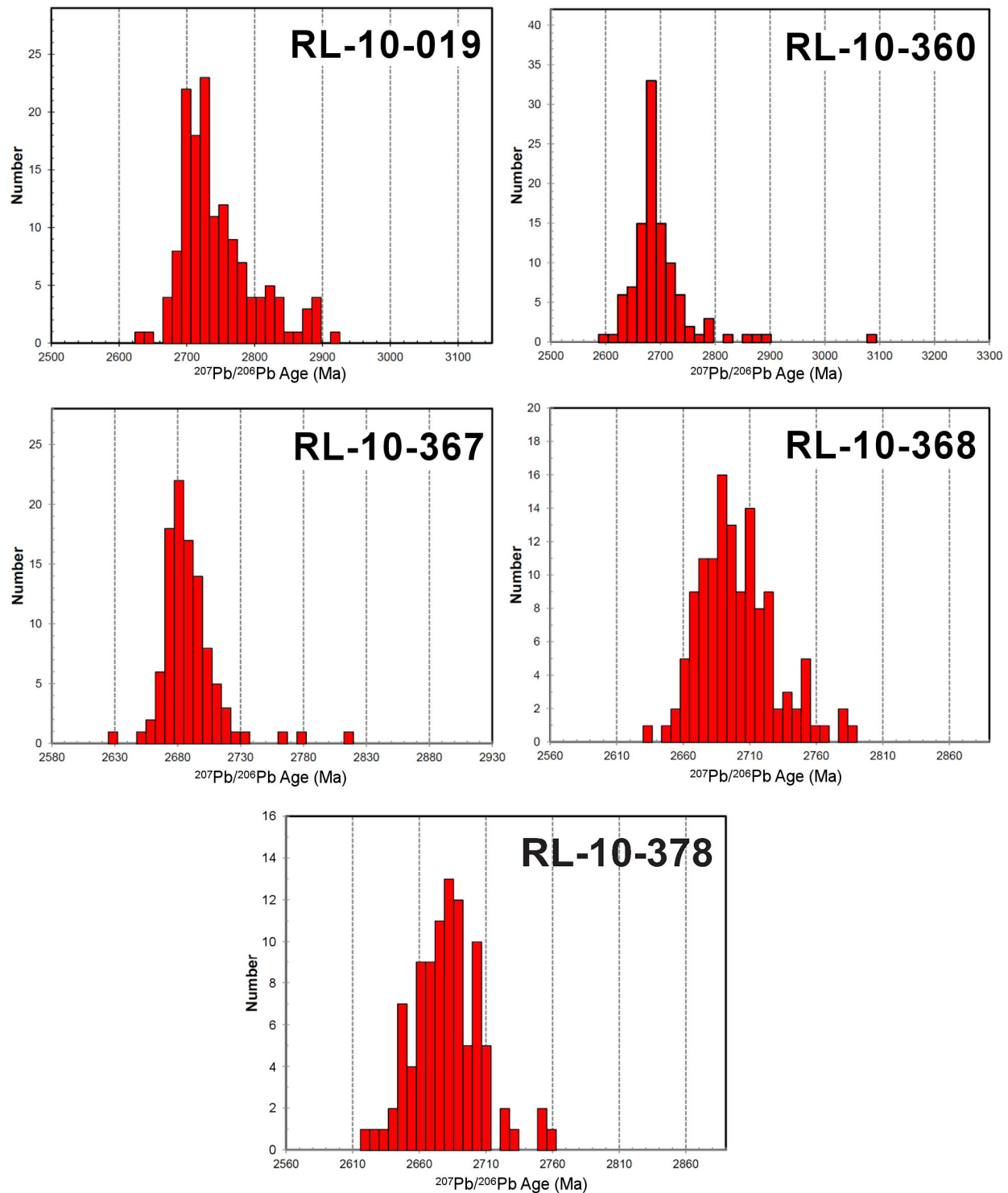


Figure 10.3. Histograms showing distribution of $^{207}\text{Pb}/^{206}\text{Pb}$ ages for detrital zircons for each sample analyzed in 2010 and 2011 from the Shebandowan and Winston Lake greenstone belts.

The ages define a broad peak centred at 2700 to 2720 Ma with zircons as young as 2620 Ma. A significant proportion of detrital zircon ages are older than 2750 Ma, which represents the oldest rocks for which ages have been determined in the Shebandowan greenstone belt (Corfu and Stott 1998). The higher proportion of older ages (>2750 Ma) suggests that the sedimentary provenance of this sample extends beyond this region of the Wawa Subprovince.

Sample RL-10-252 Bedded Felsic Tuff and Crystal Tuff

This sample is from a bedded felsic volcanoclastic unit located near the southern tip of Upper Shebandowan Lake. Bedding in this unit varied in thickness, ranging from centimetre-scale to massive metre-scale beds. The sample contained interbedded felsic crystal tuff and tuff. The crystal tuff was composed of 35 to 60% feldspar crystals. The tuff layers were composed of a silt- to sand-sized felsic ash and were locally graded. In the immediate area, this unit also had metre-scale beds of coarse monolithic tuff breccia and minor heterolithic tuff breccia. Localized chlorite-garnet-pyrite alteration resembling metamorphosed VMS-associated hydrothermal alteration was present within this volcanoclastic unit.

Four zircons were selected after treatment for analysis. These grains are generally equant to slightly prismatic, doubly terminated, euhedral, sharply faceted crystals. These single-grain analyses gave concordant and overlapping data that have a weighted mean $^{207}\text{Pb}/^{206}\text{Pb}$ age of 2693.82 ± 0.87 Ma (Kamo 2011). This is interpreted to be the age of volcanism for this unit and this unit is assigned to the Kashabowie assemblage.

Sample RL-10-302 Massive Felsic Flow

This sample was from a massive siliceous, muscovite-bearing felsic metavolcanic flow. Faint feldspar phenocrysts are visible on a freshly sawed surface and compose 1 to 2% of the rock. This felsic metavolcanic flow is associated with the VMS prospect explored by RJK Exploration Ltd. and is taken from one of the trenched outcrop exposures. Felsic volcanoclastic rocks were intersected in diamond-drill core (Franklin 2001), but were not observed in surface exposures during the 2010 field investigation. There is very little outcrop in this area other than in the trenches, so regional variation in the unit is unknown.

Four zircons were selected after treatment for analysis. Three grains are long prismatic euhedral crystals and 1 grain was more equant. The single-grain analyses produced concordant and overlapping data that have a weighted mean $^{207}\text{Pb}/^{206}\text{Pb}$ age of 2719.7 ± 1.0 Ma (Kamo 2011). This is interpreted to be the age of the felsic flow and this unit is assigned to the Greenwater assemblage.

Sample RL-10-360 Massive Pebbly Sandstone

This sample is from a dark pebbly sandstone located in Adrian Township. The heterolithic clasts are up to 1 cm in size and compose approximately 20 to 30% of the rock. The clasts are supported in a sandy feldspar-rich matrix. Clasts are subangular and are moderately sorted. Clast composition ranges from dominantly mafic volcanic to intermediate volcanic rocks. Variation in clast sizes and abundances define metre-scale bedding in this area. These sediments were interpreted to be deposited in a shallow marine to fluvial setting (Lodge 2011; Rogers and Berger 1995).

Detrital zircons from this sample ($n = 128$) range from equant to stubby to prismatic crystals. In general, the zircons are slightly rounded reflecting sedimentary transport. They are generally colourless to weakly coloured and have moderate to high opacity. Data from these zircons are mostly concordant, with some evidence for lead-loss resulting in a higher degree of discordance. Data obtained from 23 zircons were higher than 10% discordance and were not included when plotting the histogram in Figure 10.3.

Uranium–lead ages from this sample define a tight peak centred at 2685 to 2695 Ma. The dominance of detrital zircons with ages equivalent to the age of the Shebandowan assemblage suggest a localized provenance for the detritus that was likely sourced from Shebandowan assemblage metavolcanic rocks. There are some older zircons, younger than 2750 Ma, which were either inherited from basement strata (no age determined) or have a provenance outside this region of the Wawa Subprovince.

Sample RL-10-367 Weakly Bedded Wacke

This sample is from a dark wacke to sandstone located in the central part of Duckworth Township. There is faint planar bedding noted by slight, centimetre-scale colour changes. Most of the metasedimentary outcrops in the immediate area are similar to the sampled outcrop. Aside from the planar bedding, the sampled unit is featureless and exposure is generally poor because of lichen cover.

Detrital zircons from this sample ($n = 113$) range from equant to stubby to weakly prismatic crystals. In general, the degree of rounding in these grains is minimal. They are generally colourless to weakly coloured and have moderate to high opacity. Data from these zircons are mostly concordant, with some evidence for lead-loss resulting in a higher degree of discordance. Data obtained from 11 zircons exceed the 10% discordance limit and are not included in the histogram of Figure 10.3.

The sample shows a distribution of U/Pb ages that define a moderately tight peak centred at 2680 to 2695 Ma. The dominance of detrital zircons with ages equivalent to the age of the Shebandowan assemblage suggests a localized provenance for the detritus that was likely sourced from Shebandowan assemblage metavolcanic rocks. Older zircons, younger than 2750 Ma, were either inherited from basement strata (age not determined) or have a provenance outside this region of the Wawa Subprovince.

Sample RL-10-368 Heterolithic Paraconglomerate

This sample is from a foliated, heterolithic paraconglomerate located along the Shebandowan Mine road in Conacher Township. The clast composition is highly varied and includes mafic to felsic volcanic rocks, sulphide mineralization, jasper and minor mafic to intermediate intrusive rocks. The conglomerate is moderately sorted and bedding is defined by the abundance and size of clasts. The paraconglomerate has been interpreted to be deposited in an alluvial–fluvial environment (Shegelski 1980). This outcrop is in close association with a reddish green, hornblende-phyric andesite to trachyandesite tuff breccia that is the characteristic volcanic lithofacies of the Shebandowan assemblage (Carter 1993; Corfu and Stott 1998; Shegelski 1980).

Detrital zircons from this sample ($n = 126$) range from equant to stubby to prismatic crystals. In general, the zircons are euhedral and the degree of rounding in these grains was minimal. They are generally colourless to weakly coloured and have moderate to high opacity. Data from these zircons are all near concordant, with very little evidence for lead-loss. The age distribution of the detrital zircons is represented as a histogram in Figure 10.3.

The distribution of U/Pb ages form a broad peak centred at 2680 to 2695 Ma. The dominance of detrital zircons with ages equivalent to the age of the Shebandowan assemblage suggests a localized provenance for the detritus that was likely sourced from Shebandowan assemblage metavolcanic rocks. There is a significant population that have ages *circa* 2720 Ma, suggesting a provenance from the Greenwater assemblage. The few, older zircons younger than 2750 Ma were either inherited from basement strata (age not determined) or have a provenance outside this region of the Wawa Subprovince.

Sample RL-10-378 Heterolithic Paraconglomerate

This sample is from a roadside exposure of a massive heterolithic pebble paraconglomerate located in Moss Township. There is no obvious bedding in this exposure. The clasts are poorly to moderately size sorted and constitute 40 to 60% of the rock. Clasts are 1 to 2 cm in size and are composed of mafic and felsic volcanic rocks with minor felsic intrusion clasts. The clasts are supported in a sandy, green matrix. There are no other exposures of this conglomerate or any other metasedimentary rocks in the immediate area where the strata is dominated by mafic volcanic lithofacies.

Detrital zircons from this sample ($n = 113$) range from equant to weakly prismatic, euhedral crystals. In general, the degree of rounding in the zircons is minimal. They are generally colourless to weakly coloured and have moderate to high opacity. Data from these zircons are all near concordant, with evidence for minor lead-loss. Data obtained from 17 zircons were higher than the 10% discordance cut-off and were not included when plotting the histogram in Figure 10.3.

The U/Pb ages form a broad peak centred at 2660 to 2695 Ma. There are a larger proportion of younger ages (post-2680 Ma) in this sample compared to others, and this may reflect a stronger metamorphic overprint. This sample is in close proximity to the northern margin of the Shebandowan greenstone belt and may have been influenced by later thermal events in the Quetico Subprovince (e.g., Davis, Pezzutto and Ojakangas 1990). Additional work on the analyzed zircons would be required to establish whether or not the ablated material was from a metamorphic rim or if there is a younger magmatic rock contributing detritus to this basin. If the latter was the case, then this would represent one of the youngest basins, as well as youngest igneous detritus, in the Shebandowan greenstone belt. Other than the youngest zircons, the main provenance of detritus appears to be the Shebandowan and Greenwater assemblages.

Sample RL-11-305 Pumiceous Felsic Lapilli Tuff

This sample is a light-coloured felsic crystal-rich pumiceous lapilli tuff located in Moss Township. Feldspar crystals in the matrix are 1 to 3 mm in size and often show broken crystal shapes. The quartzphyric pumice fragments are 1 to 6 cm in size and compose 20 to 40% of the rock. These volcanoclastic deposits are in close association with autobrecciated to massive felsic flows that are exposed nearby.

At the time of report writing, results have not been returned from the Jack Satterly Geochronology Laboratory. These results will be published in 2013 (*see* “Future Work Planned”).

Sample RL-11-353 Pumiceous Felsic Lapilli Tuff

This sample is from a light coloured pumice-bearing, felsic lapilli tuff located on the northern shoreline of Greenwater Lake. The sample is notable for the exceptional preservation of pumice fragments and feldspar-rich siliceous matrix. Pumice ranges from 1 to 5 cm in size and composes 20 to 25% of the rock. The presence of a siliceous matrix and the high abundance of pumice is consistent with a primary volcanoclastic deposit. This felsic unit is located along strike from pyrite-chalcopyrite-bearing sericitic schist. The nature of this mineralization is uncertain, but appears to be shear hosted and the property is currently being explored by Benton Resources Ltd.

Zircons in this sample are largely subhedral and display moderately formed crystal faces. Most grains are stubby, equant, or moderately prismatic. This sample had a lower zircon yield and, therefore, only 18 grains were analyzed by LA-ICP-MS. All data obtained from this sample produced a tight group

of concordant ages. When the best analyses were isolated, they provided a concordant age of 2723.1 ± 4.4 Ma. This is interpreted to be the age of volcanism for this unit and this felsic unit is assigned to the Greenwater assemblage.

FUTURE WORK PLANNED

A Miscellaneous Release—Data (MRD) of all geochemical (major, trace, REE), isotopic (Sm/Nd, $^{207}\text{Pb}/^{204}\text{Pb}$), and U/Pb geochronological data will be released in 2013 and will be available online at GeologyOntario (www.ontario.ca/geology). This MRD will be a geographic information system (GIS)–based product and all geochemical and isotopic data and interpretations will be spatially controlled by results of the 2010 and 2011 mapping programs conducted in the Shebandowan, Winston Lake and Manitouwadge greenstone belts. All data will be released in both shape (ESRI® ArcGIS®) and Microsoft® Excel® file formats. Tables of all zircon analyses discussed in this report will be included with the MRD.

ACKNOWLEDGMENTS

This is the third report of a four-year PhD thesis project supported by the Mineral Exploration Research Centre (MERC) at the Department of Earth Sciences, Laurentian University (LU) and the Ontario Geological Survey and is co-supervised by Dr. Harold Gibson (LU) and Dr. Greg Stott (Stott Geoconsulting Ltd. (formerly OGS)). Additional members of the thesis committee are Dr. Doug Tinkham (LU) and Dr. Jim Franklin (Consultant). Additional funding is provided by the Natural Sciences and Engineering Research Council of Canada (NSERC) and the Society of Economic Geologists (SEG) Student Research Grant. Joe Petrus assisted with LA-ICP–MS analysis at Laurentian University. Michael Hamilton and Sandra Kamo completed the TIMS analyses at the Jack Satterly Geochronology Laboratory, University of Toronto.

REFERENCES

- Black, L.P., Kamo, S.L., Allen, C.M., Aleinikoff, J.N., Davis, D.W., Korsch, R.J. and Foudoulis, C. 2003. TEMORA 1: a new zircon standard for Phanerozoic U–Pb geochronology; *Chemical Geology*, v.200, p.155-170.
- Carter, M.W. 1993. The geochemical characteristics of Neoproterozoic alkaline magmatism in central Superior Province; *in* Summary of Field Work and Other Activities 1993, Ontario Geological Survey, Miscellaneous Paper 162, p.13-19.
- Corfu, F. and Stott, G.M. 1986. U–Pb ages for late magmatism and regional deformation in the Shebandowan Belt, Superior Province, Canada; *Canadian Journal of Earth Sciences*, v.23, p.1075-1082.
- 1998. Shebandowan greenstone belt, western Superior Province: U–Pb ages, tectonic implications, and correlations; *Geological Society of America Bulletin*, v.110, p.1467-1484.
- Davis, D.W., Pezzutto, F. and Ojakangas, R.W. 1990. The age and provenance of metasedimentary rocks in the Quetico Subprovince, Ontario, from single zircon analyses: implications for Archean sedimentation and tectonics in the Superior Province; *Earth and Planetary Science Letters*, v.99, p.195-205.
- Franklin, J.M. 2001. Preliminary assessment of the lithogeochemistry of the Aldina township base metal-gold-silver property; unpublished report by Franklin Geosciences Ltd. for RJK Explorations–Greater Leonora Resource Corp.
- Gerstenberger, H. and Haase, G. 1997. A highly effective emitter substance for mass spectrometric Pb isotope ratio determinations; *Chemical Geology*, v.136, p.309-312.

- Hart, T.R. 2007. Geochronology of the Hamlin and Wye lakes area, Shebandowan greenstone belt, Thunder Bay District; *in* Summary of Field Work and Other Activities 2007, Ontario Geological Survey, Open File Report 6213, p.9-1 to 9-8.
- Jaffey, A.H., Flynn, K.F., Glendenin, L.E., Bentley, W.C. and Essling, A.M. 1971. Precision measurement of half-lives and specific activities of ^{235}U and ^{238}U ; *Physical Reviews*, v.4, p.1889-1906.
- Kamo, S.L. 2011. Report on the U-Pb CA-ID-TIMS geochronology on volcanic and plutonic rocks, Grenville and Superior provinces, Ontario, for the Ontario Geological Survey; unpublished report, Jack Satterly Geochronology Laboratory, Department of Geology, University of Toronto, 22 Russell Street, Toronto, Ontario, 38p.
- Krogh, T.E. 1973. A low contamination method for hydrothermal decomposition of zircon and extraction of U and Pb for isotopic age determinations; *Geochimica et Cosmochimica Acta*, v.37, p.485-494.
- Lodge, R.W.D. 2010. Volcanology and lithofacies of the Shebandowan greenstone belt, Wawa Subprovince; *in* Summary of Field Work and Other Activities 2010, Ontario Geological Survey, Open File Report 6260, p.16-1 to 16-22.
- 2011. A progress report on the volcanology, stratigraphy and geodynamic setting of greenstone belts of age 2720 Ma near the Wawa–Quetico subprovincial boundary; *in* Summary of Field Work and Other Activities 2011, Ontario Geological Survey, Open File Report 6270, p.11-1 to 11-13.
- Ludwig, K.R. 2012. User's manual for Isoplot 3.75. A geochronological toolkit for Microsoft® Excel®; Berkley Geochronology Center, Special Publication No. 5, 75p.
- Mattinson, J.M. 2005. Zircon U-Pb chemical abrasion (“CA-TIMS”) method: combined annealing and multi-step partial dissolution analysis for improved precision and accuracy of zircon ages; *Chemical Geology*, v.220, p.47-66.
- Paton, C., Hellstrom, J., Paul, B., Woodhead, J. and Hergt, J. 2011. Iolite: freeware for the visualization and processing of mass spectrometer data; *Journal of Analytical Atomic Spectrometry*, v.26, p.2508-2518.
- Petrus, J.A. and Kamber, B.S. 2012. VizualAge: a novel approach to laser ablation ICP-MS U-Pb geochronology data reduction; *Geostandards and Geoanalytical Research*, v.36, p.247-270, DOI: 10.1111/j.1751-1908X.2012.00158.x.
- Rogers, M.C. and Berger, B.R. 1995. Precambrian geology, Adrian, Marks, Sackville, Aldina and Duckworth townships; Ontario Geological Survey, Report 295, 66p.
- Santaguida, F. 2001a. Precambrian geology compilation series–Quetico sheet; Ontario Geological Survey, Map 2663, scale 1:250 000.
- 2001b. Precambrian geology compilation series–Thunder Bay sheet; Ontario Geological Survey, Map 2664, scale 1:250 000.
- Shegelski, R.J. 1980. Archean cratonization, emergence and red bed development, Lake Shebandowan area, Canada; *Precambrian Research*, v.12, p.331-347.
- Sláma, J., Košler, J., Condon, D.J., Crowley, J.L., Gerdes, A., Hanchar, J.M., Horstwood, M.S.A., Morris, G.A., Nasdala, L., Noberg, N., Schaltegger, U., Schoene, B., Turbrett, M. and Whitehouse, M.J. 2008. Plešovice zircon - a new natural reference material for U-Pb and Hf isotopic microanalysis; *Chemical Geology*, v.249, p.1-35.
- Wiedenbeck, M., Allé, P., Corfu, F., Griffen, W.L., Meier, M., Oberli, F., Von Quadt, A., Roddick, J.C. and Spiegel, W. 1995. Three natural zircon standards for U-Th-Pb, Lu-Hf, trace element and REE analyses; *Geostandards Newsletter*, v.19, p.1-23.

11. Project Unit 10-002. Uranium–Lead Geochronological Results from the Keezhik Lake and Miminiska Lake Area, Fort Hope Greenstone Belt, Eastern Uchi Subprovince

S. Buse¹ and M.A. Hamilton²

¹Earth Resources and Geoscience Mapping Section, Ontario Geological Survey, Sudbury, Ontario P3E 6B5

²Jack Satterly Geochronology Laboratory, University of Toronto, Toronto, Ontario M5S 3B1

INTRODUCTION

The Keezhik Lake and Miminiska Lake area, located 200 km northwest of Nakina (Figure 11.1) in the eastern Uchi Subprovince, was mapped during the summers of 2010 and 2011 as part of the multiyear Fort Hope greenstone belt bedrock mapping project (Buse and Purdy 2010; Buse 2011). Both the Keezhik Lake and Miminiska Lake 1:50 000 scale bedrock maps and their accompanying geochemical and geochronological data were published in April 2012 (Buse and Purdy 2012; Buse 2012a, 2012b); a simplified version of the 2 maps is presented in Figure 11.2. The Keezhik Lake and Miminiska Lake areas were first mapped by Prest (1939) and the Miminiska Lake area was subsequently mapped by Wallace (1978a, 1978b).

Four distinct terranes—packages of rock that appear to be temporally and genetically related—were recognized in the map area based on field relationships observed during bedrock mapping. These include the Keezhik metavolcanic terrane, the South Miminiska metavolcanic terrane, the Miminiska metasedimentary terrane and the North Miminiska metavolcanic terrane (Figure 11.3).

The Keezhik metavolcanic terrane encompasses the majority of the Keezhik Lake area and comprises homoclinal, south-facing volcanic stratigraphy. The lowest stratigraphic unit, located in the northern part of the map area, is composed of platformal massive to pillowed mafic metavolcanic rocks with thin interbedded tuffaceous units, which are interpreted to have originated from a distal source. The Keezhik volcanic complex, located in the centre of the terrane, is dominantly composed of an intermediate metavolcanic succession of massive, vesiculated flows and breccias, with local tuffaceous units. The volcanic complex is cored by a tonalitic to trondhjemitic synvolcanic intrusion containing roof pendants of the material immediately surrounding the intrusion. The intrusion is interpreted to be the upper magma chamber for the volcanic centre. The Keezhik volcanic complex is overlain by mafic metavolcanic flows and an intraformational conglomerate.

The 3 remaining terranes all face to the north. The South Miminiska metavolcanic terrane is composed of mafic massive to pillowed flows with synvolcanic gabbro sills and minor felsic tuffaceous units. This is overlain by the Miminiska metasedimentary terrane, which is a wacke-dominated, basinal turbidite sequence interlayered with local iron formation. These metasedimentary rocks are overlain by a conglomerate unit and a wedge of felsic metavolcanic rocks on the western side of the sedimentary basin. Lastly, the North Miminiska metavolcanic terrane is composed of mafic massive to pillowed metavolcanic rocks with local synvolcanic gabbroic sills and felsic tuffaceous units.

Several large synvolcanic batholiths, such as the north Keezhik intrusion, form the boundaries of the greenstone belt (*see* Figure 11.2). A chain of smaller plutons, referred to as the Keezhik plutonic complex,

are located between the Keezhik metavolcanic terrane and the North Miminiska metavolcanic terrane. These intrusions are interpreted to be syntectonic to posttectonic relative to the D₁ deformational event. The Kawitos batholith, located on the eastern side of the Miminiska metasedimentary terrane, is interpreted to have intruded at the time of the D₂ deformational event. There are 3 main deformational events that effect the Keezhik and Miminiska Lakes area and are important to understand when interpreting geochronological data. These events are summarized in Table 11.1. For more information on the rocks that make up these terranes and the structural geology of the area, refer to Buse and Purdy (2010, 2012) and Buse (2011, 2012a).

SAMPLE DESCRIPTION AND RESULTS

This section provides a summary of recent U/Pb geochronological age determinations for 11 samples collected in the Keezhik and Miminiska lakes area. Age determinations, in part, were conducted at the Jack Satterly Geochronology Laboratory at the University of Toronto, using both isotope dilution thermal ionization mass spectrometry (ID-TIMS) and laser ablation inductively coupled mass spectrometry (LA-ICP-MS). For ID-TIMS analyses, zircons were pre-treated using chemical abrasion methods (e.g., Mattinson 2005). Age determinations for some igneous and detrital samples were also conducted at Laurentian University using LA-ICP-MS. Table 11.2 provides the sample locations and a summary of the age determinations; Figure 11.2 shows the sample locations relative to the geology of the area. Errors on all quoted ages presented herein are provided at the 2-sigma (2 σ) level of uncertainty.



Figure 11.1. Location of the study area.

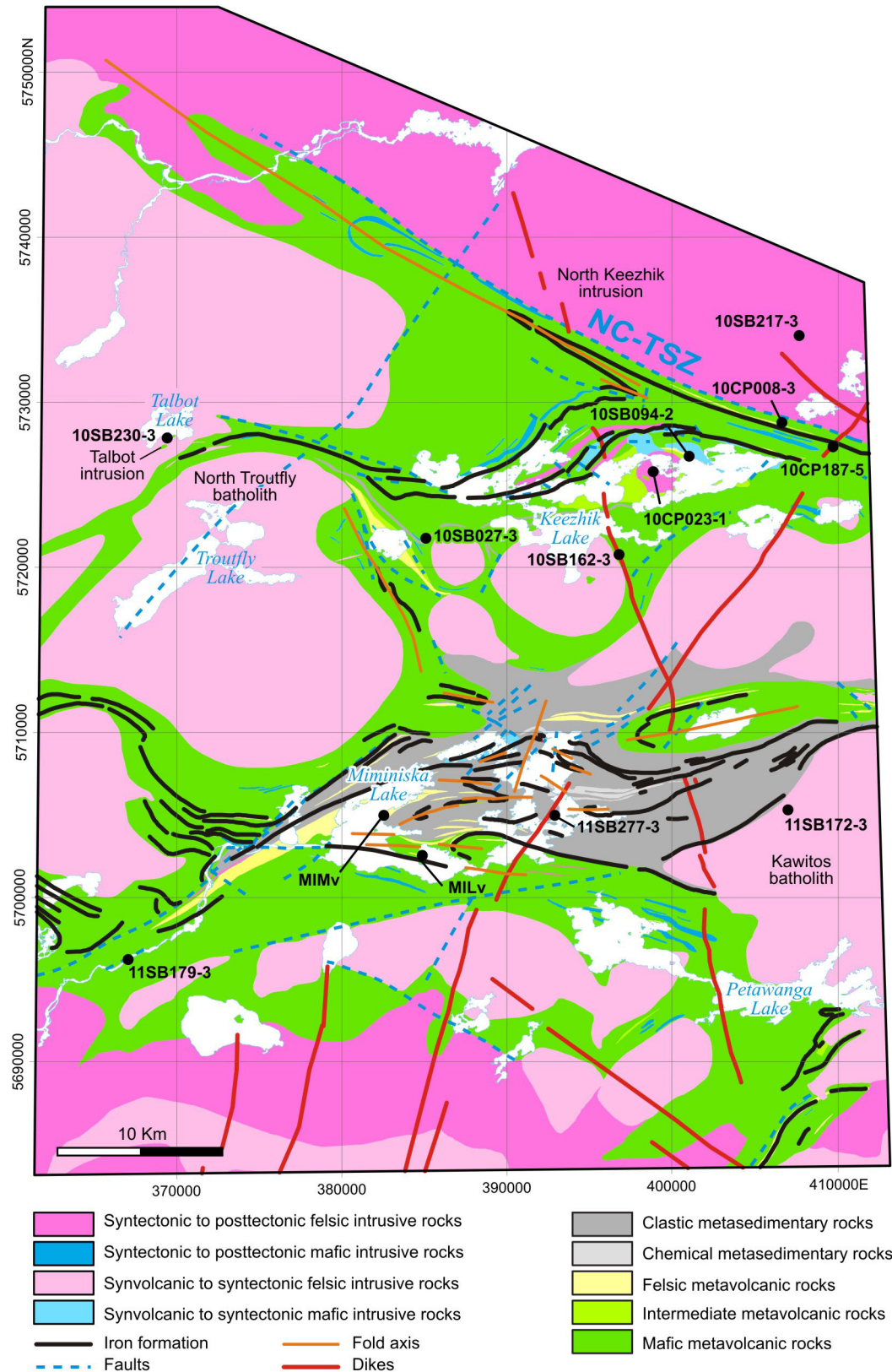


Figure 11.2. Simplified geology of the Keezhik Lake and Miminiska Lake area (after Buse 2012a; Buse and Purdy 2012) with the locations of the geochronological samples (see Table 11.2). Abbreviation: NC-TSZ, North Caribou-Totogan shear zone.

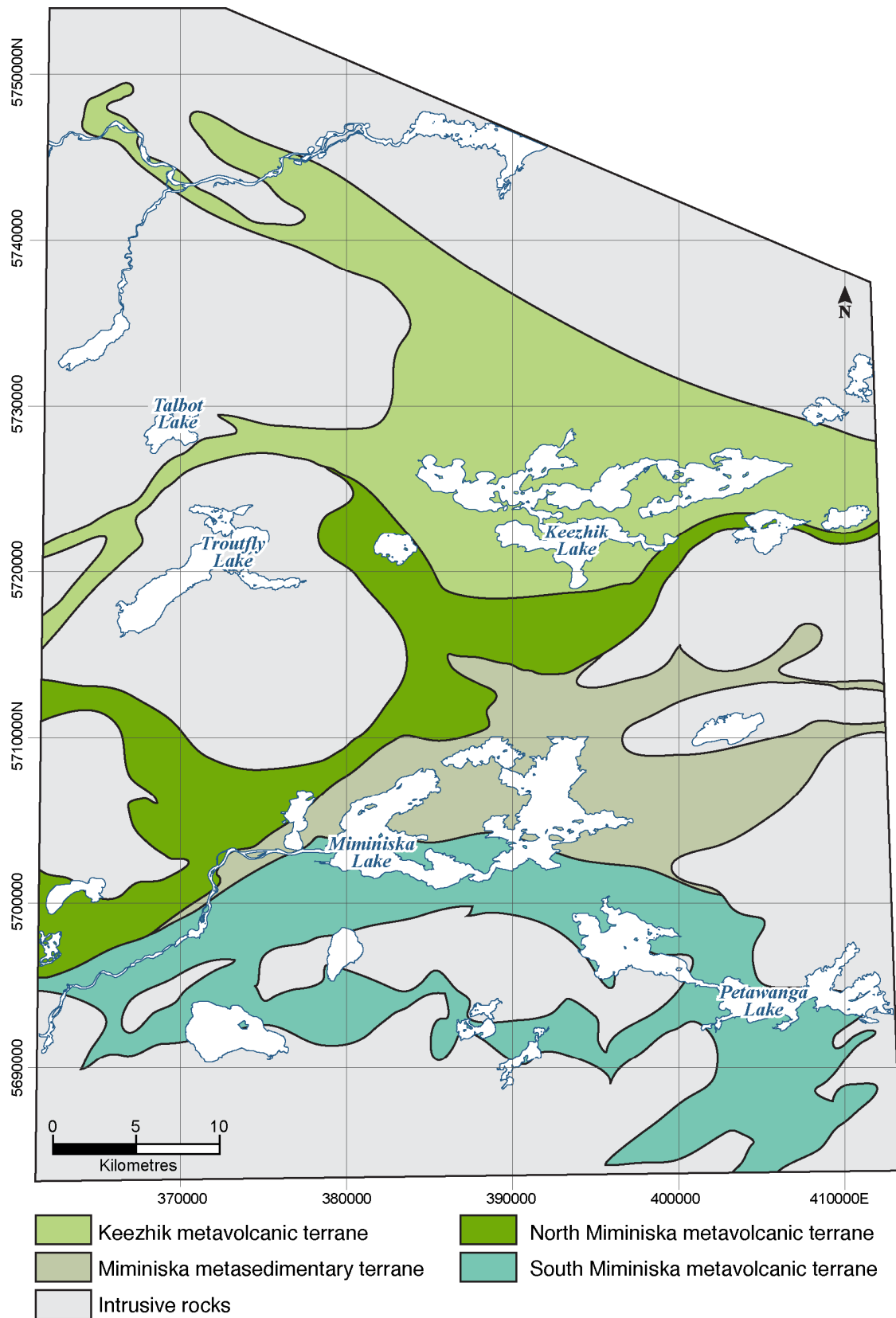


Figure 11.3. Geologic terrane map for the Keezhik Lake and Miminiska Lake area.

Table 11.1. Summary of structural events in the Keezhik Lake and Miminiska Lake area.

Deformational Event	Area	Foliation	Lineation	Folding	Comments
S ₀	Keezhik				Stratigraphy faces to the south in the northern portion of the area. An inferred fault that runs from north of Nesting Lake, into the South Keezhik pluton and south of Bresnahan Lake, marks where stratigraphy switches to north facing.
	Miminiska				Stratigraphy faces to the north
D ₁	Keezhik	Predominantly west-striking, moderate to steeply dipping S ₁ foliation defined by chlorite and weakly flattened clasts and volcanic fragments	East-trending, moderately to steeply plunging stretching lineation		This foliation is the penetrative foliation in the Keezhik Lake area, and is deformed by the intrusion of the syntectonic to posttectonic plutonic rocks as well as dextral shearing in the North Caribou–Totogan shear zone
	Miminiska	West-striking, moderate to steeply dipping S ₁ foliation defined by biotite, amphibolite, chlorite and flattened clasts and volcanic fragments	Northeast-trending, moderately to steeply plunging stretching lineation, but locally is a mineral lineation	Minor evidence for early isoclinal folding, subsequently re-folded by F ₂	This foliation is deformed by the intrusion of the syntectonic to posttectonic plutonic rocks
D ₂	Keezhik			The large-scale fold in the northernmost limb of the greenstone belt as well the anticline south of Nesting Lake may be related to this event, although no D ₂ foliations or lineations similar to those found at Miminiska Lake were observed	Very little evidence for the D ₂ event in the Keezhik Lake map area
	Miminiska	Three trajectories of S ₂ foliation at 60°, 90° and 120°. Steeply dipping and cleavage refraction in the wacke units.	Intersection lineation between S ₁ and S ₂ . Shallow stretching lineation plunging between 15° and 30° that crosscuts L ₁ .	Main F ₂ folding event producing isoclinal to tight folds with at least 2 orders of magnitude of parasitic folds. Upright folds (1-1.5 m wide), found locally, are interpreted to be late D ₂ , but no relationship between these folds and D ₃ were observed.	Metamorphism is interpreted to be coeval with D ₂ . Difference in the S ₂ foliation trajectories due to the D ₃ folding event and intrusion of surrounding granitoid rocks that deform the shape of the greenstone belt. A large shear zone associated with the gold occurrences on the west side of the belt may be late D ₂ but its relationship to D ₃ is unknown.

Table 11.1, continued.

Deformational Event	Area	Foliation	Lineation	Folding	Comments
D ₃	Keezhik	Discrete S ₃ foliation between 20° and 50° with moderate to steep dip			The S ₃ foliation is found throughout the Miminiska Lake area as well as the Keezhik Lake area to the north, and south in the Discovery Lake area, indicating that it is likely a greenstone belt-scale event
	Miminiska	Discrete S ₃ foliation between 20° and 50° with moderate to steep dip	Intersection lineation between S ₂ and S ₃	Small (1 cm) crenulation folds in quartz veins have axial planes parallel to S ₃ . The entire sedimentary belt is folded in a kilometre-scale open fold with axial plane parallel to S ₃ .	The S ₃ foliation is found throughout the Miminiska Lake area as well as the Keezhik Lake area to the north, and south in the Discovery Lake area, indicating that it is likely a greenstone belt-scale event

Table 11.2. Summary of select U/Pb geochronological determinations from the Fort Hope greenstone belt.

Sample Number ¹	Rock Type	Easting ² (m)	Northing ² (m)	²⁰⁷ Pb/ ²⁰⁶ Pb Age (Ma)	Interpretation	Method ³	Laboratory ⁴ or Source
10SB230-3	Potassium feldspar granite	369654	5738156	2706±1	Intrusive crystallization	LA-ICP-MS	JSGL
10CP023-1	Plagioclase porphyritic tonalite	398868	5736156	2738±4	Intrusive crystallization	TIMS	JSGL
10CP187-5	Northeast-trending diabase dike	409715	5737628	2102±1	Emplacement: interpreted as part of the Marathon dike swarm	TIMS	JSGL
10SB162-3	North-northwest-trending diabase dike	396727	5730861	1883±1	Emplacement: interpreted as part of the Pickle Crow dike swarm	TIMS	JSGL
10CP008-3	Felsic tuff	406133	5738723	2752±23	Eruptive	LA-ICP-MS	LU
10SB217-3	Biotite magnetite tonalite	408058	5743647	2758±6	Intrusive crystallization	LA-ICP-MS	LU
10SB027-3	Conglomerate	385040	5731799	> ca. 2731±30	Maximum age of deposition	LA-ICP-MS	LU
10SB094-2	Felsic tuff	400627	5737066	2694±3	Age is currently poorly understood and is very young for the Uchi Subprovince. Possibly eruptive age for infolded, unconformable tuff, or intrusive age of highly sheared late sill, or hydrothermally reset zircon.	LA-ICP-MS	LU
11SB172-3	S-type granite	407092	5715240	2696±8	Intrusive crystallization	LA-ICP-MS	LU
11SB179-3	Felsic tuff	366760	5706270	2739±3	Eruptive	LA-ICP-MS	LU
11SB277-3	Wacke	392956	5714624	> ca. 2705	Maximum age of deposition	LA-ICP-MS	LU
MILv	Felsic lapilli tuff	385163	5712630	2723±1	Eruptive	TIMS	see footnote ⁵
MIMv	Felsic crystal tuff breccia	382460	5714917	2716±1	Eruptive	TIMS	see footnote ⁵

¹ The locations of samples are shown by sample number on Figure 11.2.² All UTM co-ordinates are in North American Datum 1983 (NAD83), Zone 16. ³ LA-ICP-MS = laser ablation-inductively coupled plasma mass spectrometry; TIMS = thermal ionization mass spectrometry.⁴ JSGL = Jack Satterly Geochronology Laboratory, University of Toronto, Toronto, Ontario; LU = Laurentian University laboratory, Sudbury, Ontario.⁵ Source: Corfu and Stott (1993a).

10SB217-3

This sample was collected from a biotite-magnetite-bearing tonalite intrusion from the North Keezhik intrusion. The body is interpreted to be a large synvolcanic intrusion coeval with the mafic metavolcanic platformal sequence that is part of the Keezhik metavolcanic terrane (Buse and Purdy 2010). A large amount of pale brown, elongate zircon prisms, often with subhedral tips, were recovered from the sample. Eighty-nine (89) grains were analyzed using LA-ICP-MS (Laurentian University (LU)), and yielded a mean $^{207}\text{Pb}/^{206}\text{Pb}$ age of 2758 ± 6 Ma, which is interpreted to be the crystallization age for the intrusion.

10SB230-3

This sample was collected from the Talbot intrusion, a massive to weakly foliated potassium feldspar porphyritic granite, in the western portion of the Keezhik Lake area. This small intrusion is sandwiched between a thin sliver of greenstone belt to the south and several other prominent intrusions to the north and west. The intrusion commonly contains mafic xenoliths of varying sizes. North-side-up indicators in the greenstone belt indicate that the Talbot intrusion is younger than the North Troutfly batholith to the south of the greenstone belt (Buse and Purdy 2010). The North Troutfly batholith, as well as other batholiths that make up the Keezhik plutonic complex, are interpreted to be coeval with, or follow, the D_1 deformation event, indicating that the Talbot intrusion was emplaced after the D_1 event.

Zircons from this sample were analyzed using both ID-TIMS and LA-ICP-MS methods at the Jack Satterly Geochronology Laboratory. Abundant, strongly zoned, short and long prismatic zircons were recovered from the sample. Three chemically abraded single grains are 0.0 to 2.6% discordant and regress to yield an upper intercept age of 2705.9 ± 1.0 Ma. By comparison, 14 spot analyses carried out via LA-ICP-MS yielded an average $^{207}\text{Pb}/^{206}\text{Pb}$ age of 2709 ± 4 Ma, within error of the TIMS age. Two spot analyses by laser ablation gave slightly younger $^{207}\text{Pb}/^{206}\text{Pb}$ ages at 2680 ± 14 Ma and 2684 ± 12 Ma (2σ errors), but their significance is unclear. The latter 2 analyses were not measured on obvious overgrowth domains; further measurements would be required to assess whether the ages are analytically reproducible and whether they carry any geological significance. The ID-TIMS age of 2706 ± 1 Ma, which showed no signs of younger Archean secondary lead-loss or metamorphic zircon growth, is interpreted to represent the best estimate of the timing of crystallization for the intrusion. It also provides an absolute maximum age for the D_1 deformation event in the area.

11SB172-3

This sample was collected from the Kawitos batholith, a peraluminous, two-mica granite with muscovite, biotite and local tourmaline and garnet. It is interpreted to be one of the youngest intrusive suites in the greenstone belt as it intrudes the Miminiska metasedimentary basin and contains abundant xenoliths of the metamorphosed wackes from within the basin.

The sample contained abundant zircons, which included brown, generally stubby grains and clear, fracture-free elongate prisms. Spot analyses on 46 grains using LA-ICP-MS (LU) were completed and yielded an upper intercept age of 2696 ± 8 Ma, which is interpreted to be the crystallization age for the batholith. Minor inheritance was recorded in this suite, with $^{207}\text{Pb}/^{206}\text{Pb}$ model ages between *circa* 2700 and 2720 Ma, which may reflect the presence of xenocrystic cores or discrete grains from the metasedimentary basin wackes, since the intrusion is interpreted to have resulted from the partial melting of metasedimentary rocks.

10CP008-3

This sample was collected from a thin quartz porphyritic felsic tuff within a thick succession of platformal basaltic rocks located in the northernmost part of the Keezhik Lake area. This sample contained very few zircon grains, which were clear to pale yellow and elongate, but often with corroded edges. Thirty-five (35) grains were analyzed using LA-ICP-MS (LU), yielding an average $^{207}\text{Pb}/^{206}\text{Pb}$ age of 2752 ± 23 Ma, which is interpreted to be the eruptive age for this tuff. Spot analyses also revealed Mesoarchean inheritance between 2800 and 2876 Ma, indicating that the tuff may have been partially sourced from older material.

10CP023-1

This sample was collected from a plagioclase porphyritic tonalite from an intrusion located at the centre of the Keezhik volcanic complex within the Keezhik metavolcanic terrane. The intrusion contains roof pendants from the surrounding volcanic complex and is interpreted to be the synvolcanic equivalent to the effusive units. Samples collected from surrounding metavolcanic rocks that are also part of the Keezhik volcanic complex did not yield zircon; however, the age for the tonalite effectively provides ages for both the intrusion and the surrounding volcanic complex.

Zircon from the intrusion is of poor quality and quite altered. Following chemical abrasion pre-treatment, 3 single-grain fractions were analyzed using ID-TIMS methods. Two of these fractions were high in common lead and yielded slightly discordant ages, whereas the third yielded a near-concordant (99.65%) $^{207}\text{Pb}/^{206}\text{Pb}$ age of 2737.7 ± 4.3 Ma. The 2 discordant fractions, although imprecise, yielded similar ages of 2740 ± 21 Ma and 2743 ± 13 Ma. The single, most concordant age of 2738 ± 4 Ma is interpreted to best represent the time of crystallization of the interpreted synvolcanic pluton and eruption of flows within the overlying Keezhik volcanic centre.

10SB027-3

This sample was collected from a conglomerate unit in the Keezhik metavolcanic terrane, less than 10 km west of Keezhik Lake (*see* Figure 11.2). The unit contains dominantly chert clasts, with lesser local volcanic clasts and blocks set in a matrix having a dacitic composition. It is interpreted to be intraformational in origin, deposited as a result of mass wasting from the side of the Keezhik volcanic complex. Sample processing at LU recovered only 6 zircons from this unit, all of which were broken, brown and of different sizes and shapes. The low yield of zircon may reflect the abundance of chert clasts as well as the intermediate composition of the matrix that is interpreted to be sourced from the Keezhik volcanic complex, which is also zircon poor. The 6 grains yielded ages determined via LA-ICP-MS (LU) between 2731 and 2954 Ma with a mean $^{207}\text{Pb}/^{206}\text{Pb}$ age of 2761 ± 30 Ma. The sparse amount of data only constrain a maximum age of deposition of the conglomerate at *circa* 2731 Ma.

10SB094-2

This sample was collected from a felsic tuffaceous unit located directly north of the Keezhik volcanic centre and was processed at LU. The sample contains abundant, brown, elongate prismatic zircon that often have broken tips. Ninety-four (94) spot analyses yielded a reproducible, weighted average $^{207}\text{Pb}/^{206}\text{Pb}$ age of 2694 ± 3 Ma using LA-ICP-MS (LU).

Although the fit of the data for this sample is very good and many of the grains are concordant, this age is unusual since there are no other similar ages for volcanic rocks within the Uchi Subprovince.

Plutonic rocks, such as the Osnaburgh pluton in the Lac St. Joseph belt, with an age of 2693 ± 1 Ma, do occur regionally (Corfu and Stott 1993b). Nonetheless, the age of this tuffaceous unit is inconsistent with observed, surrounding field relationships that suggest the stratigraphy of the Keezhik volcanic terrane is a homoclinal, south-facing volcanic succession. The age may simply represent the eruptive age for the tuff if the unit represents an infolded and unconformable tuff deposited later in the history of the greenstone belt. If true, this represents an interesting relationship since such young volcanic activity, previously unrecorded locally, could be temporally equivalent to late volcanic activity found in other parts of the eastern portion of the Subprovince.

The age of 2694 Ma reported here is not considered to reflect an age of metamorphic zircon growth or recrystallization, as pressure–temperature conditions in the Keezhik Lake area are not interpreted to have exceeded subgreenschist to greenschist grades; moreover, the uranium–lead systematics, zircon morphologies and chemistry favour an igneous origin. Hydrothermal resetting of these zircon grains is also considered unlikely.

11SB179-3

This sample was collected from a fairly homogenous, thin felsic tuffaceous unit from within a sequence of predominantly mafic metavolcanic rocks in the South Miminiska metavolcanic terrane. Abundant pale to dark brown zircons having generally stubby, semi-prismatic and equant morphologies of varying sizes were picked for LA-ICP–MS analysis (LU). Spot U/Pb determinations on 47 grains yielded a distinct cluster overlapping with concordia giving an average $^{207}\text{Pb}/^{206}\text{Pb}$ age of 2739 ± 3 Ma, which is interpreted to be the eruptive age for the tuff.

11SB277-3

This sample was collected from the Miminiska metasedimentary terrane in an effort to determine a maximum age of deposition for the sedimentary basin. The sample was taken from a graded wacke, typical of the majority of the rocks in the basin. The sample yielded abundant zircon with a variety of grain morphologies ranging from grey to brown, stubby and equant to elongate and prismatic and some that contained visible cores. Approximately 90 zircon grains were analyzed using LA-ICP–MS methods at Laurentian University. Least discordant zircons from this sample have model $^{207}\text{Pb}/^{206}\text{Pb}$ ages ranging mostly from *circa* 2680 to 2720 Ma, with a prominent age mode near 2690 to 2700 Ma. A half-dozen grains yielded older $^{207}\text{Pb}/^{206}\text{Pb}$ ages between *circa* 2730 and 2780 Ma, and at 2805 Ma, 2840 Ma and 3010 Ma. From crosscutting relationships, the sedimentary terrane is constrained to be older than the *circa* 2696 Ma Kawitos batholith; therefore, the few spot analyses on detrital grains younger than this age may reflect secondary lead-loss and are considered suspect. On the west side of the sedimentary basin, intercalated felsic tuffaceous rocks occur, with ages of 2723 ± 1 Ma and 2716 ± 1 Ma (*see* Table 11.2; *see* Figure 11.2; samples MILv and MIMv, respectively, of Corfu and Stott 1993a), suggesting that there was coeval sedimentation and felsic volcanism within the basin during this interval. Field observations also indicate that wackes represented by this age were deformed by the D₁ deformational event, suggesting that sedimentation had to have occurred prior to *circa* 2705 Ma (the age of the Talbot intrusion which brackets the D₁ event). Therefore, despite the large number of detrital zircons examined, they are characterized by variable discordance and relatively large analytical errors: the best constraint on the age of deposition of sediments in this Miminiska terrane remains the bracket between the tuffs at 2723 Ma and 2716 Ma and the superimposed deformation event at *circa* 2705 Ma.

10CP187-5

This sample was collected from a northeast-trending diabase dike east of Keezhik Lake. Regional aeromagnetic data suggest that it could be part of a broader swarm of north-northeast- to northeast-trending mafic dikes cutting across the southern and eastern halves of the map area (*see* Figure 11.2). The sampled dike, of uncertain width, is composed of hornblende, clinopyroxene, plagioclase and magnetite. Sample 10CP187-5 yielded a modest population of fine baddeleyite of which 3 multigrain fractions, comprising 8 to 10 grains each were used for U/Pb ID-TIMS analysis. Results for the baddeleyite analyses are only slightly discordant (0.6 to 1.1%) and have model $^{207}\text{Pb}/^{206}\text{Pb}$ ages ranging narrowly between 2101.5 and 2102.9 Ma. A regression of all fractions through the origin yields an upper intercept age of 2102.0 ± 1.2 Ma, and is interpreted to represent an accurate estimate of the emplacement age for this dike.

10SB162-3

A single, long, segmented north-northwest-trending diabase dike, prominent in the regional aeromagnetic coverage, strikes across the eastern half of the map area. A sample of this dike was collected from a well-exposed outcrop immediately south of Keezhik Lake (*see* Figure 11.2). The dike at this locality has a minimum width of 25 m, and varies in composition locally from gabbro to quartz diorite. The medium-grained gabbroic phase has a mineralogy dominated by an assemblage of hornblende, clinopyroxene and plagioclase, whereas, locally, coarser pegmatitic equivalents are present. A medium-grained quartz dioritic phase of the dike was sampled for geochronological analysis, and yielded a small population of fine, elongate zircons with square cross sections. Three fractions of zircons, comprising 2 grains each, were analyzed using ID-TIMS methods, are 0.6 to 1.0% discordant and regress (through the origin) to yield an upper intercept age of 1883.3 ± 1.4 Ma. This age is interpreted to represent the primary age of emplacement and crystallization of the dike.

INTERPRETATION AND TECTONIC SIGNIFICANCE

Based on the geochronological results presented in this article, the 4 previously described terranes that make up the western portion of the Fort Hope greenstone belt most likely represent tectono-stratigraphic assemblages (*see* Figure 11.3), and can be correlated westward with other tectono-stratigraphic assemblages in the Uchi Subprovince.

The Keezhik metavolcanic terrane ranges in age from *circa* 2752 Ma to *circa* 2731 Ma and, thus, includes the oldest ages currently recognized in the greenstone belt. This span of ages is roughly correlative with those identified in the Confederation assemblage, which extends eastward from the Red Lake greenstone belt. This assemblage is interpreted to have developed within a dominantly back-arc tectonic environment amidst the Mesoarchean volcanic arc complexes that widely constituted the Uchi Subprovince prior to that time (Corfu and Stott 1993a; Percival et al. 2006). The age of the Confederation assemblage has been roughly constrained between 2760 and 2730 Ma (Corfu and Stott 1993a), but, more commonly, rocks assigned to this assemblage appear to be dominated by ages between 2745 and 2730 Ma (e.g. Percival et al. 2006). The older *circa* 2752 Ma ages of the Keezhik metavolcanic terrane suggest that there may have been an earlier stage of back-arc initiation preserved within the assemblage. Both the felsic tuff (10CP008-3) and the conglomerate (10SB027-3) yielded inherited and detrital zircons, respectively, of Mesoarchean age, suggesting that there is an ancient component to their respective magmatic and detrital sources. This is a common theme across the Uchi Subprovince, which preserves several Mesoarchean assemblages, such as the Balmer, Woman and Pickle Crow assemblages, within the Red Lake, Birch Uchi and Pickle Lake greenstone belts (Percival et al. 2006; Corfu and Stott 1993a; Young et al. 2006).

The South Miminiska metavolcanic terrane, with an age of *circa* 2739 Ma, is also correlative with the Confederation assemblage, in agreement with the 2723 Ma age defined by Corfu and Stott (1993a), although those workers interpreted their unit to be part of the St. Joseph assemblage. This assemblage extends southward from the southern margin of the Miminiska metasedimentary terrane. This suggests that 2 distinct terranes (the Keezhik metavolcanic terrane and the south Miminiska metavolcanic terrane) were developing from *circa* 2752 Ma to *circa* 2723 Ma and formed in relative proximity to each other prior to the deposition of the basinal wackes that subsequently formed the Miminiska metasedimentary terrane.

The contact between the South Miminiska metavolcanic terrane and the Miminiska metasedimentary terrane was not observed in the field because of poor exposure, but is interpreted to be an unconformity or erosional surface. The Miminiska metasedimentary terrane, which includes turbiditic metasedimentary rocks and a wedge of felsic metavolcanic rocks on the western side of the metasedimentary sequence, is suggested to be correlative with the St. Joseph assemblage (*circa* 2723 to *circa* 2713 Ma), which was originally identified in the Pickle Lake and Lake St. Joseph greenstone belts (Corfu and Stott 1993a). The St. Joseph assemblage is also temporally correlative with the Bidou, Black Island, Gem and Anderson assemblages in the western greenstone belts of the Uchi Subprovince (Percival et al. 2006). A maximum age of *circa* 2705 Ma was determined in this study for the deposition of the metasedimentary rocks in the turbiditic basin, whereas an age of *circa* 2716 Ma was determined for the felsic metavolcanic volcanic rocks on the western side of the Miminiska metasedimentary terrane (Corfu and Stott 1993a). Felsic metavolcanic rocks in the Opikeigen Lake area, located directly east of the Miminiska metasedimentary terrane, also have ages similar to the St. Joseph assemblage ages at *circa* 2722 Ma and *circa* 2716 Ma (Madon, McIlraith and Stott 2009). This suggests that development of the Miminiska sedimentary basin was coeval with volcanism both west of Miminiska Lake, preserving the felsic metavolcanic wedge, and in the Opikeigen Lake area.

No age determinations were obtained from the North Miminiska metavolcanic terrane. The felsic metavolcanic rocks from within that terrane did not yield any zircon, so the temporal relationship of the North Miminiska metavolcanic terrane relative to the other terranes in the greenstone belt remains unknown. However, the consistent north-facing stratigraphy of the metavolcanic rocks between the 3 Miminiska terranes suggests that the North Miminiska metavolcanic terrane is likely correlative with the St. Joseph assemblage.

The D₁ deformational event is poorly constrained chronologically; however, the crosscutting relationships between the supracrustal rocks and the Talbot intrusion, as well as north-side-up structural indicators suggest that the Talbot intrusion is younger than the North Troutfly pluton. This relationship indicates that the D₁ deformation predates the Talbot intrusion at *circa* 2706 Ma, but occurred following the deposition of the metasedimentary rocks. Throughout the rest of the Uchi Subprovince, penetrative deformation is constrained between *circa* 2718 Ma and 2712 Ma (Sanborn-Barrie, Skulski and Parker 2001; Dubé et al. 2004) along the southern margin of the North Caribou terrane in the Red Lake greenstone belt and between *circa* 2716 Ma and 2739 Ma in the Pickle Lake greenstone belt (Young et al. 2006). The D₁ deformation event in the Fort Hope greenstone belt is constrained by the turbiditic sedimentation that is coeval with the felsic volcanism at 2723 to 2716 Ma (and perhaps slightly younger) and the Talbot intrusion at 2706 Ma. This slightly younger timing, as compared to the events in other greenstone belts in the Uchi Subprovince, may represent the diachronous migration of deformation across the subprovince. This D₁ event has been interpreted to be part of the Uchian orogeny, which represents the northward accretion of the Uchi Subprovince onto the North Caribou terrane (Percival et al. 2006).

The felsic tuff (10SB094-2), at *circa* 2694 Ma, is the youngest recognized unit to have been deposited in the greenstone belt. This tuff is strongly foliated, even though it postdates D₁ deformation, the regional penetrative deformational fabric-forming event in the Keezhik metavolcanic terrane. However, it is spatially located within the regionally extensive strain zone of the North Caribou–Totogan

shear zone. This shear zone is interpreted to be a very late structure in the tectonic evolution of the greenstone belt and overprints much of the D₁ fabric in the northern portion of the Keezhik metavolcanic terrane. This may explain the intense foliation in the tuff.

The 2 Proterozoic diabase dike samples both yield important results in terms of our understanding of regional Paleoproterozoic magmatism within the Superior Province. Sample 10CP187-5, with an age of *circa* 2102 Ma, falls into the younger range of ages for the Marathon dike swarm, which is known to span from 2126 to 2101 Ma (Halls et al. 2008). This dike swarm has been interpreted to be part of a suite of mafic magmas related to plume magmatism that occurred near the time of final breakup of the southern margin of the Superior craton during the Paleoproterozoic. The second diabase dike, sample 10SB162-3, with an age of *circa* 1883 Ma, broadly matches that of 2 swarms of dikes with poorly constrained age limits: the large Pickle Crow dike (*circa* 1.87 Ga, Ar/Ar: Buchan et al. 2003) and its sparse, parallel satellite dikes, and the Wabigoon swarm (*circa* 1888 Ma, U/Pb: Davis and Hamilton 2010). Because of the north-northwest orientation and the geographic location of the dike, we consider it more likely to be related to the Pickle Crow dike event supporting the notion that there may be a more extensive swarm of this age in the western Superior craton.

Uranium-lead geochronological analyses within the Fort Hope greenstone belt have revealed that the assemblages tend to be younger than those in the central and western parts of the Uchi Subprovince, but that there may have been some Mesoarchean crust present during the formation of the belt. This supports the interpretation of general eastward younging across the Uchi Subprovince. Further work will be required to determine the lateral continuity of these assemblages across the rest of the eastern Uchi Subprovince.

ACKNOWLEDGMENTS

The senior author would like to thank Don Davis for analysis of sample 10SB230-3 at the Jack Satterly Geochronology Laboratory at the University of Toronto, as well as Robert Lodge and Joe Petrus for sample preparation and data regression for the samples completed at the Laurentian University laboratory.

REFERENCES

- Buchan, K.L., Harris, B.A., Ernst, R.E. and Hanes, J.A. 2003. Ar-Ar dating of the Pickle Crow diabase dyke in the western Superior craton of the Canadian Shield of Ontario and implications for a possible plume centre associated with ca. 1880 Ma Molson magmatism of Manitoba; abstract *in* Geological Association of Canada–Mineralogical Association of Canada, Joint Annual Meeting, Vancouver 2003, Program with Abstracts, v.28, p.17.
- Buse, S. 2011. Preliminary results from the eastern Uchi bedrock geology mapping project in the Miminiska Lake area, Fort Hope greenstone belt, Uchi Subprovince; *in* Summary of Field Work and Other Activities 2011, Ontario Geological Survey, Open File Report 6270, p.13-1 to 13-11.
- 2012a. Precambrian geology of the Miminiska Lake area, Fort Hope greenstone belt; Ontario Geological Survey, Preliminary Map P.3764, scale 1:50 000.
- 2012b. Geochemical and geological data from the Keezhik Lake and Miminiska Lake area, Fort Hope greenstone belt, northwestern Ontario; Ontario Geological Survey, Miscellaneous Release—Data 293.
- Buse, S. and Purdy, C. 2010. Preliminary results from the eastern Uchi bedrock mapping project in the Keezhik Lake area, Fort Hope greenstone belt, Uchi Subprovince; *in* Summary of Field Work and Other Activities 2010, Ontario Geological Survey, Open File Report 6260, p.18-1 to 18-13.

- . 2012. Precambrian geology of the Keezhik Lake area, Fort Hope greenstone belt; Ontario Geological Survey, Preliminary Map P.3763, scale 1:50 000.
- Corfu, F. and Stott, G.M. 1993a. U–Pb geochronology of the central Uchi Subprovince, Superior Province; Canadian Journal of Earth Sciences, v.30, p.1179-1196.
- . 1993b. Age and petrogenesis of two late Archean magmatic suites, northwestern Superior Province, Canada: zircon U–Pb and Lu–Hf isotopic relations; Journal of Petrology, v.34, p.817-838.
- Davis, D.W. and Hamilton, M.A. 2010. Geochronology report, Atikokan region [for the Ontario Geological Survey]; unpublished report of the Jack Satterly Geochronology Laboratory, Department of Geology, University of Toronto, Earth Sciences Centre, 22 Russell Street, Toronto, Ontario.
- Dubé, B., Williamson, K., McNicoll, V., Malo, M., Skulski, T., Twomey, T. and Sanborn-Barrie, M. 2004. Timing of gold mineralization at Red Lake, northwestern Ontario, Canada: new constraints from U–Pb geochronology at the Goldcorp high-grade zone, Red Lake Mine and the Madsen Mine; Economic Geology and the Bulletin of the Society of Economic Geologists, v.99, p.1611-1641.
- Halls, H.C., Davis, D.W., Stott, G.M., Ernst, R.E. and Hamilton, M.A. 2008. The Paleoproterozoic Marathon large igneous province: new evidence for a 2.1 Ga long-loved mantle plume event along the southern margin of the North American Superior Province; Precambrian Research, v.162, p.327-353.
- Madon, Z.B., McIlraith, S.J. and Stott, G.M. 2009. Geological compilation of the Miminiska–Fort Hope area, eastern Uchi domain; Ontario Geological Survey, Preliminary Map P.3611, scale 1:250 000.
- Mattinson, J. 2005. Zircon U–Pb chemical abrasion (CA–TIMS) method: combined annealing and multi-step partial dissolution analysis for improved precision and accuracy of zircon ages; Chemical Geology, v.220, p.47-66.
- Percival, J.A., Sanborn-Barrie, M., Skulski, T., Stott, G.M., Helmstaedt, H. and White, D.J. 2006. Tectonic evolution of the western Superior from NATMAP and Lithoprobe studies; Canadian Journal of Earth Sciences, v.43, p.1085-1117.
- Prest, V.K. 1939. Keezhik–Miminiska lakes area, District of Kenora (Patricia Portion), Ontario; Ontario Department of Mines, Annual Report Map 48E, scale 1:63 360.
- Sanborn-Barrie, M., Skulski, T. and Parker, J.R. 2001. Three hundred million years of tectonic history recorded by the Red Lake greenstone belt, Ontario; *in* Geological Survey of Canada, Current Research 2001-C19.
- Wallace, H. 1978a. Miminiska Peninsula, Kenora and Thunder Bay districts; Ontario Department of Mines, Map 2416, scale 1:31 680.
- . 1978b. Wottam Lake, Kenora and Thunder Bay districts; Ontario Department of Mines, Map 2417, scale 1:31 680.
- Young, M.D., McNicoll, V., Helmstaedt, H., Skulski, T. and Percival, J.A. 2006. Pickle Lake revisited: new structural, geochronological and geochemical constraints on greenstone belt assembly, western Superior Province, Canada; Canadian Journal of Earth Sciences, v.43, p.821-847.

12. Project Unit 11-004. Geology and Mineral Potential of the Brudenell Area, Northeastern Central Metasedimentary Belt, Grenville Province, with an Emphasis on the Syenitic Rocks

R.M. Easton¹

¹Earth Resources and Geoscience Mapping Section, Ontario Geological Survey

INTRODUCTION

The northeastern Central Metasedimentary Belt, specifically the area between Barry's Bay and Renfrew, is one of the more poorly known parts of the Grenville Province (Figure 12.1). Existing detailed mapping of this area consists of 1:63 360 scale mapping from the early 1950s (Hewitt 1954; Quinn, Wilson and Leech 1956), and 1:100 000 and 1:31 680 scale mapping from the 1970s (Lumbers 1982a, 1982b; Themistocleous 1981a, 1981b). Despite the limited mapping base for the area, several mineral deposit inventories of Renfrew County, including the study area, were conducted in the late 1970s (Carter, Colvine and Meyn 1980; Storey and Vos 1981a, 1981b; Masson and Gordon 1981). These studies, however, assumed that the basic geological framework of the Barry's Bay to Renfrew area was similar to that documented for better studied parts of the Central Metasedimentary Belt, which may not be the case. Another reason for the lack of studies in the Brudenell map area is because it has been subjected to upper amphibolite-facies metamorphism and multiple deformational events, resulting in a complicated geological history. Furthermore, almost no U/Pb zircon geochronology data are available for the area.

To address this knowledge gap, a multiyear 1:50 000 scale mapping program of the Brudenell area (NTS 31 F/6) (Project Unit 11-004) (*see* Figure 12.1) was begun in 2011 (Easton, Duguet and Magnus 2011). In conjunction with mapping of the Brudenell area, additional studies in the northeastern Central Metasedimentary Belt include a detailed geochemical study of the Raglan Hills gabbro (Magnus, Cousens and Easton, this volume, Article 14) and 1:20 000 scale mapping of the Admaston–Horton area immediately to the east of the Brudenell area (Duguet, Magnus and Ratcliffe, this volume, Article 13). A specific focus of the Brudenell mapping program is on rare metal and radioactive mineralization associated with syenitic rocks in the area, as well as examining the potential for porphyry molybdenum mineralization. The Brudenell area hosts past-producing vein-style molybdenite deposits; however, the deposit model for these veins is poorly understood.

The Brudenell area encompasses approximately 1088 km², is bounded by latitudes 45°15' to 45°30'N and longitudes 77°00' to 77°30'W, and encompasses all or parts of Brudenell, Grattan, Griffith, Hagarty, Lyndoch, Sebastopol, South Algona and Raglan townships. Approximately 13 weeks of the 2012 field season were spent conducting mapping and sampling in the area. Mapping was focussed on the goal of better understanding the rocks and mineral potential of the “alkalic suite” (units 19 to 23 of Lumbers 1982a, 1982b). In addition to field observations, mapping of granitoid rocks in the area benefitted from over 980 assay-mode scintillometer measurements for potassium, uranium and thorium using the methodology outlined by Easton (2009, 2010). All Universal Transverse Mercator (UTM) co-ordinates given in this article are provided in Zone 18, North American Datum 1983 (NAD83).

Figure 12.2 illustrates the major tectonic elements of the northeastern Central Metasedimentary Belt, which are described briefly in Table 12.1.

GENERAL GEOLOGY

The Brudenell area consists of 3 main lithologic domains (*see* Figure 12.2). The extreme northwest corner of the map area is underlain by monzonitic and granitic gneisses of the Central Gneiss Belt and by highly deformed and flattened gneisses of the Central Metasedimentary Belt Boundary Tectonic Zone (units 2 to 4 and unit 5 of Lumbers 1982a, respectively). The other 2 lithologic domains belong to the Central Metasedimentary Belt, with each domain underlying roughly half of the map area. The more northerly domain, which corresponds roughly to Bancroft terrane (*see* Figure 12.1), consists predominantly of marble tectonic breccia, cut by a variety of syenitic and granitic veins and intrusive bodies that have locally metasomatized the marbles to form pyroxene skarns. These syenitic and granitic rocks belong to the “alkalic suite” of Lumbers (1982a, 1982b), and are described in more detail (*see* “Syenite Magmatism”). The more southerly domain, which corresponds roughly to the Black Donald domain (*see* Figure 12.1), consists predominantly of calcite and dolomite marble, which has been intruded by tonalite, gabbro and syenite plutons. The southerly domain has many similarities with the northern and eastern parts of the Admaston–Horton area (Easton, Duguet and Magnus 2011; Duguet, Magnus and Ratcliffe, this volume, Article 13).

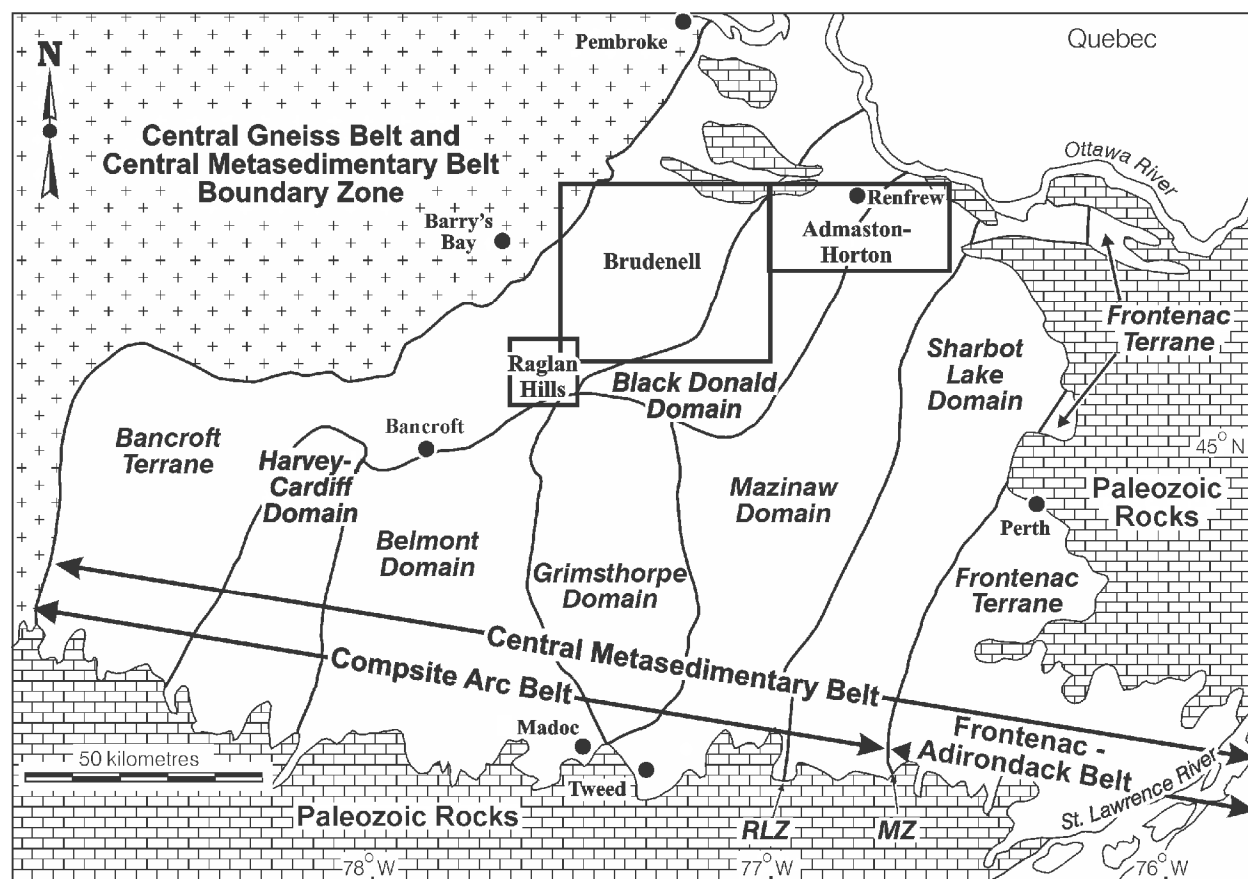


Figure 12.1. Terrane and domain subdivision of the Central Metasedimentary Belt (*modified from* Easton (1992) and Carr et al. (2000)) showing the location of the Brudenell study area as well as adjacent areas mapped by Magnus, Cousens and Easton (this volume, Article 14) and Duguet, Magnus and Ratcliffe (this volume, Article 13). The Central Metasedimentary Belt is composed of the Composite Arc Belt and Frontenac terrane. Abbreviations: RLZ, Robertson Lake mylonite zone; MZ, Maberly shear zone.

As noted in Easton, Duguet and Magnus (2011), within the northerly domain, host rocks to the marble breccias and the rocks of the alkalic suite consist of a variety of migmatitic, commonly garnet-bearing, dioritic to tonalitic grey gneiss with minor leucogabbro gneiss. These gneisses are lithologically heterogeneous over short distances, and leucosome content can vary considerably, from approximately 5% to over 20%, even over the scale of tens of metres. The migmatitic and typically garnet-rich character of these grey and leucogabbroic gneisses contrasts with the non-migmatitic and garnet-poor character of metasedimentary and mafic gneisses present in larger more intact fragments and slivers present in the marble breccia belts. As noted in Easton, Duguet and Magnus (2011), all occurrences of these grey and leucogabbroic gneisses follow an east-northeast trend from Rockingham to Hyndford, which is coincident with an east-northeast-trending gravity high visible in the first vertical derivative of the gradient of the gravity field (*see* Figure 12.2) (Ontario Geological Survey 1999).

Mapping during the current field season suggests that these migmatitic gneisses are tectonic slivers interleaved with marble breccia. This is consistent with reflection seismic imaging across the Central Metasedimentary Belt Boundary Tectonic Zone (White et al. 2000), which shows no distinction between gneiss-rich versus marble-rich zones on either side of the boundary. This begs the question as to how best to define the boundary between the Central Gneiss Belt and the Central Metasedimentary Belt, as the most northwesterly exposures of marble breccia in the area may not be the best indicator of where the Central Metasedimentary Belt ends, and the Central Gneiss Belt begins.

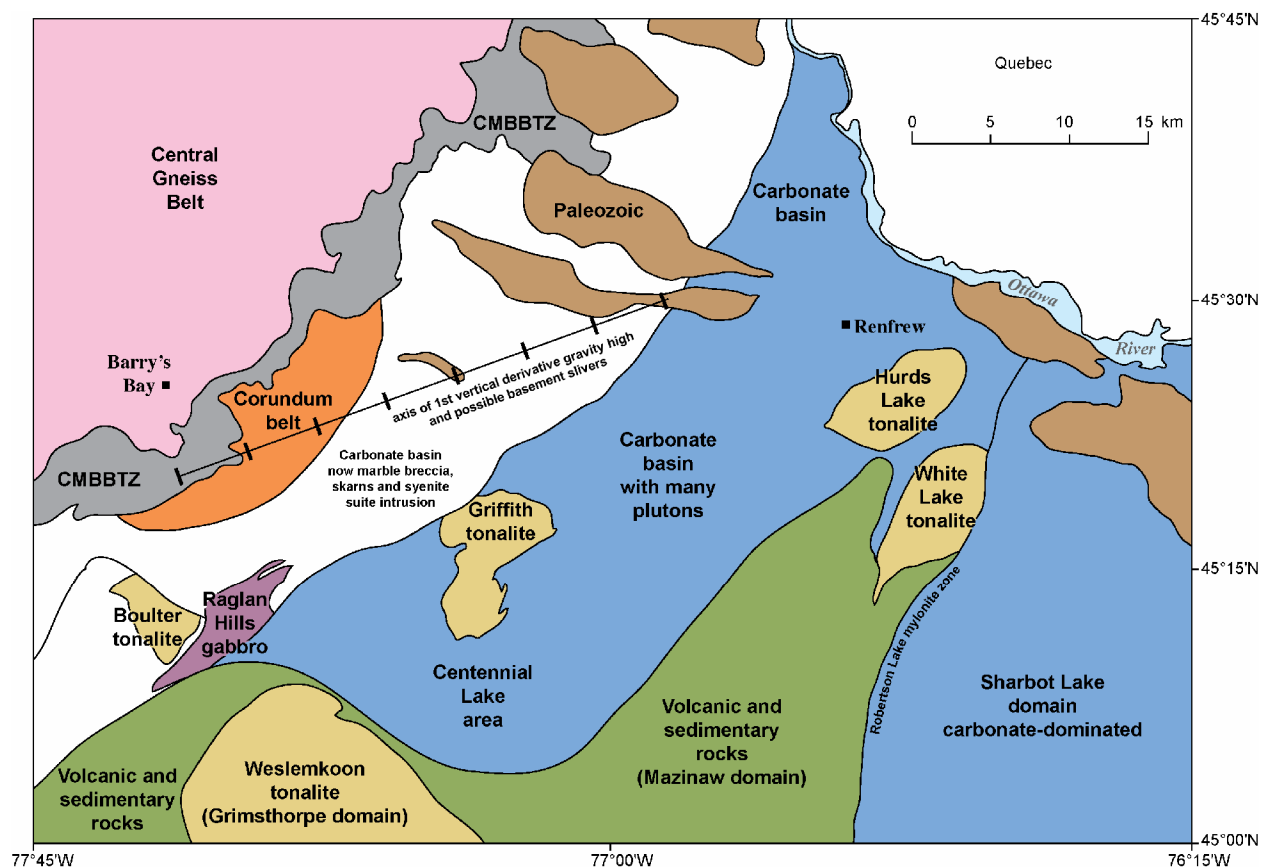


Figure 12.2. Geological sketch map of the northeastern Central Metasedimentary Belt showing the major tectonic elements of the region. The area shown in this sketch encompasses all 3 map areas shown in Figure 12.1 as well as surrounding regions. For clarity, not all intrusions are shown and east-trending Ottawa–Bonnetcherre graben faults have been omitted. *See* Table 12.1 for descriptions of each of the major tectonic elements. Geology adapted from Ontario Geological Survey (2011a). Abbreviation: CMBBTZ, Central Metasedimentary Belt Boundary Tectonic Zone.

Table 12.1. Characteristics of the major tectonic elements present in the northeastern Central Metasedimentary Belt.

Element	Typical Rock Types	Major Intrusive Phases	Age Constraints
Carbonate-belts, northern and eastern Admaston–Horton and southern Brudenell areas	Calcite marble, minor dolomite marble and interlayered immature siltstone and sandstone and rusty schist	Gabbro dikes, sills and intrusions, granodiorite to tonalite intrusions, mixed diorite-gabbro intrusive bodies, locally cut by Kensington–Skootamatta suite monzonite or syenite intrusions	Marbles older than ~1230 Ma (age of Chenaux gabbro)
Marble-breccia belt, northern Brudenell area	Matrix dominantly calcite marble containing 5-30% silicate minerals, commonly diopside, phlogopite, chondrodite and graphite with fragments of immature siltstone and sandstone, rusty schist and amphibolite. Interlayered with migmatitic grey and leucogabbroic gneisses, commonly garnet bearing	Syenite and granite veins and irregular bodies of the “alkalic suite” (Lumbers 1982a, 1982b) and associated metasomatic alteration, including pyroxenite skarn formation in the marble breccia units	“Alkalic suite” rocks ~1040 Ma (Lumbers et al. 1990)
Mazinaw terrane, central Admaston–Horton area	Amphibolite, paragneiss derived from immature siltstone and sandstone, minor calcite and dolomite marble. Garnet ± sillimanite ± muscovite gneiss of the Flinton Group.	Gabbro dikes, sills and intrusions, granodiorite to tonalite intrusions, mixed diorite-gabbro intrusive bodies, locally cut by Kensington–Skootamatta suite monzonite or syenite intrusions	None within the Brudenell area
Sharbot Lake domain	Calcite marble, minor dolomite marble and interlayered immature siltstone and sandstone and rusty schist	Gabbro dikes, sills and intrusions, granodiorite to tonalite intrusions	Marbles older than ~1224 Ma (age of Lavant gabbro)
Central Gneiss Belt Boundary tectonic zone	Thin to medium-layered, compositionally heterogeneous mafic, intermediate and felsic gneisses, highly strained and flattened	Cut by several generations of granitic pegmatite veins	Ages of 1079, 1053, 1045, 1016 Ma on granitic pegmatite veins (McEachern and van Breemen 1993)
Central Gneiss Belt	Monzonite and tonalite gneiss, local compositionally heterogeneous high-strain zones	Cut by several generations of granitic pegmatite veins	Gneisses typically older than 1340 Ma (cf. Easton 1992)

NEWLY RECOGNIZED MAFIC DIKE SWARM

Mafic dikes belonging to a previously undocumented dike swarm were identified at 5 locations in both the Brudenell and the adjacent Admaston–Horton map area (Table 12.2; Figure 12.3). These mafic dikes intruded a wide variety of rock types in both the Central Gneiss Belt and the Central Metasedimentary Belt (*see* Table 12.2; *see* Figure 12.3), cut gneissic fabric, are 2 to 5 m wide, typically fine-grained, and have chill margins (Photo 12.1). These dikes are distinct from dikes of the younger Grenville dike swarm (*circa* 590 Ma) in 3 main aspects. First, they have been recrystallized to form a sugary-textured, amphibole-biotite-plagioclase rock. Despite this recrystallization, they are still magnetic (*see* Table 12.2). In contrast, Grenville swarm dikes retain primary mineralogy and, where high-resolution magnetic data are available, can be recognized as northwest-trending, linear magnetic highs (Ontario Geological Survey 2010a, 2010b). Second, the Grenville swarm dikes show a limited range in orientation (290 to 310°, typically dipping 65 to 80°), whereas dikes of the new swarm display a wide range of azimuths (10°, 240°, 285°, 345°) and are typically vertical. Third, they are geochemically distinct, exhibiting enrichment in alkaline elements such as K₂O, barium and strontium (but not rubidium), and have light rare earth element-enriched patterns (*see* Table 12.2).

Table 12.2. Comparison of geophysical and geochemical data for mafic dikes in the Brudenell and Admaston–Horton areas.

Rock Type [Host Rock]	Stratigraphic Assignment	Sample Number	Average Magnetic Susceptibility ($\times 10^{-3}$ SI units)	K ₂ O (wt %) Scintillometer [laboratory]	Ba (ppm)	Sr (ppm)	Total REE (ppm)	Zr (ppm)
Gabbro [unknown]	Woermke gabbro	11RME-0157	85±16	1.3 to 1.7 [1.18]	1137	2466	180	96
Gabbro [unknown]	Woermke gabbro	12RME-0226	101±25	1.0 to 1.7 [pending]	1155	>1560	286	146
Gabbro [unknown]	Woermke gabbro	12RME-0318	95±45	1.8 [pending]	1194	>1560	177	122
Mafic dike [CGB gneiss]	new swarm	12RME-0025	36±10	0.8 to 1.0 [1.59]	1280	1183	163	87
Mafic dike [CMB gneiss]	new swarm	12RME-0282	2±1	0.5 to 0.7 [pending]	285	558	89	89
Mafic dike [CMB gneiss]	new swarm	12RME-0666	29±14	1.0 [pending]	<i>pending</i>	<i>pending</i>	<i>pending</i>	<i>pending</i>
Mafic dike [CMB marble breccia]	new swarm	12RME-0750	30±10	0.8 [pending]	<i>pending</i>	<i>pending</i>	<i>pending</i>	<i>pending</i>
Mafic dike [CMB mafic gneiss]	new swarm	12LR-0077b ^a	30±10	0.8 [pending]	<i>pending</i>	<i>pending</i>	<i>pending</i>	<i>pending</i>
Mafic dike [CMB gneiss]	Grenville swarm	11RME-0145	20±10	0.4 to 1.2 [0.30]	56	195	57	84
Mafic dike [CMB marble breccia]	Grenville swarm	11RME-0169	55±8	0.1 to 0.4 [0.33]	<20	186	100	163
Mafic dike [CMB marble breccia]	Grenville swarm	11SJM-0022a 12RME-0442	28±3	0.7 to 0.8 [0.23]	53	157	55	87

^asample from Admaston–Horton area. **Abbreviations:** CGB = Central Gneiss Belt; CMB = Central Metasedimentary Belt.



Photo 12.1. Sharp, irregular contact between mafic dike of the newly recognized dike swarm and leucogabbroic gneiss of the Central Gneiss Belt (UTM 306918E 5040900N, station 12RME-0025). Hammer handle is 33 cm long.

This new dike swarm is significant because it is posttectonic, but synmetamorphic, and because it occurs throughout the map area in both the Central Gneiss Belt and the Central Metasedimentary Belt. As such, it has the potential to constrain the timing of latest deformation and metamorphism within this part of the Grenville Province. It is possible that the dike swarm may be linked to “alkalic suite” magmatism, as the only mafic rock unit within the map area that is similar geochemically to the mafic dikes is the Woermke gabbro (*see* Table 12.2). Both units are enriched in K_2O , barium and strontium (but not rubidium), and have similar rare earth element patterns. The dikes, however, occur over a much larger area than do rocks of the Woermke gabbro and related mafic intrusions. A U/Pb TIMS (thermal ionization mass spectrometry) intercept age of 1073 ± 3 Ma was recently obtained from the Woermke gabbro (S.L. Kamo, Jack Satterly Geochronology Laboratory, Toronto, written communication, 2012), and probably represents a maximum age for the mafic dike swarm. A sample of one of the dikes has been collected for U/Pb geochronology.

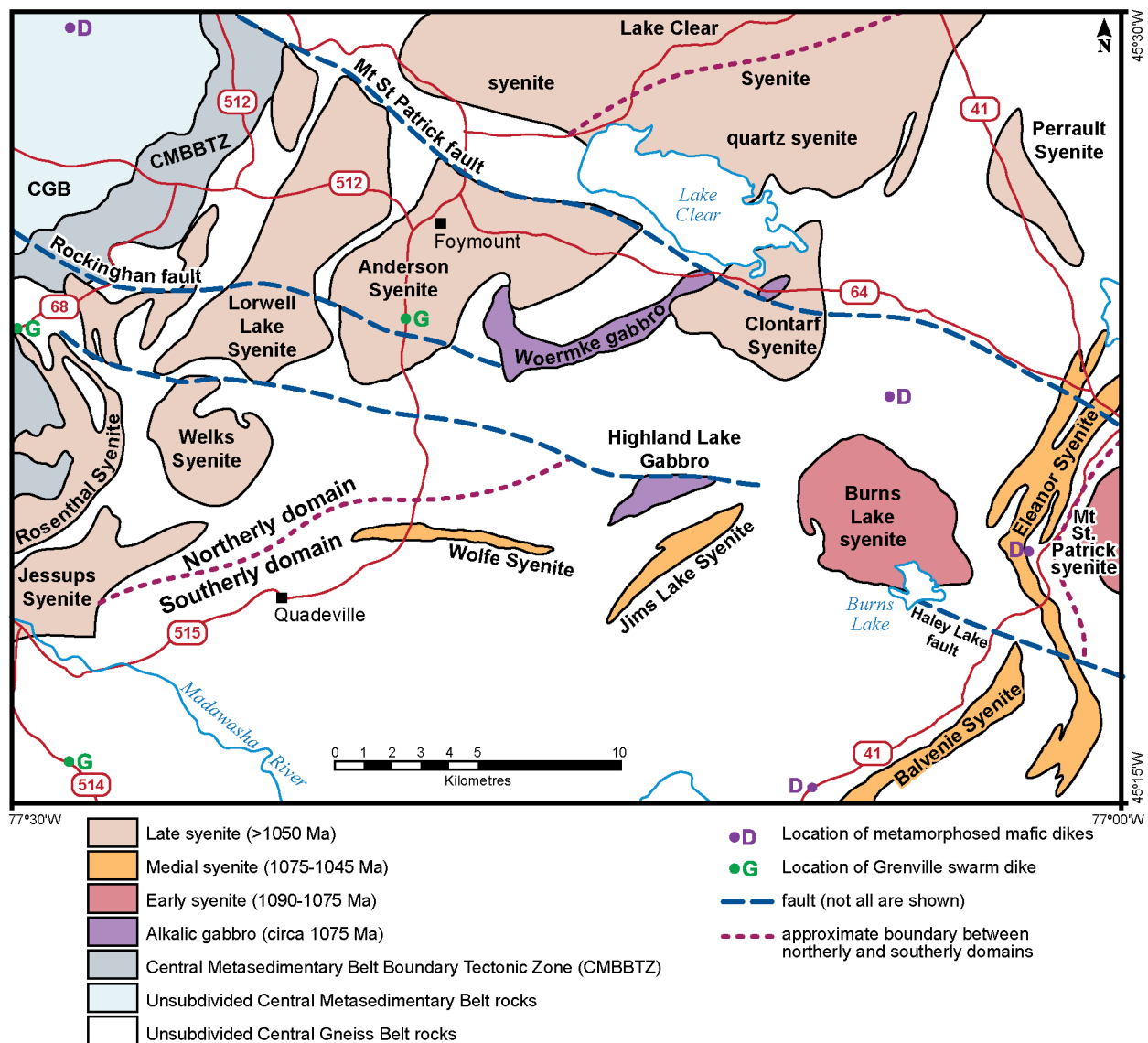


Figure 12.3. Location of major syenite intrusions and mafic dikes within the Brudenell area. Geology simplified from Lumbers (1982a). See Table 12.3 for details on the individual plutons.

Table 12.3. Summary of the features of the major syenitic bodies in the Brudenell map area. See Figure 12.3 for locations.

Pluton Name	Syenite Age Class (see text)	Main Rock Types	Radiometric Characteristics	Magnetic Characteristics (Susceptibility)	Associated Mineralization (historic workings)
Burns Lake ¹	Early	Biotite syenite	Potassium high, thorium and uranium lows	Magnetic high ($10\text{--}70 \times 10^{-3}$ SI units)	none
Mount St. Patrick ¹	Early	Biotite syenite	Potassium high, thorium and uranium lows	Magnetic high	none
Balvenie ¹	Medial	Biotite syenite	Potassium high, minor thorium expression	Weak magnetic expression ($2\text{--}5 \times 10^{-3}$ SI units)	Mo, U, Th (Spain Mine, Sunset Mine)
Eleanor (new name)	Medial	Biotite, amphibole and pyroxene syenite, monzodiorite, monzonite, minor nepheline syenite	Potassium high, moderate thorium expression	No magnetic expression ($2\text{--}10 \times 10^{-3}$ SI units)	Mo, U, Th
Perrault (new name)	Medial	Pink pyroxene syenite to quartz syenite	Potassium high, moderate thorium expression	Localized magnetic high (not whole body) ($2\text{--}20 \times 10^{-3}$ SI units)	none (Colaurti Feldspar)
Wolfe ¹	Medial 1042 \pm 3 Ma ²	Nepheline syenite, monzodiorite, amphibole monzonite, buff syenite	Signature lost in surrounding Methuen suite granitoid	Magnetic high but signature mixed with adjacent Methuen suite granitoid ($10\text{--}20, 110\text{--}145 \times 10^{-3}$ SI units)	magnetite, nepheline
Anderson ¹ , includes Foymount	Late circa 1040 Ma ³	Pyroxene and amphibole syenite	Potassium high, localized thorium highs, signature grades into adjacent Methuen suite granitoid	Localized magnetic high but adjacent Methuen-suite granite has a stronger signature ($5\text{--}35 \times 10^{-3}$ SI units)	Th
Clontarf (new name)	Late	Amphibole syenite	Potassium high, minor thorium expression	Magnetic high ($5\text{--}30 \times 10^{-3}$ SI units)	none
Jessups (new name)	Late	Leucosyenite	Potassium high, minor thorium signature	Magnetic high	beryl (Universal Light Metals)
Little Lake Clear ¹	Late 1059 to 1033 Ma, most cluster at 1040 Ma ⁴	Pink pyroxene syenite to quartz syenite, minor amphibole syenite	Localized potassium and thorium highs (not whole body)	No magnetic expression ($2\text{--}10 \times 10^{-3}$ SI units)	Th, apatite, possible REE, mineral specimens (Meany Mine, Park Mine, Smart Mine, Turners Island Mine)
Lorwall Lake (new name)	Late	Buff, pyroxene syenite	Moderate potassium, weak thorium signature	No magnetic expression ($2\text{--}5 \times 10^{-3}$ SI units)	Th, possible REE
Rosenthal (new name)	Late	Biotite syenite, amphibole syenite, minor nepheline syenite (older?)	Potassium high, minor thorium signature	Magnetic high	Corundum, numerous pits and occurrences
South Algona ¹	Late	Pink, pyroxene syenite	Potassium high, moderate thorium	Weak magnetic high ($5\text{--}35 \times 10^{-3}$ SI units)	Th, nepheline
Welks (new name)	Late	Biotite syenite, minor amphibole syenite	Potassium high, minor thorium high	Localized magnetic high (not whole body)	none

¹names from McCrank, Misiura and Brown (1981). In Figure 12.3, the Little Lake Clear syenite is the quartz syenite portion of the Lake Clear syenite (Childe, Mungall and Martin 2000) and the South Algona syenite is the syenite portion. ²U/Pb zircon, S.L. Kamo, Jack Satterly Geochronology Laboratory, written communication, 2012; ³U/Pb zircon, unpublished data as stated in Lumbers et al. (1990, p.251); ⁴U/Pb zircon, Childe, Mungall and Martin (2000). **Abbreviation:** REE = rare earth elements.

SYENITE MAGMATISM

This year's mapping program has led to improved understanding of long-standing controversial questions regarding the origin of alkalic syenite, fenite and "carbonatite" rocks within the hanging wall of the Central Metasedimentary Belt Boundary Thrust Zone (CMBBTZ), as described below and summarized in Table 12.3 and illustrated in Figure 12.3 and Photos 12.2A to 12.2F and 12.3A to 12.3D. In addition, it appears that the broad surface distribution of alkalic syenite, fenite and "carbonatite" rocks in the Brudenell area, compared to elsewhere along the Central Metasedimentary Belt Boundary Thrust Zone, is likely due to the shallow nature (dips of 5 to 10°) of the boundary zone within the Brudenell area.

Syenitic rocks within the map area belong to several previously defined lithodemic units, including the Nepheline Syenite, Kensington–Skootamatta (Monzonite-Diorite suite of Lumbers et al. 1990) and the "alkalic" (Lumbers 1982a, 1982b) or Fenite-Carbonatite suites (Lumbers et al. 1990; Easton 1992). The results described herein suggest that these different suites may represent a continuum of syenitic magmatism spanning roughly 40 million years, rather than being separate, discrete, magmatic events. As such, the stratigraphic usefulness of these lithodemic units needs to be re-considered.

Based on relative age relationships, there are at least 3 periods of syenite emplacement within the Brudenell area (*see* Table 12.3). The older period resulted in the emplacement of igneous-textured ovoid plutons of syenite (Burns Lake and Mt. St. Patrick plutons) and gabbro (Woermke and Highland plutons). These syenite plutons would correspond roughly to the Kensington–Skootamatta Suite. No absolute age information is available for the older syenite plutons in the map area; however, the similarity of their potassium, uranium and thorium contents to plutons of the Kensington–Skootamatta Suite (Easton, Duguet and Magnus 2011) suggest that they were emplaced at *circa* 1080 Ma, consistent with the age of 1073±3 Ma for the Woermke gabbro.

The medial period resulted in emplacement of linear-trending (either 90°, or 20 to 45°) heterogeneous bodies of monzodiorite, syenite and nepheline-syenite, best exemplified by the Wolfe and Eleanor intrusions (*see* Figure 12.3). These syenite plutons correspond in part to the Nepheline Syenite Suite, but, for the most part, are much younger than the age of *circa* 1290 Ma for this suite suggested by Lumbers et al. (1990). In addition, despite the name, non-foïd-bearing intrusions are more common than nepheline-bearing intrusions within this medial period of syenite emplacement. The linear shape of these intrusions suggests much greater tectonic control on their emplacement than that which occurred for the earlier ovoid syenite intrusions. In fact, portions of the Eleanor syenite show evidence for syn-emplacement deformation (Photos 12.3C and 12.3D). In addition, the nepheline syenite intrusions are spatially restricted to 20 km of the Central Metasedimentary Belt Boundary Tectonic Zone (CMBBTZ), whereas the ovoid intrusions occur throughout most of the Central Metasedimentary Belt.

A sample of igneous-textured nepheline syenite from the Wolfe intrusion was collected for geochronology in 2011. The most concordant zircon from this sample yielded a preliminary U/Pb TIMS age of 1042±3 Ma (S.L. Kamo, Jack Satterly Geochronology Laboratory, Toronto, written communication, 2012). This age is younger than that obtained from the Tory Hill nepheline syenite near Bancroft (*circa* 1055 Ma), but is similar to the ages obtained by Childe, Mungall and Martin (2000) on pyroxene syenite intrusions within the map area northeast of Lake Clear.

The latest period of syenite magmatism produced a diverse package of rocks that correspond roughly to the Fenite-Carbonatite Suite of Lumbers et al. (1990). Lumbers and Vertolli (1998) provide a brief description and some geochemical data for rocks of the Fenite-Carbonatite suite, and note that aegerine-augite is the dominant pyroxene species in these rocks. Four types of calcite-dominated rocks occur in association with this diverse package of syenitic and metasomatic rocks:

1. calcite and minor dolomite marbles derived from chemical sediments (distal to CMBBTZ, mainly in the southerly domain) (Photo 12.4A)

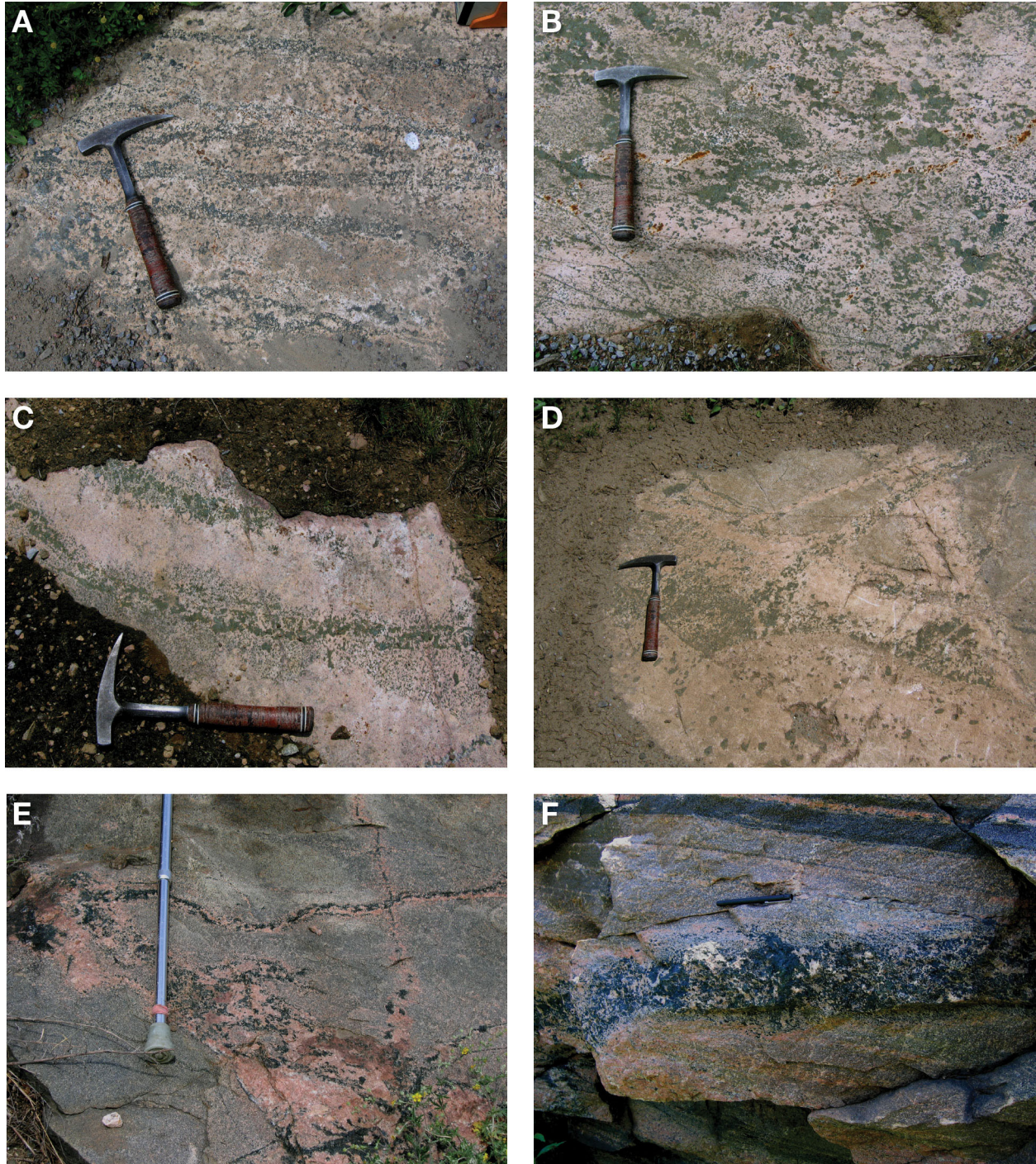


Photo 12.2. Textures in syenitic rocks from the Brudenell area. A) Varied grain size and pyroxene concentrations in the Lake Clear syenite (UTM 322885E 5040722N). B) Varied grain size and pyroxene concentrations in the Lake Clear syenite (UTM 329863E 5038501N). C) Varied grain size and pyroxene concentrations in the Lake Clear syenite (UTM 330382E 5039600N). D) Varied grain size and pyroxene concentrations in the Lake Clear syenite (UTM 324300E 5040470N). E) Metasomatism of country rocks to the Lake Clear syenite by crosscutting pyroxene-rich veins (UTM 324118E 5033825N). F) Metasomatism of country rocks to the Lake Clear syenite by crosscutting pyroxene-rich veins (UTM 326660E 5037800N). Objects used for scale: hammer handle is 33 cm long, pen is 10 cm long, cane is 95 cm long.

2. white marble tectonic breccias (Photo 12.4B) derived from 1 (proximal to CMBBTZ, mainly in the northern domain)
3. tectonic breccias (metasomatized) with pink calcite (Photo 12.4D) and abundant pyroxene (near syenite intrusions, but most abundant proximal to the CMBBTZ)
4. buff or pink calcite veins and segregations (Photos 12.2E, 12.3A and 12.3B) with pyroxene-amphibole \pm apatite rims derived from either carbonatitic liquids or immiscible segregation from syenite melts (proximal to CMBBTZ)

Types 3 and 4 occur in association with syenite and quartz syenite sills, veins and irregularly shaped bodies exhibiting a variety of textures, colours and grain sizes (*see* Photos 12.2A to 12.2D), as well as extensive fenitization and pyroxenite veining of host rocks (*see* Photo 12.2F). Martin and Sinai (2012) have described rocks similar to types 3 and 4 from the Central Metasedimentary Belt in Quebec.

Local differences in the syenite intrusions (kilometre scale) may be related in part to host composition. For example, corundum-bearing rocks appear to occur near nepheline syenite host rocks, and buff-coloured syenite appears to occur more commonly in areas underlain by large areas of marble breccia.

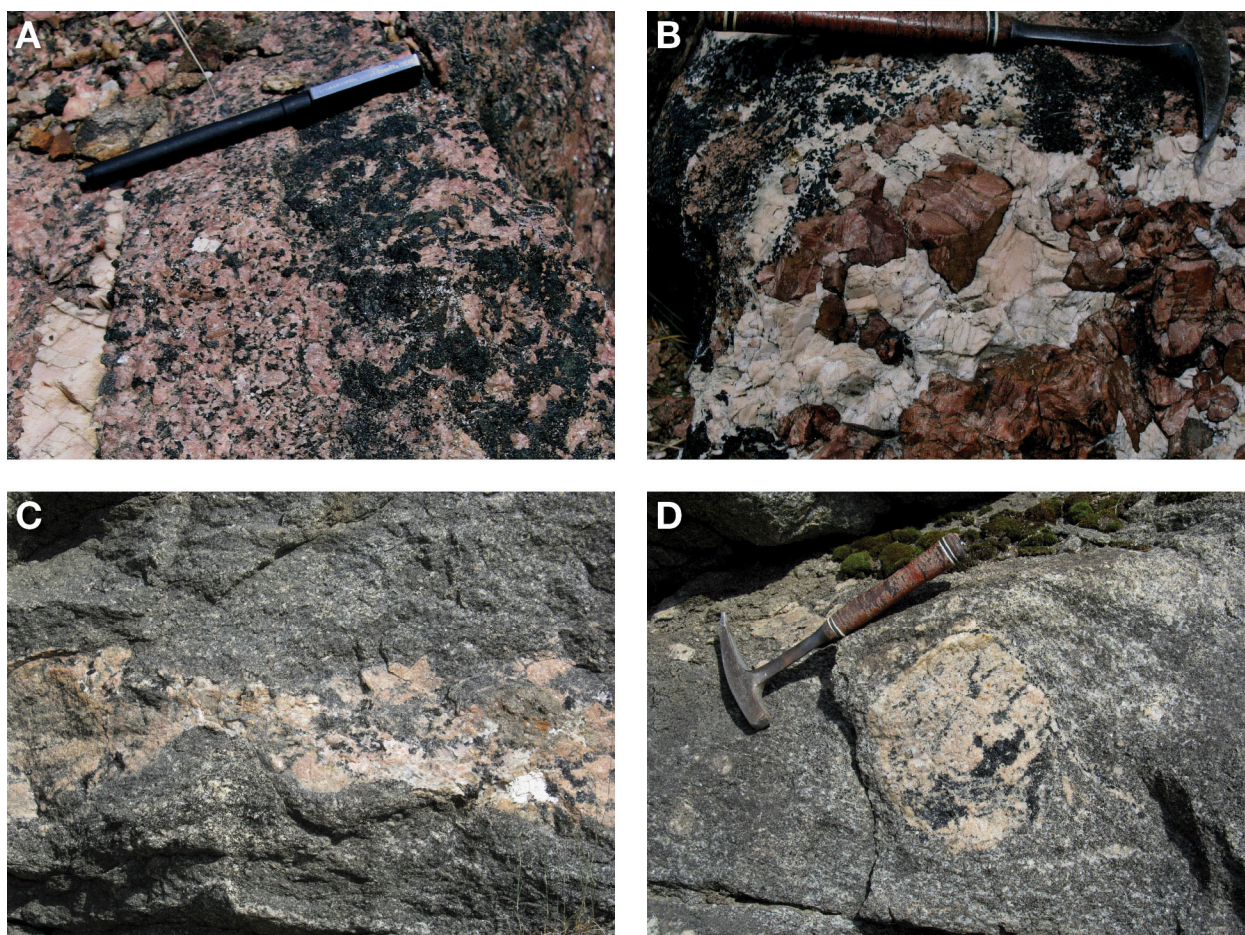


Photo 12.3. Textures in syenitic rocks from the Brudenell area, continued. A) Close-up of texture in the Lake Clear syenite, with a large coarse-grained calcite vein totally incorporated within the syenite (UTM 330780E 5040225N). B) Aggregate of coarse calcite and potassium feldspar as a segregation total encased in syenite of the Lake Clear syenite (UTM 330726E 5040388N). C) Boudinaged pink syenite vein cutting biotite-calcite-amphibole-feldspar melanocratic syenite of the Eleanor syenite (UTM 340545E 5019905N; field of view similar to Photo 12.3D). D) Isolated pink feldspar fragment in biotite-calcite-amphibole-feldspar melanocratic syenite of the Eleanor syenite, indicating syntectonic deformation of the syenite (UTM 340545E 5019905N). Objects used for scale: hammer handle is 33 cm long, pen is 10 cm long.

Emplacement of the syenitic rocks in the Brudenell area is attributed to an influx of fluids and heat between 1090 and 1035 Ma resulting from upwelling of asthenospheric mantle due to crustal delamination. This resulted in a prolonged, evolving, period of syenite production, as follows:

1. early syenites (1090 to 1070 Ma) were regionally distributed and form discrete low U-Th, magnetic plutons
2. medial syenites (*circa* 1050 Ma, low U-Th, magnetic), some of which are foid bearing, were localized along shear zones within 20 km of the CMBBTZ
3. late syenites (*circa* 1040 Ma, less magnetic, high Th) are associated with metasomatic fluids which interacted extensively with its host rocks, and are found almost exclusively within 20 km of the CMBBTZ

This progression in syenite type may reflect decreasing depth to the mantle source and increasing interaction with the lower crust during the Ottawa stage of the Grenville Orogeny.

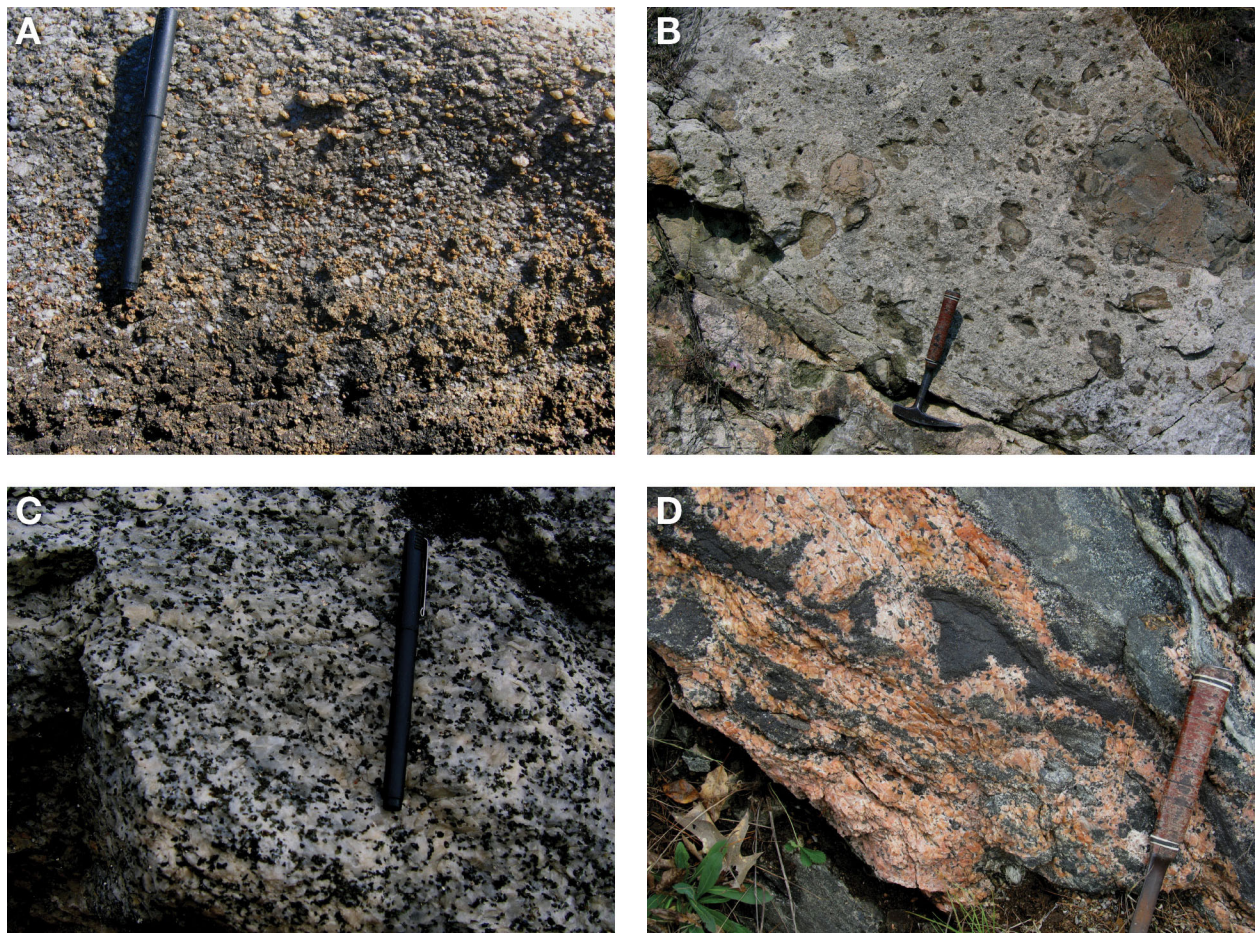


Photo 12.4. Carbonate-bearing rocks from the Brudenell area. A) Chondrodite (yellowish)-bearing marble exposed along Renfrew County Road 515 (UTM 317492E 5022006N). B) Typical marble breccia exposed along Renfrew County Road 64 near Clontarf (UTM 330988E 5030901N). C) Silicate-rich impure calcite matrix to marble breccia (UTM 326671E 5038044N). This rock contains 1112 ppm total REEs (*see* Table 12.5, sample 12RME-0055). D) Typical orange-calcite found in association with syenite intrusions and pyroxene skarn zones within marble breccia units (UTM 338574E 5018739N). Objects used for scale: hammer handle is 33 cm long, pen is 10 cm long.

IMPLICATIONS AND RECOMMENDATIONS FOR EXPLORATION

Radioactive Mineralization

Table 12.4 lists 30 assay-mode scintillometer measurements for new and old radioactive occurrences with thorium contents greater than 400 ppm, and/or uranium contents greater than 100 ppm. Most of the high uranium measurements were from previously known radioactive occurrences associated with either the Balvenie or Eleanor medial syenite intrusions. Four separate sites have thorium contents greater than 1000 ppm; only one of these localities was previously known. Few of the occurrences listed in Table 12.4 are associated with airborne gamma-ray spectrometric highs (Carson et al. 2004a, 2004b) for either uranium or thorium. This is in contrast to other parts of the Central Metasedimentary Belt, where most radioactive mineral occurrences have concurrent airborne gamma-ray spectrometric highs for either uranium and/or thorium (cf. Easton 2012).

Older syenite intrusions (*circa* 1080 Ma) have low uranium and thorium contents and, therefore, are unfavourable targets for uranium and thorium exploration. Neither the Burns Lake nor Mount Saint Patrick intrusions contain any airborne gamma-ray spectrometric anomalies for uranium or thorium (Carson et al. 2004a, 2004b). Medial syenite intrusions and their associated pegmatite veins, such as the Eleanor intrusion, contain radioactive occurrences with roughly equal amounts of uranium and thorium, and are the best targets for radioactive mineral exploration. The medial syenite intrusions are also those bodies most likely to contain molybdenum mineralization (e.g., the Balvenie and Eleanor intrusions, *see* Figure 12.3). Radioactive occurrences associated with many of the late syenite intrusions, particularly those located northeast and southwest of Lake Clear, are predominantly thorium enriched (*see* Table 12.4). Syenite colour (buff or pink) does not seem to be a factor with respect to thorium concentration. Regardless of syenite type and age, quartz is typically present in the more radioactive rocks, be they quartz syenites, alkali feldspar quartz syenites, or syenogranites. The change from uraniferous mineralization in the medial syenites to thorium mineralization in the late syenites may reflect increasing oxidation of the source fluids, which would partition uranium from thorium and transport uranium to higher crustal levels.

Rare Element Mineralization

The Brudenell area has potential for rare element and rare earth element in 3 main rock types: pegmatite veins, late syenite intrusions, and carbonate rocks associated with some of the late syenite intrusions. Unfortunately, this type of mineralization is not easily recognized in the field, but preliminary geochemical data obtained to date, and summarized in Table 12.5, provide some insight as to where such mineralization might be found.

Data for the 5 syenite intrusions presented in Table 12.5 represent the 5 highest total rare earth element contents found to date in syenitic rocks in the area. Light rare earth elements constitute the bulk of the rare earth elements present in these syenites, and the association with high phosphorous and zircon contents suggest that the rare earth elements are probably hosted in either apatite or zircon, or both. Niobium and scandium contents in these syenites are not particularly high (*see* Table 12.5), and do not represent the highest values observed in the Brudenell area. Strontium is notably enriched in all of these syenites, however.

More interesting is the fact that several of the marble breccia units that are intruded by late syenite intrusions are also enriched in the rare earth elements, again, mainly the light rare earths (*see* Table 12.5). Syenite sample 12RME-0052 is located within 100 m of the marble breccia sample 11RME-0055, but the marble breccia has a higher total rare earth element content than does the syenite (*see* Table 12.5; Photo 12.4C). As with the syenites, strontium is also high in these marbles. In the marble samples, however,

Table 12.4. Assay-mode scintillometer data for syenite and related rocks from the Brudenell area with thorium contents greater than 400 ppm Th and/or uranium contents greater than 100 ppm U, including measurements from previously known radioactive occurrences.

Sample Number	Easting (m)	Northing (m)	K ₂ O (wt %)	U (ppm)	Th (ppm)	Geological Unit	Comment
11RME-0137a*	318532	5027626	3.7	2.9	441	Anderson syenite	near airborne thorium high
11RME-0137b*	318560	5027615	6.5	3.1	406	Anderson syenite	near airborne thorium high
11RME-0143*	318167	5029007	11.2	0	1347	Anderson syenite	
12RME-0094a	325272	5032362	14.2	0	1705	Anderson syenite	highest Th from study area, near airborne thorium high
12RME-0094b	325336	5032362	9.2	9.2	737	Anderson syenite	near airborne thorium high
12RME-0106a	327622	031575	2.0	177.8	221	Anderson syenite	Opeongo Uranium, MDI31F06NE00093
12RME-0106b	327621	5031577	0.2	92.1	318	Anderson syenite	Opeongo Uranium, MDI31F06NE00093
12RME-0671a	336927	5015962	0	369.8	404	Balvenie syenite	former MDI31F06SE0030
12RME-0671b	336929	5015969	0	445.5	350	Balvenie syenite	former MDI31F06SE0030
12RME-0671c	336933	5015966	0	469.0	215	Balvenie syenite	highest U from study area, former MDI31F06SE0030
12RME-0581a	339304	5021948	8.4	182.3	1104	Eleanor syenite	Imperial Oil, former MDI31F06SE00092
12RME-0581b	339298	5021948	0	229.8	1702	Eleanor syenite	Imperial Oil, former MDI31F06SE00092
12RME-0581c	339298	5021945	7	340.7	1702	Eleanor syenite	Imperial Oil, former MDI31F06SE00092
12RME-0016a	309683	5033789	7.8	0	1545	Gorman syenite	
12RME-0016b	309683	5033789	11.3	0	1499	Gorman syenite	
12RME-0422a	303961	5020185	5.1	3.9	908	Jessups syenite	
12RME-0422b	303993	5020178	9.5	17.4	797	Jessups syenite	
12RME-0422c	303961	5020183	8.8	0.	565	Jessups syenite	
12RME-0424a	304209	5020133	8.2	5.0	450	Jessups syenite	
11RME-0075a*	312227	5035155	2.9	3.5	931	Lorwell Lake syenite	
11RME-0075b*	312227	5035155	2.2	42.6	791	Lorwell Lake syenite	
11RME-0112*	335425	5037593	6.5	61.4	458	Little Lake Clear syenite	near airborne thorium high
11RME-0113*	335441	5037595	3.6	8.8	478	Little Lake Clear syenite	near airborne thorium high
12RME-0054	326671	5038011	6.7	0	614	South Algona syenite	
12RME-0068	330712	5040382	7.7	24.1	507	South Algona syenite	
12RME-0069	330717	5040379	7.0	20.1	406	South Algona syenite	
12RME-0538a	317041	5023088	1.0	102.1	254	Wolfe syenite	small exposure
12RME-0538b	317041	5023088	1.6	119.5	296	Wolfe syenite	small exposure
11RME-0092	337907	5034609	4.5	0	414	Un-named quartz syenite	old pit
12RME-0032	313054	5037278	0	164.8	695	Syenite vein	Central Gneiss Belt

Abbreviations: ppm = parts per million, wt % = weight percent.

Notes: *previously reported in Easton, Duguet and Magnus (2011).

bold values indicate high values >1000 ppm Th or >400 ppm U.

Multiply U by 1.1793 for U₃O₈. All K, U and Th data were recorded using an Exploranium™ GR-135G MiniSpec gamma-ray spectrometer, serial number 4885, calibrated on February 22, 2006, using an NaI crystal and software version 501GEO. The instrument was stabilized daily, and data were recorded using the assay mode with a dead-time adjusted 5-minute count time. Quoted accuracy is 0.1% K, 0.4 ppm U, and 0.7 ppm Th for a sample with 2% K, 2 ppm U and 8 ppm Th. Reproducibility, accuracy and precision data for this particular instrument can be found in Easton (2009) and Banman (2009).

Table 12.5. Rare earth element data for selected syenitic and carbonate rocks from the Brudenell area.

Sample Number	Rock Type	Easting (m)	Northing (m)	Total REEs (ppm)	P ₂ O ₅ (wt %)	Zr (ppm)	Nb (ppm)	Sc (ppm)	Sr (ppm)
11RME-0082	Buff syenite	317874	5034785	1395	1.45	524	28	13	2246
11RME-0095	Buff syenite	338965	5036595	883	0.82	572	24	6	1259
12RME-0052	Buff syenite	326663	5037830	856	1.44	845	38	12	1168
12RME-0423	Syenite, Jessups	304095	5020153	850	<i>in progress</i>	480	18	4	376
12RME-0252	Pyroxene syenite, Lake Clear	330522	5036601	669	<i>in progress</i>	>1450	53	4	560
12RME-0355	Mafic gneiss interlayered with syenite	305092	5023428	1072	<i>in progress</i>	131	2	17	254
12RME-0356	Syenite with mafic gneiss	305077	5023430	359	<i>in progress</i>	98	24	1	484
12RME-0367	Buff syenite, Wolfe syenite	318181	5022678	593	436	436	61	5	>1560
12RME-0368	Calcite in buff syenite, Wolfe syenite	318181	5022678	410	<i>in progress</i>	178	0.1	0	912
12RME-0055	Marble breccia, white	326671	5038044	1112	0.01	8	1.8	2	1619
12RME-0322	Marble breccia, white	330988	5030901	584	<i>in progress</i>	148	2.4	17	249
11RME-0085	Marble breccia, pink	318280	5034420	390	0.01	19	2.0	3	1070
12RME-0030	Marble breccia, white	313256	5036390	163	0.04	32	3.8	3	713
12RME-0198	Pink calcite marble	333752	5033677	161	<i>in progress</i>	<6	0.2	<1	1228
09RME-2026	Calcite marble, Centennial Lake area	341914	5006329	27	0.02	16	0.6	4	165

there is no corresponding enrichment in either phosphorous and zircon (*see* Table 12.5); consequently, the host phase for the rare earth elements is unclear. Scanning electron microscopy is planned to determine what phase is hosting the rare earth elements in the marbles. Although the rare earth element content in the marble breccias is most likely related to metasomatic fluids, rather than being a primary compositional feature, there does not appear to be a correspondence with calcite colour, be it white or pink-orange (skarn-related); for example, compare samples 12RME-0055 (white) and 11RME-0085 (pink) (*see* Table 12.5). For reference, a typical marble from the Centennial Lake area that is unaffected by metasomatism is included in Table 12.5 (sample 09RME-2026, Easton 2011).

In summary, exploration for rare earth elements in the northern domain of the Central Metasedimentary Belt should focus on both the syenitic and carbonate rocks, not just on the syenites.

Carbonate-Hosted Mineralization

Space limitations prevent a thorough discussion of the carbonate rocks present within the Brudenell map area. However, field observations of these carbonate rocks have identified a number of features in these units relevant to mineral exploration.

- A belt of dolomite and dolomitic calcite marbles, up to 450 m wide and with a strike length of over 5 km, is present in southeastern Lyndoch and southwestern Griffith townships. A small part of this dolomite marble unit has been examined for its high-purity flux (Easton quarry, MDI31F06SE00024; GRI-01 LeBaron and MacKinnon 1990) and aggregate potential (Two Island Lake, now Dacre Industrial Minerals Inc. quarry, MDI31F06SE00026; GRI-02 LeBaron and MacKinnon 1990). The unit has not been examined for zinc mineralization and is not identified on older maps of the area (Lumbers 1982b; Themistocleous 1981b). This unit remains a favourable exploration target for zinc sulphide and zinc oxide mineralization, as well as for high-purity flux and aggregate applications.

- Chondrodite-bearing marbles in the southerly domain appear to have a high content of graphite (typically 1 to 3% graphite), of larger flake size, than other marble types. A chondrodite marble unit with graphite is exposed in several places along the Doorley Creek Forest Access Road in the southeastern corner of the map area, and is a target for graphite exploration.
- Marbles and marble breccias within both the northerly and southerly domains in the Brudenell area are predominantly calcitic, but many of these carbonate rocks contain between 10 and 20% magnesian silicate minerals, typically diopside (CaMgSiO_3), chondrodite ($\text{Mg}_5(\text{SiO}_4)(\text{F},\text{OH})_2$) and phlogopite ($\text{KMg}_3\text{AlSi}_3\text{O}_{10}(\text{F},\text{OH})_2$) (*see* Photo 12.4A). This abundance of magnesian-bearing phases suggests that the original protolith of these marbles may have been muddy calcitic dolostone or muddy dolomitic limestone, rather than muddy limestone. If so, then many of the marble units in the Brudenell may be favourable targets for zinc sulphide or zinc oxide mineralization; more so than their predominant calcite mineralogy would initially indicate.
- All of the high-purity marble occurrences that are currently listed in the Mineral Deposit Inventory (MDI) (Ontario Geological Survey 2011b) for the Brudenell area are based on geochemical data from Storey and Vos (1981a). All of these occurrences (MDI31F06SE00016, MDI31F06SW00021, MDI31F06SW00033, MDI31F06SW00008, MDI31F06NE00020, MDI31F06NE00002) are hosted in marble breccia units and, consequently, are of very limited size and volume. Thus, the ability to exploit any of these occurrences is limited. Therefore, it is recommended that these particular occurrences either be removed from future editions of MDI, or that a qualification be added to reflect the fact that they occur in compositionally heterogeneous marbles.

Fault-Related Mineralization

The Brudenell area is cut by several large west-trending faults, many of which show normal displacement resulting in the preservation of Paleozoic rocks on their down-dropped sides. Previously, these faults have been interpreted as developing during the Paleozoic or even the Mesozoic; however, during the course of mapping, it has become apparent that some of these west-trending faults may have initially developed in the Precambrian, and were subsequently reactivated during the Early Paleozoic. A recent comparison between Grenville and modern-day Tibetan geology suggests that west-trending faults should have been present in the northeastern Central Metasedimentary Belt during the late stages of the Grenville Orogeny (Rivers 2012). Elsewhere in the Central Metasedimentary Belt, Paleozoic mineralization associated with these west-trending faults includes vein systems dominated by calcite, barite, fluorite or galena (cf. Easton 1992). None of these Paleozoic vein systems are known to occur in the Brudenell area; however, there is nothing to preclude their presence.

It is also possible that Precambrian mineralization may occur adjacent to these faults. For example, along the Haley Lake fault (Themistocleous 1981b) in the southeast corner of the map area (*see* Figure 12.3), mafic gneisses only 100 m north of the fault are cut by a series of 20 to 100 cm wide diopside-potassium feldspar-sulphide veins that trend $070^\circ/90^\circ$, parallel to the Haley Lake fault. The sulphide minerals (pyrite, pyrrhotite) occur as massive pods in the veins. The silicate mineral assemblage in the veins is the same as that found in the pyroxene skarn rocks that occur adjacent to the nearby Eleanor and Balvenie syenite intrusions, suggesting that these veins formed during emplacement of the medial syenites, that is, during the Precambrian. Coincidentally, the Spain Mine (molybdenite; pyrite, pyrrhotite: MDI31F06SE00003) is located only 400 m north of the Haley Lake fault, and the abundance of pyrite and pyrrhotite at the mine suggests it too may be related to the same vein system. Also, 2 uranium occurrences (MDI31F06SE00089 and MDI31F06SE00104) are also present within 150 m of the Haley Lake fault, near these sulphide occurrences. To date, the Haley Lake fault is the only known example with possible Precambrian mineralization; however, further examination of other large west-trending faults in the area (e.g., Lake Clear, Mount St. Patrick, Rockingham, Turtle Lake faults) for similar sulphide vein systems is warranted.

REFERENCES

- Banman, S. 2009. Characterization of plutonic suites in Cavendish Township by *in-situ* geophysical measurements and geochemistry; unpublished BSc thesis, Carleton University, Ottawa, Ontario, 51p.
- Carr, S.D., Easton, R.M., Jamieson, R.A. and Culshaw, N.G. 2000. Geologic transect across the Grenville Orogen of Ontario and New York; Canadian Journal of Earth Sciences, v.37, p.193-216.
- Carson, J.M., Holman, P.B., Ford, K.L., Grant, J.A. and Shives, R.B.K. 2004a. Airborne gamma ray spectrometry compilation, equivalent uranium, Central Metasedimentary Belt, (Grenville Province), Ontario–Quebec; Geological Survey of Canada, Open File 4559, scale 1:250 000.
- 2004b. Airborne gamma ray spectrometry compilation, equivalent thorium, Central Metasedimentary Belt, (Grenville Province), Ontario–Quebec; Geological Survey of Canada, Open File 4560, scale 1:250 000.
- Carter, T.R., Colvine, A.C. and Meyn, H.D. 1980. Geology of base metal, precious metal, iron and molybdenum deposits in the Pembroke–Renfrew area; Ontario Geological Survey, Mineral Deposits Circular 20, 186p.
- Childe, F., Mungall, J.E. and Martin, R.F. 2000. U-Pb age constraints on Mesoproterozoic shoshonitic magmatism in the Bancroft terrane, Ontario; abstract *in* GeoCanada 2000: the Millennium Geoscience Summit Conference, joint meeting of the Canadian Geophysical Union, Canadian Society of Exploration Geophysicists, Canadian Society of Petroleum Geologists, Canadian Well Logging Society, Geological Association of Canada and the Mineralogical Association of Canada, May 29-June 2, 2000, Calgary, Alberta, also known as Geological Association of Canada–Mineralogical Association of Canada, Program with Abstracts, v.25, 5p.
- Easton, R.M. 1992. The Grenville Province; *in* Geology of Ontario, Chapter 19, Ontario Geological Survey, Special Volume 4, Part 2, p.713-904.
- 2009. Characterization of rock units in the Grenville and Southern Provinces by *in-situ* geophysical measurements and geochemistry; *in* Summary of Field Work and Other Activities, 2009, Ontario Geological Survey, Open File Report 6240, p.9-1 to 9-4.
- 2010. Use of a hand-held gamma-ray spectrometer as a mapping tool: examples from the Canadian Shield of Ontario; abstract, Geological Society of America, Abstracts with Program, v.42, no.5, p.276.
- 2011. Geological, geochemical and geophysical data related to the zinc scoping project, Grenville Province; Ontario Geological Survey, Miscellaneous Release—Data 286.
- 2012. Geology of Cavendish Township, Grenville Province; Ontario Geological Survey, Open File Report 6229, 141p.
- Easton, R.M., Duguet, M. and Magnus, S.J. 2011. Geology and mineral potential of the northeastern Central Metasedimentary Belt, Grenville province; *in* Summary of Field Work and Other Activities, 2011, Ontario Geological Survey, Open File Report 6270, p.5-1 to 5-23.
- Hewitt, D.F. 1954. Geology of the Brudenell–Raglan area; Ontario Department of Mines, Annual Report, 1953, v.62, pt.5, 123p.
- LeBaron, P.S. and MacKinnon, A. 1990. Precambrian dolomite resources in southeastern Ontario; Ontario Geological Survey, Open File Report 5712, 134p.
- Lumbers, S.B. 1982a. Barry’s Bay; Ontario Geological Survey, Map 2461, scale 1:100 000.
- 1982b. Renfrew; Ontario Geological Survey, Map 2462, scale 1:100 000.
- Lumbers, S.B., Heaman, L.M., Vertolli, V.M. and Wu, T.W. 1990. Nature and timing of Middle Proterozoic magmatism in the Central Metasedimentary Belt, Grenville Province, Ontario; *in* Mid-Proterozoic Laurentia–Baltica, Geological Association of Canada, Special Paper 38, p.243-276.

- Lumbers, S.B. and Vertolli, V.M. 1998. Fenite, carbonatite and other alkaline rocks in the Bancroft–Haliburton–Muskoka regions; Geological Society of America, Annual Meeting, Toronto 1998, Field Trip Guide Number 5, 14p.
- Martin, R.F. and Sinai, F. 2012. Rheomorphic fenite and crustal carbonatites: new complications in the Grenville crust, Old Chelsea area, Quebec; abstract *in* Geological Association of Canada–Mineralogical Association of Canada, St. John's 2012, Program with Abstracts, v.35, p.85.
- Masson, S.L. and Gordon, J.B. 1981. Radioactive mineral deposits of the Pembroke–Renfrew area; Ontario Geological Survey, Mineral Deposits Circular 23, 155p.
- McCrack, G.F.D., Misiura, J.D. and Brown, P.A. 1981. Plutonic rocks in Ontario; Geological Survey of Canada, Paper 80-23, 171p.
- McEachern, S.J. and van Breemen, O. 1993. Age of deformation within the Central Metasedimentary Belt boundary thrust zone, southwest Grenville Orogen: constraints on the collision of the Mid-Proterozoic Elzevir terrane; Canadian Journal of Earth Sciences, v.30, p.1155-1165.
- Ontario Geological Survey 1999. Single master gravity and aeromagnetic data for Ontario, ASCII, Excel® and Access® formats; Ontario Geological Survey, Geophysical Data Set 1035.
- 2010a. Airborne magnetic and electromagnetic surveys, colour-filled contours of the residual magnetic field and electromagnetic anomalies, Bancroft area—Purchased data; Ontario Geological Survey, Map 60 149, scale 1:20 000.
- 2010b. Airborne magnetic and electromagnetic surveys, shaded colour image of the second vertical derivative of the residual magnetic field and Keating coefficients, Bancroft area—Purchased data; Ontario Geological Survey, Map 60 164, scale 1:20 000.
- 2011a. 1:250 000 bedrock geology of Ontario; Ontario Geological Survey, Miscellaneous Release—Data 126—Revision 1.
- 2011b. Mineral Deposit Inventory—2011 (MDI 2011); Ontario Geological Survey, Mineral Deposit Inventory, December 2011 release.
- Quinn, H.A., Wilson, M.E. and Leech, G.B. 1956. Renfrew map-area; Geological Survey of Canada, Map 1046A, scale 1:63 360.
- Rivers, T. 2012. Upper-crustal orogenic lid and mid-crustal core complexes: signature of a collapsed orogenic plateau in the hinterland of the Grenville Province; Canadian Journal of Earth Sciences, v.49, p.1-42.
- Storey, C.C. and Vos, M.A. 1981a. Industrial minerals of the Pembroke–Renfrew area, part 1: Marble; Ontario Geological Survey, Mineral Deposits Circular 21, 132p.
- 1981b. Industrial minerals of the Pembroke–Renfrew area, part 2; Ontario Geological Survey, Mineral Deposits Circular 22, 214p.
- Themistocleous, S.G. 1981a. Geology of the Clontarf area; Ontario Geological Survey, Report 209, 64p.
- 1981b. Geology of the Khartum area; Ontario Geological Survey, Report 211, 56p.
- White, D.J., Forsyth, D.A., Asudeh, I., Carr, S.D., Wu, H., Easton, R.M. and Mereu, R.F. 2000. A seismic-based cross-section of the Grenville Orogen in southern Ontario and western Quebec; Canadian Journal of Earth Sciences, v.37, p.183-192.

13. Project Unit 11-003. Geology and Mineral Potential of the Admaston–Horton Area, Northeastern Central Metasedimentary Belt, Grenville Province

M. Duguet¹, S.J. Magnus² and L. Ratcliffe³

¹Earth Resources and Geoscience Mapping Section, Ontario Geological Survey, Sudbury, Ontario P3E 6B5

²Ottawa–Carleton Geoscience Centre, Department of Earth Sciences, Carleton University, Ottawa, Ontario K1S 5B6

³1664 Bruce Rd. 9, Wiarton, Ontario N0H 2T0

INTRODUCTION

The Admaston–Horton map area covers approximately over 544 km² and is bounded by 45°22'30" to 45°30'N latitude and 77°00' to 76°30'W longitude, and encompasses all or parts of Admaston, Bagot, Bromley, Brougham, Grattan, Horton and McNab townships (*see* Figure 12.1, Easton, this volume). The 2011 field season focussed on the east (Horton) half of the area (Easton, Duguet and Magnus 2011). Approximately 12 weeks of the 2012 field season were spent conducting mapping and sampling in the western (Admaston) half of the area, which is bounded by 45°22'30"N to 45°30'N latitude and 76°45'W to 77°00'W longitude.

This paper focusses on lithologic and structural aspects of the Horton area based on analysis of the 2011 and 2012 field programs; however, key aspects of the Admaston area and its relationship to the Horton area will also be addressed in this paper. In addition, a wide variety of rock types in the Horton area contain elevated rare earth element (REE) contents. As neither the Admaston nor Horton areas had been previously investigated for this commodity, this paper will also focus on the exploration potential for rare earth elements in the map area.

The Renprior zinc occurrence (MDI31F07NE00063, UTM 366130E 5030240N), hosted in dolomite, siliceous dolomite and calcite marble (Robertson 1984), is in the Admaston–Horton map area. Mineralization, consisting mainly of sphalerite and pyrite, with minor galena, is stratabound and is commonly located near the contacts of the different marble types present at the occurrence, with the siliceous dolomite marble being the most commonly mineralized unit. Based on mineral exploration work up until 1982, 4 zones of significant mineralization were outlined, with an ore reserve calculation (not National Instrument 43-101 compliant) of 280 000 metric tonnes of 9% Zn to an average depth of 130 m (Robertson 1984). Possible relationships between this zinc mineralization and a newly discovered potassium alteration zone will be discussed latter in this article.

GENERAL GEOLOGY

Geological Overview and Stratigraphy

Figure 13.1 presents the results of the 2011 mapping program in the Horton area. The Horton area lies mostly within the Mazinaw domain of the Central Metasedimentary Belt (Easton 1992), and is subdivided herein into 2 lithostructural subdomains that are fault bounded.

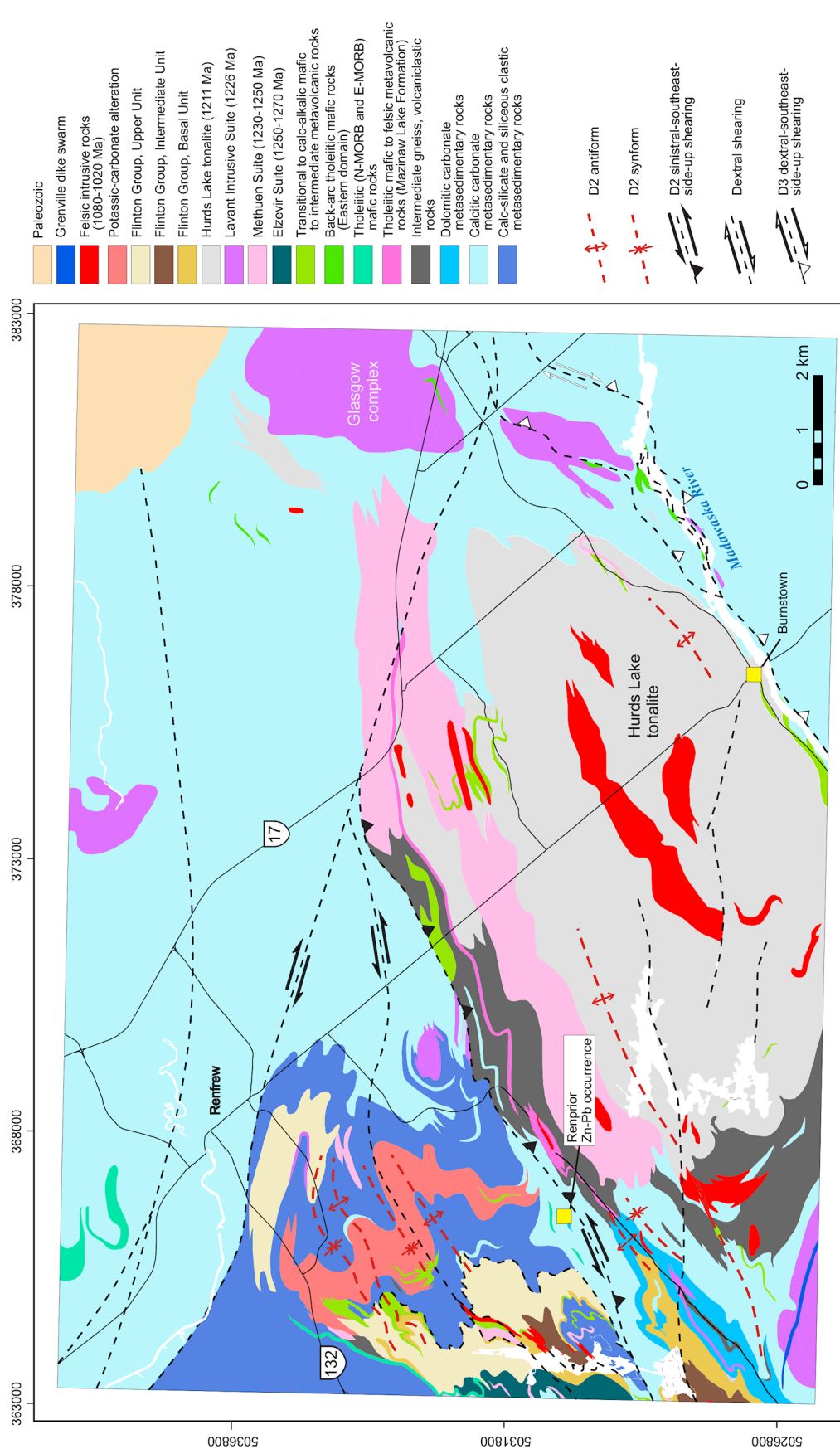


Figure 13.1. Geological map of the Horton area; Universal Transverse Mercator (UTM) co-ordinates provided in North American Datum 1983 (NAD83), Zone 18. For regional location of the study area, see Easton (this volume, Figure 12.1).

The eastern and northern parts of the Horton area are carbonate dominated and composed mainly of calcite marble and minor calc-silicate gneiss, along with minor mafic and felsic gneiss possibly derived from volcanoclastic rocks. This mixed package of mafic and felsic gneiss and mafic schist can be traced along strike over 10 km (*see* Figure 13.1). This unit was previously identified as a marker horizon in 2011 because of its anomalous garnet content in the both the mafic and felsic rocks (Easton, Duguet and Magnus 2011). Some of these mafic and felsic gneiss units display chemical characteristics similar to those documented for the Mazinaw Lake Formation (Ayer 1979; Easton and Ayer 1994).

The supracrustal units were intruded by at least 3 different intrusive suites: the Elzevir, Methuen and Lavant suites (Easton 1992). So far, plutonism representing the Gananogue (Frontenac) suite (1175 to 1150 Ma) appears to be absent in the Admaston–Horton area.

The apparently oldest intrusive suite is composed of alkali-feldspar granite and syenogranite chemically identical to those of the Methuen suite (Easton 1992; Lumbers et al. 1990). The largest granitic pluton of this suite occurs on the north side of the Hurds Lake tonalite and is oriented to the northeast (*see* Figure 13.1). A zircon from this pluton, analyzed by thermal ionization mass spectrometry (TIMS), has yielded a minimum U/Pb age of 1229 ± 3 Ma (S.L. Kamo, Jack Satterly Geochronology Laboratory, Toronto, written communication, 2012). This age is younger than the typical age of *circa* 1245 Ma for the Methuen suite, but is consistent with ages of Methuen suite granitoid rocks present in the northwestern Central Metasedimentary Belt (Easton and Kamo 2011).

A diorite from the Glasgow complex, an intrusion consisting of gabbro, diorite and syenite, yielded a slightly younger zircon age of 1223 ± 1 Ma by U/Pb TIMS (S.L. Kamo, Jack Satterly Geochronology Laboratory, Toronto, written communication, 2012). This unit is tentatively assigned to the Lavant suite. These 2 new ages are comparable to the U/Pb zircon ages of the Chenaux and Raglan Hills gabbros (1231 ± 2 Ma and 1229 ± 5 Ma, respectively: Pehrsson, Hanmer and van Breemen 1996) and the Lavant gabbro (1224 ± 2 Ma: Corfu and Easton 1997). The age on the Glasgow complex is older than previous workers had suggested based on field relationships (e.g., Lumbers 1982b).

The final plutonic unit with a newly obtained zircon age is the Hurds Lake tonalite, which yielded a U/Pb TIMS age of 1211 ± 1.4 Ma (S.L. Kamo, Jack Satterly Geochronology Laboratory, Toronto, written communication, 2012). This age is far younger than other ages obtained from the Elzevir suite, which are typically 1270 to 1250 Ma (Easton 1992; Lumbers et al. 1990). The age of the Hurds Lake tonalite would seem to confirm the hypothesis previously laid out concerning a younger age for tonalitic plutonism in this part of the Central Metasedimentary Belt (Easton, Duguet and Magnus 2011). If this young age is also found from other tonalite intrusions in the Admaston–Horton and Brudenell map area, then it is possible that a new suite of calc-alkalic intermediate to felsic plutonic rocks will have to be created within the overall tectono-stratigraphic framework of the Central Metasedimentary Belt. Additional geochronology in the region will be needed to further test this hypothesis.

The western part of the Horton area is characterized by a strong decrease in volume of the carbonate rocks. This trend of decreasing carbonate units continues west into the eastern Admaston area, which is mainly composed of plutonic rocks comprising mostly tonalitic gneiss, Methuen suite granitoids, amphibolite and minor carbonate units. To the northeast in the Horton area, a highly deformed and metamorphosed package of calc-silicates, Methuen suite granitoids, fine-grained intermediate gneisses of calc-alkalic affinity, tholeiitic and calc-alkalic gabbroic intrusions with minor calcite marble structurally overlie the plutonic-dominated package. The bulk of these structurally overlying units are likely metasedimentary in origin and are, in turn, overlain by thicker units of carbonate rocks further to the northeast. The metasedimentary-dominated package was in part subjected to an intense potassium metasomatic event that will be described latter in this article.

All of these units are unconformably overlain by rocks of the Flinton Group, which were deposited no later than 1157 ± 10 Ma (maximum age of deposition: Sager-Kinsman and Parrish 1993). Three belts of rocks assigned to the Flinton Group were identified in the field. They are all located to the southwestern side of the Horton area and continue into the southeastern corner of the Admaston area. The southernmost belt overlies marbles and is composed of metaquartzarenite, calcareous metaquartzarenite and biotite-sillimanite-bearing mylonitic schist. They are, in turn, overlain by garnet-sillimanite-bearing mica schists. The second belt is located just north of the first belt and covers the largest area of the 3 belts. The substrate to the second belt consists of the rock units present in the Admaston area, in which carbonate rocks are a minor component. This second belt is composed of the 2 rock units previously described for the first belt, plus an upper unit composed of finely laminated calc-silicate rock. The northernmost belt is almost exclusively composed of finely laminated calc-silicate rocks, with minor meta-arenites. Of all of the Flinton Group rock types, the calc-silicate rocks are the most difficult to assign to the Flinton Group, or to differentiate into the different formations of the group. This is because they are very texturally and compositional similar to Grenville Supergroup calc-silicate rocks—a task made more difficult by the metamorphism and the intense deformation that these rocks have undergone.

Mapping in 2012 in the Admaston area farther west has shown that this domain differs lithologically and structurally from the Horton area. The structural and kinematic aspects of this difference are described in the next section. Compared to the Horton area, the main difference is the overwhelming amount of late Grenvillian syenitic and monzonitic plutonism present in the Admaston area. The compositional range of these plutons is more diversified compared to the Horton area, and ranges from porphyritic syenogranite, quartz syenite, equigranular biotite-rich monzonite to equigranular pyroxene-rich syenite. This late Grenvillian plutonic event is pervasive in the Admaston area and affects every unit north and west of Highway 132. All these late Grenvillian plutons are synkinematic except for some of the pyroxene-bearing syenites, which are postkinematic. These plutons have strong compositional, structural and likely chemical affinities with those described further west in the adjacent Brudenell area (Easton, this volume, Article 12).

The host rocks of this late Grenvillian plutonism is composed mostly of a package of mafic, intermediate and felsic gneisses interlayered with calcitic marble. The majority of these gneissic rocks are likely derived from igneous protoliths. Some primary textural features can still be recognized in these gneisses in the eastern part of the Admaston area. In contrast, these gneisses are strongly deformed and locally underwent partial melting, especially in the western part of the Admaston area.

Structural Geology

The Horton area underwent a major sinistral strike-slip deformational event that was responsible for the formation of shear zones associated with northeast-trending upright to northwest-verging folds in the area (Easton, Duguet and Magnus 2011; Photo 13.1A). This strike-slip event is coeval with the emplacement of pegmatitic syenite and syenogranite bodies (Easton, Duguet and Magnus 2011). On the northern side of the Hurds Lake tonalite, a northeast-trending sinistral shear zone separates the carbonate-dominated eastern domain from the plutonic and siliciclastic-dominated western domain. This shear zone continues further south into the Admaston area where it adopts a bearing closer to north. The shear sense criteria in the Admaston area gives a consistent sinistral southeast-side-up shear sense that is particularly well developed in the mica schists of the Flinton Group (Photo 13.1B). Several second-order sinistral shear zones are also present to the northwest in the western part of Horton area.

Mapping during 2012 in the Admaston area has confirmed that this sinistral strike-slip deformational event decreases in intensity and eventually disappears in the eastern part of the Admaston area. Mapping along Highway 132 and farther to the west has shown that the deformation is predominantly characterized by thrusting. In the Admaston area, north and west of the Highway 132, the overall northeast-trending

foliation dips shallowly to the southeast. This general foliation contains a stretching and mineral lineation that plunges steeply to the southeast. No major folds were identified during mapping in this domain. Numerous intrusions, mostly composed of syenite, quartz syenite, pyroxene syenite were emplaced during this thrusting event (Photo 13.2). The fabric in these intrusive rocks was acquired at the supra solidus stage when they were emplaced parallel to the main deformational fabric. Numerous shear criteria gave a

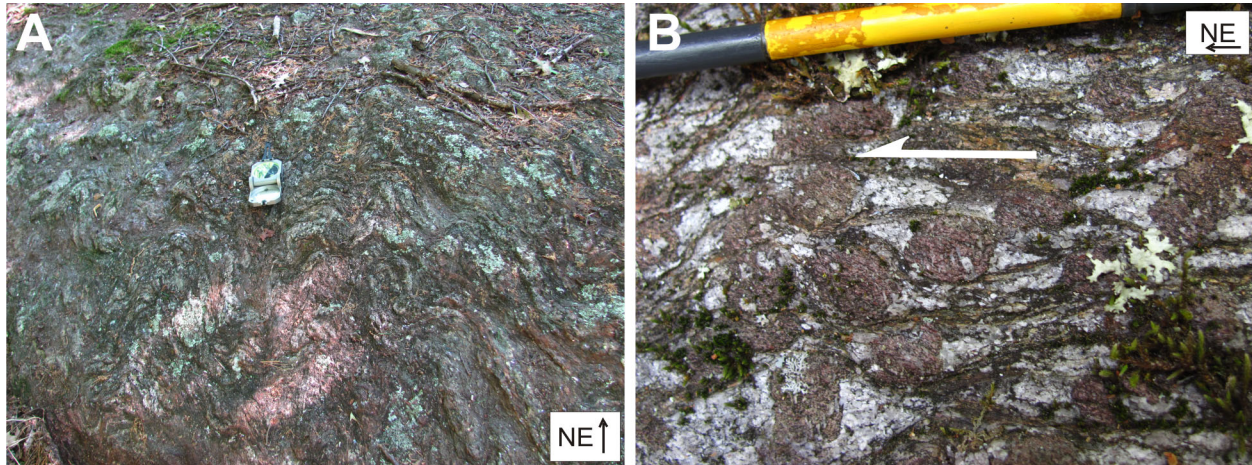


Photo 13.1. A) Northeast-trending upright folding within a garnet-sillimanite mica schist of the Flinton Group (UTM 362122E 5026219N, NAD83, Zone 18). Compass is 14.5 cm long. B) Asymmetric recrystallization tails around garnets giving a sinistral southeast-side-up shearing (Flinton Group) (UTM 362055E 5026483N, NAD83, Zone 18). Stylus is 96 mm long.



Photo 13.2. Shear bands within a synkinematic potassium feldspar porphyritic syenogranite give a top-to-the-northwest shear sense (vertical surface), Admaston area (UTM 347401E 5029067N, NAD83, Zone 18). Stylus is 96 mm long.

consistent top-to-the-northwest shear sense (*see* Photo 13.2). This thrusting event is reworked by a late normal southeast-side-down event. This late normal event is characterized in the field by localized shear zones and microfolding (Photos 13.3A and 13.3B). This late normal event nonetheless seems to have been discrete, and possibly incipient, since no major structure could be linked to the observed microstructures.

The Horton–Admaston area also underwent another ductile deformation event that has either been disregarded or unidentified. In the field, northwest-trending shear zones are associated with this event. If such structures were identified in previous mapping of the area (Lumbers 1982a, 1982b), then they were interpreted as resulting from Paleozoic faulting associated with the Ottawa–Bonnechere graben. However, our field investigations have shed new light on the nature and the age of this ductile deformation event. In the north part of Horton area, on a map scale, all of the northeast-trending structures are consistently transposed into a northwest trend (*see* Figure 13.1). This is particularly evident just south of Renfrew, where structures were bent clockwise as much as 90° from their initial orientation. Further north from Renfrew, however, the regional structures once again exhibit a regional northeast trend. Along the Highway 17, localized northwest-trending shear zones that dip steeply to the northeast crosscut the earlier regional fabric. Within the shear zone, asymmetric boudinage of pegmatitic veins gives a dextral shear sense consistent with the clockwise rotation of the structures on a map-scale view (Photo 13.4A). These pegmatites are clearly synkinematic with respect to this event since they present little to no internal plastic deformation. These features cast strong doubts on an exclusively Paleozoic age of these structures. The evidence presented herein indicates that these shear zones were contemporaneous of the Grenville Orogeny and developed roughly perpendicular to the trend of the belt. Additional studies are underway to decipher the relative timing between this late ductile deformational event and the sinistral strike-slip deformation. Such orthogonal structures are observed in younger orogens such as the Himalayas, where they have been recently described and discussed (*cf.* Rivers 2012).

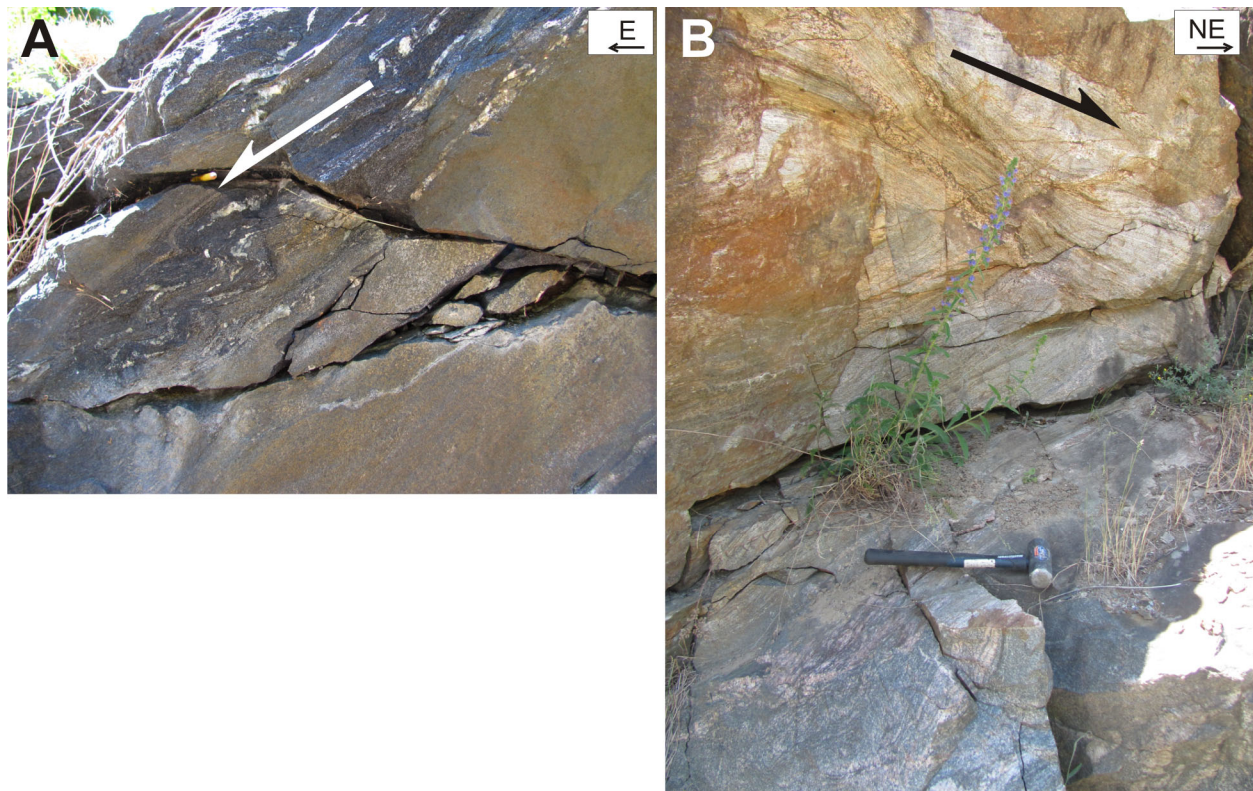


Photo 13.3. A) Drag folds outlined by thin white granitic veins. The folds give an east-side-down shear sense (vertical surface) (UTM 358990E 5035337N, NAD83, Zone 18). B) High-angle shear bands in a porphyritic tonalite gneiss giving a northeast-side-down shear sense (vertical surface) (UTM 345004E 5037532N, NAD83, Zone 18). Hammer handle is 45 cm long.

The Horton area was also affected by a late dextral thrusting event (*see* Figure 13.1). Evidence of this event can be found along the Madawaska River near Burnstown in the southeastern part of Horton area (Photo 13.4B).

As a concluding remark, it is striking that 3 of the 4 of the deformational episodes described herein are all coeval with pegmatitic syenitic to granitic magmatism. There remains the question of the relative timing of these different deformation events with magmatism. Are we dealing with a single tectonic event having different structural features and kinematic sense according to their geographic and/or stratigraphic positions in the map area, or are they several temporally distinct episodes? In the neighbouring Brudenell area, late magmatism seems to have spanned a period of 40 million years (Easton, this volume, Article 12). Unravelling these questions will require additional studies.

RECOMMENDATIONS FOR EXPLORATION

Rare Element Mineralization

The Admaston–Horton area, similar to the Brudenell area (*see* Easton, this volume, Article 12), has potential for rare element and rare earth element mineralization. However, the mineralizing processes and the age of these mineralizing events are probably different from those described for the Brudenell area. Geochemical data for those rock units with the highest rare earth element contents are presented Table 13.1.

The highest concentration of total rare earth elements (1200 ppm) was found in an impure calcite marble in a roadcut immediately southeast of Burnstown on the south side of the Madawaska River (sample 11MD001B, Figure 13.2A). This sample is located at the edge of a complex, highly strained, skarn zone infilled with several generations of sills of syenitic, tonalitic and mafic compositions. The rare earth element pattern of this sample is characterized by a strongly fractionated pattern with enrichment in the light rare earth elements (*see* Figure 13.2A). This pattern is unlike those present in typical marble units (cf. Easton 1995), and suggests that the marble was affected by a postdepositional fluids. This pattern is similar to that observed for the Hurds Lake tonalite and for calc-alkalic mafic rocks in the Horton area. Both of these rock types are located on the north shore of the Madawaska River and are proximal to sample 11MD001B. Nonetheless, the elevated phosphorus content (0.51 weight %) in sample

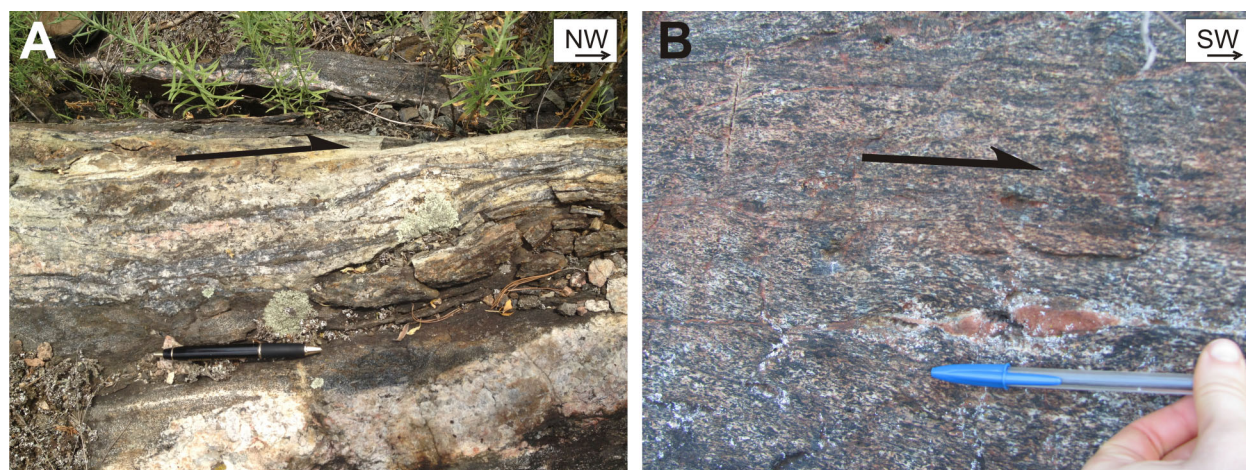


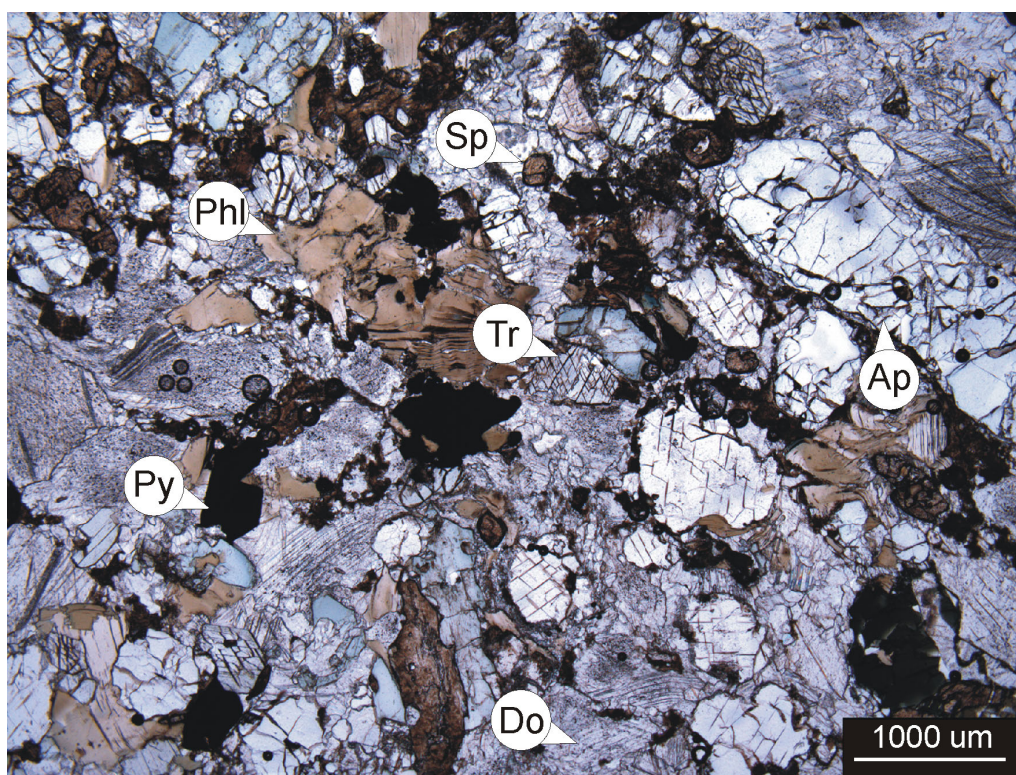
Photo 13.4. A) Asymmetric boudinage of porphyritic granite and pegmatitic veins giving a dextral shear sense (horizontal surface) (UTM 377194E 5033756N, NAD83, Zone 18). The pen is 14 cm long. B) Asymmetric boudinage of the quartz vein in this mylonitic gabbro gives a dextral shear movement (vertical surface) (UTM 379002E 5028270N, NAD83, Zone 18). The pen is 14 cm long.

Table 13.1. Selected chemistry of a variety of rock types from the Horton area, which contain elevated rare element and rare earth element (REE) contents. Data from the Geoscience Laboratories, Ontario Geological Survey.

Sample Number	Rock Type	Easting ¹ (m)	Northing ¹ (m)	Total REE (ppm)	P ₂ O ₅ (wt %)	Zr (ppm)	Nb (ppm)	Sc (ppm)	Sr (ppm)	Y (ppm)
11MD001B	Impure calcite marble	376720	5026788	1210	0.51	45	10	5	>1560	76
11SM104B	Metasomatized syenite (Methuen suite)	378003	5033774	713	0.08	>1450	40	4	104	299
11SM116A	Felsic schist (Flinton Group)	363022	5028777	619	0.04	1281	53	4	15	232
11SM175A	Quartz syenite (Methuen suite)	364228	5032013	548	0.05	1080	39	2.5	66	163
11MD038A-2	Felsic gneiss (Mazinaw Lake Formation)	366875	5030152	532	0.03	1100	45	2	56	173

¹UTM co-ordinates in NAD83, Zone 18.

11MD001B also suggests a geochemical signature more akin to the calc-alkalic mafic rocks than to the Hurds Lake tonalite, which is almost devoid of this element. In thin section, the observed mineral assemblage (presented from most to least abundant) in this sample is calcite + dolomite (55%) + tremolite + phlogopite + apatite + titanite + pyrite (Photo 13.5). Although this marble has been subjected to metasomatic fluids, it does not qualify as skarn *sensu stricto* because it lacks of the characteristic skarn mineralogy. The anomalous phosphorus content compared to typical marbles suggests that the rare earth elements may be, in part, hosted in apatite and/or monazite.

**Photo 13.5.** Photomicrograph of sample 11MD001B in plane-polarized light showing the mineral assemblage present. Abbreviations: Ap, apatite; Do, dolomite; Phl, phlogopite; Py, pyrite; Sp, titanite; Tr, tremolite.

Elevated rare earth element contents are also present in some granites and quartz syenites of the Methuen suite. On a chondrite-normalized diagram, these rocks have a flat but enriched pattern with a negative europium anomaly (Figure 13.2B). This pattern is similar to that of FIII rhyolites (Leshner et al., 1986). The highest value of total rare earth elements was found in a metasomatized quartz syenite (see Table 13.1, sample 11SM104B). Zirconium content is above the detection limit (>1000 ppm) and yttrium is high. Conversely, phosphorus, strontium, niobium and scandium are very low. The relatively enriched but unfractionated rare earth element patterns of the Methuen suite rocks make them more favourable hosts for the heavy rare earth elements than any other unit in the Horton area, as the latter all have more

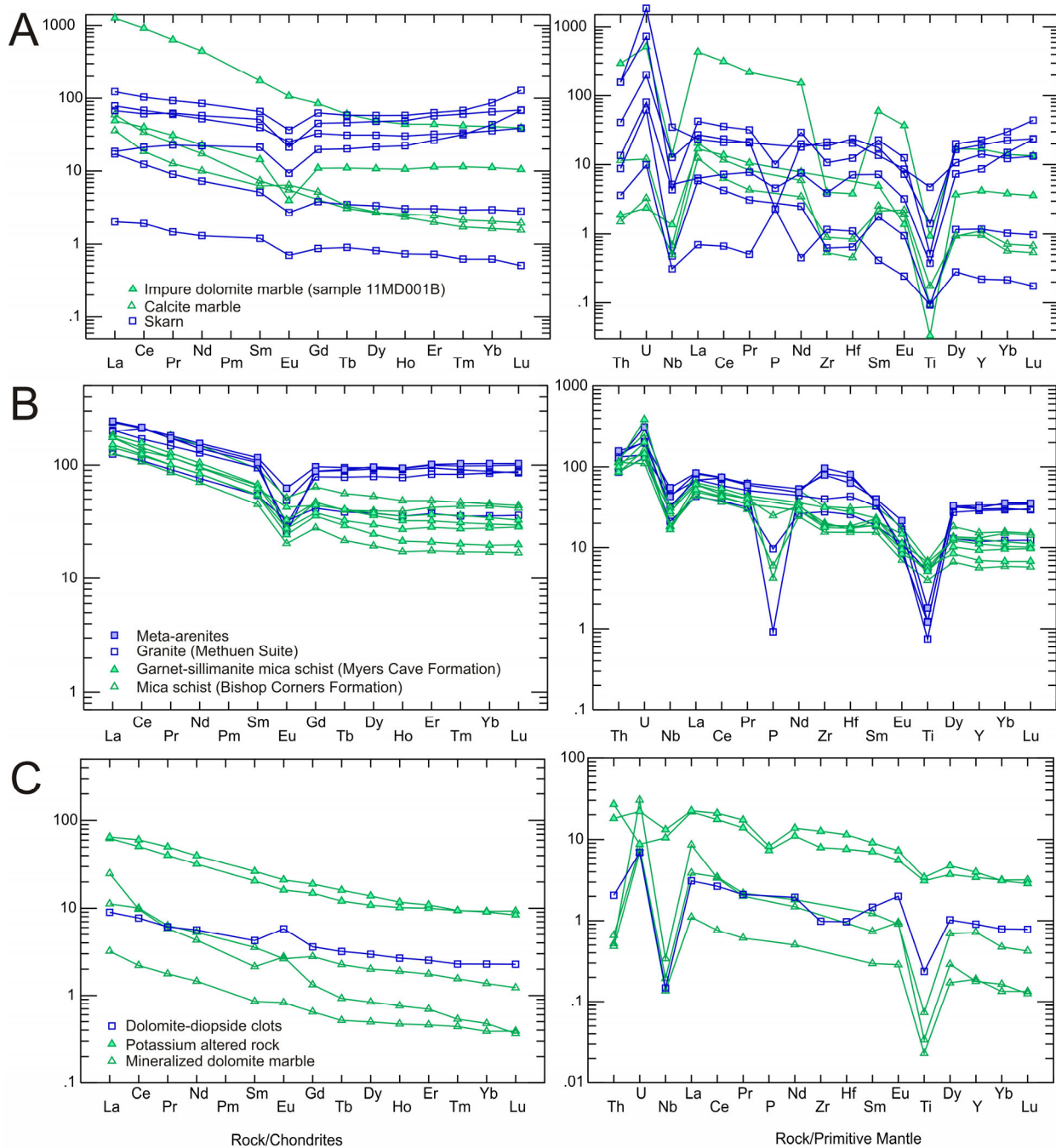


Figure 13.2. Chondrite-normalized rare earth element (REE) and incompatible element (Spider) diagrams for selected rock units from the Horton area. See text for discussion. Normalizing factors of Sun and McDonough (1989) are used.

Table 13.2. Selected chemistry of 2 samples from the potassium alteration zone. Data from the Geoscience Laboratories, Ontario Geological Survey.

Sample Number	Easting ¹ (m)	Northing ¹ (m)	CaO (wt %)	K ₂ O (wt %)	SiO ₂ (wt %)	CO ₂ (wt %)	Sr (ppm)
11MD047A	367601	5033210	5.86	11.5	52.56	3.91	394
11MD120A	365949	5034178	5.13	10.14	57.47	0.82	192

¹UTM co-ordinates in NAD83, Zone 18.

fractionated, light rare earth enriched patterns. These chemical characteristics differ notably from those found in the younger syenitic rocks that host rare earth element mineralization in the adjacent Brudenell area (Easton, this volume, Article 12). The mineral phases hosting the rare earth elements within the Methuen suite rocks have not been identified yet; however, given the high zirconium content, it is likely that zircon is one of the main rare earth element host phases. Some rocks interpreted herein as belonging to the Mazinaw Lake Formation also exhibit the same chemical features (*see* Table 13.1, sample 11MD038A-2).

It is also interesting to note that felsic intrusive rocks assigned to the Lavant suite and emplaced at *circa* 1223 Ma share some of the same chemical features as the Methuen suite, but so far have not been found to contain high rare earth element contents.

Meta-arenites and mica schists and interpreted as equivalents of the Ore Chimney and Bishop Corner formations display some of the same geochemical characteristics to the granites of the Methuen suite (*see* Figure 13.2B; *see* Table 13.1). This is not surprising since a significant part of the substrate to these units, and/or the nearest detritus sources is mostly composed of Methuen suite granites. Also noteworthy is that the rare earth element patterns for these rocks become more fractionated with increasing stratigraphic height relative to the underlying unconformity. Unfortunately, the lower units of the Flinton Group are not a primary target for exploration due to their limited areal extent.

Regional Potassium Alteration and its Relationship to Base Metal Mineralization

A prominent, ovoid, airborne gamma-ray spectrometric potassium high covering an area of approximately 12 km² is located in the northwest corner of the Horton map area (Carson et al. 2004). This anomaly was first noted in Easton, Duguet and Magnus (2011), but further mapping in 2012 has improved delineation of the extent and character of this potassium anomaly. The rocks in the area of the anomaly were previously mapped as syenite (Lumbers 1982b). Nonetheless, gamma-ray scintillometer measurements reported in Easton, Duguet and Magnus (2011) and subsequent geochemical analyses indicate K₂O contents up to 11.5 weight %, which is 2 to 3 weight % higher than the K₂O contents found even in ultrapotassic syenites. Such high K₂O contents are more typically observed in alteration zones present in a wide variety of mineralizing systems ranging from porphyry systems, iron oxide-copper-gold (IOCG), orogenic gold and sedimentary-exhalative systems (SEDEX). The chemistry for 2 samples from the potassium-rich zone is presented in Table 13.2. These 2 samples are also calcium- and CO₂-rich compared to typical syenitic rocks, although it is unclear if the calcium and CO₂ are primary features of the rock or are also the result of this hydrothermal event. Rare earth element and incompatible element diagrams are presented for the 2 rocks in Figure 13.2C (samples 11MD047A and 11MD120A). The patterns are not unique, as other rock types in the area display similar patterns; however, they are distinct from Methuen suite granitoids by the absence of a europium anomaly.

On a map scale, the potassium alteration zone seems to parallel the regional foliation. It is also affected by the northeast-trending upright folding event. The potassium alteration affects all rock types ranging from gabbro, granites of the Methuen suite and calc-silicate rocks, but can vary in intensity. It is

usually characterized by an intense, texturally destructive replacement of the protolith resulting in a light to medium pink colour on fresh surfaces (Photo 13.6A). Some of these altered rocks adopt a more greenish colour when calc-silicate minerals are present in greater amounts. Where less intensely altered, alteration of the protolith is characterized by the presence of light pink veins mostly composed of potassium feldspar that parallel the main fabric in the rock (Photo 13.6B).

In thin section (Photos 13.6C and 13.6D), pervasively altered samples 11MD047A and 11MD120A display a granoblastic texture with a groundmass composed mostly of orthoclase (65%). Two mineral assemblages have been observed so far: 1) orthoclase + biotite + diopside + hornblende + magnetite, and 2) orthoclase + biotite + calcite + hornblende + titanite + magnetite (the minerals are presented in order of most to least abundant). Quartz is absent in both assemblages. Considering the intense deformation and metamorphism that the Horton area has undergone, it is unlikely that these assemblages reflect the primary mineralogy of the alteration.

The geological context of this intense potassium alteration zone is still a mystery. One reason for this is the intense metamorphism and polyphase deformation which affected the area during the Grenville Orogeny. Nonetheless, several hypotheses remain to be tested. As previously indicated, potassium alteration

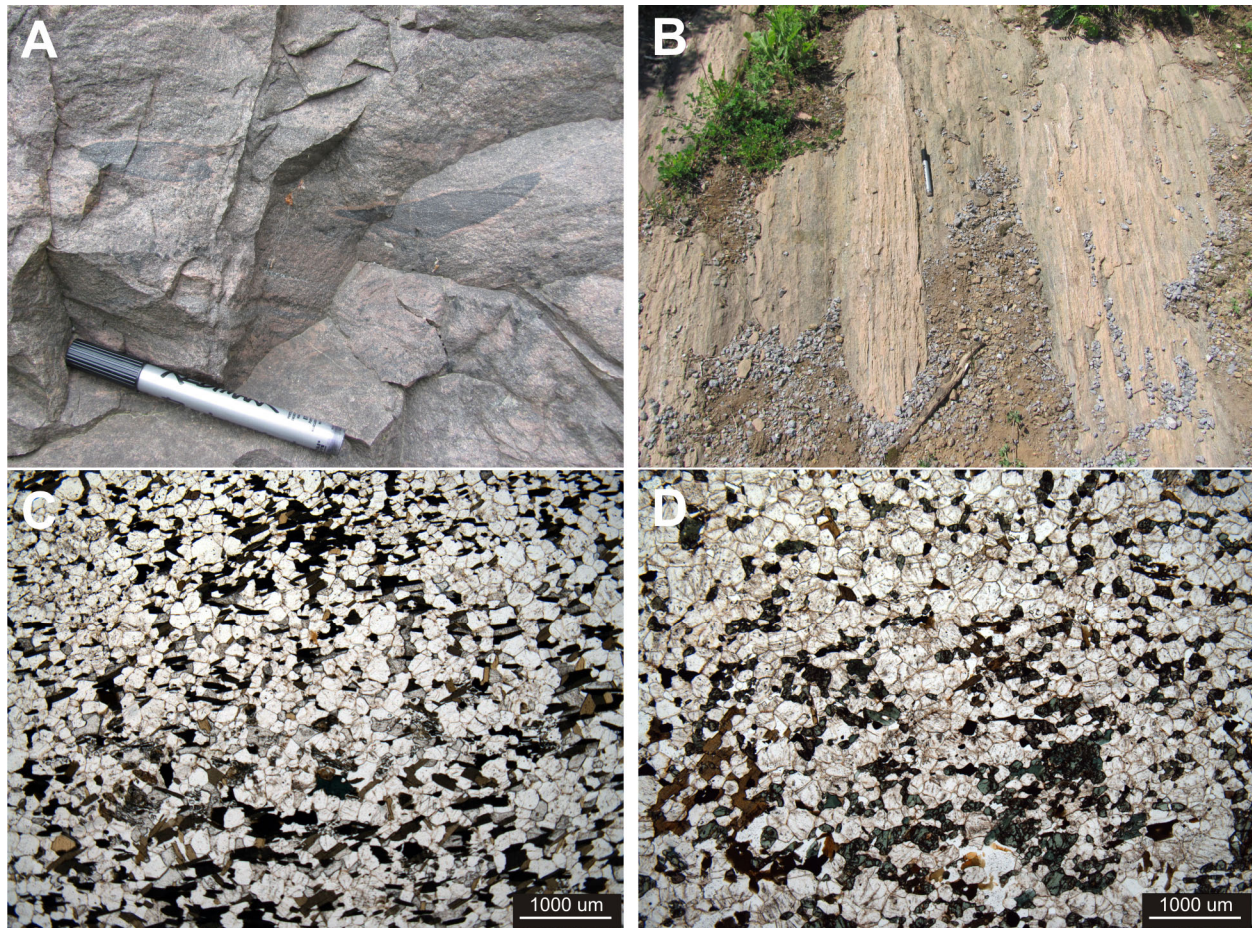


Photo 13.6. A) Rocks of unknown affinity affected by pervasive potassic alteration. Alteration halos are present around mafic “enclaves” that may be the unaltered protolith (UTM 366028E 5032764N, NAD83, Zone 18). The marker is 16 cm long. B) Potassic alteration veins parallel to the main foliation (UTM 365487E 5035312N, NAD83, Zone 18). The marker is 16 cm long. C) Photomicrograph of sample 11MD047A in plane-polarized light showing the texture and the mineral assemblage of a pervasively potassic altered rock. D) Photomicrograph of sample 11MD120A in plane-polarized light showing the texture and the mineral assemblage of a pervasively potassic altered rock.

is a ubiquitous feature in several mineralizing systems. To date, no pluton large enough to generate such a large hydrothermal system has been identified in the immediate vicinity of the alteration zone. Even if one considers that this pluton was within the alteration zone itself and was completely obliterated by the metasomatic event, it would have to be considerably smaller than either the Hurds Lake tonalite or the Glasgow complex. These 2 bodies only induced limited hydrothermal activity in their country rocks, consisting of limited local fenitization and albitization. The lack of an identifiable plutonic source makes any magmatic-related hydrothermal deposit models, such as porphyry or IOCG, highly unlikely.

On the other hand, the proximity of the Renprior zinc-lead occurrence and the Flinton Group unconformity to this potassium alteration zone favours a model of hydrothermal circulation in a sedimentary basin. The Renprior zinc-lead occurrence is located at the southeastern edge of the potassium alteration zone and is 500 m distant from the zone. Moreover, the Flinton Group unconformity in the southwestern part of the Horton area is geometrically associated with the only continuous dolomite marble unit in the area. Consequently, it is likely that Flinton Group deposition was coeval with complete dolomitization of an original calcite marble substrate by intense fluid circulation.

Similar relationships between unconformities, zinc-lead mineralization of Mississippi Valley-type (MVT) or SEDEX-type and pervasive potassium alteration by saline brines have been described elsewhere (e.g., Cooke et al. 1998). Further work will be needed to clearly assess the setting of this potassium alteration and its relationships with zinc-lead sulphide mineralization. If they are indeed genetically linked, then identifying regional potassium alteration may be an useful tool for zinc-lead exploration within the Central Metasedimentary Belt.

ACKNOWLEDGMENTS

K. Campbell and V. Dubé-Bourgeois are warmly thanked for their outstanding performance as junior assistants. Numerous discussions with R.M. Easton also proved very helpful. S. Lin's visit at our camp and his insight into the structural geology of the area was greatly appreciated. Many land owners in the area kindly granted permission to inspect their properties, and their assistance is greatly appreciated.

REFERENCES

- Ayer, J.A. 1979. The Mazinaw Lake metavolcanic complex, Grenville Province, southeastern Ontario; unpublished MSc thesis, Carleton University, Ottawa, Ontario, 100p.
- Carson, J.M., Holman, P.B., Ford, K.L., Grant, J.A. and Shives, R.B.K. 2004. Airborne gamma ray spectrometry compilation, potassium, Central Metasedimentary Belt, (Grenville Province), Ontario–Quebec; Geological Survey of Canada, Open File 4558, scale 1:250 000.
- Cooke, D., Bull, S.W., Donovan, S. and Rogers, J.R. 1998. K-metasomatism and base metal depletion in volcanic rocks from the McArthur Basin Northern Territory—implications for base metal mineralization; *Economic Geology*, v.93, p.1237-1263.
- Corfu, F. and Easton, R.M. 1997. Sharbot Lake terrane and its relationships to Frontenac terrane, Central Metasedimentary Belt, Grenville Province: new insights from U–Pb geochronology; *Canadian Journal of Earth Sciences*, v.34, p.1239-1257.
- Easton, R.M. 1992. The Grenville Province; *in* *Geology of Ontario*, Ontario Geological Survey, Special Volume 4, Part 2, p.713-904.
- 1995. Regional geochemical variation in Grenvillian carbonate rocks: implications for mineral exploration; *in* *Summary of Field Work and Other Activities, 1995*, Ontario Geological Survey, Miscellaneous Paper 164, p.6-18.

- Easton, R.M. and Ayer, J.A. 1994. VMS potential of the Mazinaw terrane, Grenville Province; *in* Summary of Field Work and Other Activities, 1994, Ontario Geological Survey, Miscellaneous Paper 163, p.27-30.
- Easton, R.M., Duguet, M. and Magnus, S.J. 2011. Geology and mineral potential of the northeastern Central Metasedimentary Belt, Grenville Province; *in* Summary of Field Work and Other Activities, 2011, Ontario Geological Survey, Open File Report 6270, p.5-1 to 5-23.
- Easton, R.M. and Kamo, S.L. 2011. Harvey–Cardiff domain and its relationship to the Composite Arc Belt, Grenville Province: insights from U–Pb geochronology and geochemistry; *Canadian Journal of Earth Sciences*, v.48, p.347-370.
- Leshner, C.M., Goodwin, A.M., Campbell, I.H. and Gorton, M.P. 1986. Trace-element geochemistry of ore associated and barren, felsic metavolcanic rocks in the Superior Province, Canada; *Canadian Journal of Earth Sciences*, v.23, p.222-237.
- Lumbers, S.B. 1982a. Barry's Bay; Ontario Geological Survey, Map 2461, scale 1:100 000.
- 1982b. Renfrew; Ontario Geological Survey, Map 2462, scale 1:100 000.
- Lumbers, S.B., Heaman, L.M., Vertolli, V.M. and Wu, T.-W. 1990. Nature and timing of Middle Proterozoic magmatism in the Central Metasedimentary Belt, Ontario; *in* Mid-Proterozoic Laurentia–Baltica, Geological Association of Canada, Special Paper 38, p.243-276.
- Pehrsson, S., Hanmer, S. and van Breemen, O. 1996. U–Pb geochronology of the Raglan gabbro belt, Central Metasedimentary Belt, Ontario: implications for an ensialic marginal basin in the Grenville Orogen; *Canadian Journal of Earth Sciences*, v.33, p.691-702.
- Rivers, T. 2012. Upper-crustal orogenic lid and mid-crustal core complexes: signature of a collapsed orogenic plateau in the hinterland of the Grenville Province; *Canadian Journal of Earth Sciences*, v.49, p.1-42.
- Robertson, D. 1984. Cadieux (Renprior) deposit; *in* Metallogeny of the Grenville Province, southeastern Ontario; Ontario Geological Survey, Open File Report 5515, p.272-285.
- Sager-Kinsman, A. and Parrish, R.R. 1993. Geochronology of detrital zircons from the Elzevir and Frontenac terranes, Central Metasedimentary Belt, Grenville Province, Ontario; *Canadian Journal of Earth Sciences*, v.30, p.465-473.
- Sun, S.-S. and McDonough, W.F. 1989. Chemical and isotopic systematics of oceanic basalts: implications for mantle composition and processes; *in* Magmatism in the ocean basins, The Geological Society, Special Publication No.42, p.313-345.

14. Project Unit 11-005. Geology and Mineral Potential of the Raglan Hills Metagabbro, Northeastern Central Metasedimentary Belt, Grenville Province

S.J. Magnus¹, B. Cousens¹ and R.M. Easton²

¹Ottawa–Carleton Geoscience Centre, Department of Earth Sciences, Carleton University, Ottawa, Ontario K1S 5B6

²Earth Resources and Geoscience Mapping Section, Ontario Geological Survey, Sudbury, Ontario P3E 6B5

INTRODUCTION

The Raglan Hills area encompasses approximately 220 km² and is bounded by 45°07'30" to 45°18'30"N latitude and 77°25'00"W to 77°33'30"W longitude. Most of the study area is in Raglan Township, but does include parts of Ashby and Mayo townships. This map area contains part of the carbonate-dominated Bancroft terrane (Easton 1992), into which the Raglan Hills metagabbro was intruded, and part of the metavolcanic and metavolcaniclastic rock dominated Elzevir terrane (Easton 1992) to the south (Figure 14.1). The Raglan Hills metagabbro has had limited study in the past. It is indicated on 2 regional bedrock maps: Hewitt (1954) at a scale of 1:63 360, and Lumbers (1982) at a scale of 1:100 000. Easton (this volume, *see* Figure 12.1) provides an indication of the regional setting of the Raglan Hills map area within the northeastern Central Metasedimentary Belt.

First Nickel Inc. has been exploring for nickel and copper within the Raglan Hills metagabbro since 2009, with the hope of expanding the previously identified resource at the Raglan copper-nickel showing located at 45°12'02"N latitude and 77°28'13"W longitude (MDI31F03NW00041; Carter, Colvine and Meyn 1980). This showing lies on a positive magnetic and electromagnetic anomaly identified by a detailed airborne geophysical survey of the Raglan Hills metagabbro and surrounding area performed by First Nickel Inc. in 2009, and subsequently purchased and published by the Ontario Geological Survey (Ontario Geological Survey 2010a, 2010b) (*see* Figure 14.1).

The purpose of this project is to study the geology of the Raglan Hills metagabbro, and to utilize whole-rock and isotope geochemistry, in combination with metamorphic and structural analyses, to better understand the processes which formed the varied rock units in the intrusion and the post-intrusive processes, including tectonism and metamorphism, that have since affected it. The mineralization within the intrusion will be analyzed using the same methods, in order to determine the source of the copper and nickel in the mineralized zones and to determine how their host sulphide minerals have been affected by deformation and metamorphism. Additionally, the Raglan Hills metagabbro will be compared to the other gabbroic intrusions within the Raglan Hills and adjacent Brudenell map areas (Easton, this volume, Article 12) and elsewhere within the Central Metasedimentary Belt, such as the Glamorgan and Lavant metagabbros.

Following the 4 weeks of field work performed during the 2011 field season (Easton, Duguet and Magnus 2011), 40 samples from the Raglan Hills metagabbro (including samples from drill core and hand samples) were analyzed for whole-rock geochemistry and cut into thin sections for petrographic analysis. Four samples taken from diamond-drill core were analyzed for Rb/Sr and Sm/Nd isotopic abundances at Carleton University in February 2011. Additional isotopic analyses will be made prior to the end of 2012.

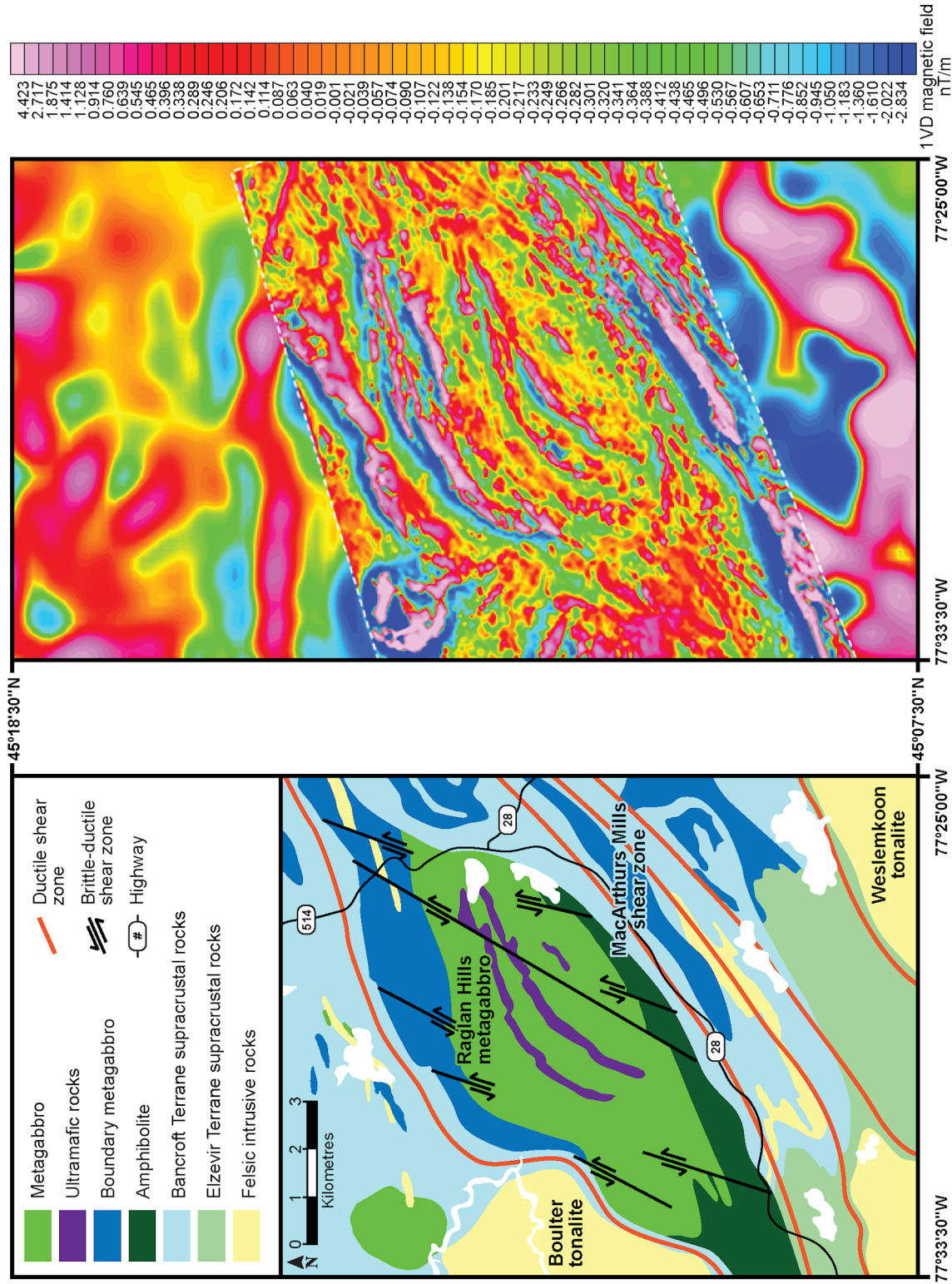


Figure 14.1. Left: Preliminary map compiled from field observations from the 2011 and 2012 field seasons. Right: Map of the second vertical derivative of the residual magnetic field at the same scale and dimensions as the geology map (from Ontario Geological Survey 2010b). Easton (this volume, see Figure 12.1) provides an indication of the regional setting of the Raglan Hills map area within the northeastern Central Metasedimentary Belt.

Approximately 3 weeks of the 2012 field season were spent mapping and sampling the Raglan Hills metagabbro and the surrounding country rocks. The interval between the 2011 and 2012 field seasons was spent studying the petrography, whole rock and isotope geochemistry of the Raglan Hills metagabbro. Preliminary results of this laboratory work were presented by Magnus, Cousens and Easton (2012a, 2012b).

RAGLAN HILLS METAGABBRO

In plan-view, the Raglan Hills metagabbro appears similar to a sigma-clast indicating a dextral shear-sense within the host carbonate rocks into which the gabbro was originally intruded (*see* Figure 14.1). Along the McArthurs Mills shear zone located along the southern edge of the intrusion (*see* Figure 14.1), the metagabbro has been recrystallized to granoblastic amphibolite. In contrast, the rocks at the northern edge of the intrusion have apparently experienced less deformation, preserving more primary gabbroic textures (Photos 14.1C and 14.1E). However, much of the bedrock between the Raglan Hills metagabbro and the Moccasin Lake anticline to the north is buried beneath overburden, obscuring the true nature of the contacts within this area. The rocks within the interior of the intrusion show no evidence of melting, although they display evidence for multiple generations of deformation.

Several distinct rock types within the Raglan Hills metagabbro were identified in the field, each of which also was observed in diamond-drill core. These rock types were first described in Easton, Duguet and Magnus (2011). Petrographic and geochemical studies on the 2011 samples from the Raglan Hills metagabbro, combined with observations in the field during the 2012 field season, have helped to better improve our understanding of the rock types within the Raglan Hill metagabbro. The rock types can be distinguished from one another by macroscopic textures visible in hand sample, as well as in thin section, in addition to their geochemical and geophysical signatures.

Metagabbro

The most abundant rock type is a melanocratic to leucocratic, green and white metagabbro consisting of mainly plagioclase and hornblende, with some relict pyroxene (Photos 14.1A and 14.1B). These rocks are nonmagnetic (average magnetic susceptibility of approximately 0.4×10^{-3} SI units), and rarely contain trace sulphides.

These rocks have been subjected to varied degrees of shearing, producing strong mylonitic fabrics in some cases (*see* Photo 14.1B). Locally, near primary textures are preserved in the lesser deformed rocks, allowing for an assessment of the paragenetic sequence of the metagabbro (*see* Photos 14.1C and 14.1E). The melanocratic and leucocratic end-members of this rock type appear to be related by plagioclase fractionation, since the melanocratic rocks contain plagioclase laths in a mafic matrix, whereas the more leucocratic rocks consist of cumulate-textured plagioclase laths with interstitial mafic material.

The metagabbroic rocks located close to the outer rim of the intrusion (boundary metagabbro) tend to be more varied in their geochemical and geophysical signatures. They also display more varied textures, including the presence of megacrystic clinopyroxene grains and the presence of tonalitic pods (Photo 14.1F), which may represent *in-situ* partial melting of the gabbro.

Amphibolite

Several types of strongly foliated amphibolites are present within the Raglan Hills metagabbro, composed mainly of fine-grained equigranular hornblende, plagioclase and biotite. The majority of these rocks have been observed along the southern rim of the intrusion. They commonly contain tonalitic pods that were likely produced during partial melting of the amphibolite, as well as calc-silicate minerals such as scapolite, titanite and diopside. The latter calc-silicate minerals may indicate interaction between the amphibolites and the surrounding carbonate rocks.



Photo 14.1. Selected photos of the Raglan Hills metagabbro. A) Melanocratic metagabbro (station 11SJM163, UTM 305553E 5007083N). B) Mylonitic leucocratic metagabbro (station 11SJM118, UTM 306582E 5007641N). C) Preserved primary igneous layering (11SJM174, 305436E 5008400N). D) Horizontal hornblende dike in gabbro, below the compass (11SJM186, UTM 303326E 5009863N). E) Preserved primary igneous texture, possibly indicative of magma mixing (11SJM099, UTM 301786E 5007589N). F) A tonalite dike (upper) crosscutting metagabbro in diamond-drill core (First Nickel Inc. diamond-drill hole FNB007, UTM 306137E 5008157N). The diffuse contact and the presence of an anorthositic component exsolved from the metagabbro suggest that the gabbro was still partially liquid when the tonalite was intruded. All UTM co-ordinates are in NAD83, Zone 18. Objects for scale: white pen is 15 cm long; yellow stylus is 8 cm long; compass is 14.5 cm long. All objects point north in all photos.

The magnetic susceptibility of the amphibolites tends to be slightly higher than that of the metagabbro phases, ranging from 0.5 to 1.8×10^{-3} SI units, but with some anomalous sites of up to at least 100×10^{-3} SI units (sample 12SJM-026A, UTM 306574E 5011904N, NAD83, Zone 18).

Several outcrops of metagabbro contain lenses of amphibolite with similar textural and magnetic characteristics (12SJM-030, 12SJM-036), and in these cases the amphibolites are interpreted as mafic xenoliths within the gabbro. It is possible that all of the granoblastic amphibolites found throughout the intrusion are xenoliths and rafts of country rock; however, it is difficult to make this inference for the amphibolites along the southern rim of the intrusion, because of both the lack of exposed contacts and the higher degree of deformation. The higher degree of deformation in the southern margin of the intrusion may be related to the McArthurs Mills shear zone, which may have mylonitized the Raglan Hills metagabbro to this fine-grained amphibolite.

Altered Metagabbro

During logging of diamond-drill core during the 2011 field season, several occurrences of “primary-textured gabbro” were documented and sampled, although none of these rocks were observed in the field. Three occurrences of this unit were observed in outcrop during the 2012 field season, indicating that these primary-textured gabbros are not just a local anomaly within part of the Raglan Hills metagabbro.

Petrographic study of the diamond-drill core samples revealed that these rocks were much more altered than previously thought. The mineral assemblage in these rocks contains olivine, orthorhombic and monoclinic amphiboles, probable pyroxenes, plagioclase, and possibly cordierite (\pm opaque minerals). The presence of cordierite and ortho-amphiboles (most likely anthophyllite with gedrite exsolution) in a metagabbro is indicative of an unusual bulk rock composition commonly attributed to hydrothermal alteration of basaltic crust prior to regional metamorphism, or possibly by metasomatism during metamorphism (Spear 1993).

Ultramafic Rocks

Occurrences of ultramafic rocks termed hornblendites were identified during the 2011 field season in both diamond-drill core and in outcrop, coincident with positive magnetic anomalies in the metagabbro (see Figure 14.1). In diamond-drill core, these ultramafic rocks (pyroxenites) contain primarily clinopyroxene with exsolution lamellae of amphibole, and minor epidote, scapolite and plagioclase, with trace sulphides (chalcopyrite and pyrrhotite with pentlandite flames). In outcrop, these rocks typically contain primarily metamorphic amphiboles with minor epidote, biotite, scapolite and diopside \pm opaque grains (probably magnetite). Outcrops of hornblendite that were observed during the 2012 field season along the positive magnetic anomalies appear similar to the ultramafic rocks observed in diamond-drill core, suggesting that the hornblendites are indeed metamorphic equivalents of the pyroxenites, and not a separate rock unit (a small dike likely similar to the hornblendites is displayed in Photo 14.1D).

The pyroxenites have CaO and CO₂ contents of about 21.0 weight % and 0.7 weight %, respectively, which is much higher than the average composition of the intrusion (13.0 weight % CaO and 0.34 weight % CO₂) (Table 14.1). The pyroxenites commonly host carbonate veinlets consisting of calcite \pm scapolite \pm diopside that have not been observed cutting the other units within the intrusion. The hornblendites have significantly lower CaO and CO₂ contents (14.0 weight % and 0.3 weight %, respectively), which may indicate that any calcium carbonate present in the parent pyroxenites were driven off during metamorphism. Future work on the petrography, whole rock and isotope geochemistry of these ultramafic units will focus on determining the genesis of these rocks and their behaviour during metamorphism.

Table 14.1. Average major element, copper and nickel concentrations for the rock types in the Raglan Hills metagabbro, as well as data from sample 11SJM-120 taken from the historic Raglan Hills copper-nickel showing. Data from the Geoscience Laboratories, Ontario Geological Survey.

Rock Type	SiO ₂ (wt %)	Al ₂ O ₃ (wt %)	TiO ₂ (wt %)	Fe ₂ O ₃ (wt %)	MnO (wt %)	MgO (wt %)	CaO (wt %)	Na ₂ O (wt %)	K ₂ O (wt %)	P ₂ O ₅ (wt %)	LOI (wt %)	Cu (ppm)	Ni (ppm)
Pyroxenite	45.31	5.25	1.45	12.89	0.17	10.38	21.97	0.71	0.13	0.91	1.19	1092.6	168.9
Hornblendite	45.61	8.02	1.27	14.76	0.21	12.89	14.36	1.24	0.29	0.15	0.56	20.1	191.8
Metagabbro	48.81	16.95	0.43	7.48	0.12	8.10	13.46	2.39	0.50	0.07	1.11	37.4	120.5
Boundary metagabbro	45.43	11.07	1.35	16.89	0.18	6.57	15.05	2.32	0.33	0.23	0.14	16.9	38.9
Altered metagabbro	49.20	12.14	0.58	13.94	0.19	11.62	11.21	2.10	0.40	0.02	0.33	3.5	170.8
Mylonitic amphibolite	47.56	15.71	1.72	12.19	0.21	4.81	11.27	2.95	0.69	0.25	0.78	113.3	40.6
11SJM-120	46.10	19.99	0.83	11.33	0.09	4.89	11.90	2.65	0.42	0.02	1.64	1252.4	1092.1

Abbreviations: LOI = loss on ignition, ppm = parts per million, wt % = weight percent.

BASE METALS AND MINERALIZATION

Preliminary examination of the whole-rock analyses of the 2011 samples has shown that copper and nickel are distributed differently within the Raglan Hills metagabbro. This distribution is presented in Table 14.1 based on the rock types described above and compared to the average concentration of copper and nickel within the Raglan copper-nickel showing.

The bulk of the metagabbro contains on average 37.4 ppm Cu and 120.5 ppm Ni, whereas the boundary metagabbros contain significantly less copper and nickel (16.8 ppm Cu, 48.4 ppm Ni, respectively). This may indicate that these metals were leached from the gabbro during regional metamorphism. Sulphide mineralization is rare within both the metagabbro and the boundary metagabbro, with very few occurrences of sulphides visible in hand sample.

The mylonitic amphibolites present at the southern edge of the intrusion contain more copper, but less nickel than the typical metagabbro; however, sulphide occurrences are more common within this unit, and the sulphide mineral assemblages are dominated by pyrite rather than chalcopyrite.

The pyroxenites contain the highest concentration of copper of all the units, with an average of 1092 ppm Cu (and 168.8 ppm Ni), whereas the hornblendites contain significantly less copper (20.0 ppm) and higher nickel (191.7 ppm). If the hornblendites do represent metamorphosed equivalents of the pyroxenites, this would indicate that copper was highly mobile during metamorphism and was expelled from the hornblendite units, whereas the nickel was more immobile (perhaps because chalcopyrite and pyrrhotite behave differently during metamorphism). The pyroxenites contain up to 2% disseminated sulphide minerals, primarily chalcopyrite and pyrrhotite, with minor pentlandite present as exsolution lamellae in pyrrhotite, whereas the hornblendites contain only trace pyrite and pyrrhotite.

The altered metagabbro, present proximal to the ultramafic rocks, contains the least amount of copper, averaging 3.5 ppm Cu and 170.7 ppm Ni. This signature is likely related to the proposed alteration of the regular gabbro prior to regional metamorphism, with leaching of copper from the gabbro and possible redeposition in the pyroxenites, whereas the nickel present in silicate phases such as olivine remained in the gabbro. So far, no sulphide minerals have been observed in these rocks.

NEODYMIUM–SAMARIUM ISOTOPE SYSTEMATICS

Four samples from the Raglan Hills metagabbro were analyzed for Rb/Sr and Sm/Nd isotopic concentrations in February 2012, including 2 samples of altered metagabbro, 1 sample of regular metagabbro and 1 sample of pyroxenite.

On a time versus ϵ_{Nd} plot (Figure 14.2), the 3 gabbroic samples from the Raglan Hills metagabbro plot together on the depleted mantle line (using a crystallization age of 1229 Ma, based on Pehrsson, Hanmer and van Breemen (1996)), which indicates that the magma that formed these rocks was likely derived from a depleted-mantle source and experienced little to no crustal contamination upon ascension. The pyroxenite sample plots slightly below the depleted-mantle line, due to its slightly more negative ϵ_{Nd} value, which may indicate more interaction with the country rocks during its ascent, or local heterogeneity within the mantle-source region.

FUTURE WORK

Samples collected during the 2012 field season are currently being analyzed for whole-rock geochemistry. These data will help to better define the different rock types within the Raglan Hills metagabbro and hopefully provide some insights into the igneous and metamorphic processes that have affected these rocks. In addition, polished and regular thin sections will be prepared for petrographic and electron microprobe analyses to help describe the nature of the mineralization present in the sulphide mineral occurrences present in the Raglan Hills metagabbro.

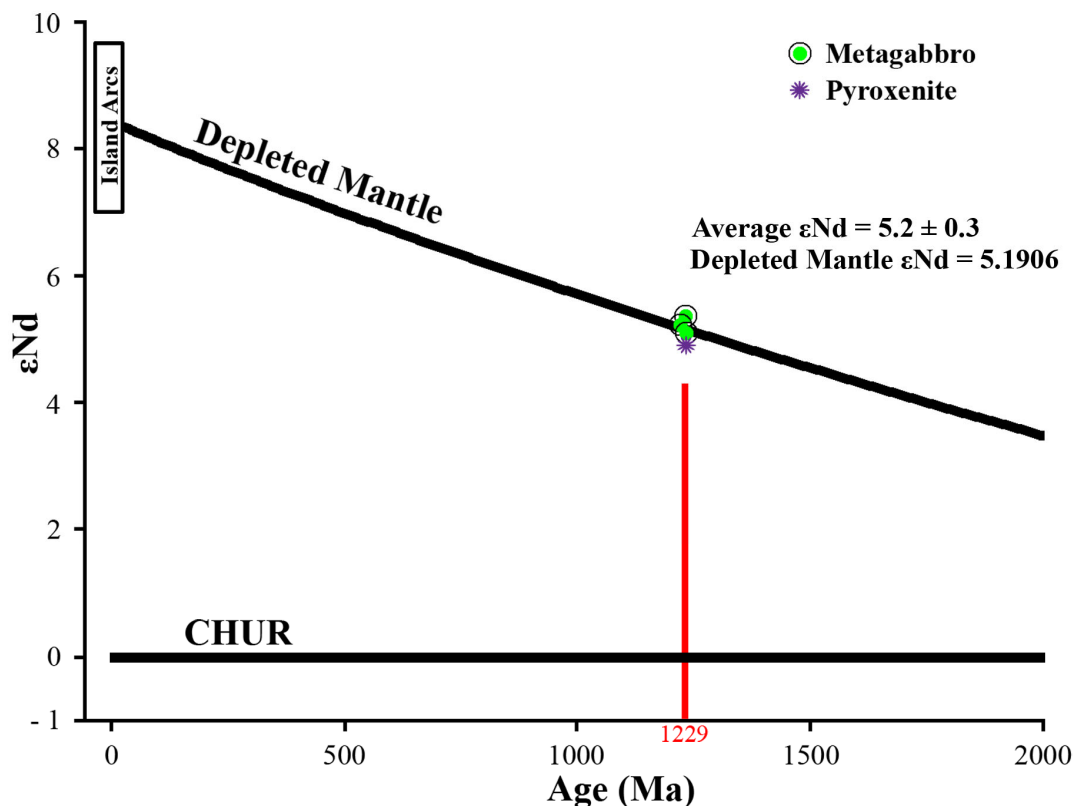


Figure 14.2. Time versus ϵ_{Nd} plot *after* DePaolo (1981), with points plotted at 1229 Ma based on a crystallization age for the Raglan Hills metagabbro obtained by Pehrsson, Hanmer and van Breemen (1996). Abbreviation: CHUR, chondritic uniform reservoir evolution line.

Additional isotopic work will focus on obtaining data from a wider range of rock types within the Raglan Hills metagabbro (e.g., melanocratic to leucocratic gabbro) in order to better constrain the Nd/Sm isochron diagram, and to allow comparison with other metagabbros from the Central Metasedimentary Belt (e.g., Gemmell 2009; Jessett 2010).

Preparation of the geological map of the Raglan Hills area will be undertaken in early 2013 for publication by the Ontario Geological Survey. In addition, a Miscellaneous Release—Data, which will contain the geochemical, isotopic, magnetic susceptibility and photographic images collected during the 2011 and 2012 field seasons, will also be prepared for publication.

ACKNOWLEDGMENTS

S.J. Magnus wrote all parts of the article, which was edited and reviewed by the co-authors. This article constitutes part of the requirements of an MSc thesis at Carleton University, Department of Earth Sciences, under the supervision of Professor Brian Cousens. The co-operation of Paul Davis and Scot Halliday of First Nickel Inc. in providing access to their properties and diamond-drill core is gratefully acknowledged by the authors.

REFERENCES

- Carter, T.R., Colvine, A.C. and Meyn, H.D. 1980. Geology of base metal, precious metal, iron and molybdenum deposits in the Pembroke–Renfrew area; Ontario Geological Survey, Mineral Deposits Circular 20, 186p.
- DePaolo, D.J. 1981. Neodymium isotopes in the Colorado Front Range and crust-mantle evolution in the Proterozoic; *Nature*, v.291, p.193-196.
- Easton, R.M. 1992. The Grenville Province; *in* Geology of Ontario, Chapter 19, Ontario Geological Survey, Special Volume 4, Part 2, p.713-904.
- Easton, R.M., Duguet, M. and Magnus, S.J. 2011. Geology and mineral potential of the northeastern Central Metasedimentary Belt, Grenville Province; *in* Summary of Field Work and Other Activities, 2011, Ontario Geological Survey, Open File Report 6270, p.5-1 to 5-23.
- Gemmell, T. 2009. Geochemical, petrographic and isotope analysis of the Lavant Gabbroic Complex within the Sharbot Lake domain; unpublished BSc thesis, Carleton University, Ottawa, Ontario, 36p.
- Hewitt, D.F. 1954. Geology of the Brudenell–Raglan area; Ontario Department of Mines, Annual Report, 1953, v.62, pt.5, 123p.
- Jessett, K. 2010. The petrology and geochemistry of the Glamorgan Gabbro, Ontario; unpublished BSc thesis, Carleton University, Ottawa, Ontario, 59p.
- Lumbers, S.B. 1982. Renfrew; Ontario Geological Survey, Map 2462, scale 1:100 000.
- Ontario Geological Survey 2010a. Airborne magnetic and electromagnetic surveys, colour-filled contours of the residual magnetic field and electromagnetic anomalies, Bancroft area—Purchased data; Ontario Geological Survey, Map 60 149, scale 1:20 000.
- 2010b. Airborne magnetic and electromagnetic surveys, shaded colour image of the second vertical derivative of the residual magnetic field and Keating coefficients, Bancroft area—Purchased data; Ontario Geological Survey, Map 60 164, scale 1:20 000.
- Magnus, S., Cousens, B. and Easton, R.M. 2012a. The Raglan Hills gabbro: a potential Ni-Cu deposit; Geological Association of Canada–Mineralogical Association of Canada, Program with Abstracts, St. John's 2012, v.35, p.83.

- 2012b. The Raglan Hills gabbro: a potential Ni-Cu deposit; abstract *in* Advances in Earth Sciences Research Conference (AESRC), March 23-25, 2012, Kingston, Ontario, Abstracts.
- Pehrsson, S., Hanmer, S. and van Breemen, O. 1996. U-Pb geochronology of the Raglan gabbro belt, Central Metasedimentary Belt, Ontario: implications for an ensialic marginal basin in the Grenville Orogen; *Canadian Journal of Earth Sciences*, v.33, p.691-702.
- Spear, F.S. 1993. Chapter 13: Metamorphism of ultramafic and cordierite-anthophyllite rocks; *in* Metamorphic phase equilibria and pressure-temperature-time paths, Mineralogical Society of America, Monograph 1, p.469-489.

15. Project Unit 11-013. Major Element, Trace Element and Isotope Geochemistry of Plutons Intruded Circa 1090 to 1065 Ma in the Southeastern Central Metasedimentary Belt, Grenville Province

J. Cutts¹, R.M. Easton² and S.D. Carr¹

¹Ottawa–Carleton Geoscience Centre, Department of Earth Sciences, Carleton University, Ottawa, Ontario K1S 5B6

²Earth Resources and Geoscience Mapping Section, Ontario Geological Survey, Sudbury, Ontario P3E 6B5

INTRODUCTION

The Kensington–Skootamatta plutonic suite in the Grenville Province (defined by Corriveau 1989, 1990; Corriveau et al. 1990; Lumbers et al. 1990; Easton 1992) is described as a syntectonic to posttectonic suite of granitic to syenitic plutons intruded *circa* 1090 to 1060 Ma (Easton 2008). Geochemically, the plutons are alkalic, shoshonitic to ultrapotassic and have been interpreted as forming in a supra-subduction zone tectonic setting (Corriveau 1990). Several late granitic plutons in the Central Metasedimentary Belt of Ontario have been included in this suite; however, there is a lack of sufficient geochemical and/or geochronological data for them to be formally assigned to the Kensington–Skootamatta suite. How, and if, these granite plutons are related to the ultrapotassic plutons of the classic Kensington–Skootamatta suite in terms of geochemistry and tectonic setting remains to be determined. This relationship has mineral exploration significance as there is a genetic link between the granites and Rössing-style uranium potential in the Central Metasedimentary Belt, as suggested by Easton (2008).

For this project, 9 plutons (Barbers Lake, Leggat Lake, Elphin, McLean, Skootamatta and Cranberry Lake plutons and the Wolfe Lake, Rideau Lake and Westport plutons, collectively referred to as the “Westport area” plutons) have been targeted for geochemical, isotopic, and geochronological study (Figure 15.1). This project is part of an MSc thesis project, by the senior author, at Carleton University, supported by the Ontario Geological Survey, the Natural Sciences and Engineering Research Council of Canada (NSERC) and Carleton University. In 2011, the plutons were sampled for petrography, whole-rock major and trace element geochemistry and isotopic analysis to determine their dominant rock-type, geochemical character and petrogenesis (Cutts, Carr and Easton 2011). Additional sampling for isotope and geochronology studies was carried out to address questions about the petrogenesis and tectonic setting of the plutons.

2012 FIELD ACTIVITIES

Approximately 4 days of field work were carried out in 2012. Detailed field descriptions were made and sampling for petrography, whole-rock major, trace element and isotope geochemistry was carried out at approximately 40 sites. Sampling for geochemistry, petrography and U/Pb geochronology of all plutons has been completed. Both the Skootamatta syenite and the Barbers Lake pluton have existing data sets of major and trace element data that will be utilized to complement the data generated in this study (e.g., Easton and Ford 1994; K.L. Ford, unpublished data (*see* “Acknowledgments”)). Table 15.1 summarizes the preliminary data and observations of the plutons examined as part of this study.

Summary of Field Work and Other Activities 2012,
Ontario Geological Survey, Open File Report 6280, p.15-1 to 15-5.

© Queen’s Printer for Ontario, 2012

2012 PRELIMINARY OBSERVATIONS AND RESULTS

The plutons of interest consist of 2 dominant rock-types: granite to alkali-feldspar granite and syenite to quartz-syenite to monzonite. In addition to the standard granitoid rock-forming minerals, the plutons locally contain up to 40% biotite, approximately 10% hornblende, and accessory zircon, apatite, monazite, garnet and pyrite. The plutons are apparently undeformed and unmetamorphosed; although, at the margins of several plutons, there are weak mineral foliations defined by the preferred orientation of minerals. It has yet to be determined if these mineral foliations represent igneous flow fabrics or solid state structural features (i.e., due to shear zones or perhaps as result of forcible emplacement into the country rocks).

Between October 2011 and May 2012, approximately 40 samples were analyzed for major and trace element analysis at the Geoscience Laboratories in Sudbury. Major elements were analyzed using X-ray fluorescence (XRF); trace elements were analyzed using a combination of inductively coupled plasma mass spectrometry (ICP-MS) and inductively coupled plasma atomic emission spectroscopy (ICP-AES). All geochemical results are expected by late October 2012. Table 15.1 summarizes the physical and geochemical characteristics of the plutons based on the data currently available.

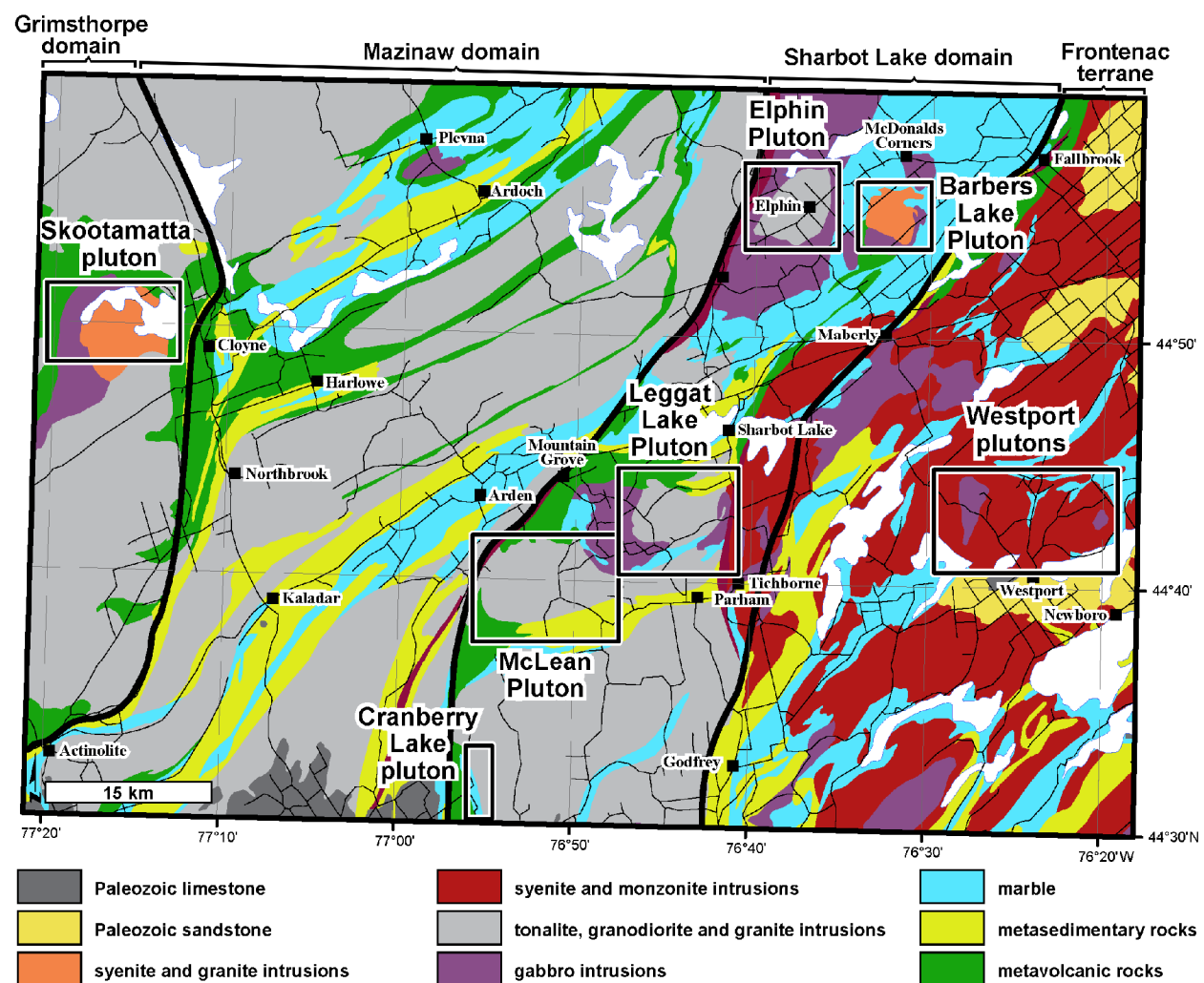


Figure 15.1. Geological map, encompassing approximately 5000 km² of southeastern Ontario, featuring the locations of the Kensington–Skootamatta suite plutons being studied as part of this project. Geology from Ontario Geological Survey (2011).

Table 15.1. Summary of the physical and geochemical characteristics for the plutons examined during the 2011 and 2012 field seasons. Number of samples in parentheses indicates collection in 2011.

Pluton	Main Rock Types (Field-Based)	Textures	State of Deformation and Metamorphism	Data from 2012, (2011) and Prior Geochemical Data	Preliminary Geochemical Results
Skootamatta	Fine- to coarse-grained biotite-rich syenite to quartz-syenite	Localized extreme coarsening of biotite	– Undeformed – Unmetamorphosed	(13) TSG; 16 SC; 8 MS; $\epsilon_{Nd} +4.46$; 26 GC analyses (no REE) ²	Mainly alkalic, total alkali 10.0–11.0 wt %, metaluminous, VAG
Wolfe Lake	Coarse-grained syenite	Local tourmaline veining	– Mineral foliation (biotite, potassium feldspar) throughout – Unmetamorphosed	3 (7) TSG; 18 SC; 6 MS; 1 GC analysis ³ ; $\epsilon_{Nd} +3.4$ ³	Alkalic, total alkali ~12.0 wt %, metaluminous, mainly WPG
Westport	Coarse-grained syenite to monzonite	Varied, ranging from fine-grained to very coarse-grained, abundant biotite	– Undeformed – Unmetamorphosed	3 (7) TSG; 13 SC; 8 MS; $\epsilon_{Nd} +1.98$; 2 GC analyses ³ ; $\epsilon_{Nd} +2.7$ to $+3.1$ ³	Alkalic (shoshonitic), total alkali ~12.3 wt %, weakly metaluminous, mainly WPG
Rideau Lake	Coarse-grained syenite, monzonite, and alkali feldspar granite	5–10% coarse biotite, local epidotization	– Weak localized mineral foliation (biotite) at margins – Unmetamorphosed	10 TSG; 1 GC analysis ³ ; $\epsilon_{Nd} +3.1$ ³	Major-element data pending, mainly WPG
Barbers Lake	Medium- to coarse-grained granite	Tourmaline veining	– Some epidotization – Undeformed – Unmetamorphosed	(3) TSG; 16 SC; 2 MS; $\epsilon_{Nd} -6.39$ and $+4.27$; 17 GC analyses ^{4,5,6}	Subalkalic, total alkali <9.0 wt %, peraluminous to metaluminous, WPG
Elphin	Medium-grained alkali feldspar granite	Leucocratic veining with epidote alteration and pegmatite veining	– Local mineral foliation (biotite) – Unmetamorphosed	4 (8) TSG; 11 SC; 6 MS; $\epsilon_{Nd} +2.82$ and $+2.94$; 4 GC analyses ^{4,5}	Subalkalic, total alkali 9.0–10.0 wt %, metaluminous to peraluminous, VAG
McLean	Medium- to coarse-grained alkali feldspar granite	Rafts of varied composition and leucocratic pegmatite veins	– Weak mineral foliation (biotite) near the margins of the pluton – Unmetamorphosed	4 (6) TSG; 22 SC; 6 MS; $\epsilon_{Nd} +4.58$; 3 GC analyses ⁴	Subalkalic and alkalic, total alkali 9.0–10.0 wt %, metaluminous, WPG
Leggat Lake	Medium- to coarse-grained quartz syenite to alkali feldspar granite	Leucocratic veins	– Mineral foliation (biotite, potassium feldspar) near the margins of the pluton – Unmetamorphosed	5 (5) TSG; 14 SC; 6 MS; $\epsilon_{Nd} +1.46$ and $+4.03$; 2 GC analyses ⁴	Alkalic and subalkalic, total alkali 10.0–12.0 wt %, metaluminous, WPG
Cranberry Lake	Coarse-grained alkali feldspar granite	No data available	– Mineral foliation (biotite, potassium feldspar) throughout – Unmetamorphosed	1 (1) TSG; $\epsilon_{Nd} +3.61$; 1 GC analysis ⁷	Subalkalic, total alkali ~10.0 wt %, metaluminous, on WPG–VAG tie-line

Abbreviations: GC = geochemical analyses; MS = magnetic susceptibility stations with measurements; SC = assay-mode scintillometer measurements; TSG = sampled for thin section petrography, whole-rock major and trace element geochemistry; VAG = volcanic arc granite; WPG = within-plate granite: both of Pearce, Harris and Tindle (1984).

Sources: ¹Easton (2001); ²Easton and Ford (1994); ³Marcantonio et al. (1990); ⁴van Breemen and Davidson (2000);

⁵Wu and Kerrich (1986); ⁶K.L. Ford, unpublished data and re-analysis of powdered samples (see “Acknowledgments”).

Analysis of the geochemical data indicates that the syenitic plutons are alkalic, whereas the granitic ones are predominantly subalkalic. All the plutons are metaluminous to weakly peraluminous. Tectonic settings, based on the geochemical discrimination scheme of Pearce, Harris and Tindle (1984), are either volcanic-arc granite or within-plate granite. Only the Westport and Wolfe Lake plutons consistently exhibit the TiO_2 greater than 0.8 weight % and P_2O_5 greater than 0.21 weight % contents, which are regarded by Corriveau (1990) as characteristic of the Kensington–Skootamatta suite. The Skootamatta pluton contains some samples with TiO_2 greater than 0.8 weight % and P_2O_5 greater than 0.21 weight %, but also contains samples with lower TiO_2 and P_2O_5 content.

Each pluton has a distinctive normalized extended trace-element profile. The Barbers Lake pluton is distinctive, relative to the other plutons, as it has greater overall enrichment in the light rare earth elements, more elevated concentrations of uranium and lead, and depletions in lanthanum and cerium. The Westport area plutons can be distinguished from all the other plutons by their lack of a significant niobium anomaly. On extended element diagrams, all 9 plutons have trends with a negative slope ($\text{La}_n/\text{Lu}_n = 10$), and negative anomalies in strontium, phosphorous and titanium.

In total, 22 samples were selected for Sm/Nd and strontium isotopic analysis. Samples were selected based on whole-rock major and trace element geochemistry trends that best represent the plutons in question, and include all samples chosen for U/Pb geochronology studies. Samples were prepared and purified at the Isotope Geochemistry and Geochronology Centre at Carleton University based on procedures outlined by Cousens (1996), and isotopic analyses were carried out using thermal ionization mass spectrometry (TIMS). Preliminary neodymium and strontium isotope geochemistry results suggest that the plutons originated from a primitive mantle source without significant crustal contamination during melting and emplacement.

Six samples were selected for geochronology analysis. Representative samples were selected based on geographic location within the pluton (typically near the centre). Heavy mineral separates were concentrated from the rock by crushing, grinding, processing by a Rogers™ table, heavy liquids and, finally, sorting of zircon using a Frantz™ isodynamic magnetic separator. Zircons have been selected based on their clarity, quality of crystal shape, and lack of inclusions and fractures. Imaging on a scanning electron microscope (SEM), as well as chemical abrasion, chemistry and isotopic analysis of zircon fractions will be completed by the end of 2012.

FUTURE WORK

Uranium–lead (U/Pb) geochronology studies are continuing at the Isotope Geochemistry and Geochronology Centre at Carleton University. The geochemical and isotopic data will be utilized to address whether or not the 2 compositional groups (syenites versus granites) have a single magmatic source or if they arose from different mantle source regions. Determining the emplacement ages of the undated plutons will address whether the 2 compositional groups are coeval or if they were emplaced at different times.

ACKNOWLEDGMENTS

J. Cutts contributed to the writing of the “Introduction”; wrote the sections “2012 Field Activities”, “2012 Preliminary Observations and Results” and “Future Work”; and prepared Table 15.1. This work constitutes part of the requirements of an MSc thesis at Carleton University under the supervision of Professors S.D. Carr and J. Blenkinsop, and Adjunct Professor R.M. Easton. S.D. Carr has been instrumental in defining the parameters of the project, and revising this article. J. Blenkinsop advised in the analysis of isotopic data. R.M. Easton co-wrote the “Introduction”, and has been invaluable providing guidance and knowledge for this project. Rhea Mitchell assisted greatly in the preparation and analysis of samples for Sm/Nd isotope geochemistry. The support of the Grenville Supergroup at Carleton University is acknowledged.

The authors thank K.L. Ford, Geological Survey of Canada, for providing access to his unpublished major-element analyses of samples from the Barbers Lake pluton, as well as providing powders of representative samples from the intrusion for geochemical and isotopic analysis as part of this study.

REFERENCES

- Corriveau, L. 1989. Potassic alkaline plutonism in the southwestern Grenville Province; unpublished PhD thesis, McGill University, Montreal, Quebec, 263p.
- 1990. Proterozoic subduction and terrane amalgamation in the southwestern Grenville Province, Canada: evidence from ultrapotassic to shoshonitic plutonism; *Geology*, v.18, p.614-617.
- Corriveau, L., Heaman, L.M., Marcantonio, F. and van Breemen, O. 1990. 1.1 Ga K-rich alkaline plutonism in the SW Grenville Province, U-Pb constraints for the timing of subduction-related magmatism; *Contributions to Mineralogy and Petrology*, v.105, p.473-485.
- Cousens, B.L. 1996. Magmatic evolution of Quaternary mafic magmas at Long Valley Caldera and the Devils Postpile, California: effects of crustal contamination on lithospheric mantle-derived magmas; *Journal of Geophysical Research*, v.101, p.27 673-27 689.
- Cutts, J., Carr, S.D. and Easton, R.M. 2011. Characterization of syntectonic to posttectonic intrusions of *circa* 1090 to 1065 Ma age in the southeastern Central Metasedimentary Belt, Grenville Province; *in* Summary of Field Work and Other Activities, 2011, Ontario Geological Survey, Open File Report 6270, p.6-1 to 6-7.
- Easton, R.M. 1992. The Grenville Province; *in* *Geology of Ontario*, Chapter 19, Ontario Geological Survey, Special Volume 4, Part 2, p.713-904.
- 2001. Geology and mineral potential of the Puzzle Lake area, Central Metasedimentary Belt, Grenville Province; Ontario Geological Survey, Open File Report 6064, 26p.
- 2008. Rössing-style uranium potential of late granites and pegmatites from the Central Metasedimentary Belt, Grenville Province; *in* Summary of Field Work and Other Activities, 2008, Ontario Geological Survey, Open File Report 6226, p.16-1 to 16-10.
- Easton, R.M. and Ford, F.D. 1994. Geology of the Grimsthorpe area; Ontario Geological Survey, Open File Report 5894, 153p.
- Lumbers, S.B., Heaman, L.M., Vertolli, V.M. and Wu, T.W. 1990. Nature and timing of Middle Proterozoic magmatism in the Central Metasedimentary Belt, Grenville Province, Ontario; *in* Mid-Proterozoic Laurentia–Baltica, Geological Association of Canada, Special Paper 38, p.243-276.
- Marcantonio, F., McNutt, R.H., Dickin, A.P. and Heaman, L.M. 1990. Isotopic evidence for the crustal evolution of the Frontenac Arch in the Grenville Province of Ontario, Canada; *Chemical Geology*, v.83, p.297-314.
- Ontario Geological Survey 2011. 1:250 000 bedrock geology of Ontario; Ontario Geological Survey, Miscellaneous Release—Data 126–Revision 1.
- Pearce, J.A., Harris, N.B.W. and Tindle, A.G. 1984. Trace element discrimination diagrams for the tectonic interpretation of granitic rocks; *Journal of Petrology*, v.25, p.956-983.
- van Breemen, O. and Davidson, A. 2000. Late Grenvillian granite plutons in the Central Metasedimentary Belt, Grenville Province, southeastern Ontario; *in* Radiogenic Age and Isotopic Studies: Report 13, Geological Survey of Canada, Paper 2000-F5, 9p.
- Wu, T.W. and Kerrich, R. 1986. Combined oxygen isotope-compositional studies of some granitoids from the Grenville Province of Ontario, Canada: implications for source regions; *Canadian Journal of Earth Sciences*, v.23, p.1412-1432.

16. Project Unit 12-003. Lithological and Structural Mapping of Albanel Township, Southern and Superior Provinces

D. Lewis¹

¹Earth Resources and Geoscience Mapping Section, Ontario Geological Survey

INTRODUCTION

A two-year bedrock mapping project was initiated in 2012 to map the geology of Albanel and Varley townships (formerly townships 169 and 176), located northwest of Elliot Lake, Ontario. These townships cover 200 km² and straddle the contact between the Superior Province to the north and the Southern Province to the south. The area has potential for hosting a variety of metals (including uranium, copper, nickel, zinc, lead, silver, rare earth elements, and potentially gold and platinum group elements) in a variety of deposit types. The area had been suggested as having potential for magmatic deposits (Lightfoot, Prevec and Keays 1995), and several lake sediment anomalies for copper were documented in Albanel and Varley townships by Dyer (2010a, 2010b). Albanel Township was mapped during the 2012 field season, with an emphasis on its structural geology and styles of mineralization.

REGIONAL GEOLOGY

Albanel Township is located at the intersection between the Archean Ramsey–Algoma granitoid complex to the north and the unconformably overlying Paleoproterozoic Huronian Supergroup of the Southern Province to the south. The unconformable contact is significant regionally because the basal formation of the Huronian Supergroup, the Matinenda Formation, is the host to the low-grade placer uranium deposits that were mined historically at Elliot Lake. Recent mineral exploration by Pele Mountain Resources has focussed on the rare element potential of the Matinenda Formation, with uranium as a secondary commodity (Pele Mountain Resources Inc., news release, July 4, 2012, www.pelemountain.com/news-release.php?id=730 [accessed October 15, 2012]).

The Ramsey–Algoma granitoid complex ranges in composition from tonalite and diorite to alkali-feldspar syenite (Card 1979). In Albanel Township, it contains granite, granodiorite and granitic gneissic rocks, greenstone enclaves, and numerous variably foliated granitic, granodioritic and syenitic intrusions. Uranium–lead zircon ages from the Ramsey–Algoma granitoid complex range from 2651 to 2697 Ma (Prevec 1993; Easton 2006; R.M. Easton, OGS, written communication, 2012). The granitoid rocks are intruded by north-northwest-trending Paleoproterozoic Matachewan mafic dikes.

The Huronian Supergroup is a cyclic sequence of sedimentary rocks that were unconformably deposited on the Superior Province, and extends from Sault Ste. Marie into the province of Quebec. The Huronian Supergroup is divided into 4 groups (from oldest to youngest): the Elliot Lake, Hough Lake, Quirke Lake and Cobalt groups (Figure 16.1; Robertson, Card and Frarey 1969; Bennett, Dressler and Robertson 1991). With the exception of the Elliot Lake Group, the individual groups follow a general sequence of unconformable basal conglomerate, overlain by siltstone, overlain by sandstone, although there is some variation to this repetition. The sedimentary rocks are cut by several groups of mafic dikes (Nipissing, Sudbury and unclassified dikes).

*Summary of Field Work and Other Activities 2012,
Ontario Geological Survey, Open File Report 6280, p.16-1 to 16-11.*

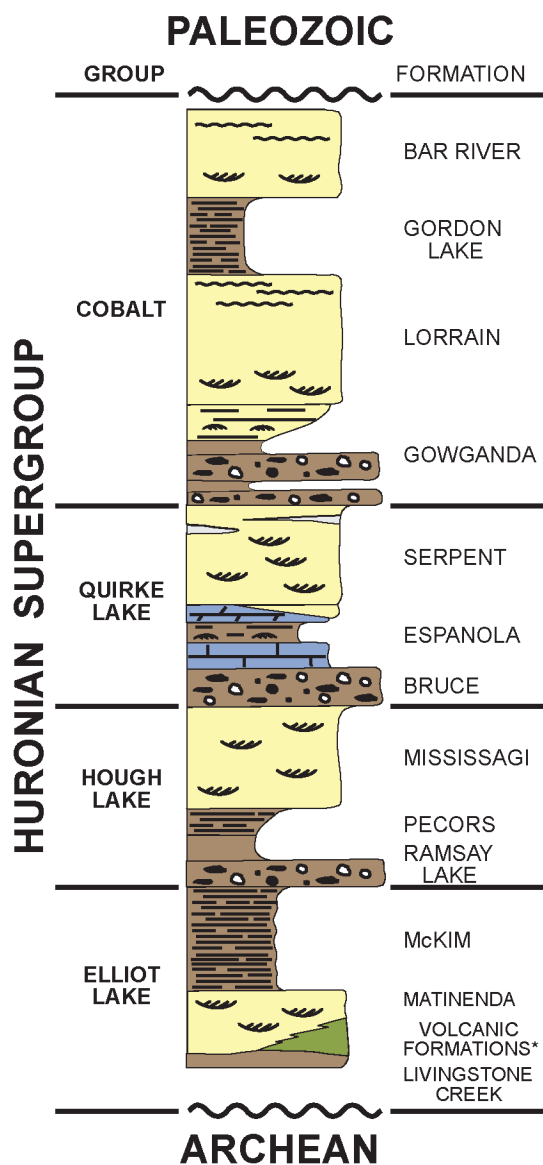
© Queen's Printer for Ontario, 2012

LOCAL GEOLOGY

A generalized stratigraphic section is presented in Figure 16.1. Note that rocks within the Huronian Supergroup are variably metamorphosed and the prefix “meta” is omitted for brevity. All bedding thickness values given are true, not apparent, thicknesses (i.e., perpendicular to bedding).

Ramsey–Algoma Granitoid Complex, Superior Province

In Albanel Township, the Archean rocks consist dominantly of felsic intrusive rocks and lesser mafic volcanic rocks, both of which are cut by mafic dikes of the Paleoproterozoic Matachewan dike swarm. Mapping of the felsic intrusive rocks indicates that they are syenogranitic to granitic in composition. They are medium- to coarse-grained rocks that contain hornblende, potassium-feldspar, minor plagioclase and



*Thessalon, "Dollyberry Volcanics", Salmay Lake, Elsie Mountain, Stobie, Copper Cliff

Figure 16.1. The stratigraphic section for the Huronian Supergroup (modified after Jackson 2001).

quartz, and rarely biotite. There are 2 areas of exposure of these granites in the map area, at the north and south end of Endikai Lake (Figure 16.2), but there is little to no textural or mineralogical difference between them. The rocks are typically massive and are commonly jointed. Quartz and epidote veins are the only alteration mineralogy observed.

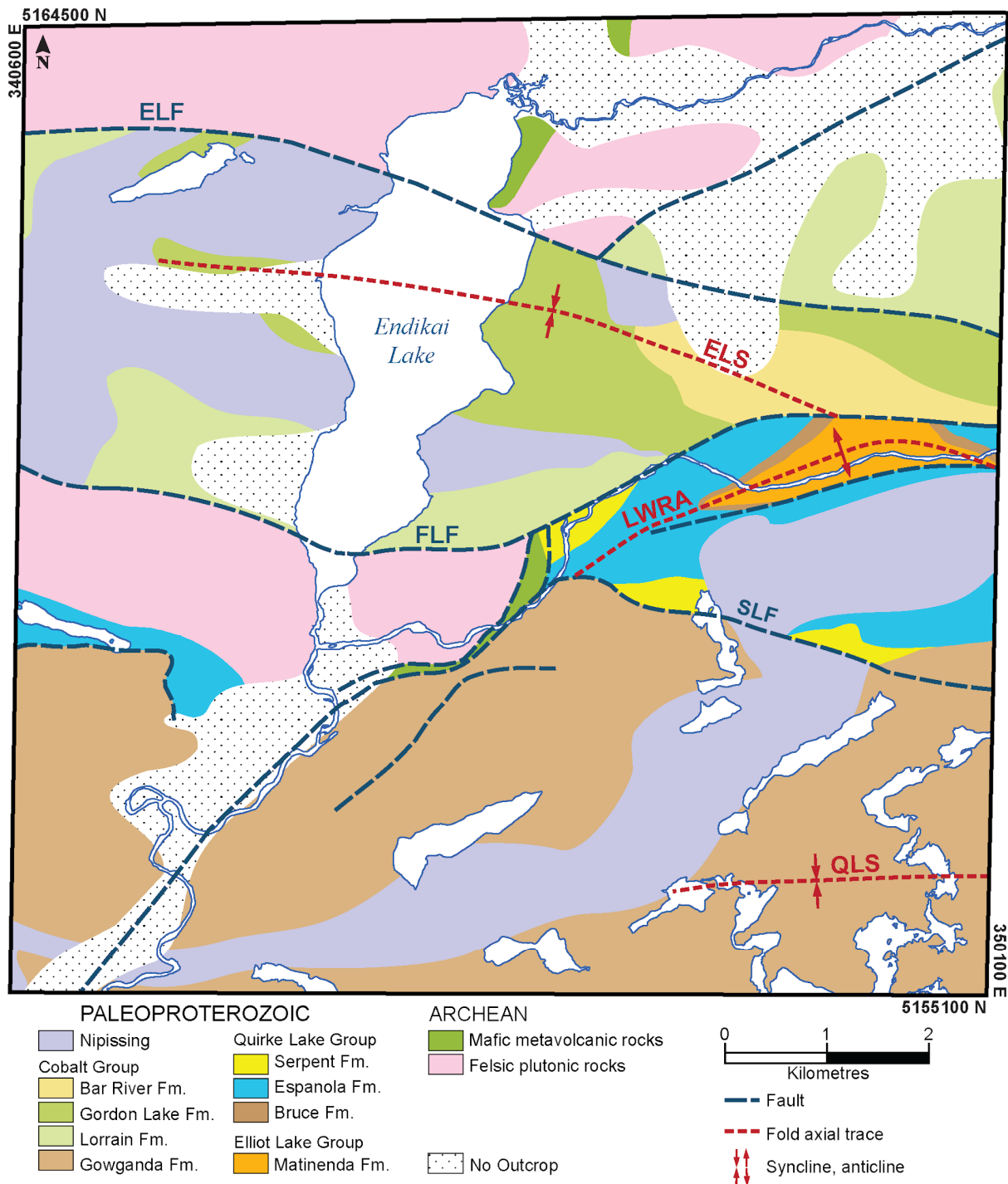


Figure 16.2. Simplified geological map of Albnel Township (geology modified from Siemiatkowska 1977). Abbreviations: ELF, Endikai Lake fault; ELS, Endikai Lake syncline; FLF, Flack Lake fault; Fm, Formation; LWRA, Little White River anticline; QLS, Quirke Lake syncline; SLF, Scarbo Lake fault. Universal Transverse Mercator (UTM) co-ordinates provided using North American Datum 1983 (NAD83) in Zone 17.

The Matachewan dikes are a series of mafic intrusions that cut the Archean rocks. They are equigranular, fine- to medium-grained mafic dikes that contain hornblende and plagioclase. The magnetic susceptibility of these dikes is varied, ranging from poorly to moderately magnetic (0.6 to 40×10^{-3} SI units). The dikes range in width from 2 to 20 m and can be traced for more than 1 km with a north-northwest trend.

Huronian Supergroup, Southern Province

ELLIOT LAKE AND HOUGH LAKE GROUPS

The Elliot Lake Group contains a variety of intercalated volcanic and sedimentary rocks. It includes the Livingstone Creek Formation, various volcanic formations, the Matinenda Formation and the McKim Formation (*see* Figure 16.1). The Hough Lake Group includes the Ramsay Lake, Pecors and Mississagi formations (*see* Figure 16.1); however, no rocks that could be identified as belonging to the Hough Lake were observed during the 2012 field season. In Alban Township, the basal rock unit of the Huronian Supergroup was mapped by Siemiatkowska (1977) as Mississagi Formation sandstone, although, as discussed in more detail in “Stratigraphic Reclassification”, texturally and compositionally, it is more consistent with descriptions of the Matinenda Formation.

The basal sandstone is a light yellow to light green arkose that contains high plagioclase and quartz content with lesser sericite. The grains range in size from approximately 0.5 to 3 mm in diameter and are subangular to angular. These features, combined with the high feldspar and sericite content, suggest that the rock is immature to submature and derived from a relatively proximal environment. The Matinenda Formation within the map area has a minimum thickness of 250 m. Thin (<1 m thick) quartz-pebble conglomerate layers are present within the sandstone (Photo 16.1A). The quartz pebbles are up to 1.5 cm in diameter and are subrounded and moderately well sorted. Bedding is thick to massive, although it can best be measured accurately when the conglomerate layers are present. The entire rock unit is anomalously high in uranium, with typical portable gamma-ray spectrometer values of 300 cpm (counts per minute; ~20 ppm U) throughout the sandstone. On fractured surfaces and especially in the quartz-pebble conglomerate layers, maximum gamma-ray spectrometer readings of 5000 cpm total (200 ppm U) were measured (Table 16.1).

QUIRKE LAKE GROUP

The Quirke Lake Group includes the Bruce, Espanola and Serpent formations and is the group most identifiable in the field because of the unique calcareous Espanola Formation (*see* Figure 16.1). These 3 formations are in conformable contact with one another and, although the contact was not directly observed, seem to be conformable with the basal sandstone of the Matinenda Formation.

The Bruce Formation is a polymictic matrix-supported conglomerate that conformably overlies the basal sandstone of the Matinenda Formation. The conglomerate clasts vary in composition, are subangular to angular and vary in size from approximately 1 to 10 cm in diameter. The Bruce Formation is approximately 100 to 150 m thick within the map area.

In Alban Township, the Espanola Formation is a thin- to medium-bedded calcareous to dolomitic siltstone. Quartz is the dominant mineral and the calcareous minerals occur in lesser quantities. Bedding is generally planar and is preserved as thin grey cherty bands within thickly bedded calcareous silty layers. Postdepositional folds are relatively common in the Espanola Formation, partly because of its proximity to regional structures (*see* Figure 16.2), in addition to weak internal competency compared to other rock units.

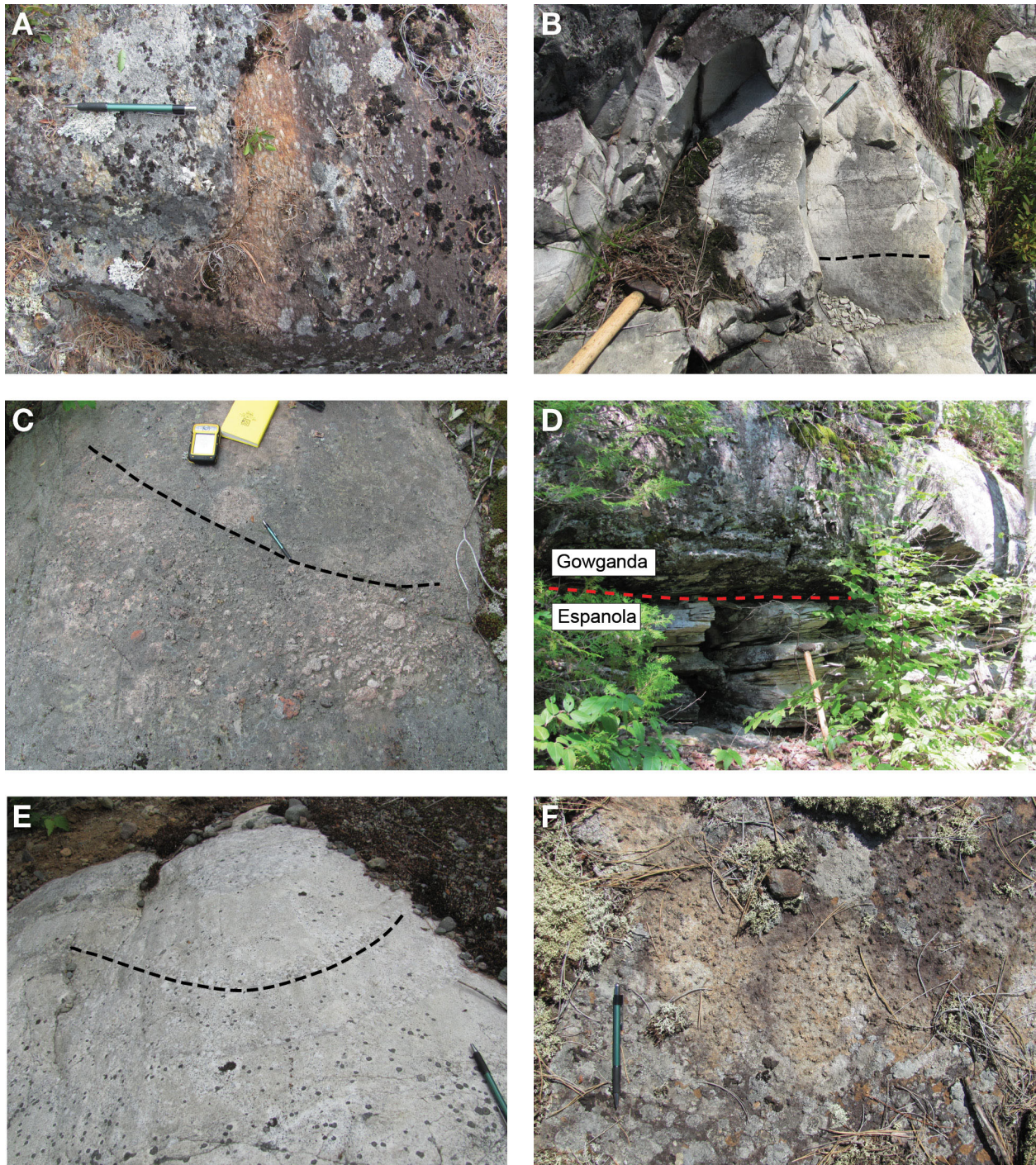


Photo 16.1. A) Quartz-pebble conglomerate of the Matinenda Formation (UTM 348555E 5160635N). B) Bedded quartz arenite of the Serpent Formation (UTM 347311E 5159103N). The black dashed line is parallel to bedding. Hammer head is approximately 10 cm wide. C) Bedded conglomerate of the Gowganda Formation (UTM 343484E 5156739N). Bedding is graded normally. Note the pink clasts that are typical of the Gowganda Formation. D) Faulted contact between the older Espanola Formation and younger Gowganda Formation (UTM 342135E 5158281N). The curvilinear fault surface is represented by the red dashed line. Note the pink granitic clasts in the Gowganda Formation, the intensely foliated Espanola Formation, and the weakly foliated Gowganda Formation. E) Rhythmically bedded Lorrain Formation sandstone and conglomerate (UTM 345721E 5160158N). Bedding is represented by the black dashed line. F) Medium-grained Nipissing mafic dike with coarse-grained hornblende phenocrysts (UTM 346656E 5161302N). In the photos, the pencil is approximately 15 cm long and points north. UTM co-ordinates provided using NAD83 in Zone 17.

Table 16.1. Assay-mode gamma-ray spectrometric readings from quartz-pebble conglomerate within the Matinenda Formation.

Easting (m)	Northing (m)	K (wt %)	U (ppm)	Th (ppm)
348555	5160635	7.6	199.6	355.9
348555	5160635	9.1	192.1	511.3

Abbreviation: ppm = parts per million, wt % = weight percent.

Notes: 1. UTM co-ordinates are in Zone 17, NAD83.

2. multiply U by 1.1793 for U_3O_8 . All K, U and Th data were recorded using an Exploranium™ GR-135G MiniSpec gamma-ray spectrometer, serial number 4884, calibrated on February 22, 2006, using an NaI crystal and software version 501GEO. The instrument was stabilized daily, and data were recorded using the assay mode with a dead-time adjusted 5-minute count time. Quoted accuracy is 0.1% K, 0.4 ppm U, and 0.7 ppm Th for a sample with 2% K, 2 ppm U and 8 ppm Th.

The Serpent Formation is a fine- to medium-grained, white quartz arenite that conformably overlies the Espanola Formation (Photo 16.1B). The quartz grains are subrounded to rounded, moderately to well sorted and the sandstone is submature to mature. Bedding in the Serpent Formation is generally either massive or cross-bedded, although, in some instances, it is planar bedded.

COBALT GROUP

The Cobalt Group includes the Gowganda, Lorrain, Gordon Lake and Bar River formations (see Figure 16.1). The Gowganda Formation is known foremost as a conglomerate unit, but it also contains sandstone and bedded siltstone (Photos 16.1C and 16.1D). The lowermost subunit is a monomictic, matrix-supported conglomerate that contains subangular to subrounded pink granitic to syenitic clasts and a medium-grained, reddish to beige arkosic matrix. The transition into the sandstone is gradual; infrequent conglomerate beds persist into the sandstone. This sandstone is identical to the matrix of the conglomerate unit. The siltstone is a black fine-bedded to laminated rock.

The Lorrain Formation, similar to the Gowganda Formation, contains several subunits (Photo 16.1E). The basal conglomerate unit contains subrounded to rounded polymictic clasts that are dominated by white translucent quartz pebbles, with lesser jasper and rare ironstone clasts. The conglomerate unit is generally thickly bedded and it grades into the overlying sandstone. The sandstone is a white massive-bedded quartz arenite with rounded grains.

The Gordon Lake Formation conformably overlies the Lorrain Formation. It is a thinly bedded siltstone with grey, tan and purple beds. Bedding is planar and ranges from 1 to 10 cm thick.

The Bar River Formation is a fine- to medium-grained quartz arenite sandstone. The quartz grains vary from subangular to rounded, but rounded grains dominate. Bedding is massive to planar bedded (with beds ranging from 1 to 100 cm thick), although some cross-bedding is present locally.

MAFIC INTRUSIVE ROCKS

Gabbroic intrusions of the Nipissing intrusive suite (Photo 16.1F) are medium-grained phaneritic leucocratic to melanocratic mafic intrusive rocks containing plagioclase and hornblende with varied magnetite content. On a map scale (local), the gabbros trend either northwest or southwest. The southwest-trending gabbros are generally hosted by foliated wall rocks, which may indicate that they were intruded along faults. The Nipissing gabbros occasionally contain sulphide minerals, specifically pyrite and pyrrhotite, and these sulphide minerals do not appear to be associated with alteration. The sulphide content in mineralized areas is low (<1%), but may indicate higher concentrations of sulphides at depth. Diabase dikes of the Sudbury swarm are fine-grained diabase with a high magnetic susceptibility (Palmer, Merz and Hayatsu 1977).

The Nipissing and Sudbury mafic intrusive rocks are historically the only 2 mafic intrusive suites known to cut the Huronian Supergroup (Siemiatkowska 1977), although a third suite may also be present. A suite of weakly plagioclase-phyric, fine- to medium-grained mesocratic mafic intrusive rocks cut the Nipissing gabbros. These intrusive rocks have been noted along road cuts on Highway 539 (R.M. Easton, OGS, personal communication, 2012). In Albanel Township, these intrusive rocks are distinguished from the Nipissing gabbros by their distinct west trend.

Stratigraphic Reclassification

Previous mapping by Siemiatkowska (1977) identified the basal sandstone in Albanel Township as part of the Mississagi Formation, although the high uranium content in this unit is more consistent with the Matinenda Formation. Below, the textural features of this basal sandstone are compared to published descriptions of the Matinenda and Mississagi formations.

The Matinenda Formation is a green to pink, medium- to coarse-grained, poorly to moderately sorted feldspathic arkose, with interbedded quartz-pebble conglomerate, and minor mudstone, with significant sericite and pyrite content (Pienaar 1963; Robertson 1968; Roscoe 1969; Card, Innes and Debicki 1977). The feldspathic arkose is the dominant rock type, with lesser mudstone and quartz-pebble conglomerate (Card, Innes and Debicki 1977). The quartz-pebble conglomerates are concentrated mainly near the base and the top of the Matinenda Formation. Bedding in the Matinenda Formation can be massive, planar and cross-bedded, and is defined by variations in grain size (cf. Pienaar 1963; Young 1991).

In contrast, the Mississagi Formation is a medium- to coarse-grained, moderately to well-sorted sandstone that is persistently planar to trough cross-bedded (Long 1976). The sandstone varies from subarkose to arkose and, with increasing mud content toward the top of the formation, it grades into greywacke with or without thin mudstone beds (Card, Innes and Debicki 1977). Rare quartz-pebble conglomerate beds that are similar to those of the Matinenda Formation do occur, although they contain little to no radioactive minerals (Card, Innes and Debicki 1977).

As noted earlier, the textural characteristics of the basal sandstone, as well as its radioactive character, are most similar to the Matinenda Formation. Consequently, the basal sandstone is reinterpreted herein to be part of the Matinenda Formation, not the Mississagi Formation.

STRUCTURAL GEOLOGY

Within the Huronian Supergroup in Albanel Township, there are 2 distinct generations of faults and 2 generations of folds. The major faults in Albanel Township include the Flack Lake, Endikai Lake and Scarbo Lake faults (*see* Figure 16.2). These structures trend west, but a second group of faults trend southwest. Previous work on the major west-trending faults suggests that they originated as south-dipping normal (slump) faults and were reactivated as reverse (thrust) faults (Zolnai, Price and Helmstaedt 1984).

The east-trending faults offset younger Huronian Supergroup rocks over older Superior Province rocks suggesting an early reverse sense of displacement. In outcrop, the faults are defined by a narrow (<5 m wide) zone of brittle brecciation, fault gouge and strongly developed foliation. Kinematic indicators that may have been formed initially are poorly preserved, but subsequently formed kinematic indicators, such as quartz-tension gashes and drag folds, suggest dextral transcurrent displacement along these faults.

The Flack Lake fault is well exposed at a roadcut on Highway 546, where it offsets bedded carbonate rocks of the Espanola Formation with conglomerates of the Bruce Formation. Here, the fault is defined by transposed bedding in the Espanola Formation that has been realigned into the Flack Lake fault. The Z-shaped folds, shown in the top left of Photo 16.2A, are interpreted to be related to early reverse movement.

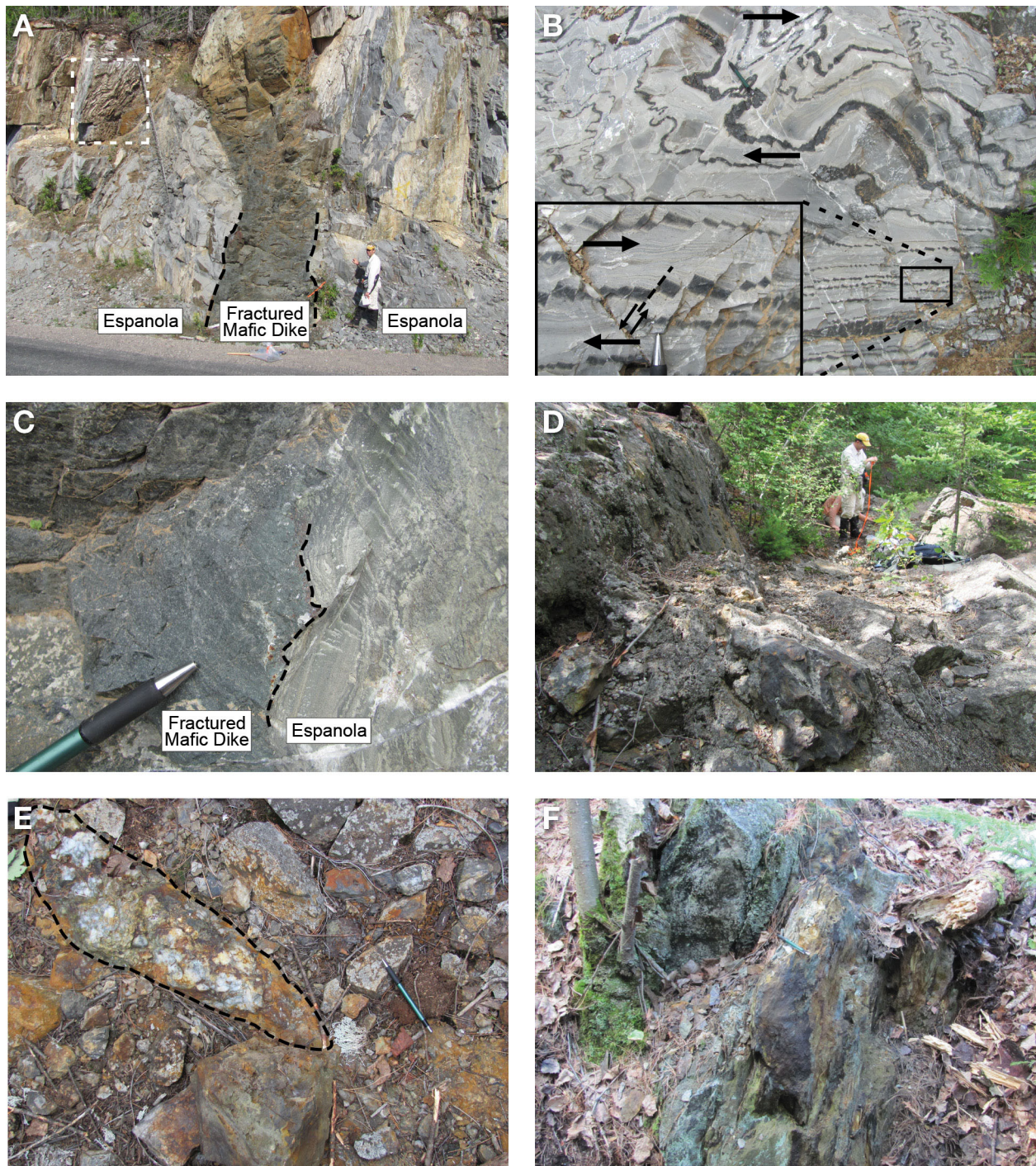


Photo 16.2. A) Roadside outcrop of the Flack Lake fault (UTM 350208E 5160521N). The bedded calcareous siltstone of the Espanola Formation has been transposed into the Flack Lake fault and overprinted by a mafic (Nipissing?) intrusion that is subsequently internally fractured. The white dashed box highlights Z-shaped folds; the black dashed lines outline the dike contact. Person for scale. Photo is taken facing west. B) Dextral Z-shaped folds and dextral back-rotation of beds of the Espanola Formation within the Flack Lake fault (UTM 350208E 5160521N). C) Contact between Espanola Formation and mafic intrusion at the Flack Lake fault (UTM 350208E 5160521N). The black dashed line outlines this contact. Note the sulphide mineralization at the contact. D) Trench in mineralized zone located within brittle-faulted Nipissing gabbro of the Scarbo Lake fault (UTM 347826E 5158751N). Important carbonate and sulphide minerals include malachite, sphalerite and galena. Person for scale. Photo taken facing west. E) Mineralized quartz vein of the Scarbo Lake fault (UTM 347826E 5158751N). F) Mineralized fault zone that offsets Archean mafic volcanic rocks (UTM 345849E 5159646N). In the photos, the pencil is approximately 15 cm long and points north. UTM co-ordinates provided using NAD83 in Zone 17.

This interpretation is further supported based on the juxtaposition of upper Huronian Supergroup rocks beneath lower units. Subsequent deformation includes subvertically plunging Z-shaped folds and dextral back-rotation of the bedded Espanola Formation calcareous siltstone (Photo 16.2B). These kinematic indicators are consistent with dextral strike-slip (transcurrent) reactivation of the fault. In outcrop, the Flack Lake fault is cut by an internally fractured mafic dike that trends northwest (*see* Photo 16.2A). This dike, which is interpreted to be of Nipissing age, contains pyrrhotite and pyrite along the margins with the Espanola Formation (*see* Photo 16.1C). It is interpreted to have been emplaced following reverse movement and internally fractured by strain partitioning during dextral fault reactivation. Pyrrhotite mineralization is hosted at the contact between the mafic dike and Espanola Formation (Photo 16.2C).

Layer-cake-style folded rock units can be demonstrated at a local scale. Two of the more readily identifiable folds include the Little White River anticline and the Endikai Lake syncline (*see* Figure 16.2). The Little White River anticline is defined by the curvilinear contacts between the Matinenda, Bruce, Espanola and Serpent formations, whereas the Endikai Lake syncline is defined by the folded contact between the Gordon Lake and Bar River formations. Bedding measurements within these formations mimic the folded contacts between formations.

The Little White River anticline is defined by the contact between the Matinenda, Bruce, Espanola and Serpent formations. These contacts trend southwest (north limb) and wrap sharply anticlockwise to the east (south limb). Bedding on the north limb dips northwest, bedding on the south limb dips shallowly south and the oldest rock unit is located in the centre of the fold. The fold axial trace trends northeast and the fold plunges moderately toward the southwest. Parasitic folds, particularly well preserved in the Espanola Formation, have the Z-shaped asymmetry on the north limb and S-shaped asymmetry on the south limb.

The Endikai Lake syncline is defined by the contact between the Gordon Lake and Bar River formations. This contact trends west (north limb), bends to the south (defining the fold hinge) and curves southeast (south limb). It is a closed fold with an axial trace that strikes west and an axial plunge oriented shallowly to the east-southeast (approximately 11° toward 104°). A fissile, slaty foliation in the Gordon Lake Formation and a spaced fracture foliation in the Bar River Formation are observed in the fold. The slaty foliation is parallel to the axial plane of Z-shaped parasitic folds along the southwest limb of the syncline. This foliation intensifies in large- and small-scale fold hinges and it is oriented anticlockwise to bedding on the south limb, perpendicular in the hinge area and clockwise to bedding on the north limb. The fold plunges shallowly to the east.

The Little White River anticline and the Endikai Lake syncline are interpreted to be of different generations for the following reasons:

- Both folds have an approximately east-trending axial trace, but, in an anticline–syncline pair, the fold noses should close in opposite directions. In this case, both fold noses close to the west.
- The fold plunge is not co-linear (the folds plunge in opposite directions).
- The Endikai Lake syncline has an axial planar foliation that is developed in the Bar River sandstone. The Matinenda Formation preserves a foliation in the core of the Little White River anticline, but this foliation overprints the fold and is broadly parallel to the Flack Lake fault.

These observations are consistent with the presence of 2 fold generations affecting the Huronian Supergroup, as noted by Jackson (2001) and Easton (2006).

ECONOMIC GEOLOGY

There are several styles of mineralization recognized in Albanel Township, including stratabound and hydrothermal mineralization, and there is also the potential for magmatic mineralization.

The basal conglomerates within the newly reclassified Matinenda Formation in Albanel Township are economically significant as they contain the highest concentration of uranium within the formation (Roscoe 1969; Card, Innes and Debicki 1977). The uranium concentration in the conglomerate layers is interpreted as the result of erosion of uraniferous granites and subsequent placer deposition in fluvial channels in a reducing environment (cf. Roscoe 1969; Robertson 1978; Young 1991). Within the Matinenda Formation, high uranium content relative to background was measured; typical gamma-ray scintillometer readings were in the 20 to 50 ppm U range. Higher values occur in the quartz-pebble conglomerate layers, with a maximum value of 199.6 ppm U (*see* Table 16.1; *see* Photo 16.1A).

In addition to the uranium potential of the Matinenda Formation, the results from the Pele Mountain Resources Eco Ridge Mine project at Elliot Lake (Pele Mountain Resources Inc., news release, July 4, 2012, www.pelemountain.com/news-release.php?id=730 [accessed October 15, 2012]) suggest that rare elements may be associated with the quartz-pebble conglomerate layers within the Matinenda Formation in the map area.

The hydrothermal mineralization is controlled by brittle faults in the map area (Photos 16.2D, 16.2E and 16.2F). These faults are characterized by narrow, moderately to strongly altered cataclastite zones with fault gouge. Generally, the deformation is limited to within a few metres of the wall rock, suggesting intense strain partitioning within rock units and along contacts. The more significant mineralized zones are located where the fault systems are adjacent to (or cut) mafic intrusive rocks, suggesting that fluid precipitation, rock competency and a source of iron are important for sulphide generation.

As well as stratabound and hydrothermal mineralization, the Nipissing intrusions, although rarely, do contain areas of sulphide mineralization that are not conspicuously associated with rock contacts or structures and which are not obviously altered. The nature of these mineralized zones is under investigation.

ACKNOWLEDGMENTS

The author is grateful for the enthusiastic assistance of A. Shushan and N. Szumylo. Field advice and discussions were provided by R.M. Easton and A. Pace. Figures were drafted by P. Gervais.

REFERENCES

- Bennett, G., Dressler, B.O. and Robertson, J.A. 1991. The Huronian Supergroup and associated intrusive rocks; *in* Geology of Ontario, Ontario Geological Survey, Special Volume 4, Part 1, p.549-591.
- Card, K.D. 1979. Regional geological synthesis, Central Superior Province; *in* Current Research, Geological Survey of Canada, Paper 79-1A, p.87-90.
- Card, K.D., Innes, D.G. and Debicki, R.L. 1977. Stratigraphy, sedimentology, and petrology of the Huronian Supergroup in the Sudbury–Espanola area; Ontario Division of Mines, Study 16, 99p.
- Dyer, R.D. 2010a. Elliot Lake–Sault Ste. Marie area lake sediment geochemical survey, northeastern Ontario; Ontario Geological Survey, Open File Report 6251, 195p.

- 2010b. Lake sediment and water geochemical data from the Elliot Lake–Sault Ste. Marie area, northeastern Ontario; Ontario Geological Survey, Miscellaneous Release—Data 267.
- Easton, R.M. 2006. Precambrian geology, Porter and Vernon townships; Ontario Geological Survey, Preliminary Map P.2845, scale 1:20 000.
- Jackson, S.L. 2001. On the structural geology of the Southern Province between Sault Ste. Marie and Espanola, Ontario; Ontario Geological Survey, Open File Report 5995, 55p.
- Lightfoot, P.C., Prevec, S. and Keays, R.R. 1995. Mineral potential of the Nipissing Gabbro; *in* Summary of Field Work and Other Activities 1995, Ontario Geological Survey, Miscellaneous Paper 164, p.113-115.
- Long, D.G.F. 1976. The stratigraphy and sedimentology of the Huronian (Lower Aphebian) Mississagi and Serpent formations; unpublished PhD thesis, University of Western Ontario, London, Ontario, 291p.
- Palmer, H.C., Merz, B.A. and Hayatsu, A. 1977. The Sudbury dikes of the Grenville Front region: paleomagnetism, petrochemistry and K-Ar studies; Canadian Journal of Earth Sciences, v.14, p.1867-1887.
- Pienaar, P.J. 1963. Stratigraphy, petrography and genesis of the Elliot Group, Blind River, Ontario, including the uraniferous conglomerate; Geological Survey of Canada, Bulletin 83, 140p.
- Prevec, S.A. 1993. An isotopic, geochemical and petrographic investigation of the genesis of Early Proterozoic mafic intrusions and associated volcanics near Sudbury, Ontario; unpublished PhD thesis, University of Alberta, Edmonton, Alberta, 223p.
- Robertson, J.A. 1968. Geology of Township 149 and Township 150, District of Algoma; Ontario Department of Mines, Report 57, 162p.
- 1978. Uranium deposits in Ontario; *in* Uranium deposits: their mineralogy and origin, Mineralogical Association of Canada, Short Course Volume 3, p.229-280.
- Robertson, J.A., Card, K.D. and Frarey, M.J. 1969. The Federal–Provincial Committee on Huronian Stratigraphy Progress Report; Ontario Department of Mines, Miscellaneous Paper 31, 26p.
- Roscoe, S.M. 1969. Huronian rocks and uraniferous conglomerates; Geological Survey of Canada, Paper 68-40, 205p.
- Siemiatkowska, K.M. 1977. Precambrian geology, Endikai Lake area, District of Algoma; Ontario Geological Survey, Map 2399, scale 1:31 680.
- Young, G.M. 1991. Stratigraphy, sedimentology and tectonic setting of the Huronian Supergroup; Geological Association of Canada–Mineralogical Association of Canada–Society of Economic Geologists, Toronto '91, Field Trip B5, Guidebook, 34p.
- Zolnai, A.I., Price, R.A. and Helmstaedt, H. 1984. Regional cross section of the Southern Province adjacent to Lake Huron, Ontario: implications for the tectonic significance of the Murray fault zone; Canadian Journal of Earth Sciences, v.21, p.447-456.

17. Project Unit 12-004. Preliminary Results from the Otter–Morin Townships Bedrock Mapping Project, Southern and Superior Provinces

C.A. Gordon¹

¹Earth Resources and Geoscience Mapping Section, Ontario Geological Survey

INTRODUCTION

The bedrock mapping project of Otter and Morin townships began in 2012 with the 1:20 000 scale mapping of Otter Township. Otter Township, which covers 100 km², is located approximately 35 km north of the town of Thessalon. Although the area was mapped in detail in the early 1970s (Chandler 1973, 1976), several outstanding geological problems remain to be resolved and explored, some of which are listed below.

- Several large mafic intrusions occur in the map area and have previously been assigned to the Nipissing intrusive suite (2220 Ma), and have associated nickel-copper mineralization. Work by Easton (2009, 2010) in the Elliot Lake area to the west suggests that intrusions belonging to the East Bull Lake intrusive suite (2475 Ma) may be present in the study area. Mapping aided by geochemical and geochronological analyses will help to classify and evaluate the nickel-copper-platinum group element (PGE) mineral potential of the different mafic intrusions in the map area.
- The southern portion of Otter and Morin townships contain one of the larger exposures of Matinenda Formation rocks west of Elliot Lake. The Matinenda Formation is not known to be mineralized (uranium) in the study area, but mapping will assess the mineral potential of the formation as well as the character of the Archean basement. This work will assist with forming regional interpretations regarding the source of uranium mineralization in the Huronian Supergroup and whether the Matinenda Formation exhibits significant regional lateral-facies variation.
- A large portion of the study area is underlain by rocks of the Archean Ramsey–Algoma granitoid complex. Little information is currently available on this complex. Mapping, sampling and geochemical and geochronological analyses will help to characterize this large basement terrane.

This article summarizes the preliminary results from the 2012 field season with field descriptions and discussion of the major rock units, structural geology and mineralization.

GEOLOGICAL SETTING AND PREVIOUS WORK

Otter Township and Morin Township straddle the boundary between the Superior and Southern provinces, and are located approximately 40 km north of Lake Huron (Figure 17.1, inset map). The majority of the study area is underlain by the Archean Ramsey–Algoma granitoid complex of the southern Abitibi Subprovince. Little information is available on this part of the Superior Province; however, the complex is known to contain granitic, granodioritic and granitic gneiss with numerous greenstone enclaves and massive to foliated granite, granodiorite and syenite intrusions (Card 1979). The Ramsey–Algoma granitoid complex is bounded to the south by the Paleoproterozoic Huronian Supergroup of the Southern Province. The Huronian Supergroup is subdivided into 4 groups: the Elliot

*Summary of Field Work and Other Activities 2012,
Ontario Geological Survey, Open File Report 6280, p.17-1 to 17-10.*

© Queen's Printer for Ontario, 2012

Lake Group, the Hough Lake Group, the Quirke Lake Group and the Cobalt Group. Beginning with the Hough Lake Group, these divisions define cycles involving conglomerates at the base, followed by finer grained mudstone-dominated rocks and capped by sandstones (Bennett, Dressler and Robertson 1991).

Previous mapping of Otter and Morin townships includes that of Bennett, Leahy and Walmsley (1990), Chandler (1973, 1976), Frarey (1959), Emmons (1927) and Collins (1925). Existing regional compilations that include the area are those of Johns, McIlraith and Muir (2003) and Giblin, Leahy and Robertson (1979).

PRELIMINARY RESULTS

Archean Ramsey–Algoma Granitoid Complex, Mafic Dikes and Greenstone Remnants

Archean basement comprises two thirds of the map area and is part of the Ramsey–Algoma granitoid complex. The dominant rock type is syenogranite, with minor monzogranite, granodiorite and syenite phases. The dominant rock unit consists of medium-grained, homogeneous, equigranular alkali feldspar, quartz, plagioclase, minor biotite and amphibole. It is typically massive, but a northwest-trending foliation is locally developed and defined by feldspar and quartz grains. An alkali feldspar phyrlic phase is locally present and consists of 0.5 cm up to 2 cm wide, round alkali feldspar oikocrysts enclosing medium-grained quartz, plagioclase and biotite. A pegmatitic phase occurs at the eastern edge of Desayeux Lake and approximately 1.5 km south of Burden Lake. Within the Ramsey–Algoma granitoid complex, medium- to fine-grained mafic xenoliths are common and range from 5 to 30 cm wide; the xenoliths tend to be elongate and angular with sharp contacts with the granitoid phases. Alteration of the basement rocks is varied across the township, but is predominantly patchy and/or concentrated along fractures and consists of potassic and minor epidote alteration.

The unconformable contact between the Ramsey–Algoma complex and the Huronian Supergroup is well exposed along the eastern edge of Desayeux Lake. At this location, quartz arenite, interpreted to belong to the Matinenda Formation, overlies a significantly altered granitoid, possible regolith, where quartz and alkali feldspar grains are embedded in a fine-grained pale green matrix. Near the contact with the overlying sandstone, a 35 cm wide granitoid clast is wholly enclosed by the quartz arenite and the quartz arenite appears to have filled fractures in the underlying granitoid.

The Archean basement is crosscut by numerous mafic dikes, most of which are interpreted to be Proterozoic; however, 2 sets of older mafic dikes were identified in the map area. These older mafic dikes are fine to medium grained, locally plagioclase phyrlic and weakly foliated. The main feature that suggests these are Archean is the abundance of fine aplite to medium-grained granitoid dikes that crosscut the mafic dikes.

A sliver of Archean metavolcanic rock is preserved northeast of Burden Lake (Photo 17.1A). The metavolcanic rocks consist of deformed pillow basalts, with pillows approximately 15 by 8 cm in size. This pillowed unit is plagioclase phyrlic and contains approximately 5% round, quartz-filled amygdules that are 2 to 3 mm in size and are concentrated near the margins of the pillows. Pillow selvages are thick, 3 to 8 cm wide, and weather beige compared to the more bluish weathered surface of the pillows.

Paleoproterozoic Dikes

A significant geological problem faced in the mapping was unravelling the complex history of mafic intrusive events in the area. In addition to the aforementioned Archean mafic dikes and the large mafic

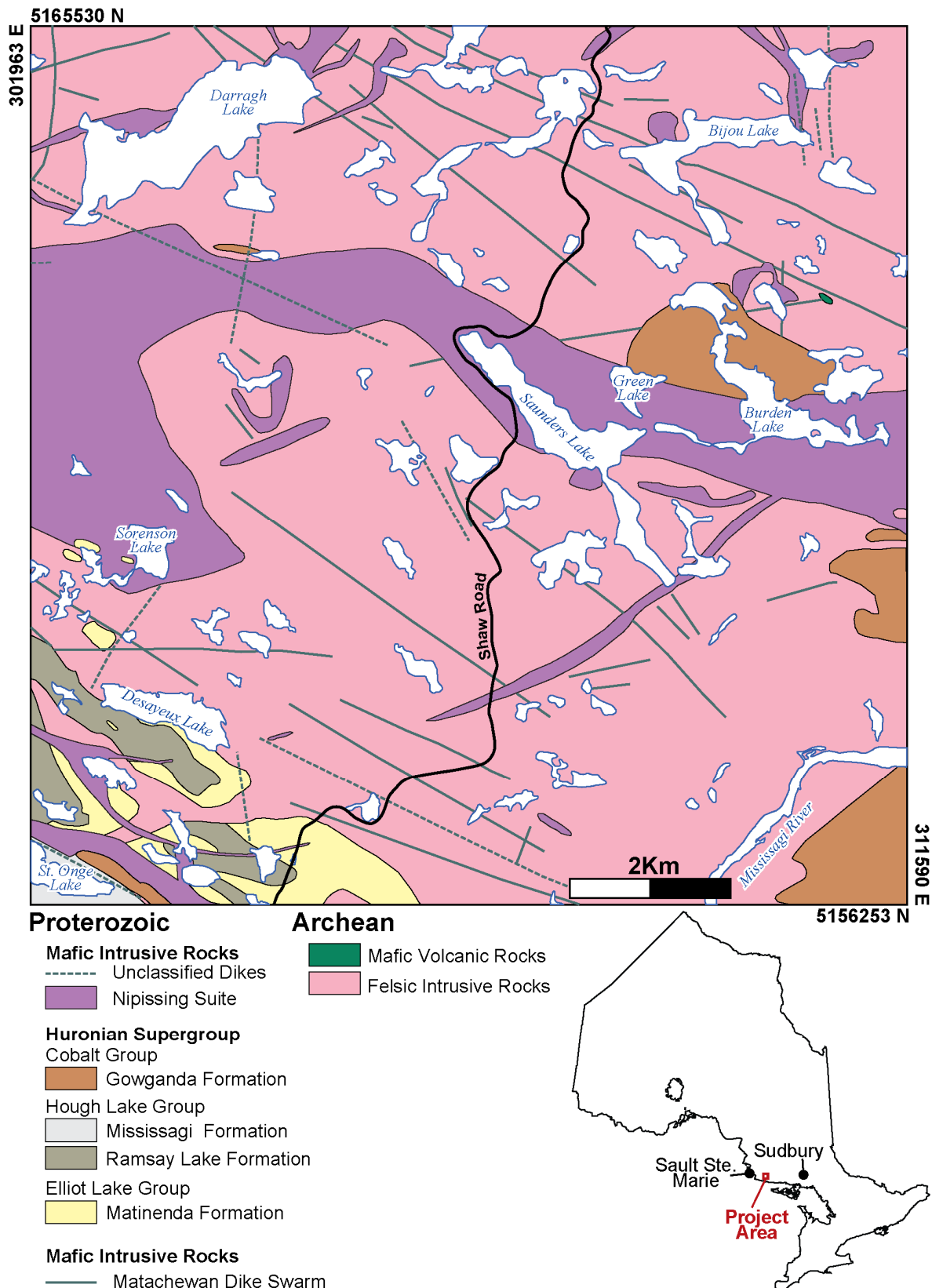


Figure 17.1. Simplified geological map of Otter Township, Superior and Southern provinces. Universal Transverse Mercator (UTM) co-ordinates provided using on North American Datum 1983 (NAD83) in Zone 17.

intrusion that occurs in the map area, which will be discussed below, there are numerous, relatively narrow (0.5 m up to 50 m wide), northwest- and west-trending mafic dikes that appear to predate the larger mafic intrusions in the area and the sedimentary rocks of the Huronian Supergroup. These dikes range from mesocratic to melanocratic, nonmagnetic to moderately magnetic, fine to medium grained and, locally, are plagioclase phyric. Plagioclase phenocrysts are typically 3 to 4 mm in size, subhedral to anhedral with rare occurrences of plagioclase glomerocrysts up to 3 cm in diameter (Photo 17.1B).

To the east, in the Elliot Lake area, many of the mafic dikes within the Archean basement were interpreted to belong to the Matachewan and Hearst dike swarm (Easton 2009). Unfortunately, there are currently no field criteria to clearly identify the Matachewan dikes from other mafic intrusive events. Therefore, some, or all, of the mafic dikes described in this section may belong to the plagioclase-phyric and non-plagioclase-phyric varieties of the Matachewan dike swarm. Samples were collected of the various mafic dikes for petrographic and geochemical analysis to aid in the further characterization of these dikes.

Huronian Supergroup and Feeders to Huronian Supergroup Metavolcanic Rocks

Sedimentary rocks of the Huronian Supergroup crop out in the southwestern and southeastern parts of Otter Township and within a few outliers across the township (*see* Figure 17.1). These units are tentatively assigned to the Elliot Lake Group, Hough Lake Group and the lower member of the Cobalt Group (broadly keeping with their original designation by Chandler (1976)). As noted in previous investigations, formations of the Quirke Lake Group are either not preserved or were not deposited within the map area.

ELLIOT LAKE GROUP AND FEEDERS TO THE HURONIAN SUPERGROUP METAVOLCANIC ROCKS

The Livingstone Creek Formation, lowermost formation of the Elliot Lake Group, is exposed in 3 locations within the southern part of Otter Township. The southernmost occurrence, which has been described in detail by Bennett, Leahy and Walmsley (1990), is along Shaw Road at the southern boundary of Otter Township, where the side of a hill exposes a thickly laminated, fine- to medium-grained, grey subfeldspathic sandstone that grades upward into quartz arenite. These units are overlain by pyritic quartz pebble conglomerate of the Matinenda Formation. Bennett, Leahy and Walmsley (1990) suggested, based on this occurrence and one directly south of the map area in Houghton Township, that the Matinenda Formation lies disconformably upon the Livingstone Creek Formation and that the Thessalon Formation volcanic rocks were removed by “pre-Matinenda” erosion. Approximately 1 km north of the Shaw Road exposure, additional outcrops observed by the author exhibit an irregular contact between rocks interpreted as the Livingstone Creek Formation and the Matinenda Formation. The lower contact of pyritic quartz pebble conglomerate of the Matinenda Formation can be traced cutting downward into the underlying sandstones of Livingstone Creek Formation (Photo 17.1C).

The grey subfeldspathic sandstone of Livingstone Creek Formation is crosscut by fine-grained, east-trending, vertically dipping quartz- and chlorite-filled amygdaloidal mafic dikes (Photo 17.1D). The mafic dikes do not appear to crosscut the overlying quartz pebble conglomerate, but additional stripping of the outcrop would be needed to fully confirm this relationship. The contacts of the mafic dike are locally sheared. Shallow level dikes identified in the map area may represent feeders to the Thessalon Formation volcanic rocks and have been sampled for geochemistry in order to confirm this relationship.

With the exception of the locations described above, typically the Matinenda Formation directly overlies rocks of the Ramsey–Algoma granitoid complex. East of Shaw Road, the Matinenda Formation is composed of interlayered pyritic quartz pebble conglomerate (Photo 17.1E) and quartz arenite. To the west of Shaw Road, the “classic” pyritic quartz pebble conglomerate is less common, and the presence of medium- to coarse-grained pink arkose, grey siltstone and green, coarse-grained quartz arenite have tentatively been assigned to the Matinenda Formation. Most of these units contain minor quartz pebbles and/or quartz pebble-rich conglomerate beds and appear to be either massive or cross-bedded (Photo 17.1F). Bedding trends roughly northwest and dips shallowly (10 to 20°) to the southwest.

Throughout the map area, the McKim Formation appears to be absent or not exposed with the exception of an outcrop of thickly laminated mudstone and siltstone that is overlain by polymictic orthoconglomerate. The mudstone–siltstone unit may represent the McKim Formation with the overlying conglomerate representing the lowermost unit of the Ramsay Lake Formation.

HOUGH LAKE GROUP

The Ramsay Lake Formation overlies the Matinenda Formation and is commonly exposed within higher topographic areas. The dominant unit is a massive, poorly sorted, polymictic paraconglomerate with a medium- to coarse-grained, grey sandy matrix. Angular, white quartz and pink feldspar fragments are abundant and range from 2 to 5 mm in diameter. Clasts, which compose 10 to 15% of the outcrops, range from pebble to cobble sized, and are predominantly grey granodiorite with lesser fine-grained mafic clasts and quartz pebbles. A second conglomerate unit, tentatively assigned to the Ramsay Lake Formation, is a thick-bedded, poorly sorted, polymictic orthoconglomerate (Photo 17.2A). Clasts are predominantly medium-grained, grey granodiorite, well rounded, cobble sized and weakly oriented with a sandy, pink, arkosic matrix.

Southwest of the Ramsay Lake Formation conglomerates, sandstones of the Mississagi Formation crop out along the north shore of St. Onge Lake (*see* Figure 17.1). The contact between these 2 units is overlapped by polymictic conglomerates of the Gowganda Formation and crosscut by medium-grained quartz gabbro and fine-grained mafic dikes. The sandstones of the Mississagi Formation are composed of massive, well-sorted, white to light pink-grey, coarse-grained and gritty subfeldspathic arenite.

COBALT GROUP

The Gowganda Formation is exposed in the southeast and southwest of the township and as small outliers in and around Burden Lake and Green Lake, northwest of Sorenson Lake and south of Darragh Lake (*see* Figure 17.1). The formation directly overlies the Archean basement with the exception of where it overlaps the Mississagi Formation in the southeast corner of the map area. The predominant rock types are a thickly bedded polymictic paraconglomerate with a mica-rich argillaceous matrix interlayered with coarse-grained, very pink, arkosic sandstones and/or a polymictic paraconglomerate with a sandy arkosic matrix (Photos 17.2B and 17.2C). The polymictic conglomerates are poorly sorted and contain pebbles and cobbles of dominantly pink granitoid clasts with lesser medium- to fine-grained mafic intrusive rocks, quartz pebbles, sandstone and very rare, red chert clasts. Mixing between the argillaceous and arkosic matrix polymictic conglomerates is common, as is soft sediment deformation of bedding.

A small outlier just south of Darragh Lake contains thickly laminated mudstone with east-trending, steeply dipping beds. Similar mudstones occur in the Gowganda Formation east of the map area along Highway 129 and the mudstones south of Darragh Lake are tentatively assigned to the same formation.



Photo 17.1. A) Deformed pillow basalts from remnant greenstone sliver in the Ramsey–Algoma granitoid complex (UTM 310573E 5162534N). B) Plagioclase-phyric Matachewan dike (UTM 310137E 5162689N). C) Pyritic quartz-pebble conglomerate of the Matinenda Formation cutting down into the underlying subfeldspathic sandstone of the Livingstone Creek Formation (contact shown by dashed line) (UTM 304820E 5157042N). D) Quartz and chlorite amygdaloidal basaltic dike, possible feeder to the Thessalon Formation volcanic rocks (UTM 304742E 5156127N). E) Greenish-grey, cross-bedded sandstone, Matinenda Formation (UTM 304820E 5157042N). F) Pyritic quartz-pebble conglomerate, Matinenda Formation (UTM 310204E 5165307N). Objects used for scale: compass = 14.5 cm; hammer = 40 cm; pen = 14 cm; pencil = 15 cm. UTM co-ordinates provided using NAD83 in Zone 17.



Photo 17.2. A) Polymictic orthoconglomerate with sandy arkosic matrix, Ramsay Lake Formation (UTM 302728E 5157027N). B) Polymictic paraconglomerate with mica-rich argillaceous matrix, Gowganda Formation (UTM 309957E 5161743N). C) Pink, coarse-grained arkose interbedded with polymictic paraconglomerate, Gowganda Formation (UTM 317164E 5149847N). D) Medium-grained monzogabbro, Nipissing intrusion (UTM 305039E 5162404N). E) Vari-textured quartz gabbro with centimetre-sized sulphide burns, Nipissing intrusion (UTM 306815E 5162445N). F) Medium-grained gabbro-norite xenolith from local Nipissing intrusion in fine-grained, highly magnetic mafic dike (UTM 302484E 5162065N). Objects used for scale: compass = 14.5 cm; hammer = 40 cm; pen = 14 cm; pencil = 15 cm. UTM co-ordinates provided using NAD83 in Zone 17.

Mesoproterozoic Mafic Intrusive Rocks

NIPISSING INTRUSIVE SUITE

A large, roughly east-trending mafic sill that is up to 2 km wide at its thickest point, but typically 800 to 1000 m wide, is present in Otter Township (*see* Figure 17.1). The intrusion is relatively evolved and differentiated. A transect, approximately north-to-south, begins with medium- to coarse-grained gabbro followed by quartz gabbro, monzogabbro (possible granophyre; Photo 17.2D) and lastly a fine- to medium-grained gabbro. Near the southern margin of the large intrusion, a vari-textured, locally pegmatitic, quartz gabbro horizon is present and can be traced for several kilometres (Figure 17.2E). The large sill intruded Archean basement. Several, relatively smaller, 100 to 200 m wide, discontinuous mafic intrusions in the map area are interpreted to be related. These intrusions directly cut Huronian Supergroup sedimentary rocks, which suggests that they are Mesoproterozoic and younger than the abundant, northwest- and west-trending dikes of the Matachewan–Hearst dike swarm. The smaller intrusions are medium- to coarse-grained, locally contain pyroxene phenocrysts, and are composed of quartz gabbro, gabbro and minor phases of monzogabbro.

The large sill and the related smaller intrusions were previously mapped as part of the Nipissing intrusive suite and, based on lithological, textural and crosscutting relationships, the author agrees with this interpretation.

YOUNGER DIKES

A series of fine-grained to aphanitic, northwest-trending and approximately north-trending mafic dikes with high magnetic susceptibility (74 to 103×10^{-3} SI units), cut the large Nipissing sill that transects the central portion of the Otter Township (*see* Figure 17.1). Intrusion breccia containing clasts of medium- to coarse-grained Nipissing gabbro was observed in the fine-grained, highly magnetic, mafic dikes in 2 locations (Photo 17.2F). These dikes may be related to the Sudbury dike swarm, which is typically composed of olivine gabbro. The strong magnetic character of these dikes may be related to serpentinization of olivine. Detailed petrographic and geochemical analysis will aid in the classification of these and all of the aforementioned mafic intrusions.

Structural Geology

One of the geological questions about this area, prior to the 2012 field season, was whether there are any regional faults affecting the Archean basement or Huronian Supergroup, such as those that occur in abundance in the Elliot Lake area. For the most part, the syenogranites of the Ramsey–Algoma granitoid complex are massive with local development of a northwest-trending foliation. Minor west- to northwest-trending shear zones, 5 cm up to 3 m wide, with dextral shear sense, do transect the map area, but could not be consistently traced; their full extent is still under investigation. Furthermore, contacts between mafic intrusive units and both granitoid and sedimentary units are commonly sheared.

A reversal in bedding dip direction occurring along Highway 129, parallel to, and approximately 1.5 km east of the map area, indicates a possible syncline with an axial plane trending roughly southwest. This fold may affect the Gowganda Formation in the southeastern part of the map area, east of the Mississagi River. West of the Mississagi River, the bedding in the Huronian Supergroup units are consistently northwest striking, with shallow southwest dips. Schistosity is locally developed, but may be related to northwest-trending shear zones seen throughout the map area. Outliers, such as the small exposure of laminated argillite, south of Darragh Lake, contain the only west-striking, steeply southward-dipping beds, which may be attributed to a local, primary, depositional environment.

Mineralization

Sulphide mineralization in the map area is associated with mafic dikes, grey siltstone and quartz pebble conglomerate of the Matinenda Formation and along quartz veins that cut the various rock units. Many of the Archean and Proterozoic mafic intrusive rocks contain trace amounts of fine disseminated sulphide minerals, including chalcopyrite, pyrrhotite and pyrite. Elevated concentrations of sulphide minerals, up to 5 to 7%, are associated with the quartz gabbro, monzogabbro and vari-textured gabbro-norite phases of the large Nipissing intrusions. The amygdaloidal mafic dikes that cut the Livingstone Creek Formation contain 5 to 10%, subhedral to euhedral, cubic pyrite crystals that are 2 to 5 mm in size and occur in centimetre-sized highly concentrated patches. The quartz pebble conglomerate and local grey siltstones of the Matinenda Formation contain subhedral to euhedral, cubic pyrite grains that range from less than 0.1 mm up to 2 mm in size. These exposures tend to be very rusty in the field. The highest concentration of sulphide mineralization encountered was associated with quartz veins that transect the various rock types in the map area. The quartz veins trend roughly westerly and northwesterly, and are 2 to 15 cm in width. Mineralization consists of a silver-coloured sulphide mineral, identified in the field as molybdenite, and minor copper sulphide minerals within fracture surfaces and surrounding drusy cavities in the white quartz veins.

FUTURE WORK

A sample from the vari-textured quartz gabbro unit, tentatively classified as a Nipissing sill, was collected for geochronology in order to confirm the age of the intrusion. Magnetic susceptibility and scintillometer measurements were collected this summer and are undergoing analysis to aid in the division of the different mafic rocks units, as well as to evaluate potential uranium sources in the granitoid basement and the uranium mineral potential of the Matinenda Formation within the Otter–Morin map area. The latter information will also allow for regional comparison with data from the Elliot Lake area (Easton 2009, 2010). Bedrock mapping for the summer 2013 field season will extend westward into Morin Township.

ACKNOWLEDGMENTS

The author would like to thank C. Laws for her assistance during the 2012 field season. R.M. Easton is thanked for his ongoing guidance and assistance on this project and to P. Gervais for drafting of the figure. Special thanks are extended to the owner–operators of Carpenter Lake Cabins and Limberlost Lodge for their exceptional service and hospitality this past summer.

REFERENCES

- Bennett, G., Dressler, B.O. and Robertson, J.A. 1991. The Huronian Supergroup and associated intrusive rocks; *in* Geology of Ontario, Chapter 14, Ontario Geological Survey, Special Volume 4, Part 1, p.549-591.
- Bennett, G., Leahy, E.J. and Walmsley, J. 1990. The Sault Ste. Marie Resident Geologist's District—1989; *in* Report of Activities, Regional and Resident Geologists, Ontario Geological Survey, Miscellaneous Paper 147, p.205-215.
- Card, K.D. 1979. Regional geological synthesis, central Superior Province; *in* Current Research, Part A, Geological Survey of Canada, Paper 79-1A, p.87-90.
- Chandler, F.W. 1973. Geology of McMahon and Morin townships, District of Algoma; Ontario Geological Survey, Report 112, 77p.

- 1976. Geology of the Saunders Lake area, District of Algoma; Ontario Geological Survey, Report 155, 46p.
- Collins, W.H. 1925. North shore of Lake Huron; Geological Survey of Canada, Memoir 143, 160p.
- Easton, R.M. 2009. Compilation mapping, Pecors–Whiskey Lake area, Superior and Southern provinces; *in* Summary of Field Work and Other Activities, 2009, Ontario Geological Survey, Open File Report 6240, p.10-1 to 10-21.
- 2010. Compilation mapping, Pecors–Whiskey Lake area, Southern and Superior provinces; *in* Summary of Field Work and Other Activities, 2010, Open File Report 6260, p.8-1 to 8-12.
- Emmons, R.C. 1927. Wakomata Lake map-area, Algoma District, Ontario; Geological Survey of Canada, Summary Report 1926, Part C, p.1C-15C.
- Frarey, M.J. 1959. Geology, Echo Lake, District of Algoma, Ontario; Geology Survey of Canada, Map 23-1959, scale 1:63 360.
- Giblin, P.E., Leahy, E.J. and Robertson, J.A. 1979. Sault Ste. Marie–Elliot Lake area, geological compilation series, Algoma, Manitoulin and Sudbury districts; Ontario Geological Survey, Map 2419, scale 1:253 440.
- Johns, G.W., McIlraith, S.J. and Muir, T.L. 2003. Precambrian geology compilation series—Sault Ste. Marie–Blind River map sheet; Ontario Geological Survey, Map 2670, scale 1:250 000.

18. Project Unit 11-007. Whole Rock and Isotope Data from the Midcontinent Rift: Implications for Crustal Contamination History

R.M. Cundari^{1,2}, P. Hollings¹, M.C. Smyk², J.F. Scott^{2,3} and D.A. Campbell²

¹Department of Geology, Lakehead University, Thunder Bay, Ontario P7B 5E1

²Resident Geologist Program, Ontario Geological Survey, Thunder Bay, Ontario P7E 6S7

³*Present Address:* Thunder Bay Geological Services, 236 S. Algonquin Ave., Thunder Bay, Ontario P7B 4T3

INTRODUCTION

This article presents the results from a Master of Science (MSc) thesis project by the senior author focussed on magmatism associated with the 1.1 Ga Mesoproterozoic (Keweenaw) Midcontinent Rift in Ontario. This work is part of multiyear project (Project Units 08-021 and 10-012) most recently summarized by Hollings et al. (2010) and Hollings, Smyk and Cousens (2012). Details regarding field work associated with this study were summarized in Cundari et al. (2011). Three study areas are included in this article: the Pigeon River area (National Topographic System (NTS) map areas 52 A/3 and A/4), the Nipigon Embayment (NTS 52 H and 52 I) and the Coldwell Complex (NTS 42 D/16). Work in the Pigeon River area was focussed on determining the timing relationship between 3 main dike swarms in that area (Pigeon River, Cloud River and Mount Mollie dikes). Once the timing relationships were established, geochemical and isotopic data were applied to the units in order to investigate the geochemical evolution of the units through time. The second portion of the study was a re-evaluation of geochemical and isotopic data for the intrusive rocks of the Nipigon Embayment, focussing on the Nipigon sills. The third portion of the study was related to a volcanic unit exposed near Geordie and Coubran lakes in the north-central portion of the Coldwell Complex, near Marathon. The goal of the study was to investigate the relationship between these volcanic rocks and the intrusive units in this alkalic complex. Isotopic data were used to aid in evaluating the crustal contamination history as well as placing the Coubran Lake basalts within the magmatic context of the Midcontinent Rift.

DIKE SWARMS OF THE LOGAN BASIN

From field, paleomagnetic and geochemical evidence, the following timing sequence for intrusive units of the Logan Basin was proposed (from oldest to youngest): the Riverdale sill, the Devon volcanic rocks, the Logan sills, the Pigeon River dikes, the Cloud River dikes, the Mount Mollie dike and the Crystal Lake gabbro. The Pigeon River dikes are geochemically similar to the Nipigon sills to the north, although they are not thought to be feeders to the sills given the distance between them. Carl (2010) suggested that the Pigeon River-style, east-northeast-trending dikes on Sibley Peninsula (here referred to as the Sibley dikes) are geochemically similar to and thus belong to the Pigeon River suite. Re-evaluation of the geochemical data from the Pigeon River dikes in the Logan Basin and the Sibley dikes in relation to the Nipigon sills has shown geochemical differences between the Pigeon River dikes and the Sibley dikes. On the plot of Nb/Yb_{pm} versus Th/Yb_{pm} (Figure 18.1A), the Pigeon River dikes form arrays separate to those of the Nipigon sills, with the Sibley dikes dominantly plotting within the Nipigon field.

The field evidence shows that the Cloud River dikes perpendicularly crosscut Pigeon River dikes, with the Mount Mollie dike crosscutting both Pigeon River dikes and Cloud River dikes (Cundari et al. 2011), which is not consistent with the geochronological data of Hollings et al. (2010). The age of 1078 ± 3 Ma for the Arrow River dike (a Pigeon River dike) supports the observation that the Pigeon River dikes postdate the Logan sills (1114.7 ± 1.1 Ma), which they crosscut. However, the 1078 Ma Pigeon River dike age is contradicted by the age of 1109.2 ± 4.2 Ma for the Cloud River dike and the age of 1109.3 ± 6.3 Ma for the Mount Mollie dike, both of which have been shown to crosscut Pigeon River dikes. The age of 1141 ± 20 Ma for the Rita Bolduc dike (a Pigeon River dike) does not support the Pigeon River dikes crosscutting the Logan sills, but supports the Pigeon River dikes being crosscut by the Cloud River and the Mount Mollie dikes. Further geochronology is needed to resolve these inconsistencies.

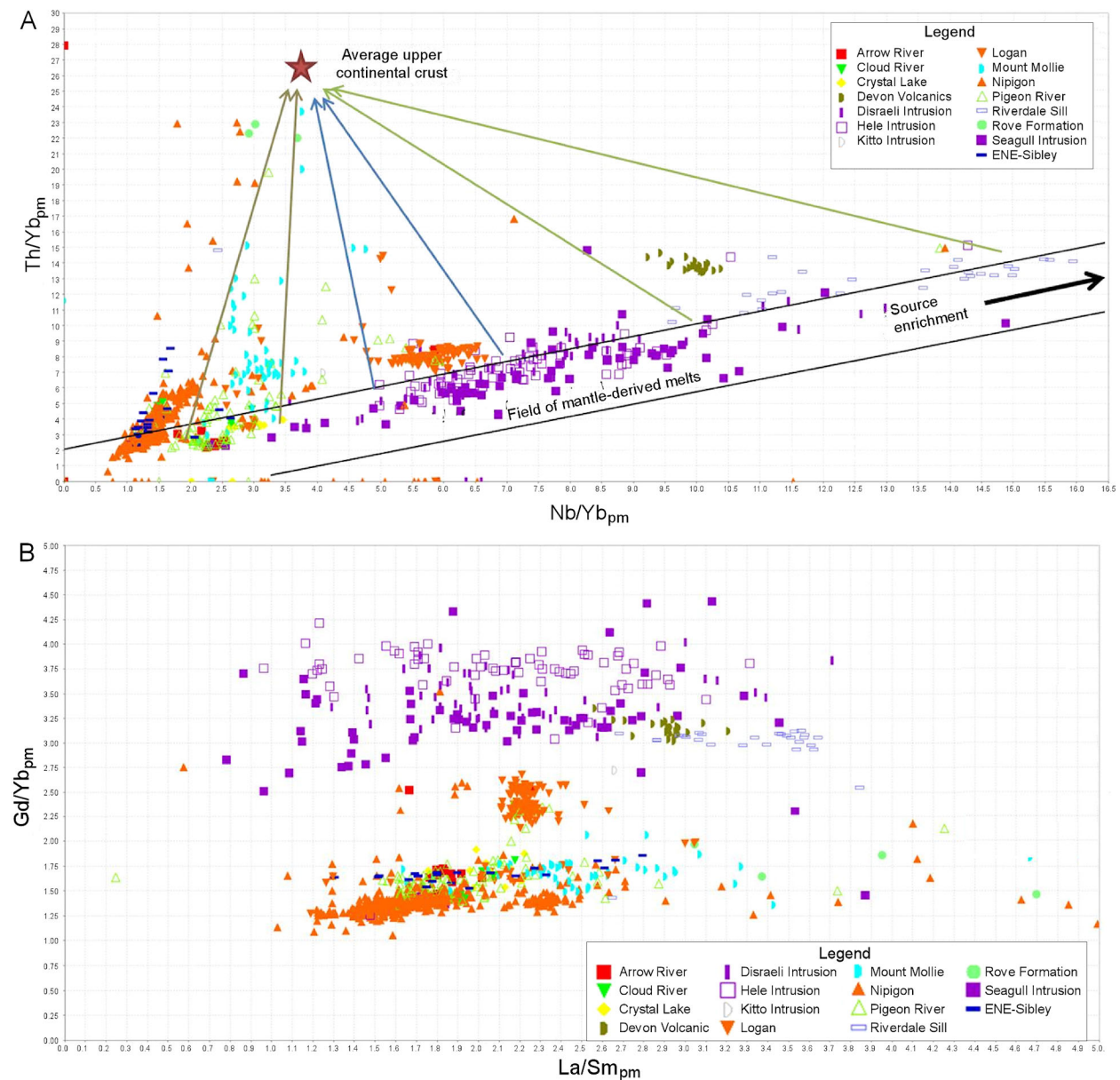


Figure 18.1. A) Diagram showing variations in Th/Yb_{pm} and Nb/Yb_{pm} ratios for Midcontinent Rift-related mafic rocks. B) Diagram showing La/Sm_{pm} versus Gd/Yb_{pm} ratios for Midcontinent Rift-related mafic rocks. Normalizing values from Sun and McDonough (1989). Abbreviation: “pm” indicates normalized to primitive mantle.

Table 18.1. Isotope data for Logan Basin units analyzed in this study. Supplementary data for ranges and averages from Hollings, Smyk and Cousens (2012).

Unit	Sample Numbers	$^{87}\text{Sr}/^{86}\text{Sr}_i$	$\epsilon_{\text{Nd}(t=1100\text{Ma})}$ Values	$\epsilon_{\text{Nd}(t=1100\text{Ma})}$ Range	$\epsilon_{\text{Nd}(t=1100\text{Ma})}$ Average
Devon volcanic rocks	SP-RC-008	0.70931	-2.9	-2.9 to -3.5	-3.2 (n=2)
Logan	112	0.71196	-4.2	0.1 to -4.2	-0.9 (n=17)
Arrow River	136	0.70343	-0.2	see Pigeon River sample 113	
Pigeon River	SP-RC-014	0.6891	0		
Pigeon River	113	0.70461	0	1.5 to -7.9	-1.1 (n=8)
Pigeon River	111	0.70498	1.5		
Cloud River	126	0.70722	-4	0.3 to -4.0	-2.2 (n=3)
Mount Mollie	110	0.71662	-13.3	0.9 to -13.3	-4.5 (n=4)

Abbreviations: n = number of samples, $^{87}\text{Sr}/^{86}\text{Sr}_i = ^{87}\text{Sr}/^{86}\text{Sr}$ initial ratio, t = time.

The varied orientation between the 3 dike sets, as well as textural differences between them, allows for inferences into the geodynamic controls on the emplacement, as well as the source of the dikes. The Pigeon River dikes were emplaced at a roughly rift axis-parallel orientation likely due to magma exploiting normal faulting as extension progressed. Along with normal faulting, it is likely that accommodation or transverse faults propagated perpendicularly to the normal faults and were infilled by Cloud River dikes. The Cloud River dikes contain abundant plagioclase phenocrysts, unlike the Pigeon River dikes. This plagioclase likely formed in a staging chamber where the Cloud River dike may have experienced a longer residence time given the fact that it was emplaced after the Pigeon River dikes. The longer residency time of the Cloud River dike is consistent with the neodymium isotope data, as 2 of the 3 available samples display $\epsilon_{\text{Nd}(t=1100\text{Ma})}$ values of -3.0 and -4.0, which are more negative than the majority of the Pigeon River dike samples, indicative of a greater degree of crustal contamination (Table 18.1).

A similar process may explain the geochemical and textural characteristics of the Mount Mollie dike, which may have had a similar source to that of the Pigeon River and Cloud River dikes. It is possible that the Mount Mollie dike was sourced from the same magma chamber as the Pigeon River and Cloud River dikes, but had a longer residence time allowing for additional fractionation and the formation of a felsic component, manifested as extensive granophyric zones. The longer residence time of the Mount Mollie dike is supported by the more contaminated geochemical signature; the Mount Mollie dike displays the highest $\text{Th}/\text{Yb}_{\text{pm}}$ ratios (see Figure 18.1A) of the 3 dike sets as well as the broadest range of $\text{La}/\text{Sm}_{\text{pm}}$ values (Figure 18.1B). Furthermore, the Mount Mollie dike displays a wide range of $\epsilon_{\text{Nd}(t=1100\text{Ma})}$ from 0.9 to -13.3, suggesting a complex crustal contamination history. The strontium data for the 3 dike sets in the Logan Basin do not show any correlation to the emplacement sequence. Elevated $^{87}\text{Sr}/^{86}\text{Sr}_i$ values are interpreted to be a result of shallow-level contamination by Paleoproterozoic Rove Formation sedimentary rocks (Hollings, Smyk and Cousens 2012). The $^{87}\text{Sr}/^{86}\text{Sr}_i$ values for the Pigeon River dikes, the Cloud River dikes and the Mount Mollie dike (see Table 18.1) show considerable overlap and broad ranges, suggesting that individual dikes underwent variable shallow-level contamination during emplacement.

The similar source characteristics of all 3 dikes sets support the model of their being tapped from the same magma chamber, and subsequently undergoing varied degrees of crustal contamination through time (i.e., similar $\text{Nb}/\text{Yb}_{\text{pm}}$ values: Figure 18.1A, and $\text{Gd}/\text{Yb}_{\text{pm}}$: Figure 18.1B). The average $\epsilon_{\text{Nd}(t=1100\text{Ma})}$ values for each of the 3 dike sets is consistent with the progressively more contaminated nature of the dikes with time; Pigeon River = -1.1, Cloud River -2.2 and Mount Mollie = -4.5 (Figure 18.2). The data presented here begin to explain the magmatic evolution of dikes within the Logan Basin in light of their crosscutting relationships, dike-specific textures and lithologic variability, similar geochemistry and their different crustal contamination signatures. Further work is warranted on this topic in order to better support this proposed model. This involves refinement of the emplacement ages of the dike swarms and a better understanding of the composite nature of the Mount Mollie dike.

PETROGENESIS OF THE NIPIGON SILLS

Many authors have proposed that the main volume of Midcontinent Rift basalt was produced from an enriched-mantle plume with a $\epsilon_{\text{Nd}(t=1100\text{Ma})}$ value close to 0 and $\text{La}/\text{Sm}_\text{N}$ of 2 to 3 (cf. Nicholson and Shirey 1990; Nicholson et al. 1997; Hollings et al. 2007a). Data for the Nipigon sill suites from Hollings et al. (2007b), combined with analyses from this study, show that the Nipigon sills have $\epsilon_{\text{Nd}(t=1100\text{Ma})}$ values from -0.29 to -6.42 , which is consistent with contamination by an older crustal source. The most plausible sources of contamination for the intrusive rocks of the Nipigon Embayment are the Mesoproterozoic Sibley Group sedimentary rocks and the Archean metasedimentary and migmatitic rocks of the Quetico Subprovince. Rocks of the Quetico Subprovince display strongly negative $\epsilon_{\text{Nd}(t=1100\text{Ma})}$ values ranging from -16 to -23 , with lower Sr_i values than rocks of the Sibley Group. Sibley Group sedimentary rocks have $\epsilon_{\text{Nd}(t=1100\text{Ma})}$ values of -5.20 and -5.38 , with higher Sr_i values than the Quetico Subprovince rocks. Quetico Subprovince rocks form the basement to the overlying Mesoproterozoic Sibley Group rocks, which are spatially restricted to a few hundred metres of the present-day surface. It is possible to distinguish between contaminant sources. Sibley Group rocks have a stronger control on strontium values, whereas the Quetico Subprovince rocks have a stronger control on $\epsilon_{\text{Nd}(t=1100\text{Ma})}$ values (Figure 18.3C).

The degree of crustal contamination that a magma experienced during emplacement can be assessed using the plot of $\text{Nb}/\text{Yb}_{\text{pm}}$ versus $\text{Th}/\text{Yb}_{\text{pm}}$ (see Figure 18.1A and 18.3A), with $\text{Th}/\text{Yb}_{\text{pm}}$ controlling contamination by crustal material. Progressively elevated $\text{Th}/\text{Yb}_{\text{pm}}$ values for a given source region suggest that the source magma has undergone progressively increased interaction with continental crust (i.e., higher $\text{Th}/\text{Yb}_{\text{pm}}$ value indicating more crustal contamination). Using $\text{Th}/\text{Yb}_{\text{pm}}$ as a proxy for crustal contamination, 3 distinct Nipigon sill units are proposed here. The plot of $\text{Nb}/\text{Yb}_{\text{pm}}$ versus $\text{Th}/\text{Yb}_{\text{pm}}$ (see Figure 18.1A and 18.3A) shows proposed Nipigon sill types I, II and III, displaying progressively increased crustal contamination. The $\text{Th}/\text{Yb}_{\text{pm}}$ values for the more-contaminated Nipigon sill types trend toward

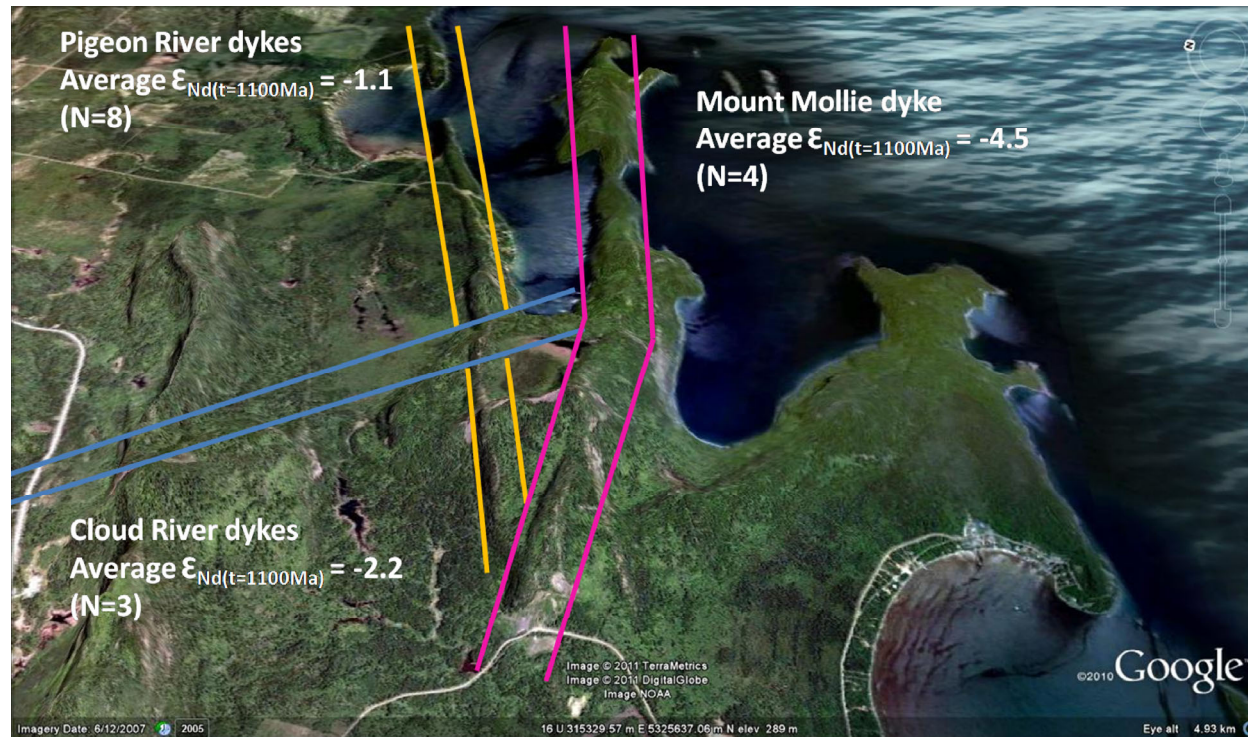


Figure 18.2. Satellite image of the Mount Mollie study area showing crosscutting relationships between a Pigeon River dike (yellow), a Cloud River dike (blue) and the Mount Mollie dike (pink). Topography displayed at 3× vertical exaggeration. Satellite photo from Google Earth™ mapping service.

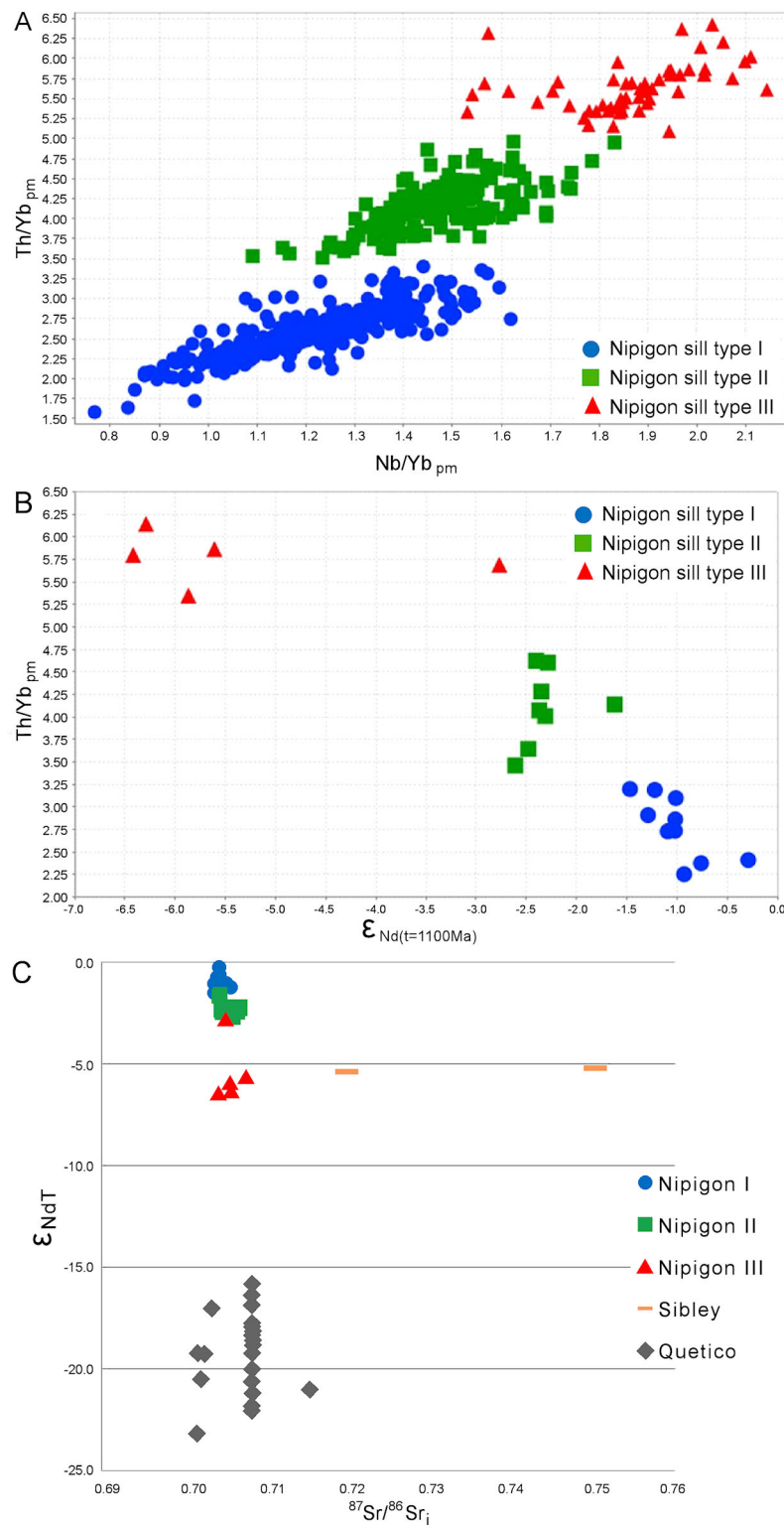


Figure 18.3. A) Plot of Nb/Yb_{pm} versus Th/Yb_{pm} showing Nipigon sill types I, II and III. B) $\epsilon_{\text{Nd}(t=1100\text{Ma})}$ versus Th/Yb_{pm} showing Nipigon sill types I, II and III. C) $^{87}\text{Sr}/^{86}\text{Sr}_i$ versus $\epsilon_{\text{Nd}(t=1100\text{Ma})}$ for Nipigon sill types I, II and III, Quetico Subprovince rocks and Sibley Group rocks. Normalizing values from Sun and McDonough (1989). Additional data from Henry, Stevenson and Garipey (1998), from Pan, Fleet and Longstaffe (1999) and unpublished data from R.T. Metsaranta (Ontario Geological Survey, personal communication, 2011). Abbreviations: $\epsilon_{\text{Nd}T}$ where T = time; “pm” = normalized to primitive mantle; $^{87}\text{Sr}/^{86}\text{Sr}_i$ = $^{87}\text{Sr}/^{86}\text{Sr}$ initial ratio.

Table 18.2. Summary of geochemical data for Nipigon sill types I, II and III. Supplementary data for ranges and averages from Hollings, Smyk and Cousens (2012).

	Nipigon I	Nipigon II	Nipigon III
Number of Samples	395	171	55
Th/Yb_{pm}	1.97 to 3.4	3.4 to 5.0	5.0 to 6.5
Nb/Yb_{pm}	0.75 to 1.65	1.2 to 1.8	1.5 to 2.2
Nb/Nb*	0.425 to 0.65	0.35 to 0.55	0.3 to 0.5
La/Sm_{pm}	1.2 to 1.8	1.60 to 2.0	2.2 to 2.6
Gd/Yb_{pm}	1.0 to 1.9	1.0 to 1.9	1.0 to 1.9
ε_{Nd(t=1100Ma)}	−0.5 to −1.5	−1.5 to −3.0	−5.0 to −7.0
⁸⁷Sr/⁸⁶Sr_i	0.70403 to 0.70556	0.70459 to 0.70681	0.70431 to 0.70761

Abbreviations: *pm* = primitive mantle, $^{87}\text{Sr}/^{86}\text{Sr}_i = ^{87}\text{Sr}/^{86}\text{Sr}$ initial ratio, *t* = time.

the Th/Yb_{pm} values for Quetico Subprovince and Sibley Group rocks, which are broadly consistent with the values for average upper continental crust defined by Taylor and McLennan (1985). The Nipigon sill types defined by Th/Yb_{pm} values show consistent results with the neodymium isotope data on the plot of ε_{Nd(t=1100Ma)} versus Th/Yb_{pm} with more negative ε_{Nd(t=1100Ma)} values correlating with higher Th/Yb_{pm} (Figure 18.3B). Geochemical analyses for all 3 Nipigon sill types are summarized in Table 18.2.

The varied crustal contamination signatures detected throughout the Nipigon sills have implications for the emplacement history of the sills. It is likely that the least-contaminated type I magmas were emplaced relatively quickly along faults, resulting in less crustal interaction, as previously proposed for the ultramafic intrusions within the Nipigon Embayment (e.g., Hart and MacDonald 2007). The more-contaminated type II and III magmas were emplaced after a longer residence in a crustal-level magma chamber where they likely assimilated more crustal material. Based on the evidence presented here, it is likely that the more-contaminated signatures of type II and III sills are dominantly controlled by the Quetico Subprovince rocks, as in the “ponding” model described above.

THE COUBRAN LAKE BASALTS

Kilometre-scale basaltic xenoliths within Centre II syenites located in the centre of the Coldwell Complex were described by Puskas (1967) and Walker et al. (1993). They have been recently recognized by the staff of Stillwater Canada Incorporated who exposed them in the Geordie–Coubran lakes area during overburden stripping. Field observations for the Coubran Lake basalts have been reported by Cundari et al. (2011). The goal of this portion of the study was to characterize these volcanic rocks and put them into the context of the larger Midcontinent Rift system.

The Coubran Lake volcanic unit comprises 3 basalt types (A, B and C), distinguished by their incompatible element abundances displayed on primitive mantle–normalized spider plots (Figure 18.4A). Basalt type A lies toward the base of the unit, forming the lowermost 10% of the exposed sequence and displaying strong light rare earth element (LREE) enrichment (La/Sm_N = 7.4 to 9.3), with heavy rare earth element (HREE) ratios comparable to types B and C (Gd/Yb_N = 2.4 to 2.5). Rocks of this type are distinguishable from basalt types B and C by the pronounced enrichment in LREE (lanthanum, cerium, praseodymium and neodymium). Basalt type B dominates the succession and displays LREE enrichment (La/Sm_N = 2.4 to 4.7) and HREE fractionation (Gd/Yb_N = 1.9 to 2.3). Rocks of this type display LREE enrichment as well as pronounced high field-strength element (HFSE) anomalies displayed by relatively lower abundances of niobium, zirconium, hafnium, titanium, vanadium and scandium. Basalt type C comprises only 3 samples, sporadically located through the sequence. It displays LREE enrichment (La/Sm_N = 1.9 to 2.9) and HREE fractionation (Gd/Yb_N = 1.9 to 2.1). It is distinguishable from basalt type A and B, based on the absence of a negative niobium anomaly and lower abundances of LREE (lanthanum and cerium).

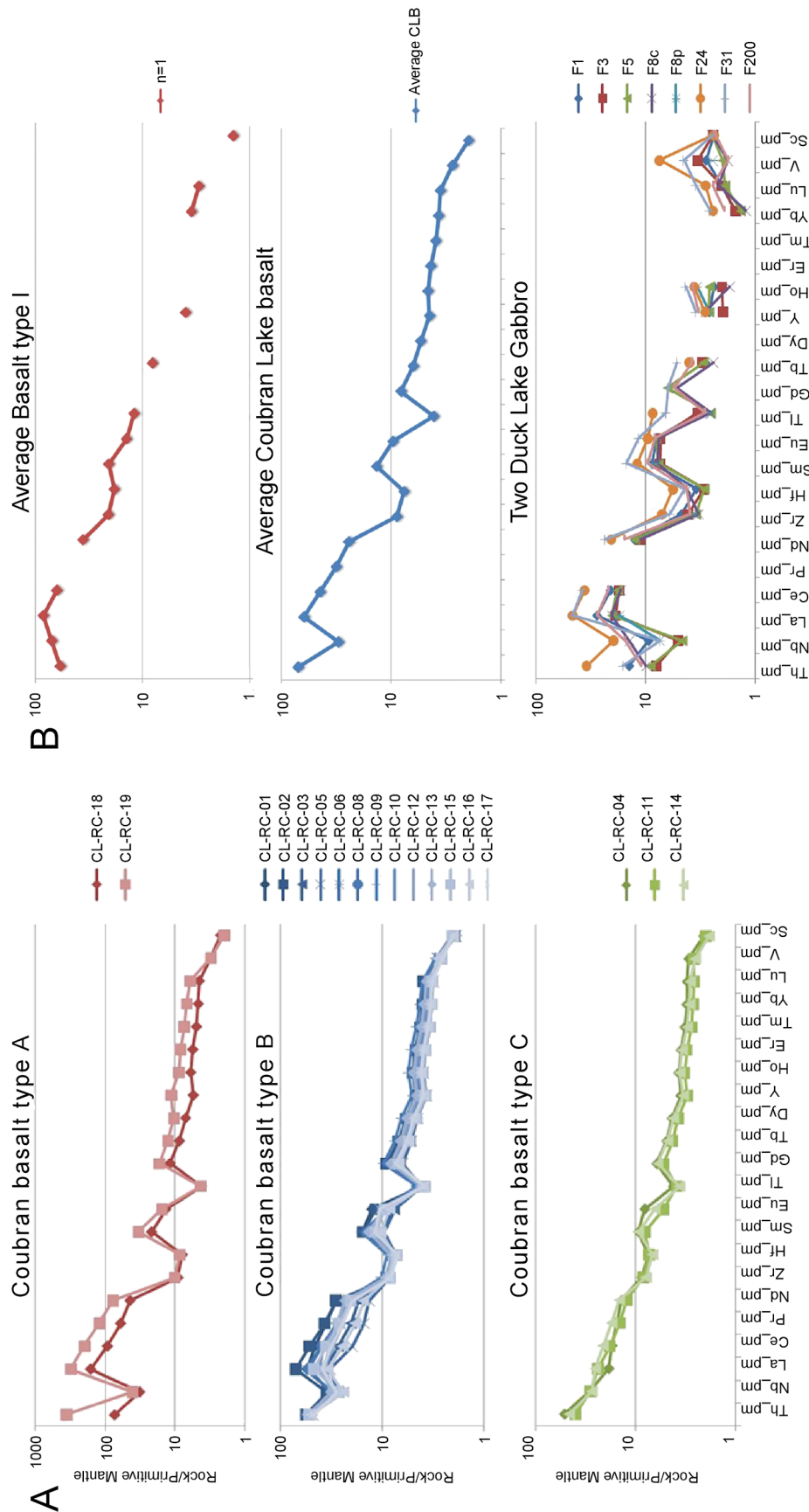


Figure 18.4. Primitive mantle-normalized (“pm”) spider plots showing Coubran Lake basalts type A, B and C. B) Primitive mantle-normalized spider plots showing average basalt type I composition, average Coubran Lake basalt composition and Two Duck Lake gabbro composition. Supplementary data from Nicholson et al. (1997) and Good (1993). Normalizing values from Sun and McDonough (1989).

Table 18.3. Summary of isotope data for the Coubran Lake basalts.

Sample	Basalt Type	$\epsilon_{\text{Nd}(t=1100\text{Ma})}$	$^{87}\text{Sr}/^{86}\text{Sr}_i$	$^{143}\text{Nd}/^{144}\text{Nd}$
CL-RC-01	B	-0.7	0.70442	0.511958
CL-RC-04	C	-0.9	0.70407	0.512139
CL-RC-09	B	-0.9	0.70386	0.512119
CL-RC-13	B	-0.7	0.70387	0.51202
CL-RC-17	B	-1	0.70356	0.51202
CL-RC-019	A	-0.5	0.70484	0.511799

Abbreviations: $^{87}\text{Sr}/^{86}\text{Sr}_i = ^{87}\text{Sr}/^{86}\text{Sr}$ initial ratio, $t = \text{time}$.

Isotopic analyses were carried out on 6 samples from the Coubran Lake basalts. Samples were chosen to represent each of the 3 basalt types recognized by trace element chemistry: 1 sample from basalt type A, 1 sample from basalt type B and 4 samples from basalt type C. The results of the isotopic analyses are summarized in Table 18.3. All 6 samples show very similar $\epsilon_{\text{Nd}(t=1100\text{Ma})}$ values ranging from -0.5 to -1.0, with an average of -0.8. The basalts show a positive correlation between $\epsilon_{\text{Nd}(t=1100\text{Ma})}$ and $^{87}\text{Sr}/^{86}\text{Sr}_i$ with samples displaying more negative $\epsilon_{\text{Nd}(t=1100\text{Ma})}$ and having lower $^{87}\text{Sr}/^{86}\text{Sr}_i$ values.

The varied LREE enrichment of basalt types A, B and C may be attributed to varied degrees of contamination by underlying Archean crustal rocks. Basalt type A is characterized by elevated thorium values, as well as the highest $^{87}\text{Sr}/^{86}\text{Sr}_i$ values. Although the elevated thorium values may be attributed to contamination by Archean crust, this is not supported by the neodymium isotope data as all 3 basalt types display broadly similar $\epsilon_{\text{Nd}(t=1100\text{Ma})}$ values (-0.5 to -1.0). Vervoort and Green (1997) calculated that Archean tonalite-trondhjemite-granodiorite (TTG) suite underlying the Midcontinent Rift would have $\epsilon_{\text{Nd}(t=1100\text{Ma})}$ values of -18 to -13. If LREE enrichment signatures are to be attributed to a high degree of contamination by Archean crust, one would expect to see more negative $\epsilon_{\text{Nd}(t=1100\text{Ma})}$ values in conjunction with LREE enrichment (e.g., Nicholson et al. 1997; Hollings et al. 2007b). As the LREE enrichment of basalt type A is not consistent with more negative $\epsilon_{\text{Nd}(t=1100\text{Ma})}$ values, it cannot be solely attributed to contamination by Archean crustal rocks with negative $\epsilon_{\text{Nd}(t=1100\text{Ma})}$ values.

There is a correlation between the strontium and neodymium isotope data, with the least negative $\epsilon_{\text{Nd}(t=1100\text{Ma})}$ values correlating with higher $^{87}\text{Sr}/^{86}\text{Sr}_i$ values as well as elevated thorium abundances (Table 18.3). Basalt type A, as represented by sample CL-RC-019, shows the highest $^{87}\text{Sr}/^{86}\text{Sr}_i$, as well as elevated thorium values. It is, therefore, likely that the elevated thorium and $^{87}\text{Sr}/^{86}\text{Sr}_i$ signatures displayed by basalt type A may be attributed to a contaminant with elevated thorium and $^{87}\text{Sr}/^{86}\text{Sr}_i$ signatures, albeit with a positive $\epsilon_{\text{Nd}(t=1100\text{Ma})}$ signature. No strontium isotope data are available for the underlying mafic metavolcanic rocks of the Archean Schreiber-Hemlo greenstone belt into which the Coldwell Complex has been intruded. Positive $\epsilon_{\text{Nd}(t=1100\text{Ma})}$ signatures have been reported for Wabigoon Subprovince mafic metavolcanic rocks to the north by Tomlinson et al. (2003), which may serve as an analogue for the underlying mafic metavolcanic rocks of the Schreiber-Hemlo greenstone belt. However, no strontium isotope data are available for the Wabigoon Subprovince rocks. Alternatively, the strong thorium enrichment present in basalt type A may be attributed to a greater abundance of hornblende in those samples. Thorium has a partition coefficient of 0.50 for hornblende compared to 0.03 for clinopyroxene and 0.10 for plagioclase (Fujimaki, Tatsumoto and Aoki 1984). The abundance of amygdules infilled with hornblende toward the base of the section may explain the elevated thorium abundances in those samples.

The Coubran Lake basalts exhibit very similar trace element patterns to those of the Two Duck Lake gabbro in the eastern part of the Coldwell Complex (see Figure 18.4B). The trace element patterns are characterized by strong LREE enrichment and moderate HREE fractionation, as well as negative HFSE anomalies (zirconium, hafnium and titanium). The similar trace element characteristics of the Two Duck Lake gabbro and the Coubran Lake basalts suggests that the 2 units may have been derived from the same source, with the Coubran Lake basalts representing the extrusive equivalent of the Two Duck Lake

gabbro. Nicholson et al. (1997) proposed that basalt type I melts were erupted during the first phase of Midcontinent Rift volcanism (>1105 Ma). These melts are manifested by the Lower Siemens Creek volcanic rocks, the basal units in the Ely's Peak and Grand Portage areas of the North Shore Volcanic Group, and as the lower suite of the Osler Group in Ontario. Primitive mantle-normalized plots of the Coubran Lake basalts and of average basalt type I composition (Figure 18.4B) both display broadly similar trends of LREE enrichment and moderate HREE fractionation. The only difference is the average trend for the Coubran Lake basalts exhibits a negative niobium anomaly. However, Coubran Lake basalt type C does not display a negative niobium anomaly supporting a basalt type I composition. Basalt type I exhibits $\epsilon_{\text{Nd}(t=1100\text{Ma})}$ values of -0.7 to 0.7 with an average of -0.1 (n=10 samples) comparable to values for the Coubran Lake basalts ($\epsilon_{\text{Nd}(t=1100\text{Ma})}$ values ranging from -0.5 to -1.0 with an average of -0.8) with the slightly more negative values of some Coubran Lake basalt samples being attributed to slightly greater degrees of crustal contamination, which may also account for the negative niobium values.

ACKNOWLEDGMENTS

The authors would like to thank the Ontario Geological Survey for “in-kind” support of this project by providing sample preparation and analytical work at the Geoscience Laboratories, Sudbury, as well as providing financial support for isotopic analyses at the Isotope Geochemistry and Geochronology Research Centre at Carleton University, Ottawa. Also, thanks to Dave Good and the staff of Stillwater Canada Inc. for allowing access to, and sampling of, the Coubran Lake basalts. This work constitutes part of the requirements of a Master of Science (MSc) thesis by R.M. Cundari at Lakehead University under the supervision of Professor P. Hollings.

REFERENCES

- Carl, C.F.J. 2011. Geochemistry and petrology of intrusive rocks of the Sibley Peninsula; unpublished BSc (Honours) thesis, Lakehead University, Thunder Bay, Ontario, 79p.
- Cundari, R.M., Hollings, P., Smyk, M., Scott, J.F. and Campbell, D.A. 2011. Mesoproterozoic Midcontinent Rift-related mafic magmatism: project update and field observations; *in* Summary of Field Work and Other Activities 2011, Ontario Geological Survey, Open File Report 6270, p.7-1 to 7-6.
- Fujimaki, H., Tatsumoto, M. and Aoki, K. 1984. Partition coefficients of Hf, Zr and REE between phenocrysts and groundmasses; *in* Proceedings of the 14th Lunar and Planetary Science Conference, Part 2; Journal of Geophysical Research, v.89, Suppl. p.B662-B672.
- Good, D.J. 1993. Genesis of copper-precious metal sulfide deposits in the Port Coldwell alkalic complex, Ontario; Ontario Geoscience Research Grant Program, Grant No. 341, Ontario Geological Survey, Open File Report 5839, 231p. [PhD thesis, McMaster University, Hamilton, Ontario]
- Hart, T.R. and MacDonald, C.A. 2007. Proterozoic and Archean geology of the Nipigon Embayment: implications for emplacement of the Mesoproterozoic Nipigon diabase sills and mafic to ultramafic intrusions; Canadian Journal of Earth Sciences, v.44, p.1021-1040.
- Henry, P., Stevenson, R.K. and Gariépy, C. 1998. Late Archean mantle composition and crustal growth in the western Superior Province of Canada: neodymium and lead isotopic evidence from the Wawa, Quetico and Wabigoon subprovinces; *Geochimica et Cosmochimica Acta*, v.62, p.143-157.
- Hollings, P., Hart, T.R., Richardson, A. and MacDonald, C.A. 2007a. Geochemistry of the mid-Proterozoic intrusive rocks of the Nipigon Embayment, northwestern Ontario; Canadian Journal of Earth Sciences, v.44, p.1087-1110.

- Hollings, P., Richardson, A., Creaser, R. and Franklin, J. 2007b. Radiogenic isotope characteristics of the mid-Proterozoic intrusive rocks of the Nipigon Embayment, northwestern Ontario; *Canadian Journal of Earth Sciences*, v.44, p.1111-1129.
- Hollings, P., Smyk, M.C. and Cousens, B. 2012. The radiogenic isotope characteristics of dikes and sills associated with the Mesoproterozoic Midcontinent Rift near Thunder Bay, Ontario, Canada; *Precambrian Research*, v.214-215, p.269-279.
- Hollings, P., Smyk, M.C., Heaman, L.M. and Halls, H.C. 2010. The geochemistry, geochronology and paleomagnetism of dikes and sills associated with the Mesoproterozoic Midcontinent Rift near Thunder Bay, Ontario, Canada; *Precambrian Research*, v.183, p.553-571.
- Nicholson, S.W. and Shirey, S.B. 1990. Midcontinent Rift volcanism in the Lake Superior Region: Sr, Nd and Pb isotopic evidence for a mantle plume origin; *Journal of Geophysical Research*, v.95, p.10,851-10,868.
- Nicholson, S.W., Shirey, S., Schulz, K. and Green, J. 1997. Rift-wide correlation of 1.1 Ga Midcontinent rift system basalts: implications for multiple mantle sources during rift development; *Canadian Journal of Earth Sciences*, v.34, p.504-520.
- Pan, Y., Fleet, M.E. and Longstaffe, F.J. 1999. Melt-related metasomatism in mafic granulites of the Quetico Subprovince, Ontario: constraints from O–Sr–Nd isotopic and fluid inclusion data; *Canadian Journal of Earth Sciences*, v.36, p.1449-1462.
- Puskas, F.P. 1967. The geology of the Port Coldwell area, Thunder Bay, Ontario; Ontario Department of Mines, Open File Report 5014, 115p.
- Sun, S-S. and McDonough, W.F. 1989. Chemical and isotopic systematics of oceanic basalts: implications for mantle composition and processes; *in* *Magmatism in the ocean basins*, The Geological Society, Special Publication No.42, p.313-345.
- Taylor, S.R. and McLennan, S.M. 1985. The continental crust: its composition and evolution; Blackwell Scientific, London, United Kingdom, 328p.
- Tomlinson, K.Y., Davis, D.W., Stone, D. and Hart, T.R. 2003. U–Pb ages and Nd isotopic evidence for crustal recycling and Archean terrane development in the south-central Wabigoon Subprovince, Canada; *Contributions to Mineralogy and Petrology*, v.144, p.684-702.
- Vervoort, J.D. and Green, J.C. 1997. Origin of evolved magmas in the Midcontinent Rift system, northeast Minnesota: Nd-isotope evidence for melting of Archean crust; *Canadian Journal of Earth Sciences*, v.34, p.521-535.
- Walker, E.C., Sutcliffe, R.H., Shaw, C.S.J., Shore, G.T. and Penczak, R.C. 1993. Precambrian geology of the Coldwell alkalic complex; Ontario Geological Survey, Open File Report 5868, 30p.

19. Summary of Geophysical Projects and Activities

D.R.B. Rainsford¹ and T.L. Muir¹

¹Earth Resources and Geoscience Mapping Section, Ontario Geological Survey

SUPPORT FOR THE BEDROCK MAPPING PROGRAM

Geophysical support for the bedrock mapping program comprised the compilation of regional Geophysical Data Sets to generate geographic information system (GIS)-compatible images and layers for use by the project geologists. In most cases, this was supplemented with in-house, collaborative workshops where multi-disciplinary geoscience data sets were integrated and interpreted in order to better understand the geology prior to the field season and to highlight areas requiring further study.

Geophysical support was provided for the following projects:

- geology of Otter and Morin townships
- geology of Varley and Albanel townships
- Price–Thornloe townships bedrock geology mapping project
- Wabigoon Subprovince synthesis
- McFaulds Region bedrock geology mapping and compilation

SUPPORT FOR THE GROUNDWATER PROGRAM

Over the past several years, ground gravity surveys have become a commonplace part of groundwater programs (e.g., Bajc and Rainsford 2010; Burt and Rainsford 2010). Ground gravity has proven to be an effective tool for the detection and delineation of buried-river valleys incised into bedrock. The method does, however, have a number of limitations, namely the inability to distinguish between porous and non-porous valley fill, uneven distribution of data points (restricted to road traverses) and the uncertainties associated with the separation of regional and residual signals.

Airborne electromagnetic (EM) methods have been used with success to map groundwater aquifers in other jurisdictions (e.g., Oldenborger et al. 2010; Jørgensen and Sandersen 2006). If the electrical property contrasts are sufficient, it may be possible to map buried-river valleys and identify areas that bear significant quantities of fresh groundwater using airborne EM. Airborne geophysical methods also have the advantage of being quick to perform, achieving nearly uniform data coverage and are capable of being performed over areas not suitable for ground data acquisition. As a result, it was decided to fly an airborne EM survey to test the suitability of this method to the OGS groundwater program. A test site was chosen in the southern portion of the County of Simcoe (referred to as “south Simcoe County survey”). This site was selected because of the depth of knowledge about the surficial geology including surface mapping, borehole information, ground gravity and water-well records. The site also offered a variety of surficial and bedrock materials.

Owing to the fact that depth-to-bedrock ranges from 70 to 180 m in the test area, it was decided to fly the survey using a time-domain electromagnetic (TDEM) system that offers greater depth penetration

than comparable frequency domain electromagnetic (FDEM) systems. As a result of competitive bidding, the AeroTEM IV system operated by Aeroquest Ltd. was chosen for this survey. The survey was completed over a six-day period in March and comprised a total of 1898 line-kilometres acquired at a nominal line spacing of 200 m. In addition to standard airborne EM deliverables, such as conductance and decay constant maps, laterally constrained one-dimensional (1-D) inversions were performed along each flight line to create multiple electrical conductivity sections across the survey area. The laterally constrained 1-D inversions were performed by Aarhus Geophysics of Denmark.

The results of the survey were published in October 2012 as Geophysical Data Set 1070 (Ontario Geological Survey 2012). A discussion of the preliminary assessment of the test results is presented by Bajc, Rainsford and Mulligan (this volume, Article 31).

ACQUISITION OF NEW AIRBORNE GEOPHYSICAL DATA IN 2011–2012

The OGS completed 2 new airborne geophysical surveys during the 2011–2012 fiscal year. The south Simcoe County test survey has already been discussed above. The second survey was flown in the Winisk River area in the Hudson Bay Lowland commencing in November 2011 and was completed in February 2012 (Figure 19.1). The survey acquired a total of 76 744 line-kilometres of horizontal magnetic gradiometer data over a surface area of approximately 20 707 km² at 300 m line spacing.

The Winisk River survey was designed to help map Precambrian basement geology below the overlying Paleozoic sediments and complements targeted geoscience activities being conducted by the Geological Survey of Canada (GSC), Natural Resources Canada, as part of their GEO-mapping for Energy and Minerals (“GEM”) initiative, which is focussed on conducting geological mapping for informed resource development in the extreme Far North of Canada (generally north of latitude 60°). The magnetic data will be used to estimate depth to basement, identify major basement structures that may extend northward into Hudson Bay, detect magnetic kimberlite bodies and provide geoscience knowledge for land-use planning purposes. The survey was flown by Fugro Airborne Surveys and quality assurance–quality control for the survey was provided under contract by Paterson, Grant and Watson Ltd. Publication of the data has been delayed pending discussions with affected First Nation communities.

PLANNED ACQUISITION OF NEW GEOPHYSICAL DATA IN 2012–2013

The OGS will be conducting an airborne magnetic gradiometer geophysical survey of the Fort Severn region in the Hudson Bay Lowland commencing in the fall of 2012 and continuing through the winter. The survey will be completed under contract and will require approximately 127 704 line-kilometres of flying over a surface area of approximately 34 692 km² at 300 m line spacing. Project management and quality assurance–quality control for the survey will be conducted under contract by Paterson, Grant and Watson Ltd.

The airborne geophysical survey complements targeted geoscience activities being conducted by the GSC as part of their GEM initiative. The airborne survey is part of an OGS collaboration with GSC to address various geoscience problems in the Hudson Bay Lowland as part of the GEM initiative (*see* Armstrong, this volume, Article 30). The geoscience data will also provide information for land-use planning and energy development as part of the Ontario government’s Far North Land-Use Planning Initiative.

The Fort Severn survey area (*see* Figure 19.1) is located in the Northern Superior superterrane of the northwest Superior Province and is underlain by steeply dipping Precambrian basement rocks that are covered by relatively flat-lying Paleozoic marine sedimentary rocks. The Fort Severn survey will assist in establishing the extent of a north-trending Ordovician trough in the Hudson Bay Lowland; specifically,

the survey will identify the possible onshore extension of a major horst structure in Hudson Bay and also identify possible north-trending basement structures that may have controlled Paleozoic sedimentation. This information will help to constrain the stratigraphic distribution of potential hydrocarbons in the region. The existing half-mile line spacing, 1960s vintage magnetic coverage provides insufficient resolution to adequately map the structures of interest. The scheduled survey is expected to double or triple resolution and yield generally much higher quality data than are currently available.

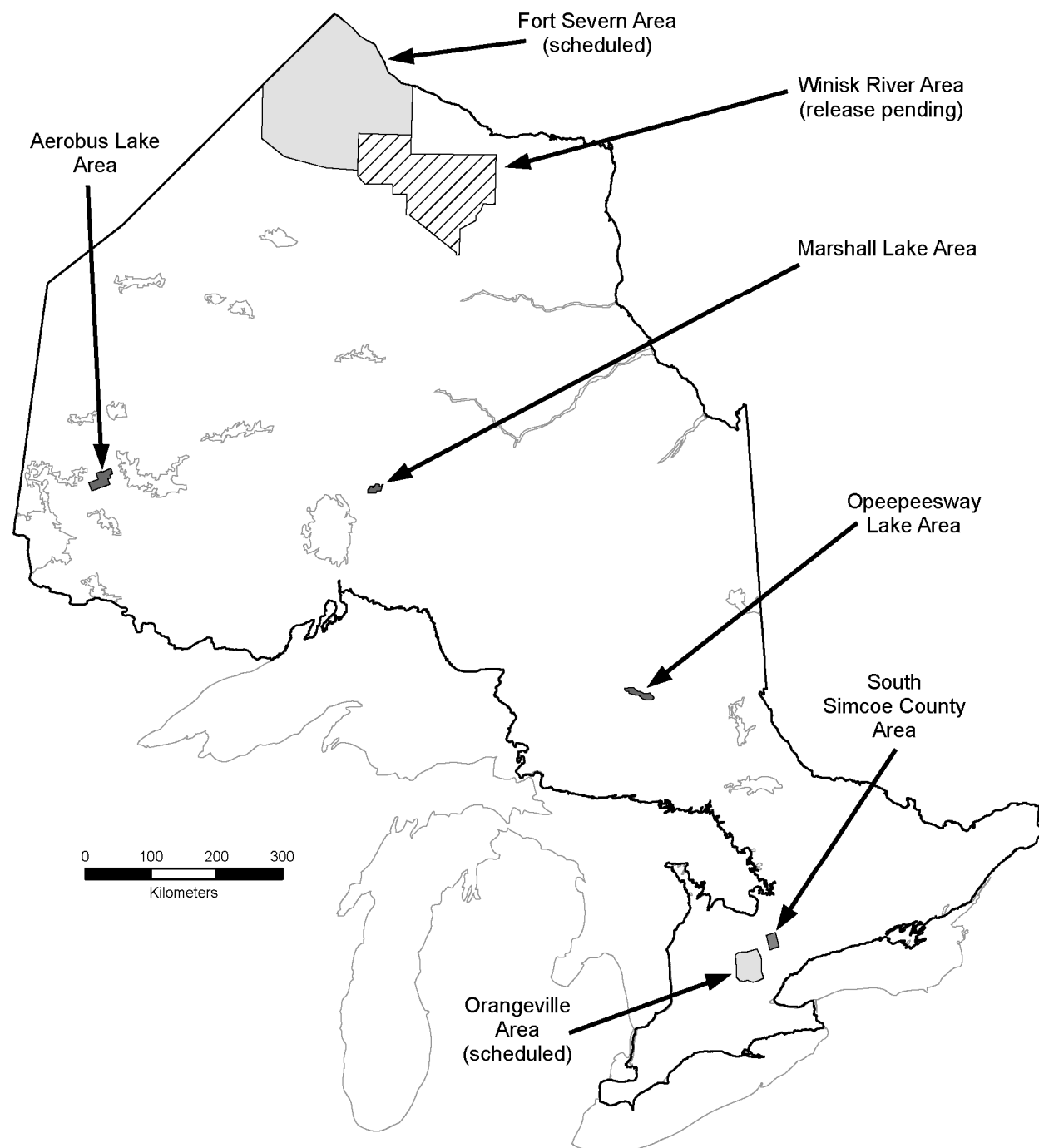


Figure 19.1. Locations of geophysical surveys released as Geophysical Data Sets during 2012, scheduled surveys commencing in 2012, and a survey pending release.

The OGS will also be conducting a ground gravity geophysical survey in the Orangeville region of southern Ontario commencing in the fall of 2012 and expected to be completed in December. The survey area encompasses approximately 1550 km² centred on the Orangeville moraine (*see* Figure 19.1) and extends from the Regional Municipality of Waterloo to north of Orangeville. The survey will be completed under contract and consists of approximately 6270 stations of new ground gravity data. This ground gravity survey is part of the OGS groundwater mapping program and will support 3-D mapping of surficial sediments in the Orangeville region. The gravity data will be used to map bedrock surfaces and identify buried valleys and potential groundwater aquifers (*see* Burt, this volume, Article 32).

GEOPHYSICAL DATA SET RELEASES FOR 2012

Four Geophysical Data Sets (GDS) were released during 2012. Table 19.1 lists the data sets and Figure 19.1 shows the locations of the geophysical surveys.

The data sets comprise a total of 12 961 line-kilometres of airborne surveys. Of the 4 data sets, the south Simcoe Country area survey was newly commissioned as part of the OGS core program, whereas the Opepeesway Lake, Marshall Lake and Aerobus Lake areas were purchased proprietary data sets.

The 3 purchased data sets, comprising 4 separate surveys, were reprocessed to be consistent with OGS standards and formats prior to publication. The reprocessing work was carried out under contract by Scott Hogg & Associates.

Table 19.1. Summary of Geophysical Data Sets (GDS) released by the Ontario Geological Survey in 2012.

GDS	Survey Name	Year of Survey	Survey Type	Line-Kilometres	Line Spacing (metres)
1238	Opepeesway Lake	2007	Magnetic total field and FDEM (purchased survey)	3035	150
1239	Marshall Lake	2007	Magnetic total field and TDEM (purchased survey)	1616	150
1240	Aerobus Lake	2008	Magnetic total field (purchased survey)	6412	200
1070	south Simcoe County area	2012	Magnetic total field and TDEM	1898	200

McFAULDS LAKE COMPILATION

Subsequent to the completion of the McFaulds Lake airborne gravity gradiometer survey (Rainsford et al. 2011), those results, along with other OGS Geophysical Data Sets and geophysical information gleaned from assessment files, were compiled into a GIS-compatible version.

High-resolution digital aeromagnetic data, from several OGS geophysical data sets, cover most of the study area. Much of the area has previously been covered by helicopter TDEM surveys flown for mineral exploration companies working in the area. The results of many of these surveys have been submitted for assessment credits and the scanned files are available through the Assessment File Resources Inventory (AFRI) on the GeologyOntario Web portal. Approximately 200 airborne EM maps from the assessment files have been geo-referenced and used to build an EM interpretation layer. As much of the airborne EM data were acquired using coincident loop systems, it is possible to interpret conductor dip direction from the EM profiles. In a region where outcrop is very sparse, dip information interpreted from the geophysics can be a valuable tool to help interpret structure. The compilation and interpretation work is on-going and will be used to augment the geological mapping and compilation

program being carried out in the McFaulds Lake area by the OGS and GSC. Modelling of the gravity gradiometer and magnetic data is being carried out by the GSC (P. Keating, GSC, personal communication², 2012).

During the course of this compilation and interpretation work, a number of instances were noted where it was apparent that gravity data are a better predictor of rock type than magnetic data. One such example is in the area that hosts most of the known chromite mineralization in the McFaulds Lake area and is shown in Figure 19.2. The pre-existing compiled geology (see Figure 19.2C), which was compiled mainly from an interpretation of the aeromagnetic data (see Figure 19.2A) and very sparse outcrop, is significantly different from the image of the vertical gravity gradient (see Figure 19.2B). This is

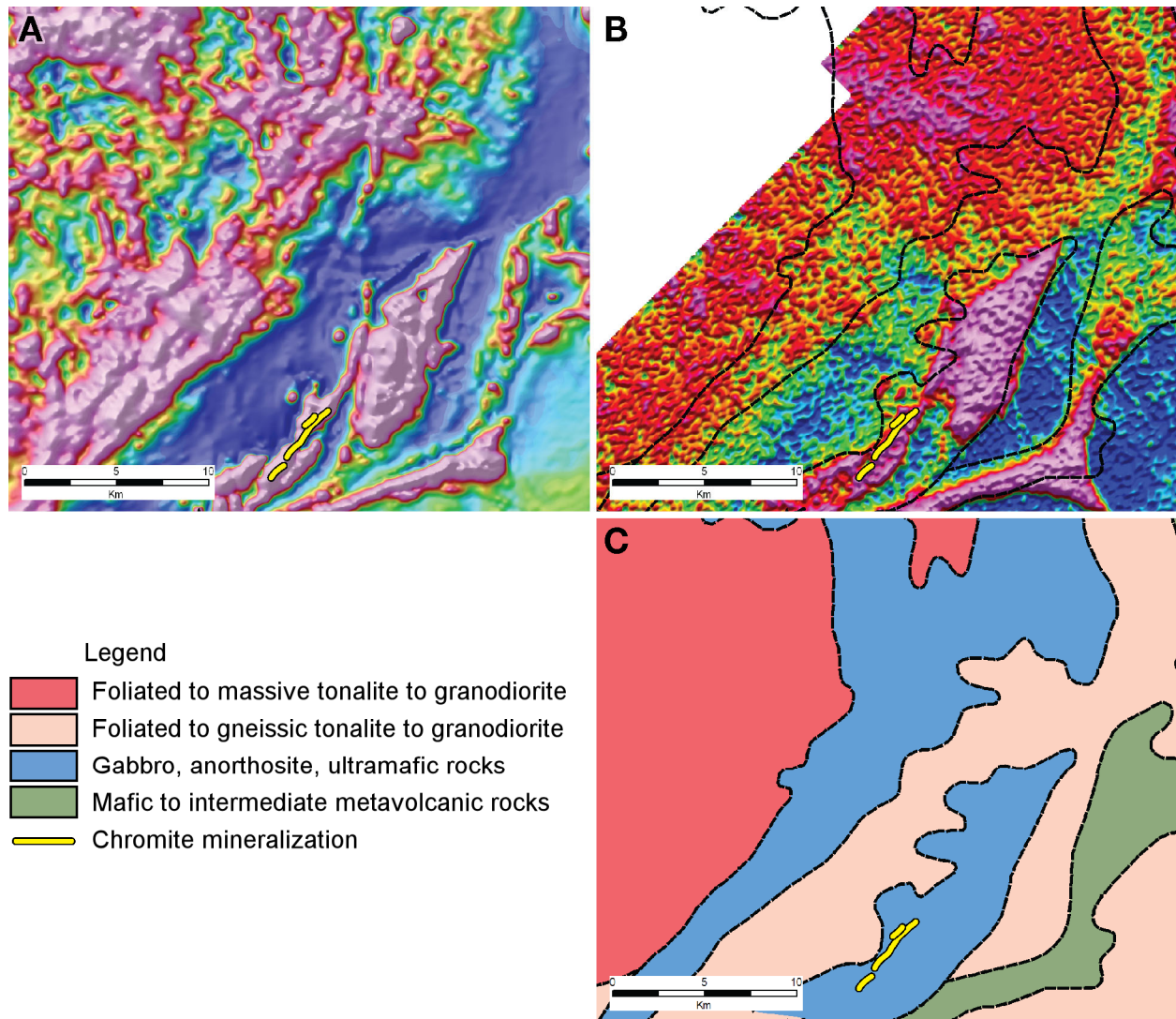


Figure 19.2. Illustration of how airborne gravity gradiometry can provide a better understanding of lithology than magnetic data: A) total magnetic field, B) vertical gravity gradient with contacts inferred from the magnetic data superimposed and C) geology compiled mainly from the magnetic data.

²Beiki, M., Keating, P. and Clark, D., "Interpretation of magnetic and gravity gradient tensor data using normalized source strength (NSS)"; submitted to *Geophysical Prospecting*.

particularly evident in the western part of the area where a northeast-striking gabbro, anorthosite and ultramafic unit is interpreted from the high magnetic responses. The gravity data show no evidence of elevated gravity values that would be expected with these higher density rocks and, as a result, it is likely that the area of high magnetic field is a more magnetic phase of the tonalitic rocks that pervade the area. The second gabbroic, anorthositic and ultramafic unit, indicated in the south-central part of the area (*see* Figure 19.2C), on the other hand, is accompanied by a distinct gravity gradient high (*see* Figure 19.2B), which is consistent with the high densities associated with these rock types and is confirmed by extensive drilling in the vicinity. Even in this second area, the gravity data suggest that the shape of the contacts, inferred from the magnetic data, need modification. The superiority of gravity information (relative to magnetic) for the interpretation of rock type is mainly due to the fact that density is a bulk physical property, whereas magnetic susceptibility is primarily an indication of magnetite content, which is itself an accessory mineral and not necessarily indicative of rock type.

OTHER ACTIVITIES

The GeologyOntario Web portal (www.ontario.ca/geology) allows the free download of the OGS geophysical data sets, except for halfwave electromagnetic (EM) and some profile data due to their file size. Alternatively, hard-copy (paper) maps and physical media (CD or DVD) of digital data (including profile and halfwave EM data) continue to be available for purchase through

Publication Sales

Tel: 705-670-5691 (local)

Toll-free: 1-888-415-9845 ext. 5691 (Canada and United States)

Fax: 705-670-5770

E-mail: pubsales.ndm@ontario.ca

The Ontario Geological Survey has in the past posted a separate Web-based, “Geophysical Atlas”. Recent changes to government Web sites have been made to improve accessibility for all users. As a result, the Geophysical Atlas is no longer available. Geoscience data collected by the OGS can also be viewed geographically using the OGSEarth (www.ontario.ca/ogsearth) application, which provides keyhole mark-up language (.kml) files for use with applications such as Google Earth™ mapping service. A modified version of the Geophysical Atlas for future availability is under consideration.

The Ontario Geological Survey purchased 23 new KT-10 magnetic susceptibility meters for use by the geological mapping crews. The new instruments were acquired in order to replace the KT-9 units that had seen service over approximately 10 field seasons and are no longer being manufactured. The KT-10 instruments offer a number of advances over the previous model, the most significant being a ten-fold increase in sensitivity. Several thousand sets of magnetic susceptibility readings continue to be collected in the field each year. These new data are being added to the previously published magnetic susceptibility database (Muir 2010).

REFERENCES

- Bajc, A.F. and Rainsford, D.R.B. 2010. Three-dimensional mapping of Quaternary deposits in the southern part of the County of Simcoe, southern Ontario; *in* Summary of Field Work and Other Activities 2010, Ontario Geological Survey, Open File Report 6260, p.30-1 to 30-10.
- Burt, A.K. and Rainsford, D.R.B. 2010. The Orangeville Moraine project: buried valley targetted gravity study; *in* Summary of Field Work and Other Activities 2010, Ontario Geological Survey, Open File Report 6260, p.31-1 to 31-6.

- Jørgensen, F. and Sandersen, P.B.E. 2006. Buried and open tunnel valleys in Denmark—erosion beneath multiple ice sheets; *Quaternary Science Reviews*, v.25, p.1339-1363.
- Muir, T.L. 2010. Ontario Precambrian bedrock magnetic susceptibility geodatabase for 2001 to 2008; Ontario Geological Survey, Miscellaneous Release—Data 273.
- Oldenborger, G.A., Pugin, A.J.-M., Hinton, M.J., Pullen, S.E., Russell, H.A.J. and Sharpe, D.R. 2010. Airborne time-domain electromagnetic data for mapping and characterization of the Spiritwood Valley aquifer, Manitoba, Canada; Geological Survey of Canada, Current Research 2010-11, 13p.
- Ontario Geological Survey 2012. Ontario airborne geophysical surveys, magnetic and electromagnetic data, grid and profile data (ASCII and Geosoft® formats) and vector data, south Simcoe County area; Ontario Geological Survey, Geophysical Data Set 1070.
- Rainsford, D.R.B., Houlié, M.G., Metsaranta, R.T., Keating, P. and Pilkington, M. 2011. An overview of the McFaulds Lake airborne gravity gradiometer and magnetic survey, northwestern Ontario; *in* Summary of Field Work and Other Activities 2011, Ontario Geological Survey, Open File Report 6270, p.39-1 to 39-8.

20. Summary of Aggregate Resources and Industrial Minerals Projects and Activities, Southern Ontario

V.L. Lee¹ and D.J. Rowell¹

¹Earth Resources and Geoscience Mapping Section, Ontario Geological Survey

INTRODUCTION

As in previous years, the focus of the Ontario Geological Survey's aggregate program has been to map aggregate resources across southern Ontario. New publications this year include the *Aggregate Resources Inventory of the County of Bruce, Southern Ontario* (Rowell 2012a) and the *Aggregate Resources Inventory of the County of Frontenac, Southern Ontario* (Marich 2012). A number of Aggregate Resources Inventory Papers (ARIP) are due to be released in the near future (Figure 20.1) along with a report and accompanying data on shale resources in southern Ontario (Rowell 2012b, 2012c). Future projects will include the mapping of areas that are currently lacking aggregate mapping and updating older reports.

Ontario Geological Survey publications and data are available for download at no charge through GeologyOntario (www.ontario.ca/geology). In addition, geoscience data, collected by the OGS, can be viewed geographically using the OGSEarth application (www.ontario.ca/ogsearth), which provides keyhole markup language (.kml) files for use with applications such as Google Earth™ mapping service. OGSEarth also provides an index map for ARIPs (similar to Figure 20.1).

AGGREGATE RESOURCES PROJECT UPDATES

- Final report writing and editing was completed on the aggregate resources inventory of the County of Lanark, southeastern Ontario (Lee 2010). The publication will be released in 2012–2013.
- Final report writing and editing was completed on the aggregate resources inventory of the County of Simcoe, southern Ontario (Rowell 2010). The publication will be released in 2012–2013.
- Work continued on the aggregate resources inventory of the City of Ottawa, southeastern Ontario (Lee 2011). A short amount of time was spent in the field to complete site visits of newly accessible land and to fill in gaps from the previous year's field work. In addition, down-hole geophysical logs were obtained through the co-operation of quarry operators. This information will help to assess the known problems of the bedrock mapping in the area and to make recommendations for future projects. The project is in its final writing stages, and it is anticipated that the publication will be released in 2013.
- Field work for the aggregate resources inventory of the County of Perth, southwestern Ontario was completed this year (Rowell, this volume, Article 21). Some township-based aggregate studies were completed in the 1980s. This report will provide an up-to-date countywide aggregate resources inventory. It is anticipated that the publication will be released in 2013.

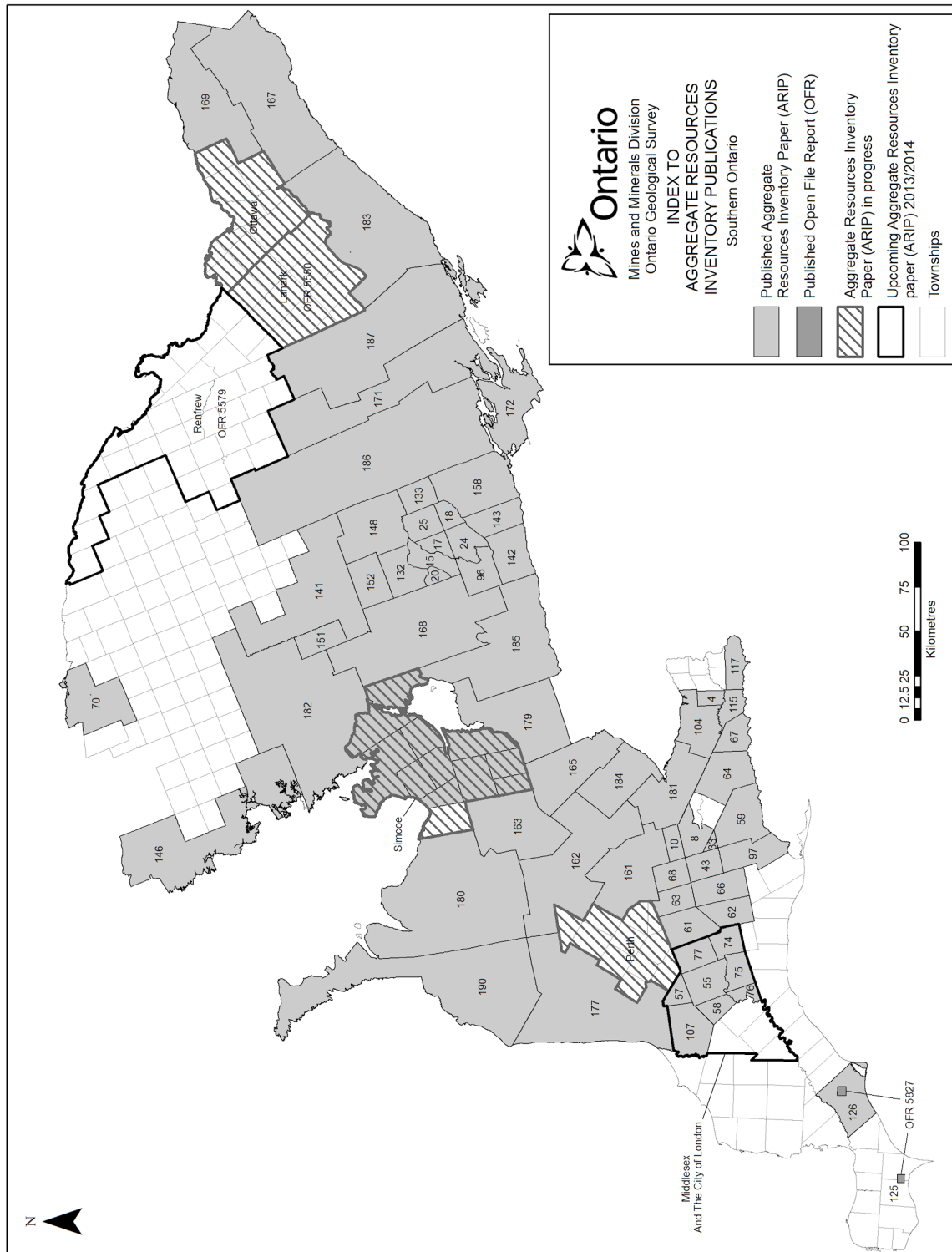


Figure 20.1. Index map for Aggregate Resources Inventory Papers (ARIP) for southern Ontario released as Open File Report or ARIP publications, work to be published in 2012–2013 (“in progress”) and planned publications (“upcoming”).

OTHER AGGREGATE RESOURCES PROJECTS

- *Aggregate Test Results for Various Rock Types in Ontario* (Rowell and Dodge 2012) was published. This digital data set provides a compilation of previously published and unpublished “standard” aggregate test data across Ontario.
- Rowell and Brunton (this volume, Article 22) had an opportunity to collect samples from drill-hole core on Manitoulin Island and have standard aggregate tests done on the samples from the St. Edmund Formation. Initial test results indicate that the St. Edmund Formation is a promising new crushed stone prospect for the aggregate industry.

INDUSTRIAL MINERALS PROJECT UPDATES

- A report and associated data (Rowell 2012b, 2012c) evaluate the state of available shale resource areas in southern Ontario, and the use of this resource by brick and tile manufacturers.

FUTURE AGGREGATE RESOURCES PROJECTS

There are 2 aggregate resources inventory projects planned for 2013–2014 (*see* Figure 20.1):

- An update of the aggregate resources inventory for the County of Renfrew in eastern Ontario. Previous aggregate mapping of the municipality was completed, but is now considered to be out of date. The goal of the proposed project is to provide up-to-date aggregate resources inventory mapping and reporting for the county.
- An update of the aggregate resources inventory for the County of Middlesex in southwestern Ontario. Previous township-based aggregate studies are now more than 25 years old; therefore, the goal of the proposed project is to provide an up-to-date countywide aggregate resources inventory paper with accompanying maps.

REFERENCES

- Lee, V.L. 2010. Aggregate resources inventory of the County of Lanark, southeastern Ontario; *in* Summary of Field Work and Other Activities 2010, Ontario Geological Survey, Open File Report 6260, p.29-1 to 29-9.
- 2011. Aggregate resources inventory of the City of Ottawa, southeastern Ontario; *in* Summary of Field Work and Other Activities 2011, Ontario Geological Survey, Open File Report 6270, p.18-1 to 18-8.
- Marich, A.S. 2012. Aggregate resources inventory of the County of Frontenac, southern Ontario; Ontario Geological Survey, Aggregate Resources Inventory Paper 187, 50p.
- Rowell, D.J. 2010. Aggregate resources inventory of the County of Simcoe, southern Ontario; *in* Summary of Field Work and Other Activities 2010, Ontario Geological Survey, Open File Report 6260, p.28-1 to 28-13.
- 2012a. Aggregate resources inventory of the County of Bruce, southern Ontario; Ontario Geological Survey, Aggregate Resources Inventory Paper 190, 94p.
- 2012b. Shale resources of southern Ontario: an update; Ontario Geological Survey, Open File Report 6278, 46p.
- 2012c. Geochemical, mineralogical and brick testing results for shale resources of southern Ontario; Ontario Geological Survey, Miscellaneous Release—Data 301.
- Rowell, D.J. and Dodge, J.E.P. 2012. Aggregate test results for various rock types in Ontario; Ontario Geological Survey, Miscellaneous Release—Data 297.

21. Project Unit 12-008. Aggregate Resources of the County of Perth, Southwestern Ontario

D.J. Rowell¹

¹Earth Resources and Geoscience Mapping Section, Ontario Geological Survey

INTRODUCTION

The County of Perth (herein referred to as “Perth County”) occupies 221 846 ha in southwestern Ontario (Statistics Canada 2011). It is bounded to the east by the Regional Municipality of Waterloo; by the County of Wellington to the east and northeast; by the County of Huron to the west and northwest; and to the south by the counties of Middlesex and Oxford (Figure 21.1). The county is covered by all or parts of 7 National Topographic System (NTS) 1:50 000 scale map sheets. The 7 map sheets from north to south are Wingham (40 P/14), Palmerston (40 P/15), Seaforth (40 P/11), Conestogo (40 P/10), St. Marys (40 P/6), Stratford (40 P/7) and Lucan (40 P/3).

SURFICIAL GEOLOGY

The distribution of surficial materials in Perth County, including sand and gravel deposits, are primarily the result of glacial activity that took place in the Late Wisconsinan (Barnett 1992). This period, which lasted from approximately 23 000 to 10 000 years before present (BP), was marked by the repeated advance and retreat of glacial ice originating in the Huron–Georgian Bay and the Erie–Ontario basins (Cowan 1979; Karrow 1977, 1991). The direction of ice movement in the study area is generally recorded

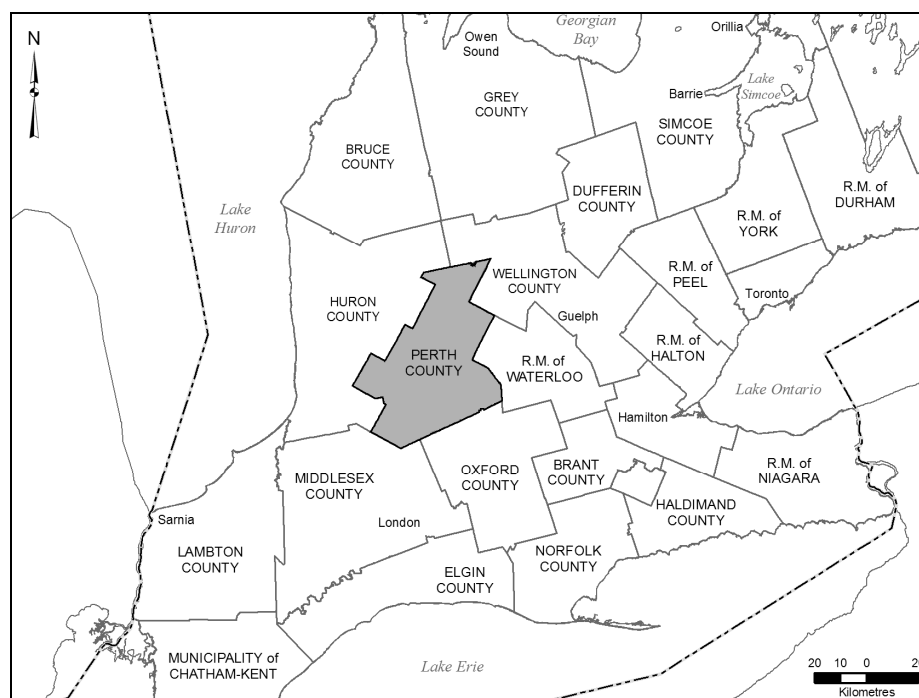


Figure 21.1. Map of southwestern Ontario showing the location of Perth County.

*Summary of Field Work and Other Activities 2012,
Ontario Geological Survey, Open File Report 6280, p.21-1 to 21-6.*

© Queen's Printer for Ontario, 2012

by depositional forms (drumlins, moraines and fluted ground moraine). As the ice advanced across the study area, debris from the underlying soil and bedrock accumulated within and beneath the ice. The debris—a mixture of stones, sand, silt and clay—was deposited over large areas of Perth County as till plains, drumlins and moraines.

Till

Overlying the Paleozoic bedrock in the study area is a complex sequence of unconsolidated Quaternary sediments. Because the area has been affected by multiple ice lobes over an extended period of time, the area has a rather complicated depositional history. One of the oldest buried till units in the study area is the Catfish Creek Till. Its presence has been widely documented in water-well records, boreholes and subsurface exposures (e.g., deeply cut river valleys) throughout a large portion of the study area. The till was deposited during the Nissouri Phase (Stadial) approximately 23 000 to 17 000 years BP. It is an extremely compact, stony to bouldery, sandy silt to silty sand till that can range from 3 to 6 m thick in the study area. The till appears yellow to buff to olive in colour when oxidized and grey when unoxidized. Pebble lithology and till fabric analysis suggests that the till was deposited by ice advancing into the area from the north-northeast (Georgian Bay lobe). There are areas where the Catfish Creek Till lies directly on the bedrock surface. In other areas, the Catfish Creek Till overlies older unconsolidated sediments including older till units.

The only named pre-Catfish Creek till in the study area is the Canning Till (Karrow 1991). The till is described as a reddish, clayey to silty, nearly stonefree till. The reddish colour of this till, and the presence of granules of red shale, are indicative of the Queenston Formation located along the base of the Niagara Escarpment, suggesting that this till was deposited by ice moving from the Erie–Ontario basin (i.e., the ice advanced to the north-northwest) (Karrow 1991). The Canning Till is believed to have been deposited approximately 45 000 to 49 000 years BP, suggesting a middle Wisconsinan depositional age (Barnett 1992). Fine-textured glaciolacustrine or lacustrine sediments have been recorded overlying the Canning Till.

Overlying the Catfish Creek Till in the study area is the Stirton Till. The till has been described as a dolomitic, strongly calcareous, stiff, very dark grey to greyish brown, silty to silty clay till with low to moderate plasticity. Where the till exists, the unit is generally from 1 to 3 m thick. Cowan (1979) reports a very limited distribution of the Stirton Till in the northern part of Perth County. Pebble lithology and fabric analysis conducted by Cowan (1979) and Karrow (1991) suggests that the till was deposited by the Georgian Bay lobe at approximately 15 000 years BP (Port Bruce Phase (Stadial)). The Stirton Till can lie directly on top of the Catfish Creek Till or overlie a relatively thin sequence of glaciolacustrine–lacustrine sediments (laminated sand, silt and clay) deposited over the Catfish Creek Till. The Stirton Till does not appear as a surface till in the study area. It is believed that the Stirton Till is correlative to the Maryhill Till deposited by the Erie–Ontario lobe.

Overlying the Stirton Till is the Tavistock Till. The till has been described as a dolomitic, highly calcareous, stiff to very stiff, brown to yellowish-brown, silt to clayey silt till (Cowan 1979). The clast content is low, usually less than 5%, and is dominated by carbonate and shale clasts. It has been suggested that the Tavistock Till was deposited by a major readvance of the Huron–Georgian Bay lobe during the Port Bruce Phase (Stadial), and is correlative with the Port Stanley Till of the Erie–Ontario lobe. The till has a thickness that varies from 1 to 9 m in the study area. The till has been identified in the subsurface along the Middle Maitland River near Listowel and is present as a surface till in other areas of the study area (southeast corner of the study area near the community of Tavistock). The Tavistock Till can be overlain by glaciolacustrine–lacustrine sediments, the Stratford or Mornington tills, or in some locations directly overlain by the Elma Till. Where glaciolacustrine–lacustrine sediments appear between the Tavistock and Mornington tills, they have been described as 0.5 to 2 m of rhythmic, laminated sand, silt and clay.

Overlying the Tavistock Till is the Mornington Till. This till is named after the former Township of Mornington, Perth County. The till has been observed in the subsurface near Drayton (just east of the

study area in the County of Wellington) with a thickness of about 1 m, and has been mapped as a surface till near the eastern boundary of Perth County in North Easthope Ward. It is described as a dark grey to grey, mottled, strongly calcareous clay till with rare pebbles believed to be derived from underlying glaciolacustrine silt and clay, and older till units. It is believed to have been deposited by a minor readvance of the Georgian Bay lobe, after the deposition of the Tavistock Till (Cowan 1979; Karrow 1991).

Generally located south of the Milverton moraine and north of the community of Harmony, westward to the North Thames River and east to the Easthope moraine, is the strongly calcareous, stony, sandy silt Stratford Till. It is generally a thin till often lying directly on the Tavistock Till in the south and the Mornington Till in the north (Karrow 1991). Based on the general thickness of this till unit, it has been suggested that the Stratford Till represents a minor readvance of the Huron–Georgian Bay ice.

Overlying the Stratford Till, only in a small portion of the study area, is the Wartburg Till. The till lies on surface in an area near the Milverton moraine and from Brunner to Fullarton. The till has been described as a strongly calcareous, almost stone-free clay till. It represents a very brief and minor advance of the Huron–Georgian Bay ice during the Port Bruce Phase (Stadial).

The Elma Till is one of the youngest tills in the study area and, as such, is located on the surface over a good portion of Perth County. The till is generally located in the northwest corner of the county and extends southeastward to the central part of the county (Cowan 1979; A.J. Cooper, OGS, unpublished report). The till has been estimated to be up to 9 m thick. It is described as a stony, sandy silt to silt till with low plasticity that can be very stiff at depth. It is generally yellowish brown and the colour can range from brown to light yellowish brown. It has a high total carbonate content and is strongly dolomitic. In the northern part of Perth County (Wallace Ward), the chert content can be up to 17% (Cowan 1979). The till was deposited by the Georgian Bay lobe and is middle to late Port Bruce Phase (Stadial) in age. The till continues to the north into Huron, Wellington and Bruce counties. It is drumlinized and fluted.

The Rannoch Till was deposited by ice of the Huron lobe. It is characterized by a strongly calcareous, silt to silty clay matrix, except where deposited over sand, when the matrix may become quite loose and exhibit a sandy silt texture (Karrow 1977; A.J. Cooper, OGS, unpublished report). The till occurs in the southwest corner of Perth County and along the western part of the study area.

Moraines

Old landforms are often difficult to recognize in the study area because of the obscuring effects of subsequent geological events. There are a number of older landforms that have been partially obscured and buried, which affect the present assemblage of landforms. The term palimpsest has been applied to these landforms, which include a number of large moraines in, and to the east of, the study area (Karrow 1991). An example of a palimpsest landform in the study area is the Easthope moraine, whose origin remains undetermined.

The Gads Hill moraine consists of 2 surface tills: the Tavistock and Stratford tills. Within this morainic area are about 20 ice marginal positions (Karrow 1991). The Milverton moraine is composed predominantly of Elma Till and, therefore, is believed to be associated with the Georgian Bay lobe. The Mitchell, Dublin and Lucan moraines are composed of, or capped by, Rannoch Till and are associated with the Huron lobe.

Glaciofluvial Deposits

In addition to the glacial deposits noted above, there are a number of glaciofluvial ice-contact deposits located throughout the study area. As the ice retreated, sediment-laden meltwater flowing within

and beneath the ice deposited numerous southeast-trending esker ridges or segments, particularly in the northwest corner of Perth County. West of the North Thames River, many of these esker segments trend easterly, whereas many of the morainic ridges trend south. Granular material within esker deposits is generally clean and varies from sand to gravel to crushable sized clasts. The aggregate potential of these types of deposits is generally good, although lithological constraints may limit usage. In Perth County, these deposits have been extracted extensively in the past.

Glaciofluvial outwash deposits occur as meltwater channel fills and outwash plains throughout much of the northern part of the county. Sand and gravel-rich channel-fill and terrace deposits occur south of the community of Palmerston, along the Little Maitland and Middle Maitland river systems and from Treacastle to Treviotdale (Wallace Ward). Many of these deposits are limited in size or thickness, and may lack desirable gradation for high-specification aggregate products. The outwash deposits are generally 1 to 3 m thick, whereas outwash terraces can be up to 5 m thick. Although these deposits have been extracted extensively in the past, the lithology of some of the coarse aggregate clasts may limit the suitability of these granular resources in the production of high-end aggregate products. A complex of glaciofluvial ice-contact and outwash deposits occurs near Staffa in the Municipality of Perth West. This complex hosts a number of licenced aggregate operations.

Glaciolacustrine and/or Lacustrine Deposits

Unlike many areas of southwestern Ontario, there is a general lack of glaciolacustrine or lacustrine sand deposits located throughout the study area, other than a small area to the north of the City of Stratford. The study area has a reasonably high surface elevation and, therefore, was less susceptible to being inundated by glacial lake waters. Fine-grained glaciolacustrine or lacustrine deposits (silt and clay) do exist, but these were generally deposited in small, isolated, low-lying “ponds” that were not part of a much larger glacial lake. Older proglacial lakes occurred sporadically between the till sheets, depositing older glaciolacustrine–lacustrine deposits (laminated or rhythmites of sand, silt and clay). No glaciolacustrine beach deposits were mapped in the study area, although Karrow (1991) noted that a small lake formed north of Stratford at an elevation of about 372 m asl. A similar lake formed west of the Milverton moraine at approximately the same elevation.

BEDROCK GEOLOGY AND RESOURCE POTENTIAL

The oldest Paleozoic rocks in Perth County are the buff, fine-crystalline dolostones; greenish grey and reddish shales; and evaporites of the Upper Silurian Salina Formation (or Group, e.g., *see* Armstrong and Carter 2010), which are located in the northeast corner of the study area. The Salina Formation has not been utilized for the production of aggregate because of a thick overburden cover, poor accessibility, a high shale content, and poor physical properties. The Salina Formation is believed to have formed because of uplift along the Algonquin Arch and reasonably rapid basin subsidence, drastically changing the depositional environment (Armstrong and Carter 2010). Repeated carbonate, evaporite and argillaceous sedimentation characterize the Salina Formation as represented by the various rock units. Salt extraction from the Salina Formation occurs in southwestern Ontario near Windsor and Goderich, as well as a number of salt brine wells. A significant thickness of 205.2 m of Salina Formation was intersected at the Bruce Nuclear site (Raven et al. 2009), northwest of the study area.

The Upper Silurian Bass Islands Formation conformably overlies the Salina Formation. The lithology of the Bass Islands Formation strata consists of buff to brown, fine-grained dolostone in even, vertically jointed thin to medium beds (Armstrong and Carter 2010). Locally, thick beds up to 60 cm are present. The Bass Islands Formation has not been utilized for aggregate in the study area; however, some strata have historical use for the manufacture of lime (Hewitt 1960). The formation is overlain by a thick

overburden cover and does not crop out in the study area. A drill hole at the Bruce Nuclear site intersected 45.3 m of Bass Islands Formation (Raven et al. 2009). The Bass Islands Formation is roughly equivalent to the Bertie Formation located farther south in Ontario (Johnson et al. 1992).

Overlying the Bass Islands Formation are the greenish-grey to grey-brownish, thin- to medium-bedded, fine- to medium-grained, fossiliferous, bioturbated, cherty limestones and dolostones of the Middle Devonian Bois Blanc Formation (Armstrong and Carter 2010). The unit is locally very fossiliferous containing rugose and tabulate corals, brachiopods and some amphipora. Perhaps most characteristic of this unit is the presence of abundant nodules and lenses of white weathered chert. In some exposures, the chert can form up to 90% of the rock. The formation is between 3 and 50 m thick and is generally thicker toward the centre of the Michigan Basin (Johnson et al. 1992). At the Bruce Nuclear site, drill holes intersected about 49 m of the Bois Blanc Formation (Raven et al. 2009). The formation is covered by a thick and extensive overburden cover and does not crop out in the study area. South of the study area, the formation has been quarried at Hagersville, Cayuga and Port Colborne for crushed stone suitable for base course. The high chert content of this unit makes it unsuitable for asphalt and concrete aggregate.

The Amherstburg Formation is a Middle Devonian formation with the lower part of the formation quite possibly Lower Devonian in age (Armstrong and Carter 2010). The formation varies from 0 to 50 m thick and consists of tan to grey-brown to dark brown, fine- to coarse-grained, bituminous, bioclastic, fossiliferous, commonly cherty limestones and dolostones. Drill holes at the Bruce Nuclear site intersected 44.6 m of Amherstburg Formation (Raven et al. 2009). Fossils that have been noted in the formation include rugose and tabulate corals, brachiopods, crinoids, cephalopods and trilobites. In the Teeswater–Formosa area of southern Bruce County, biohermal limestone and dolostone units are considered to belong to the Amherstburg Formation (Uyeno, Telford and Sanford 1982). This biohermal facies is known as the Formosa Reef Limestone or Formosa reef facies. The formation is covered by thick overburden and does not crop out in the study area. Historically, the main utility of the strata has been for the production of cement, metallurgical flux, agricultural lime and chemical stone (Hewitt 1960). Use of the stone for aggregate is less likely, because of the porous and sometimes soft nature of the rock.

Overlying the Amherstburg Formation in the study area is the Lucas Formation. The formation consists of brownish-grey, brown and cream, thin- to thick-bedded, fine crystalline dolostone. Minor interbeds of limestone occur in association with small bioherms and brecciated beds (Armstrong and Carter 2010). Locally, the strata contain chert nodules, bituminous streaks and algal laminae. Anhydritic beds have also been observed and recorded within the formation. Rutka and Birchard (1993) and Birchard, Rutka and Brunton (2004) have proposed 4 depositional environments for the various lithologies noted within the Lucas Formation in the Michigan Basin. These include upper sabkha mud-flat evaporate, lower sabkha mud-flat evaporate, supratidal to shallow intertidal and subtidal depositional environments. The formation is exposed along Trout Creek and the Thames River near St. Marys, and in the subsurface at the St. Marys quarry site. Drill holes at the Bruce Nuclear site intersected 10.4 m of Lucas Formation (Raven et al. 2009). Historically, the Lucas Formation has been used for chemical and metallurgical stone, especially in the Ingersoll area of southern Ontario. Within the study area, the formation has been utilized for lime production, aggregate for road construction and the manufacture of cement.

Overlying the Lucas Formation are the grey to tan to brown, fossiliferous, medium- to thick-bedded limestone and minor dolostone of the Dundee Formation. The formation is about 35 to 45 m thick and does display bituminous partings and oil staining in more porous segments and along fractures. Chert nodules are locally abundant. Fossils are generally abundant and include crinoid debris, brachiopods, rugose and tabulate corals, trilobites and algal cysts. The Dundee Formation is an oil-bearing formation. It has been quarried near Port Dover and on Pelee Island for crushed stone. It is also extracted near St. Marys for the manufacture of cement. The St. Marys quarry operation exposes 11.1 m of the basal part of the Dundee Formation, which sharply overlies 8.1 m of the Lucas Formation.

SUMMARY

Bedrock-derived aggregate resource development opportunities are limited within Perth County by a thick overburden cover and lithology. Rock units that have a high percentage of shale or chert (Ingham and Dunikowska-Koniuszy 1965) are not conducive to the production of high-specification aggregate products. Sand and gravel aggregate resource development opportunities are also restricted by the lack of extensive surface deposits (glaciofluvial ice-contact and outwash deposits) and lithology. Many of the gravel and crushable clasts consist of chert (Cowan 1979). The sand and gravel deposits that are available have been extracted extensively and are nearing depletion. Buried granular resources near the City of Stratford have, and continue, to provide aggregate material. Many dredging operations exist throughout Perth County, since these types of operations prolong the life of a resource area by allowing extraction below the water table. The Aggregate Resources Inventory report and maps for Perth County will delineate the remaining aggregate resources and detail the quality and limitations of these resources.

REFERENCES

- Armstrong, D.K. and Carter, T.R. 2010. The subsurface Paleozoic stratigraphy of southern Ontario; Ontario Geological Survey, Special Volume 7, 301p.
- Barnett, P.J. 1992. Quaternary geology of Ontario; *in* Geology of Ontario, Ontario Geological Survey, Special Volume 4, Part 2, p.1011-1088.
- Birchard, M.C., Rutka, M.A. and Brunton, F.R. 2004. Lithofacies and geochemistry of the Lucas Formation in the subsurface of southwestern Ontario: a high-purity limestone and potential high-purity dolostone resource; Ontario Geological Survey, Open File Report 6137, 180p.
- Cooper, A.J. [no date] Quaternary geology of the Goderich–Seaforth area, southern Ontario; Ontario Geological Survey, unpublished report.
- Cowan, W.R. 1979. Quaternary geology of the Palmerston area, southern Ontario; Ontario Geological Survey, Report 187, 64p.
- Hewitt, D.F. 1960. The limestone industries of Ontario; Ontario Department of Mines, Industrial Minerals Circular 5, 177p.
- Ingham, K.W. and Dunikowska-Koniuszy, Z. 1965. The distribution, character and basic properties of cherts in southwestern Ontario; Department of Highways of Ontario, No. RB106, 35p.
- Johnson, M.D., Armstrong, D.K., Sanford, B.V., Telford, P.G. and Rutka, M.A. 1992. Paleozoic and Mesozoic geology of Ontario; *in* Geology of Ontario, Ontario Geological Survey, Special Volume 4, Part 2, p.907-1008.
- Karrow, P.F. 1977. Quaternary geology of the St. Marys area, southern Ontario; Ontario Division of Mines, Report 148, 59p.
- 1991. Quaternary geology, Stratford–Conestogo area; Ontario Geological Survey, Report 283, 104p.
- Raven, K., Sterling, S., Gaines, S., Wigston, A. and Frizzell, R. 2009. Regional and site geological frameworks—proposed deep geologic repository, Bruce County, Ontario; *in* GeoHalifax 2009, 62nd Canadian Geotechnical Conference and 10th Joint Canadian Geotechnical Society (CGS) and the International Association of Hydrogeologists (IAH)—Canadian National Chapter (CNC) Groundwater Conference, Halifax, Nova Scotia, September 20-24, Proceedings, p.1348-1355.
- Rutka, M.A. and Birchard, M.C. 1993. Facies and geochemical analysis and evaluation of carbonate resources from the Lucas Formation cores in the subsurface, southwestern Ontario; *in* Summary of Field Work and Other Activities 1993, Ontario Geological Survey, Miscellaneous Paper 163, p.160-166.
- Statistics Canada 2011. Population and dwelling counts for Canada, province and territories; Government of Canada, 2011 Census of Population.
- Uyeno, T.T., Telford, P.G. and Sanford, B.V. 1982. Devonian conodonts and stratigraphy of southwestern Ontario; Geological Survey of Canada, Bulletin 332, 55p.

22. Project Unit 12-012. The St. Edmund Formation—The Next Major Bedrock-Derived Aggregate Source in Ontario?

D.J. Rowell¹ and F.R. Brunton¹

¹Earth Resources and Geoscience Mapping Section, Ontario Geological Survey

INTRODUCTION

An opportunity to acquire an Early Silurian bedrock drill core spanning the Gasport Formation (commonly mapped as, or included with, the Amabel Formation) through to the Cabot Head Formation in west-central Manitoulin Island was presented to OGS staff in December 2011. The main purpose of acquiring the core was to enable better characterization and correlation of Silurian strata along the northern rim of the Niagara Escarpment from Cockburn Island across Manitoulin Island through to the Bruce Peninsula region. Such data are important for both basin analysis and regional bedrock aquifer mapping along the escarpment, and from an industrial minerals and aggregate resources perspective. Figure 22.1 shows the location of drill hole FRB-11-DDH#4, located just east of Silver Lake and southwest of Barrie Island (UTM location: 360983E 5079866N, NAD83, Zone 17).

Table 22.1 is the drill-core log for FRB-11-DDH#4. As can be seen in the table, the drill hole intersected 7.01 m of Gasport Formation, which is quarried extensively by the aggregate industry throughout south-central Ontario. While logging the hole, what became of particular interest was the look and competency of the St. Edmund Formation. Because the St. Edmund Formation does not crop out extensively in southern Ontario (only along the face of the Niagara Escarpment, along the western shoreline of Georgian Bay in the northern part of the Bruce Peninsula) and aggregate testing of the

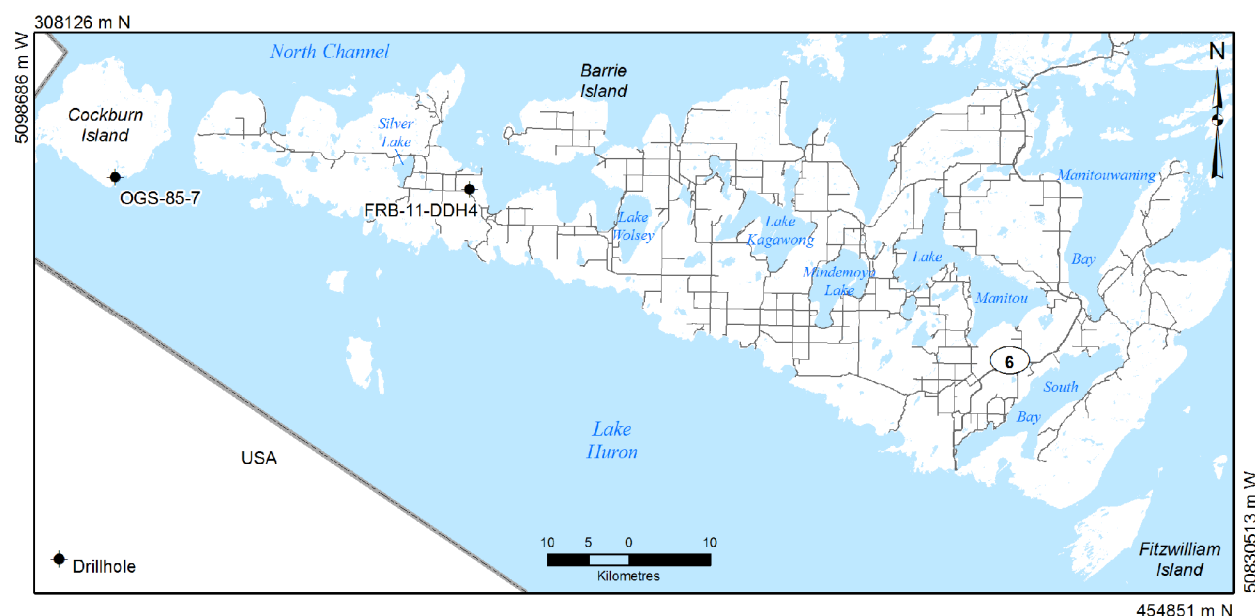


Figure 22.1. Location of drill hole FRB-11-DDH#4. Universal Transverse Mercator (UTM) co-ordinates provided using North American Datum 1983 (NAD83) in Zone 17.

*Summary of Field Work and Other Activities 2012,
Ontario Geological Survey, Open File Report 6280, p.22-1 to 22-11.*

© Queen's Printer for Ontario, 2012

Table 22.1. Drill-core log for drill hole FRB-11-DDH#4.

Stratigraphic Description	Depth (m)	Formation Thickness (m)	Elevation (m)
Top of Hole: Gasport Fm.	0.00		226.00
<i>Gasport Fm.</i>		7.01	
Gasport Fm.–Fossil Hill Fm. contact	7.01		218.99
<i>Fossil Hill Fm.</i>		21.95	
Fossil Hill Fm.–St. Edmund Fm. contact	28.96		197.04
<i>St. Edmund Fm.</i>		39.31	
St. Edmund Fm.–Wingfield Fm. contact	68.27		157.73
<i>Wingfield Fm.</i>		12.20	
Wingfield Fm.–Dyer Bay Fm. contact	80.47		145.53
<i>Dyer Bay Fm.</i>		4.36	
Dyer Bay Fm.–Cabot Head Fm. contact	84.83		141.17
<i>Cabot Head Fm.</i>		8.52	
End of Hole (EOH): Cabot Head Fm.	93.35		132.65

Notes: False Mindemoya noted between 27.28 m (89.5 feet) and 28.96 m (95 feet).
Cabot Head Formation continues but end of hole.

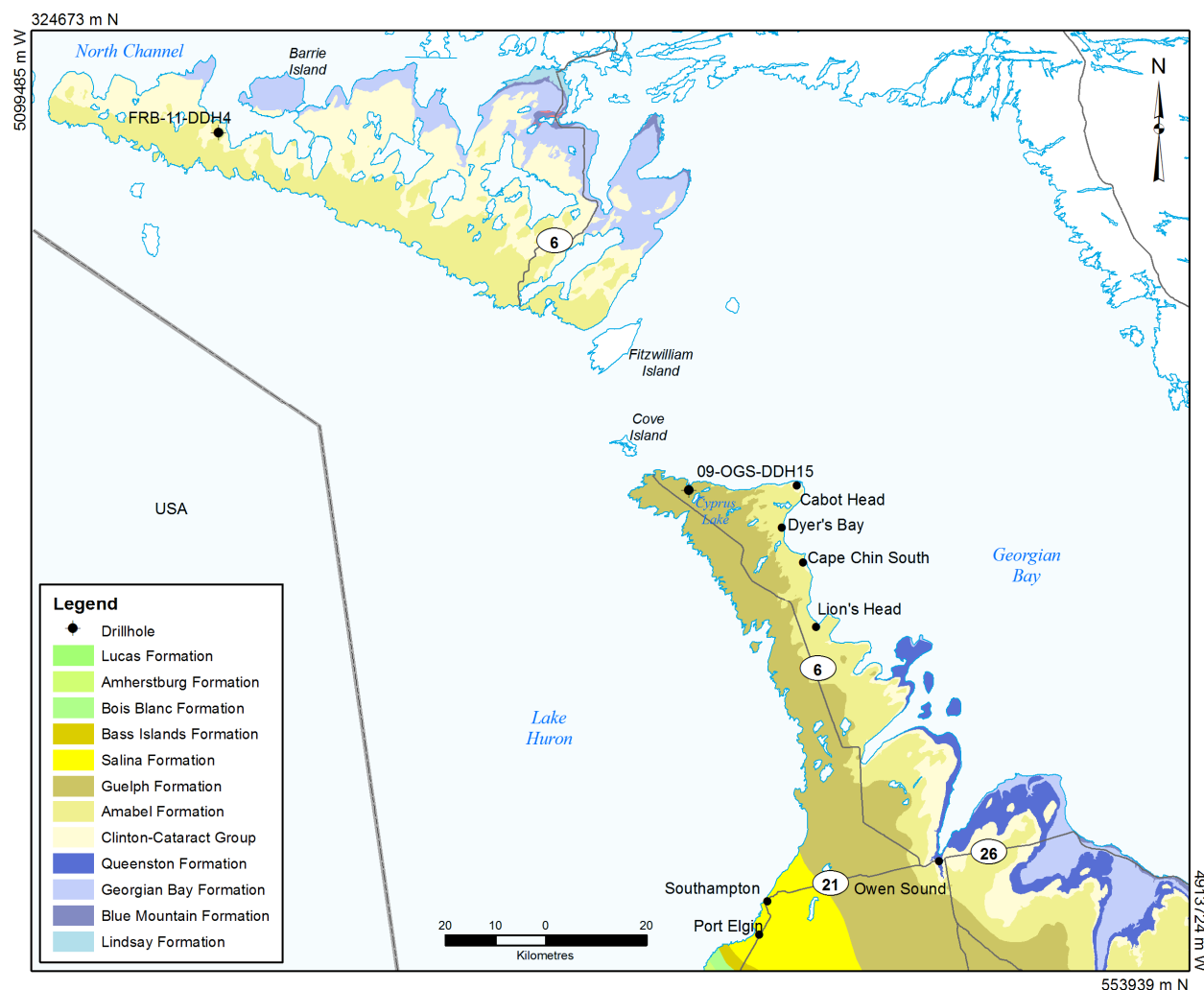


Figure 22.2. Geographic distribution of the St. Edmund Formation. Paleozoic geology from Armstrong and Dodge (2007). UTM co-ordinates provided using NAD83 in Zone 17.

formation is scarce, this was the perfect opportunity to perform standard aggregate tests on the St. Edmund Formation. Furthermore, examination of the core revealed that the St. Edmund Formation was of similar thickness to that observed on Cockburn Island (Wolf 1986, 2006) and possessed rock characteristics similar to that found in the Port Inland Quarry on the Upper Peninsula of Michigan (F.R. Brunton, personal observations).

The opportunity to test the St. Edmund Formation is important because the aggregate industry contributes to a \$37 billion construction industry that employs 292 000 Ontarians (Ministry of Natural Resources 2009). It is also important because competing land use interests in southern Ontario are making it difficult to licence new aggregate properties, thereby restricting supply.

ST. EDMUND FORMATION

The St. Edmund Member was first described on the Bruce Peninsula as a dolostone lens of the Cabot Head Formation by Williams (1919). Sanford (1978) was the first to “promote” the St. Edmund to formational rank as he questioned Liberty’s (1968) introduction of the term Mindemoya Formation for part of the St. Edmund and Wingfield rock units that underlie the Fossil Hill Formation on Manitoulin Island. Subsequent mapping by Johnson and Telford (1981, 1985a-f) on Manitoulin Island further demonstrated that the strata as defined by Williams (1919) as the St. Edmund lentil is a single rock unit, and should be “promoted” to formational rank.

The formation has a sharp upper contact with the overlying Fossil Hill Formation, but possesses a similar dolostone lithology and, therefore, is difficult to identify in borehole geophysical logs. These 2 formations are very distinctive lithologically in core and the contact is always sharp and disconformable. The top is reported to be locally marked by a thin green shale bed that may produce a small gamma-ray spike (evident at the type section west of the community of Cabot Head along the Bruce Peninsula, Figure 22.2). The lower contact with the Wingfield Formation has been defined as the first appearance of green shale. This contact has been reported to be sharp, but other reports suggest the contact is somewhat gradational as the upper Wingfield Formation can be rich in green shale interbedded with small dolomite cycles, masking the contact. Geophysics can help to establish the presence of the shale beds and can therefore be used to help define this contact.

Geographic Distribution

The St. Edmund Formation is located in the subsurface of the northern part of the Bruce Peninsula, and extends northward onto Manitoulin and Cockburn islands. The formation crops out along the face of the Niagara Escarpment, along the western shoreline of Georgian Bay; in fact, the type locality for the St. Edmund Formation is at Rocky Bay, east of Cabot Head. The formation is also exposed south of Cabot Head at Boulder Bluff, and along the eastern shoreline of the Bruce Peninsula near Dyer’s Bay and Cape Chin South (*see* Figure 22.2). The formation is included as part of the Clinton–Cataract Group (*see* Figure 22.2). The formation crops out along the northern part of Cockburn and Manitoulin islands and the northeastern shoreline of Fitzwilliam Island (*see* Figure 22.1; Johnson and Telford 1985a-f; Wolf 1986, 2006; F.R. Brunton, personal observation).

Formation Thickness

The St. Edmund Formation was estimated to be 25 m thick on Manitoulin Island (Johnson et al. 1992). Drill-hole FRB-11-DDH#4 intersected 39.31 m (*see* Table 22.1). Wolf (2006) intersected approximately 40 m of St. Edmund Formation on Cockburn Island, at Ontario Geological Survey (OGS) drill-site OGS-85-7 (*see* Figure 22.1). Rowell and Brunton (2011) intersected 5.32 m of St. Edmund Formation at the Cyprus Lake drill site along the northeastern part of the Bruce Peninsula (*see* Figure 22.2,

drill-hole 09-OGS-DDH15). No St. Edmund Formation was intersected at the Bruce Nuclear site, south of Port Elgin (Raven et al. 2009). AMEC (2010) did not drill deep enough to intersect the St. Edmund Formation on Fitzwilliam Island, although it is expected that the formation would underlie the island. The St. Edmund Formation is absent in outcrop and the subsurface south of Lion's Head (Johnson et al. 1992). The St. Edmund Formation is cut out tectonically south of the town of Wiarton on the Bruce Peninsula.

Lithology

Brintnell et al. (2009) identified 2 facies within the St. Edmund Formation. The first is defined as a pale- to medium-grey, microcrystalline, thin-bedded dolostone (5 to 10 cm beds). Individual beds may contain fine laminae. Photo 22.1 shows this first facies, which weathers from white to cream. The second facies is a medium brown, fine- to medium-crystalline, medium-bedded dolostone (10 to 25 cm beds). The second facies weathers from light brown to tan. The microcrystalline facies appears to be more prevalent in the upper part of the formation. Wolf (2006) reports the odd occurrence of vuggy texture with the vugs lined with either dolomite or quartz crystals. Wolf (2006) also reported almost pure limestone beds, which can actually be separated and identified using major oxide geochemical data presented in Table 22.3c. Rhythmites, sparse green shaly partings, and rip-up clasts have also been observed. The lower St. Edmund Formation contains a correlative coral-rich transgressive bed and a diagnostic intraformational conglomerate (Brintnell et al. 2009). A *Diplocraterion* marker bed is also common in the lower part of the formation.

Johnson et al. (1992) have suggested that the first facies was deposited in a quiet intertidal to supratidal environment (desiccation cracks were noted), whereas the second facies was deposited in a deeper intertidal to supratidal environment.



Photo 22.1. Facies 1 of the St. Edmund Formation.

Table 22.2. Details of samples collected.

Sample No.	Bag No.	Core Depth (feet)	Total Interval (feet)
11DJR-0040	Bag 1 of 2	95–110	15
11DJR-0040	Bag 2 of 2	110–125	15
11DJR-0041	Bag 1 of 2	125–140	15
11DJR-0041	Bag 2 of 2	140–155	15
11DJR-0042	Bag 1 of 2	155–170	15
11DJR-0042	Bag 2 of 2	170–185	15
11DJR-0043	Bag 1 of 2	185–200	15
11DJR-0043	Bag 2 of 2	200–224	24

ST. EDMUND FORMATION SAMPLES

The St. Edmund Formation drill core was cut longitudinally and divided into samples (as detailed in Table 22.2) in order to provide sufficient material for proper aggregate testing (half the core was consumed for aggregate tests). As a result, geochemical samples were collected according to the same drill-core intervals in order to provide consistency. This sampling was chosen to represent a bench or lift of 30 feet (9.14 m) if quarry development were to occur, with the last bench height being 39 feet (11.9 m).

Geochemistry

Geochemical analyses completed as part of this study are presented in Tables 22.3a and 22.4a (major oxides and trace elements, respectively). Analytical data from samples that were clearly identified as St. Edmund Formation in Johnson and Telford (1981) and in Wolf (2006) have been provided in Tables 22.3b and 22.3c, respectively, for comparative purpose. These samples have been averaged to represent a bench or lift, instead of a single analytical result within a certain small interval along the drill core. For individual geochemical results, refer to the original published reports. The “benched” samples from this study clearly have a lower MgO content (average 17.31%) and, therefore, are slightly less dolomitic than previous geochemical results have indicated. Therefore, the Ca/Mg ratio is on average higher at 1.56 compared to an average of 1.29 to 1.33 (Johnson and Telford 1981; Wolf 2006). Magnesium oxide content in the Johnson and Telford (1981) and Wolf (2006) analyses average from 20.26 to 21.54.

Based on the limited amount of data, one major oxide that does show some variability is silica (SiO₂). The suggestion by Wolf (2006) that the vugs were lined with dolomite or quartz crystals may explain the variations in the silica results (essentially vugs may cause a “nugget” effect). An increase in the frequency and thickness of shale partings or beds, or the presence of silica as a “cementing” compound may also explain the variance. The rest of the major oxides appear to be reasonably consistent based on the limited data available. Minor variations in Al₂O₃ and K₂O may be explained by concentration of minor shale partings or beds, particularly in the lower portion of the formation.

Despite having a limited set of trace element data (*see* Table 22.4a), one trend that seems to appear is the increase in most trace elements down the stratigraphic sequence. This increase in trace element concentration is probably a reflection of an increase in the frequency and thickness of shale beds, since shale tends to have higher values of trace elements (Drever 1982). For example, Drever (1982) reports that the typical concentration of barium in shale is 580 ppm, whereas the typical concentration of barium in limestone is 10 ppm. More trace element geochemical data would have to be available to make more detailed analyses and trends.

Table 22.3a. Major element analytical results for St. Edmund Formation, Manitoulin Island samples (this study).

Sample No.	11DJR-0040	11DJR-0041	11DJR-0042	11DJR-0043	Average	Standard Deviation
SiO ₂ (%)	4.26	1.96	6.71	5.84	4.69	2.08
Al ₂ O ₃	0.43	0.42	0.85	1.14	0.71	0.35
MnO	0.01	0.01	0.01	0.01	0.01	0.00
MgO	17.51	17.76	16.89	17.08	17.31	0.40
CaO	27.14	27.80	26.33	26.58	26.96	0.65
Na ₂ O	<0.01	<0.01	<0.01	<0.01	0.00	–
K ₂ O	0.15	0.16	0.52	0.69	0.38	0.27
P ₂ O ₅	<0.01	<0.01	0.01	0.01	0.01	–
TiO ₂	0.02	0.02	0.05	0.08	0.04	0.03
Fe ₂ O ₃ ^{total}	0.16	0.14	0.28	0.49	0.27	0.16
LOI	49.73	51.25	47.59	47.50	49.02	1.81
Total	99.24	99.35	99.10	99.30	99.25	0.11
S	0.03	0.01	0.04	0.09	0.04	0.03
CO ₂	46.90	44.30	49.50	43.30	46.00	2.78
Ca/Mg	1.55	1.57	1.56	1.56	1.56	0.01

Table 22.3b. Major element analytical results for St. Edmund Formation samples (from Johnson and Telford 1981).

Sample No.	M5-31	M5-32	M5-33	M5-34	M5-35	M5-36	M5-37	Average	Std. Dev.
SiO ₂ (%)	6.36	8.30	6.75	13.90	1.68	11.80	7.68	8.07	3.95
Al ₂ O ₃	1.35	1.67	1.35	2.14	0.52	2.71	1.59	1.62	0.69
MnO	0.00	0.00	0.00	0.00	0.00	0.00	0.00	0.00	–
MgO	20.60	20.30	20.60	19.30	21.20	19.60	20.20	20.26	0.64
CaO	25.20	26.70	25.20	25.50	28.90	24.40	26.80	26.10	1.50
Na ₂ O	<0.01	<0.01	<0.01	<0.01	<0.01	<0.01	<0.01	<0.01	–
K ₂ O	0.92	1.11	0.92	1.14	0.18	1.60	1.06	0.99	0.42
P ₂ O ₅	0.00	0.01	0.00	0.05	0.00	0.02	0.00	0.01	0.02
TiO ₂	0.06	0.07	0.05	0.17	0.02	0.17	0.10	0.09	0.06
Fe ₂ O ₃ ^{total}	0.46	0.60	0.45	0.75	0.61	0.72	0.51	0.59	0.12
LOI	42.90	41.70	42.80	37.80	45.50	37.60	41.50	41.40	2.84
Total	97.85	100.46	98.12	100.75	98.61	98.62	99.44	99.12	1.13
S	0.09	0.20	0.03	0.20	0.11	0.18	0.07	0.13	0.07
CO ₂	45.20	43.80	45.20	39.90	45.60	41.00	44.30	43.57	2.24
Ca/Mg	1.22	1.32	1.22	1.32	1.36	1.24	1.33	1.29	0.06

Sample No.	M6-28	M6-29	M6-31	M6-32	M6-33	M6-34	M6-35	M6-36	Average	Std. Dev.
SiO ₂ (%)	4.65	4.61	1.60	2.87	2.32	9.34	9.38	9.47	5.53	3.37
Al ₂ O ₃	0.72	1.07	1.17	0.77	0.64	2.20	1.86	1.68	1.26	0.58
MnO	0.00	0.00	0.00	0.00	0.00	0.00	0.00	0.00	0.00	0.00
MgO	20.90	20.90	21.10	21.20	21.20	19.60	19.80	19.90	20.58	0.68
CaO	28.40	28.00	28.20	27.20	27.90	26.00	26.30	26.40	27.30	0.95
Na ₂ O	0.00	0.00	0.01	0.00	0.02	0.00	0.01	0.02	0.01	0.01
K ₂ O	0.43	0.68	0.15	0.56	0.40	1.45	0.78	0.92	0.67	0.40
P ₂ O ₅	0.00	0.00	0.00	0.00	0.00	0.00	0.00	0.00	0.00	–
TiO ₂	0.06	0.06	0.01	0.03	0.02	0.13	0.12	0.13	0.07	0.05
Fe ₂ O ₃ ^{total}	0.58	0.46	0.37	0.49	0.42	0.91	0.62	0.94	0.60	0.22
LOI	43.80	43.80	45.60	44.50	45.20	40.00	40.10	40.20	42.90	2.40
Total	99.54	99.58	98.21	97.62	98.12	99.63	98.97	99.66	98.92	0.82
S	0.07	0.04	0.02	0.04	0.01	0.26	0.29	0.36	0.14	0.14
CO ₂	46.10	46.40	47.30	47.30	47.20	42.30	42.40	42.60	45.20	2.33
Ca/Mg	1.36	1.34	1.34	1.28	1.32	1.33	1.33	1.33	1.33	0.02

Table 22.3c. Major element analytical results for St. Edmund Formation samples (*from* Wolf 2006).

Sample No.	31D	31C	31B	31A	21	22	23B	23A	60	57B	57A	53B	58	Average	Standard Deviation
SiO ₂ (%)	0.80	8.18	5.80	2.93	0.84	5.97	1.23	1.24	1.20	2.08	7.56	0.48	1.50	3.06	2.78
Al ₂ O ₃	0.15	1.70	1.21	0.65	0.21	1.29	0.28	0.26	0.30	0.24	0.13	0.10	0.16	0.51	0.53
MnO	0.01	0.01	0.01	0.01	0.01	0.01	0.01	0.01	0.02	0.01	0.01	0.01	0.02	0.01	0.00
MgO	22.00	20.30	21.00	21.45	22.10	20.90	22.10	21.90	21.30	22.00	21.20	22.10	21.70	21.54	0.57
CaO	29.80	24.80	26.50	28.20	29.80	26.20	29.60	29.60	30.00	29.20	27.00	29.90	29.70	28.48	1.76
Na ₂ O	0.00	0.00	0.00	0.00	0.00	0.00	0.00	0.00	0.00	0.10	0.00	0.00	0.00	0.01	0.03
K ₂ O	0.06	1.07	0.74	0.37	0.05	0.77	0.13	0.10	0.08	0.01	0.02	0.01	0.06	0.27	0.36
P ₂ O ₅	0.02	0.03	0.02	0.02	0.01	0.02	0.02	0.01	0.02	0.02	0.04	0.02	0.01	0.02	0.01
TiO ₂	0.00	0.08	0.05	0.03	0.00	0.05	0.01	0.01	0.00	0.01	0.00	0.00	0.01	0.02	0.03
Fe ₂ O ₃ ^{total}	0.19	0.46	0.38	0.26	0.14	0.36	0.22	0.22	0.20	0.21	0.19	0.14	0.30	0.25	0.10
LOI	46.60	41.60	43.50	45.30	47.00	43.40	46.30	46.60	46.80	46.00	43.30	47.10	46.20	45.36	1.79
Total	99.63	98.23	99.21	99.22	100.16	98.97	99.90	99.95	99.92	99.88	99.45	99.86	99.66	99.54	0.53
S	—	—	—	—	—	—	—	—	—	—	—	—	—	—	—
CO ₂	45.50	42.20	43.30	44.00	44.80	43.80	45.60	44.10	44.80	45.30	41.30	44.50	44.90	44.16	1.28
Ca/Mg	1.35	1.22	1.26	1.31	1.35	1.25	1.34	1.35	1.41	1.33	1.27	1.35	1.37	1.32	0.05

Continued. Analytical results for St. Edmund Formation samples (*from* Wolf 2006) not included in the average above.

Sample No.	34	59C	59A
SiO ₂ (%)	1.11	1.02	0.75
Al ₂ O ₃	0.20	0.14	0.11
MnO	0.01	0.01	0.01
MgO	4.85	1.15	0.93
CaO	50.60	54.10	54.50
Na ₂ O	0.06	0.08	0.10
K ₂ O	0.07	0.04	0.03
P ₂ O ₅	0.02	0.02	0.02
TiO ₂	0.00	0.00	0.00
Fe ₂ O ₃ ^{total}	0.21	0.12	0.12
LOI	43.10	43.20	42.90
Total	100.23	99.88	99.47
S	—	—	—
CO ₂	43.10	42.80	39.90
Ca/Mg	10.43	47.04	58.60

Table 22.4a. Trace element analytical results (in ppm) for St. Edmund Formation, Manitoulin Island samples (this study).*Analysis by Atomic Absorption Spectroscopy (AAS)*

Sample No.	11DJR-0040	11DJR-0041	11DJR-0042	11DJR-0043
Cd (ppm)	<5	<5	<5	<5
Co	<30	<30	<30	<30
Cu	<3	<3	<3	3
Li	22	24	34	39

	11DJR-0040	11DJR-0041	11DJR-0042	11DJR-0043
Ni (ppm)	<6	9	<6	10
Pb	<12	<12	<12	<12
Zn	6	6	6	9

Analysis by Inductively Coupled Plasma Mass Spectrometry (ICP-MS)

Sample No.	11DJR-0040	11DJR-0041	11DJR-0042	11DJR-0043		11DJR-0040	11DJR-0041	11DJR-0042	11DJR-0043
Ba (ppm)	17.6	16.3	65.2	47.9	Ni (ppm)	7.0	7.5	8.3	10.1
Be	0.13	0.09	0.14	0.19	Pb	1.3	1.3	1.6	3.7
Bi	0.19	<0.15	<0.15	<0.15	Pr	0.418	0.431	0.971	1.278
Cd	0.017	0.016	0.013	0.018	Rb	4.17	4.42	10.74	13.50
Ce	3.62	3.93	8.98	11.65	Sb	0.06	<0.04	0.04	0.06
Co	0.64	0.81	1.21	1.60	Sc	2.5	2.1	2.5	3.3
Cr	8	6	7	12	Sm	0.293	0.274	0.637	0.814
Cs	0.150	0.168	0.279	0.472	Sn	0.18	<0.16	0.18	0.20
Cu	<1.4	<1.4	<1.4	2.0	Sr	59.1	48.7	55.3	59.6
Dy	0.219	0.200	0.460	0.537	Ta	0.024	0.027	0.066	0.114
Er	0.135	0.111	0.262	0.305	Tb	0.0356	0.0340	0.0753	0.0921
Eu	0.0599	0.0602	0.1408	0.1786	Th	0.417	0.480	1.182	1.215
Ga	0.56	0.61	1.11	1.60	Ti	102	118	234	417
Gd	0.253	0.248	0.548	0.641	Tl	0.028	0.025	0.051	0.065
Hf	0.22	0.29	1.09	0.65	Tm	0.0175	0.0149	0.0391	0.0431
Ho	0.0439	0.0374	0.0915	0.1064	U	0.570	0.520	0.646	0.640
In	0.0022	0.0022	0.0037	0.0058	V	3.5	3.8	5.3	9.6
La	2.16	1.91	4.49	6.20	W	<0.5	0.05	0.08	0.13
Li	11.9	10.2	26.9	35.5	Y	1.62	1.01	2.64	3.01
Lu	0.0162	0.0143	0.0388	0.0394	Yb	0.108	0.100	0.248	0.272
Mo	0.41	0.95	0.33	0.44	Zn	<7	<7	<7	<7
Nb	0.495	0.676	1.120	2.474	Zr	9	12	47	27
Nd	1.50	1.54	3.53	4.62					

Table 22.4b. Fluorine analytical results (in ppm) for St. Edmund Formation, Manitoulin Island samples (*from* Johnson and Telford 1981).*Analysis by Atomic Absorption Spectroscopy (AAS)*

Sample No.	F (ppm)	Sample No.	F (ppm)
M5-31	540	M6-28	185
M5-32	600	M6-29	325
M5-33	385	M6-31	215
M5-34	650	M6-32	215
M5-35	325	M6-33	140
M5-36	490	M6-34	600
M5-37	450	M6-35	580
<i>average</i>	<i>491</i>	M6-36	465
		<i>average</i>	<i>341</i>

Table 22.5. Coarse aggregate quality test data for dolostone from the St. Edmund Formation.

Sample Number	Petrographic Number		MgSO ₄ Soundness (%)	Micro-Deval Abrasion (% Loss)	Los Angeles Abrasion and Impact Test	Unconfined Freeze–Thaw (% Loss)	Absorption Capacity (%)	Bulk Relative Density	Accelerated Mortar Bar Expansion (14 days) (% Loss)
	Granular and 16 mm	Asphalt and Concrete							
<i>Generally acceptable values:</i>		<125–140	<12–15%	<14–17%	<35%	<6%	<2%	>2.5	<0.150%
11DJR-0040*	–	104.0	5.6	9.4	–	6.3	0.820	2.765	0.038
11DJR-0041*	–	102.0	3.8	6.0	–	2.5	0.720	2.782	0.020
11DJR-0042*	–	107.0	8.4	10.7	–	11.2	1.240	2.732	0.058
11DJR-0043*	–	107.0	15.5	8.5	–	24.4	1.320	2.726	0.061
10**	100.0	101.0	2.7	–	21.1	–	0.803	2.774	–
average, multiple analyses***	–	105.0	1–2	–	19–21	–	0.6–0.7	2.78–2.79	–

* *this study*; ** *Russell and Johnson (1981)*; ****data from Ministry of Transportation (MTO)*.

Aggregate Test Results

As mentioned earlier, the St. Edmund Formation appears quite competent in drill-core FRB-11-DDH#4. Aggregate test results presented in Table 22.5 indicate that the St. Edmund Formation would meet specification for a number of high-end aggregate products, including Select Subbase Material (SSM), Granular B, Granular A, asphalt and concrete aggregate. Generally acceptable aggregate testing specifications have been provided in Table 22.5.

Where the formation does not appear to consistently meet specification is in the lowermost bench sample (Sample 11DJR-0043), which is encroaching on the Wingfield Formation contact, and may indeed incorporate some of the interbedded shale–dolomite cycles, as noted earlier. At this point, the magnesium sulphate soundness test result is slightly higher than the recommended 15%. Unconfined freeze–thaw test results may also be of concern. Beyond these specific test results, the St. Edmund Formation would appear suitable for a wide variety of high-specification aggregate products with proper beneficiation. Previous testing by Russell and Johnson (1981) and Ministry of Transportation of Ontario (MTO) test results (ranges) are also included in Table 22.5. Their data also indicate that the St. Edmund Formation may be of interest to the aggregate industry.

SUMMARY AND RECOMMENDATIONS

1. An opportunity to test the St. Edmund Formation for standard aggregate testing from a drill hole on Manitoulin Island was presented in December 2011. The results from this testing clearly indicate that the St. Edmund Formation has potential for the production of a wide variety of high-specification aggregate products.
2. The upper stromatoporoid-bearing beds of the St. Edmund Formation that crop out along the Cup and Saucer trail on Manitoulin Island are equivalent to the small microbial-dominated coral and stromatoporoid reef mounds in the upper Fiborn Member of the Hendricks Formation at the Port Inland Quarry, in the Upper Peninsula of Michigan. This suggests that the St. Edmund Formation on Cockburn and Manitoulin islands have similar lithofacies characteristics to the Hendricks Formation, which has been quarried in Michigan for more than a century. The Port Inland Quarry is one of the largest aggregate-industrial minerals quarries in North America.

3. Furthermore, a rock unit that is situated a few metres above the contact between the Fossil Hill and St. Edmund formations is similar to the St. Edmund Formation, which is referred to as the “False Mindemoya” of Liberty (1968) (noted in drill-hole FRB-11-DDH#4 at 27.28 m, *see* Table 22.1 and is mentioned in Cockburn Island core; Wolf 2006). Therefore, one of the next steps for the authors of this paper will be to test the Fossil Hill Formation (including the “False Mindemoya”) for standard aggregate testing. This material may also be suitable for the production of high-specification aggregate and, if so, could add another bench or lift to a potential quarry operation. This concept could be an exciting development.
4. Because of the geographic and topographic distribution of the St. Edmund and potentially the bottom of the Fossil Hill formations on Fitzwilliam, Manitoulin and Cockburn islands, there may be an opportunity for underground aggregate extraction (room-and-pillar-type extraction).

It is always highly recommended that where extraction and development are being contemplated, that extensive testing be conducted to verify aggregate quality and quantity. Site-specific investigations provide greater detail on the nature of the local deposit.

REFERENCES

- AMEC Earth and Environmental 2010. Evaluation of bedrock for construction aggregate; unpublished report, 20p.
- Armstrong, D.K. and Dodge, J.E.P. 2007. Paleozoic geology of southern Ontario; Ontario Geological Survey, Miscellaneous Release—Data 219.
- Brintnell, C., Brunton, F.R., Brett, C.E. and Jin, J. 2009. Characterization of the Fossil Hill–Cabot Head formational disconformity between Tobermory and Guelph, Niagara Escarpment region, southern Ontario; *in* Summary of Field Work and Other Activities 2009, Ontario Geological Survey, Open File Report 6240, p.26-1 to 26-10.
- Drever, J.L. 1982. The geochemistry of natural waters, Prentice-Hall Inc., Englewood Cliffs, New Jersey, 388p.
- Johnson, M.D., Armstrong, D.K., Sanford, B.V., Telford, P.G. and Rutka, M.A. 1992. Paleozoic and Mesozoic geology of Ontario; *in* Geology of Ontario, Ontario Geological Survey, Special Volume 4, Part 2, p.907-1008.
- Johnson, M.D. and Telford, P.G. 1981. Preliminary results of 1978–1979 drilling program, Manitoulin Island Limestone-Dolostone Assessment Project; Ontario Geological Survey, Open File Report 5360, 81p.
- 1985a. Paleozoic geology of the Meldrum Bay area, District of Manitoulin; Ontario Geological Survey, Preliminary Map P.2667, scale 1:50 000.
- 1985b. Paleozoic geology of the Silver Water area, District of Manitoulin; Ontario Geological Survey, Preliminary Map P.2668, scale 1:50 000.
- 1985c. Paleozoic geology of the Kagawong area, District of Manitoulin; Ontario Geological Survey, Preliminary Map P.2669, scale 1:50 000.
- 1985d. Paleozoic geology of the Providence Bay area, District of Manitoulin; Ontario Geological Survey, Preliminary Map P.2671, scale 1:50 000.
- 1985e. Paleozoic geology of the Little Current area, District of Manitoulin; Ontario Geological Survey, Preliminary Map P.2670, scale 1:50 000.
- 1985f. Paleozoic geology of the Manitowaning area, District of Manitoulin; Ontario Geological Survey, Preliminary Map P.2672, scale 1:50 000.
- Liberty, B.A. 1968. Ordovician and Silurian stratigraphy of Manitoulin Island, Ontario; *in* The geology of Manitoulin Island, Michigan Basin Geological Society, Annual Field Trip Guidebook, p.14-37.

- Ministry of Natural Resources 2009. State of the Aggregate Resource in Ontario Study, Paper 2 – Future Aggregate Availability and Alternative Analysis; Ministry of Natural Resources, Paper No. 2, 126p.
- Raven, K., Sterling, S., Gaines, S., Wigston, A. and Frizzell, R. 2009. Regional and site geological frameworks—proposed deep geologic repository, Bruce County, Ontario; *in* GeoHalifax 2009, 62nd Canadian Geotechnical Conference and 10th Joint Canadian Geotechnical Society (CGS) and the International Association of Hydrogeologists (IAH)—Canadian National Chapter (CNC) Groundwater Conference, Halifax, Nova Scotia, September 20-24, Proceedings, p.1348-1355.
- Rowell, D.J. and Brunton, F.R. 2011. Geochemical and brick testing results for the Queenston and Cabot Head formations from drill hole 09OGS-DDH-15, Bruce County, southern Ontario; Ontario Geological Survey, Miscellaneous Release—Data 279.
- Russell, D.J. and Johnson, M.D. 1981. Aggregate test results for Silurian carbonate rocks on Manitoulin Island; Ontario Geological Survey, Open File Report 5370, 21p.
- Sanford, J.T. 1978. General stratigraphy of the Manitoulin area; *in* Geology of the Manitoulin area, Michigan Basin Geological Society, Special Paper No. 3, p.31-41.
- Williams, M.Y. 1919. The Silurian geology and fauna of the Ontario Peninsula, and Manitoulin and adjacent islands; Geological Survey of Canada, Memoir 111, 195p.
- Wolf, R.R. 1986. Paleozoic geology of Cockburn Island, District of Manitoulin; Ontario Geological Survey, Preliminary Map P.2987, scale 1:50 000.
- 2006. Paleozoic geology of Cockburn Island, Manitoulin area; Ontario Geological Survey, Open File Report 5424, 55p.

23. Project Unit 08-005. Surficial Mapping in the Detour Lake–Burntbush Areas: A Progress Report

C. Gao¹

¹Earth Resources and Geoscience Mapping Section, Ontario Geological Survey

INTRODUCTION

Six 1:50 000 scale surficial geology maps are currently being compiled for the Detour Lake–Burntbush area located along the Ontario–Quebec provincial border in northern Ontario, covering the areas of National Topographic (NTS) map sheets 32 E/4 (Abbotsford Lake), 32 E/5 (Payntouk Lake), 32 E/13 (Detour Lake), 32 L/4 (Hopper Creek), 42 H/1 (Mistango Lake) and 42 H/8 (Twopeak Lake) (Figure 23.1). During the course of the compilation, 2 weeks of field work were completed in the area of the Detour gold mine. Accessibility was poor in this part of the map area, which has rendered detailed mapping difficult (Gao and Day 2008; Gao and Kodors 2009; Gao 2010). Currently, Detour Gold Corporation is developing an open pit gold mine, which has generated well-exposed geologic sections at several localities. As such, it is important to check and sample these sites to increase the density of data points for better maps, but also for a better understanding of the recent glacial and deglacial history of this region.

MAP COMPILATION

Apart from field work (Gao and Day 2008; Gao and Kodors 2009), 1:10 000 scale aerial photographs taken in 1986, and imagery from SPOT and Google Earth™ mapping service are used in the map compilation. At the time of writing this report, drafts have been generated for most of the maps.

The surficial deposits and landforms show pronounced changes in the map area. Prominent, southeast-aligned glacial lineations, mostly flutings, occur in the areas covered by NTS maps 32 E/13 and the southern half of 32 L/4; these lineations developed during the Cochrane ice readvance *circa* 8200 calibrated (calendar) years before present (cal years BP) or shortly before this date in the early Holocene (Hughes 1965; Prest 1969; Veillette 1994; Roy et al. 2011; Breckenridge et al. 2012). A silty to clayey till, commonly mapped below the surface in this area, has been correlated with the Cochrane Till, which is likely associated with this landform feature (Boissonneau 1966; Smith 1992; Veillette 2007; Veillette and Thibaudeau 2007; Gao and Day 2008; Gao and Kodors 2009; Gao 2010). The lineations persist to the south until across the northern borders of the areas covered by NTS maps 42 H/8 and 32 E/5, where they become less prominent to nonexistent (*see* Figure 23.1). However, in the southwestern part of the area covered by NTS map 32 E/5, the Cochrane Till still occurs above a sandy and bouldery till correlated to the Matheson Till (Gao and Day 2008; Gao 2010). To the south, at the southern border of the area covered by NTS map 32 E/5, the Cochrane Till occurs as a wedge in glaciolacustrine sand, probably indicating the terminal location of the Cochrane ice readvance in this area (Figure 23.2). Further to the south, as well as to the west, the Matheson Till commonly occurs (Gao and Day 2008; Gao and Kodors 2009; Gao 2010).

Moraine ridges, probably similar in age to the Matheson Till, occur north of bedrock ridges and hillocks commonly present along the boundary between the areas covered by NTS maps 42 H/8 and 42 H/1, which indicate the stagnant positions of the retreating ice sheet. In this area, broad sand and

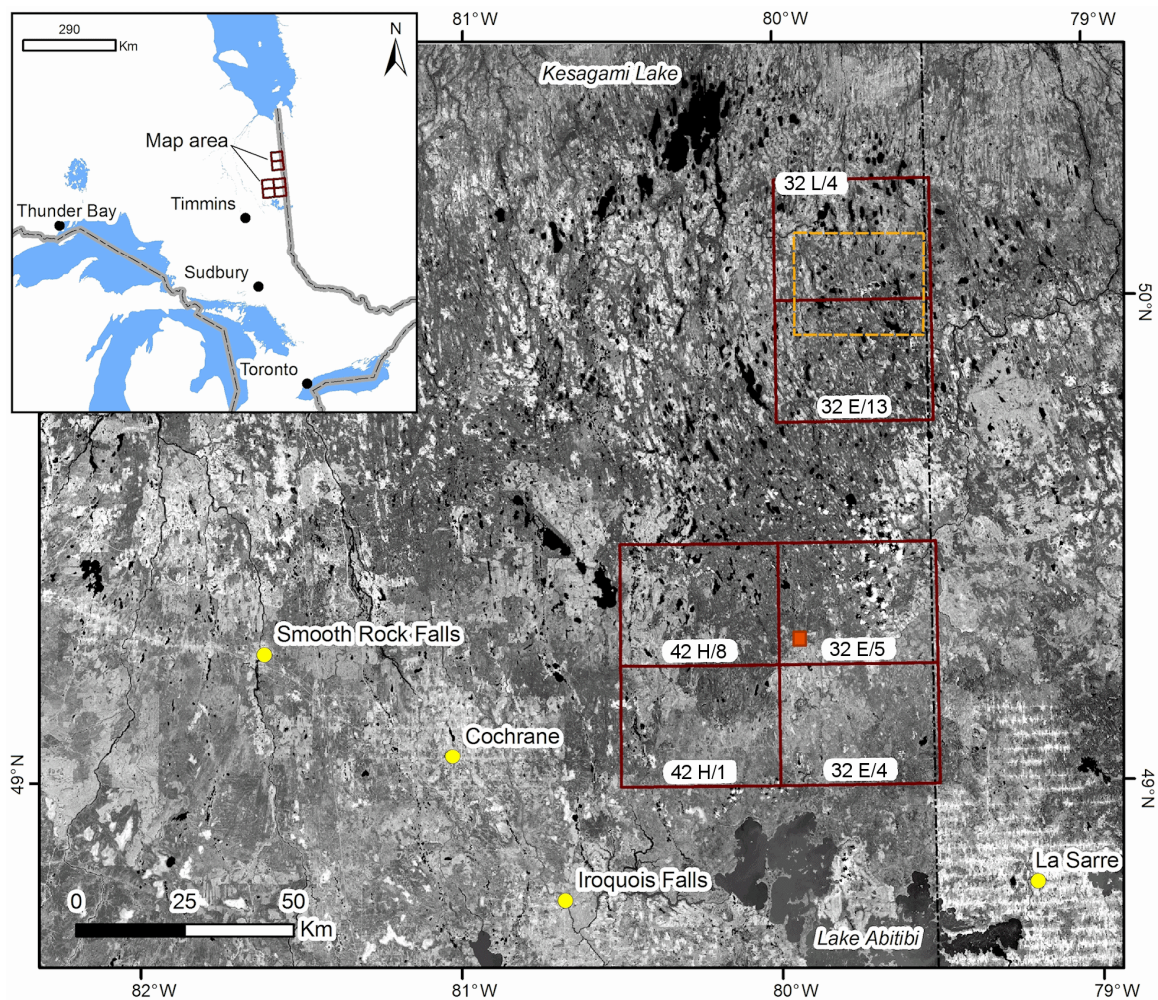


Figure 23.1. Location map showing the 1:50 000 scale NTS map sheets covering the area for which geologic data are being compiled. The small square in NTS 32 E/5 is the location of a section depicted in Figure 23.2. Boxed area with dashed outline is enlarged in Figure 23.5.

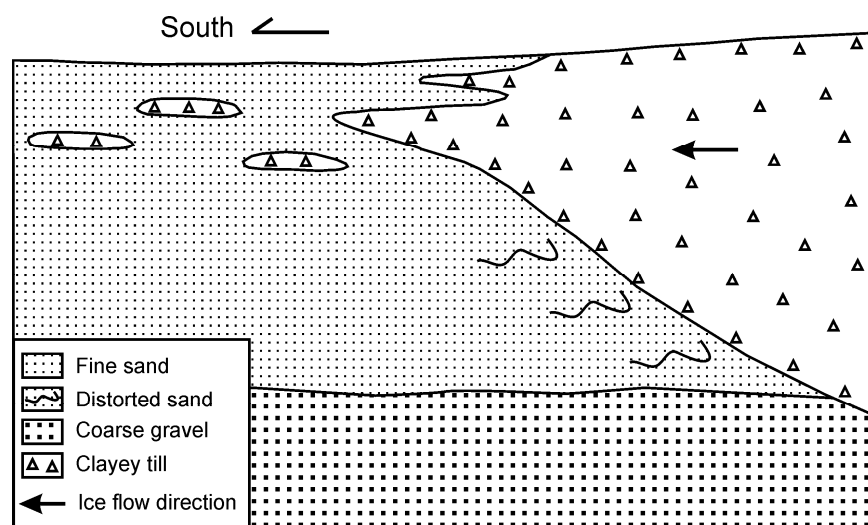


Figure 23.2. Sketched section (not to scale) showing the Cochrane Till in a glaciolacustrine sand as a result of the advance of Cochrane ice sheet into proglacial Lake Ojibway in the early Holocene. The gravel deposit at the base is part of an esker formed during the preceding Matheson ice advance of Late Wisconsinan. Refer to Figure 23.1 for location.

gravel ridges of glaciofluvial origin occur, which become narrower along the southward-dip direction. These wedge-like deposits have a northern slope that is oversteepened and concave with the apex pointing down ice, formed typically under ice-walled conditions in front of a stagnant ice sheet. Sporadic moraine ridges, probably of Cochrane affinity, occur in a southwest alignment in the northeastern corner of the area covered by NTS map 42 H/8, from which southeast-aligned eskers emanate. Because the Cochrane Till occurs approximately 20 km to the southeast (*see* Figure 23.2), these moraines likely resulted from the stagnation of the retreating ice sheet. In the areas covered by NTS maps 32 L/4 and 32 E/13, elongated moraine ridges transversal to the surface flutings occur 6 to 7 km north-northwest and southeast of the tailings pond of the Detour gold mine. A field check shows that the one located to the southeast consists predominantly of a sandy material.

Glaciolacustrine silt and clay mantles the majority of the map area, reaching at least 4 m thickness in this region (Smith 1992). It is related to proglacial Lake Ojibway (Veillette 1994, 2007). This deposit contains, without exception, ice-rafted pebble-sized clasts. In areas covered by such a deposit, crosscutting linear marks (grooves), interpreted as iceberg keel marks, occur, in particular, in grounds slightly higher than the clay plain. The glaciolacustrine silt and clay directly overlies the Matheson Till in the areas

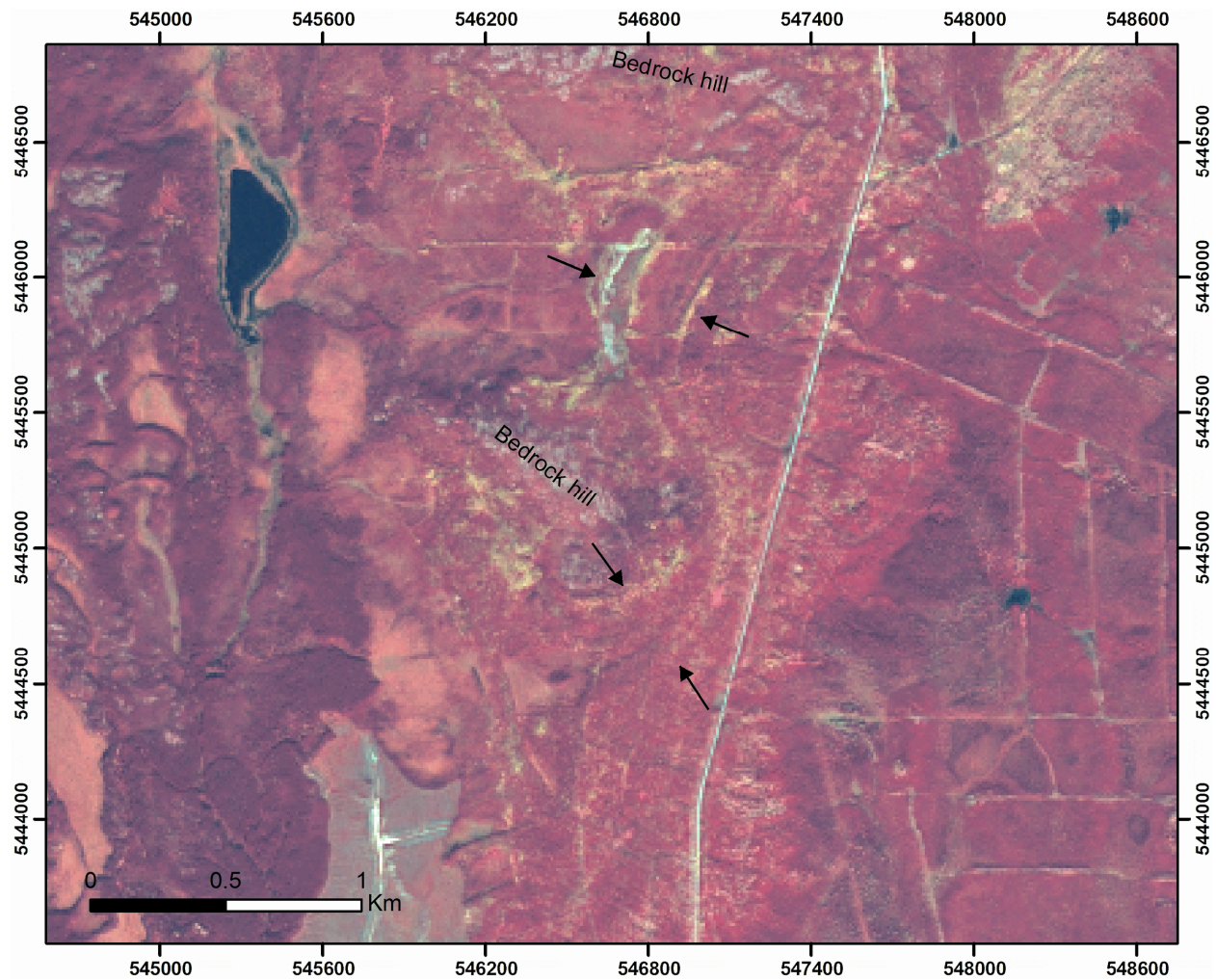


Figure 23.3. Strandlines of lake beaches (between opposing arrows) at 360 to 340 m above sea level as shown in this false-colour SPOT imagery in the northern part of the area covered by NTS map 42 H/1. The lake beaches are thought to represent the level of proglacial Lake Ojibway prior to its final drainage in the early Holocene (Veillette 1994; Roy et al. 2011). Elevations are estimated from contours of the 1:50 000 scale NTS map with an interval of 10 m. Universal Transverse Mercator (UTM) co-ordinates are provided using North American Datum 1983 (NAD83) in Zone 17.

covered by NTS maps 32 E/4 and 42 H/1, whereas in the area covered by NTS map 32 E/5 and further to the north, this deposit drapes the Cochrane Till. Given its massive texture and high content of ice-rafted clasts, it is always difficult in the field to separate this deposit from the underlying Cochrane Till (Gao and Day 2008; Gao and Kodors 2009).

Lake beaches and wave-cut benches occur, in particular, along the boundary between the areas covered by NTS maps 42 H/8 and 42 H/1, and at the eastern border of the area covered by NTS map 32 E/4, reaching at least 390 m above sea level (asl). The maximum level of Lake Ojibway could be higher, but it cannot be reconstructed because of the lack of higher terrain to record it. Since lake washing limits up to 460 m asl are documented east of the map area in northern Quebec (Veillette 1994), it would indicate that similar lake levels could have been in this area. It is noteworthy that well-developed strandlines occur commonly at 360 to 340 m asl on bedrock hills (Figure 23.3). Many authors consider these elevations to be the level of Lake Ojibway prior to its final drainage into Hudson Bay *circa* 8200 cal years BP (e.g., Veillette 1994; Dyke 2004; Roy et al. 2011).

Eskers in the areas covered by NTS maps 32 E/4, 42 H/1 and in the western half of 42 H/8 (see Figure 23.1), have, in general, a southward alignment, whereas, in 32 L/4 and 32 E/13, they tend to align

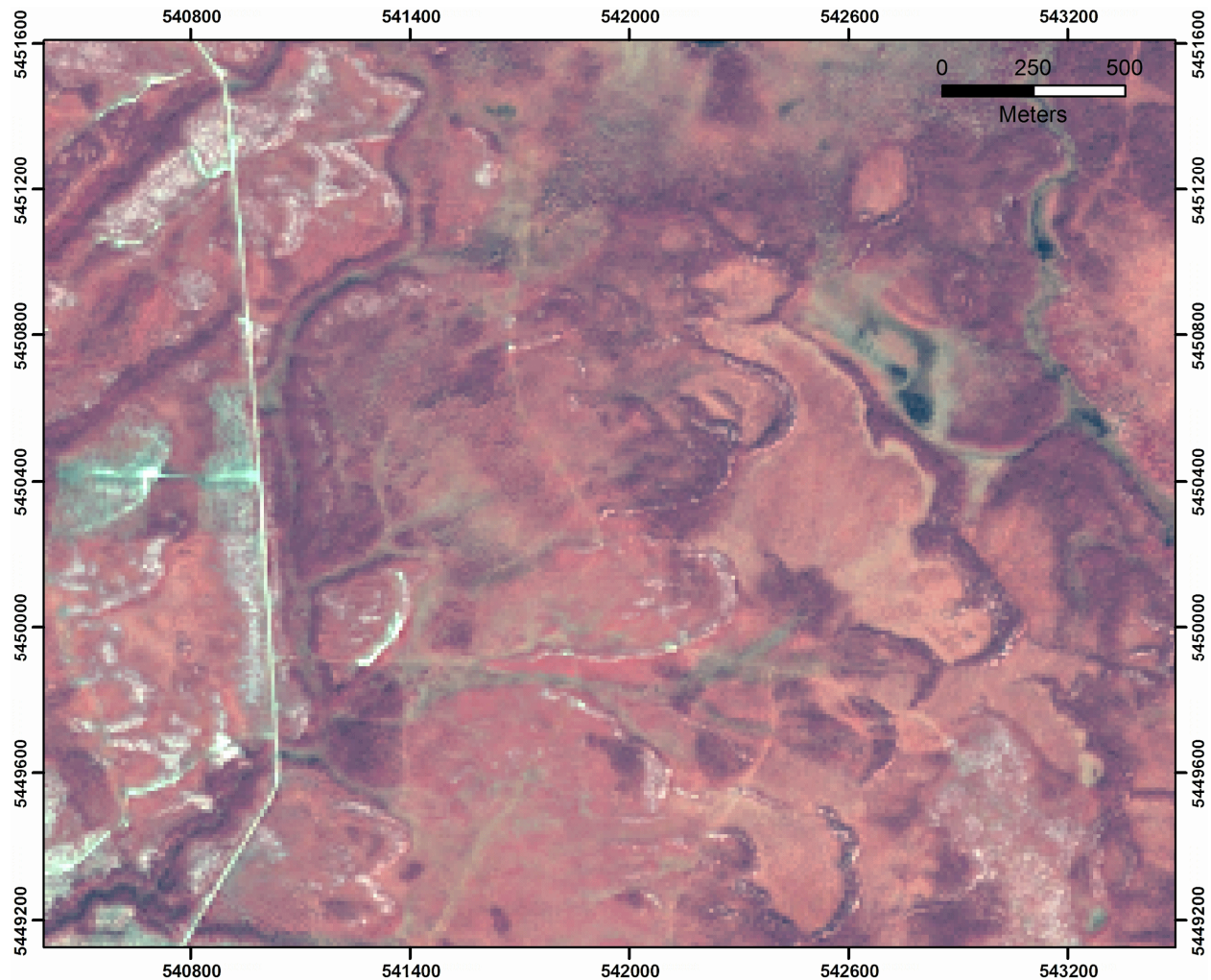


Figure 23.4. Well-developed parabolic sand dunes with a height of at least 2 m as shown in this false-colour SPOT imagery in the northwestern part of the area covered by NTS map 42 H/1. They developed under an eastward prevailing wind probably on a newly formed lake plain after the drainage of Lake Ojibway in the early Holocene prior to the colonization of this area by vegetation. UTM co-ordinates are provided using NAD83 in Zone 17.

southeastward. The 2 groups of eskers are broadly in line with the spatial distribution of the Matheson and Cochrane tills, respectively. It is, thus, not surprising to see that eskers in the former area contain abundant boulders with limited amount of limestone clasts, comparable to the Matheson Till in pebble lithology, whereas, in comparison, eskers in the latter-mentioned area contain smaller gravel clasts, fewer boulders and a higher proportion of limestone clasts, matching the clast lithology of Cochrane Till (Gao and Day 2008; Gao and Kodors 2009). As such, these 2 groups of eskers likely developed during the Late Wisconsin glacial maximum and Cochrane readvance, respectively. In an esker ascribed with a Cochrane affinity, diamict balls of Cochrane Till were recorded (Gao and Day 2008).

Well-developed parabolic or U-shaped sand dunes occur over an area exceeding 60 km² in the northwestern part of the area covered by NTS map 42 H/1. They have a gentle stoss and a steep lee with their elongated arms pointing upwind; some are joined together to form chains of dunes transversal to the prevailing eastward wind (Figure 23.4). Their source of material is likely the extensive sand deposit of Lake Ojibway in this region. Although no radiometric ages are available, formation of these dunes is estimated to be shortly after the drainage of the lake, *circa* 8200 cal years BP (Roy et al. 2011), but prior to the colonization of this area by vegetation in the early Holocene.

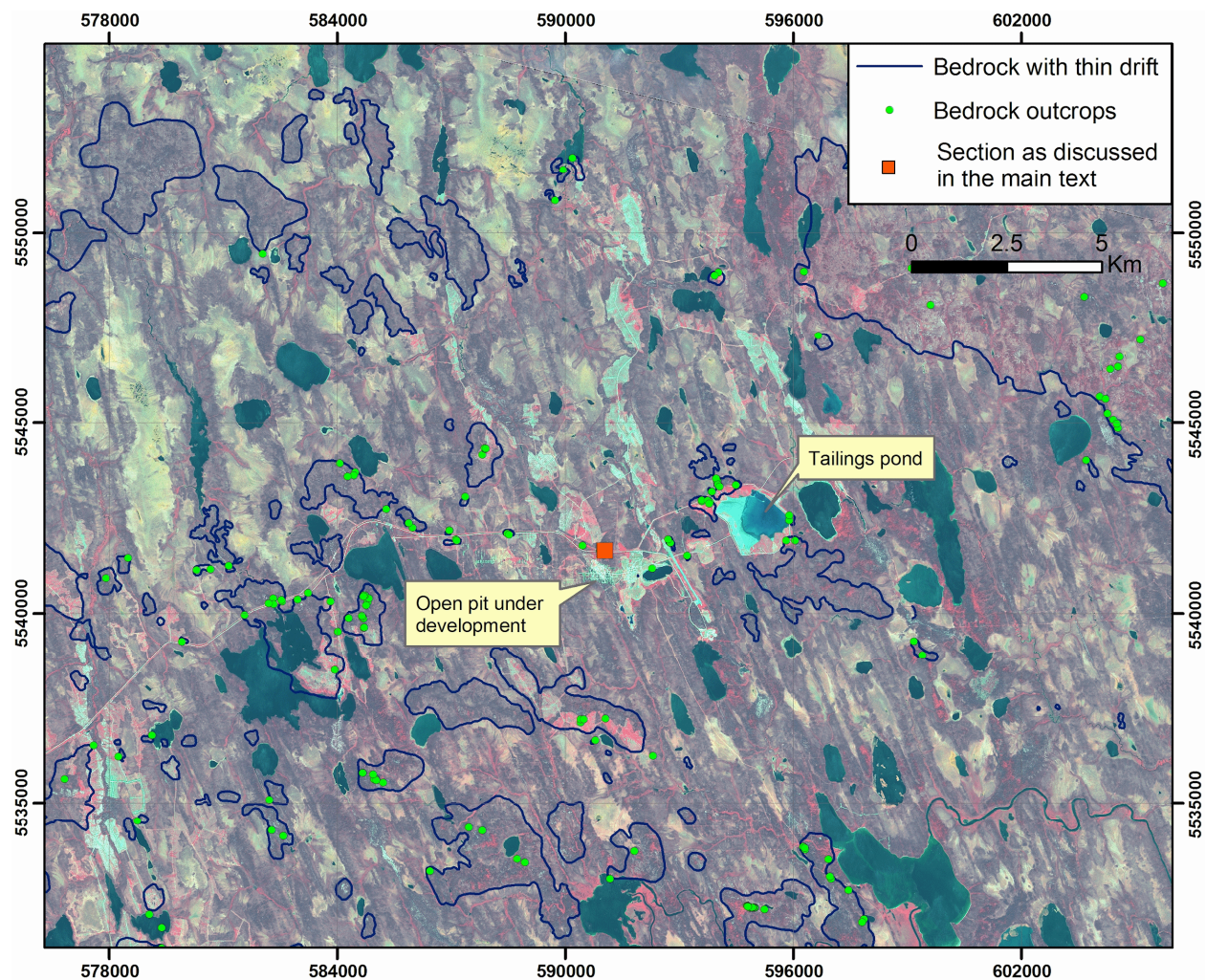


Figure 23.5. Bedrock areas with thin drift around the Detour gold mine, interpreted on the basis of field data and aerial photographs taken in 1986 (part of the bedrock outcrop data provided by Detour Gold Corporation). Orange-red square is the location of the section shown in Photo 23.1. Background: SPOT imagery. Refer to Figure 23.1 for location. UTM co-ordinates are provided using NAD83 in Zone 17.

FIELD WORK

Field work was undertaken in the vicinity of the Detour gold mine. Sections were checked in newly exposed areas including road ditches, the open pit and test pits for aggregates. In addition, Detour Gold Corporation provided helicopter support for access to areas with poor accessibility.

The Detour gold mine is located in a strongly fluted area formed during the Cochrane ice readvance (Figure 23.5). In this flat, boggy lowland, bedrock sporadically crops out in low-relief ridges (*see* Figure 23.5). The lithostratigraphy above the bedrock for this area is well exposed in a recently excavated road ditch at the mine, which consists of a lower sandy to bouldery till (Unit A), an upper clayey till (Unit B), and overlying glaciolacustrine fines (Unit C) beneath a colluvial deposit and peat (Unit D) (Photo 23.1). The lower till, about 1.5 m thick, is pale to greyish in colour, has a sand-rich matrix and contains abundant cobbles and boulders dominated with granite and paragneiss or metasedimentary rocks. Limestone clasts are present but low in concentration in comparison with the upper till. The matrix is soft and lacks compactness and fissility in wet conditions. It shows weak reaction to 10% HCl. Because the till rests directly on basalt bedrock, the striae at 150° (measured from the underlying bedrock) likely indicate the direction of the ice flow that emplaced the till. The brownish, upper clayey till, 0.3 m thick, is stone poor, contains a high proportion of limestone clasts, and shows apparent compactness and well-developed fissility (Photo 23.2). It has an irregular, sharp lower contact (*see* Photos 23.1 and 23.2). Its matrix reacts strongly to 10% HCl. The ice-flow direction is estimated to be 146° as measured from the bedrock that directly underlies this till approximately 40 m east of this section along the same ditch. Approximately 1 km southwest of this site, this till reaches 6 to 8 m thickness in the open pit mine currently under development.



Photo 23.1. Greyish bouldery Matheson Till (A) overlain by the brownish clayey Cochrane Till (B), which is overlain, in turn, by a massive to laminated glaciolacustrine clay of Lake Ojibway (C) beneath a colluvial silty sand (D). The glaciolacustrine deposit can be divided into a clast-rich lower part with lamination (C1) and a massive clay with fewer clasts (C2). Recent peat is less than 10 cm thick at this locality. Hammer 32 cm long. Refer to Figure 23.5 for location.

The sandy to bouldery till commonly occurs in the areas covered by NTS maps 32 E/4, 32 E/5, 42 H/1 and 42 H/8, and its direct contact with an overlying clayey till has been recorded from a site at the western border of the area covered by NTS map 32 E/4 (Gao and Day 2008). However, this till has not been well documented in exposures in the northern part of the map area, that is, from the previous work done in the areas covered by NTS maps 32 E/13 and 32 L/4 (Gao and Day 2008; Gao and Kodors 2009). This section as described above thus attests to a consistent surficial till stratigraphy in the map area that spans 140 km from the north to the south. As discussed above, the sandy to bouldery till and the overlying clayey till can be conveniently correlated to the Matheson Till and the Cochrane Till, respectively (Gao and Day 2008; Gao and Kodors 2009; Gao 2010). Till deposits older than the Matheson Till have been reported from boreholes (Smith 1992; Gao and Day 2008); however, their stratigraphic status remains to be confirmed.

Unit C is a massive, clay-rich deposit interpreted as being of a glaciolacustrine origin. It contains ice-rafted pebble-sized clasts and clayey till balls and has a sharp lower contact (*see* Photos 23.1 and 23.2). It can be subdivided into a lower and an upper part. The lower part (C1) has a diamict facies and, in many cases, it seemingly resembles the Cochrane Till below. However, it lacks compactness and fissility and contains, characteristically, laminations that attest to a glaciolacustrine origin (*see* Photo 23.2). That said, it is not readily separable from the underlying clayey till in the field without well-exposed sections such as this one for reference. The abundance of ice-rafted debris in this deposit indicates ice proximal conditions. This deposit grades upward into a massive clay (C2) (*see* Photo 23.1). About 0.8 km east of this site, this subunit is rich in silt, with well-developed, but distorted, lamination. Although pebble clasts are present, they are fewer than the underlying subunit C1. A decrease in the concentration of ice-rafted debris was probably related to a progressive retreating ice sheet that was farther away from this site.

The glaciolacustrine deposit indicates the inundation of this area in a proglacial lake (Lake Ojibway). However, it is, in general, thin and has not completely masked off the surface lineations generated during the Cochrane ice readvance. In the northern half of the area covered by NTS map 32 L/4 and further



Photo 23.2. Enlarged view of the Matheson and Cochrane tills and the overlying Lake Ojibway deposit. Note the sharp contact between these deposits (white arrows) and lamination in the lake deposit (black arrow). The Cochrane Till contains sand lenses and streaks in the upper part. Dark areas in the Matheson Till are weathered gneiss. Trowel 28 cm long.

northwest to Kesagami Lake, the surface lineations are less recognizable to nonexistent (*see* Figure 23.1 for location). This may be partly explained by the presence of a thick glaciolacustrine deposit there. Stratigraphically, this glaciolacustrine deposit is associated with Lake Ojibway that fronted the retreating Cochrane ice sheet and drained into the Hudson Bay in the early Holocene (Veillette 1994; Dyke 2004; Roy et al. 2011; Breckenridge et al. 2012).

Unit D at the top of the section has an irregular, sharp lower contact and contains a poorly sorted, massive to stratified silty sand with pebbles and occasional cobbles beneath a peat about 0.1 to 0.3 m thick (*see* Photo 23.1). In the vicinity, this deposit is no more than a few centimetres thick and, in many cases, consists of a thin layer of pebbles and coarse sand below the peat. The massive to stratified texture suggests a colluvial origin for this deposit probably related to wave washing along the shores of shallow, ephemeral lakes or ponds developed on the newly exposed lake plain after the drainage of Lake Ojibway. At that time, wave erosion was likely intense given a thin vegetation and the presence of strong wind as indicated by the development of extensive eolian deposit (*see* Figure 23.4).

SUMMARY

Six 1:50 000 scale surficial geology maps are being compiled for the Detour Lake–Burntbrush area along the Ontario–Quebec provincial border, northern Ontario (*see* Figure 23.1). In the map area that spans 140 km from the north to the south, a consistent stratigraphy exists for the Late Wisconsin to Holocene, which consists of, up section, a sandy to bouldery till, glaciolacustrine deposits, a silty to clayey till, glaciolacustrine deposits, and post-Lake Ojibway deposits. The 2 tills can be correlated to the Matheson Till and the overlying Cochrane Till. The glaciolacustrine deposits accumulated in Lake Ojibway. The Matheson Till is the principal deposit emplaced during the Late Wisconsin glacial maximum. The associated ice flow had a direction of 150°, at least during its most recent phase. Glaciolacustrine fines developed in Lake Ojibway in front of the retreating ice sheet. Later, the ice sheet readvanced into the lake during the Cochrane Stadial in the early Holocene (Photo 23.3; *also see* Figure 23.2). The Cochrane ice advanced in

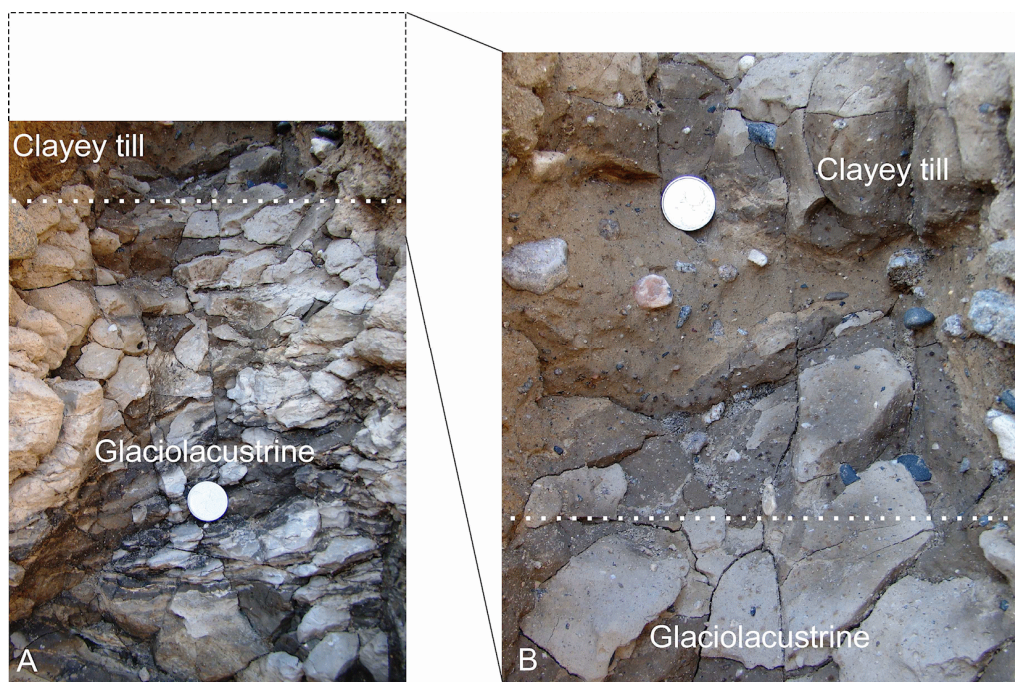


Photo 23.3. Glaciolacustrine clay of Lake Ojibway grades into the overlying clayey Cochrane Till from a section in Cochrane. Their boundary is highlighted by dotted white line. A) Glaciolacustrine clay that shows distorted but well-developed lamination. B) Enlarged view of the overlying Cochrane Till. Note its gradational lower contact. Coin 3.2 cm diameter.

a southeast-aligned path centred at 146° in this region. With the retreat of the Cochrane ice sheet, Lake Ojibway was drained in the early Holocene. After its drainage, the area covered by this study saw a strong eolian and wave-washing process that resulted in the development of extensive sand dunes and accumulation of colluvial deposits in ephemeral lakes prior to the colonization by vegetation of the newly formed lake plain.

In contrast to the Matheson Till, which is suitable for sampling for indicator minerals because of its local source of rock fragments, the Cochrane Till is not an ideal deposit for sampling because its distal source of lithogenic material is in Hudson Bay. The common occurrence of the Cochrane Till, together with overlying thick glaciolacustrine fines, renders till sampling difficult. Reverse-rotary drill is recommended for future till sampling projects in these areas.

ACKNOWLEDGMENTS

The author wishes to thank David Zhu for field assistance. Thanks are also extended to Detour Gold Corporation, in particular, to Guy MacGillivray, Michael Bingham, Charles Hartley and Adree Delazzer for providing logistics and helicopter support for the field work. Jack Parker reviewed the manuscript and put forward many suggestions and comments that helped improve the quality of this paper.

REFERENCES

- Boissonneau, A.N. 1966. Glacial history of northeastern Ontario; *Canadian Journal of Earth Sciences*, v.3, p.559-578.
- Breckenridge, A., Lowell, T.V., Stroup, J.S. and Evans, G. 2012. A review and analysis of varve thickness records from glacial Lake Ojibway (Ontario and Quebec, Canada); *Quaternary International*, v.260, p.43-54.
- Dyke, A.S. 2004. An outline of North American deglaciation with emphasis on central and northern Canada; *in* *Quaternary glaciations—extent and chronology, Part II: North America*, Elsevier, Amsterdam, p.373-424.
- Gao, C. 2010. Surficial geology and till stratigraphy in the Detour Lake and Burntbush areas, northeastern Ontario; *in* *Summary of Field Work and Other Activities 2010*, Ontario Geological Survey, Open File Report 6260, p.26-1 to 26-5.
- Gao, C. and Day, A. 2008. Quaternary geology of the Burntbush area, north of Lake Abitibi, northeastern Ontario; *in* *Summary of Field Work and Other Activities 2008*, Ontario Geological Survey, Open File Report 6226, p.21-1 to 21-5.
- Gao, C. and Kodors, C. 2009. Update on surficial mapping and till sampling in the Detour Lake and Burntbush areas, northeastern Ontario; *in* *Summary of Field Work and Other Activities 2009*, Ontario Geological Survey, Open File Report 6240, p.18-1 to 18-6.
- Hughes, O.L. 1965. Surficial geology of part of the Cochrane District, Ontario, Canada; *in* *International Studies on the Quaternary, 7th International Quaternary Association (INQUA) Congress*, Geological Society of America, Special Paper 84, p.535-565.
- Prest, V.K. 1969. Retreat of Wisconsin and recent ice in North America glacial map; Geological Survey of Canada, Map 1253A, scale 1:5 000 000.
- Roy, M., Dell'Oste, F., Veillette, J.J., de Vernal, A., Hélie, J.-F. and Parent, M. 2011. Insights on the events surrounding the final drainage of Lake Ojibway based on James Bay stratigraphic sequences; *Quaternary Science Reviews*, v.30, p.682-692.
- Smith, S.L. 1992. Quaternary stratigraphic drilling transect, Timmins to the Moose River Basin, Ontario; Geological Survey of Canada, Bulletin 415, 94p.

Veillette, J.J. 1994. Evolution and paleohydrology of glacial lakes Barlow and Ojibway; *Quaternary Science Reviews*, v.13, p.945-971.

——— 2007. Géologie des formations en surface et histoire glaciaire, Rivière Harricana, Québec; Geological Survey of Canada, Map 1993A, scale 1:100 000.

Veillette, J.J. and Thibaudeau, P. 2007. Géologie des formations en surface et histoire glaciaire, Rivière Wawagasic, Québec; Geological Survey of Canada, Map 1995A, scale 1:100 000.

24. Project Unit 08-008. Field Investigations for Remote Predictive Terrain Mapping in the Far North of Ontario

P.J. Barnett¹ and K.H. Yeung¹

¹Earth Resources and Geoscience Mapping Section, Ontario Geological Survey

INTRODUCTION

Field observations for the Far North Terrain Mapping project continued during the summer of 2012 (Figure 24.1; Barnett et al. 2008; Barnett, Webb and Hill 2009; Barnett and Yeung 2009a, 2009b, 2010, 2011). There were 2 areas of field investigation. The first area of investigation included the examination of river exposures along selected tributaries of the Kenogami River, in particular the Ridge, Little Current and Drowning rivers, to provide information on material change with depth; and the second area, located southwest of the “Ring of Fire” chromite occurrences west to Pickle Lake, was designed to obtain information on the areal distribution and properties of the various surficial materials that occur in this part of the Far North. The study of exposures along the Ridge River will form part of a Master of Science (MSc) thesis being undertaken by M.K. Nguyen at Western University (*see* Nguyen, Hicock and Barnett, this volume, Article 25). The areas investigated straddle the boundary between the Precambrian Shield and the Hudson Bay Lowland within the southernmost part of the Far North. The 2 areas are displayed on National Topographic System (NTS) maps: 42 K/E and 42 J/W (riverbank exposure study) and 52 P, 52 O/N, 53 A/W, 42 M/W (surface mapping). This summary will discuss primarily the findings of the surface observation study; for preliminary observations from the study of riverbank exposures, *see* Nguyen, Hicock and Barnett (this volume, Article 25).

FINDINGS

The Agutua moraine is the most prominent landform in the study area, rising over 100 m above the surrounding landscape in several places along its length (Photo 24.1). Its width can commonly exceed 4 km wide. This moraine appears to be composed almost entirely of stratified sand and gravel. In part, it appears to be formed of coalescing subaqueous fans, in others, deltas. A large, deep proglacial lake (glacial Lake Agassiz) fronted the ice margin as the moraine formed. One large ice-marginal delta, located 12 km northeast of Windigo Lake, indicates lake level once occurred above 410 m above sea level (asl) in this area during moraine formation. Subsequent reworking by waves and currents of falling levels of this lake formed a spectacular series of raised shorelines around exposed parts of the moraine.

As suggested by Prest (1963a), there is evidence of a readvance of the ice margin to override parts of this landform, but the extent of the readvance of at least 25 miles as suggested by Prest (1963a) could not be verified due to poor and limited natural exposures during the time of field observations. Parts of the moraine immediately south of Troutfly Lake to approximately Pringle Lake have been augmented by surface fluting oriented toward the west-southwest as previously indicated by Prest (1963a, 1963b).

Interesting relationships exist between the Agutua moraine and the many esker systems that are located nearby. Some appear to be buried by the sediments of the moraine (pre-existing), others terminate in fan-shaped bodies that become part of the moraine (contemporaneous) and still others appear to pass right through the moraine at odd angles apparently unaffected by moraine sedimentation (postdate the moraine?).

*Summary of Field Work and Other Activities 2012,
Ontario Geological Survey, Open File Report 6280, p.24-1 to 24-5.*

© Queen's Printer for Ontario, 2012

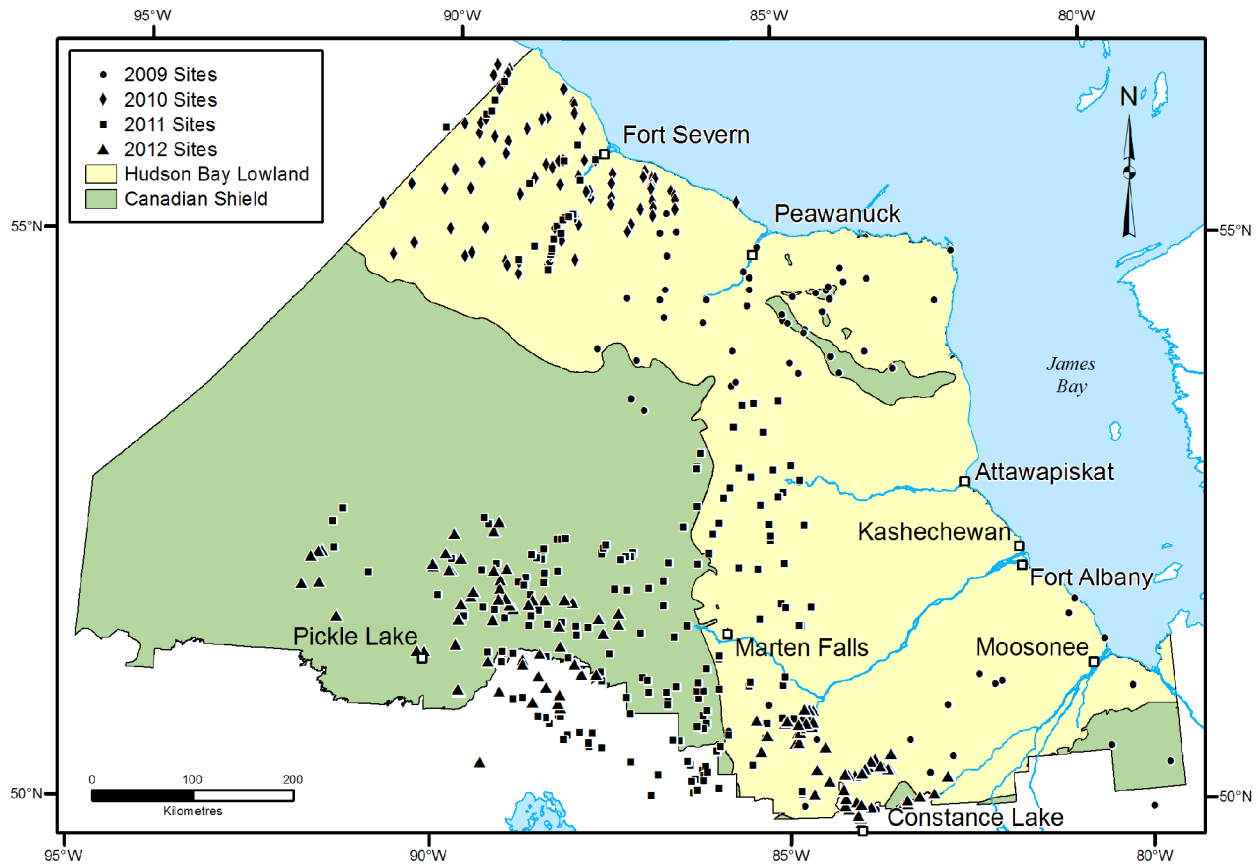


Figure 24.1. Location of field sites visited during the summers of 2009, 2010, 2011 and 2012.



Photo 24.1. Distal view of the Agutua moraine (photo courtesy of Z. Pironkova, Ministry of Natural Resources).

The glaciofluvial systems are extensive in the area. Large branching networks of eskers are near continuous across the landscape in the area mapped. For example, the esker ridge, on which the community of Pickle Lake is built, is nearly continuous from the Agutua moraine southwestward for 135 km and a branching esker south of Keezhik Lake can also be traced eastward beyond 135 km from the Agutua moraine. Esker ridges are of various sizes and can obtain heights of greater than 45 m above the surrounding landscape. They are composed predominantly of sand and gravelly sand where observed, with the exception of boulder gravel ridges exceeding 15 m in height within the feature mapped by Prest (1963b) as the Windigo interlobate moraine. In places, esker ridges have been modified by waves and currents associated with the shoreline of a proglacial lake; elsewhere, the esker ridges appear to be pristine or unmodified.

It has been difficult to determine to date whether certain northwest-trending ridges that in places cross the dominant south-southwest and southwest esker ridges are end moraines or part of the esker systems. In places, parts of the northwest-trending ridges are strongly asymmetrical, but, elsewhere along the same ridge, they can be sinuous with a symmetrical profile. Up to 7 west-northwestward-trending end moraines occur west of (in front of) the Agutua moraine in the vicinity of Windigo Lake in addition to the series of landforms identified by Prest (1963b) as the Windigo interlobate moraine. Other moraines in the area are the 2 main ridges of the Nakina moraines, a moraine southeast of Opapimiskan Lake and the Big Beaver House moraine that is associated with fine-grained till.

Till occurs as ground moraine, in drumlins, Røgen or ribbed moraine and De Geer or washboard moraine. The latter landform occurs primarily in the vicinity of North Caribou Lake. Streamline landforms (drumlins, flutes) vary greatly in long-axis orientation across the area from southwestward through to westward (*see* Barnett, Webb and Hill 2009; Barnett and Yeung 2011). Till west of the Agutua moraine varies from a sandy silt to a silty, very-fine sand till with variable clast content. East of the moraine, the till in drumlins is commonly a sandy silt diamicton.

The flanks of some drumlins and the area between them appear to have been intensely eroded in places producing a suite of landforms from classic Røgen or ribbed moraine through scabland-type erosion surfaces to trains of large-scale megaripples composed of large boulders (Photo 24.2). Boulder lags are common in these areas of scour, and these areas will be mapped as being underlain by boulder silty sand to sand till on the series of surficial geology maps being produced in this project. It is suggested that the erosion event occurred subglacially during the release of large volumes of stored subglacial meltwater (a jökulhlaup).

Interestingly, eskers commonly located within these areas of scour are themselves not affected by the erosion event and, therefore, must have formed subsequent to it, possibly as flows began to subside. Their long continuous extent and their extensive tributary network may suggest that ice stagnation may have followed the subglacial discharge event(s). Small tunnel channels can be associated with the eskers in areas of elevated terrain. The Agutua moraine may be a product of this release of meltwater as well, possibly through a similar mechanism as suggested by Sharpe and Cowan (1990) for the Eagle–Findlayson, Hartman and Lac Seul moraines that occur to the west of the area investigated this past summer.

Extensive areas of silt and clay and wetland deposits occur between the Big Beaver House moraine and the Agutua moraine, generally west of Attawapiskat Lake. The remainder of the terrain is underlain primarily by bedrock at or near the surface. The bedrock occurs as prominent ridges or along the floor of valleys where the low-relief bedrock surface (Photo 24.3) is partially buried by extremely bouldery and sandy till. Bedrock surfaces have been washed cleaned in areas that occurred within wave base of the former proglacial lake.

Two new exposures containing interglacial sediments below till were described and sampled in addition to 54 sites along the tributaries of the Kenogami River within the Far North of Ontario.

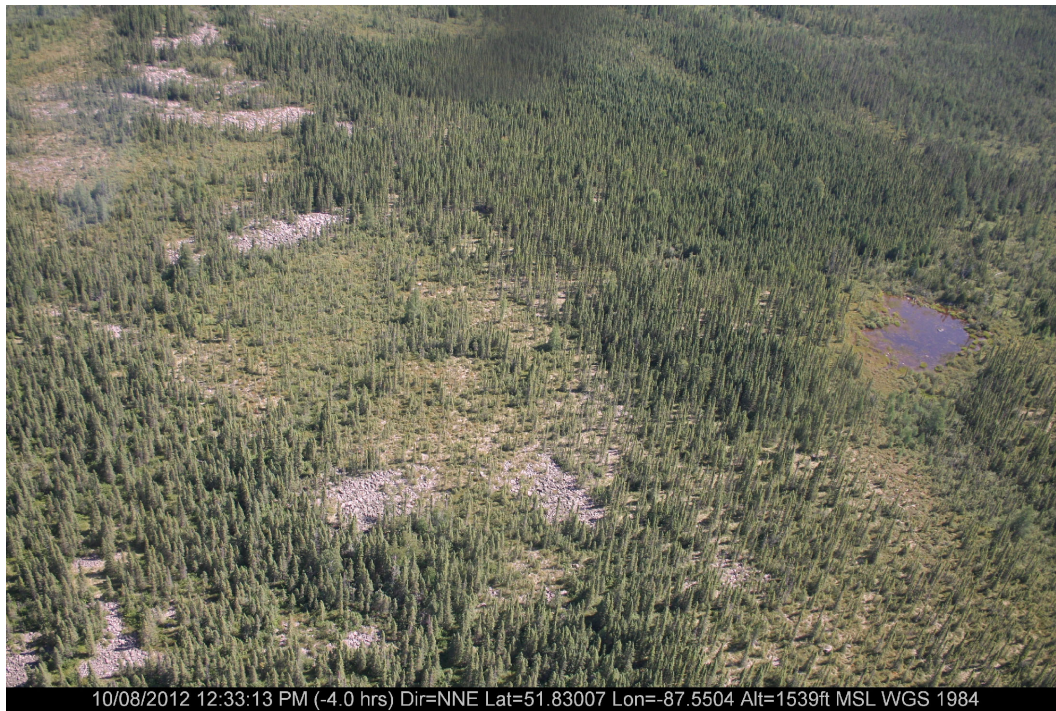


Photo 24.2. Train of bouldery megaripples (photo courtesy of Z. Pironkova, Ministry of Natural Resources).



Photo 24.3. Low-relief bedrock surface and thin bouldery till cover (photo courtesy of Z. Pironkova, Ministry of Natural Resources).

Remote predictive mapping procedures continue to be modified as terrain conditions and relationships between surface material, vegetation and topography change. Extensive areas of disturbance, such as previously burned or logged areas, continue to provide problems for the remote predictive mapping process. Maps for the traditional land of the Moose Cree and Weenusk First Nations have been released, with work continuing within the traditional land of the Washaho Cree Nation and within the area of the “Ring of Fire” chromite occurrences and potential transportation corridors.

ACKNOWLEDGMENTS

The authors would like to thank the First Nation communities whose traditional areas were covered by this study for their overall support. The assistance of M.K. Nguyen and Dr. S.R. Hicock (Western University) and Dr. Z. Pironkova (Ministry of Natural Resources) in the field and J.D. McCallum (OGS) for her help in map production is greatly appreciated.

The Ministry of Natural Resources (MNR) provided helicopter support throughout the project. The assistance of Rick Olar (MNR) and Gord Pearson of the Aviation Services Centre with flight planning and the help and dedication of Bill Spiers, Rob Fletcher, Dan Steckly, and Andy Brunet, MNR helicopter pilots are gratefully appreciated.

REFERENCES

- Barnett, P.J., Dodge, J.E.P., Webb J.L. and Hill, J.L. 2008. Far North Information Knowledge Management planning initiative terrain mapping project; *in* Summary of Field Work and Other Activities 2008, Ontario Geological Survey, Open File Report 6226, p.25-1 to 25-5.
- Barnett, P.J., Webb, J.L. and Hill, J.L. 2009. Flow indicator map of the far north of Ontario; Ontario Geological Survey, Preliminary Map P.3610, scale 1:1 000 000.
- Barnett, P.J. and Yeung, K.H. 2009a. Far North terrain mapping project; *in* Summary of Field Work and Other Activities 2009, Ontario Geological Survey, Open File Report 6240, p.17-1 to 17-5.
- 2009b. Remote predictive mapping of surficial geology in aid of regional land-use planning in the Far North of Ontario, Canada; Prairie Summit 2010, Regina, Saskatchewan, Proceedings, p.41-44.
- 2010. Far North terrain mapping project—Fort Severn; *in* Summary of Field Work and Other Activities 2010, Ontario Geological Survey, Open File Report 6260, p.25-1 to 25-6.
- 2011. Far North Terrain Mapping Project—“Ring of Fire” and the Severn River area; *in* Summary of Field Work and Other Activities 2011, Ontario Geological Survey, Open File Report 6260, p.22-1 to 22-7.
- Prest, V.K. 1963a. Red Lake–Lansdowne House area, northwestern Ontario, surficial geology; Geological Survey of Canada, Paper 63-6, 23p.
- 1963b. Surficial geology, Red Lake–Lansdowne House area, Ontario; Geological Survey of Canada, Preliminary Map 5-1863, scale 1:506 880.
- Sharpe, D.R. and Cowan, W.R. 1990. Moraine formation in northwestern Ontario: product of subglacial fluvial and glaciolacustrine sedimentation; *Canadian Journal of Earth Sciences*, v.27, p.1478-1486.

25. Project Unit 08-008. Quaternary Stratigraphy of the Ridge River Area in Support of Far North Terrain Mapping

M.K. Nguyen¹, S.R. Hicock¹ and P.J. Barnett²

¹Department of Earth Sciences, Western University, London, Ontario N6A 5B7

²Earth Resources and Geoscience Mapping Section, Ontario Geological Survey, Sudbury, Ontario P3E 6B5

INTRODUCTION

The examination of natural river exposures was conducted in the Ridge River area of the Hudson Bay Lowland in northeastern Ontario during the summer of 2012 (Figure 25.1). The purpose of the study is to investigate the Quaternary stratigraphy and glacial geology of the Ridge River area as part of a larger mapping project encompassing the Far North region of Ontario (*see* Barnett and Yeung, this volume, Article 24).

The study of the riverbank exposures will provide details on Laurentide Ice Sheet behaviour in an area previously studied only in reconnaissance (Skinner 1973; Geological Survey of Canada 1967). It will also form the basis of a Master of Science (MSc) thesis at Western University in the Department of Earth Sciences under the supervision of Dr. S.R. Hicock.

A detailed stratigraphic study will determine facies characteristics, distribution and depositional environments in the region. This should reveal the number of distinct till units and their associated ice-flow directions. Such information should provide a better understanding of local glacial history including ice-flow patterns and past glacial and nonglacial episodes. Furthermore, the location of the area near the southern margin of the James Bay Lowland will improve our understanding of the link between the distribution and composition of Quaternary sediments in the Hudson Bay Lowland and the Canadian Shield to the south.

LOCATION AND FIELD WORK

Field work was conducted during 2 separate excursions in June and August and took place primarily in the Ridge River area approximately 85 km northwest of the town of Hearst, Ontario. Field studies consisted of helicopter-supported exploration of riverbank exposures within an area of nearly 6000 km². This included a 60 km stretch of the Ridge River, a 50 km stretch of the Kenogami River (including parts of its southern tributaries), south from its confluence with the Ridge River and as far east as the Pivabiska River.

The stratigraphic units of every exposed section examined were carefully measured and described. Till matrix samples were collected and will be analyzed for particle size distribution (ASTM 2007), carbonate content (including calcite and dolomite proportions; Dreimanis 1962) and heavy mineral content (Gwyn and Dreimanis 1979). Supplementary data include pebble counts (pebble lithology identification), till fabrics (pebble long-axis orientation; Hicock et al. 1996), and various structural measurements (including the orientation of shear planes, extension fracture, etc.) within and below the till units (Photo 25.1; Hicock and Dreimanis 1985). In addition, preserved striations found on boulder tops were recorded. These data will allow us to construct stratigraphic fence diagrams and maps of the study area. Furthermore, radiocarbon dating of collected buried organic material may improve the existing geochronology.

*Summary of Field Work and Other Activities 2012,
Ontario Geological Survey, Open File Report 6280, p.25-1 to 25-3.*

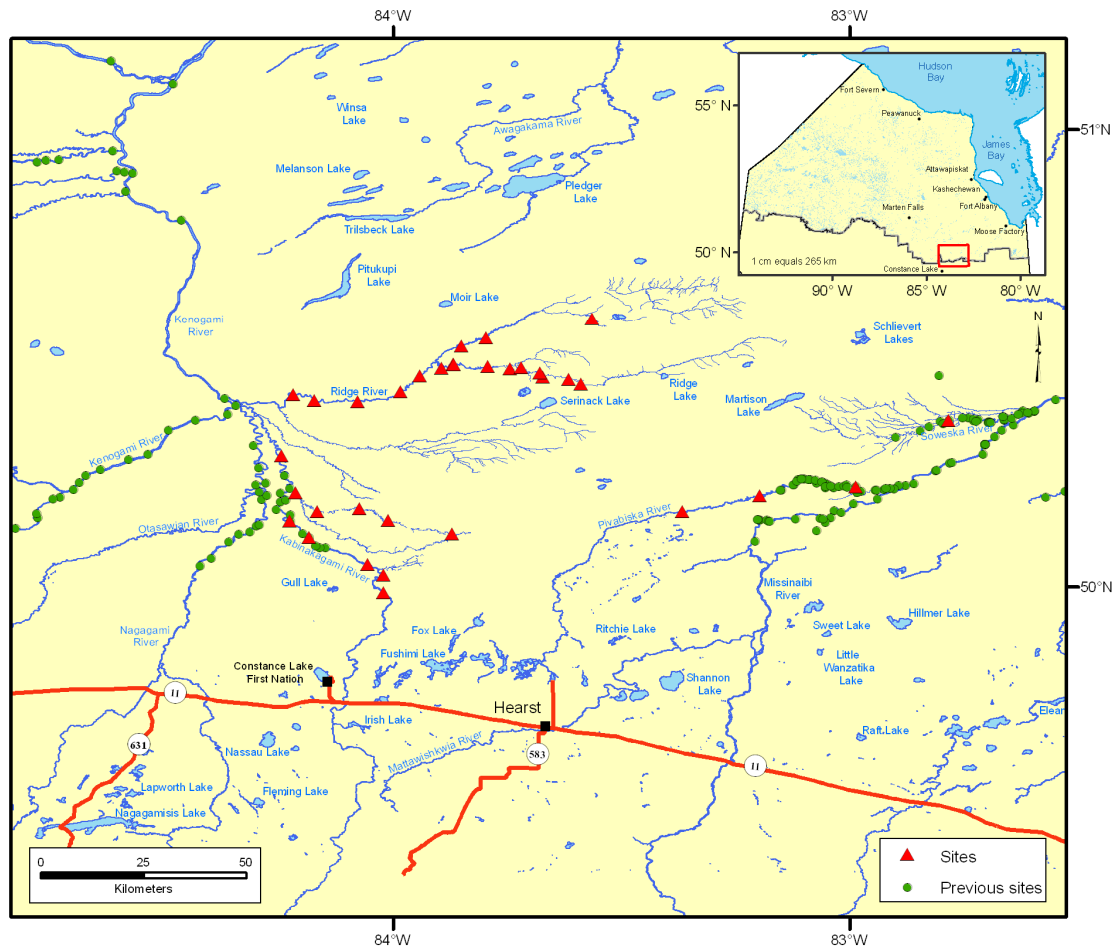


Figure 25.1. Location of the Ridge River study area: sites investigated and previously studied sites (Skinner 1973; Geological Survey of Canada 1967).



Photo 25.1. Measuring the orientation of the long axis of stones within till (till fabric), Ridge River study area.

ACKNOWLEDGMENTS

The authors thank the Constance Lake First Nation for their overall support of this study. The senior author thanks the Ontario Geological Survey, Ministry of Northern Development and Mines for the in-kind support for this MSc thesis.

The Ministry of Natural Resources (MNR) provided helicopter support throughout this study. The assistance of Rick Olar (MNR) and Gord Pearson of the Aviation Services Centre with flight planning and the help and dedication of Bill Spiers, Dan Steckly and Andy Brunet, MNR helicopter pilots are greatly appreciated.

REFERENCES

- American Society for Testing and Materials 2007. D422-63. Standard test method for particle-size analysis of soils; ASTM International, West Conshohocken, Pennsylvania, p.112-122.
- Dreimanis, A. 1962. Quantitative gasometric determination of calcite and dolomite by using Chittick apparatus; *Journal of Sedimentary Petrology*, v.32, p.520-529.
- Geological Survey of Canada 1967. Operation Winisk; Geological Survey of Canada, unpublished field notes.
- Gwyn, Q.H.J. and Dreimanis, A. 1979. Heavy mineral assemblages in tills and their use in distinguishing glacial lobes in the Great Lakes Region; *Canadian Journal of Earth Sciences*, v.16, p.2219-2235.
- Hicock, S.R. and Dreimanis, A. 1985. Glaciotectonic structures as useful ice-movement indicators in glacial deposits: four Canadian case studies; *Canadian Journal of Earth Sciences*, v.22, p.339-346.
- Hicock, S.R., Goff, J.R., Lian, O.B. and Little, E.C. 1996. On the interpretation of subglacial till fabric; *Journal of Sedimentary Research*, v.66, p.928-934.
- Skinner, R.G. 1973. Quaternary stratigraphy of the Moose River Basin, Ontario; Geological Survey of Canada, Bulletin 225, 77p.

26. Project Unit 11-027. Greenstone Area High-Density Lake Sediment and Water Survey, Northwestern Ontario

R.D. Dyer¹ and H.E. Burke¹

¹Earth Resources and Geoscience Mapping Section, Ontario Geological Survey

INTRODUCTION

Field work for a high-density lake sediment and water geochemical survey of the Greenstone area, in northwestern Ontario, was carried out between July 18 and August 7, 2012. This is the second year of a two-year project (*see* Dyer 2011) to survey the area extending from the town of Longlac westward to Lake Nipigon. This survey area straddles the boundary between the Wabigoon and Quetico subprovinces of the Superior Province, and covers most of the Beardmore–Geraldton and Onaman–Tashota greenstone belts.

This summer's activities focussed primarily on the southern and northwestern portions of the Greenstone study area (Figure 26.1). Coverage over the areas represented by National Topographic System (NTS) map sheets 42 E/10 and 42 E/11 was completed and, in addition, the survey was extended to include NTS map sheet 42 L/4 in order to cover the northern extent of the Onaman–Tashota greenstone belt. Infill sampling was also carried out in the area outlined by map sheets 42 E/13 and 42 E/14 and some of 42 H/15.

This field season, a total of 953 water samples and 1732 lake sediment samples were collected over an area of approximately 4960 km². The 1732 sediment samples comprise 907 shallow samples (0 to 15 cm sediment depth) and 843 deep samples (>20 cm sediment depth). The total for the combined 2011 and 2012 Greenstone surveys is 2246 sample sites over an area of 6170 km² corresponding to an average sample density of 1 sample site per 2.7 km². The Greenstone region was previously sampled at a much lower density during the late 1970s and early 1980s for the National Geochemical Reconnaissance (NGR) lake sediment program carried out jointly by the Geological Survey of Canada (GSC) and the Ontario Geological Survey (OGS) (Hornbrook, Coker and Lynch 1978a, 1978b; Hornbrook et al. 1990). The results from this new two-year OGS Greenstone survey will provide updated high-resolution geochemical data for both mineral exploration and environmental baseline purposes.

REGIONAL SETTING AND GEOLOGY

The study area contains Archean rocks of the Wabigoon (Blackburn et al. 1991) and Quetico subprovinces (Williams 1991) of the Superior Province. Younger Proterozoic Nipigon diabase sills (Sutcliffe 1991) of the Southern Province are located in the western extremity of the study area. The southern half of the survey area (which was the focus of this year's field work) is underlain by monotonous metasedimentary rocks, paragneiss, migmatite and granite that dominate the rocks of the Quetico Subprovince. The northern half is underlain mostly by supracrustal rocks of the Beardmore–Geraldton and Onaman–Tashota greenstone belts, later intrusive rocks (e.g., gabbro, granodiorite) and basement granitoids. Two regional bedrock compilation maps covering the area have been completed at a scale of 1:250 000 (Johns, McIlraith and Stott 2003; Stott et al. 2002).

*Summary of Field Work and Other Activities 2012,
Ontario Geological Survey, Open File Report 6280, p.26-1 to 26-5.*

Mineral exploration activity within the study area has been focussed historically on gold, with the first production occurring in 1934 (Mason and White 1986). Since 1934, approximately 4.3 million ounces of gold have been recovered from the region from 24 past-producing mines (Speed and Craig 1992). Very little exploration work in the region was carried out between the early 1990s and 2006; however, renewed interest in the gold potential of the Beardmore–Geraldton area was spurred on by discovery of a new gold zone (“the golden mile”) by Kodiak Exploration (now Prodigy Gold Inc.) in 2007 (Kociumbas and Power-Fardy 2010). Since 2007, Premier Gold Mines Ltd. has also been very active in the Geraldton camp, focussing efforts on the past-producing Hardrock Mine area, where they have reported measured and indicated resources of 2.5 million ounces of gold (www.premiergoldmines.com/s/Hardrock.asp [accessed September 13, 2012]).

The project area lies within uplands of the James Region physiographic division of the Canadian Shield (Bostock 1970). In most of the eastern and central portions of the area, the topography is rolling or relatively flat coinciding with the presence of either granitoid bedrock or thick glacial deposits; relief rarely exceeds 60 m. The topography of the western half of the study area is more bedrock controlled, with the presence of volcanic rocks and, at the western extremity, Proterozoic Nipigon sill rocks, where the incidence of cliffs and dramatic topographic changes is significant. Two large areas within the survey area are dominated by glaciolacustrine sand and contain very few lakes; these are located in Bickle Township and at the northwestern end of the survey area between Lake Nipigon and Onaman Lake.

The regional surficial geology of the area was first compiled by Zoltai (1965). The surficial deposits were outlined in more detail with the publication of 1:100 000 scale engineering geology terrain (NOEGTS) maps that cover the study area (Gartner 1979a, 1979b; Mollard and Mollard 1981). The most recent Quaternary mapping and till sampling of the area was undertaken by Thorleifson and Kristjansson (1993), which coincides almost exactly with the present lake sediment survey area. These studies indicate

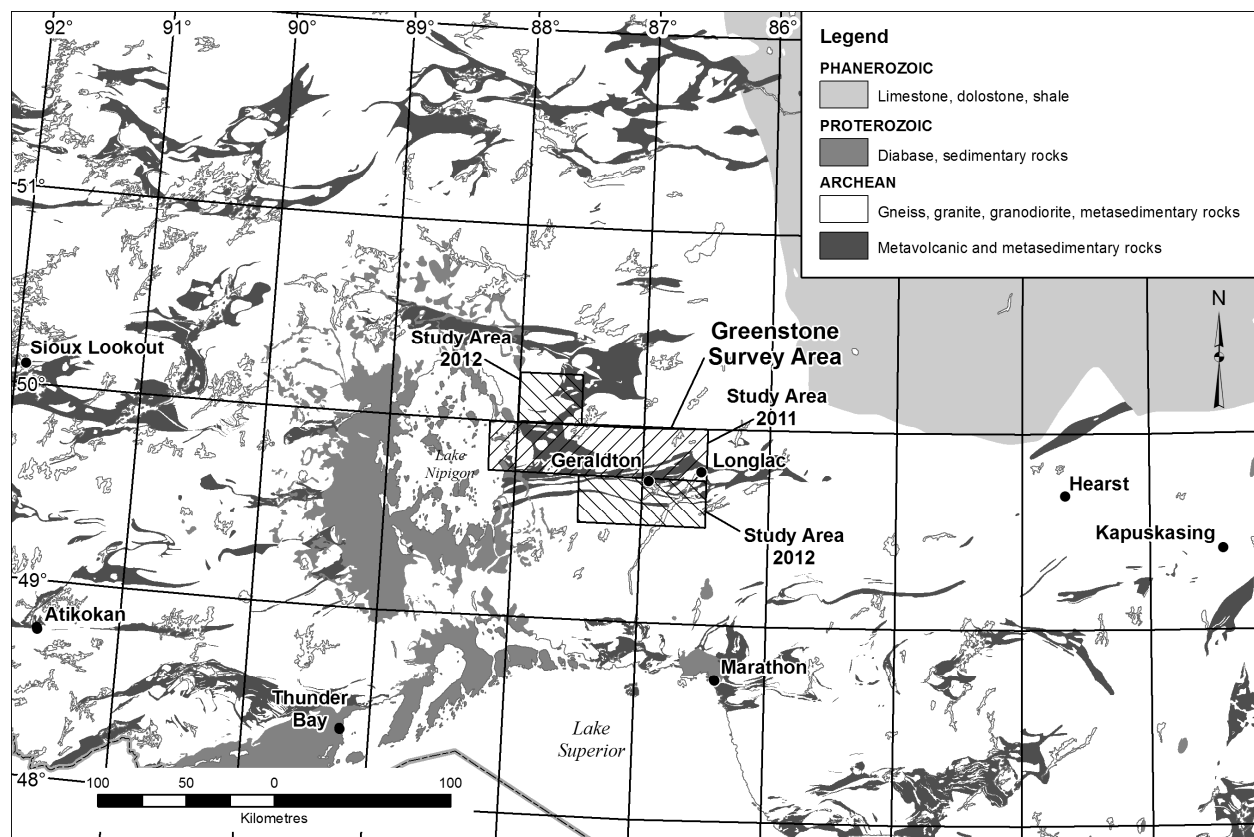


Figure 26.1. Location map of the 2011 and 2012 Greenstone area lake sediment and water surveys.

that the most common surficial material within the survey area is till, which ranges from thin (<1 m thick) and discontinuous to laterally extensive and thick; the latter is present in the central portion of the survey area centred on Wildgoose Lake. Glaciofluvial (esker) deposits (sand and gravel) form prominent belts across the study area with a general trend to the southwest. Glaciolacustrine deposits are also common and associated with areas of low topography within and around the perimeters of large lakes, especially Lake Nipigon. Dominant ice direction, based on bedrock striae and other ice-flow indicators, features a radiating pattern from 250° in the western portion of the study area, gradually becoming 210° at Longlac (Thorleifson and Kristjansson 1988).

SAMPLING METHODS

Organic-rich lake sediment samples were collected from a helicopter float using the OGS-designed gravity corer. Wherever possible, both shallow (0 to 15 cm) and deep (>20 cm) sediment samples were obtained at each sampling site. Based on average sediment rates of approximately 1.5 cm per decade within lakes on shield landscapes (e.g., Hunt 2003; Dickman and Fortescue 1991), the shallow sample is considered to represent sedimentation during the past 100 years (approximately) and, therefore, may be subject to anthropogenic contamination. The deep sediment sample represents sedimentation older than 100 years; therefore, this portion better reflects the effects of natural geochemical inputs that may be traced to local geology and/or mineralization.

Lake water samples were collected from a depth of between 0.5 and 1.0 m using a weighted intake hose and pump. Water-quality parameters, including pH and conductivity, were measured at each lake site using a flow cell attached to a multiparameter probe. Lake water was pumped from each lake and allowed to purge the sampling system prior to the collection of a water sample and the recording of water quality parameters. Water samples were kept cool after collection and processed (filtered and acidified) within 6 hours of collection.

A global positioning system (GPS) receiver was utilized to record accurate sample-site positions and to record each flight track. In addition, a GPS receiver connected to a tablet computer was utilized to provide “heads up” real-time navigation between lake sites.

SAMPLE PREPARATION AND ANALYTICAL METHODS

Lake sediment samples were placed in breathable fabric bags and allowed to partially air dry prior to shipment to Sudbury. Final drying was done in ovens at a temperature of less than 40°C prior to partial pulverization in a ceramic ring and puck pulverizer and sieving to obtain the –60 mesh (<250 µm) size fraction. Laboratory analysis will include nitric acid–aqua regia digestion followed by inductively coupled plasma mass spectrometry (ICP–MS) to determine approximately 50 trace elements. Nitric acid–aqua regia digestion attacks all sample matrix constituents, except for silicate minerals and, therefore, is considered a nonselective, relatively strong partial extractant. Quality control will be monitored through the use of certified and internal reference materials and sample pulp duplicates. Loss-on-ignition (LOI) is determined at 500°C, using an automated gravimetric technique. The deep (>15 cm) sediment samples will undergo further analysis for arsenic, gold and rare earth elements (REE) by instrumental neutron activation analysis (INAA).

Water samples were passed through 0.45 µm syringe filters and acidified to 1% ultrapure nitric acid within 6 hours of collection. Analysis of water will include direct aspiration ICP–MS to determine approximately 50 elements. Quality of the analyses is monitored through the use of sample duplicates, CANMET-certified reference standard SLRS-5 and distilled water blanks.

ACKNOWLEDGMENTS

Special thanks to Essential Helicopters, specifically to pilot Dave Ross, and to the summer student field crew comprising Kaya Zoratto, Laura Colgrove, Will Hamilton and Cedric Mayer. Thanks are extended to Greg and Jacque Riou of Wild Goose Lake Resort for their kindness, prudence and hospitality.

REFERENCES

- Blackburn, C.E., Johns, G.W., Ayer, J.A. and Davis, D.W. 1991. Wabigoon Subprovince; *in* Geology of Ontario, Ontario Geological Survey, Special Volume 4, Part 1, p.303-382.
- Bostock, H.S. 1970. Physiographic subdivisions of Canada; *in* Geology and economic minerals of Canada, Part A, Geological Survey of Canada, Economic Geology Report No.1, p.10-30.
- Dickman, M. and Fortescue, J. 1991. The role of lake deacidification as inferred from sediment core diatom stratigraphies; *AMBIO – A Journal of the Human Environment*, v.20, no.3-4, p.129-135.
- Dyer, R.D. 2011. Greenstone area high-density lake sediment and water survey, northwestern Ontario; *in* Summary of Field Work and Other Activities 2011, Ontario Geological Survey, Open File Report 6270, p.24-1 to 24-5.
- Gartner, J.F. 1979a. Jellicoe area (NTS 42E/NW), District of Thunder Bay; Ontario Geological Survey, Northern Ontario Engineering Geology Terrain Study 27, 16p., accompanied by Map 5077, scale 1:100 000.
- 1979b. Longlac area (NTS 42E/NE), District of Thunder Bay; Ontario Geological Survey, Northern Ontario Engineering Geology Terrain Study 28, 21p., accompanied by Map 5078, scale 1:100 000.
- Hornbrook, E.H.W., Coker, W.B. and Lynch, J.J. 1978a. National geochemical reconnaissance release NGR 18-1977, regional lake sediment and water geochemical reconnaissance data, Ontario–north shore Lake Superior; Geological Survey of Canada, Open File 507.
- 1978b. National geochemical reconnaissance release NGR 17-1977, regional lake sediment and water geochemical reconnaissance data, Ontario–north shore Lake Superior; Geological Survey of Canada, Open File 506, 275p.
- Hornbrook, E.H.W., Friske, P.W.B., Lynch, J.J., McCurdy, M.W., Gross, H., Galletta, A.C. and Durham, C.C. 1990. National geochemical reconnaissance lake sediment and water data, central northern Ontario (parts of NTS 42E, 42L and 52H); Geological Survey of Canada, Open File 2177.
- Hunt, C. 2003. Metal concentrations and algal microfossil diversity in pre-industrial (pre-1880) sediment of lakes located on the Sudbury Igneous Complex in Sudbury, Ontario; unpublished MSc thesis, Laurentian University, Sudbury, Ontario, 124p.
- Johns, G.W., McIlraith, S. and Stott, G.M. 2003. Precambrian geology compilation map – Longlac sheet; Ontario Geological Survey, Map 2667, scale 1:250 000.
- Kociumbas, M.W. and Power-Fardy, D. 2010. A technical review and mineral resource estimate of the Hercules property, Elmhurst and Rickaby Townships, Ontario, Canada, prepared for Kodiak Exploration Limited by Watts, Griffiths and McOuat, May 26, 2010; technical report under NI 43-101, filed May 28, 2010, with SEDAR®, see [SEDAR Home Page](#), 118p.
- Mason, J. and White, G. 1986. Gold occurrences, prospects, and deposits of the Beardmore–Geraldton area, districts of Thunder Bay and Cochrane; Ontario Geological Survey, Open File Report 5630, v.1 and v.2, 670p.
- Mollard, D.G. and Mollard, J.D. 1981. Mount Royal area (NTS 52H/NE), District of Thunder Bay; Ontario Geological Survey, Northern Ontario Engineering Geology Terrain Study 26, 18p., accompanied by Map 5050, scale 1:100 000.

- Speed, A.A. and Craig, S. 1992. Beardmore–Geraldton historical research project; Ontario Geological Survey, Open File Report 5823, 283p.
- Stott, G.M., Davis, D.W., Parker, J.R., Straub, K.J., and Tomlinson, K.Y. 2002. Geology and tectonic assemblages, eastern Wabigoon Subprovince, Ontario; Ontario Geological Survey, Preliminary Map P.3449, or Geological Survey of Canada, Open File 4285, scale 1:250 000.
- Sutcliffe, R.H. 1991. Proterozoic geology of the Lake Superior area; *in* Geology of Ontario, Ontario Geological Survey, Special Volume 4, Part 1, p.627-661.
- Thorleifson, L.H. and Kristjansson, F.J. 1988. Visible gold content and lithology of till from overburden drillholes, Beardmore–Geraldton area, District of Thunder Bay, northern Ontario; Geological Survey of Canada, Open File 1756, 21p.
- 1993. Quaternary geology and drift prospecting, Beardmore–Geraldton area, Ontario; Geological Survey of Canada, Memoir 435, 146p.
- Williams, H.R. 1991. Quetico Subprovince; *in* Geology of Ontario, Ontario Geological Survey, Special Volume 4, Part 1, p.383-405.
- Zoltai, S.C. 1965. Surficial geology, Thunder Bay; Ontario Department of Lands and Forests, Map S265, scale 1:506 880.

27. Project Unit 12-013. Current Lake Area High-Density Lake Sediment and Water Survey, Northwestern Ontario

R.D. Dyer¹

¹Earth Resources and Geoscience Mapping Section, Ontario Geological Survey

INTRODUCTION

Field work for a high-density lake sediment and water geochemical survey of the Current Lake area, in northwestern Ontario, was carried out between August 12 and August 15, 2012. The survey area is near the town of Dorion and is centred approximately 50 km northeast of the city of Thunder Bay (Figure 27.1). This area covers a gap in lake sediment geochemistry coverage within the southeast corner of the Lac des Iles survey area (Dyer and Russell 2002) that was omitted during the original sampling activities under the Operation Treasure Hunt program in 2002. Lake sediment sampling through this region was previously completed at a much lower density during the early 1980s for the National Geochemical Reconnaissance (NGR) lake sediment program carried out jointly by the Geological Survey of Canada (GSC) and the Ontario Geological Survey (OGS) (Friske et al. 1990). The results from this new OGS study will provide updated higher resolution geochemical data for both mineral exploration and environmental baseline purposes.

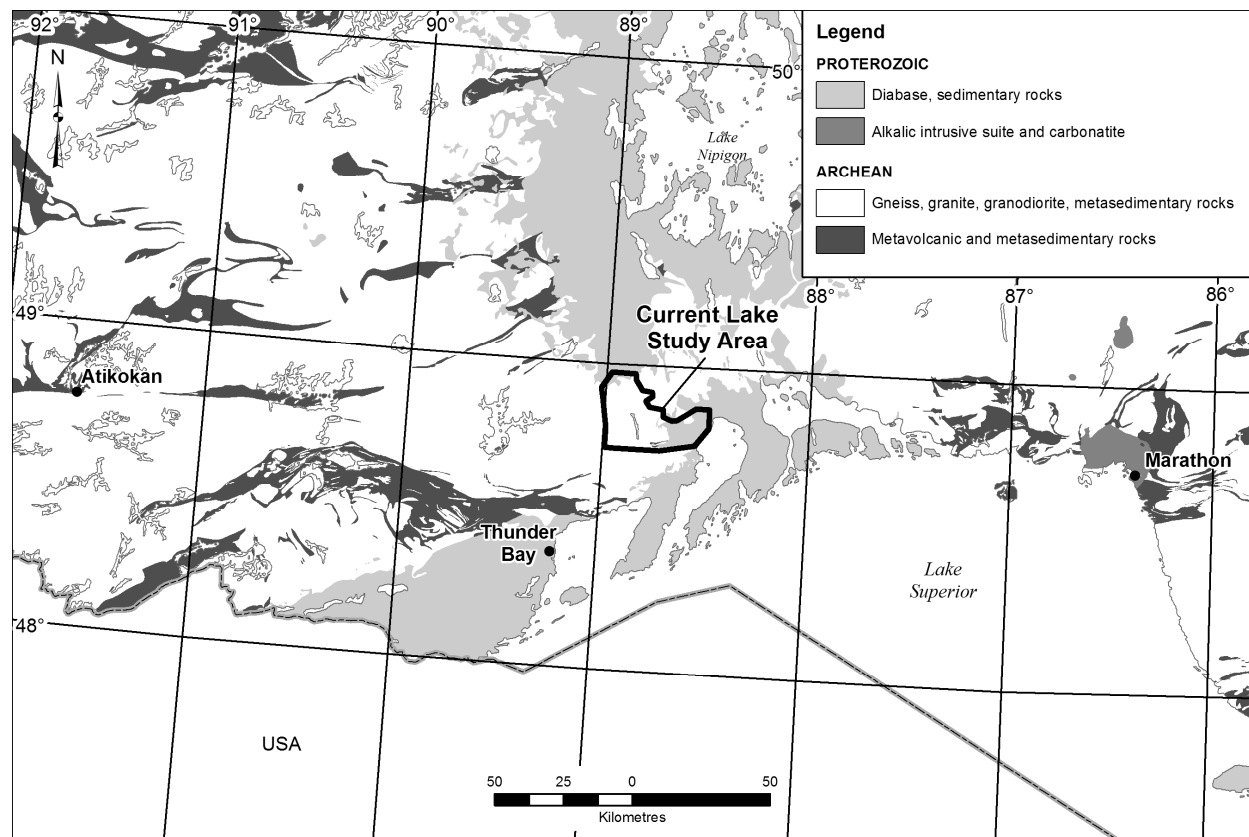


Figure 27.1. Location map of the Current Lake survey area.

Summary of Field Work and Other Activities 2012,
Ontario Geological Survey, Open File Report 6280, p.27-1 to 27-5.

This Current Lake area became a focus for mineral exploration in 2006 after the discovery of a nickel-copper-platinum group element (PGE) deposit underneath Current Lake by Magma Metals Ltd. This deposit, known as the Thunder Bay North (TBN) deposit, has been reported to contain 790 000 ounces of platinum-equivalent (Pt-Eq) mineralization (Thomas et al. 2011). The location of this deposit, almost entirely beneath Current Lake, is a setting for which lake sediment geochemistry may be advantageous as an exploration tool in the area. Ideally, the combination of geophysics and geochemistry should be effective to map out the extent of, and prioritize exploration targets; however, to date, the use of lake sediment geochemistry has only been marginally effective as a vector to identify mineralization over the Current Lake area (R. Weston, Magma Metals Ltd., personal communication, 2011). Therefore, the goals of this project are to not only fill the gap in regional lake sediment geochemistry coverage, but also test the effectiveness of OGS lake sediment geochemical methodology and techniques to detect buried mineralized ultramafic rocks. The latter will be done with both conventional geochemical techniques and soil gas hydrocarbons (SGHSM) analysis, the latter being a relatively new and unconventional technique that has demonstrated promise in a recent lake sediment survey in the McFaulds Lake (“Ring of Fire”) area in the Far North (Dyer and Burke 2012).

REGIONAL SETTING AND GEOLOGY

The survey area contains rocks of the Superior Craton and the Southern Province. Major geological subdivisions include the Mesoarchean Quetico Subprovince (2.70 to 2.69 Ga; Williams 1991), the Proterozoic Sibley Group and the Proterozoic Nipigon diabase sills. The most recent bedrock geology mapping was completed by Hart and Tolsen (2005) and Hart (2006) and a regional compilation was assembled by Santaguida (2001). The study area is underlain primarily with granitoid and metasedimentary rocks of the Quetico Subprovince. Proterozoic Nipigon diabase sills and Sibley Group sedimentary rocks unconformably overlie the Archean rocks in the northern and eastern portions of the survey area. The Sibley Group sedimentary rocks are unmetamorphosed and are a red-bed sequence consisting of conglomerates, sandstones and shales. The flat-lying Nipigon diabase sills form prominent ridges and hills, particularly in the eastern portion of the survey area.

In 2006, diamond drilling by Magma Metals Ltd. intersected ultramafic rocks beneath Current Lake containing nickel and copper sulphides and PGE mineralization. This ultramafic body, termed the Current Lake intrusive complex, is part of a network of magma conduits or chonoliths thought to have formed in association with the Keweenaw Supergroup of the Midcontinent Rift (Thomas et al. 2011). Subsequent exploration in the region has revealed the presence of other similar intrusive complex “conduits” (e.g., Steepledge Lake, Lone Island Lake, EWC intrusive complexes) parts of which lie beneath lakes (Thomas et al. 2011). A significant mineralized drill intercept (10.9 m at 2.35 g/t Pt+Pd+Au, 0.46% Cu, 0.24% Ni) along the trend of the EWC intrusive complex was reported by Kennecott Canada Exploration Inc. (2008).

In the western portion of the area, relief rarely exceeds 60 m between widely scattered points. The land surface is rolling and relatively flat. The incidence of cliffs and topographic changes increases to the north and particularly to the east because of differential erosion of the Sibley Group rocks and the flat-lying relatively resistant Nipigon diabase sills. Local relief approaches 200 m at the eastern end of the survey area.

The regional surficial geology of the area was first compiled by Zoltai (1965). The surficial deposits were outlined in more detail with the completion of an engineering geology terrain (NOEGTS) report that covers the study area (Mollard and Mollard 1981). More recent regional compilations of the Quaternary geology of the area have been completed by Barnett, Henry and Babuin (1991) and Sado, Fullerton and Farrand (1994). These sources indicate the presence of thin drift, mostly till deposits, throughout most of the survey area. Exceptions include an area of laterally continuous glaciolacustrine deposits in low-lying portions of the eastern end of the survey area and thicker till deposits overlying bedrock at the northern end of the survey area.

The predominant glacial ice direction across the study area was toward the south-southwest between 190 and 200° (Sado, Fullerton and Farrand 1994).

SOIL GAS HYDROCARBONS (SGHSM) ANALYSIS

The analysis of lake sediments for soil gas hydrocarbons, a proprietary deep-penetrating geochemical technique offered by Activation Laboratories Inc., was undertaken for the first time by the OGS on samples collected in the McFaulds Lake (“Ring of Fire”) area (Dyer and Burke 2012). The results were promising because the interpretation of the data delineated the general area of the known nickel-copper and chromium mineral deposits, despite being masked by thick (>50 m) of glacial overburden and organic deposits. However, it was recognized that a more regularly spaced and higher density sampling would likely result in better target resolution and confidence. The application of this technique on Current Lake area sediments is particularly appropriate because of the presence of intrusive ultramafic rock “conduits”, many of which lie hidden beneath lakes or granitoid rocks. Therefore, the impetus for the application of the SGHSM technique on Current Lake area lake sediments is twofold: 1) in an area of lower landscape complexity than the Far North, to determine the effectiveness of the method for the detection of buried ultramafic rocks; and 2) to test the ability of the method to discriminate between mineralized ultramafic conduits (such as at Current Lake) and unmineralized conduits.

As a further test of the SGHSM method, 2 “B”-horizon soil-sampling transects were carried out over the Current Lake intrusive complex (Figure 27.2). The top of the ultramafic rock conduit underneath transects #1 and #2 are buried beneath approximately 60 m and 125 m of granitoid rocks, respectively. Sulphide mineralization is reported to be continuous and relatively high grade throughout this zone (Thomas et al. 2011). A total of 24 “B”-horizon samples were collected from soil developed in till deposits and the sampling traverses extended well beyond the vertical trace of the ultramafic conduit.

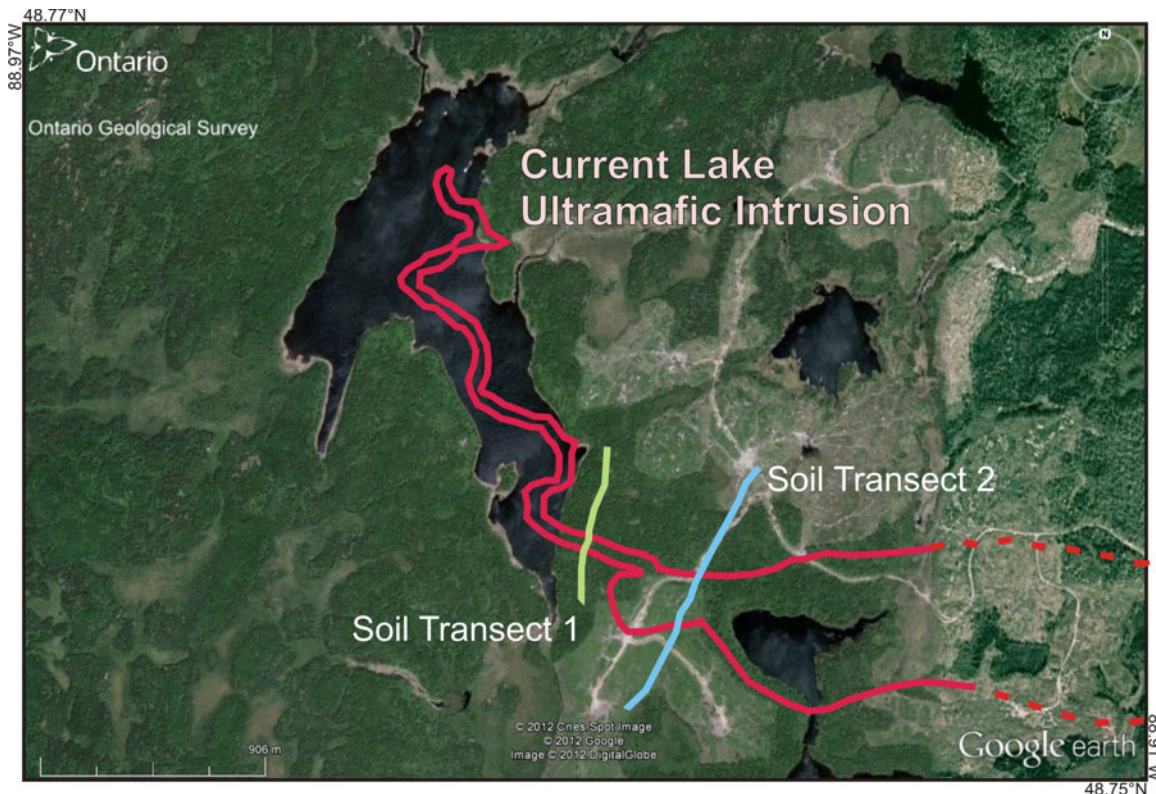


Figure 27.2. Location of “B”-horizon soil-sampling traverses completed over the Current Lake ultramafic complex (image modified from Google Earth™ mapping service).

SAMPLING METHODS

Organic-rich lake sediment samples were collected from a helicopter float using the OGS-designed gravity corer. A total of 440 lake sediment samples were collected over an area of approximately 650 km². Wherever possible, both shallow (0 to 15 cm) and deep (>20 cm) sediment samples were obtained at each sampling site. Therefore, the 440 sediment samples comprise 225 shallow samples (0 to 15 cm sediment depth) and 215 deep samples (>20 cm sediment depth). Based on average sediment rates of approximately 1.5 cm per decade within lakes on shield landscapes (e.g., Hunt 2003; Dickman and Fortescue 1991), the shallow sample is considered to represent sedimentation during the past 100 years (approximately) and, therefore, may be subject to anthropogenic contamination. The deep sediment sample represents sedimentation older than 100 years; therefore, this portion better reflects the effects of natural geochemical inputs that may be traced to local geology and/or mineralization.

A total of 237 water samples were collected over the study area. These were collected from a depth of between 0.5 and 1.0 m using a weighted intake hose and pump. Water-quality parameters, including pH and conductivity, were measured at each lake site using a flow cell attached to a multiparameter probe. Lake water was pumped from each lake and allowed to purge the sampling system prior to the collection of a water sample and the recording of water-quality parameters. Water samples were kept cool after collection and processed (filtered and acidified) within 6 hours of collection.

Soil samples were collected by auger or from small test pits dug by hand with a shovel. The average sample interval was 50 m along transect #1 and 70 m along transect #2. Samples were placed in breathable fabric bags which in turn were placed in plastic Ziploc[®] bags for shipment to Sudbury for drying and further preparation as described below.

SAMPLE PREPARATION AND ANALYTICAL METHODS

Lake sediment samples were placed in breathable fabric bags and allowed to partially air dry prior to shipment to Sudbury. Final drying was done in ovens at a temperature of less than 40°C prior to partial pulverization in a ceramic ring and puck pulverizer and sieving to obtain the -60 mesh (<250 µm) size fraction. Laboratory analysis will include nitric acid–aqua regia digestion followed by inductively coupled plasma mass spectrometry (ICP–MS) to determine approximately 50 trace elements. Nitric acid–aqua regia digestion attacks all sample matrix constituents, except for silicate minerals and, therefore, is considered a nonselective, relatively strong partial extractant. Quality control will be monitored through the use of certified and internal reference materials and sample pulp duplicates. Loss-on-ignition (LOI) is determined at 500°C, using an automated gravimetric technique. The deep (>15 cm) sediment samples will undergo further analysis for arsenic and gold by instrumental neutron activation analysis (INAA), platinum group elements by fire assay–ICP–MS (FA–ICP–MS) and SGHSM.

Water samples were passed through 0.45 µm syringe filters and acidified to 1% ultrapure nitric acid (HNO₃) within 6 hours of collection. Analysis of water will include direct aspiration ICP–MS to determine approximately 50 elements. Quality of the analyses is monitored through the use of sample duplicates, CANMET-certified reference standard SLRS-5 and distilled water blanks.

The breathable fabric bags containing soil samples were placed in ovens at a temperature of 35°C. After drying, samples were sieved at 5 mesh (4 mm) to remove pebbles for later identification. An aliquot of approximately 200 g of -5 mesh material was separated for submission to Activation Laboratories for SGHSM preparation and analysis. The remaining material was submitted to the OGS Geoscience Laboratories for sieving at -230 mesh (63 µm) prior to nitric acid–aqua regia digestion followed by ICP–MS analysis to determine approximately 50 trace elements. The samples will undergo further analysis for arsenic and gold by INAA and platinum group elements by FA–ICP–MS.

ACKNOWLEDGMENTS

Thanks are extended to Essential Helicopters, specifically to pilot Dave Ross; the summer student field crew comprising Kaya Zoratto, Laura Colgrove, Will Hamilton and Cedric Mayer; and finally Shannon Evers and Hannah Burke for the production of figures.

REFERENCES

- Barnett, P.J., Henry, A.P. and Babuin, D. 1991. Quaternary geology of Ontario, west-central sheet; Ontario Geologic Survey, Map 2554, scale 1:1 000 000.
- Dickman, M. and Fortescue, J. 1991. The role of lake deacidification as inferred from sediment core diatom stratigraphies; *AMBIO – A Journal of the Human Environment*, v.20, no.3-4, p.129-135.
- Dyer, R.D. and Burke, H.E. 2012. Preliminary results from the McFaulds Lake (“Ring of Fire”) area lake sediment geochemistry pilot study, northern Ontario; Ontario Geological Survey, Open File Report 6269, 26p.
- Dyer, R.D. and Russell, D.F. 2002. Lac des Iles–Black Sturgeon River area lake sediment survey: Operation Treasure Hunt; Ontario Geological Survey, Open File Report 6096, 134p.
- Friske, P.W.B., Hornbrook, E.H.W., Lynch, J.J., McCurdy, M.W., Gross, H., Galletta, A.C. and Durham, C.C. 1990. National geochemical reconnaissance lake sediment and water data, Thunder Bay region, northwestern Ontario (NTS 52A and 52H south); Geological Survey of Canada, Open File 2179.
- Hart, T.R. 2006. Precambrian geology of the southwest portion of the Nipigon Embayment, northwestern Ontario; Ontario Geological Survey, Preliminary Map P.3580, scale 1:100 000.
- Hart, T.R. and Tolsen, A. 2005. Southern Black Sturgeon River–Seagull Lake area geological cross-sections, Nipigon Embayment, northwestern Ontario; Ontario Geological Survey, Preliminary Map P.3563, scale 1:100 000.
- Hunt, C. 2003. Metal concentrations and algal microfossil diversity in pre-industrial (pre-1880) sediment of lakes located on the Sudbury Igneous Complex in Sudbury, Ontario; unpublished MSc thesis, Laurentian University, Sudbury, Ontario, 124p.
- Kennecott Canada Exploration Inc. 2008. Assessment report on 2008 diamond drilling, Current Lake project, Greenwich Lake area, NTS 52 A/15, Thunder Bay Mining Division, Ontario, Canada; Thunder Bay South Resident Geologist’s office, assessment file AFRO# 2.38816, 42p.
- Mollard, D.G. and Mollard, J.D. 1981. Black Bay area (NTS 52A/NE and part of NTS 52A/SE), District of Thunder Bay; Ontario Geological Survey, Northern Ontario Engineering Geology Terrain Study 58, 30p., accompanied by Map 5046, scale 1:100 000.
- Sado, E.V., Fullerton, D.S. and Farrand, W.R. 1994. Quaternary geological map of the Lake Nipigon 4° × 6° quadrangle, United States and Canada; United States Geological Survey, Miscellaneous Investigations Series, Map I-1420 (NM-16), scale 1:1 000 000.
- Santaguida, F. 2001. Precambrian geology compilation series–Thunder Bay sheet; Ontario Geological Survey, Map 2664, scale 1:250 000.
- Thomas, D.G., Melnyk, J., Gormely, L., Searston, S. and Kulla, G. 2011. Magma Metals Limited Thunder Bay North polymetallic project, Ontario, Canada, NI 43-101 technical report on preliminary assessment; prepared for Magma Metals Limited by AMEC Americas Limited, March 17, 2011; Technical Report under NI 43-101, filed March 24, 2011, with SEDAR®, see [SEDAR Home Page](#), 209p.
- Williams, H.R. 1991. Quetico Subprovince; *in* *Geology of Ontario*, Ontario Geological Survey, Special Volume 4, Part 1, p.383-405.
- Zoltai, S.C. 1965. Surficial geology, Thunder Bay; Ontario Department of Lands and Forests, Map S265, scale 1:506 880.

28. Project Unit 11-024. McFaulds Lake (“Ring of Fire”) Area Lake Sediment and Water Sampling Pilot Study, Far North, Ontario

R.D. Dyer¹

¹Earth Resources and Geoscience Mapping Section, Ontario Geological Survey

INTRODUCTION

Field work for a lake sediment and water sampling geochemical pilot study over the McFaulds Lake (“Ring of Fire”) region of far northern Ontario was carried out over a four-day period in August 2012 to augment the initial survey carried out during the previous field season (Dyer 2011). This work consisted primarily of in-fill lake sediment and water sampling to increase the sampling resolution following the success from the preliminary lake sediment soil gas hydrocarbon (SGHSM) analytical results and interpretation recently published (Dyer and Burke 2012). The survey area was also expanded to the north as shown in Figure 28.1.

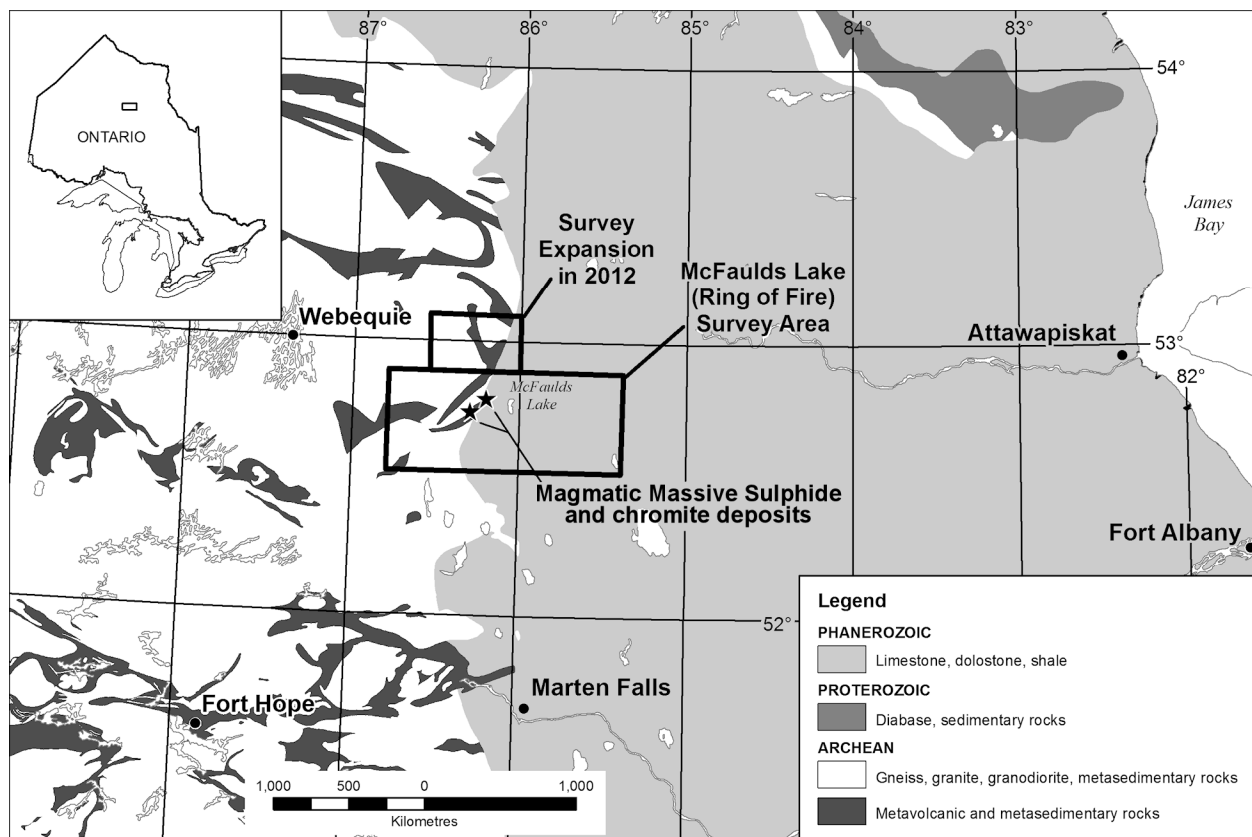


Figure 28.1. Location map of the McFaulds Lake (“Ring of Fire”) area lake sediment and water sampling pilot study.

The study area is centred on McFaulds Lake and covers the nickel-copper-platinum group elements (PGE) magmatic massive sulphide and chromite deposits currently being explored by a number of mineral exploration companies. The initial concept of this pilot study was conceived to determine the suitability of conventional lake sediment and water geochemistry for mineral exploration over the James Bay Lowland landscape and to create a database of the baseline geochemical and environmental conditions of the area prior to any mine or infrastructure development. Subsequently, it was decided to carry out SGHSM analysis of the lake sediment samples to test the effectiveness of a relatively new and non-traditional exploration technique over the complex landscapes of the James Bay Lowland. The preliminary results and interpretation of the SGHSM analysis of lake sediments were promising in detecting the known “Ring of Fire” deposit area; however, it was recognized that a more regularly spaced and higher sample density would contribute to better resolution and constraint on data interpolation, resulting in a higher level of interpretation confidence (Dyer and Burke 2012).

The 2012 field operations, utilizing a Bell 206B helicopter on floats, were carried out from the Noront Resources Limited Esker exploration camp located approximately 15 km west of McFaulds Lake. A total of 164 water samples and 321 lake sediment samples were collected (Figure 28.2); the sediment samples comprised 162 shallow samples (<15 cm sediment depth) and 159 deep samples (>15 cm sediment depth).

GEOLOGY

The nickel-copper-PGE and chromite deposits are contained within the Archean McFaulds Lake ultramafic complex, a deformed, layered, largely ultramafic, sill-like intrusion consisting mainly of dunite and peridotite with lesser pyroxenite, chromitite and possibly gabbro (Metsaranta 2010; Metsaranta and Houl   2011; Metsaranta and Houl  , this volume, Article 43). The bedrock west and northwest of this complex consists primarily of felsic plutonic rocks (Ontario Geological Survey 1991; Buse et al. 2009); to the east, the underlying Precambrian bedrock is a mix of supracrustal rocks (metavolcanic and metasediment) and granitoids (Metsaranta 2010). The unconformably overlying Paleozoic stratigraphy consists of Upper Ordovician limestone and dolostone and Lower Silurian limestone rocks (Ontario Geological Survey 1991). The Paleozoic cover rocks are intermittently present over the known magmatic massive sulphide and chromite deposits and typically consist of fossiliferous beige limestone and rare muddy dolostones; this stratigraphy thickens considerably toward the east, where, at McFaulds Lake, up to 100 m of strata have been observed (Golder Associates Ltd. 2010).

Detailed surficial mapping coverage of the McFaulds Lake area does not exist. A surficial geology map at a scale of 1:100 000 covering the Webequie area, immediately to the west of the present study area, was published in 2008 (Barnett 2008). It is anticipated that the OGS “Ring of Fire” surficial sampling project (Gao 2011) will advance the understanding of the Quaternary deposits over the “Ring of Fire” area and result in surficial mapping coverage of the immediate McFaulds Lake area.

Some details on the character and thickness of the Quaternary deposits can be gleaned from the exploration activities in the “Ring of Fire” area. For example, diamond drilling by Noront Resources Inc. indicates that thickness of surficial cover ranges from approximately 33 to 76 m (Golder Associates Ltd. 2010). The Quaternary sequence typically encountered in diamond-drill holes in the region consists of 1 to 2 m of sandy till overlain by varved sand grading upward into clays and finally marine clays (Thomas 2004). The limit of marine incursion from the east has been estimated to be a north-trending line approximately 5 km west of McFaulds Lake (Prest 1963a, 1963b). Most of the survey area is considered to be in a zone of sporadic permafrost (Brown et al. 1998).

The dominant ice direction of the most recent glaciation, based on bedrock striations and streamlined forms (e.g., flutes), was toward the south-southeast (Barnett, Webb and Hill 2009).

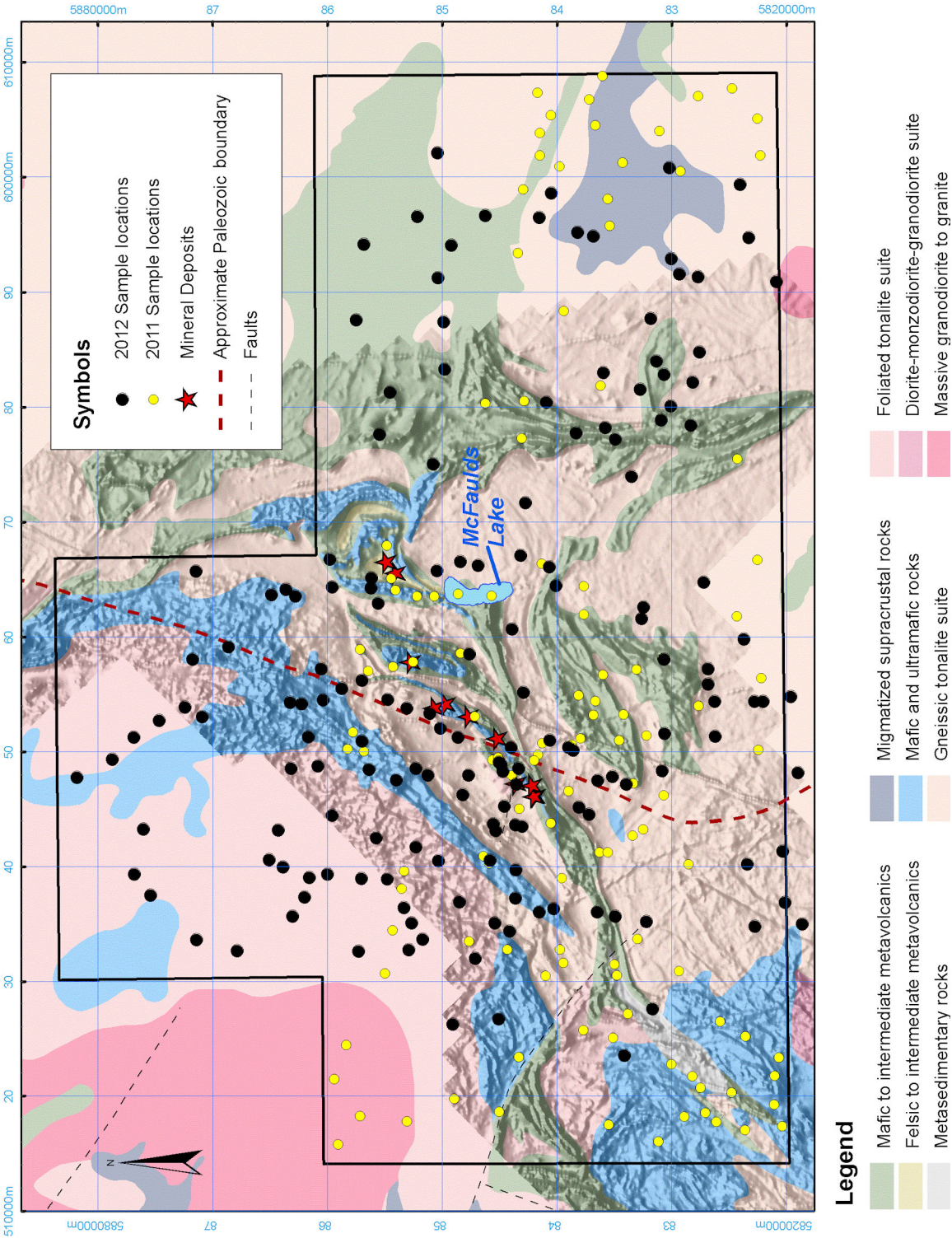


Figure 28.2. McFaulds ("Ring of Fire") study area showing lake sampling coverage completed in 2011 and 2012 (geology from Ontario Geological Survey 1991). Universal Transverse Mercator (UTM) co-ordinates provided using North American Datum 1983 (NAD83) in Zone 16.

SAMPLING METHODS

Organic-rich lake sediment samples were collected from a helicopter float using the OGS-designed gravity corer. Wherever possible, both shallow (0 to 15 cm) and deep (>15 cm) sediment samples were obtained at each sampling site. The expectation that the shallow sample would represent sedimentation during the past 100 years (approximately) and, therefore, perhaps reflect some airborne anthropogenic component, is based on experience from southern Boreal forest lakes, with an average sedimentation rate of approximately 1.5 cm per decade (e.g., Hunt 2003; Dickman and Fortescue 1991). Therefore, assuming an undisturbed stratigraphic record, the deep sediment sample would represent sedimentation older than 100 years and, therefore, reflect natural geochemical inputs that may be traced to local geology and landscape.

Lake water samples were collected from a depth of between 0.5 and 1.0 m using a weighted intake hose connected to a diaphragm pump inside the helicopter. Water-quality parameters, including pH and conductivity, were measured at each lake site using a flow cell attached to a multiparameter probe. Lake water was pumped from each lake and allowed to purge the sampling system prior to the collection of a water sample and the recording of water-quality parameters. Water samples were kept cool after collection and processed (filtered and acidified) within 6 hours of collection.

A global positioning system (GPS) receiver was utilized to record accurate sample site positions and to record each flight track. In addition, a GPS receiver connected to a tablet computer was utilized to provide “heads up” real-time navigation between lake sites.

SAMPLE PREPARATION AND ANALYTICAL METHODS

Lake sediment samples for geochemical analysis were collected in breathable fabric bags and then placed into plastic Ziploc[®] bags to prevent leakage. The samples were shipped to Sudbury, where drying was done in ovens at a temperature of less than 40°C prior to partial pulverization in a ceramic ring and puck pulverizer and sieving to obtain the –60 mesh (<250 µm) size fraction. Laboratory analysis will include nitric acid–aqua regia digestion followed by inductively coupled plasma mass spectrometry (ICP–MS) to determine approximately 50 trace elements. Nitric acid–aqua regia digestion attacks all sample matrix constituents, except for silicate minerals and, therefore, is considered a nonselective, relatively strong partial extractant. Quality control will be monitored through the use of sample pulp duplicates and certified reference materials. Loss-on-ignition (LOI) is determined at 500°C, using an automated gravimetric technique. The deep (>15 cm) sediment samples will undergo further analysis for gold by instrumental neutron activation analysis (INAA), platinum group elements by fire assay–ICP–MS and SGHSM.

Water samples for geochemical analysis were passed through 0.45 µm syringe filters and acidified to 1% ultrapure nitric acid (HNO₃) within 6 hours of collection. Analysis of water will include direct aspiration ICP–MS to determine approximately 50 elements. Major anions will also be determined on an aliquot of unacidified water that has been kept cool since collection. Quality of the analyses is monitored through the use of sample duplicates, CANMET-certified reference standard SLRS-5 and distilled water blanks.

ACKNOWLEDGMENTS

Thanks are extended to pilot Dave Ross of Essential Helicopters for efficient flying, summer student Cedric Mayer for very capable field assistance and Hannah Burke for production of figures.

REFERENCES

- Barnett, P.J. 2008. Surficial geology of the Winisk Lake area, northern Ontario; Ontario Geological Survey, Preliminary Map P.3602, scale 1:100 000.
- Barnett, P.J., Webb, J.L. and Hill, J.L. 2009. Flow indicator map of the Far North of Ontario; Ontario Geological Survey, Preliminary Map P.3610, scale 1:1 000 000.
- Brown, J., Ferrians, O.J., Jr., Heginbottom, J.A. and Melnikov, E.S. 1998 (revised February 2001). Circum-Arctic map of permafrost and ground ice conditions; National Snow and Ice Data Center/World Data Center for Glaciology, Boulder, Colorado, digital media.
- Buse, S., Smar, L., Stott, G.M. and McIlraith, S.J. 2009. Precambrian geology of the Winisk Lake area; Ontario Geological Survey, Preliminary Map P.3607, scale 1:100 000.
- Dickman, M. and Fortescue, J. 1991. The role of lake deacidification as inferred from sediment core diatom stratigraphies; *AMBIO – A Journal of the Human Environment*, v.20, no.3-4, p.129-135.
- Dyer, R.D. 2011. McFaulds Lake area lake sediment and water pilot study, northern Ontario; *in* Summary of Field Work and Other Activities 2011, Ontario Geological Survey, Open File Report 6270, p.25-1 to 25-6.
- Dyer, R.D. and Burke, H.E. 2012. Preliminary results from the McFaulds Lake (“Ring of Fire”) area lake sediment geochemistry pilot study, northern Ontario; Ontario Geological Survey, Open File Report 6269, 26p.
- Gao, C. 2011. Surficial geology mapping and drift sediment sampling in the McFaulds Lake (“Ring of Fire”) area, northern Ontario; *in* Summary of Field Work and Other Activities 2011, Ontario Geological Survey, Open File Report 6270, p.23-1 to 23-7.
- Golder Associates Ltd. 2010. Technical report and resource estimate, McFaulds Lake project James Bay Lowlands, Report Number 10-1117-0001, for Noront Resources Ltd. by Golder Associates Ltd., April 23, 2010; Technical Report under NI 43-101, filed April 23, 2010, with SEDAR[®], see [SEDAR Home Page](#), 241p.
- Hunt, C. 2003. Metal concentrations and algal microfossil diversity in pre-industrial (pre-1880) sediment of lakes located on the Sudbury Igneous Complex in Sudbury, Ontario; unpublished MSc thesis, Laurentian University, Sudbury, Ontario, 124p.
- Metsaranta, R.T. 2010. McFaulds Lake area regional compilation and bedrock geology mapping project; *in* Summary of Field Work and Other Activities 2010, Ontario Geological Survey, Open File Report 6260, p.17-1 to 17-5.
- Metsaranta, R.T. and Houlé, M.G. 2011. McFaulds Lake area regional compilation and bedrock mapping project update; *in* Summary of Field Work and Other Activities 2011, Ontario Geological Survey, Open File Report 6270, p.12-1 to 12-12.
- Ontario Geological Survey 1991. Bedrock geology of Ontario, northern sheet; Ontario Geological Survey, Map 2541, scale 1:1 000 000.
- Prest, V.K. 1963a. Red Lake–Lansdowne House area, northwestern Ontario, surficial geology; Geological Survey of Canada, Paper 63-6, 23p.
- 1963b. Surficial geology, Red Lake–Lansdowne House area, Ontario; Geological Survey of Canada, Preliminary Map 5-1863, scale 1:506 880.
- Thomas, R.D. 2004. Technical report Spider # 1 and # 3 projects (James Bay Joint Venture), James Bay, Ontario, for Spider Resources Inc. and KWG Resources Inc. by R.D. Thomas and Associates, June 30, 2004, 95p.; KWG Resources Inc., www.kwgresources.com/resources/Kyle/20040630Mcfaulds_spider1_n_3.pdf [accessed September 27, 2012]

29. Project Unit 09-024. Preliminary Results: Potential Ordovician Shale Gas Units in Southern Ontario

C. Béland Otis¹

¹Earth Resources and Geoscience Mapping Section, Ontario Geological Survey

INTRODUCTION

In 2009, the Ontario Geological Survey (OGS) initiated a project to evaluate the shale gas potential of Paleozoic shale units present in southern Ontario. Several units were initially identified for assessment based upon several criteria: high organic content; being the source rocks of economic hydrocarbon accumulations; and correlatives to shale gas units in contiguous states of the United States and/or Canadian provinces (Barker 1985; Béland Otis 2009, 2010, 2011). These units consist of the Upper Devonian Kettle Point and Marcellus formations, the Upper Ordovician Georgian Bay and Blue Mountain formations and the Upper Ordovician Collingwood Member of the Lindsay Formation, equivalent of the Cobourg Formation.

In the spring of 2010, 2 boreholes were drilled through the Kettle Point Formation (Béland Otis 2010, 2011). Core samples were collected to evaluate gas concentration and other key parameters. Similar work was performed in 2011 near Mount Forest in the County of Wellington to assess the shale gas potential of the Ordovician shale succession. Furthermore, in the summer of 2012, additional rock samples were collected from previously drilled wells from southern Ontario and were analyzed for mineralogy and Rock-Eval[®] 6 pyrolysis parameters. These analyses may assist in refining stratigraphic correlations across provincial and international borders.

ORDOVICIAN SHALES

The Ordovician shale sequence present in southern Ontario comprises, in descending stratigraphy, the Queenston, the Georgian Bay and the Blue Mountain formations and the Collingwood Member of the Lindsay Formation. Since the Queenston Formation is composed of a succession of red and green shales, has low organic content and, therefore, almost no shale gas potential, it is not being studied as part of this current project. The Georgian Bay Formation consists of up to 200 m of greenish- to bluish-grey shale, interbedded with limestone, siltstone and sandstone (Armstrong and Carter 2010). Its lower contact is gradational with the Blue Mountain Formation, which is characterized by up to 60 m of blue-grey to grey-brown shales with thin, minor interbeds of limestone and siltstone. The lowest part of the Blue Mountain Formation is called the Rouge River Member, a dark brown to black, noncalcareous shale that can reach up to 35 m in thickness (Armstrong and Carter 2010).

The Collingwood Member of the Lindsay Formation is referred to as an impure limestone or lime marlstone (Macauley et al. 1990). It is a dark grey to black, organic-rich, calcareous shale with very thin, fossiliferous bioclastic interbeds (Armstrong and Carter 2010). It is considered a shale unit because of its well-developed fissility (Macauley et al. 1990). Total organic carbon values of up to 8.31% have been reported in Ontario (Macauley and Snowdon 1984). The Collingwood Member is situated stratigraphically beneath the Blue Mountain Formation and the 2 units are separated by a phosphatic bed. This phosphate layer suggests a depositional time break between the units (Churcher et al. 1991; Rancourt 2009). A similar phosphatic horizon has been reported in some cores completed in the Montreal area of Quebec (Lavoie and Thériault 2012).

*Summary of Field Work and Other Activities 2012,
Ontario Geological Survey, Open File Report 6280, p.29-1 to 29-12.*

© Queen's Printer for Ontario, 2012

Table 29.1. Wells sampled for mineralogy and Rock-Eval® 6 pyrolysis in 2012.

Well Information		Location		Depth of Top of Unit (m)				
				Georgian Bay Formation	Blue Mountain Formation		Cobourg Formation	
Name	Number of Samples	Latitude (°N)	Longitude (°W)	—	—	Rouge River Member	Collingwood Member	—
CORE								
GSC #2 Russell	52	45.32047222	75.39594444	21.6	172.8	260.3	273.8	283.2
OGS 82-2 Chatham	31	42.38782250	82.07989500	731.5	848.7	872.9	899.4	899.6
OGS 82-4 Warton	21	44.79185583	81.23234972	156.1	265.8	287.7	291.1	292.9
OGS 82-3 Port Stanley	47	42.67076833	81.16139472	639.4	795.1	822.5	859.8	861.2
OGS 83-1 Halton	38	43.53479139	79.95857611	182.7	358.2	433.2	435.5	437.3
OGS 83-3 Pickering	13	43.81651639	79.05789056	N/A	22.8*	40.2	46.8	48.2
OGS 83-5 Little Current	23	45.94118222	81.94684528	4.0**	90.5	94.4	105.0	113.0
OGS 83-6 St. Joseph	31	46.09623778	83.92743250	43.3**	98.8	135.5	158.5	168.4
OGS-SG11-02 Mount Forest	30	43.95996417	80.63534694	304.1	444.5	473.5	479.9	488.6
CUTTINGS								
Imperial Lincoln	48	43.21346361	79.17188917	220.7	338.3	414.5	445.0	460.2
Texaco #6 Bruce	26	44.30411111	81.54727778	518.0	608.9	647.0	651.6	659.5

Abbreviations: Mbr, Member; N/A, not analyzed.

Notes: *The Blue Mountain Formation is the first geological unit intercepted by the well.

**The Georgian Bay Formation is the first geological unit intercepted by the well.

In neighbouring provinces and states, Ordovician shale gas potential has been confirmed for units thought to be equivalent to those found in southern Ontario. These include the Collingwood Member found in Michigan and the Utica Shale present in the province of Quebec and in the northeastern United States (Smith and Leone 2010; Rock, Harrison and Barranco 2010; Lavoie 2011). The Ordovician shale succession in southern Ontario has previously been extensively studied by the OGS for its potential as an oil shale resource (Barker 1985; Barker et al. 1983; Churcher et al. 1991; Harris 1984; Johnson 1983; Johnson, Russell and Telford 1983a, 1983b, 1985; Snowdon 1984; Stromquist, Dickhout and Barker 1984).

METHODOLOGY

In 2011, the well OGS-SG11-02, located 20 km east of the town of Mount Forest, in Arthur Township, was drilled down to the Cobourg Formation. The entire Ordovician shale succession, with the exception of the Queenston Formation, was intersected. Core samples, approximately 30 cm in length, were collected approximately every 3 m and stored in specialized canisters designed to measure gas content over time. These were also analyzed for gas composition, isotopic composition of methane, adsorption isotherms and rock mechanics; additional core samples were collected for total organic carbon, density, gas, oil and water saturation, permeability and porosity. The well was also geophysically logged for various parameters (gamma-ray, density, sonic, porosity, televiwer, etc.) and was then plugged.

In June and July 2012, also as part of the shale gas assessment project, 360 core and cuttings samples from 11 previously drilled wells (including OGS-SG11-02) were sampled and analyzed for mineralogy by X-ray diffraction (XRD) and for pyrolysis by Rock-Eval® 6 analyzer. Rock-Eval® 6 pyrolysis indicates the quantity, type and thermal maturity of organic matter. All cores and cuttings can currently be found either at the Ontario Oil, Gas and Salt Resources Library in London or at the Willet Green Miller Centre in Sudbury. Table 29.1 presents information about the sampled wells: location, the number of samples per well and the associated stratigraphy.

INITIAL RESULTS

Drilling and Sampling Program of Well OGS-SG11-02

The Ordovician shale stratigraphy of well OGS-SG11-02 is presented in Table 29.1 and in Figures 29.1 to 29.3. The well was bored through Quaternary deposits, Silurian bedrock and the Queenston Formation, to a depth of 304.1 m. Then, the well was cored through 140.4 m of Georgian Bay Formation and 35.4 m of Blue Mountain Formation down to a total depth of 496.5 m; the last 7.9 m were drilled into the Cobourg Formation. The Rouge River Member of the Blue Mountain Formation and the Collingwood Member of the Cobourg Formation are 6.4 m and 8.7 m thick, respectively, in this well.

All analytical results of well OGS-SG11-02, except the adsorption isotherms, were available at the time of publication (Tables 29.2 to 29.6). Gas analyses, which include desorption, gas composition, calorific value and isotopic composition of methane, are presented in Table 29.2. Total gas values (up to 18.4 standard cubic feet per ton (scft/ton)) are highest in the black shale units of the Rouge River and the Collingwood members, which are also the units with the greatest total organic carbon content values (up to 4.55 weight %) (*see* Table 29.3; *see* Figure 29.1). Some interesting total gas content values (up to 8.6 scft/ton) are also observed for the Georgian Bay Formation even if the total organic carbon is low (≤ 0.60 weight %). The calorific values can also be quite high in the Georgian Bay Formation. Throughout the Ordovician shale succession, gas is mostly composed of methane (73.92 to 94.57%) with varying amounts of ethane (3.94 to 8.76%), heavier hydrocarbons (1.49 to 14.70%) and carbon dioxide (0.00 to 7.19%) (*see* Figure 29.2). Carbon ($> -60\text{‰}$) and hydrogen ($> -250\text{‰}$) isotopic compositions of methane, as well as a $C_1/(C_2+C_3)$ ratio less than 10, all suggest a thermogenic origin for the gas (*see* Tables 29.2 and 29.3).

Core analyses indicate a clear relation between grain and bulk densities with total organic carbon content (*see* Table 29.4; *see* Figure 29.1). Also, permeability and porosity values are much lower in the Rouge River and Collingwood members (*see* Figure 29.3). However, the Rouge River Member has a good oil saturation (31.5%), whereas the Collingwood Member has a much higher gas saturation (77.2%). Rock mechanics results are presented in Tables 29.5 and 29.6. As shown in Figure 29.4, the Ordovician shales fall mostly in the ductile area with some exceptions for the Georgian Bay and Blue Mountain formations. Also, a brittleness index can also be calculated with rock mechanics parameters (Rickman et al. 2008). The values obtained give brittleness indices between 29 and 41%, which can be considered low (Buller 2010; Hall 2010). Finally, with the televIEWER log, structural features in the wells were recorded; these are summarized in Figure 29.5.

Sampling Program of Summer 2012

Some of the lithostratigraphic contacts within the Upper Ordovician shale succession are somewhat unclear in previous literature (Churcher et al. 1991; Johnson et al. 1992; Russell and Telford 1983); therefore, new contacts were defined for this study. The lower contact of the Collingwood Member was described as the first appearance of a 10 cm bed of black calcareous shale or mudstone, in contrast with the underlying Cobourg Formation (subsurface equivalent to the Lindsay Formation), generally defined as a grey nodular limestone. The upper contact of the Collingwood Member with the Rouge River Member of the Blue Mountain Formation was easily recognized in most wells by the presence of a phosphatic and/or pyritic bed. The upper contact of the Rouge River Member was identified as the first appearance of a bluish-gray bed, characteristic of the overlying unnamed part of the Blue Mountain Formation. Finally, the Georgian Bay Formation was delimited at the bottom by the first appearance of a 1 cm fossiliferous limestone bed and, at the top, by the lowermost red shale beds of the overlying Queenston Formation. Results of the present study, including mineralogy and Rock-Eval[®] 6 pyrolysis analysis, may assist in refining these contacts.

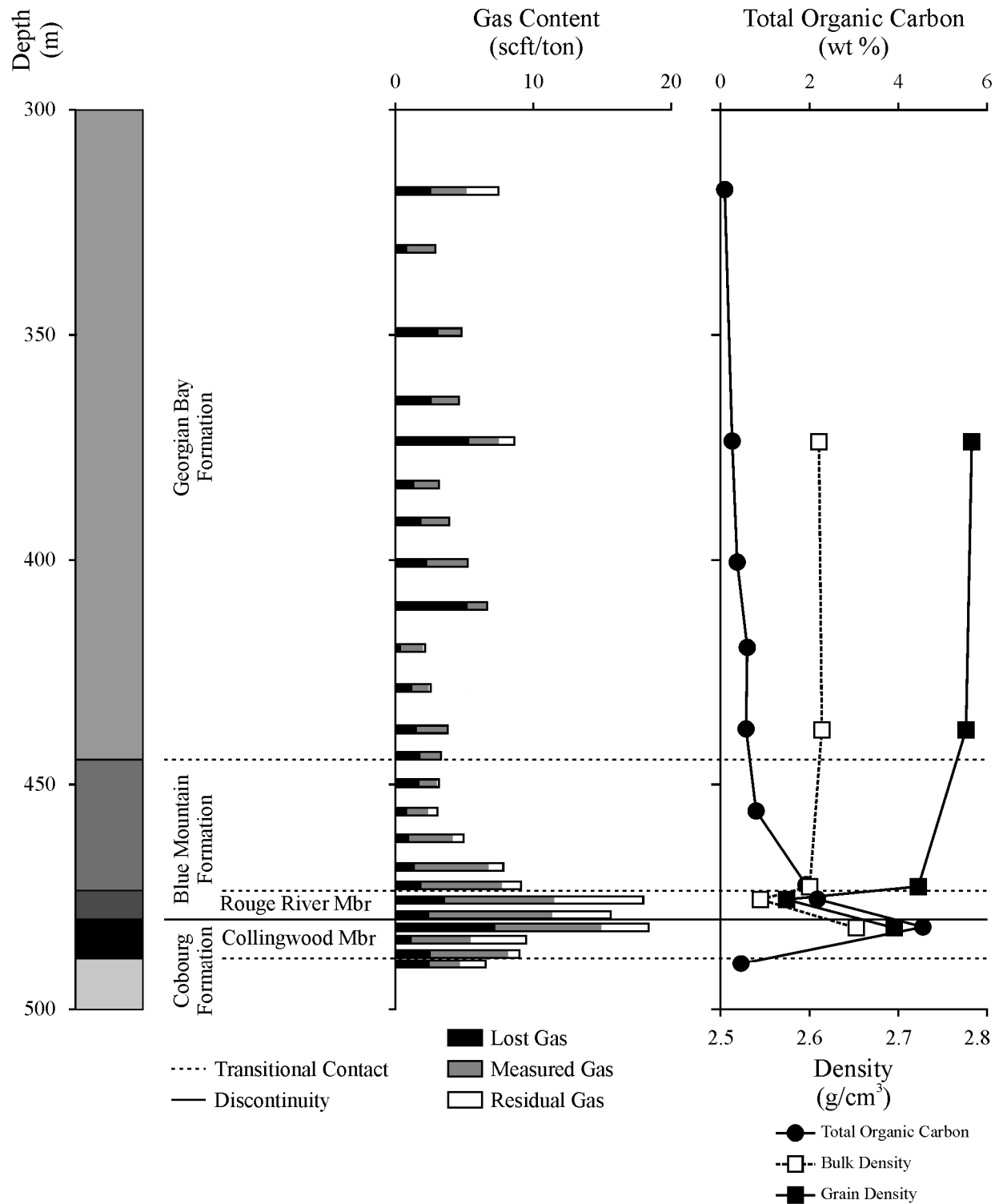


Figure 29.1. Stratigraphy, total gas content (standard cubic feet per ton (scft/ton)), total organic carbon (weight % (wt %)) and density (g/cm^3) logs of well OGS-SG11-02. Abbreviation: Mbr = Member.

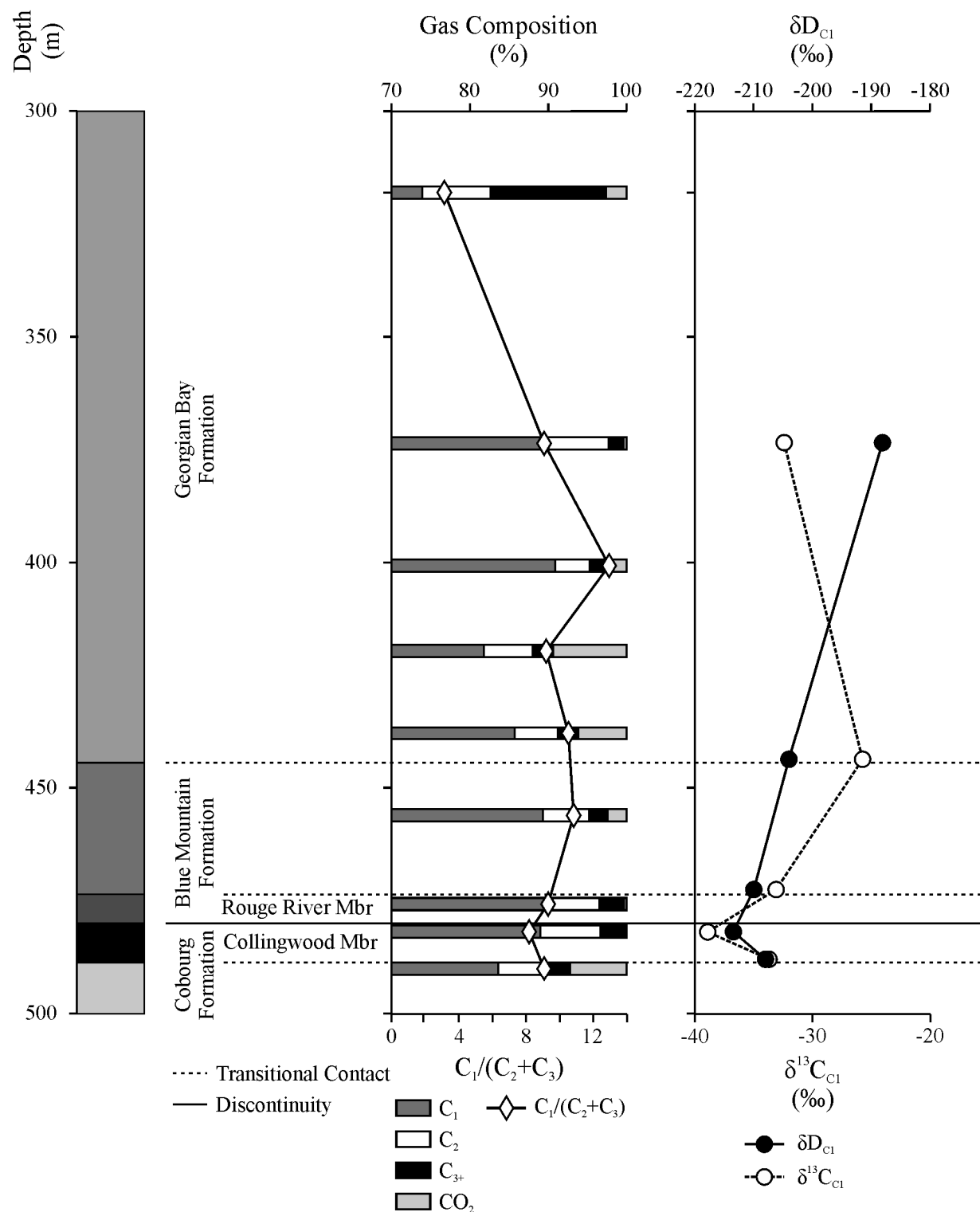


Figure 29.2. Stratigraphy, gas composition (%) and isotopic composition of methane (‰) logs of well OGS-SG11-02. Abbreviation: Mbr = Member.

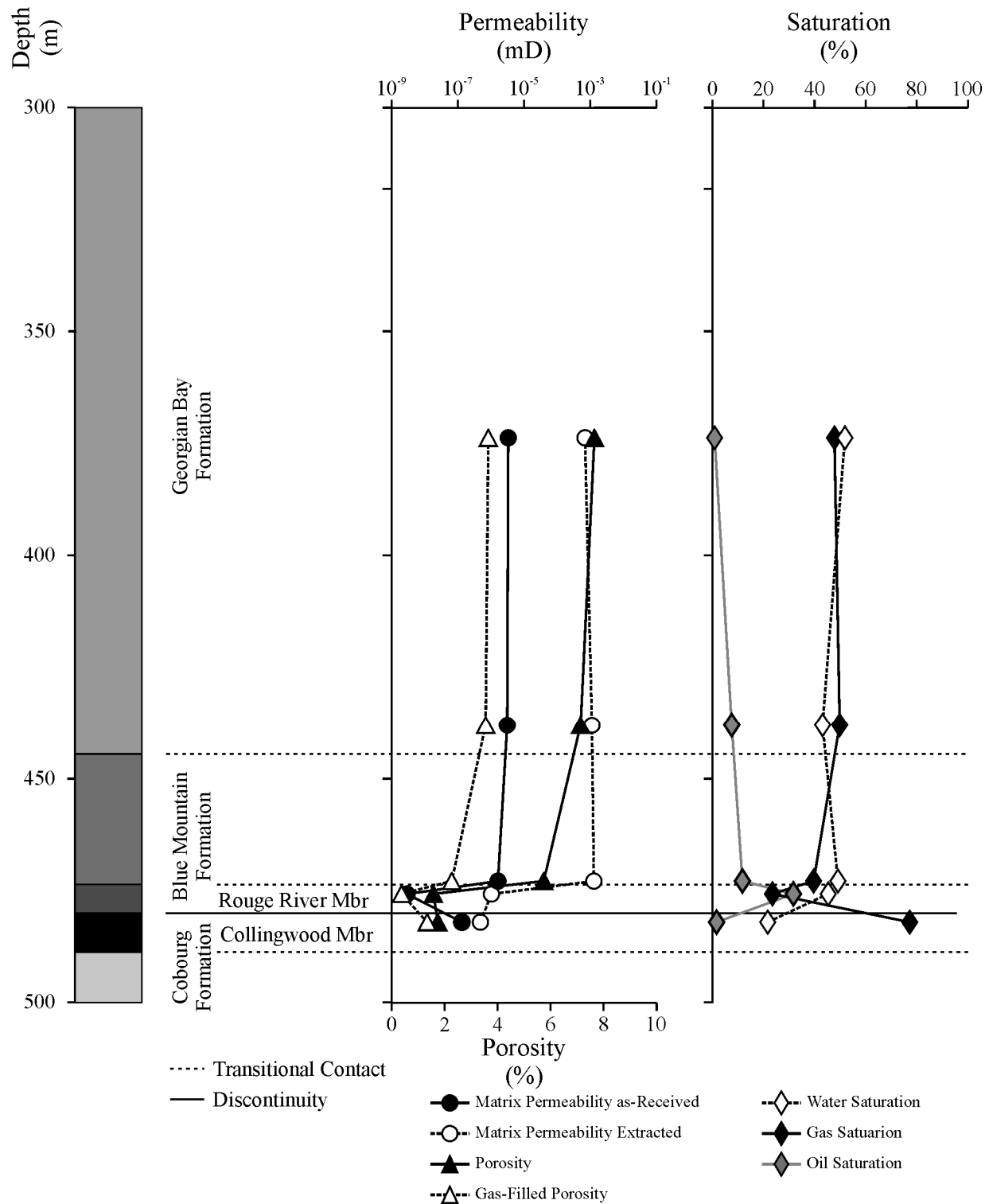


Figure 29.3. Stratigraphy, permeability (mD), porosity (%) and saturation (%) logs of well OGS-SG11-02.
Abbreviation: Mbr = Member.

Table 29.2. Gas results from well OGS-SG11-02 (from samples CAN-01 to CAN-24).

Lithology	Sample ID (CAN-)	Depth Interval (m)	Desorption					Average Composition						Isotopes	
			Lost	Desorb.	Residual		Total Gas	C ₁	C ₂	C ₃₋₁₀	CO ₂	Calorific Value		δ ¹³ C	δD
					Proj.	Meas.						Dry	Sat.		
Georgian Bay Formation	01	317.85-318.15	2.6	2.6	0.0	2.3	7.5	73.92	8.76	14.70	2.62	1326.0	1302.9	—	—
	02	330.74-331.04	0.9	2.0	0.0	0.0	2.9	—	—	—	—	—	—	—	—
	03	349.24-349.54	3.1	1.7	0.9	—	4.8	—	—	—	—	—	—	—	—
	04	364.48-364.78	2.7	1.9	0.0	—	4.6	—	—	—	—	—	—	—	—
	05	373.41-373.72	5.4	2.2	0.0	1.1	8.6	89.71	7.98	1.89	0.42	1100.8	1081.6	-32.4	-188
	06	383.07-383.38	1.4	1.8	0.9	—	3.2	—	—	—	—	—	—	—	—
	07	391.24-391.55	1.8	2.1	0.0	0.0	3.9	—	—	—	—	—	—	—	—
	08	400.48-400.75	2.3	2.9	1.7	0.0	5.2	90.90	4.37	2.65	2.09	1073.2	1054.4	—	—
	09	409.99-410.29	5.3	1.4	0.0	—	6.7	—	—	—	—	—	—	—	—
	10	419.40-419.71	0.4	1.6	0.6	0.1	2.1	81.77	6.27	2.61	9.36	1010.6	992.9	—	—
	11	428.27-428.58	1.2	1.2	0.0	0.0	2.5	—	—	—	—	—	—	—	—
	12	437.63-437.94	1.6	2.2	0.0	—	3.8	85.70	5.52	2.61	6.16	1038.6	1020.4	—	—
	Blue Mountain Formation	13	443.51-443.82	1.8	1.5	0.0	—	3.3	90.91	6.97	2.12	0.00	1100.3	1081.2	-25.7
14		449.61-449.92	1.8	1.3	0.0	0.1	3.1	—	—	—	—	—	—	—	—
15		455.92-456.22	0.8	1.6	0.0	0.7	3.0	89.31	5.89	2.34	2.46	1073.7	1055.0	—	—
16		461.86-462.17	1.0	3.2	0.8	—	4.9	—	—	—	—	—	—	—	—
17		468.20-468.51	1.4	5.4	1.0	—	7.8	—	—	—	—	—	—	—	—
18		472.26-472.56	1.9	5.8	1.1	1.4	9.1	94.57	3.94	1.49	0.00	1068.8	1048.2	-33.1	-210
Rouge River Member	19	475.49-475.79	3.6	7.9	0.4	6.4	18.0	90.02	6.49	3.16	0.33	1113.1	1093.6	<u>-15.5</u>	<u>-200</u>
Collingwood Member	20	478.81-479.12	2.5	8.9	5.0	4.2	15.6	—	—	—	—	—	—	—	—
	21	481.61-481.92	7.3	7.7	2.6	3.4	18.4	89.02	7.63	3.23	0.12	1125.4	1105.7	-38.9	-214
	22	484.36-484.66	1.2	4.3	1.4	4.0	9.5	—	—	—	—	—	—	—	—
Cobourg Formation	23	487.53-487.83	2.5	5.7	3.8	0.8	9.0	89.01	7.74	3.25	0.00	1123.1	1103.5	-33.7	-208
	24	489.81-490.12	2.5	2.2	1.8	—	6.5	83.61	6.63	2.56	7.19	1036.4	1018.3	<u>-18.7</u>	<u>-205</u>

Abbreviations: BTU/ft³ = British thermal units per cubic feet; Desorb. = desorbed; Meas. = measured; Proj. = projected, Sat. = saturated, scft = standard cubic feet per ton.

Notes: values underlined and in italics = presents air contamination. Total gas represents the sum of lost, desorbed and residual gas. When available, measured residual gas values are used instead of projected values.

Table 29.3. Total organic carbon (TOC) results from well OGS-SG11-02.

Lithology	Sample ID	Depth (m)	Total Organic Carbon (wt %)
Georgian Bay Formation	TOC-01	317.72	0.09
	TOC-10	373.53	0.26
	TOC-15	400.42	0.37
	TOC-20	419.40	0.60
	TOC-24	437.66	0.57
Blue Mountain Formation	TOC-28	455.86	0.80
	TOC-34	472.23	1.92
Rouge River Member	TOC-37	475.46	2.18
Collingwood Member	TOC-39	481.61	4.55
Cobourg Formation	TOC-42	489.81	0.46

Abbreviation: wt % = weight percent.

Table 29.4. Core analysis results from well OGS-SG11-02.

Lithology	Sample ID	Depth Interval (m)	Density		Matrix Permeability		Porosity		Saturation		
			Bulk (g/cm ³)	Grain (g/cm ³)	As-Received (mD)	Extracted (mD)	— (%)	Gas-Filled (%)	Oil (%)	Water (%)	Gas (%)
Georgian Bay Formation	GRI-05	373.51 - 373.81	2.611	2.783	3.25×10^{-6}	6.90×10^{-4}	7.66	3.65	0.6	51.7	47.6
	GRI-12	437.74 - 438.05	2.614	2.777	3.04×10^{-6}	1.12×10^{-3}	7.15	3.55	7.4	43.0	49.7
Blue Mountain Formation	GRI-18	472.78 - 472.68	2.601	2.723	1.59×10^{-6}	1.27×10^{-3}	5.75	2.27	11.5	49.0	39.5
Rouge River Member	GRI-19	475.46 - 475.76	2.545	2.574	2.85×10^{-9}	1.015×10^{-6}	1.58	0.37	31.5	45.2	23.3
Collingwood Member	GRI-21	481.74 - 482.04	2.653	2.696	1.30×10^{-7}	4.74×10^{-7}	1.74	1.34	1.4	21.4	77.2

Abbreviation: mD = millidarcy ($\approx 10^{-12} \text{ m}^2$).

Table 29.5. Triaxial static Young's modulus, Poisson's ratio and compressive strength results from well OGS-SG11-02.

Lithology	Sample ID	Depth Interval (m)	Confining Pressure (psi)	Bulk Density (g/cm ³)	Compressive Strength (psi)	Young's Modulus ($\times 10^6$ psi)	Poisson's Ratio
Georgian Bay Formation	CAN-03	349.24 - 349.54	250	2.58	16138	1.95	0.23
	CAN-12	437.63 - 437.94	310	2.55	9747	1.19	0.25
Blue Mountain Formation	CAN-18	472.26 - 472.56	330	2.6	15105	3.04	0.24
Rouge River Member	CAN-20	482.05 - 482.36	340	2.37	16968	1.59	0.24
Cobourg Formation	CAN-24	489.81 - 490.12	340	2.44	10444	1.13	0.26

Abbreviation: psi = pounds per square inch.

Table 29.6. Acoustic velocities and dynamic moduli at triaxial stress conditions from well OGS-SG11-02.

Lithology	Sample ID	Depth Interval (m)	Pressure		Bulk Density (g/cm ³)	Acoustic Velocity		Modulus			Poisson's Ratio
			Confining (psi)	Axial (psi)		Compressional (ft/s)	Shear (ft/s)	Bulk ($\times 10^6$ psi)	Young's ($\times 10^6$ psi)	Shear ($\times 10^6$ psi)	
Georgian Bay Formation	CAN-03	349.24 - 349.54	250	250	2.58	12 075	7288	2.61	4.49	1.85	0.21
			250	8000	2.58	13 499	7859	3.47	5.34	2.15	0.24
	CAN-12	130.76 - 131.06	310	310	2.55	7184	4183	0.97	1.5	0.6	0.24
			310	5000	2.55	7550	4251	1.13	1.58	0.62	0.27
Blue Mountain Formation	CAN-18	23.47 - 23.77	330	330	2.6	14 066	8442	3.61	6.09	2.5	0.22
			330	6000	2.6	14 745	8732	4.06	6.58	2.68	0.23
Rouge River Member	CAN-20	482.05 - 482.36	340	340	2.37	11 207	6482	2.22	3.35	1.34	0.25
			340	8000	2.37	12 004	6674	2.71	3.63	1.42	0.28
Cobourg Formation	CAN-24	112.47 - 112.79	340	340	2.44	10 708	6398	1.97	3.29	1.35	0.22
			340	5000	2.44	11 588	6608	2.5	3.61	1.43	0.26

Abbreviation: psi = pounds per square inch.

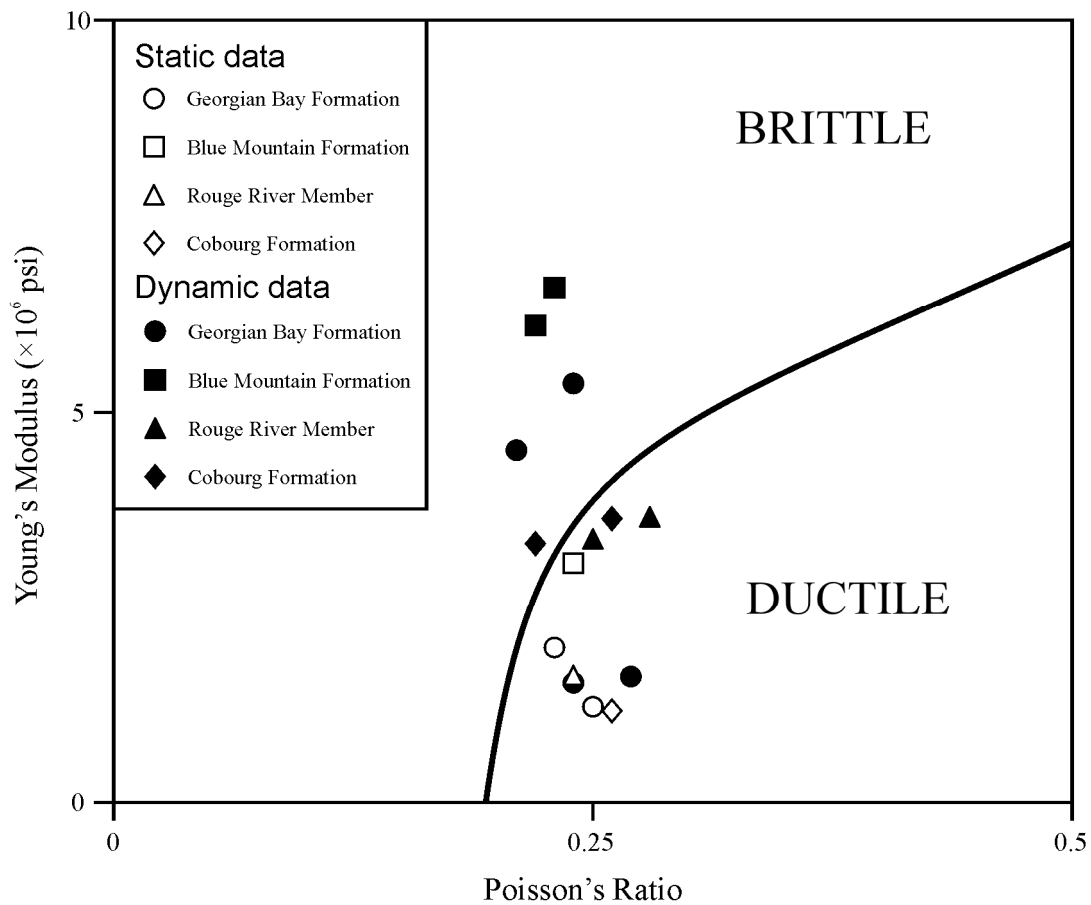


Figure 29.4. Cross-plot of Poisson's ratio and Young's modulus indicating brittle and ductile areas and well OGS-SG11-02 samples (*modified from Grieser and Bray 2007*).

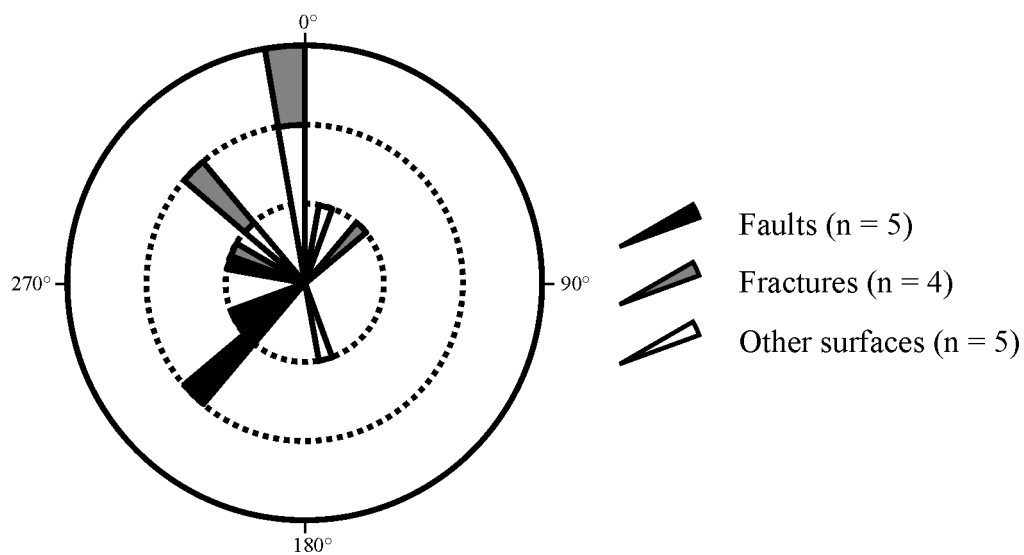


Figure 29.5. Rose diagram presenting structural features of well OGS-SG11-02 measured by the televiewer log.

At the time of publication, mineralogical and Rock-Eval[®] 6 pyrolysis results were not available from the 2012 sampling program. However, initial geological observations from the selected wells allow some regional trends in stratigraphy to be discerned. Indeed, the entire section of Ordovician shales tends to increase from the northwest to the southeast. This is even more pronounced for the Georgian Bay and Blue Mountain formations. However, the Collingwood Member shows a reverse trend based on the thickest section observed in the north. Also, the Rouge River Member, observed in cores located along lakes Erie and Ontario, seems more calcareous than in the other cores.

DISCUSSION AND CONCLUSION

Initial results from the OGS-SG11-02 drilling and sampling program show that the Rouge River Member of the Blue Mountain Formation and the Collingwood Member of the Cobourg Formation have the best potential for shale gas productive units when considering total organic carbon, gas content and hydrocarbon saturation. Indeed, the Rouge River Member has high oil saturation, whereas the Collingwood Member has a high gas saturation. However, the Georgian Bay and Blue Mountain formations can also have higher gas content values. In the case of the Georgian Bay Formation, the higher gas content samples are probably associated with limestone beds that are characterized by greater porosity (*see* Figure 29.3). For the Blue Mountain Formation, the best gas desorption values are associated with the transition into the Rouge River Member, which can also be observed with the increase of total organic carbon with depth (*see* Figure 29.1).

The first geological observations of the 2012 sampling program present different trends depending if the units are located under or above the phosphatic bed. This marker is stratigraphically situated between the limestone and calcareous mudstone of the Collingwood Member and of the Cobourg Formation and the black and bluish-grey shales from the Rouge River Member of the Blue Mountain Formation. Under this marker, the increase in thickness of the Collingwood Member to the north also corresponds to the depocentres identified in the northeast of Michigan by Rock, Harrison and Barranco (2010). The fact that the Georgian Bay and Blue Mountain formations increase in thickness to the southeast suggests these units originate from the erosion of the Appalachian Mountains. This is supported by the concordance between previously published mineralogy data of the Georgian Bay and Blue Mountain formations and similar data from the Utica Shale located in Quebec and New York State (Jackson and Murphy 2011; Martin et al. 2008; Martini and Kwong 1986; Skowron and Hoffman 2009; Thériault 2008; Wigston and Jackson 2010a, 2010b).

Future results from mineralogy and Rock-Eval[®] 6 pyrolysis analyses may help determine factors influencing important shale gas parameters such as reservoir capacity and brittleness. Furthermore, it may assist identifying organic-rich intervals, gas versus oil-prone zones and regional mineralogical variations within the same units, as preliminarily observed with the Rouge River Member. Finally, it may also help correlate Ontario's Ordovician stratigraphy with other jurisdictions.

REFERENCES

- Armstrong, D.K. and Carter, T.R. 2010. The subsurface Paleozoic stratigraphy of southern Ontario; Ontario Geological Survey, Special Volume 7, 301p.
- Barker, J.F. 1985. Geochemical analyses of Ontario oil shales; Ontario Geological Survey, Open File Report 5568, 77p.
- Barker, J.F., Russell, D.J., Johnson, M.D. and Telford, P.G. 1983. Oil shale assessment project, volume 3, organic geochemical results 1981–82; Ontario Geological Survey, Open File Report 5460, 36p.
- Béland Otis, C. 2009. Shale gas assessment project, southern Ontario; *in* Summary of Field Work and Other Activities, 2009, Ontario Geological Survey, Open File Report 6240, p.30-1 to 30-4.

- . 2010. Shale gas assessment project, southern Ontario: preliminary results from the Kettle Point Formation; *in* Summary of Field Work and Other Activities, 2010, Ontario Geological Survey, Open File Report 6260, p.38-1 to 38-7.
- . 2011. Preliminary results: shale gas assessment of the Devonian Kettle Point Formation and the Ordovician shale units, southern Ontario; *in* Summary of Field Work and Other Activities, 2011, Ontario Geological Survey, Open File Report 6270, p.26-1 to 26-9.
- Buller, D. 2010. Haynesville Shale reservoir evaluation and stimulation topics; Society of Petroleum Engineers, luncheon address, Tulsa, Oklahoma, March 11, 2010.
- Churcher, P.L., Johnson, M.D., Telford, P.G. and Barker, J.F. 1991. Stratigraphy and oil shale resource potential of the Upper Ordovician Collingwood Member, Lindsay Formation, southwestern Ontario; Ontario Geological Survey, Open File Report 5817, 98p.
- Grieser, B. and Bray, J.B. 2007. Identification of production potential in unconventional gas; Society of Petroleum Engineers, Production and Operations Symposium, March 31–April 3, 2007, Oklahoma City, Oklahoma.
- Hall, C.D. 2010. A comparison of gas shale reservoir properties – Muskwa, Marcellus, Barnett, Montney, Haynesville and Eagle Ford; oral presentation, 4th British Columbia Unconventional Gas Technical Forum, Victoria, British Columbia, April 9, 2010.
- Harris, D. 1984. Graphic logs of oil shale intervals: Ordovician Collingwood Member and the Devonian Kettle Point and Marcellus formations; Ontario Geological Survey, Open File Report 5527, 225p.
- Jackson, R. and Murphy, S. 2011. Mineralogical and lithogeochemical analyses of DGR-5 and DGR-6 core; report by Geofirma Engineering Ltd., Ottawa, Ontario, under contract to Nuclear Waste Management Organization, Ontario Power Generation (OPG) Deep Geologic Repository (DGR) project, Site Characterization Technical Report TR-09-06 (rev.0), 158p., www.nwmo.ca/dgrsitecharacterizationtechnicalreports [accessed September 19, 2012].
- Johnson, M.D. 1983. Oil shale assessment project, deep drilling results 1982/83, Toronto region; Ontario Geological Survey, Open File Report 5477, 17p.
- Johnson, M.D., Armstrong, D.K., Sanford, B.V., Telford, P.G. and Rutka, M.A. 1992. Paleozoic and Mesozoic geology of Ontario; *in* Geology of Ontario, Ontario Geological Survey, Special Volume 4, Part 2, p.907-1008.
- Johnson, M.D., Russell, D.J. and Telford, P.G. 1983a. Oil shale assessment project, volume 1, shallow drilling results 1981–1982; Ontario Geological Survey, Open File Report 5458, 39p.
- . 1983b. Oil shale assessment project, volume 2, drillholes for regional correlation 1981–1982; Ontario Geological Survey, Open File Report 5459, 20p.
- . 1985. Oil shale assessment project, drillholes for regional correlation 1983/84; Ontario Geological Survey, Open File Report 5565, 49p.
- Lavoie, D. 2011. The Upper Ordovician Utica and Lorraine shales in southern Quebec: a regional overview; abstract, American Association of Petroleum Geologists, AAPG Geosciences Technology Workshop, “Success in the Marcellus and Utica shales: Case studies and new developments”, Baltimore, Maryland, May 23-25, 2011.
- Lavoie, D. and Thériault, R. 2012. Upper Ordovician shale gas and oil in Quebec: sedimentological, geochemical and thermal frameworks; oral presentation, Canadian Society of Petroleum Geologist, GeoConvention 2012: Vision, Calgary, Alberta, May 14-18, 2012.
- Macauley, G., Fowler, M.G., Goodarzi, F., Snowdon, L.R. and Stasiuk, L.D. 1990. Ordovician oil shale-source rock sediments in the central and eastern Canada mainland and eastern arctic areas, and their significance for frontier exploration; Geological Survey of Canada, Paper 90-14, 51p.

- Macauley, G. and Snowdon, L.R. 1984. A Rock-Eval appraisal of the Ordovician Collingwood shales, southern Ontario; Geological Survey of Canada, Open File 1092, 15p.
- Martin, J.P., Nyahay, R., Leone, J. and Smith, L.B. 2008. Developing a new gas resource in the heart of the northeastern U.S. market: New York's Utica Shale play; oral presentation, American Association of Petroleum Geologists, Convention, San Antonio, Texas, April 20-23, 2008.
- Martini, I.P. and Kwong, J.K.P. 1986. Geology and ceramic properties of selected shales and clays of southwestern Ontario; Ontario Geological Survey, Open File Report 5583, 116p.
- Rancourt, C.C. 2009. "Collingwood" strata in south-central Ontario – a petrophysical chemostratigraphic approach to comparison and correlation using geophysical borehole logs; unpublished MSc thesis, University of Toronto, Toronto, Ontario, 65p.
- Rickman, R., Mullen, M., Petre, E., Grieser, B. and Kundert, D. 2008. A practical use of shale petrophysics for stimulation design optimization: all shale plays are not clones of the Barnett Shale; Society of Professional Engineers, Annual Technical Conference and Exhibition, September 21-24, 2008, Denver, Colorado.
- Rock, F., Harrison, W.B. and Barranco, R.K. 2010. Geological and petrophysical characterization of unconventional gas play, the Middle Ordovician Collingwood Member of Trenton Formation, in north-central lower Michigan, USA; American Association of Petroleum Geologists, Eastern Section Meeting, Kalamazoo, Michigan, September 25-29, 2010.
- Russell, D.J. and Telford, P.G. 1983. Revisions to the stratigraphy of the Upper Ordovician Collingwood beds of Ontario – a potential oil shale; Canadian Journal of Earth Sciences, v.20, p.1780-1790.
- Skowron, A. and Hoffman, E. 2009. XRD Mineralogical analysis of DGR-1 and DGR-2 core; report by Activation Laboratories, Ancaster, Ontario, for Intera Engineering Ltd., Ottawa, Ontario, under contract to Nuclear Waste Management Organization, Ontario Power Generation (OPG) Deep Geologic Repository (DGR) project, Site Characterization Technical Report TR-08-01 (rev.0), 112p., www.nwmo.ca/dgrsitecharacterizationtechnicalreports [accessed September 19, 2012].
- Smith, L.B. and Leone, J. 2010. Integrated characterization of Utica and Marcellus black shale gas plays, New York State; oral presentation, American Association of Petroleum Geologists, Annual Convention and Exhibition, New Orleans, Louisiana, April 11-14, 2010.
- Snowdon, L.R. 1984. A comparison of RockEval pyrolysis and solvent extract results from the Collingwood and Kettle Point oil shales, Ontario; Bulletin of Canadian Petroleum Geology, v.32, p.327-334.
- Stromquist, J.K., Dickhout, R. and Barker, J.F. 1984. Oil shale assessment project, volume 4, analytical geochemistry of selected potential oil shales (Ontario and New Brunswick); Ontario Geological Survey, Open File Report 5461, 46p.
- Thériault, R. 2008. Caractérisation géochimique et minéralogique des shales de l'Utica et du Lorraine, Basses-Terres du Saint-Laurent, Base de données; Ministère des Ressources naturelles et de la Faune du Québec, 2008-EG-01.
- Wigston, A. and Jackson, R. 2010a. Mineralogy and geochemistry of DGR-3 core; report by Intera Engineering Ltd., Ottawa, Ontario, under contract to Nuclear Waste Management Organization, Ontario Power Generation (OPG) Deep Geologic Repository (DGR) project, Site Characterization Technical Report TR-08-22 (rev.0), 183p., www.nwmo.ca/dgrsitecharacterizationtechnicalreports [accessed September 19, 2012].
- 2010b. Mineralogy and geochemistry of DGR-4 core; report by Intera Engineering Ltd., Ottawa, Ontario, under contract to Nuclear Waste Management Organization, Ontario Power Generation (OPG) Deep Geologic Repository (DGR) project, Site Characterization Technical Report TR-08-23 (rev.0), 156p., www.nwmo.ca/dgrsitecharacterizationtechnicalreports [accessed September 19, 2012].

30. Project Unit 10-028. Update on the Hudson Platform Paleozoic Mapping Project: Results from the Northwestern Moose River Basin

D.K. Armstrong¹

¹Earth Resources and Geoscience Mapping Section, Ontario Geological Survey

INTRODUCTION

This project was initiated in 2010 by the Ontario Geological Survey (OGS) in support of the Federal GEO-mapping for Energy and Minerals (“GEM”) initiative conducted by the Geological Survey of Canada (GSC), Natural Resources Canada. This initiative is focussed on geological mapping for informed resource development in the extreme Far North of Canada (generally north of latitude 60°). Activities under GEM in the Far North of Ontario are designed to assist in re-assessing the hydrocarbon resource potential of the Hudson Platform (Armstrong and Lavoie 2010a).

In 2010, the OGS project involved logging and sampling of archival cores from the James and Hudson Bay lowlands (Armstrong and Lavoie 2010a). The most significant finding of that first year was the confirmation of the presence of Upper Ordovician organic-rich lime mudstones (i.e., “black shales”) in northern Ontario. These were initially discovered in 2 archived mineral industry cores and were assigned to the Boas River Formation (Sanford and Grant 1990; McCracken 1990). This unit is roughly equivalent to the Collingwood Member of the Lindsay Formation in southern Ontario and the Utica Shale of Quebec and northeastern United States. Organic analysis of the Boas River Formation indicates it has good potential as a source of hydrocarbons (Armstrong and Lavoie 2010b).

In 2011, field investigations were carried out across the Far North from the upper Attawapiskat River to the lower Severn River (Figure 30.1; Armstrong 2011). The objectives of that work included 1) examination of previously mapped outcrops (i.e., Sanford, Norris and Bostock 1968), especially in areas considered to be “type” or representative for particular formations; and 2) logging and sampling of mineral industry exploration drill cores that had been left at drill sites in the lowlands (Armstrong 2011). Locations of outcrops and cores examined in 2011 are shown in Figure 30.1. An outcrop of the Boas River Formation was discovered along the Asheweig River, in what appears to be an outlier, approximately 40 km south of the drill core occurrences confirmed in 2010.

Field work for 2012 was planned to follow up this discovery and explore for more occurrences of the Boas River Formation along the Ordovician outcrop belt. Unfortunately, field work in 2012 was deferred due to ongoing discussions with affected First Nation communities. Instead, selected diamond-drill cores from the northwestern Moose River Basin were logged in Sudbury. These diamond-drill holes were completed in the mid-1990s by KWG–Spider Resources; the core was subsequently donated to the OGS. The cores studied in 2012 intersected only Upper Ordovician to Lower Silurian strata. Location and basic stratigraphic information for these cores is presented in Table 30.1. These cores provide a more detailed picture of the Paleozoic geology in this part of the basin. This report presents preliminary results from the study of these cores, combined with results of field work done in 2011.

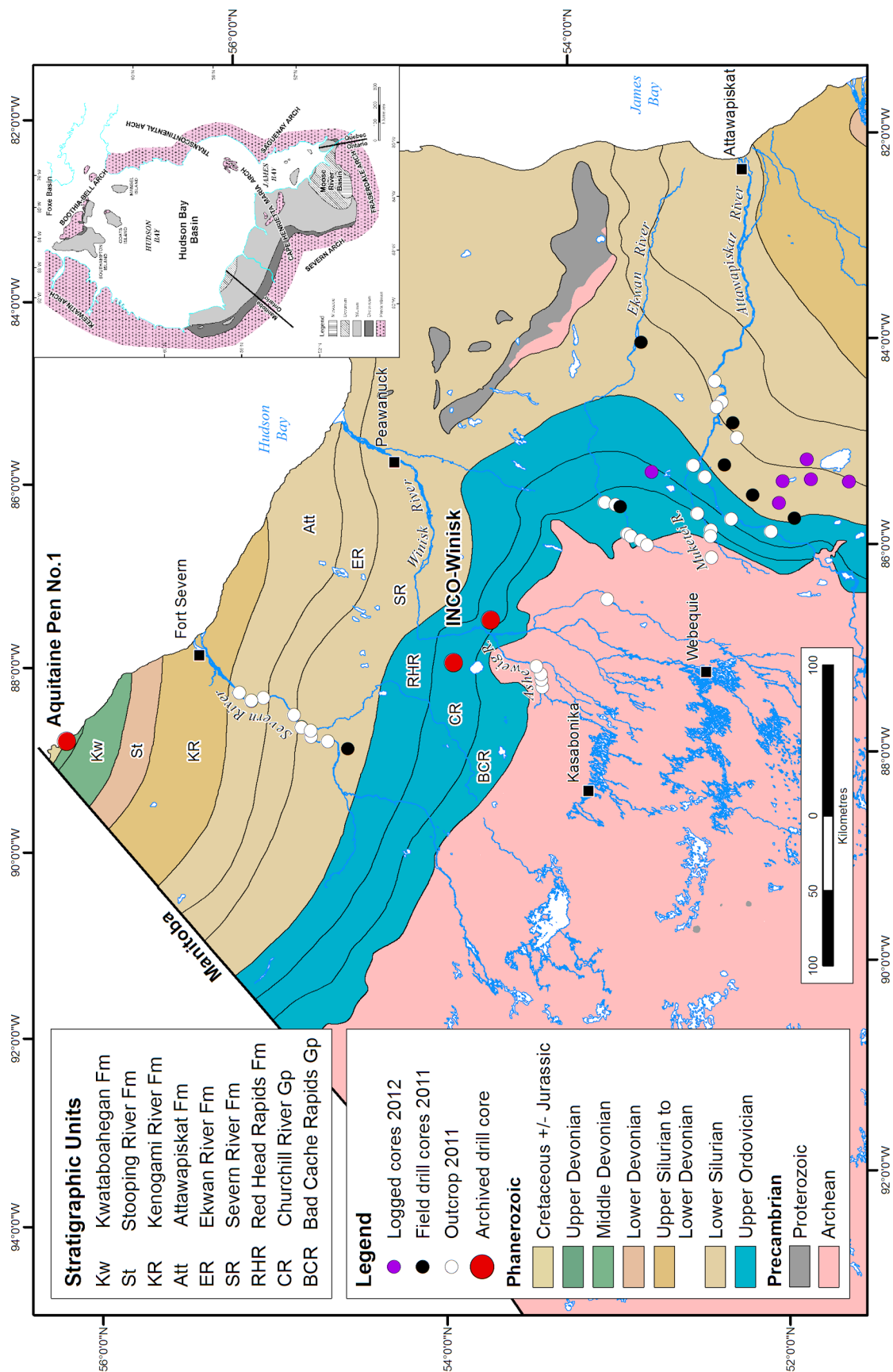


Figure 30.1. Paleozoic geology of the Hudson Platform in northern Ontario showing locations of cores and outcrops examined for this project in 2011 and 2012. Geology modified from Ontario Geological Survey (1991). Inset map from Zhang (2010).

Table 30.1. Drill cores studied in 2012, with corresponding OGS station number, location and basic stratigraphic information.

OGS Station #	Company Hole #	UTM NAD83, Zone 16		Latitude (N)	Longitude (W)	Elevation (m asl)	Top Bedrock Unit	Top of Bedrock Depth (m bs)	Depth to Precambrian Basement (m bs)
		Easting (m)	Northing (m)						
12DKA001	DR-94-09	608446	5813808	52°27'49.20"	85°24'13.38"	178	Severn River Fm	57.83	133.05*
12DKA002	DR-94-10	608882	5788342	52°14'05"	85°24'20"	170	Red Head Rapids Fm	64.62	154.53
12DKA003	DR-95-29	621316	5817411	52°29'36"	85°12'47"	195	Severn River Fm	39.00*	182.20*
12DKA004	DR-95-27	605495	5832388	52°37'52.38"	85°26'28.44"	175	Severn River Fm	23.00	123.50*
12DKA005	DR-94-24	591024	5833437	52°38'35.76"	85°39'16.86"	165	Red Head Rapids Fm	30.50	100.00
12DKA006	DR-95-37	604494	5919557	53°24'53"	85°25'40"	122	Red Head Rapids Fm	10.40	81.80*

Notes: * depth from company core logs. Elevations were estimated from 1:250 000 scale topographic maps.

Abbreviations: Fm = Formation; m bs = metres below surface; m asl = metres above sea level;

NAD83 = North American Datum 1983; UTM = Universal Transverse Mercator co-ordinates .

GEOLOGIC SETTING

Overviews of the geologic setting and Paleozoic stratigraphy of the Hudson Platform and its constituent sedimentary basins are provided by Hamblin (2008), Norris (1993), Sanford (1987) and Sanford, Norris and Bostock (1968). The platform consists of the Hudson Bay Basin and 2 subordinate basins, the Foxe Basin to the north in Nunavut, and the Moose River Basin to the south in northern Ontario (*see inset, Figure 30.1*).

The Hudson Bay Basin contains up to 2500 m of Upper Ordovician to Upper Devonian shallow marine strata with thin remnants of Cretaceous and Cenozoic sedimentation. The Moose River Basin contains approximately 500 m of Upper Ordovician to Upper Devonian shallow marine to terrestrial sediments, partially covered by as much as 200 m of Jurassic and Cretaceous lacustrine and fluvial sediments (Johnson et al. 1992).

NORTHWESTERN MOOSE RIVER BASIN

The cores examined in 2012 resulted from diamond drilling in the northwestern part of the Moose River Basin, south of the Cape Henrietta Maria Arch (*see inset, Figure 30.1*). The arch is a Precambrian basement topographic high that presently separates the Moose River Basin from the Hudson Bay Basin to the north. The arch was apparently not a positive topographic feature during the Upper Ordovician and Silurian (Sanford 1987). The Paleozoic succession in the northern Moose River Basin ranges from the Upper Ordovician Bad Cache Rapids Group up to the Siluro-Devonian Kenogami River Formation (Figures 30.1 and 30.2). The cores studied in 2012 were collared in the Lower Silurian Severn River Formation or older units.

The Bad Cache Rapids Group generally consists of basal quartz-rich, typically carbonate-cemented sandstones that grade upward into thick-bedded, bioturbated, fossiliferous limestones and/or dolostones with local chert toward the top. A variety of burrow types occur in this unit; however, small, blue-rimmed burrows are characteristic. The formal subdivisions of this unit, as identified in Manitoba (e.g., Nelson 1963), are not presently recognized in Ontario. In most of the cores examined, the Bad Cache Rapids Group was almost entirely dolomitized.

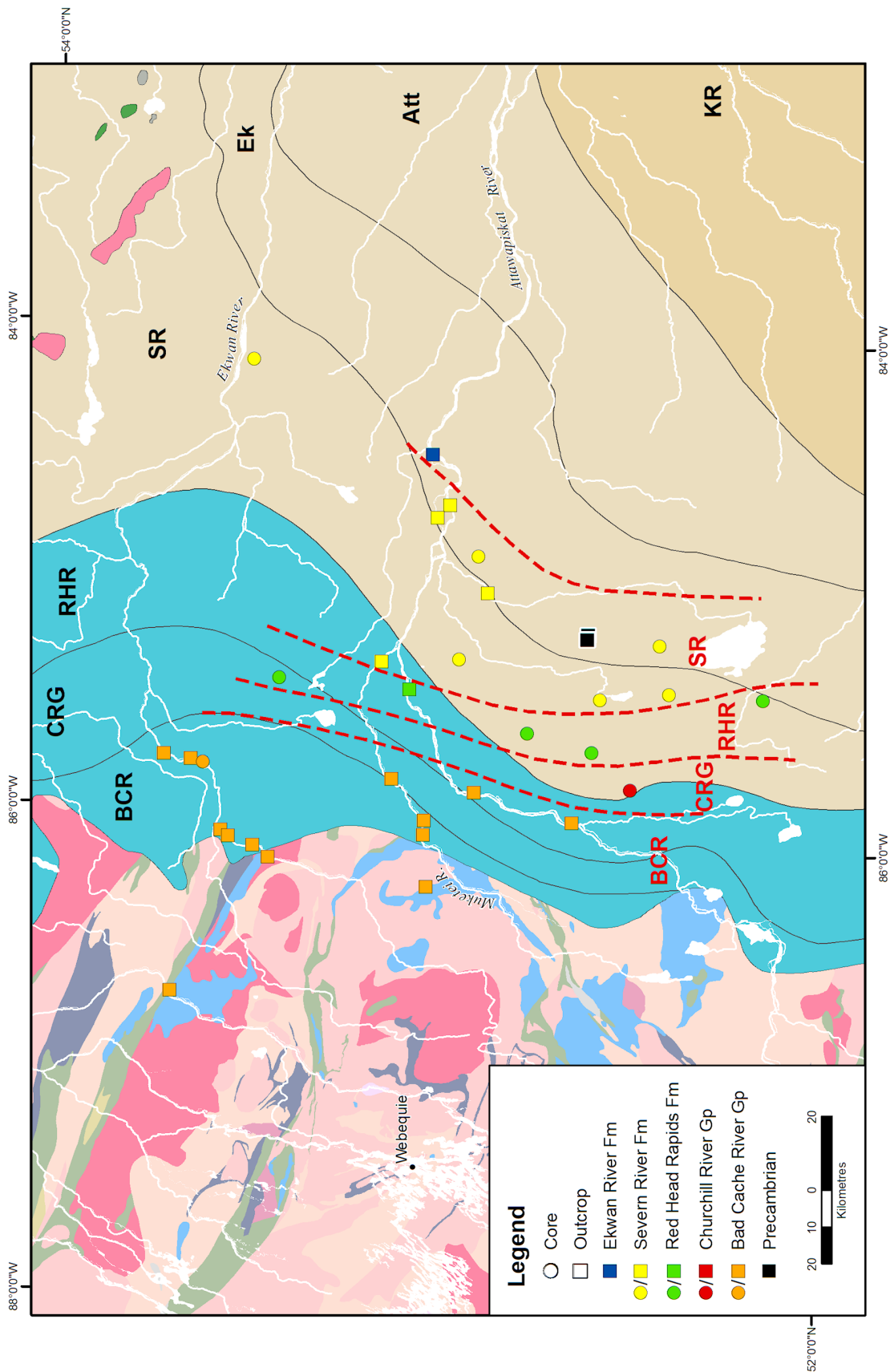


Figure 30.2. Bedrock geology of the northwestern Moose River Basin showing locations of cores and outcrops studied in 2011 and 2012, colour-coded to indicate the topmost stratigraphic unit. Red dashed lines and labels indicate proposed new distribution of stratigraphic units and contacts. Colours and acronyms for Paleozoic units are the same as in Figure 30.1. Geology is *from* Ontario Geological Survey (2011).

To date, only one occurrence of possible Boas River Formation has been found in the northwest Moose River Basin. It is a thin bed of black, apparently organic-rich, shelly, lime mudstone that occurs near the top of a core drilled near the upper Ekwan River (station 11DKA004, *see* Table 27.1 in Armstrong 2011). Organic and biostratigraphic analyses of this bed are ongoing. A few other very thin dark brown beds of shale or sandstone were found in the Churchill River Group in cores logged this year. Samples of these beds have been submitted for organic analysis.

In Ontario, the Churchill River Group can be divided into lower and upper units. The correlations of these informal units to formations as defined in northern Manitoba (e.g., Nelson 1963) are unclear. The lower Churchill River Group is characterized by thin-bedded dolostones and green shales, with gypsum (or anhydrite) nodules and seams, and local sandstones. It is interpreted to have been deposited in a very shallow restricted environment. The upper Churchill River Group consists of thicker bedded, massive textured, sparsely to moderately fossiliferous limestones and dolostones. The upper Churchill River Group unit is interpreted to have been deposited in a shallow subtidal setting, similar to the Bad Cache Rapids Group. In places in the northern Moose River Basin, the upper Churchill River Group appears to thin and the evaporitic lower Churchill River Group appears to merge with similar strata of the overlying Red Head Rapids Formation.

The uppermost Ordovician unit, the Red Head Rapids Formation, consists of a mixture of siliciclastic mudstones (shales), siltstones and sandstones, dolo-mudstones, argillaceous dolostones, limestones and gypsum or anhydrite. In the Hudson Bay Basin, shallowing-upward evaporative cycles are well developed in this formation. The cycles begin with normal subtidal marine bioturbated, fossiliferous limestone, grade up into barren dolostones and then into anhydrite-bearing dolostones. Cycles are capped by green, argillaceous, and sometimes silty, dolostones, which may, in part, represent subaerial deposition. Halite is reported in the Red Head Rapids Formation toward the centre of the Hudson Bay Basin (Norris 1993). In the Moose River Basin, fossiliferous limestones are sparse in this unit and red sandy mudstones are more prevalent. These suggest a shallower, perhaps periodically terrestrial environment during the latest Ordovician in this region.

The Lower Silurian Severn River Formation consists of a basal unit characterized by fossiliferous, tan to grey, burrow-mottled limestone and minor dolostone with up to 2 zones containing abundant thick-shelled *Virgiana* brachiopods. Most of the rest of this formation consists of cycles of similarly fossiliferous and burrow-mottled carbonates, overlain by anhydrite- (or gypsum-) bearing dolostones, capped with thin-bedded argillaceous and sometimes silty dolostones.

Implications for the Bedrock Geology Map of the Northwestern Moose River Basin

During field work in 2011, an outcrop of the Severn River Formation containing *Virgiana* brachiopods was discovered on the lower Muketei River in an area that had been mapped as Red Head Rapids Formation (station 11DKA019, *see* Table 27.1 in Armstrong 2011). Also, some cores drilled in areas mapped as Severn River Formation were actually collared in the underlying Red Head Rapids Formation. Clearly, as new data are acquired in this region, significant refinements may be made to bedrock geology maps.

This summer, archival cores drilled in this area were examined, specifically to identify the uppermost unit in each core. Many of the Paleozoic units in the Hudson Platform have similar lithologic characteristics, so the stratigraphic assignment of a small outcrop or short interval of core is often difficult. Continuous cores provide stratigraphic context and lithostratigraphic patterns can be identified and correlated from core to core.

An important stratigraphic marker in this part of the Moose River Basin is the *Virgiana*-rich horizon near the base of the Severn River Formation. These white, thick-shelled brachiopods (Photo 30.1) are abundant in 1 or 2 zones, with total stratigraphic section of up to 12 m thick. The base of the “*Virgiana* beds” was found to occur from 5 to 8 m above the base of the formation in this region.

Using the occurrence of *Virgiana* in cores and outcrops, mapping of the Severn River–Red Head Rapids formational contact is much better constrained. As shown in Figure 30.2, south of the Attawapiskat River, this contact shifts from its currently mapped location to the east. North of the Attawapiskat River, it appears to shift to the west. From the distribution of formation tops in drill cores and outcrops west of this contact, it appears as though the bases of the Red Head Rapids Formation and Churchill River Group are subparallel to this. The upper contact of the Severn River Formation with the overlying Ekwon River Formation appears to trend to the northeast; however, there are few new data points to constrain this contact.

ONGOING RESEARCH AND FUTURE WORK

Results of biostratigraphic, chemostratigraphic and geochemical analyses are pending. These will be incorporated with lithostratigraphic core logs and petrographic characterization of units. Synthesis of all these data will enable a more robust stratigraphic architecture and mapping of the Paleozoic of the Hudson Platform in Ontario.

Analysis of the abundant new diamond-drilling data resulting from the McFaulds Lake (“Ring of Fire”) area mineral exploration activities at the western edge of the Paleozoic cover will assist mapping in the northwestern Moose River Basin.



Photo 30.1. Abundant white, thick-shelled *Virgiana* brachiopods of the lower Severn River Formation in core pieces next to the tape measure, at approximately 65 m depth in core DR-94-09 (station 12DKA001; see Table 30.1). Small red and white divisions on the tape measure are 0.5 cm long.

More field work is required to explore for more occurrences of the Boas River Formation. Accessing more industry core (if available) or acquiring new cores, especially in the Hudson Bay Lowland, would add significantly in our understanding of this unit and its potential resources.

In northern Ontario, the Boas River Formation has only been discovered in the upper Winisk River area (Sanford and Grant 1990; Armstrong and Lavoie 2010a; Armstrong 2011). It is absent in the Aquitaine Pen No. 1 well (*see* Figure 30.1) and also appears absent (although there are missing intervals of core) in Wallbridge core (station 11DKA026, *see* Armstrong 2011). It is not clear what controls the deposition and/or preservation of the Boas River Formation. Understanding these controls is critical to predicting its potential as a hydrocarbon source rock deeper in the Hudson Bay Basin. St. Jean (2012) undertook a petrographic study of the Boas River Formation occurrences in Ontario. She found the organic-rich laminated facies to exhibit grading and that its fossil content is almost exclusively ostracods. Together, these suggest deposition as distal tempestites in an outer shelf or ramp setting with restricted anoxic to dysoxic waters.

Claire Bibby is starting a Bachelor of Science thesis at the University of Ottawa, under the supervision of Dr. André Desrochers. She will be undertaking a petrographic examination of the Bad Cache Rapids and Churchill River groups in order to better define the environments in which the Boas River Formation facies may (or may not) have developed.

ACKNOWLEDGMENTS

The efforts of Neil Novak, formerly of Spider Resources, in arranging for and facilitating the donation of diamond-drill core from the Spider-KWG Joint Venture in the James Bay Lowland to the OGS in the 1990s is greatly appreciated. Dr. Jisuo Jin, Western University (formerly the University of Western Ontario), is thanked for his assistance in the initial identification of *Virgiana* brachiopods in our samples. The assistance of Claire Bibby this summer is appreciated, as is the supervision by Dr. André Desrochers, University of Ottawa, of Bachelor of Science theses by Nadia St. Jean and Claire Bibby. Denis Lavoie (GSC–Quebec), as lead of the Hudson Platform GEM project, has been instrumental in facilitating analytical support for this project at the GSC, especially in the form biostratigraphic and organic geochemical analyses. This project has also benefitted from his guidance, encouragement and commitment. Thank you to Shannon Evers for preparing figures for this report and for other presentations.

REFERENCES

- Armstrong, D.K. 2011. Re-evaluating the hydrocarbon resource potential of the Hudson Platform: interim results from northern Ontario; *in* Summary of Field Work and Other Activities 2011, Ontario Geological Survey, Open File Report 6270, p.27-1 to 27-11.
- Armstrong, D.K. and Lavoie, D. 2010a. Re-evaluating the hydrocarbon resource potential of the Hudson Platform: project introduction and preliminary results from northern Ontario; *in* Summary of Field Work and Other Activities 2010, Ontario Geological Survey, Open File Report 6260, p.39-1 to 39-9.
- 2010b. Re-appraisal of the hydrocarbon resource potential of the Hudson Platform: project introduction and preliminary results from northern Ontario; *in* Proceedings of the Ontario Petroleum Institute, 49th Annual Conference, Niagara Falls, Ontario, Technical Paper 15, 12p.
- Hamblin, A.P. 2008. Hydrocarbon potential of the Paleozoic succession of Hudson Bay/James Bay: preliminary conceptual synthesis of background data; Geological Survey of Canada, Open File 5731, 12p.
- Johnson, M.D., Armstrong, D.K., Sanford, B.V., Telford, P.G. and Rutka, M.A. 1992. Paleozoic and Mesozoic geology of Ontario; *in* Geology of Ontario, Ontario Geological Survey, Special Volume 4, Part 2, p.907-1008.

- McCracken, A.D. 1990. Report on 38 Ordovician conodont samples from drill core of the Bad Cache Rapids Formation, Boas River Formation, and Churchill River Group in the Hudson Bay Lowlands (Clendenning River map sheet, Winisk River area), northern Ontario submitted by B.V. Sanford (GSC–LCSD) and A.C. Grant (GSC–AGC) (NTS 43 L/6, 43 L/12); Geological Survey of Canada, Paleontological Report 03-ADM-1990, 30p.
- Nelson, S.J. 1963. Ordovician paleontology of the Hudson Bay Lowlands; Geological Society of America, Memoir 90, 152 p.
- Norris, A.W. 1993. Hudson Platform – geology; *in* Sedimentary cover of the craton in Canada, Geological Survey of Canada, Geology of Canada, no.5, p.653–700. [*also* Geological Society of America, The geology of North America, v.D-1.]
- Ontario Geological Survey 1991. Bedrock geology of Ontario, northern sheet; Ontario Geological Survey, Map 2541, scale 1:1 000 000.
- 2011. 1:250 000 scale bedrock geology of Ontario; Ontario Geological Survey, Miscellaneous Release—Data 126—Revision 1.
- St. Jean, N.F. 2012. Mineralogical, petrographic and geochemical characterization of organic-rich carbonate of the Upper Ordovician Boas River Formation in northern Ontario: implications for petroleum exploration; unpublished Bachelor of Science thesis, University of Ottawa, Ottawa, Ontario, 61p.
- Sanford, B.V. 1987. Paleozoic geology of the Hudson Platform; *in* Sedimentary basins and basin-forming mechanisms, Canadian Society of Petroleum Geologists, Memoir 12, p.483-505.
- Sanford, B.V. and Grant, A.C. 1990. New findings relating to the stratigraphy and structure of the Hudson Platform; *in* Current Research, Part D, Geological Survey of Canada, Paper 90-1D, p.17–30.
- Sanford, B.V., Norris, A.W. and Bostock, H.H. 1968. Geology of the Hudson Bay Lowlands (Operation Winisk); Geological Survey of Canada, Paper 67-60, 118p.
- Zhang, S. 2010. Upper Ordovician stratigraphy and oil shales on Southampton Island, field trip guidebook; Geological Survey of Canada, Open File 6668, 42p.

31. Project Unit 10-026. An Update on Three-Dimensional Mapping of Quaternary Deposits in the Southern Part of the County of Simcoe, Southern Ontario

A.F. Bajc¹, D.R.B. Rainsford¹ and R.P.M. Mulligan²

¹Earth Resources and Geoscience Mapping Section, Ontario Geological Survey, Sudbury, Ontario P3E 6B5

²School of Geography and Earth Sciences, McMaster University, Hamilton, Ontario L8S 4K1

INTRODUCTION

Field work for a three-dimensional (3-D) mapping project of Quaternary deposits in the southern part of the County of Simcoe (herein referred to as “south Simcoe County”) (Figure 31.1) was initiated in 2010 (Bajc and Rainsford 2010, 2011) and continued during the spring and summer of 2012. The project is one of several currently being undertaken as part of the Ontario Geological Survey groundwater mapping program and is a continuation of a similar project recently completed within the Barrie–Oro moraine area to the north (Burt and Dodge 2011).

The objectives of this project are to develop interactive 3-D models of the Quaternary geology that can 1) aid in studies involving groundwater extraction, protection and remediation; 2) assist with the development of policies surrounding land use and nutrient management; and 3) help to better understand the interaction between ground and surface waters. A better understanding of the geometry and inherent properties of the Quaternary sediments that overlie the bedrock surface within this region will assist with the development of source water protection plans and with the development of a geoscience-based management plan for the groundwater resource.

The 2010 program consisted of reconnaissance mapping of surficial deposits, which included detailed inspection and logging of significant natural and man-made exposures. In addition, a pilot project of ground-based gravity surveying was conducted along 3 west-trending transects to evaluate the method as a tool for refining the position of buried-bedrock channels associated with the Laurentian trough. The results of this work are summarized in Bajc and Rainsford (2010). Following on the positive results of this pilot project, a full-scale regional gravity survey was conducted across the entire study area in 2011 to not only refine the position of deeply buried bedrock channels, but also assist with the selection of sites suitable for follow-up coring during the summer of 2011. The results of this geophysical survey as well as the first campaign of drilling are reported on in Bajc and Rainsford (2011).

An airborne electromagnetic survey was conducted over the south-central part of the study area during the spring of 2012 to determine the effectiveness of this method for mapping bedrock topography and important hydrostratigraphic units that overlie the bedrock surface. A follow-up drill program during the summer of 2012 was undertaken to help calibrate the electromagnetic geophysical model as well as to provide additional stratigraphic information in outlying areas. Detailed section logging along the Nottawasaga River was also undertaken in support of a Master of Science thesis at McMaster University as well as to provide additional shallow stratigraphic information within this area for construction of the 3-D model.

CONTINUOUS CORING

At the time of writing, 7 continuously cored boreholes were completed to bedrock within the study area with an eighth borehole planned for the fall of 2012. Of the 7 holes drilled during the summer months, 4 were located on the Simcoe uplands, 2 in tunnel-channel settings and 1 within the Oak Ridges Moraine adjacent to the Niagara Escarpment (Figure 31.2). The eighth borehole (SS-12-08) was drilled in October south of the town of Cookstown within the Cookstown tunnel channel.

A total of 813.65 m were drilled in the 7 boreholes with depth-to-bedrock ranging between 5.65 and 161.25 m (Figure 31.3). Core recovery was generally very good with a mean recovery rate of greater than 90 to 95%. Deep monitoring wells were installed at 4 sites (SS-12-02, -04, -05 and -07) with a fifth planned for site SS-12-08. Shallow monitors were installed adjacent to the deep ones in order to compare water parameters and establish groundwater flow gradients.

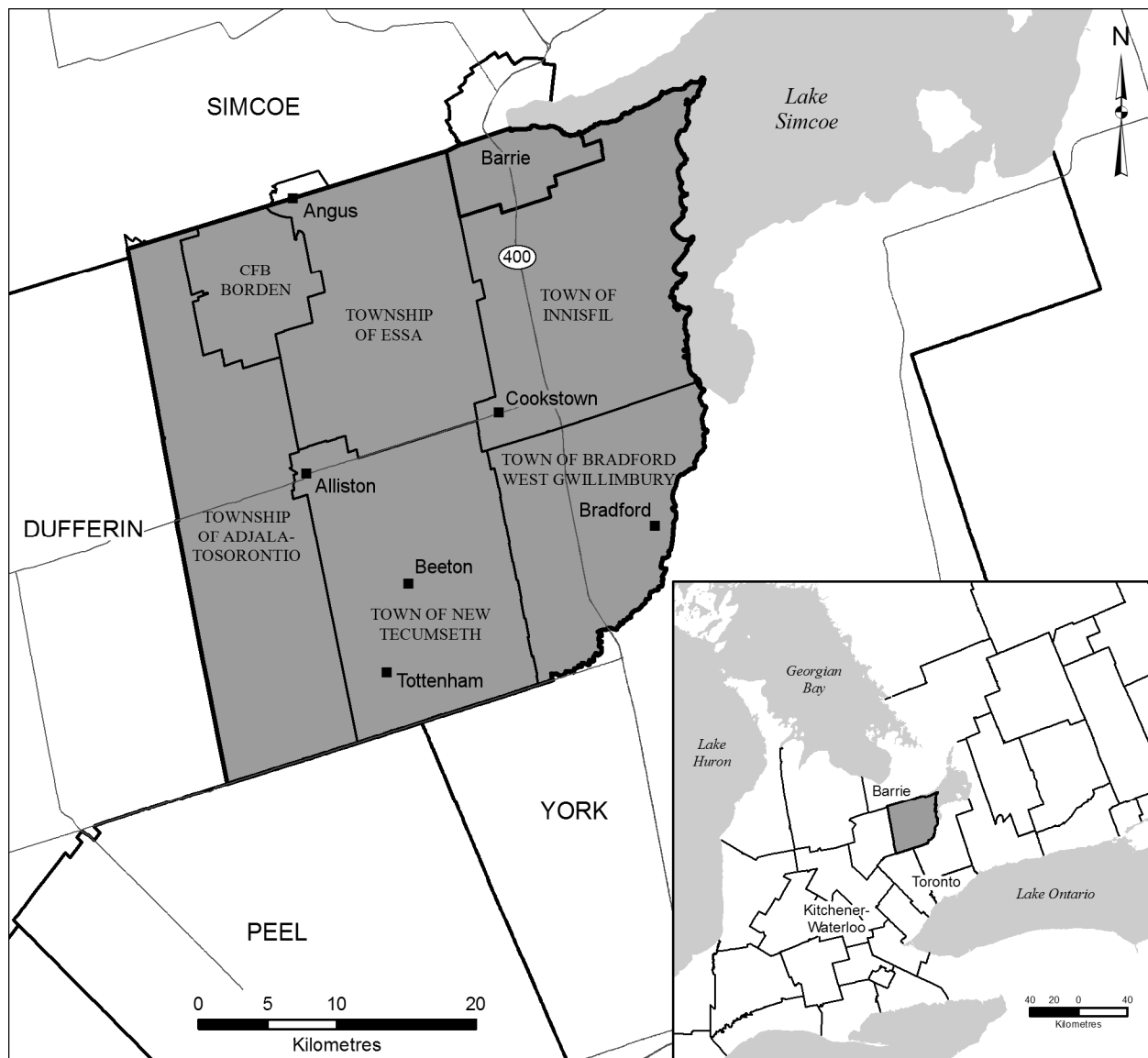


Figure 31.1. Location of the study area, southern part of Simcoe County, southern Ontario.

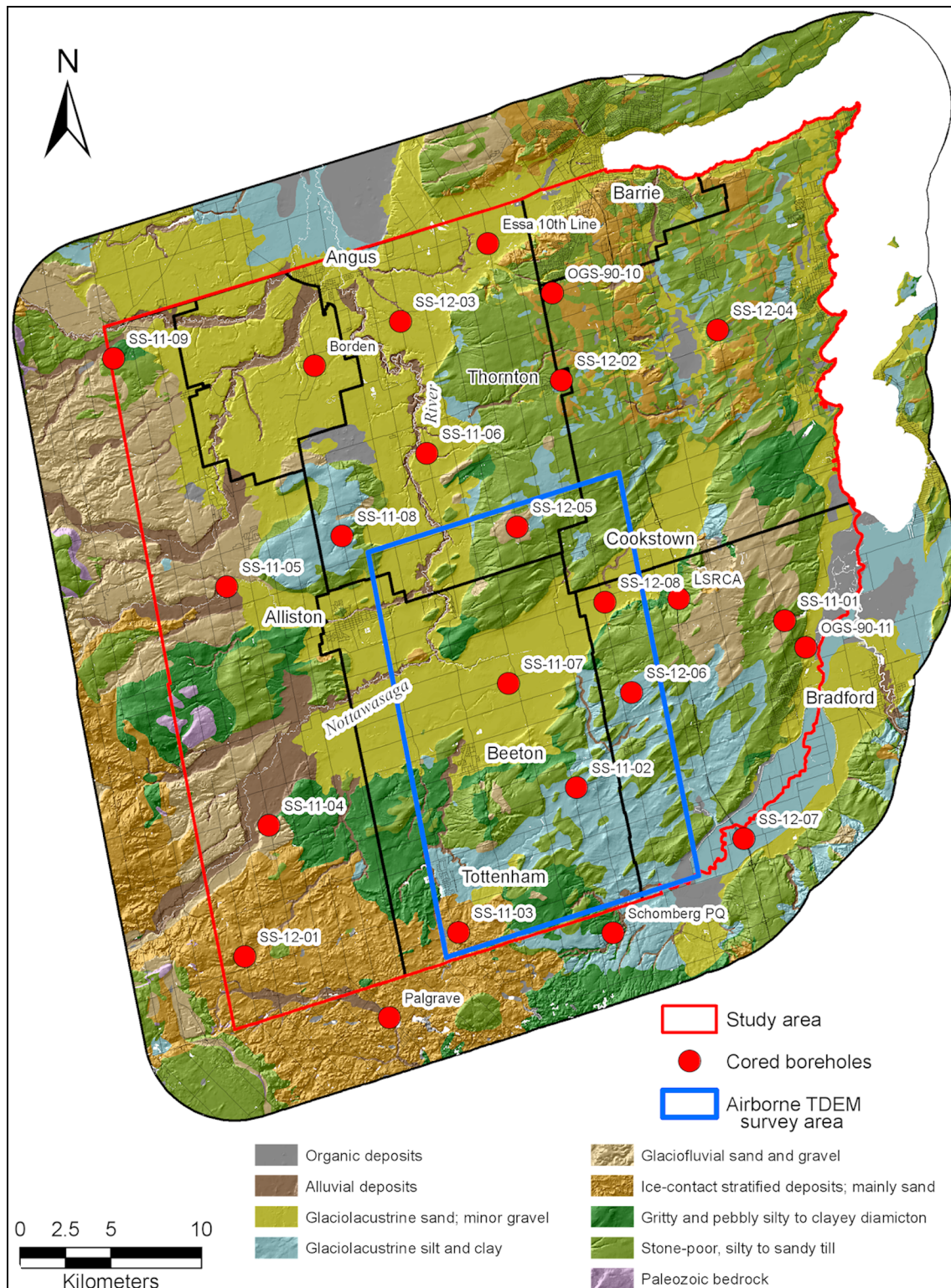


Figure 31.2. Location of cored boreholes and the time-domain electromagnetic (TDEM) survey, southern part of Simcoe County, southern Ontario. Boreholes with labels prefixed by “SS-12-” were drilled during the 2012 field season. Geology from Ontario Geological Survey (2010) and is overlain with shaded relief (“hillshade”) imagery.

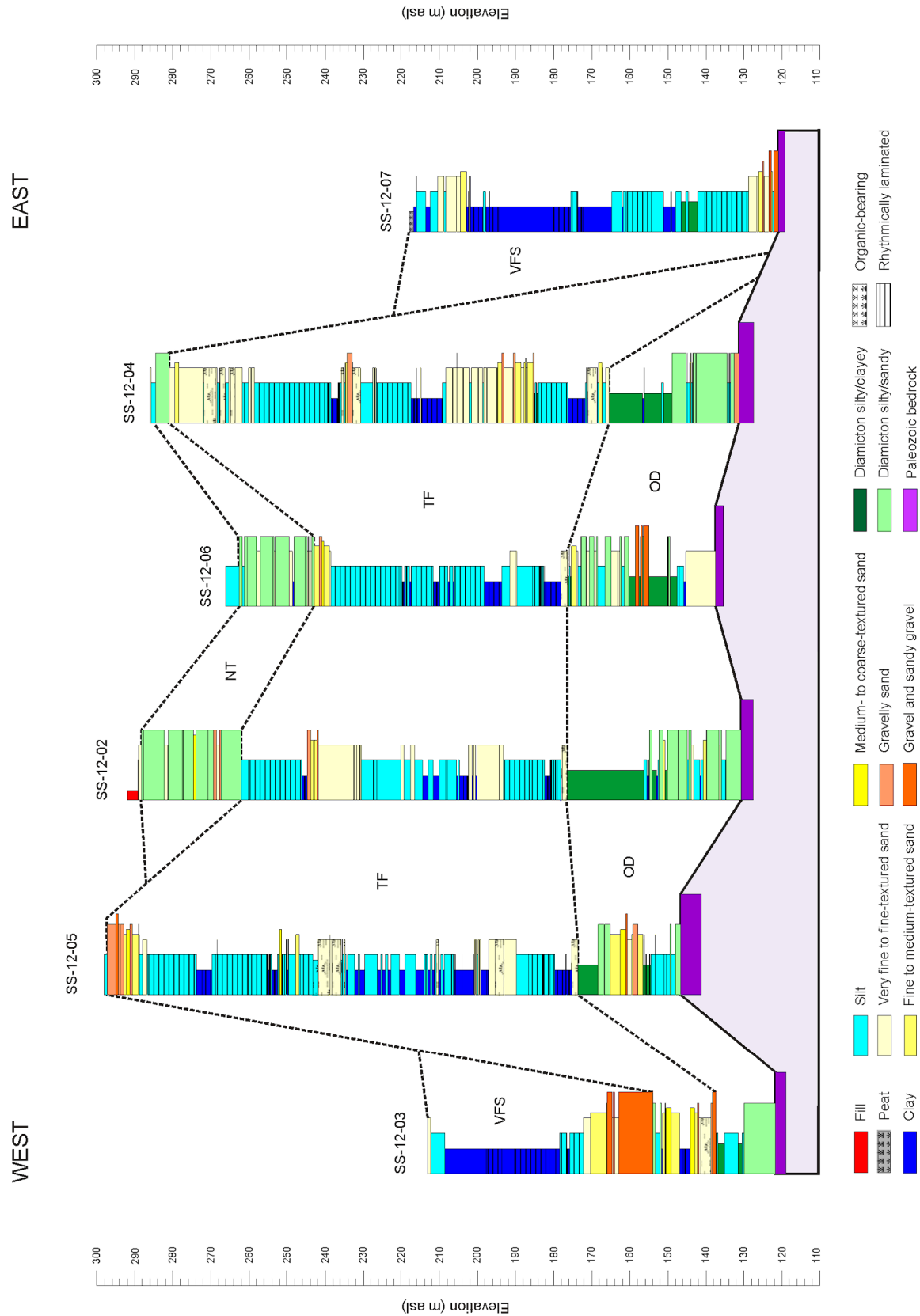


Figure 31.3. Graphic logs of boreholes drilled during 2012. The graphic log of borehole SS-12-01 is not shown as depth to bedrock was only 5.65 m. Important stratigraphic packages highlighted with dashed lines. Abbreviations: NT, Newmarket Till; TF, Thorncliffe Formation; OD, Older drift; VFS, valley-fill sequence.

Stratigraphy

A distinctive, yet consistent, stratigraphic sequence is emerging across the study area in the upland, tunnel valley and Oak Ridges Moraine physiographic regions. Upland regions generally record an older sedimentary record, whereas the tunnel valleys and Oak Ridges Moraine regions record a sequence that, for the most part, postdates the last advance of ice across the region (*see* Figure 31.3).

Boreholes SS-12-02, -04, -05 and -06 were collared in uplands within the eastern half of the study area (*see* Figure 31.2). Late Wisconsin Newmarket Till forms the uppermost stratigraphic unit in all boreholes except SS-12-05 where it was likely removed by nearshore processes associated with glacial Lake Schomberg. A thin layer of till was, however, observed to overlie glaciofluvial sand and gravel just a few hundred metres northwest of the drill site. Newmarket Till attains a thickness of 30 m in borehole SS-12-02. Massive, moderately compact diamicton is interrupted by thin interbeds, seams and stringers of silt, fine- to very fine-grained sand and pebbly sand. This represents the upper range of thickness observed to date for Newmarket Till within the study area.

A thick sequence of glaciolacustrine silt and clay rhythmites with as many as 3 packages of ripple- to planar-laminated, fine- to very fine-grained sand with lesser fine- to medium-grained sand and pebble gravel underlies the Newmarket Till. Thicknesses of up to 125 m have been observed for this unit. Sandy glaciolacustrine facies occur immediately below Newmarket Till in 5 of the 7 upland holes drilled to date and their occurrence likely reflects proximity to an ice margin. The lower sandy sediment units were probably deposited during changes in the position of feeder channels delivering sediment from the glacier into the deep basinal glaciolacustrine setting. Lobe switching and reoccupation of distributary channels in the subaquatic fan setting can result in alternating sequences of rippled sands and silt-clay rhythmites. There is a suggestion that some of the sand bodies may be correlatable across the uplands where the 2012 drilling was undertaken with one sand body occurring at approximately 230 to 245 m asl and the other at 185 to 210 m asl. The base of the glaciolacustrine sequence generally becomes clay rich, very finely laminated and often contains fine detrital organic accumulations along the foresets of starved silty to sandy ripples (Photo 31.1). This organic matter is likely reworked from the underlying organic sequence. Tracks and burrows are commonly observed along silty parting planes as well. The contact between the 2 units is often abrupt suggesting a sudden change in depositional environments. The entire glaciolacustrine sequence underlying Newmarket Till is correlative with the Thorncliffe Formation as defined to the south in the Scarborough bluff exposures (Karrow 1967).

Organic-rich, nonglacial, alluvial and lacustrine deposits were intersected beneath the Thorncliffe Formation in all 4 boreholes drilled on the uplands. They generally range between 1.5 and 5.0 m in thickness and consist of peaty gyttja and plant-bearing silts and sands sometimes containing fossil molluscs. This unit occurs at a remarkably consistent elevation in the subsurface with its top ranging between 165 and 180 m asl. Radiocarbon dating of fossil wood recovered from the same stratigraphic unit in 2011 boreholes returned finite radiocarbon ages ranging between 39.8 and 44.0 ka BP as well as ages of >46.9, >49.2 and 54.8 ka BP. Fossil pollen assemblages are dominated by spruce and pine suggesting boreal conditions (J.H. McAndrews, written communication, 2012). This Middle Wisconsin interstadial unit has now been encountered in 8 of the boreholes drilled to date and suggests a period of significant ice retreat allowing for the drainage of proglacial lakes and the establishment of subaerial conditions on a newly deglaciated landscape.

A pervasive unit of stone-poor, fine-grained diamicton with occasional sandy debris-flow facies underlies the organic horizon and exhibits features indicative of subaerial exposure and weathering on its upper surface (oxidation-reduction, carbonate leaching). Thicknesses ranging between 5 and 80 m have been observed for this unit with the greatest accumulations generally being associated with ice-marginal deposition. Significant thicknesses of diamicton and associated glaciolacustrine deposits were

encountered in boreholes SS-11-01 (*see* Bajc and Rainsford 2011) and SS-12-06 suggesting a possible ice margin. Pebbles of black, bituminous limestone–shale (Collingwood Member of the Lindsay Formation) are commonly observed in this till and indicate a Georgian Bay source lobe. This unit may be correlative with the Sunnybrook Formation (Early Wisconsin) as defined to the south in the Lake Ontario basin (Karrow 1967).

A stony, sandy silt diamicton occasionally interbedded with glaciolacustrine silt and sand often occurs at the base of the stratigraphic succession. This till more closely resembles Newmarket Till than the overlying fine-grained diamicton. A northeasterly source area is suggested because of the abundance of buff-brown and grey limestone clasts and the notable absence of black limestones. Follow-up heavy mineral studies should help to confirm these observations.

Boreholes SS-12-03 and SS-12-07 were drilled along the central axes of the Kempenfelt Bay and Cook's Bay tunnel valleys, respectively (*see* Figure 31.2). Both boreholes contain a thick fining-upward sequence that postdates deposition of Newmarket Till (*see* Figure 31.3). In the case of borehole SS-12-03, 12 m of pebble to cobble gravel is overlain by 6 m of very fine- to medium-grained sand, then 41 m of glaciolacustrine clay and silt rhythmites. At SS-12-07, Lindsay Formation limestone is overlain by 7 m of cobble to boulder gravel grading up to medium-, then fine- and very fine-grained sand. This is, in turn, overlain by 90 m of silt and clay rhythmites associated with glacial Lake Schomberg, then glacial Lake Algonquin. Fine-grained diamicton layers between 72 and 76 m are probably attributed to a slight fluctuation of the retreating ice margin and fluvial sands between 7.5 and 15 m depth are attributed to an early low-water stage of glacial Lake Algonquin. The coarse-grained glaciofluvial units in both boreholes are potentially attributed to the meltwater event that eroded the tunnel channels. Additional drilling and sediment architectural studies may assist with determining the origin of these deposits. The fining-upward



Photo 31.1. Contact between the lower part of the Thorncliffe Formation glaciolacustrine unit and older, organic-rich pond deposits (depth in metres).

sequence at borehole SS-12-03 is floored by a thin layer of possible Newmarket Till, then older Thorncliffe Formation sands, silts and clays. An organic-rich, fining-upward sequence of pebble gravel to very fine-grained sand underlies the Thorncliffe Formation. Poorly preserved valves of unionid clams and gastropods were noted within the lower gravel facies. A notable occurrence of *Pleurocera acuta*, a gastropod recovered from the interglacial Don beds in Toronto (Kerr-Lawson, Karrow and Edwards 1992) suggests a possible interglacial assignment to this organic unit. Follow-up radiocarbon dating and paleoecological studies should help to shed some light on the age of this deposit. Stone-poor, fine-grained diamicton and associated glaciolacustrine deposits, similar to the unit found regionally in the subsurface, underlies the organic bed. This till is, in turn, underlain by 8 m of pebbly and cobbly sandy silt till, which rests directly on Lindsay Formation limestone.

Borehole SS-12-01 was drilled in the extreme southwest corner of the study area within the Oak Ridges Moraine. Queenston Formation red shale was encountered at a depth of 5.65 m and was overlain by a fining-upward sequence of glaciofluvial gravel grading up to glaciolacustrine silt and sand. A highly irregular bedrock surface is suggested for this area, as water-well records in close proximity to the drill site indicate depths to rock of up to 53 m.

AIRBORNE TIME-DOMAIN ELECTROMAGNETIC TEST SURVEY

A 1898 line-kilometres AeroTEM IV time-domain electromagnetic (TDEM) survey was flown over a 328 km² area of south Simcoe County (see Figure 31.2) in order to test whether the airborne TDEM method could be an effective tool for detecting and delineating buried valleys incised into bedrock as well as important hydrostratigraphic units in the overlying Quaternary sequence. Aquifers that occur within these buried-bedrock valleys as well as higher up in the sedimentary sequence can host significant groundwater resources.

Ground gravity surveys have previously been used with some success to define buried-bedrock valleys, but EM methods have been shown to have the potential to be able to discriminate between fill material that is an aquifer versus an aquitard (see “Support for Groundwater Program” in Rainsford and Muir, this volume, Article 19). The survey deliverables, in addition to standard EM products such as decay constant and apparent conductance, included laterally constrained 1-D inversions of the EM data. The inversions resulted in a 3-D database of electrical conductivity that can be imaged in plan and section form. The results of this survey have been published (Ontario Geological Survey 2012).

The objective of this test survey is to determine

- whether buried-bedrock valleys and channels within surficial materials are detectable
- whether important hydrostratigraphic units are mappable in the subsurface
- the optimum flight-line spacing and orientation
- whether the TDEM data provides more information than ground gravity
- the effect of cultural sources on the survey results

Surficial deposit mapping, continuously cored borehole logs, ground gravity data and water-well records are available to help answer these questions. At this point, very little electrical property information from downhole geophysical logging is available for the area.

It was clear from the preliminary survey results that man-made cultural interferences such as power lines, telephone cables, pipelines, rail lines and metal fences had a deleterious effect on the data. This outcome was not unexpected and resulted in about a 50% loss of useable data. Such challenges have

previously been noted with similar surveys elsewhere (Viezzoli, Soerenson and Jørgensen 2011). The effect could have been mitigated somewhat by orienting the flight lines oblique to the road network along which most of the cultural infrastructure is situated rather than parallel with it.

From an inspection of the inverted EM conductivity sections, a good deal of vertical variation coupled with continuity in the horizontal direction (along the flight line) is observed. The vertical variations suggest the presence of mappable electrical conductivity contrasts within the Quaternary layers, and the lateral continuity implies consistency of the inversions. The majority of the electrical conductivity sections show a similar pattern with a low conductivity response (<0.015 S/m) starting near the surface and extending down to a depth of between 75 and 150 m. This low-conductivity unit is underlain by a higher conductivity (>0.03 S/m) horizon. This lower unit appears in the sections to be approximately 100 m thick, although the confidence in the model at these depths is limited. A more conductive “cap” overlies the upper low-conductivity unit over much of the area. This cap unit appears to be associated with Newmarket Till in places; however, as it is expressed in the upper 30 m of the conductivity section where there is little early-time EM data to support it, the validity of this feature is open to question.

The 5 boreholes drilled by the OGS within the test area provide high-quality geological logs of the Quaternary cover as well as the upper part of the Paleozoic bedrock. As these holes have been drilled on the sides of public roads, which are themselves often associated with cultural conductors, the borehole locations frequently correspond to gaps in the inverted conductivity sections. However, the lateral continuity of the conductivity sections is such that it is usually easy to visually extrapolate features across the gaps.

Parts of 2 inverted conductivity sections are presented in Figures 31.4a and 31.4b in order to illustrate the correlation with the geological sections obtained from 2 boreholes. As is typical of many of the conductivity sections, the deeper parts are characterized by a region of high conductivity (imaged as red) overlain by a lower conductivity upper layer (imaged as blue). The very near surface around borehole SS-12-05 (*see* Figure 31.4b) exhibits elevated conductivities (green hues). Although both electrical conductivity sections are quite similar, the Quaternary geology, intersected by drilling, is quite different. SS-11-03 encountered mostly fine sandy material, whereas SS-12-05 encountered predominantly silts and clays along with some sandy intervals. Based solely on the geological logs, it would be expected that SS-12-05 would be within an area demonstrating higher conductivities, due to the higher clay content of the surficial materials. Conversely, the section containing SS-11-03 would be expected to exhibit lower conductivities due to the predominance of sandy materials. In this regard, the conductivity section appears consistent with SS-11-03, but not with SS-12-05. In both holes, the bedrock interface appears to be associated with a transition to markedly higher conductivities. As the bedrock is limestone in SS-12-05, a decrease in conductivity would be expected rather than the observed increase. The results are counter-intuitive and demonstrate the need for downhole electrical conductivity logging to help interpret the airborne test survey results. One explanation that has been suggested to account for the higher conductivities imaged in the bedrock is the presence of a saline aquifer. This explanation could easily be tested with downhole geophysical logging. However, the EM data may also be influenced by the residual effects of a major powerline corridor 600 m west of the borehole and, as a result, the inversions may be less reliable in this area (A. Viezzoli, Aarhus Geophysics ApS., personal communication, 2012). At borehole SS-11-03, the bedrock encountered at the base of the hole is Georgian Bay Formation shale, which appears to be consistent with the elevated conductivity measurements.

The next steps in this study are to georeference all of the inverted conductivity sections and import them into Datamine Studio[®] software in order to better understand how the electrical conductivity and geology are related. Downhole geophysical logging (including electrical conductivity logs) is planned for the OGS boreholes within the test area.

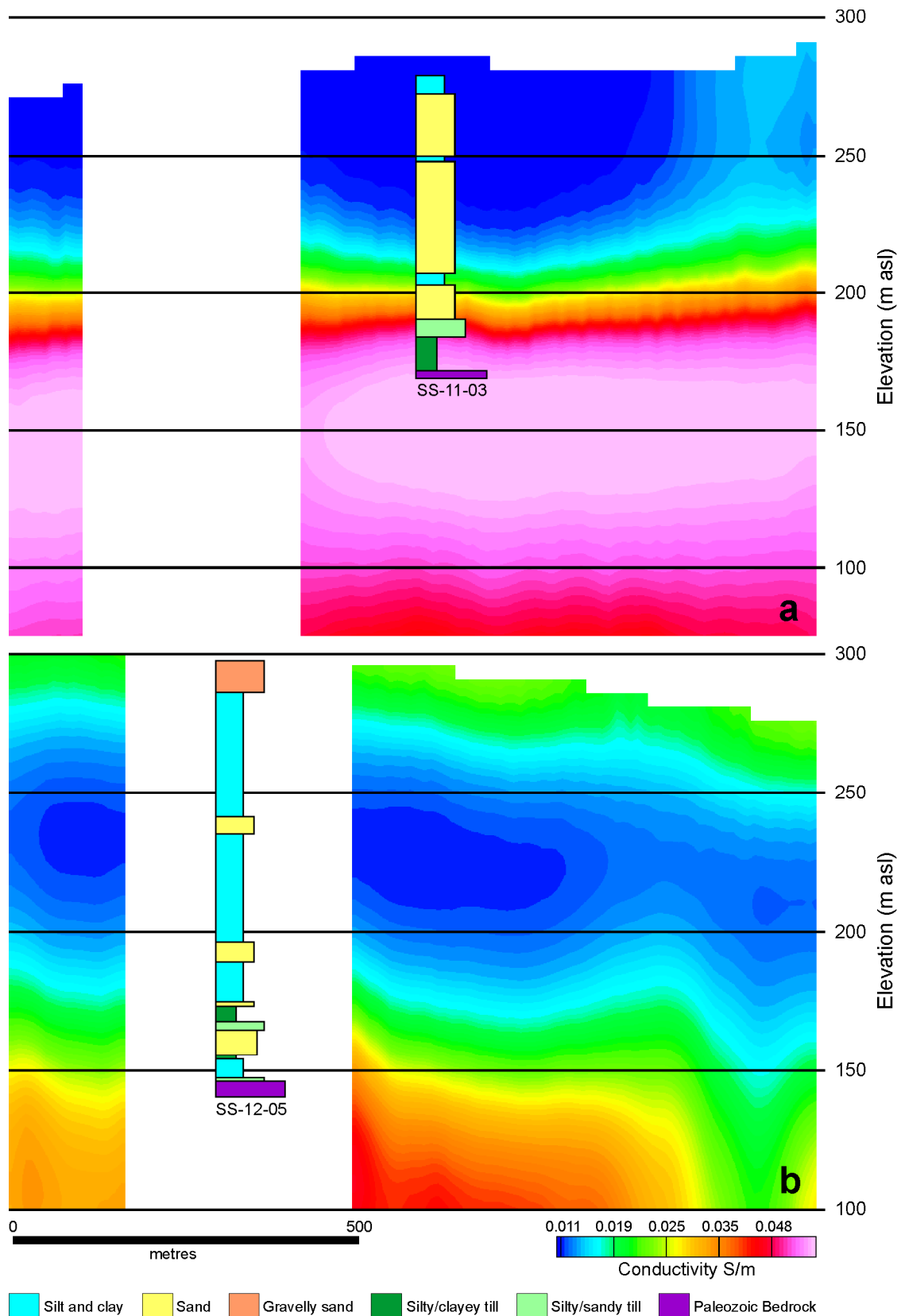


Figure 31.4. Laterally constrained inversion of TDEM test data results. Inverted electrical conductivity is displayed along with graphic logs of drill holes.

STRATIGRAPHIC STUDIES ALONG THE NOTTAWASAGA RIVER

Melting of the Laurentide Ice Sheet produced large volumes of meltwater and redistributed glacially derived sediments. Basins were exposed in the southern part of Simcoe County, and were occupied by a series of proglacial lakes during ice recession (Bajc and Rainsford 2010; Mulligan 2011). These low-lying areas host abundant shallow aquifers within sediments deposited in glacial Lake Algonquin approximately 12.5 to 10.5 ka BP (Lewis et al. 2008). A detailed sedimentological investigation of 56 outcrop exposures along cut banks of the Nottawasaga River was performed during the summer of 2012 (Figures 31.2 and 31.5). This work provides valuable data on the near-surface sediment stratigraphy beneath the glacial Lake Algonquin plain and allows for greatly improved characterization of major hydrostratigraphic units within valley areas of southern Simcoe County.

Facies Associations

The stratigraphy is floored by the Newmarket Till. Silt and clay rhythmites rest on the till and are unconformably overlain by a coarse-grained, fluvial unit that passes upward into fine-grained sand to silt-rich rhythmites. These sediments can be grouped into 4 facies associations (FAs) that reflect common, contemporaneous depositional environments for the sedimentary units identified across the study area.

FACIES ASSOCIATION 1

Widespread silt and clay rhythmites overlie an undulating Newmarket Till surface that is observable in places at the base of river sections. Rhythmite couplets are typically 1 to 4 cm thick and consist of a thicker silt layer with a thin clay-rich cap. Rippled, very fine-grained sand beds, generally less than 1 cm thick, occur throughout the succession. Locally, a transitional succession of fine- to coarse-grained diamictons interbedded with sand and silt rests directly on the massive Newmarket Till.

FACIES ASSOCIATION 2

Northward-migrating, trough cross-bedded gravel and gravelly sand, in places containing mollusc remains, unconformably overlies the fine-grained facies (FA 1) in the southern and western parts of the basin. These gravels often show iron and manganese oxide staining, suggestive of active groundwater flow, and are composed of well-rounded clasts, averaging 1 to 3 cm in diameter. Toward the north and central parts of the basin, this unit loses its coarse character and consists of channelized, fine- to medium-grained sand with type-A and -B current ripples containing large silt rip-up clasts. Radiocarbon dating of delicate and well-preserved *Dryas integrifolia* leaves recovered from FA 2 in borehole SS-11-06 returned a radiocarbon age of $12\,410 \pm 25$ years BP (A2060).



Figure 31.5. Cut-bank exposure along the Nottawasaga River near the hamlet of Baxter showing important facies associations recognized within the Lake Algonquin lowland. Depth of section (shown in graphic logs) is approximately 15 m. Colours in graphic logs: light yellow, fine- to very fine-grained sand; dark yellow, medium- to coarse-grained sand; light blue, silt; dark blue, clay; brown, slump covered.

FACIES ASSOCIATION 3

An upward-fining, mollusc-bearing (glacio)lacustrine package overlies FA 2. This unit, which occurs throughout the lowland lake plain, consists of sandy silt rhythmites with minor silt and clay laminae. Couplets are generally 2 to 4 cm thick, but display undulating and discontinuous contacts as well as greater heterogeneity in grain sizes within individual beds. Starved ripples are observed in sandy beds throughout the Alliston area and wave ripples with deformation structures characterize the sands in the Cookstown valley to the east.

FACIES ASSOCIATION 4

Outcrops of FA 4 show ripple- to planar-laminated, very fine-grained sand and silt-rich deposits passing upward into very well-sorted, mollusc-bearing, fine-grained sand displaying large- and small-scale ball-and-pillow and dish structures and hummocky cross-stratification, then type-A and -B current ripples. Granular to pebbly coarse-grained sands with north-northwest to northwest paleocurrents often cap the succession in this region. Deposits of FA 4 are locally incised and backfilled with channelized, pebbly fine- to medium-grained, rippled and planar-bedded sands containing wood, bones and molluscs with notable unionid clams. Buried woody peat and soil horizons occur below this younger succession and have returned radiocarbon ages ranging between 5.88 and 7.51 ka BP.

Depositional History and Paleoenvironmental Evolution

The fine-grained deposits of FA 1 record a time when lows in the Newmarket Till sheet were inundated by early Lake Algonquin as the ice front retreated northward away from the Niagara Escarpment approximately 12.5 ka BP. Lower sediments contain ice-proximal debris flows and fine upward into deep-water glaciolacustrine facies containing localized ice-rafted debris. The outlet for early Lake Algonquin was to the south, via Port Huron and Chicago (Larson and Shaetzl 2001). Elevated wave-cut terraces at approximately 235 to 245 m asl near Alliston may mark the position of the early Lake Algonquin water plane (Eschman and Karrow 1985).

The unconformity at the top of FA 1 records a drop in water level resulting from continued recession of the Simcoe ice lobe toward the northeast and the uncovering of a lower level outlet at Kirkfield (Finamore 1985). Water levels dropped by as much as 30 m and the shoreline migrated northward to a position just south of Angus. The drop in base level caused erosion and reworking of previously deposited early Algonquin glaciolacustrine deposits and of older sediments laid down along the flanks of the Niagara Escarpment. This low-level lake is referred to as the Kirkfield phase of Lake Algonquin and is represented by FA 2 (Karrow et al. 1975).

The succession comprising FA 3 records a steady basin-wide transgression that occurred in response to isostatic uplift of the outlet at Kirkfield and the return of outflow to Port Huron and Chicago. This transgressive phase is referred to as “main Lake Algonquin” and resulted in prominent wave-cut bluffs, beach ridges and spits in south Simcoe County at approximately 225 m asl (Deane 1950). Wave ripples and associated soft sediment deformation in the sandy upper sediments of the Cookstown Embayment indicate a shallow (<5 m water depth), high-energy environment. Sandy rhythmites across the Alliston Embayment likely record waning fluvio-deltaic deposition during the transgression, as well as reworking of unconsolidated sediments along the basin margins.

At approximately 10.5 ka BP, the margin of the Laurentide Ice Sheet receded northward uncovering a series of low-level outlets in the French River and North Bay areas resulting in the drainage of main Lake Algonquin (Fitzgerald 1985). The sediments of FA 4 record delta development along a stormy shore face during the early stages of falling lake levels. The gradation of deformation features observed in the

fine-grained sands is consistent with rapid sediment accumulation on a delta front influenced by storm and wave activity. Uplift of the North Bay outlet once again resulted in a basin-wide transgression and the establishment of the Nipissing shoreline in the vicinity of Angus at approximately 190 m asl. Buried peat beds and paleosols unconformably overlie FA 4 and record the Stanley low-water phase of the Huron basin. Transgressive sheet sands bury the peats and paleosols and record fluvio-deltaic valley-fill and nearshore deposits associated with the Nipissing high stand.

The sediments exposed along the Nottawasaga River offer a complete and detailed picture of the paleoenvironmental evolution of glacial Lake Algonquin in southern Simcoe County. Correlation of major facies associations identified in this study helps to characterize the three-dimensional geometry of the infill succession within the valley areas. This holds important implications for shallow groundwater flow beneath the former lake plain. The thicknesses and distribution of the major units identified in this work appear to depend largely on the topography of the upper surface of the Newmarket Till sheet, which forms the floor of the glacial Lake Algonquin succession. The fluvio-deltaic sediments of FA 2 form an extensive shallow aquifer beneath the lake plain and both the underlying silt rhythmites of FA 1 and the Newmarket Till form important aquitards that promote abundant shallow groundwater discharge into the Nottawasaga River.

NEXT STEPS

A third phase of coring is planned for the 2013 field season to assist with the interpretation of the airborne TDEM survey data as well as to collect additional stratigraphic information from outlying areas. Borehole geophysics will be undertaken to assist with the interpretation of the EM data as well. The possibility of undertaking a seismic reflection survey along key transects covered by the TDEM survey is also being investigated. Modelling of the bedrock surface and important hydrostratigraphic units will commence early in the new year using Datamine Studio® software with the vision of having a 3-D model completed late in the year.

ACKNOWLEDGMENTS

The section written by R.P.M. Mulligan (“Stratigraphic Studies Along the Nottawasaga River”) forms the basis of an ongoing MSc thesis at McMaster University, School of Geography and Earth Sciences, under the supervision of Dr. Carolyn Eyles. A portion of this research is supported under Ontario Geological Survey Project Unit 11-034.

REFERENCES

- Bajc, A.F. and Rainsford, D.R.B. 2010. Three-dimensional mapping of Quaternary deposits in the southern part of the County of Simcoe, southern Ontario; *in* Summary of Field Work and Other Activities 2010, Ontario Geological Survey, Open File Report 6260, p.30-1 to 30-10.
- 2011. Three-dimensional mapping of Quaternary deposits in the southern part of the County of Simcoe, southern Ontario: A progress report; *in* Summary of Field Work and Other Activities 2011, Ontario Geological Survey, Open File Report 6270, p.29-1 to 29-8.
- Burt, A.K. and Dodge, J.E.P. 2011. Three-dimensional modelling of surficial deposits in the Barrie–Oro moraine area of southern Ontario; Ontario Geological Survey, Groundwater Resources Study 11, 125p.
- Deane, R.E. 1950. Pleistocene geology of the Lake Simcoe District, Ontario. Geological Survey of Canada, Memoir 256, 108p.

- Eschman, D.F. and Karrow, P.F. 1985. Huron basin glacial lakes: a review; *in* Quaternary evolution of the Great Lakes, Geological Association of Canada, Special Paper 30, p.79-93.
- Finamore, P.F. 1985. Glacial Lake Algonquin and the Fenelon Falls outlet; *in* Quaternary evolution of the Great Lakes, Geological Association of Canada, Special Paper 30, p.125-132.
- Fitzgerald, W.D. 1985. Postglacial history of the Minesing basin, Ontario; *in* Quaternary evolution of the Great Lakes, Geological Association of Canada, Special Paper 30, p.133-146.
- Karrow, P.F. 1967. Pleistocene geology of the Scarborough area; Ontario Department of Mines, Report 46, 108p.
- Karrow, P.F., Anderson, T.W., Clarke, A.H., Delorme, L.D. and Sreenivasa, M.R. 1975. Stratigraphy, paleontology, and age of Lake Algonquin deposits in southwestern Ontario, Canada; *Quaternary Research*, v.54, p.49-87.
- Kerr-Lawson, L.J., Karrow, P.F. and Edwards, T.W.D. 1992. A paleoenvironmental study of the molluscs from the Don Formation (Sangamonian?), Don Valley Brickyard, Toronto, Ontario; *Canadian Journal of Earth Sciences*, v.29, p.2406-2417.
- Larson, G. and Shaetzel, R. 2001. Origin of the Great Lakes watershed; *Journal of Great Lakes Resources*, v.27, p.518-546.
- Lewis, C.F.M., Karrow, P.F., Blasco, S.M., McCarthy, F.M., King, J.W., Moore, T.C., Jr. and Rea, D.K. 2008. Evolution of lakes in the Huron basin: deglaciation to present; *Aquatic Ecosystem Health and Management*, v.11, p.127-136.
- Mulligan, R.P.M. 2011. Surficial geology of the Alliston area, southern Ontario; *in* Summary of Field Work and Other Activities 2011, Ontario Geological Survey, Open File Report 6270, p.21-1 to 21-7.
- Ontario Geological Survey 2010. Surficial geology of southern Ontario; Ontario Geological Survey, Miscellaneous Release—Data 128—Revised.
- 2012. Ontario airborne geophysical surveys, magnetic and electromagnetic data, grid and profile data (ASCII and Geosoft® formats) and vector data, south Simcoe County area; Ontario Geological Survey, Geophysical Data Set 1070.
- Viezzoli, A., Soerenson, C. and Jørgensen, F. 2011, Does accurate processing of airborne EM data have an impact on derived hydrogeological units?; expanded abstract, Canadian Society of Exploration Geophysicists convention, Calgary, Alberta, 2011.

32. Project Unit 08-003. Conceptual Geologic Model for the Orangeville Moraine Three-Dimensional Project

A.K. Burt¹

¹Earth Resources and Geoscience Mapping Section, Ontario Geological Survey

INTRODUCTION

The Orangeville moraine three-dimensional (3-D) project, the fourth in a series of highly successful regional-scale 3-D surficial mapping projects for groundwater applications, encompasses approximately 1550 km² centred on the Orangeville moraine and extends from the Regional Municipality of Waterloo to north of Orangeville in southwestern Ontario (Figure 32.1). This year, the Ontario Geological Survey (OGS) is launching the approximately 2000 km² Mount Forest–Elmira 3-D project immediately to the west (Burt, this volume, Article 33). This new project will connect the Orangeville moraine 3-D project area with the Regional Municipality of Waterloo (Bajc and Shirota 2007) and Brantford–Woodstock (Bajc and Dodge 2011) 3-D project areas eventually forming a laterally continuous 3-D mapped area of 7135.5 km² (see Figure 32.1).

As with previous studies, key objectives of the Orangeville moraine 3-D project are the reconstruction of the Quaternary history of the study area, the development of a 3-D model of Quaternary sediments, and the characterization of the properties of the modelled sediment packages (see Burt 2008, 2009, 2011; see Burt and Rainsford 2010 for more information on the project area and work completed to date).

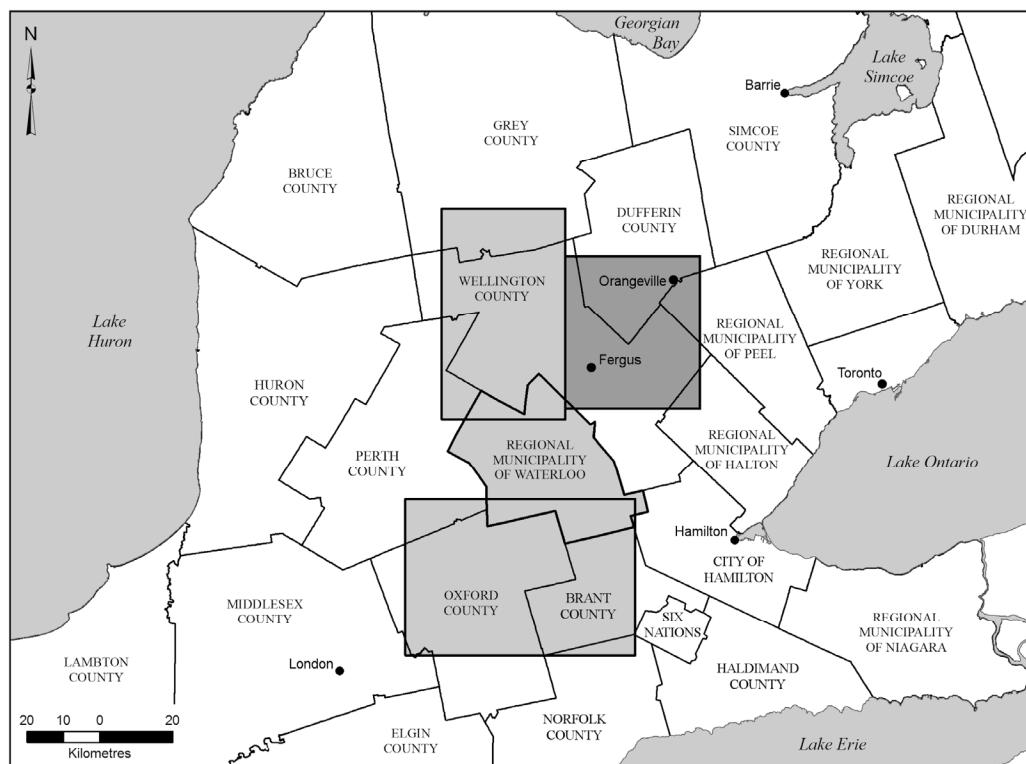


Figure 32.1. Location of the Orangeville moraine (dark grey) and other (light grey) 3-D project areas.

*Summary of Field Work and Other Activities 2012,
Ontario Geological Survey, Open File Report 6280, p.32-1 to 32-6.*

© Queen's Printer for Ontario, 2012

Table 32.1. Comparison of the hydrostratigraphic units in the completed Regional Municipality of Waterloo and Brantford–Woodstock 3-D project areas with units in the Orangeville moraine 3-D project area (*see* Bajc and Shirota (2007) and Bajc and Dodge (2011) for information on the completed projects).

	Regional Municipality of Waterloo	Brantford–Woodstock	Orangeville Moraine
Younger	—	AFA0	—
	ATA1	ATA1	—
	AFA1	AFA1	AFA1
	ATA2	ATA2	ATA2
	AFA2	AFA2	AFA2
	ATA3	ATA3	ATA3
	ATB1	ATB1	ATB1
	AFB1	AFB1	AFB1
	ATB2	ATB2	ATB2
	AFB2	AFB2	AFB2
	ATB3	ATB3	ATB3
	AFB3	AFB3	AFB3
	ATC1	ATC1	ATC1
	AFC1	AFC1	AFC1
	ATC2	ATC2	ATC2
	AFD1	AFD1	AFD1
	ATE1	ATE1	ATE1
	AFF1	AFF1	AFF1
	ATG1	ATG1	ATG1
Older	—	—	AFH1
	BR	BR	BR

CONCEPTUAL GEOLOGICAL MODEL

A series of 19 hydrostratigraphic units were modelled in the Regional Municipality of Waterloo 3-D project (Bajc and Shirota 2007). These units were based on the stratigraphic relationships between the till formations and intervening stratified sediments that form key aquifers and aquitards across the region. To date, these original hydrostratigraphic units have been robust enough to extend into subsequent 3-D mapping project areas while remaining flexible enough to allow for the incorporation of new units where necessary. For example, the Brantford–Woodstock 3-D project (Bajc and Dodge 2011) used the same 19 hydrostratigraphic units plus 1 additional younger unit (Table 32.1). It is expected that, as our 3-D mapping efforts are extended into more distant areas, there will be challenges in correlating both geologic formations and hydrostratigraphic units. Some formations, for example Catfish Creek Till, have a widespread distribution and, as such, are key marker beds. Other formations not only have a much more limited extent, but were deposited during local ice fluctuations.

A conceptual geological model has been developed for the Orangeville moraine 3-D project area based on new and existing subsurface data as well as published reports on the Quaternary history of the area (Figure 32.2; Table 32.2). Some of the formations presented previously (Burt 2011) have been either grouped together into a single hydrostratigraphic unit or subdivided into upper and lower units following the conventions established during previous projects (Bajc and Shirota 2007; Bajc and Dodge 2011). For example, the upper Maryhill, Tavistock, Port Stanley and the upper sandy tills have been grouped together into hydrostratigraphic unit ATB1, whereas the Catfish Creek Till has been subdivided into main and lower units. From oldest to youngest, the hydrostratigraphic units for the Orangeville moraine 3-D project area consist of the following:

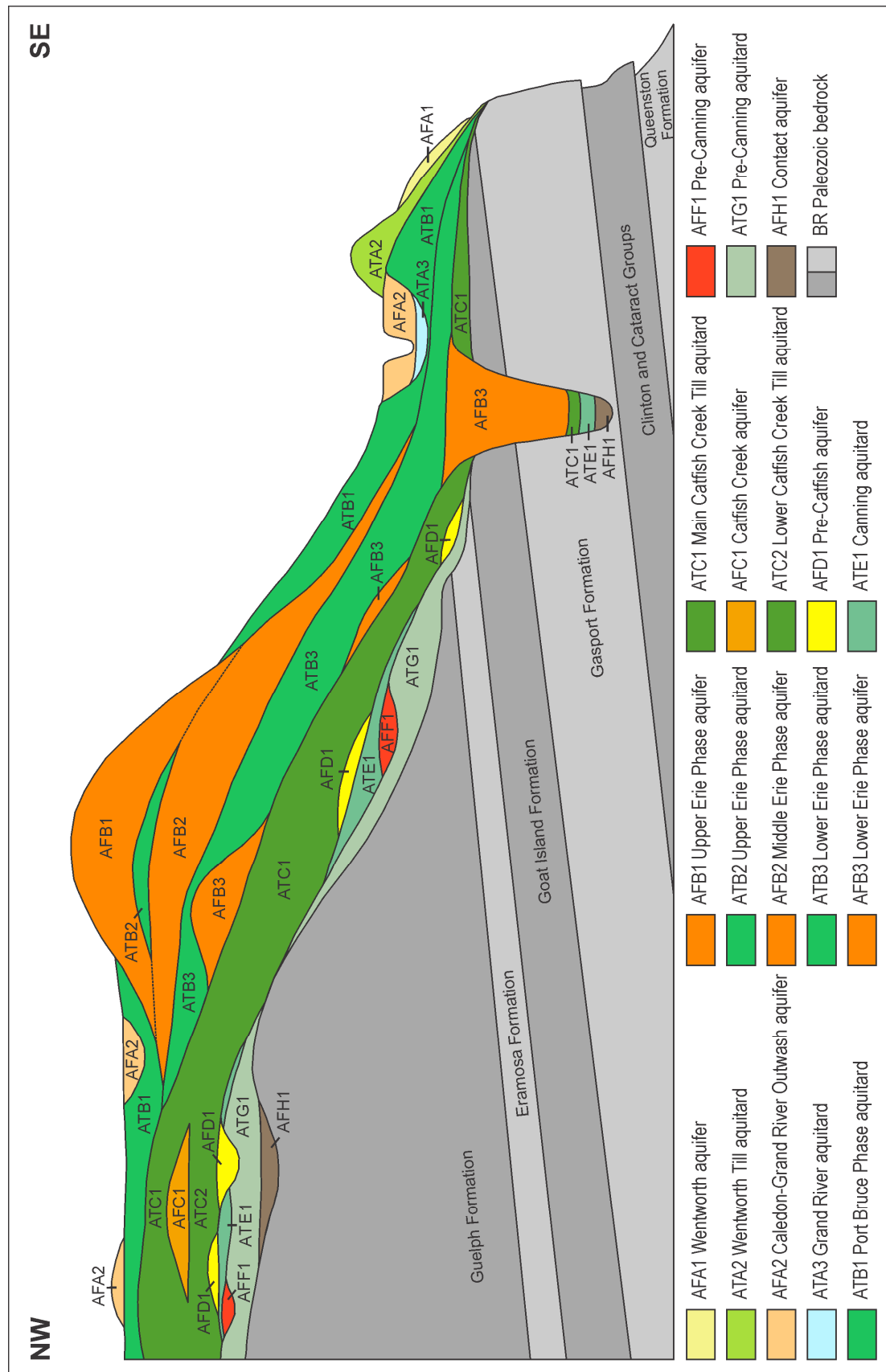

















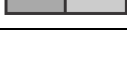



Figure 32.2. Conceptual geologic model for the Orangeville moraine 3-D project area.

Table 32.2. The 19 hydrostratigraphic units in the Orangeville moraine 3-D project area with their corresponding lithostratigraphic units and primary lithologic descriptions.

Hydrostratigraphic Unit	Lithostratigraphic Unit	Lithology
 AFA1	Wentworth aquifer: glaciofluvial and coarse-textured glaciolacustrine sediments, alluvium and recent organics overlying Wentworth Till	Sand; gravel
 ATA2	Wentworth Till aquitard: Wentworth Till and associated fine-textured glaciolacustrine sediments, Paris moraine	Dirty sand and gravel; sand and gravel; stony sandy till to silty sandy till; stony sandy diamicton (debris flow deposits)
 AFA2	Caledon–Grand River Outwash aquifer: Caledon and Grand River outwash, glaciofluvial and coarse-textured glaciolacustrine sediments, alluvium and recent organics	Sand; gravel and cobbles; rare sand and silt; rare dirty sand and gravel; rare peat and wetland deposits
 ATA3	Grand River aquitard: fine-textured deposits confined to the Grand River valley under AFA2	Sandy silt; silt
 ATB1	Port Bruce Phase aquitard: Tavistock Till, Port Stanley Till, upper sandy tills, upper Maryhill drift and associated fine-textured glaciolacustrine sediments	Stone-poor clayey silt to silt till (Tavistock Till); stony sandy silt till (Port Stanley Till); stony sand till (upper sandy till); clayey silt till, silt and clay (Maryhill drift)
 AFB1	Upper Erie Phase aquifer: upper Orangeville moraine stratified sediments and equivalents	Sand; silt and sand rhythmites; gravel and cobbles
 ATB2	Upper Erie Phase aquitard: Maryhill drift	Clayey silt till, silt and clay rhythmites; silt
 AFB2	Middle Erie Phase aquifer: lower Orangeville moraine stratified sediments and equivalents	Sand; silt and sand rhythmites; gravel and cobbles
 ATB3	Lower Erie Phase aquitard: lower Maryhill drift, fine-textured glaciolacustrine sediments and equivalents	Clayey silt till, silt and clay rhythmites; sand and silt rhythmites; silt
 AFB3	Lower Erie Phase aquifer: stratified sediments associated with the breakup of the main Late Wisconsin (Catfish Creek) ice	Sand; gravel; dirty sand and gravel; sand and silt (buried-bedrock valley fill)
 ATC1	Main Catfish Creek Till aquitard: upper / main Catfish Creek Till and associated fine-textured glaciolacustrine sediments	Stony sandy silt till; rare silt and sand
 AFC1	Catfish Creek aquifer: Catfish Creek stratified sediments	Sand; sand and gravel
 ATC2	Lower Catfish Creek Till aquitard: lower Catfish Creek Till and associated fine-textured glaciolacustrine sediments	Stony sand silt till; rare silt and sand
 AFD1	Pre-Catfish aquifer: pre-Catfish Creek glaciofluvial and coarse-textured glaciolacustrine sediments	Sand; sand and silt
 ATE1	Canning aquitard: Canning drift	Clayey silt till; silt till; silt and clay
 AFF1	Pre-Canning aquifer: pre-Canning glaciofluvial and coarse-textured glaciolacustrine sediments	Sand; gravel
 ATG1	Pre-Canning aquitard: pre-Canning coarse-textured till	Very stony sandy silt till
 AFH1	Contact aquifer: stratified sediments and highly weathered bedrock	Gravel and cobbles; dirty sand and gravel; rubble
 BR	Paleozoic bedrock: Guelph, Eramosa, Goat Island, Gasport and Queenston formations, Clinton and Cataract groups	Dolostone; limestone; shale

1. Paleozoic bedrock (Paleozoic bedrock: BR). This unit is continuous across the study area. From oldest to youngest, the Ordovician Queenston Formation and Silurian Gasport, Eramosa and Guelph formations were intersected during drilling. Individual formations will not be modelled as part of this project.
2. A contact aquifer (Contact aquifer: AFH1) consisting of stratified sediments, likely of various ages, and highly weathered bedrock found at the bottom of the Rockwood buried-bedrock valley and other bedrock lows (the extent of this and overlying units is based on the results of the 2008, 2009 and 2010 overburden drilling programs).
3. A sequence of 1, or occasionally 2, older tills (pre-Canning aquitard: ATG1) overlying bedrock or the contact aquifer and localized coarse-textured stratified sediments (pre-Canning aquifer: AFF1) likely deposited during ice retreat. These units are typically located in the western and rarely central portions of the study area farther away from the escarpment. The age of the deposits and direction of ice flow are not known.
4. Canning drift (Canning aquitard: ATE1) consisting of fine-textured till and fine-textured glaciolacustrine deposits. Canning drift is found in buried-bedrock valleys and sporadically in the western and central portions of the study area.
5. A pre-Catfish aquifer (pre-Catfish aquifer: AFD1) that occasionally contains organic material (e.g., the new Eramosa site (Burt 2011)). This unit has a sporadic distribution across the south-central and western parts of the study area.
6. Nissouri Phase Catfish Creek Till and stratified sediments (Main Catfish Creek Till aquitard: ATC1; Catfish Creek aquifer: AFC1; Lower Catfish Creek Till aquitard: ATC2). Main Catfish Creek Till is typically an overconsolidated stony sandy silt till that was deposited during the main Late Wisconsin ice advance, whereas lower Catfish Creek Till is often finer textured and may represent early lobate flow. Catfish Creek Till is found across the study area, although it typically thins toward the escarpment.
7. A series of Erie Phase aquifers and aquitards (Upper Erie Phase aquifer: AFB1; Upper Erie Phase aquitard: ATB2; Middle Erie Phase aquifer: AFB2; Lower Erie Phase aquitard: ATB3; Lower Erie Phase aquifer: AFB3) deposited during and following the break-up of Catfish Creek ice consisting of coarse-textured glaciofluvial and subaquatic fan sediments, fine-textured glaciolacustrine sediments and diamicton. The centrally located Orangeville moraine and Rockwood buried-bedrock valley sandy fill are part of this sequence and form the largest overburden aquifers within the study area. The Lower Erie Phase aquitard is dominated by thick glaciolacustrine sediments deposited in an interlobate zone in the central portion of the study area.
8. Port Bruce Phase Tavistock, Port Stanley and upper sandy tills and upper Maryhill drift (Port Bruce Phase aquitard: ATB1) deposited during lobate ice advances from the northwest (Georgian Bay Lobe Tavistock Till), northeast (Simcoe Lobe upper sandy till) and southeast (Erie–Ontario Lobe Port Stanley Till) (Figure 32.3). These deposits form the upper aquitard across much of the study area.
9. Outwash gravels (Caledon–Grand River outwash aquifer: AFA2) deposited in channels incised into Tavistock and Port Stanley till. Coarse-textured glaciolacustrine and localized glaciofluvial and ice-contact stratified deposits overlying the Port Bruce phase aquitard have been included in this unit. Fine-textured deposits (Grand River aquitard: ATA3) confined to the Grand River valley were mapped in the Waterloo project area (Bajc and Shiota 2007) and may extend into the Orangeville moraine area.
10. Mackinaw Phase Wentworth Till and debris flows forming the Paris moraine (Wentworth Till aquitard: ATA2). The Paris moraine, located in the far southeast of the study area, marks the maximum advance of the final Erie–Ontario lobe ice advance within the study area (*see* Figure 32.3).
11. Glaciofluvial and coarse-textured glaciolacustrine sediments overlying Wentworth Till (Wentworth aquifer: AFA1) in the far southeast of the study area.

The Orangeville moraine project area does not contain the youngest hydrostratigraphic units mapped in the Waterloo and Brantford–Woodstock areas (units ATA1 and AFA0 in Table 32.1) and 1 older unit has been added to the sequence. If a hydrostratigraphic unit is not present within a particular project area, it is still included in the stratigraphic sequence used during the modelling process, but will have zero thickness assigned (*see* Burt and Dodge 2011 for information on the modelling process). Adopting this methodology will make it easier to integrate individual 3-D project areas ensuring that the 3-D project areas are functionally continuous as well as geographically continuous.

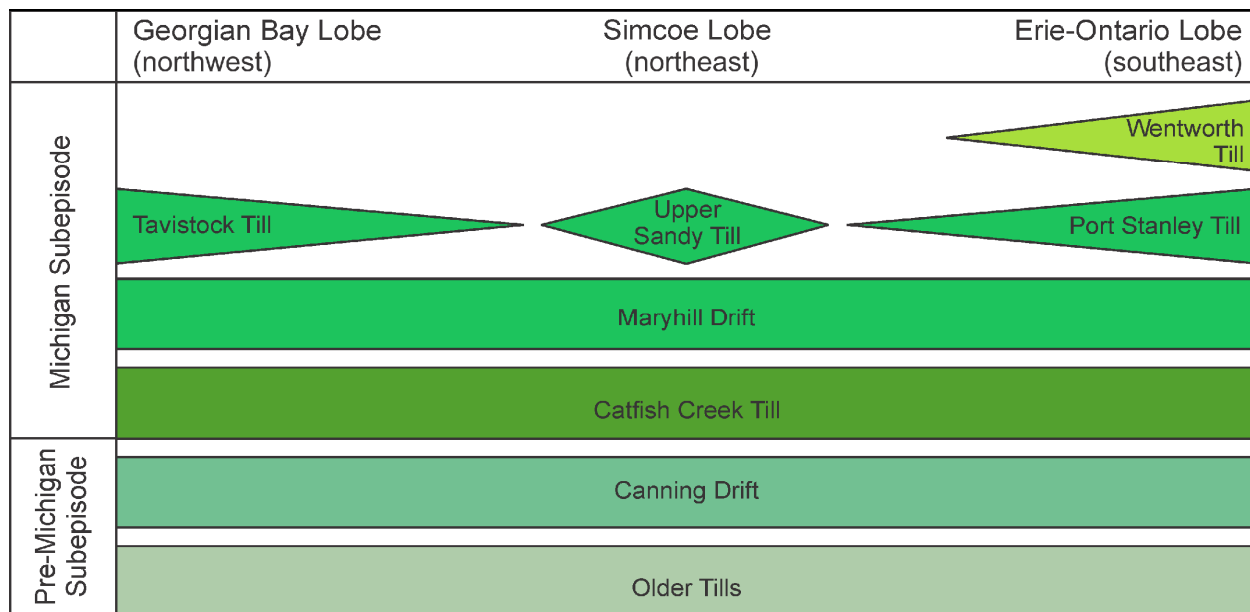


Figure 32.3. Time–distance distance diagram showing till units in the Orangeville moraine 3-D project area.

REFERENCES

- Bajc, A.F. and Dodge, J.E.P. 2011. Three-dimensional mapping of surficial deposits in the Brantford–Woodstock area, southwestern Ontario; Ontario Geological Survey, Groundwater Resources Study 10, 86p.
- Bajc, A.F. and Shirota, J. 2007. Three-dimensional mapping of surficial deposits in the Regional Municipality of Waterloo, southwestern Ontario; report *in* Ontario Geological Survey, Groundwater Resources Study 3, 42p.
- Burt, A.K. 2008. The Orangeville moraine study: a new three-dimensional Quaternary mapping project; *in* Summary of Field Work and Other Activities 2008, Ontario Geological Survey, Open File Report 6226, p.30-1 to 30-9.
- 2009. The Orangeville moraine project: an update of field activities; *in* Summary of Field Work and Other Activities 2009, Ontario Geological Survey, Open File Report 6240, p.22-1 to 22-3.
- 2011. The Orangeville moraine project: preliminary results of drilling and section work; *in* Summary of Field Work and Other Activities 2011, Ontario Geological Survey, Open File Report 6270, p.28-1 to 28-34.
- Burt, A.K. and Dodge, J.E.P. 2011. Three-dimensional modelling of surficial deposits in the Barrie–Oro moraine area of southern Ontario; Ontario Geological Survey, Groundwater Resources Study 11, 125p.
- Burt, A.K. and Rainsford, D.R.B. 2010. The Orangeville moraine project: buried valley targeted gravity study; *in* Summary of Field Work and Other Activities 2010, Ontario Geological Survey, Open File Report 6220, p.31-1 to 31-6.

33. Project Unit 12-005. The Mount Forest–Elmira Study: A New Three-Dimensional Quaternary Mapping Project

A.K. Burt¹

¹Earth Resources and Geoscience Mapping Section, Ontario Geological Survey

INTRODUCTION

The May 2000 Walkerton tragedy and resulting *Clean Water Act* focussed the attention of all levels of government, conservation authorities and members of the public on the importance of protecting Ontario's groundwater resource. A critical component of mapping the resource is a thorough understanding of the three-dimensional (3-D) distribution of Quaternary (surficial) sediments. The 3-D distribution of these sediments influences groundwater recharge and discharge zones and the location of both regional and local aquitards and aquifers. Accurate 3-D models will improve volumetric estimations of the provincial groundwater resource and may allow undiscovered aquifers to be located. Of equal importance, the models can be used to identify aquifers susceptible to contamination and potential pathways for contaminants.

The Ontario Geological Survey (OGS) is initiating a new 3-D mapping project in the Mount Forest–Elmira area of southern Ontario. This area was selected for study for several reasons. First, groundwater is the primary source of water for domestic, agricultural and industrial uses. Much of the proposed area falls within the Greater Golden Horseshoe Growth Plan Area and, as such, is poised to receive accelerated population growth placing increasing pressure on the groundwater resource (www.ontario.ca/placestogrow, accessed September 25, 2012). The 3 conservation authorities (Grand River, Saugeen Valley and Maitland Valley) mandated to protect the groundwater resource in this area require detailed subsurface information for source water protection planning. Second, there is significant potential regional groundwater recharge via the Elmira moraine in the south and Saugeen kames (Singhampton moraine) in the north. Third, areas with a thick sedimentary cover mean there may be near-surface as well as deeper aquifers. A buried-bedrock valley connecting the thick drift zones may form an important local aquifer as well as transfer water between watersheds. Fourth, the project will connect the Orangeville moraine project area (Burt, this volume, Article 32) with the Regional Municipality of Waterloo and Brantford–Woodstock project areas (Bajc and Shirota 2007; Bajc and Dodge 2011) creating a laterally continuous 3-D mapped area of 7135.5 km² (Figure 33.1). It is also laterally continuous with the Dundas buried-bedrock valley project area (Marich et al. 2011).

The goal of the Mount Forest–Elmira project is to build an interactive 3-D model of Quaternary deposits that form both regional and local aquifers and aquitards. Key objectives are 1) reconstruction of the Quaternary history of the Mount Forest–Elmira area, 2) development of a 3-D model of Quaternary sediments, 3) characterization of the properties of the modelled sediment packages and 4) examination of the connection between the surface topography of the moraine and groundwater recharge. The model will be based on the interpretation of natural and man-made exposures, existing subsurface records (water wells, geotechnical records, etc.) and new geophysical data and drilling. It is anticipated that the final block model of Quaternary deposits will be used for studies involving groundwater recharge, exploration, extraction, protection and remediation; studies to support the *Clean Water Act*; detailed planning for healthy community growth (*Places to Grow Act*); development of policies surrounding land use and nutrient management; and enhanced understanding of the interaction between ground and surface waters.

Summary of Field Work and Other Activities 2012,
Ontario Geological Survey, Open File Report 6280, p.33-1 to 33-16.

© Queen's Printer for Ontario, 2012

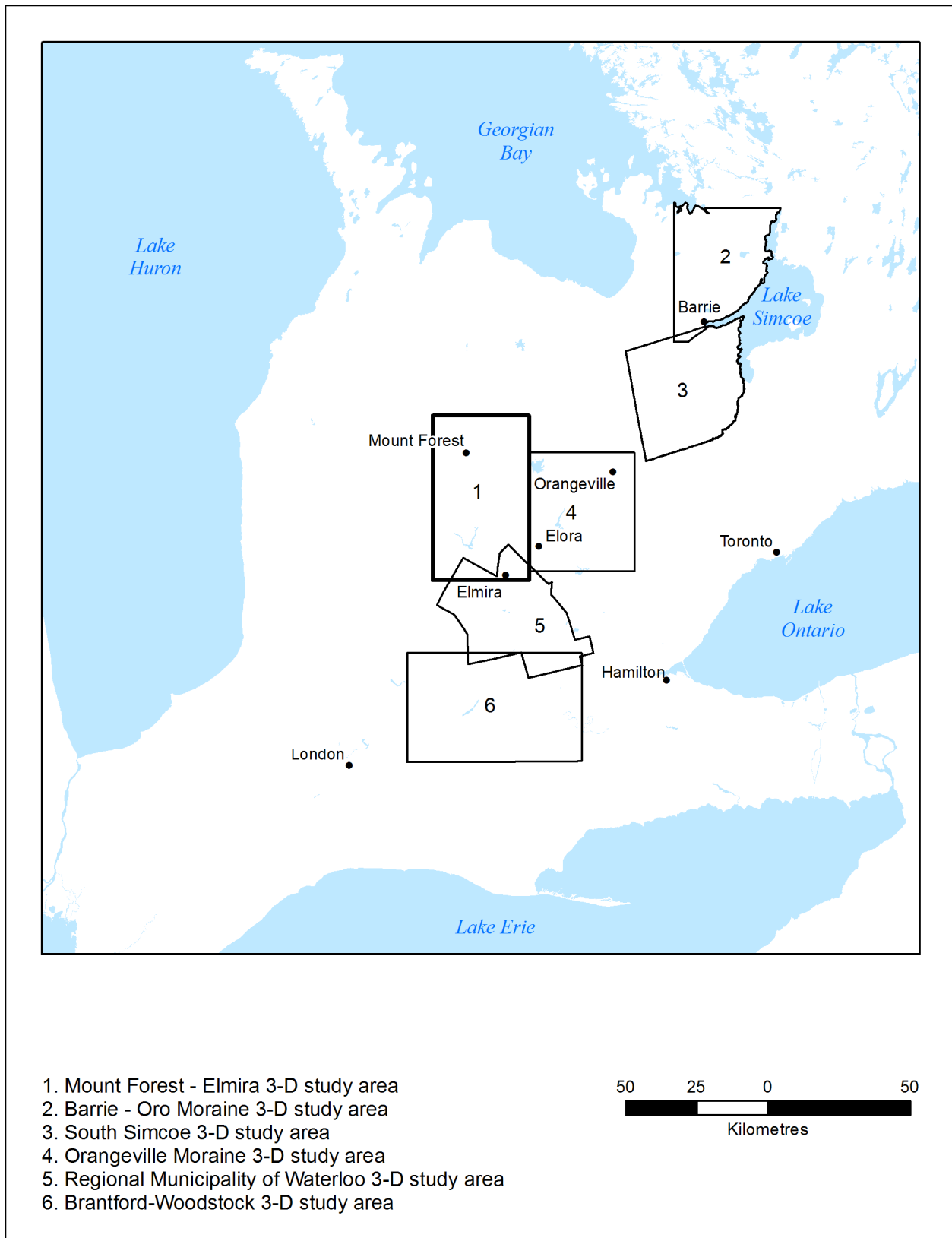


Figure 33.1. Location of the Mount Forest–Elmira study area in southwestern Ontario.

LOCATION

The Mount Forest–Elmira study area encompasses approximately 2000 km² extending from Grey Road 9 northwest of Mount Forest south to Elmira (Figures 33.1 and 33.2). Portions of the County of Grey (Town of West Grey and Township of Southgate), the County of Wellington (Town of Minto, Township of Wellington North, Township of Mapleton and Township of Centre Wellington), the County of Perth (Municipality of North Perth and Township of Perth East) and the Regional Municipality of Waterloo (Township of Wellesley and Township of Woolwich), represented on 1:50 000 scale NTS map sheets 40 P/9, 40 P/10, 40 P/15, 40 P/16, 41 A/1 and 41 A/2, are included within the study area. The towns of Mount Forest, Harriston, Palmerston, Arthur and Elmira are the largest urban centres within the study area. The communities of Holstein, Kenilworth, Teviotdale, Moorefield, Drayton, Alma and Linwood, as well as numerous smaller hamlets, are also located within the study area.

REGIONAL SETTING

Bedrock Geology

The Mount Forest–Elmira study area is underlain by southwest-dipping Silurian and Devonian bedrock formations (Ontario Geological Survey 2011). Upper and lower Silurian Guelph Formation subcrops across the northeast and in a 2.5 to 6 km wide band along most of the eastern side of the study area (Figure 33.3). A series of 14 continuous-cored overburden boreholes drilled along the western 10 km of the adjacent Orangeville moraine project area (*see* Burt 2011 for borehole locations) terminated in the Guelph Formation (F.R. Brunton, OGS, personal communication, 2012). The Guelph Formation is characterized by brown or tan fine- to medium-crystalline, sucrosic, fossiliferous and biostromal to biohermal dolostone (Armstrong and Carter 2010). The Guelph Formation is overlain by the Upper Silurian Salina Formation mapped as a 25 km wide band extending from the northwest to south of the study area. The Salina Formation is characterized by thin-bedded grey and brown argillaceous dolostone and green and red shale with beds and nodules of gypsum (Ontario Geological Survey 2011). The Upper Silurian Bass Islands Formation overlies the Salina Formation. It subcrops in a 2.5 km wide band west of the Salina Formation. The Bass Islands Formation is dark brown to light grey-tan very fine- to fine-crystalline dolostone that is variably laminated, mottled, argillaceous and bituminous (Armstrong and Carter 2010). The Lower Devonian Bois Blanc Formation subcrops along the western side of the study area where it disconformably overlies the Bass Islands Formation. The Bois Blanc Formation is characterized by grey to brown, fine- to medium-grained, cherty, fossiliferous limestone and dolostone with thin beds of glauconitic quartz sandstone locally near the base (Ontario Geological Survey 2011). The Bois Blanc Formation is overlain by the Middle Devonian Amherstburg Formation. The Amherstburg Formation is characterized by tan to grey-brown to dark brown fine- to coarse-grained bituminous, bioclastic, fossiliferous and commonly cherty limestone and dolostone. Although not occurring within the current study area boundary, the Amherstburg Formation is mapped less than 2 km to the southwest.

The regional bedrock surface dips from a high of 500 m above sea level (asl) west of Luther Lake on the eastern side of the study area to 290 m asl in the Grand Basin (Cowan 1979) near Elmira in the southwest and 300 m asl in the Saugeen Basin northwest of Mount Forest (Figure 33.4). The 2 distinct bedrock lows are separated by a broad, gently southwest-dipping regional-scale bedrock high. This regional bedrock high is bisected by a clearly defined bedrock valley, referred to by Karrow (1973) as the Walkerton Valley, that can be traced from the Mount Forest bedrock low south as far as Drayton before becoming obscured by the pit and hummock nature of the interpolated bedrock surface. The water-well records suggest that this channel is approximately 70 m deep. There are several additional poorly defined channels that show up as 2 or more adjacent circular depressions (e.g., southeast of Mount Forest and south of Kenilworth) or as short sections of channel (e.g., south of Arthur and north of Elmira). Knowledge

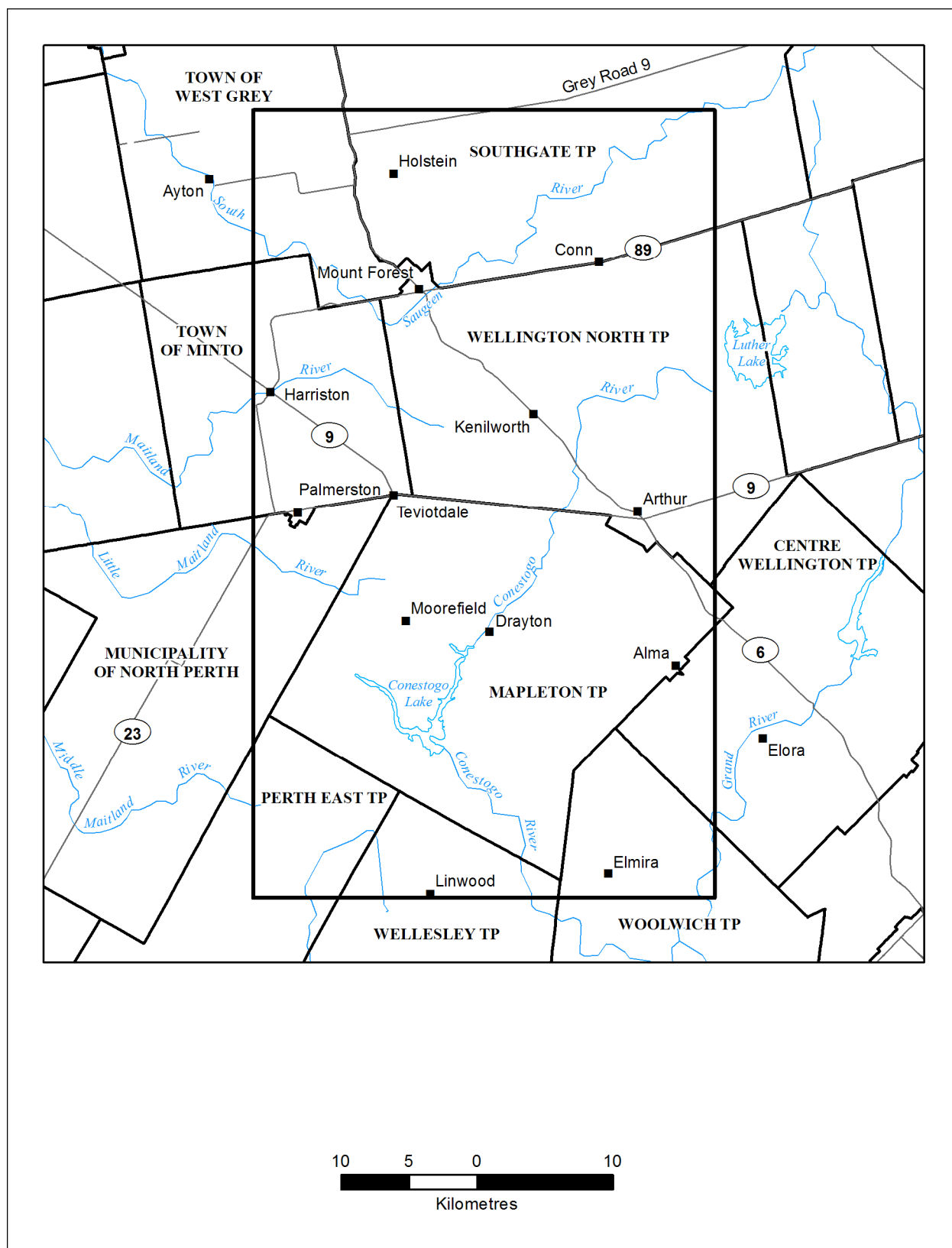


Figure 33.2. Townships, larger communities, lakes and rivers within the Mount Forest–Elmira study area.

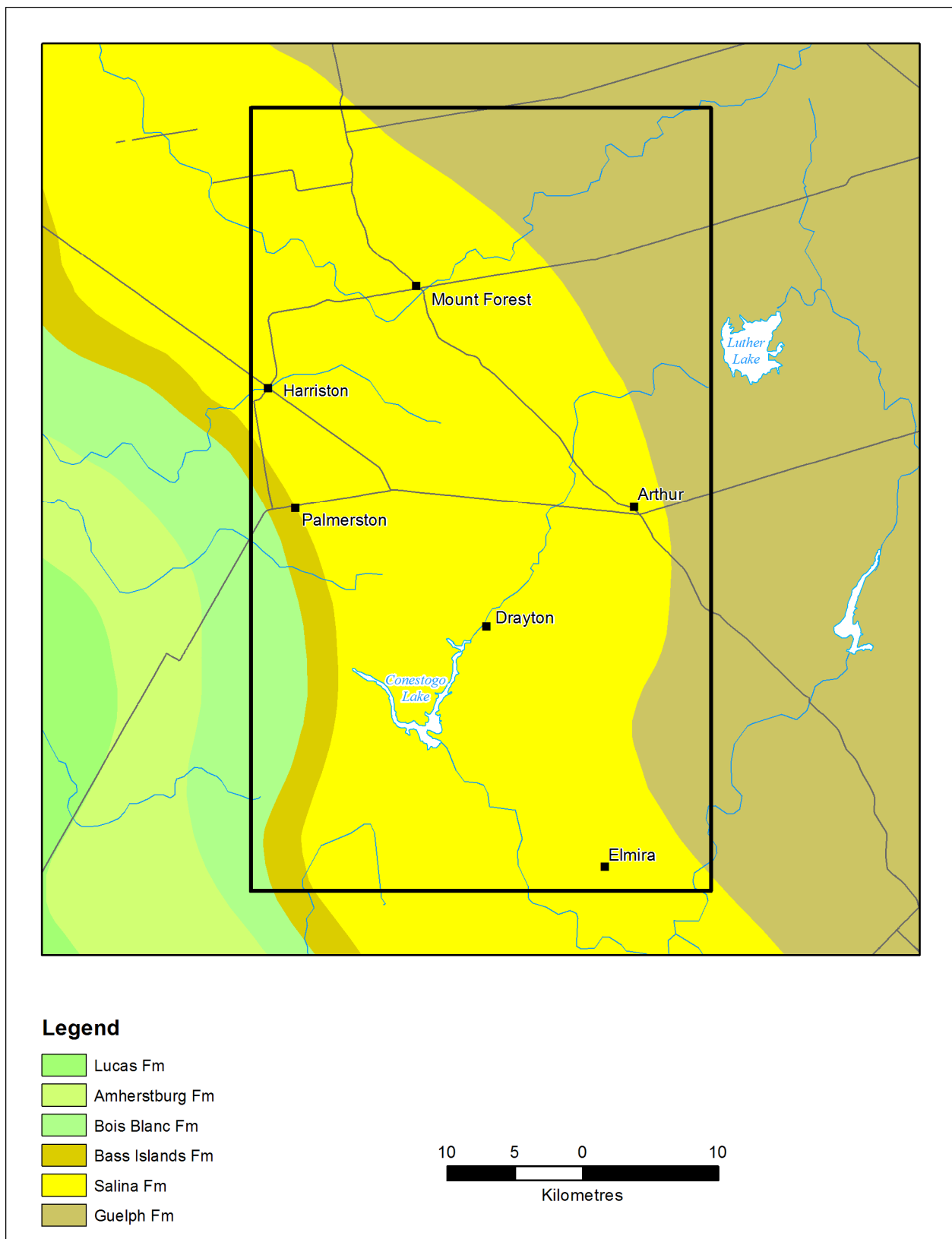


Figure 33.3. Bedrock geology of the Mount Forest–Elmira study area (*from* Ontario Geological Survey 2011).

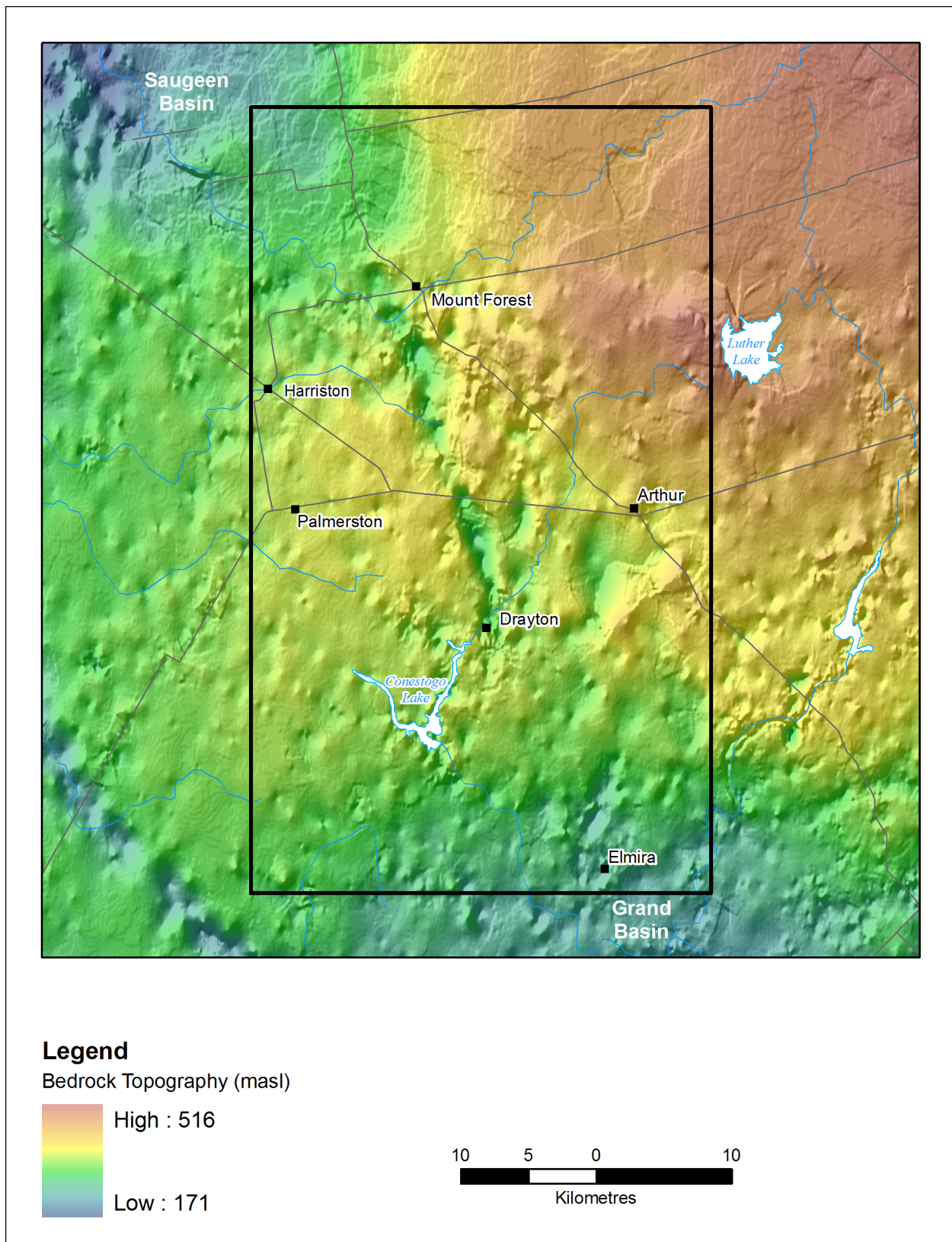


Figure 33.4. Bedrock topography of the Mount Forest–Elmira study area (*from* Gao et al. 2006).

of the regional bedrock surface, particularly the locations of bedrock channels, will be improved by a geophysical survey that will be conducted during the early stages of the project. Further refinements will come from overburden drilling.

Surface Drainage and Watersheds

There are 3 major watersheds and, therefore, 3 conservation authorities—the Saugeen Valley Conservation Authority, the Maitland Valley Conservation Authority and the Grand River Conservation Authority—within the Mount Forest–Elmira study area (Figure 33.5). The northern third of the study area forms the headwater region of the Saugeen Valley Conservation Authority. Northwest of Holstein, drainage is southwest then northwest through the Beatty Saugeen River and tributaries. The South Saugeen River drains the majority of the watershed flowing from the far northeast of the study area southwest toward Mount Forest then northwest toward Ayton. Between Holstein and Mount Forest, drainage is westward through Fairbanks Creek into the South Saugeen River. The Beatty Saugeen and South Saugeen rivers join the Saugeen River and flow northwest into Lake Huron. In addition, there are numerous small lakes and wetlands within areas of closed drainage in the Saugeen kame moraine.

The west-central portion of the study area forms the headwater region of the Maitland Valley Conservation Authority. Between Harriston and Palmerston drainage is westward through the North Maitland River. South of Palmerston, drainage is westward through the Little Maitland River and, in the far south of the study area, drainage is westward through the Middle Maitland River. These rivers join the Maitland River and flow southwest then northwest into Lake Huron.

The east-central and southern portions of the study area are part of the Grand River Conservation Authority. The northern portion of the watershed drains from Kenilworth southwest then east through the Mallet River and from Arthur southwest through the Conestogo River into Conestogo Lake (a man-made reservoir). Drainage then continues south through the Conestogo River and into the Grand River south of Elmira. From Alma, drainage is southeast through the Irvine River into the Grand River at Elora. In the central area, drainage is south into the Woolwich Reservoir and then southeast into the Grand River east of Elmira. The Grand River flows south and southeast into Lake Erie.

Drift Thickness

Drift thicknesses within the study area ranges from less than 10 m up to 115 m (Ontario Geological Survey 2010) (Figure 33.6). There are large areas of thin drift in the northeast and along most of the western side of the study area with a small thin drift area in the far southeast. In these areas, bedrock is exposed, such as along rivers and streams, or is covered by only a few tens of metres of sediment.

North of Mount Forest, generally corresponding with the Saugeen kames (Figure 33.7), the drift thickens to 30 to 75 m. Dominating the central portion of the study area are 1 distinct continuous, and several intermittent, 30 to 110 m thick linear bands of sediment that radiate south and southeast of Mount Forest (see Figure 33.6). These thick drift bands are formed of sediments that are filling in the bedrock valleys. There is a broad zone of thick drift extending from Arthur south to Elmira and southwest to Linwood. Sediments typically range from 40 m up to 115 m in thickness in the central portion of the zone. These thick drift areas are significant as they may host near-surface as well as deeper aquifers. The bedrock valley sediments may form an important local aquifer as well as transfer water between watersheds.

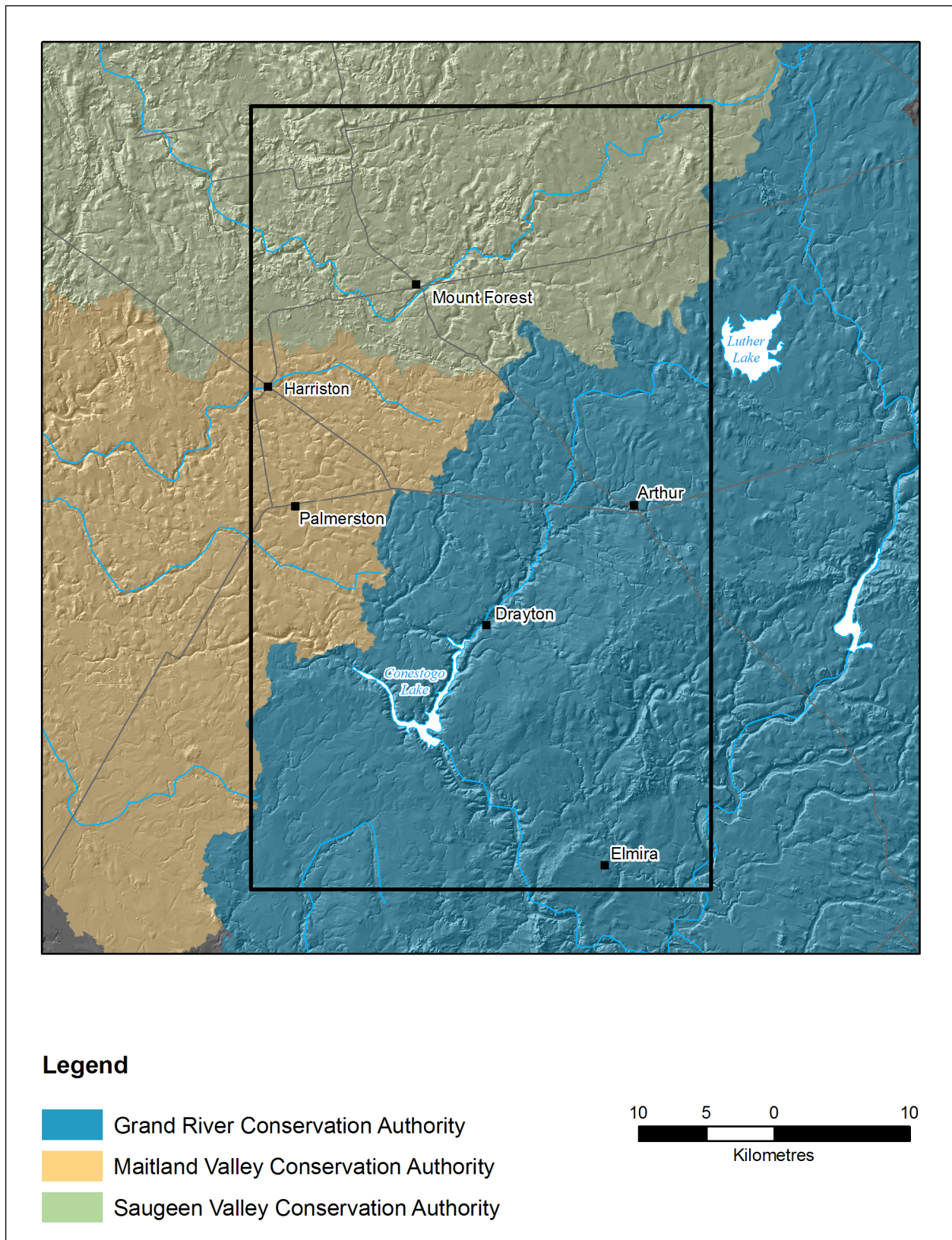


Figure 33.5. Watershed and drainage map of the Mount Forest–Elmira study area.

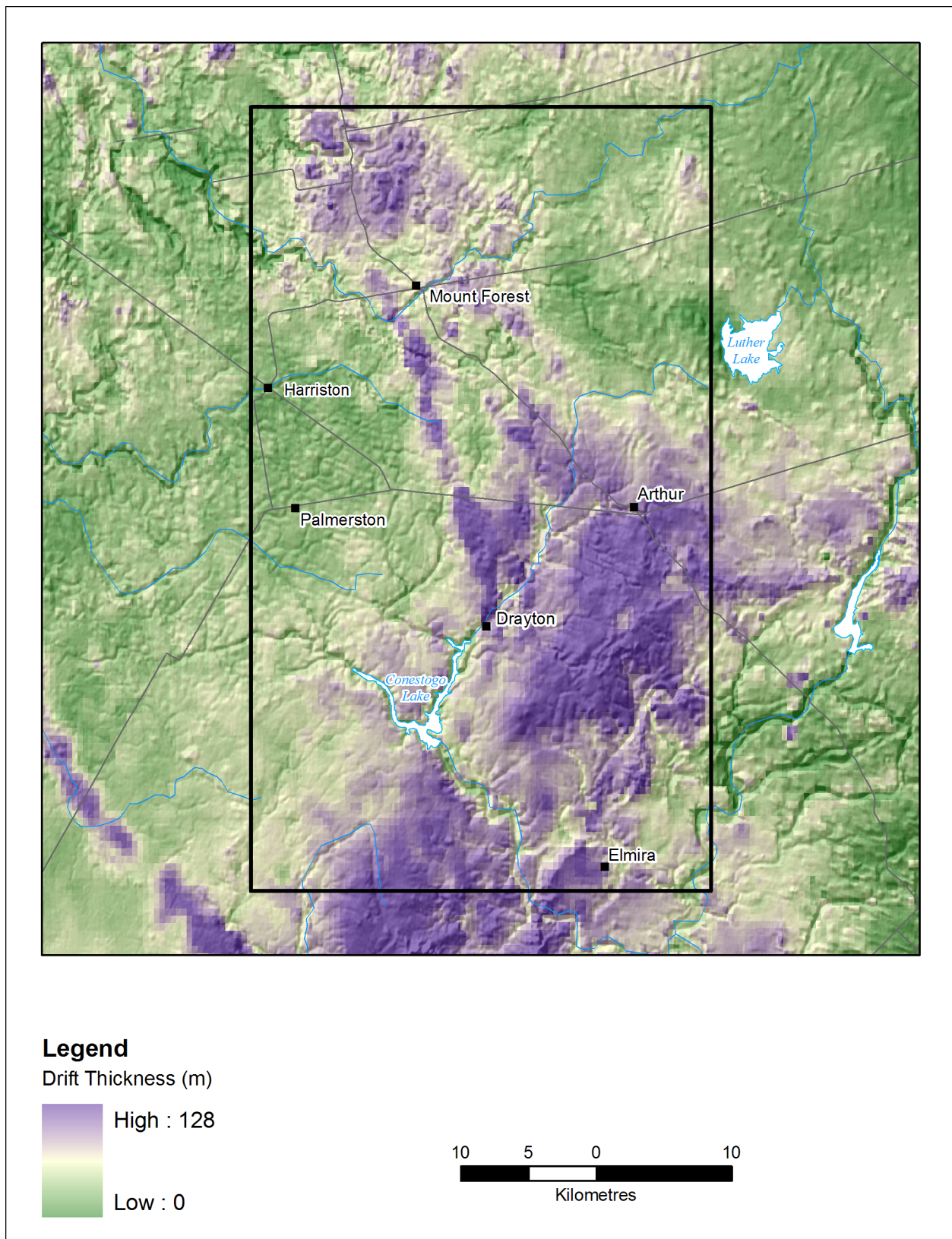


Figure 33.6. Drift thickness of the Mount Forest–Elmira study area (*from* Gao et al. 2006).

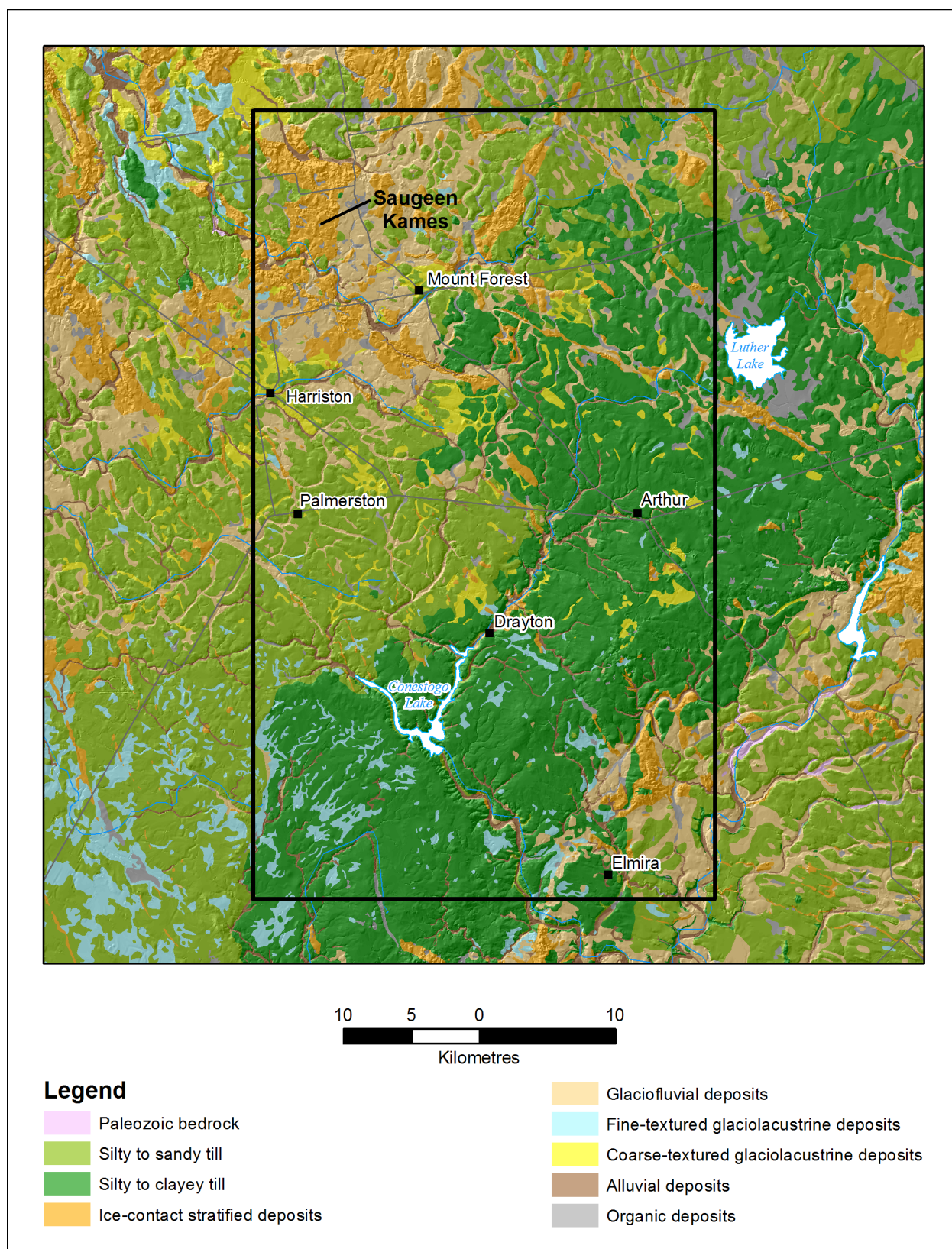


Figure 33.7. Surficial geology of the Mount Forest–Elmira study area (*from* Ontario Geological Survey 2010).

Surficial Geology

The oldest till mapped at surface is Nissouri Phase Catfish Creek Till representing the main Laurentide ice advance as far south as Ohio. The till is mapped along some rivers in the southern and eastern portions of the study area with additional small outcrops east of Conn (Figure 33.8; *see also* Figure 33.2). Catfish Creek Till is typically a grey to greyish brown overconsolidated stony sandy silt till. There is a high percentage of dolostone clasts and a low calcite-dolomite ratio in the till matrix, both of which are likely derived from Silurian dolostones to the north (Cowan 1979). Catfish Creek Till characteristically has a relatively high percentage of Precambrian clasts reflecting its northern source. Early and late lobate facies of Catfish Creek Till are typically stone poor and finer textured than the main regional Catfish Creek Till (Bajc and Dodge 2011; Burt, this volume, Article 32). Catfish Creek Till is an important marker bed in southwestern Ontario: it was intersected during drilling in the Orangeville moraine 3-D study area to the east and the Regional Municipality of Waterloo and Brantford–Woodstock 3-D study areas to the south (Bajc and Shiota 2007; Bajc and Dodge 2011; Burt 2011).

An interlobate zone formed during the breakup of the Nissouri Phase Laurentide Ice Sheet extending from the Dorchester moraine, through the Waterloo moraine and up to the Orangeville moraine. The main moraine-building phase was likely initiated as the ice thinned and took on the lobate form that was to characterize subsequent cycles of advance and retreat (*see* Bajc and Dodge (2011) and Burt (2011) for more information on the Waterloo and Orangeville moraines). The Elmira moraine, located between Elmira and Alma, has been interpreted as forming within a re-entrant along the retreating ice margin (Bajc and Karrow 2004). This may have been in the interlobate zone between the Erie–Ontario and Huron–Georgian Bay ice lobes. Paleocurrent measurements in the Waterloo moraine record paleoflows to the west and northwest indicative of an Erie–Ontario lobe source (Bajc and Shiota 2007), whereas paleocurrent measurements in the Orangeville moraine record paleoflows to the southwest indicative of a Simcoe lobe source (Burt 2011). Preliminary observations have been made in 1 pit in the Elmira moraine and these suggest paleoflows to the southwest (Burt 2011), whereas observations made by Bajc and Karrow (2004) record paleoflows ranging from the southeast to the southwest.

During the Port Bruce Phase, a series of tills were deposited by ice flowing out of the Erie–Ontario and Huron–Georgian Bay lake basins. Maryhill drift, traditionally attributed to the Erie–Ontario lobe, is mapped at surface along river cuts southeast and southwest of Elmira (*see* Figure 33.8). Maryhill drift consists of stone-poor silt and clay-rich till with low calcite-dolomite ratios (Karrow 1993) and associated fine-textured glaciolacustrine sediments. Port Stanley Till, deposited by Erie–Ontario lobe ice, is mapped at surface east of Elmira (*see* Figure 33.8). In the adjacent Orangeville moraine 3-D study area, Port Stanley Till is typically a stony silty sandy till, is heavily drumlinized (forming the Guelph drumlin field physiographic region of Chapman and Putnam (1984)) and is also bisected by numerous outwash channels that form part of the Grand River outwash (Burt 2011). These outwash channels are found within the Mount Forest–Elmira 3-D study area as well as the Regional Municipality of Waterloo 3-D study area (Bajc and Shiota 2007).

The surface sediments within the study area are dominated by tills deposited by Georgian Bay lobe ice. The oldest of these, stone-poor silt and clay-rich Stirton Till, has been attributed to a minor ice fluctuation within the Conestogo River basin (Cowan 1979; Karrow 1993). This till is not mapped at surface, but may be encountered during drilling. Feenstra (1975) observed Stirton Till in cuts along Conestogo Lake north of Conestogo Dam. This local ice fluctuation was followed by the main Port Bruce Phase ice advance to the Orangeville moraine which deposited the stone-poor to slightly stony, silt to clayey silt Tavistock Till. Pebble counts yield generally high numbers of dolostone clasts throughout the study area, but limestone and chert is reported to increase in the south and west (Cowan 1979; Karrow 1993). Tavistock Till is mapped at surface across much of eastern portion of the study area and exhibits a very gently rolling topography with localized east-southeast- to southeast-trending low streamlined landforms. There are several large eskers associated with the Tavistock Till ice advance (*see* Figure 33.8).

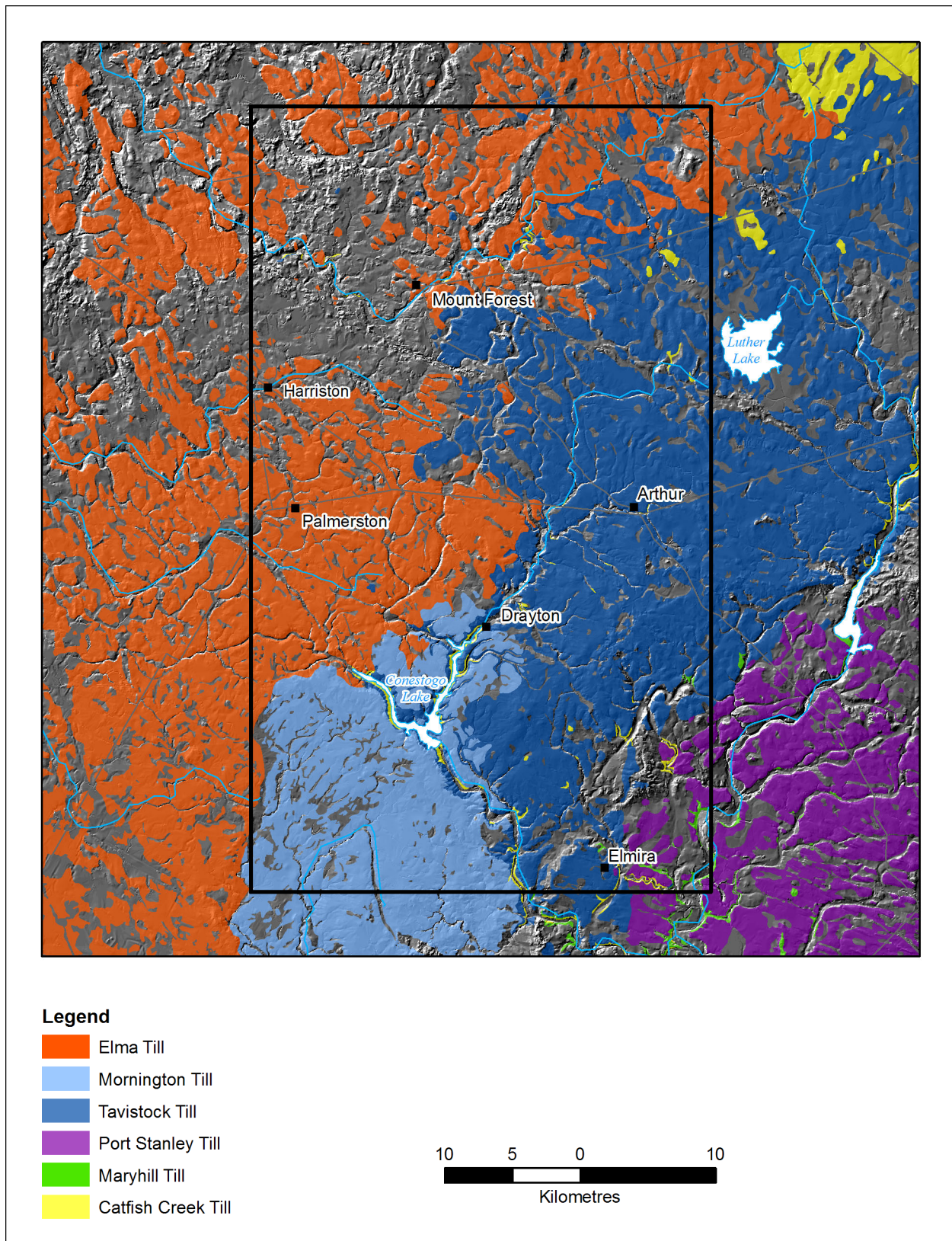


Figure 33.8. Surficial tills of the Mount Forest–Elmira study area (from Ontario Geological Survey 2010). Grey areas on figure indicate areas of no till.

A minor fluctuation of the Tavistock Till ice resulted in the over-riding of esker deposits near Mount Forest (Cowan 1979) and deposition of the localized Mornington Till southwest of Drayton (*see* Figure 33.8). Mornington Till is grey to dark grey, has a silty clay texture and is stone poor to somewhat stony (Karrow 1993). The outer margin of the till roughly coincides with the low-lying Macton moraine west of Conestogo Lake and Conestogo River. The subdued relief of the Macton moraine is due, in part, to draping with glaciolacustrine sediments as described by Bajc and Karrow (2004). Mornington Till has a surface topography of small low ridges, which has been attributed to deposition by stagnant ice (Karrow 1993). Tavistock and Mornington tills crosscut the boundaries of the Stratford till plain and Dundalk till plain physiographic regions (Chapman and Putnam 1984) (Figure 33.9).

A late Port Bruce Phase advance of Georgian Bay lobe ice deposited Elma Till across the northwest portion of the study area (*see* Figure 33.8). Elma Till ranges from a light brown silty till to a cream coloured stony sandy till. Pebble lithologies reflect the underlying bedrock with a very high percentage of dolostone clasts and locally high percentages of chert clasts south and west of Palmerston, which is down ice from where the Bois Blanc Formation subcrops (Cowan 1979). In the southern part of the study area, the surface topography of Elma Till is characterized by shallow flutes; however, between Palmerston and Harriston, it forms the southern part of the Teeswater drumlin field. Elma Till thins toward its outer margin resulting in a patchy and discontinuous distribution, particularly between Teviotdale and Conn. It has been suggested that Elma ice locally flowed beyond the mapped extent of the Elma Till modifying and resculpting the underlying Tavistock and Mornington tills (Cowan 1979; Karrow 1993). There are numerous small and occasional large eskers, meltwater channels and outwash associated with the advance and retreat of Elma ice.

A series of standstills or minor fluctuations as the Elma ice retreated resulted in the deposition of the Saugeen kames, part of the Singhampton moraine (i.e., the Horseshoe moraine physiographic region of Chapman and Putnam (1984)) in the northwest part of the study area (*see* Figures 33.7 and 33.9). Elma Till is mapped both south and north of the kames providing chronologic control for their deposition. The Saugeen kames are hummocky with areas of closed drainage resulting in small lakes and wetlands (Photo 33.1). They consist of belts of ice-contact stratified drift, outwash, small pockets of glaciolacustrine silt and a localized brown silty till. These deposits have been interpreted as a series of 2 or 3 ice-marginal positions with associated small glacial lakes and a very minor ice advance that deposited the till (Cowan 1979). A 25 km long esker-bead complex extending northwest of Kenilworth may record the ice margins and will be investigated during this project.



Photo 33.1. Hummocky topography of the Saugeen kames.

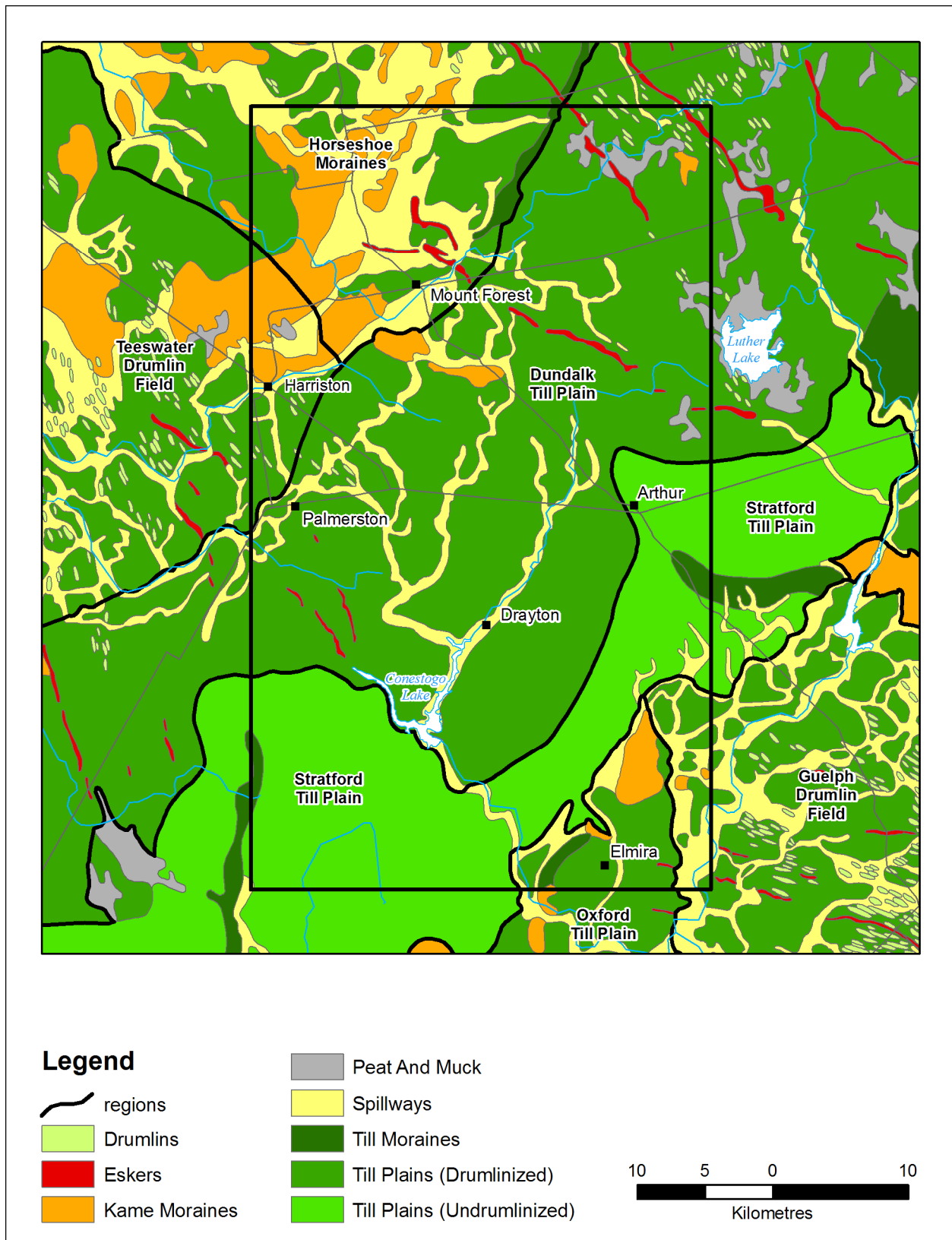


Figure 33.9. Physiography of the Mount Forest–Elmira study area (*from* Chapman and Putnam 2007).

Small pockets of glaciolacustrine sediments are located in shallow depressions across the study area. These deposits consist of fine-textured silt and clay south of a line extending from Moorefield through Drayton to Alma, whereas coarser textured silt and sand were deposited to the north. It is not known whether these sediments were deposited in one lake or were deposited in a series of lakes relating to multiple phases of ice advance and retreat. Glaciolacustrine sediments have been reported between Port Bruce Phase tills in the Mount Forest–Elmira study area (Cowan 1979; Karrow 1993) and were observed by the author in the adjacent Orangeville moraine study area. It is certainly plausible, however, for the surface deposits to have been deposited in one lake as the margin between fine- and coarse-textured sediments does not correspond with the mapped extent of the tills and individual deposits frequently straddle till margins.

There is postglacial alluvium along rivers and streams throughout the region. Significant organic deposits and wetlands are found in depressions within the Saugeen kames in the northwest and around Luther Lake in the northeast. There are occasional small accumulations of organic material further south, often associated with modern rivers and streams.

PROJECT PLAN

The Mount Forest–Elmira 3-D mapping project has been initiated, but field work will not commence until 2013. A ground gravity geophysical survey will be conducted in the survey area this year to define bedrock surfaces. This will aid in the selection of drill targets, particularly in the buried-bedrock valleys. Continuous coring of the overburden and upper 3 m of bedrock will take place during the 2013, 2014 and possibly 2015 field seasons. Natural and man-made exposures will be logged and reconnaissance level geomorphological and surficial sediment observations made during each field season.

A database will be assembled from existing subsurface information including Ministry of the Environment water-well records, Ministry of Transportation geotechnical records, Ontario Oil, Gas and Salt Resources Library oil and gas well records, geotechnical records from the Urban Geology Automated Information System (UGAIS) and Waterloo Area Geology Automated Information System (WAGAIS), and archived field notes. The data will be standardized in preparation for modelling. As with previous OGS 3-D modelling projects, Datamine Studio[®] software, a software package developed for the mining industry and adapted for overburden mapping for groundwater modelling applications with a series of scripts, will be used for modelling and the preliminary generation of products (*see* Bajc and Newton (2005) and Bajc and Shiota (2007) for more information on the scripts and Burt and Dodge (2011) for more information on database standardization).

REFERENCES

- Armstrong, D.K. and Carter, T.R. 2010. The subsurface Paleozoic stratigraphy of southern Ontario; Ontario Geological Survey, Special Volume 7, 301p.
- Bajc, A.F. and Dodge, J.E.P. 2011. Three-dimensional mapping of surficial deposits in the Brantford–Woodstock area, southwestern Ontario; Ontario Geological Survey, Groundwater Resources Study 10, 86p.
- Bajc, A.F. and Karrow, P.F. 2004. 3-Dimensional mapping of Quaternary deposits in Waterloo Region, southwestern Ontario; Geological Association of Canada–Mineralogical Association of Canada, Joint Annual Meeting, Field Trip FT-7, 72p.
- Bajc, A.F. and Newton, M.J. 2005. Three-dimensional modelling of Quaternary deposits in Waterloo Region, Ontario: a case study using Datamine Studio[®] software; *in* Summary of Field Work and Other Activities 2005, Ontario Geological Survey, Open File Report 6172, p.25-1 to 25-8.

- Bajc, A.F. and Shiota, J. 2007. Three-dimensional mapping of surficial deposits in the Regional Municipality of Waterloo, southwestern Ontario; report *in* Ontario Geological Survey, Groundwater Resources Study 3, 42p.
- Burt, A.K. 2011. The Orangeville moraine project: preliminary results of drilling and section work; *in* Summary of Field Work and Other Activities 2011, Ontario Geological Survey, Open File Report 6270, p.28-1 to 28-34.
- Burt, A.K. and Dodge, J.E.P. 2011. Three-dimensional modelling of surficial deposits in the Barrie–Oro moraine area of southern Ontario; Ontario Geological Survey, Groundwater Resources Study 11, 125p.
- Chapman, L.J. and Putnam, D.F. 1984. The physiography of southern Ontario; Ontario Geological Survey, Special Volume 2, 270p.
- 2007. Physiography of southern Ontario; Ontario Geological Survey, Miscellaneous Release—Data 228.
- Cowan, W.R. 1979. Quaternary geology of the Palmerston area, southern Ontario; Ontario Geological Survey Report 187, 64p. Accompanied by Maps 2383 and 2384, scale 1:50 000.
- Feenstra, B.H. 1975. Late Wisconsin stratigraphy in the northern part of the Stratford–Conestogo area, southern Ontario; unpublished MSc thesis, University of Western Ontario, London, Ontario, 233p.
- Gao, C., Shiota, J., Kelly, R.I., Brunton, F.R. and van Haaften, S. 2006. Bedrock topography and overburden thickness mapping, southern Ontario; Ontario Geological Survey, Miscellaneous Release—Data 207.
- Karrow, P.F. 1973. Bedrock topography in southern Ontario: a progress report; Geological Association of Canada, Proceedings, v.25, p.67-77.
- 1993. Quaternary geology, Stratford–Conestogo area; Ontario Geological Survey, Report 283, 104p. Accompanied by Maps 2558 and 2559, scale 1:50 000.
- Marich, A.S., Priebe, E.H., Bajc, A.F., Rainsford, D.R.B. and Zwiers, W.G. 2011. A geological and hydrogeological investigation of the Dundas buried-bedrock valley, southern Ontario; Ontario Geological Survey, Groundwater Resources Study 12.
- Ontario Geological Survey 2010. Surficial geology of southern Ontario; Ontario Geological Survey, Miscellaneous Release—Data 128—Revised.
- 2011. 1:250 000 scale bedrock geology of Ontario; Ontario Geological Survey, Miscellaneous Release—Data 126—Revision 1.

34. Project Unit 12-006. A Preliminary Assessment of Subsurface Sediments in the Central Norfolk Sand Plain, Norfolk County and the County of Oxford, Southern Ontario

A.S. Marich¹

¹Earth Resources and Geoscience Mapping Section, Ontario Geological Survey

INTRODUCTION

This report briefly summarizes the results of an overburden drilling program completed within the central part of the Norfolk sand plain, southern Ontario. The drill program is part of a Tier 3 Water Quality Risk Assessment currently being undertaken by the Grand River Conservation Authority (GRCA), Norfolk County, the County of Oxford (herein referred to as “Oxford County”) and the Long Point Region Conservation Authority, as well as the Ontario Ministry of Natural Resources (MNR) and the Ontario Ministry of the Environment (MOE). All of these groups are working within the Lake Erie Source Water Protection Region. The local population draws water primarily from private and municipal water wells screened within the Norfolk sand plain sediments. With increasing pressures on groundwater resources, a better understanding of the deep aquifers is required to properly assess the quality and quantity of water within the groundwater system.

The study area covers the central portion of Norfolk County as well as part of southeastern Oxford County. Access to the study area is via Highways 3, 24 and 19 as well as a dense network of township and county roads. The towns of Tillsonburg, Delhi and Simcoe are located within the study area (Figure 34.1).

A series of 26 PQ diameter (85 mm) overburden boreholes were drilled between September 2010 and January 2011. Depths ranged between 29 and 67 m with approximately 1300 m of drill core being collected. All 26 boreholes reached bedrock. Following collection, the drill cores were shipped to the Ontario Geological Survey office in Sudbury for detailed logging and sampling. All samples will be analyzed for grain size and diamictons for carbonate content as well. The tests are being completed by the Ontario Geological Survey Geoscience Laboratories in Sudbury. Pebbles were also collected from the various diamicton units for lithological identification and provenance determination.

BEDROCK GEOLOGY

The bedrock surface slopes gently toward the Lake Erie basin and is overlain by a thick sequence of Quaternary deposits. In some areas, the drift is up to 100 m thick.

The bedrock formations underlying the study area are of Upper Silurian to Middle Devonian age (Figure 34.2). No outcrops of these formations have been identified within the study area (Barnett 1982).

The oldest bedrock unit, located in the extreme northeastern edge of the study area, is the Upper Silurian Salina Group, which consists primarily of shale and gypsum with lesser dolostone (Armstrong and Carter 2010). The Bass Islands Formation is dark brown to light grey-tan, variably laminated,

mottled, argillaceous and bituminous, very fine- to fine-crystalline and sucrosic dolostone with local intraclastic breccia, evaporitic mineral moulds, blue-grey mottling, minor anhydritic beds and rare thin sandstone beds. The Bass Islands Formation grades into the Bertie Formation eastward in the study area. The Bertie Formation consists of dark brown to light grey-tan, very fine- to fine-grained, variably laminated and bituminous, sparsely fossiliferous dolostones, and argillaceous dolostones and minor shale (Armstrong and Carter 2010).

Overlying the Bass Islands and the Bertie formations is the Lower Devonian Bois Blanc Formation. This unit is a resistant cherty and fossiliferous limestone that disconformably overlies the Silurian strata. This formation is commonly greenish-grey to grey-brown, thin- to medium-bedded and fine- to medium-textured rock. Some sections are fossiliferous and cherty limestone and dolostone units have been observed (Armstrong and Carter 2010).

The Middle Devonian Amherstburg Formation consists of tan to grey-brown to dark brown, fine- to coarse-grained, bituminous, bioclastic, fossiliferous limestones and dolostones. Fossil crinoids, corals, brachiopods and cephalopods are present locally. The Amherstburg Formation grades into the Onondaga Formation to the east exhibiting similar characteristics with cherty sections (Armstrong and Carter 2010).

The Middle Devonian Lucas Formation limestone and dolostones contain anhydritic beds and local sandy limestones. The bedrock is thin to medium bedded, light to dark grey-brown, fine crystalline and poorly fossiliferous.

The Dundee Formation is grey to tan to brown, fossiliferous, medium- to thick-bedded limestones and minor dolostones. Chert nodules are locally abundant, and the unit exhibits bituminous partings and microstylolites (Armstrong and Carter 2010).

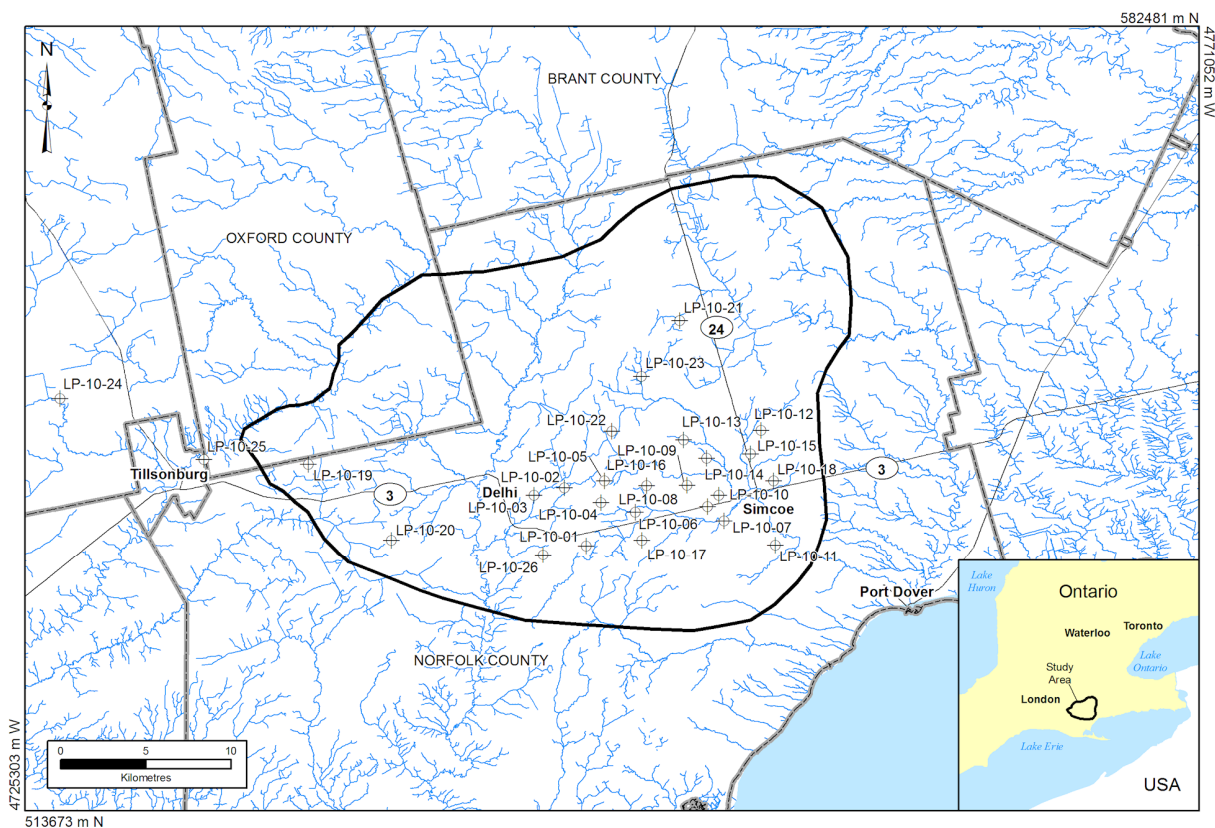


Figure 34.1. Location of the study area in southern Ontario. The study area is outlined in black. Locations of the 26 boreholes are also indicated. Universal Transverse Mercator (UTM) co-ordinates provided in North American Datum 1983 (NAD83), Zone 17.

QUATERNARY GEOLOGY

Physiography

Chapman and Putnam (1984) identified 2 physiographic regions within the current study area: the Norfolk sand plain and the Mount Elgin ridges. The study area is dominated at surface by gently undulating glaciolacustrine deposits of the Norfolk sand plain. These sediments were deposited within glacial Lake Warren and glacial Lake Whittlesey and represent the sandy topset beds of a large delta. The plain dips gently toward Lake Erie.

The Mount Elgin ridges physiographic region is located in the northwest corner of the study area and is represented by the St. Thomas and Norwich moraines. The ridge crests gradually increase in height from northwest to southeast with local relief being approximately 30 m (Chapman and Putnam 1984). These ridges are cored by the clayey silt Port Stanley Till.

A series of near-parallel northeast- to southwest-trending moraines transect the study area and were constructed during brief pauses in the retreat or slight readjustments of the Erie lobe. From west to east, the moraines are the St. Thomas, Norwich, Tillsonburg, Courtland, Mabee, Paris and Galt moraines (Figure 34.3).

Glacial History and Stratigraphy

The last major advance of glacial ice into southern Ontario occurred during the Nissouri Phase of the Michigan Subepisode approximately 17 000 to 25 000 years before present (BP).

The Catfish Creek Till and associated stratified deposits were laid down during this phase. The till displays a compact, stony and sandy texture that is commonly finer grained in the earlier and later lobate phases (Barnett 1992, 1993; Bajc and Dodge 2011). The till is often characterized by high matrix carbonate and a low calcite to dolomite ratio. It is also often associated with fine-textured glaciolacustrine sediments as well as glaciofluvial sands and gravels that are found above, below and interbedded with the till (Barnett 1992, 1993; Bajc and Shirota 2007; Bajc and Dodge 2011). Pre-Catfish Creek Till sediments were found in several boreholes, but are not consistently observed throughout the study area.

Following the deposition of the Catfish Creek Till, ice retreated from the study area during the Erie Phase approximately 15 000 years BP (Barnett 1982). At this time, a series of high-level lakes occupied the Lake Erie Basin. The fine-textured sediments, including rhythmically bedded silts and clays as well as glaciofluvial sands overlying Catfish Creek Till, are attributed to the Erie Interstadial. These deposits were encountered in several boreholes drilled for this study.

During the Port Bruce Phase, glacial ice overrode the Erie Interstadial glaciolacustrine and glaciofluvial deposits. The ice margins during this advance are marked by the series of moraines near Tillsonburg and St. Thomas (Barnett 1978, 1982). As the ice advanced westward, it incorporated the fine-textured glaciolacustrine sediments and re-deposited them as Port Stanley Till. In places, the till is interbedded with debris-flow deposits and associated stratified sediments. The Port Stanley Till is a clayey silt to very fine-textured sandy silt diamicton with minor grits and granules. The Courtland and Mabee moraines are composed of Port Stanley Till (Barnett 1978, 1998). The Tillsonburg moraine is capped by Port Stanley Till and cored by till interbedded with ice-contact stratified deposits (Barnett 1982; Bajc and Dodge 2011).

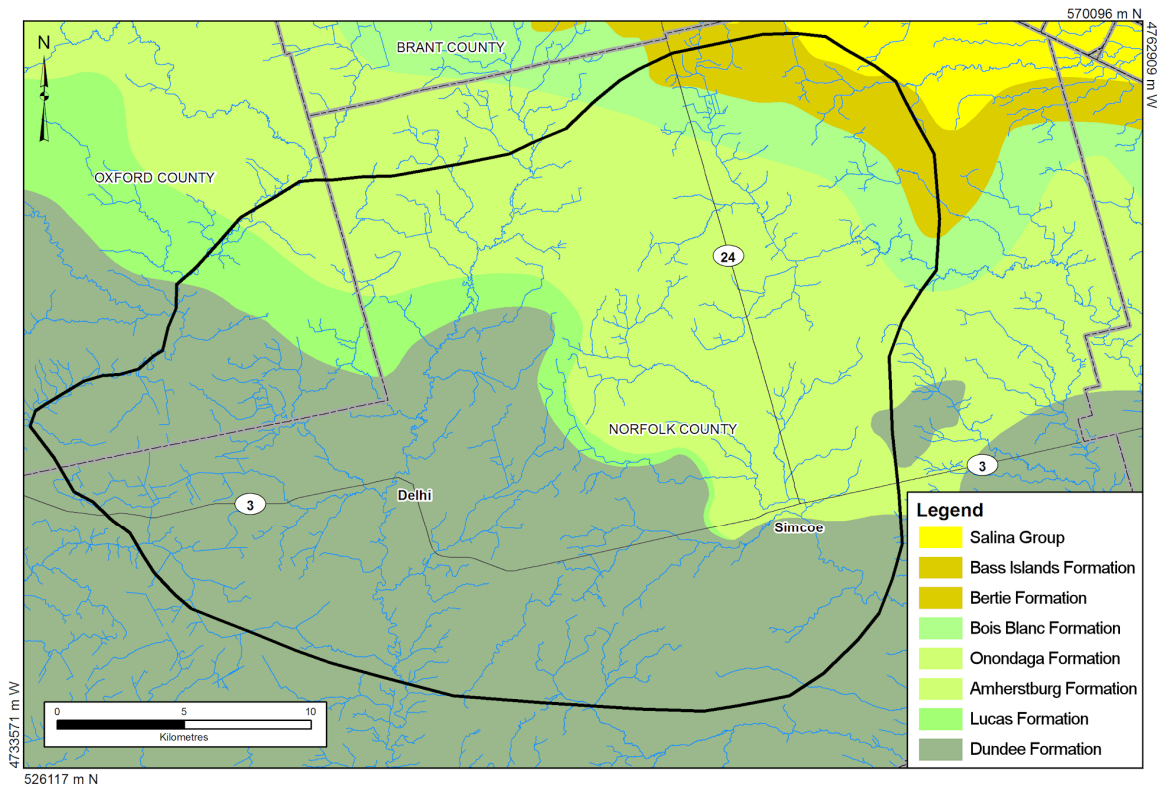


Figure 34.2. Simplified bedrock geology of the study area (after Armstrong and Carter 2010). UTM co-ordinates provided in NAD83, Zone 17.

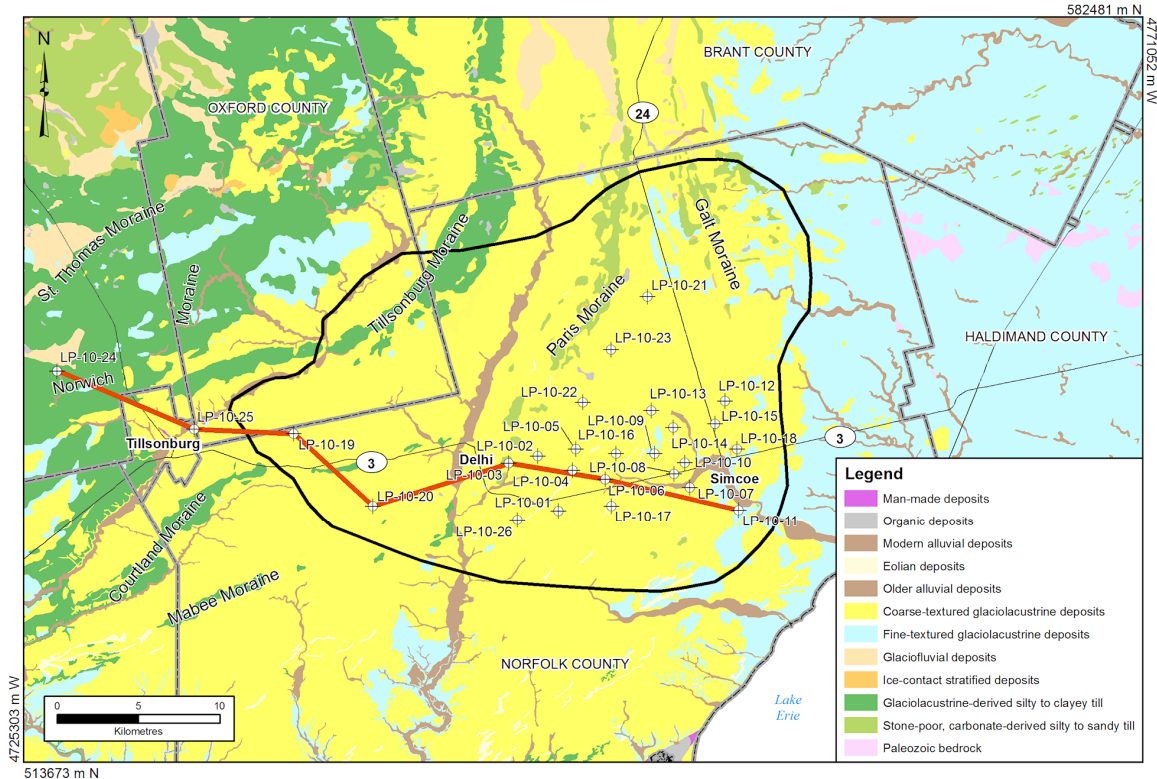


Figure 34.3. Simplified surficial geology of the study area including the locations of the boreholes (after Ontario Geological Survey 2010). UTM co-ordinates provided in NAD83, Zone 17.

Late in the Port Bruce Phase, as the ice retreated from the Norwich moraine, deltaic sands were deposited within the proglacial lake. Slight fluctuations of the ice margin resulted in the formation of the Courtland and Mabee moraines. The final glacial advance to enter the study area occurred during the Mackinaw Phase resulting in the deposition of the Wentworth Till and the formation of the Paris and Galt moraines (Barnett 1982). The Wentworth Till is a stony, sandy to silty till, and is exposed mainly along the crests of the Paris and Galt moraines.

Following the final retreat of glacial ice from the area approximately 12 000 years BP, a series of glacial lakes formed within the Erie Basin, the most recent of which was glacial Lake Whittlesey. The extensive deltaic sands of the Norfolk sand plain were laid down in these lakes (Chapman and Putnam 1984; Barnett 1982).

OVERBURDEN DRILLING

Logging and interpretation of the 26 boreholes drilled for this study revealed a relatively simple and consistent stratigraphic sequence reflecting the fluctuations in the ice margins and development of glacial lakes. Figure 34.4 shows the graphic logs for 7 of these boreholes along a west-east transect (the transect is shown on Figure 34.3). These boreholes display the general sequence of sediments identified within the study area.

There is a general coarsening-upward sequence observed within these boreholes. Directly overlying bedrock is the compact silty sandy Catfish Creek Till and related fine-textured glaciolacustrine sediments; this sedimentary package is identified as the Catfish Creek Drift (*see* CCD on Figure 34.4). The Catfish Creek Drift ranges between 3 and 15 m in thickness with the thickest section occurring in borehole LP-10-19. In the westernmost borehole (LP-10-24), the Catfish Creek Drift is absent. There, the Port Stanley Drift was deposited directly on the bedrock surface.

Thin deposits of fine-textured glaciolacustrine sediments overlying the Catfish Creek Drift have been attributed to the Erie Phase of deposition. This unit ranges from 1 to 5 m in thickness and represents the period of ice retreat following deposition of the Catfish Creek Drift. The next sedimentary package that occurs in several of the boreholes is the silty and clayey, stone-poor, Port Stanley Till and related fine-textured glaciolacustrine sediments. This package, called the Port Stanley Drift, varies in thickness from just under a metre to approximately 15 m, except in borehole LP-10-24 where the drift package accounts for almost the entire borehole record, approximately 55 m. Borehole LP-10-24 is the westernmost borehole and is located just to the north of a segment of the Norwich moraine. This borehole record suggests that the Norwich moraine is capped with Port Stanley Till and cored with glaciofluvial sands and gravels similar to the Tillsonburg moraine. Occasionally in this drift package, 2 till units were observed, at the base and at the top. In the central part of the drift package, fine-textured glaciolacustrine sediments or glaciofluvial sands and gravels are present (*see* boreholes LP-10-24 and LP-10-06). The Port Stanley Drift is absent from boreholes LP-10-25, LP-10-19 and LP-10-11. It is possible that these fine-textured diamictons were either never deposited or reworked with the development of glacial lakes and eventually re-deposited as stratified sediments.

Overlying the Port Stanley Drift is a thick package of glaciolacustrine sediments, the Lake Whittlesey deltaic deposits. At the base of this package are interbedded to laminated silts and clays that coarsen into very fine-textured sands, which are rhythmically bedded in sections. The sands coarsen gradually upward into medium- to medium-coarse-textured sands. Throughout the Lake Whittlesey package, irregular beds and laminae of silts and clay have been observed. The deltaic sands account for the largest portion of this drift sequence and the borehole records are commonly capped with this sand.

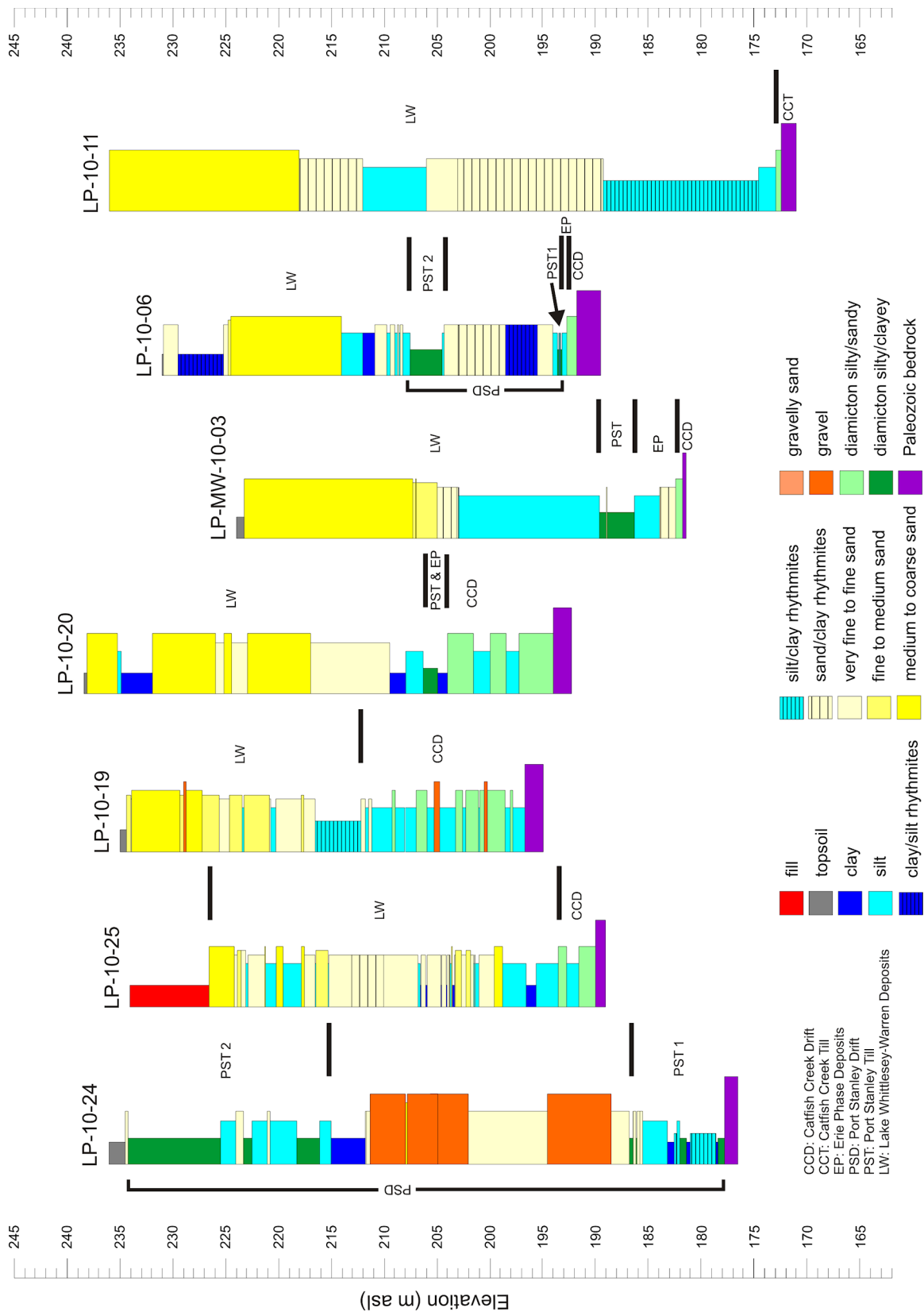


Figure 34.4. A west-to-east selection of borehole graphic logs.

FUTURE WORK

Interpretation of the sedimentary sequence contained within the 26 boreholes is ongoing. Grain size and carbonate analyses are being completed. Also, a conceptual model of the subsurface including the identification of possible aquifer units will be produced.

REFERENCES

- Armstrong, D.K. and Carter, T.R. 2010. The subsurface Paleozoic stratigraphy of southern Ontario; Ontario Geological Survey, Special Volume 7, 301p.
- Bajc, A.F. and Dodge, J.E.P. 2011. Three-dimensional mapping of surficial deposits in the Brantford–Woodstock area, southwestern Ontario; report *in* Ontario Geological Survey, Groundwater Resources Study 10, 86p. [PDF document]
- Bajc, A.F. and Shirota, J. 2007. Three-dimensional mapping of surficial deposits in the Regional Municipality of Waterloo, southwestern Ontario; report *in* Ontario Geological Survey, Groundwater Resources Study 3, 42p.
- Barnett, P.J. 1978. Quaternary geology of the Simcoe area, southern Ontario; Ontario Geological Survey, Report 162, 81p.
- 1982. Quaternary geology of the Tillsonburg area, southern Ontario; Ontario Geological Survey, Report 220, 95p.
- 1992. Quaternary geology of Ontario; *in* Geology of Ontario, Ontario Geological Survey, Special Volume 4, Part 2, p.1011-1088.
- 1993. Quaternary geology of the Long Point–Port Burwell area; Ontario Geological Survey, Open File Report 5873, 229p.
- 1998. Quaternary geology, Long Point–Port Burwell area; Ontario Geological Survey, Report 298, 153p.
- Chapman, L.J. and Putnam, D.J. 1984. The physiography of southern Ontario, 3rd ed.; Ontario Geological Survey, Special Volume 2, 270p.
- Ontario Geological Survey 2010. Surficial geology of southern Ontario; Ontario Geological Survey, Miscellaneous Release—Data 128—Revised.

35. Project Unit 11-032. Regional-Scale Groundwater Mapping in Early Silurian Carbonate Rocks of the Niagara Escarpment Cuesta: Multi-Level Monitoring Well Sampling

E.H. Priebe¹, F.R. Brunton¹ and V.L. Lee¹

¹Earth Resources and Geoscience Mapping Section, Ontario Geological Survey

INTRODUCTION

Groundwater is an invaluable resource in Ontario, with approximately 30% of residents relying on it as their sole source of drinking water (Statistics Canada 1996). The information that is currently collected to support groundwater management in Ontario is *ad hoc*, addressing many objectives across the province at different scales and using a variety of methods. Most groundwater resource exploration activities are narrow in scope, conducted to satisfy domestic, industrial or municipal requirements, leaving a knowledge gap in the area of broader unexplored groundwater potential. To address these knowledge gaps and to create bedrock groundwater maps, the Ontario Geological Survey (OGS) initiated a bedrock groundwater mapping program in 2008 (Brunton 2009; Brunton and Brintnell 2011). The program objectives are to systematically map groundwater flow systems and karst in Paleozoic sedimentary rocks across southern Ontario. This is the first attempt by the OGS to develop a multidisciplinary approach to regional-scale groundwater mapping in sedimentary rocks by integrating hydrogeological information with a predictive, basin-scale sequence stratigraphic geologic model. The combination of hydrogeological field methods and modelling tools with an understanding of geological controls on regional groundwater flow and chemistry, will result in the delineation of hydrogeologic units (HGUs). Because an HGU, by definition, is not constrained by stratigraphy, it is most appropriate for describing the Paleozoic sedimentary rocks of southern Ontario, which are variably karsted and jointed, enabling cross-formational flow. The creation of groundwater potential bedrock maps in which HGUs are delineated will provide a baseline for future groundwater exploration programs.

Beginning in 2005, pilot-scale bedrock groundwater characterization work was initiated in partnership with the City of Guelph, Ontario. Results from the pilot-scale work demonstrated that bedrock aquifers consistently take advantage of sequence stratigraphic boundaries and spatially associated karst conduits. It was subsequently demonstrated that regional flow systems reside above a regional-scale shale aquitard known as the Cabot Head Formation (Brunton et al. 2007; Brunton and Dodge 2008; Brunton et al. 2011; Brunton and Brintnell 2011). In support of the development of the broader geological model, further regional-scale mapping of Silurian rock units along the Niagara Escarpment and away from the Guelph–Cambridge area suggests similar geological controls on groundwater movement (Brunton et al. 2011; Brunton and Brintnell 2011).

BACKGROUND

The field work and laboratory activities described in this article have been completed as part of an ongoing four-year regional study (2011–2015) to characterize the hydrogeology of the Early Silurian

*Summary of Field Work and Other Activities 2012,
Ontario Geological Survey, Open File Report 6280, p.35-1 to 35-11.*

rocks of the Niagara Escarpment cuesta, which is an outgrowth of the four-year bedrock geology mapping project that is planned to be completed in the spring of 2013. The study area encompasses the Michigan Basin portion of southwestern Ontario focussing on the north-to-south-trending region bounded by the Bruce Peninsula to the north, the erosional edge of the Niagara Escarpment cuesta to the east, the edge of the Appalachian Basin to the south-southeast and the subcrop boundary of the Salina Group to the west.

The Lockport Group, which is the Early Silurian package of dolostones that form the Niagara Escarpment cuesta, outcrop or subcrop across the study area and overlie the regional aquitard shales of the Cabot Head Formation. The Cabot Head Formation, which forms part of the underlying Clinton Group, is laterally continuous across the study area, and hydraulic testing (Water FLUTe™ profiling) has demonstrated its competency as a regional hydraulic barrier. The well-cemented dolostones of the upper Fossil Hill (equivalent to the Merrittton Formation of Brett et al. 1995), Rockway and Irondequoit formations, in ascending order (Brunton 2009), overlie the regional Cabot Head Formation aquitard. These thin dolostone rock units typically have very low vertical hydraulic conductivities and they provide hydraulic separation between the karstic bedrock groundwaters of the Lockport Group and the regional Cabot Head Formation aquitard across most of the study area, with the exception of the cuesta margin.

The study area was selected because it comprises the potable water zones of the eastern and northern erosional edge of the Niagara Escarpment in southwestern Ontario (Brunton and Brintnell 2011). The Lockport Group rocks have been described by Funk (1979) as containing some of the most productive aquifers in Ontario. Singer, Cheng and Scafe (2003) identified great inconsistency in specific capacity values within Lockport Group wells, although these observations may be misleading given that many of the wells from which they gathered hydraulic information were completed in the overburden–bedrock interface rather than within the deep bedrock groundwater flow zones that the OGS is currently mapping.

As described in Lee et al. (2011), a hydrogeological monitoring network was established in 2011. Groundwater data presented in this report are from 12 multi-level wells that use the Water FLUTe™ system (Flexible Liner Underground Technology), extending from the City of Guelph in the south to the Town of Wiarton in the north (Figure 35.1). The sampling of the 12 multi-level wells conducted in 2011 and 2012 represents a small subset of the larger sampling and monitoring program that will be conducted in support of the hydrogeologic characterization work for this project. Future data collection, sampling and monitoring will include additional high-quality data from multi-level installations in the vicinity of the City of Guelph, strategically located wells within the City of Cambridge, monitoring wells within Hamilton Region and a number of municipal and private industrial installations across the study area.

Field data collected and work completed during the 2011 field season included 1) hydraulic conductivity testing at each of the well installation sites; 2) design and installation of the multi-level wells; 3) installation of pressure transducers; and 4) three separate sets of groundwater sampling at each multi-level well. Multi-level monitoring well ports were installed at target zones where hydraulic testing had demonstrated the groundwater flow zones.

Field work completed in the 2012 season included 1) early spring (April) sampling of ports; 2) an evaluation of the FLUTe™ air coupled transducer (ACT) systems; and 3) the evaluation of a field method for the calculation of acid-neutralizing capacity (ANC) or alkalinity. A preliminary interpretation of groundwater chemical data available at the time of publication is also included below.

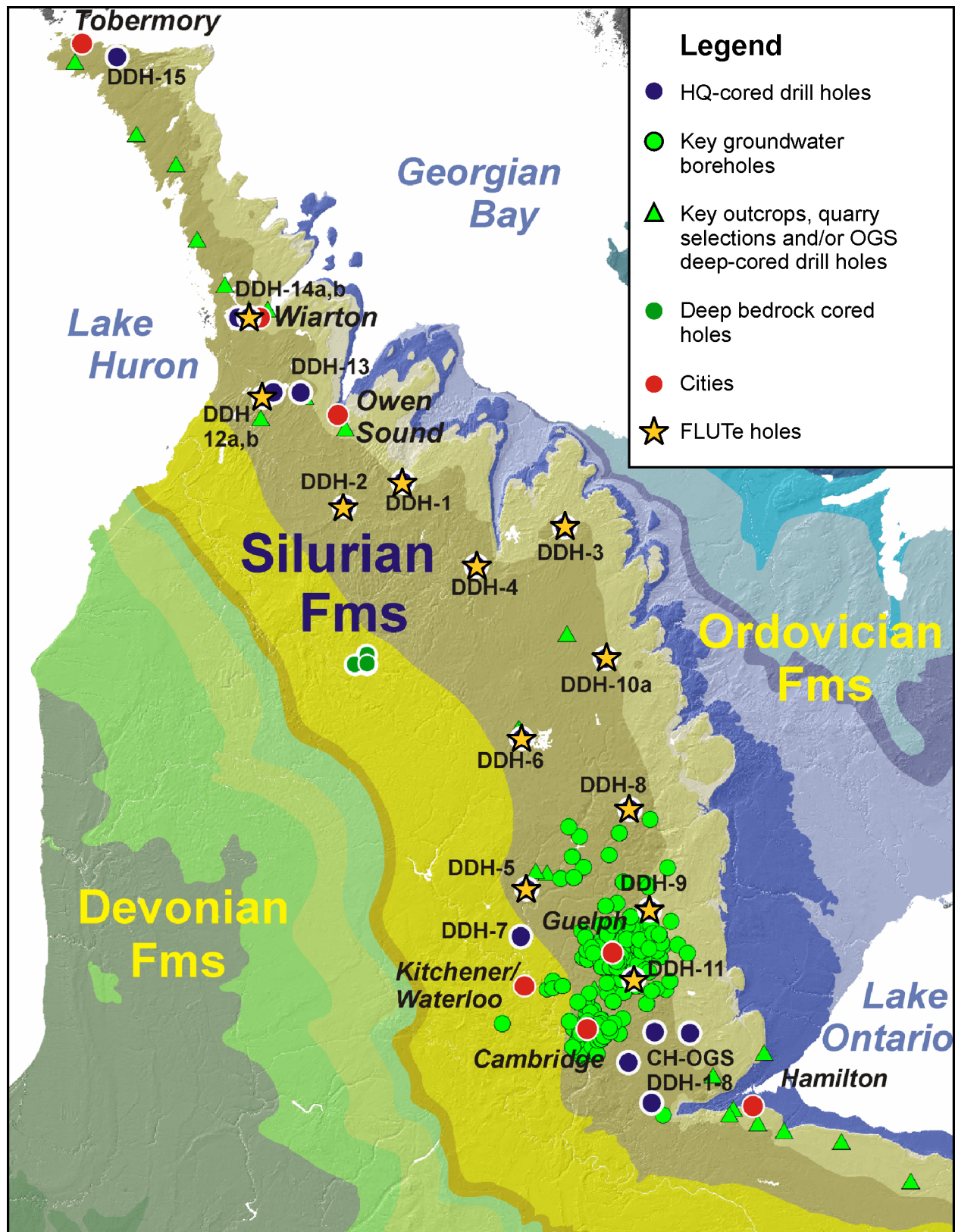


Figure 35.1. Study area showing borehole, well and outcrop locations.

FIELD AND LABORATORY ACTIVITIES COMPLETED IN 2012

Seasonal Groundwater Monitoring at Multi-Level Water FLUTe™ Wells

Groundwater sampling and water-level monitoring were conducted at each of the 12 multi-level wells 4 times between mid-2011 and early 2012. These events were timed to target seasonal extreme wet and dry conditions throughout the course of 1 year to evaluate trends in water levels, vertical groundwater gradients and water chemistry. Sampling was undertaken in July, October and December 2011 and April 2012 during which a total of 160 samples were collected. The purging and sampling protocol developed and outlined by Flexible Liner Underground Technologies Ltd. (2009) was followed for sampling the wells. In addition, water-quality parameters were monitored using a Manta 2™ Sub 2™ multiprobe and flow-through cell. Sample collection and analysis of groundwater for geochemical properties followed the protocols of the OGS Ambient Groundwater Geochemistry program (*see* Hamilton, Brauner and Mellor 2007; Hamilton and Brauner 2008; Hamilton and Freckleton 2009; Hamilton, Freckleton and Mariotti 2010). The only deviation from the Ambient Groundwater Geochemistry program was the use of a different brand of multiparameter sonde (the Manta 2™ Sub 2™). This multiprobe was used for the measurement and recording of parameters including pH, oxidation–reduction potential (ORP), electrical conductivity (EC), dissolved oxygen (DO) and temperature. This sonde uses an optical DO sensor as opposed to the Clark-type DO sensor used in the Ambient Groundwater Geochemistry program. Although the optical DO sensor has a slower response time than the Clark-type sensor, the advantages of the optical DO sensor include low maintenance, anti-fouling characteristics and resistance to damage from exposure to H₂S.

An Evaluation of the FLUTe™ Air Coupled Transducer System

Part of the field work completed in 2011 included the installation of pressure transducers to measure water-level fluctuations at most of the sampling ports of the multi-level systems. To facilitate future repair and replacement of transducers within the FLUTe™ multi-level systems, without the removal of the liner, the FLUTe™ air coupled transducer (ACT) system was employed. The ACT system allows the pressure transducer to be installed at surface with a tube connecting to the sampling port from which the head measurement is required. The system operates under the assumption that the volume of air initially trapped in the tube is fixed. As the water level in the port rises and falls, the pressure of that fixed volume of air responds accordingly, is measured by the transducer (Figure 35.2, *modified from* Keller 2011) and the water levels can then be calculated (Keller 2011). At each location, an additional pressure transducer was also installed in the well casing to measure changes in barometric pressure. All pressure transducers were programmed to take measurements every 4 hours.

Pressure transducer data were downloaded at each sampling and monitoring event throughout 2011 and 2012. These data were submitted to Flexible Liner Underground Technologies Ltd. for the initial conversion of pressure data to water levels. Once the data conversion was complete, it became evident that the process of sampling the Water FLUTe™ systems had introduced significant errors into the ACT system. The introduced error resulted in calculated water levels displaying unnatural offsets in both positive and negative directions at different magnitudes. These offsets likely resulted from gases either entering or leaving the ACT tubing system during the process of sampling. This effect was not anticipated because the sampling port is constructed with a check valve to prevent the interaction of the nitrogen gas, used for sampling, with the air pressure in the ACT tubing. These water-level offsets, which apparently resulted from sampling, occurred in 31 of the 40 ACT systems installed in Water FLUTe™ systems across the study area.

In June 2012, short-term testing was completed on a subset of the affected ACT systems to determine if a change in sampling procedure could eliminate the water-level offset induced by sampling. Results of this testing are pending; if it proves unsuccessful, the ACT tubes will be equipped with a bleed valve that will allow for pressure to be reset to atmospheric pressure after sampling, thereby re-setting the system.

Evaluation of Field Method for Estimating Acid-Neutralizing Capacity or Alkalinity

The Ambient Groundwater Geochemistry program sampling protocol used in this study, employs the HACH alkalinity test kit (Cat. No. 20637-00) for alkalinity determinations in the field at the time of sampling. Each groundwater sample is titrated with sulphuric acid (H_2SO_4) to 3 fixed pH endpoints. These points are visually identifiable when a bromocresol green-methyl red indicator powder is added to the sample prior to starting the titration. The endpoint of the alkalinity titration occurs when all of the reactive species that contribute to alkalinity have reacted. The pH at which this endpoint occurs will depend on the temperature and the ionic strength of the sample solution (Hem 1985), making the fixed-endpoint method employed here appropriate for only a range of values. To better understand the range of values for which the fixed-endpoint method is appropriate, and to evaluate the ease with which the colour changes can be

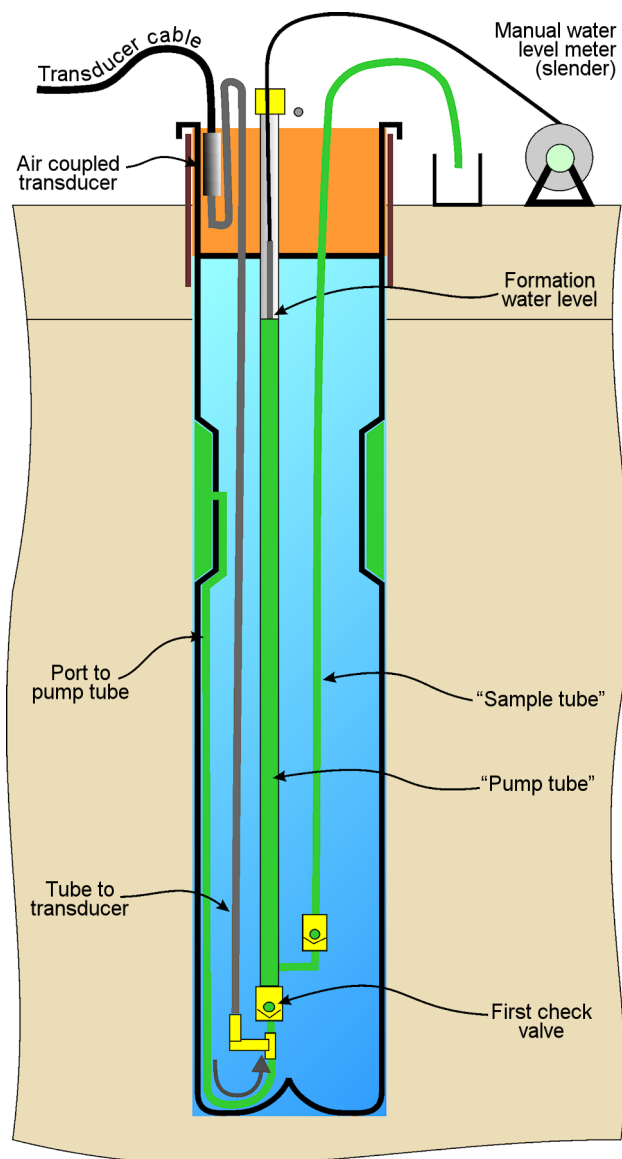


Figure 35.2. The FLUTE™ air coupled transducer (ACT) system in a single sampling port well (drawing *modified from Keller 2011*).

identified, a matrix-appropriate selection of samples were titrated in the laboratory. The samples selected for additional alkalinity determination covered the full range of electrical conductivity values, measured in the field, and also alkalinity estimates from HACH fixed-endpoint titrations. After sampling was complete, titrations were performed a second time in the laboratory using the HACH kit as well as a pH meter. Each titration was carried through to a final pH of about 3.5, well below the bicarbonate equivalence point, to provide an alkalinity determination using the Gran function plot method for comparison with the HACH fixed-endpoint method. The Gran method uses functions to linearize the titration curve, thereby simplifying the estimation of the quantity of acid used to reach the equivalence point. This is then used to calculate alkalinity (Figure 35.3). The bicarbonate equivalence point function (F1) is defined as

$$F1 = (V_t - V_s) \times Ca$$

where, V_t is the volume of acid titrant added, V_s is the titrant volume at the bicarbonate endpoint, Ca is the concentration of the acid titrant (for the full derivation, *see* Stumm and Morgan 1996).

The percent difference between the alkalinity values determined using the fixed-endpoint versus the Gran method is between 0.1 and 1.2%. This level of error in alkalinity is not anticipated to influence the bicarbonate concentration estimate enough to result in unacceptable cation–anion charge balance errors. Although the HACH fixed-endpoint method has its limitations, results from this exercise demonstrate that it is an appropriate method to use for alkalinity determination for the groundwater sampling within the bedrock aquifers of this study area. The effect of filtration on alkalinity estimates was also examined in this study. For comparison, titrations were completed in the laboratory on unfiltered and filtered samples. Filtering was completed by passing the sample through a 0.45 μm filter. The percent difference between the filtered and unfiltered results were less than 2%; therefore, filtration prior to HACH fixed-endpoint alkalinity determinations is not necessary or recommended unless turbidity is visible.

This alkalinity testing exercise also provided the opportunity to use a pH meter to monitor the pH at the moment that the colour change signals the pH 4.5 endpoint. Thus, the light pink colour that identifies the pH 4.5 endpoint was visually noted between a pH range from 4.4 to 4.6. It is recommended that the user of each HACH fixed-endpoint kit go through the exercise of identifying the colour change while using a pH meter to “calibrate” their technique, which will improve the precision and accuracy of these observations in the field.

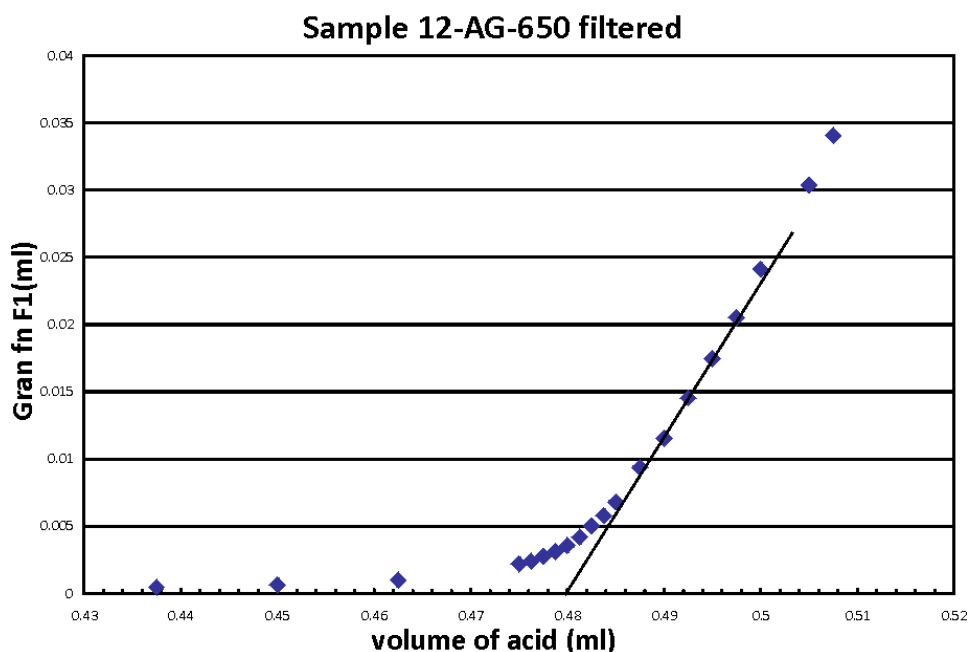


Figure 35.3. An example of a GRAN titration function F1 for one of the groundwater samples in the study area.

This alkalinity testing exercise also provided the opportunity to use a pH meter to monitor the pH at the moment that the colour change signals the pH 4.5 endpoint. Thus, the light pink colour that identifies the 4.5 pH endpoint was visually noted between a pH range from 4.4 to 4.6. It is recommended that the user of each HACH fixed-endpoint kit go through the exercise of identifying the colour change while using a pH meter to “calibrate” their technique, which will improve the precision and accuracy of these observations in the field.

PRELIMINARY INTERPRETATION OF GROUNDWATER SAMPLING RESULTS

The groundwater chemistry data collected during the 2011 and 2012 field seasons are currently undergoing quality-control assessment. The sampling program was designed with a sufficient number of analytical duplicate pairs to allow for Thompson–Howarth precision estimates (Thompson and Howarth 1978), in addition to certified reference materials (CRMs) for accuracy determinations. Data available for discussion at the time of this publication include field parameters and water isotopes, including tritium. These data allow for a preliminary interpretations regarding a) the type and quality of the connection(s) between the groundwater sampling zones and the surface, and b) the chemical distinctions between zones at each monitoring location.

Groundwater samples analyzed for water isotopes and tritium were collected in the summer of 2011. Samples were analyzed by Isotope Tracer Technologies Inc. in Waterloo, Ontario. The deuterium (^2H) and ^{18}O values for groundwater samples collected across the study area fit directly on the Ottawa meteoric water line demonstrating that the isotopic composition of regional bedrock groundwaters mirrors that of precipitation (Figure 35.4). With respect to the individual water isotopes, the range of ^{18}O values across the study area are between -13.14 and -10.32 ‰ Vienna Standard Mean Ocean Water (VSMOW). This range of values is only slightly more depleted than that reported by Fritz et al. (1987) who described ^{18}O levels in shallow groundwater ranging between -9 and -12 ‰ VSMOW.

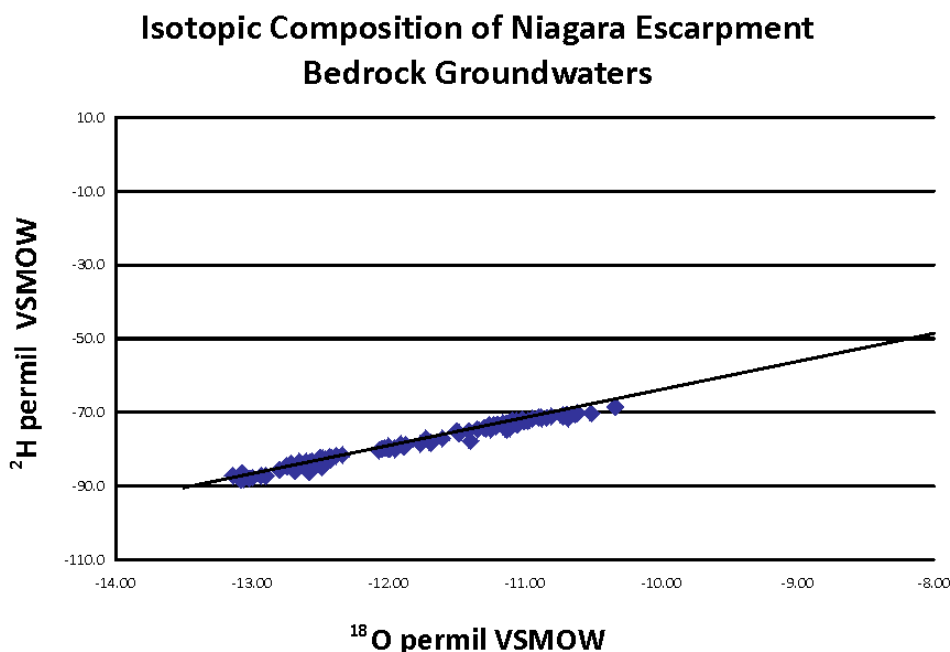


Figure 35.4. Oxygen-18 (^{18}O ‰ VSMOW (per mil Vienna standard mean ocean water)) and deuterium (^2H ‰ VSMOW) values are compared with those of Ottawa precipitation (Ottawa meteoric water line (OMWL) from Fritz et al. 1987).

Depletion in ^{18}O attributed to glacial-age recharge has been observed by others in groundwater at several North American locations, with values ranging from -14 to -17 ‰ VSMOW and water ages estimated to be older than 10 000 years (Desaulniers, Cherry and Fritz 1981; Remenda, Cherry and Edwards 1994). To evaluate whether the observed ^{18}O depletion in the study area groundwaters can be attributed to glacial recharge, or variability in the isotopic composition of local modern recharge across the study area, ^{18}O values were plotted against tritium (enriched; ^3H). An ^{18}O depletion resulting from glacial water input would not carry a relatively modern tritium signature. Figure 35.5 demonstrates the absence of a correlation between tritium values and ^{18}O values; in fact, even some of the most depleted waters carry a tritium signature. As such, the ^{18}O depletion observed at many locations across the study area is the result of the isotopic signature of local recharge.

Deuterium excess across the study area ranges from 13.39 to 18.05‰ VSMOW with a mean of 16.06‰ VSMOW and a standard deviation of 0.95. These values are higher than yearly averages reported for both Ottawa and Simcoe, Ontario, though they fall within the winter range of 12.8 to 25.9‰ VSMOW reported for Ottawa (Fritz et al. 1987) indicating that recharge in the study area is likely derived primarily from snowmelt.

Groundwater samples analyzed for enriched tritium were collected in the summer of 2011. Samples were analyzed by Isotope Tracer Technologies Inc., Waterloo, Ontario, to a detection limit of 0.8 tritium units (TU). Although it is not possible to estimate an absolute water age using tritium alone, its presence can still provide insight into how young and active a flow system is. Assuming closed-system conditions and plug flow, decay calculations using tritium values for Ottawa precipitation (International Atomic Energy Association 2007) indicate that samples with tritium values greater than 30 TU likely contain considerable recharge from the 1960s and 1970s when the peak of tritium from surface nuclear testing was observed. Samples with tritium values less than the 0.8 TU detection limit can be interpreted to have been recharged prior to 1953, when tritium from nuclear testing was starting to be observed in Ottawa precipitation. The annual average tritium level in Ottawa precipitation for 2007, the most recent data available, is 17.6 TU (International Atomic Energy Association 2007).

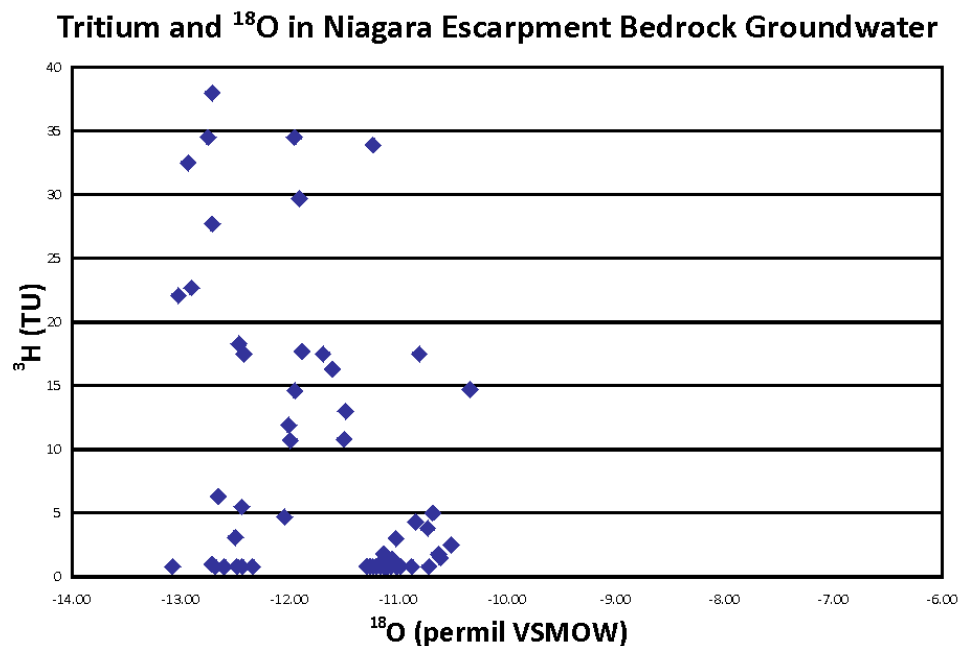


Figure 35.5. Oxygen-18 (^{18}O ‰ VSMOW (per mil Vienna standard mean ocean water)) are compared with tritium (^3H , tritium units (TU)) values to evaluate whether ^{18}O depletion is related to glacial recharge or a seasonal bias resulting from recharge patterns.

Comparing tritium levels with sample-port depth provides a preliminary view of how well connected the bedrock aquifers across the study area are to meteoric water. Figure 35.6 illustrates that many ports, regardless of depth, yield waters that were recharged prior to 1953. Signature waters, containing peak tritium from nuclear testing, appear to penetrate to 70 m into rock at several locations, and mixed waters penetrate all strata. These data provide insight into the variability of recharge patterns across the study area, and the utility of understanding geological control on the hydrologic cycle. Some of the key geological controls include glacial history and subsequent overburden permeability, short-circuiting of groundwaters in bedrock through penetrative joints and regional stress field release features (especially in the region near the cuesta scarp) and temporal karstic features associated with sequence stratigraphic architecture.

The field water-quality parameters collected at each sampling port included pH, oxidation–reduction potential (ORP), dissolved oxygen, electrical conductivity and temperature. Similar to the results of the isotope data, variability in recharge patterns is also interpreted from the dissolved oxygen values across the study area. The pattern of dissolved oxygen results are similar to that of tritium, in that the presence of dissolved oxygen was observed at some of the deepest ports at several wells; however, samples from many wells showed reducing conditions at all ports regardless of depth. The range of electrical conductivity values observed between sampling ports at individual wells showed great variability, with values differing by up to 6 times between sampling ports, likely resulting from distinct flow zones. Variability in water levels between sampling ports also indicate the presence of hydraulic separation between these zones of differing electrical conductivity.

SUMMARY AND FUTURE WORK

Air coupled transducer system issues are expected to be resolved by spring of 2013. Alkalinity testing and interpretation have been revised to reflect the laboratory work completed during the summer of 2012. A total of 160 samples were collected from 12 wells installed with the Water FLUTE™ system during the 2011–2012 field seasons. Field parameters and isotopes were the only data available for review at the time of this publication. Water isotope values demonstrate that the groundwater across the

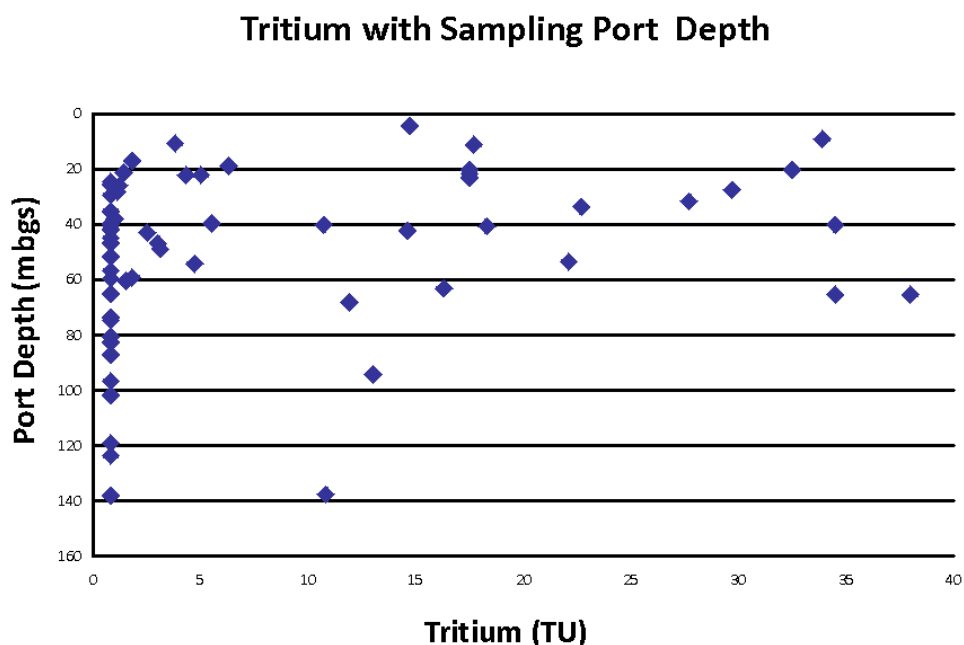


Figure 35.6. Tritium (^3H , tritium units (TU)) values are compared with sampling port depth (mbgs, metres below ground surface).

escarpment carries a meteoric water signature, indicating the absence of glacial age recharge. Deuterium excess values indicate that the primary recharge source is likely from snowmelt. Tritium numbers show pre-1953, peak and younger recharge across the study area with no trend in relative water age with depth. Conductivity values highlight the presence of distinct hydrochemical zones between sampling ports at many wells. Hydraulic head data show great variability in the direction and magnitude of vertical gradients at the wells. An understanding of geologic control on vertical connection between port zones will assist in future interpretation of both hydraulic head and chemistry data.

Future work in the Niagara Escarpment study area will focus on the development of a conceptual hydrogeological model and, ultimately, the delineation of HGUs. Although vertical gradients, hydraulic properties and chemistry at each well provide an indication of the presence of discrete flow zones, the lateral continuity and connection between these zones for the mapping of HGUs is yet to be characterized. Hydrochemical and water-level variability at each well, and additional available wells within the study area, are being gathered and evaluated relative to the regional bedrock topography and geological controls (sequence stratigraphic framework and karstic features) for the Early Silurian strata of eastern Michigan Basin of the Niagara Escarpment cuesta.

This multidisciplinary approach to regional groundwater mapping is the first of its kind in Ontario. Prior to the initiation of this project, regional groundwater flow in bedrock aquifers has remained uncharacterized. This contrasts greatly with the amount of work that has been done to understand the overlying glacial sediments and groundwater flow that comprise overburden aquifers in the province. Well-characterized bedrock aquifer systems in the Province can be protected and managed in the face of possible water shortages, climate change, population growth and development. Therefore, it is anticipated that this regional bedrock groundwater mapping project will provide an excellent baseline for informing and empowering water managers across the province.

REFERENCES

- Brett, C.E., Tepper, D.H., Goodman, W.M., LoDuca, S.T. and Eckert, B.Y. 1995. Revised stratigraphy and correlations of the Niagaran provincial series (Medina, Clinton, and Lockport Groups) in the type area of western New York; United States Geological Survey, Bulletin 2086, 66p.
- Brunton, F.R. 2009. Update of revisions to the Early Silurian stratigraphy of the Niagara Escarpment: integration of sequence stratigraphy, sedimentology and hydrogeology to delineate hydrogeologic units; *in* Summary of Field Work and Other Activities 2009, Ontario Geological Survey, Open File Report 6240, p.25-1 to 25-20.
- Brunton, F.R., Belanger, D., DiBiase, S., Yungwirth, G. and Boonstra, G. 2007. Caprock carbonate stratigraphy and bedrock aquifer character of the Niagara Escarpment – City of Guelph Region, southern Ontario; *in* Proceedings of the 60th Canadian Geotechnical Conference and the 8th joint Canadian Geotechnical Society–International Association of Hydrogeologists conference, Canadian Geotechnical Society, Ottawa, Ontario, p.371-377.
- Brunton, F.R. and Brintnell, C. 2011. Final update of Early Silurian stratigraphy of the Niagara Escarpment and correlation with subsurface units across south western Ontario and the Great Lakes Basin; *in* Summary of Field Work and Other Activities 2011, Ontario Geological Survey, Open File Report 6270, p.30-1 to 30-11.
- Brunton, F.R. and Dodge, J.E.P. 2008. Karst of southern Ontario and Manitoulin Island; Ontario Geological Survey, Groundwater Resources Study No.5, 100p.
- Brunton, F.R., Priebe, E., Brintnell, C., Bingham, M. and Belanger, D. 2011. Exploring for deep bedrock groundwaters along the Niagara Escarpment cuesta of southern Ontario; abstract *in* Special Session 1 Regional and basin-scale groundwater flow systems, Geological Association of Canada–Mineralogical Association of Canada–Society of Economic Geologists, Ottawa 2011, Abstracts and Programs, v.34, p.28.

- Desaulniers, D.E., Cherry, J.A. and Fritz, P. 1981. Origin, age and movement of pore water in argillaceous Quaternary deposits at four sites in southwestern Ontario; *Journal of Hydrology*, v.50, p.231-257.
- Flexible Liner Underground Technologies Ltd. 2009. Sampling guidelines for water FLUTE systems installed after May, 2009, 8p.
- Fritz, P., Drimmie, R.J., Frape, S.K. and O'Shea, K. 1987. The isotopic composition of precipitation and groundwater in Canada; *in* Proceedings of the International Symposium on the use of isotope techniques in water resources; International Atomic Energy Agency, Vienna, Austria, p.539-550.
- Funk, G. 1979. Geology and water resources of the East and Middle Oakville Creeks IHD representative drainage basin; Ministry of the Environment, Toronto, Ontario, Water Resources Report 12, 68p.
- Hamilton, S.M. and Brauner, K. 2008. The Ambient Groundwater Geochemistry Project: Year 2; *in* Summary of Field Work and Other Activities, 2008, Ontario Geological Survey, Open File Report 6226, p.34-1 to 34-7.
- Hamilton, S.M., Brauner, K. and Mellor, K.J. 2007. The Ambient Groundwater Geochemistry Project – southwestern Ontario; *in* Summary of Field Work and Other Activities, 2007, Ontario Geological Survey, Open File Report 6213, p.23-1 to 23-5.
- Hamilton, S.M. and Freckelton, C.N. 2009. Ambient Groundwater Project: Grey–Bruce counties and area, 2009; *in* Summary of Field Work and Other Activities, 2009, Ontario Geological Survey, Open File Report 6240, p.27-1 to 27-9.
- Hamilton, S.M., Freckelton, C.N. and Mariotti, R. 2010. The Ambient Groundwater Project: completion of sampling of southwestern Ontario; *in* Summary of Field Work and Other Activities, 2010, Ontario Geological Survey, Open File Report 6260, p.34-1 to 34-4.
- Hem, J.D. 1985. Study and Interpretation of the chemical characteristics of natural water, 3rd ed.; United States Geological Survey, Water Supply Paper 2254, 264p.
- International Atomic Energy Association 2007. Global network of isotopes in precipitation: the GNIP database; International Atomic Energy Association, Vienna, Austria, www.iaea.org/water .[accessed October 9, 2012]
- Keller, C. 2011. FLUTE Air coupled pressure transducer design and function (a new multi level sampling system innovation); unpublished internal publication, Flexible Liner Underground Technologies, Ltd.
- Lee, V.L., Priebe, E.H., Brunton, F.R., Piersol, J., Monier-Williams, M., Pendleton, B., Bingham, M., Keller, C. and Sharp, I. 2011. Bedrock aquifer mapping of Niagara Escarpment cuesta: installation and sampling of multi-level monitoring wells; *in* Summary of Field Work and Other Activities 2011, Ontario Geological Survey, Open File Report 6270, p.31-1 to 31-6.
- Remenda, V.H., Cherry, J.A. and Edwards, T.W.D. 1994. Isotopic composition of old ground water from Lake Agassiz: implications for Late Pleistocene climate; *Science*, v.266, p.1975-1978.
- Singer, S.N., Cheng, C.K. and Scafe, M.G. 2003. The hydrogeology of southern Ontario, 2nd ed.; Ministry of the Environment, Environmental Monitoring and Reporting Branch, Hydrogeology of Ontario Series (Report 1), 395p.
- Stumm, W. and Morgan, J.J. 1996. Aquatic chemistry: chemical equilibria and rates in natural waters, 3rd ed.; Wiley Interscience, New York, 1022p.
- Statistics Canada 1996. Special compilation using data from Environment Canada, Environment Accounts and Statistics Division, Ottawa, Ontario, Municipal Water Use Database, Catalogue No. 91-001.
- Thompson, M. and Howarth, R.J. 1978. A new approach to the estimation of analytical precision; *Journal of Geochemical Exploration*, v.9, p.23-30.

36. Project Unit 07-025. Description and Mitigation of Domestic Well Sampling Biases

S.M. Hamilton¹ and V.L. Lee¹

¹Earth Resources and Geoscience Mapping Section, Ontario Geological Survey

INTRODUCTION

The Ambient Groundwater Geochemistry program has the basic goal of mapping the natural chemistry of groundwater in Ontario's major aquifers (Hamilton, Brauner and Mellor 2007; Hamilton and Brauner 2008). To do this, 2 groundwater samples are collected from each "node" in a uniform 10 by 10 km grid. One sample is from a well finished in bedrock and the second from a well finished in glacial overburden materials, provided wells of each type are available in the node. With the co-operation of the owners, domestic or farm wells are sampled most often, but monitoring wells are also used occasionally. On average, this density will result in the Ambient Groundwater Geochemistry program sampling approximately 1% of the available wells in southern Ontario.

Groundwater is accessed via the existing domestic or farm plumbing systems and only untreated waters are considered for sampling. Water is purged at a high rate and a substream of the water is sent through a flow cell housing the probes of a multiparameter instrument. This measures and continuously logs pH, electrical conductivity, dissolved oxygen, temperature and oxidation–reduction potential. These readings are important parameters and hundreds of readings are logged at 5 second intervals for each parameter at each site. One reading for each parameter is recorded in the field on a sample form. However, the final discrete data that will be considered representative of that sample are determined later by choosing the most stable values from the logs for each parameter. The other reason for gathering these data in the field is to allow monitoring during purging as a way of determining when stagnant water in the plumbing system has been sufficiently removed.

The purging protocol has changed somewhat with new instruments and better understanding, but the basic principle of waiting for stable readings has been used throughout the 6 years of the program so far. After purging begins, the parameters are monitored and sample collection does not start until the parameters show reasonable stability. Temperature has proven to be the most important parameter for determining the onset of freshwater from the well. The current protocols are to wait until the absolute temperature variation on a 1 minute display screen drops to less than 0.1°C or, for cyclical readings, until temperatures on the lower part of cycle are repeated several times to 2 decimal places.

The length of purging time varies, but rarely involves less than 10 minutes and 150 L of purged water. The variable rate depends, in particular, on the size and nature of the pump and the pressure tank. Pressure tanks are installed in almost all domestic plumbing systems that utilize wells (Figure 36.1). Modern pressure tanks have a rubber membrane inside the tank that separates water from pressurized air. As the tank fills, the air above the membrane becomes increasingly compressed until the pump shut-off pressure is reached. This allows for a certain amount of water to be supplied from storage, the amount of which depends on the capacity of the tank, before the pressure drops to the pump-on pressure. The use of pressure tanks prolongs the life of pumps, saves electricity and can provide a limited amount of water, even if the well runs dry. The objective of waiting for stable readings is to ensure that either the pressure tank is fully purged or that the flow is high enough so the pump never shuts off and, therefore, water is supplied only from the well and not the tank (unless the pump pressure drops).

*Summary of Field Work and Other Activities 2012,
Ontario Geological Survey, Open File Report 6280, p.36-1 to 36-15.*

© Queen's Printer for Ontario, 2012

In all forms of groundwater sampling, measurement biases are a potential concern. Groundwater sampling and measurement of water from domestic wells has the potential to add a number of specific biases to geochemical data. These measurement biases are of less concern if they are well understood and, less still, if they are mitigated. This paper discusses known biases in domestic well sampling and describes the procedures the Ambient Groundwater Geochemistry program uses to mitigate them.

DOMESTIC WELL SAMPLING AND MEASUREMENT BIASES

Biases Related to Well Construction and Design

Of the various biases that can occur in domestic well sampling, several relate to the inherent nature and construction of domestic wells. These include

1. non-discrete capture zones in uncased open holes in bedrock or due to multiple screened zones in overburden. This can cause mixing of incompatible waters resulting in possible mineral precipitation, degassing and biofouling and a water chemistry that is unrepresentative of any of the water-bearing zones.
2. large capture zones resulting from long-term daily pumping. This can cause the movement of water, over time, from different geological units (e.g., overburden) and result in chemistry that is unrepresentative of the unit that the well is finished in. Long-distance transport is especially a possibility in bedrock where fracture-flow predominates.

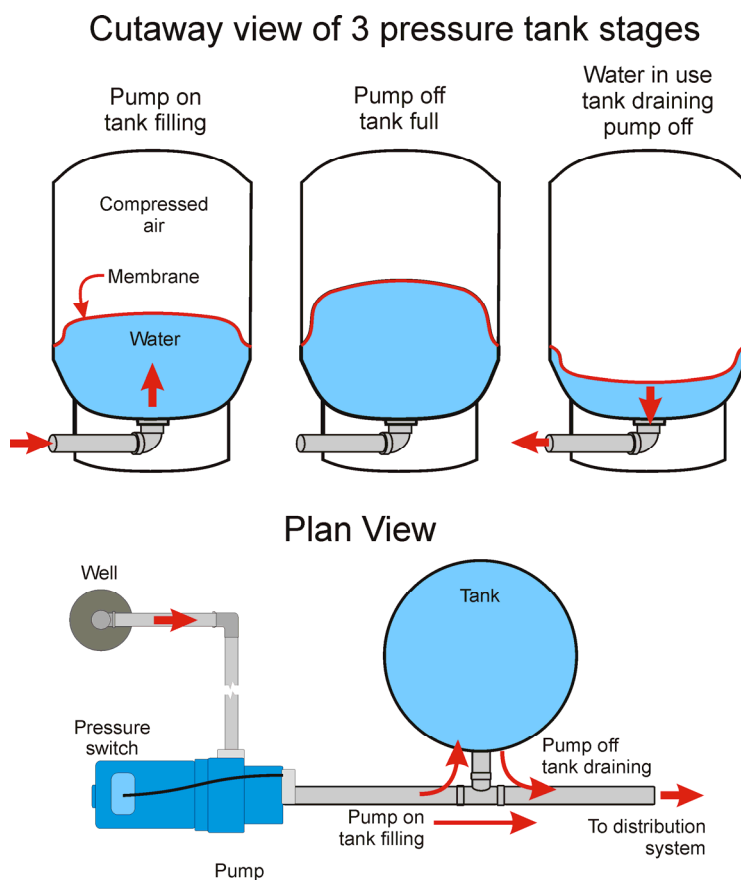


Figure 36.1. Cutaway of a modern pressure tank at 3 stages and a plan-view schematic of the tank and pump hook-up.

Both these potential biases are manageable in the case of the Ambient Groundwater Geochemistry program. Although the bedrock portion of domestic wells are largely uncased, multiple water-bearing zones are unusual and, when they occur, one zone usually predominates over another. This is because they are drilled for vigilant homeowners who are paying by the metre. When a sufficient quantity of water is encountered, the drilling usually ceases and, therefore, in most domestic wells, the main water-bearing zone often occurs near the bottom of the hole. A notable exception is where low flow is encountered and the well is drilled deeper to add storage capacity. Multiple screened intervals in overburden wells are difficult to install and rarely occur in the Ambient Groundwater Geochemistry program data set.

Large capture zones due to long-term pumping can be problematic for contaminant transport studies, but are generally an advantage for the Ambient Groundwater Geochemistry program. We are characterizing geochemistry on the geological formation and group level and these are large units with typical surface widths of many tens of kilometres. Except in cases where a sampled well is at a formation boundary, the chemistry is likely to be ideally representative of the host lithology in the vicinity of the sampling point. At the scale of the sampling, dozens of wells will be sampled in each major unit and, therefore, the few wells sampled near contact boundaries will not be significant. Drawing water down from overburden in bedrock interface wells would seem to be a potential bias, but, in fact, the opposite is true. In Ontario, groundwater from interface wells, whether in bedrock or overburden, tends to exhibit the chemistry of the underlying bedrock (Singer, Cheng and Scafe 2003). This is presumably because most of the till in the “basal till / fractured rock aquifer” is a pulverized component of the underlying bedrock and increased surface area likely results in increased dissolution of this host rock material.

However, there are other biases that can occur with sampling domestic wells that are related to the plumbing and, since these vary from site to site, it is essential to the viability of the geochemical data that they be understood and, where possible, mitigated.

Biases Related to Septic Influence

In the particular case of bored or dug wells, the capture zone is non-discrete and usually extends from surface to the bottom of the well. This makes the well a groundwater discharge zone for the shallow unconfined aquifer and, in flat areas, it is likely to be the most significant point of discharge on a domestic lot. Considering that the most significant source of recharge to the unconfined aquifer on any rural lot is likely to be the septic system, an obvious potential bias exists with these types of wells. In the Ambient Groundwater Geochemistry program data, dug and bored wells are much more likely to show elevated bacteria and nitrate levels than other well types and this is consistent with observations by others (e.g., Goss et al. 1998).

The bias due to possible septic influence cannot be mitigated, but can generally be detected with a close examination of the chemical data. Nitrate, dissolved organic carbon, bacteria, chloride, potassium and, surprisingly, rare earth elements in water together in a sample can be indicative of septic influence. It is not a primary objective of this program to characterize anthropogenic contamination, but it is important to identify it so as to not confuse it with the natural ambient signal. Since a significant proportion of dug and bored well waters show evidence of septic influence, these wells are generally avoided except where drilled overburden wells are not present in an area.

Biases Related to Water Treatment Systems

The Ambient Groundwater Geochemistry program samples only untreated water, but, nonetheless, the possibility exists for contamination by treatment systems. This can occur, for example, by back-feeding from the pressure tank if sampling is carried out at a hydrant near the well. Most treatment

systems are located after the pressure tank, making back-feeding unlikely. However aeration, chlorine and peroxide are usually applied ahead of the tank and ultraviolet light treatment may also be applied. In addition, homeowners are sometimes mistaken when they claim that a particular tap is untreated.

Biases due to water treatment are unacceptable in the Ambient Groundwater Geochemistry data set. The influence of softeners, whether they utilize NaCl or KCl, is very easily identified both in the field and later when examining the data. Since 2010, inexpensive test strips have been used to test for softened water prior to sampling; this testing prevents the accidental sampling of softened water 5 to 10 times per field season. This is consistent with the number of accidentally sampled softened waters in previous years (e.g., 6 in 2009). When this occurred in the past, the waters were resampled the following summer ahead of treatment, or if no bypass is possible, the data were removed from the data set and, where necessary, another well was found in that node to sample.

Half-a-dozen near-misses with softened water per summer is disconcerting since some other types of treatment are not so easily detected; and one might assume that undetected accidents with these systems occur at the same frequency. This is not the case because softening is far more common than other forms of treatment and because many other forms of treatment are used in conjunction with softeners. The presence of greensand iron filters, carbon filters or ultraviolet (UV) treatment is impossible to detect in the field. Fortunately, these iron filters are rarely used except in conjunction with softeners, which are quite effective at removing iron and much cheaper to operate. System-wide, as opposed to under-counter, carbon filters are vanishingly rare and only one such system was encountered in the first 6 years of this program. Ultraviolet light treatment kills bacteria, but does not otherwise compromise our results.

Deionizers, distillers, reverse osmosis, chlorine, peroxide and air-bleed iron filters can be detected in the field, but only by well-trained samplers. For new staff, a certain amount of on-the-job training is inevitable and if one of these treatments systems is encountered early in a field season, it may be missed if no experienced person is present. Deionizers, distillers and reverse osmosis can be detected by anomalously low electrical conductivity; although these are very rarely used on system-wide applications and are usually installed for kitchen use only. Chlorine is fairly commonly used on dairy farms and hydrogen peroxide is an occasional treatment to combat high H_2S (i.e., “sulphur”). Both can be detected because they give very high oxidation–reduction potential readings and can cause the alkalinity test solution to turn yellow instead of pink. Peroxide treatment for sulphur also produces a distinct smell (burnt matches) and this can be detected during the smell test.

Biases Related to Construction Materials

Drilled well casings are overwhelmingly composed of steel and distribution systems of copper, and/or brass pipes and fittings. Even the components such as black polyvinyl chloride (PVC) riser pipes and rubber seals and membranes (Hall 1998) can leach metals into water, especially when the components are new. In oxidized environments, steel well casings can rust, increasing the acidity of the water and producing an orange flocculant that can be hard to filter and which interferes with alkalinity readings. In reducing, H_2S -rich environments, the steel casing is attacked producing amorphous FeS and increasing the pH of the water. The resulting black slime on the casing is easily dislodged with pumping or during water-level measurement and can interfere with alkalinity readings and positively bias H_2S readings.

Biases due to construction materials are minimized in the Ambient Groundwater Geochemistry program by the philosophy of maximum purging. The leaching and chemical processes that cause material-related biases are slow and are most likely to affect stagnant water. Purging a large volume of water at a high rate removes the stagnant water and minimizes the effects of biasing processes on the chemistry of the water. This large amount of purging often surprises well owners, but they are generally accepting of it when the reasons are explained. Since a small number of low-yield wells cannot produce

the approximately 25 L per minute flow rate at which purging is typically done, the first question well owners are asked in the interview is if they have ever had quantity problems. If they have, the flow is scaled back, the overall quantity is reduced to about 100 L and the flow is further restricted during sampling to the minimum quantity required to purge the flow-cell and fill the sample bottles.

Domestic wells that are in service have a natural advantage in preventing biases due to construction materials because they are constantly in use. Domestic well plumbing systems can supply up to 50 000 L per day and many dwellings use a substantial fraction of this. Our additional purging of several hundred litres is a precaution that is likely not necessary in many cases.

Biases Related to Pressure Tank Design

Modern pressure tanks, like the one shown in Figure 36.1, store less than half of their rated capacity; the remainder of which is compressed air. Most of the stored water drains during the pump-off part of the cycle and, each time the pump turns on, the remaining component is successively diluted with a larger component of freshwater. This leads to rapid cleansing of stagnant water from the plumbing system. An older design, referred to here as “flow-through” tanks (Figure 36.2), has the inlet and outlet on opposite sides of the tank. These tanks have no internal membrane and the cushion of air that is compressed during the pumping cycles eventually dissolves into the water and must be maintained with periodic (e.g., bi-yearly) manual addition of compressed air. However, this is often not done; leading, over time, to a large water–air ratio in the tank, very short pump cycles and decreased pump life. Since these tanks rarely have “bypass” valves on the upstream side of the tank, the water must be discharged for very long periods to obtain freshwater from the well.

The only strategy for mitigating the effects of flow-through tanks is long-term purging. Figure 36.3 shows the temperature curves for 3 plumbing configurations. Not shown are curves where the water is pumped directly from the well or where there is no tank or only an in-line tank, since none of these configurations store a significant amount of water. Figure 36.3 shows that flow-through tanks take far longer than standard tanks to fully purge and none of the temperature curves has ceased dropping by the end of measurements. When water is taken from a hydrant by the well (Photo 36.1), curves are similar to those of standard tanks because they are connected to the main water supply line with a T-junction. Hydrants must always be located after the pump and, therefore, only submersible pumps and never suction or jet pumps can supply a well-side hydrant. Hydrants located elsewhere on the property are often fed by a separate line from the pressure tank and, if so, their temperature curves would be controlled by the tank type like any other faucet.

Cycling is also apparent in one of the flow-through tank curves, but is more gradual due to partial mixing of the freshwater with older water in the tank during the pump-on and pump-off phases.

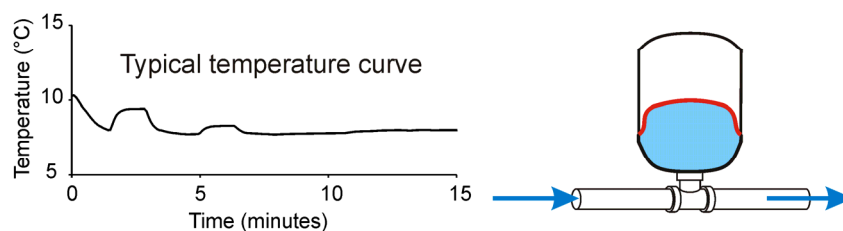
One each of the hydrant and standard tank curves shows cyclical drops in temperature punctuated by increases that decline over time. These are the pumping and tank phases, respectively, on systems with high-capacity pumps that are strong enough to supply the required purging stream and refill the tank simultaneously. The decline in the high phases shows the progress of the tank flushing, but it should be noted that the low-phase temperature equilibrates much sooner. This provides a stable temperature that we consider to be representative of the groundwater at that site.

All but one of the other curves for hydrants and standard tanks are flat, demonstrating that either

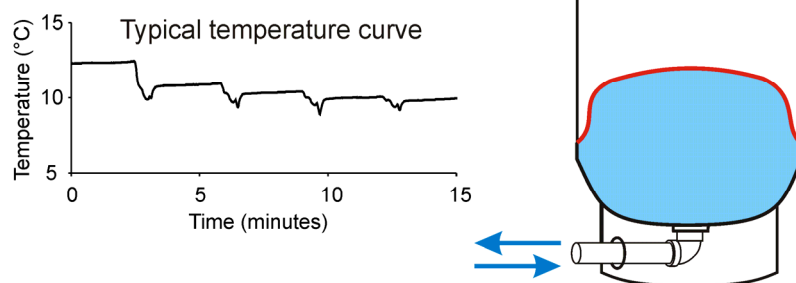
1. the purging stream is flowing at a rate that is equal to or greater than the capacity of the pump and, therefore, no water comes from the tank; or
2. the tank has been completely flushed and has the same ambient temperature as the groundwater

Both these scenarios are desirable for sample representivity. An anomaly in the hydrant curves is the curve at the bottom showing perpetual on-off cycles. This is pump cycling resulting either from an incorrectly adjusted high–low pressure range on the pressure switch or more likely from a flow-through tank that has no cushion of air left to store pressure. The pump provides water from the well at a rate that exceeds the purging rate, the pressure rises in the tank and the pump shuts off almost immediately, causing backflow from the tank along the long pipe to the hydrant. Without the air cushion, the pressure drops rapidly and only a small portion of tank water makes it back to the hydrant before the pump turns on again. Hardly any purging of the tank occurs and so the upper temperature limit never drops. The lower limit, however, is representative of the ambient groundwater temperature.

In-line tank (effectively no storage)



Standard tank (T-junction)



Flow-through tank without membrane

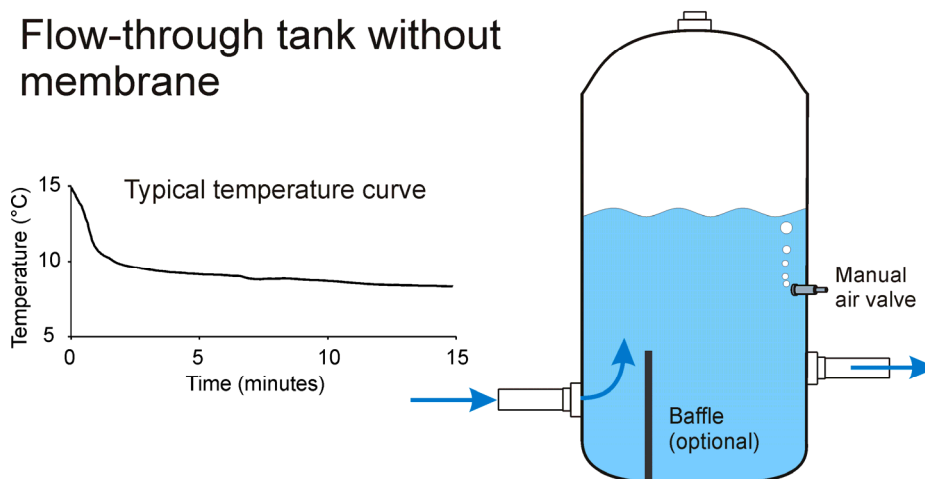


Figure 36.2. Three types of pressure tanks and typical temperature logs for each. Temperature is measured while purging the system at a point in the plumbing beyond the tank.

The lesson, illustrated in Figure 36.3, is that, at a minimum, flow-through tanks must be purged for 20 minutes. After this time, the temperature indicates the vast majority of water in the tank is fresh and should yield an acceptable geochemical sample. However, fully stable temperature readings may require between 30 and 60 minutes of purging, which is unacceptable both in terms of sample cost and inconvenience to the homeowner. Furthermore, temperature readings after flow-through tanks may never

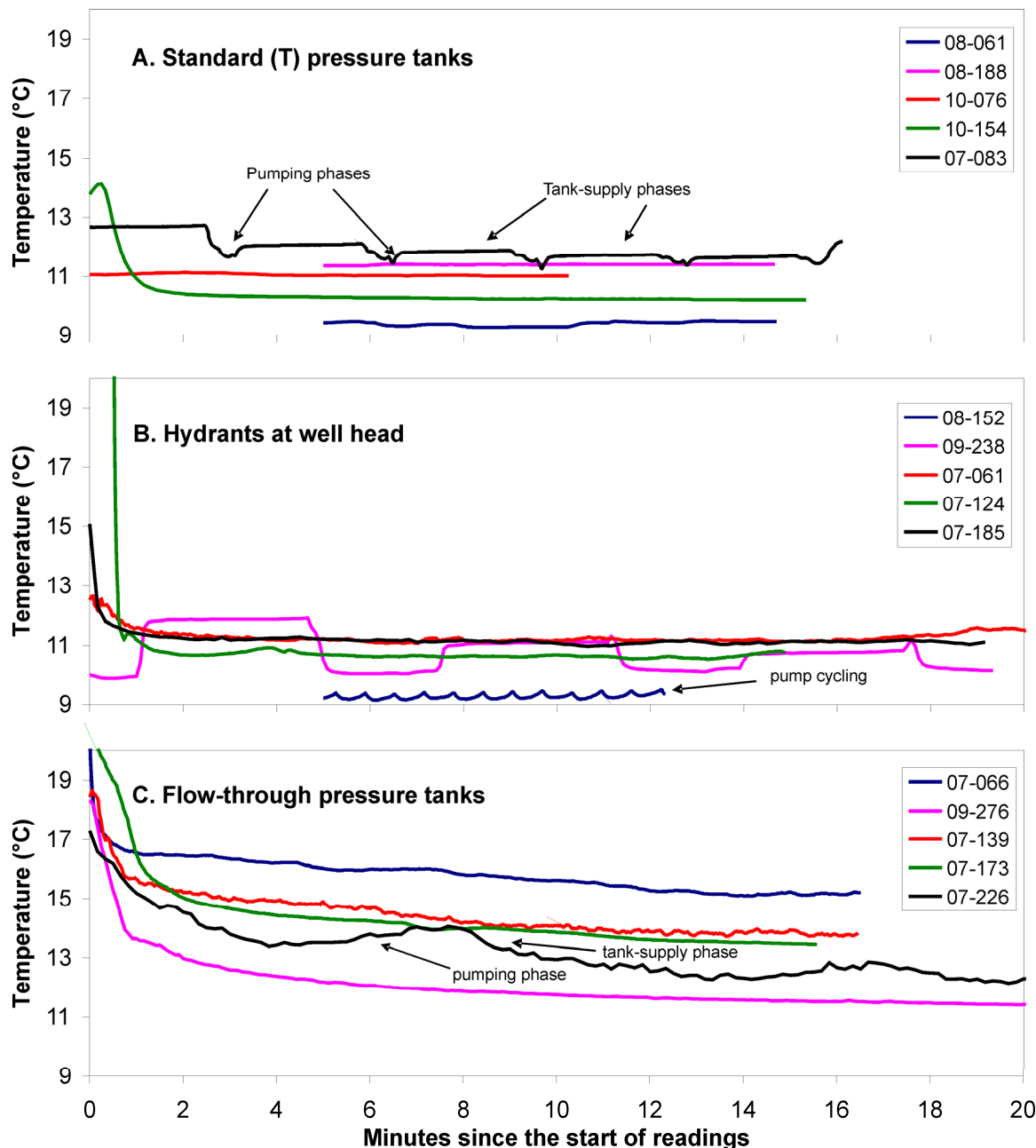


Figure 36.3. Temperature logs for 3 types of plumbing configurations. A) Standard tanks with a T-junction are most common. B) Hydrants near the wellhead produce similar curves because they are connected with a T-junction ahead of the pressure tank. C) Flow-through tanks are an older design and usually do not have pressure membranes. Note that the temperature equilibrates more quickly during the pumping phase than the tank-supply stage. The other curves show no obvious pump cycles, demonstrating that either the water in the tank is fully flushed or that the flow from the purging stream has matched the capacity of the pump and, therefore, no water comes from the tank. Temperature was determined on surface with a multiparameter instrument in a flow cell. The distance of the sampling point from the well varies.

have comparable temperature representivity as standard tanks because of radiative gains in heat as the water swirls inside the tank. As such, temperature from flow-through tanks probably cannot ever be directly compared with temperature from standard tanks or with that derived from direct pumping of the well.

ASSESSING TEMPERATURE REPRESENTIVITY

Temperature is a very important parameter for assessing when the purging stream becomes representative of freshwater from the well. Field monitoring of the temperature and other parameters and later assessment of the field parameter logs has provided assurance that the geochemical samples collected are representative of ambient groundwater at almost all sites sampled. The field protocol of waiting for near stability of temperature readings is suitable for all plumbing arrangements, even flow-through tanks, although the latter require longer purging times.

In addition to this important use of temperature data, the distribution of actual groundwater temperatures across the study area has intrinsic value of its own. Early plots of the temperature readings for the Ambient Groundwater Geochemistry program used final temperatures for any logs that showed stable readings. The plots (e.g., Figure 36.4) showed distinct patterns related to geological and topographic conditions and latitude. There were some other patterns that were of interest because they could not easily be explained. One of these was a broad anomaly north of Lake Erie, extending from St. Thomas in the east to Essex County in the west, with its highest magnitude expression around the City of Chatham.

Temperature anomalies in groundwater have potential economic significance and environmental benefit because of the possibility of geothermal exploitation. Field checking of these anomalies was, therefore, prudent and a program was set up to re-test the water and examine the plumbing to determine if any other factors might be influencing the end-of-line temperatures that were observed. In particular, we requested homeowners to allow us to see and photograph their pressure tank, since it is known to have the greatest effect on temperature of any of the plumbing components.



Photo 36.1. A well-side hydrant. Hydrants can be used year round because the pipes automatically drain into a gravel bed below the frost line when the valve is closed.

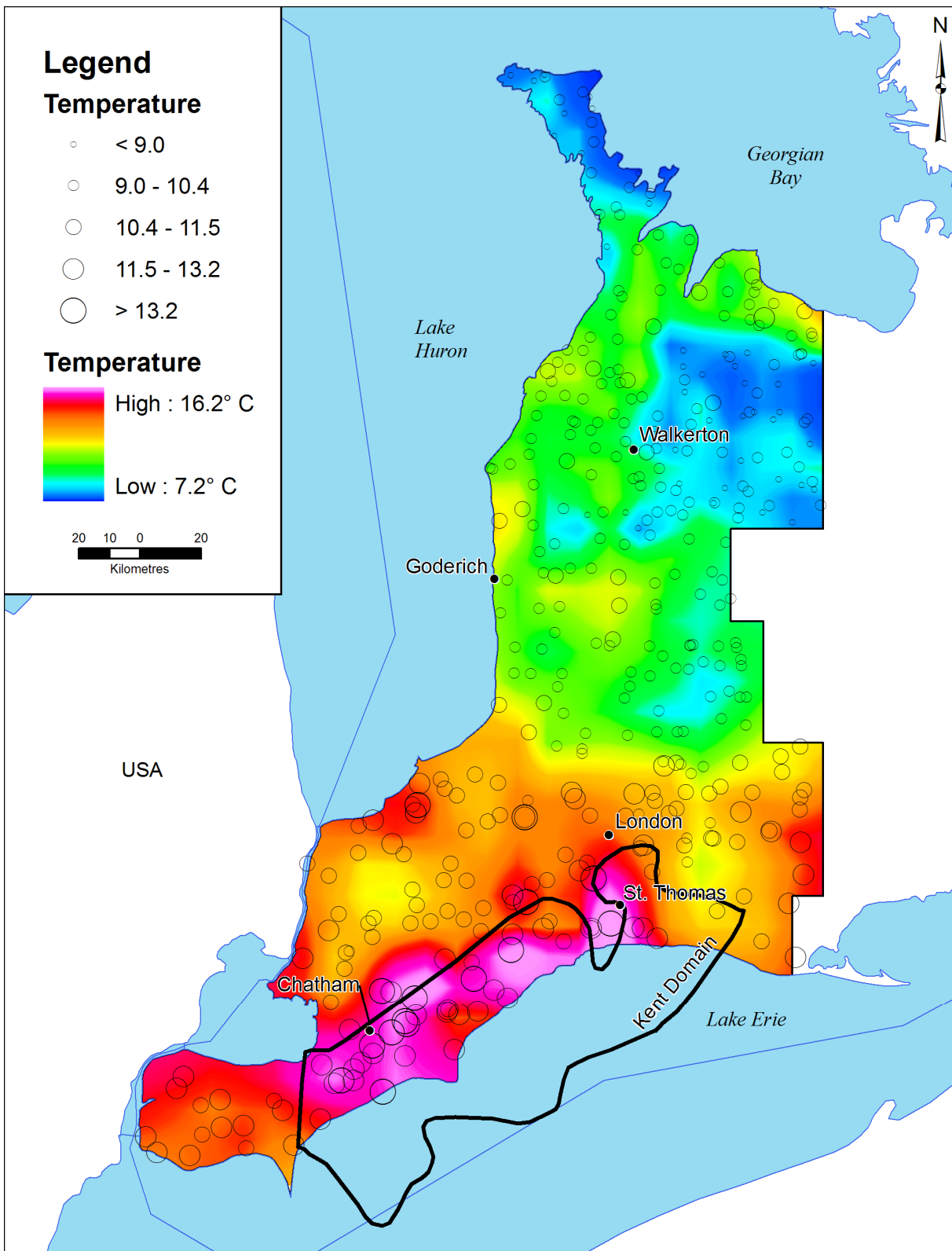


Figure 36.4. Groundwater temperature of drilled wells using all sites that exhibited stable or near-stable temperature logs (from Hamilton and Freckleton 1999).

The program was carried out in October of 2011, during which a number of Ambient Groundwater Geochemistry sites in and around the known anomaly were re-visited. In total, 16 former stations were selected in such a way to test many of the higher temperature sites, but also to test a selection from outside the anomaly to determine if the observed temperature contrast still exists, even if seasonal or other regional changes have occurred. After checking the plumbing, the water was purged and temperature logs collected for a much longer period of time than during the original sampling. In most cases, the flowing water was logged for more than 30 minutes.

The results showed there are an unusually high number of flow-through tanks in this area. Over the 6 year program, we estimate that less than 20% of plumbing systems have tanks that are of the flow-through type. In the resampled wells, almost all of the high-temperature sites had flow-through tanks. Once this became apparent, a re-assessment of all the logs collected from 2007 to 2010 was carried out to determine if there were regional patterns in plumbing that might be adding biases to the temperature plot. Based on the shape of the temperature curves, each station was classified as flow-through, standard-T, possible-standard-T or unknown. Well-side hydrants were considered to be the same as standard-T tanks regardless of the nature of the tank. Unknowns occurred because of missing or very unstable logs. Once the exercise was complete, the results were tested by examining field photographs in the approximately 10% of cases where we had actual photographs of the tanks. The photos showed that examining the curve shape is an effective way of predicting tank type.

The result of the tank assessment shows that there are indeed regional patterns to plumbing, with the area around Chatham having a disproportionate number of flow-through tanks (Figure 36.5). This is not due to older infrastructure in this area because a plot of pump types (Figure 36.6) shows no difference in this area in the expected dispersal pattern of pump-types, that is, no unusual accumulation of older suction or jet pumps here. Here and elsewhere in southwestern Ontario, pump types follow a pattern related to the depth to the water level. Although modern submersible pumps occur everywhere, older suction pumps occur often in areas of very shallow water table (<10 m), whereas jet pumps occur mostly in areas of shallow to intermediate water table depth (<40 m). In areas of deeper water level, submersible pumps are used almost exclusively.

At first, the accumulation of flow-through tanks in this area was perplexing. However, the area around Chatham and to the northeast is a known area of natural gas (i.e., methane: CH₄) in well water. By comparing the field notes with the results from the temperature curve assessment, it was determined that most of the wells in this area that were recorded to have significant amount of gas also have flow-through tanks. Natural gas concentration was measured as part of the Ambient Groundwater Geochemistry program and Figure 36.5 shows the areas where the *in situ* (i.e., in the ground) CH₄ saturation level exceeds 10%. Inside these areas, 65% of plumbing systems use flow-through tanks in comparison to only 21% in the rest of the study area. It appears that one of the major disadvantages of flow-through tanks does not apply in this area. Free gas is often pumped up with groundwater in this area and, since the in-tank pressure of 40 to 50 pounds per square inch (PSI) would often be lower than the in-ground pressure, gas would also exsolve in the tank. This will prevent the need to pump an air cushion and eliminate one of the advantages of modern tanks. Furthermore, modern tanks with a membrane would actually be a disadvantage because the membrane unnecessarily prevents storage in more than half the tank and, because the water outlet is at the bottom, allowing gas to entirely fill the tank, thereby degrading its water storage capacity.

Figure 36.7 shows a re-plotting of the temperature across southwestern Ontario. Preliminary data from the 2011 study area north of Toronto are also shown. Only results where the curves are stable are shown and all known or suspected flow-through tanks have been removed. The data have been corrected for the averaged radiative temperature gain in standard tank systems of 0.83°C (Hamilton and Freckelton 2009). The temperature gain where the water is pumped directly from the well is not known, but must occur due to pump heating and heat gain in the pipes and flow-cell. For plotting purposes, we have used an arbitrary estimate of 0.2°C for the small percentage of wells that were directly pumped.

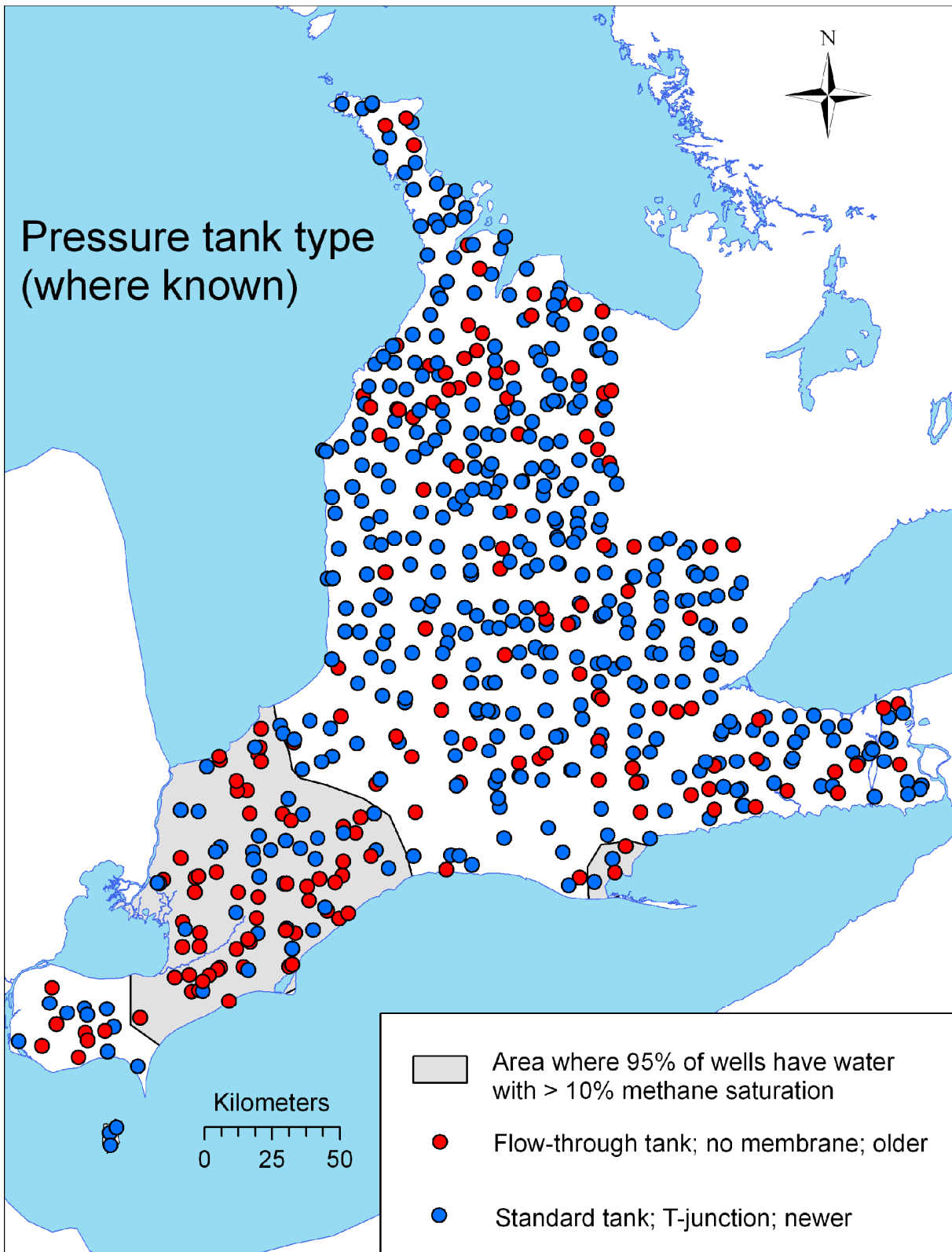


Figure 36.5. The distribution of modern standard and older flow-through pressure tanks based on the shape of the temperature curve. Unknown tank types are not shown. Note the 3 times greater usage of flow-through tanks in areas where gas (i.e., methane) occurs naturally in groundwater.

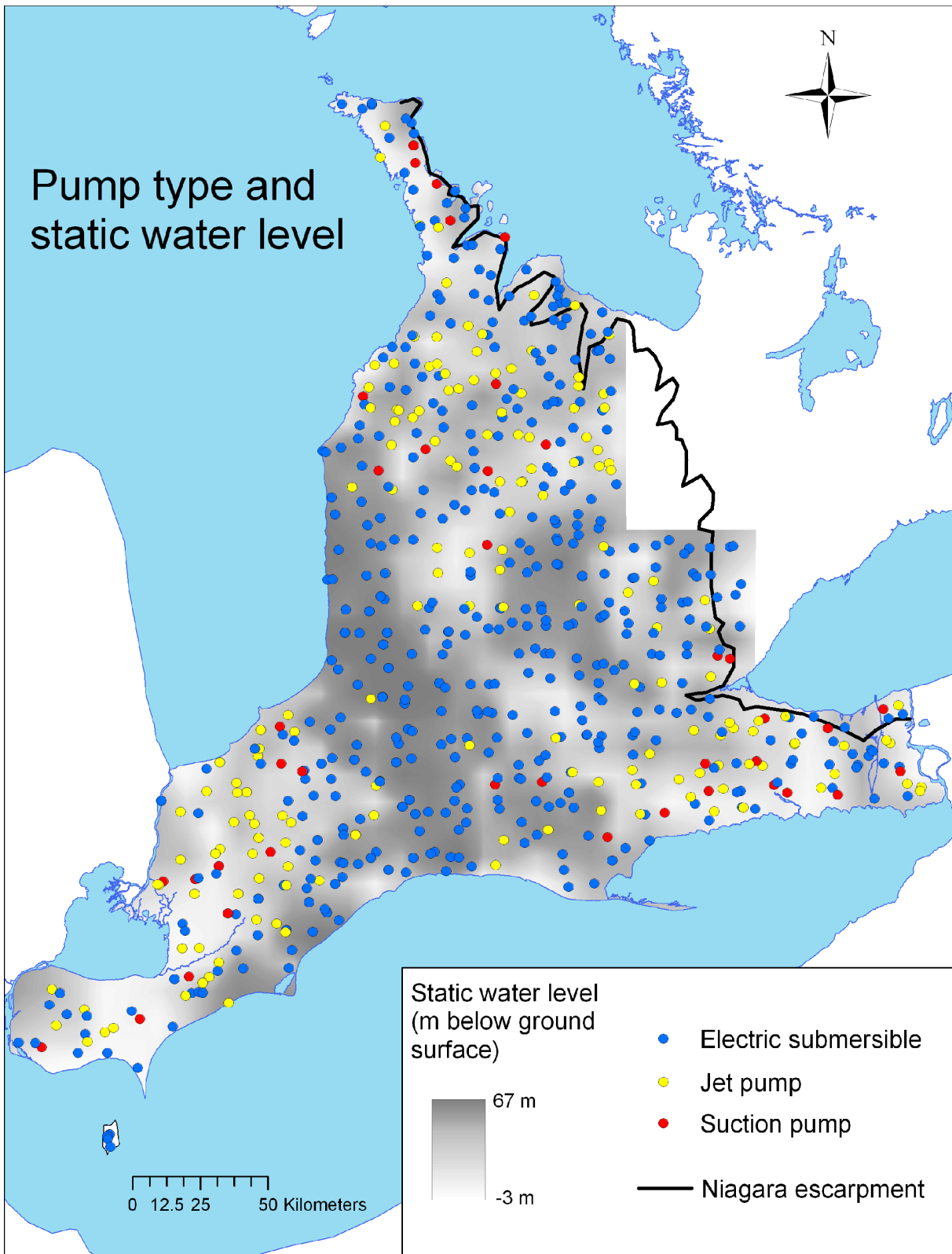


Figure 36.6. Distribution of the 3 dominant pump types. Although modern submersible pumps are used almost everywhere, jet pumps and suction pumps are used where the depth of the water table allows. There is no evidence of older infrastructure in the same area where flow-through tanks are common (see Figure 36.5).

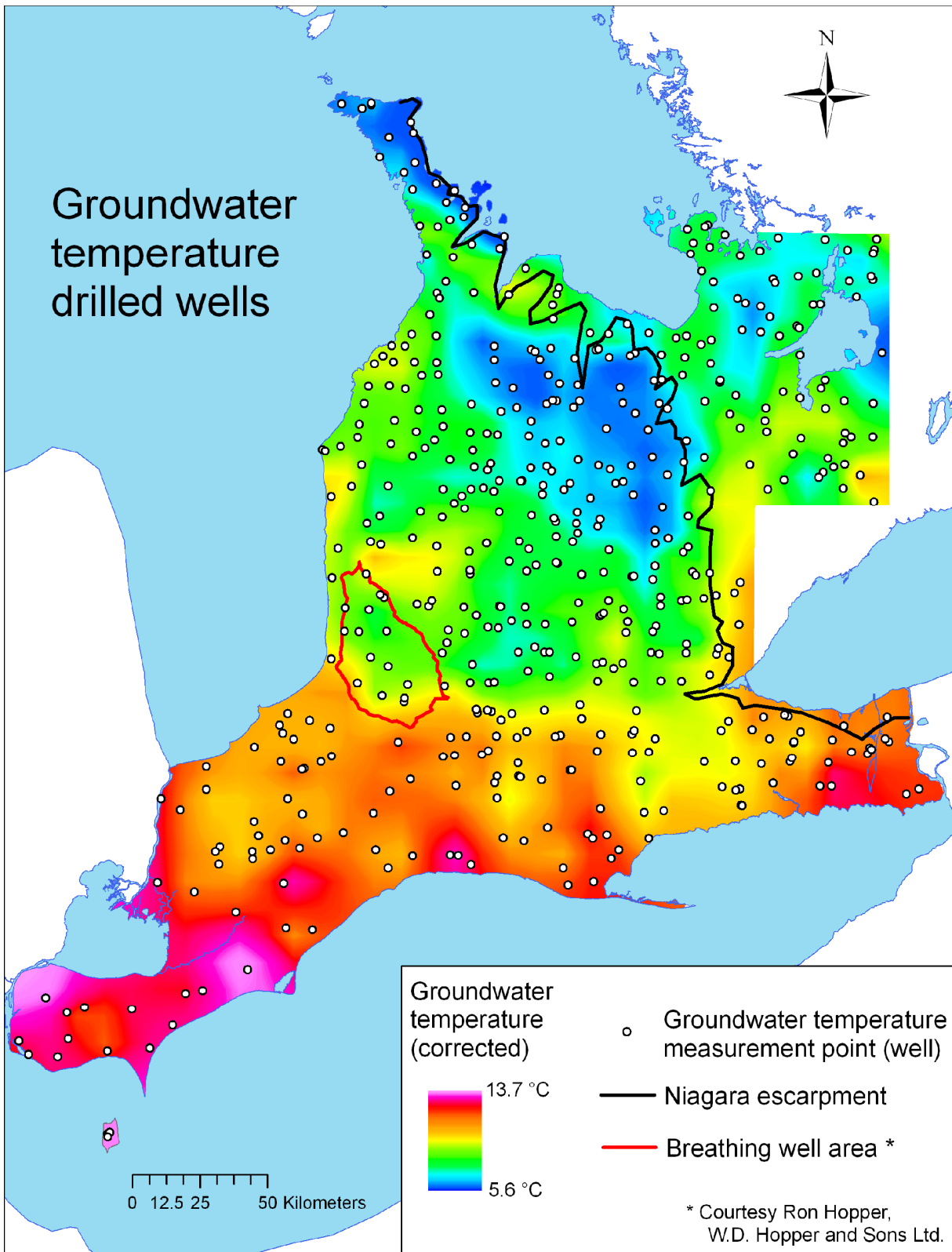


Figure 36.7. Groundwater temperatures corrected for estimated radiative gain in distribution systems. Data were only used from systems where the water was pumped directly from the well or where they were estimated to have standard pressure tanks based on the shape of the temperature curve.

Most of Figure 36.7 shows similar results to the earlier plot (*see* Figure 36.4) including the temperature low above the northern half of the Niagara Escarpment and the latitudinal gradient. The exception is the anomalous area near Lake Erie, which shows a lower magnitude and a different shape, but still exists. However, the large number of flow-through wells in this area has decreased the sample density and, consequently, the reliability of this result. The overall temperature range has changed. The warmest groundwater in the province, not surprisingly, is on Pelee Island, which shows an average temperature of about 13°C. The coldest, so far, is on the eastern side of the northern Bruce Peninsula, with a typical temperature of less than 6°C. These latter waters may be influenced by a direct connection with Georgian Bay surface waters.

CONCLUSIONS

In most cases, the biases related to the sampling of domestic wells are either manageable or can be mitigated by sufficient purging of the system. To assess if the system has been sufficiently purged, dissolved oxygen, conductivity, pH and oxidation–reduction potential are useful, but temperature is the most instructive parameter. Our protocols use a loose rule that the temperature change or fluctuations over a 1 minute time period must drop to less than 0.1°C, or alternatively when readings are cyclical, the same lower temperature must be repeated several times. The rule is loose because on low-yield wells, it cannot be adhered to. The normal protocol takes between 10 and 15 minutes, purging at 20 to 25 L per minute. However, the nature of the pressure tank can greatly affect the length of time required to purge. Flow-through tanks encompass less than 20% of all tanks, but, when encountered, can take 20 minutes or more to fully purge using the standard criteria.

The distribution of groundwater temperature across southern Ontario has been revised from earlier estimates (e.g., Hamilton and Freckelton 2009). Temperature logs were examined and assessed as being influenced by flow-through tanks (i.e., old), standard membrane tanks (i.e., new) or unknown configurations. Our ability to separate tank types based on the shape of the temperature curve is good, based on crosschecking with the few photos of tanks that had been taken at the time of sampling. In the final plot, temperatures were only used from known or probable T-junction tanks or from logs where the well had been directly pumped. The result shows that the originally identified temperature anomalies between St. Thomas and particularly around Chatham are still present, although their magnitude and configuration has changed. The sample density has greatly decreased because of an unusual accumulation of flow-through tanks in this region, which also reduces the reliability of the temperature assessment. The presence of natural gas (i.e., methane: CH₄) in the water is the presumed cause of the clustering of flow-through tanks, because, in gas-rich waters, this type of tank is advantageous over modern membrane tanks.

It is unlikely that better temperature resolution can be obtained using the Ambient Groundwater Geochemistry data. Variations in the length of plumbing and the distance between the well and the sampling point also contribute to temperature changes and these factors are not quantifiable with the existing data. The amount that these and other factors affect absolute temperatures cannot be determined, but, based on down-hole testing and empirical observation, it is likely to be less than 1°C. Ideally temperature should be measured *in situ*, but this would be very difficult, since many of the wells are buried or have sanitary seals that cannot easily be removed. A better approach might be to obtain lower density but higher quality temperature data from other sources to further investigate the groundwater temperature distribution. For example, the Provincial Groundwater Monitoring Network has wells in this area to monitor chemical and water-levels changes. All the water-levels loggers are equipped with extremely accurate temperature sensors and these data are recorded alongside the water-level data. Although the Ministry of the Environment does not publish the temperature data, they must exist and could be utilized to further investigate this phenomenon.

REFERENCES

- Goss, M.J., Barry, D.A.J. and Rudolph, D.L. 1998. Contamination in Ontario farmstead domestic wells and its association with agriculture. 1. Results from drinking water wells; *Journal of Contaminant Hydrology*, v.32, p.267-293.
- Hall, G.E.M. 1998. Cost-effective protocols for the collection, filtration and preservation of surface waters for detection of metals and metalloids at ppb ($\mu\text{g L}^{-1}$) and ppt (ng L^{-1}) levels; Aquatic Effects Technology Evaluation Program (Task Force on Water Quality Issues), CANMET, Natural Resources Canada, Ottawa, Ontario, AETE Project 3.1.3, 57p. plus appendices.
- Hamilton, S.M. and Brauner, K. 2008. The Ambient Groundwater Geochemistry Project: Year 2; *in* Summary of Field Work and Other Activities 2008, Ontario Geological Survey, Open File Report 6226, p.34-1 to 34-7.
- Hamilton, S.M., Brauner, K. and Mellor, K.J. 2007. The Ambient Groundwater Geochemistry Project – southwestern Ontario; *in* Summary of Field Work and Other Activities 2007, Ontario Geological Survey, Open File Report 6213, p.23-1 to 23-5.
- Hamilton, S.M. and Freckleton, C.N. 2009. Ambient Groundwater Project: Grey–Bruce counties and area, 2009; *in* Summary of Field Work and Other Activities 2009, Ontario Geological Survey, Open File Report 6240, p.27-1 to 27-9.
- Singer, S.N., Cheng, C.K. and Scafe, M.G. 2003. The hydrogeology of southern Ontario, 2nd ed.; Ministry of the Environment, Environmental Monitoring and Reporting Branch, Hydrogeology of Ontario Series (Report 1), 395p.

37. Project Unit 07-025. Ambient Groundwater Geochemistry Project of the Ottawa–St. Lawrence River Area

C.N. Freckelton¹ and S.M. Hamilton¹

¹Earth Resources and Geoscience Mapping Section, Ontario Geological Survey

INTRODUCTION

Groundwater geochemical samples were collected in an area between the Ottawa and St. Lawrence Rivers (Figure 37.1) as a part of the multiyear Ambient Groundwater Geochemistry Program. The primary objective of this program is to map the baseline geochemical conditions in groundwater across Ontario, using a wide variety of parameters at a consistent scale and high standard of quality. Groundwater is a very important source of fresh water throughout the province, and plays an important role in domestic, municipal and agricultural sectors. It is, therefore, important to know the processes controlling groundwater chemistry.

The results from the first 4 years of study (2007 to 2010), encompassing all of southwestern Ontario, were released in the summer of 2011 as Miscellaneous Release—Data 283 (Hamilton 2011). The 2011 field season covered the Aurora–Orillia area (excluding Lake Simcoe), which extended from the boundary of urban Toronto northward to Port Severn and from approximately Collingwood east to Beaverton (Hamilton et al. 2011).

STUDY AREA

The 2012 study area is located in the St. Lawrence Platform, and is bound by the Ottawa River and the St. Lawrence River to the north and south, respectively. The eastern boundary is the Ontario–Quebec provincial border and the area extends west to the Town of Perth (*see* Figure 37.1). The study area encompasses approximately 12 500 km² and is in the physiographic region of the St. Lawrence Lowland.

The underlying bedrock comprises Cambrian–Ordovician sedimentary units that unconformably overlie crystalline Precambrian rocks. In the western portion of the study area, the Precambrian basement rocks subcrop in the many areas where the Paleozoic bedrock is absent. The Paleozoic sedimentary strata are generally flat lying and have comparatively uniform thickness, resulting from deposition on a tectonically stable, shallow shelf, largely unaffected by Paleozoic orogenic events (Johnson et al. 1992). Block faulting, a result of the Atlantic Ocean opening during the Late Mesozoic, exists in the northern part of the study area along the Ottawa River (Johnson et al. 1992). Consequently, bedding is subhorizontal except in close proximity to fault zones, where steeply dipping normal faults with up to 1000 m of vertical displacement have been determined (Johnson et al. 1992).

The overlying Quaternary sediments are thin toward the western edge of the study area, making overburden wells hard to find. Glacial sediments are more prevalent in the central to westward part of the study area. A significant portion of the Quaternary deposits are composed of sandy deltaic and estuarine deposits and clay and silty-rich offshore marine deposits, both of which are related to the Champlain Sea. The Champlain Sea covered the St. Lawrence Lowland, and was an inlet of the Atlantic Ocean existing

Summary of Field Work and Other Activities 2012,
Ontario Geological Survey, Open File Report 6280, p.37-1 to 37-7.

© Queen's Printer for Ontario, 2012

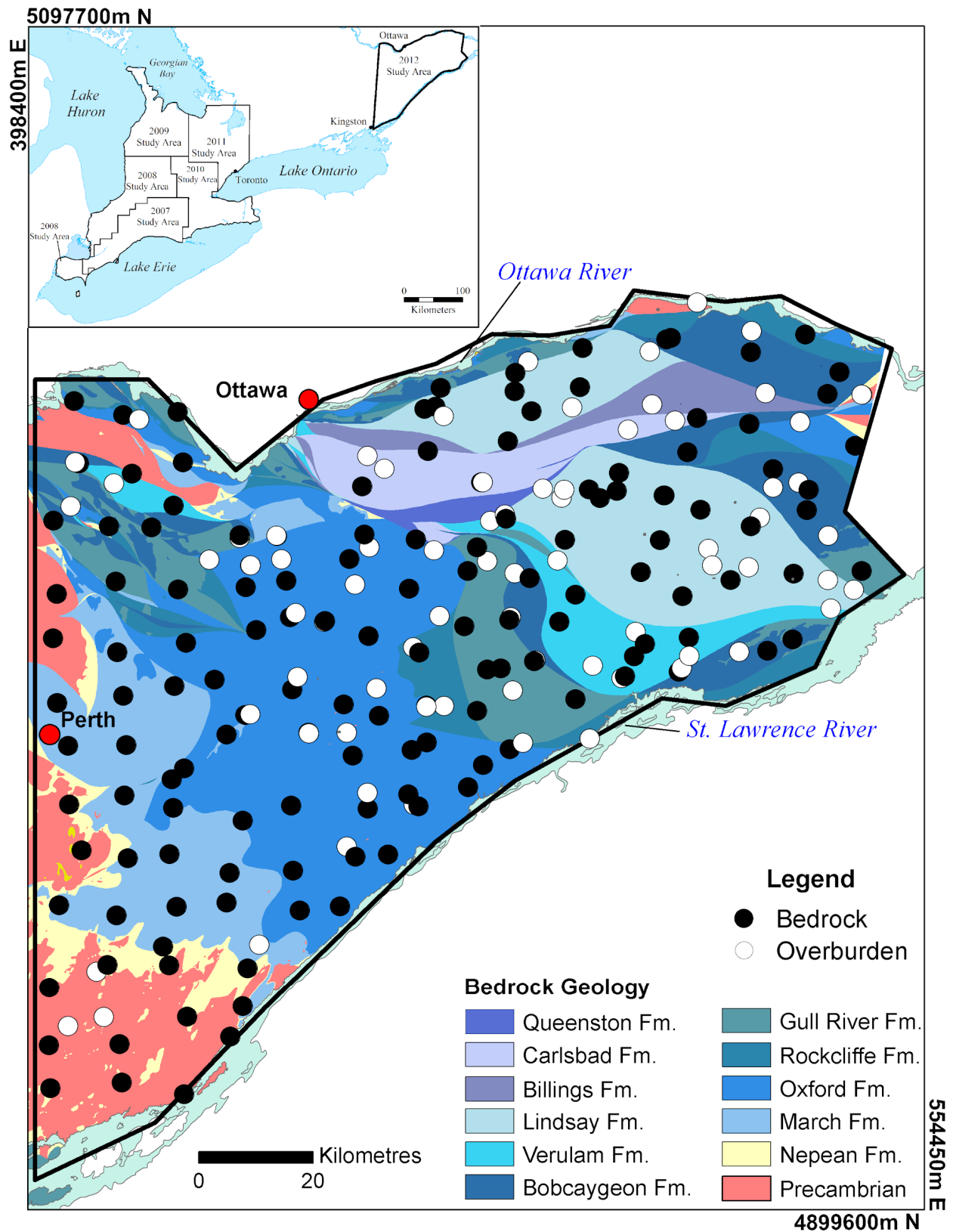


Figure 37.1. Location and geology of 2012 study area (bedrock geology from Armstrong and Dodge (2007)). Universal Transverse Mercator (UTM) co-ordinates in Zone 18, North American Datum 1983 (NAD83).

between 12 000 and 10 000 years before present (BP). The sea drained as the continental crust underwent isostatic rebound. Much of the remaining glacial strata (e.g., buried eskers) are sources of potable groundwater (Fulton and Richard 1987; Russell, Brooks and Cummings 2011).

METHODS

The field methodology used in the Ambient Groundwater Geochemistry Program is described in Hamilton, Brauner and Mellor (2007) and Hamilton and Brauner (2008). Using the Ontario Ministry of Environment (MOE) water-well database records, both a bedrock and overburden well are selected on a 10 by 10 km grid node. These are usually domestic wells. Homeowners are then contacted and, if permission is granted, the well is sampled using the existing domestic pump and distribution system, provided any water treatment systems the home may have can be bypassed.

At each site, notes are taken regarding the nature of the well and plumbing, the sampling point, the nature of the water (e.g., gaseous, odours, colour, turbidity, etc), and field-determined chemical and physical parameters. Temperature, dissolved oxygen (DO), pH, conductivity and oxidation–reduction potential (ORP) are measured using a multiparameter instruments equipped with a flow cell. During the initial purging of the well, these 5 parameters are continuously monitored and logged until they become stable or until long-term trends (up or down) are established. Generally, the systems are purged of at least 160 L and sometimes in excess of 400 L before sampling can begin. A total of 11 sample bottles are then collected, individually prepared (including filtration and acidification, where appropriate) and transported to the laboratory for analysis. Several additional parameters are determined in-field including bicarbonate (HCO_3^-), hydrogen sulphide (H_2S), dissolved gases (CO_2 , O_2 , CH_4) and iodide (I^-).

PRELIMINARY RESULTS

A total of 267 samples were collected from 224 wells (stations): 79 overburden and 145 bedrock wells. The well depths of overburden sample stations varied from 2.0 to 64.0 m, whereas bedrock sample stations varied from 7.6 to 104.2 m. It is believed that of the 145 bedrock sample stations, groundwater was obtained from 10 units: the Paleozoic Nepean (7), March (15), Oxford (40), Rockcliffe (3), Gull River (14), Bobcaygeon (17), Verulam (10), Lindsay (20) and Carlsbad (5) formations and Precambrian bedrock (14).

Temperature for all well types varied between 7.7 and 13.3°C. Conductivity varied from 105.7 to 311 111 $\mu\text{S}/\text{m}$, with the highest measurements having been sampled from an area containing Quaternary deposits from the Champaign Sea (Figure 37.2). Champlain Sea waters are interpreted to have been comprised from meltwater from the Laurentide Ice Sheet and local precipitation mixed with salt water from the St. Lawrence Gulf (Hillaire-Marcel 1999; as stated in Russell, Brooks and Cummings 2011). Groundwater that has come into contact with the older glacial sediments would incorporate their geochemical signature. The abnormally high conductivity values that were measured are therefore likely a result of groundwater interacting with the marine sediments, in areas where groundwater flow is extremely sluggish.

Oxidation–reduction measurements ranged from 155.3 to –345.8 and pH ranged from 5.7 to 8.6. Variable dissolved oxygen (DO) was detected ranging from 0.0 to 84.0% saturation, with the median values of 0.0% saturation. Elevated concentrations of DO were measured in groundwater obtained from wells completed in the glacial overburden sediments (Figure 37.3) and bedrock (Figure 37.4). In the southwestern portion of the study area, DO concentrations ranged between 2.3 to 58.6% saturation. This is an area where groundwater wells are drilled through, and terminated in, the March Formation, which is an Ordovician sandstone–dolostone unit.

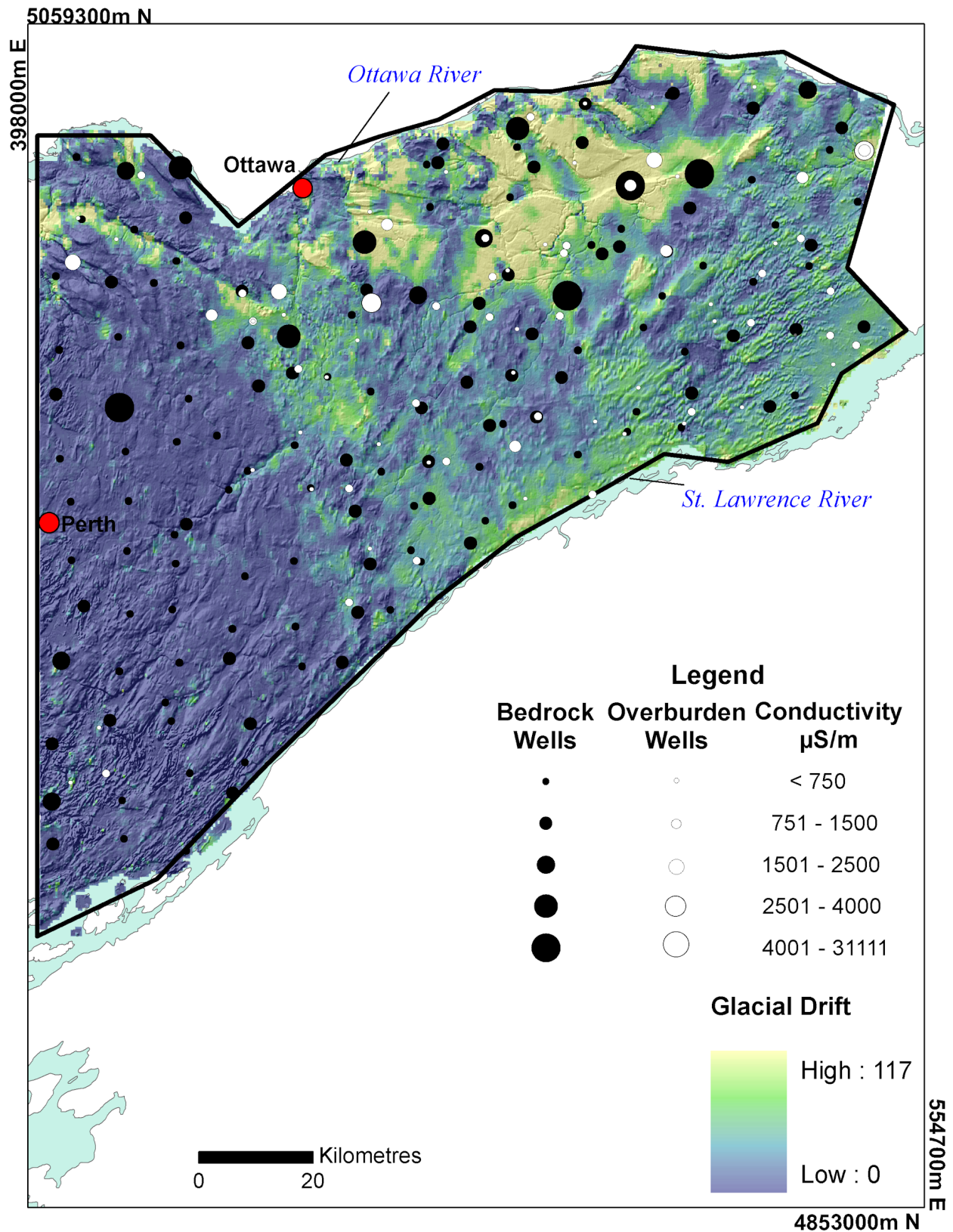


Figure 37.2. Electrical conductivity as measured in both bedrock and overburden wells in the study area, with respect to the regional glacial drift geology. Bedrock geology from Armstrong and Dodge (2007). UTM co-ordinates in Zone 18, NAD83.

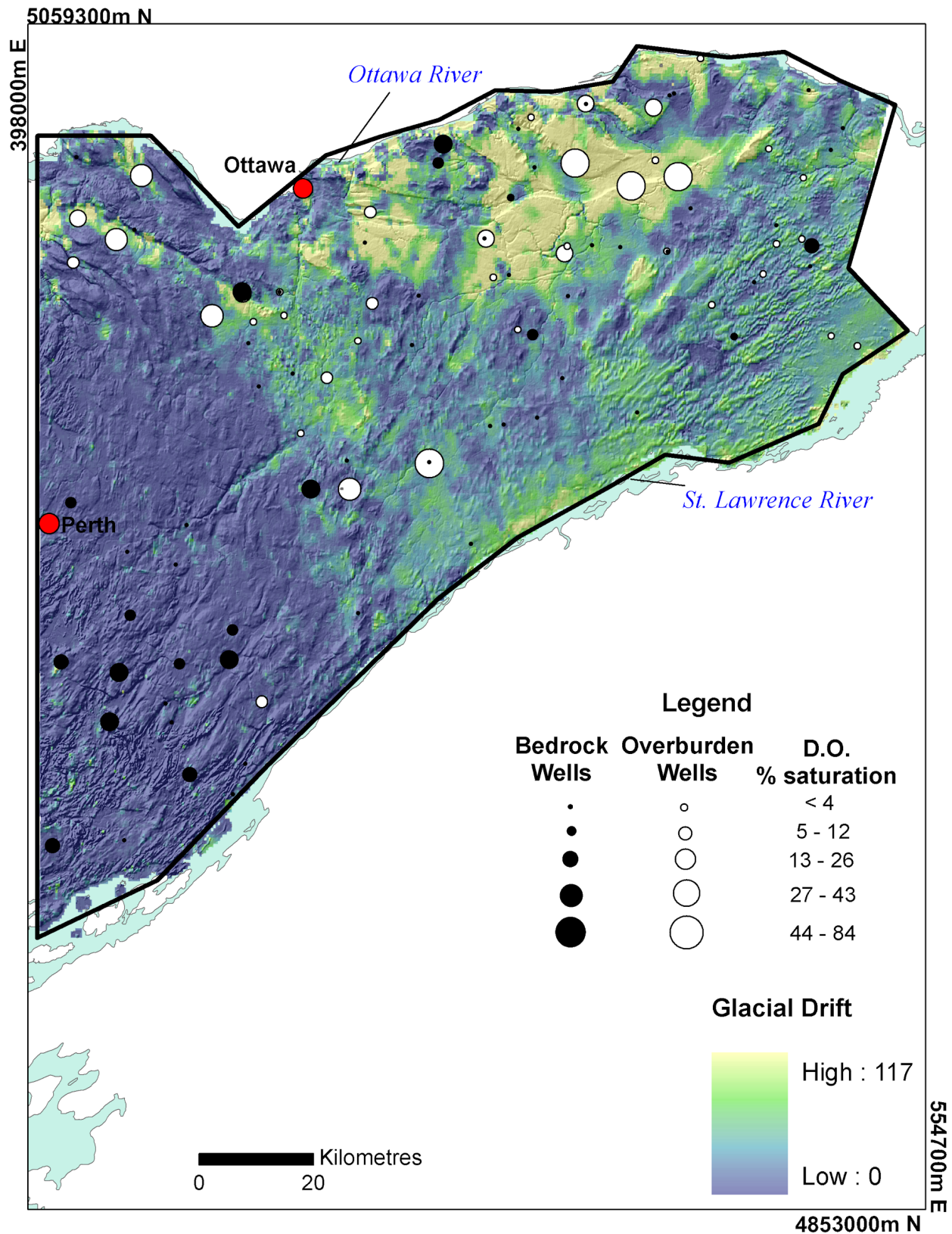


Figure 37.3. Dissolved oxygen concentrations as measured in overburden and bedrock wells for the study area, with respect to the regional glacial drift geology. Bedrock geology from Armstrong and Dodge (2007). UTM co-ordinates in Zone 18, NAD83.

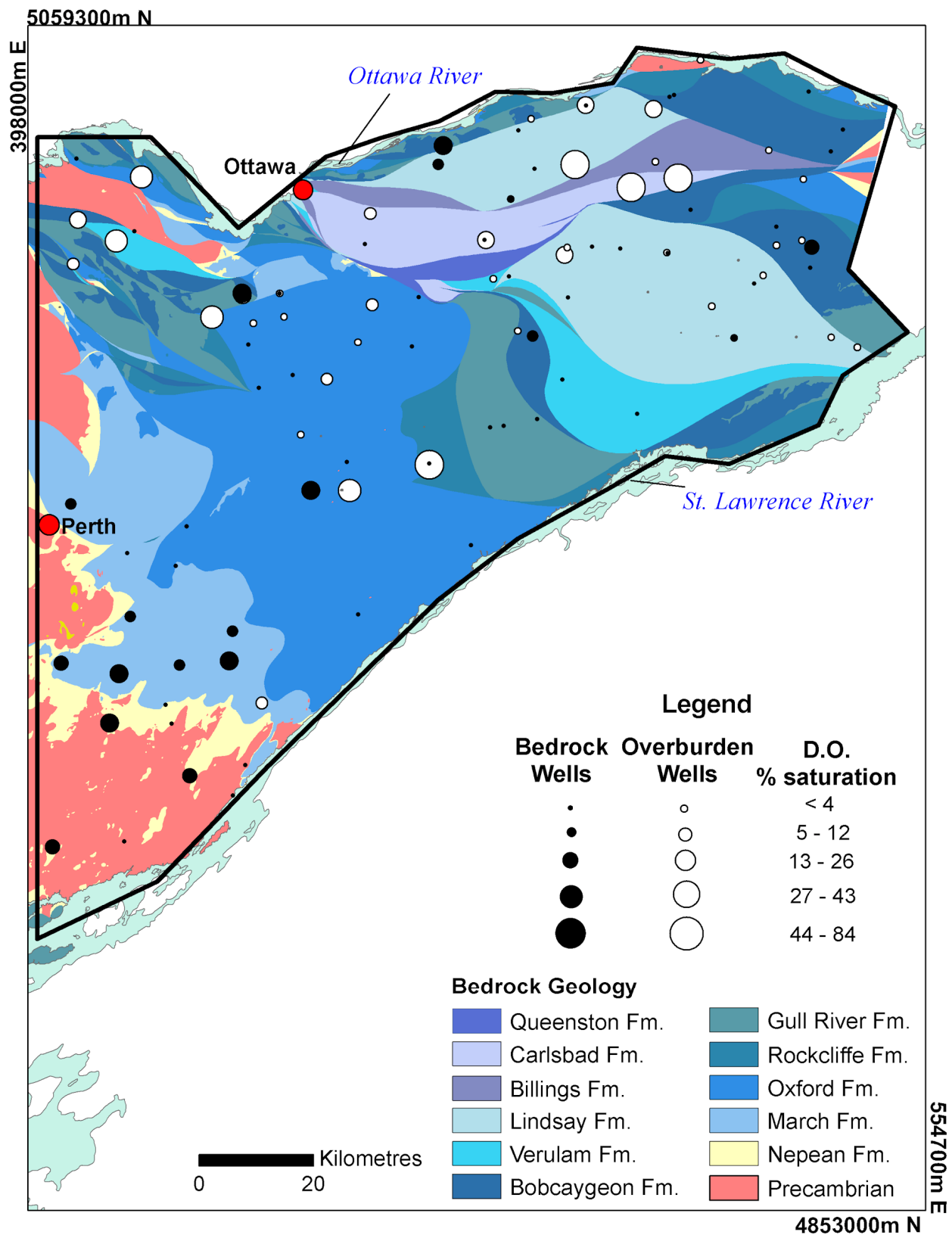


Figure 37.4. Dissolved oxygen concentrations as measured in overburden and bedrock wells for the study area, with respect to the bedrock geology. Bedrock geology from Armstrong and Dodge (2007). UTM co-ordinates in Zone 18, NAD83.

SUMMARY

During the 2012 field season, 267 samples were collected from 224 stations in a 12 500 km² area between the Ottawa and St. Lawrence rivers. Overburden wells were difficult to find in the western portion of the study area, since the glacial overburden was extremely thin to absent. Preliminary interpretation from field results reveals that wells drilled in sandstone of the March Formation contain moderate amounts of dissolved oxygen and elevated levels of conductivity were measured in areas that were inundated by the Champlain Sea. Further results and interpretations will be made once laboratory analysis is completed.

ACKNOWLEDGMENTS

Very able and professional field assistance was provided by Kaya Zoratto, Laura Colgrove, Cedric Mayer, Harry Cortis, Meaghan Francis and Jeremy Dalton.

REFERENCES

- Armstrong, D.K. and Dodge, J.E.P. 2007. Paleozoic geology of southern Ontario; Ontario Geological Survey, Miscellaneous Release—Data 219.
- Fulton, R.J. and Richard, S.H. 1987. Chronology of Late Quaternary events in the Ottawa region; *in* Quaternary geology of the Ottawa region, Ontario and Quebec, Geological Survey of Canada, Paper 86-23, p.24-30.
- Hamilton, S.M. 2011. Ambient groundwater geochemistry data for southwestern Ontario, 2007–2010; Ontario Geological Survey, Miscellaneous Release—Data 283.
- Hamilton, S.M. and Brauneder, K. 2008. The Ambient Groundwater Geochemistry Project: Year 2; *in* Summary of Field Work and Other Activities, 2008, Ontario Geological Survey, Open File Report 6226, p.34-1 to 34-7.
- Hamilton, S.M., Brauneder, K. and Mellor, K.J. 2007. The Ambient Groundwater Geochemistry Project – southwestern Ontario; *in* Summary of Field Work and Other Activities, 2007, Ontario Geological Survey, Open File Report 6213, p.23-1 to 23-5.
- Hamilton, S.M., Matheson, E.J., Freckelton, C.N. and Burke H. 2011. Ambient Groundwater Geochemistry Program: the 2011 Aurora–Orillia study area and selected results for the Bruce and Niagara peninsulas; *in* Summary of Field Work and Other Activities, 2011, Ontario Geological Survey, Open File Report 6270, p.32-1 to 32-11.
- Hillaire-Marcel, C. 1988. Isotopic composition (¹⁸O, ¹³C, ¹⁴C) of biogenic carbonates in Champlain Sea sediments; *in* The Late Quaternary development of the Champlain Sea basin, Geological Association of Canada, Special Paper 35, p.177-194.
- Johnson, M.D., Armstrong, D.K., Sanford, B.V., Telford, P.G. and Rutka, M.A. 1992. Paleozoic and Mesozoic geology of Ontario; *in* Geology of Ontario, Ontario Geological Survey, Special Volume 4, Part 2, p.907-1008.
- Russell, H.A.J., Brooks, G.R. and Cummings, D.I., eds. 2011. Deglacial history of the Champlain Sea basin and implications for urbanization; Geological Survey of Canada, Open File 6947, 96p.

38. Project Unit 07-025. Assessing Laboratories' Capabilities for Water Analysis: Results of a Round-Robin Study

O.M. Burnham¹, J. Schroeder² and S.M. Hamilton²

¹Geoscience Laboratories, Ontario Geological Survey

²Earth Resources and Geoscience Mapping Section, Ontario Geological Survey

INTRODUCTION

A critical part of the quality-control (QC) program of any geochemical study and any application of an analytical method is the monitoring of the resulting data through the analysis of quality-control materials. Whereas the most comprehensive monitors are certified reference materials (CRMs) in which the matrices match those of the samples and for which the compositions are characterized for all the analytes of interest through interlaboratory testing, such materials are not always available and, when they are, the CRMs can be too costly for routine use. Under such conditions, it is common to use in-house quality-control materials (QCMs) to monitor within- and between-batch variations. Because in-house QCMs can be tailored to specific sample types, they can provide the truest measure of analytical precision in the matrix of interest. However, in most cases, the “true” compositions of in-house QCMs are unknown, preventing their use for the assessment of accuracy.

The question of accuracy arose in the case of the 2 in-house QCMs used for QC during the collection and analysis of waters as part of the ongoing Ambient Groundwater Geochemistry program being carried out by the Earth Resources and Geoscience Mapping Section of the Ontario Geological Survey (Hamilton, Brauner and Mellor 2007; Hamilton and Brauner 2008) and the in-house QCM used during routine quality control of the analyses of trace elements in waters at the Geoscience Laboratories (Geo Labs; method codes IMW-100 and IAW-100). Having been used for several field seasons, abundant data exist with which to assess the precision of the data, but the QCMs give no indication of accuracy. Therefore, in order to characterize these materials better, a round-robin study was undertaken, with aliquots of each solution being sent out to a number of laboratories for full chemical analyses. The accuracy of the data was verified by the inclusion of the CRMs SLRS-4 and SLRS-5 (river water reference materials for trace element analysis distributed by the National Research Council of Canada (NRC), Ottawa). In addition to providing better constraints on the compositions of the QCMs, the results of these analyses also allowed an assessment of the laboratories' abilities to analyze a range of elements and/or a sample matrix not covered by existing proficiency tests³.

³ Proficiency tests for the analysis of water samples are routinely run by several organizations that specialize in QC in analytical laboratories, in particular Environment Canada's biannual “Major Ions and Nutrients in Water” and “Trace Elements in Water” proficiency tests and the Canadian Association for Laboratory Accreditation (CALA) biannual “Major Ions in Water” and “Metals in Water” proficiency tests. However, in most cases, the major elements are analyzed in separate samples from those in which the trace elements are analyzed, the major element concentrations of the samples in which trace elements are analyzed are normally relatively low, the range of trace elements considered in these studies is smaller than that encountered in many geochemical surveys, and the range of concentrations is uncharacteristic of “natural” samples (e.g., in proficiency test samples, nickel typically ranges from ~10 ppb to >1 ppm in matrices that contain <20 ppm Ca, but the majority of lake water and/or groundwaters collected by regional surveys carried out by the OGS contain <3 ppb Ni in matrices containing >70 ppm Ca and, in 5% samples, >400 ppm Ca).

This report summarizes the results of the round-robin study and presents externally verified working values for the in-house and interlaboratory water QCMs used during analyses at the Geo Labs, including initial data for many trace elements not currently characterized in the NRC river water CRM SLRS-5.

EXPERIMENTAL DESIGN

The 3 in-house QCMs (BLK-1, BLK-2 and WANA-1) and 2 NRC river water CRMs (SLRS-4 and SLRS-5) were circulated in a blind study to 8 laboratories that offer geological and/or environmental analyses. BLK-1 was collected from a water well finished in the Hamilton Group shale (station 08-AG-004), 12 km northeast of Strathroy, Ontario. It is a slightly basic and reducing groundwater with elevated Na and Cl and is high in many trace elements. BLK-2 was collected from a water well finished in the Lucas Formation (08-AG-010), 13 km south-southeast of Exeter, Ontario. It is a slightly basic and oxidizing water that has very high Ca, Mg, Sr and SO_4^{2-} . Almost all major and trace elements determined in the ambient groundwater sampling are elevated in at least one of the two BLK standards. The exception was Mn and, therefore, BLK-1 was spiked to achieve a target concentration of about 45 ppm Mn. WANA-1 was collected from the Wapitei River, 500 m downstream from Highway 17 in Wahnapiatae, Ontario. It represents typical river water with marginally elevated base metal (Ni and Cu) contents from historic mining activities in the Sudbury area. Whereas the bulk solutions of the 3 in-house water QCMs used for metals analysis were acidified to 1% v/v HNO_3 , the splits of BLK-1 and BLK-2 used for anion analysis were untreated, but kept refrigerated. Each of the laboratories was sent 3 aliquots of each acidified QCM, 2 aliquots of SLRS-5, and 1 aliquot of SLRS-4 for metals analysis, together with 2 aliquots of unacidified BLK-1 and BLK-2 for anion analysis. The laboratories were also supplied with a list of the analytes normally obtained during the Ambient Groundwater Geochemistry program, and the expected concentration ranges, and were asked to use their most appropriate methods to analyze for as many analytes as they could. To obtain the maximum amount of data for each material, laboratories were requested to submit data unscreened for reporting limits. Although data outside of reporting limits were considered during the assignment of values to the reference materials, they were not used to assess laboratories' capabilities.

Data reduction was carried out following the protocols employed by the International Association of Geoanalysts (IAG) for their GeoPTTM proficiency testing program (for details, *see* www.geoanalyst.org/documents/GeoPT-protocol.pdf [accessed October 29, 2012]). The mean results reported by each laboratory (X) were converted to "z-scores", defined by $z = (X - X_a)/\sigma_p$, where X_a is the "assigned value", representing the best estimate of the "true" value of the concentration of the analyte, and σ_p is the target precision, a value similar in function to a standard deviation that describes an acceptable range of variation among the results. Absolute z-scores greater than 3 indicate that an unacceptable source of error may be present in the laboratory's data and that remedial action should be taken. Absolute z-scores between 2 and 3 may also be taken to indicate the existence of errors. However, because such values can occur by chance (~5% chance based on classical Gaussian statistics), these isolated values are less significant.

During the initial stage of data reduction for BLK-1, BLK-2 and WANA-1, the assigned value was taken as the "consensus" of the laboratories' results for each analyte. Ideally, this would have been the robust mean of the individual laboratory means after the rejection of outliers. However, owing to the small number of data for each analyte and the large number of outliers, for consistency it was deemed preferable to use the median of the individual laboratory means, with outlier rejection, as the consensus value for all analytes. For SLRS-4 and SLRS-5, the assigned values were taken from the NRC certificates and previously published analyses of the CRMs (Yeghicheyan et al. 2001; Roduskin et al. 2005).

The target precision, σ_p , was based on fitness-for-purpose criteria derived from the Horwitz function ($H_a = 0.02c^{0.8495}$, where H_a is the target between-laboratory reproducibility observed at analyte concentration c and both c and H_a are expressed as mass ratios (Horwitz, Kamps and Boyer 1980; Horwitz and Albert 1995). Because this function is an empirical observation that may be applicable over a wide range of concentrations, test materials, analytes and analytical methods and depends solely on the

Table 38.1. Relative standard deviations (RSD) implied by the target value σ_p .

Concentration	σ_p	%RSD
10 ppm (10 mg/mL)	0.57 ppm	5.7%
100 ppb (100 µg/mL)	11.3 ppb	11.3%
1 ppb (1 µg/mL)	0.226 ppb	22.6%
10 ppt (10 ng/mL)	4.52 ppt	45.2%
0.1 ppt (0.1 ng/mL)	0.091 ppt	90.5%

Unit abbreviations: ppm, parts per million; ppb, parts per billion; ppt, parts per trillion.

assigned value rather than the observed spread in values, it allows the assessment of small data sets that may contain several outlying values. In the GeoPT™ program, 2 levels of uncertainty are recognized as fit-for-purpose: “Class 1”, which is appropriate for high-precision analysis for “pure” geological research, for which $\sigma_p = H_a/2$; and “Class 2”, more appropriate for “applied geochemistry”, for which $\sigma_p = H_a$. Because H_a may be over generous at low concentrations (<10 µg/L; Thompson 2000; Table 38.1), during this study, it was decided to apply the criteria used to judge “pure” geological research laboratories when assessing the data.

Because the assigned value was often calculated on a limited number of analyses that show considerable spread, σ_p was also used as a benchmark for the uncertainty on the assigned value X_a ($u(X_a)$). Because X_a was taken from the median value of the reported data, $u(X_a)$ was estimated as half the spread of the values either side of the median (e.g., when there were 6 determinations, $u(X_a)$ was set at half the difference between the third and fourth largest values). Consistent with the GeoPT™ protocol, where there was large uncertainty in the assigned value (specifically, $u(X_a) > 0.6\sigma_p$; Uriano and Gravatt 1977), the resulting z-scores were viewed as being too uncertain and were designated as provisional and for guidance only.

Having determined the laboratories capable of producing good-quality data for each analyte in the 5 materials, final working values were calculated for the 3 in-house QCMs and SLRS-5, including values for analytes that were previously uncharacterized in the NRC CRM. For each of the in-house QCMs, only data within $X_a \pm 2\sigma_p$ ($|z| < 2$) for each element were used to calculate the final working values. For SLRS-5, only data from laboratories with $|z| < 2$ for the same analyte in SLRS-4 were used to calculate the final working values, allowing the new data for SLRS-5 to be traceable to well-constrained analyses of a CRM with a similar matrix and composition. Target expanded uncertainties for the final values were set at $0.33 H_a$ ($U/H_a < 0.33$), consistent with those suggested in the IAG “Protocol for the Certification of Geological Reference Materials” (Kane et al. 2003; Kane and Potts 2007).

RESULTS

Proficiency Test Results

The assigned values (X_a), target precisions (σ_p) and individual laboratories scores for each of the 5 waters are shown in Tables 38.A1 to 38.A5. The number of analytes reported by each laboratory and quality of data varied greatly. Based on the results of the tests, the following observations can be made.

- Very few analytes are consistently available and satisfactorily analyzed by all laboratories in the 5 waters. Only Ca, Mg, Cl^- and SO_4^{2-} were available and accurately analyzed (>80% of labs reporting satisfactory data) by all 8 laboratories (Figure 38.1). Na, K, Ba, Cu, Fe, Sr, and Zn were reported by 6 to 7 of the laboratories and normally analyzed satisfactorily, but at least 2 laboratories had difficulties analyzing Cu or K in BLK-1 or BLK-2, or Zn in the 2 NRC CRMs.
- Satisfactory data for many of the trace and ultra-trace elements (e.g., B (at ppb levels), Be, Bi, Cr, Cs, Hf, Li, Nb, Sb, Th, Tl, Zr and the rare earth elements (REE)) are available from only a few laboratories when present at the levels found in natural samples. At the level of single to

tens parts per trillion (ppt) (e.g., in BLK-1 and WANA-1), only 2 or 3 laboratories would have routinely reported satisfactory data. The situation gets worse at lower concentrations, with only 1 laboratory reporting data for many of the REE at sub-ppt-levels present in BLK-2; however, the situation improves with increasing concentrations: REE data for samples with concentrations at the level of single to hundreds parts per trillion, for example SLRS-4 and SLRS-5, are routinely reported by 3 or 4 of the 8 participating laboratories. Examination of the raw data provided by several of the laboratories indicates that they were able to produce accurate data for many of these analytes at low levels, but that such concentrations would not have been reported as they are below the laboratories reporting limits. Therefore, the problem appears to be less each laboratory's capacity to determine accurate concentrations at low levels and more their scope to report such data routinely. Based on the current study, many laboratories may actually under-represent their capabilities for several analytes.

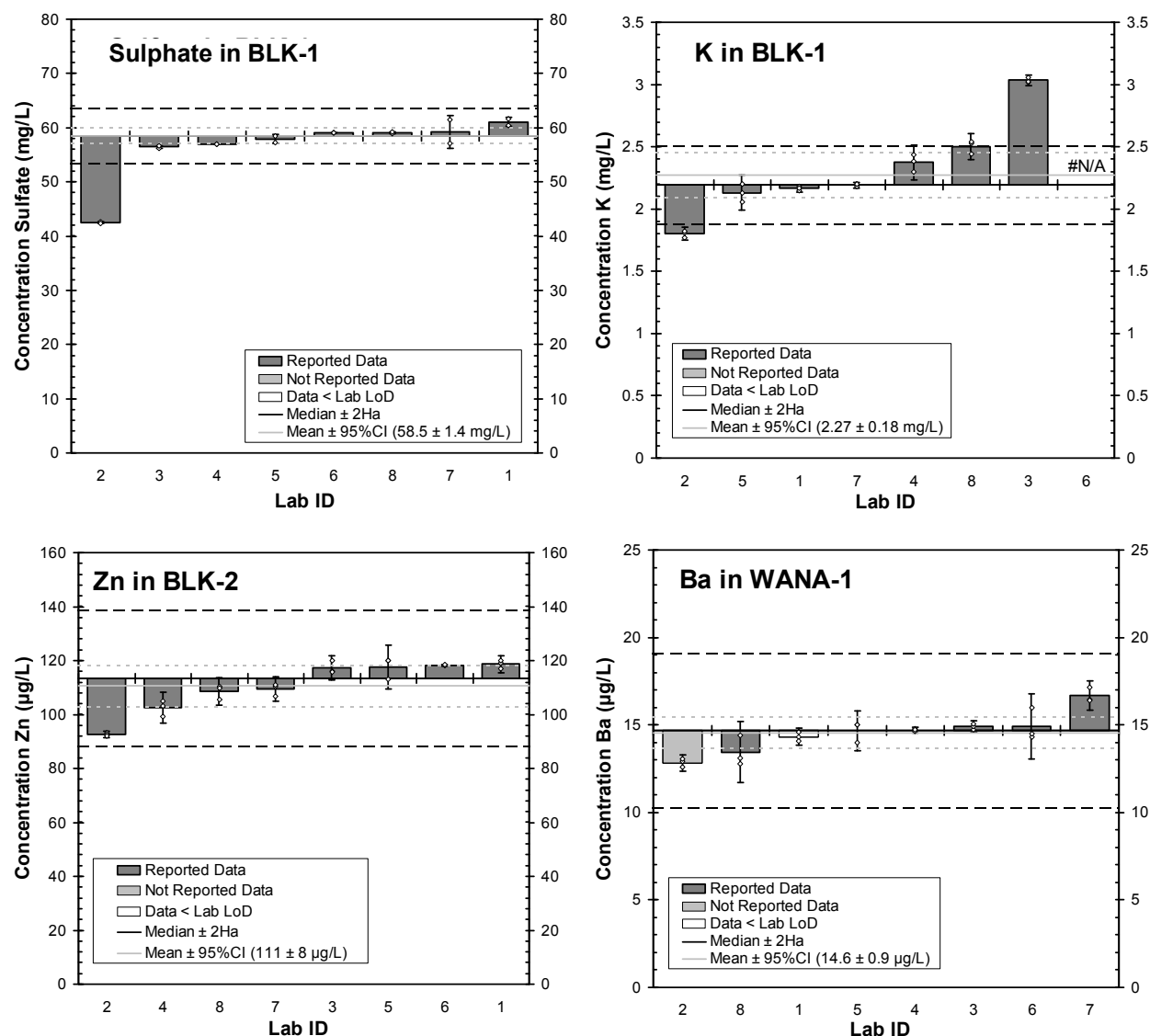


Figure 38.1. Data distribution plots for which satisfactory data could be obtained from most laboratories. Small diamonds and error bars indicate individual analyses and mean \pm 2 σ for each laboratory. Not Reported Data: data for an analyte not normally reported by the indicated laboratory; CI: confidence interval.

- Several of the participating laboratories had difficulty analyzing many of the elements that may be of importance to regional geochemical studies, with fewer than half the laboratories reporting data for As, Co, Ni, Pb, Se or V in most of the samples and frequently poor internal and/or external agreement between the reported values and/or the certified values, when available. Because the majority of the analyses of these elements at low levels are performed using inductively coupled plasma mass spectrometry (ICP-MS), it is not surprising that some of the least satisfactory agreement is seen for BLK-1 and BLK-2 and analytes affected by the spectroscopic interferences expected during the analyses of samples with complex matrices (Figure 38.2). The problems are most acute for analytes such as As and V in BLK-1, presumably due to pronounced interferences from chloride-bearing polyatomic species ($[\text{Cl}]_{\text{BLK-1}} \sim 200 \text{ ppm}$; $^{35}\text{ClO}^+$ is isobaric with $^{51}\text{V}^+$ and $^{40}\text{Ar}^{35}\text{Cl}^+$ is isobaric with $^{75}\text{As}^+$), or Co and Ni in BLK-2 ($[\text{Ca}]_{\text{BLK-2}} \sim 162 \text{ ppm}$) owing to pronounced interferences from $^{43}\text{Ca}^{16}\text{O}^+$ on $^{59}\text{Co}^+$ and $^{44}\text{Ca}^{16}\text{O}^+$ on $^{60}\text{Ni}^+$.

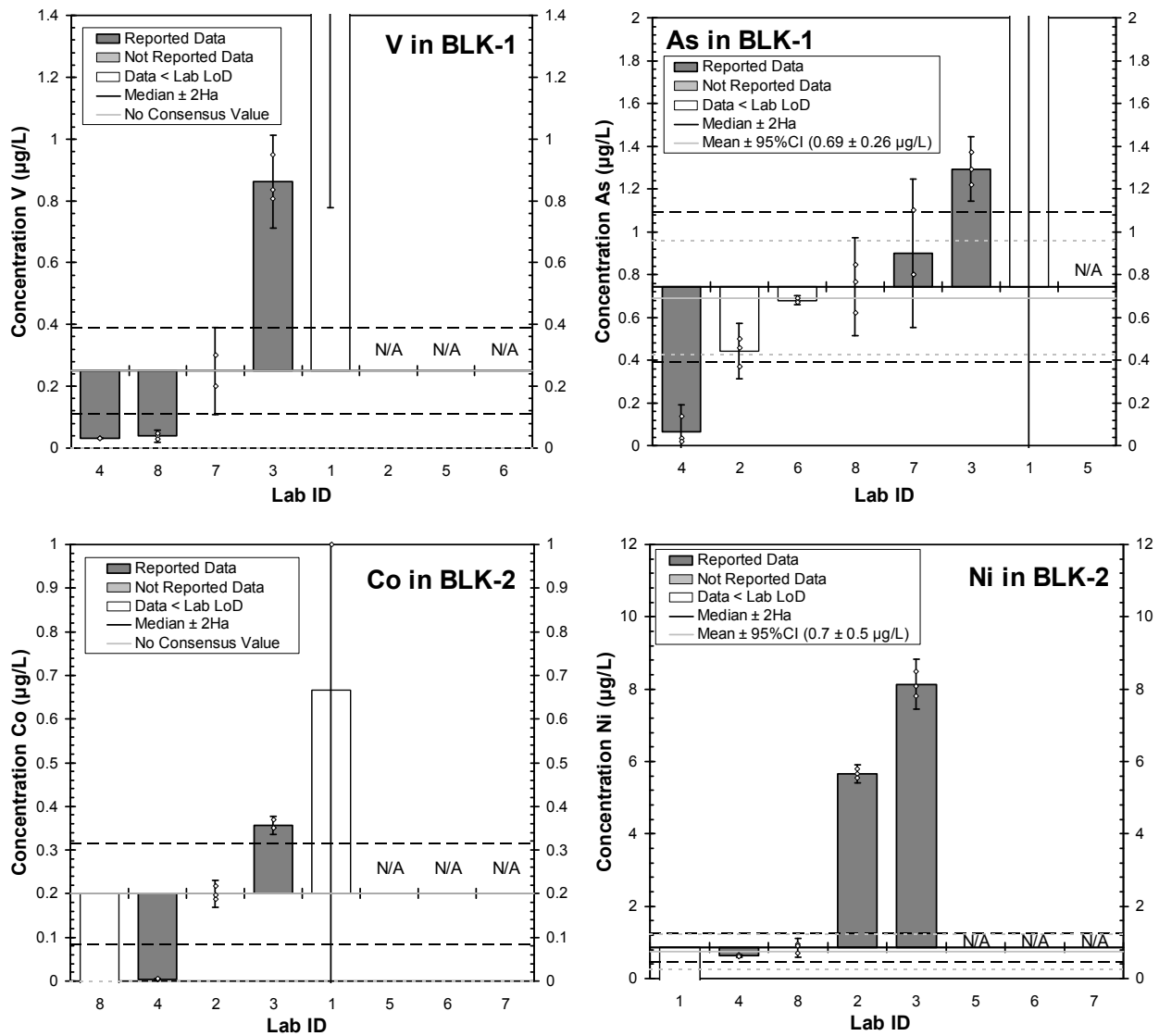


Figure 38.2. Data distribution plots for analytically challenging analytes of potential importance to regional geochemical studies. Upper plots: V and As in the chlorine-rich BLK-1 in-house QCM. Lower plots: Co and Ni in the calcium-rich BLK-2 in-house QCM. Small diamonds and error bars indicate individual analyses and mean $\pm 2\sigma$ for each laboratory. Not Reported Data: data for an analyte not normally reported by the indicated laboratory; CI: confidence interval.

- In view of the variable quality of data available from different laboratories, when using a laboratory as part of regional study, it is advisable, not only to submit within-batch blind QC samples to monitor analytical precision (preferably using aliquots of a matrix-matched bulk in-house QCM), but also to determine the accuracy of candidate laboratories' results for the analytes of interest *before* committing to their use.

Characterization of Quality-Control Materials

Tables 38.A6 and 38.A7 present final consensus values for the 3 in-house QCMs and the NRC certified reference material SLRS-5. As described above, in order to minimize the uncertainty, only data from laboratories who demonstrated the ability to produce satisfactory results were used in the calculation of the final values. For BLK-1, BLK-2 and WANA-1, the selection was based on the z-scores for the material ($|z| < 2$) during the proficiency-testing part of the study. For SLRS-5, the selection was based on the z-scores calculated for SLRS-4 using either its NRC certificate or literature values.

The values in Table 38.A6 and 38.A7 represent the means of the chosen laboratories' averages, the expanded uncertainties of these means (U) and, in accordance with ISO Guide 33 (2000), the within- and between-laboratory standard deviations (σ_{within} and σ_{between}) of the data. Whereas ISO Guide 35 (2006) identifies several components of variance that should be included in the uncertainties of all reference values for compliance with the "Guide on Measurement Uncertainty" (in particular, material instability (u_{stabil}), material heterogeneity (u_{matl}), analytical bias (u_{bias}) and random measurement variability (u_{mean})), not all were applicable or could be constrained during the current study and only the uncertainty due to random measurement variability (u_{mean}) was considered in detail.

Because sample heterogeneity was not expected for solutions poured from a single stock, it is reasonable to exclude a heterogeneity component from the uncertainty budgets for the water QCMs. However, less easily excluded are components that account for sample instability or analytical bias. Although most of the major cations and trace metals may be expected to be reasonably stable in a dilute nitric acid-stabilized solution, the long-term stability of some metals (e.g., the high-field strength elements (HFSE): Zr, Nb, Mo, Hf, Ta and W) in such a matrix at low concentrations is not well constrained. Similarly, without chemical stabilization, short holding times before analysis are recommended for many of the anions (e.g., 48 hours for $\text{NO}_2^-/\text{NO}_3^-$ and PO_4^{3-} or 28 days for Br^- , Cl^- , F^- , and SO_4^{2-} ; Pfaff, Hautman and Munch 1999), suggesting that, even after equilibration following sample collection, there is scope for concentrations to change should the sample not be stored correctly. Owing to the limited scope of the current study, the stability component could not be considered in detail and so the uncertainties for the anion contents in BLK-1 and BLK-2 should be considered as underestimates of the total uncertainties. Similarly, because samples were submitted for the "most appropriate methods" to analyze for the analytes of interest, there was little control and often no information on the analytical methods that were used. In the absence of such information, an assessment of analytical method bias was also beyond the scope of this study. In the absence of estimates of u_{stabil} , u_{matl} and u_{bias} , the uncertainties in the final values were calculated from u_{mean} alone, using the standard errors of the laboratory average and the t-factor appropriate for the number of set analyses that were used⁴.

According to the guidelines set out by ISO Guide 35 (2006) or the IAG Certification Protocol (Kane et al. 2003; Kane and Potts 2007), certification for an analyte requires at least 15 individual laboratory

⁴ For an infinite number of analyses, n , the number of degrees of freedom, $df = n - 1$, also approaches infinity, and $t \rightarrow 1.96$ for 95% confidence, but as the number of analyses decreases, t increases to 2.36 for 8 analyses ($df = 7$) and 4.3 for 3 analyses ($df = 2$). Because t increases rapidly with decreasing number of analyses, the spread in data for analytes characterized by only a few laboratories must be considerably smaller than that for a widely analyzed analyte if the final uncertainty is to be within an acceptable range.

measurements or 10 results that originate from at least 2 different methods of analysis that are in agreement. Owing to the low number of laboratories participating in the current study (and even lower number of results available for many of the analytes) and the inability to demonstrate inter-method agreement for most of the data, none of the final values presented in Table 38.A6 and 38.A7 can be considered to be certified, despite the close agreement between laboratories for many analytes, and so must be designated a lower status. When it comes to non-certified values, there is less rigour in the definition of terms. For the purposes of this study, the following designations were used:

- “Provisional” values:
 $n \geq 6$ and $U/H_a < 0.33$ (good agreement between many of the laboratories)
- “Indicative” values:
 $n \geq 6$ and $U/H_a = 0.33 - 1$ (reasonable agreement between many of the laboratories) or
 $n \geq 3$ and $U/H_a < 0.33$ (good agreement between a few of the laboratories)
- “Information” values:
 $n \geq 3$ and $U/H_a = 0.33 - 1$ (reasonable agreement between a few of the laboratories) or
 $n = 2$ and $U/H_a < 0.33$ (very good agreement between two laboratories).

Based on these designations, it was possible to assign provisional values to 6 analytes (Ca, Mg, Mn, Cl⁻, SO₄²⁻, Ba and Mo) and indicative values to a further 19 analytes in BLK-1; and provisional values to 8 analytes (Ca, Mg, B, Ba, Mo, Tl, U and Zn) and indicative values to a further 9 analytes in BLK-2. Owing to the low number of values and/or less interlaboratory agreement, a further 24 to 27 analytes were assigned information values and 8 to 21 of the analytes were given no rating. Although both materials were challenging due to their complex matrix (either Na, Cl and Mn in BLK-1 or Ca, Mg and SO₄²⁻ in Bulk-2), the characterization of BLK-2 appears to have been less successful owing to its overall lower trace element contents.

On account of their simpler matrices, it was possible to assign provisional values to 8 analytes (Ca, Mg, As, Ba, Cu, Sr and/or Al, Mn, Ni and Zn) and indicative values to a further 18 analytes (including Na, Rb, Si, U, Y and most of the REE) in the 2 river waters (WANA-1 and SLRS-5). A further 18 to 27 analytes were assigned information values. It was not possible to assign values with any surety to only 3 (WANA-1) to 12 (SLRS-5) analytes. The higher number of un-rated analytes in SLRS-5 resulted primarily from the large spread in the data received and/or the poor agreement obtained for the concentrations of these analytes (Ag, B, Bi, Hf, Sc, Se, Sn, Ta or W) in SLRS-4 with their certificate or literature values.

Where values are available, most of the concentrations obtained for SLRS-5 in the current study are in agreement with the values given on the NRC certificate, albeit with considerably greater spread for several of the less abundant trace elements (e.g., Be, Ni, Zn and Pb) and marginally lower values for some analytes (e.g., 45 ± 4 versus 49.5 ± 5 µg/L Na; 4.95 ± 0.25 versus 5.38 ± 0.1 mg/L Al). Whereas the indicative values obtained for Sb and U (0.33 ± 0.06 and 0.091 ± 0.004 µg/L, respectively) are in good agreement with the information values on the certificate (0.3 and 0.1 µg/L, respectively) and yield values that have estimates of precisions, the information value obtained for Mo (0.18 ± 0.06 µg/L) is considerably lower than that given by the NRC (0.5 µg/mL). Given reasonable agreement from 5 separate laboratories, it is possible that the certificate significantly overestimates the Mo content of the CRM and that a lower value may be more accurate.

In addition to corroborating the existing values for SLRS-5, this study gives new indicative or information values for many analytes not previously characterized in SLRS-5, including Cs, Ga, Li, Nb, Rb, Si, Th, Ti, Tl, Y, Zr and many of the REE. To the best of our knowledge, these are the first well-characterized values for these elements in this CRM.

The new values for SLRS-5 and robust values for the other 3 water-quality control materials obtained during this study increase the range of analytes for which SLRS-5 can be used for quality control during analysis and, more significantly for the work at the OGS, expands the scope of their in-house QCMs from simple monitors of precision to indicators of both precision and accuracy during internal and external analyses of samples collected as part of regional geochemical surveys.

SUMMARY

Through a round-robin study of several commercial and government laboratories that offer geological or environmental analyses, it was found that not all laboratories can offer the same range and quality of data, in particular:

- Most laboratories can offer satisfactory data for the major cations and anions (Ca, Mg, Na, K, Cl^- , and SO_4^{2-}) in lake, river and groundwater typical of those collected as part of regional surveys carried out by the OGS.
- Only a handful of laboratories are capable of offering satisfactory data for all the analytes routinely needed as part of such surveys (including data for As, Co, Cr, Cs, Li, Ni, Pb, REE, Sb, Se, Th, Tl and V).
- Several of the participating laboratories had particular difficulty analyzing many of the elements that may be of importance to regional geochemical studies, especially when present in samples with challenging matrices.
- In view of the variable quality of data available from different laboratories, it is strongly advised that researchers determine the laboratories capability to produce accurate data for the analytes of interest before committing to the use of a particular laboratory.

Using data from the best-performing laboratories, robust consensus values have been obtained for the compositions of the 3 in-house QCMs and additional information values have been produced for many of analytes not currently available on the certificate for the NRC river water CRM SLRS-5. These new values enable these materials to be used within a QC program to now check both the precision and accuracy of data obtained at the OGS as part of ongoing regional survey programs.

REFERENCES

- Hamilton, S.M. and Brauner, K. 2008. The Ambient Groundwater Geochemistry Project: Year 2; *in* Summary of Field Work and Other Activities, 2008, Ontario Geological Survey, Open File Report 6226, p.34-1 to 34-7.
- Hamilton, S.M., Brauner, K. and Mellor, K.J. 2007. The Ambient Groundwater Geochemistry Project – southwestern Ontario; *in* Summary of Field Work and Other Activities, 2007, Ontario Geological Survey, Open File Report 6213, p.23-1 to 23-5.
- Horwitz, W. and Albert, R. 1995. Precision in analytical measurements: expected values and consequences in geochemical analyses; *Fresenius' Journal of Analytical Chemistry*, v.351, p.507-511.
- Horwitz, W., Kamps, L.R. and Boyer, K.W. 1980. Quality assurance in the analysis of foods for trace constituents; *Journal of the Association of Official Analytical Chemists*, v.63, p.1344-1354.
- ISO Guide 33 2000. Uses of certified reference materials, 2nd ed.; International Organisation for Standardisation, Geneva, 64p.
- ISO Guide 35 2006. Certification of reference materials – general and statistical principles, 3rd ed.; International Organisation for Standardisation, Geneva, 64p.

- Kane, J.S. and Potts, P.J. 2007. ISO best practices in reference material certification and use in geoanalysis; *Geostandards and Geoanalytical Research*, v.31, p.361-378.
- Kane, J.S., Potts, P.J., Wiedenbeck, M., Carignan, J. and Wilson, S. 2003. International Association of Geoanalysts' protocol for the certification of geological and environmental reference materials; *Geostandards Newsletter: The Journal of Geostandards and Geoanalysis*, v.27, p.227-244.
- Pfaff, J.D., Hautman, D.P. and Munch, D.J. 1999. Method 300.1. Determination of inorganic anions in drinking water by ion chromatography, revision 1.0; United States Environmental Protection Agency, www.epa.gov/sam/pdfs/EPA-300.1.pdf [accessed October 24, 2012], [also in *Methods for the determination of organic and inorganic compounds in drinking water*, volume 1, EPA 815-R-00-014, p.300.1-1 to 300.1-42].
- Rodushkin, I., Nordlund, P., Engström, E. and Baxter, D.C. 2005. Improved multi-elemental analyses by inductively coupled plasma-sector field mass spectrometry through methane addition to the plasma; *Journal of Analytical Atomic Spectrometry*, v.20, p.1250-1255.
- Thompson, M. 2000. Recent trends in inter-laboratory precision at ppb and sub-ppb concentrations in relation to fitness for purpose criteria in proficiency testing; *Analyst*, v.125, p.385-386.
- Uriano, G.A and Gravatt, C.C. 1977. The role of reference materials and reference methods in chemical analysis; *CRC Critical Reviews in Analytical Chemistry*, v.6, p.361-411.
- Yeghicheyan, D., Carignan, J., Valladon, M., Bouhnik Le Coz, M., Le Cornec, F., Castrec-Rouelle, M., Robert, M., Qaailina, L., Aubry, E., Churlaud, C., Dia, A., Debertdt, S., Dupré, B., Freydier, R., Gruau, G., Hénin, O., deKersabiec, A., Macé, J., Marin, L., Morin, N., Petitjean, P. and Serrat, E. 2001. A compilation of silicon and thirty-one trace elements measured in the natural river water reference material SLRS-4 (NRC-CNRC); *Geostandards Newsletter: The Journal of Geostandards and Geoanalysis*, v.25, p.465-474.

APPENDIX

Table 38.A1. Parameters used in the calculation of z-scores and laboratory z-scores for the analysis of in-house QCM BLK-1.

	Laboratory ID											
	X _a	u(X _a)	H _a	u(X _a)/H _a	1	2	3	4	5	6	7	8
Majors (ppm)												
Ca	8.73	0.21	0.5	0.41	0.56	-2.12	0.41	0.87	-0.49	-0.62	1.50	-0.41
Mg	5.32	0.0051	0.3309	0.02	-0.16	-1.73	1.84	0.02	-0.20	0.08	0.85	-0.02
Na	203.7	0.45	7.32	0.06	0.20	-25.17	1.58	2.32	-0.04		0.00	-0.87
K	2.19	0.052	0.156	0.34	-0.18	-2.51	5.39	1.16	-0.41		0.00	1.98
Traces (ppb)												
Ag	0.0073	0.0031	0.0035	0.9			(0.00) ²	2.96				-0.63
Al	12.41	0.15	1.92	0.08		(0.00) ¹	0.88	-1.47	-1.77	0.10	-0.21	0.49
As	0.74	0.06	0.18	0.31	BDL	(-1.71) ²	3.13	-3.87		(-0.36) ²	0.89	0.00
B	1817	54	133	0.41	0.00	NNR	-0.86	1.51	0.82		-0.81	2.30
Ba	38.38	0.12	5.01	0.02	-0.02	(-1.08) ¹	0.02	0.95	0.39	-0.18	0.79	-0.86
Be	0.00427	0.00029	0.0022	0.13	BDL		(0.56) ²	0.13				(-0.13) ²
Bi	0.0011	0.0004	0.0007	0.5				0.50				(-0.50) ²
Cd	0.108	0.005	0.034	0.16			0.00	0.70		0.30	-0.53	-0.33
Co	0.078	0.005	0.026	0.19	BDL	(-0.98) ²	2.69	-0.19			-1.47	0.19
Cr	0.25	0.007	0.07	0.1	BDL	(-0.01) ²	12.83	0.00		0.39	3.59	-0.39
Cs	0.033	0.004	0.012	0.34		(-0.82) ¹	BDL	0.00			0.84	-0.52
Cu	2.948	0.012	0.567	0.02	BDL	5.32	0.02	-1.35	0.09	3.39	-0.44	-0.02
Fe	511	4	45	0.1	0.10	(-1.75) ¹	0.62	0.75	-0.93	-0.62	-0.10	0.89
Ga	0.54	0.24	0.13	1.76		NNR	-1.69	-3.94			0.00	5.99
Hf	0.0005	0.0153	0.0004	41.92			167.15	0.00				(-0.52) ²
Li	51	2.8	6.4	0.45		(2.09) ¹	-0.45	0.45	-0.99		-1.44	1.27
Mn	38190	690	1770	0.39	0.60	NR	-1.22	0.47	-0.39	0.39	-0.42	3.55
Mo	7.65	0.017	1.274	0.01	(0.38) ²	-0.38	-0.37	0.06	0.01	-0.33	-0.01	0.52
Nb	0.00057	0.00008	0.0004	0.19				-0.19				(0.19) ²
Ni	0.16	0.06	0.05	1.35	BDL	BDL	19.98	-1.32				0.00
Pb	0.106	0.004	0.034	0.13	BDL	(-0.67) ²	9.14	0.34		(-1.35) ²	-0.19	0.00
Rb	2.05	0.04	0.42	0.1		(-0.37) ¹	0.20	0.03			-0.45	0.00
Sb	0.0223	0.0014	0.0089	0.16	BDL		BDL	0.16				-0.16
Sc	0.76	0.13	0.18	0.73		(0.00) ¹	0.55	-4.27			1.33	-2.37
Se	1.53	0.05	0.32	0.15	BDL	-0.15	8.53	(-2.05) ²			0.22	0.15
Si	3653	57	240	0.24	0.24	NNR	0.70		-0.62	-0.24	0.70	
Sn	0.04	0.019	0.015	1.27	BDL		-0.37	-0.27			4.82	0.00
Sr	555.5	0.7	48.5	0.01	-0.01	(-1.57) ¹	0.01	0.90	0.66	-0.70	-0.07	0.56
Ta	0.00021	0.0046	0.00017	27.07			107.64	(-0.64) ²				(0.00) ²
Th	0.0028	0.0101	0.0015	6.63		(-1.17) ¹	26.51	-0.01			133.30	0.00
Ti	0.819	0.022	0.191	0.12	BDL	(0.12) ¹	-0.12	-3.47	BDL			16.66
Tl	0.00024	0.00015	0.00019	0.78				-0.78				(0.78) ²
U	0.00416	0.00011	0.00215	0.05		(-0.85) ¹	0.85	-0.05				0.05
V	0.25	0.21	0.07	2.96	BDL		8.80	-3.14			0.00	-3.03
W	0.113	0.004	0.036	0.11		(-0.10) ¹	5.96	-0.16			0.00	0.33
Y	0.03	0.0004	0.0115	0.04		(-0.41) ¹	-0.09	0.06			0.00	0.11
Zn	9.2672	0.0005	1.4994	0	(-1.51) ²	-0.31	1.20	0.00	3.82	0.00	-0.53	0.42
Zr	0.025	0.005	0.01	0.49		(0.49) ¹	BDL	-0.70		349.6	-0.49	(-0.85) ²

Notes: Italics: provisional scores for elements with large uncertainty on the assigned value X_a . **Bold:** Unacceptable data ($|z| > 3$).

¹Acceptable ($|z| < 3$) data reported for an element not normally reported. NNR: Data unacceptable ($|z| > 3$), but for an element not normally reported.

²Acceptable ($|z| < 3$) data reported below normal reporting limits for laboratory. BDL: Data unacceptable ($|z| > 3$), but below normal reporting limits.

Table 38.A1, continued.

	X _a	u(X _a)	H _a	u(X _a)/H _a	Laboratory ID							
					1	2	3	4	5	6	7	8
REE (ppt)												
La	9	0.9	4.1	0.22		(-1.61) ¹	(0.00) ²	4.38			0.24	-0.63
Ce	23.3	1	9.3	0.11		(-0.65) ¹	(0.25) ²	2.43			0.00	-0.18
Pr	3.09	0.18	1.67	0.11			(0.14) ²	0.00				-0.28
Nd	15.7	0.7	6.6	0.11			(-0.11) ²	-0.31			0.14	0.11
Sm	4.53	0.12	2.31	0.05			(-0.09) ²	0.13				0.00
Eu	6.3	2.3	3.1	0.76		(1.08) ¹	-0.76	0.76				-2.23
Gd	4.8	0.4	2.4	0.16			(0.06) ²	-0.58				0.00
Tb	0.79	0.25	0.52	0.47			1.36	0.00				-0.51
Dy	3.71	0.09	1.95	0.05			-0.02	0.17				0.00
Ho	1	0.16	0.64	0.24			0.00	0.44				-0.54
Er	2	0.027	1.153	0.02			0.00	0.02				-0.07
Tm	0.23	0.2	0.18	1.12			BDL	0.00				-0.20
Yb	1.29	0.14	0.79	0.18			(0.48) ²	0.00				-0.25
Lu	0.2	0.03	0.17	0.20				0.20				-0.20
Anions (ppm)												
Br ⁻	0.441	0.73	0.04	18.22		-0.94	-0.73	0.73		2.73	-1.03	4.05
Cl ⁻	200.4	0.15	7.2	0.02	-0.33	-0.43	1.15	-0.15	2.09	0.15	-1.44	0.71
F ⁻	2.4	0.18	0.17	1.05	0.00	-5.65	-0.08	1.66	-4.41	0.62		1.93
NO ₃ ⁻	0.145	0.37	0.016	23.96	-0.52	-4.61	0.00	-0.64		3.55	0.97	39.01
PO ₄ ⁻	0.0187				0.00							
SO ₄ ⁻	58.5	0.22	2.5	0.09	1.02	-6.29	-0.80	-0.61	-0.22	0.22	0.32	0.24

Notes: *Italics:* provisional scores for elements with large uncertainty on the assigned value X_a . **Bold:** Unacceptable data ($|z| > 3$).

¹Acceptable ($|z| < 3$) data reported for an element not normally reported. NNR: Data unacceptable ($|z| > 3$), but for an element not normally reported.

²Acceptable ($|z| < 3$) data reported below normal reporting limits for laboratory. BDL: Data unacceptable ($|z| > 3$), but below normal reporting limits.

Table 38.A2. Parameters used in the calculation of z-scores and laboratory z-scores for the analysis of in-house QCM BLK-2.

	Laboratory ID											
	X _a	u(X _a)	H _a	u(X _a)/H _a	1	2	3	4	5	6	7	8
Majors (ppm)												
Ca	161.7	0.7	6	0.12	0.53	-3.71	0.35	-2.80	-1.22	0.12	-0.12	0.59
Mg	47.9	0.6	2.1	0.3	-0.30	-1.08	1.00	-3.92	-0.32	1.09	0.30	0.53
Na	7.88	0.11	0.46	0.23	0.22	-0.98	3.25	-1.96	0.00		-0.70	1.39
K	0.833	0.0017	0.0685	0.02	BDL	-1.39	14.29	0.00	-0.09		0.00	7.62
Traces (ppb)												
Ag	0.0066	0.0022	0.0032	0.68		(-2.08) ¹		0.00				0.64
Al	2.09	0.09	0.42	0.22	BDL		-1.65	-1.14		BDL	-0.22	(0.22) ²
As	0.204	0.01	0.058	0.17	BDL	(0.17) ²	6.66	-1.31		(-0.17) ²		-1.42
B	61.6	1.3	7.5	0.17	0.00	(0.04) ¹	0.04	-1.19	-0.65		0.06	-2.25
Ba	47.8	0.9	6	0.15	0.17	(-1.23) ¹	0.15	-4.61	0.42	-0.15	0.72	-2.64
Be	0.003	0.0008	0.0016	0.49			(0.00) ²	0.73				(-1.25) ²
Bi	0.0007	0.0014	0.0004	3.21			BDL	(-0.83) ²				(0.00) ²
Cd	0.046	0.003	0.017	0.21		BDL	-0.56	0.28		0.00		-0.64
Co	0.2	0.09	0.06	1.531	BDL	0.00	2.71	-3.40				-4.23
Cr	0.13	0.06	0.04	1.48	BDL	(1.48) ²	(2.23) ²	-1.58			17.26	-1.48
Cs	0.0006	0.0082	0.0004	18.94			BDL	(0.00) ²				-0.50
Cu	1.86	0.1	0.38	0.25	BDL	0.16	2.30	-1.65		-0.86	5.84	0.00
Fe	33.2	1.3	4.4	0.29	-1.03	NNR	0.94	0.00	-2.91	0.79		0.11
Ga	0.0039	0.0119	0.002	5.85		NNR	(-0.69) ²	0.00			22.73	-0.77
Hf	0.00037	0.01843	0.00028	66.82			267.01	0.00				(-0.28) ²
Li	4.23	0.07	0.77	0.09		NNR	0.35	-0.02			0.00	-0.50
Mn	2.7	0.22	0.53	0.41	(0.39) ²	(0.14) ¹	-1.51	-3.27	4.38		0.00	BDL
Mo	3.22	0.04	0.61	0.07	BDL	-0.90	-0.07	-0.67	-0.36	0.07	0.13	0.39
Nb	0.0007	0.0042	0.0005	8.9			36.64	-0.98				(0.00) ²
Ni	0.85	1.26	0.2	6.38	BDL	24.36	36.84	-1.15				0.00
Pb	0.051	0.065	0.018	3.55	BDL	(-0.68) ²	13.67	-0.53			24.67 ³	0.00
Rb	0.535	0.015	0.133	0.12		(0.00) ¹	0.51	-0.68			-0.24	0.22
Sb	0.01	0.044	0.005	9.81	BDL		BDL	0.00				-0.43
Sc	0.91	0.19	0.21	0.92		(0.56) ¹	0.00	-4.34			(0.41) ²	-3.29
Se	0.32	0.16	0.09	1.86	BDL	BDL	BDL	(0.00) ²				-0.61
Si	4352	124	279	0.44	0.44	(-2.05) ¹	0.50		-1.11	-0.44	0.59	
Sn	0.0044	0.0055	0.0022	0.38	BDL		1.67	-1.67				-1.74
Sr	12011	37	661	2.45	1.37	NNR	-0.06	-18.18	0.49	-0.31	0.06	2.32
Ta	0.00014	0.00723	0.00012	59.72			238.24	(0.00) ²				(-0.64) ²
Th	0.0008	0.0073	0.0005	14.3			56.40	-0.81			174.2 ³	(0.00) ²
Ti	0.53	0.28	0.13	2.12	BDL	(2.12) ¹	2.14	-3.92	77.01			-2.12
Tl	0.0638	0.0005	0.0218	0.02		(-1.23) ¹	(-0.02) ²	0.07		0.02	-0.02	0.12
U	1.527	0.005	0.324	0.02		(0.02) ¹	-0.31	-0.04	-1.63	0.00	0.03	0.22
V	0.097	0.017	0.031	0.55	BDL	(0.55) ¹	1.12	-0.55		BDL		-0.73
W	0.00185	0.00030	0.003	0.28				5.00 ⁴		16700 ³		(-0.14) ²
Y	0.068	0.006	0.023	0.27		(-0.48) ¹	0.00	1.30			-0.49	0.60
Zn	113	4	13	0.31	0.42	-1.65	0.31	-0.86	0.34	0.39	-0.31	-0.38
Zr	0.013	0.053	0.006	9.24			16.38	0.00		10160 ³		(-2.09) ²

Notes: Italics: provisional scores for elements with large uncertainty on the assigned value X_a . **Bold:** Unacceptable data ($|z| > 3$).

¹Acceptable ($|z| < 3$) data reported for an element not normally reported. NNR: Data unacceptable ($|z| > 3$), but for an element not normally reported.

²Acceptable ($|z| < 3$) data reported below normal reporting limits for laboratory. BDL: Data unacceptable ($|z| > 3$), but below normal reporting limits.

³Removed from data set before calculation of assigned value.

⁴One replicate removed before calculation of assigned value. All replicates used for calculation of z-score.

Table 38.A2, continued.

	X _a	u(X _a)	H _a	u(X _a)/H _a	Laboratory ID							
					1	2	3	4	5	6	7	8
REE (ppt)												
La	4.8	1.5	2.4	0.63			(0.63) ²	-0.63			2.14	-0.93
Ce	1.297	0.03	0.798	0.04				0.04				(-0.04) ²
Pr	0.55	0.15	0.38	0.39			(1.19) ²	0.00				-0.37
Nd	2.8	0.6	1.6	0.36			(0.75) ²	0.00				(-0.67) ²
Sm	1	0.16	0.64	0.26			(0.00) ²	0.02				-1.00
Eu	4.7	3.1	2.4	1.32			0.00	2.55				-2.73
Gd	0.7608	0.0025	0.5072	0.00				0.00				(0.00) ²
Tb	0.36	0.24	0.27	0.89			2.36	0.00				-1.19
Dy	0.79	0.17	0.52	0.33			(0.41) ²	0.00				(-0.89) ²
Ho	0.9	0.8	0.6	1.28				1.28				-1.28
Er	0.69	0.13	0.47	0.27			0.66	0.00				(-0.42) ²
Tm	0.13	0.23	0.11	2.04			7.84	0.00				-0.31
Yb	0.45	0.16	0.33	0.49			(1.68) ²	0.00				(-0.28) ²
Lu	0.099	0.008	0.089	0.09				-0.09				(0.09) ²
Anions (ppm)												
Br ⁻	0.1											0.00
Cl ⁻	5.42	0.47	0.34	1.38	0.82	-4.61	-0.47	-0.81	2.02	-1.24	1.29	0.47
F ⁻	1.51	0.13	0.11	1.15	0.00	-5.32	0.40	2.20	-5.79	-0.12		2.69
NO ₃ ⁻	3.17	0.088	0.21	0.41	0.74	-5.28	0.09	-0.09	-0.09	-0.79	1.72	58.39
PO ₄ ⁻	0.0132	1.6	0.002	774.2	1.56					-1.56		
SO ₄ ⁻	384	0.05	13	0	0.05	0.84	-0.05	-0.75	0.64	-0.39	-1.95	1.57

Notes: *Italics:* provisional scores for elements with large uncertainty on the assigned value X_a . **Bold:** Unacceptable data ($|z| > 3$).

¹Acceptable ($|z| < 3$) data reported for an element not normally reported. NNR: Data unacceptable ($|z| > 3$), but for an element not normally reported.

²Acceptable ($|z| < 3$) data reported below normal reporting limits for laboratory. BDL: Data unacceptable ($|z| > 3$), but below normal reporting limits.

³Removed from data set before calculation of assigned value.

⁴One replicate removed before calculation of assigned value. All replicates used for calculation of z-score.

Table 38.A3. Parameters used in the calculation of z-scores and laboratory z-scores for the analysis of in-house QCM WANA-1.

	Laboratory ID											
	X _a	u(X _a)	H _a	u(X _a)/H _a	1	2	3	4	5	6	7	8
Majors (ppm)												
Ca	8	0.05	0.47	0.11	0.96	-2.04	0.78	-0.69	0.11	-0.11	2.07	-0.38
Mg	2.0443	0.0023	0.1468	0.02	-0.55	-1.69	0.24	-0.99	0.02	-0.02	2.49	0.21
Na	1.82	0.02	0.133	0.15	0.91	-1.85	12.06	-0.72	0.00		-0.11	0.50
K	0.4767	0.0007	0.0426	0.02	(-1.70) ²	-2.74	42.45	-0.07	0.31		0.00	0.00
Traces (ppb)												
Ag	0.051	0.006	0.018	0.31			0.38	-2.28		0.31		-0.31
Al	22.03	0.03	3.13	0.01	BDL	NNR	1.25	0.01	-0.01	1.75	2.65	-0.23
As	0.641	0.017	0.155	0.11	BDL	(-0.40) ²	1.22	0.00		(-0.35) ²	0.38	-0.06
B	17	1.6	2.5	0.62	(-1.70) ²	(1.28) ¹	1.12	-3.47	0.00		0.80	-2.74
Ba	14.686	0.019	2.217	0.01	(-0.16) ²	(-0.83) ¹	0.10	0.01	-0.01	0.11	0.90	-0.56
Be	0.00845	0.00012	0.00392	0.03		(-0.29) ¹	(-0.03) ²	0.59				(0.03) ²
Bi	0.0031	0.0006	0.0017	0.36			(-1.26) ²	0.00				(0.19) ²
Cd	0.0255	0.0016	0.01	0.16		(-0.68) ²	0.62	0.75		-0.01		0.00
Co	0.0435	0.0016	0.0158	0.1	BDL	(-0.85) ²	6.68	0.10			-1.49	-0.10
Cr	0.23	0.021	0.065	0.32	BDL	(-0.68) ²	6.62	0.33		-0.32		0.32
Cs	0.003106	0.000023	0.001676	0.01				0.01				-0.01
Cu	4.9	0.1	0.87	0.12	BDL	0.12	0.38	-0.12	0.12	-0.63	0.15	-0.23
Fe	67	5	8	0.63	-0.63	NNR	0.82	0.63	-1.94	0.92	-0.70	0.98
Ga	0.008	0.024	0.004	6.32		NNR	(0.00) ²	-0.80			24.95	-0.34
Hf	0.02027	0.00027	0.00824	0.03			1.26	0.03			-0.03	-0.36
Li	0.42	0.06	0.11	0.57		(1.56) ¹	(1.71) ²	-0.71			-0.77	0.00
Mn	4.4	1.4	0.8	1.8	18.34	NNR	-1.80	-2.45	3.62	-3.58	1.80	-2.16
Mo	0.1351	0.0006	0.0413	0.01	BDL		1.42	-0.01		0.27	-0.85	0.01
Nb	0.0192	0.0008	0.0079	0.1		(-0.70) ¹		0.12			0.10	-0.10
Ni	17.7	0.25	2.6	0.1	(-1.62) ²	0.10	0.18	-0.10	0.11	-0.53	0.31	-0.38
Pb	0.133	0.01	0.041	0.24	BDL	(-0.83) ²	10.73	0.00		(-1.27) ²	-0.80	0.15
Rb	1.169	0.011	0.258	0.04		(0.00) ¹	0.07	-0.17			0.16	-0.10
Sb	0.073	0.004	0.025	0.15	BDL		(1.49) ²	0.37			0.00	-0.21
Sc	0.09	0.023	0.029	0.78		(-0.78) ¹	13.46	-2.96				0.78
Se	0.2516	0.0019	0.0701	0.03	BDL		BDL	(0.03) ²				-0.03
Si	2290	41	162	0.25	0.29	NNR	0.25		-0.91	-0.25	0.84	
Sn	0.065	0.007	0.022	0.32	BDL		0.00	-0.47			0.96	-0.31
Sr	20.96	0.04	3	0.01	0.45	(-1.16) ¹	0.62	-0.01	0.01	-0.12	0.96	-0.08
Ta	0.02	0.004	0.008	0.43			1.63	-0.43			(0.43) ²	-0.72
Th	0.0059	0.00007	0.00289	0.03		(-1.47) ¹	5.45	0.03				-0.03
Ti	0.55	0.07	0.14	0.49	BDL	(0.00) ¹	2.45	-1.23				0.71
Tl	0.0037	0.0004	0.002	0.18				-0.18				0.18
U	0.0383	0.0004	0.0142	0.03		(0.07) ¹	0.00	-0.17			0.12	-0.04
V	0.139	0.011	0.042	0.26	BDL	(-1.23) ¹	0.98	0.00				-0.04
W	0.0297	0.0003	0.0114	0.03			18.77	-0.69			0.03	-0.03
Y	0.0508	0.0007	0.018	0.04		(-0.08) ¹	0.07	-0.12			0.14	0.00
Zn	26.77	0.1	3.69	0.03	-0.10	-1.14	0.39	1.55	-0.03	0.42	0.03	-0.04
Zr	0.07	0.012	0.024	0.51		(2.85) ¹	1.98	-0.07			0.00	(-0.33) ²

Notes: *Italics:* provisional scores for elements with large uncertainty on the assigned value X_a . **Bold:** Unacceptable data ($|z| > 3$).

¹Acceptable ($|z| < 3$) data reported for an element not normally reported. NNR: Data unacceptable ($|z| > 3$), but for an element not normally reported.

²Acceptable ($|z| < 3$) data reported below normal reporting limits for laboratory. BDL: Data unacceptable ($|z| > 3$), but below normal reporting limits.

³Removed from data set before calculation of assigned value.

Table 38.A3, continued.

Laboratory ID												
	X _a	u(X _a)	H _a	u(X _a)/H _a	1	2	3	4	5	6	7	8
REE (ppt)												
La	50	1.2	17.8	0.07		(-0.32) ¹	0.04	0.01			0.00	-0.26
Ce	59.3	1.4	20.5	0.07		(-0.60) ¹	(0.00) ²	0.00			0.04	-0.27
Pr	11.5	0.5	5.1	0.1			0.16	0.10			-0.30	-0.10
Nd	49.76	0.24	17.68	0.01			0.01	-0.01			0.39	-0.27
Sm	9.4	0.8	4.3	0.18			(-0.09) ²	0.26	230.9 ³			0.00
Eu	4.4	1.1	2.2	0.47		(0.57) ¹	-0.47	0.47				-1.47
Gd	8.83	0.17	4.07	0.04			(0.04) ²	-0.04			(2.74) ²	-0.14
Tb	1.8	0.6	1	0.56			1.69	0.00				-0.56
Dy	7.38	0.05	3.49	0.01			-0.01	0.01			(0.75) ²	-0.48
Ho	1.42	0.25	0.86	0.29			-0.10	1.05				0.00
Er	4.8	0.11	2.43	0.05			-0.06	0.12				0.00
Tm	0.8	0.5	0.6	0.82			3.01	0.00				-0.26
Yb	4.75	0.19	2.4	0.08			0.10	0.00				-0.21
Lu	0.99	0.05	0.63	0.08			0.02	0.00				-0.29

Notes: *Italics:* provisional scores for elements with large uncertainty on the assigned value X_a . **Bold:** Unacceptable data ($|z| > 3$).

¹Acceptable ($|z| < 3$) data reported for an element not normally reported. NNR: Data unacceptable ($|z| > 3$), but for an element not normally reported.

²Acceptable ($|z| < 3$) data reported below normal reporting limits for laboratory. BDL: Data unacceptable ($|z| > 3$), but below normal reporting limits.

³Removed from data set before calculation of assigned value.

Table 38.A4. Parameters used in the calculation of z-scores and laboratory z-scores for the analysis of CRM SLRS-4.

	Laboratory ID											
	X _a	u(X _a)	H _a	u(X _a)/H _a	1	2	3	4	5	6	7	8
Majors (ppm)												
Ca	6.2	0.2	0.38	0.53	0.25	-2.45	-0.01	-3.03	-0.37	-0.92	1.03	-1.11
Mg	1.6	0.1	0.12	0.83	-0.25	-0.91	0.26	-1.37	0.50	0.08	2.85	0.24
Na	2.4	0.2	0.17	1.18	-1.07	-1.94	-2.07	-1.96	-0.36		-0.63	-1.08
K	0.68	0.02	0.058	0.34	(-2.30) ²	-2.40	-0.26	-0.96	-0.17		-0.17	0.35
Traces (ppb)												
Ag	0.035	0.01	0.013	0.76				-2.53				-2.64
Al	54	4	7	0.60	(-1.03) ²	(-1.39) ¹	-0.40	-0.65	0.15	0.12	2.54	-0.45
As	0.68	0.06	0.16	0.37	BDL	(0.45) ²	0.18	0.20		(0.67) ²	0.74	0.47
B	5.95	0.22	1	0.21	BDL		4.75	-0.54			1.99	-0.24
Ba	12.2	0.6	1.9	0.32	(-0.21) ²	(-0.89) ¹	0.43	0.22	0.42	0.21	0.96	-0.10
Be	0.007	0.002	0.003	0.60			(-1.20) ²	0.68				(0.23) ²
Bi	0.0022	0.0002	0.0012	0.16				-2.04				(-0.93) ²
Cd	0.012	0.002	0.005	0.38		(-0.19) ²	1.33	1.05				0.09
Co	0.033	0.006	0.012	0.48	BDL	(-1.68) ²	1.84	0.02				-0.01
Cr	0.33	0.02	0.09	0.23	BDL	(0.15) ²	(1.59) ²	-0.19		-0.85		-0.37
Cs	0.009	0.002	0.004	0.48			(0.24) ²	-0.76				-0.59
Cu	1.81	0.08	0.4	0.21	BDL	0.47	0.61	-0.04		0.02	1.04	0.12
Fe	103	5	12	0.43	-1.28	NNR	0.33	-0.09	-2.76	-3.59	-0.95	0.22
Ga	0.0119	0.0008	0.005	0.15		NNR	-0.17	-1.02				0.72
Hf	0.0033	0.0006	0.0018	0.34			0.96	-0.58				(-0.15) ²
Li	0.54	0.14	0.13	1.04		(2.86) ¹	(-0.30) ²	-0.49			0.45	-0.52
Mn	3.37	0.18	0.6	0.28	(-1.06) ²	(0.84) ¹	1.08	-0.06	0.99	-0.27	1.07	-0.33
Mo	0.21	0.02	0.06	0.33	BDL		0.45	-1.69		-0.47	-1.83	-0.02
Nb	0.0041	0.0003	0.0021	0.14				-0.69				-0.26
Ni	0.67	0.08	0.16	0.50	BDL	(1.22) ²	4.29	-0.16			-1.06	-0.05
Pb	0.086	0.007	0.028	0.25	BDL	(-1.92) ²	18.23	-0.29		(-2.06) ²		-0.27
Rb	1.53	0.1	0.3	0.31		(0.15) ¹	0.28	-0.10			0.37	0.15
Sb	0.23	0.04	0.06	0.62	BDL		1.39	0.83		0.77	0.62	0.30
Sc	0.012	0.001	0.005	0.19			73.27	-1.91				BDL
Se	0.23	0.06	0.06	0.92	BDL	BDL	(-0.46) ²	(-1.47) ²				-0.25
Si	1864	96	136	0.71	0.89	(-2.49) ¹	0.88		0.85	0.29	1.62	
Sn	0.01	0.002	0.005	0.44	BDL			-2.80				-1.47
Sr	26.3	3.2	4	0.88	2.69	(-0.30) ¹	1.18	0.48	2.39	0.36	1.86	0.67
Ta	0.0003	0.0002	0.00023	0.87				(-0.60) ²				-1.30
Th	0.018	0.006	0.007	0.81			0.40	-0.76				-0.70
Ti	1.46	0.16	0.31	0.51	BDL	(-0.91) ¹	0.67	-0.93	(-1.47) ²			-0.64
Tl	0.0076	0.0012	0.004	0.33				-0.43				-0.27
U	0.05	0.003	0.018	0.17		(-0.39) ¹	0.34	-0.14			0.00	-0.04
V	0.32	0.03	0.09	0.35	BDL	(0.06) ¹	0.70	0.17			-1.40	0.51
W	0.0133	0.002	0.006	0.35				-2.19				-1.72
Y	0.146	0.016	0.04	0.36		(-0.18) ¹	-0.11	-0.32			0.32	-0.18
Zn	0.93	0.1	0.21	0.47	(-2.02) ²	11.22	13.02	0.42			0.33	1.89
Zr	0.12	0.03	0.04	0.80		(0.51) ¹	-0.35	-1.69			-1.34	-0.94

Notes: *Italics:* provisional scores for elements with large uncertainty on the assigned value X_a . **Bold:** Unacceptable data ($|z| > 3$).

¹Acceptable ($|z| < 3$) data reported for an element not normally reported. NNR: Data unacceptable ($|z| > 3$), but for an element not normally reported.

²Acceptable ($|z| < 3$) data reported below normal reporting limits for laboratory. BDL: Data unacceptable ($|z| > 3$), but below normal reporting limits.

Table 38.A4, continued.

	Laboratory ID											
	X _a	u(X _a)	H _a	u(X _a)/H _a	1	2	3	4	5	6	7	8
REE (ppt)												
La	287	16	80	0.2		(-0.47) ¹	-0.28	0.08			-0.22	-0.22
Ce	360	24	90	0.25		(-0.35) ¹	-0.28	0.12			-0.11	-0.23
Pr	69.3	3.6	23	0.15			-0.27	-0.11			0.03	-0.23
Nd	269	28	70	0.38			-0.39	-0.39			-0.26	-0.27
Sm	57.4	5.6	20	0.28			-0.42	-0.12			-0.37	-0.26
Eu	8	1.2	4	0.32		(0.27) ¹	0.27	0.57				-0.34
Gd	34.2	4	13	0.31			(-0.02) ²	-0.14			-0.33	0.15
Tb	4.3	0.8	2.2	0.36			-0.14	0.51				-0.15
Dy	24.2	3.2	10	0.33			-0.23	-0.17			0.61	0.13
Ho	4.7	0.6	2.4	0.25			-0.29	0.19				-0.01
Er	13.4	1.2	6	0.21			-0.24	0.12			-0.59	0.12
Tm	1.7	0.4	1	0.4			0.30	-0.05				-0.15
Yb	12	0.8	5	0.15			-0.38	-0.01			1.51	-0.27
Lu	1.9	0.2	1.1	0.18			0.09	-0.13				0.30

Notes: *Italics:* provisional scores for elements with large uncertainty on the assigned value X_a . **Bold:** Unacceptable data ($|z| > 3$).

¹Acceptable ($|z| < 3$) data reported for an element not normally reported. NNR: Data unacceptable ($|z| > 3$), but for an element not normally reported.

²Acceptable ($|z| < 3$) data reported below normal reporting limits for laboratory. BDL: Data unacceptable ($|z| > 3$), but below normal reporting limits.

Table 38.A5. Parameters used in the calculation of z-scores and laboratory z-scores for the analysis of CRM SLRS-5.

	Laboratory ID											
	X _a	u(X _a)	H _a	u(X _a)/H _a	1	2	3	4	5	6	7	8
Majors (ppm)												
Ca	10.5	0.4	0.59	0.68	0.76	-2.63	0.01	-1.33	-0.25	-0.51	0.34	-0.75
Mg	2.54	0.16	0.18	0.89	-0.40	-1.69	0.00	-1.57	0.00	0.03	1.05	-0.22
Na	5.38	0.1	0.33	0.30	-0.46	-2.22	-1.71	-1.68	-0.27		-1.62	-1.43
K	0.839	0.036	0.069	0.52	0.47	-2.30	0.37	0.20	0.67		-0.49	1.90
Traces (ppb)												
Ag												
Al	49.5	5	6	0.80	(-0.88) ²	(-2.08) ¹	-0.39	-0.12	-0.48	0.14	1.29	-0.80
As	0.413	0.039	0.11	0.37	BDL	(0.03) ²	1.99	0.84		(0.11) ²	(0.82) ²	0.25
B												
Ba	14	0.5	2.1	0.23	(0.28) ²	(-0.85) ¹	0.14	0.04	-0.23	0.00	0.40	-0.84
Be	0.005	0.001	0.0025	0.40			(-1.19)	1.52				(1.06) ²
Bi												
Cd	0.006	0.0014	0.0029	0.48			0.17	1.25				(0.72) ²
Co	0.05	0.01	0.018	0.56	BDL	(-0.76) ²	2.73	0.12				-0.02
Cr	0.208	0.023	0.06	0.39	BDL	(-1.28) ²	(2.38)	0.36				0.55
Cs												
Cu	17.4	1.3	2.6	0.51	(-0.62)	0.38	0.39	0.22	0.43	-0.25	0.31	0.14
Fe	91.2	5.8	10	0.55	-1.13	NNR	0.23	0.09	-2.50	-3.51	-1.36	0.55
Ga												
Hf												
Li												
Mn	4.33	0.18	0.8	0.23	(2.38) ²	(1.21) ¹	1.67	0.01	0.85	-0.29	1.13	-0.32
Mo	0.5	0.1	0.13	0.80	BDL		-2.08	-3.09		-2.57	-2.79	-2.16
Nb												
Ni	0.476	0.064	0.12	0.53	BDL	(2.03) ²	5.14	-0.34			-1.46	-0.31
Pb	0.081	0.006	0.027	0.22	BDL	(-1.46) ²	14.94	0.54		(-2.13) ²		-0.03
Rb												
Sb	0.3	0.06	0.08	0.74	BDL		1.41	0.44		0.37	-0.18	-0.21
Sc												
Se												
Si												
Sn												
Sr	53.6	1.3	7	0.20	1.24	(-1.15) ¹	0.36	-0.22	0.14	-0.23	0.28	-0.13
Ta												
Th												
Ti												
Tl												
U	0.1	0.02	0.03	0.63		(-0.41) ¹	-0.13	-0.33		-0.53	-0.31	-0.31
V	0.317	0.033	0.09	0.39	BDL	(-0.56) ¹	0.97	0.32			-1.37	0.46
W												
Y												
Zn	0.845	0.095	0.2	0.48	BDL	BDL	BDL	-0.20			-0.23	(1.93) ²
Zr												

Notes: *Italics:* provisional scores for elements with large uncertainty on the assigned value X_a . **Bold:** Unacceptable data ($|z| > 3$).

¹Acceptable ($|z| < 3$) data reported for an element not normally reported. NNR: Data unacceptable ($|z| > 3$), but for an element not normally reported.

²Acceptable ($|z| < 3$) data reported below normal reporting limits for laboratory. BDL: Data unacceptable ($|z| > 3$), but below normal reporting limits.

Table 38.A6. Consensus values (“C.V.”) and uncertainties (“± U”) for in-house QCMs BLK-1 and BLK-2. All data in ppb (µg/mL) unless otherwise stated.

BLK-1						BLK-2					
	C.V.	± U	n	σ _{between}	σ _{within}		C.V.	± U	n	σ _{between}	σ _{within}
Provisional						Provisional					
Ca (ppm)	8.9	0.4	7	0.4	0.11	Ca (ppm)	162	4	6	4	1.3
Mg (ppm)	5.35	0.27	8	0.33	0.05	Mg (ppm)	48.2	1.5	7	1.7	0.4
Mn (ppm)	38.03	1.25	6	1.25	0.41	B	59	4	6	4	4
Cl ⁻ (ppm)	200	5	7	6	1	Ba	48	4	6	4	0.7
SO ₄ ²⁻ (ppm)	58.5	1.4	7	1.6	1.1	Mo	3.1	0.25	7	0.28	0.05
Ba	38.4	2.9	8	3.6	0.8	Tl	0.06	0.011	6	0.011	0.005
Mo	7.6	0.4	8	0.4	0.5	U	1.45	0.18	7	0.2	0.022
						Zn	111	8	8	9	2.3
Indicative						Indicative					
Al	11.9	1.7	7	1.9	3.1	Na (ppm)	7.7	0.5	6	0.5	0.13
Be	0.0047	0.0014	3	0.0008	0.0011	Cl ⁻ (ppm)	5.4	0.3	6	0.3	0.13
Cd	0.109	0.019	5	0.017	0.011	F ⁻ (ppm)	1.52	0.06	3	0.031	0.004
Cr	0.25	0.031	4	0.022	0.021	NO ₃ ⁻ (ppm)	3.22	0.18	6	0.18	0.02
Fe	505	34	8	42	17	SO ₄ ²⁻ (ppm)	384	11	8	13	1.2
Rb	2	0.13	5	0.12	0.03	Cd	0.042	0.01	4	0.007	0.0028
Se	1.55	0.12	3	0.06	0.11	Li	4.2	0.4	4	0.27	0.19
Sn	0.037	0.005	3	0.0028	0.007	Rb	0.53	0.07	5	0.06	0.04
Sr	554	32	8	39	8	Sc	0.98	0.11	3	0.29	0.015
W	0.114	0.011	4	0.008	0.008	Information					
Y	0.0293	0.0027	5	0.0024	0.0017	K (ppm)	0.81	0.06	4	0.05	0.008
Zn	9.1	1.1	7	1.3	0.8	Sr (ppm)	12.22	0.50	5	0.44	0.099
Ce (ppt)	22	4.9	4	4	3	Al	1.8	0.5	4	0.4	1
Pr (ppt)	3.02	0.66	3	0.4	0.4	As	0.16	0.07	4	0.05	0.018
Nd (ppt)	15.5	1.9	4	1.4	3.2	Cu	1.6	0.4	4	0.3	0.05
Sm (ppt)	4.57	0.46	3	0.25	0.4	Fe	34	4	5	3	2
Dy (ppt)	3.81	0.38	3	0.21	0.4	Ga	0.0029	0.0016	3	0.0009	0.0018
Er (ppt)	1.98	0.1	3	0.06	0.29	Hf	0.00033	0.00017	2	0.00006	0.0001
Yb (ppt)	1.35	0.54	3	0.29	0.4	Mn	2.6	0.6	4	0.5	1.4
Information						Pb	0.044	0.012	3	0.007	0.004
Na (ppm)	205	7	5	6	1.9	Si	4351	239	5	207	52
K (ppm)	2.27	0.18	5	0.16	0.04	V	0.1	0.04	4	0.027	0.011
Br ⁻ (ppm)	0.42	0.05	4	0.03	0.03	Y	0.072	0.02	5	0.018	0.004
F ⁻ (ppm)	2.53	0.18	5	0.16	0.08	La (ppt)	4	3.7	3	2	0.4
NO ₃ ⁻ (ppm)	0.144	0.016	4	0.011	0.0023	Ce (ppt)	1.3	0.13	2	0.04	0.33
As	0.69	0.26	4	0.19	0.07	Pr (ppt)	0.65	0.57	3	0.31	0.07
B	1835	158	5	137	27	Nd (ppt)	2.9	2	3	1.1	0.3
Co	0.062	0.027	4	0.019	0.011	Sm (ppt)	0.79	0.69	3	0.4	0.13
Cs	0.031	0.013	4	0.009	0.0026	Gd (ppt)	0.761	0.011	2	0.004	0.228
Cu	2.8	0.4	5	0.3	0.1	Dy (ppt)	0.7	0.64	3	0.3	0.05
Li	50	8	5	7	2.3	Er (ppt)	0.73	0.47	3	0.25	0.06
Nb	0.0006	0.0003	2	0.00011	0.00027	Tm (ppt)	0.111	0.074	2	0.024	0.03
Pb	0.094	0.025	5	0.022	0.013	Yb (ppt)	0.6	0.64	3	0.3	0.18
Sb	0.022	0.006	2	0.002	0.004	Lu (ppt)	0.099	0.035	2	0.012	0.05
Sc	0.87	0.22	3	0.67	0.04	Not Rated					
Si	3691	161	5	140	27	Br ⁻ (ppm)	0.1		1		
Th	0.0022	0.0019	3	0.001	0.00015	PO ₄ ³⁻ (ppm)	0.013	0.014	2	0.004	0.006
Ti	0.82	0.1	2	0.032	0.017	Ag	0.008	0.004	2	0.0014	0.003
U	0.0042	0.0021	4	0.0015	0.0006						
Zr	0.021	0.008	4	0.006	0.003						

Table 38.A6, continued.

BLK-1						BLK-2					
	C.V.	± U	n	σ _{between}	σ _{within}		C.V.	± U	n	σ _{between}	σ _{within}
Information (cont'd.)						Not Rated (cont'd.)					
La (ppt)	6.9	4.7	4	3	0.6	Be	0.0027	0.003	3	0.0016	0.0006
Eu (ppt)	7.5	5.6	3	3	0.7	Bi	0.0005	0.0008	2	0.00026	0.0004
Gd (ppt)	4.4	1.6	3	0.9	0.27	Co	0.2		1		
Tb (ppt)	0.94	0.93	3	0.5	0.13	Cr	0.11	0.12	3	0.07	0.016
Ho (ppt)	0.98	0.57	3	0.31	0.27	Cs	0.0005	0.0005	2	0.00015	0.00005
Tm (ppt)	0.208	0.078	2	0.026	0.013	Nb	0.0005	0.001	2	0.0003	0.0003
Lu (ppt)	0.2	0.14	2	0.05	0.04	Ni	0.7	0.5	2	0.16	0.05
Not Rated						Sb	0.009	0.004	2	0.0014	0.0007
PO ₄ ³⁻ (ppm)	N/A					Se	0.29	0.11	2	0.04	0.07
Ag	0.006	0.005	2	0.0016	0.0022	Sn	0.011	0.023	3	0.0003	0.0016
Bi	0.0011	0.0015	2	0.0005	0.0011	Ta	0.0001	0.00017	2	0.00005	0.000027
Ga	0.4	0.5	2	0.16	0.021	Th	0.0006	0.0009	2	0.00029	0.00025
Hf	0.0004	0.0004	2	0.00013	0.00004	Ti	N/A				
Ni	0.12	0.13	2	0.04	0.01	W	0.0018	0.0007	2	0.0002	0.0004
Ta	0.00016	0.00023	2	0.00008	0.00004	Zr	0.013		1		
Tl	0.0002	0.0006	2	0.00021	0.00018	Eu (ppt)	4.7		1		
V	0.25		1			Tb (ppt)	0.2	0.69	2	0.23	0.05
						Ho (ppt)	0.9	3.3	2	1.1	0.9

N/A: No consensus value available.

Table 38.A7. Consensus values (“C.V.”) and uncertainties (“± U”) for in-house QCM WANA-1 and CRM SLRS-5. All data in ppb (µg/mL) unless otherwise stated.

WANA-1						SLRS-5							
	C.V.	± U	n	σ_{between}	σ_{within}		C.V.	± U	n	σ_{between}	σ_{within}	Cert.	±
Provisional						Provisional							
Ca (ppm)	8.1	0.3	6	0.3	0.08	Ca (ppm)	10.5	0.3	6	0.3	0.09	10.5	0.4
Mg (ppm)	1.99	0.1	7	0.11	0.019	Mg (ppm)	2.44	0.12	7	0.13	0.026	2.54	0.16
As	0.66	0.09	6	0.09	0.07	Al	45	4	7	4	8	49.5	5
Ba	14.6	0.9	8	1.1	0.5	As	0.48	0.08	6	0.08	0.19	0.413	0.039
Cu	4.87	0.26	7	0.29	0.12	Ba	13.7	0.8	8	1	0.4	14	0.5
Ni	17.1	1.3	8	1.6	2.4	Cu	17.9	0.6	6	0.6	0.26	17.4	1.3
Sr	21.2	1.6	8	1.9	0.6	Mn	5	0.6	8	0.8	0.7	4.33	0.18
Zn	27.3	2.2	8	2.8	0.8	Sr	52	4	6	4	1.2	53.6	1.3
Indicative						Indicative							
Na (ppm)	1.79	0.13	6	0.13	0.08	Na (ppm)	4.95	0.25	6	0.25	0.05	5.38	0.1
Be	0.0087	0.002	4	0.0014	0.0025	Ga	0.0143	0.0031	3	0.0017	0.0035		
Cd	0.027	0.007	5	0.006	0.006	Li	0.44	0.06	4	0.04	0.026		
Fe	67	8	7	9	2.7	Rb	1.29	0.14	5	0.12	0.11		
Nb	0.018	0.004	4	0.003	0.0012	Sb	0.33	0.06	5	0.05	0.05	0.3	
Rb	1.17	0.04	5	0.03	0.02	Si	1920	38	5	33	50		
Si	2298	123	5	107	19	Ti	2.00	0.29	5	0.25	0.10		
U	0.0383	0.0018	5	0.0016	0.0007	U	0.091	0.004	5	0.003	0.004	0.1	
Y	0.0508	0.0022	5	0.0019	0.003	Y	0.1098	0.0028	5	0.0025	0.0019		
La (ppt)	48.1	3.5	5	3	2.6	La (ppt)	187	14	5	12	7		
Ce (ppt)	55.9	6.4	5	6	3.1	Ce (ppt)	229	22	5	19	8		
Pr (ppt)	11.4	1.5	4	1.1	0.7	Pr (ppt)	43	5	4	4	1.4		
Nd (ppt)	50.3	6.6	4	5	4	Nd (ppt)	167	16	4	12	7		
Sm (ppt)	9.6	1.4	3	0.8	0.7	Sm (ppt)	29.7	2.9	4	2.1	1.5		
Gd (ppt)	8.64	0.67	3	0.4	0.7	Dy (ppt)	16.0	1.9	4	1.3	3.7		
Er (ppt)	4.86	0.41	3	0.22	0.7	Er (ppt)	9.7	1.9	4	1.4	3.6		
Yb (ppt)	4.66	0.71	3	0.4	0.15	Tm (ppt)	1.52	0.13	3	0.07	0.41		
Lu (ppt)	0.93	0.2	3	0.11	0.22	Yb (ppt)	9.1	1.1	4	0.8	0.4		
Information						Information							
K (ppm)	0.46	0.04	5	0.03	0.026	K (ppm)	0.88	0.07	5	0.06	0.016	0.839	0.036
Ag	0.053	0.013	3	0.007	0.005	Cd	0.0081	0.0029	3	0.0016	0.0005	0.006	0.0014
Al	24	3	5	2.8	1.4	Co	0.06	0.04	4	0.027	0.003	0.05	
B	18	4	5	3.1	7	Cr	0.24	0.12	4	0.09	0.027	0.208	0.023
Bi	0.0025	0.0024	3	0.0013	0.0008	Cs	0.00380	0.00019	2	0.00006	0.00052		
Co	0.034	0.016	4	0.011	0.006	Fe	88	10	5	9	1.6	91.2	5.8
Cr	0.22	0.05	4	0.03	0.029	Mo	0.18	0.06	5	0.05	0.03	0.5	
Cs	0.0031	0.0001	2	0.00003	0.0002	Nb	0.00271	0.00005	2	0.00002	0.00018		
Ga	0.0069	0.0029	3	0.0016	0.0015	Th	0.008	0.007	3	0.004	0.0025		
Hf	0.022	0.008	4	0.006	0.0025	Tl	0.0035	0.0004	2	0.00012	0.0003		
Li	0.45	0.15	5	0.13	0.04	V	0.31	0.09	5	0.08	0.06	0.317	0.033
Mo	0.14	0.04	5	0.03	0.007	Zn	0.9	0.4	3	0.24	0.2	0.845	0.095
Pb	0.11	0.028	5	0.025	0.006	Zr	0.030	0.014	5	0.012	0.011		
Sb	0.083	0.026	4	0.019	0.02	Eu (ppt)	6.5	2.8	4	2	1.2		
Se	0.252	0.008	2	0.0028	0.076	Gd (ppt)	29	11	4	8	0.5		
Sn	0.066	0.02	4	0.014	0.006	Tb (ppt)	3.1	2.1	3	1.1	0.8		
Ta	0.022	0.012	4	0.009	0.0031	Ho (ppt)	3.6	1.4	3	0.8	0.4		
Th	0.004	0.004	3	0.0024	0.0004	Lu (ppt)	1.6	0.7	3	0.4	0.01		
Ti	0.53	0.25	3	0.13	0.06								
V	0.14	0.05	4	0.04	0.01								

Table 38.A7, continued.

WANA-1						SLRS-5							
	C.V.	± U	n	σ _{between}	σ _{within}		C.V.	± U	n	σ _{between}	σ _{within}	Cert.	±
Information (cont'd.)						Not Rated							
W	0.027	0.008	3	0.005	0.0005	Ag	N/A						
Zr	0.08	0.03	4	0.025	0.007	B	9	5	3	2.7	2.5		
Eu (ppt)	3.9	3	4	2.1	0.8	Be	0.006	0.007	3	0.004	0.0021	0.005	
Tb (ppt)	2.1	2.2	3	1.2	0.3	Bi	0.00012		1				
Dy (ppt)	7.6	2.5	4	1.8	0.9	Hf	0.003	0.006	3	0.003	0.003		
Ho (ppt)	1.7	1	3	0.5	0.5	Ni	0.47	0.25	4	0.18	0.02	0.476	0.064
Tm (ppt)	0.77	0.31	2	0.1	0.21	Pb	0.07	0.05	3	0.028	0.019	0.081	0.006
Not Rated						Sc	N/A		1				
Mn	4	6	2	2	1	Se	0.3	0.3	3	0.17	0.12		
Sc	0.09	0.1	2	1.1	0.016	Sn	0.0031		1				
Tl	0.0037	0.0015	2	0.0005	0.00023	Ta	0.00005	0.00019	2	0.00006	0.00003		
						W	0.008		1				

N/A: No consensus value available.

Geoscience Laboratories

39. Revision of the Calibration for Major Element Analysis of Geological Samples by Wavelength Dispersive X-Ray Fluorescence at the Geoscience Laboratories

G.L. Keating¹ and O.M. Burnham¹

¹Geosciences Laboratories, Ontario Geological Survey

INTRODUCTION

Analysis of geological samples for major elements in the Geoscience Laboratories (Geo Labs) by wavelength dispersive X-ray fluorescence spectrometry (WD-XRF) has been very successful for many years. In order to maintain the high quality of routine analyses, calibration maintenance, review of the robustness of the calibrations and verification of lower limits of detection (LLD) should be performed regularly, keeping in mind the requirements of the majority of clients. At the beginning of 2012, with a change in staff and a shift in the needs of a significant number of clients, a comprehensive review of the calibrations was undertaken.

In March 2012, it was determined that, after 7 years, the monitors used to compensate for instrument drift were no longer able to correct the calibrations adequately for instrument drift and the range of reference materials in the calibrations was not adequate to produce data that were suited to the needs of most clients. At that time, it was decided that an overhaul of the calibration for the major element method (method code XRF-M01) was required, and that a verification of the LLD should be undertaken as quickly as possible. The overhaul of the calibration allowed the implementation of several improvements, leading to a more comprehensive and robust method. The work to prepare the new calibrations, expand the list of measured elements and verify the LLDs and upper limits (UL) for reporting was completed in July 2012.

BACKGROUND

The performance of each method employed at the Geo Labs is monitored using control charts of the analysis of interlaboratory and in-house reference materials. In February and March of 2012, a review of the active control charts for the XRF-M01 method indicated that some of the light elements (e.g., Na and Al) were no longer in control, initiating an investigation into the overall performance and status of the calibrations and drift corrections for all the major elements. It was determined that the drift corrections were too large, leading to inaccuracies in the resulting data. Sample preparation was also reviewed and it was concluded that no modifications or significant revisions were necessary at this time. Due to the age of the previous calibrations, the only remedy for the inaccuracies caused by the drift monitors was an update to all the calibration measurements and a full reset of the measuring application on the spectrometers. The update offered an ideal and rare opportunity to implement critical improvements to the calibrations in order to meet the criteria for good XRF analysis using fundamental parameters (Lachance 1989; Willis and Duncan 2008), which was no longer being met for certain types of samples received by the Geo Labs, in particular, those with high concentrations of “minor” elements (e.g., Cr, Co, Ni, Cu, Zn, Sr and/or Ba).

With any change to a calibration, it is mandatory to verify the performance of the revised method and update the LLDs and ULs as necessary. This article presents a summary of the work done to update the calibrations and the revised figures of merit for the method.

*Summary of Field Work and Other Activities 2012,
Ontario Geological Survey, Open File Report 6280, p.39-1 to 39-4.*

© Queen's Printer for Ontario, 2012

ANALYTICAL WORK

The new spectrometer measuring application was built based on parameters provided by the instrument manufacturer (PANalytical) and those in use by Geo Labs in the previous version, using the fundamental parameters technique. It was expanded based on similar successful applications used in other research laboratories. In addition to the 10 major elements (Na, Mg, Al, Si, P, K, Ca, Ti, Mn, Fe), 8 other elements (S, V, Cr, Co, Ni, Cu, Zn, Ba) are now measured to complete the major element spectra and ensure optimal corrections are in place for XRF-M01 analysis². All of the measuring parameters were carefully optimized based on the types of samples received in the past and anticipated projects.

Fifty-two (52) certified reference materials (CRMs) were used to calibrate the spectrometer. Although both old and new fused-bead preparations were used to calibrate the spectrometer, some of the fused beads that were used in earlier calibrations were no longer viable because of devitrification. Where additional material was available, those materials were prepared anew with a high degree of accuracy and using the same sample:flux ratio as that used to prepare samples from ignited material. Some new materials were added to the calibrations to fill out and extend the ranges. The calibrations and sample analyses are based on “volatile free” values as determined by measurement of the loss on ignition. The loss-on-ignition values are integrated into the results from the spectrometers in a separate spreadsheet and then incorporated into the analytical results to the client.

An independent set of CRMs (AL-I, BCS-353, BCS-368, BCS-381, BHVO-2, BXMG-3, DTS-2, FeR-2, FeR-3, FeR-4, FK-N, GSP-2, MO-7, NIM-P, NIST-694, SARM-40, AN-G, BCR-32, BIR-1, GSR-2, GYP-A, IPT-62, JDo-1, JLS-1, JP-1, TIG-1 and UB-N) with a wide variety of compositions were freshly prepared to check the calibration regressions for all 19 elements over an extended range.

METHOD VERIFICATION

The ULs were estimated using a combination of the calibration and test set of CRMs. The highest value of either the calibration standards or successfully measured test standard was chosen, with a +10% window for extrapolation (Table 39.1 provides a summary of the final values).

The LLDs were estimated using measurements of 91 duplicate client samples and CRMs prepared routinely in the Geo Labs in the past year. By using duplicate analyses carried out on separate sample splits and analyzed on different days, it was possible to obtain an overall “method” LLD for each analyte that includes most of the major sources of variation (including those from sample preparation and within-run or between-run instrumental variations). The sample pairs were chosen based on their composition to ensure a broad sampling of rock types and ensure completeness over the entire desired range of analysis. The LLD calculations were based on the seminal article published by Thompson and Howarth (1976).

The data were grouped into 13 groups of 7 samples, each sample pair averaged and relative difference calculated. For each group, the mean concentration, group median difference, relative difference (%) and expected (95% relative) were calculated. The LLDs and optimal precisions that are achievable by the method were estimated from the regression of median differences against the group means. To minimize the effect of the highest concentration groups on the regression and the uncertainty in the calculated LLDs, only the lowest concentration groups (points closest to the LLD) were used for most elements. In most cases, a minimum of 5 groups (35 sample pairs) were used in the calculation, but, for elements for which most samples were considerably above the LLD (e.g., SiO₂ and Fe₂O₃), the most reliable estimates of the LLD were obtained using as few as 3 or 4 groups (21 to 28 samples). A typical set of plots used to evaluate the statistics for the data are in Figure 39.1. The final LLDs and best precisions are listed in Table 39.1 along with the number of groups used in their estimation.

² Although measured and quantified, the additional elements have yet to be added to the suite that is routinely reported from the method as their optimal counting times have yet to be established. This will be done in the coming months.

SUMMARY

The overhaul of the XRF-M01 method was informative and provided a detailed analysis of its performance for routine and many atypical samples. Based on the analyses used to verify the technique, several conclusions were reached:

- The method is accurate over a wide range of concentrations (up to 100% oxide) for many elements and yields results that are within accepted published uncertainties for a wide suite of CRMs.
- All figures of merit (LLD, UL, precision and accuracy) are now confirmed empirically for the total method, including preparation of fused beads.
- For several of the lighter element oxides (e.g., Al_2O_3 , SiO_2 and Na_2O), there *may* be room for improvement with respect to precision and/or LLD; the revised LLDs (0.02–0.04 weight %) are higher than those previously offered at the Geo Labs (0.01 weight % for all elements). However, higher detection limits for these elements may be expected owing to their poorer sensitivity and ease of contamination and it is likely that the previous values overestimated the abilities of the method.
- On the other hand, several of the other oxides yielded results that exceeded previous expectations, in particular CaO , MnO and P_2O_5 . For these analytes, in the process of verifying the updated calibrations, it has been possible to demonstrate LLDs as low as 0.002 to 0.006 weight %.

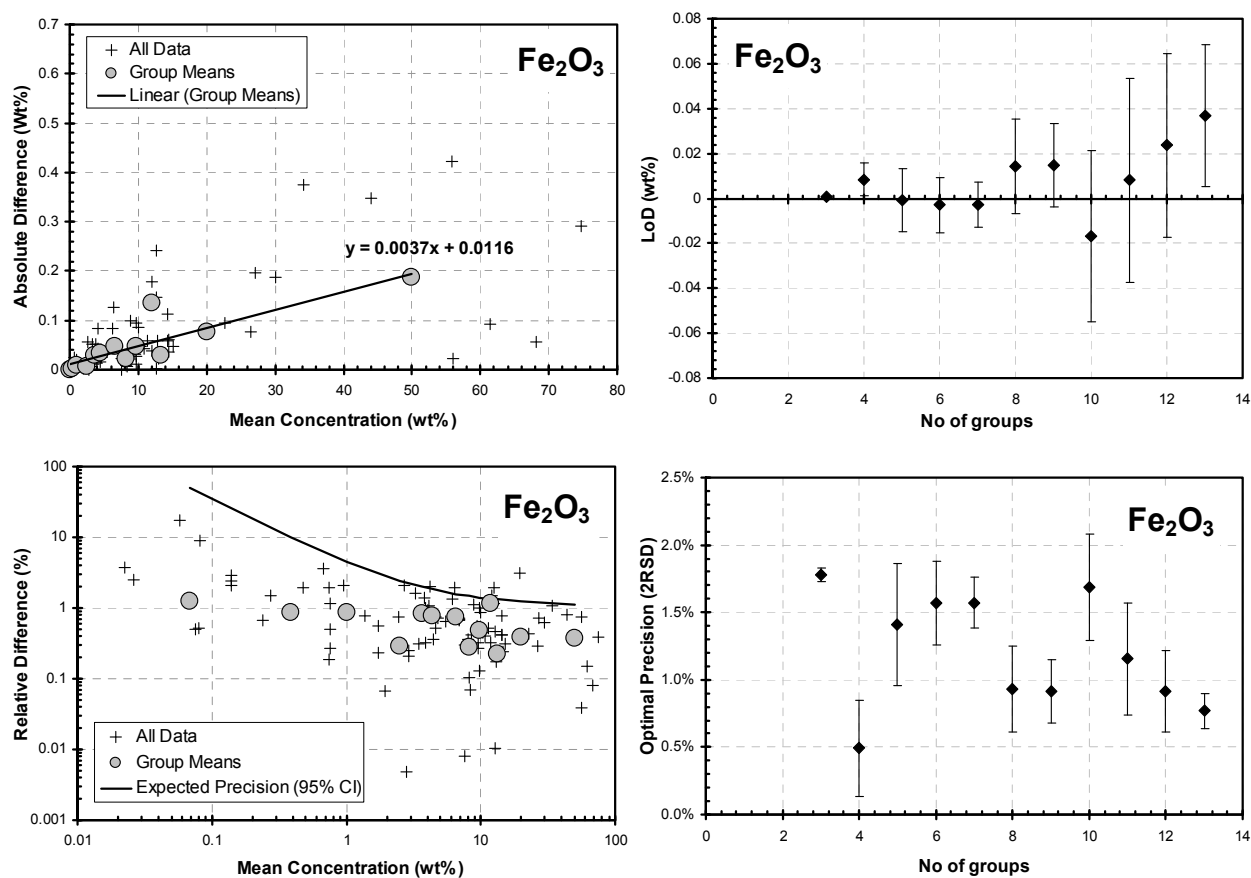


Figure 39.1. Plots summarizing the data used for the estimation of LLD and optimal precision for Fe_2O_3 analyses under method code XRF-M01. The most reliable estimate of the LLD was obtained using the 4 lowest concentration groups, whereas the most reliable estimate of the precision of the method at higher concentrations (>10 weight % Fe_2O_3) was obtained using the entire data set.

Table 39.1. Summary of lower limit of detection (LLD), precision and upper limit of reporting (UL).

Analyte	LLD (weight %)			Precision			UL
	# of Groups	Value	± 2SD	# of Groups	Value	± 2SD	
Major Elements							
SiO ₂	3	0.04	± 0.07	10	0.9%	± 0.2%	100 wt %
TiO ₂	10	0.01	± 0.003	13	0.8%	± 0.3%	8 wt %
Al ₂ O ₃	5	0.02	± 0.007	13	1.3%	± 0.2%	100 wt %
Cr ₂ O ₃	13	0.002	± 0.0004	13	1.2%	± 0.3%	5 wt %
Fe ₂ O ₃	4	0.01	± 0.007	13	0.8%	± 0.1%	100 wt %
MnO	9	0.002	± 0.0008	13	1.7%	± 0.5%	5 wt %
MgO	5	0.01	± 0.004	12	1.3%	± 0.1%	50 wt %
CaO	6	0.006	± 0.005	13	0.5%	± 0.1%	100 wt %
BaO	5	0.004	± 0.0008	13	0.1%	± 0.5%	1 wt %
Na ₂ O	8	0.02	± 0.0027	13	1.8%	± 0.2%	15 wt %
K ₂ O	7	0.01	± 0.0031	13	0.8%	± 0.1%	20 wt %
P ₂ O ₅	9	0.002	± 0.0005	13	0.45%	± 0.01%	40 wt %
SO ₃	13	0.027	± 0.006	13	3.2%	± 0.8%	60 wt %
Minor Elements							
Co	13	11.2	± 2.4	13	6.1%	± 1.9%	5000 ppm
Cu	12	13.9	± 2.7	13	0.7%	± 0.4%	15 000 ppm
Ni	13	8.3	± 1.1	13	0.9%	± 0.1%	15 000 ppm
V	8	7.8	± 0.9	13	1.9%	± 1.1%	7500 ppm
Zn	11	5.1	± 1.2	13	2.9%	± 0.2%	5000 ppm

Minor elements were determined with longer than optimal counting times. Estimated LLD may, therefore, be lower than those in final method.

ACKNOWLEDGMENTS

The effort to prepare and roll out a new calibration with improvements was quite extensive and many people contributed to the quality of the final product. In particular, 2 individuals were very instrumental in expediting the process: Natalie Chretien, who prepared many of the new fused beads for the reference materials and provided invaluable support to everyone (in addition to keeping ongoing sample preparation on track); and Georgina Rainsford, who prepared the groundwork of the spreadsheet for the statistical evaluation.

REFERENCES

- Lachance, G.R. 1989. Algorithms for the correction of matrix effects in X-ray fluorescence; *in* X-ray fluorescence analysis in the geological sciences: advances in methodology, Geological Association of Canada, Short Course Notes Volume 7, p.55-90.
- Thompson, M. and Howarth, R.J. 1976. Duplicate analysis in geochemical practice. Part I. Theoretical approach and estimation of analytical reproducibility; *Analyst*, v.101, p.690-698.
- Willis, J.P. and Duncan, A.R. 2008. Understanding XRF spectrometry, volume I: Basic concepts and instrumentation; PANalytical B.V., Almelo, Netherlands.

40. QA/QC: Summary of 2010–2012 Quality-Control Data at the Geoscience Laboratories

J. Hargreaves¹

¹Geoscience Laboratories, Ontario Geological Survey

INTRODUCTION

This paper summarizes the quality-control checks for 3 laboratory methods in the Geoscience Laboratories (Geo Labs) for the years 2010–2012: loss on ignition (LOI), inductively coupled plasma mass spectrometry (ICP–MS) with hydride-generation for the analysis of selenium and tellurium and ICP–MS water analysis. The information provided will help evaluate the precision and bias of the methods listed above.

In addition to the routine LOI analyses that are included in the determination of major elements by X-ray fluorescence (XRF) spectrometry (method code XRF-M01), the Geo Labs offer 4 LOI packages (Geoscience Laboratories 2009): 2 step (method code LOI-2ST), 3 step (method code LOI-3ST), 4 step (method code LOI-4ST) and lake sediment (LOI-LK1). In the routine method, the sample is heated to 105°C under N₂ atmosphere, then to 1000°C under O₂ atmosphere and the mass change is measured after each heating stage. The LOI-2ST and LOI-3ST method are similar in the first 2 steps of the procedure, measuring the mass change after heating samples to 100°C under N₂ atmosphere, then after heating to 500°C under O₂ atmosphere. However, the LOI-3ST method continues to a third step by heating to 1000°C under O₂ atmosphere. The LOI-4ST method heats samples first to 105°C under N₂ atmosphere, then to 371°C, 538°C and 900°C under O₂ atmosphere. The LOI-LK1 method heats the sample directly to 500°C and measures the mass change. In each method, the “Total LOI” reported represents the total change in mass up to the highest temperature achieved by the sample, so, the LOI-2ST and LOI-LK1 methods may not represent the total volatile content of the sample. These methods have been developed to accommodate 3 different types of samples: cement, lake sediment and geological samples. This summary will review results for certified reference material (CRM) BCS-353 and in-house reference material TLC used as quality assurance samples with the routine LOI method for cements (Table 40.1); LKSD-2, LKSD-3 and LKSD-4 used with the LOI-LK1 and LOI-2ST methods (Table 40.3); and a number of in-house materials, including LDI-2, LK-NIP-1, LLH-1, MRB-15, NPD-1, ODL-1, OKUM-1, ORCA-1 and QS-1, used with the routine LOI and LOI-4ST methods for geological samples (*see* Tables 40.1 and 40.2, respectively). Because the LOI-3ST method was performed infrequently in the period 2010–2012, there are insufficient data to present.

The hydride-generation ICP–MS method (IMH-100) utilizes in-house standards MRB-29 and OKUM-1 and CRMs GSR-3, GSR-4, MRG-1 and UB-N. Certified values for selenium and tellurium for the CRMs were not listed on the certificates for these materials; thus, the published results of Hall and Pelchat (1997), Terashima (2001) and Terashima and Imai (2000) have been provided for comparison (Table 40.4).

The ICP–MS waters method utilizes the CRMs SLRS-4 (discontinued) and SLRS-5 (river water reference materials for trace element analysis distributed by the National Research Council of Canada (NRC), Ottawa: Table 40.5). Whereas SLRS-4 has been characterized for a wide range of trace elements not present on the original certificate (e.g., Yeghicheyan et al. 2001; Rodushkin et al. 2005), the range of elements for which data are available for SLRS-5 is much smaller. With its inclusion in the round-robin study for the characterization of the in-house quality-control materials described by Burnham, Schroeder

and Hamilton (this volume, Article 38), it has been possible to characterize SLRS-5 for a greater number of elements. In March 2010, SLRS-5 replaced SLRS-4 as the primary CRM for the IMW-100 method.

Table 40.1. Summary of reference material data for the routine LOI method. All values in weight %.

Certified Reference Material		N ₂ at 105°C	O ₂ at 1000°C	Total LOI
Cements				
BCS-353	average ± SD	0.07 ± 0.13 (13)	1.89 ± 0.28 (13)	1.98 ± 0.26 (13)
In-House Reference Materials				
Cements				
TLC	average ± SD	0.29 ± 0.18 (50)	1.77 ± 0.33 (50)	2.08 ± 0.30 (50)
Geological Samples				
LDI-2	average ± SD	0.07 ± 0.07 (278)	2.66 ± 0.18 (278)	2.74 ± 0.18 (278)
LK-NIP-1	average ± SD	0.12 ± 0.08 (286)	0.001 ± 0.10 (278)	0.13 ± 0.07 (286)
LLH-1	average ± SD	0.77 ± 0.20 (63)	5.23 ± 0.31 (63)	6.02 ± 0.24 (63)
NPD-1	average ± SD	0.08 ± 0.06 (475)	1.28 ± 0.08 (475)	1.37 ± 0.09 (475)
ODL-1	average ± SD	0.20 ± 0.11 (146)	42.0 ± 1.7 (146)	42.4 ± 1.7 (146)
OKUM-1	average ± SD	0.16 ± 0.10 (511)	4.76 ± 0.21 (146)	4.95 ± 0.20 (511)
ORCA-1	average ± SD	0.05 ± 0.09 (279)	0.77 ± 0.13 (279)	0.82 ± 0.08 (279)
QS-1	average ± SD	0.71 ± 0.35 (230)	10.9 ± 0.6 (230)	11.7 ± 0.5 (230)

Note: average ± SD (n) is mean ± one standard deviation of results (number of measurements).

Table 40.2. Summary of reference material data for the LOI-4ST method. All values in weight %.

In-House Reference Materials		N ₂ at 105°C	O ₂ at 371°C	O ₂ at 538°C	O ₂ at 900°C	Total LOI
Geological Samples						
LDI-2	average ± SD	0.03 ± 0.06 (6)	0.15 ± 0.09 (6)	−0.01 ± 0.03 (6)	2.44 ± 0.06 (6)	2.60 ± 0.07 (6)
LK-NIP-1	average ± SD	0.16 ± 0.07 (4)	0.14 ± 0.01 (4)	0.06 ± 0.06 (4)	−0.17 ± 0.12 (4)	0.20 ± 0.10 (4)
NPD-1	average ± SD	0.08 ± 0.01 (4)	0.13 ± 0.02 (4)	0.09 ± 0.07 (4)	0.93 ± 0.07 (4)	1.25 ± 0.07 (4)
OKUM-1	average ± SD	0.18 ± 0.09 (6)	1.0 ± 1.7 (6)	0.08 ± 0.07 (6)	4.08 ± 0.02 (6)	4.63 ± 0.08 (6)
QS-1	average ± SD	0.56 ± 0.15 (5)	0.40 ± 0.11 (5)	0.42 ± 0.34 (5)	9.7 ± 0.4 (5)	11.18 ± 0.31 (5)

Note: average ± SD (n) is mean ± one standard deviation of results (number of measurements).

Table 40.3. Summary of reference material data for the LOI-LK1 and LOI-2ST methods. All values in weight %.

Certified Reference Materials		N ₂ at 100°C	O ₂ at 500°C	Total LOI
LOI-LK1 Method				
Sediments				
LKSD-2	average ± SD	N.M.	12.16 ± 0.32 (375)	12.16 ± 0.32 (375)
	Certificate		12.3 ± 0.4	12.3 ± 0.4
LKSD-3	average ± SD	N.M.	11.95 ± 0.21 (321)	11.95 ± 0.21 (321)
	Certificate		11.8 ± 0.6	11.8 ± 0.6
LKSD-4	average ± SD	N.M.	41.1 ± 0.4 (532)	41.1 ± 0.4 (532)
	Certificate		40.8 ± 0.7	40.8 ± 0.7
LOI-2ST Method				
Sediments				
LKSD-2	average ± SD	1.6 ± 0.5 (9)	10.22 ± 0.08 (9)	11.8 ± 0.5 (9)
	Certificate	na	12.3 ± 0.4	12.3 ± 0.4

Notes: average ± SD (n) is mean ± one standard deviation of results (number of measurements).

Abbreviations: na: data not available; N.M.: not measured.

Table 40.4. Summary of reference material data for the IMH-100 method. All values in ppb.

Certified Reference Materials		Se	Te
GSR-3	average \pm SD	35.3 \pm 2.5 (4)	2.4 \pm 0.7 (4)
	Reference	37 \pm 2*	< 1*
GSR-4	average \pm SD	62 \pm 11 (6)	21.3 \pm 6.0 (6)
	Reference	76 \pm 4*	38 \pm 1*
MRG-1	average \pm SD	195 \pm 19 (13)	29 \pm 7 (13)
	Reference	199 \pm 10*	32 \pm 1*
UB-N	average \pm SD	123 \pm 11 (11)	9.2 \pm 2.2 (11)
	Reference	112 \pm 3 [†]	8 \pm 2 [‡]
In-House Reference Materials			
MRB-29	average \pm SD	144 \pm 20 (29)	4.7 \pm 1.8 (29)
OKUM-1	average \pm SD	138 \pm 11 (22)	17 \pm 4 (22)

Note: average \pm SD (n) is mean \pm one standard deviation of results (number of measurements).

References: * Hall and Pelchat (1997); [†] Terashima (2001); [‡] Terashima and Imai (2000).

Table 40.5. Summary of data for the IMW-100 method for certified reference materials. All values in ppb ($\mu\text{g/L}$).

Certified Reference Materials		Ag	Al	As	Au
SLRS-4	average \pm SD	0.00007 \pm 0.00126 (31)	58 \pm 3 (31)	0.72 \pm 0.06 (31)	−0.0003 \pm 0.0019 (31)
	Reference	0.035 \pm 0.005 [†]	54 \pm 4*	0.68 \pm 0.06*	0.0009 \pm 0.0001 [‡]
SLRS-5	average \pm SD	0.0009 \pm 0.0013 (205)	50 \pm 4 (203)	0.42 \pm 0.03 (206)	0.00043 \pm 0.00043 (206)
	Reference	na	49.5 \pm 5*	0.413 \pm 0.039*	na
		Ba	Be	Bi	Ca
SLRS-4	average \pm SD	13.5 \pm 0.6 (31)	0.0082 \pm 0.0030 (31)	0.007 \pm 0.004 (31)	5810 \pm 300 (30)
	Reference	12.2 \pm 0.6*	0.007 \pm 0.002*	0.0021 \pm 0.0001 [‡]	6200 \pm 200*
SLRS-5	average \pm SD	14.77 \pm 0.59 (200)	0.0063 \pm 0.0022 (206)	0.0025 \pm 0.0022 (206)	10,290 \pm 450 (205)
	Reference	14.0 \pm 0.5*	0.005*	na	10,500 \pm 400*
		Cd	Ce	Co	Cr
SLRS-4	average \pm SD	0.0143 \pm 0.0027 (31)	0.371 \pm 0.0004 (31)	0.037 \pm 0.004 (31)	0.325 \pm 0.020 (31)
	Reference	0.012 \pm 0.002*	0.360 \pm 0.012 [†]	0.033 \pm 0.006*	0.33 \pm 0.02*
SLRS-5	average \pm SD	0.011 \pm 0.008 (206)	0.254 \pm 0.014 (206)	0.053 \pm 0.004 (206)	0.25 \pm 0.04 (206)
	Reference	0.0060 \pm 0.0014*	0.229 \pm 0.022 [#]	0.05* (0.06 \pm 0.04 [#])	0.208 \pm 0.023*
		Cs	Cu	Dy	Er
SLRS-4	average \pm SD	0.0072 \pm 0.0008 (31)	2.02 \pm 0.16 (30)	0.0247 \pm 0.0018 (31)	0.0137 \pm 0.0013 (31)
	Reference	0.009 \pm 0.001 [†]	1.81 \pm 0.08*	0.0242 \pm 0.0016 [†]	0.0134 \pm 0.0006**
SLRS-5	average \pm SD	0.0046 \pm 0.0006 (206)	18.5 \pm 0.8 (205)	0.0193 \pm 0.0015 (206)	0.0109 \pm 0.0011 (206)
	Reference	0.00380 \pm 0.00019	17.4 \pm 1.3*	0.0160 \pm 0.0019 [#]	0.0097 \pm 0.0019 [#]
		Eu	Fe	Ga	Gd
SLRS-4	average \pm SD	0.0078 \pm 0.0009 (31)	106 \pm 5 (31)	0.0140 \pm 0.0012 (31)	0.038 \pm 0.003 (31)
	Reference	0.0080 \pm 0.0006 [†]	103 \pm 5*	0.0119 \pm 0.0004 [†]	0.0342 \pm 0.0020 [†]
SLRS-5	average \pm SD	0.0056 \pm 0.0009 (0)	95 \pm 6 (205)	0.0163 \pm 0.0015 (206)	0.028 \pm 0.003 (206)
	Reference	0.0065 \pm 0.0028 [#]	91.2 \pm 5.8*	0.0143 \pm 0.0031 [#]	0.029 \pm 0.011 [#]
		Hf	Ho	La	Li
SLRS-4	average \pm SD	0.0047 \pm 0.0010 (31)	0.0049 \pm 0.0006 (31)	0.299 \pm 0.019 (31)	0.55 \pm 0.04 (31)
	Reference	0.003 \pm 0.0002 [‡]	0.0047 \pm 0.0003 [†]	0.287 \pm 0.008 [†]	0.54 \pm 0.07 [†]
SLRS-5	average \pm SD	0.0014 \pm 0.0007 (206)	0.0039 \pm 0.0005 (206)	0.209 \pm 0.009 (205)	0.49 \pm 0.04 (206)
	Reference	na	0.0036 \pm 0.0014 [#]	0.187 \pm 0.014 [#]	0.44 \pm 0.06 [#]

Table 40.5, continued. All values in ppb (µg/L).

Certified Reference Materials		Lu	Mg	Mn	Mo
SLRS-4	average ± SD	0.00196 ± 0.00021 (31)	1640 ± 210 (31)	3.72 ± 0.28 (31)	0.225 ± 0.014 (31)
	Reference	0.0019 ± 0.0001 [†]	1600 ± 100 [*]	3.37 ± 0.18 [*]	0.21 ± 0.02 [*]
SLRS-5	average ± SD	0.0016 ± 0.0002 (206)	2530 ± 130 (205)	4.47 ± 0.25 (206)	0.231 ± 0.011 (206)
	Reference	0.0016 ± 0.0007 [#]	2540 ± 160 [*]	4.33 ± 0.18 [*]	0.5 [*] (0.18 ± 0.06 [#])
		Nb	Nd	Ni	Pb
SLRS-4	average ± SD	0.0047 ± 0.0006 (28)	0.25 ± 0.09 (31)	0.69 ± 0.07 (31)	0.091 ± 0.015 (31)
	Reference	0.0041 ± 0.0003 [‡]	0.269 ± 0.014 [†]	0.67 ± 0.08 [*]	0.086 ± 0.007 [*]
SLRS-5	average ± SD	0.0038 ± 0.0005 (203)	0.197 ± 0.018 (204)	0.53 ± 0.17 (204)	0.081 ± 0.009 (198)
	Reference	0.00271 ± 0.00005 [#]	0.167 ± 0.016 [#]	0.476 ± 0.064 [*]	0.081 ± 0.006 [*]
		Pr	Rb	Sb	Sc
SLRS-4	average ± SD	0.072 ± 0.005 (31)	1.63 ± 0.09 (31)	0.246 ± 0.012 (31)	−0.17 ± 0.03 (31)
	Reference	0.0693 ± 0.0018 [†]	1.53 ± 0.05 [†]	0.23 ± 0.04 [†]	0.0113 ± 0.0006 [‡]
SLRS-5	average ± SD	0.0505 ± 0.0028 (206)	1.30 ± 0.06 (206)	0.300 ± 0.015 (206)	−0.04 ± 0.09 (206)
	Reference	0.043 ± 0.0049 [#]	1.29 ± 0.14 [#]	0.3 [*] (0.33 ± 0.06 [#])	na
		Se	Sm	Sn	Sr
SLRS-4	average ± SD	0.20 ± 0.05 (31)	0.059 ± 0.006 (31)	0.009 ± 0.005 (31)	30.5 ± 5.2 (31)
	Reference	0.23 ± 0.03 [†]	0.0574 ± 0.0028 [†]	0.01 ± 0.002 [†]	26.3 ± 3.2 [*]
SLRS-5	average ± SD	0.12 ± 0.05 (206)	0.0342 ± 0.0032 (206)	0.007 ± 0.005 (206)	55.3 ± 2.1 (205)
	Reference	na	0.0297 ± 0.0029 [#]	na	53.6 ± 1.3 [*]
		Ta	Tb	Th	Ti
SLRS-4	average ± SD	0.0004 ± 0.0002 (31)	0.0048 ± 0.0004 (31)	0.0181 ± 0.0024 (31)	1.28 ± 0.16 (31)
	Reference	0.0003 ± 0.0002 [‡]	0.0043 ± 0.0004 [†]	0.018 ± 0.003 [†]	1.46 ± 0.08 [†]
SLRS-5	average ± SD	0.00020 ± 0.00024 (206)	0.0036 ± 0.0006 (206)	0.008 ± 0.003 (206)	1.98 ± 0.16 (206)
	Reference	na	0.0031 ± 0.0021 [#]	0.008 ± 0.007 [#]	2.00 ± 0.29 [#]
		Tl	Tm	U	V
SLRS-4	average ± SD	0.0065 ± 0.0006 (31)	0.00190 ± 0.00023 (31)	0.0509 ± 0.0081 (31)	0.357 ± 0.017 (31)
	Reference	0.0076 ± 0.0006 [†]	0.0017 ± 0.0002 [†]	0.050 ± 0.003 [*]	0.32 ± 0.03 [*]
SLRS-5	average ± SD	0.0037 ± 0.0004 (206)	0.0015 ± 0.0002 (206)	0.090 ± 0.005 (206)	0.340 ± 0.026 (204)
	Reference	0.0035 ± 0.0004 [#]	0.00152 ± 0.00013 [#]	0.1 [*] (0.091 ± 0.004 [#])	0.317 ± 0.033 [*]
		W	Y	Yb	Zn
SLRS-4	average ± SD	0.0052 ± 0.0011 (31)	0.144 ± 0.008 (31)	0.0125 ± 0.0013 (31)	1.22 ± 0.24 (31)
	Reference	0.0133 ± 0.0010 [†]	0.146 ± 0.008 [†]	0.0120 ± 0.0004 [†]	0.93 ± 0.10 [*]
SLRS-5	average ± SD	0.0100 ± 0.0014 (206)	0.1149 ± 0.0056 (206)	0.0100 ± 0.0014 (206)	1.10 ± 0.16 (200)
	Reference	na	0.1098 ± 0.0028 [#]	0.0091 ± 0.0011 [#]	0.845 ± 0.095 [*]
		Zr			
SLRS-4	average ± SD	0.139 ± 0.026 (31)			
	Reference	0.12 ± 0.015 [†]			
SLRS-5	average ± SD	0.032 ± 0.023 (206)			
	Reference	0.030 ± 0.014 [#]			

Note: average ± SD (n) is mean ± one standard deviation of results (number of measurements).

Abbreviation: na: data not available.

References: ^{*} NRC Certificate (including information values);

[†] Yeghicheyan et al. (2001);

[‡] Rodushkin et al. (2005);

[#] Burnham, Schroeder and Hamilton (this volume, Article 38; indicative and information values).

SUMMARY OF REFERENCE MATERIAL RESULTS

The 2010–2012 average, standard deviation and number of determinations are shown for all certified reference materials and in-house reference materials; the certified or published values are also provided for the CRMs (*see* Tables 40.1 to 40.5). Provisional values are given for the lake sediment standards. Provisional values have a lower degree of confidence compared to certified values due to either a limited number of results were used to calculate the mean, a limited number of methods used, or high variability was observed between laboratories.

FUTURE WORK

The Geo Labs have recently received new furnaces for lead fire-assay analyses and are in the process of initiating work on ISO 17025:2005 accreditation for the lead-fire assay with gravimetric finish (method code GFA-PBG). The new method validation and quality assurance–quality control (QA/QC) summary for this method will be published in the future.

ACKNOWLEDGMENTS

The author would like to thank Marcus Burnham and Natalie Chrétien for their help in compiling the data presented in this paper.

REFERENCES

- Geoscience Laboratories 2009. Geoscience Laboratories Schedule of Fees and Services, Issue 5.
- Hall, G.E.M. and Pelchat, J.C. 1997. Determination of As, Bi, Sb, Se and Te in fifty-five reference materials by hydride generation ICP-MS; *Geostandards Newsletter: The Journal of Geostandards and Geoanalysis*, v.21, p.85-91.
- Rodushkin, I., Nordlund, P., Engström, E. and Baxter, D.C. 2005. Improved multi-elemental analyses by inductively coupled plasma-sector field mass spectrometry through methane addition to the plasma; *Journal of Analytical Atomic Spectrometry*, v.20, p.1250-1255.
- Terashima, S. 2001. Determination of indium and tellurium in fifty-nine geological reference materials by solvent extraction and graphite furnace atomic absorption spectrometry; *Geostandards Newsletter: The Journal of Geostandards and Geoanalysis*, v.25, p.127-132.
- Terashima, S. and Imai, N. 2000. Determination of selenium in fifty-two geochemical reference materials by hydride generation atomic absorption spectrometry; *Geostandards Newsletter: The Journal of Geostandards and Geoanalysis*, v.24, p.83-86.
- Yeghicheyan, D., Carignan, J., Valladon, M., Bouhnik Le Coz, M., Le Cornec, F., Castrec-Rouelle, M., Robert, M., Qauilina, L., Aubry, E., Churlaud, C., Dia, A., Debertdt, S., Dupré, B., Freydier, R., Gruau, G., Hénin, O., deKersabiec, A., Macé, J., Marin, L., Morin, N., Petitjean, P. and Serrat, E. 2001. A compilation of silicon and thirty-one trace elements measured in the natural river water reference material SLRS-4 (NRC-CNRC); *Geostandards Newsletter: The Journal of Geostandards and Geoanalysis*, v.25, p.465-474.

Targeted Geoscience Initiative 4

41. Update on Research Activities in the Targeted Geoscience Initiative 4 Magmatic-Hydrothermal Nickel-Copper-Platinum Group Elements Ore System Subproject: System Fertility and Ore Vectors

D.E. Ames¹, S.A.S. Dare², J.J. Hanley³, P. Hollings⁴, S.E. Jackson¹, P.J. Jugo⁵, D.J. Kontak⁵, R.L. Linnen⁶ and I.M. Samson⁷

¹Geological Survey of Canada, Ottawa, Ontario K1A 0E8

²Département des sciences de la Terre, Université du Québec à Chicoutimi, Saguenay, Québec G7H 2B1

³Department of Earth Sciences, Saint Mary's University, Halifax, Nova Scotia B3H 3C3

⁴Department of Geology, Lakehead University, Thunder Bay, Ontario P7B 5E1

⁵Department of Earth Sciences, Laurentian University, Sudbury, Ontario P3E 2C6

⁶Department of Earth Sciences, Western University, London, Ontario N6A 5B7

⁷Department of Earth and Environmental Sciences, University of Windsor, Windsor, Ontario N9B 3P4

INTRODUCTION

The nickel-copper-platinum group elements (PGE)-chromium ore systems project is one of 6 national minerals projects in the Geological Survey of Canada's Targeted Geoscience Initiative 4 (TGI-4) program. The TGI-4 has a mandate to employ public geoscience in the development of new geoscience knowledge and techniques in support of more effective exploration for buried ore deposits (Villeneuve 2011). Nickel-copper-platinum group element (PGE) deposits are key exploration targets given high precious metal prices. These ore deposits occur in highly varied geological settings with complex geochemical, mineralogical and geophysical signatures that challenge successful exploration, particularly in the deeper or covered parts of established and emerging terranes.

This project focusses on data-rich, established and emerging mining camps in Canada to optimize exploration-related geoscience knowledge with national district- and deposit-scale studies in selected areas (*see* Ames and Houlé 2011). A multidisciplinary approach is adopted, focussed on improving the geological knowledge of the ore environments by determining footprints of fertile ore systems and defining better vectors towards their mineralized parts. This report, which focusses on hydrothermal-magmatic copper-PGE-rich systems, is accompanied by a report on other ore deposit styles in high-magnesium ultramafic to mafic systems, with a subproject report by Houlé, Leshner and Metsaranta (this volume, Article 42). The TGI-4 project will also provide an opportunity to acquire knowledge on less-understood, and mostly underexplored deposit types, such as the orogenic nickel-copper systems that host the Giant Mascot and Turnagain deposits in British Columbia.

This contribution highlights research activities within the hydrothermal-magmatic copper-PGE subproject carried out in collaboration with provincial and territorial governments and agencies, academia and the exploration and mining sector.

HYDROTHERMAL-MAGMATIC COPPER-PLATINUM GROUP ELEMENT-RICH ORE SYSTEMS SUBPROJECT

There is a substantial body of evidence for significant water–rock interaction in mafic intrusions that host copper-nickel-PGE deposits resulting in hydrothermal modification and enrichment of metals. A spectrum of different geological settings are being studied to determine 1) the conditions necessary to concentrate hydrothermal fluids and precipitate copper-PGE±nickel minerals; 2) what defines a fertile versus economically barren ore system; and 3) to further develop definitive criteria for deposit vectoring within the broader halo that defines the ore system, or the broader area of rock that has been affected by hydrothermal-magmatic alteration. Research areas requiring further refinement include 1) discerning the difference between fertile and infertile intrusions or parts thereof; 2) defining distal footwall and hanging-wall vectors toward deep hydrothermal-magmatic copper-PGE systems and sulphur-poor PGE deposits (i.e., which ore indicators are most robust and diagnostic); 3) identifying pathways for fluids, volatiles and melts that transport metals; and 4) determining the effect of later tectonic-metamorphic-magmatic events on the distribution and grade of mineralization.

Research Activities

METHOD DEVELOPMENT: TOWARDS FERTILITY

Trace Elements in Iron Oxides from Fertile and Barren Intrusions: Investigating Their Use as a Vector to Nickel-Copper-Platinum Group Element Deposits, Sudbury and Voisey's Bay

(Participants: S.A.S. Dare and S.-J. Barnes, Université du Québec à Chicoutimi; D.E. Ames, GSC; G. Beaudoin, Laval University)

The nickel and chromium trace element chemistry of magnetite has recently received much attention on its use as an indicator mineral for exploration for many types of ore deposits (Dupuis and Beaudoin 2011). Studies have shown that the trace element chemistry of magnetite from the ore zones of magmatic nickel-copper deposits can be used to discriminate these from other deposits of hydrothermal origin (such as banded-iron formation gold, porphyry copper-molybdenum, volcanogenic massive sulphide, iron oxide-copper-gold deposits). Previous studies on magnetite from massive sulphides of Sudbury and Voisey's Bay nickel-copper-PGE deposits show that magnetite trace element chemistry is very sensitive to fractionation of the sulphide liquid and to the changing sulphide mineralogy (Dare, Barnes and Beaudoin 2012).

The aim of this TGI-4 study by postdoctoral fellow Sarah Dare at the University of Québec at Chicoutimi is to determine the diagnostic iron-oxide compositions in silicate igneous rocks that may discriminate between barren and fertile mafic to intermediate intrusions. The key objectives include

- investigating whether the trace element geochemistry of iron oxides (magnetite, titanomagnetite and ilmenite), found in intrusion-hosted nickel deposits, record sulphide saturation and segregation, which could then be used to vector toward a sulphide deposit at the base of, and in the footwall of the intrusion,
- gaining a better understanding of the evolution of iron-oxide geochemistry during fractionation of the silicate liquid, and
- comparing and contrasting the geochemical signature of iron oxides in both barren and mineralized or fertile intrusions of similar composition and genesis, in order to determine whether these can be used to discriminate the presence of mineralization.

Two case studies are being carried out, one at the Sudbury Igneous Complex (SIC) where data generation is complete after the first year, and the other at Voisey's Bay where data collection has started recently. Barren site testing will be an important method of validating the use of mineral-specific pathfinder elements both within a large intrusion that hosts many deposits, smaller intrusions with just 1 deposit and barren intrusions.

The lower mafic part of the SIC was sampled along 4 transects that include known mineralized and assumed barren regions, above and away from footwall contact embayments that are common ore environments on the north and south margins of the intrusive complex. A whole rock geochemistry database with over 250 samples will aid in determining the degree of silicate fractionation in the intrusion and verify the fertile or barren nature of the samples using useful element indicators of sulphide segregation as guides, for example, nickel, magnesium, copper and zirconium (Darling et al. 2010). A total of 190 polished thin sections were investigated by iron-oxide petrography, from which 60 samples containing iron-oxide mineral grains suitable for electron microprobe and laser ablation inductively coupled plasma mass spectrometric (LA-ICP-MS) trace element analysis of magnetite and/or ilmenite. Mineral chemical and petrographic data acquisition has been completed on the SIC sites, and preliminary iron-oxide mineralogy initiated on the barren Newark intrusion in Labrador. Final results and knowledge gained on the use of iron oxides in large mafic intrusions as a fertility indicator will be published in a peer-reviewed journal with the associated full database released as a Geological Survey of Canada Open File.

Constraining Melt Chemistry and Evolution Within the Sudbury Igneous Complex Through the Use of Melt Inclusions: A Potential Tool to Determining Metal Fertility and Hidden Magmatic Sulphide Deposits

(Participants: K. Watts and J.J. Hanley, Saint Mary's University; D.E. Ames, GSC; D.J. Kontak, Laurentian University)

Understanding of the processes that lead to the formation of nickel-copper-PGE deposits is limited by knowledge of the composition of the intrusions at the time of their emplacement and their subsequent crystallization history. Many mafic to ultramafic intrusions have undergone intense deformation and hydrothermal alteration since their formation. These processes have modified the composition of the rocks, making it, in some cases, difficult to use the current chemical composition of the intrusion as a proxy for ore-forming processes that occurred 1.85 billion years ago when the Sudbury deposits were formed. For example, a major limitation of mass balance exercises, which focus on determining the amount of magma needed to generate the sulphide deposits, is the knowledge of the metal and sulphur content of the magma before and after the deposits formed, and before the intrusion was subjected to deformation and alteration.

A melt inclusion study of the SIC, which is one of the largest known repositories for nickel-copper-PGE ore, is the focus of the TGI-4-sponsored Master of Science (MSc) thesis research by Kathleen Watts at Saint Mary's University, Halifax, under the supervision of Drs. J.J. Hanley and D.E. Ames (GSC). The study of melt inclusions (i.e., trapped droplets of various stages of the Sudbury magma hosted in minerals that grew from the magma) is believed to be the key toward

- understanding the early events that made the SIC and enriched its original melt sheet in ore metals,
- gaining insight into the origin of the nickel and PGE deposits by identifying the geological contributions (mantle and crustal reservoirs) to the intrusion chemistry and, ultimately, a mining district mass-balance calculation of the amount of ore-forming magma that was required to generate its overall contained resources, and

- developing exploration criteria to discriminate between “metal-fertile” and “metal-depleted” areas of the intrusion with application to Sudbury and other intrusions globally where similar processes have operated.

Preliminary results from a regional reconnaissance study of apatite in the lower part of the Sudbury Igneous Complex using mineral chemistry (electron microprobe), scanning electron microscopic (SEM) and cathodoluminescence data from a preliminary suite of SIC samples, analyzed at the GSC, indicated that the melt inclusion record would be more than suitable for a detailed study. A collection of several hundred rock samples from the main rock units (i.e., gabbro, norite and quartz diorite) in the lower part of the intrusion, crystallization of which was critical to the saturation of sulphides and fluids on both the northern and southern margins (North Range, South Range) of the intrusive complex, is being examined. From this larger sample suite, 20 samples determined to have the best inclusion assemblages (well-preserved, texturally representative and abundant) will be selected for melt-inclusion analysis.

In the first 8 months of this study, the types and composition of melt inclusions hosted in apatite have been characterized and analyzed for major elements by electron microprobe and SEM–electron dispersive spectrometry (SEM-EDS) and trace elements using LA-ICP–MS. Analysis of mineral separates from 6 samples (4 gabbros, 1 norite, 1 quartz diorite) from the North Range lower mafic part of the intrusion has been completed so far. These represent a barren and mineralized portion of the Levack embayment–Windy Lake area and quartz diorite from the Whistle offset environment. An additional 8 samples are being analyzed currently from the South Range. Importantly, colour cathodoluminescence and trace element mapping of the apatite demonstrates that the inclusions in apatite are primary and that the apatite represents an early, cumulus phase within all rock types studied. Preliminary trace element analyses of melt inclusions in apatite from North Range gabbro and norite by LA-ICP–MS have provided partition coefficient data for melt–apatite pairs and for iron-rich liquid–silicon-rich liquid pairs in homogenized melt inclusions. The primary melt composition at the time of crystallization of various phases of the lower SIC is being examined and, most importantly, may constrain the original metal content of the intrusion. We have been able to quantify nickel, copper, cobalt, silver, antimony and bismuth in melt inclusions and show that immiscibility of felsic and iron-rich liquids occurred in the SIC, a feature common to the Skaergaard system of Greenland, another PGE-rich environment.

This study will provide new insights into the origin and emplacement of the Sudbury district nickel-copper-PGE and copper-PGE ores within a complex, multi-stage ore system that encompasses the SIC and its host wall rocks. In those environments where post-magmatic processes have taken their toll on the effectiveness of applying routine whole-rock geochemistry, the analysis of melt inclusion chemistry could significantly enhance exploration success. Additionally, the study represents the first significant attempt to quantify melt chemistry in mafic plutonic rocks.

GEOLOGY, MINERAL CHEMISTRY AND GEOCHEMISTRY: VECTORS TO ORE

Hydrothermal Interactions in Platinum Group Element Deposits: Implications for Deposit Genesis and New Exploration Vectors, Georgie Lake and Marathon Copper-Palladium, Coldwell Complex

(Participants: M. Shahabi Far, M. Brzowski, I.M. Samson and J. Gagnon, University of Windsor; I. Meghji, R. Smoke and R.L. Linnen, Western University; D.J. Good, Stillwater Canada; and D.E. Ames, GSC)

The Marathon deposit is one of the largest PGE-copper reserves in Canada and is expected to grow with the development of additional nearby resources and exploration targets in the Coldwell Complex of the Midcontinent Rift. These include the Georgie Lake deposit which is the focus of an active exploration program. The exploration implications of the effects of post-magmatic modification by hydrothermal–late magmatic activity are poorly understood. There is a growing body of evidence that demonstrates that

significant water–rock interaction occurred in mafic intrusions hosting copper-PGE deposits, and that this resulted in modification of the deposit and dispersion of elements characteristic of these systems. The hydrothermal dispersion of key indicator elements presents an opportunity to use their variation in concentration with respect to the PGE deposits as a vector to ore. The copper-PGE deposits in the Midcontinent Rift, such as those hosted within the Coldwell Complex and the Thunder intrusion near Thunder Bay, are not metamorphosed or structurally remobilized and, therefore, provide an ideal environment to study the effects of last-stage hydrothermal remobilization.

The knowledge gaps, addressed by a group of 4 graduate student projects (1 PhD, 3 MSc) at the University of Windsor and Western University, are a) the consequences of hydrothermal fluid–rock interaction on the mineralogy and geochemistry of PGE-copper deposits hosted by mafic igneous rocks; and b) the degree of hydrothermal dispersion of characteristic elements and their incorporation into distal hydrothermal minerals around such deposits. These studies will provide a better understanding of the role that fluids play in these systems.

The Origin of Platinum Group Element Mineralization, Georgie Lake Deposit, Marathon

(Participants: I. Meghji and R.L. Linnen, Western University; D.E. Ames, GSC)

Field work was initiated in the summer of 2011 for the MSc study of Imran Meghji at Western University supervised by Drs. R.L. Linnen, I.M. Samson, D.J. Good (Stillwater Canada Inc.) and D.E. Ames (GSC). Preliminary investigations indicate that, as with the Main Zone at Marathon, the Georgie Lake copper-palladium mineralization is spatially associated with moderate to intense alteration within a heterogeneous gabbro. The host gabbro at Georgie Lake is unusual owing to the presence of abundant skeletal fayalitic olivine and ubiquitous pink albite alteration. It also has a distinct geochemical signature relative to other gabbros generated in rift-related tectonic settings. In addition, the northern part of the Georgie Lake intrusion is partly covered by subhorizontal submarine basaltic flows of similar (Keweenawan) age. There are numerous occurrences of copper mineralization in the pillowed basaltic flows, which may indicate remobilization of copper and precious metals from the underlying gabbros or deposits. This could have implications for other copper mineralization in Keweenawan flows as distal indicators to underlying gabbro-hosted mineralization. The geologic setting of the mineralization at the Georgie Lake copper-palladium deposit needs to be first defined in order to characterize the mineralogy and paragenesis of the alteration and precious metal minerals.

Therefore, the objectives are to

- determine the distribution of, and controls on, PGE in the Georgie Lake deposit relative to its host rocks, associated albite-actinolite alteration and paleofaults,
- determine the distribution of PGE ratios in the Georgie Lake deposit relative to alteration, structure and intrusive units and evaluate whether these can be used as vectors toward additional resources,
- identify the proximal alteration signature through trace-element chemistry of hydrothermal minerals within the deposit,
- compare the Georgie Lake deposit to other deposits within the Coldwell Complex, e.g., the Main Zone and W horizon mineralization at the Marathon deposit, and
- establish a practical guide to mineralogical and geochemical exploration for hidden magmatic-hydrothermal copper-PGE deposits. It is critical to establish the relationship between mineralization and fluid activity, and the role that fluids play on the localization of precious metals.

Four drill holes along a north-south section of the Geordie Lake deposit (G-10-02, G-10-04-, G-10-16, G-10-17) have been logged in detail with particular emphasis on the lithology, alteration type and alteration intensity, texture, and sulphide mineralogy. A total of 58 gabbro samples representing the major lithological and textural variations along the north-south section were collected in the summer of 2011. Of these 58 representative samples, 41 were selected for major and trace element geochemistry, and petrography was initiated on 76 polished sections. Preliminary geochemical results for the albite-altered gabbro indicates that it is more rare earth element (REE)-enriched than the skeletal olivine gabbro, likely indicating that the albitization resulted from interaction with a much more fractionated liquid. In the summer of 2012, an additional 12 samples of homogenous plagioclase-pyroxene cumulates and 3 samples of footwall quartz-syenite were collected from the 4 drill holes for major and trace element geochemistry. Additionally, 3 large albite pods on outcrop were sampled to determine their alteration signatures relative to the host gabbro using trace element geochemistry. All geochemistry samples will have detailed petrographic descriptions and analysis.

Chemistry of Alteration Minerals as a Vector for Platinum Group Element Mineralization, Marathon and Geordie Lake Deposits, Coldwell Complex

(Participants: M. Brzozowski, I.M. Samson and J. Gagnon, University of Windsor; D.J. Good, Stillwater Canada; D.E. Ames, GSC)

Hydrothermal alteration and vein- or vug-filling minerals occur both proximally and distally to deposits perhaps indicative of a halo to be used to detect the ore system and vector toward its high-grade core. Certainly in the proximal case, the trace element chemistry of hydrous silicate minerals, such as amphibole, can reflect the local environment. The extent to which the concentrations of elements such as copper, nickel and arsenic are anomalous at increasing distances from a deposit needs to be determined. If this is the case, analysis of common minerals such as amphibole, chlorite, pyrite, rutile and titanite distally to orebodies may be used to indicate the presence of buried deposits and, if geochemical gradients exist over significant distances, be used in vectoring.

The main objectives of this activity are to

- identify and examine the occurrence, types and paragenesis of hydrothermal mineral assemblages in proximal and distal settings to the copper-PGE mineralization at the Marathon and Geordie Lake deposits,
- determine the trace element characteristics of key minerals (e.g., amphibole, chlorite, pyrite, rutile and titanite) relative to mineralization using laser ablation inductively coupled mass spectrometry to identify the extent to which the concentrations of elements are anomalous at increasing distance from a deposit, and
- establish diagnostic criteria with geochemical and mineralogical indicators targeting copper-palladium ore environments.

A BSc study by Matthew Brzozowski (2012) was completed at the University of Windsor and supervised by Dr. I.M. Samson. This BSc project focussed on identifying the variations in fracture mineral chemistry, if any, between fractures within mineralized and nonmineralized zones as a means of indicating copper-PGE mineralization below. Field methods used involved describing rock quality designation, fracture density, including broken and intact fractures, fracture mineralogy (e.g., chlorite, carbonate, or a mixture), fracture roughness and rock hardness. Such a description provides an overview of the fracture density and fracture mineral chemistry throughout the length of the drill hole. Results from logging and mineral chemistry found that chlorite is the dominant fracture mineral and that of the trace elements analyzed, the transition metals copper, nickel, cobalt, vanadium and manganese have the highest concentration.

This preliminary study provided the groundwork for the MSc project of Matthew Brzozowski at the University of Windsor under the supervision of Drs. I.M. Samson and D.E. Ames (GSC). The fundamental objective of this study is to characterize variations in fracture mineral chemistry, if any, which may be used as exploration vectors for copper-PGE in the Marathon deposit. The effects of fluids within the deposit have been described by Watkinson and Ohnenstetter (1992) and Barrie et al. (2002) and, along with pervasive fracturing throughout the deposit, provide support for fluid movement through the deposit and its subsequent alteration of neighbouring rock. It is hypothesized that fluids passing through the deposit mobilized metals (e.g., copper, nickel) out of the mineralized and into the nonmineralized parts of the Two Duck Lake gabbro and Eastern Gabbro and was recorded in the chemistry of the vein minerals. Fracture minerals (principally chlorite and carbonate) will be analyzed by electron microprobe (wavelength dispersive spectrometry), SEM-EDS and LA-ICP-MS to determine their major (e.g., iron, magnesium and manganese) and trace (e.g., nickel, copper and vanadium) element chemistry. These data will be assessed in terms of their spatial relationships to known mineralization to determine the influence on mineral chemistry of proximity to mineralization. Variations in fracture and vesicle mineral chemistry will be assessed at the Geordie Lake deposit and compared to those at the Marathon deposit. Geordie Lake is a similar copper-PGE deposit to Marathon, also within the Coldwell Complex, but hosted by a different gabbro.

Field work was carried out this summer along a fence of drill holes through the Marathon deposit ore zones and nonmineralized or barren areas. Five holes were logged for fracture density and general fracture mineralogy. These 5 holes, plus sections of 2 other holes containing WD zone and W horizon mineralization, were systematically logged. They were also sampled at approximately 20 m intervals for chlorite and carbonate fractures, vugs and patchy alteration. This resulted in the collection of 138 samples, augmented by the 43 samples that were collected and prepared in 2011. In addition, a total of 10 samples containing chlorite fractures were obtained from the Geordie Lake property, at various distances from mineralization.

Petrology, Mineralization (Copper-Platinum Group Elements) and Alteration (Skarn) of the Thunder Mafic Intrusion Midcontinent Rift, Thunder Bay

(Participants: B. Trevisan and P. Hollings, Lakehead University; D.E. Ames, GSC)

The Midcontinent Rift of North America is host to a number of high-grade nickel-copper-PGE deposits including Marathon PGE and Current Lake in Canada and Eagle and Tamarack in the USA. Many of these deposits are small, buried and difficult to identify on regional magnetic surveys. In order to increase the success of exploration programs for this style of mineralization, it is necessary to characterize the intrusions themselves and the alteration halos that they generate in the surrounding country rocks. The Thunder mafic to ultramafic intrusion is distinct from other mineralized Midcontinent Rift intrusions as it has consistently lower nickel grades, but a relatively large range of PGE tenors; consequently, it offers an excellent opportunity to fingerprint this type of intrusion and see how it fits with other mineralized and nonmineralized intrusions within the rift. To date, it also represents the only mineralized Midcontinent Rift intrusion that is emplaced within a greenstone belt and, consequently, offers a unique opportunity to identify the alteration footprint generated in these units.

This Master of Science (MSc) thesis study by Brent Trevisan at Lakehead University is underway under the supervision of Drs. P. Hollings and D.E. Ames (GSC). The main objectives are to

- define the mineralogical and geochemical signature of the Thunder intrusion and PGE mineralization,
- establish the geochemical vectoring capability by characterizing the alteration footprint of the intrusion in the surrounding country rocks, and

- establish practical mineralogical and geochemical exploration criteria for hidden mafic to ultramafic ore systems by relating the intrusion and/or mineralization to other fertile and barren intrusive units within the Midcontinent Rift.

The MSc study started in September 2012. However, a few days of field work were undertaken in May with the assistance of Dean Rossell from Rio Tinto. The remainder of the initial phase of mapping and sampling is ongoing and will be completed in the fall of 2012. Lithological, geochemical and geochronological criteria that can be used by the mining and exploration industry to identify prospective portions of the rift and focus exploration activities at an early stage will be published in a peer-reviewed journal with publication of integrated results released as a Geological Survey of Canada Open File.

Sulphide and Metal Isotope Ratio as Tracers in Evolving Mafic Mineralizing Systems Through Ore Environments: Hydrothermal-Magmatic Indicators and Timing of Low-Sulphide Platinum Group Element-Rich Deposits

(Participants: D.E. Ames, GSC; J.J. Hanley, Saint Mary's University; J.B. Chapman, S.E. Jackson, W. Doherty and N. Rayner, GSC; D.J. Kontak, Laurentian University)

This activity involves the development and use of non-traditional (nickel, copper) and traditional isotopes to establish their usefulness in tracking the magmatic, magmatic-hydrothermal and hydrothermal processes in the generation or remobilization of metals in mafic to ultramafic ore systems. Well-constrained, spatially controlled studies are being carried out in collaboration with other researchers in the TGI-4 research group both at the Marathon deposit and within the exceptional natural laboratory of the Sudbury mining district to identify isotopic signatures of the distal and proximal manifestation of mineralization. New geoscience data generated will develop the geochronological framework that will improve the current knowledge of the timing of the mineralizing events and processes and will be integrated with metal and stable isotope results.

Deep Footwall Copper-Nickel-Platinum Group Element Ores, Sudbury: Constraints on Platinum Group Element Mobilization and Ore Genesis

(Participants: M. Adibpour and P.J. Jugo, Laurentian University; D.E. Ames, GSC)

The main challenge in the exploration of copper-nickel-PGE mineralization within the footwall of the SIC is due to the complexity of magmatic, magmatic-hydrothermal, hydrothermal and metamorphic processes resulting in formation of the Sudbury suite of ore deposits. Chemical fingerprinting related to processes and mineralization types is critical to developing robust exploration vectors for these deep deposits.

This laboratory-oriented study is the topic for a Master of Science (MSc) thesis by Mojgan Adibpour at Laurentian University, under the supervision of Drs. P.J. Jugo and D.E. Ames (GSC). The main objective of this activity is to determine the key processes that control formation of the precious-metal-rich footwall deposits through application of element distribution mapping. This will involve the use of LA-ICP-MS analysis at Laurentian University to examine the sulphide assemblages of the various "ore types" in a Sudbury nickel-copper-platinum-palladium-gold-silver ore system. This includes examples of contact ore, sharp-walled vein, low-sulphur and high-PGE, and hybrid ores (Ames and Farrow 2007).

Representative samples of sulphide assemblages from each deposit type listed above will be analyzed using a 193 nm excimer laser (Resonetics RESOLUTION M-50) coupled to a quadrupole ICP-MS (Thermo X Series II). Scanning areas of interest have created trace element maps with beam diameters ranging from 30 µm down to 5 µm (the appropriate resolution depending on the size of features present). The generated spectra are integrated using the Iolite software to generate the trace element maps. Prior to

ablation, SEM and reflected light photomicroscopic images will be obtained to have a record of sulphide assemblages and textures. Reflected light petrography and available information pertaining to the paragenesis of the sulphide assemblages (e.g., Kjarsgaard and Ames 2010) will be used to assess whether geochemical features, resolved using LA-ICP-MS mapping, can be ascribed to a particular process (magmatic, metamorphic, hydrothermal).

In the first 8 months, 20 representative nickel-copper-PGE ore samples were selected from different Sudbury ore types from the Sudbury mining district ore collection at the GSC-Ottawa (Ames et al. 2010) for initial petrographic documentation of textural and paragenetic relationships of minerals and identification of key areas (i.e., with multiple sulphide phases: chalcopyrite, pyrrhotite, pentlandite, pyrite, millerite, bornite). A subset of ores from the North Range Levack-Morrison ore system were selected to focus the study because of the apparent continuum with depth, from contact nickel-copper ores, to transitional nickel-copper-PGE ores of the Rob's zone, to massive sharp-walled copper-(nickel-) PGE vein ores and deeper to low-sulphide PGE-rich disseminated ores of the lower Morrison deposit (Ames, Golightly and Zierenberg 2010). Photomicroscopy, scanning electron microscope (SEM) analysis and image capture of key textures were documented for the first batch of 6 samples prior to LA-ICP-MS chemical analysis.

Constraining the Footwall Alteration Footprint for Effective Vectoring: A Case Study in the Grey Gabbro, Podolsky Copper-Platinum Group Element Deposit

(Participants: L. MacInnis, D.J. Kontak, Laurentian University; D.E. Ames and N. Rayner, GSC)

The high-grade copper-(nickel)-PGE deposits in the footwall environment around the Sudbury Igneous Complex (SIC) have, in recent years, become prime exploration targets because of increases in metal prices and discovery of a relatively new deposit type in a mature mining region. The footwall mineralization styles differ from the traditional nickel-copper-rich contact-ore deposits in their setting and geometry (mineralization occurring as veins and disseminations). Important also is that this ore type may be associated with intense alteration (e.g., epidote, albite, actinolite, magnetite), which may provide a significantly larger target for exploration and also a vector if such alteration can unambiguously be characterized when associated with sulphide mineralization.

The study of L. MacInnis (MSc candidate) at Laurentian University was initiated in 2012 and is supervised by Drs. D.J. Kontak and D.E. Ames (GSC). There are 2 clear objectives to unambiguously characterizing the alteration associated with copper-(nickel)-PGE mineralization in the footwall environment:

- The first objective is to determine the least-altered composition of the gabbroic host rock to the Podolsky copper-palladium mineralization in terms of both its mineralogy and geochemistry. This characterization of the least-altered rock will allow documentation of the macro- and micro-scale changes in rock texture, mineralogy and chemistry due to fluid-rock interaction (i.e., the interaction of the mineralizing fluids with the relatively uniform medium).
- The second and most important objective is to assess the nature and origin of the alteration types that are variably associated with the ore zones within this unit and compare these to the alteration types present in the footwall environment of the SIC. The characterization and chemical fingerprinting of the alteration-specific mineralization could then be used to provide criteria for targeting mineralization in other footwall environments.

In the first 6 months, 12 drill holes that transect the gabbroic host to copper-palladium-platinum-gold mineralization were relogged using an existing drill-core database and archived photos of all drill cores along with underground maps. The results included the documentation of texture, alteration types, mineralization and lithology. A series of geological plan and longitudinal sections across the "Grey

gabbro” unit were prepared, identifying the mineralized zones, textural and compositional variations, within the unit and the distribution of alteration types. The “Grey gabbro” is a local mine term used to describe the altered gabbroic host to part of the Podolsky copper-PGE deposit. Representative samples of the copper-PGE ores and the gabbroic host of the Podolsky deposit (n=103) were collected underground and in drill core. This Podolsky deposit collection is composed mostly (60%) of the altered and least-altered gabbroic host rock, with the remaining samples being copper-PGE veins that were systematically sampled with depth on each of 8 levels in the mine. Sample subsets were made for initial petrographic analysis (n=36) and 25 samples were submitted for whole-rock geochemical analysis to compare with other pertinent mafic igneous rocks in the mining district. Sulphur isotope analysis of chalcopyrite minerals sampled at various depths in the mine are all consistent ($\delta^{34}\text{S} = 4.3 \pm 0.2\%$, n= 16) and similar to those from the Podolsky north zone and other North Range footwall sulphides (Ames, Golightly and Zierenberg 2010). Oxygen isotope analysis of actinolite, in addition to analysis of contained fluid inclusions in this mineral phase, will provide new information on the source of the altering and mineralizing fluids. Data interpretation and results from the first year of work, which will define the composition of the least-altered “Grey gabbro” and production of maps of alteration types, will be published in 2013 as a GSC *Current Research* paper.

CONCLUSION

In summary, the nickel-copper-PGE-chromium project of the TGI-4 program is a collaborative research effort that will provide new geoscience-based knowledge of the mafic to ultramafic ore systems where significant gaps exist in our understanding of these major mineral systems in Canada and abroad. This subproject is a multidisciplinary effort done in close collaboration with provincial and territorial governments and agencies, academia and mineral industry sectors. Thus far, the subproject encompasses activities in 3 provinces, with significant in-kind support from industry and collaboration with over 20 university and government researchers and graduate students from 8 universities across Canada.

Presently, 15 graduate and undergraduate students and postdoctoral fellows are being trained and mentored in the magmatic-hydrothermal copper(-nickel)-PGE ore system subproject to increase the number of highly qualified personnel available to Canada’s mineral industry, research institutes, universities and government.

ACKNOWLEDGMENTS

Thanks are extended to the following mining companies for their logistical support, access to properties, information and, foremost, for discussions throughout project development: Hard Creek Mining Ltd., KGHM/QuadraFNX Mining Ltd., RioTinto, Stillwater Canada Inc., Vale Limited and Wallbridge Mining Co. This is Geological Survey of Canada/ESS contribution number 2012-0228.

REFERENCES

- Ames, D.E. and Farrow, C.E.G. 2007. Metallogeny of the Sudbury mining camp, Ontario; *in* Mineral deposits of Canada: a synthesis of major deposit-types, district metallogeny, the evolution of geological provinces, and exploration methods, Geological Association of Canada, Mineral Deposits Division, Special Publication No. 5, p.329-350.
- Ames, D.E., Golightly, J.P., Kjarsgaard, I.M. and Farrow, C.E.G. 2010. Minor element composition of Sudbury ores: implications for source contributions, genesis and exploration of Ni-Cu-PGE in diverse settings; extended abstract, *in* Abstracts, 11th International Platinum Symposium, 21–24 June 2010, Sudbury, Ontario, Canada, Ontario Geological Survey, Miscellaneous Release—Data 269, p.1-4.

- Ames, D.E., Golightly, J.P. and Zierenberg, R.A. 2010. Trace element and sulfur isotope composition of Sudbury Ni-Cu-PGE ores in diverse settings; abstract *in* Society of Economic Geologists 2010 Conference, Keystone, Colorado, October 2–5, 2010, Extended Abstracts (DVD), 4p.
- Ames, D.E. and Houl  , M.G. 2011. Overview of the Targeted Geoscience Initiative 4 nickel-copper-platinum group elements-chromium project (2010–2015)—mafic to ultramafic ore systems: footprint, fertility and vectors; *in* Summary of Field Work and Other Activities 2011, Ontario Geological Survey, Open File Report 6270, p.37-1 to 37-7.
- Barrie, C.T., MacTavish, A.D., Walford, P.C., Chataway, R. and Middaugh, R. 2002. Contact-type and magnetite reef-type Pd-Cu mineralization in ferroan olivine gabbros of the Coldwell Complex, Ontario; *in* The geology, geochemistry, mineralogy and mineral beneficiation of platinum-groups, Canadian Institute of Mining, Metallurgy and Petroleum, Special Volume 54, p.13-129.
- Brzozowski, M. 2012. Variation in fracture mineralogy and mineral chemistry around the Marathon Cu-PGE deposit; unpublished BSc thesis, University of Windsor, Windsor, Ontario, 59p.
- Dare, S.A.S., Barnes, S.-J. and Beaudoin, G. 2012. Variation in trace element content of magnetite crystallized from a fractionating sulfide liquid, Sudbury Canada: implications for provenance discrimination; *Geochimica et Cosmochimica Acta*, v.88, p.27-50.
- Darling, J.R., Hawkesworth, C.J., Lightfoot, P.C., Storey, C.C. and Tremblay, E. 2010. Isotopic heterogeneity in the Sudbury impact melt sheet; *Earth and Planetary Science Letters*, v.289, p.347-356.
- Dupuis, C. and Beaudoin, G. 2011. Discriminant diagrams for iron oxide trace element fingerprinting of mineral deposit types; *Mineralium Deposita*, v.46, p.319-335.
- Kjarsgaard, I.M. and Ames, D.E. 2010. Ore mineralogy of Cu-Ni-PGE deposits in the North Range footwall environment, Sudbury, Canada; extended abstract, *in* Abstracts, 11th International Platinum Symposium, 21–24 June 2010, Sudbury, Ontario, Canada, Ontario Geological Survey, Miscellaneous Release—Data 269, p.5-9.
- Villeneuve, M.E. 2011. An overview of Natural Resources Canada’s Targeted Geoscience Initiative 4: enhancing the effectiveness of deep exploration; *in* Summary of Field Work and Other Activities 2011, Ontario Geological Survey, Open File Report 6270, p.36-1 to 36-4.
- Watkinson, D.H. and Ohnenstetter, D. 1992. Hydrothermal origin of platinum group mineralization in the Two Duck Lake intrusion, Coldwell Complex, northwestern Ontario; *The Canadian Mineralogist*, v.30, p.121-136.

42. Overview of the High-Magnesium Ultramafic to Mafic Systems Subproject under the Targeted Geoscience Initiative 4: An Ontario Perspective

M.G. Houlé¹, C.M. Leshner² and R.T. Metsaranta³

¹Geological Survey of Canada, Québec City, Québec G1K 9A9

²Department of Earth Sciences, Laurentian University, Sudbury, Ontario P3E 2C6

³Earth Resources and Geoscience Mapping Section, Ontario Geological Survey P3E 6B5

INTRODUCTION

This report provides an update on the results of the high-magnesium ultramafic to mafic systems subproject conducted in collaboration between the Earth Resources and Geoscience Mapping Section of the Ontario Geological Survey (OGS) and the Geological Survey of Canada (GSC) as part of the nickel-copper-platinum group elements (PGE)-chromium ore systems project of the Targeted Geoscience Initiative 4 (TGI-4) (*see* Ames et al., this volume, Article 41). The main TGI-4 objectives and the different themes associated with the nickel-copper-PGE-chromium project were published last year (for more details, *see* Ames and Houlé 2011).

This year's contribution highlights research activities within the high-magnesium ultramafic to mafic system subproject carried out in collaboration with provincial governments (Ontario Geological Survey, Manitoba Geological Survey and Géologie Québec), academia and the exploration and mining sector.

HIGH-MAGNESIUM ULTRAMAFIC TO MAFIC SYSTEMS

The metal (e.g., nickel-copper-chromium-PGE) endowments of high-magnesium ultramafic to mafic systems are well-known in Canada (e.g., Thompson, Raglan) and other countries (e.g., Perseverence, Kambalda, Mt. Keith). However, these world-class deposits are becoming more and more difficult to find and operate, requiring a global perspective and better understanding of their geological settings, processes of transport, deposition and modification.

Several parameters are considered critical to the genesis of economically significant orthomagmatic nickel-copper-chromium-PGE deposits. Economically significant deposits are thought to require a number of factors: initial magmas with enough dissolved metals (i.e., not depleted through prior sulphide segregation); a dynamic system (i.e., a system that can achieve a high magma:sulphide mass ratio to form high ore tenors); an external sulphur source to achieve saturation prior to significant fractionation; a physical trap (e.g., footwall depression in magma pathway, dilational jog in magma conduit); and, finally, a good degree of preservation. However, the ore system approach recognizes that ore deposits represent very small expressions of a larger earth process system that operates at various scales to focus the magmas and metals (McCuaig et al. 2010). Despite the importance of these key parameters, one of the most critical controls is the immediate geological environment as it governs how the high-magnesium ultramafic to mafic magma will ascend through the crust and determine its magmatic architecture (i.e., plumbing system: plutonic → subvolcanic-volcanic → volcanic settings). This architecture will ultimately control the localization of nickel-copper-chromium-PGE mineralization within the ore system and will establish key exploration guidelines for targeting environments permissive for mineralization at the regional-, district- and unit-scale.

This Canada-wide subproject focusses on district- and deposit-scale studies in selected areas directed toward outlining the key components for detecting hidden or deeply buried nickel-copper-PGE-chromium mineralization by using and developing methods to characterize the fertility of intrusions, expanding target indicators (the “vectoring toolbox”) and improving the geological knowledge of the ore environments. Canada contains a variety of prospective areas for these types of deposits within both established and frontier areas throughout the Precambrian Shield. However, most of the activities within this subproject have been directed toward the most exciting emerging camp since the discovery of Voisey’s Bay in the 1990s, the “Ring of Fire” (i.e., McFaulds Lake). Numerous mafic and ultramafic intrusions have been found in the McFaulds Lake area, similar in type to those that host many other major magmatic nickel-copper-(PGE), PGE and chromium deposits worldwide and which have been recently shown to contain world-class chromite (e.g., Black Thor, Black Label, Blackbird), significant nickel-copper-PGE (e.g., Eagle’s Nest), and minor (thus far) iron-titanium-vanadium mineralization (e.g., Thunderbird) (Mungall, Azar and Hamilton 2011; Tuchscherer et al. 2010). The high level of current exploration activity in this emerging area provides unparalleled access to additional geoscience data sets and provides an ideal environment to test genetic and exploration models for chromium-PGE, nickel-copper-PGE and vanadium deposits in ultramafic to mafic systems, and will benefit from knowledge derived in complementary TGI-4 studies elsewhere in Canada. Other areas have been selected within the Bird River greenstone belt (southern Manitoba), and La Grande–Eastmain domains across James Bay (Quebec), both the potential geological extension of the Oxford–Stull domain in Ontario, and also the Abitibi greenstone belt. Together, these domains appear to define what appears to be a major new chromium-nickel-copper-PGE superdomain (metallotect) that is fundamentally different from the nickel-copper-PGE dominated systems in the Abitibi greenstone belt or, thus far, the relatively unmineralized North Caribou terrane and Goudalie domain (Figure 42.1). This subproject will hopefully highlight the likelihood of discovering additional major deposits within the frontier areas throughout Canada.

Research Activities

All the activities within this subproject have been designed to provide new, innovative and up-to-date geoscience data to support more effective exploration across Canada by developing better predictive and/or exploration models for finding buried nickel-copper-chromium-PGE deposits. Almost all of these activities are conducted in close collaboration with the OGS and could be grouped under 3 main categories: geological, method development and mineralogical. Activities under the geological heading aim to delineate key geological features that determine the ore localization within prospective mafic to ultramafic systems. Activities under the method development category seek to conduct or develop innovative exploration methods or strategies to explore for buried deposits using airborne or enhanced airborne gravity and magnetic geophysical surveys. Activities under the mineralogical category look to establish new mineralogical and geochemical factors that could indicate and/or target fertile ultramafic to mafic systems. All ongoing activities in Ontario (McFaulds Lake, Abitibi) are also intended to be complementary to other ongoing activities in southeastern Manitoba and in the James Bay area of Quebec.

GEOLOGICAL FRAMEWORK: SYSTEM FERTILITY

Bedrock Geological Mapping and Compilation

(Participants: R.T. Metsaranta, M.G. Houllé, V.J. McNicoll, M.A. Hamilton, S.L. Kamo, R.W.D. Lodge)

In 2010, the OGS started a multiyear regional compilation and bedrock geological mapping project in the McFaulds Lake region. This project is part of the core program of the OGS, but also represents an in-kind contribution to the Targeted Geoscience Initiative 4 (TGI-4), a multidisciplinary collaboration effort between geological surveys, mineral industry sector, and academia.

The main objective of this work is to update the regional geological mapping in the McFaulds Lake area, but also to increase our overall understanding of the evolution of this emerging, well-endowed Archean greenstone belt in northern Ontario. Many scientific contributions have been made since the beginning of this study and are highlighted in Metsaranta and Houlé (this volume, Article 43) but also from previous contributions over the past 2 years (Metsaranta 2010; Metsaranta and Houlé 2011).

Regional Characterization of Ultramafic to Mafic Intrusions in the Oxford–Stull and Uchi Domains, Superior Province

(Participants: M.G. Houlé, A.-A. Sappin, C.M. Leshner, R.T. Metsaranta, V.J. McNicoll)

It is well known that mafic to ultramafic rocks within Precambrian terranes similar to the Canadian Shield form large and economically prospective targets for magmatic nickel-copper-PGE, chromium and iron-titanium-vanadium deposits. Recent discoveries of world-class chromium deposits and significant nickel-copper-PGE deposits in the McFaulds Lake area highlight the likelihood of discovering additional

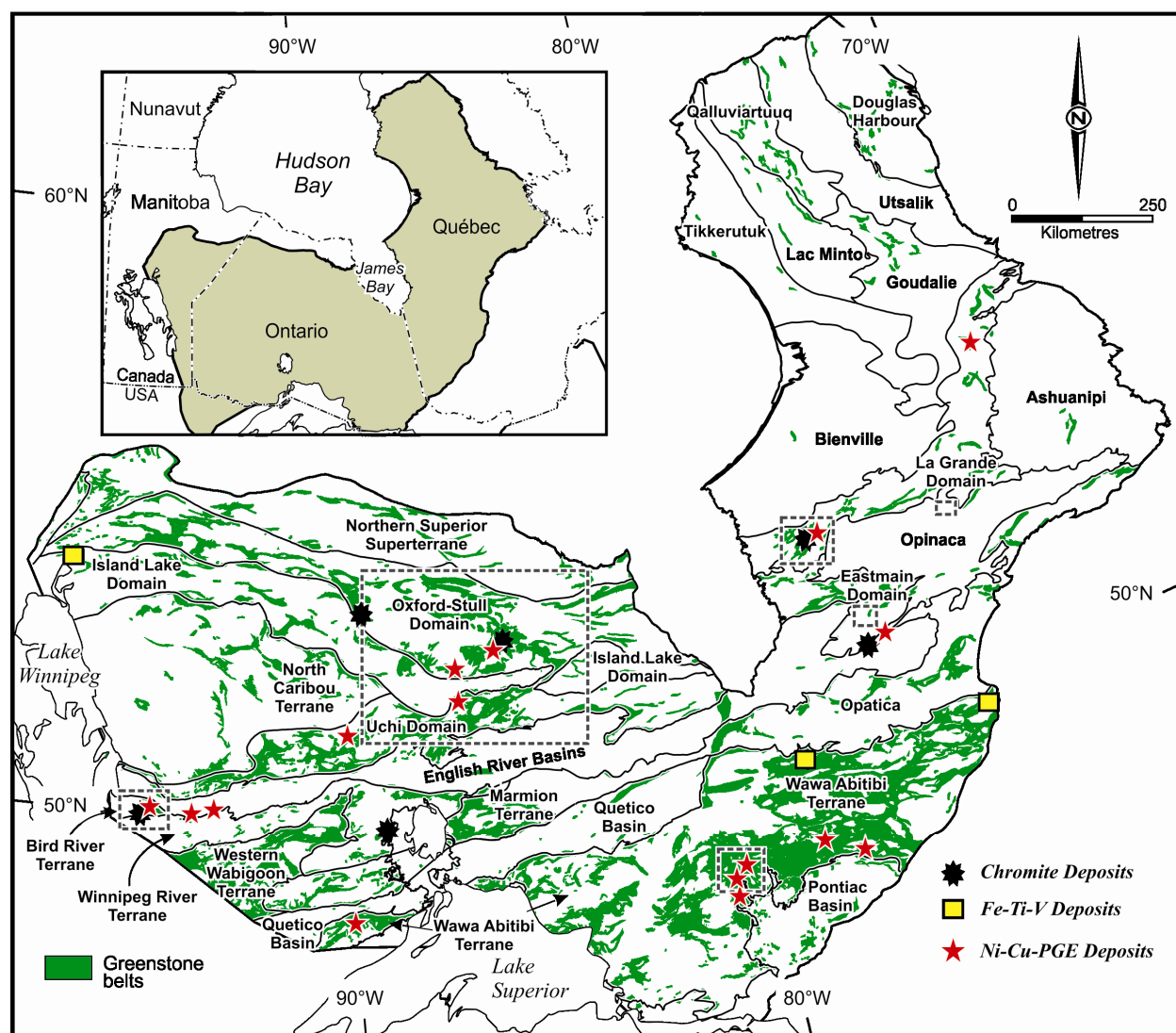


Figure 42.1. Schematic geological map showing the main nickel-copper-(PGE) sulphide and chromite deposits of the Oxford–Stull, LaGrande and Eastmain domains, and the Bird River and the Abitibi greenstone belts within the Superior Province. Note that outline boxes indicate the main location under investigation within the high-magnesium ultramafic to mafic systems subproject. Terranes, domains and boundaries are *modified from Stott and Mueller (2009)*.

major deposits within the frontier areas of Ontario. Work on this topic proposes to characterize the mafic to ultramafic intrusions in McFaulds Lake area in an effort to assess their mineral potential and stimulate further exploration for nickel-copper-PGE-chromium within the Oxford–Stull domain and in the diverse geologic terranes throughout northern Ontario.

The work will be carried out in 2 geographic areas, the eastern Oxford–Stull and eastern Uchi domains, and will include 2 components. The first component will consist of creating an inventory of all known mafic to ultramafic intrusions within these areas. The second component will involve the generation of new geoscience data on selected mafic to ultramafic complexes to develop a classification framework, based on form, petrology, lithogeochemistry, mineralization style(s), volcanic-subvolcanic setting and tectonic setting. The focus will be on intrusions that host nickel-copper-PGE, chromium and/or iron-titanium-vanadium deposits or occurrences in the Oxford–Stull and Uchi domains, but barren intrusions will be also studied to a lesser extent. This classification may be used to help delineate areas where exploration should be focussed. Ultimately, the main objectives are 1) to evaluate the critical factors that govern the localization of nickel-copper-PGE, chromium and/or iron-titanium-vanadium mineralization hosted in the mafic to ultramafic plutons; 2) to characterize the geological, geochemical, volcanic-subvolcanic and tectonic footprints of mineralized intrusions; and 3) to improve mineral exploration effectiveness in poorly exposed or surficially covered areas.

Petrology of the Ultramafic to Mafic Black Label–Black Thor Intrusive Complex in the McFaulds Lake Greenstone Belt

(Participants: H. Carson, C.M. Lesher, M.G. Houlé, R.T. Metsaranta, D. Shinkle, R. Weston)

Several graduate projects within this topic are being undertaken at Laurentian University (Sudbury) under the supervision of Drs. C.M. Lesher (Laurentian University) and M.G. Houlé (GSC) to better understand the critical parameters that are responsible for the generation of world-class chromite deposits such as the Black Thor deposit of Cliffs Natural Resources Inc. in the McFaulds Lake area. The proposed projects seek to establish the geological and geochemical footprints and how those signatures can be used as new exploration tools to target prospective ore settings.

Field work conducted by H. Carson (PhD candidate) in the summer of 2012 consisted of logging core from 18 drill holes on the Cliffs Natural Resources property. Carson's thesis focusses on the geology, geochemistry and petrogenesis of the Black Label–Black Thor intrusive complex. The logging was undertaken in order to identify the main rock types (e.g., dunite, peridotite, pyroxenite, gabbro and chromitite) within the intrusions and to define their stratigraphy. In total, 1312 samples were collected and a representative subset of 350 samples is being prepared for petrographic, mineralogical and whole-rock geochemical analyses. At least 2 other field seasons are planned for this study. A Master of Science (MSc) thesis project on the petrogenesis of nickel-copper-PGE mineralization in the Black Label–Black Thor complex will begin in January 2013, a second MSc thesis project on the petrogenesis of chromite mineralization in the Black Label is planned for the summer of 2013, and a third MSc thesis project on the petrogenesis of the Black Label pyroxenite is planned for the summer of 2014.

Petrology of Iron-Vanadium-Titanium Mafic Intrusions in the McFaulds Lake Greenstone Belt

(Participants: B. Kuzmich, P. Hollings, M.G. Houlé, R.T. Metsaranta, V.J. McNicoll, Q. Yarie, C. Hunt, E. Mosley, R. MacNally)

For this topic, a Master of Science (MSc) thesis project is being undertaken by B. Kuzmich at Lakehead University (Thunder Bay) under the supervision of Drs. P. Hollings (Lakehead University) and M.G. Houlé (GSC). The primary objective of this study is to characterize several gabbroic intrusions that host iron-titanium-vanadium mineralization at the Butler Lake property (MacDonald Mines Ltd.) and the

Thunderbird property (Noront Resources Ltd.) in the McFaulds Lake greenstone belt in order to compare their petrogenesis.

Field work conducted in the spring of 2012 consisted of logging core from 10 drill holes on the Butler Lake property; however, the actual study began in September 2012. The logging was undertaken to identify the main rock types (e.g., gabbro, anorthosite, peridotite) within the intrusions and also to define their stratigraphy. During the initial field work, 133 samples were collected and a representative subset of 54 samples was prepared for geochemical analysis. Study of the Thunderbird property began this fall with core logging followed by geochemical and petrographic work.

METHOD DEVELOPMENT: TOWARD FERTILITY

Geochemistry of Detrital Chromite: Investigating Their Use to Target Nickel-Copper-Platinum Group Element, Chromium and Iron-Titanium-Vanadium Deposits

(Participants: O.M. Burnham, D.C. Crabtree, M.G. Houlé, R.T. Metsaranta, S.E. Jackson)

This topic was designed to follow up on a stream sediment sampling program in the James Bay Lowland, carried out by the OGS under the Operation Treasure Hunt (OTH) program in 2003 (Crabtree 2003). Over 1000 stream sediment samples were collected and processed for kimberlite and metamorphic/magmatic massive sulphide indicator minerals (MMSIM^{®4}) and gold grains. A large chromite anomaly was identified by Crabtree (2003) based on the heavy mineral separates recovered and was interpreted to be associated with large mafic intrusive complexes in the area. However, at the time, the focus was placed on the compositions of the garnet fraction to evaluate the potential of this area to host additional kimberlite pipes such as the Victor Mine in the vicinity of the Attawapiskat River.

In light of recent discoveries of world-class chromite deposits, a significant nickel-copper-PGE deposit and several iron-vanadium-titanium occurrences in the McFaulds Lake area, the current proposed study aims to identify indicator mineral signatures for these types of deposits in stream sediments of the area. The study also aims to develop vectoring tools based on indicator mineral signatures to increase exploration effectiveness for deeply buried orthomagmatic chromium-nickel-copper-PGE-vanadium deposits in this thickly drift-covered area. The chemistry of detrital chromite grains is being re-investigated through statistical analysis of the original data set (>5500 electron microprobe analyses) and suggests that at least 9 compositional groups can be recognized (Burnham et al. 2012). These groups show spatial associations with bedrock geology as indicated by their titanium, ferric iron (Fe^{3+}), ferrous iron (Fe^{2+}) and vanadium contents.

Airborne Gravity Gradiometer and Magnetic Survey, McFaulds Lake Greenstone Belt

(Participants: P. Keating, D.R.B. Rainsford, M. Pilkington, M.G. Houlé, R.T. Metsaranta)

Geophysical surveys are essential tools used by geologists and explorationists to constrain geological observations, identify prospective terrains and generate specific exploration targets. This is particularly true in areas with limited bedrock exposure. An airborne gravity gradiometer and magnetometer survey was flown over the central part of the “Ring of Fire” area and jointly released in August 2011 by the OGS and GSC under the TGI-4 program to complement the regional mapping in the area (Metsaranta 2010; Metsaranta and Houlé 2011, Metsaranta and Houlé, this volume, Article 43). This regional survey has already provided the mineral industry with new and innovative tools to explore for and target buried deposits (MacDonald Mines Ltd., press release, February 16, 2012).

⁴MMSIM is a registered trademark of Overburden Drilling Management Limited, Nepean Ontario.

The high-resolution airborne magnetic and gravity gradiometry imagery helps to better define the regional geology of the area and outlines key lithological units that may host significant mineralization in the McFaulds Lake area (Rainsford et al. 2011). Continued processing of the geophysical data will focus on 1) generating pseudo-geologic contact maps that highlight lateral contrasts in magnetization and density as an aid to geological mapping and 2) three-dimensional (3-D) inversions of both gradiometer and magnetic data to retrieve structural information (at depth) for the major anomalies.

Geophysical Modelling of Gravity Survey

(Participants: M. Pilkington, P. Keating, M. Beiki, D.R.B. Rainsford, M.G. Houlé, R.T. Metsaranta)

The airborne geophysical data are being used to test new interpretation techniques (Pilkington and Beiki 2012; Beiki, Keating and Clark 2012) and study the usefulness of measuring and using all components of the gravity gradient tensor for interpretation (Pilkington 2012). A geostatistical three-dimensional (3-D) gravity inversion technique is being modified to interpret gravity gradient data. The technique will allow the inclusion of constraints such as measured densities from surface samples or boreholes when they become available.

CHEMISTRY AND GEOCHEMISTRY: VECTORS TO ORE

Chromite Geochemistry Black Label–Black Thor–Big Daddy, McFaulds Lake Greenstone Belt

(Participants: J.E. Laarman, N.A. Duke, R.L. Barnett, S.E. Jackson, M.G. Houlé)

A doctoral study on this topic is being undertaken by J.E. Laarman at Western University (London) under the supervision of Dr. N.A. Duke (Western University). The primary objective of this study is to characterize the variability of the chromite geochemistry at 3 of the chromite deposits in the McFaulds Lake area (Black Label, Black Thor and Big Daddy).

Field work was conducted during the period between 2009 and 2012 and consisted of logging core from 80 drill holes on the properties, 3 of which were chosen for detailed geochemical analysis. In total, 600 samples were collected with a representative subset of 334 samples for detailed textural and mineralogical characterization of chromites in mineralized and barren chromite-bearing lithologies. Extensive electron microprobe analysis (EMPA) has been completed on chromite grains (>4000 points) that clearly demonstrate both primary magmatic signatures as well as various degrees of replacement by ferrichromite rims. Furthermore, this analytical work will be complemented by the ultratrace geochemistry of the chromite (laser ablation inductively coupled plasma mass spectrometry (LA-ICP-MS)) to better characterize potential geochemical variation within and between each deposit, to establish the geochemical footprint and to constrain the genesis of the chromite deposits. For further details, *see* Laarman, Barnett and Duke (this volume, Article 44).

Chromite Geochemistry of Komatiitic Rocks in the Abitibi Greenstone Belt

(Participants: J. Méric, P. Pagé, S.-J. Barnes, M.G. Houlé)

A Master of Science (MSc) thesis project on this topic is being undertaken by J. Méric at Université du Québec à Chicoutimi (UQAC, Saguenay) under the supervision of Drs. P. Pagé (UQAC), S.-J. Barnes (UQAC) and M.G. Houlé (GSC). The primary objective of this study is to develop criteria, based on the chromite geochemistry, to be used as a diagnostic exploration tool for mineralized komatiitic systems.

The Hart nickel-copper-(PGE) komatiite-associated deposit, in the Shaw Dome area (Abitibi greenstone belt), was initially selected as the type locality for this study. However, preliminary petrographic work conducted on 17 samples from the Hart deposit led to focus being concentrated on the

Alexo Mine, because it is hosted in less-altered rocks. A total of 54 samples were selected from previous studies (Barnes, Gorton and Naldrett 1983; Houlé, Leshner and Davis 2012) to establish the geochemical variation of the chromite from mineralized and barren komatiitic lava flows. For further details, *see* Méric et al. (this volume, Article 46).

Multiple Sulphur Isotopes Associated with Nickel Sulphide Deposits in the Abitibi Greenstone Belt

(Participants: R.S. Hiebert, A. Bekker, M.G. Houlé, C.M. Leshner, B.A. Wing, O. Rouxel)

A doctoral study on this topic is being undertaken by R.S. Hiebert at University of Manitoba (Winnipeg) under the supervision of Drs. A. Bekker (University of Manitoba) and M.G. Houlé (GSC). The main objective of this study on multiple sulphur, iron and nickel isotopes seeks to determine the sulphur source, factors controlling stable isotope fractionation in magmatic sulphide deposits, and how those fractionation signatures might be used as a new exploration tool to target prospective ore settings.

Field work was conducted in 2011 and consisted of logging core from 11 drill holes on the Shaw Dome property (Liberty Mines Ltd.) around the Hart nickel-copper-(PGE) komatiite-associated deposits in the Abitibi greenstone belt. The field work established the main rock types (e.g., komatiite, iron formation, felsic to intermediate volcanic rocks and graphitic argillite) occurring within this succession. Sampling within the deposit area (including along strike and through the stratigraphy) was also undertaken. For this project, 108 samples were collected and 76 of these samples were selected to be used for stable isotope analyses, and further characterization through geochemical and petrographic work. For more information, *see* Hiebert et al. (this volume, Article 45).

CONCLUSIONS

In summary, the high-magnesium ultramafic and mafic system subproject is a multidisciplinary project designed to improve and expand geoscience knowledge within emerging and/or establish mining districts and develop better predictive or exploration models to support exploration for buried nickel-copper-PGE-chromium-vanadium mineral deposits across Canada.

New advances in our understanding of the geology of the McFaulds Lake greenstone belt are being made, demonstrating the merit of a collaborative approach using the traditional strengths of the OGS bedrock geology mapping, the thematic strengths of the GSC, the research skills of academia, and the comprehensive geological knowledge of mining companies in their working areas. A significant effort was also devoted to developing collaborations with universities to aid in the creation of new highly qualified geoscientific personnel, which is one of the major goals of the TGI-4 program. Thus far, for the entire subproject, activities are being conducted in 4 provinces and involve 1 postdoctoral fellow, 3 PhD candidates, 3 MSc candidates, and 1 BSc candidate at 6 universities across Canada.

We believe that an integrated approach is needed to advance our understanding of the geology of the highly prospective McFaulds Lake area and its numerous mineral deposit types. We are also confident that the new geoscience information resulting from this program will provide many innovative scientific ideas and concepts that are, and that will continue to be, relevant to exploration in this area, but also elsewhere within Archean terranes.

ACKNOWLEDGMENTS

First of all, we would like to express our appreciation to numerous companies for their logistical support, access to properties, information and, foremost, for discussions throughout project development including Cliffs Natural Resources Inc. (Andrew Mitchell, Richard Fink, David Shinkle, Daron Slaney), formerly Freewest Resources Canada Inc.—Cliffs Natural Resources Inc. (Don Hoy, Martin Tuchscherer), Noront Resources Ltd. (Ralph MacNally, Eric Mosley, Eric Downey), KWG Resources Inc. (Moe Lavigne), MacDonald Mines Ltd. (Quentin Yarie, Jacob McKinnon, Craig Sherba, Craig Hunt, and James Masters), Melkior Resources Inc. (Nathalie Hansen, Éric Hébert and Ian Lawyer) and Northern Shield Resources Inc. (Christine Vaillancourt, Ian Bliss, Rénée-Luce Simard). Thanks are also extended to Jim Franklin, Larry Hulbert, Jim Mungall and Greg Stott for valuable discussions and insight into the geology of the McFaulds Lake area. Finally, we want to greatly acknowledge the involvement and the participation, at many stages including some inputs on this contribution, of numerous researchers and students in the TGI-4 high-magnesium ultramafic to mafic system subproject including V.J. McNicoll, P. Keating, M. Pilkington, S.E. Jackson, and A.-A. Sappin (Geological Survey of Canada); H. Carson and R.W.D. Lodge (Laurentian University, Sudbury); B. Kuzmich and P. Hollings (Lakehead University, Thunder Bay); O.M. Burnham, D.R.B. Rainsford, and D.C. Crabtree (Ontario Geological Survey); J.E. Laarman, N.A. Duke (Western University, London); J. Méric, P. Pagé and S.-J. Barnes (Université du Québec à Chicoutimi, Saguenay); R.S. Hiebert and A. Bekker (University of Manitoba, Winnipeg); and B.A. Wing (McGill University, Montréal). This is Geological Survey of Canada contribution number 20120244.

REFERENCES

- Ames, D.E. and Houlé, M.G. 2011. Overview of the Targeted Geoscience Initiative 4 nickel-copper-platinum group elements-chromium project (2010–2015)—mafic to ultramafic ore systems: footprint, fertility and vectors; *in* Summary of Field Work and Other Activities 2011, Ontario Geological Survey, Open File Report 6270, p.37-1 to 37-7.
- Barnes, S.-J., Gorton, M.P. and Naldrett, A.J. 1983. A comparative study of olivine and clinopyroxene spinifex flows from Alexo, Abitibi greenstone belt, Ontario, Canada; *Contributions to Mineralogy and Petrology*, v.83, p.293-308.
- Beiki, M., Keating, P. and Clark, D. 2012. Depth estimation of magnetic and gravity sources using normalized source strength calculated from gradient tensor; abstract, Society of Exploration Geophysicists, 2012 annual meeting, Las Vegas, Nevada.
- Burnham, M., Crabtree, D. and Metsaranta, R. 2012. Identification of chromitite and kimberlite occurrences in the James Bay lowland using statistical analysis of detrital chromite compositions; abstract, The 22nd Annual V.M. Goldschmidt Conference™, Montreal, Quebec, June 24–29, 2012.
- Crabtree, D.C. 2003. Preliminary results from the James Bay Lowland indicator mineral sampling program; Ontario Geological Survey, Open File Report 6108, 115p.
- Houlé, M.G., Leshar, C.M. and Davis, P.C. 2012. Thermomechanical erosion at the Alexo Mine, Abitibi greenstone belt, Ontario: implications for the genesis of komatiite-associated Ni-Cu-(PGE) mineralization; *Mineralium Deposita*, v.47, p.105-129, DOI: 10.1007/s00126-011-0371-6.
- McCuaig, T.C., Beresford, S. and Hronsky, J. 2010. Translating the mineral systems approach into an effective exploration targeting system; *Ore Geology Reviews*, v.38, p.128–138.
- Metsaranta, R.T. 2010. McFaulds Lake area regional compilation and bedrock mapping project; *in* Summary of Field Work and Other Activities 2010, Ontario Geological Survey, Open File Report 6260, p.17-1 to 17-5.

- Metsaranta, R.T. and Houlé, M.G. 2011. McFaulds Lake area regional compilation and bedrock mapping project update; *in* Summary of Field Work and Other Activities 2011, Ontario Geological Survey, Open File Report 6270, p.12-1 to 12-12.
- Mungall, J.E., Azar, B. and Hamilton, M.A. 2011. Ni-Cu-PGE-Cr-Fe-Ti-V and VMS mineralisation of the Ring of Fire intrusive suite, Ontario; abstract *in* Geological Association of Canada–Mineralogical Association of Canada, Ottawa 2011 Joint Annual Meeting, Program with Abstracts, v.34, p.148.
- Pilkington, M. 2012. Analysis of gravity gradiometer inverse problems using optimal design measures; *Geophysics*, v.77, no.2, G25-G31.
- Pilkington, M. and Beiki, M. 2012, Mitigating remanent magnetization effects in magnetic data using the normalized source strength; extended abstract, Society of Exploration Geophysicists, Las Vegas 2012 Annual Meeting, session GM3 - Mostly Magnetism, presentation GM3.3, DOI: 10.1190/segam2012-0079.1.
- Rainsford, D.R.B., Houlé, M.G., Metsaranta, R.T., Keating, P. and Pilkington, M. 2011. An overview of the McFaulds Lake airborne gravity gradiometer and magnetic survey, northwestern Ontario; *in* Summary of Field Work and Other Activities 2011, Ontario Geological Survey, Open File Report 6270, p.39-1 to 39-8.
- Stott, G.M. and Mueller, W.U. 2009. Superior Province: the nature and evolution of the Archean continental lithosphere; *Precambrian Research*, v.168, p.1-3.
- Tuchscherer, M.G., Hoy, D., Johnson, M., Shinkle, D. and Holmes, M. 2010. Fall 2008 to winter 2009 technical drill report on the Black Thor chromite deposit–Black Label chromite zone and associated Ni-Cu-PGEs, McFaulds Lake property, James Bay Lowlands, northern Ontario; unpublished technical report, Freewest Resources Canada Inc., 57p.

43. Project Unit 10-004. Progress on the McFaulds Lake (“Ring of Fire”) Region Data Compilation and Bedrock Geology Mapping Project

R.T. Metsaranta¹ and M.G. Houlé²

¹Earth Resources and Geoscience Mapping Section, Ontario Geological Survey, Sudbury, Ontario P3E 6B5

²Geological Survey of Canada, Québec City, Québec G1K 9A9

INTRODUCTION

This report provides an update on continued, regionally focussed, geological compilation and bedrock mapping in the McFaulds Lake or “Ring of Fire” region in northern Ontario. The project is part of the Ontario Geological Survey’s (OGS) core bedrock geology mapping program, but it is also an in-kind contribution to the Targeted Geoscience Initiative 4 (TGI-4) of the Geological Survey of Canada (GSC), which is part of the Earth Sciences Sector (ESS) of Natural Resources Canada (NRCan). As outlined in Metsaranta (2010) and Metsaranta and Houlé (2011), the main objectives at the outset of the project were to

- update the regional bedrock geological mapping in the McFaulds Lake region;
- clarify and characterize the major lithologic units;
- better understand the stratigraphy and age relationships between the various lithologies;
- develop a better understanding of the actual extent of the mafic to ultramafic intrusions hosting recently discovered nickel-copper-platinum group elements (PGE) and chromium deposits in the region;
- develop a better understanding of the structural and metamorphic history of the area;
- improve our understanding of the relationship of geophysical features to bedrock geology.

More specifically, this report outlines some new observations and ideas on the broad stratigraphy of the McFaulds Lake greenstone belt, with a focus on supracrustal rocks based on field observations from outcrop mapping and diamond-drill holes carried out during the past summer. Further information on the project is also available to the reader in previously published articles (Metsaranta 2010; Metsaranta and Houlé 2011; Rainsford et al. 2011).

PROJECT STATUS

The McFaulds Lake geological compilation and bedrock mapping project was initiated during the summer of 2010 and covers an area of approximately 17 550 km² (~135 by 130 km; Figure 43.1) in far northern Ontario. A summary of data compilation and field work carried out on the project to date is shown on Figure 43.1 and includes compiled diamond-drill hole and outcrop locations, the locations of re-logged diamond-drill holes and the locations of outcrops visited in the course of the project. Field work in 2012 consisted of 2 main activities: continued re-logging of exploration company diamond-drill core and helicopter-based outcrop mapping over the entire area.

*Summary of Field Work and Other Activities 2012,
Ontario Geological Survey, Open File Report 6280, p.43-1 to 43-12.*

© Queen’s Printer for Ontario, 2012

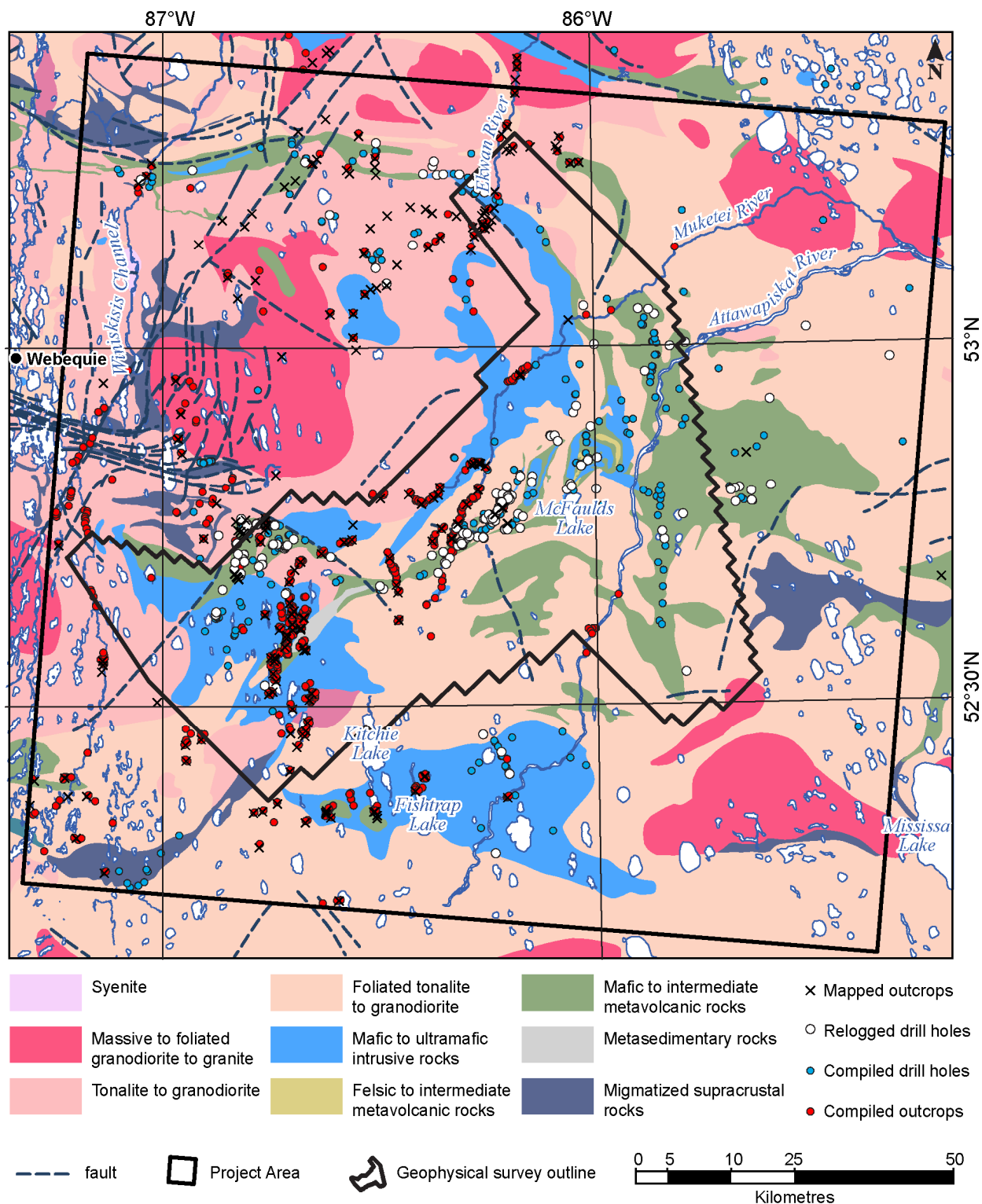


Figure 43.1. Compiled outcrop and diamond-drill hole locations as well as locations of re-logged diamond-drill core and mapped outcrops. Also shown is the area of the 2011 OGS–GSC airborne geophysical survey (Ontario Geological Survey 2011a). Compiled outcrop locations are from Bostock (1962), Thurston, Sage and Siragusa (1971a, 1971b), and Thurston and Carter (1969). Geology from Stott and Josey (2009).

Re-logging of diamond-drill core was carried out mainly at the MacDonald Mines Exploration Ltd. Butler Lake camp and, to a lesser extent, at various other inactive exploration camps and at the First Nation community of Webequie. During the 2012 field season, 50 diamond-drill holes, totalling approximately 10 200 m, were re-logged in varying detail. Helicopter-supported outcrop mapping, based from Webequie, was carried out between July 5 and 31, 2012. This mapping provided new geological information on 175 outcrops across the project area. Since the beginning of the project, 212 diamond-drill holes, totalling approximately 53 000 m, have been re-examined and 230 outcrops have been mapped. Field work in the McFaulds Lake region will likely continue for one more field season to fill a few significant gaps in data collection in the area (see Figure 43.1) that need to be addressed prior to completion of regional geological bedrock maps.

Further work being carried out in conjunction with this project includes several thematic studies on mafic and ultramafic rocks in the McFaulds Lake area initiated to address more specific scientific gaps relating to nickel-copper-PGE-chromium mineralization. Houlé, Leshner and Metsaranta (this volume, Article 42) provide more details on these ongoing thematic studies conducted in collaboration between the GSC and the OGS under the TGI-4 program.

PRELIMINARY SUBDIVISIONS OF THE MCFAULDS LAKE GREENSTONE BELT

The regional geological bedrock mapping and compilation conducted to date in the McFaulds Lake greenstone belt has highlighted a number of potentially distinct supracrustal rock packages with spatially related mafic to ultramafic intrusive rocks. These preliminary packages have been identified based on lithological mapping and geophysical interpretation supplemented by new and compiled geochronology. Based on this new geological knowledge acquired in the area, the supracrustal rocks are tentatively subdivided into 5 supracrustal rock packages that range in age from older than 2808 Ma to younger than 2702 Ma. These packages include the:

- *Kitchie Lake supracrustal package*, consisting of potential remnants of Mesoarchean crust occurring west of, and intruded by, the Highbank Lake–Fishtap Lake intrusive complex (*circa* 2808 Ma: M.A. Hamilton, Jack Satterly Geochronology Laboratory, unpublished data cited by Stott 2008);
- *Butler Lake supracrustal package*, consisting of ultramafic to felsic volcanic rocks and a variety of mafic to ultramafic intrusive rocks of unknown age in the Butler Lake area. Felsic metavolcanic rocks in this package host significant volcanogenic massive sulphide (VMS)-style mineralization and alteration, nickel-sulphide-bearing gabbro and iron-titanium-vanadium-rich magnetite gabbro;
- *Muketei River supracrustal package*, consisting of northeast-striking mafic and felsic metavolcanic rocks, minor clastic metasedimentary rocks and iron formation. At least 2 ages of volcanic strata are present in this package: *circa* 2770 Ma and *circa* 2737 Ma. The younger (*circa* 2737 Ma) felsic-dominated metavolcanic rocks host VMS mineralization. Ultramafic rocks, intruding the older (*circa* 2770 Ma) supracrustal rocks, are host to the various chromium and nickel-copper-PGE deposits in the region. The greenstone belt hosts magnetite-bearing gabbro intrusions varying from large layered gabbro bodies (e.g., Thunderbird iron-titanium-vanadium showing of Noront Resources Ltd.) to thinner sills which are characteristic of this package;
- *Winiskisis Channel supracrustal package*, consisting of roughly east-striking dominantly mafic metavolcanic rocks with lesser felsic to intermediate metavolcanic rocks and intercalated metasedimentary rocks. At least in part, these rocks are younger than 2714 Ma based on detrital zircon geochronology (Buse et al. 2009). Both ultramafic and mafic igneous bodies intrude

supracrustal rocks of this package, including ferrogabbro similar to the Butler Lake supracrustal package and Muketei River supracrustal package;

- *Attawapiskat River supracrustal package*, consists of a mafic- to felsic-dominated volcanic succession with subordinate magnetite-gabbro intrusions in the western part, a sedimentary-dominated succession in the central part (with preliminary detrital zircon ages as young as *circa* 2702 Ma) and a mafic-dominated volcanic succession in the eastern part.

The simplified geological map (Figure 43.2) outlines the geographic distribution of these supracrustal-dominated packages and provides a new geological framework for the McFaulds Lake greenstone belt. Other geological units, comprising a variety of felsic and intermediate intrusive rocks, are also present; however, because of space constraints, observations on these units are limited. Descriptions of the supracrustal packages outlined above, highlighting the main characteristics of each, are provided below. It is important to note that, at this point, subdivision into these supracrustal packages is done primarily for description and clarification purposes and will most likely be modified in the future in the light of the new geochronological and geochemical data being gathered during this project.

Kitchie Lake Supracrustal Package

The Kitchie Lake supracrustal package occurs in the south-central part of the map area. Based on limited outcrops and no diamond-drill holes, it forms a 15 km long, east-striking band to the south of Kitchie Lake and west of Highbank Lake. Despite the scarcity of diamond drilling and outcrop exposure that makes this interpretation equivocal, the Kitchie Lake supracrustal package appears to be engulfed by mafic and ultramafic rocks related to the Fishtrap Lake and Highbank Lake intrusions (*see* Figure 43.2). To the north and south, this package appears to be bounded by younger granitoid intrusions, which may, in part, also control the map pattern of the Highbank Lake–Fishtrap Lake intrusive complex. The westward extension of the Kitchie Lake supracrustal package remains unclear. As mentioned above, these supracrustal rocks are tentatively assigned an age of older than 2808 Ma, the existing age constraint for the Highbank Lake intrusion reported by Stott (2008). A sample of a quartz-rich metasedimentary unit from this package has been collected for detrital zircon U/Pb geochronology to test this hypothesis.

This area was mapped previously by Bostock (1962) as a sedimentary-dominated succession including many lithologies such as quartzite, greywacke, paragneiss, schist with lesser mafic metavolcanic pillowed flows. Re-mapping of these outcrops (in 2012) suggests that those sedimentary units could be re-interpreted as medium-grained, buff coloured, moderately foliated, poorly bedded, quartz-rich, garnet-biotite-bearing metasandstones with prominent steeply southeast-plunging stretching lineations (Photo 43.1A). Fine-grained, weakly to moderately magnetic, foliated gabbro dikes were observed to crosscut this metasedimentary succession and could be related to the Fishtrap Lake intrusion. Re-mapping of some of the “pillowed flow” outcrops revealed dark green, homogeneous, fine- to medium-grained amphibolites with moderate foliations and rare relict pillow structures (Photo 43.1B). It is not clear whether these are, in fact, amphibolite-grade metamorphosed mafic metavolcanic rocks or, at least in part, fine-grained gabbro.

Thus far, this area is not known to contain significant mineralization. The only mineralization identified occurs within the Highbank Lake mafic to ultramafic layered intrusion and consist of thin magnetite-bearing horizons that grade up to 0.75% V₂O₅ over 5.2 m including a higher grade interval of 0.98% V₂O₅ over 2.2 m (Northern Shield Resources Inc., Highbank Lake property, www.northern-shield.com/properties/highbank [accessed September 27, 2012]). However, Northern Shield Resources Inc. have also reported numerous boulders of chromite-bearing peridotite and grains of nickel and platinum sulphide-bearing minerals in stream sediments in the area suggesting that this mafic to ultramafic intrusion may have the potential to host other styles of magmatic mineralization.

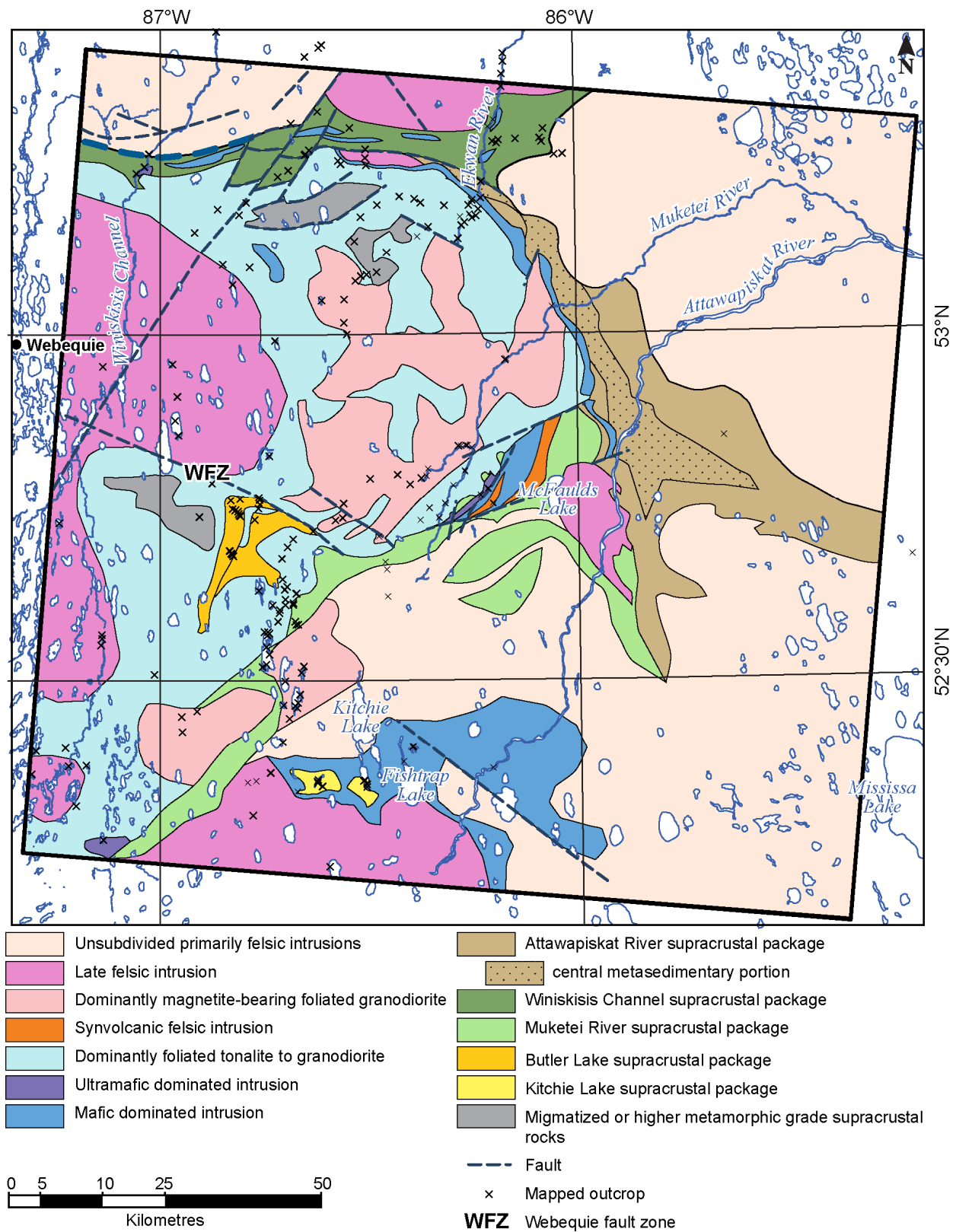


Figure 43.2. Simplified geology of the McFaulds Lake project area showing the distribution of preliminary supracrustal packages.



Photo 43.1. A) Quartz-rich metasandstone from the Kitchie Lake supracrustal package (UTM 533264E 5800356N). B) Amphibolite-grade mafic metavolcanic rocks or fine-grained gabbro with crosscutting fine-grained granite dike, Kitchie Lake supracrustal package (UTM 525659E 5799909N). C) Igneous layering in stripped outcrop of magnetite-bearing gabbro, western section of Butler Lake supracrustal package (UTM 511953E 5844024N). D) Intense anthophyllite-garnet alteration in felsic volcanic rock near the Butler 3 VMS occurrence in the western part of the Butler Lake supracrustal package (UTM 513077E 5842933N). E) Weakly deformed and relatively unaltered felsic tuff, *circa* 2737 Ma portion of Muketei River supracrustal package (UTM 566403E 5855024N). F) Mafic volcanic rock and oxide-facies iron formation from the *circa* 2770 Ma part of the Muketei River supracrustal package (UTM 552186E 5849798N). G) Weakly deformed, pillowed, mafic metavolcanic rocks from the eastern part of the Winiskisis Channel supracrustal package (UTM 557379E 5903875N). H) Deformed, pillowed, mafic flows from the mafic-dominated, eastern portion of the Attawapiskat River supracrustal package (UTM 621396E 5837115N). I) Black argillite interbedded with fine-grained sandstone from the central metasedimentary portion of the Attawapiskat River supracrustal package (UTM 578319E 5842799N). Universal Transverse Mercator (UTM) co-ordinates are provided using North American Datum 1983 (NAD83), Zone 16.

Butler Lake Supracrustal Package

The Butler Lake supracrustal package occurs in the west-central part of the project area and was a major focus of mapping during 2012 (*see* Figure 43.2). To the north, the package is bounded by the Webequie fault zone, which is a major, dextral, regional structure. To the west, the package appears to be bounded by older tonalitic rocks, and migmatized supracrustal rocks (Buse et al. 2009). To the east, a variety of tonalitic to granodioritic intrusive rocks are present. The southward extension of the Butler Lake supracrustal package is not well delineated, but it is best detected by recent airborne gravity gradiometry data (OGS–GSC 2011). Based on geological compilation, mapping and geophysics, the Butler Lake supracrustal package is subdivided into a western and eastern domain separated by an area of low magnetic response. Both domains appear to merge in the southwest of the Butler Lake supracrustal package. No previous geochronology exists for this area. In 2012, felsic metavolcanic rocks from both the eastern and western domains and an anorthositic gabbro were sampled for U/Pb age determinations.

The western domain, strikes approximately north to northeast over a length of about 30 km and has an average width of 3 to 4 km. At its north end, it folds to the east as a result of dextral motion along the Webequie fault zone, which appears to create a broad regional drag fold. This domain consists of felsic-dominated metavolcanic rocks with subordinate mafic to ultramafic metavolcanic rocks intruded by mafic-dominated intrusions. Along its eastern edge, it is dominated by felsic volcanic strata with abundant hydrothermal alteration and a number of significant VMS-style copper-zinc showings. Preservation of primary features in these metavolcanic rocks is poor, resulting from extensive subvolcanic alteration and subsequent metamorphism to amphibolite facies (Photo 43.1D). Metamorphosed alteration zones are variable, and further work is required to establish some mappable units based on more detailed mineralogical and geochemical investigations. Ultramafic metavolcanic rocks are present in the far northwest corner of this section near the hinge of the fold created by the Webequie fault. Mafic to ultramafic intrusive rocks, including layered magnetite-bearing gabbro, gabbro and anorthosite underlie the area to the west of the felsic metavolcanic rocks. Within this intrusive-dominated part of the section, it is not clear whether there are multiple thin gabbroic sills intruding volcanic strata, or if there is a single, differentiated mafic intrusive body. A number of gabbro outcrops were mapped in this area, of which some display well-preserved igneous interlayering of gabbro, anorthositic gabbro and magnetite-bearing gabbro with minor sulphide mineral veining and rare crosscutting ultramafic dikes (Photo 43.1C). The majority of observed facing directions suggest younging to the east, based on a variety of somewhat tenuous indicators, such as mineralogical variation in igneous layers, sedimentary structures such as displacements along small-scale synsedimentary normal faults and alteration patterns around VMS mineralization zones. However, small-scale folding as well as evidence for multiple structural fabrics in some diamond-drill holes indicate that several deformation episodes have affected the area.

The eastern domain of the Butler Lake supracrustal package strikes northeast and has an approximate width of 4 to 5 km and contains a variety of supracrustal lithologies, but is generally dominated by high-magnesium to mafic metavolcanic rocks with lesser iron formation and felsic metavolcanic rocks. However, this domain is characterized by numerous mafic to ultramafic units, mostly intrusive in origin, throughout the entire section. The diverse mafic to ultramafic intrusive rocks in this area include ultramafic intrusive rocks composed essentially of dunitic and peridotitic rocks and several variations of mafic intrusive phases. At least 3 types of mafic intrusive rocks are recognized in that area: 1) iron-rich, magnetite-gabbro-bearing intrusions similar to magnetite-bearing gabbroic rocks within other supracrustal package, 2) non-magnetic gabbro intrusions commonly spatially associated with type 1 and 3) equigranular gabbroic intrusions intercalated with mafic metavolcanic rocks and iron formation similar in appearance to some gabbroic rocks found along the western edge of the Muketei River supracrustal package. The magnetic low between the western and eastern domains of the Butler Lake supracrustal package is underlain, in part, by gabbroic rocks and, in part, by a tonalite to quartz-diorite intrusion, based on isolated outcrops.

The Butler Lake supracrustal package contains numerous occurrences of copper-zinc VMS-style mineralization, dominantly within the western domain. Gabbro-hosted nickel-copper-PGE-style mineralization occurs primarily within the eastern domain and iron-vanadium-titanium oxide mineralization is present in both domains. This supracrustal package is currently being explored by MacDonald Mines Exploration Ltd. for copper-zinc VMS, nickel-copper-PGE and iron-vanadium-titanium mineral potential, but also to assess its potential to host chromite mineralization. Four areas are currently targeted for its VMS mineralization (Butler 1 to 4). The best results, obtained to date on the Butler 3 occurrence, grade up to 3.26% Zn, 0.4% Cu and 6 g/t Ag over 41.5 m (MacDonald Mines Exploration Ltd., news release, August 16, 2012, www.macdonaldmines.com/news/2012, [accessed September 27, 2012]). The best nickel assay results grade up to 0.26% Ni over 27 m associated with a gabbroic phase on the eastern domain. Iron-vanadium-titanium assays from magnetite-bearing gabbro units vary. Analyses reported by MacDonald Mines Exploration Ltd. revealed, for example, 1.17% V₂O₅, 7.97% TiO₂ and 40.73% Fe over 4.2 m, as a higher grade intersection, and 0.54% V₂O₅, 0.46% TiO₂ and 23.78% Fe over 36 m as a wider, lower grade interval (MacDonald Mines Exploration Ltd., news release, May 11, 2012, www.macdonaldmines.com/news/2012 [accessed September 27, 2012]).

Muketei River Supracrustal Package

The Muketei River supracrustal package trends in a northeast-southwest orientation and appears to extend, over a strike length of up to 110 km (*see* Figure 43.2). However, the southwest extension of this package is highly speculative as a result of sparse drilling and lack of outcrop data. To the northeast and east, the package appears to be truncated by rocks of the Attawapiskat River supracrustal package trending roughly northwest. To the west, this unit is bounded primarily by foliated tonalitic rocks and, to the east-southeast, by a variety of granitoid rocks, including a prominent oval-shaped posttectonic pluton adjacent to McFaulds Lake. Northeast-trending shear zones transect the package and, based on limited outcrop evidence, appear to be dextral. In addition, later, north- and northwest-trending faults are also present. The geology of the central domain of this area is perhaps the best understood of any part of the McFaulds Lake area, as it is the site of world-class chromium deposits and significant nickel-copper-PGE deposits.

This supracrustal rock package is characterized by 2 ages of volcanic strata: 1) 2770.7±0.8 Ma (Mungall, Azar and Hamilton 2011) and 2) 2737±7 Ma (Rayner and Stott 2005). Chromium and nickel-copper-PGE mineralized ultramafic intrusive bodies appear to be emplaced near the contact between the metavolcanic rocks (*circa* 2770 Ma), and tonalite (*circa* 2773 Ma) (Mungall et al. 2010). These mineralized ultramafic intrusions are considered to be emplaced *circa* 2735 Ma (Mungall et al. 2010), the age of a potentially co-magmatic ferrogabbro phase and, as such, appear to be roughly coeval with the mainly intermediate to felsic metavolcanic rocks (*circa* 2737 Ma). In addition, deformed tonalitic to granodioritic, likely synvolcanic, intrusions are present within the section (*see* Figure 43.2). In places, gabbroic rocks, with mafic metavolcanic rocks and iron formation (Photo 43.1F), similar in appearance to the eastern portion of the Butler Lake supracrustal package, rather than tonalite, are in contact with the mineralized ultramafic suite on its western side (*see* Figure 43.2). These may be part of the supracrustal unit *circa* 2770 Ma inferred by Mungall, Azar and Hamilton (2011) and, as such, supracrustal rocks of that age are present in the hanging wall and footwall of the mineralized ultramafic intrusion. This older unit may form the bulk of the metavolcanic rocks in the Muketei River supracrustal package and it includes both mafic- and felsic-dominated successions, but these have not yet been delineated in detail. Felsic to intermediate metavolcanic rocks of age *circa* 2737 Ma (Photo 43.1E) appear to be restricted to the area east of the large layered, iron-titanium-vanadium-mineralized gabbro that hosts the Thunderbird occurrence held by Noront Resources Ltd.

The Muketei River supracrustal package is the most endowed supracrustal package in the McFaulds Lake area with several world-class chromite deposits (e.g., Black Thor, Big Daddy, Black Label, Black Creek), the Eagle's Nest nickel-copper-PGE deposit, small VMS deposits (e.g., McFaulds #1 and #3 deposits). This package also hosts a number of additional VMS occurrences, magmatic nickel-sulphide occurrences and iron-titanium-vanadium occurrences (e.g., Noront Resources Ltd. Thunderbird zone). The reader is referred to Metsaranta and Houlé (2011) for more detailed information on the geological resources of these deposits.

Winiskisis Channel Supracrustal Package

The Winiskisis Channel supracrustal package forms a significant, broadly east-striking supracrustal package that extends over a length of 80 to 90 km and widths of 5 to 10 km in the northern part of the project area. To the north, it is bound primarily by foliated tonalite and granodiorite as well as younger granite to granodiorite plutons. To the south, foliated tonalitic rocks are also present, along with an area of highly metamorphosed supracrustal rocks (*see* Figure 43.2). To the west, the Winiskisis Channel supracrustal package appears to extend toward Kasabonika Lake, whereas, to the east, it is bound by granitoid plutons. A fault contact is interpreted between the supracrustal rocks of the Winiskisis Channel supracrustal package and the Muketei River supracrustal package to the southeast, but the overall geological context is still unclear (*see* Figure 43.2). Detrital zircons from a reworked tuff unit in the extension of this package to the west yielded ages as young as *circa* 2714 Ma (Buse et al. 2009). This indicates that, at least in part, the Winiskisis Channel supracrustal package is younger than the Muketei River supracrustal package. Another sample of felsic metavolcanic rock from this package has been collected for geochronological assessment to see if it will confirm this younger age. Prominent, east-trending and also north-northeast-trending faults crosscut the Winiskisis Channel supracrustal package and the east-trending faults appear to represent a regional fault zone of similar scale to the Webequie fault zone.

Based on limited mapping and core logging, the Winiskisis Channel supracrustal package contains felsic to mafic metavolcanic rocks and minor intercalated metasedimentary units. Notably, during outcrop mapping, a substantial area of supracrustal rocks, dominated by pillowed to massive mafic metavolcanic flows was observed in the central and eastern part of this supracrustal package. Typical outcrops varied from nearly undeformed with vesicular, amoeboid pillow forms (Photo 43.1G) near the central part of the package, to highly strained near contacts with inferred neighbouring felsic plutons. This strain gradient also appeared to mirror metamorphic grades where less deformed sections are characterized by greenschist facies and more amphibolite facies toward the margins. The Winiskisis Channel supracrustal package is also intruded by subconcordant mafic to ultramafic igneous bodies. A few diamond-drill holes at the west end of this package contain thick intervals of dunite to peridotite. A separate diamond-drill hole contains a crudely layered magnetite-bearing gabbro. The magnetite-bearing gabbro section is very similar in appearance to those described in the other packages so far. On previous regional compilation maps, this eastern area was shown to be underlain by granitoid rocks, likely due to their non-magnetic geophysical signature. There is a strong, north-northeast-striking vertical gravity gradient anomaly associated with this part of the greenstone belt (at the northern margin of the geophysical survey area), which is coincident with a smaller ovoid magnetic anomaly (OGS–GSC 2011). There are also a number of similar linear magnetic anomalies outside of the gravity gradiometer survey area (OGS–GSC 2011). These are tentatively interpreted as mafic to ultramafic intrusions, although no outcrops were found to support this interpretation. This area contains several large outcrop areas that were not examined in detail because of the reconnaissance nature of the mapping project. At present, much of this area is not staked and would make an interesting prospecting target.

This supracrustal package is characterized by the presence of significant VMS-style mineralization associated with very altered felsic and mafic metavolcanic rocks. Some of the best intervals of massive to semi-massive sulphides grade up to 13.8% Zn, 0.50% Cu, 0.05% Pb, 2 g/t Ag over 26 m and up to 2.67% Zn were obtained on the 5.01 and the Northern Star Eagle (TMX-08-02) occurrences, respectively (Ontario Geological Survey 2011; MDI000000000912 and MDI000000000861). Thus far, no other mineralization has been reported within the Winiskisis Channel supracrustal package.

Attawapiskat River Supracrustal Package

The Attawapiskat River supracrustal package is almost entirely overlain by Paleozoic strata where the preliminary geological interpretation of this part of the belt is based only on limited scattered observations from diamond-drill cores and outcrops. To the northeast and the southeast, the Attawapiskat River supracrustal package is bounded by a large area of inferred felsic to intermediate intrusive rocks. Reconnaissance geochronology by Rayner and Stott (2005) yielded U/Pb ages for 3 quartz diorite to diorite samples, respectively, of *circa* 2710 Ma to the northeast of this package and *circa* 2724 to 2728 Ma to the southeast of this package. To the west, this package is in contact with the Muketei River supracrustal package, but the nature of the contact remains unclear. Although this area remains poorly characterized, it can be crudely divided into 3 domains (western, central and eastern domains) as outlined below.

The western domain is defined by a prominent generally north-striking vertical gravity gradient anomaly (OGS–GSC 2011) that appears to be dominated by ferrogabbroic sills intruding the felsic to mafic volcanic succession, and may be correlative with supracrustal rocks *circa* 2737 Ma in the eastern part of the Muketei River supracrustal package. The central domain, characterized by a low magnetic signature, consists of felsic to intermediate tuffaceous metavolcanic rocks in the north, and a clastic metasedimentary succession including graphitic argillite and greywacke farther east (Photo 43.1I). The eastern domain appears to be more mafic in character, based on examined diamond-drill core and outcrops. Two Archean inliers within this eastern domain consist of an exposure of fairly homogenous medium-grained gabbro and an exposure of mafic metavolcanic flows (Photo 43.1H) with subordinate gabbroic intrusions, respectively. During the summer of 2012, a number of diamond-drill holes were logged from the eastern domain within this package where the dominant lithology is massive and pillowed mafic metavolcanic flows. Locally, in drill core, many pervasive zones of carbonatization, sericitization and silicification were observed along with minor veins of sulphide mineralization. In places, zones of silicification, brecciation and sulphide minerals were associated with contacts of feldspar porphyritic tonalite to quartz diorite intrusions and may be prospective hosts for gold mineralization. Preliminary detrital zircon U/Pb geochronology, carried out during this study, yielded zircon as young as *circa* 2702 Ma from the central metasedimentary unit, supporting a generally younger age for this package.

This supracrustal package is not especially well mineralized, but contains several VMS mineralization occurrences associated with felsic volcanoclastic rocks similar in style to mineralization within the McFaulds #1, #2 and #3 copper-zinc occurrences in the eastern part of the Muketei River supracrustal package. The best intersection reported by the company (Probe Mines Ltd.) shows up to 0.86% Zn, 0.03% Pb and 0.13% Cu over 2.0 m associated with a sequence of coherent and fragmental intermediate metavolcanic rocks crosscut by carbonate-chlorite-quartz veinlets (Ontario Geological Survey 2011; MDI000000000264). Interestingly, almost all the VMS occurrences seem to be spatially associated with high magnetic anomaly interpreted to be related to the presence of ferrogabbro sills. Furthermore, locally, some of these ferrogabbro sills have potential to contain iron-titanium-vanadium mineralized intersection within magnetite-bearing lithologies.

SUMMARY

The stratigraphic framework outlined above highlights our improving understanding of the geology of the McFaulds Lake greenstone belt. Continuing field work and laboratory studies, including the geochronology sampling mentioned above, lithogeochemistry and petrography, will likely provide refinements to this preliminary framework. In particular, the sampling of materials for geochronology should permit further refinements on the timing of various metavolcanic successions within the greenstone belt and provide insight into correlations of VMS mineralized areas in the region. Further, sampling of various gabbroic intrusions, for age determinations and whole rock geochemistry, will hopefully shed light on the origins of the diverse suite of mafic and ultramafic intrusive rocks associated with these supracrustal packages and their relationship to the exceptional chromium and nickel-copper-PGE mineralization in the “Ring of Fire”.

ACKNOWLEDGMENTS

This project has benefitted greatly, for a second summer, from the able and enthusiastic assistance of Jean-François Beausoleil. Patrick Gervais is thanked for drafting the figures. Thanks are extended to all mining companies involved in the McFaulds Lake area. In particular, we would like to thank: Andrew Mitchell, Richard Fink, David Shinkle, Daron Slaney (Cliffs Natural Resources Inc.); Don Hoy, Martin Tuchscherer (formerly with Freewest Resources Inc.—Cliffs Natural Resources Inc.); Ralph MacNally, Eric Mosley, Eric Downey (Noront Resources Ltd.); Mike Flanagan and Peter Smith (Fancamp Exploration Ltd.); Moe Lavigne (KWG Resources Inc.); Quentin Yarie, Jacob McKinnon, Craig Sherba, Craig Hunt, James Masters (MacDonald Mines Exploration Ltd.); David Palmer (Probe Mines Ltd.); Jim Voisin (UC Resources Ltd.); David Clarke (Canterra Minerals Corporation); Nathalie Hansen, Éric Hébert, Ian Lawyer (Melkior Resources Inc.); and Christine Vaillancourt and Ian Bliss (Northern Shield Resources Inc.) for their generous assistance, numerous discussions, permission to access properties and/or diamond-drill cores, and corporate geological databases. Mike Hamilton, Sandra Kamo, Robert Lodge and Vicki McNicoll are thanked for preliminary geochronological analyses. Jim Franklin, Larry Hulbert, Jim Mungall and Greg Stott are thanked for valuable discussions and insight into the geology of the McFaulds Lake area. Hearst Air Service and the Ministry of Natural Resources are thanked for float plane and helicopter services during the summer. We also thank Elijah Jacob, Jonas Whitehead, Travis Spence, Leah Wabasse and Chris McKay for assistance with various aspects of our work carried out in Webequie. We also thank Jack Parker (OGS), Anne-Aurélien Sappin (GSC) and Monica Gaiswinkler Easton (OGS) for reviews that helped us improve the final version of this report. This is Geological Survey of Canada contribution number 20120245.

REFERENCES

- Bostock, H.H. 1962. Geology, Lansdowne House, Ontario; Geological Survey of Canada, Preliminary Map 4-1962, scale 1:253 440.
- Buse, S., Smar, L., Stott, G.M. and McIlraith, S.J. 2009. Precambrian geology of the Winisk Lake area; Ontario Geological Survey, Preliminary Map P.3607, scale 1:100 000.
- Metsaranta, R.T. 2010. McFaulds Lake area regional compilation and bedrock mapping project; *in* Summary of Field Work and Other Activities 2010, Ontario Geological Survey, Open File Report 6260, p.17-1 to 17-5.
- Metsaranta, R.T. and Houlé, M.G. 2011. McFaulds Lake area regional compilation and bedrock mapping project update; *in* Summary of Field Work and Other Activities 2011, Ontario Geological Survey, Open File Report 6270, p.12-1 to 12-12.

- Mungall, J.E., Azar, B. and Hamilton, M. 2011. Ni-Cu-PGE-Cr-Fe-Ti-V and VMS mineralisation of the Ring of Fire intrusive suite, Ontario; abstract, Geological Association of Canada–Mineralogical Association of Canada, Joint Annual Meeting, Ottawa, Program with Abstracts, v.34, p.148.
- Mungall, J.E., Harvey, J.D., Balch, S.J., Atkinson, J. and Hamilton, M.A. 2010. Eagle's Nest: a magmatic Ni-sulfide deposit in the James Bay Lowlands, Ontario, Canada; *in* The challenge of finding new mineral resources: global metallogeny, innovative exploration, and new discoveries, Volume II: Zinc-lead, nickel-copper-PGE, and uranium, Society of Economic Geologists, Special Publication 15, p.539-557.
- Ontario Geological Survey 2011. Mineral Deposit Inventory—2011; Ontario Geological Survey, December 2011 release.
- Ontario Geological Survey–Geological Survey of Canada 2011. Ontario airborne geophysical surveys, gravity gradiometer and magnetic data, grid and profile data (ASCII and Geosoft® formats) and vector data, McFaulds Lake area; Ontario Geological Survey, Geophysical Data Set 1068.
- Rainsford, D.R.B., Houlé, M.G., Metsaranta, R.T., Keating, P. and Pilkington, M. 2011. An overview of the McFaulds Lake airborne gravity gradiometer and magnetic survey, northwestern Ontario; *in* Summary of Field Work and Other Activities 2011, Ontario Geological Survey, Open File Report 6270, p.39-1 to 39-8.
- Rayner, N. and Stott, G.M. 2005. Discrimination of Archean domains in the Sachigo Subprovince: a progress report on the geochronology; *in* Summary of Field Work and Other Activities 2005, Ontario Geological Survey, Open File Report 6172, p.10-1 to 10-21.
- Stott, G.M. 2008. Superior Province: terranes, domains and autochthons; presentation, Northwestern Ontario Mines and Minerals Symposium, December 9, 2008.
- Stott, G.M. and Josey, S.D. 2009. Regional geology and mineral deposits of northern Ontario, north of latitude 49°30'; Ontario Geological Survey, Miscellaneous Release—Data 265.
- Thurston, P.C. and Carter, M.W. 1969. Operation Fort Hope: Attawapiskat River sheet, districts of Kenora (Patricia Portion) and Thunder Bay; Ontario Department of Mines, Preliminary Map P.563, scale 1:126 720.
- Thurston, P.C., Sage, R.P. and Siragusa, G.M. 1971a. Operation Winisk Lake: Winiskisis Channel sheet, District of Kenora (Patricia Portion); Ontario Department of Mines, Preliminary Map P.714, scale 1:126 720.
- 1971b. Operation Winisk Lake: Winisk Lake sheet, District of Kenora (Patricia Portion); Ontario Department of Mines, Preliminary Map P.716, scale 1:126 720.

44. Preliminary Results of Chromite Geochemistry at the Black Label, Black Thor and Big Daddy Chromite Deposits, McFaulds Lake Greenstone Belt, Ontario

J.E. Laarman¹, R.L. Barnett² and N.A. Duke¹

¹Department of Earth Sciences, Western University, London, Ontario N6A 5B7

²R.L. Barnett Geoanalytical Consulting Ltd., London, Ontario N6P 1P2

INTRODUCTION

Three new chromite deposits have been discovered in the McFaulds Lake (“Ring of Fire”) area in the James Bay Lowland of northern Ontario. The largest—the Black Thor deposit—is up to 46.3 m thick with 40.4% Cr₂O₃ in massive chromitite that extends along strike for 2.6 km. These new discoveries of high-grade chromite have associated platinum group element (PGE)—enrichment and are only exceeded by deposits such as the Bushveld Complex in South Africa and the Great Dyke of Zimbabwe for global chromium resources. Historically, the main source of chromite has been in South Africa; however, this new resource will allow North America to sustain itself. Mining is planned to start by 2015 and a 30 year mine life is predicted. This operation will have a major impact on the economic development of northern Ontario. These new chromite deposits are classified with the group of stratiform magmatic chromium-PGE ores in layered complexes (Duke 1988). Better understanding of their formation will facilitate stratigraphic correlation and, thus, be instrumental in defining an exploration vector. The occurrence of multiple zones of basal massive versus disseminated styles of mineralization indicates primary magmatic cumulate concentration of the chromite.

The objective of this project is to investigate the origin of the McFaulds Lake chromite deposits. The deposits are hosted by the McFaulds Lake ultramafic complex for which an age of 2734.5±1.0 Ma has been determined (Mungall et al. 2010). This ultramafic sill is up to 500 m thick and has been traced for over 15 km along strike. The McFaulds Lake ultramafic complex is located in the Oxford–Stull domain, northern Superior Province (Stott et al. 2010). Intermediate volcanic rocks located to the east of the intrusion have approximately the same age at 2737±7 Ma (Rayner and Stott 2005) indicating high-level subvolcanic emplacement. The age of the granodiorite basement occurring west of the deposit has not been determined; however, plutons of tonalite, granodiorite and granite underlie large parts of the terrane and yield ages between 2.83 and 2.69 Ga (Percival 2007). Structurally, the intrusion is overturned with stratigraphy of the layered units younging to the southeast.

This project is both field and laboratory based, focussing on drill core because there is only sparse outcrop in the muskeg-covered lowlands. The logging of drill core allows stratigraphic sampling of chromitite layers in igneous rocks. Basal lithologies of the intrusion consist of dunite-peridotite and oikocrystic harzburgite with disseminated to heavily disseminated chromite with intermittent beds of semi-massive chromite to massive chromite and local magmatic chromite breccia. Overlying units include heterogeneous olivine pyroxenite and pyroxenite capped by leucogabbro-gabbro-norite. These lithologies are pervasively hydrated with essentially complete serpentinization of olivine; the serpentine coexists with talc, tremolite, chlorite, kämmererite and magnetite.

The mineral chemistry of the various chromitites at Big Daddy, Black Label and Black Thor needs to be considered in the interest of their metallurgical response. The higher and more consistent Cr# in the more massive chromitite makes such zones most profitable to mine. The Cr# measured in 3 strategic drill holes can be correlated to trends of chromitites in other drill holes along strike. In addition to bulk rock weight % Cr₂O₃, microprobe data are crucial in documenting chromite mineral chemistry of the ore.

METHODOLOGY

To define igneous stratigraphy at the McFaulds Lake deposits, the cores from 13 drill holes were logged and photographs taken of the key textures. Logging commenced in September 2009 and, as a result, 3 strategic drill holes were selected from each of the 3 deposits (Black Thor, Black Label and Big Daddy) for detailed sampling of 600 samples. Core from 13 additional drill holes were logged over the summer of 2010 at McFaulds Lake; these were sited on the same section line as the strategic drill holes chosen for study. Also, at that time, all 3 strategic drill holes were re-examined to better detail the textures of the lithologies hosting the chromitite intervals. DDH BT-09-17 was re-examined in the summer of 2011 to characterize the uppermost chromitite hosted in leucogabbro. From June 2011 to March 2012, the cores from 53 drill holes were logged in conjunction with infill drill programs performed by Cliffs Natural Resources Inc. on the Black Label, Black Thor and Big Daddy chromite deposits. Additional textures of lithologies and mineralization were documented and photographed to supplement the petrographic analysis. The petrographic investigation of the lithologies was carried out in April–May 2011 and in the summer of 2012.

A major effort was made to define the mineral chemical variation in the McFaulds Lake chromite deposits. Electron microprobe analyses have been carried out on 300 samples with over 4000 point analyses on samples spaced 20 to 100 cm apart across individual gravitational cycles. Generally, up to 8 point analyses were made of each chromite sample. More point analyses are needed where there is a) evident textural variation in modal chromite (i.e., mineral zoning), b) variation in grain size, and/or c) higher ferrichromite content. The microprobe work outlines the primary differentiation sequences as well as the effects of secondary hydration on chromite mineral chemistry.

All microprobe analyses were performed by R.L. Barnett in London, Ontario, using a JEOL Model 733 electron microprobe equipped with 5 wavelength spectrometers and using the Tracor-Northern automation system. The preliminary microprobe work was initiated in the spring of 2010 on samples from Black Thor. Electron microprobe analyses continued from December 2010 to January 2011 and from March to May 2011 completing analyses on Black Thor samples and starting on Black Label samples. Analyses on samples from Black Label were completed during May to July 2011. Samples from Big Daddy were analyzed in the summer of 2011.

PRELIMINARY RESULTS OF ELECTRON MICROPROBE ANALYSES

Chromite Morphology and Composition

The electron microprobe analyses best document original igneous compositions preserved in the cores of large chromite grains in massive chromitite. The smaller, more isolated disseminated chromites and zoned margins of larger grains have undergone greater silicate exchange. Primary compositions retained in larger grains best define igneous fractionation. Ferrichromite developed on the rims of original grains relates to secondary hydration. Specific chromite mineral chemistry, therefore, relates to both primary adcumulate sintering and secondary hydrous retrogression.

Current microprobe data show Cr_2O_3 loss from 55 to 51 weight % for centres of grains up section. Grain margins and disseminated smaller grains show up section chemistries of 49 to 47 weight % Cr_2O_3 . Disseminated chromites have generally undergone more silicate exchange, reporting 48 weight % Cr_2O_3 . Other elemental variation in the chromites includes increasing iron, slightly decreasing aluminum and decreasing magnesium due to magmatic differentiation. Aluminum may be the exception to that observed in other layered intrusions in having near-constant compositions. High-grade chromite with higher weight % FeO_T forms as retrograde ferrichromite rims. The rims of original magmatic chromites are leached of magnesium and aluminum leaving high chromium and iron behind as ferrichromite.

In comparing trends, the Black Thor chromites are higher grade with more primitive magmatic compositions in terms of chromium and magnesium than the Black Label chromites. Heterogeneous pyroxene oikocrystic harzburgites host the Black Label chromitite, and more heterogeneous textures are displayed by the chromite ores themselves. With higher modal % silicate in the chromitite, there is more silicate exchange accounting for the lower 50 to 46 weight % Cr_2O_3 in Black Label chromite compared to 53 to 49 weight % Cr_2O_3 in Black Thor chromite. In addition to the more primitive composition of Black Thor chromite, magmatic variation grossly accounts for the lower weight % Cr_2O_3 in disseminated chromite grains. Although lower Cr_2O_3 contents occur with more silicate exchange in disseminated grains, a strong linear regression from massive to disseminated grains reflects magmatic differentiation in forming massive through to disseminated chromites.

The massive chromitite at Big Daddy shows remarkable homogeneity at 50 to 51 weight % Cr_2O_3 . This is higher than the reported assay data for weight % Cr_2O_3 , accounted for by the minor silicate. The homogeneity of the massive ores is attributed to development of chromite layers by double diffusive convection (Rice and von Gruenewaldt 1994). With little silicate in the massive zones, there is less silicate exchange, much less than observed in the exchanged chromitites of the Black Thor and Black Label intersections. Variations from core to rim in all chromite are most likely due to diffusion during secondary hydration.

Up-Section Chromite Variation

Binary plots showing variation of weight % MgO and weight % Cr_2O_3 versus depth are provided for the 3 chromite deposits: Black Label analyses are from DDH BT-09-31; Black Thor from DDH BT-08-10; and Big Daddy from DDH FW-08-19 (Figures 44.1, 44.2 and 44.3). Note that, since the host sill is overturned, increasing drill-hole depths register increasing height in sill stratigraphy.

BLACK LABEL

The 2 chromitite intervals analyzed in core from DDH BT-09-31 have markedly different mineral chemistries (*see* Figure 44.1). From 158 to 161 m, the Cr_2O_3 and MgO values in disseminated chromite are low with maximum contents of 42 to 44 weight % Cr_2O_3 and up to 4.67 weight % MgO. Notably, FeO contents are high ranging from 26 to 30 weight %. The first chromitite interval from 161 to 203 m comprises 3 zones defined by 3 pulses of decreasing weight % MgO with height. The first pulse from 161 to 164 m contains the lowest weight % MgO and weight % Cr_2O_3 . The next 2 pulses are larger, approximately 20 m thickness for each, and contain well-defined differentiation sequences of decreasing weight % MgO. Within these 2 zones are individual replenishments with MgO peaks followed by decreasing weight % MgO. The second pulse contains 2 subzones of decreasing weight % Cr_2O_3 with height, following the pattern of differentiation shown by the MgO contents. However, in the third pulse, with each new replenishment, the Cr_2O_3 contents remained high at about 50 weight % Cr_2O_3 . However, individual differentiation sequences of decreasing Cr_2O_3 weight % with height can be picked out with up to 6 m thick mini-pulses. These mini cycles possibly formed by convection cells within the larger pulse of magma (Rice and von Gruenewaldt 1994; Naldrett et al. 2011).

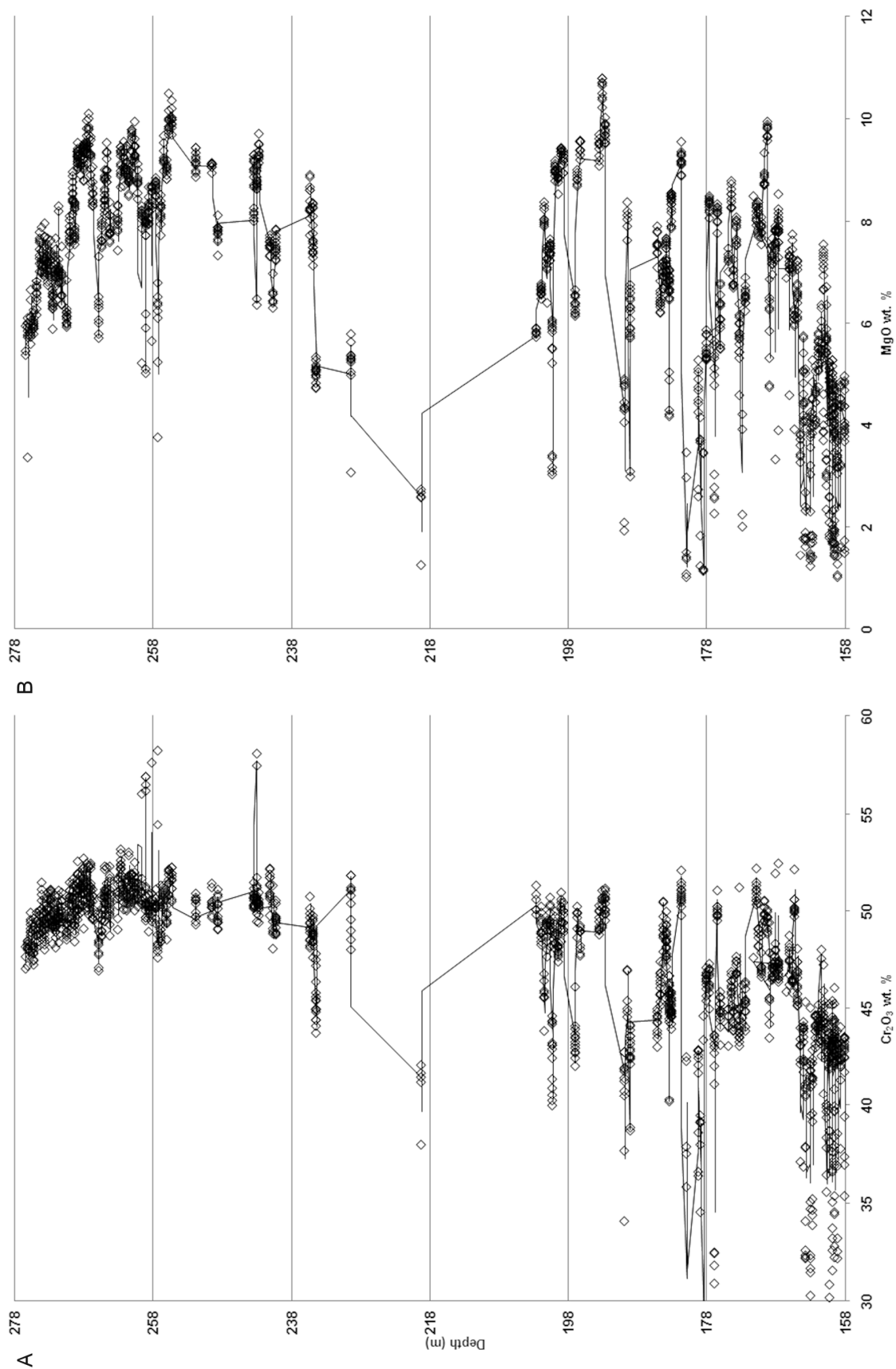


Figure 44.1. Plots of Cr_2O_3 (weight %) and MgO (weight %) versus depth (m) for Black Label DDH BT-09-31.

The second chromitite interval is from 229 to 276 m and contains 3 zones from 229 to 257 m, 257 to 265 m and from 265 to 276 m characterized by separate subsets of elevated weight % Cr_2O_3 separated by troughs of low weight % Cr_2O_3 . Notably, the Cr_2O_3 values are consistently high at above 50 weight % suggesting a primitive chromitite interval. In the first zone, 3 pulses of replenished MgO are followed by decreasing MgO trends. With each successive replenishment, there is an overall increase in the MgO values. This suggests the influx of more primitive magma. The high peaks above 53 weight % Cr_2O_3 with low weight % MgO are ferrichromites due to secondary hydration. In the second zone, there are 2 pulses with the first being larger, and having higher weight % MgO and Cr_2O_3 than the second. Notably, more secondary ferrichromite has been detected in this first pulse. The second pulse shows marked decreasing weight % MgO with height while the Cr_2O_3 values decrease to a lesser extent. The third zone contains 3 to 4 pulses on an overall trend of decreasing Cr_2O_3 weight % with height. The first pulse from 259 to 270 m contains higher weight % MgO than the others and is well differentiated. The second pulse is poorly developed. The third to fourth pulses from 272 to 276 m begin with more elevated MgO contents that decrease past 274 m. The overall decreasing trend in Cr_2O_3 weight % in this zone also reflects igneous differentiation.

BLACK THOR

The core from Black Thor DDH BT-08-10 contains chromite of more variable composition due to diffusion processes accompanying greater ferrichromite replacement during retrogression (*see* Figure 44.2). Therefore, plots of core + margin of igneous chromite have been separated from replacement rims of ferrichromite. From 114 to 124 m, there are 2 zones of low MgO chromite disseminated in dunite. The first zone, from 114 to 118.5 m, comprises 2 pulses with trends of decreasing weight % MgO with height. The second zone from 118.5 to 124 m also contains 2 pulses with decreasing weight % MgO with height.

Above 124 m, chromite shows elevated weight % Cr_2O_3 in intermittent beds of massive chromitite. Between 124 and 127 m, there is a well-differentiated sequence showing decreasing weight % MgO and Cr_2O_3 with height. A large zone of chromitite between 127 and 150 m can be subdivided into 2 zones from 127 to 136 m and 136 to 150 m based on Cr_2O_3 contents. These chromitites begin with high Cr_2O_3 weight % contents and show a marked trend of decreasing MgO and Cr_2O_3 with height. In the first subzone, Cr_2O_3 contents reach 54 weight % suggesting very primitive magma.

The upper zone, from 150 to 174 m, also show trends of decreasing MgO and Cr_2O_3 weight % with height. Notably, there is only a slight decrease in weight % Cr_2O_3 . This may be explained by development of chromite convection cells. A number of replenishments of high MgO may be also attributed to successive convection cells (Rice and von Gruenewaldt 1994).

BIG DADDY

The core from the interval in the Big Daddy DDH FW-08-19 is all massive chromitite and, therefore, demonstrates a markedly different compositional trend than Black Thor and Label (*see* Figure 44.3). The MgO and Cr_2O_3 compositions are more uniform in the chromites. This is especially reflected in constant Cr_2O_3 values from one zone to another. The main chromitite interval in DDH FW-08-19 is from 183 to 230 m and is divided into 4 main zones as defined by troughs in weight % MgO. The first zone, from 183 to 192 m, begins with 2 minor replenishments in weight % MgO followed by decreasing weight % MgO with height from 187 to 192 m. Chromite compositions are at 51 weight % Cr_2O_3 . The second zone, from 192 to 206 m, begins with a pulse from 192 to 194 m at lower weight % MgO followed by 3 successive pulses beginning at 11.46 weight % MgO that decrease successively upward. Chromite compositions are constant at 50 weight % Cr_2O_3 . The third zone, from 206 to 227 m, starts with a pulse at 11.27 weight % MgO that decreases with height from 206 to 211 m. From 211 to 227 m, there is a large well-defined differentiation sequence. Chromite compositions decrease subtly from 51 to 47 weight % Cr_2O_3 as the

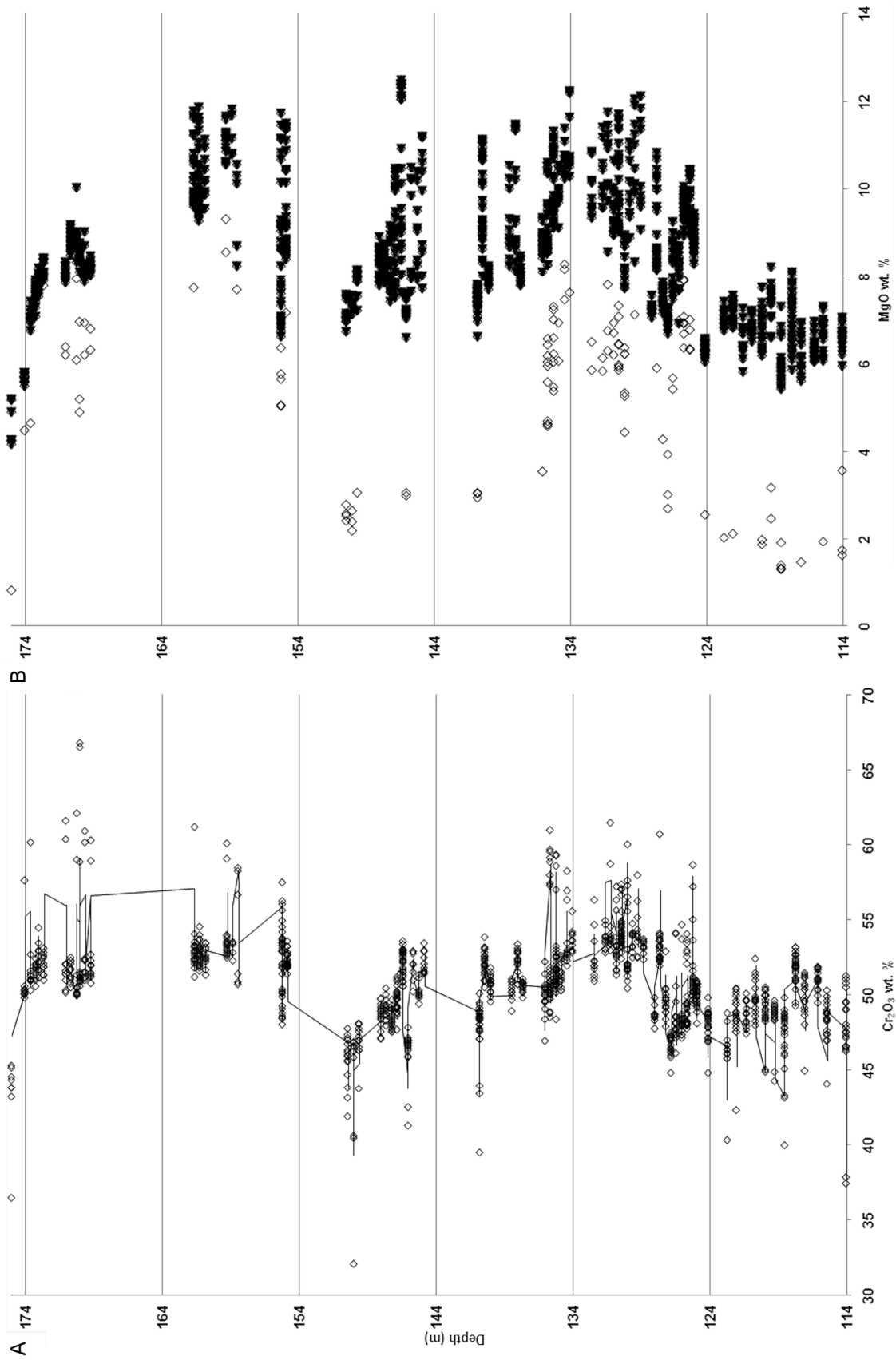


Figure 44.2. Plots of Cr_2O_3 (weight %) and MgO (weight %) versus depth (m) for Black Thor DDH BT-08-10. On the MgO plot, dark triangles are chromite cores + margins; white diamonds are ferrichromites.

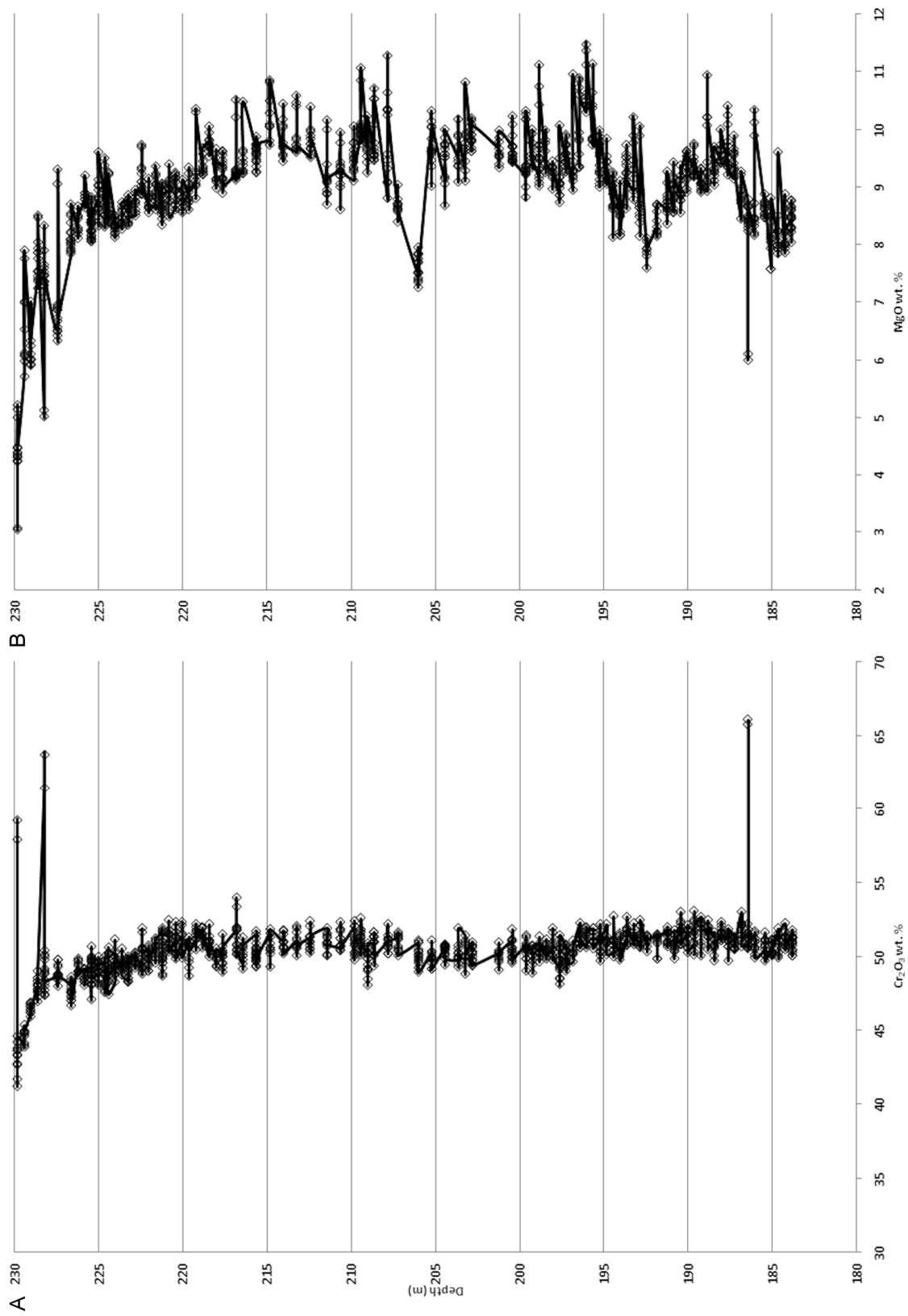


Figure 44.3. Plots of Cr_2O_3 (weight %) and MgO (weight %) versus depth (m) for Big Daddy DDH FW-08-19.

interval approaches the upper contact with pyroxenite. From 227 to 230 m, there is a contact zone with a pronounced decrease to 3 weight % MgO and 41 weight % Cr₂O₃ toward the contact. This zone is probably depleted due to silicate exchange with pale grey to white globular shaped aggregates of pyroxene. Also, there is more ferrichromite in this zone indicating higher degrees of hydration.

SUMMARY

Results of the electron microprobe analyses define well primary igneous cycles from a few metres to up to 50 m thick intervals, reflecting primary magma replenishment and fractionation within the McFaulds Lake chromitites. Complex filling histories identify numerous magma batches that occurred over the course of chromite crystallization. Individual differentiation sequences are well defined at below the metre scale and chromite chemistry is supportive of mineralization by double diffusive convective processes. Pervasive retrograde hydration, attributed to the shallow subvolcanic environment of sill emplacement, forms secondary ferrichromite rims on primary igneous chromite grains at all 3 deposits.

ACKNOWLEDGMENTS

The senior author would like to thank Cliffs Natural Resources Inc. and KWG Resources Inc. for funding the microprobe analyses and living expenses incurred during this project. The research was also made possible by the Natural Sciences and Engineering Research Council of Canada (NSERC), Society of Economic Geologists (SEG) Canada Foundation and Western University internal grants and research scholarships. This work constitutes part of the requirements of a PhD thesis by J.E. Laarman at Western University under the supervision of Professor N.A. Duke.

REFERENCES

- Duke, J.M. 1988. Magmatic segregation deposits of chromite; *in* Ore deposit models, Geological Association of Canada, Geoscience Canada Reprint Series 3, p.133-144.
- Mungall, J.E., Azar, B., Atkinson, J. and Harvey, J.D. 2010. The Eagle's Nest komatiite-hosted Ni-Cu-PGE sulphide deposit in the James Bay Lowlands, Ontario; *in* Abstracts, 11th International Platinum Symposium, 21–24 June 2010, Sudbury, Ontario, Canada, Ontario Geological Survey, Miscellaneous Release—Data 269.
- Naldrett, A., Kinnaird, J., Wilson, A., Yudovskay, M. and Chunnett, G. 2011. Genesis of the PGE-enriched Merensky Reef and chromitite seams of the Bushveld Complex; *in* Magmatic Ni-Cu and PGE deposits: geology, geochemistry, and genesis, Society of Economic Geologists, Reviews in Economic Geology, v.17, p.235-296.
- Percival, J.A. 2007. Geology and metallogeny of the Superior Province, Canada; *in* Mineral deposits of Canada: a synthesis of major deposit-types, district metallogeny, the evolution of geological provinces, and exploration models, Geological Association of Canada, Mineral Deposits Division, Special Publication No.5, p.903-928.
- Rayner, N. and Stott, G.M. 2005. Discrimination of Archean domains in the Sachigo Subprovince: a progress report on the geochronology; *in* Summary of Field Work and Other Activities 2005, Ontario Geological Survey, Open File Report 6172, p.10-1 to 10-21.
- Rice, A. and von Gruenewaldt, G. 1994. Convective scavenging and cascade enrichment in Bushveld Complex melts: possible mechanism for concentration of PGEs and chromite in mineralized layers; Applied Earth Science (Transactions of the Institute of Materials, Minerals and Mining, Section B), v.103, p.B31-B38.
- Stott, G.M., Corkery, M.T., Percival, J.A., Simard, M. and Goutier, J. 2010. A revised terrane subdivision of the Superior Province; *in* Summary of Field Work and Other Activities 2010, Ontario Geological Survey, Open File Report 6260, p.20-1 to 20-10.

45. Multiple Sulphur Isotopes as a Method to Evaluate Sulphur Sources and a Potential Exploration Tool in the Komatiite-Associated Nickel-Copper-(Platinum Group Elements) Hart Deposit, Shaw Dome, Abitibi Greenstone Belt, Ontario

R.S. Hiebert¹, A. Bekker¹, M.G. Houlié², C.M. Lesher³ and B.A. Wing⁴

¹Department of Geological Sciences, University of Manitoba, Winnipeg, Manitoba R3T 2N2

²Geological Survey of Canada, Québec City, Québec G1K 9A9

³Department of Earth Sciences, Laurentian University, Sudbury, Ontario P3E 2C6

⁴Department of Earth and Planetary Sciences, McGill University, Montreal, Quebec H3A 2A7

INTRODUCTION

Exploration models for magmatic nickel-copper-platinum group element (PGE) sulphide deposits are relatively well understood, and it is well accepted that the metals (e.g., nickel, copper and PGE) come from mantle-derived magmas. Most deposits are thought to have been formed by sulphur-undersaturated magmas melting sulphur-bearing country rocks to generate sulphide xenomelts (Lesher and Campbell 1993; Lesher and Burnham 2001), but the source(s) of the sulphur remains poorly constrained in a few cases. The addition of sulphur is required, as melting of the mantle generates a sulphur-undersaturated magma as it rises to near-surface environments because of increased solubility of sulphur in mafic and ultramafic melts as pressure decreases (Wendlandt 1982; Lesher and Groves 1986; Mavrogenes and O'Neill 1999).

Earlier attempts to identify the sulphur source using sulphur isotopes relied only on $\delta^{34}\text{S}$ values, but the range of sulphur isotope values recorded in Archean supracrustal deposits is much smaller than that in Phanerozoic examples, resulting in near-mantle $\delta^{34}\text{S}$ values (Ripley 1999), which makes these data inconclusive in some cases. The value for $\delta^{34}\text{S}$ in parts per thousand (‰ or per mil) is defined as

$$\delta^{34}\text{S} = \left(\frac{{}^{34}\text{S}/{}^{32}\text{S}_{\text{sample}}}{{}^{34}\text{S}/{}^{32}\text{S}_{\text{V-CDT}}} - 1 \right) \times 1000 \quad (1)$$

where V-CDT is a reference scale defined by the isotopic composition of IAEA-S-1 (a sulphur reference material distributed by the International Atomic Energy Agency (IAEA, Vienna)) and calibrated to $\delta^{34}\text{S}_{\text{IAEA-S-1}} \equiv -0.3\text{‰}$. When measurements of ${}^{33}\text{S}$ - ${}^{32}\text{S}$ ratios are made, the above expression can be used to define $\delta^{33}\text{S}$ values.

Under present terrestrial conditions, sulphur isotope fractionation is controlled strictly by relative isotope mass differences and, therefore, is a completely mass-dependent process. However, as a result of photochemical reactions in the Archean anoxic atmosphere, atmospherically processed Archean sulphur also exhibits mass-independent fractionation that can be considered as the difference between the $\delta^{33}\text{S}$

value expected from normal mass-dependent fractionation and the observed $\delta^{33}\text{S}$ value (Farquhar and Wing 2003). It can be calculated as

$$\Delta^{33}\text{S} = \delta^{33}\text{S} - \left[\left(\frac{\delta^{34}\text{S}}{1000} + 1 \right)^{\lambda_{\text{RFL}}} - 1 \right] \times 1000 \quad (2)$$

where the λ_{RFL} has been defined as the slope of the reference fractionation line for sulphur isotopes equal to 0.515. In this contribution, we take the $\Delta^{33}\text{S}$ value of IAEA-S-1 to be -0.094‰ .

The photochemically fractionated sulphur was then delivered to Archean seawater and ultimately sediments. Additionally, unlike modern oceans, the Archean oceans had relatively low sulphate concentrations, which resulted in small isotopic fractionation during bacterial sulphate reduction, a common process of sulphide formation in sediments. As such, Archean sediments do not exhibit large variations in $\delta^{34}\text{S}$ values, hampering discrimination between crustal and mantle sulphur. However, these sediments typically exhibit mass-independent fractionation even when $\delta^{34}\text{S}$ values show a small range centred on the average mantle value. Multiple sulphur isotope ratios can, therefore, constrain the sulphur source for nickel-copper-(PGE) sulphide mineralization in mafic to ultramafic systems and target prospective areas, where crustal sulphur incorporation occurred and triggered sulphide saturation (e.g., Bekker et al. 2009).

OBJECTIVES

Previous work by Bekker et al. (2009) has shown that the multiple sulphur isotope method can be used to differentiate between crustal and mantle sulphur sources in Archean terrains. Under that premise, the proposed research will use new techniques for analyzing multiple sulphur isotope ratios to investigate the role of crustal sulphur in the formation of ultramafic- and mafic-hosted nickel-copper-(PGE) sulphide mineralization.

The main objectives targeted in this project are

- to determine the sulphur source involved in the genesis of komatiite-associated nickel-copper-(PGE) sulphide deposits, the factors controlling sulphur isotope fractionation in these deposits, and how these signatures might be used as a new exploration tool to target prospective ore settings through a detailed investigation at the Hart deposit in the Shaw Dome area;
- to study the iron formation, thought to be the most likely source of sulphur for the Hart deposit and to determine if there is a systematic difference in sulphur isotope composition of sulphides between oxide facies and sulphide facies of the iron formation. This information will be used to establish if sulphide-facies iron formations had an oxide-facies iron formation precursor and were later sulphidized by hydrothermal fluids; and finally
- to use isotopic analysis of ores and country rocks throughout the Shaw Dome of the Abitibi greenstone belt in Ontario to establish regional variations and relationship between ores and host rocks in different stratigraphic and volcanic to subvolcanic settings within an extremely well-constrained (geologically, stratigraphically and geochronologically) greenstone belt in the Superior Province that is known to contain significant komatiite-hosted nickel-copper-(PGE) mineralization.

This contribution presents preliminary sulphur isotope data from the komatiite-associated nickel-copper-(PGE) sulphide Hart deposit within the Shaw Dome area in the Abitibi greenstone belt in Ontario.

METHODOLOGY

The multiple sulphur isotope data will be evaluated in 2 ways: the first is to calculate the degree of mass-independent fractionation and the second is to determine the relationship between $\delta^{34}\text{S}$ and $\Delta^{33}\text{S}$ values. The degree of mass-independent fractionation is not altered by magmatic and metamorphic reactions unless significant amounts of sulphur are added, making it a robust tracer. However, mass-independent fractionation is not always present even in Archean deposits; in these cases, the relationship between $\delta^{34}\text{S}$ and $\Delta^{33}\text{S}$ values may be used to place constraints on ore genesis.

Sample Selection

So far our study has been focussed on the Hart deposit and has been undertaken through the collection of several representative samples of felsic volcanic, iron formation, komatiite and sulphide horizons from trenches excavated by Liberty Mines Inc. on the surface projection of the ore zone. All samples processed to this point have come from 3 trenches over a distance of 100 m along the basal contact between the komatiite and the footwall rock. Additional detailed drill-core examination and sampling was conducted in order to characterize and constrain the sulphur isotope variations vertically through the stratigraphy (from footwall to hanging wall) and laterally from proximal to distal settings with respect to the ore zone to explore the potential of multiple sulphur isotopes to target prospective environments that may host mineralization. Considering that the magma directly above mineralization in the komatiite channels was likely emplaced after the mineralization due to continued flow in the channel, the komatiite material involved in the formation of the sulphide mineralization may only be preserved on the flow flanks (e.g., Leshner and Keays 2002; Arndt, Leshner and Barnes 2008). Therefore, sampling laterally into the flanks of komatiite channels may be critical for development of a geochemical tool that can target mineralization using isotopic data from the mineralization, the footwall lithologies and the flanks of the komatiite flows.

Analytical Method

Samples with coarse sulphide grains were micro-drilled to produce a pure sulphide powder. Samples with finely disseminated sulphide grains were pulverized to produce an impure powder. Sulphur was extracted from all powders (both pure and impure sulphide powders) through a chemical Cr(III) reduction process as described by Canfield et al. (1986) to produce pure Ag_2S .

Pure Ag_2S was fluorinated and analyzed for multiple sulphur isotopes as SF_6 on a ThermoFinnigan MAT 253 mass spectrometer at McGill University. Repeat analyses throughout the entire analytical procedure returned 2σ uncertainties on $\delta^{34}\text{S}$ and $\Delta^{33}\text{S}$ values that are <0.25 and $<0.01\text{‰}$, respectively, for the reported results herein.

GEOLOGICAL SETTING

Komatiites and komatiite-associated nickel-copper-(PGE) deposits in the Abitibi greenstone belt are recognized worldwide for their outstanding preservation and exposure. Most of the past and ongoing nickel production from this type of deposit in the Abitibi greenstone belt has come from the Shaw Dome area (Figure 45.1), which hosts the Hart deposit located approximately 30 km southeast of the City of Timmins (Houlé and Leshner 2011).

The volcano-sedimentary succession in the Shaw Dome comprises, from oldest to youngest, 1) massive and pillowed intermediate volcanic rocks and thin, but laterally extensive, iron formations of the 2734–2724 Ma volcanic episode (Deloro); 2) felsic volcanoclastic rocks intercalated with komatiitic

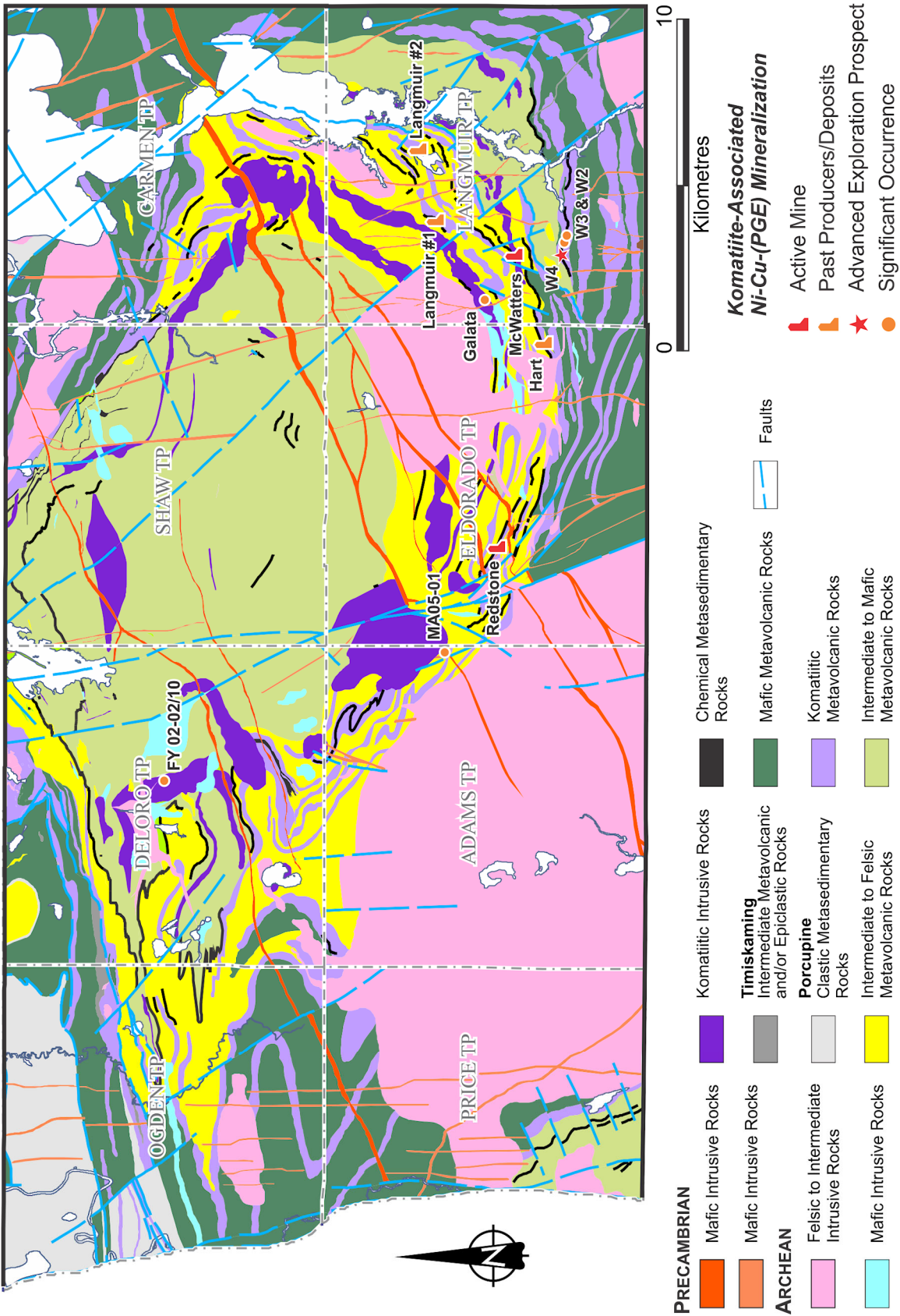


Figure 45.1. Geological map of the Shaw Dome area showing the major lithological units and the most significant nickel-copper-PGE deposits and occurrences throughout the area (modified from Houli  et al. 2010a).

Table 45.1. Preliminary sulphur isotope data for the Hart deposit.

Sample	Lithology	Location		$\delta^{33}\text{S}_{\text{V-CDT}}$ (‰)	$\delta^{34}\text{S}_{\text{V-CDT}}$ (‰)	$\delta^{36}\text{S}_{\text{V-CDT}}$ (‰)	$\Delta^{33}\text{S}_{\text{V-CDT}}$ (‰)	$\Delta^{36}\text{S}_{\text{V-CDT}}$ (‰)
		Trench	Stratigraphy					
MGH502	IF	A	FW	−6.21	−11.00	−20.06	−0.53	0.74
MGH600A	IF	B	FW1	−2.09	−2.78	−4.24	−0.66	1.03
MGH600B	IF (S)	B	FW2	2.09	5.49	11.55	−0.73	1.10
MGH600C	N\$	B	K1	−1.96	−2.61	−4.02	−0.61	0.94
MGH600D	D\$	B	K2	−2.09	−2.85	−4.83	−0.62	0.58
MGH600E	T\$	B	K3	−1.87	−2.41	−3.58	−0.62	0.99
MGH600F	BKk	B	K4	−1.47	−1.61	−5.17	−0.64	−2.11
MGH600G	BKk	B	K5	−1.34	−1.45	−1.75	−0.59	1.01
MGH601A	FV	C	FW1	0.75	1.87	4.25	−0.22	0.69
MGH601B	IF	C	FW2	−5.77	−10.00	−17.74	−0.61	1.18
MGH601C	M\$	C	K1	−2.28	−3.23	−5.06	−0.62	1.07
MGH601D	BKk	C	K2	−2.66	−4.09	−6.58	−0.55	1.17

Abbreviations: BKk: barren komatiite, D\$: disseminated sulphide in komatiite, FV: felsic volcanic rocks, IF: iron formation, IF (S): secondary pyrite within iron formation, M\$: massive sulphide in komatiite, N\$: net-textured sulphide in komatiite; T\$: trace of sulphide in komatiite;

FW: footwall rocks, K: komatiite, 1, 2, 3, etc.: number refers to the stratigraphic position from the base to the top.

Note: V-CDT refers to a troilite (FeS) standard from the Cañon Diablo meteorite calibrated with respect to sulphur reference materials distributed by the International Atomic Energy Agency (IAEA) (Vienna) and is reported as $\delta^{34}\text{S}$ values in parts per thousand (‰ or per mil).

dikes, sills, lavas and less extensive iron formations of the 2704 Ma volcanic episode (Tisdale); 3) intercalated tholeiitic mafic and komatiitic volcanic rocks of the 2704 Ma volcanic episode (Tisdale); and 4) calc-alkalic felsic to intermediate volcanic rocks in the upper part of the 2710–2704 Ma volcanic episode (Tisdale) (Houlé et al. 2010a).

The Hart deposit is a classic Type I stratiform basal deposit hosted by thick olivine, orthocumulate to mesocumulate komatiite units in which the mineralization is localized in the wide embayment into its footwall rocks that comprise banded iron formations and felsic volcanoclastic rocks. The embayment (>200 m wide) is interpreted to have been produced by thermomechanical erosion (Houlé et al. 2010b).

PRELIMINARY RESULTS

Field observations based on drill-core examination have allowed interpretation of a broad internal stratigraphy of the Hart komatiite succession, which is essentially composed of spinifex-textured flows of varying thickness, where the thicker units are generally found at the base of the succession. In addition to multiple horizons of iron formation, several intercalated layers of graphitic argillite were identified in the footwall rock package, providing a previously unrecognized potential sulphur source. The iron formation locally contains massive sulphide layers or zones, whereas the graphitic argillite contains up to 35% by volume of pyrite nodules and bands; as such, both lithologies could be potential sources of sulphur to the komatiite-associated mineralization. Multiple generations of sulphide have also been identified within the iron formation, with early generation, fine-grained pyrite being replaced locally by secondary, medium-grained, blocky pyrite.

Preliminary data from the Hart deposit exhibits significant variations in sulphur isotope values (Table 45.1; Figure 45.2). Only one sample of felsic volcanic rock was analyzed: it has $\delta^{34}\text{S}$ and $\Delta^{33}\text{S}$ values of 1.87‰ and −0.22‰, respectively. Sulphur isotope data for komatiites, including barren komatiites, komatiites with trace amounts of sulphides, disseminated, net-textured and massive sulphide mineralization range from −1.45 to −4.09‰ for $\delta^{34}\text{S}$ values and cluster between −0.55 and −0.64‰ for

$\Delta^{33}\text{S}$ values. The small range of $\Delta^{33}\text{S}$ values in komatiites and sulphide mineralization reflects the degree and efficiency of mixing of sulphur in the komatiite magma, resulting in little to no difference between sulphide horizons in the Hart deposit at the scale of the preliminary sampling. The larger range of $\delta^{34}\text{S}$ values in the same samples, on another hand, likely reflects sulphur isotope fractionation during precipitation of sulphides with different chemical compositions. The sulphur isotope data for iron formation appear to be clustered into 2 groups. The first group exhibits $\delta^{34}\text{S}$ values of -10.00 to -11.00‰ and $\Delta^{33}\text{S}$ values of -0.53 to -0.61‰ , whereas the single sample from the second group has a $\delta^{34}\text{S}$ value of -2.78‰ and $\Delta^{33}\text{S}$ value of -0.66‰ . The single sample of secondary pyrite in iron formation has a similar $\Delta^{33}\text{S}$ value of -0.73‰ and a significantly different $\delta^{34}\text{S}$ value of $+5.49\text{‰}$.

Assuming that iron-nickel-copper-(PGE) deposits associated with komatiites formed by thermochemical erosion and sulphur incorporated from their footwall, values of $\delta^{34}\text{S}$ and $\Delta^{33}\text{S}$ in the komatiite samples are likely to lie somewhere between the bulk value of the country rock sulphur source and the composition of the magma, depending on the magma:sulphide ratio (Leshner and Stone 1996; Leshner and Burnham 2001). Both felsic volcanic rocks and the secondary pyrite in iron formation show distinctly different values for $\delta^{34}\text{S}$ and $\Delta^{33}\text{S}$ suggesting that they have not contributed significant amounts of sulphur to the ores. The sulphide-facies iron formation and komatiite with associated mineralization show very similar $\Delta^{33}\text{S}$ values, but the former has a much broader range of $\delta^{34}\text{S}$ values. The isotopic data suggest that the sulphur source for the mineralization could have been sulphide-facies iron formation, based on $\Delta^{33}\text{S}$ values, which is consistent with field observations that the iron-formation horizons are truncated by the ores zones (Coad 1979). Notably, whereas the larger range of $\delta^{34}\text{S}$ values in sulphide-facies iron formation with respect to those in komatiite and associated mineralization might reflect homogenization of this range during assimilation by komatiite, similarity in their $\Delta^{33}\text{S}$ signature strongly suggests a genetic link between sulphide-facies iron formation in the footwall and mineralization in

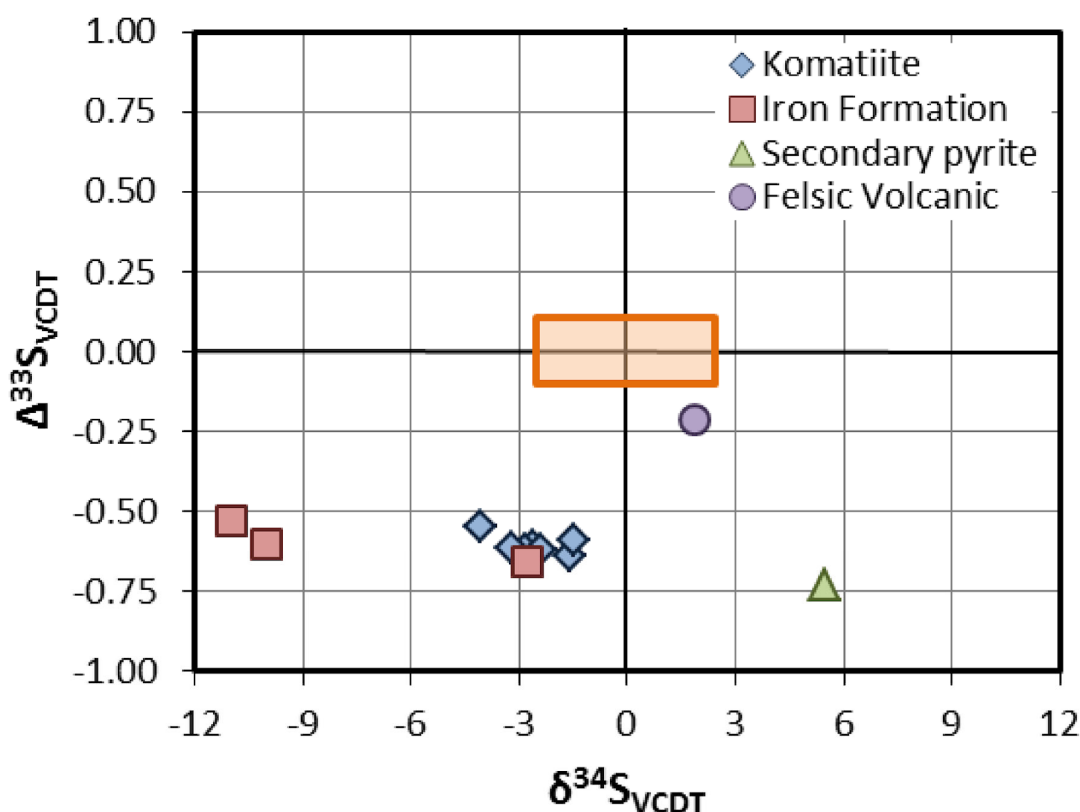


Figure 45.2. Preliminary sulphur isotope data for samples analyzed from komatiite, sulphide-bearing iron formation, secondary pyrite in iron formation and felsic volcanic rocks. Typical mantle range shown by orange box.

komatiite, and highlights the value of a $\Delta^{33}\text{S}$ proxy in establishing sulphur source for komatiite-hosted iron-nickel-copper-(PGE) deposits. Although sulphur isotope systematics of graphitic argillites that have been found recently during regional mapping and the core logging have not yet been tested for potential sulphur contribution to the nickel sulphide deposit, available data for a similar graphitic argillite unit from the Dundonald Township (Bekker et al. 2009) do not suggest significant argillite contribution to the sulphur budget of komatiite at the Hart deposit. However, as these graphitic argillite units may have distinctly different sulphur isotope values, no conclusions can be reached at this point.

FUTURE WORK

Additional samples of komatiite, iron-nickel-copper-(PGE) sulphide mineralization, and all footwall lithologies have been collected and will be analyzed in the upcoming year. Furthermore, this study is attempting to assess the variability seen in nickel-copper-(PGE) deposits associated with komatiites throughout the Shaw Dome. Comparison of other deposits in the Shaw Dome to the Hart deposit might provide further insight into which country rock lithologies are the most important sulphur source rocks to these deposits, and could allow for another guide to exploration in the region.

Finally, the study will also characterize the nature of the sulphur source rocks, including evaluating the source of sulphur for the iron formations. Recently, several authors have questioned the validity of the term “sulphide-facies” iron formation (e.g., Beukes and Gutzmer 2008; Bekker et al. 2010), introduced by James (1954), suggesting that these are either sulphide-bearing shales or formed by proximal hydrothermal processes. However, the iron formations observed in the Shaw Dome area contain locally abundant sulphide minerals, which might be replacing iron oxides in the iron formation. As the iron oxides are thought to form from recrystallization of sedimentary iron-oxyhydroxides during diagenesis (Beukes and Gutzmer 2008), another objective of this study will be to determine if the sulphur in these iron formations is derived from the seawater or from circulating proximal hydrothermal fluids below the sediment–water interface.

CONCLUDING REMARKS

Traditionally, exploration for nickel-copper-(PGE) is guided by direct and indirect geological knowledge; however, indicators for hidden mineral systems are not always present at or near the surface. Multiple sulphur isotope geochemistry provides a new exploration tool to identify the source of sulphur, allowing prioritization of prospective areas leading to a more efficient and cost-effective exploration program for nickel-copper-(PGE) deposits. The new method has been applied to the komatiite-associated nickel-copper-(PGE) Hart deposit located in the Shaw Dome area of the Abitibi greenstone belt and has proven a certain potential at a reconnaissance level.

ACKNOWLEDGMENTS

This project has been funded by the Geological Survey of Canada (GSC) under the Targeted Geoscience Initiative Phase 4 (TGI-4), a Natural Sciences and Engineering Research Council of Canada (NSERC) operating grant to Dr. Andrey Bekker, and a graduate fellowship from the University of Manitoba to Russel Hiebert. Olivier Rouxel (Institut Universitaire Européen de la Mer at Brest, France) is thanked for valuable discussions on isotope geochemistry in general. We are very grateful to Peter Caldbick (formerly with Liberty Mines Ltd.), Todd Mathieu (Liberty Mines Ltd.), and other Liberty Mines staff members for their advice and assistance with the field work and core examination of the Hart deposit at the Redstone Mine site. We also thank Valérie Bécu (GSC) for her review of the manuscript that helped us improve the final version of this report. This is Geological Survey of Canada contribution number 20120250.

REFERENCES

- Arndt, N.T., Leshner, C.M. and Barnes, S.J. 2008. Komatiite; Cambridge University Press, New York, 467p.
- Bekker, A., Barley, M.E., Fiorentini, M.L., Rouxel, O.J., Rumble, D. and Beresford, S.W. 2009. Atmospheric sulfur in Archean komatiite-hosted nickel deposits; *Science*, v.326, p.1086-1089.
- Bekker, A., Slack, J.F., Planavsky, N., Krapez, B., Hofmann, A., Konhauser, K.O. and Rouxel, O.J. 2010. Iron formation: the sedimentary product of a complex interplay among mantle, tectonic, oceanic, and biospheric processes; *Economic Geology*, v.105, p.467-508.
- Beukes, N.J. and Gutzmer, J. 2008. Origin and paleoenvironmental significance of major iron formations at the Archean–Paleoproterozoic boundary; *in* Banded iron formation-related high-grade iron ore, Society of Economic Geologists, *Reviews in Economic Geology*, v.15, p.5-47.
- Canfield, D.E., Raiswell, R., Westrich, J.T., Reaves, C.M. and Berner, R.A. 1986. The use of chromium reduction in the analysis of reduced inorganic sulfur in sediments and shales; *Chemical Geology*, v.54, p.149-155.
- Coad, P.R. 1979. Nickel sulfide deposits associated with ultramafic rocks of the Abitibi belt and economic potential of mafic–ultramafic intrusions; Ontario Geological Survey, Study 20, 84p.
- Farquhar, J. and Wing, B.A. 2003. Multiple sulfur isotopes and the evolution of the atmosphere; *Earth and Planetary Science Letters*, v.213, p.1-13.
- Houlé, M.G. and Leshner, C.M. 2011. Komatiite-associated Ni-Cu-(PGE) deposits, Abitibi greenstone belt, Superior Province, Canada; *in* Magmatic Ni-Cu and PGE deposits: geology, geochemistry, and genesis, Society of Economic Geologists, *Reviews in Economic Geology*, v.17, p.89-121.
- Houlé, M.G., Leshner, C.M., Gibson, H.L., Ayer, J.A. and Hall, L.A.F. 2010a. Localization of komatiite-associated Ni-Cu-(PGE) deposits in the Shaw Dome, Abitibi greenstone belt, Superior Province; *in* Abstracts, 11th International Platinum Symposium, 21–24 June 2010, Sudbury, Ontario, Canada, Ontario Geological Survey, Miscellaneous Release—Data 269.
- Houlé, M.G., Leshner, C.M., Préfontaine, S., Ayer, J.A., Berger, B.R., Taranovic, V., Davis, P.C. and Atkinson, B. 2010b. Stratigraphy and physical volcanology of komatiites and associated Ni-Cu-(PGE) mineralization in the western Abitibi greenstone belt, Timmins area, Ontario: a field trip for the 11th International Platinum Symposium; Ontario Geological Survey, Open File Report 6255, 99p.
- James, H.L. 1954. Sedimentary facies of iron-formation: *Economic Geology*, v.49, p.235-293.
- Leshner, C.M. and Burnham, O.M. 2001. Multicomponent elemental and isotopic mixing in Ni-Cu-(PGE) ores at Kambalda, Western Australia; *The Canadian Mineralogist*, v.39, p.421-446.
- Leshner, C.M. and Campbell, I.H. 1993. Geochemical and fluid dynamic modeling of compositional variations in Archean komatiite-hosted nickel sulfide ores in Western Australia; *Economic Geology*, v.88, p.804-816.
- Leshner, C.M. and Groves, D.I. 1986. Controls on the formation of komatiite-associated nickel-copper sulfide deposits: geology and metallogenesis of copper deposits; *Proceedings of the Twenty-Seventh International Geological Congress*, Berlin, Springer Verlag, p.43-62.
- Leshner, C.M. and Keays, R.R. 2002. Komatiite-associated Ni-Cu-(PGE) deposits: mineralogy, geochemistry, and genesis; *in* The geology, geochemistry, mineralogy, and mineral beneficiation of the platinum-group elements, Canadian Institute of Mining, Metallurgy and Petroleum, Special Volume 54, p.579-617.
- Leshner, C.M. and Stone, W.E. 1996. Exploration geochemistry of komatiites: igneous trace element geochemistry applications for massive sulphide exploration; *Geological Association of Canada, Short Course Notes*, v.12, p.153-204.

- Mavrogenes, J.A. and O'Neill, H. StC. 1999. The relative effects of pressure, temperature and oxygen fugacity on the solubility of sulfide in mafic magmas; *Geochimica et Cosmochimica Acta*, v.63, p.1173-1180.
- Ripley, E.M. 1999. Systematics of sulphur and oxygen isotopes in mafic igneous rocks and Cu-Ni-PGE mineralization; *in* Dynamic processes in magmatic ore deposits and their application in mineral exploration, Geological Association of Canada, Short Course Notes, v.13, p.111-158.
- Wendlandt, R.F. 1982. Sulfide saturation of basalt and andesite melts at high pressures and temperatures; *American Mineralogist*, v.67, p.877-885.

46. Geochemistry of Chromite from the Alexo Komatiite, Dundonald Township: Preliminary Results from Electron Microprobe and Laser Ablation Inductively Coupled Plasma Mass Spectrometric Analyses

J. Méric¹, P. Pagé¹, S.-J. Barnes^{1,2} and M.G. Houlé³

¹Département des sciences de la Terre, Université du Québec à Chicoutimi, Saguenay, Québec G7H 2B1

²Chaire de Recherche du Canada en Métallogénie Magmatique, Université du Québec à Chicoutimi, Saguenay, Québec

³Geological Survey of Canada, Québec City, Québec G1K 9A9

INTRODUCTION

Komatiite-associated nickel-copper-platinum group element (PGE) sulphide deposits exhibit generally a relatively small footprint and are becoming more and more difficult to find especially within poorly exposed and extensively overburden covered Archean and Proterozoic greenstone belts. It has been proposed that lithogeochemistry can be used to discriminate between rocks from mineralized and barren environments (e.g., Leshner et al. 2001). However, despite the fact these lithogeochemical indicators can be used as exploration guidelines, Barnes et al. (2004) suggests that, overall, the most reliable indicator of the presence of nickel sulphide mineralization, by far, is the presence of nickel-enriched sulphides.

Experimental studies have suggested some PGE fractionation between chromium-rich spinel and silicate melts where iridium, rhenium and ruthenium are found to be compatible and to be preferentially incorporated into the chromium-rich spinel, whereas palladium and platinum are found to be incompatible and stay in the magma during fractional crystallization (e.g., Richter et al. 2004). More recently, the work of Locmelis et al. (2011, in press) and Pagé et al. (2012) demonstrated from natural samples that PGE, particularly ruthenium, are preferentially incorporated into chromite in the absence of immiscible sulphide melt, and into sulphide when immiscible sulphide melt droplets are present (Figure 46.1). Therefore, it has been suggested that a better understanding of the behaviour of ruthenium in komatiitic systems might lead to some application for the exploration of magmatic nickel sulphide deposits and might be a good indicator for the presence of nickel-copper and PGE sulphide mineralization in those systems.

The main goal of this study, which is part of the high-magnesium ultramafic to mafic system subproject under the Targeted Geoscience Initiative 4 (TGI-4) (*see* Houlé, Leshner and Metsaranta, this volume, Article 42), is to develop the use of chromite as an indicator mineral for ore-forming processes related to nickel-copper-PGE mineralization associated with komatiites. In addition to ruthenium, other chalcophile elements, such as nickel, copper, cobalt, zinc, tin and also osmium and iridium, could be used to predict the presence of sulphide mineralization. Furthermore, the variations of the concentration of chromium, aluminum, iron, magnesium, titanium, nickel, manganese, vanadium, zinc, cobalt, gallium, scandium, osmium, iridium and ruthenium will be addressed in order to constrain different magmatic and secondary processes (i.e., post-cumulate) involved in the generation and the evolution of komatiitic rocks, such as

- magmatic processes: the melting degree of the mantle source, cooling history, fractional crystallization and crystallization sequence, country rock assimilation and sulphide segregation, and
- secondary processes: subsolidus re-equilibration, metamorphism and alteration.

Furthermore, our data set builds on major, minor and trace elements of chromite in komatiitic systems and will also be used to define a typical chromite signature associated with nickel-copper-PGE sulphide mineralization, which can be used in studies of detrital chromites within poorly exposed and/or extensively overburden covered areas.

More specifically, in this contribution are presented the preliminary results of electron microprobe and laser ablation inductively coupled plasma mass spectrometry (LA-ICP-MS) analyses of chromite from mineralized and unmineralized komatiitic flows or sills from the Alexo Mine area in Dundonald Township within the Abitibi greenstone belt in Ontario.

GEOLOGICAL SETTING

The komatiites of the Alexo Mine area are recognized as one of the classic and well-preserved examples of komatiites associated with a nickel-copper-(PGE) deposit not only in the Abitibi greenstone belt, but also worldwide. The Alexo Mine is hosted within a volcano-sedimentary succession recognized as the 2720–2710 Ma volcanic episode (e.g., Thurston et al. 2008) located in the northeastern part of Dundonald Township, approximately 45 km northeast of the City of Timmins. This volcanic episode has been subdivided into 3 informal formations by Houlié et al. (2008), which are, from oldest to youngest, 1) the McIntosh Lake formation, 2) the Dundonald formation and 3) the Frederick House Lake formation (Figures 46.2 and 46.3).

The Dundonald formation is composed of felsic volcanoclastic rocks, sulphidic-graphitic argillites, and komatiitic sills and flows. The komatiitic units of the Dundonald formation are subdivided into 4 informal members (oldest to youngest): 1) the Foundation member, 2) the Empire member, 3) the Dundonald South member and 4) the Alexo member (Houlié et al. 2008; *see* Figure 46.3). Iron-nickel-copper sulphide mineralization occurs at or near the base of all 4 komatiite members, but only those from the Alexo member (Alexo Mine) and the Foundation member (Kelex deposit) have been mined.

More specific to this project, samples investigated through this study are located within i) the Empire member (Small Pit area) that corresponds to a 100 m thick massive komatiitic peridotite sill; ii) the upper part of Dundonald South member, which is represented by thin well-differentiated (i.e., spinifex-textured and cumulate-textured zones) komatiitic flows with hyaloclastite top-flow breccias (described in detail by Barnes, Gorton and Naldrett (1983) and Arndt (1986)); and iii) the Alexo member (Alexo Mine zone) that comprises thick, poorly differentiated olivine orthocumulate to mesocumulate komatiitic flows (Houlié et al. 2008; Houlié, Leshner and Davis 2012).

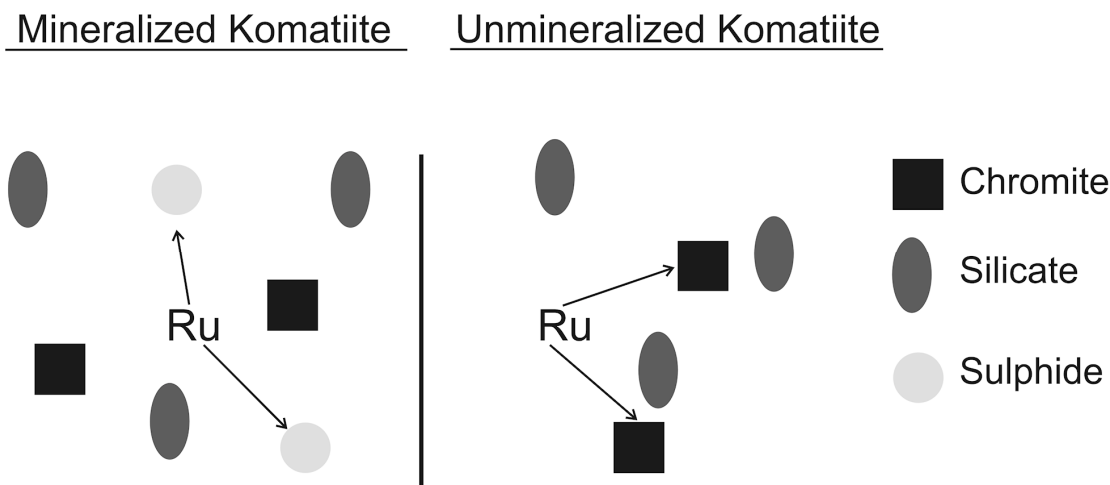


Figure 46.1. Cartoon showing the behaviour of ruthenium in a komatiitic magma where the ruthenium is incorporated within sulphide phases in a sulphide-rich system (left) and incorporated within chromite in sulphide-poor system (right).

METHODOLOGY

Sample Selection

Initially, the komatiite-associated nickel-copper-(PGE) Hart deposit in the Shaw Dome area of the Abitibi greenstone belt, was targeted as a good site for this study, similar to the ongoing companion study on multiple sulphur isotopes also at this site (*see* Hiebert et al., this volume, Article 45). However, preliminary petrographic investigation conducted on samples from the Hart deposit showed that chromites were absent from most of the selected samples and they were also locally pervasively serpentinized, which could have altered the primary geochemical signature of the chromite. As an alternative, the Alexo Mine area was finally selected as the new locality; this was justified by several factors: i) the komatiites are at the prehnite-pumpellyite up to lower greenschist metamorphic facies (Arndt 1986), ii) the deformation is non-penetrative, iii) the primary volcanic textures and structures are very well preserved and, finally, iv) a large suite of samples were available in a well-characterized geological setting. All

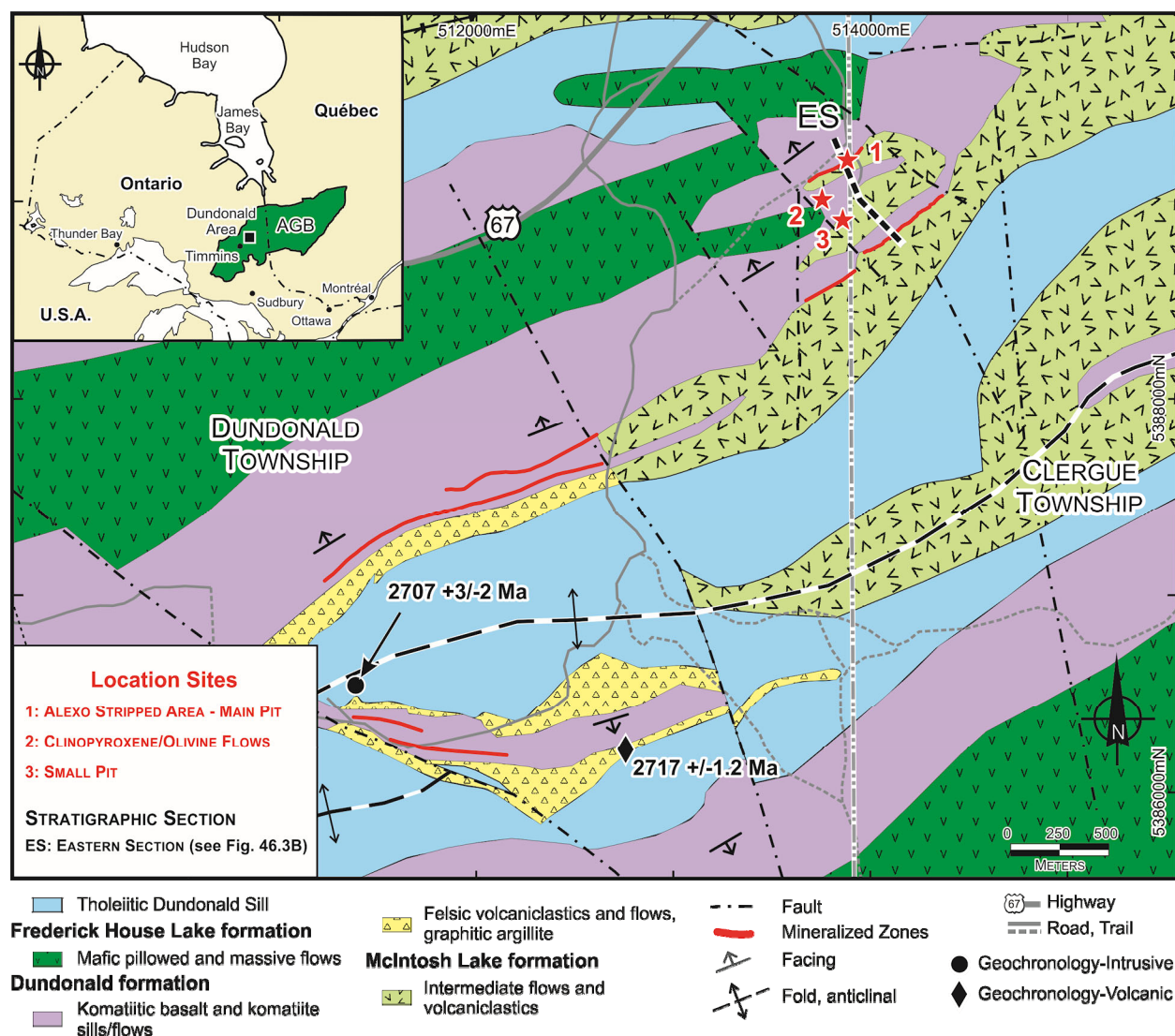


Figure 46.2. Simplified geological map of the Dundonald Township area, Abitibi greenstone belt (AGB), showing major geological units and location sites for this study (*adapted from* Houllé, Leshner and Davis 2012). Section ES (Eastern Section: Alexo Mine) is the location of the stratigraphic column shown in Figure 46.3B.

these considerations led us to use pre-metamorphic igneous and volcanic nomenclature as rock names in the course of this study. The impact of metamorphism on trace elements content of chromite is not well constrained in comparison to major and minor elements (Barnes 2000). Thus, the low metamorphic grade of the samples (1/3 of the thin sections contain fresh olivine relicts) enhanced the quality and the confidence over the actual and future results on the chromite chemistry. A total of 47 samples have been

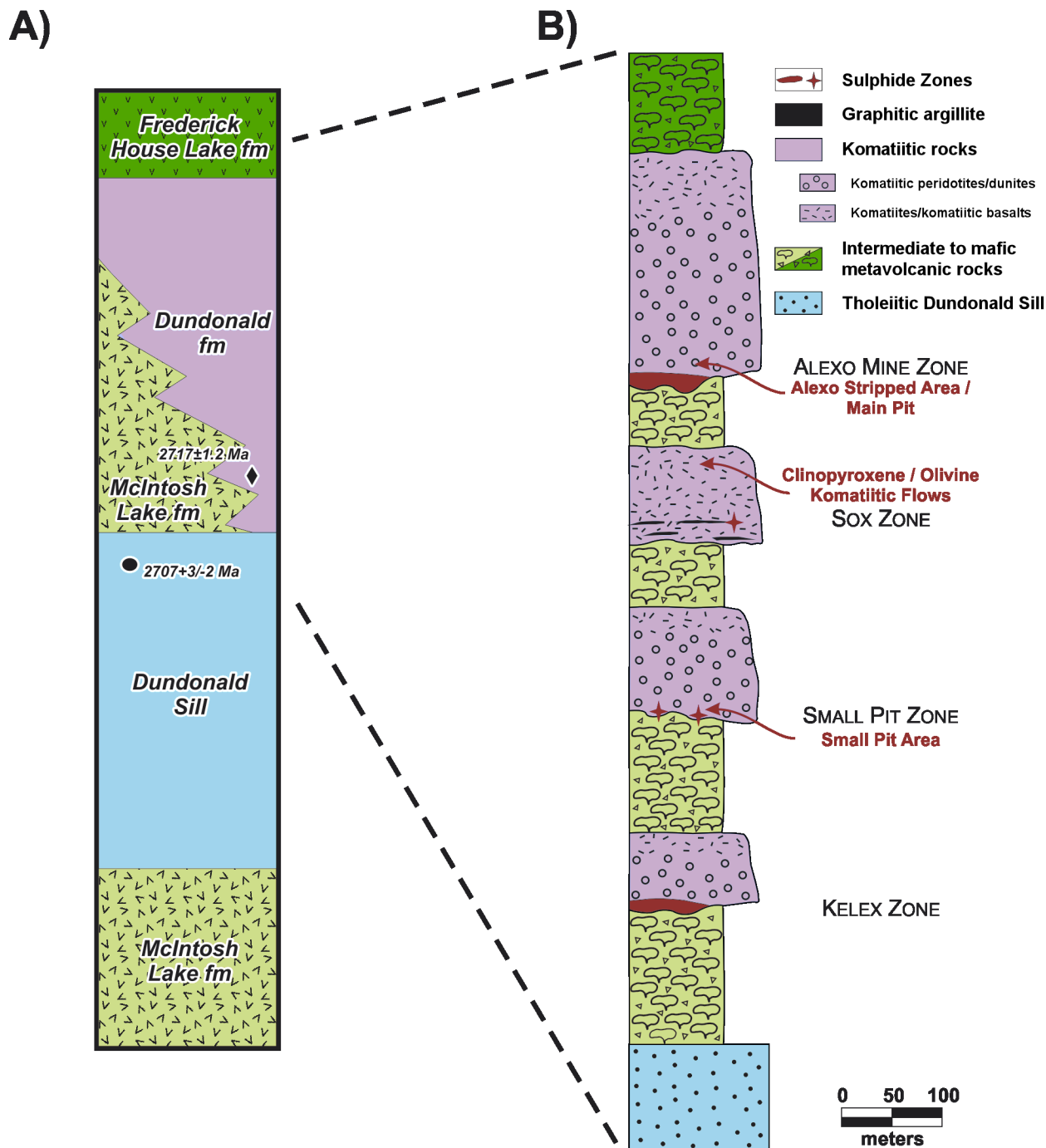


Figure 46.3. A) General schematic stratigraphic column of Dundonald Township (after Houlié et al. 2008). B) Schematic stratigraphy of the Dundonald formation at the Alexo Mine, showing the locations of komatiite-associated nickel-copper-(PGE) deposits or occurrences and location sites for this study (adapted from Houlié, Leshner and Davis 2012).

selected, all from 2 previous studies conducted at the Alexo Mine area, and are allocated as follows: 24 samples are from the PhD thesis of Dr. S.-J. Barnes (Barnes 1983), and 23 samples are from the PhD thesis of Dr. M.G. Houllé (Houllé 2008). At each location, samples were selected along a stratigraphic transect from the basal mineralization up to the olivine cumulate higher up-section, but also laterally to investigate the influence of the proximity of the mineralization.

In this investigation, all samples were grouped into 2 unit-types: the mineralized komatiitic units (i.e., flows and/or sills) and the barren or unmineralized komatiitic units. As an initial attempt, each sample was assigned into one of the unit-types (or groups) based on their actual stratigraphic location. Samples from the Alexo member (Alexo stripped area: 23 samples; and the Main Pit area: 5 samples) and the Empire member (Small Pit area: 6 samples) were assigned to the mineralized komatiitic units and the samples from the upper section of the Dundonald South member (clinopyroxene and olivine komatiitic flows: 13 samples) were assigned to the unmineralized komatiitic units (*see* Figure 46.3). However, the confidence in this preliminary classification scheme is unknown thus far; despite the fact that the samples from the clinopyroxene and the olivine komatiitic flows are known to be unmineralized, some nickel-copper-(PGE) sulphide mineralization is recognized farther to the east and to the west (e.g., Sox zone; Houllé, Leshner and Davis 2012).

Analytical and Laboratory Work

The methodology of the project consists of 4 different and complementary approaches to characterize the chromite geochemistry within mineralized and unmineralized komatiitic units:

- selection of the samples according to their position relative to the mineralization, their facies (cumulate, spinifex, net-textured sulphide, etc.) and the size of chromite (large enough to be analyzed by LA-ICP-MS);
- classic petrographic study with emphasis on the characterization of the chromite morphology, size, texture, alteration and its relation with the other phases that coexist with them;
- electron microprobe analyses of chromite at Laval University (Québec) to determine their major elements content; LA-ICP-MS at Laboratoire des Matériaux Terrestres de l'UQAC (LabMaTer, Saguenay) to determine the minor and trace element and PGE content of chromite; and
- whole rock analyses for major and trace elements and PGE content to perform mass balance calculations to determine which elements are influenced by the chromite and sulphide crystallization. Major element analyses, trace element analyses, and PGE analyses were carried out at Activation Laboratories Ltd. (ActLabs, Ancaster), at the Geosciences Laboratories (Geo Labs, Sudbury), and at Laboratoire des Matériaux Terrestres de l'UQAC (LabMaTer, Saguenay), respectively.

PRELIMINARY RESULTS

Petrographic Observations

The morphology of chromite within the komatiitic rocks at the Alexo Mine area is similar to those observed in other komatiitic units elsewhere around the world (Barnes 1998). Typically, chromite from the spinifex-textured komatiite of the A zone exhibits subeuhedral and skeletal crystal shapes (Figure 46.4A). In contrast, chromite from the olivine cumulate of the B zones exhibits euhedral to subeuhedral crystal shapes and is distributed as small clusters of several grains (Figure 46.4B). Euhedral chromite grains were also observed within massive sulphides at the base of the mineralized flow (sample MGH140; Figure 46.4D); however, Houllé, Leshner and Davis (2012) have also reported “hopper” to skeletal

chromite crystals along the basal contact between the komatiite unit and its footwall rocks. These observations suggest that chromite morphology is clearly dependant of the cooling environment within each komatiitic units (Barnes 1998).

In all samples investigated, almost all chromites exhibit some evidence of different degrees of alteration, which is expressed by the presence of thin rim of ferrichromite to magnetite surrounding a preserved primary chromite core (Figure 46.4C). To obtain the primary magmatic composition of the chromite, analyses were done within the core of each chromite grain (avoiding any fractures and/or inclusions).

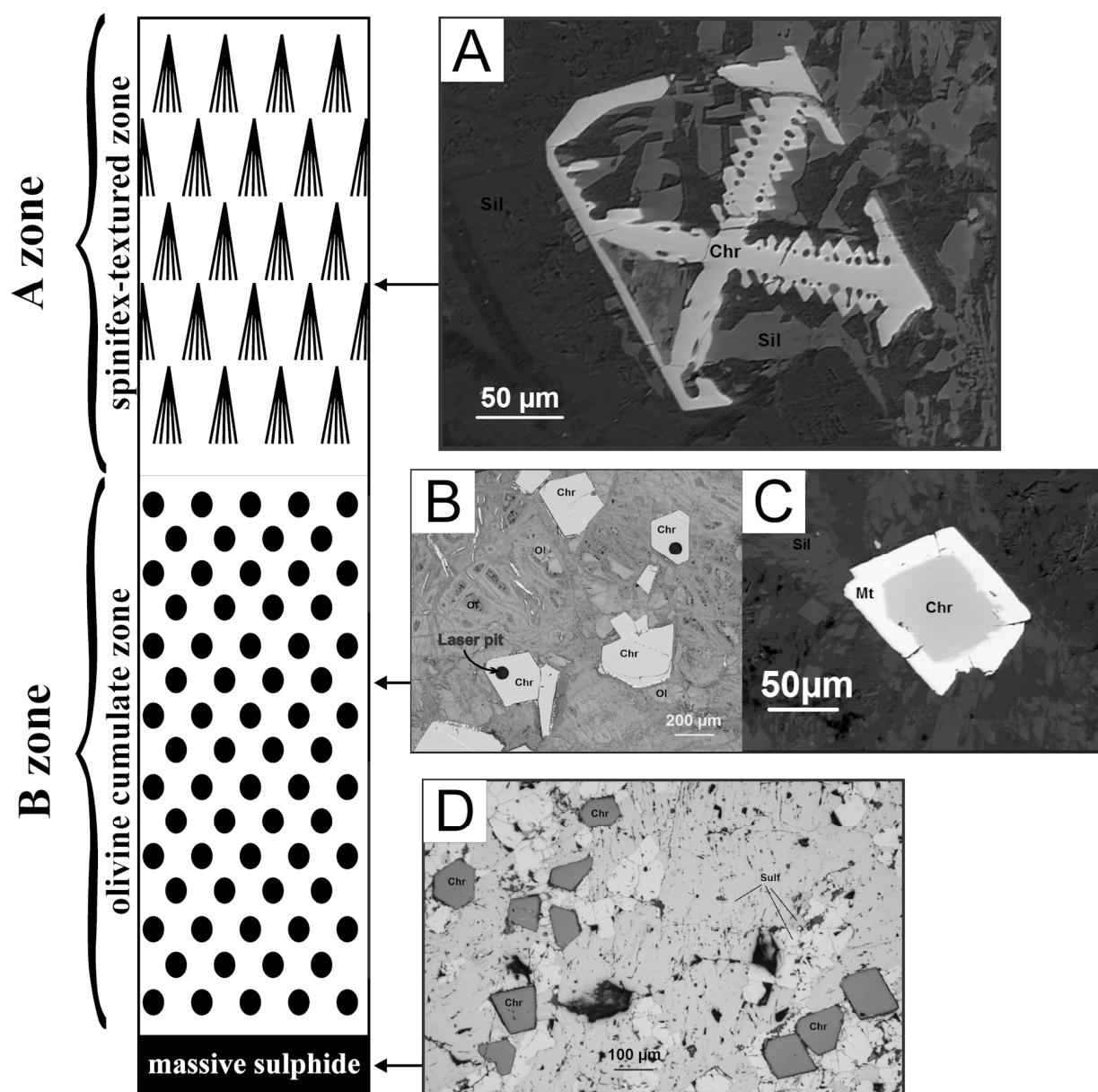


Figure 46.4. Idealized and schematic profile (not to scale) through a komatiitic unit (left) and photos of chromite with different morphologies relative to their position at the Alexo Mine area (right). A) Skeletal chromite from the spinifex-textured zone (A zone); B) euhedral chromite from an olivine cumulate (B zone); C) euhedral-altered chromite characterized by a well-preserved chromite core surrounded by a rim of magnetite within an olivine cumulate (B zone); D) euhedral chromite within a massive sulphide horizon at the base of a komatiitic flow within (Alexo member). Abbreviations: Chr = chromite; Sil = silicate; Ol = olivine; Mt = magnetite; sulf = sulphide.

Mineralogical Analysis

Chromites from mineralized and unmineralized komatiitic units were analyzed by electron microprobe and LA-ICP-MS to characterize their composition in terms of major (Cr, Al, Fe, Mg), minor and trace (Ti, Ni, Mn, V, Zn, Co, Ga, Sc), and ultra-trace (Os, Ir, Ru and Rh) elements. This section presents the preliminary results from 36 and 26 thin sections analyzed by electron microprobe and LA-ICP-MS, respectively. Between 2 to 5 chromite grains were analyzed per thin section.

ELECTRON MICROPROBE ANALYSIS

Figure 46.5 presents $\text{Fe}^{2+}\#$ ($100 \times \text{Fe}^{2+}/(\text{Fe}^{2+}+\text{Mg})$) versus $\text{Cr}\#$ ($100 \times \text{Cr}/(\text{Cr}+\text{Al})$) of chromite from our preliminary data for the mineralized and unmineralized komatiitic units at the Alexo Mine area in comparison with the broad field of chromite (shown in light grey) from komatiites from the compilation by Barnes and Roeder (2001). Figure 46.5 also includes a subgroup of chromite (shown in medium grey) from komatiites exhibiting low metamorphic grade (greenschist facies; Barnes and Roeder 2001). The chromite grains from our samples show $\text{Cr}\#$ ranging from 63 to 78 and $\text{Fe}^{2+}\#$ ranging from 31 to 78. As expected, the chromite from our samples compared well with the chromite from slightly metamorphosed komatiites. However, one of our samples (MGH140), containing massive sulphide, shows chromite grains with a composition clearly different from the chromite from the unmineralized komatiites. The chromites from this sample (MGH140) show high $\text{Fe}^{2+}\#$ (61 to 65) and much higher $\text{Cr}\#$ (96 to 99).

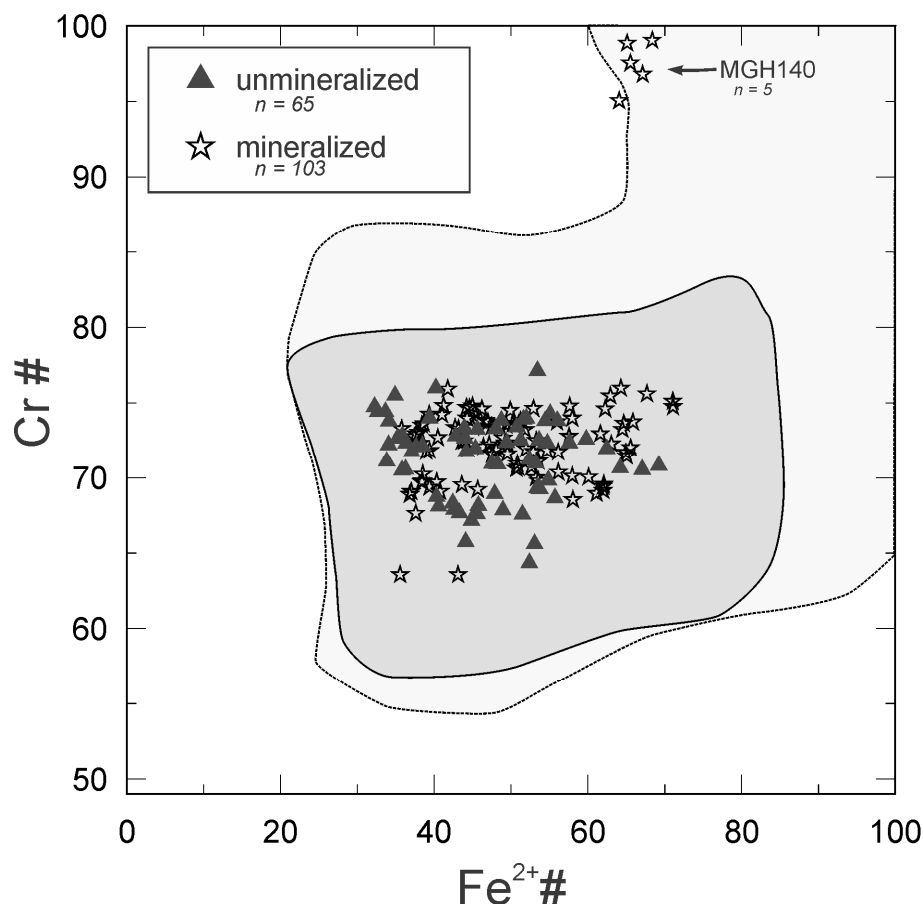


Figure 46.5. $\text{Fe}^{2+}\#$ ($= 100 \times \text{Fe}^{2+}/(\text{Fe}^{2+}+\text{Mg})$) versus $\text{Cr}\#$ ($= 100 \times \text{Cr}/(\text{Cr}+\text{Al})$) of chromite in komatiites from the Alexo Mine area (this study) compared with the compilation of chromite in komatiites from Barnes and Roeder (2001); light grey field = all chromites from komatiites around the world ($n=4095$); medium grey field = chromites from komatiites at greenschist facies ($n=1036$).

LASER ABLATION INDUCTIVELY COUPLED PLASMA MASS SPECTROMETRIC ANALYSES

Chromite cores were analyzed using LA-ICP-MS and concentrations of 32 elements were measured, 10 of which (Mg, Al, Si, S, Ca, Cr, Cu, Sr, Pt and Pd) were used to control the nature of the ablated material and the potential presence of inclusions in the chromite. A number of elements (Sc, Ti, V, Mn, Co, Ni, Cu, Zn, Ga, Ge, As, Zr, Nb, Mo, Ru, Rh, In, Os and Ir) are well above detection limits, whereas other elements (Y, Pd, Sn, Sb, Hf and Ta) were mostly below detection limits. Figure 46.6 presents binary plots for Cr # versus scandium, gallium, titanium and vanadium and for Fe^{2+} # versus nickel, cobalt, manganese and zinc for mineralized and unmineralized samples. In terms of minor and trace elements, chromites from Alexo Mine komatiites show 700 to 2100 ppm V, 1400 to 3700 ppm Ti, 3 to 37 ppm Ga and 1 to 14 ppm Sc. These multivalent (3^+ and 4^+) elements show negative correlations with Cr #. For the divalent elements, chromites from Alexo Mine komatiites show 470 to 3700 ppm Zn, 1200 to 2300 ppm Mn, 150 to 350 ppm Co and 350 to 2000 ppm Ni. Zinc, manganese and cobalt show positive correlations with Fe^{2+} #. Nickel shows a contrasting behaviour compared with the other divalent elements; it shows a negative correlation with Fe^{2+} #. All these trends can be interpreted as being the result of fractionation. During the magmatic differentiation, Cr # decreases whereas Fe^{2+} # increases. We note that with Cr # there is no discrimination between mineralized and unmineralized for almost all samples, but with Fe^{2+} # some samples present a higher Fe^{2+} #, a higher content in zinc, manganese and cobalt, and a lower content in nickel; however, such contents could be explained by a stronger alteration of these samples (*see* Figure 46.6; Barnes 2000). Sample MGH140 was excluded from the diagrams because of a very different content in all of these elements; indeed, this sample presents very high contents of 9300 to 12 000 ppm Ti, 5200 to 6300 ppm Mn, 1750 to 2250 ppm Zn and 2650 to 3200 ppm V; high contents of 38 to 47 ppm Ga and 10 to 16 ppm Sc; and lower contents of 160 to 260 ppm Co and 320 to 410 Ni. Sample Ax33 is excluded from fractionation trends (*see* Figure 46.6) because of differences in content for all elements presented. In Cr # diagrams, sample Ax33 presents a high content relative to other samples of 1600 to 2000 ppm V and a low content of 1500 to 1700 ppm Ti, 3 to 25 ppm Ga and 1 to 6 ppm Sc. In Fe^{2+} # diagrams, sample Ax33 presents a high Fe^{2+} # (~76); a higher content of 15 000 to 26 000 ppm Zn, 4300 to 5900 ppm Mn and 350 to 400 ppm Co; and a lower content of 95 to 175 ppm Ni. Sample Ax33 is the only sample where chromites a) show evidence of alteration by the presence of a large magnetite rim and by distinctive geochemical signatures that could reflect the effect of alteration, and b) show lower scandium, gallium and nickel contents and enrichment in iron, zinc, manganese and cobalt; all these characteristics are indicators of metamorphosed chromites (Barnes 2000).

As was mentioned previously, platinum group elements are extremely sensitive, especially ruthenium, to the presence of an immiscible sulphide liquid that has the capacity to scavenge most of the PGE available in the komatiitic magma, thus affecting the composition of chromite formed subsequently (e.g., Righter et al. 2004). The results obtained so far indicate analytical signals above detection limits for osmium, iridium, rhenium and ruthenium for most of the chromite from the mineralized and unmineralized samples. Ruthenium is detected above detection limit from most of the 26 samples for which chromites have been analyzed, but 3 of the samples have ruthenium concentrations close to or below the detection limit (60 ppb): these samples include 2 samples from the mineralized flows, Ax33 (n=4) and the massive sulphide MGH140 (n=5), and 1 sample from the unmineralized flow, Ax69 (n=3) (Figure 46.7). The chromites from Alexo Mine contain low concentrations (close to the detection limit) of osmium, iridium and rhenium varying from 7 ppb (detection limit) to 30 ppb. On the other hand, most of the chromites from Alexo Mine contain significantly higher concentrations of ruthenium varying from 6 ppb (below detection limit) up to 430 ppb (*see* Figure 46.7). As shown on Figure 46.7, we note ruthenium shows a weak positive correlation with Cr #, a trend that could also be related to fractionation.

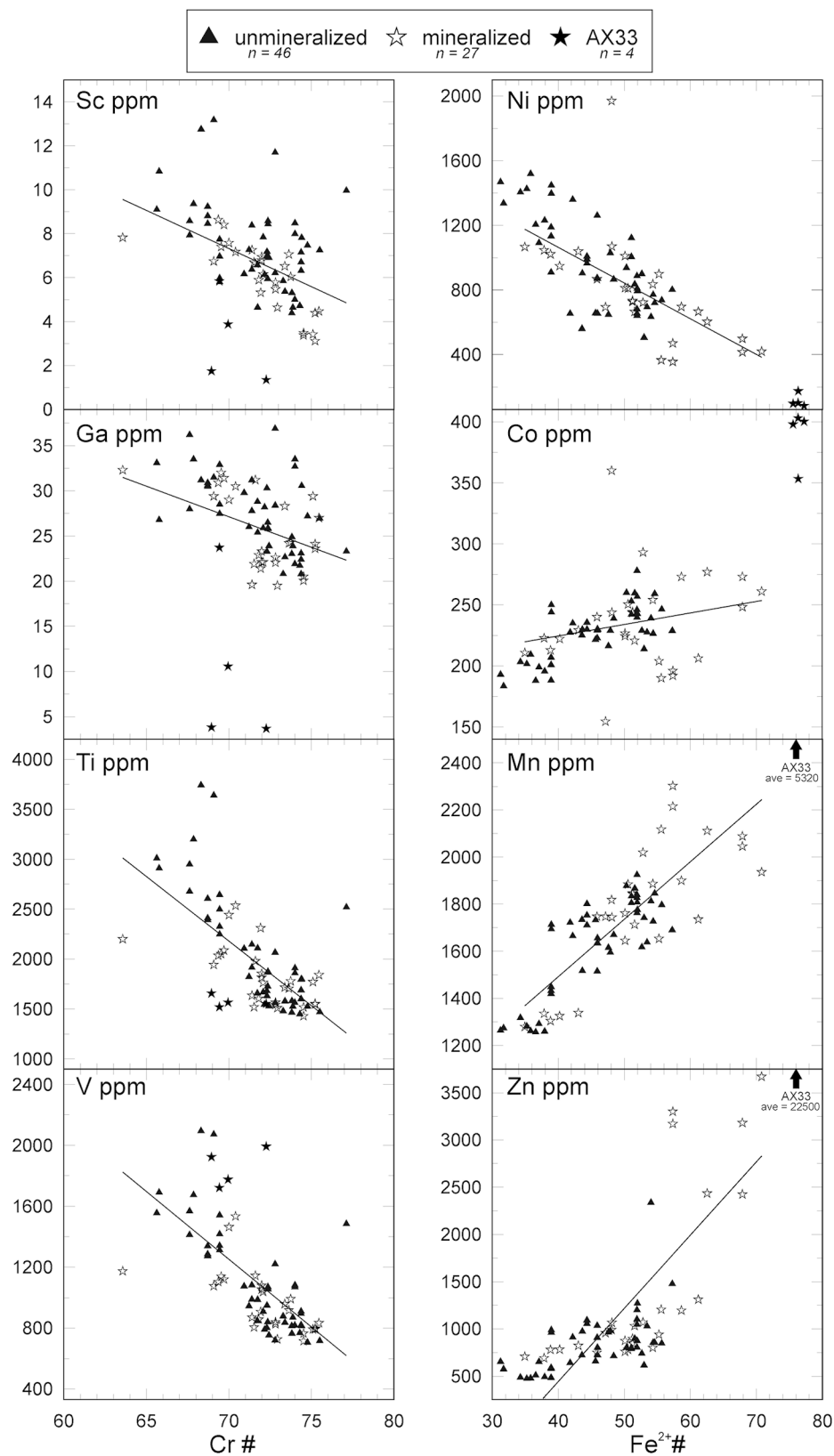


Figure 46.6. Binary plots showing, on the left, Cr # versus scandium, gallium, titanium and vanadium content, respectively; and, on the right, Fe²⁺ # versus nickel, cobalt, manganese and zinc content, respectively. Solid lines = linear regression lines.

SUMMARY

Preliminary results of the chromite geochemistry shows that vanadium, titanium, gallium, scandium, zinc, manganese and cobalt contents of the chromite from Alexo Mine komatiites increase with magmatic differentiation, represented by the decrease of Cr # and the increase of Fe^{2+} #. However, nickel shows an inverse correlation with Fe^{2+} #, and correlates very well with the magnesium content of chromites. Overall, these relationships seem to reflect the effect of fractionation of komatiitic magmas. Ruthenium concentrations range from below detection level to 430 ppb, and the positive correlation could also be related to the effect of fractionation of komatiitic magmas. It is noted that, based on analyses to date, trace elements and ruthenium do not discriminate between mineralized and unmineralized units at the Alexo Mine area. However, it is interesting to note that at least some of the chromite formed with sulphide droplets exhibits depletion in ruthenium that results from a much higher partition coefficient for sulphide than for chromite (e.g., sample MGH140). One of the main goals of this study is to evaluate whether the PGE content of chromite can be used as an exploration tool for mineralized komatiitic systems. In the light of these new results, the high concentration of ruthenium in chromites from some of the mineralized samples could be explained either by i) the fact that Alexo Mine komatiites are probably an open system as proposed by Houllé, Leshner and Davis (2012) (i.e., flow-through systems) and the ruthenium depletion signature of the chromite within these mineralized units have been flushed out of this system or ii) the fact that chromite could have crystallized before the sulphide segregation, or concomitantly with sulphide segregation (i.e., pre- to syn- sulphide). However, further investigation is needed to confirm these hypothesis.

FUTURE WORK

These preliminary results still need to be analyzed and evaluated further to better understand the behaviour of the PGE, especially ruthenium, in the presence or absence of an immiscible sulphide liquid. Additional chromite electron microprobe and LA-ICP-MS analyses will be carried out on mineralized and barren komatiitic units from the Alexo Mine area, after which we will be able to observe if there is a

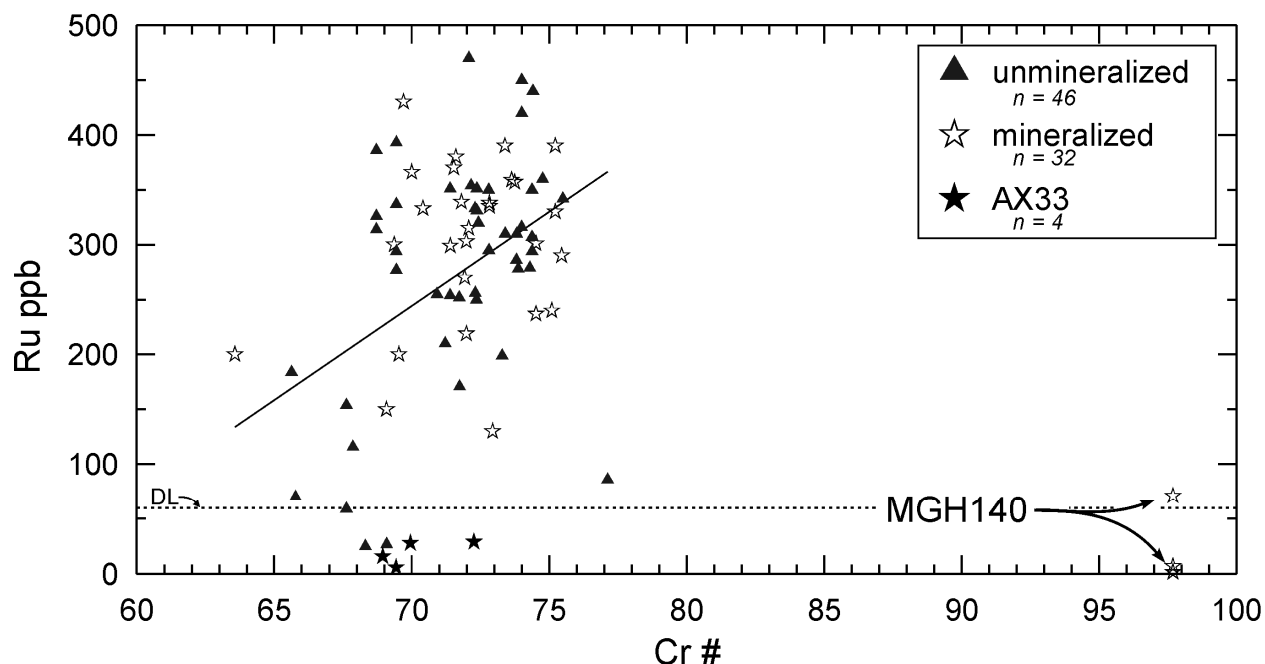


Figure 46.7. Diagram showing the concentrations of Cr # versus ruthenium (ppb) for chromites from the Alexo komatiites. Solid line = linear regression line; DL = detection limit.

variation in chromite geochemistry relative to the position of the mineralization (from distal to proximal). In addition, whole rock analyses will be used to perform mass balance calculations to determine which elements are controlled and influenced by the chromite and sulphide crystallization.

ACKNOWLEDGMENTS

This study is part of a Master of Science (MSc) thesis project based at Université du Québec à Chicoutimi (UQAC, Saguenay) under the supervision of Drs. P. Pagé (UQAC), S.-J. Barnes (UQAC), and M.G. Houlé (GSC-Québec). The project has been funded by the Geological Survey of Canada under the Targeted Geoscience Initiative 4 (TGI-4) and the Canada Research Chair of Magmatic Ore Deposits. We also thank Anne-Aurélien Sappin (GSC) for her review of the manuscript that helped us improve the final version of this report. This is Geological Survey of Canada contribution number 20120251.

REFERENCES

- Arndt, N.T. 1986. Differentiation of komatiite flows; *Journal of Petrology*, v.27, p.279-301.
- Barnes, S.-J. 1983. The origin of the fractionation of platinum group elements in Archean komatiites of the Abitibi greenstone belt, northern Ontario, Canada; unpublished PhD thesis, University of Toronto, Toronto, Ontario, 231p.
- Barnes, S.-J., Gorton, M.P. and Naldrett, A.J. 1983. A comparative study of olivine and clinopyroxene spinifex flows from Alexo, Abitibi greenstone belt, Ontario, Canada; *Contributions to Mineralogy and Petrology*, v.83, p.293-308.
- Barnes, S.-J., Hill, R.E.T., Perring, C.S. and Dowling, S.E. 2004. Lithogeochemical exploration for komatiite-associated Ni-sulfide deposits: strategies and limitations; *Mineralogy and Petrology*, v.82, p.259-293.
- Barnes, S.J. 1998. Chromite in komatiites, I. Magmatic controls on crystallization and composition; *Journal of Petrology*, v.39, p.1689-1720.
- 2000. Chromite in komatiites, II. Modification during greenschist to mid-amphibolite facies metamorphism; *Journal of Petrology*, v.41, p.387-409.
- Barnes, S.J. and Roeder, P.L. 2001. The range of spinel compositions in terrestrial mafic and ultramafic rocks; *Journal of Petrology*, v.42, p.2279-2302.
- Houlé, M.G. 2008. Physical volcanology and metallogenesis of komatiitic rocks in the Abitibi greenstone belt, Superior Province, Ontario, Canada; unpublished PhD thesis, University of Ottawa, Ottawa, Ontario, 203p.
- Houlé, M.G., Gibson, H.L., Leshner, C.M., Davis, P.C., Cas, R.A.F., Beresford, S.W. and Arndt, N.T. 2008. Komatiitic sills and multigenerational peperite at Dundonald Beach, Abitibi greenstone belt, Ontario: volcanic architecture and nickel sulfide distribution; *Economic Geology*, v.103, p.1269-1284.
- Houlé, M.G., Leshner, C.M. and Davis, P.C. 2012. Thermomechanical erosion at the Alexo Mine, Abitibi greenstone belt: implications for the genesis of komatiite-associated Ni-Cu-(PGE) mineralization; *Mineralium Deposita*, v.47, p.105-128.
- Leshner, C.M., Burnham, O.M., Keays, R.R., Barnes, S.J. and Hulbert, L. 2001. Geochemical discrimination of barren and mineralized komatiites associated with magmatic Ni-Cu-(PGE) sulphide deposits; *The Canadian Mineralogist*, v.39, p.673-696.
- Locmelis, M., Fiorentini, M.L., Barnes, S.J. and Pearson, N.J. in press. Ruthenium variation in chromite from komatiites and komatiitic basalts – a potential mineralogical indicator for nickel-sulfide mineralization; *Economic Geology*.

- Locmelis, M., Pearson, N.J., Barnes, S.J. and Fiorentini, M.L. 2011. Ruthenium in komatiitic chromite; *Geochimica et Cosmochimica Acta*, v.75, p.3645-3661.
- Pagé, P., Barnes, S.-J., Bedard, J.H. and Zientek, M.L. 2012. *In situ* determination of Os, Ir and Ru in chromites formed from komatiite, tholeiite and boninite magmas: implications for chromite control of Os, Ir and Ru during partial melting and crystal fractionation; *Chemical Geology*, v.302-303, p.3-15.
- Righter, K., Campbell, A.J., Humayun, M. and Hervig, R.L. 2004. Partitioning of Ru, Rh, Pd, Re, Ir, and Au between Cr-bearing spinel, olivine, pyroxene and silicate melts; *Geochimica et Cosmochimica Acta*, v.68, p.867-880.
- Thurston, P.C., Ayer, J.A., Goutier, J. and Hamilton, M.A. 2008. Depositional gaps in Abitibi greenstone belt stratigraphy: a key to exploration for syngenetic mineralization; *Economic Geology*, v.103, p.1097-1134.

47. Targeted Geoscience Initiative 4. Lode Gold Deposits in Ancient Deformed and Metamorphosed Terranes: The Role of Extension in the Formation of Timiskaming Basins and Large Gold Deposits, Abitibi Greenstone Belt—A Discussion

W. Bleeker¹

¹Geological Survey of Canada, Ottawa, Ontario K1A 0E8

INTRODUCTION

Lode gold deposits or “orogenic gold deposits” (Groves et al. 1998) have generally been understood in the context of terrane accretion, thrusting, crustal shortening and an attendant metamorphic cycle. In recent years, however, there has been a growing recognition in moderately eroded Archean greenstone belt environments that synorogenic extension may have played a critical role (e.g., Blewett and Czarnota 2007; Bleeker, van Breemen and Berger 2008; Blewett, Czarnota and Henson 2010; Czarnota et al. 2010). Looking at a terrain such as the Abitibi greenstone belt (AGB), there are a number of attributes that are indeed puzzling in light of an accretion and shortening-only model:

- Fold-thrust systems are characterized by a network of upward-branching faults; why would they focus fluid flow en route to the upper crust?
- Why are shallow crustal levels and their low-grade, or even sub-greenschist facies, rocks and vein systems preserved?
- Why are the synorogenic clastic basins preserved and not quickly eroded off the top during general post-orogenic uplift?
- Why do some of these basins show a rapid transition to deep-water facies?
- Why is there a sudden flare-up of alkaline magmatism, overlapping in time with these late basins?
- Crustal thickening would lead to a delayed lower crustal metamorphic cycle and a peak in metamorphic fluid production tens of millions of years after accretion. Yet, some ages on gold deposits do indicate relatively early ages (e.g., see brief discussion in Ayer et al. 2003) close in time to that of the synorogenic basins and associated magmatism.

Although local explanations could probably account for some of these observations at any particular locality, a distinct synorogenic phase of extension may help to explain all these observations in a single coherent model. The reason this synorogenic phase of extension has been slow to be fully recognized in places such as the AGB is because of the general complexity of the multiphase structural history (e.g., Bleeker 1999), involving 1) an early phase of folding and thrusting and, on the larger scale, terrane imbrication (e.g., Bleeker and van Breemen 2011), all predating the extensional phase; 2) then the sharp phase of synorogenic extension; 3) a later phase of thick-skinned thrusting that inverted the extensional architecture; 4) further shortening and steepening of all structures; and finally, 5) transpression and degeneration to and overprinting by strike-slip deformation, first sinistral and then dextral.

Here I show in a series of simple conceptual cartoons how the critical phase of extension manifests itself in the south-central AGB and why it may be important, on the belt scale, in generating a world-class lode gold environment. Although these cartoons and underlying structural evolution are indeed modelled on the AGB, they can be applied step-by-step to other (Archean) lode gold districts, for example, Yellowknife (Slave craton), Agnew (Eastern Goldfields, Yilgarn craton) and several others.

EARLY FOLD-THRUST BELT FORMATION AND TERRANE IMBRICATION

In the Timmins to Kirkland Lake area of the south-central AGB, there is a major phase of tight folding, and probably some thrusting, imbricating stratigraphy at various scales (Figure 47.1). It occurred immediately following deposition of generally deep-water greywacke turbidites of the Porcupine Group (Bleeker and Parrish 1996), which was deposited at *circa* 2695 to 2687 Ma overlying the volcanic stratigraphy. Bleeker and van Breemen (2011) have shown that entire assemblages such as the Kidd–Munro, and probably also the Blake River, were emplaced as high-level thrust nappes on top of these younger turbidites, prior to being folded. There is no convincing evidence that the major faults, locally known as the “breaks” and which clearly play a critical role in later gold distribution, were active or even present at this point in time. The general tectonic transport direction at this early stage seems to have been toward the west or southwest (Bleeker 1999; Bleeker and van Breemen 2011). The strong easterly plunge of stretched pillows in the Timmins area lies in the east-dipping axial plane of this fold-thrust event and is inherited from this very first phase of regional deformation. At the subprovince scale, the onset of thrusting in one place may have led to “Porcupine-type” turbidite sedimentation in foreland to the south (*see* Figure 47.1).

SECOND PHASE OF FOLDING OF ALREADY IMBRICATED STRATIGRAPHY

In the classic and well-studied Timmins area, because of a fortuitous relationship and the way overprinting relationships are laid out in the field, one can actually demonstrate a second phase of (re)folding prior to the onset of synorogenic clastic basin development. This second folding event is represented by the “Porcupine Syncline”, both limbs of which are cut by the next critical time-marker in the area, the

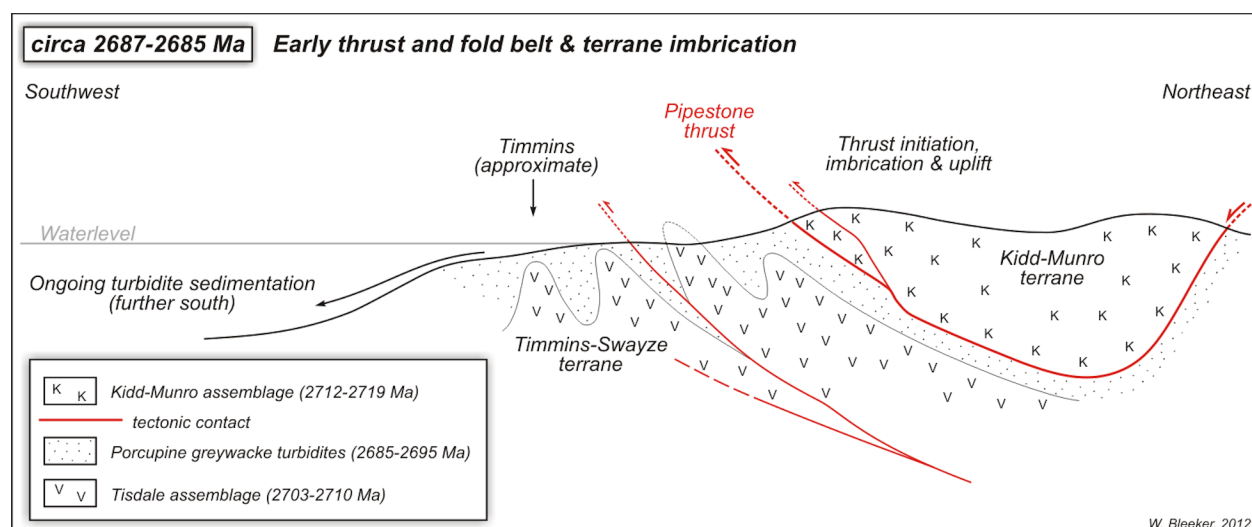


Figure 47.1. Cartoon showing a section through the early fold-thrust belt affecting the south-central Abitibi greenstone belt, Timmins area, at about 2687 to 2685 Ma, just prior to the onset of alkaline magmatism. Porcupine Group greywacke turbidites are being fold- and thrust-imbricated with older volcanic rocks. Major thrust slices such as the Kidd–Munro terrane are emplaced on top of the structural pile. Overall vergence of the folds is toward the west (southwest). There is no indication at this stage that the major “breaks” such as the Porcupine–Destor fault zone were present.

unconformity at the base of the synorogenic clastic sequence (Hurst 1939; Ferguson 1966; Ferguson et al. 1968; Bleeker 1999). The synorogenic clastic sedimentary rocks are locally known as the “Timiskaming sequence”. Similarly complex structural histories are likely to exist in many other areas, but, depending on the interference patterns and the presence or absence of unequivocal truncations or crosscutting relationships, they may go unnoticed. The Porcupine Syncline and the earlier tight to isoclinal folds form a Type 2 (“mushroom”) fold interference pattern (Davies 1977; Bleeker 1999), and this entire fold interference pattern predates the Timiskaming unconformity. A structural section parallel to the axial plane of the younger Porcupine Syncline eliminates this younger fold from the geometry and clearly demonstrates the rather strong westerly vergence of the early fold-thrust belt (*see* Bleeker 1999). This is important for several reasons, but, most pertinent to the present discussion, it demonstrates that the strong east-west structure of this part of the AGB is a structural feature that is acquired later; it is not an early feature.

UPLIFT AND EROSION

The response to these early folding and thickening events, in Timmins bracketed to a time interval of *circa* 2687 to 2680 Ma, was uplift, rapid emergence of the fold-thrust belt, and erosion. This was followed by the formation of a terrestrial unconformity surface that became covered by initially proximal erosional debris: coarse conglomerates and immature sandstones (Figure 47.2). These “synorogenic” clastic sequences are recognized in many orogenic belts. In the AGB, they are generally referred to as “Timiskaming-type” clastic sequences after a type locality in the Lake Temiskaming area (note the spelling difference!). So far this structural–stratigraphic evolution is unremarkable, but key attributes of

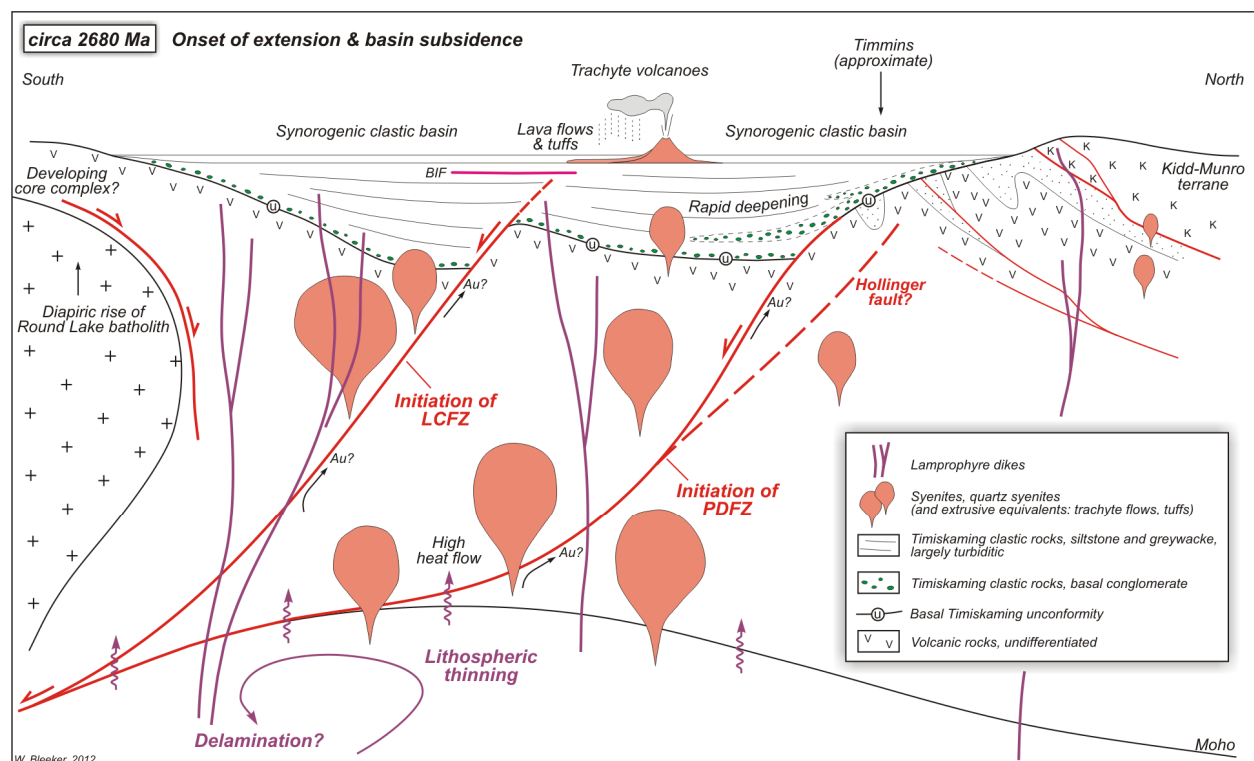


Figure 47.2. Formation of synorogenic clastic basins at *circa* 2680 Ma. Rapid deepening of these basins, as well as a sudden flare-up of alkaline magmatism, suggests a link with extension and upper mantle processes (delamination?). The major “breaks”, that is, the Porcupine–Destor fault zone (PDFZ) in the north and the Larder–Cadillac fault zone (LCFZ) farther south, were likely initiated at this time as crustal-scale extensional faults, listric to the south. Numerous syenitic plutons were emplaced and lithospheric thinning increased the heat flow into the lower crust. During this extensional deformation, composite granitoid batholiths such as the Round Lake may have risen diapirically, their ascent aided by additional extensional shear zones. (*See* previous and next figures for additional symbols.)

the Timiskaming sequences in the AGB tell us that there is more to the story: a sharp onset of regional extension and alkaline magmatism and the initiation of the first-order faults (the so-called “breaks”) as crustal-scale extensional faults (see Figure 47.2).

WHY EXTENSION?

One of the more important characteristics of Timiskaming-type clastic sequences is the first appearance of a variety of granitoid clasts in the sedimentary record of these greenstone belts, with some clasts showing a strong fabric (i.e., relatively deep, hot deformation). This indicates uplift and erosion (exhumation) of different crustal levels. An onset of extensional faulting and unroofing of mid-crustal levels, at the same time as creating accommodation space for sediment accumulation, is an attractive scenario to explain this observation (Figures 47.2 and 47.3). Other observations support an extensional scenario: in Timmins, the synorogenic unconformity is overlain by a thin locally derived conglomerate or slope breccia deposit, which then rapidly grades up into deeper water siltstones and mudstones with a turbiditic character. Sheets of polymict conglomerate occur within this lower sequence, but much of the lower half of the Timiskaming sequence consists of relatively deep-water deposits. Both extension and strike-slip basin development could explain this very rapid deepening, but there are few if any strike-slip indicators at this time (e.g., demonstrable pull-apart basins). While Timiskaming basins were developing, there was a sudden flare-up in alkaline magmatism in the area, represented by syenitic and lamprophyric intrusions. Locally, this magmatism erupted into developing Timiskaming-type basins as flows and tuffs. The time frame for this extension and rapid basin deepening in the AGB is *circa* 2680 to 2670 Ma. In Timmins, an age of 2687 ± 3 Ma (Barrie 1990) has been determined for the very oldest alkaline intrusive rocks, perhaps indicating a slightly earlier onset of extension.

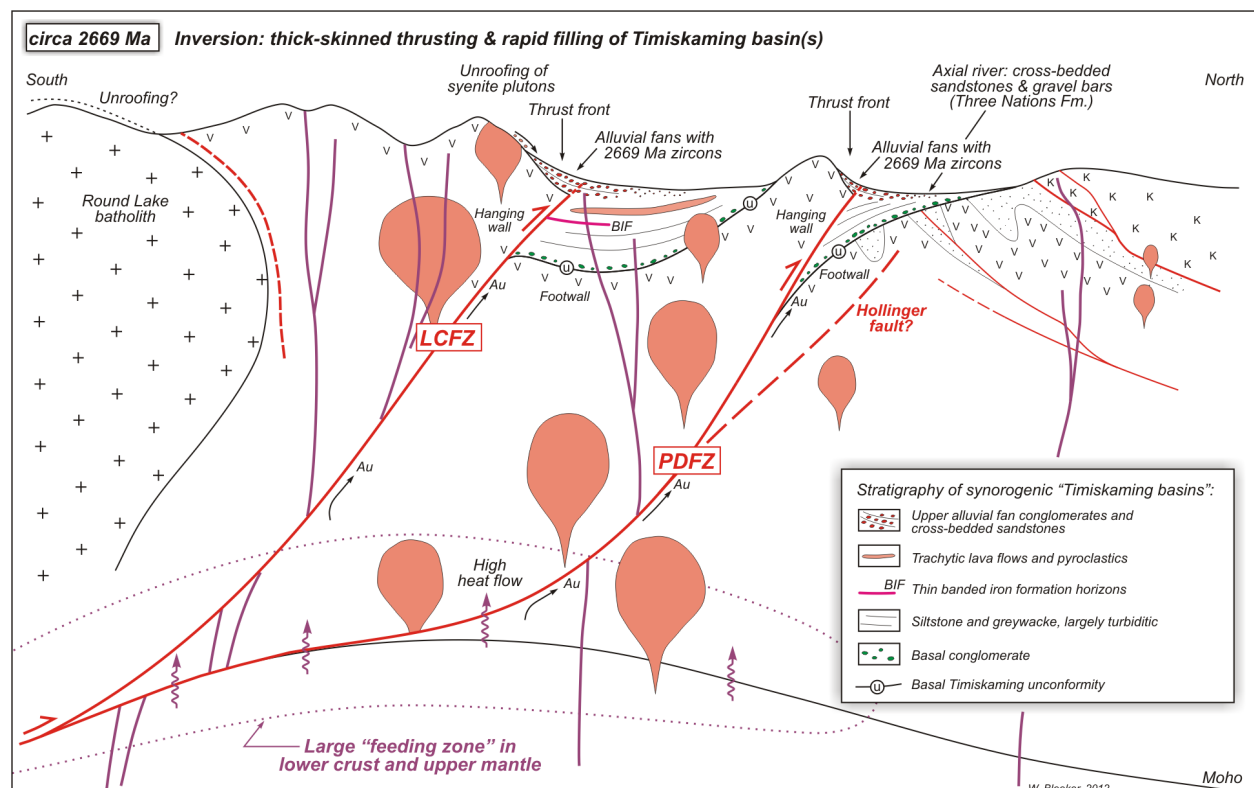


Figure 47.3. Transition from extension to renewed north-south shortening, with the major breaks being inverted as thick-skinned thrusts, overriding and burying remnants of the synorogenic clastic basins in their footwalls. Rising mountain fronts were flanking the basin remnants on their south side, shedding alluvial fans to the north. Conglomerates and cross-bedded fluvial sandstones filled the basin. This stage is timed by precise ages (2669 Ma) on detrital zircons that were captured in the uppermost clastic rocks. (See previous figures for additional symbols.)

THE MAJOR “BREAKS”: CRUSTAL-SCALE EXTENSIONAL FAULTS

In the AGB and in several other similar belts (Yellowknife, Agnew), there is little or no debate that the first-order “breaks” play a critical role in the spatial distribution of major gold deposits. These first-order faults are few in number, are spaced tens of kilometres apart and are likely crustal in scale. In Timmins, and also in Yellowknife (Bleeker et al. 2007), there is no evidence of these faults having been part of the early fold-thrust architecture; instead, they slice through and truncate these early structures. On the other hand, there is strong evidence, from numerous belts and cratons, including the AGB, that the breaks are spatially associated with the synorogenic clastic basins, or, more specifically, with the preserved and metamorphosed remnants of such basins. Thus, it is natural to link the breaks and the synorogenic clastic basins. As the latter indicate an extensional origin, it is thus logical to propose that these major crosscutting breaks were initiated as the first-order extensional faults (*see* Figure 47.2). They are major listric faults reaching deep into the crust if not the lithosphere. Associated lithospheric thinning led to the onset of alkaline magmatism and the major faults provided the pathways for some of these magmas to reach the surface. These deep-reaching listric faults, few in number, and with a large “feeding zone” in the lower crust or even the upper mantle lithosphere, also became the key structures to focus gold-bearing fluids to the upper crust, perhaps starting at the time they were initiated (e.g., in the AGB at *circa* 2680 Ma). Seismic imaging has been somewhat successful in imaging some of the major faults, supporting a listric to the south overall geometry for the Porcupine–Destor fault zone (Green et al. 1990).

RENEWED SHORTENING, FAULT INVERSION AND THICK-SKINNED THRUST BURIAL OF THE CLASTIC BASINS

Most of the Timiskaming-type synorogenic clastic basin remnants in the AGB have the following key attributes:

- The very fact that they are preserved, despite 5 to 15 km of post-Archean uplift, must mean that they were tectonically buried.
- They are metamorphosed, to approximately the same metamorphic grade as adjacent greenstones, again consistent with substantial tectonic burial.
- They are typically preserved as “asymmetric panels” with or without minor internal folding, and with or without internal imbrication, with a marked unconformity on one side while younging into and being bounded by one of the major faults on the other.
- And, in the south-central AGB, the majority of the panels occur on the north side of the major breaks and young to the south (Figures 47.3 and 47.4). (There are a few exceptions to this rule, each of them interesting, but they can be explained and do not negate the model described here.)

All these observations are most easily explained by late-stage thrust burial, to substantial depth, by some of the main extensional faults having undergone inversion and becoming thick-skinned thrust. As a consequence of thrust inversion, they overrode the “leading edges” of the extensional basin(s) and placed older greenstones on top of the synorogenic clastic rocks (*see* Figure 47.3). The present erosion surface merely preserves these leading edges of the basins as thin panels in the original footwalls of the thick-skinned thrusts. The fault-bounded asymmetric panels of synorogenic clastic rocks, thus, are the key diagnostic for recognizing *those* faults that were initiated as extensional faults and then became the principal thick-skinned thrust planes during renewed shortening. A “late extension only” scenario cannot explain the substantial burial and preservation of the clastic rocks, neither their asymmetry nor their metamorphic state. Whereas a “strike-slip only” scenario could explain deep largely clastic pull-apart basins, it again has trouble explaining all the additional observations. Continued strike-slip would slice apart basin remnants and distribute them on either side of a major faults, not preferentially on the northern

side and all younging south; and it would not necessarily bury them to be preserved. In Timmins, in the old Buffalo–Ankerite pits, kinematic indicators near the fault that placed volcanic rocks on top of the synorogenic clastic rocks indicate dip-slip, with volcanic rocks south of the fault having moved up relative to the clastic rocks north of the fault (*see* Photo 47.1 for photos of highly deformed conglomerates). At this and many other localities, the kinematic picture is complicated, however, by later north-south shortening that has rotated the original thrust to vertical, or locally even overturned (*see* Figure 47.4, inset).

STRATIGRAPHIC CONSEQUENCES OF INVERSION AND THICK-SKINNED THRUST BURIAL

The model described thus far makes a strong prediction: that following the switch from extension to renewed shortening, a rising mountain front similar to a Laramide-type range front (e.g., west side of the Wind River Mountains, or southeast side of the Bighorns, Wyoming) would rise up on one side of the clastic basins, shedding coarse debris into the basin and filling it up with alluvial fans and fluvial outwash (*see* Figure 47.3). Further thrust advance would finally fully bury (and preserve!) the leading edge of the

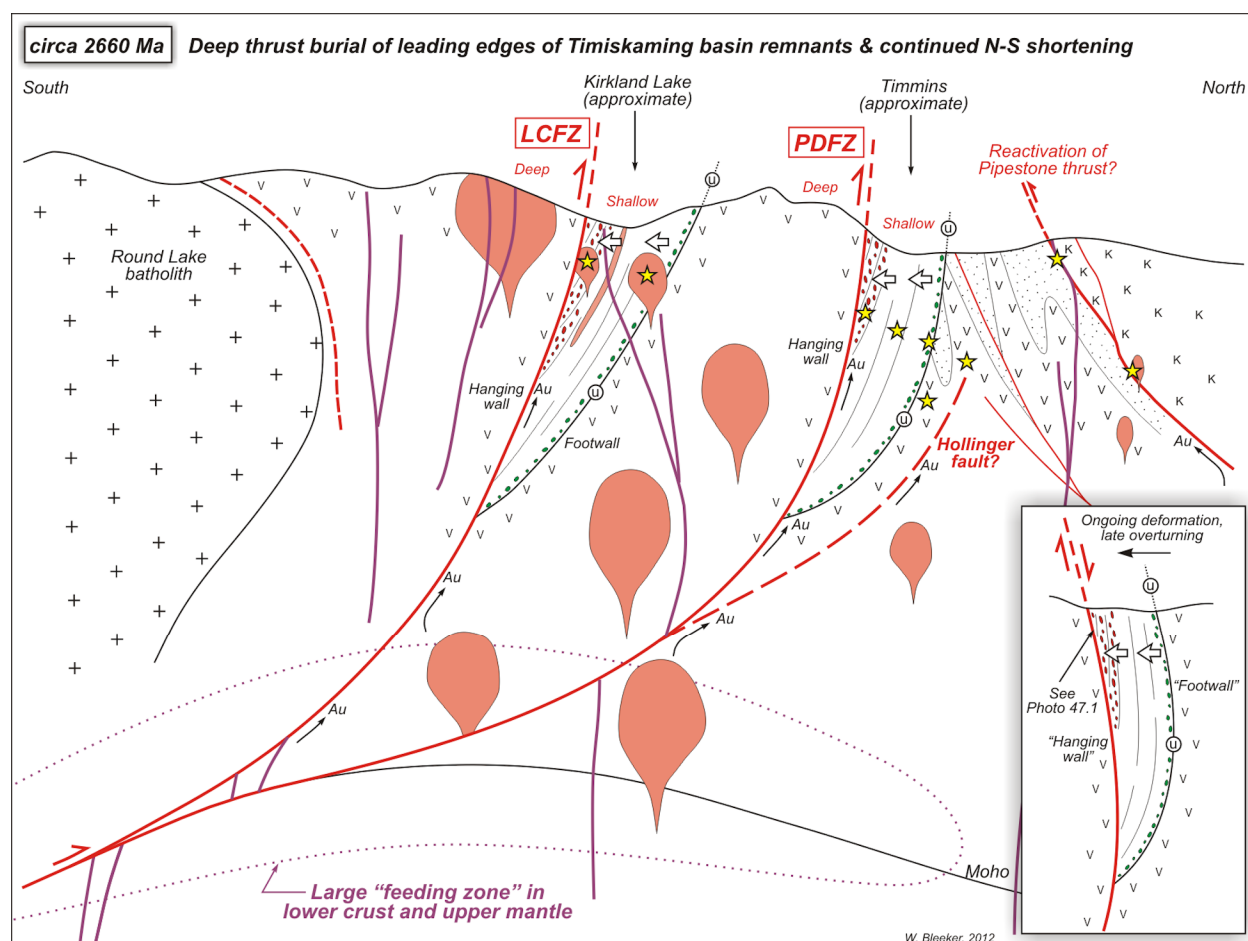


Figure 47.4. Deep burial and steepening of the basin remnants underneath the thick-skinned thrusts. Deeper exhumation of the southern structural hanging walls, as indicated by deeper stratigraphy and larger plutons being exposed south of the faults. Continued north-south shortening steepened all structures to near vertical, likely also reactivating other discontinuities (e.g., the earlier Pipestone thrust). Locally, the basin remnants and bounding structures were overturned, leading to confusing kinematics (*see* inset). Approximate positions of gold deposits are indicated by yellow stars. Note their asymmetry with respect to the main faults. The unfilled arrows indicate the overall younging direction in the fundamentally asymmetric panels of synorogenic clastic rocks. (*See* previous figures for additional symbols.)

basins (*see* Figure 47.4). Indeed, in the Timiskaming basin in Timmins, this is exactly what is observed: after rapid deepening in the lower half of the basin, it fills up and coarsens upward into cross-bedded sandstones (the Three Nations Formation) and finally conglomerates. Large-scale cross-bedding in the uppermost interlayered conglomerates and sandstones suggest alluvial fan-type deposition shedding off a southern highland comprising older and deeper greenstones and unroofing plutons. This particular aspect is superbly laid out in Kirkland Lake, with alluvial fan-type deposits dipping into the main fault to the south, and paleocurrent directions indicated by cross-bedding being up-dip and to the north, that is, away from the fault (as schematically shown in Figure 47.4). The youngest detrital zircons, concordant and precise, from the uppermost clastic rocks underneath the main thrust faults have an age of 2669 Ma (*see* Figure 47.3), indicating final burial at 2669 Ma or shortly thereafter. This is fully consistent with an extension-dominated interval lasting from *circa* 2680 to 2670 Ma, followed by thick-skinned thrusting starting at *circa* 2670 Ma.

FINAL SHORTENING AND DEGENERATION TO LARGE-SCALE STRIKE SLIP

As the main thrusts that buried the clastic basin remnants are now essentially vertical or even overturned (Figures 47.4 and 47.5), there must have been very significant shortening postdating the thick-skinned thrust burial. Local overturning complicates the overall structural picture significantly. For instance, a fault that shows thrust kinematic indicators prior to overturning becomes an apparent extensional fault after overturning (*see* Figure 47.4, inset). Hence, only by examining the full picture of these major fault systems, over long enough strike lengths, can one see through these local complications. Finally, the steepened, thick-skinned thrust faults (which earlier were initiated as the main extensional faults) became strike-slip faults. In Timmins, and in Kirkland Lake, early kinematic indicators *and* net fault offsets, amounting to tens of kilometres, are clearly sinistral (as highlighted in Figure 47.5), whereas later kinematic indicators indicate a late, more easily demonstrated, dextral overprint. Spectacular dextral (Z) asymmetric folds are formed during this last phase, but net offsets nevertheless remain sinistral.

WHAT CONCLUSIONS AND PREDICTIONS CAN BE DISTILLED FROM THIS MODEL?

One conclusion is that there is no special, direct, genetic relationship between the synorogenic clastic basins (remnants) and gold mineralization. The important relationship is that the buried and preserved leading edges of the clastic basins merely indicate the location of the master faults—those first-order, crustal-scale faults that were initiated and played a critical role during extension and were later inverted as thick-skinned thrusts. It is *these* faults, with their lower crustal feeding zones and possibly tapping into a disturbed upper mantle (*see* Figures 47.2 and 47.3), that are the key to prolific gold mineralization. The panels of synorogenic clastic rocks, thus, allow us to tell these faults apart from a more general population of faults. In a few places, however, such as at the Pamour Mine, graphitic siltstones and wackes of the synorogenic clastic basin may have added special redox conditions that may have played a role locally in gold deposition.

The recurring relationship between major faults and alkaline igneous rocks is likely significant as noted by previous workers (e.g., Wyman and Kerrich 1988, 1989), and it may be that it is the alkaline magmatism that is the ultimate driver behind the overall gold endowment (e.g., Beakhouse 2007). This magmatism suggests that extension involved the mantle and that the faults are deep reaching. Extension, lithospheric thinning and/or delamination, and mantle-generated magmatism would also increase the overall heat flow into the crust and steepen geothermal gradients, factors that likely promoted hydrothermal processes. So it is the superposition of extension, major faults with large feeding zones, and alkaline magmatism that appear essential ingredients in generating an AGB-type gold corridor. Remnants of the synorogenic clastic basins are a key diagnostic of these types of environments and, where preserved, they identify the critical faults.

WHEN DID GOLD MINERALIZATION PEAK?

Given the overall evolution of these systems, with the numerous discrete structural (i.e., kinematic) phases, it is still not entirely clear which phase was the most productive in terms of multi-million ounce gold deposition. The diversity of gold mineralization documented in many of these camps likely tells us that there is some gold mineralization at more than one part of this history. But when was the peak? In the specific context of Timmins, when did the giant Hollinger deposit form? During full-blown extension (e.g., *circa* 2675 Ma), everything else being local remobilization; or during the tail end of extension and the transition to thick-skinned thrusting and tectonic burial of the footwall (*circa* 2670–2665 Ma)? Or even later, during the transition to strike-slip, when jogs in the fault traces would have had special significance (*circa* 2660–2650 Ma and younger). If so, was it during the sinistral phase, when the bend in Timmins would have been dominantly dilational, or was it the latest dextral phase when this same jog would have seen contraction? We only have preliminary answers to these questions. In the main

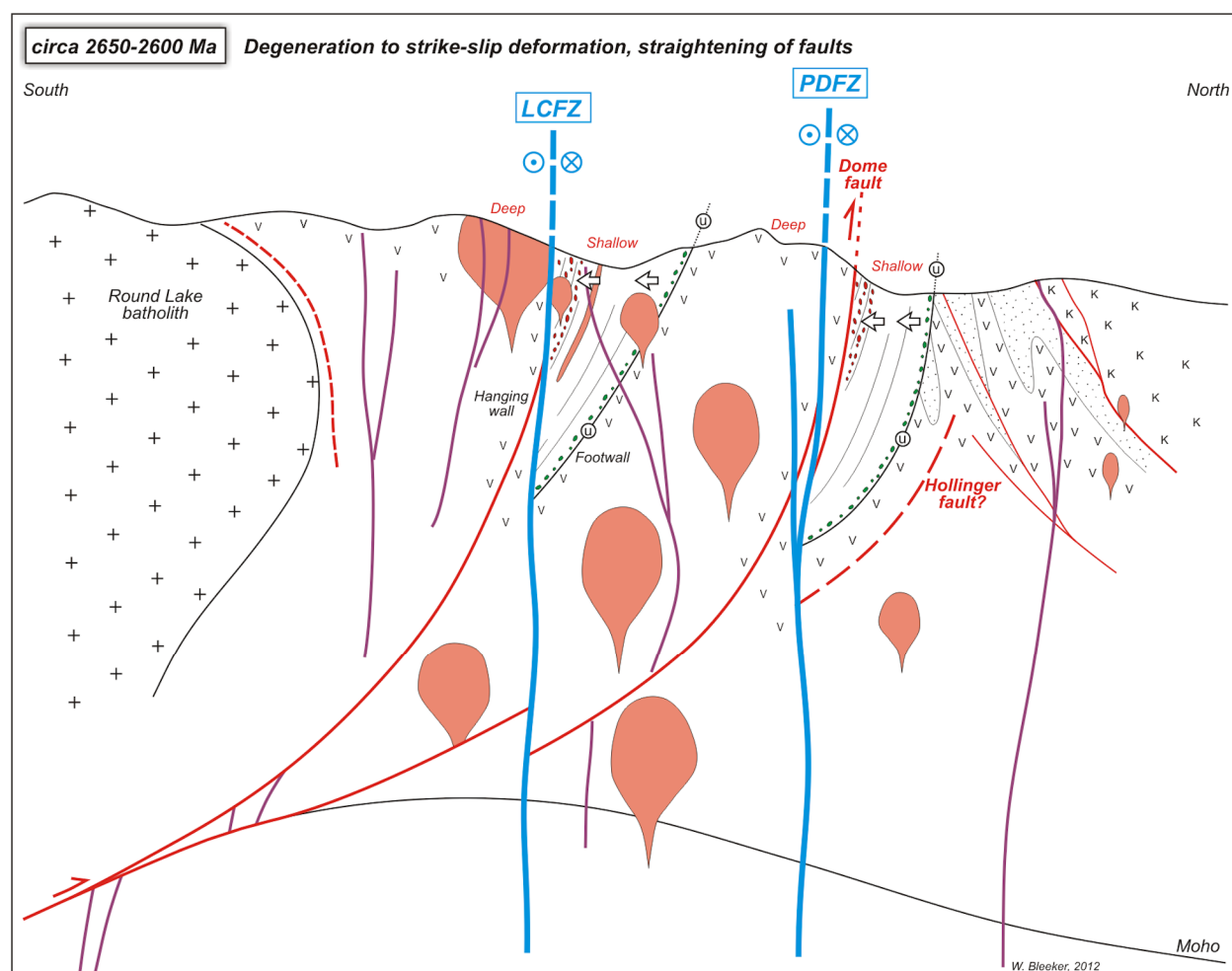


Figure 47.5. Degeneration of the fault systems to strike-slip fault zones. Major strike-slip fault planes (in blue), now typically mapped as the “breaks”, broke through to minimize local asperities. Locally, they may follow and overprint the earlier steepened thrust structures, but, elsewhere, they deviate from and isolate the main thrust faults in separate slices, such as the Dome fault in the Dome Mine. Hence, in some cases, the fault trace referred to as “the break” is actually not the most important fault of the system. Staying with the example of the Dome Mine near Timmins (illustrated above), it is the Dome fault (red) that is the key structure and it is mineralized. In contrast, the Porcupine–Destor fault zone (PDFZ, in blue) broke through later, farther to the south, and is a dominantly strike-slip barren fault zone. Both in Timmins and Kirkland Lake, there is evidence for early sinistral strike-slip, followed by a latest phase of dextral deformation. Net offsets, determined by matching up pairs of most likely piercing points on either side of the faults, indicate large sinistral net displacements (e.g., 10 to 50 km). (See previous figures for symbols.)

Hollinger–McIntyre system, gold mineralization overprints *circa* 2673 Ma lamprophyre (“albitite”) dikes (Burrows and Spooner 1986; Marmont and Corfu 1989; Corfu et al. 1989), but this age is imprecise enough to allow a syn-extensional onset of gold mineralization. Other ages suggest a timing of gold deposition probably coincident with the later thrust inversion interval. For instance, several Re/Os ages on molybdenite are in the 2670 to 2660 Ma range (*see* brief discussion in Ayer et al. 2003, and references therein). Still younger, monazite ages (U/Pb, SHRIMP (sensitive high-resolution ion microprobe)) from gold-bearing quartz veins in the Dome deposit, suggest gold deposition may have been as young as *circa* 2640 Ma (data by B. Salier, *see* discussion in Ayer et al. 2003), apparently ruling out formation of these veins during the active extension phase. At the Pamour Mine, stacked flat veins in the Pamour conglomerate and in overlying Timiskaming greywackes indicate emplacement during strong horizontal shortening, which must have followed the thick-skinned thrust burial of the Timiskaming basin remnant. So, even though extension may have set up the overall system, and led to alkaline magmatism and syenite stock emplacement, peak gold mineralization likely occurred during or following the thick-skinned thrusting.

These questions of timing remain critical because accurate timing helps determine at what kinematic phase the fluid systems were most productive. This, in turn, determines what secondary structures to target along the overall fault corridors. In any case, even with incomplete answers, it seems clear that the earliest fold and thrust structures, more high-level and thin-skinned in nature, did not play a major role. Not only are they structurally less favourable, they predated the critical phase of extension and associated magmatism.

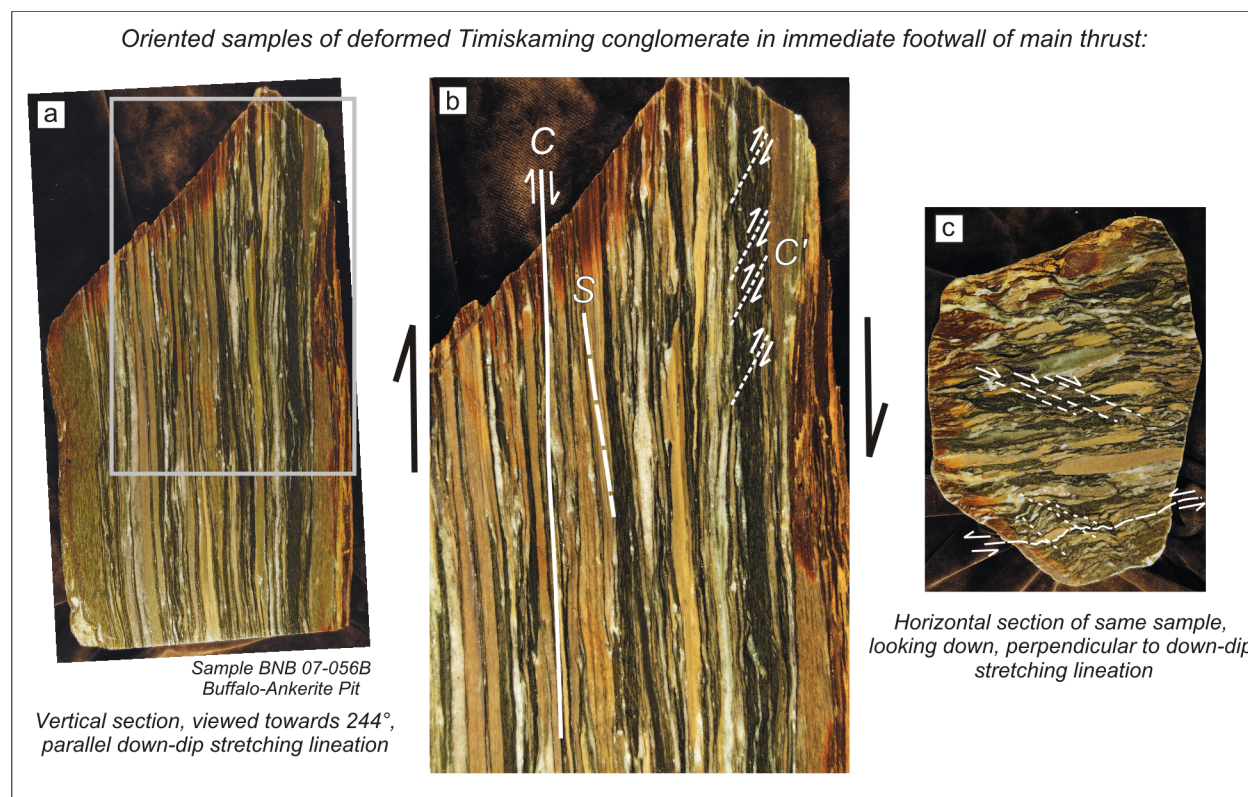


Photo 47.1. An example of highly deformed polymict conglomerate, Buffalo–Ankerite pit, immediately “below” (i.e., to the north of) the major fault that buried them, in this case the Porcupine–Destor fault zone (or strictly speaking, the Dome fault). Photo a) shows a vertical view, looking towards 244° along the trace of the fault, perpendicular to foliation and parallel to the down-dip stretching lineation. The slab is 16 cm wide. An enlargement is shown in b), with foliation (S) and shear (C and C’) planes highlighted. These composite fabrics and map-scale relationships indicate that older volcanic rocks south of the fault moved up and over the conglomerates, even though the structures are now vertical if not slightly overturned. Original pebbles are barely recognizable, but a cut looking down, as in photo c), perpendicular to the stretching lineation, clearly reveals the origin of this rock as a polymict conglomerate. This view also shows younger crenulation cleavages consistent with late strike-slip overprints. Detrital zircons from this sample contain a young population of zircons of age *circa* 2575 Ma.

Another strong observation is that gold deposits in both Timmins and Kirkland Lake are strongly asymmetric with respect to the major fault traces. For instance, the large Dome deposit occurs essentially all on one side of the major fault. The general conclusion must be that major gold deposition terminated well before large-scale movements on the faults (thick-skinned thrusting, and later strike slip) ceased, otherwise the vein systems and gold mineralization would straddle broadly across the faults, occurring in both footwall and hanging wall. The corollary of this is that, if it was final strike-slip that truncated the major deposits, the “other halves” may still be located along strike on the opposite side of the major breaks.

FUTURE WORK

With a reasonably self-consistent model of the structural and kinematic evolution of camps such as Timmins and Kirkland Lake, and key temporal constraints for when extension was initiated and when it was terminated, it will now be possible to date major gold deposition relative to this kinematic framework (e.g., *see* Figures 47.1 to 47.5; brief discussion above) and, thus, determine which kinematic phase was the most productive. This will require better and more detailed uranium-lead dating of accessory phases in veins from some of the major deposits.

A more detailed geometrical evaluation of vein systems, allowing certain kinematic frameworks but ruling out others, is also needed. Much of the required data already exists, but is scattered through the literature and has not been systematically synthesized across the AGB or even the Timmins to Kirkland Lake area.

On a larger scale, a “compare and contrast exercise” of these kind of gold camps in Canada and across cratons worldwide may help establish whether alkaline magmatism is indeed correlated with overall gold endowment, and whether a sharp extensional phase is critical in creating deep-reaching listric faults.

CONCLUSIONS

The multiphase structural evolution of the Timmins and Kirkland Lake gold camps can be captured in a number of conceptual cartoons that rationalize all major phases and fully explain the setting and preservation of the synorogenic clastic panels. From the overall model, it is concluded that the major breaks were initiated as first-order extensional faults (Bleeker, van Breemen and Berger 2008) reaching deep into the crust, if not the uppermost mantle. Lithospheric thinning, basin formation and alkaline magmatism accompanied the extensional phase and may have been critical to overall gold endowment, even though peak gold deposition may have occurred somewhat later during renewed shortening. Following extension, the main breaks were inverted as thick-skinned thrusts that tectonically buried the leading edges of the synorogenic clastic basins. Further shortening rotated the faults to near vertical, with local overturning. Finally, the faults were overprinted by major strike-slip movement and mapped breaks may locally deviate from the critical fault planes that controlled the extension and thrust inversion history. It appears that gold mineralization started during extension, but likely peaked during and following thick-skinned thrust inversion. Deposits along the faults were sliced apart by continued fault movement, with the “missing halves” either advected out of the section and lost to erosion or, more interestingly from an exploration point of view, occurring somewhere along strike along the major strike-slip faults.

ACKNOWLEDGMENTS

This research is part of the Targeted Geoscience Initiative 4 (TGI-4) program of the Geological Survey of Canada, carried out in co-operation with the Ontario Geological Survey (OGS). Ben Berger, Brian Atkinson and Gary Beakhouse of the OGS are thanked for sharing their knowledge of the Abitibi greenstone belt. Discussions with GSC colleagues, especially Benoît Dubé and Otto van Breemen, are acknowledged. Gary Beakhouse provided useful comments on a draft of this discussion, and Monica Gaiswinkler Easton was helpful in the editorial handling. The diagrams and underlying observations formed the basis for a well-attended field trip in September 2012.

REFERENCES

- Ayer, J.A., Barr, E., Bleeker, W., Creaser, R.A., Hall, G., Ketchum, J.W.F., Powers, D., Salier, B., Still, A. and Trowell, N.F. 2003. Discover Abitibi. New geochronological results from the Timmins area: implications for the timing of late-tectonic stratigraphy, magmatism and gold mineralization; *in* Summary of Field Work and Other Activities 2003, Ontario Geological Survey, Open File Report 6120, p.33-1 to 33-11.
- Barrie, C.T. 1990. U–Pb garnet and titanite age for the Bristol Township lamprophyre suite, western Abitibi Subprovince, Canada; *Canadian Journal of Earth Sciences*, v.27, p.1451-1456.
- Beakhouse, G.P. 2007. Structurally controlled, magmatic hydrothermal model for Archean lode gold deposits: a working hypothesis; Ontario Geological Survey, Open File Report 6193, 133p.
- Bleeker, W. 1999. Structure, stratigraphy, and primary setting of the Kidd Creek volcanogenic massive sulphide deposit: a semiquantitative reconstruction; *in* The Giant Kidd Creek volcanogenic massive sulfide deposit, western Abitibi Subprovince, Canada, *Economic Geology Monographs* 10, p.71-121.
- Bleeker, W., LeCheminant, A.N., Davis, W.J., Buchan, K., Ketchum, J.W., Sircombe, K., Snyder, D., van Breemen, O. and Ootes, L. 2007. Transect across the southwestern Slave Craton: from Phanerozoic platform edge to the core of the Yellowknife supracrustal domain; Geological Association of Canada, Yellowknife 2007 meeting, Field Trip A1 Guidebook, 232p.
- Bleeker, W. and Parrish, R.R. 1996. Stratigraphy and U–Pb zircon geochronology of Kidd Creek: implications for the formation of giant volcanogenic massive sulphide deposits and the tectonic history of the Abitibi greenstone belt; *Canadian Journal of Earth Sciences*, v.33, p.1213-1231.
- Bleeker, W. and van Breemen, O. 2011. New geochronological, stratigraphic, and structural observations on the Kidd–Munro assemblage and the terrane architecture of the south-central Abitibi greenstone belt, Superior Craton, Canada; Chapter 2 (35p.), *in* Results from the Targeted Geoscience Initiative III, Kidd–Munro Project, Ontario Geological Survey, Open File Report 6258, 142p.
- Bleeker, W., van Breemen, O. and Berger, B. 2008. The Pipestone Thrust and the fundamental terrane architecture of the south-central Abitibi greenstone belt, Superior craton, Canada; Geological Association of Canada–Mineralogical Association of Canada, joint annual meeting, Quebec City 2008, Abstracts, v.33, p.24.
- Blewett, R.S. and Czarnota, K. 2007. Diversity of structurally controlled gold through time and space of the central Goldfields Superterrane: A field guide; Geological Survey of Western Australia, Record 2007/19, 65p.
- Blewett, R.S., Czarnota, K. and Henson, P.A. 2010. Structural-event framework for the eastern Yilgarn Craton, Western Australia, and its implications for orogenic gold; *Precambrian Research*, v.183, p.203-229.
- Burrows, D.R. and Spooner, T.C. 1986. The McIntyre Cu–Au deposit, Timmins, Ontario, Canada; *in* Proceedings of Gold '86, an international symposium on the geology of gold, Konsult International, Toronto, Ontario, p.23-39.

- Corfu, F., Krogh, T.E., Kwok, Y.Y. and Jensen, L.S. 1989. U–Pb zircon geochronology in the southwestern Abitibi greenstone belt, Superior Province; *Canadian Journal of Earth Sciences*, v.26, p.1747-1763.
- Czarnota, K., Champion, D.C., Goscombe, B., Blewett, R.S., Cassidy, K.F., Henson, P.A. and Groenewald, P.B. 2010. Geodynamics of the eastern Yilgarn Craton; *Precambrian Research*, v.183, p.175-202.
- Davies, J.F. 1977. Structural interpretation of the Timmins mining area, Ontario; *Canadian Journal of Earth Sciences*, v.14, p.1046-1053.
- Ferguson, S.A. 1966. Tisdale Township, Cochrane District; Ontario Department of Mines, Map 2075, scale 1:12 000.
- Ferguson, S.A., Buffam, B.S.W., Carter, O.F., Griffis, A.T., Holmes, T.C., Hurst, M.E., Jones, W.A., Lane, H.C. and Longley, C.S. 1968. Geology and ore deposits of Tisdale Township; Ontario Department of Mines, Report 58, 177p.
- Green, A.G., Milkereit, B., Mayrand, L.J., Ludden, J.N., Hubert, C., Jackson, S.L., Sutcliffe, R.H., West, G.F., Verpaalst, P. and Simard, A. 1990. Deep structure of an Archean greenstone terrane; *Nature*, v.344, p.327-330.
- Groves, D.I., Goldfarb, R.J., Gebre-Mariam, M., Hageman, S.G. and Robert, F. 1998. Orogenic gold deposits: a proposed classification in the context of their crustal distribution and relationship to other gold deposit types; *Ore Geology Reviews*, v.13, p.7-27.
- Hurst, M.E. 1939. Porcupine area, District of Cochrane, Ontario; Ontario Department of Mines, Annual Report Map 47a, scale 1: 24 000.
- Marmont, S. and Corfu, F. 1989. Timing of gold introduction in the late Archean tectonic framework of the Canadian Shield: Evidence from U-Pb zircon geochronology of the Abitibi Subprovince; *in* The geology of gold deposits: the perspective in 1988, *Economic Geology Monograph* 6, p.101-111.
- Wyman, D. and Kerrich, R. 1988. Alkaline magmatism, major structures, and gold deposits: implications for greenstone belt gold metallogeny; *Economic Geology*, v.83, p.454-461.
- 1989. Archean lamprophyre dikes of the Superior Province, Canada: distribution, petrology, and geochemical characteristics; *Journal of Geophysical Research*, v.94, p.B4667-B4696.

48. Targeted Geoscience Initiative 4. Lode Gold Deposits in Ancient Deformed and Metamorphosed Terranes: Geological Setting of Banded Iron Formation–Hosted Gold Mineralization in the Geraldton Area, Northern Ontario

B. Lafrance¹, Z. Tóth¹, B. Dubé² and P. Mercier-Langevin²

¹Mineral Exploration Research Centre, Laurentian University, Sudbury, Ontario P3E 2C6

²Geological Survey of Canada, Québec, Québec G1K 9A9

INTRODUCTION

The characterization of banded iron formation (BIF)-hosted gold ore systems is one of the main themes of the Targeted Geoscience Initiative 4 (TGI-4) Lode Gold project of the Geological Survey of Canada (Dubé et al. 2011). The main goals of the project are to 1) improve knowledge of the geological settings and footprints of selected gold deposits or districts in mature and emerging camps; 2) provide key descriptive and genetic parameters and improved geological and exploration models; 3) develop more robust exploration vectors and means to help identify fertile mineral systems; and 4) train and mentor students in order to increase the number of highly qualified personnel. The Geraldton area was selected as 1 of 4 areas to study BIF-hosted ore systems because of excellent descriptions of its deposits by Pye (1952), Horwood and Pye (1955) and Macdonald (1988), easy accessibility to large stripped outcrops exposing the ore-hosting structures and iron formation, and availability of new exploration data and drill cores across the main deposits and ore zones in the area. This project is carried out in collaboration with the Ontario Geological Survey and Premier Gold Mines Limited.

The project began this past summer with detailed mapping of 2 large stripped outcrops and sampling of drill cores along 2 sections across the 2 main ore zones (F zone and North zone) of the Hardrock–MacLeod–Cockshutt deposit. The preliminary results of the mapping are presented in this report.

BACKGROUND

The Geraldton area is located east of Lake Nipigon in the eastern part of the Beardmore–Geraldton belt along the southern margin of the Wabigoon Subprovince of the Archean Superior Province (Figure 48.1). The Beardmore–Geraldton belt comprises 3 metasedimentary rock panels (southern, central and northern sedimentary units) that are fault bounded and interleaved with 3 volcanic rock panels (southern, central and northern volcanic units). The southern volcanic unit has mid-ocean ridge basalt geochemical affinity and it represents ocean floor crust that formed south of an oceanic island arc (central volcanic unit) and back-arc basin (northern volcanic unit) (Tomlinson et al. 1996). A felsic flow and a synvolcanic dike in the central and northern volcanic units, respectively, have U/Pb zircon crystallization ages of 2724.9 ± 1.2 Ma (Hart, ter Meer and Jollette 2002). Thus, at 2725 Ma, these 2 volcanic units stood as an island-arc and back-arc system outboard and south of the Wabigoon Subprovince. The 3 volcanic units collided and were accreted to the southern margin of the Wabigoon Subprovince prior to the deposition of the sedimentary units at *circa* 2696 Ma to *circa* 2691 Ma (Lafrance, DeWolfe and Stott 2004). From

Summary of Field Work and Other Activities 2012,
Ontario Geological Survey, Open File Report 6280, p.48-1 to 48-10.

© Queen's Printer for Ontario, 2012

north to south, the sedimentary units record progressively deeper depositional environments. They were emplaced unconformably above the volcanic units as fluvial to alluvial fan deposits (northern sedimentary unit), deltaic to subaqueous fan deposits (central sedimentary unit), and deeper water turbidite deposits (southern sedimentary unit) (Devaney and Williams 1989). They represent a southward-prograding clastic wedge that was fed by the erosion of the uplifted Wabigoon Subprovince (Devaney and Williams 1989).

Thrust imbrications of the volcanic and sedimentary units began shortly after deposition of the sedimentary units during an early D_1 deformation event (Devaney and Williams 1989; Lafrance, DeWolfe and Stott 2004). Rare isoclinal F_1 folds are the only manifestation of the D_1 event as structural contacts and possible thrust faults between volcanic and sedimentary units were later reactivated as transcurrent shear zones. During D_2 north-south compression, the southern sedimentary unit was regionally folded into tight to isoclinal, east-striking, F_2 folds with an axial planar S_2 cleavage (Lafrance, DeWolfe and Stott 2004). The S_2 cleavage is oriented at high angle to bedding in F_2 fold hinges and is generally parallel to bedding along the limbs of the folds. The S_2 foliation is expressed by the flattening of clasts and pillows in the volcanic units and by a bedding-parallel cleavage in the central and northern sedimentary units. Late, regional, D_3 dextral transposition produced most penetrative structures in the belt. During the D_3 event, F_2 and S_2 were folded by outcrop- to map-scale, west-plunging, Z-shaped F_3 folds. The D_2 structures were overprinted by a regional S_3 cleavage oriented anticlockwise to bedding, and they were transected by east-trending, dextral, transcurrent D_3 shear zones (Lafrance, DeWolfe and Stott 2004). The

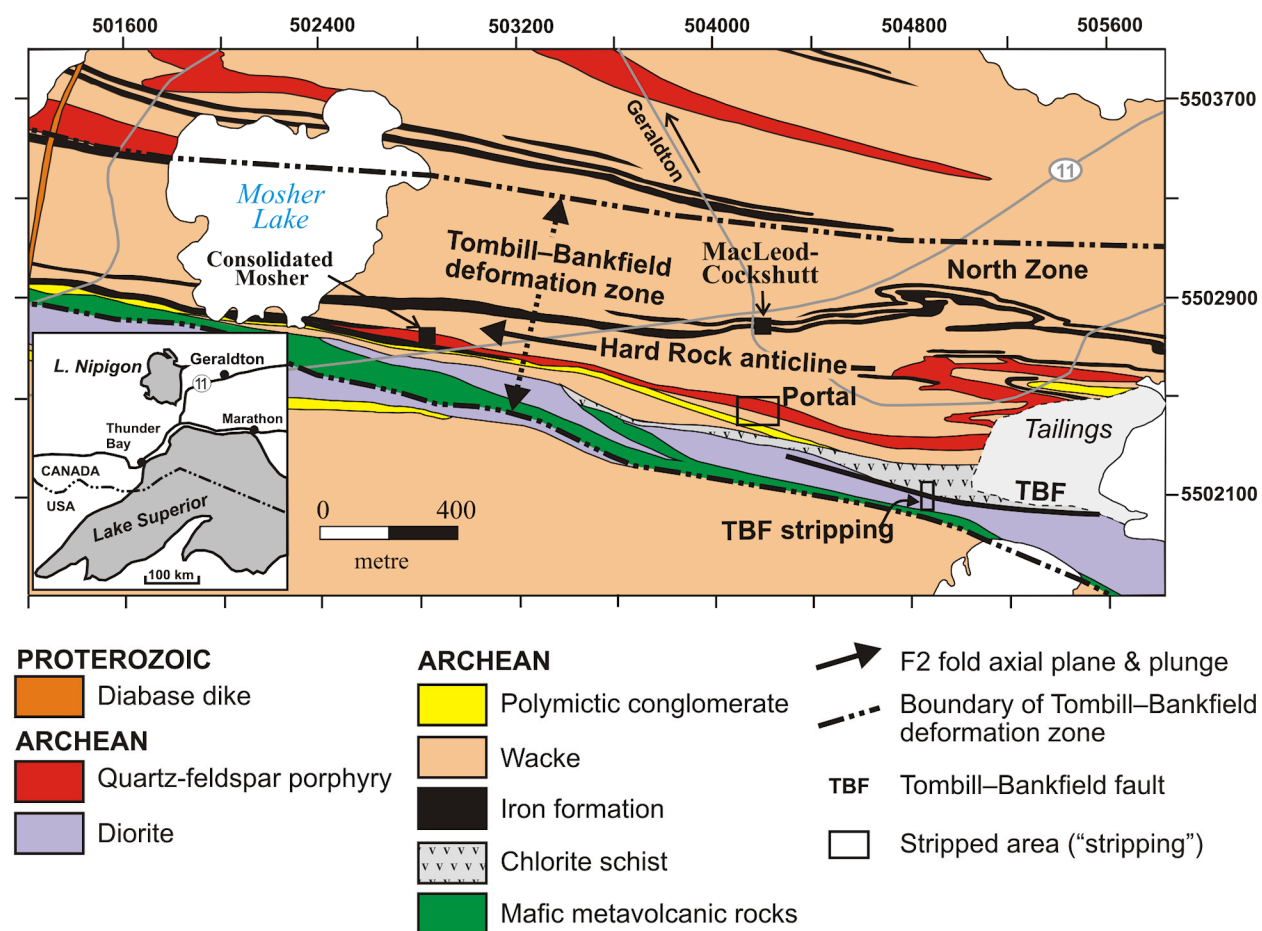


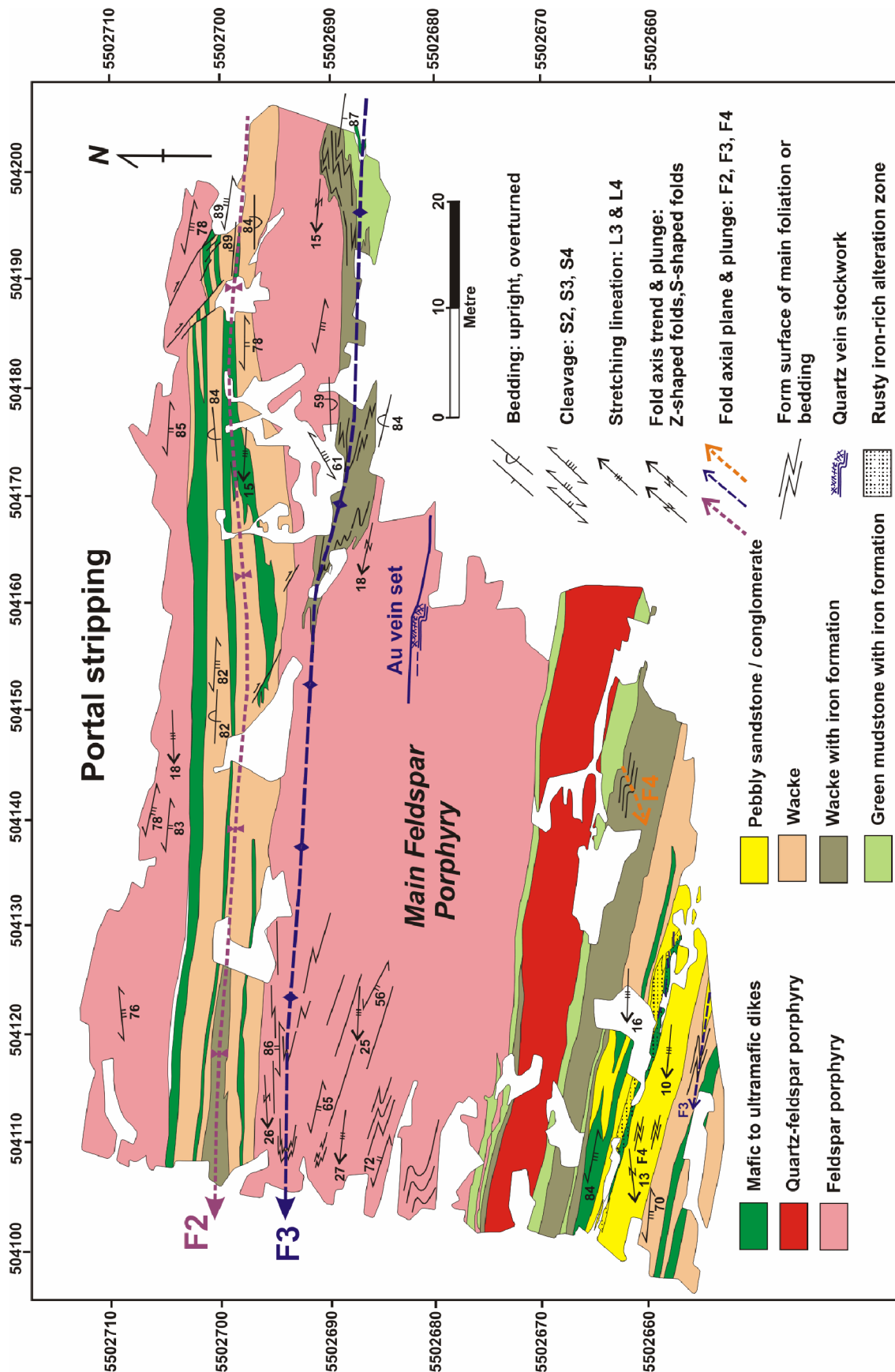
Figure 48.1. Simplified geological map of the Geraldton area (after Horwood and Pye (1955) and Pye (1952) with modifications by authors). "Portal" indicates area named Portal stripping. UTM co-ordinates are based on North American Datum 1927 (NAD27), Zone 16. Inset map shows the location of Geraldton.

F₃ folds and S₃ cleavage are, in turn, overprinted by Z-shaped F₃' folds and associated S₃' cleavage, which formed during the same progressive D₃ deformation event (Lafrance, DeWolfe and Stott 2004). Felsic porphyry dikes and sills with a U/Pb crystallization age of 2691 ⁺³/₋₂ Ma (Anglin 1987; Anglin et al. 1987) are folded by F₂ and overprinted by S₃, providing a maximum deformation age of *circa* 2691 Ma for both the D₂ and D₃ events.

All past-producing gold mines in the Geraldton area (e.g., Little Long Lac, Hardrock, MacLeod–Cockshutt, Consolidated Mosher, Magnet, Bankfield) are in the southern sedimentary unit. Most ore zones are hosted in a 1 km wide high-strain zone, called the Tombill–Bankfield deformation zone (*see* Figure 48.1), located close to the contact between the southern sedimentary unit and the Quetico Subprovince sedimentary rocks to the south (Lafrance, DeWolfe and Stott 2004). A discrete brecciated fault zone known as the Tombill–Bankfield fault, occurs within the wider, more ductile, deformation zone. The deposits hosted by the deformation zone collectively produced 2.36 million ounces of gold (Mason and White 1986). Gold occurs in sulphide-rich replacement lenses and quartz-carbonate veins in the hinge of F₂ and F₃ folded iron formation (e.g., North zone). It also occurs in quartz veins and associated sericitic selvages in folded porphyry bodies and in wacke near or at the contact with porphyry (e.g., F zone) (Horwood and Pye 1955). It is further found in quartz stringer zones within wacke and diorite (Horwood and Pye 1955). Gold mineralization is interpreted to be syn-D₃ and to have been emplaced in faults, shear zones and fractures that formed along sheared contacts and across the hinge of F₂ and F₃ folds (Anglin 1987; Macdonald 1988; Lafrance, DeWolfe and Stott 2004). A stripped outcrop exposing the Tombill–Bankfield fault, and a second larger stripped outcrop, informally named the Portal stripping, showing excellent overprinting relationships between structures and mineralization along the Tombill–Bankfield deformation zone, provide new key information and were mapped in detail. They are described below.

PORTAL STRIPPING

The Portal stripping is a 60 by 90 m stripped outcrop located along the south limb of the Hard Rock anticline, 300 m south of the MacLeod–Cockshutt headframe (*see* Figure 48.1). A feldspar porphyry body takes up more than half of the outcrop (Figure 48.2). It is pinkish white on outcrop surface, pinkish grey on fresh surface, and it consists of 40 volume % feldspar phenocryst (1 to 4 mm in size) and 10 volume % quartz phenocryst (1 to 1.5 mm in size) within a fine-grained homogeneous matrix. It contains rare xenoliths of iron formation and altered mafic rock, and it is in intrusive contact with surrounding wacke, iron formation and green mudstone. The wacke is greenish grey on outcrop and fresh surfaces, and it consists of sandstone beds (≤15 cm thick) interlayered with mudstone beds (<1 to 3 cm thick). Excellent, normal grading, top indicators are observed in the sandstone beds. Iron formation consists of up to 20 cm thick, finely laminated, black cherty magnetite beds, interspersed within thickly bedded (≤25 cm) wacke similar to that described above. Iron formation beds, millimetres to 2.5 cm thick, are further associated with laminated to thinly bedded (0.5 to 2.5 cm) mudstone, varying in colour from dark greenish grey on fresh and outcrop surfaces to dark green on outcrop surface. A polymictic pebbly sandstone or conglomerate occupies the southern part of the outcrop. It is brownish light grey to dark grey on outcrop and fresh surfaces, respectively, and it contains strongly deformed, elongate clasts of mafic to intermediate volcanic rocks and sandstone, as well as more spherical clasts of granitic composition. The percentage of clasts is difficult to estimate due to the strong deformation and gradational contacts between clasts and the sandy matrix. Another porphyry, which contains more quartz (10 to 15 volume %) and less feldspar (30 volume %) phenocrysts than the main feldspar porphyry, was emplaced into the green mudstone and wacke with iron formation beds. Numerous, greenish grey to dark brown, gabbroic to ultramafic dikes are roughly parallel to bedding in all rock types. The dikes vary in thickness from a few centimetres up to 2 m. They are strongly chloritic, commonly iron carbonatized and they contain elongate white streaks of carbonatized feldspar(?).



The Portal stripping displays excellent structural overprinting relationships: ductile structures observed on outcrop can be ascribed to 3 generations of structures. The oldest generation of structures is represented by an isoclinal synform that occupies the entire width of the wacke panel north of the main feldspar porphyry body (*see* Figure 48.2). The synform is defined by folded bedding-parallel mafic dikes and by folded sandstone beds that young away from the core of the fold (Photo 48.1A). The synform youngs downward; thus, it has the younging characteristic of a downward-facing synform or synformal anticline. It has a subvertical, west-striking, penetrative axial plane cleavage, and a shallowly (15 to 20°), west-plunging, fold axis. The latter is parallel to a strong mineral stretching lineation defined by stretched amygdules and discontinuous dark green chlorite and white carbonatized feldspar in mafic dikes. The cleavage is parallel to the contact between the wacke and the main feldspar porphyry, where it is expressed as a strong sericitic foliation that is penetrative throughout the porphyry. Because early F_1 folds in Geraldton typically lack an axial plane cleavage and because S_2 is the oldest cleavage observed in folded porphyry in the hinge of the F_2 Hard Rock anticline (Lafrance, DeWolfe and Stott 2004), the downward-facing synform and its axial plane cleavage are interpreted as F_2 and S_2 structures that formed during D_2 north-south shortening across the belt. The synform is overprinted by a cleavage (S_3) oriented clockwise to bedding on both limbs of the fold (*see* Figure 48.2). The S_3 cleavage is a differentiated cleavage defined by chloritic and sericitic foliation planes alternating with 1 to 2 mm wide white felsic microlithons. It is axial planar to S-shaped F_3 folds in the wacke north of the main porphyry (Photo 48.1B and 48.1C). In the porphyry, where the penetrative sericitic S_2 cleavage is folded by F_3 folds, the S_3 cleavage forms a composite S_2 – S_3 fabric expressed by the intensification and decreased spacing of the S_2 cleavage planes along the long limbs of asymmetrical F_3 folds (Photo 48.1D). From north to south across the main porphyry body, the asymmetry of the F_3 folds changes from S-shaped to M-shaped to Z-shaped and, thus, the porphyry is folded by a large F_3 fold that has a thin north limb and a thick south limb (*see* Figure 48.2). The attitude of F_3 folds is similar to that of F_2 folds. Their axial plane is steep and west striking, and they plunge shallowly to the west (~20°) parallel to a strong stretching lineation represented by rods of presumably recrystallized quartz and feldspar aggregates in the porphyry.

A small, parasitic, F_3 fold on the north limb of the folded porphyry is overprinted by a cleavage (S_4), striking 240 to 250° and dipping 80° to the north. The S_4 cleavage is oriented anticlockwise to bedding and is axial planar to local asymmetrical Z-shaped F_4 folds overprinting the S_3 cleavage. The folds are, in turn, overprinted by steeply dipping dextral shear bands striking approximately 115° to 125°. The orientation of the shear bands is similar to that of dextral shear fractures shown in Figure 48.2. Shear bands are observed across the main porphyry and wacke, but they become more abundant south of the main porphyry where they form a penetrative dextral slip cleavage (Photo 48.1E). A bedding- and contact-parallel, composite S_2 – S_3 foliation is present in all rock types south of the main porphyry. A shallowly west-plunging stretching lineation, which is defined by rod-like elongate pebbles in conglomerate, lies along the composite foliation plane. The intersection lineation between the dextral shear bands and composite S_2 – S_3 foliation is roughly perpendicular to the shallowly plunging stretching lineation, which is consistent with the formation of these structures during dextral transcurrent shear. On horizontal surface, strong granitic pebbles are surrounded by dextral asymmetrical strain shadows. The clasts locally contain northwest-southeast oriented, steeply dipping, extensional quartz veinlets and weak elongate volcanic clasts are folded by Z-shaped F_4 folds, further suggesting dextral transcurrent shear (Photo 48.1F). Although these structures occur throughout the Portal stripping, they are more abundant or pronounced in the southern part of the stripping where dextral transcurrent shear was more intense. The F_4 folds and S_4 cleavage correspond to the F_3' folds and S_3' cleavage of Lafrance, DeWolfe and Stott (2004), which are interpreted as late structures that formed during a progressive D_3 dextral transpressional event that began with the formation of F_3 folds, a regional S_3 cleavage, and dextral transcurrent shear zones.

A set of milky fault-fill white quartz veins with minor ankerite yielded high gold values (Premier Gold Mines Ltd. staff, personal communication, 2012). The veins were emplaced in the main porphyry body on the south limb of the large F_3 fold (*see* Figure 48.2). The veins strike east (100°), dip south (60°)

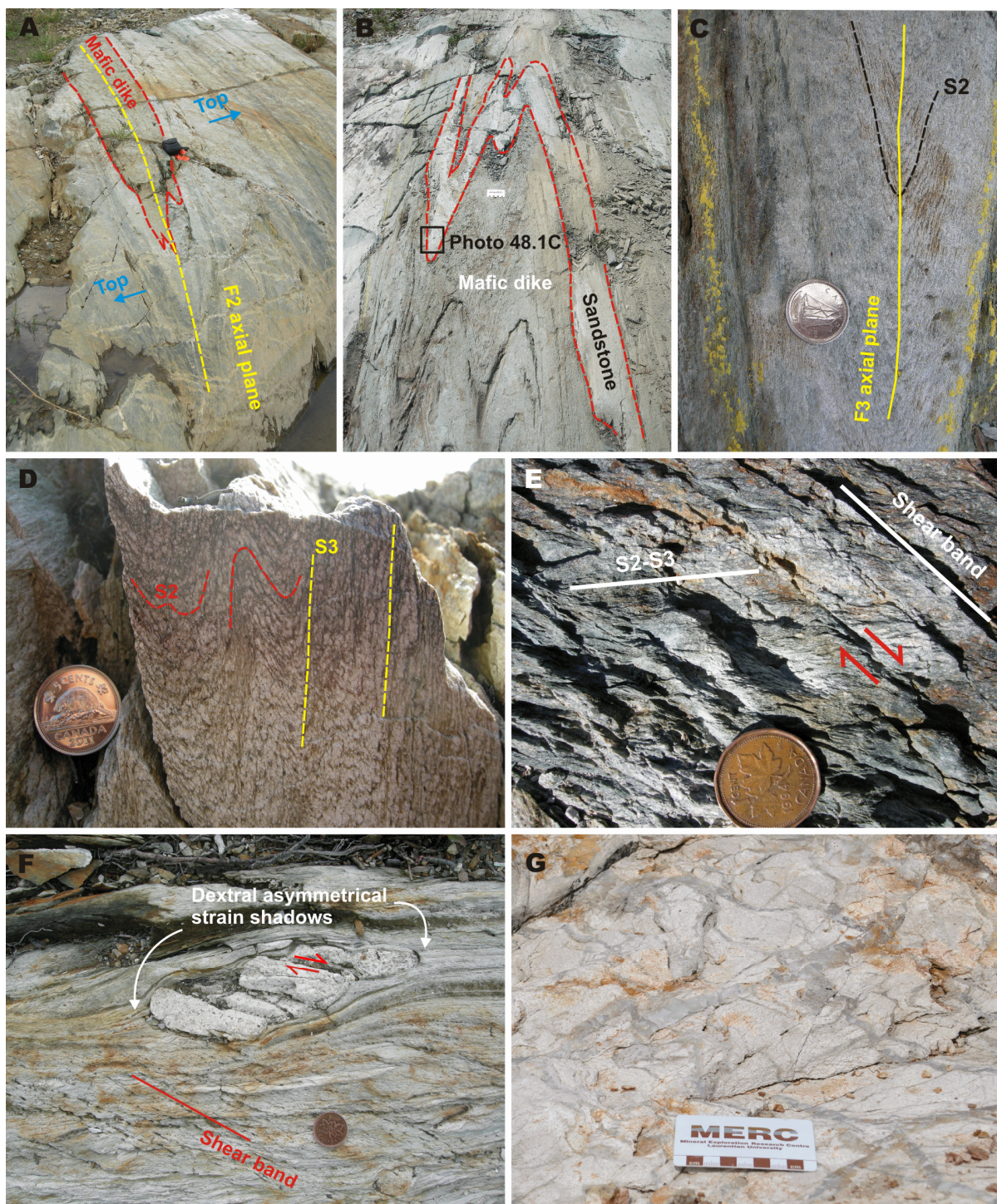


Photo 48.1. Field photographs of the Portal stripping. A) Downward-facing synformal F_2 fold. A mafic dike occupies the hinge of the fold. Blue arrows indicate younging direction in wacke. Camera casing, 15 cm in length, for scale. B) S-shaped F_3 fold defined by folded wacke and mafic dikes, north of the main feldspar porphyry body. Photo scale is 9 cm in length. C) Close-up of F_3 fold hinge shown in Photo 48.1B. S_2 cleavage in wacke is folded by F_3 . Coin (18 mm diameter) for scale. D) S_2 cleavage folded by S-shaped F_3 folds along the northern margin of the main feldspar porphyry body. S_3 cleavage is defined by the intensification of S_2 along the long limb of the folds. Coin (20 mm diameter) for scale. E) Penetrative dextral shear bands indicating dextral transcurrent movement, south of the main feldspar porphyry body. Coin (19 mm diameter) for scale. F) Dextral shear bands and dextral asymmetrical strain shadow around granitic clast in conglomerate. Coin (19 mm diameter) for scale. G) Mineralized quartz vein stockwork in the main feldspar porphyry body. Photo scale is 9 cm in length.

and are up to 10 cm thick. They are associated with a stockwork of smaller quartz veins and surrounded by silicified porphyry containing minor pyrite (Photo 48.1G). The quartz veins are folded by a Z-shaped F_3 fold that is parasitic to the large F_3 fold, and they are transposed and locally boudinaged suggesting either early- or pre- D_3 emplacement of the gold-bearing veins.

TOMBILL–BANKFIELD FAULT STRIPPING

The Tombill–Bankfield fault is described as a zone of intense shearing, brecciation, silicification and carbonatization (Pye 1952; Horwood and Pye 1955). It was thought to be a major break that influenced the location of most deposits in Geraldton (Pye 1952). This recently led Premier Gold Mines Ltd. to excavate 3 to 4 m of overburden to expose bedrock where a drill hole intersected black smoky quartz veins along the trace of the fault. This new stripping is the best known exposure of the fault at surface, but it will be reburied during the coming year.

The fault occurs at the contact between diorite to the south and sandstone to the north (Figure 48.3). The sandstone is interleaved with diorite, mafic pillowed flows and a fine-grained, synvolcanic, mafic dike. Diorite is greenish dark grey on outcrop and fresh surfaces. It consists of approximately 45% chloritized green amphibole, up to 1 cm in size, surrounded by greenish white feldspar. Epidote-quartz-amphibole patches and veins occur throughout the rock and are cut by late quartz-iron carbonate veins. Local tourmaline-rich quartz veins and breccias are present. Sandstone varies in colour and composition from a more sericitic, greenish light grey rock with bed thicknesses of 2 to 10 cm and grain size of 1 to 2 mm, to a more chloritic, brownish dark grey, interlayered sandstone–mudstone with bed thicknesses of 2 to 5 cm. Mafic pillowed flow consists of dark green, aphyric pillows with thin (~1 cm thick) selvages (Photo 48.2A). The synvolcanic dike is dark green, aphyric and massive. It is in sharp contact with the diorite and mafic pillowed flow. The mafic pillowed flow and synvolcanic dike are cut by multiple epidote-quartz veins that are, in turn, transected by quartz-iron carbonate-tourmaline veins.

The diorite has a strong differentiated foliation (S_2) defined by feldspar-rich felsic bands, alternating with amphibole-rich mafic bands (average thickness of 3 to 5 mm). The S_2 foliation strikes east (~100°) and dips steeply (70 to 85°) to the south. It is folded by Z-shaped F_3 folds associated with an axial plane S_3 cleavage defined by chlorite. The S_3 cleavage is oriented anticlockwise to the S_2 foliation; it strikes east-northeast (70 to 85°) and dips steeply (70 to 85°) to the south. The S_3 cleavage becomes more intense and closely spaced in narrow shear zones (<50 cm thick) surrounding less deformed, metre wide, lozenges of diorite. The shear zones contain a shallowly west-plunging (~15°), chloritic, mineral lineation, similar in orientation to F_3 fold axes. Dextral shear bands, striking approximately 120° or approximately 300° and dipping steeply (80 to 85°) to the south or north, and Z-shaped drag folds defined by folded quartz-iron carbonate veins, are present along most shear zones, suggesting dextral transcurrent shear. Pillows in the mafic pillowed flow are flattened parallel to the S_2 foliation. The strain appears to increase in intensity within sandstone and mudstone where the S_2 foliation is oriented parallel to bedding and the S_3 cleavage is oriented anticlockwise to the S_2 foliation as observed in the diorite. Similar dextral shear sense indicators, that is, shear bands and drag folds, are developed in sheared sandstone–mudstone and mafic pillowed flows, but, in addition, spectacular dextral asymmetrical strain shadows are present around pillow fragments (Photo 48.2B).

Black smoky fault-fill quartz veins occur along the fault. The fault is parallel to S_2 and so it formed either during or after the D_2 deformation event. The veins are individually 1 to 15 cm thick and collectively approximately 1 m thick, and they strike 90 to 105° and dip 75 to 85°S parallel to the fault. They are cut by multiple, millimetre-thick, milky white, quartz veins, filling fractures that are perpendicular to the margins of the black smoky quartz veins and that span the width of those veins. A 1.5 m thick, bleached (light grey), alteration halo surrounds the black smoky quartz veins. The veins were broken up and brecciated (Photo 48.2C), and an anticlockwise S_3 cleavage formed in the alteration halo,

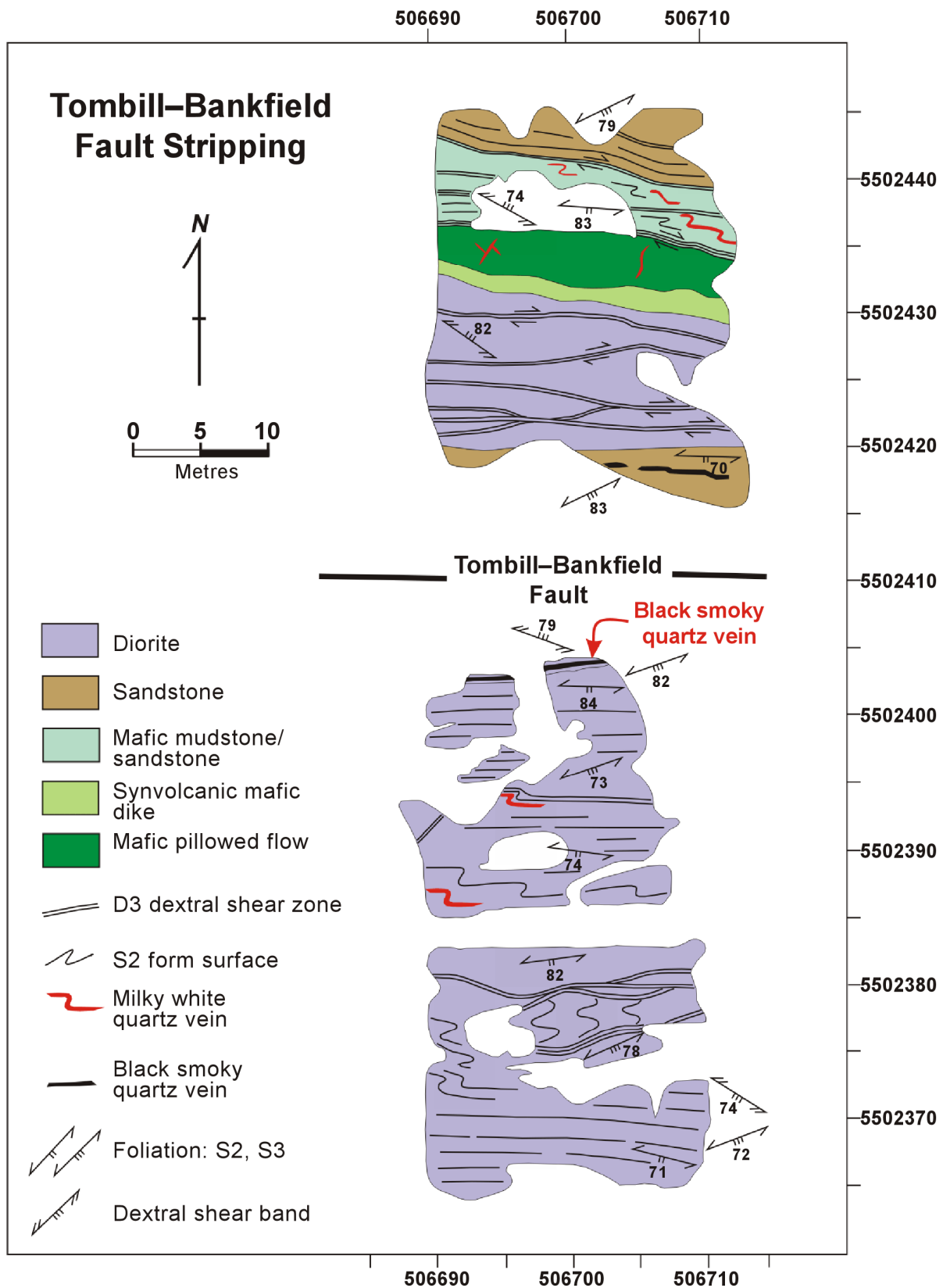


Figure 48.3. Geological map of the Tombill–Bankfield fault stripping. Location of the map is shown in Figure 48.1. UTM co-ordinates provided using NAD83, Zone 16.

during D₃ dextral shear reactivation of the fault. Pyrite and chalcopyrite(?) occupy dextral shear bands that have a strike of 125 to 140° and a dip of approximately 70° to the south (Photo 48.2D), similar to the orientation of shear bands associated with narrow dextral shear zones north and south of the fault. Thus, the smoky quartz veins were emplaced either during D₂ deformation or early during D₃ dextral shear, and sulphide mineralization was remobilized into shear bands during D₃ dextral shear. Grab samples of the veins yielded low gold values, so no further work is planned for this stripping and fault (Premier Gold Mines Ltd. staff, personal communication, 2012).

CONCLUSIONS

The Portal and Tombill–Bankfield strippings occur in a high-strain corridor that encompasses the south limb of the Hard Rock anticline. Rocks at both stripped outcrops underwent intense deformation during the D₂ event, which resulted in the development of a penetrative S₂ foliation, and were further folded and deformed during D₃ dextral transcurrent shear. The timing of mineralization differs between the 2 stripped outcrops. At the Portal stripping, the auriferous quartz veins are pre- or early D₃ dextral shear, whereas at the Tombill–Bankfield fault stripping, fault-fill veins are either syn-D₂ event or early D₃ shear and sulphide mineralization is syn-D₃ dextral shear. This suggests that at least 2 mineralizing events occurred in the Geraldton area. Thus, the ore zones may have formed, and were possibly upgraded, during more than one mineralization event. As the earliest mineralization event predates F₄ and F₃ folding, polyphase folding is likely an important control on the actual geometry and distribution of the ore zones.

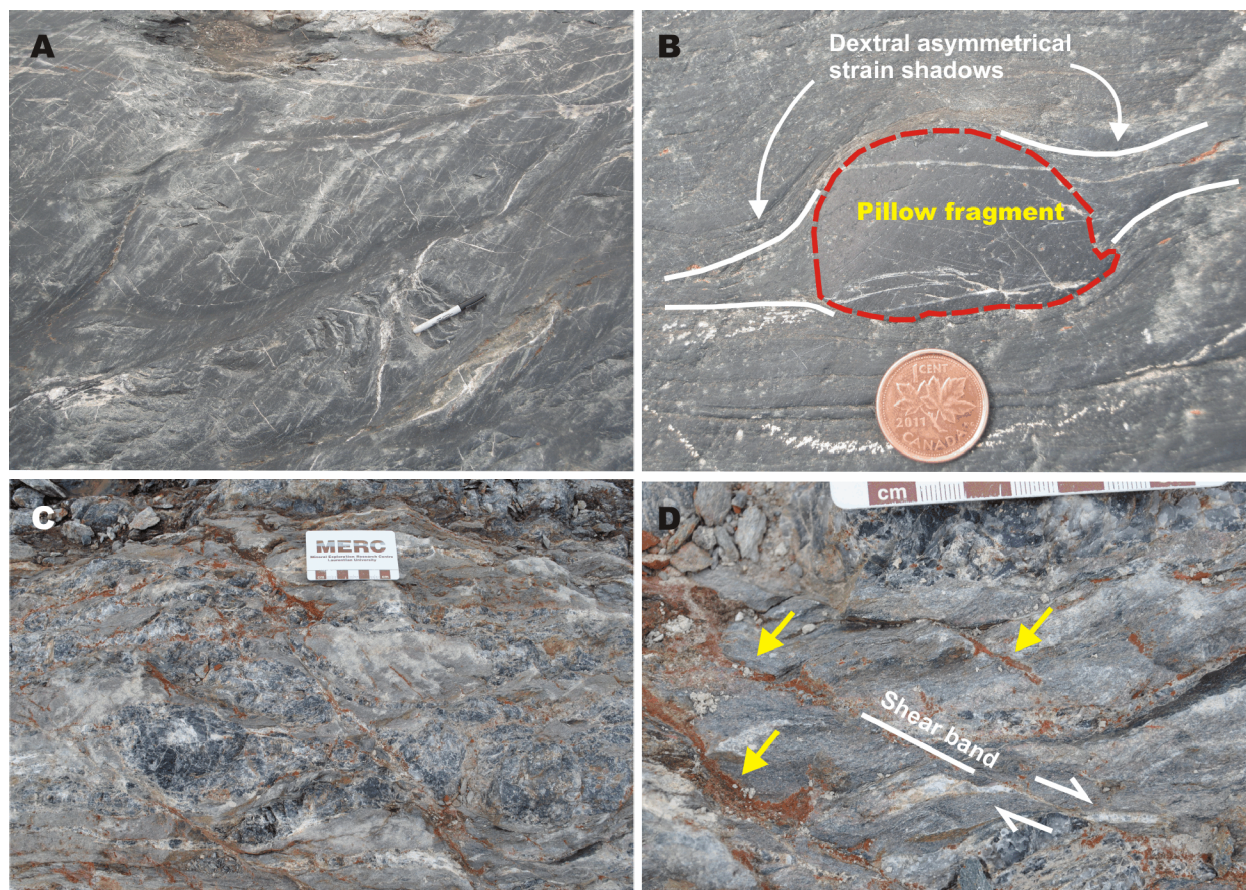


Photo 48.2. Field photographs of the Tombill–Bankfield stripping. A) Pillow in mafic pillow flow. Pencil is 10 cm in length. B) Dextral asymmetrical strain shadows around pillow fragment. Coin (19 mm diameter) for scale. C) Fractured and broken-up black smoky quartz vein along the Tombill–Bankfield fault. Photo scale is 9 cm in length. D) Sulphide mineralization (indicated by yellow arrows) was emplaced along dextral shear bands during D₃.

ACKNOWLEDGMENTS

This project is part of a PhD thesis undertaken by Z. Tóth at Laurentian University, Sudbury, supervised by B. Lafrance. We gratefully acknowledge the support of the Ontario Geological Survey and funding of the project through the TGI-4 program of Natural Resources Canada. We thank Nicholas Whynot, Andrew Hackner, Tammy Lehtinen and Tim Twomey for discussions on gold mineralization in the Geraldton area and access to drill cores, outcrops and historical data. Phil Thurston (Laurentian) and Vicki McNicoll (GSC) contributed to discussions on the geology of the Beardmore–Geraldton belt. Williams Oswald (Institut national de la recherche scientifique (INRS)) provided essential training on the use of the differential global positioning system (GPS) for mapping.

REFERENCES

- Anglin, C.D. 1987. Geology, structure and geochemistry of gold mineralization in the Geraldton area, northwestern Ontario; unpublished MSc thesis, Memorial University of Newfoundland, St. John's, Newfoundland, 283p.
- Anglin, C.D., Franklin, J.M., Loveridge, W.D., Hunt, P.A. and Osterberg, S.A. 1988. Use of zircon U-Pb ages of felsic intrusive and extrusive rocks in eastern Wabigoon Subprovince, Ontario, to place constraints on base metal and gold mineralization; *in* Radiogenic Age and Isotopic Studies: Report 2, Geological Survey of Canada, Paper 88-2, p.109-115.
- Devaney, J.R. and Williams, H.R. 1989. Evolution of an Archean subprovince boundary: a sedimentological and structural study of part of the Wabigoon–Quetico boundary in northern Ontario; *Canadian Journal of Earth Sciences*, v.26, p.1013-1026.
- Dubé, B., Mercier-Langevin, P., Castonguay, S., McNicoll, V.J., Pehrsson, S.J., Bleeker, W., Schetselaar, E.M. and Jackson, S. 2011. Targeted Geoscience Initiative 4. Lode gold deposits in ancient, deformed and metamorphosed terranes—footprints and exploration implications: a preliminary overview of themes, objectives and targeted areas; *in* Summary of Field Work and Other Activities 2011, Ontario Geological Survey, Open File Report 6270, p.38-1 to 38-10.
- Hart, T.R., ter Meer, M. and Jolette, C. 2002. Precambrian geology of Kitto, Eva, Summers, Dorothea, and Sandra townships, northwestern Ontario: Phoenix bedrock mapping project; Ontario Geological Survey, Open File Report 6095, 206p.
- Horwood, H.C. and Pye, E.G. 1955. Geology of Ashmore Township; Ontario Department of Mines, Annual Report, 1951, v.60, pt.5, 105p.
- Lafrance, B., DeWolfe, J.C. and Stott, G.M. 2004. A structural reappraisal of the Beardmore–Geraldton belt at the southern boundary of the Wabigoon Subprovince, Ontario, and implications for gold mineralization; *Canadian Journal of Earth Sciences*, v.41, p.217-235.
- Macdonald, A.J. 1988. The Geraldton gold camp: the role of banded iron formation; Ontario Geological Survey, Open File Report 5694, 176p.
- Mason, J. and White, G. 1986. Gold occurrences, prospects, and deposits of the Beardmore–Geraldton area, districts of Thunder Bay and Cochrane; Ontario Geological Survey, Open File Report 5630, 680p.
- Pye, E.G. 1952. Geology of Errington Township, Little Long Lac area; Ontario Department of Mines, Annual Report, 1951, v.60, pt.6, 140p.
- Tomlinson, K.Y., Hall, R.P., Hughes, D.J. and Thurston, P.C. 1996. Geochemistry and assemblage accretion of metavolcanic rocks in the Beardmore–Geraldton greenstone belt, Superior Province; *Canadian Journal of Earth Sciences*, v.33, p.1520-1533.

Index of Authors (with corresponding article numbers)

A

Ames, D.E., 41
Armstrong, D.K., 30

B

Bajc, A.F., 31
Barnes, S.-J., 46
Barnett, P.J., 24, 25
Barnett, R.L., 44
Beakhouse, G.P., 7, 8
Bekker, A., 45
Béland Otis, C., 29
Berger, B.R., 3, 4
Bleeker, W., 48
Brunton, F.R., 22, 35
Burke, H.E., 26
Burnham, O.M., 38, 39
Burt, A.K., 32, 33
Buse, S., 11

C

Campbell, D.A., 18
Carr, S.D., 15
Cousens, B., 14
Cundari, R.M., 18
Cutts, J., 15

D

Dare, S.A.S., 41
Dubé, B., 48
Duguet, M., 8, 13
Duke, N.A., 44
Dyer, R.D., 26, 27, 28

E

Easton, R.M., 12, 14, 15

F

Freckelton, C.N., 37
Fyon, J.A., 1

G

Gao, C., 23
Gordon, C.A., 17

H

Hamilton, M.A., 11
Hamilton, S.M., 36, 37, 38
Hanley, J.J., 41
Hargreaves, J., 40
Hicock, S.R., 25
Hiebert, R.S., 45
Hollings, P., 18, 41
Houlé, M.G., 42, 43, 45, 46

J

Jackson, S.E., 41
Jugo, P.J., 41

K

Kamo, S.L., 9
Keating, G.L., 39
Kontak, D.J., 41

L

Laarman, J.E., 44
Lafrance, B., 48
Lee, V.L., 20, 35, 36
Leshner, C.M., 42, 45
Lewis, D., 9, 16
Linnen, R.L., 41
Lodge, R.W.D., 4, 9, 10

M

Magnus, S.J., 13, 14
Marich, A.S., 34
Mercier-Langevin, P., 48
Méric, J., 46
Metsaranta, R.T., 42, 43
Muir, T.L., 19
Mulligan, R.P.M., 31

N

Nguyen, M.K., 25

P

Pagé, P., 46
Parker, J.R., 2
Préfontaine, S., 5
Priebe, E.H., 35

R

Rainsford, D.R.B., 19, 31
Ratcliffe, L., 13
Robichaud, L., 6
Rowell, D.J., 20, 21, 22

S

Samson, I.M., 41
Schroeder, J., 38
Scott, J.F., 18
Smyk, M.C., 18

T

Tóth, Z., 48

W

Wing, B.A., 45

Y

Yeung, K.H., 24

Metric Conversion Table

Conversion from SI to Imperial			Conversion from Imperial to SI		
<i>SI Unit</i>	<i>Multiplied by</i>	<i>Gives</i>	<i>Imperial Unit</i>	<i>Multiplied by</i>	<i>Gives</i>
LENGTH					
1 mm	0.039 37	inches	1 inch	25.4	mm
1 cm	0.393 70	inches	1 inch	2.54	cm
1 m	3.280 84	feet	1 foot	0.304 8	m
1 m	0.049 709	chains	1 chain	20.116 8	m
1 km	0.621 371	miles (statute)	1 mile (statute)	1.609 344	km
AREA					
1 cm ²	0.155 0	square inches	1 square inch	6.451 6	cm ²
1 m ²	10.763 9	square feet	1 square foot	0.092 903 04	m ²
1 km ²	0.386 10	square miles	1 square mile	2.589 988	km ²
1 ha	2.471 054	acres	1 acre	0.404 685 6	ha
VOLUME					
1 cm ³	0.061 023	cubic inches	1 cubic inch	16.387 064	cm ³
1 m ³	35.314 7	cubic feet	1 cubic foot	0.028 316 85	m ³
1 m ³	1.307 951	cubic yards	1 cubic yard	0.764 554 86	m ³
CAPACITY					
1 L	1.759 755	pints	1 pint	0.568 261	L
1 L	0.879 877	quarts	1 quart	1.136 522	L
1 L	0.219 969	gallons	1 gallon	4.546 090	L
MASS					
1 g	0.035 273 962	ounces (avdp)	1 ounce (avdp)	28.349 523	g
1 g	0.032 150 747	ounces (troy)	1 ounce (troy)	31.103 476 8	g
1 kg	2.204 622 6	pounds (avdp)	1 pound (avdp)	0.453 592 37	kg
1 kg	0.001 102 3	tons (short)	1 ton(short)	907.184 74	kg
1 t	1.102 311 3	tons (short)	1 ton (short)	0.907 184 74	t
1 kg	0.000 984 21	tons (long)	1 ton (long)	1016.046 908 8	kg
1 t	0.984 206 5	tons (long)	1 ton (long)	1.016 046 9	t
CONCENTRATION					
1 g/t	0.029 166 6	ounce (troy) / ton (short)	1 ounce (troy) / ton (short)	34.285 714 2	g/t
1 g/t	0.583 333 33	pennyweights / ton (short)	1 pennyweight / ton (short)	1.714 285 7	g/t

OTHER USEFUL CONVERSION FACTORS

	<i>Multiplied by</i>	
1 ounce (troy) per ton (short)	31.103 477	grams per ton (short)
1 gram per ton (short)	0.032 151	ounces (troy) per ton (short)
1 ounce (troy) per ton (short)	20.0	pennyweights per ton (short)
1 pennyweight per ton (short)	0.05	ounces (troy) per ton (short)

*Note: Conversion factors in **bold** type are exact. The conversion factors have been taken from or have been derived from factors given in the Metric Practice Guide for the Canadian Mining and Metallurgical Industries, published by the Mining Association of Canada in co-operation with the Coal Association of Canada.*

ISSN 0826-9580 (Print)
ISBN 978-1-4606-0488-5 (Print)

ISSN 1916-6117 (online)
ISBN 978-1-4606-0489-2 (PDF)